International Journal of Mathematical Analysis and Modelling

(Formerly Journal of the Nigerian Society for Mathematical Biology)

Volume 7 Issues 1&2, 2024

ISSN (Print): 2682 - 5694
ISSN (Online): 2682 – 5708
www.tnsmb.org

International Journal of Mathematical Analysis and Modelling (Formerly Journal of the Nigerian Society for Mathematical Biology)

Volume 7, Issues 1&2, 2024

ISSN (Print): 2682 – 5694

ISSN (Online): 2682 - 5708

Disclaimer: The articles published herein do not necessarily reflect the opinion of the editorial board of this journal or the Nigerian Society for Mathematical Biology (NSMB). The editorial board or the NSMB do not accept any legal responsibility for any errors or omissions that may be made in this volume of the International Journal of Mathematical Analysis and Modelling (Formerly Journal of the Nigerian Society for Mathematical Biology).

A publication of the Nigerian Society for Mathematical Biology

©NSMB

Editorial Board

Prof. Daniel Okuonghae, Ph.D., FNYA — Editor-in-Chief
Department of Mathematics
University of Benin
Benin City, Nigeria.
daniel.okuonghae@uniben.edu
danny.okuonghae@ccc.oxon.org
mcsb@uniben.edu

Editors

Prof. Samuel O. Okoya	Obafemi Awolowo University, Ile-Ife, Nigeria
Prof. Godwin C.E. Mbah	University of Nigeria, Nsukka, Nigeria
Prof. Ninuola Akinwande	Federal University of Technology, Minna, Nigeria
Prof. A.R. Kimbir	Federal University of Agriculture, Makurdi, Nigeria
Prof. Olufemi A. Adesina	Obafemi Awolowo University, Ile-Ife, Nigeria
Prof. Philip O. Olanrewaju	Federal University, Wukari, Nigeria
Prof. Augustine Iduseri	University of Benin, Benin City, Nigeria
Prof. Sirajo Abdulrahman	Federal University, Birnin Kebbi, Nigeria
Andrew Omame, Ph.D.	Federal University of Technology, Owerri, Nigeria
Prof. Bolarinwa Bolaji	Kogi State University, Ayingba, Nigeria
Dennis Agbebaku, Ph.D.	University of Nigeria, Nsukka, Nigeria
George Akuchu, Ph.D.	University of Nigeria, Nsukka, Nigeria
Prof. Robert Okuonghae	University of Benin, Benin City, Nigeria
Prof. Monday N.O. Ikhile	University of Benin, Benin City, Nigeria

Mathematical analysis for the dynamics of Feline immunodeficiency virus in cats population

Salisu Usaini[*†], **Musa Usman**[†‡]

Abstract

In this paper, we present an extended version of the deterministic model of feline immunodeficiency virus (FIV) within cats population to carry out the stability analysis with regards to the total population of cats and disease prevalence. For the extension, we incorporate the compartment of latently infected domestic cats since it is evident that such cats transmit the virus as well. Stability analysis of the presented model is carried out. The analysis reveals that the retrovirus cannot invades the population at carrying capacity state if the threshold parameter, $\mathcal{R}_0$ is less than unity. Indeed, we obtain an additional equilibrium point known as semi-trivial state for which the disease exterminate the host population. Moreover, the carrying capacity state can exchange stability with non-trivial equilibrium at $\mathcal{R}_0 = 1$ so that the latter will be the only attractor when $\mathcal{R}_0 > 1$, a phenomenon called transcritical bifurcation.

Keywords and phrases: Feline immunodeficiency virus; FIV latency; domestic cats.

1 Introduction

The feline immunodeficiency virus (FIV) is detected worldwide and is among the most common infectious diseases of domestic cats, other small felids and wild cats. It belongs to a Lentivirus subfamily which was first isolated and described by Pedersen, 1987 in the city of Petaluma, USA [1]. The FIV distinct subtypes are designated A through E [2]. The immunodeficiency disease from FIV infection in domestic cats is similar to human acquired immune deficiency syndrome (AIDS) [3]. This is an important Lentivirus that causes immune disorders in both domestic and nondomestic cats. The high incidence of the virus is associated with density of cat population and males have high risk of infection than females since transmission mode is through bites inflicted during fights and biting is more apt to occur between male cats [4]. Therefore, the risk of FIV transmission is low in socially well-adapted cats [2, 5]. Veneral transmission from infected males to females is also possible as experimental studies shows that infection occurs not only via a vaginal route, but also via rectal mucous membrane [6]. The seroprevalence of FIV is highly variable between geographic locations ranging from 2% in Germany and 16% in the United States to 33% in the United Kindom to 44% in Japan [7].

Feline immunodeficiency virus infection can be divided into five stages similar to those of human immunodeficiency virus (HIV) infection namely: acute phase which begins about four weeks after infection and lasts for four month, asymptomatic carrier (AC), persistent generalized lymphadenopathy (PGL), AIDS-related complex (ARC) and AIDS stages [5]. Although many cats exhibit no clinical signs during acute infection but fever, leucopenia, gingivitis, lethargy, signs of enteritis, stomatitis, dermatitis, conjunctivitis, respiratory tract disease, neutropenia, and generalized lymphadenopathy may be observed. There are no clinical signs in AC stage which lasts several months to years but there is a progressive decline in CD4+ T lymphocyte numbers. The PGL phase is associated with unspecific clinical signs including apathy, weight loss, lymphadenopathy, fever, anorexia, depression, chronic

[*]Corresponding Author; E-mail: salisu.usaini@kustwudil.edu.ng
[†]Department of Mathematics, Aliko Dangote University of Science and Technology, Wudil, Nigeria
[‡]Department of Statistics, Jigawa State Polytechnic, Dutse, Nigeria; E-mail: musausman39yayari@gmail.com

gingivostomatitis (difficulty eating), chronic rhinitis, lymphadenopathy, immune-mediated glomerulo nephritis, leucopenia and behavioral abnormalities. Even though the ARC and AIDS phases of disease are not clearly defined, cats with ARC usually experience chronic respiratory, gastrointestinal, and skin disorders, accompanied by PGL. While some signs that signal a progression to AIDS include more opportunistic infections, severe emaciation, neoplasia, lymphoid depletion and seizures, and neurological abnormalities [2, 5, 8].

A deterministic mathematical model of susceptible-infectious (SI) type is proposed in [9] to study the circulation of FIV within populations of domestic cats. The model analysis reveals that FIV is endemic in domestic feline populations. In 1997, a deterministic model for the transmission dynamics of two retrovirus, namely: a Feline Immunodeficiency Virus (FIV) and Feline Leukaemia Virus (FeLV) simultaneously infecting a single host (domestic cat Felis catus) was presented in [10]. Stability analysis and simulations of the model reveal that FIV persists and is maintained in the population when introduced, while FeLV is either persists or goes extinct. Further, the combined impact of the diseases is observed to be higher than the sum of the impact of the two individual diseases. This is perhaps due to a higher mortality rate when both viruses infect a single individual. A generic SEIRS model with application to cat retroviruses and fox rabies is developed in [11]. An explicit criterion for the stability of the largest disease-free stationary state is provided. The result is applied to the Feline Immunodeficiency Virus and to the Feline Leukemia Virus, two retroviruses of domestic cats (Felis catus), and to the rabies virus for red foxes (Vulpes vulpes).

In the last decade, a stochastic dynamics of FIV in cats populations was studied in [12] to get insight on the effects of environmental driving forces on its dynamics. The analysis reveals that FIV outbreak can be suppressed by large environmental fluctuations and a threshold parameter R_s^h governs the virus distributions. Moreover, susceptible-free dynamics is possible by white noise perturbations of the birth rate for infected cats. Recently, a discrete-time zoonotic infectious disease model with strong Allee effect was proposed in [13]. They shown that the presence of the strong Allee effect in the disease-free equation rendered the model bistable. The authors examined the structures of the coexisting attractors using the threshold parameter $\mathcal{R}_0$ and the spectral radius, λ_k. Numerical simulations reveals that the disease can enlarge and shrink the basic of attraction of the catastrophic extinction state as well as breaking it into several disjoint sets.

In this study, we extend the susceptible-infectious (SI) model proposed in [9] by incorporating the compartment of latently infected (as FIV supports latent infection both *in vitro* and *in vivo*, [14]) cats to carry out the stability analysis with regards to the total population of cats and disease prevalence. In fact, after a prolonged latent period that last for years, the progressive loss of T-lymphocytes results in an immunodeficiency syndrome characterised by chronic and recurrence infections. The analysis reveals that in addition to the three equilibrium points reported in [9], an additional equilibrium point exists for which the disease exterminate the host population known as semi-trivial equilibrium [15, 16]. We show that disease persistence depends on two threshold parameters $\mathcal{R}_0$ and $\mathcal{R}_1$. In fact, the uniqueness of the non-trivial equilibrium if it exists leads to occurrence of a transcritical bifurcation at $\mathcal{R} = 1$. This phenomenon results in the exchange of stability between the carrying capacity state and the nontrivial equilibrium at $\mathcal{R}_0 = 1$. That is, if $\mathcal{R}_0 < 1$, the only local asymptotic stable equilibrium is the carrying capacity state, whereas the non-trivial equilibrium will be the only attractor for $\mathcal{R}_0 > 1$ and $\mathcal{R}_1 > 1$.

We organised the remaining part of this paper as follows: In Section 2, we describe the proposed model. Stability analysis of the model equilibria is carried out in Section 3. Then we discuss on the model results and give a concluding remarks in the last section.

2 Model formulation

We denote by $N(t)$, the total number of cats at time t. Let b be the natural birth rate and m be the natural death rate in the absence of infection. Thus, the intrinsic growth-rate of the cat population in the absence of resource limitation and epidemic is $r = b - m$. We assume that resource limitation acts through density-dependence on the death rate, while the birth rate remains constant [9]. Therefore,

we split the Logistic growth rate, $G(N) = r(1 - \frac{N}{K})$ as

$$G(N) = B(N) - D(N),$$

with $B(N) = b$ is the birth rate which is constant and $D(N) = m + r\frac{N}{K}$ is the death rate which is linearly related to N, where m is the natural death rate, K is the carrying capacity of the habitat, $r = b - m \geq 0$ is the population growth rate in absence of resource limits which adjusts the maximum per capita growth rate. That is resource limitation is assumed to act through density-dependence on the death rate.

When the population is free from FIV infection, the dynamics of the total population is governed by the logistic model.

$$\frac{dN}{dt} = rN\left(1 - \frac{N}{K}\right). \tag{1}$$

To describe the dynamics of the FIV through cats population, we divide the population into three classes of susceptibles denoted by $S(t)$, latent denoted by $L(t)$ and infectious denoted by $I(t)$, so that $S(t) + L(t) + I(t) = N(t)$. Although there are several stages of illness, for the sake of simplicity we assume that there is only one stage of illness combining acute, seropositivity, persistent generalized lymphadenopathy (PGL), Aids-related complex (ARC) and AIDS stages. Furthermore, we assume that the latently infected cats transmit the disease in a reduced rate (i.e., there is a modification parameter $0 < \epsilon < 1$, accounting for the reduction of infectiousness of latently infected individuals in comparison to the infectious ones) since there is a clinical evidence of FIV latent infection [17]. As in [9], we also assume that:

(i) FIV transmission is via proportionate mixing and a cat's infection status does not affect the probability of having direct contacts with other cats,

(ii) The frequency of an aggressive contacts resulting in a bite when an encounter occurs is β, and c is the efficiency of the FIV transmission by biting,

(iii) A cat comes into contact with others in the population at a constant rate ρ,

(iv) Of all the contacts had by a single susceptible cat, a proportion $\frac{\epsilon L+I}{N}$ is with infected cats. Therefore the rate at which contacts between susceptibles and infected cats occur is $\rho\frac{S(\epsilon L+I)}{N}$ so that the force of infection is $c\rho\beta\frac{S(\epsilon L+I)}{N}$, i.e., $\sigma\frac{S(\epsilon L+I)}{N}$,

(v) There is no vertical transmission and there is no recovery of infectious cats by any means.

The respective rates of transfer between the three compartments are presented in Figure 1. Then combining the above assumptions the model equations describing the dynamics of cats population infected with FIV are given by the following system of ordinary differential equations.

$$\begin{cases} \frac{dS}{dt} = b(S + L + I) - \left(m + r\frac{N}{K}\right)S - \frac{\sigma(\epsilon L + I)}{N}S, \\ \frac{dL}{dt} = \frac{\sigma(\epsilon L + I)}{N}S - \left(m + r\frac{N}{K}\right)L - \gamma L, \\ \frac{dI}{dt} = \gamma L - \left(m + r\frac{N}{K}\right)I - \alpha I \\ \frac{dN}{dt} = rN\left(1 - \frac{N}{K}\right) - \alpha I, \end{cases} \tag{2}$$

The parameter σ is the rate of effective bites for FIV transmission. The disease related mortality rate is α and so, $\frac{1}{\alpha}$ is the rate of infectious period.

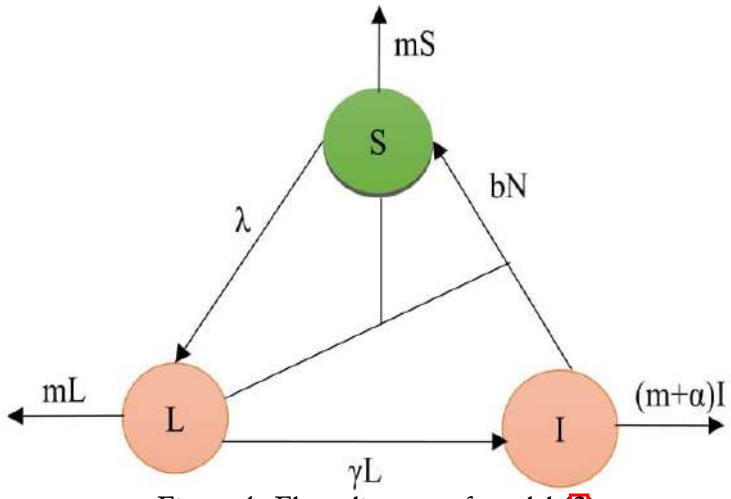


Figure 1: Flow diagram of model (2)

Introducing the prevalence $i(t)$, we have

$$s = \frac{S}{N}, e = \frac{L}{N}, i = \frac{I}{N}, \text{ and } p = \frac{N}{K}, \tag{3}$$

so that model (2) is rescaled to

$$\begin{cases} \frac{dp}{dt} = [r(1-p) - \alpha i]p, \\ \frac{de}{dt} = \sigma\epsilon e + \sigma i(1-i) - [b + \gamma + (\sigma - \alpha)i + \sigma\epsilon(e+i)]e, \\ \frac{di}{dt} = \gamma e - [b + \alpha(1-i)]i, \end{cases} \tag{4}$$

with $s = 1 - e - i$.

Theorem 2.1. *The system of equations (4) defines a dynamical system in the biologically feasible region*

$$\mathcal{D} = \{(p, e, i) \in \mathbb{R}^3_+ : 0 \leq e, i, e + i \leq p \leq 1\}.$$

In the following analysis, we assume that $\sigma > \alpha$ as in [9]. This is because when the effective contact rate σ is less than or equal to the disease-induced death rate α, the influx of infectious compartment is lower than the out flux as the number of latently infected cats decreases, resulting in the reduction of the number of infectious cats. This scenario can be seen from the second and third equations of (2).

All the model parameters are assumed to be non-negative and are described in Table 2.

Table 1: Parameter values

Parameter	Description	Nominal value	Reference
b	Natural birth rate	2.4	[9]
m	Natural death rate	1.8	[9]
α	disease-induced death rate	0.2	[9]
σ	Rate of effective bite	3	[9]
ϵ	Modification parameter	(0, 1]	Assumed
γ	Progression rate	0.3	Assumed

3 Analysis of the model

3.1 Trivial equilibria

In the absence of infection, model (4) exhibits the following equilibrium points.

(i) The trivial equilibrium: $E_0 = (p_0, e_0, i_0) = (0, 0, 0)$,

(ii) The carrying capacity state: $E_1 = (p_1, e_1, i_1) = (1, 0, 0)$,

It is well known that a disease can be controlled by either one of the two ways for disease transmission models with varying population size due to demographic effects [18, 19]. The first one requires that the proportion of infected individuals $i(t)$ goes to zero, while the second requirement is that the absolute number of infectives $I(t)$ approaches to zero. Therefore, the conditions for the linear stability of disease free equilibria and for the endemic proportion equilibria are required. The pertinent threshold parameter is as follows

$$\begin{aligned} \mathcal{R}_0 &= \frac{\sigma\gamma}{(b+\alpha)(b+\gamma)} + \frac{\sigma\epsilon}{(b+\gamma)} \\ &= \frac{\sigma[\gamma + \epsilon(b+\alpha)]}{(b+\alpha)(b+\gamma)}. \end{aligned} \tag{5}$$

Theorem 3.1. *The equilibrium point of model* (4)

(i) E_0 *is unstable if* $\mathcal{R}_0 < 1$,

(ii) E_1 *is locally asymptotically stable if* $\mathcal{R}_0 < 1$ *and is unstable when* $\mathcal{R}_0 > 1$.

Proof. By linearization, we obtain the Jacobian matrix of system (4) as

$$J(p, e, i) = \begin{pmatrix} r(1-2p) - \alpha i & 0 & -\alpha p \\ 0 & Q & \sigma(1-2i) - [\sigma\epsilon + (\sigma - \alpha)]e \\ 0 & \gamma & -[b + \alpha(1-2i)] \end{pmatrix}, \tag{6}$$

$Q = \sigma\epsilon(1 - 2e - i) - (b + \gamma) - (\sigma - \alpha)i$. Thus, the Jacobian matrix evaluated at trivial equilibrium, E_0, is given by

$$J(E_0) = \begin{pmatrix} r & 0 & 0 \\ 0 & \sigma\epsilon - (b+\gamma) & \sigma \\ 0 & \gamma & -(b+\alpha) \end{pmatrix}.$$

Then, the eigenvalues of $J(E_0)$ are: r and the eigenvalues of the matrix $J_0(E_0)$ which is obtained by deleting the first row and the first column of $J(E_0)$. It can be verified that the trace and determinant of $J_0(E_0)$ are respectively,

$$tr[J_0(E_0)] = -\left[(b+\gamma)\left(1 - \frac{\sigma\epsilon}{b+\gamma}\right) + b + \alpha\right] < 0$$

and

$$\det[J(E_0)] = (b+\gamma)(b+\alpha)(1 - \mathcal{R}_0) > 0$$

if $\mathcal{R}_0 < 1$. Then the eigenvalues of the matrix $J_0(E_0)$ have negative real parts. Hence, E_0 is unstable whenever $\mathcal{R}_0 < 1$.

Similarly, the eigenvalues of $J(E_1)$ are: $-r$ and the eigenvalues of the matrix $J_1(E_1)$, which is equivalent to $J_0(E_0)$. Therefore, all the eigenvalues of $J(E_1)$ have negative real parts. Hence E_1 is locally asymptotically stable. ■

3.2 Semi-trivial and non-trivial equilibrium points

Setting the right hand sides of (4) to zero, we have from the first and third equations of (4) that

$$p = 0 \text{ or } i = \frac{r(1-p)}{\alpha} \text{ and } e = \frac{b+\alpha(1-i)}{\gamma} i, \tag{7}$$

respectively. Moreover, if $p \neq 0$ then $p = \frac{r-\alpha i}{r}$. Thus, i satisfies $f(i) = 0$, with

$$f(i) = a_3 i^3 + a_2 i^2 + a_1 i + a_0, \tag{8}$$

where

$$\begin{aligned}
a_3 &= \alpha^2 \sigma \epsilon, \\
a_2 &= -\alpha\{\sigma\epsilon[\gamma + 2(b+\alpha) + \gamma(\sigma - \alpha)], \\
a_1 &= \sigma\{\epsilon(b+\alpha)^2 + \gamma[b(1+\epsilon) + \alpha + \gamma]\} + 2\alpha\gamma(b+\gamma)\left(\frac{\sigma\epsilon}{b+\gamma} - 1\right), \\
a_0 &= \gamma(b+\alpha)(b+\gamma)(1-\mathcal{R}_0).
\end{aligned}$$

It can be seen that the coefficient a_3 is always positive and a_2 is always negative. While the sign of the coefficients a_1 and a_0 depend on the value of $\mathcal{R}_0$. Then by Descartes' rule of sign, we have the following results.

(i) If $\mathcal{R}_0 > 1$ such that $\frac{\sigma\epsilon}{b+\gamma} > 1$, then $a_1 > 0, a_0 < 0$ and so, there are three positive roots or one positive root of (8);

(ii) If $\mathcal{R}_0 > 1$ such that $\frac{\sigma\epsilon}{b+\gamma} < 1, a_1$ can be positive or negative and $a_0 < 0$. Thus, if $a_1 > 0$ two positive roots exist while there are three positive roots or one positive root when $a_1 < 0$;

(iii) If $\mathcal{R}_0 < 1, a_1$ can be positive or negative and $a_0 > 0$. Then (8) has two or no positive roots.

It follows that, the possible number of non-trivial equilibria of system (4) could be one or two or three.

Let $E^s = (p^s, e^s, i^s)$ be an arbitrary semi-trivial equilibrium point, then from (7) and (8), we have

$$p^s = 0, e^s = \frac{b+\alpha(1-i^s)}{\gamma} i^s$$

and i^s solves $f(i) = 0$ as defined in equation (8). In a similar note, let $E^* = (p^*, e^*, i^*)$ with $p^* = \frac{r-\alpha i^*}{r}, e^* = \frac{b+\alpha(1-i^*)}{\gamma} i^*$ and i^* solves $f(i) = 0$ as defined in equation (8) be an endemic equilibrium point of (4). Then, we have the following stability results.

Theorem 3.2. *A unique semi-trivial equilibrium, E^s if it exist, is locally asymptotically stable when $\mathcal{R}_1 < 1$ and $\mathcal{R}_0 > 1$ such that $\frac{\sigma\epsilon}{b+\alpha} < 1$. It is unstable when $\mathcal{R}_1 > 1$.*

Proof. The Jacobian matrix of the linearized system of (4) evaluated at E^s is obtained from (9) as

$$J(E^s) = \begin{pmatrix} r - \alpha i^s & 0 & 0 \\ 0 & Q & \sigma(1-2i^s) - [\sigma\epsilon + (\sigma - \alpha)]e^s \\ 0 & \gamma & -[b + \alpha(1-2i^s)] \end{pmatrix}, \tag{9}$$

$Q = \sigma\epsilon(1 - 2e^s - i^s) - (b+\gamma) - (\sigma - \alpha)i^s$. Then the eigenvalues of $J(E^s)$ are:

$$r - \alpha i^s = b - (m + \alpha i^s) = (m + \alpha i^s)(\mathcal{R}_1 - 1) < 0,$$

if $\mathcal{R}_1 = \frac{b}{m+\alpha i^s} < 1$ and the eigenvalues of the matrix $J_0(E^s)$ which is obtained by deleting first row and the first column of $J(E^s)$. Then the trace and determinant of $J_0(E^s)$ are respectively, given by

$$\begin{aligned} tr[J_0(E^s)] &= \sigma\epsilon - (b+\gamma) - \sigma\epsilon(2e^s + i^s) - (\sigma-\alpha)i^s - b - \alpha(1-i^s) + \alpha i^s \\ &= -\left\{(b+\gamma)\left(1 - \frac{\sigma\epsilon}{b+\gamma}\right) + \sigma\epsilon(2e^s + i^s) + (\sigma-\alpha)i^s + b - \alpha i^s + \alpha(1-i^s)\right\} \\ &< 0 \end{aligned}$$

and

$$\begin{aligned} \det[J_0(E^s)] &= \left[(b+\gamma)\left(1 - \frac{\sigma\epsilon}{b+\alpha}\right) + \sigma\epsilon(2e^s + i^s) + (\sigma-\alpha)i^s\right][b - \alpha i^s + \alpha(1-i^s)] \\ &\quad + \gamma[\sigma\epsilon + (\sigma-\alpha)e^s + \sigma(2i^s - 1)] \\ &> 0, \end{aligned}$$

if $\mathcal{R}_1 < 1$ so that $m > 0 > b - \alpha i^s$ and $\mathcal{R}_0 > 1$ such that $\frac{\sigma\epsilon}{b+\alpha} < 1$. Therefore, the eigenvalues of $J_0(E^s)$ have negative real parts. Hence $J(E^s)$ have eigenvalues with negative real parts and so, E^s is locally asymptotically stable. ■

Theorem 3.3. *The non-trivial equilibrium E^* of system (4) if it exists is stable locally asymptotically in the interior of the domain $\mathcal{D}$, when $\mathcal{R}_0 > 1$ such that $\frac{\sigma\epsilon}{b+\gamma} > 1$ and $\mathcal{R}_1 > 1$.*

Proof. Linearizing model (4) around E^*, we obtain the Jacobian matrix

$$J(E^*) = \begin{pmatrix} r(1-2p^*) - \alpha i^* & 0 & -\alpha p^* \\ 0 & j_{22} & \sigma(1-i^*) - \sigma i^* - [\sigma\epsilon + (\sigma-\alpha)] \\ 0 & \gamma & \alpha i^* - b - \alpha(1-i^*) \end{pmatrix}$$

where $j_{22} = \sigma\epsilon - b - \gamma - (\sigma-\alpha)i^* - \sigma\epsilon(e^* + i^*) - \sigma\epsilon e^*$. One can see by inspection that the first eigenvalue of this matrix is

$$\begin{aligned} -rp^* + r(1-p^*) - \alpha i^* &= -(b-m)(2p^* - 1) - \alpha i \\ &= -[2p^* r - (m + \alpha i^*)(1 - \mathcal{R}_1)] < 0, \end{aligned}$$

for $\mathcal{R}_1 > 1$. For the remaining two eigenvalues, it suffices to show that the trace and determinant of the 2×2 sub-matrix $\tilde{J}(E^*)$ of $J(E^*)$ which is obtained by deleting the first row and the first column of $J(E^*)$ are negative and positive respectively.

$$\begin{aligned} \text{tr}(\tilde{J}) &= \sigma\epsilon - b - \gamma - (\sigma-\alpha)i^* - \sigma\epsilon(e^* + i^*) - \sigma\epsilon e^* + \alpha i^* - b - \alpha(1-i^*) \\ &= (b+\gamma)\left(\frac{\sigma\epsilon}{b+\gamma} - 1\right) - (\sigma-\alpha)i^* - \sigma\epsilon(2e^* + i^*) - m \\ &\quad + (m + \alpha i)(1 - \mathcal{R}_1) - \alpha(1-i) \\ &= -[(\sigma-\alpha)i^* + \sigma\epsilon(2e^* + i^*) + (m + \alpha i)(\mathcal{R}_1 - 1) + \alpha(1-i)] \\ &\quad - m + (b+\gamma)\left(\frac{\sigma\epsilon}{b+\gamma} - 1\right) \end{aligned}$$

$$\begin{aligned} \det(\tilde{J}) &= \left[(\sigma-\alpha)i^* + \sigma\epsilon(2e^* + i^*) + (b+\gamma)\left(1 - \frac{\sigma\epsilon}{b+\gamma}\right)\right] \\ &\quad \times \left[\alpha i^*\left(\frac{b}{\alpha i^*} - 1\right) + \alpha(1-i^*)\right] \\ &\quad + \gamma\{\sigma i^* + [\sigma\epsilon + (\sigma-\alpha)]e^* - \sigma(1-i^*)\} \end{aligned}$$

If $\mathcal{R}_0 > 1$ and $\mathcal{R}_1 > 1$ then these trace and determinant are negative and positive, respectively. Thus the eigenvalues of $\tilde{J}$ have negative real parts. Hence, the eigenvalues of $J(E^*)$ have negative real parts and so, the equilibrium point E^* locally stable asymptotically whenever $\mathcal{R}_0 > 1$ and $\mathcal{R}_1 > 1$. ■

3.3 Bifurcation analysis

The uniqueness of the non-trivial equilibrium point E^* if it exist, indicates that there is an exchange of stability between E^* and the carrying capacity state E_1 when $\mathcal{R}_0 = 1$ or equivalently $\sigma = \sigma^* = \frac{(b+\alpha)(b+\gamma)}{\epsilon(b+\gamma)+\gamma}$ (a phenomenon known as transcritical/forward bifurcation). That is, there is an exchange of stability between E_1 and E^* when $\sigma > \sigma^*$. Suppose such an equilibrium exists, then we establish the following result.

Theorem 3.4. *The system of equations (4) exhibits a transcritical bifurcation at E_1 if the bifurcation parameter $\sigma = \sigma^* = \frac{(b+\alpha)(b+\gamma)}{\epsilon(b+\gamma)+\gamma}$.*

Proof. Let f be the vector field defined by the right hand side of system (4). Then

$$f(p,e,i;\sigma) = \begin{pmatrix} [r(1-p)-\alpha i]p \\ \sigma\epsilon e + \sigma i(1-i) - [b+\gamma+(\sigma-\alpha)i + \sigma\epsilon(e+i)]e \\ \gamma e - [b+\alpha(1-i)]i \end{pmatrix}. \tag{10}$$

The Jacobian matrix evaluated at E_1, denoted by J_1 is

$$J_1 = \begin{pmatrix} -r & 0 & 0 \\ 0 & \sigma\epsilon - (b+\gamma) & \sigma \\ 0 & \gamma & -(b+\alpha) \end{pmatrix}.$$

The determinant of the matrix J_1 is

$$\det J_1 = r(b+\gamma)(b+\alpha)(\mathcal{R}_0 - 1),$$

which is zero if $\mathcal{R}_0 = 1$ or equivalently $\sigma = \sigma^* = \frac{(b+\alpha)(b+\gamma)}{\epsilon(b+\gamma)+\gamma}$. The trace of J_1 is

$$\mathrm{tr}J_1 = -\left[m + \alpha + (b+\gamma)\left(-\frac{\sigma\epsilon}{b+\gamma}\right)\right] \neq 0.$$

This guarantees that the Jacobian J_1 has a simple zero eigenvalue. Therefore the existence of transcritical bifurcation at E_1 can be established using Sotomayor theorem [20]. To verify the conditions for transcritical bifurcation given in this theorem, let $U = (u_1, u_2, u_3)^T$ be an eigenvector of the matrix J_1 corresponding to the eigenvalue $\lambda = 0$. Then using the standard computation of an eigenvector, we obtain

$$U = \begin{pmatrix} -\frac{\alpha}{r} & \frac{b+\alpha}{\gamma} & 1 \end{pmatrix}^T. \tag{11}$$

Next, let $V = (v_1, v_2, v_3)^T$ be an eigenvector of the transpose of the Jacobian matrix J_1. The eigenvector V corresponding to the eigenvalue $\lambda = 0$ is then given by

$$V = \begin{pmatrix} 0 & 1 & \frac{\sigma}{b+\alpha} \end{pmatrix}^T.$$

The derivative of the vector field $f(p,e,i;\sigma)$ in (10) with respect to the bifurcation parameter σ at the equilibrium point E_1 is

$$f_\sigma(E_1;\sigma) = \begin{pmatrix} 0 & 0 & 0 \end{pmatrix}^T$$

and so,

$$U^T f_\sigma(E_1;\sigma) = \begin{pmatrix} -\frac{\alpha}{r} & \frac{b+\alpha}{\gamma} & 1 \end{pmatrix} \begin{pmatrix} 0 \\ 0 \\ 0 \end{pmatrix} = 0. \tag{12}$$

The expression $Df_\sigma(p,e,i;\sigma)U$ as defined in [20] is

$$Df_\sigma(p,e,i;\sigma)U = \frac{\partial f_\sigma}{\partial p}u_1 + \frac{\partial f_\sigma}{\partial e}u_2 + \frac{\partial f_\sigma}{\partial i}u_3.$$

Evaluating this expression at E_1 and using (11) gives

$$Df_\sigma\left(E_1;\sigma\right)U = \begin{pmatrix} 0 & \epsilon\frac{b+\alpha}{\gamma} & 0 \end{pmatrix}^T.$$

Thus,

$$\begin{aligned} V^T\left[Df_\sigma\left(E_1;\sigma\right)\right] &= \begin{pmatrix} 0 & 1 & \frac{\sigma}{b+\alpha} \end{pmatrix}\begin{pmatrix} 0 \\ \epsilon\frac{b+\alpha}{\gamma} \\ 0 \end{pmatrix} \\ &= \epsilon\frac{b+\alpha}{\gamma} \neq 0. \end{aligned} \tag{13}$$

Also $D^2f(x;\sigma)(U,U)$ is defined in [20] as follows:

$$D^2f(x;\sigma)(U,U) = \sum_{k,i,j=1}^{3}\frac{\partial^2 f_k}{\partial x_i \partial x_j}u_i u_j.$$

Expanding and evaluating this using (11) at the point E_1, we obtain

$$D^2f(E_1;\sigma)(U,U) = \begin{pmatrix} 0 \\ -\frac{1}{\gamma^2}[2\sigma\alpha^2 + (\sigma-\alpha)\gamma + 2\sigma\epsilon(b+\alpha)(b+\alpha+\gamma)] \\ 0 \end{pmatrix}.$$

Hence,

$$\begin{aligned} V^T[D^2f(E_1;\sigma)(U,U)] &= \begin{pmatrix} 0 & 1 & \frac{\sigma}{b+\alpha} \end{pmatrix}\begin{pmatrix} 0 \\ -\frac{1}{\gamma^2}[2\sigma\alpha^2 + (\sigma-\alpha)\gamma + \varpi] \\ 0 \end{pmatrix} \\ &= -\frac{1}{\gamma^2}[2\sigma\alpha^2 + (\sigma-\alpha)\gamma + Q] \neq 0, \end{aligned} \tag{14}$$

with $\varpi = 2\sigma\epsilon(b+\alpha)(b+\alpha+\gamma)$.

It follows from [20, Theorem 1] together with conditions (12), (13) and (14) that system (4) exhibits a transcritical bifurcation at E_1 (see Figure 2). ■

This result indicates that FIV cannot invade cats population at the carrying capacity state when $\mathcal{R}_0 < 1$. While, there will be an endemic persistence of the virus for $\mathcal{R}_0 > 1$ at the non-trivial equilibrium E^* if $\mathcal{R}_1 > 1$. Moreover, Theorem 3 reveals that if E^* does not exists then the virus will exterminate the host population and persists at semi-trivial equilibrium E^s when $\mathcal{R}_1 < 1$.

4 Discussions and conclusion

In this paper, we extend the model of feline immunodeficiency virus of susceptible-infectious (SI) proposed in [9], by adding the compartment of latently infected cats. The stability analysis is carried out and it reveals that stability results of the disease persistence equilibria does not depend solely on the basic reproduction number,$\mathcal{R}_0$. In fact, we show that the disease could exterminate the host population when the virus persists in the population for ($\mathcal{R}_0 > 1$) provided the other threshold parameter, $\mathcal{R}_1 < 1$. More precisely, if $\mathcal{R}_0 < 1$ the only stable equilibrium point is the carrying capacity state E_1, while either the semi-trivial equilibrium E^s or the non-trivial equilibrium E^* is asymptotically

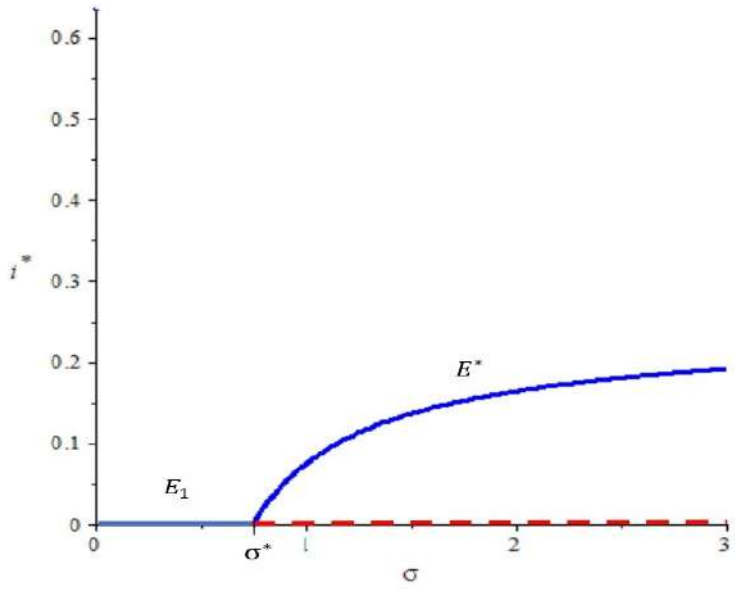


Figure 2: Transcritical bifurcation diagram showing the exchange of stability between the carrying capacity state, E_1 and the endemic equilibrium E^* at $\mathcal{R}_0 = 1$. E_1 is stable when $\mathcal{R}_0 < 1$ (Solid line) and becomes unstable if $\mathcal{R}_0 > 1$ (Dash line) so that E^* is stable. Parameter values used are as given in Table 1

stable if $\mathcal{R}_0 > 1$ depending on whether $\mathcal{R}_1 < 1$ or $\mathcal{R}_1 > 1$, respectively. It is to be noted that the semi-trivial extinction state (E^s) coincides with trivial equilibrium, E_0 when expressed in the (N, E, I) or (S, E, I) state variables. The non-trivial equilibrium, E^* if it exists, leads to an exchange of stability between it and the carrying capacity state (E_1) at $\mathcal{R}_0 = 1$ or equivalently $\sigma = \sigma^* = \frac{(b+\alpha)(b+\gamma)}{\epsilon(b+\gamma)+\gamma}$. Such a phenomenon is known as transcritical bifurcation (or forward bifurcation). That is, the equilibrium point E_1 which is stable when $\mathcal{R}_0 < 1$ ($\sigma < \sigma^*$) losses stability when $\mathcal{R}_0 > 1$ ($\sigma > \sigma^*$), leading to the emergence of a locally stable endemic equilibrium E^* (Figure 2). The occurrence of this phenomenon indicates that FIV cannot invades cats population at the carrying capacity state when $\mathcal{R}_0 < 1$, rather the disease persist if $\mathcal{R}_0 < 1$.

Complex dynamics of the presented model can be investigated when multiple non-trivial equilibrium points exist for further research. As the existence of such equilibria in disease transmission models leads to complex dynamics of a system [16, 21, 22].

The following provides a sample reference list with entries for journal articles [1], conference proceeding [2], a URL [3], as well as a book [4]. [Note that the reference list should be arranged in the order in which the articles are cited in the work, and not in alphabetical order]

References

[1] Pedersen N. C., Ho E. W., Brown M. L. and Yamamoto J. K. (1987), Isolation of a T-lymphotropic virus from domestic cats with an immunodeficiency-like syndrome. Science 235 , 790-793.

[2] Alves F. and Pimenta dos Reis J. K., Feline Immunodeficiency, http://dx.doi.org/10.5772/51631

[3] Elder J. H., Lin Y. C., Fink E., Grant C. K. (2010), Feline immunodeficiency virus (FIV) as a model for study of lentivirus infections: parallels with HIV. Curr HIV Res. 8 (2010), 73-80.

[4] Yamamoto J. K., Hansen H., Ho E. W. *et al.* (1989), Epidemiologic and clinical aspects of feline immunodeficiency virus infection in cats from the continental United States and Canada and

possible mode of transmission, Journal of American Veterinary Medecine Association, 194, 213-220.

[5] Margaret C. (1994), Feline retrovirus infections, Condensed from "Feline Viral Diseases," Textbook of Veterinary Internal Medicine, 4th Edition

[6] Moench T. R., Whaley K. J., Mandrell T. D., Bishop B. D. and Witt C. J. (1993), The cat/feline immunodeficiency virus model for transmucosal transmission of AIDS: nonoxynol-9 contraceptive jelly blocks transmission by an infected cell inoculum, AIDS 7, 797-802.

[7] Hartmann K. (1998), Feline immunodeficiency virus infection: An overview, Veterinary Journal, 155, 123-137.

[8] Ishida T., and Tomoda I. (1990), Clinical staging of feline immunodeficiency virus infection. Japanees Journal of Vetenary Sciences, 52, 645-648.

[9] Courchamp F., Pontier D., Langglais M. and Artois M. (1995), Population dynamics of Feline immunodeficiency virus within cat populations, Journal of Theoretical Biology, 175, 553-560.

[10] Courchamp F., Suppo Ch., Fromont E. and Bouloux C. (1997), Population dynamics for two feline retroviruses (FIV and FeLV) within one population of cats, Proc. R. Sot. Land. B 264 , 785-794.

[11] Langlais M. and Suppo CH. (2000), A remark on a generic SEIRS Model and application to cat retroviruses and fox rabies, Mathematics and Computer Modeling, 31, 117-124

[12] Jingli L., Shan M., Barnerjee M. and Wang W. (2016), Stochastic dynamics of feline immunodeficiency virus within cat populations, Preprint submitted to Journal of Franklin Institute, https://www.elsevier.com/open-access/userlicence/1.0/

[13] Yakubu A. and Ziyadi N. (2022), Strong Allee effect and basins of attraction in a discrete-time zoonotic infectious disease model, Natural resource modeling, 35:e12310. https://doi.org/10.1111/nrm.12310

[14] Samantha J. M., Ellen E. S., and Brian G. M. (2013), Feline immunodeficiency virus latency, Retrovirology, 10(69) https://dx.doi:10.1186/1742-4690-10-69

[15] Roberts M. G. and Jowett J. (1996), An SEI model with density-dependent demographics and epidemiology, Journal of Mathematics Applied in Medicine and Biology, 13, 245-257

[16] Usaini S., Lloyd A. L., Anguelov R. and Garba S. M. (2017), Dynamical behavior of an epidemiological model with a demographic Allee effect, Math. Comp. Simul. 133, 311-325.

[17] McDonnel S. J., Sparger E. E. and Murphy B. G. (2013), Feline immunodeficiency virus latency, Retrovirology, 10 (69), 1-8. doi:10.1186/1742-4690-10-69.

[18] Busenberg S., Cooke K.L. and Thieme H. (1991), Demographic change and persistence of HIV/AIDS in a heterogeneous population, SIAM Journal of Applied Mathematics, 51 (4), 1030-1052.

[19] Busenberg S. and Van den Driessche P. (1990), Analysis of a disease transmission model in a population with varying size, Journal of Mathematical Biology, 28, 257-270.

[20] Perko L. (2001), *Differential Equations and Dynamical Systems*. Third Edition, New York.

[21] Buonomo B. and Lacitignolo D. (2011), On the backwrd bifurcation of a vaccination model with nonlinear incidence, Nonlinear Analysis: Modelling and Control, 16 (1), 30-46.

[22] Hilker F. M., Population collapse to extinction: the catastrophic combination of parasitism and Allee effect, Journal of Biological dynamics, 4 (1), 86-101.

Uniqueness of solution of multi-term fractional order Volterra Integro-differential equations with convergence analysis

D. Umar[†*], and **S.L. Bichi**[†‡]

Abstract

This paper focused on multi-term fractional order Volterra integro-differential equations. The multi-term fractional order derivative part of the multi-term fractional order Volterra integro-differential equations is converted into its equivalent integral equation then Banach contraction principle is utilised in the establishment of the uniqueness of solution for multi-term fractional order Volterra integro-differential equations under some condition. Furthermore, the convergence of the solution is also studied and proved. Some examples were considered to test the applicability of the proposed uniqueness theorem for the solution of multi-term fractional order Volterra integro-differential equations.

Keywords and phrases: Uniqueness of solution; fractional integro-differential equation; Convergence; Volterra integro-differential equation

1 Introduction

In the past few decades, Fractional calculus have attracted so much attention of scholars in various field of mathematics and sciences at large. In recent times, numerous scholars have studied the existence and uniqueness of solutions of these equations such as [1] proved the existence results for fractional integro-differential equations with non-local condition via resolvent operators. Also, the existence of solutions of various types of fractional differential equations and fractional integro-differential equations of boundary value problems and initial value problems were explored recently by [2 - 20] and so many more. Furthermore, the application of these equations has been recorded in many discipline of engineering, social sciences and management. This is to say, fractional calculus is widely applied to described many important phenomena in the field of sciences such as Chaotic systems [21], Chemical Reactions [22], Biology [23], Fluid Mechanics [24]. In Economics [25], Social Sciences [26], Finance [27] and so on. Many physical phenomena are more favourably described by fractional operators because it considers the evolution of these phenomena into account. However, it is sometimes difficult to find analytical solutions for some of these equations. Therefore, the need for a numerical approach. In the past few decades, numerical approaches to find approximations to the solutions to this class of equations were studied. See [18, 28 - 33]. A special class of these equations are the Volterra type, it has been used to describe heat transfer issues, nano hydrodynamics, mass diffusion processes, neutron diffusion, biological species coexisting together with diminishing and increasing rate of growth, and electromagnetic theory [34]

In this paper, we considered the multi-term fractional order Volterra integro-differential equation of the form

$$D^{\beta}\xi\left(x\right)=\sum_{j=0}^{k}c_{j}(x)D^{\delta_{j}}\xi\left(x\right)+h\left(x\right)+\int_{0}^{\sigma}K\left(\sigma,\tau\right)H\left(\xi\left(\tau\right)\right)d\tau \tag{1}$$

[*]Department of Mathematics Modibbo Adama University Yola, Adamawa, Nigeria; E-mail: dah4bab@mau.edu.ng
[†]Department of Mathematical Sciences Bayero University Kano, Kano, Nigeria
[‡]Corresponding Author; E-mail: slawanbh@gmail.com

subject to the initial condition

$$\begin{aligned} \xi^{(n)}(0) &= d_n,\ n = 0, 1, 2, ..., m-1, \\ m-1 &< \delta_0 < \delta_1 < \cdots < \delta_j < \beta \leq m,\ m, k \in \mathbb{N}, \end{aligned} \tag{2}$$

where D is the differential operator defined in Caputo sense, $\xi : Q \longrightarrow \mathbb{R},\ Q = [0, 1]$ is a continuous function which needs to be determined, $c_j, h : Q \longrightarrow \mathbb{R}$ are given continuous functions, $K : Q \times Q \longrightarrow \mathbb{R}$ is the kernel of integration which is also continuous, $H : \mathbb{R} \longrightarrow \mathbb{R}$ is a Lipschitz function.

2 Peliminaries

Definition 2.1. *(Contraction Map [35]). Let X be a metric space, a mapping $T : X \longrightarrow X$ is a contraction if there exists $L \in [0, 1)$ such that $\|Tx - Ty\| \leq L \|x - y\|$ for all $x, y \in X$.*

Definition 2.2. ***(Fixed Point [36]).*** *Given a map $T : A \longrightarrow B$, every solution y of the equation*

$$Ty = y$$

is called a fixed point of T.

Definition 2.3. (***Banach Contraction Principle*** [37]). *Let X be a complete metric space, then each contraction mapping $T : Y \longrightarrow Y$ has a unique fixed point y of T in Y; that is, $Ty = y$.*

Definition 2.4. ***(Riemann-Liouville Fractional Integral [38]).*** *Reimann-Liouville fractional integral of order β of a function ξ is defined as*

$$I^{\beta}\xi(x) = \frac{1}{\Gamma(\beta)} \int_0^x (x-s)^{\beta-1} \xi(s)\, ds, \qquad x > 0,\ \beta \in \mathbb{R}^+, \tag{3}$$

where $\mathbb{R}^+$ is the set of positive real numbers.

Definition 2.5. ***(Riemann-Liouville Fractional Derivative [38]).*** *Reimann-Liouville fractional derivative of order β of a function ξ is defined as*

$$\begin{aligned} D^{\beta}\xi(x) &= D^m I^{m-\beta}\xi(x), \qquad m-1 < \beta \leq m,\ m \in \mathbb{N} \\ &= \frac{d^m}{dt^m}\left(\frac{1}{\Gamma(m-\beta)} \int_0^x (x-s)^{m-\beta-1} \xi(s)\, ds\right). \end{aligned}$$

Definition 2.6. ***(Caputo Fractional Derivative [38]).*** *The fractional derivative of $\xi(x)$ in the Caputo sense is defined by*

$$\begin{aligned} D^{\beta}\xi(x) &= I^{m-\beta} D^m \xi(x) \\ &= \frac{1}{\Gamma(m-\beta)} \int_0^x (x-s)^{m-\beta-1} \frac{d^m \xi(s)}{ds^m} ds, \quad m-1 < \beta \leq m. \end{aligned} \tag{4}$$

With the following properties

i. $I^{\beta} D^{\beta}\xi(x) = \xi(x) - \sum_{n=0}^{m-1} \frac{\xi^{(n)}(0)}{n!} x^n,\ m-1 < \beta \leq m,$

ii. $I^{\beta} D^{\gamma}\xi(x) = I^{\beta-\gamma}\xi(x),\ 0 < \gamma < \beta,$ *and* $m-1 < \beta \leq m, m \in \mathbb{N},$

iii. $I^{\alpha}\xi(x) = \frac{x^{\alpha}}{\Gamma(\alpha+1)},$ *where* $y(x) = 1,\ x \in [0, 1]$.

3 Main Result

In this work, we denote by

(i) $\|\cdot\|_\infty$ the sup norm on $C(Q,\mathbb{R})$, i.e for $c \in C(Q,\mathbb{R})$, $\|c\|_\infty = \sup_{x\in Q}|c(x)|$.

(ii) $\|\cdot\|_\infty$ the sup norm on $C(Q,\mathbb{R})$, i.e for $h \in C(Q,\mathbb{R})$, $\|h\|_\infty = \sup_{x\in Q}|h(x)|$.

We make the following hypotheses:

(p_1) there exists a constant $\Psi > 0$ such that for any $\xi_1, \xi_2 \in C(Q,\mathbb{R})$ we have

$$|H(\xi_1(x)) - H(\xi_2(x))| \leq \Psi \|\xi_1 - \xi_2\|_\infty \quad x \in Q$$

(p_2) there exists a constant Π such that

$$\Pi = \sup_{\sigma\in[0,1]} \int_0^\sigma |K(\sigma,\tau)|\, d\tau < \infty.$$

Lemma 1. Let $\xi : Q \longrightarrow \mathbb{R}$ and $g : Q \longrightarrow \mathbb{R}$ be continuous functions. Then, a function ξ is a solution to the fractional integro-differential equation (1) – (2) if, and only if,

$$\xi(x) = \sum_{n=0}^{m-1} \frac{d_n}{n!}x^n + \sum_{j=0}^{k} c_j(x) I^{\beta-\delta_j}\xi(s) + I^\beta h(x) + I^\beta\left(\int_0^\sigma K(\sigma,\tau)\, H(\xi(\tau))\, d\tau\right). \quad (5)$$

Proof. Applying equation (3) on equation (1) and using property (i), (ii) together with the initial condition (2) we have,

$$\begin{aligned}
I^\beta\left(D^\beta\xi(x)\right) &= I^\beta\left(\sum_{j=0}^{k} c_j(x) D^{\delta_j}\xi(x)\right) + I^\beta(h(x)) + I^\beta\left(\int_0^\sigma K(\sigma,\tau)\, H(\xi(\tau))\, d\tau\right) \\
&= \sum_{j=0}^{k} c_j(x) I^\beta\left(D^{\delta_j}\xi(x)\right) + I^\beta(h(x)) + I^\beta\left(\int_0^\sigma K(\sigma,\tau)\, H(\xi(\tau))\, d\tau\right) \\
&= \sum_{n=0}^{m-1} \frac{\xi^{(n)}(0)}{n!}x^n + \sum_{j=0}^{k} c_j(x) I^{\beta-\delta_j}\xi(x) + I^\beta g(x) + \\
&\quad I^\beta\left(\int_0^\sigma K(\sigma,\tau)\, H(\xi(\tau))\, d\tau\right) \\
&= \sum_{n=0}^{m-1} \frac{d_n}{n!}x^n + \sum_{j=0}^{k} c_j(x) I^{\beta-\delta_j}\xi(x) + I^\beta h(x) + I^\beta\left(\int_0^\sigma K(\sigma,\tau)\, H(\xi(\tau))\, d\tau\right).
\end{aligned}$$

Thus, ξ solves (1) – (2) if, and only if, ξ solves (5)

Theorem 3.1. *(Uniqueness of Solution) Assume that (p_1) and (p_2) holds, and if,*

$$\left(\sum_{j=0}^{k} \frac{\|c_j\|_\infty}{\Gamma(\beta-\delta_j+1)} + \frac{\Pi\Psi}{\Gamma(\beta+1)}\right) < 1, \quad (6)$$

then there is a unique solution $\xi \in C(Q,\mathbb{R})$ to problem (1) – (2).

Proof. Let T be an operator such that $T : C(Q,\mathbb{R}) \longrightarrow C(Q,\mathbb{R})$ defined from equation (5) as

$$\begin{aligned}(T\xi)(x) &= \sum_{n=0}^{m-1}\frac{d_n}{n!}x^n + \sum_{j=0}^{k}\frac{1}{\Gamma(\beta-\delta_j)}\int_0^x (x-\sigma)^{\beta-\delta_j-1}c_j(\sigma)\xi(\sigma)d\sigma \\ &+\frac{1}{\Gamma(\beta)}\int_0^x (x-\sigma)^{\beta-1}g(\sigma)\,d\sigma \\ &+\frac{1}{\Gamma(\beta)}\int_0^x (x-\sigma)^{\beta-1}\left(\int_0^\sigma K(\sigma,\tau)H(\xi(\tau))\,d\tau\right)d\sigma. \qquad (7)\end{aligned}$$

The objective here is to apply Banach contraction principle. To do that, we will show that T is a contraction.

First, we note that T is well defined. Indeed, since $x \longmapsto \sum_{n=0}^{m-1}\frac{d_n}{n!}x^n$, $x \longmapsto \sum_{j=0}^{k} c_j(x)\left(I^{\beta-\delta_j}\xi\right)(x)$, $x \longmapsto \left(I^{\beta}h\right)(x)$, $x \longmapsto \int_0^\sigma K(\sigma,\tau)H(\xi(\tau))\,d\tau$ are continuous, the right hand of equation (8) is well defined and $x \longmapsto (T\xi)(x)$ is continuous. Thus, for $\xi \in C(Q,\mathbb{R})$, $T\xi$ is also in $C(Q\mathbb{R})$.

Let $\xi_1, \xi_2 \in C(Q,\mathbb{R})$ and let $x \in [0,1]$. By definition of T we have

$$\begin{aligned}|(T\xi_1)(x)-(T\xi_2)(x)| &= \left|\sum_{j=0}^{k}\frac{1}{\Gamma(\beta-\delta_j)}\int_0^x (x-\sigma)^{\beta-\delta_j-1}c_j(\sigma)(\xi_1(\sigma)-\xi_2(\sigma))\,d\sigma\right. \\ &\left.+\frac{1}{\Gamma(\beta)}\int_0^x (x-\sigma)^{\beta-1}\left(\int_0^\sigma K(\sigma,\tau)(H(\xi_1(\tau))-H(\xi_2(\tau)))\,d\tau\right)d\sigma\right| \\ &\le \left|\sum_{j=0}^{k}\frac{1}{\Gamma(\beta-\delta_j)}\int_0^x (x-\sigma)^{\beta-\delta_j-1}c_j(\sigma)(\xi_1(\sigma)-\xi_2(\sigma))\,d\sigma\right| \\ &+\left|\frac{1}{\Gamma(\beta)}\int_0^x (x-\sigma)^{\beta-1}\left(\int_0^\sigma K(\sigma,\tau)(H(\xi_1(\tau))-H(\xi_2(\tau)))\,d\tau\right)d\sigma\right| \\ &\le \sum_{j=0}^{k}\frac{1}{\Gamma(\beta-\delta_j)}\int_0^x (x-\sigma)^{\beta-\delta_j-1}|c_j(\sigma)|\,|\xi_1(\sigma)-\xi_2(\sigma)|\,d\sigma \\ &+\frac{1}{\Gamma(\beta)}\int_0^x (x-\sigma)^{\beta-1}\left(\int_0^\sigma |K(\sigma,\tau)|\,|H(\xi_1(\tau))-H(\xi_2(\tau))|\,d\tau\right)d\sigma \\ &\le \sum_{j=0}^{k}\frac{\|c_j\|_\infty\|\xi_1-\xi_2\|_\infty}{\Gamma(\beta-\delta_j)}\int_0^x (x-\sigma)^{\beta-\delta_j-1}d\sigma \\ &+\frac{\Pi\Psi\|\xi_1-\xi_2\|_\infty}{\Gamma(\beta)}\int_0^x (x-\sigma)^{\beta-1}d\sigma \\ &\le \sum_{j=0}^{k}\frac{\|c_j\|_\infty\|\xi_1-\xi_2\|_\infty}{\Gamma(\beta-\delta_j+1)}x^{\beta-\delta_j}+\frac{\Pi\Psi\|\xi_1-\xi_2\|_\infty}{\Gamma(\beta+1)}x^{\beta}\end{aligned}$$

Thus,

$$\|T\xi_1-T\xi_2\|_\infty \le \left(\sum_{j=0}^{k}\frac{\|c_j\|_\infty}{\Gamma(\beta-\delta_j+1)}+\frac{\Pi\Psi}{\Gamma(\beta+1)}\right)\|\xi_1-\xi_2\|_\infty, \text{ for all } x\in[0,1].$$

We conclude that T is a contraction since by equation (6), $\left(\sum_{j=0}^{k}\frac{\|c_j\|_\infty}{\Gamma(\beta-\delta_j+1)}+\frac{\Pi\Psi}{\Gamma(\beta+1)}\right) < 1$. By Banach contraction principle, T has a unique solution ξ in $C(Q,\mathbb{R})$.

Theorem 3.2. (*Convergence of Solution*). *If the solution is convergent, then it converges to the exact solution of the Volterra fractional integro-differential equation.*

Proof. Let S_u, S_v be arbitrary partial sums with $v \leq u$. We show that S_u is a Cauchy sequence. Let $S_u = \sum_{j=0}^{u} \xi_j(x)$ and $S_v = \sum_{j=0}^{v} \xi_j(x)$. Since $v \leq u$, then, we have from equation (5)

$$\begin{aligned} S_u - S_v &= \sum_{j=v+1}^{u} \xi_j(x) \\ &= \sum_{j=0}^{k} \frac{1}{\Gamma(\beta-\delta_j)} \int_0^x (x-\sigma)^{\beta-\delta_j-1} c_j(\sigma) \sum_{j=v+1}^{u} \xi_j(\sigma)\, d\sigma \\ &\quad + \frac{1}{\Gamma(\beta)} \int_0^x (x-\sigma)^{\beta-1} \left(\int_0^\sigma K(\sigma,\tau) H\left(\sum_{j=v+1}^{u} \xi_j(\tau) \right) d\tau \right) d\sigma. \end{aligned} \tag{8}$$

Let $H\left(\sum_{j=v+1}^{u} \xi_j(\tau)\right) = \sum_{j=v+1}^{u} G_j(\tau)$, then equation (8) becomes

$$\begin{aligned} |S_u - S_v| &= \left| \sum_{j=v+1}^{u} \xi_j(x) \right| \\ &= \left| \sum_{j=0}^{k} \frac{1}{\Gamma(\beta-\delta_j)} \int_0^x (x-\sigma)^{\beta-\delta_j-1} c_j(\sigma) \sum_{j=v+1}^{u} \xi_j(\sigma)\, d\sigma \right. \\ &\quad \left. + \frac{1}{\Gamma(\beta)} \int_0^x (x-\sigma)^{\beta-1} \left(\int_0^\sigma K(\sigma,\tau) \sum_{j=v+1}^{u} G_j(\tau)\, d\tau \right) d\sigma \right|. \end{aligned} \tag{9}$$

If, we let $\sum_{j=v}^{u-1} \xi_j(x) = S_{u-1} - S_{v-1}$, $\sum_{j=v}^{u-1} G_j(t) = H(S_{u-1}) - H(S_{v-1})$ in equation (9), then we have

$$\begin{aligned} \|S_u - S_v\|_\infty &\leq \max_{\forall x \in Q} \left(\left| \sum_{j=0}^{k} \frac{1}{\Gamma(\beta-\delta_j)} \int_0^x (x-\sigma)^{\beta-\delta_j-1} c_j(\sigma) (S_{u-1} - S_{v-1})\, d\sigma \right. \right. \\ &\quad \left. \left. + \frac{1}{\Gamma(\beta)} \int_0^x (x-\sigma)^{\beta-1} \left(\int_0^\sigma K(\sigma,\tau) (H(S_{u-1}) - H(S_{v-1}))\, d\tau \right) d\sigma \right| \right) \\ &\leq \max_{\forall x \in Q} \left(\sum_{j=0}^{k} \frac{1}{\Gamma(\beta-\delta_j)} \int_0^x (x-\sigma)^{\beta-\delta_j-1} |c_j(\sigma)|\, |S_{u-1} - S_{v-1}|\, d\sigma \right. \\ &\quad \left. + \frac{1}{\Gamma(\beta)} \int_0^x (x-\sigma)^{\beta-1} \left(\int_0^\sigma |K(\sigma,\tau)|\, |H(S_{u-1}) - H(S_{v-1})|\, d\tau \right) d\sigma \right) \\ &\leq \sum_{j=0}^{k} \frac{\|c_j\|_\infty \|S_{u-1} - S_{v-1}\|_\infty}{\Gamma(\beta-\delta_j)} \int_0^x (x-\sigma)^{\beta-\delta_j-1} d\sigma \\ &\quad + \frac{\Pi\Psi \|S_{u-1} - S_{v-1}\|_\infty}{\Gamma(\beta)} \int_0^x (x-\sigma)^{\beta-1} d\sigma \\ &\leq \left(\sum_{j=0}^{k} \frac{\|c_j\|_\infty}{\Gamma(\beta-\delta_j+1)} + \frac{\Pi\Psi}{\Gamma(\beta+1)} \right) \|S_{u-1} - S_{v-1}\|_\infty. \end{aligned}$$

Thus,

$$\|S_u - S_v\|_\infty \leq \rho \|S_{u-1} - S_{v-1}\|_\infty. \tag{10}$$

where $\rho = \sum_{j=0}^{k} \frac{\|c_j\|_\infty}{\Gamma(\beta-\delta_j+1)} + \frac{\Pi\Psi}{\Gamma(\beta+1)}$.
Observe that, from equation (10)

$$\|S_u - S_v\|_\infty \leq \rho \|S_{u-1} - S_{v-1}\|_\infty \leq \rho \|S_{u-2} - S_{v-2}\|_\infty \leq \ldots \leq \rho \|S_1 - S_0\|_\infty$$

Also from equation (10)

$$\|S_{u-1} - S_{v-1}\|_\infty \leq \rho \|S_{u-2} - S_{v-2}\|_\infty , \ \|S_{u-2} - S_{v-2}\|_\infty \leq \rho \|S_{u-3} - S_{v-3}\|_\infty , \ldots$$

Therefore,

$$\|S_u - S_v\|_\infty \leq \rho \|S_{u-1} - S_{v-1}\|_\infty \leq \rho^2 \|S_{u-2} - S_{v-2}\|_\infty \leq \ldots \leq \rho^v \|S_1 - S_0\|_\infty \tag{11}$$

Let $u = v + 1$, accordingly in equation (11) then we have

$$\|S_u - S_v\|_\infty \leq \rho \|S_v - S_{v-1}\|_\infty \leq \rho^2 \|S_{v-1} - S_{v-2}\|_\infty \leq \ldots \leq \rho^v \|S_1 - S_0\|_\infty .$$

That is,

$$\|S_p - S_q\|_\infty \leq \rho^v \|S_1 - S_0\|_\infty \tag{12}$$

$\|S_u - S_v\|_\infty$ can be written as follows

$$\begin{aligned} \|S_u - S_v\|_\infty &= ||S_{v+1} - S_v + S_{v+2} - S_{v+1} + S_{v+3} - S_{v+2} + S_{v+4} - S_{v+3} \\ &\quad + \cdots + S_{v+(u-v-2)} - S_{v+(u-v-1)} + S_{v+(u-v)} - S_{v+(u-v-1)}||_\infty \\ &= ||S_{v+1} - S_v + S_{v+2} - S_{v+1} + S_{v+3} - S_{v+2} + S_{v+4} - S_{v+3} \\ &\quad + \cdots + S_{u-2} - S_{u-1} + S_u - S_{u-1}||_\infty \\ &\leq \|S_{v+1} - S_v\|_\infty + \|S_{v+2} - S_{v+1}\|_\infty + \|S_{v+3} - S_{v+2}\|_\infty + \\ &\quad \|S_{v+4} - S_{v+3}\|_\infty + \cdots + \|S_{u-2} - S_{u-1}\|_\infty + \|S_u - S_{u-1}\|_\infty . \end{aligned} \tag{13}$$

From equation (12) , let $u = v + 1$, then

$$\begin{aligned} \|S_{v+1} - S_v\|_\infty &\leq \rho^v \|S_1 - S_0\|_\infty \\ \|S_{v+2} - S_{v+1}\|_\infty &\leq \rho^{v+1} \|S_1 - S_0\|_\infty \\ \|S_{v+3} - S_{v+2}\|_\infty &\leq \rho^{v+2} \|S_1 - S_0\|_\infty \\ &\vdots \\ \|S_u - S_{u-1}\|_\infty &\leq \rho^{u-1} \|S_1 - S_0\|_\infty . \end{aligned}$$

Therefore, equation (13) can be written as

$$\begin{aligned} \|S_u - S_v\|_\infty &\leq \left(\rho^v + \rho^{v+1} + \rho^{v+2} + \cdots + \rho^{u-1}\right) \|S_1 - S_0\|_\infty \\ &= \rho^v \left(1 + \rho^1 + \rho^2 + \cdots + \rho^{u-v-1}\right) \|S_1 - S_0\|_\infty . \end{aligned}$$

By geometric series, let $q = u - v - 1$, this implies,

$$\|S_u - S_v\|_\infty \leq \rho^v \left(\frac{1 - \rho^{u-v}}{1 - \rho}\right) \|S_1 - S_0\|_\infty$$

since $0 < \rho < 1$, this means $1 - \rho^{u-v} < 1$, then

$$\|S_u - S_v\|_\infty \leq \frac{\rho^v}{1 - \rho} \|\xi_1\|_\infty .$$

But $|\xi_1 (x)| < \infty$ and $\lim_{v \longrightarrow \infty} \frac{\rho^v}{1-\rho} = 0$, since $\rho^v \longrightarrow 0$ as $v \longrightarrow \infty$. Therefore, $\|S_u - S_v\|_\infty \longrightarrow 0$ as $v \longrightarrow \infty$. We conclude that S_u is a Cauchy sequence in $C[0, 1]$. Therefore, $\lim_{n \longrightarrow \infty} \xi_n = \xi$. Thus, the solution is convergent.

4 Examples

Example 1 [39]. Consider the fractional order Volterra type integro-differential equation

$$D^{\frac{3}{4}}\xi(x)+\frac{x^2e^x}{5}\xi(x)-\int_0^x e^x\tau\xi(\tau)\,d\tau=\frac{6x^{\frac{9}{4}}}{\Gamma\left(\frac{13}{4}\right)} \tag{14}$$

Subject to $\xi(0)=0$ with exact solution $\xi(x)=x^3$.

Solution

Following Theorem 1, we have

$$\begin{aligned}
|(T\xi_2)(x)-(T\xi_1)(x)| &= \left|-\frac{1}{5\Gamma\left(\frac{3}{4}\right)}\int_0^x(x-\sigma)^{\frac{-1}{4}}\sigma^2e^\sigma\left(\xi_2(\sigma)-\xi_1(\sigma)\right)d\sigma\right.\\
&\quad\left.+\frac{1}{\Gamma\left(\frac{3}{4}\right)}\int_0^x(x-\sigma)^{\frac{-1}{4}}\left(\int_0^\sigma e^\sigma\tau\left(\xi_2(\tau)-\xi_1(\tau)\right)d\tau\right)d\sigma\right|\\
&\leq \left|\frac{1}{5\Gamma\left(\frac{3}{4}\right)}\int_0^x(x-\sigma)^{\frac{-1}{4}}\sigma^2e^\sigma\left(\xi_2(\sigma)-\xi_1(\sigma)\right)d\sigma\right|+\\
&\quad\left|\frac{1}{\Gamma\left(\frac{3}{4}\right)}\int_0^x(x-\sigma)^{\frac{-1}{4}}\left(\int_0^\sigma e^\sigma\tau\left(\xi_2(\tau)-\xi_1(\tau)\right)d\tau\right)d\sigma\right|\\
&\leq \frac{1}{5\Gamma\left(\frac{3}{4}\right)}\int_0^x(x-\sigma)^{\frac{-1}{4}}\sigma^2e^\sigma\left|\xi_2(\sigma)-\xi_1(\sigma)\right|d\sigma+\\
&\quad\frac{1}{\Gamma\left(\frac{3}{4}\right)}\int_0^x(x-\sigma)^{\frac{-1}{4}}\left(\int_0^\sigma e^\sigma\tau\left|\xi_2(\tau)-\xi_1(\tau)\right|d\tau\right)d\sigma\\
&\leq \frac{\|\xi_2-\xi_1\|_\infty}{5\Gamma\left(\frac{3}{4}\right)(n)!}\int_0^x(x-\sigma)^{-\frac{1}{4}}\sigma^{n+2}d\sigma+\\
&\quad\frac{\|\xi_2-\xi_1\|_\infty}{2\Gamma\left(\frac{3}{4}\right)(n)!}\int_0^x(x-\sigma)^{-\frac{1}{4}}\sigma^3d\sigma\\
&\leq \left(\frac{\Gamma(4)x^{3.75}}{5\Gamma(4.75)}+\frac{\Gamma(4)x^{3.75}}{2\Gamma(4.75)}\right)\|\xi_2-\xi_1\|_\infty.
\end{aligned}$$

Thus,

$$\|T\xi_2-T\xi_1\|_\infty\leq(0.253\,22)\|\xi_2-\xi_1\|_\infty.$$

Since $0.253\,22<1$, we say that the problem satisfies the condition of $Theorem\ 1$.

Example 2 [40]. Consider the multi fractional order differential equation of the form

$$aD^2\xi(x)+b(x)D^{\beta_1}\xi(x)+c(x)D\xi(x)+e(x)D^{\beta_2}\xi(x)+k(x)\xi(x)+\lambda\int_0^x x\tau\xi(\tau)\,d\tau=f(x). \tag{15}$$

Subject to $\xi(0)=2,\ \xi'(0)=0$ with exact solution $\xi(x)=2-\frac{x^2}{2}$,

where $f(x)=-a-\frac{b(x)}{\Gamma(3-\gamma_1)}x^{2-\gamma_1}-c(x)x-\frac{e(x)}{\Gamma(3-\gamma_2)}x^{2-\gamma_2}+k(x)\left(2-\frac{x^2}{2}\right)$, $a=1$, $b(x)=x^{\frac{1}{2}}$, $c(x)=x^{\frac{1}{3}}$, $e(x)=x^{\frac{1}{4}}$, $k(x)=x^{\frac{1}{5}}$, $\lambda=0$, $\gamma_2=0.333$ and $\gamma_1=1.234$.

Solution

Following Theorem 1, we have

$$
\begin{aligned}
|(T\xi_2)(x) - (T\xi_1)(x)| &= \Big| -\frac{1}{\Gamma(2)\Gamma(1.766)}\int_0^x (x-\sigma)\,\sigma^{1.266}\,(\xi_2(\sigma)-\xi_1(\sigma))\,d\sigma \\
&\quad -\frac{1}{\Gamma(2)}\int_0^x (x-\sigma)\,\sigma^{1.333}\,(\xi_2(\sigma)-\xi_1(\sigma))\,d\sigma \\
&\quad -\frac{1}{\Gamma(2)\Gamma(1.667)}\int_0^x (x-\sigma)\,\sigma^{0.917}\,(\xi_2(\sigma)-\xi_1(\sigma))\,d\sigma \\
&\quad -\frac{1}{\Gamma(2)}\int_0^x (x-\sigma)\,\sigma^{0.2}\,(\xi_2(\sigma)-\xi_1(\sigma))\,d\sigma\Big| \\
&\leq \frac{1}{\Gamma(2)\Gamma(1.766)}\int_0^x (x-\sigma)\,\sigma^{1.266}\,|\xi_2(\sigma)-\xi_1(\sigma)|\,d\sigma \\
&\quad +\frac{1}{\Gamma(2)}\int_0^x (x-\sigma)\,\sigma^{1.333}\,|\xi_2(\sigma)-\xi_1(\sigma)|\,d\sigma \\
&\quad +\frac{1}{\Gamma(2)\Gamma(1.667)}\int_0^x (x-\sigma)\,\sigma^{0.917}\,|\xi_2(\sigma)-\xi_1(\sigma)|\,d\sigma \\
&\quad +\frac{1}{\Gamma(2)}\int_0^x (x-\sigma)\,\sigma^{0.2}\,|\xi_2(\sigma)-\xi_1(\sigma)|\,d\sigma \\
&\leq \frac{\|\xi_2-\xi_1\|_\infty}{\Gamma(2)\Gamma(1.766)}\int_0^x (x-\sigma)\,\sigma^{1.266}d\sigma \\
&\quad +\frac{\|\xi_2-\xi_1\|_\infty}{\Gamma(2)}\int_0^x (x-\sigma)\,\sigma^{1.333}d\sigma \\
&\quad +\frac{\|\xi_2-\xi_1\|_\infty}{\Gamma(2)\Gamma(1.667)}\int_0^x (x-\sigma)\,\sigma^{0.917}d\sigma \\
&\quad +\frac{\|\xi_2-\xi_1\|_\infty}{\Gamma(2)}\int_0^x (x-\sigma)\,\sigma^{0.2}d\sigma
\end{aligned}
$$

By property (iii) we have

$$
\|T\xi_2 - T\xi_1\|_\infty \leq \left(\frac{\Gamma(2.266)}{\Gamma(1.766)\Gamma(4.266)} + \frac{\Gamma\left(\frac{7}{3}\right)}{\Gamma\left(\frac{13}{3}\right)} + \frac{\Gamma(1.917)}{\Gamma(1.667)\Gamma(3.917)} + \frac{\Gamma\left(\frac{6}{5}\right)}{\Gamma\left(\frac{16}{5}\right)}\right)\|\xi_2-\xi_1\|_\infty .
$$

Thus,

$$
\|T\xi_2 - T\xi_1\|_\infty \leq (0.851\,87)\,\|\xi_2-\xi_1\|_\infty .
$$

Since $0.851\,87 < 1$, we say that the problem satisfies the condition of the $Theorem\ 1$.

5 Discussions and Conclusion

In this paper, a new class of multi-term fractional order Volterra integro-differential equation has been transformed to its equivalent integral form with the help of Riemann-Liouville integral of fractional order. Banach contraction principle was utilised in proving the uniqueness of the solution of the multi-term fractional order Volterra integro-differential equation. Furthermore, the convergence analysis was also studied and proved using the Chauchy convergence creteria. To demonstrate the applicability and solvability of the problem, examples were presented to prove that the condition is met. The results obtained were in perfect agreement with the condition of the uniqueness of solution theorem.

References

[1] Balachandran, K., & Kiruthika, S. (2011). Existence results for fractional integrodifferential equations with nonlocal condition via resolvent operators. Computers & Mathematics with Applications, 62(3), 1350-1358.

[2] Samko, S. G., Kilbas, A. A., & Marichev, O. I. (1993). Fractional integrals and derivatives (Vol. 1). Yverdon-les-Bains, Switzerland: Gordon and breach science publishers, Yverdon.

[3] Diethelm, K., & Ford, N. J. (2002). Analysis of fractional differential equations. Journal of Mathematical Analysis and Applications, 265(2), 229-248.

[4] Yuste, S. B., & Acedo, L. (2005). An explicit finite difference method and a new von Neumann-type stability analysis for fractional diffusion equations. SIAM Journal on Numerical Analysis, 42(5), 1862-1874.

[5] Kilbas, A. A., & Marzan, S. A. (2005). Nonlinear differential equations with the Caputo fractional derivative in the space of continuously differentiable functions. Differential Equations, 41, 84-89.

[6] Pilipović, S., & Stojanović, M. (2006). Fractional differential equations through Laguerre expansions in abstract spaces: Error estimates. Integral Transforms and Special Functions, 17(12), 877-887.

[7] Agarwal, R. P., Benchohra, M., & Hamani, S. (2010). A survey on existence results for boundary value problems of nonlinear fractional differential equations and inclusions. Acta Applicandae Mathematicae, 109, 973-1033.

[8] Baleanu, D., & Mustafa, O. G. (2010). On the global existence of solutions to a class of fractional differential equations. Computers & Mathematics with Applications, 59(5), 1835-1841.

[9] Tian, Y., & Bai, Z. (2010). Existence results for the three-point impulsive boundary value problem involving fractional differential equations. Computers & Mathematics with Applications, 59(8), 2601-2609.

[10] Wei, Z., Li, Q., & Che, J. (2010). Initial value problems for fractional differential equations involving Riemann–Liouville sequential fractional derivative. Journal of Mathematical Analysis and Applications, 367(1), 260-272.

[11] Anguraj, A., Karthikeyan, P., & Trujillo, J. J. (2011). Existence of solutions to fractional mixed integrodifferential equations with nonlocal initial condition. Advances in Difference Equations, 2011, 1-12.

[12] Aghajani, A., Banaś, J., & Jalilian, Y. (2011). Existence of solutions for a class of nonlinear Volterra singular integral equations. Computers & Mathematics with Applications, 62(3), 1215-1227.

[13] Idczak, D., & Kamocki, R. (2011). On the existence and uniqueness and formula for the solution of RL fractional Cauchy problem in $\mathbb{R}$ n. Fractional Calculus and Applied Analysis, 14, 538-553.

[14] Kostić, M. (2011). Abstract time-fractional equations: existence and growth of solutions. Fractional Calculus and Applied Analysis, 14(2), 301-316.

[15] Agarwal, R. P., & Ahmad, B. (2011). Existence theory for anti-periodic boundary value problems of fractional differential equations and inclusions. Computers & Mathematics with Applications, 62(3), 1200-1214.

[16] Hu, Z., & Liu, W. (2011). Solvability for fractional order boundary value problems at resonance. Boundary Value Problems, 2011(1), 1-10.

[17] Aghajani, A., Jalilian, Y., & Trujillo, J. J. (2012). On the existence of solutions of fractional integro-differential equations. Fractional Calculus and Applied Analysis, 15, 44-69.

[18] Hamoud, A., Ghadle, K., & Atshan, S. (2019). The approximate solutions of fractional integro-differential equations by using modified Adomian decomposition method. Khayyam Journal of Mathematics, 5(1), 21-39.

[19] Rui, W. (2011). Existence of solutions of nonlinear fractional differential equations at resonance. Electronic Journal of Qualitative Theory of Differential Equations, 2011(66), 1-12.

[20] Caballero, J., Harjani, J., & Sadarangani, K. (2011). On existence and uniqueness of positive solutions to a class of fractional boundary value problems. Boundary Value Problems, 2011(1), 1-9.

[21] Huang, L., & Bae, Y. (2018). Chaotic dynamics of the fractional-love model with an external environment. Entropy, 20(1), 53.

[22] Zabadal, J., Vilhena, M., & Livotto, P. (2001). Simulation of chemical reactions using fractional derivatives. Nuovo Cimento. B, 116(5), 529-545.

[23] Ertürk, V. S., Odibat, Z. M., & Momani, S. (2011). An approximate solution of a fractional order differential equation model of human T-cell lymphotropic virus I (HTLV-I) infection of CD4+ T-cells. Computers & Mathematics with applications, 62(3), 996-1002.

[24] Zheng, L., & Zhang, X. (2017). Modeling and analysis of modern fluid problems. Academic Press. London, UK.

[25] Tarasov, V. E. (2020). Mathematical economics: application of fractional calculus. Mathematics, 8(5), 660.

[26] Baleanu, D., & Lopes, A. M. (2019). Handbook of Fractional Calculus with Applications. Applications in Engineering, Life and Social Sciences, Part A, Southampton: Comput Mech Publicat, 7.

[27] Fallahgoul, H., Focardi, S., & Fabozzi, F. (2016). Fractional calculus and fractional processes with applications to financial economics: Theory and application. Academic Press.

[28] Avcı, İ., & Mahmudov, N. I. (2020). Numerical solutions for multi-term fractional order differential equations with fractional Taylor operational matrix of fractional integration. *Mathematics*, 8(1), 96.

[29] Chen, X., Lei, S., & Wang, L. (2020). Bernoulli Polynomials Collocation Method for Multi-term Fractional Differential Equations. IAENG International Journal of Applied Mathematics, 50(3), 1-8.

[30] Bragdi, A., Frioui, A., & Guezane Lakoud, A. (2020). Existence of solutions for nonlinear fractional integro-differential equations. Advances in Difference Equations, 2020(1), 1-9.

[31] Ghomanjani, F. (2020). A new approach for solving linear fractional integro-differential equations and multi variable order fractional differential equations. Proyecciones (Antofagasta), 39(1), 199-218.

[32] Uwaheren, O. A., Adebisi, A. F., Olotu, O. T., Etuk, M. O., & Peter, O. J. (2021). Legendre Galerkin method for solving fractional integro-differential equations of Fredholm type. The Aligarh Bulletin of Mathematics, 40(1), 1-13.

[33] Căruntu, B., & Paşca, M. S. (2021). The Polynomial Least Squares Method for Nonlinear Fractional Volterra and Fredholm Integro-Differential Equations. Mathematics, 9(18), 2324.

[34] Wazwaz, A. M. (2011). Linear and nonlinear integral equations. Berlin: Springer.

[35] Rudin, W. (1953). Priciple of Mathematical Analysis. McGraw Hill. New York, NY.

[36] Zeidler, E. (1986). Nonlinear Functional Analysis and its Applications, Part 1: Fixed-Point Theorems. Springer.

[37] Zhou, Y. (2014). Basic theory of fractional differential equations, World Scientific, Singapore.

[38] Kilbas, A. A., Srivastava, H. M., & Trujillo, J. J. (2006). Theory and applications of fractional differential equations (Vol. 204). elsevier.

[39] Huang, L., Li, X. F., Zhao, Y., & Duan, X. Y. (2011). Approximate solution of fractional integro-differential equations by Taylor expansion method. Computers & Mathematics with Applications, 62(3), 1127-1134.

[40] Mahmudov, N. I. (2017). Finite-approximate controllability of evolution equations. Appl. Comput. Math, 16(2), 159-167.

The application of Least Squares Method and Shifted Chebychev Polynomials for solving fourth order Volterra Integro-Differential Equations

A.K. Bello[*], A.M. Ayinde[†], A.S. Daodu[‡] and A.A. Ishaq[§]

Abstract

This study employs the least squares method in conjunction with shifted Chebyshev polynomials as a framework to approximate solutions for fourth-order Volterra integro-differential equations. By leveraging this numerical approach, the method effectively tackles various fourth-order Volterra integro-differential equations, yielding results closely aligned with exact solutions. The utilization of the least squares method with shifted Chebyshev polynomials demonstrates its efficacy in solving such equations with exact and converges faster than existing methods. The tables and graphical representation below display this

Keywords and phrases: Chebyshev polynomials; least square method; numerical method; utilized effectively; Volterra integro-differential equations.

1 Introduction

Integro-differential equations, amalgamating integral and derivative operators within an unknown function, find extensive utility across engineering and scientific domains [1]. These equations manifest in forms such as Fredholm, Volterra, or their hybrid, Fredholm-Volterra integro-differential equations, necessitating numerical methods for resolution. Existing literature presents diverse numerical approaches for tackling integro-differential equations, including the collocation method [2-4] and the hybrid linear multistep method [5-7]. Notably, Volterra integro-differential equations, prevalent in realms like fluid mechanics and viscoelasticity, have garnered significant attention [8]. Given the analytical complexity inherent in solving such equations, the pursuit of accurate numerical

[*]Department of Mathematics, University of Ilorin, Ilorin, Nigeria. E-mail: bello.ak@unilorin.edu.ng
[†] Corresponding Author; Department of Mathematics, University of Abuja, Abuja, Nigeria. E-mail: ayinde.abdullahi@uniabuja.edu.ng
[‡] Department of Mathematics, University of Ilorin, Ilorin, Nigeria. E-mail: samthizidrock@gmail.edu.ng
[§] Department of Physical Sciences, Al-Hikmah University, Ilorin, Nigeria. E-mail: aaishaq@alhikmah.edu.ng

approximations becomes imperative for comparative analysis against exact solutions [9]. Integral equations, particularly Volterra integral equations, constitute a cornerstone in solving myriad natural science predicaments. These equations, encapsulating variable boundary techniques, serve as fundamental tools in modeling numerous phenomena within the natural sciences [10]. The examination of such integral equations has facilitated the translation of various real-world problems into mathematical frameworks, thereby enabling their resolution [10]. Moreover, a pivotal advancement in contemporary mathematics lies in the successful resolution of Volterra integral equations, underscoring their significance in both theoretical and practical domains.

Numerical solutions for various classes of integral equations remain scarce, with only a handful of approximate methods available. Among these methods are several approaches tailored specifically for integral equations with variable boundaries, each presenting its own limitations. In this study, we employ the least squares method in conjunction with shifted Chebyshev polynomials as a basis to approximate solutions for fourth-order Volterra integro-differential equations [11, 12].

An integral equation is an equation in which the unknown function $u(x)$ to be determined appears under the integral sign. A typical form of an integral equation in $u(x)$ is of the form

$$u(x) = f(x) + \int_{\alpha(x)}^{\beta(x)} K(x,t)u(t)dt \tag{1}$$

where $K(x,t)$ is called the kernel of the integral equation, and $\alpha(x), \beta(x)$ are the limits of integration.

In equation (1), it is easily observed that the unknown function $u(x)$ appears under the integral sign as stated above, and out of the integral sign in most other cases [13]. It is important to point out that the kernel $K(x,t)$ and the function $f(x)$ in (1) are given in advance. Our goal is to determine $u(x)$ that will satisfy (1), and this may be achieved by using the Volterra Integro-differential equation

$$u^{(n)}(x) = f(x) + \lambda \int_0^x K(x,t)u(t)dt \tag{2}$$

This equation (2) is called an integral-differential equation because differential and integral operators are involved in the same equation. The concept of integral and integro-differential equations has inspired a lot of study in recent years [14]. Generally, methods for solving integro-differential equations combine approaches used for both integral and differential equations, which contain both integral and differential operators. Also, since closed-form solutions may not be tractable for most applications, numerical methods are employed to obtain an approximation to exact solutions.

Numerical methods like variational iteration, homotopy pertubation, domain decomposition methods, and others have been used to solve these equations. Other methods, such as least squares methods, where Chebyshev and Legendre's polynomials are used as basis functions, have been applied to obtain solutions to some higher-order linear-type integro-difference equations and their function derivatives [14]. Integro-differential equations emerge frequently as mathematical models in diverse disciplines. The study of integral and integro-differential equations may be traced to the work of Abel, Lotka, Fredholm, Malthus, Verhulst, and Volterra on problems in mechanics, mathematical biology, and economics [15]. The work of Volterra on the problem of competing species is of fundamental importance for the development of mathematical modeling of real-world problems. Volterra explored the effect of inherited characteristics when he was examining a population growth model. The research work led to a specific topic where a distinctive equation emerged, featuring both differential and integral operators [15].

Numerous descriptions of physical occurrences in mathematics contain integro-differential equations. These equations arise in fluid dynamics, biological models, and chemical kinetics. The Adomian decomposition approach for solving boundary value problems for fourth-order integro-

differential equations was developed by Hashim [16]. While [17] delved into the numerical solution of Volterra-Fredholm integral equations by moving least squares method and Chebyshev polynomials.

In this study, a method based on the least squares approximation method and the Chebyshev polynomial is introduced to address the following fourth-order integro-differential equation:

$$u^n(x) = f(x) + \lambda \int_0^x k(x,t)u(t)dt \qquad 0 \le t, t \le 1 \tag{3}$$

where $u^n(x) = \frac{d^n u}{dx^n}$ because the resulted equation in (3) combines the differential operator and the integral operator, then it is necessary to define initial conditions $u(0), u'(0), u(0), \cdots, u''(0)$ for the determination of the particular solution $u(x)$ of the Volterra integro-differential equation. The method is proposed by using shifted Chebyshev polynomials for solving the integro-differential equations [18]. One of the most significant advantages of the least square technique is that it improves the accuracy of the model problem predictions. By minimizing the sum of the squared residuals, the method ensures that the model fits the observed data as closely as possible. This approach helps to reduce the errors and uncertainties associated with the model predictions, making it more reliable and robust than the other methods.

1.1 Basic Definitions

This section defines the basic terms that will be frequently used during the research work.

Definition 1: Standard Collocation Method [1]: This is the method partitioning intervals into different points. For example, let say an interval $[a, b]$, N be the number of collocation points to get the desired collocation points, we use;

$x_p = a + \frac{(b-a)}{N} p$, where $p = 1, 2, \cdots N$.

Definition 2: Power Series Polynomial [1]: A power series is basically an infinite degree polynomial that represents some function. It is generally written in the form ; $y(x) = \sum_{n=0}^{\infty} a_n x^n$, where a_n is the coefficient of the polynomials which are real numbers.

Definition 3: Shifted Chebyshev Polynomials [1]: This is a special type of polynomial generated from Chebyshev polynomial. The shifted Chebyshev has interval $[0, 1]$, while Chebyshev has an interval of $[-1, 1]$.

2 Methodology

In this section, the derivation of the method based on the numerical solution of the Volterra Integro-differential equation using the least squares method and the shifted Chebyshev polynomial of the interval [0, 1] and some examples of the fourth-order Volterra Integro-differential equations will be solved using the shifted Chebyshev polynomial as the basis function [17, 18].

2.1 Construction of Chebyshev Polynomials

The Chebyshev polynomial defined on interval $[-1, 1]$ denoted by $T_n(x)$ is defined as

$$T_n(x) = \cos\left[n \cos^{-1} x\right] \tag{4}$$

when $n = 0$

$$T_0(x) = \cos\left[0\cos^{-1}x\right] \tag{5}$$

$\cos 0 = 1$

Thus $T_0(x) = 1$

when $n = 1$

$$T_1(x) = \cos 1\cos^{-1}x \tag{6}$$

$\cos\left[\cos^{-1}x\right] - x$

Thus $T_1(x) = x$.

Hence, from the recurrence relation, i.e.

$$T_{n+1}(x) = 2xT_n(x) - T_{n-1}(x) \tag{7}$$

when $n = 1$, we have

$$\begin{aligned} T_2(x) &= 2x(x) - 1 \\ &= 2x^2 - 1 \end{aligned} \tag{8}$$

when $n = 2$, we have

$$\begin{aligned} T_3(x) &= 2x\left(2x^2 - 1\right) - T_1(x) \\ &= 4x^3 - 3x \end{aligned} \tag{9}$$

The first few Chebychev polynomial of interval $[-1, 1]$ are as follows

$$\left.\begin{aligned} T_0(x) &= 1 \\ T_1(x) &= x \\ T_2(x) &= 2x^2 - 1 \\ T_3(x) &= 4x^4 - 3x \\ T_4(x) &= 4x^4 - 8x^2 + 1 \\ T_5(x) &= 16x^4 - 20x^3 + 5x \end{aligned}\right\} \tag{10}$$

2.2 Shifted Chebyshev Polynomial on interval $[a, b]$

The nth degree shifted Chebyshev polynomials of the first kind valid in the interval $[a, b]$ is given as

$$T_n^*(x) - \cos\left[n\cos^{-1}\left(\frac{2x-b-a}{b-a}\right)\right], \quad n \geq 0 \text{ and } n \in N \tag{11}$$

and the recurrence relation is given as

$$T_{n+1}^*(x) = 2\left(\frac{2x-b-a}{b-a}\right)T_n^*(x) - T_{n-1}^*(x) \tag{12}$$

To use shifted Chebyshev polynomials on interval $[0, 1]$ we need to change the domain using the following substitution

$$X = 2x - 1, \; 0 \leq x \leq 1 \tag{13}$$

The Chebyshev polynomials valid on $[0, 1]$ denoted by $T_n(x)$ is defined as

$$T_n(x) - \cos\left\{N\cos^{-1}(2x-1)\right\}, \quad 0 \leq x \leq 1 \tag{14}$$

The recurrence relation is given as

$$T_N(x) = 2(2x-1)T_N(x) - T_N(x), \quad N \geq 1$$

From equation (11) we obtain

when $N=0$, we obtain

$$T_0(x)=\cos\left[0\cos^{-1}(2x-1)\right]=1$$

when $N=1$, we obtain

$$T_1(x)=\cos\left[\cos^{-1}(2x-1)\right]=2x-1$$

So the shifted Chebyshev polynomials $T_n(x)$ on $[0,1]$ are obtained as follows

$$\left.\begin{aligned}
T_0^*(x)&=1\\
T_1^*(x)&=2x-1\\
T_2^*(x)&=8x^2-8x+1\\
T_3^*(x)&=32x^3-48x^2+18x-1\\
T_4^*(x)&=128x^4-256x^3+160x^2-32x+1\\
T_5^*(x)&=512x^5-128x^4+1120x^3-400x^2-50x-1\\
T_6^*(x)&=2048x^6-6144x^5+6912x^4-3584x^3+840x^2-72x+1\\
T_7^*(x)&=8192x^7-2867x^6+39936x^5-2688x^4+9408x^3-1560x^2+98x-1
\end{aligned}\right\} \quad (15)$$

2.3 Existence and Uniqueness Solution [19]

In this section, we shall give an existence and Uniqueness solution of equation (3) and its initial conditions.

$$\frac{d^n u}{dx^n}\alpha u+\beta v+\int_\rho^\sigma H(\tau,s)\big(u(s)-v(s)\big)ds \quad (16)$$

$$\frac{d^n v}{dx^n}\varphi u+\xi v+\int_\rho^\sigma Q(\tau,s)\big(u(s)-v(s)\big)ds \quad (17)$$

Here,$u\in D$ and $\in D_1\subseteq R^m$, where each D and D_1 is a closed and bounded domain subset of Euclidean spacesR^m.

Suppose that$\alpha=(\alpha_{ij}),\beta=(\beta_{ij}),\varphi=(\varphi_{ij}),$ and $\xi=(\xi_{ij})$ $(m\times m)$ are non-negative matrices.

The functions

$H(\tau,s)$ and $Q(\tau,s)$ is defined on the domain

$$\left.\begin{aligned}&(\tau,s,u)\in[0,T]\times[0,T]\times D\\&(\tau,s,u)\in[0,T]\times[0,T]\times D_1\end{aligned}\right\} \quad (18)$$

Also, the function $H(\tau,s)$ and $Q(\tau,s)$satisfies the following inequality

$$\|H(\tau,s)\|\le H_1,\ \|Q(\tau,s)\|\le Q_1 \quad (19)$$

$\forall\, u\in[0,T], s\in[0,T]$ and $u,u_1,u_2\in D, v,v_1,v_2\in D_1$ where H_1,Q_1 are positive constants, $0\le s\le\tau\le T$.

We define the non-empty sets as follow

$$D_j=D-\alpha_1\|u_0\|+\beta T\|v_0\|+\alpha_2 T\Lambda_1\|u_0-v_0\| \quad (20)$$

$$D_{1_j}=D_1-\varphi_1\|v_0\|+\xi T\|u_0\|+\varphi_2 T\Lambda_2\|u_0-v_0\| \quad (21)$$

2.3.1 Existence Solution

The study of existence solution of the problem above will be introduced by the following theorem without proof.

Theorem 1

Let the functions $H(\tau,s)$ and $Q(\tau,s)$ be defined in the domain (18), continuous in τ and satisfy the inequalities (19), then

$$u(\tau,u_0)=u_0e^{\alpha\tau}+\int_0^\tau\beta v_0ds+\int_0^\tau e^{\alpha(\tau-s)}\left[\int_\rho^\sigma H(\tau,s)\big(u(s)-v(s)\big)ds\right]$$

$$v(\tau, v_0) = v_0 e^{\varphi\tau} + \int_0^\tau \xi u_0 ds + \int_0^\tau e^{\varphi(\tau-s)} \left[\int_\rho^\sigma Q(\tau, s)\big(u(s) - v(s)\big)ds\right]$$

are the solution of the equations (16) and (17) Source: [19]

2.3.2 Uniqueness Solution

The uniqueness solution of the equation (16) and (17) will be introduced by the following theorem without proof

Theorem 2

Let all assumptions and conditions of the theorem 1 be given then the problem (16) and (17) has a unique solution$u = u_\infty(\tau, u_0, v_0)$, $v = v_\infty(\tau, u_0, v_0)$ on the domain (20) Source: [19]

3 Numerical application and results

Description of the least square method on the general problem considered.

Problem 1

Consider the general fourth order integro- differential equation of the form

$$u^{(iv)}(x) = f(x) + \lambda \int_0^x K(x, t)u(t)dt \tag{22}$$

Together with the initial condition $u(0), u'(0), \cdots u^{n-1}(0)$.

Let the assumed equation be

$$u_n(x) = \sum_{i=0}^{n} a_i T_i^*(x), \quad 0 \le x \le 1 \tag{23}$$

where

$$\sum_{i=0}^{n} a_i T_i^*(x) = a_0 T_0^*(x) + a_1 T_1^*(x) + a_2 T_2^*(x) + a_3 T_3^*(x) + \cdots + a_n T_n^*(x) \tag{24}$$

(24) is modified to satisfy the condition and becomes

$$u_n^*(x) = \sum_{i=4}^{N} a_i T_n^{(iv)}(x) \tag{25}$$

Substituting equation (24) and (25) in (22) and replacing x by t in the integrand

$$\sum_{i=4}^{N} a_i T_n^{(iv)}(x) - f(x) + \lambda \int_0^x k(x, t) \sum_{i=0}^{n} a_i T_i^*(t)dt \tag{26}$$

which could be expressed as

$$\begin{aligned} &a_0 T_0^{(*iv)}(x) + a_1 T_1^{(*iv)}(x) + a_2 T_2^{(*iv)}(x) + a_3 T_3^{(*iv)}(x) + \cdots a_n T_n^{(*iv)}(x) = \\ &f(x) + \lambda \int_0^x \left(a_0 T_0^*(t) + a_1 T_1^*(t) + a_2 T_2^*(t) + a_3 T_3^*(t) + \cdots + a_n T_n^*(t)\right)dt \end{aligned} \tag{27}$$

The residual equation from equation (27) is written as

$$R(a_0, a_1, a_2, a_3, \cdots, a_n) = \left\{ \begin{array}{l} a_0 T_0^{(*iv)}(x) + a_1 T_1^{(*iv)}(x) + a_2 T_2^{(*iv)}(x) + a_3 T_3^{(*iv)}(x) + \cdots a_n T_n^{(*iv)}(x) \\ -\lambda \int_0^x k(x, t)[a_0 T_0^{(*iv)}(t) + a_1 T_1^{(*iv)}(t) + a_2 T_2^{(*iv)}(t) + \\ \quad a_3 T_3^{(*iv)}(t) + \cdots a_n T_n^{(*iv)}(t)]dt - f(x) \end{array} \right\} \tag{28}$$

Let

$$S(a_0, a_1, a_2, a_3, \cdots, a_n) = \int_0^1 [R(a_0, a_1, a_2, a_3, \cdots, a_0)]^2 w(x)dx \tag{29}$$

where $S(a_0, a_1, a_2, a_3, \cdots, a_n)$ is to be minimized, $w(x)$ which is the weight function is taken to be 1.

Equation (29) is express as

$$S(a_0, a_1, a_2, a_3, \cdots, a_n) = \int_0^1 \left(a_0 T_0^{(*iv)}(x) + a_1 T_1^{(*iv)}(x) + a_2 T_2^{(*iv)}(x) + a_3 T_3^{(*iv)}(x) + \cdots a_n T_n^{(*iv)}(x)\right) -$$
$$\lambda \int_0^1 k(x,t)\left[a_0 T_0^{(*iv)}(t) + a_1 T_1^{(*iv)}(t) + a_2 T_2^{(*iv)}(t) + a_3 T_3^{(*iv)}(t) + \cdots a_n T_n^{(*iv)}(t)\right]dt - f(x) \tag{30}$$

Now, S is to minimized and to do this, we set

$$\frac{\delta S}{\delta a_j} = 0, 1, 2, 3, \cdots, n \tag{31}$$

for $j = 0$, we get

$$\frac{\delta S}{\delta a_0} = 2\left[\begin{array}{l} \int_0^1 \left(T_0^{(*iv)}(x) - \lambda \int_a^b k(x,t) T_0^*(t)dt\right)a_0 + \left(T_1^{(*iv)}(x) - \lambda \int_a^b k(x,t) T_1^*(t)dt\right)a_1 \\ + \left(T_2^{(*iv)}(x) - \lambda \int_a^b k(x,t) T_2^*(t)dt\right)a_2 + \left(T_3^{(*iv)}(t) - \lambda \int_a^b k(x,t) T_3^*(t)dt\right)a_3 + \cdots \end{array}\right]$$
$$+ \left(T_n^{(*iv)}(t) - \lambda \int_0^x k(x,t) T_n^*(t)dt\right)a_n - f(x)\left(T_0^{(*iv)}(x) - \lambda \int_0^x k(x,t) T_0^*(t)dt\right)dx = 0 \tag{32}$$

for $j = 1$, we get

$$\frac{\delta S}{\delta a_1} = 2\left[\begin{array}{l} \int_0^1 \left(T_0^{(*iv)}(x) - \lambda \int_a^b k(x,t) T_0^*(t)dt\right)a_0 + \left(T_1^{(*iv)}(x) - \lambda \int_a^b k(x,t) T_1^*(t)dt\right)a_1 \\ + \left(T_2^{(*iv)}(x) - \lambda \int_0^x k(x,t) T_2^*(t)dt\right)a_2 + \left(T_3^{(*iv)}(t) - \lambda \int_a^b k(x,t) T_3^*(t)dt\right)a_3 + \cdots \end{array}\right]$$
$$+ \left(T_n^{(*iv)}(t) - \lambda \int_a^b k(x,t) T_n^*(t)dt\right)a_n - f(x)\left(T_1^{(*iv)}(x) - \lambda \int_0^x k(x,t) T_1(t)dt\right)dx = 0 \tag{33}$$

for $j = 2$, we get

$$\frac{\delta S}{\delta a_2} = 2\left[\begin{array}{l} \int_0^1 \left(T_0^{(*iv)}(x) - \lambda \int_0^x k(x,t) T_0^*(t)dt\right)a_0 + \left(T_1^{(*iv)}(x) - \lambda \int_0^x k(x,t) T_1^*(t)dt\right)a_1 \\ + \left(T_2^{(*iv)}(x) - \lambda \int_a^b k(x,t) T_2^*(t)dt\right)a_2 + \left(T_3^{(*iv)}(t) - \lambda \int_0^x k(x,t) T_3^*(t)dt\right)a_3 + \cdots \end{array}\right]$$
$$+ \left(T_n^{(*iv)}(t) - \lambda \int_0^x k(x,t) T_n^*(t)dt\right)a_n - f(x)\left(T_2^{(*iv)}(x) - \lambda \int_9^x k(x,t) T_2^*(t)dt\right)dx = 0 \tag{34}$$

for $j = 3$, we get

$$\frac{\delta S}{\delta a_3} = 2\left[\begin{array}{l} \int_0^1 \left(T_0^{(*iv)}(x) - \lambda \int_0^x k(x,t) T_0(t)dt\right)a_0 + \left(T_1^{(*iv)}(x) - \lambda \int_0^x k(x,t) T_1(t)dt\right)a_1 \\ + \left(T_2^{(*iv)}(x) - \lambda \int_0^x k(x,t) T_2(t)dt\right)a_2 + \left(T_3^{(*iv)}(x) - \lambda \int_0^x k(x,t) T_3(t)dt\right)a_3 + \cdots \end{array}\right]$$
$$+ \left(T_n^{(iv)}(x) - \lambda \int_0^x k(x,t) T_n(t)dt\right)a_n - f(x)\left(T_3^{(iv)}(x) - \lambda \int_0^x k(x,t) T_3^*(t)dt\right)dx = 0 \tag{35}$$

$\vdots$

for $j = n$, we get

$$\frac{\delta S}{\delta a_n} = 2\left[\begin{array}{l}\int_0^1\left(T_0^{(iv)}(x)-\lambda\int_0^x k(x,t)T_0(t)dt\right)a_0+\left(T_1^{(iv)}(x)-\lambda\int_0^x k(x,t)T_1(t)dt\right)a_1\\+\left(T_2^{(iv)}(x)-\lambda\int_0^x k(x,t)T_2(t)dt\right)a_2+\left(T_3^{(iv)}(x)-\lambda\int_0^x k(x,t)T_3(t)dt\right)a_3+\cdots\end{array}\right]$$
$$+\left(T_n^{(iv)}(x)-\lambda\int_0^x k(x,t)T_n(t)dt\right)a_n - f(x)\left(T_n^{(iv)}(x)-\lambda\int_0^x k(x,t)T_n^*(t)dt\right)dx = 0 \tag{36}$$

Evaluating the integrals in (32)-(36) gives $(n+1)$ algebraic linear equations $n\times n$ unknown constants $a_0, a_1, a_2, a_3, \cdots, a_n$ which are then substituted back into equation (34) to obtain the required approximate solution.

4 Numerical applications

We have two numerical problems that consist of fourth order linear Volterra integro-differential equation.

Problem 1

The fourth order nonlinear Volterra integro-differential equation of the form

$$u^{(iv)}(x) = 24 + x + \frac{1}{30}x^6 - \int_0^x (x-t)u(t)dt, \tag{37}$$
$$u(0) = 0,\ u'(0) = 1,\ u''(0) = -1$$

is consider with the exact solution as

$$u(x) = x^4 + \sin x \tag{38}$$

Source: [20]

Solution

For $n = 7$, equation (34) is given as

$$u(x) = a_0T_0(x) + a_1T_1(x) + a_2T_2(x) + a_3T_3(x) + a_4T_4(x)$$
$$+ a_5T_5(x) + a_6T_6(x) + a_7T_7 \tag{39}$$
$$u(x) = a_0 + a_1(2x-1) + a_2(8x^2-8x+1) + a_3(32x^3-48x^2+18x-1) +$$
$$a_4(128x^4-256x^3+160x^2-32x+1) + a_5(512x^5-128x^4+1120x^3-400x^2-50x-1)$$
$$+ a_6(2048x^6-6144x^5+6912x^4-3584x^3+840x^2-72x+1)$$
$$+ a_7(8192x^7-2867x^6+39936x^5-2688x^4+9408x^3-1560x^2+98x-1) \tag{40}$$

Remember that

$$u(0) = 0$$
$$0 = a_0 - a_1 + a_2 - a_3 + a_4 - a_5 + a_6 - a_7 \tag{41}$$
$$a_0 = a_1 - a_2 + a_3 - a_4 + a_5 - a_6 + a_7$$

substitute (41) in $u(x)$

$$u(x)=a_1-a_2+a_3-a_4+a_5-a_6+a_7+a_1(2x-1)+a_2(8x^2-8x+1)+a_3(32x^3-48x^2+18x-1)+$$
$$a_4(128x^4-256x^3+160x^2-32x+1)+a_5(512x^5-128x^4+1120x^3-400x^2-50x-1)+$$
$$a_6(2048x^6-6144x^5+6912x^4-3584x^3+840x^2-72x+1)+$$
$$a_7(8192x^7-2867x^6+39936x^5-2688x^4+9408x^3-1560x^2+98x-1) \quad (42)$$

$$u(x)=a_1(2x)+a_2(8x^2-8x)+a_3(32x^3-48x^2+18x-1)+$$
$$a_4(128x^4-256x^3+160x^2-32x)+a_5(512x^5-128x^4+1120x^3-400x^2-50x)+$$
$$a_6(2048x^6-6144x^5+6912x^4-3584x^3+840x^2-72x)+$$
$$a_7(8192x^7-2867x^6+39936x^5-2688x^4+9408x^3-1560x^2+98x) \quad (43)$$

Differentiate equation (43)

$$u'(x)=2a_1+a_2(16x-8)+a_3(96x^2-96x+18)+$$
$$a_4(512x^3+768x^2+320x-32)+a_5(2560x^4-5120x^3+3360x^2-800x+50)+ \quad (44)$$
$$a_6(12288x^5-30720x^4+276648x^3+1680x^2-72)+$$
$$a_7(57344x^6-172032x^5+199680x^4-107520x^3+282246x^2-3136x+98)$$

Recall $u'(x)=1$

$$1=2a_1-8a_2+18a_3-32a_4+50a_5-72a_6+98a_7 \quad (45)$$
$$2a_1=1+8a_2-18a_3+32a_4-50a_5+72a_6-98a_7$$

Substitute (45) in (43)

$$u(x)=[1+8a_1-18a_2+32a_4-50a_5+72a_6-98a_7]x+a_2(8x^2-8x)+a_3(32x^3-48x^2+18x)$$
$$+a_4(128x^4-256x^3+160x^2-32x)+a_5(512x^5-1280x^4+1120x^3-400x^2+50x) \quad (46)$$
$$+a_6(2048x^6-6144x^5+6912x^4-3584x^3+840x^2-72x)+$$
$$a_7(8192x^7-28672x^6+39936x^5-26880x^4+9408x^3-1568x^2+9x)$$

$$u(x)=x+a_2(8x^2)+a_3(32x^3-48x^2)+a_4(128x^4-256x^3+160x^2)$$
$$+a_5(512x^5-1280x^4-1120x^3+400x^2) \quad (47)$$
$$+a_6(2048x^6-6144x^5+6912x^4-3584x^3+840x^2)+$$
$$+a_6(2048x^6-6144x^5+6912x^4-3584x^3+840x^2)$$
$$+a_7(8192x^7-28672x^6+39936x^5-26880x^4+9408x^3-1568x^2)$$

Differentiating equation (47) once and twice

$$u'(x)=1+a_2(16x)+a_3(96x^2-96x)+a_4(512x^3-768x^2+320x)+a_5(2560x^4$$
$$-5120x^3+3360x^2-800x)+a_6(122888x^5+30720x^4+27648x^3 \quad (48)$$
$$-10752x^2+1680x)+a_7(57344x^6-172032x^5+199680x^4$$
$$-107520x^3+28224x^2-3136x)$$

$$u''(x)=16a_2+a_3(192x^2-96)+a_4(1536x^2-1536x+320)+a_5(10240x^3$$
$$-15360x^2+6720x-800)+a_6(61440x^4-122880x^3+82944x^2-21504x+1680)+$$
$$a_7(344064x^5-860160x^4+798720x^3-322560x^2+56448x-3136) \quad (49)$$

Remember $u''(x)=0$, so that

$$0 = 16a_2 - 96a_3 + 320a_4 - 800a_5 + 1680a_6 - 3136a_7$$
$$16a_2 = 96a_3 - 320a_4 + 800a_5 - 1680a_6 + 3136a_7 \quad (50)$$
$$8a_2 = 48a_3 - 160a_4 + 400a_5 - 840a_6 + 1568a_7$$

Substitute equation (50) into (47)

$$u(x) = x + a_3\left[32x^2\right] + a_4\left[128x^4 - 256x^3\right] + a_5\left[512x^5 - 1280x^4 + 1120x^3\right] + a_6[2048x^6 - 6144x^5 + 6912x^4 - 3584x^3] + a_7\left[8192x^7 - 28672x^6 + 39936x^5 - 26880x^4 + 9408x^3\right] \quad (51)$$

Differentiating equation (50) three times, we have

$$u'(x) = a_3\left[96x^2\right] + a_4\left[512x^3 - 768x^2\right] + a_5\left[2560x^4 - 5120x^3 + 3360x^2\right] + a_6\left[122888x^5 - 30720x^4 + 2764x^3 - 10752x^2 - 10752x\right] + a_7\left[57344x^6 - 172032x^5 + 199680x^4 - 107520x^3 + 28224x^2\right] \quad (52)$$

$$u''(x) = a_3[192x] + a_4\left[1536x^2 - 1536x\right] + a_5\left[10240x^3 - 15360x^2 + 6720x\right] + a_6\left[61440x^4 - 122880x^3 + 82944x^2 - 21504x\right] + a_7\left[344064x^5 - 860160x^4 + 798720x^3 - 322560x^2 + 56448x\right] \quad (53)$$

$$u'''(x) = 192a_3 + a_4[3072x - 1536x] + a_5\left[30720x^2 - 30720x + 6720\right] + a_6\left[245760x^3 - 36864x^2 + 165888x - 21504\right] + a_7\left[344064x^5 - 860160x^4 + 798720x^3 - 322560x^2 + 56448x\right] \quad (54)$$

Remember $u'''(x) = -1$

$$-1 = 192a_3 - 1536a_4 + 6720a_5 - 21504a_6 + 56448a_7$$
$$192a_3 = -1 + 1536a_4 - 6720a_5 + 21504a_6 - 56448a_7$$
$$32a_3 = \frac{-1}{6} + 256a_4 - 1120a_5 + 3584a_6 - 9408a_7 \quad (55)$$

Substitute (55) into (44), we have

$$u(x) = x - \frac{x^3}{6} + a_4\left[128x^4\right] + a_5\left[512x^5 - 1280x^4\right] + a_6\left[737280x^2 - 737280x + 165888\right] + a_7\left[6881280x^3 - 10321920x^2 + 4792320x - 645120\right] \quad (56)$$

Differentiating four times

$$u^{(iv)}(x) = a_4[3072] + a_5[61440x - 30720] + a_6\left[737280x^2 - 737280x + 165888\right] + a_7\left[6881280x^3 - 10321920x^2 + 4792320x - 645120\right] \quad (57)$$

Replacing x by t (57) we have

$$u(t) = t - \frac{t^3}{6} + a_4\left[128t^4\right] + a_5\left[512t^5 - 1280t^4\right] + a_6\left[737280t^2 - 737280t + 165888\right] + a_7\left[6881280t^3 - 10321920t^2 + 4792320t - 645120\right] \quad (58)$$

From equation (31)

$$u^{(iv)}(x) = 24 + x + \frac{x^6}{30} - \int_0^x (x-1)u(t)dt \quad (59)$$

Substitute equation (59) into (37), which yield

$$u^{(iv)}(x) = 24 + x + \frac{x^6}{30} - \int_0^x (x-1)\left[\begin{array}{l} t - \frac{t^3}{6} + a_4\left[128t^4\right] + a_5\left[512t^5 - 1280t^4\right] + a_6[737280t^2 \\ - 737280t + 165888] + a_7[6881280t^3 - 10321920t^2 \\ + 4792320t - 645120 \end{array}\right] dt \quad (60)$$

$$u^{(iv)}(x)=24+x+\frac{x^6}{30}-\left[\begin{array}{l}\frac{x^3}{6}-\frac{x^5}{120}+a_4\left[\frac{64x^6}{15}\right]+a_5\left[\frac{256x^7}{21}-\frac{128x^6}{3}\right]+a_6\left[\frac{256x^8}{7}-\frac{1024x^7}{7}+\frac{1152x^6}{5}\right]\\+a_7\left[\frac{1024x^9}{9}-512x^8+\frac{6656x^7}{7}-896x^6\right]\end{array}\right] \tag{61}$$

Equating equation (57) we have our residual equation

$$\begin{array}{l}R[a_4, a_5, a_6, a_7]=-24-x-\frac{x^6}{30}+a_4\left[\frac{x^3}{6}+30720\right]+a_5\left[\frac{256x^7}{21}-\frac{128x^6}{3}+6144x-30720\right]\\+a_6\left[\frac{256x^8}{7}-\frac{1024x^7}{7}+\frac{1152x^6}{5}+737280x^2-737280x+165888\right]\\+a_7\left[\frac{1024x^9}{9}-512x^8+\frac{6656x^7}{7}-896x^6+6881280x^3-10321920x^2+4792320x-645120\right]\end{array} \tag{62}$$

Since $S[a_4, a_5, a_6, a_7]=\int_0^1 w(x)R[a_4, a_5, a_6, a_7]^2 dt$ (63)

We take $w(x)=\left(x-\frac{x^3}{6}\right)$, which satisfy the boundary condition above.

$$S[a_4, a_5, a_6, a_7]=\int_0^1\left[\begin{array}{l}-24-x-\frac{x^6}{30}+a_4\left[\frac{x^3}{6}+30720\right]+a_5\left[\frac{256x^7}{21}-\frac{128x^6}{3}+6144x-30720\right]\\+a_6\left[\frac{256x^8}{7}-\frac{1024x^7}{7}+\frac{1152x^6}{5}+737280x^2-737280x+165888\right]\\+a_7\left[\frac{1024x^9}{9}-512x^8+\frac{6656x^7}{7}-896x^6+6881280x^3-10321920x^2\\+4792320x-645120\end{array}\right]\left(x-\frac{x^3}{6}\right)dx \tag{64}$$

Finding the values of $a'_j\ s=4,5,6,7$ which minimizes S is equivalent to finding the best approximation for (28). The minimized value of S is obtained by setting $\frac{\partial S}{\partial a_j}=0$, where $j=4,5,6,7$.

For $j=4$, we have

$$\frac{\partial S}{\partial a_4}=\frac{3859046311}{111375} \tag{65}$$

For $j=5$, we have

$$\frac{\partial S}{\partial a_5}=\frac{4019687935}{3711015} \tag{66}$$

For $j=6$, we have

$$\frac{\partial S}{\partial a_6}=\frac{5583084741}{1206079875} \tag{67}$$

For $j=7$, we have

$$\frac{\partial S}{\partial a_7}=\frac{6208544974343752}{4124793175} \tag{68}$$

The various values obtained in solving the equations (65)-(68) above using gaussian elimination are as follows

$$\left.\begin{aligned} a_4 &= 0.00796682375 \\ a_5 &= 0.00001415248812 \\ a_6 &= -3.20592\times10^{-7} \\ a_6 &= -2.03596\times10^{-8} \end{aligned}\right\} \tag{69}$$

While the values of $a_1, a_2, a_3 = 0.8627230691271666, 0.1894068028279015, 0.05800099542799082$

The values of $a_1, a_2, a_3, a_4, a_5, a_6, a_7$ are substituted into $u(x)$ to get

$$\begin{aligned} u(x) &= x - 5.082739784612264\times10^{-16}x^2 - 0.1666666666666665x^3 + 0.9999695369863625x^4 \\ &+ 0.008402706266117185x^5 - 0.0000728221644465463x^6 - 0.0001667862003381444x^7 \end{aligned} \tag{70}$$

4.1 Tables

Table 1. The numerical result of problem 1

x	Exact solution	Approximate Solution	Absolute Error
0.1	-0.8951707486	-0.8951707494	2.50e-09
0.2	-0.7813972528	-0.7813972471	3.09e-08
0.3	-0.6598162090	-0.6598162825	1.24e-07
0.4	-0.5316426245	-0.5316426517	3.17e-07
0.5	-0.3981568190	-0.3981570232	6.32e-07
0.6	-0.2606922898	-0.2606931415	1.67e-06
0.7	-0.1206216388	-0.1206245001	1.73e-06
0.8	0.0206576891	0.0206493816	2.57e-06
0.9	0.1617383810	0.1617169414	3.66e-06
1.0	0.3012188203	0.3011686789	5.02e-06

Problem 2

Consider the fourth order Volterra-integro differential equation

$$u^{(iv)}(x) = -1 + x - \int_0^x (x-t)u(t)dt \tag{71}$$

with initial condition as $u(0) = -1, u'(0) = 1, u''(0) = 1, u'''(0) = -1$ well it's the exact solution as

$$u(x) = \sin x - \cos x \tag{72}$$

Source: [20].

Table 2: the numerical result of problem 2

x	Exact Solution	Computed Solution	Absolute Error
0.1	-0.8951707486	- 0.8951707494	2.546e-08
0.2	-0.7813972528	- 0.78139724705	2.177e-07
0.3	-0.6598162090	- 0.6598162825	7.350e-08
0.4	-0.5316426245	- 0.5316426517	2.720e-08
0.5	-0.3981568190	- 0.3981570232	2.041e-07
0.6	-0.2606922898	- 0.2606931415	8.517e-07
0.7	-0.1206216388	- 0.1206245001	2.940e-06
0.8	0.0206576891	0.0206493816	8.310e-06
0.9	0.1617383810	0.1617169414	2.144e-05
1.0	0.3012188203	0.3011686789	5.014e-05

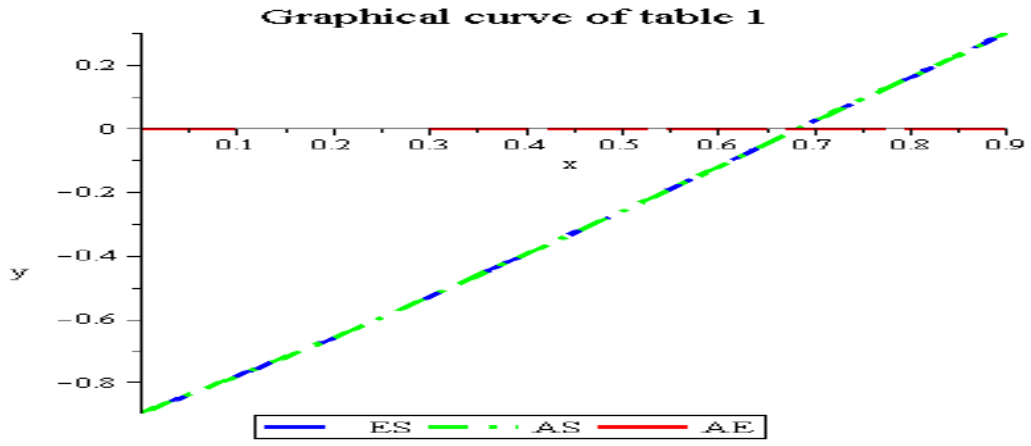


Fig. 1. Graphical Illustration of problem 1

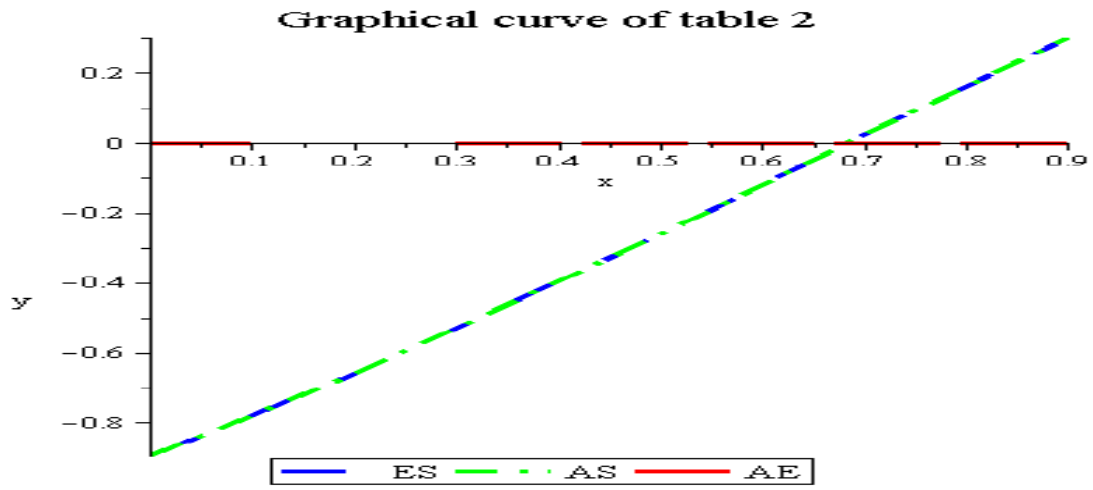


Fig. 2. Graphical Illustration of problem 2

5. Discussion and conclusion

The study focuses on the numerical solution of fourth-order Volterra integro-differential equations using the Least Squares Method and shifted Chebyshev polynomials as the basis function. The numerical method of solving and some numerical problems on fourth order Volterra integro-differential equation using the Least squares method and shifted Chebychev polynomials as basis function were consider. Table 1 and 2 shows the numerical results of problem 1 and 2, while figure 1 and 2 shows the curve of table 1 and 2. The computation of results obtained from the application of the method shows that, the Least Square method using shifted Chebyshev Polynomial as basis function has been utilized effectively to solve the fourth order Volterra Integro-Differential Equations. The solution obtained through this method produce results very close to the exact solution compare to [1]. The simplicity of the method is an included advantage and thus, it is dependable and a power tool for solving the class of problem considered. Conclusively, the study considered the solution of Volterra integro-differential equations of fourth order. All computations are done with the aid of **Maple 18** software.

References

[1] Ayinde, M.A., Ishaq, A.A., Latunde, T. and Sabo, J. (2021). Efficient numerical approximation methods for solving high-order integro-differential equations. Caliphate Journal of Science & Technology. 2, 188-195.

[2] Ajileye, G. and Aminu F.A. (2022). Approximate Solution to First-Order Integro-differential Equations Using Polynomial Collocation Approach. J. Appl Computat Math. 11, 1-4.

[3] Shahooth, M.K., Ahmad, R., Salman, U. and Swidan, W. (2016). Approximation solution of solving linear Volterra Fredholm integro differential equations of the second kind by using Bernstein

polynomial method. J. Appl. Computat. Math. 5(2), 298. doi:10.4172/2168-9679.1000298

[4] Ajileye G., Oyedepo T., Adiku Lydia, and Sabo, J. (2023). Collocation based numerical method for multi-order fractional integro-diffeerential equation. Iranian Journal of Numerical Analysis and Optimization. 13(4), 604-626.

[5] Ajileye, G., Amoo, S.A. and Ogwumu, O.D. (2018). Hybrid block method algorithms for solution of first order initial value problems in ordinary differential equations. J. Appl. Computat. Math. 7:2. doi: 10.4172/2168-9679.1000390.

[6] Ajileye, G., Okedayo, G.T. and Aboiyar, T. (2017). Laguerre collocation approach for continuous hybrid block method for solving initial value problems of second order ordinary differential equations. Trends Food Sci. Techn. 2, 379- 383.

[7] Al-Bugami, A.M. and Al-Juadi, J.G. (2020). Runge-Kutta method and block by block method to solve nonlinear fedholm-volterra integral equation with continuous kernel. Journal of Applied Mathematics and Physics, 8(9), 20-43.

[8] Shoukralla, E.S. and Ahmed, B.M. (2016). Numerical solutions of Volterra integral equations of the second using lagrange interpolation via thee vandermonde matrix. Int. Journal of Physics: Conference eries. IOP publish, 1447(1), 12003.

[9] Adesanya, A.O. Yahaya, Y.A. Ahmed, B. and Onsachi, R.O. (2019). Numerical solution of linear integral and integro-differential equations using boubakar collocation method. International Journal of Mathematical Analysis and Optimization: Theory and Application, 2, 592-598.

[10] Aggarwal, S., Sharma, N. and Chauhan, R. (2018). Solution of linear Volterra integral equations of second kind using mohand transform. International Journal of Research and Advance Technology, 6, 3098-3102.

[11] Abubakar, A. and Taiwo O.A. (2014). Integral collocation approximation methods for the numerical solution of high-orders linear Fredholm-Volterra integro-differential equations. J. Comput. Appl. Math. 4, 111-117.

[12] Ajileye, G. James, A.A. Ayinde, A.M. Oyedepo, T. (2022). Collocation approach for the computational solution of Fredholm-Volterra fractional order of integro-differential equations. J. Nig. Soc. Phys. Sci. 4, 834.

[12] Butris, R.N. and Noori, N.R. (2022). A study in the existence and uniqueness solution of Volterra-Fredholm Integro-differential equations. Journal of Applied Computer Science and Mathematics. 16(2), 26-30.

[13] Bôcher, M. (1926). An introduction to the study of integral equations. University Press. 10.

[14] Wazwaz, A.M. (2015). A first course in integral equations. Second edition. Saint Xavier University, USA.

[15] Volterra, V. (1860-1940). Obituary Notices of fellows of the royal society, 3, (1941): 690-729.

[16] Hashim, I. (2006). Adomian decomposition method for solving BVPs for fourth-order integro-differential equations. Journal of Computational and Applied Mathematics. 193(2), 658-664.

[17] Dastjerdi, H.L., and Ghaini, F.M. (2012). Numerical solution of Volterra-Fredholm integral equations by moving least square method and Chebyshev polynomials. Applied Mathematical Modelling. 36 (7), 3283-3288.

[18] Kythe, P. and Puri, P. (2002). Computational methods for linear integral equations. Springer Science & Business Media.
[19] Wazwaz, A.M. (2011). Linear and nonlinear integral equations: methods and applications. Springer.

Type II Half Logistic Inverse Exponential distribution: properties and application to tax data

D.O. Omosigho*, K.T. Amzat†, and O.E. Adeniji‡

Abstract

We defined, studied and inventive distribution called Type II half logistic Inverse Exponential ($TIIHL-IE$) distribution. Some well-known mathematical properties: moments, Bonferroni and Lorenz curves, mean deviation, quantile function, Reliability function, and Renyi entropy of $TIIHL-IE$ distribution is studied. The expressions of order statistics are derived. Parameters of the derived distribution are obtained using maximum likelihood method. The applicability of proposed distribution is exemplified by using a tax revenue dataset.

Keywords and phrases Lorenz curves, quantile function, Reliability function, Mean deviation.

1 Introduction

In the recent decade, there has been an overwhelming demand of probability distribution with a more adaptability properties in several fields of study. This has enabled the development of many generalized distributions. Many of these distributions have been developed by the addition of one or more shape parameters to baseline distribution that exist in literature to make them more flexible and adaptable in modeling various kinds of data exhibiting different shapes of the hazard function. These distributions have to found applications area such as in reliability studies, seismography, insurance, medicine among several others because of their flexibility in modeling failure rate. For example, the Kumaraswamy odd log-logistic family by [1], Weibull-G family of distributions by [3], Kumaraswamy generalized family was studied by [4], exponentiated generalized class of distribution was studied by [5], exponentiated half-logistic was introduced by [6], the type I half-logistic by [7], [8] proposed and developed the Zografos-Balakrishnan odd log-logistic family of distributions,], [9] developed the Zografos Balakrishnan odd log-logistic family of distributions, [10] developed the generalized beta family of distributions. the Kumaraswamy Weibull proposed and developed by [11, a new generalized odd log-logistic family by [12], the kummer beta was developed and studied by [13] among many

*Department of Mathematics and Statistics, Federal Polytechnic Ado-Ekiti; E-mail: etindon@yahoo.co.uk
† Department of Mathematical Sciences Crescent University Abeokuta, Ogun State; E-mail: Kafayat.amzat@cuab.edu.ng
‡ Corresponding Author. Department of Statistics, University of Ibadan, Ibadan, Oyo State; E-mail: emmanuel4444real@yahoo.com

others. This study further extends the inverse exponential distribution to further enhance its scope of applications.

A random variable X follows an Inverse exponential distribution, if its cumulative distribution function (CDF) can be represented as

$$F(x;\omega) = \exp(-\omega x^{-1}), \tag{1}$$

and the related probability density function (PDF) to (1) is

$$F(x;\omega) = \omega x^{-2}\exp(-\omega x^{-1}), x;\omega,\alpha > 0. \tag{2}$$

where w is the scale parameter.

1.1 Motivation of study

The chief motivation for this study is to exploy the flexibility offers by the Type II half logistic-G family of distribution to any baseline distribution, which makes the baseline distribution to be more flexible and adaptable to any kind of data exhibiting any form of the shapes of the failure rate. On this ground we are proposing the Type II half logistic Inverse Exponential ($TIIHL-IE$) distribution.

2 The $TIIHL-IE$ Distribution

[11] proposed and developed Type II half logistic-G (TIIHL-G) family of distributions with the CDF given by

$$G(x;\alpha,\varphi) = 1 - \int_0^{-logF(x;\varphi)} \frac{2\alpha e^{-\alpha t}}{(1+e^{-\alpha t})^2}\,dt \tag{3}$$

$$= \frac{2[F(x;\varphi)]^{\alpha}}{1+[F(x;\varphi)]^{\alpha}}, \qquad x>0,\alpha>0,$$

where $F(x;\varphi)$ the CDF of baseline model with parameter is vector φ and $G(x;\alpha,\varphi)$ is CDF obtained by using the T-X generator developed by [2]. The PDF of the $TIIHL-G$ family is given by

$$g(x;\alpha,\varphi) = \frac{2\alpha f(x;\varphi)[F(x;\varphi)]^{\alpha-1}}{[1+[F(x;\varphi)]^{\alpha}]^2}, \qquad x>0,\theta>0, \tag{4}$$

A random variable (r.v) X follows Type II half logistic Frechet ($TIIHL-IE$) distribution if its CDF is obtained by inserting (1) in (3) as follows:

$$G(x;\alpha,\omega) = \frac{2\left[e^{-\omega x^{-1}}\right]^{\alpha}}{1+\left[e^{-\omega x^{-1}}\right]^{\alpha}}, x>0;\omega,\alpha>0 \tag{5}$$

The PDF corresponding to (5) is given by

$$g(x;\alpha,\omega) = 2\alpha\omega x^{-2}e^{-\omega\alpha x^{-1}}\left(1+e^{-\omega\alpha x^{-1}}\right)^{-2}, x>0;\omega,\alpha>0 \tag{6}$$

An expression for the reliability function and the failure rate function is given respectively as

$$R(x;\alpha,\omega) = 1 - \frac{2\left[e^{-\omega x^{-1}}\right]^{\alpha}}{1+[e^{-\alpha x^{-\alpha}}]^{\alpha}}. \tag{7}$$

and

$$h(x;\alpha,\omega) = \frac{2\alpha\omega\alpha x^{-2} e^{-\omega x^{-2}}\left(1+e^{-\omega\alpha x^{-1}}\right)^{-1}}{1-e^{-\omega\alpha x^{-1}}} \quad . \tag{8}$$

Figures 1 and 2 demonstrate the flexibility of the $TIIHL-IE$ distribution. The plots for the PDF of $TIIHL-IE$ distribution is given in figure 1, and plot of the hazard rate function (hrf) is given in Figure 2 for various values of the parameters

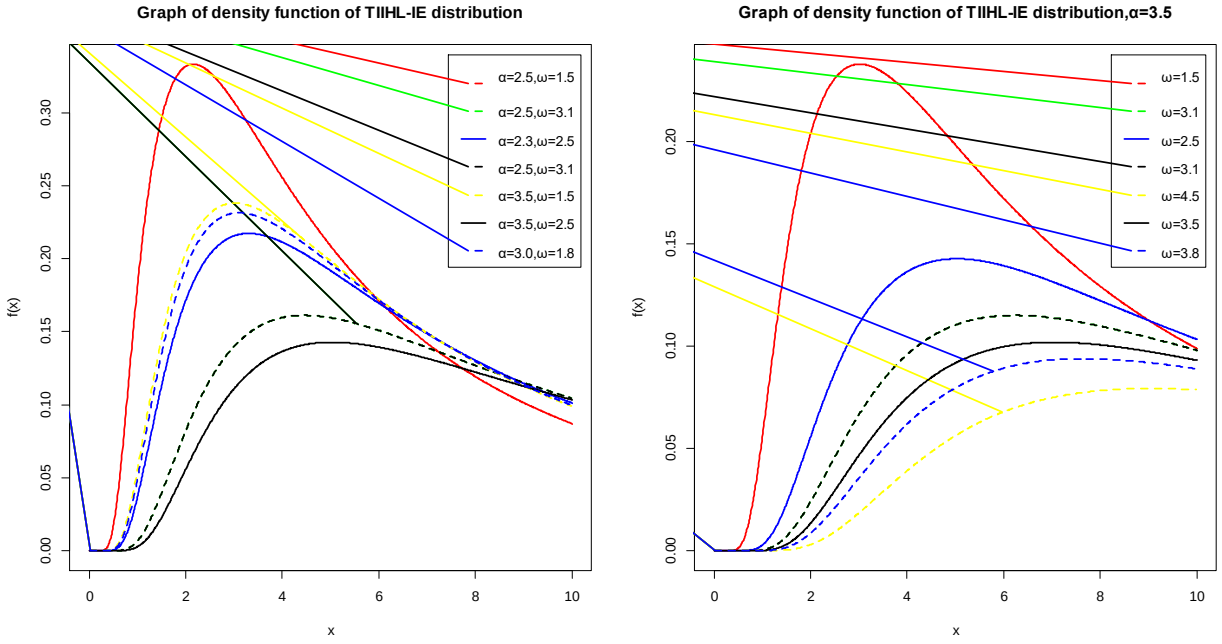


Figure 1. Plots of the PDF of $TIIHL-IE$ distribution for selected values of the parameters

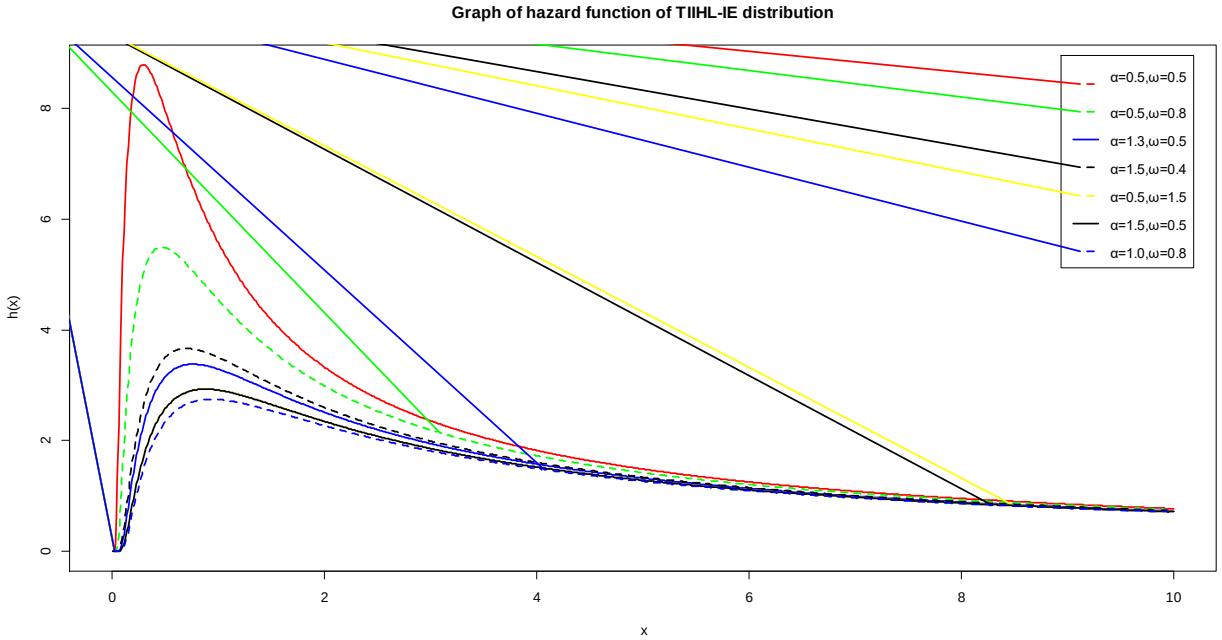


Figure 2. Plots of the PDF of $TIIHL-IE$ distribution for selected values of the parameters

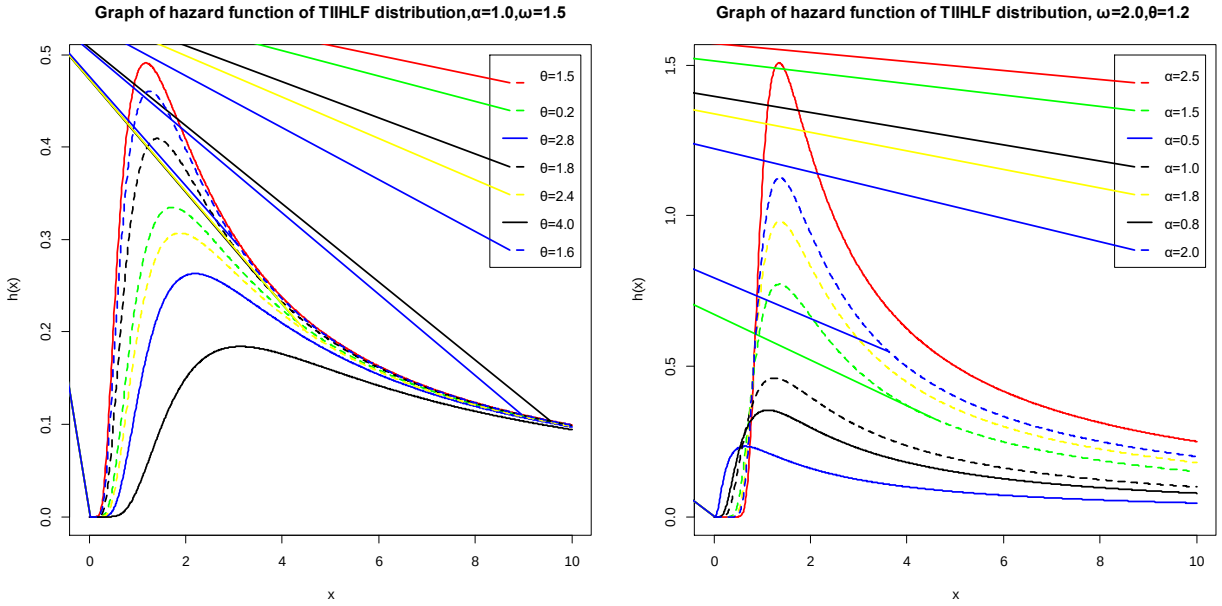


Figure 3. Plots of the hf of TIIHL-IE distribution for selected values of the parameters

subsections

3 Some Mathematical Properties

Here, we derived some properties of $TIIHL-IE$ distribution.

3.1 Quantile function.

The quantile function of X is denoted by $Q(u)$, defined as

$$Q(u) = F^{-1}\left(\frac{u}{2-u}\right)^{1/\theta}, u \in (0,1), \tag{9}$$

The inverse function of $F(.)$ is $F^{-1}(.)$, given in (1)
Also,

$$x_u = \left[-\frac{1}{\omega\alpha}\left(ln\left\{\frac{u}{2-u}\right\}\right)\right]^{-1} . \tag{10}$$

It should be noted that simulated values from the quantile function of $TIIHL-IE$ distribution given in (10) can be utilized to demonstrates the effectiveness of the method of estimation approach adopted. The random variable q follows a uniform distribution on the interval $0,1$; i.e $x_u = Q(u)$ follows $TIIHL-IE$ distribution in particular, the lower, middle and upper quartiles are obtained by taking $u = 0.25, 0.5$ and 0.75 respectively in (10).

3.2 Alternate representation.

Here, we present the expansion of the PDF and CDF for $TIIHL-IE$ distribution for further mathematical simplification. The binomial theorem, for $z>0$ and $|m|<1$, can be expressed as

$$(1+y)^{-z}=\sum_{i=0}^{\infty}(-1)^i\binom{z+i-1}{i}y^i, \tag{11}$$

Then, by applying (11) in (6), the PDF of $TIIHL-IE$ distribution becomes

$$g(x)=2\alpha\omega\sum_{i=0}^{\infty}(-1)^i\binom{i+1}{i}x^{-2}e^{-\alpha\omega(i+1)x^{-1}} \tag{12}$$

Proposition 1. Let "s" be a positive integer. The expansion of the CDF can be written in the form:

$$[F(x)]^s=2^s\sum_{j=0}^{\infty}(-1)^j\binom{s+j-1}{j}e^{-\omega\alpha(j+s)x^{-2}}, \tag{13}$$

Proof. The CDF $[F(x)]^s$ is obtained, for 's' an integer by using (12)

$$[F(x)]^s=\left[\frac{2\left[e^{-\omega x^{-1}}\right]^{\alpha}}{1+\left[e^{-ax^{-1}}\right]^{\alpha}}\right]^s,$$

$$[F(x)]^s=2^s\sum_{j=0}^{\infty}(-1)^j\binom{s+j-1}{j}e^{-\omega\alpha(j+s)x^{-2}} \tag{14}$$

3.3 Moments of $TIIHL-IE$ distribution

The moment plays an important role in distribution study and real data application(s). Now, we obtain the k^{th} moment of the $TIIHL-IE$ distribution under certain regularity condition; the k^{th} moment of $TIIHL-IE$ distribution is obtained as

$$\mu_k'=\int_{-\infty}^{\infty}x^kf(x)dx=2\alpha\omega\theta\sum_{i=0}^{\infty}(-1)^i\binom{i+1}{i}Q(x) \tag{15}$$

where

$$Q(x)=\int_{-\infty}^{\infty}x^{k-2}\,e^{-\omega\alpha(i+1)x^{-\alpha}}dx \tag{16}$$

taking $p=\omega\alpha(i+1)x^{-1}$,$dx=-\frac{p^{-2}}{[\omega\alpha(i+1]^{-1}}dp$ and substitute in (16), we have

$$Q(x)=\frac{1}{[\omega\alpha(i+1]^{1-k}}\int_0^{\infty}p^{-k}e^{-p}dp=\frac{1}{[\omega\alpha(i+1]^{1-k}}\Gamma(1-k)$$

Finally, we have an expression for the kth moment of $TIIHL-IE$ distribution given as

$$\mu_k'=2\omega\alpha\sum_{i=0}^{\infty}(-1)^i\binom{i+1}{i}\frac{1}{[\omega\alpha(i+1]^{1-k}}\Gamma(1-k) \tag{17}$$

3.4 Incomplete moments of $TIIHL-IE$ distribution

The incomplete moment of $TIIHL-IE$ distribution can be obtained using (13) as

$$\varphi_k(t) = \int_{-\infty}^{t} x^k f(x)dx = 2\alpha\omega \sum_{i=0}^{\infty} (-1)^i \binom{i+1}{i} M(x) \tag{18}$$

where

$$M(x) = \int_{-\infty}^{t} x^{k-2}\, e^{-\omega\alpha(i+1)x^{-1}} dx \tag{19}$$

taking $= \omega\alpha(i+1)x^{-1}$,$dx = -\frac{p^{-2}}{[\omega\alpha(i+1]^{-1}} dp$ and substitute in (19), we have

$$M(x) = \frac{1}{[\omega\alpha(i+1]^{1-k}} \int_{0}^{t} p^{-k/\alpha} e^{-p} dp = \frac{1}{[\omega\alpha(i+1]^{1-k}} \Gamma(1-k, \omega\alpha(i+1)t^{-1})$$

Where

Finally, we have

$$\varphi_k(t) = 2\omega\alpha \sum_{i=0}^{\infty} (-1)^i \binom{i+1}{i} \frac{1}{[\omega\alpha(i+1]^{1-k}} \Gamma(1-k, \omega\alpha(i+1)t^{-1}) \tag{20}$$

For $k = 1, 2, 3, \ldots$.

3.5 Moment generating function of $TIIHL - IE$ distribution

The moment generating function of a random variable X $TIIHL - IE$ distribution is obtained as

$$M_X(t) = \sum_{k=0}^{\infty} \frac{t^k}{k!} \mu_k' = 2\omega\alpha \sum_{i,k=0}^{\infty} (-1)^i \binom{i+1}{i} \frac{t^k}{k!} \frac{1}{[\omega\alpha(i+1]^{1-k}} \Gamma(1-k) \tag{21}$$

The mean deviation: the expression to obtain the mean deviation about the mean and median are respectively given by

$M_1(x) = 2\mu F(\mu) - 2\phi(\mu)$ and $M_2(x) = 2\mu F(\mu) - 2\phi(M_d)$, where M_d is the median of X and $\phi(q) = \int_{-\infty}^{q} xf(x)dx$ is the incomplete moment given in (21).

Now

$$T(\mu) = \int_{0}^{\mu} xf(x)dx = \sum_{i=0}^{\infty} (-1)^i \binom{i+1}{i} \frac{1}{[\omega\alpha(i+1]^{1-k/\alpha}} \Gamma(1-k, \omega\alpha(i+1)\mu^{-1})$$

$$T(M_d) = \int_{0}^{M_d} xf(x)dx = \sum_{i=0}^{\infty} (-1)^i \binom{i+1}{i} \frac{1}{[\omega\alpha(i+1]^{1-k}} \Gamma\left(1-k, \omega\alpha(i+1){M_d}^{-1}\right)$$

3.6 Bonferroni and Lorenz curves

Bonferroni and Lorenz curves are mostly applied in different fields of life such as demography studies, medical technology, life insurance, life testing, and reliability analysis among others. The Lorenz and Bonferroni Curves are computed using the expression from the first incomplete moment and can respectively be obtained as follows:

$$L_F(x) = \frac{1}{E(X)}\int_0^x tf(t)dt = \frac{\sum_{i=0}^{\infty}(-1)^i\binom{i+1}{i}\frac{1}{[\omega\alpha(i+1]^{1-k}}\Gamma(1-k,\omega\alpha(i+1)t^{-1})}{\sum_{i=0}^{\infty}(-1)^i\binom{i+1}{i}}$$

and

$$B_F(x) = \frac{L_F(x)}{F(x)} = \frac{\sum_{i=0}^{\infty}(-1)^i\binom{i+1}{i}\frac{1}{[\omega\alpha(i+1]^{1-k/\alpha}}\Gamma(1-k,\omega\alpha(i+1)t^{-1}) / \sum_{i=0}^{\infty}(-1)^i\binom{i+1}{i}}{2e^{-\omega\alpha x^{-1}}/(1+e^{-\omega\alpha x^{-1}})}$$

3.7 Probability weighted moment

The probability weighted moments (PWMs) of a distribution are further used to study some characteristics of probability distribution. Denoted by $\eta_{k,s}$, can be defined as

$$\eta_{k,s} = E[X^k F(X)^s] = \int_{-\infty}^{\infty} x^k F(x)^s f(x)dx \tag{22}$$

Considering and expression in (12) and (14) and putting it in (23), we have

$$\eta_{k,s} = 2^{s+1}\alpha\omega\theta\sum_{i,j=0}^{\infty}(-1)^{i+j}\binom{i+1}{i}\binom{j+s-1}{j}\int_{-\infty}^{\infty} x^{k-\alpha-1}e^{-\omega\alpha x^{-1}(i+j+s+1)}dx \tag{23}$$

Letting $m = \omega\alpha x^{-1}(i+j+s+1)$ and putting it (23), we have

$$\eta_{k,s} = 2^{s+1}\omega\alpha\sum_{i,j=0}^{\infty}\frac{(-1)^{i+j}\binom{i+1}{i}\binom{j+s-1}{j}}{[\omega x^{-\alpha}(i+j+s+1)]^{1-k}}\int_{-\infty}^{\infty} m^{-k}e^{-m)}dm \tag{24}$$

Finally, we have,

$$\eta_{k,s} = 2^{s+1}\omega\alpha\sum_{i,j=0}^{\infty}\frac{(-1)^{i+j}\binom{i+1}{i}\binom{j+s-1}{j}}{[\omega\alpha x^{-\alpha}(i+j+s+1)]^{1-k}}\Gamma(1-k) \tag{25}$$

3.8 Renyi entropy

Renyi entropy was proposed by [14]. It can be obtained by

$$I_\lambda(x) = \frac{1}{1-\lambda}logM \tag{26}$$

Where

$$M = \int_{-\infty}^{\infty} f^\lambda(x)dx, \qquad \lambda > 0, \lambda \neq 1 \tag{27}$$

Putting (6) in (27), we have

$$M = \int_{-\infty}^{\infty}\left[2\alpha\omega x^{-(\alpha+1)}e^{-\omega\alpha x^{-1}}\left(1+e^{-\omega\alpha x^{-1}}\right)^{-2}\right]^\lambda dx \tag{28}$$

$$= (2\alpha\omega)^\lambda\int_{-\infty}^{\infty} x^{-2\lambda}e^{-\omega\alpha\lambda x^{-\alpha}}\left(1+e^{-\omega\alpha x^{-1}}\right)^{-2\lambda}dx$$

Using binomial expansion given in (12) for the expression above, we have

$$M = (2\alpha\omega)^{\lambda}\sum_{i=0}^{\infty}(-1)^{i}\binom{2\lambda+1-1}{i}\int_{-\infty}^{\infty}x^{-2\lambda}e^{-\omega\alpha(\lambda+i)x^{-1}}dx \tag{29}$$

Taking $z = \omega\alpha(\lambda+i)x^{-2}$, $x = \frac{z^{-1}}{[\omega\theta(\lambda+i)]^{z^{-1}}}$, $dx = -1/\alpha\frac{z^{-2}}{[\omega\alpha(\lambda+i)]^{-1}}dz$ and putting it in (29), we obtain

$$M = \sum_{i=0}^{\infty}(-1)^{i}\binom{2\lambda+1-1}{i}\frac{2^{\lambda}\omega^{\lambda}\alpha^{\lambda}\alpha^{\lambda-1}}{[\omega\theta(\lambda+i)]^{-\frac{\lambda(\alpha+1)-1}{\alpha}}}\int_{0}^{\infty}z^{\frac{(\lambda-1)(\alpha+1)}{\alpha}}e^{-z}dz \tag{30}$$

$$= \sum_{i=0}^{\infty}(-1)^{i}\binom{2\lambda+1-1}{i}\frac{2^{\lambda}\omega^{\lambda}\alpha^{\lambda}}{[\omega\theta(\lambda+i)]^{-2\lambda-1}}\Gamma[(\lambda-1)+1]$$

Finally, the entropy of TIIHL distribution is given by

$$I_{\lambda}(x) = \frac{1}{1-\lambda}log\left(\sum_{i=0}^{\infty}(-1)^{i}\binom{2\lambda+1-1}{i}\frac{2^{\lambda}\omega^{\lambda}\alpha^{\lambda}}{[\omega\alpha(\lambda+i)]^{2\lambda-1}}\Gamma[(\lambda-1)+1]\right) \tag{31}$$

3.9 Stress-strength reliability

Here we obtain the stress-strength parameter of $TIIHL-IE$ distribution. Suppose X_1 represent the strength of a structure with stress X_2, and if X_1 follows $TIIHL-IE$ (ω_1,α_1) and X_2 follows $TIIHL-IE$ (ω_2,α_2), given that $X_1$and X_2 are statistically independent random variables, then the Stress-strength Reliability (R) of TIIHLIE is obtained as follows:

$$R = P(X_2 < X_1) = \int_{0}^{\infty} f_1(x;\omega_1,\alpha_1)F_2(x;\omega_2,\alpha_2)dx \tag{32}$$

Then we can express (32) as

$$R = 4\omega_1\alpha_1\sum_{j=0}^{\infty}(-1)^{i+j}\binom{i+1}{i}\int_{0}^{\infty}x^{-1}e^{-[\omega_1\alpha_1(j+1)+\omega_2\alpha_2(i+1)]x^{-1}}dx \tag{33}$$

Taking $v = [\omega_1\alpha_1(j+1)+\omega_2\alpha_2(i+1)]x^{-1}$, finally we have

$$R = \frac{4\omega_1\alpha_1}{[\omega_1\alpha_1(j+1)+\omega_2\alpha_2(i+1)]}\sum_{i,j=0}^{\infty}(-1)^{i+j}\binom{i+1}{i}$$

3.10 Order statistics

Order statistics is widely applied in statistical theory. Suppose $X_1, X_2, \ldots, X_n$ be a random sample having CDF $F(x)$. Let $x_{1:1}, x_{2:n}, \ldots, x_{n:n}$ be the ordered sample of size n, then the density of r^{th} order statistics is given as

$$f_{r:n}(x) = P\sum_{l=0}^{n-r}(-1)^{l}\binom{n-r}{l}f(x)F(x)^{l+r-1} \tag{34}$$

where $P = \frac{n!}{(n-r)!r!}$. The PDF of the r^{th} order statistics of $TIIHL-IE$ distribution is obtained by putting (13) and (14) in (34), changing s with $l+r-1$ followed by simple algebraic manipulation, we have

$$f_{r:n}(x) = P\alpha\omega \sum_{l=0}^{n-r} \sum_{i,j=0}^{\infty} H_l \, x^{-2} e^{-\omega\alpha x^{-1}(i+j+l+r)} \tag{35}$$

where

$$\boldsymbol{H_l} = 2^{l+r}(-1)^{i+j+l} \binom{n-r}{l} \binom{i+1}{i} \binom{l+r+j-2}{j}$$

Consequently, the s^{th} moment of the r^{th} order statistics for $TIIHL-IE$ distribution is given by

$$E(X_{r:n}^{s}) = \int_{-\infty}^{\infty} x^{s} f_{r:n}(x) dx. \tag{36}$$

By substituting (35) in (36), we have

$$E(X_{r:n}^{s}) = \alpha\omega P \sum_{l=0}^{n-r} \sum_{i,j=0}^{\infty} \boldsymbol{H_l} \int_{-\infty}^{\infty} x^{s-2} e^{-\omega\alpha x^{-1}(i+j+l+r)} dx. \tag{37}$$

Letting $= \omega\alpha x^{-1}(i+j+l+r)$, $x = \frac{y^{-1}}{[\omega\alpha(i+j+l+r)]^{-1}}$, $dx = -\frac{y^{-2}}{\alpha[\omega\theta(i+j+l+r)]^{-1}} dy$ and putting it (39), we have

$$E(X_{r:n}^{s}) = P \sum_{l=0}^{n-r} \sum_{i,j=0}^{\infty} \frac{\omega\alpha \boldsymbol{H_l}}{[\omega\alpha(i+j+l+r)]^{1-s/\alpha}} \int_{-\infty}^{\infty} y^{-s/r} e^{-y} dx \tag{38}$$

Then,

$$E(X_{r:n}^{s}) = P \sum_{l=0}^{n-r} \sum_{i,j=0}^{\infty} \frac{\omega\alpha H_l}{[\omega\alpha(i+j+l+r)]^{1-s/\alpha}} \Gamma(2-s) \tag{39}$$

4 Maximum likelihood estimation

Given a random sample of $x_1, x_2, \ldots, x_n$ from the TIIHLF (α, ω) distribution, the likelihood function for $\xi = (\alpha, \omega)$ is

$$L(\underline{x}, \xi) = \prod_{i=1}^{n} 2\alpha\omega x^{-2} e^{-\omega\alpha x^{-1}} \left(1 + e^{-\omega\alpha x^{-1}}\right)^{-2} \tag{40}$$

And the log-likelihood function $logL(\underline{x}, \xi) = l$ is given as

$$l = nlog(2\alpha\omega) + (\alpha - 1) \sum_{i=1}^{n} log\,(x_i) - \omega\alpha \sum_{i=1}^{n} x_i^{-1} - 2 \sum_{i=1}^{n} log\left(1 + e^{-\omega\alpha x_i^{-1}}\right) \tag{41}$$

The element of the score vector $U(\xi) = (U_\alpha, U_\omega)$ are given below

$$U_\omega = \frac{n}{\theta} - \omega \sum_{i=1}^{n} x_i^{-\alpha} + 2 \sum_{i=1}^{n} \left[\frac{\omega x_i^{-\alpha} e^{-\omega\theta x_i^{-\alpha}}}{1 + e^{-\omega\theta x_i^{-\alpha}}}\right] \tag{42}$$

$$U_\alpha = \frac{n}{\omega} - \alpha \sum_{i=1}^{n} x_i^{-1} + 2 \sum_{i=1}^{n} \left[\frac{\alpha x_i^{-1} e^{-\omega\alpha x_i^{-1}}}{1 + e^{-\omega\alpha x_i^{-1}}}\right] \tag{43}$$

The maximum likelihood estimator $\hat{\xi} = (\hat{\alpha}, \hat{\omega})^T$ can be obtained by solving simultaneously the likelihood equations

$$\frac{\partial l(\xi)}{\partial \alpha} \Big|_{\xi=\hat{\xi}} = 0, \quad \frac{\partial l(\xi)}{\partial \omega} \Big|_{\xi=\hat{\xi}} = 0,$$

There is no closed-form expression for the maximum likelihood estimator and its computation can only be handled numerically using a nonlinear optimization algorithm. We can employ the use of iterative techniques such as a Newton–Raphson-type algorithm to obtain the numerical value of $\hat{\xi}$. The observed information matrix used for computing confidence intervals for the model parameters can be obtained from standard maximization routines numerically such as the use of the R functions optim or nlm, the SAS procedure NL Mixed, the Ox function Max BFGS, and many others, to compute the observed information matrix numerically.

5 Application

In this section, two real data sets are used to demonstrate the flexibility and applicability of the Type II half logistic Frechet model over some of some other competitive model. We consider some important measures of goodness-of-fit: Akaike information criterion (AIC), Bayesian information criterion (BIC), the corrected Akaike information criterion (CAIC) and p-value (PV) are used. For the data set, we shall compare the fits of the TIIHL-IE model with other models: the Lomax -Inverse Exponential (L-IE), Inverse Exponential (IE), and Exponential model. The smaller these statistics are, the better the fit except for the p value. However, the better model corresponds to the smaller values of AIC, BIC, CAIC, and larger value of P value (PV) criteria.

The data set is a taxes revenue's data, the values of tax revenue data are 3.7, 3.11, 4.42, 3.28, 3.75, 2.96,3.39, 3.31, 3.15, 2.81, 1.41, 2.76, 3.19, 1.59, 2.17, 3.51, 1.84, 1.61, 1.57, 1.89, 2.74, 3.27, 2.41, 3.09, 2.43, 2.53,2.81, 3.31, 2.35, 2.77, 2.68, 4.91, 1.57, 2.00, 1.17, 2.17, 0.39, 2.79, 1.08, 2.88, 2.73, 2.87, 3.19, 1.87, 2.95, 2.67,4.20, 2.85, 2.55, 2.17, 2.97, 3.68, 0.81, 1.22, 5.08, 1.69, 3.68, 4.70, 2.03, 2.82, 2.50, 1.47, 3.22, 3.15, 2.97, 2.93,3.33, 2.56, 2.59, 2.83, 1.36, 1.84, 5.56, 1.12, 2.48, 1.25, 2.48, 2.03, 1.61, 2.05, 3.60, 3.11, 1.69, 4.90, 3.39, 3.22,2.55, 3.56, 2.38, 1.92, 0.98, 1.59, 1.73, 1.71, 1.18, 4.38, 0.85, 1.80, 2.12, 3.65.

Table 1 present the Exploratory data analysis of the Tax revenue data. Table 2 presents the maximin likelihood estimate (MLEs) and the measures of goodness of fits for the model considered. Figure 4 is the represent the box plot for Tax revenue data. Table 1.0 indicates that the Tax revenue data is positively skewed, with excess kurtosis of 0.18 and under-dispersed.

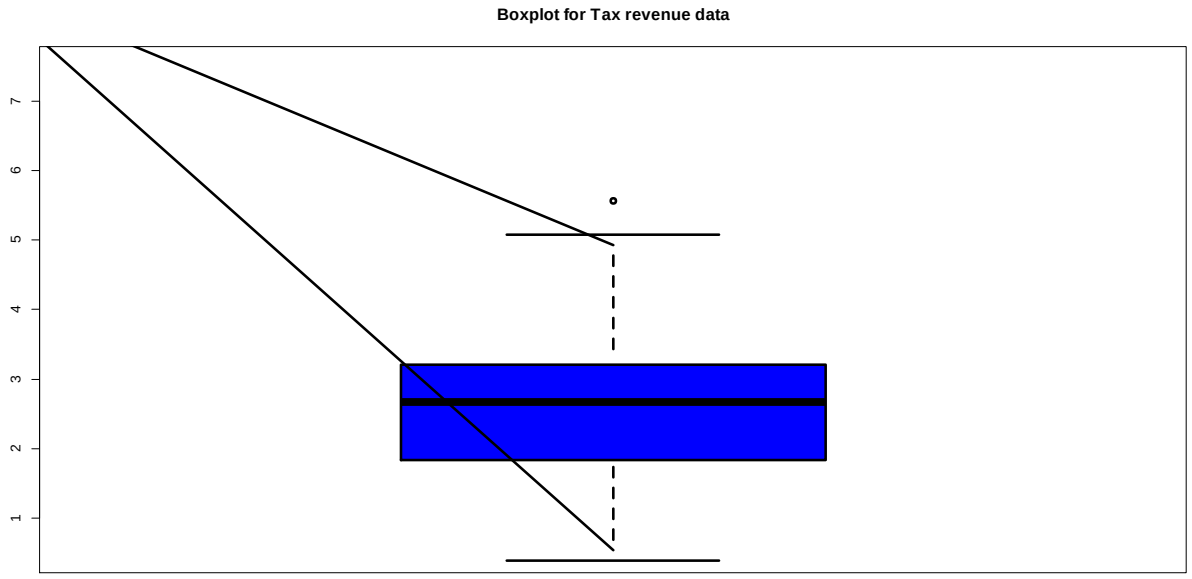


Figure 4: Box plot for Tax revenue data

Table 1.0 Exploratory data Analysis for Tax revenue data

n	Min.	q_1	$median$	q_3	$mean$	$Max.$	$skewness$	$kurtosis$	$variance$
100	0.39	1.84	2.68	3.20	2.61	5.56	0.39	3.18	1.02

Table 2.0: MLEs, standard error (parenthesis), and Measures of goodness of fits

$Model$	$\hat{\alpha}$	$\hat{w}$	$-l$	AIC	$CAIC$	HQIC	BIC
$TIIHLIE$	1.29 (0.27)	1.0901 (0.82)	92.85	189.81	189.82	191.80	194.90
IE	2.1353 (1.98)	– (–)	198.98	399.96	299.99	401.01	402.56
E	0.38 (0.04)		195.99	393.98	394.02	395.03	396.58
$L-IE$	2.77 (0.23)	1.67 (0.07)	150.42	304.83	304.96	306.94	310.04

6 Conclusion

We have developed the $TIIHL-IE$ distribution and studied its properties such as: descriptive measures based on the quantiles, moments, stress-strength reliability and incomplete moments and order statistics. Goodness of fit shows that $TIIHL-IE$ distribution provides a better fit. Applications of the TIIHL-IE model to taxes revenue's data demonstrate its significance and flexibility. We have

shown that the TIIHL-IE distribution real life data than all other competitive models considered in this study.

References

[1] Alizadeh, M., Emadi, M., Doostparast, M., Cordeiro, G. M., Ortega, E. M. M. and Pescim, R. R. (2015). Kumaraswamy odd log-logistic family of distributions: Properties and applications, Hacettepe Journal of Mathematics and Statistics, Vol. 44, No. 6, pp. 1491-1512.

[2] Alzaatreh, A., Lee, C., and Famoye, F. (2011). A new method for generating families of continuous distributions. METRON (2013) 71:63–79. DOI 10.1007/s40300-013-0007-y

[3] Bourguignon, M., Silva, R.B. and Cordeiro, G. M. (2014). The Weibull– G family of probability distributions. Journal of Data Science, 12, 53-68.

[4] Cordeiro, G. M. and de Castro, M. (2011). A new family of generalized distribution. Journal of Statistical Computations and Simulation, 81, 883-898.

[5] Cordeiro, G. M., Ortega, E. M. M. and da Cunha, D. C. C. (2013). The exponentiated generalized class of distributions. Journal of Data Science, 11, 1-27.

[6] Cordeiro, G. M., Alizadeh, M. and Ortega, E. M. (2014). The exponentiated half-logistic family of distributions: Properties and applications, Journal of Probability and Statistics.

[7] Cordeiro, G. M., Alizadeh, M. and Marinho, E. P. R. D. (2015). The type I half-logistic family of distributions. Journal of Statistical Computation and Simulation, 86, 707-728.

[8] Cordeiro, G. M., Alizadeh, M. and Ortega, E. M. M. (2014). The exponentiated half- logistic family of distributions: Properties and applications. Journal of Probability and Statistics, Article ID 864396, 21 pages. http://dx.doi.org/10.1155/2014/864396.

[9] Cordeiro, G.M., Alizadeh, M., Ortega, E.M.M. and Serrano, L.H.V. (2016). The Zografos Balakrishnan odd log-logistic family of distributions: Properties and Applications, Hacet. J. Math. Stat., Vol. 45.

[10] Eugene, N., Lee, C. and Famoye, F. (2002). The beta-normal distribution and its applications. Communications in Statistics & Theory and Methods, 31, 497-512.

[11] Hassan, A. S. and Elgarhy, M. (2016). Kumaraswamy Weibull-generated family of distributions with applications. Advances and Applications in Statistics, 48, 205-239.

[12] Haghbin, H., Ozel, G., Alizadeh, M. and Hamedani, G. G. (2017). A new generalized odd loglogistic family of distributions, Communications in Statistics-Theory and Methods, Vol. 46, No. 20, pp. 9897-9920.

[13] Pescim, R. R., Cordeiro, G. M., Demetrio, C. G. B., Ortega, E. M. M. and Nadarajah, S. (2012). The new class of Kummer beta generalized distributions. Statistics and Operations Research Transactions, 36, 153-180.

[14] Renyi A. (1961). On measures of entropy and information. In: Proceedings of the 4th Fourth Berkeley Symposium on Mathematical Statistics and Probability, 547-561. University of California Press, Berkeley.

.

Transient analysis of short circuit faults in hybrid networks

J.S. Zangina[*†], M.A. Suleiman[‡], and A. Ahmed[†§]

Abstract

Hybrid power systems, integrating renewable energy sources, energy storage devices, and conventional generators, are at the vanguard of the transition towards sustainable energy solutions. However, ensuring the robustness and reliability of these systems under fault conditions, particularly short circuit faults, remains a challenge. This research explores the complexity of hybrid networks, conducting a comprehensive transient analysis of short-circuit faults to enhance the understanding of their impact. The study employs advanced simulation techniques and state-of-the-art modeling approaches to examine the dynamic behavior of hybrid networks during fault events. Through detailed investigations, this research aims to unravel the transient responses of various fault locations, including fault resistance, and transmission line length, renewable energy sources, when subjected to short circuit faults. The findings of this study not only contribute to the academic discourse surrounding hybrid power systems but also provide invaluable insights for industry practitioners, guiding the development of reliable and efficient hybrid energy infrastructures for a sustainable future.

Keywords and phrases: First Fault resistance, hybrid power system, sustainable energy solution, transient analysis, transmission line

1 Introduction

Short-circuit analysis of a given power system is executed at the design stage to achieve optimum transformer system layout, conductor, and system voltage selection. Also, in the case of an existing power system, fault studies are essential in the events of system expansion and design of protection systems [1] – [3]. Various fault categories are present within power systems, broadly classified as symmetrical and unsymmetrical faults [4] – [8]. Determination of currents and voltage waveforms arising from various faults occurring at different locations within the power system network is essential [9], [10]. This information is crucial for designing an effective protective scheme, as highlighted in prior research [11] – [14]. It has been shown in [15] and [16] that the severity of the fault and its

[*]Corresponding Author; E-mail: jaafzangs@gmail.com
[†]Food and Industrial Biotechnology Department, National Biotechnology Development Agency, Abuja, Nigeria.
[‡]Software Engineering Department, Nile University of Nigeria, Abuja, Nigeria. E-mail: muhammad.suleiman @ nileuniversity.edu.ng
[§]Faculty of Engineering Science, Department of Electrical and Electronics Engineering, University of Nyala, Nyala, Sudan. E-mail: elamin2018@gmail.com

transient component in transmission systems depends on several factors, such as fault type, the magnitude of the system voltage at the instant of the fault occurrence, and fault location [17] – [19]. These factors significantly impact the shapes and amplitudes of voltage and current waveforms as well as the damping rates and frequencies across the transmission system.

The simulation of transient voltage and current, coupled with an analysis of diverse fault conditions that may arise during short circuit events, holds significant importance in the power system engineering practice. Transient overvoltage and current are widely recognized for inducing harmful thermal stress and fire hazards, potentially causing damage to power system equipment [20]. Short circuit on power system network is inevitable, but protective devices like circuit breakers and fuses should be able to cut off fault at a given location with considerable damage. Similarly, buses, cables, and disconnecting switches should be robust to withstand the mechanical and thermal stresses of short-circuit currents that flow through them [21], [22]. The selections of this equipment are subject to the magnitude of short circuit currents. The interaction of several apparatuses used for generating, transmitting, and distributing hybrid electrical power makes it somewhat of a complex system. The extreme complexity of these systems proposes ineluctable failures regardless of system perfection during the design stage. Rotating electrical machinery was considered the source of fundamental frequency currents that flow during a short circuit [23]. Power capacitors within the systems can also develop very high transient short-circuit discharge currents.

This research contributes to a deeper understanding of the dynamic behavior of hybrid power systems during short-circuit fault events. In particular, the study employs advanced simulation techniques that include numerical modeling, dynamic simulations, and state-of-the-art modeling approaches. These techniques are valuable in examining the complex transient phenomena during short-circuit faults in hybrid networks. The findings of this research offer practical guidance to industry practitioners involved in the design and operation of hybrid energy infrastructures. By understanding the transient behavior of these systems during short-circuit faults, practitioners can make informed decisions to enhance the reliability and efficiency of hybrid power systems. The work also contributes to the broader goal of creating a more sustainable and resilient energy infrastructure. It adds to the academic discourse surrounding hybrid power systems, which is critical in the perspective of global efforts to reduce greenhouse gas emissions and promote renewable energy. The research serves as a foundation for further studies in the field of fault analysis in hybrid networks. It provides a starting point for researchers to further explore the subject, investigate new fault scenarios, and develop mitigation strategies to enhance the robustness of hybrid power systems.

2 System description

The system comprises a conventional generation unit with a nominal capacity of 50MVA. The power system is outfitted with a synchronous generator connected via a hybrid transformer and a double-circuit line of 132 kV. The specific line configuration is illustrated in Fig. 1, with the total line length varying from 20 to 100 km. Detailed parameters are provided in Table 1.

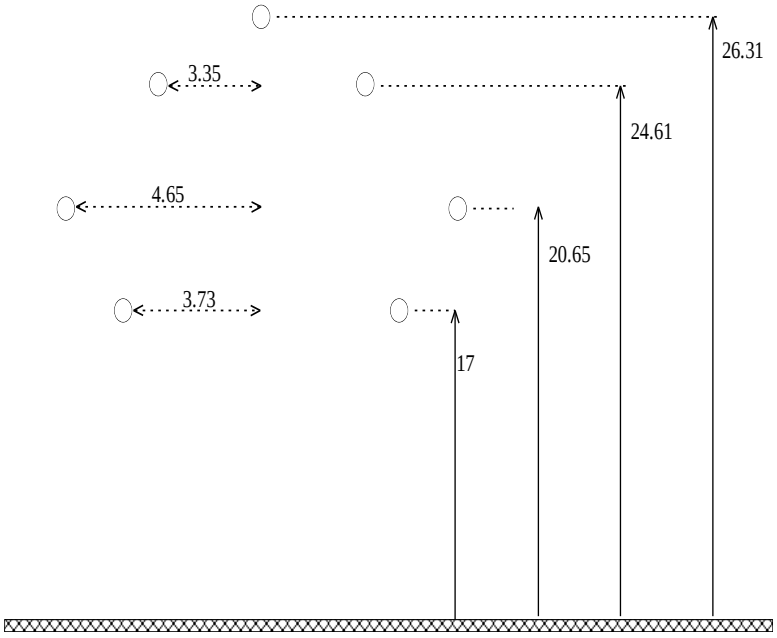


Fig. 1. Configuration of the overhead line (dimension in meters)

The transmission line is energized at one end by both conventional and wind generation, but in different locations, while the other end is open-circuited and on no-load.

Table 1. Details of the transmission line conductors

	Phase Conductor	Earth Wire
DC resistance (ohm/km)	0.156489	0.1469
Conductor radius (cm)	0.976	0.976
Number of conductors	1	1
Resistivity of the soil (Ω-m)	20	

2.1 Hybrid system configuration

Simulating transient voltages in a hybrid power network of transmission systems requires electromagnetic transient (EMT) simulation software. This simulation process is usually accompanied by time-consuming, which can hinder the efficiency of research and engineering tasks [24]. For this reason, it's essential to avoid unnecessary model assumptions and adopt a sufficient system model. It is imperative to recognize model elements with fast-front wave characteristics as they account for critical variables in the transient study. The hybrid power system component like transformer and generators in the ATPDraw program is suitable for a system with fast-front waves as it accounts for the magnetic saturation effects, main and leakage flux losses, and coil capacitances [25]. These variables are essential in power system transient study. The wind farm model from the ATPDraw Windsyn is employed to complete the hybrid power system setup. The Windsyn control mechanism

operates to maintain more than 0.89 lagging power factor at the terminal bus of the wind farm. The nominal power generation of the wind farm is 35 MW. The equivalent diagram of the system is shown in Fig. 2.

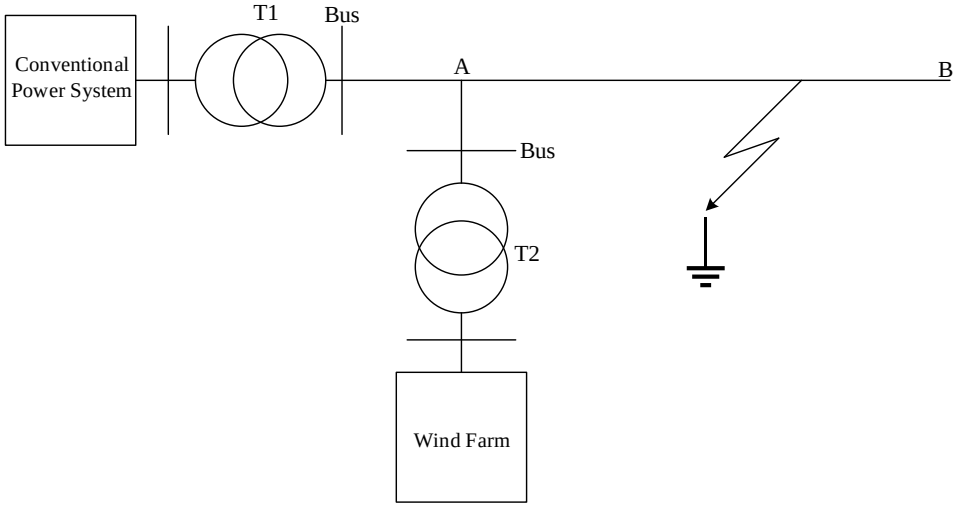


Fig. 2. Single line equivalent diagram of the hybrid power system

2.2 Transmission Line Model

To accurately model the transmission line for the transient study, a frequency-dependent distributed line mode is adopted. Consider a small portion of the long segment of the line as shown in Fig. 3. Let the total line be x and a small segment of it Δy, then the wave propagation along the line is described as follows:

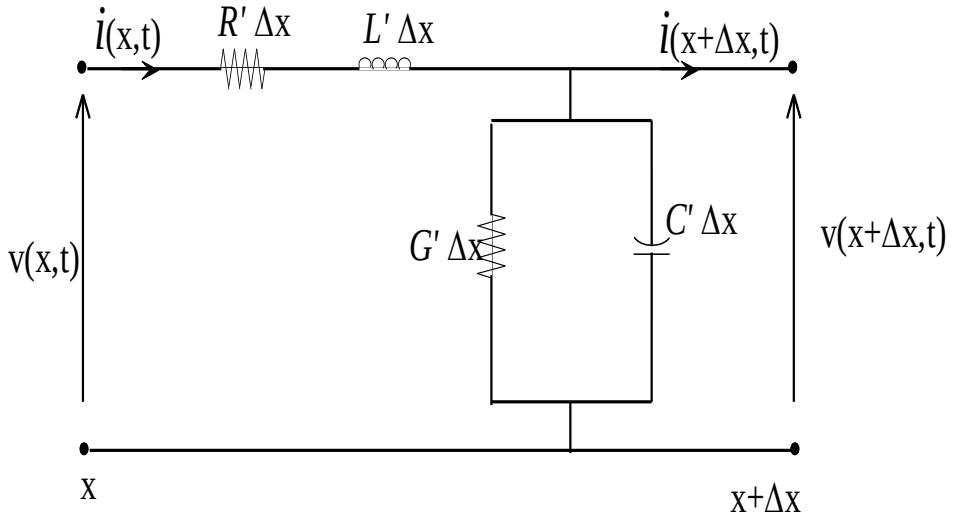


Fig. 3. Transmission line segment

$$\frac{\partial i}{dy} = -vG' - \frac{\partial v_o}{\partial t}C' \quad (1)$$

$$\frac{\partial v}{\partial y} = -iR' - \frac{\partial i_i}{\partial t}L' \quad (2)$$

where R' is the transmission line resistance in Ω/km, L' denote inductance in H/km, C' is the capacitance in F/km, G' denote the shunt conductance in Ω-1/km.

$$\frac{\partial^2 v}{\partial y^2} = -R'\frac{\partial i}{\partial y} - L'\frac{\partial^2 i}{\partial y \partial t} \quad (3)$$

$$\frac{\partial^2 v}{\partial y \partial t} = -R'\frac{\partial i}{\partial t} - L'\frac{\partial^2 i}{\partial t^2} \quad (4)$$

$$\frac{\partial^2 i}{\partial y \partial t} = -G'\frac{\partial v}{\partial t} - C'\frac{\partial^2 v}{\partial t^2} \quad (5)$$

$$\frac{\partial^2 i}{\partial y^2} = -G'\frac{\partial v}{\partial t} - L'\frac{\partial^2 v}{\partial y \partial t} \quad (6)$$

$$\frac{\partial^2 v}{\partial y^2} = v(R'G') + \frac{\partial v}{\partial t}(L'G' + R'C') + (C'L')\frac{\partial^2 v}{\partial t^2} \quad (7)$$

$$\frac{\partial^2 i}{\partial y^2} = i(R'G') + \frac{\partial i}{\partial t}(L'G' + R'C') + (C'L')\frac{\partial^2 i}{\partial t^2} \quad (8)$$

$$\frac{\partial^2 v}{\partial y^2} = v(R'G') + j\omega v(y,t)(L'G' + R'C') - (C'L')\omega^2 v(y,t) \quad (9)$$

$$\frac{\partial^2 v}{\partial y^2} = v(y,t)[(R + j\omega L)(G + j\omega C)] \quad (10)$$

$$v(y) = K_0 e^{-\gamma y} + K_1 e^{\gamma y} \quad (11)$$

$$\gamma = \sqrt{[(R' + j\omega L')(G' + j\omega C')]} \quad (12)$$

where γ is the propagation constant, ω represents angular velocity.

The current wave propagation along the line and the characteristics impedance becomes:

$$i(y,t) = \frac{-\gamma K_0 e^{-\gamma y} + \gamma K_1 e^{\gamma y}}{(R' + j\omega L')} \quad (13)$$

$$\frac{v(y,t)}{i(y,t)} = Z_0 \quad (14)$$

$$Z_0 = \sqrt{\frac{R' + j\omega L'}{G' + j\omega C'}} \quad (15)$$

However, in the case of frequency-dependent factors, the wave propagation characterized by impedance and propagation constant is determined by the following expression:

$$Z_c(\omega) = \sqrt{\frac{R'(\omega) + j\omega L'(\omega)}{G'(\omega) + j\omega C'(\omega)}} \quad (16)$$

$$Z_c(\omega) = \sqrt{\frac{Z'(\omega)}{Y'(\omega)}} \quad (17)$$

where $Z'(\omega)$ is the series impedance matrix, $Y'(\omega)$ is the shunt admittance matrix.
The fault in a power system is known to cause distortion in the current and voltage waveform along the transmission line. This fault can be represented by the equations, which describe the relationship between voltage and current along the line:

$$V(x) = V_{in}e^{-\gamma x} + V_r e^{\gamma x} \quad (18)$$

$$I(x) = \frac{V_{in}}{Z_0}e^{-\gamma x} - \frac{V_r}{Z_0}e^{\gamma x} \quad (19)$$

where $V(x)$ is the voltage at a distance x along the line, $I(x)$ is the current at a distance x, V_{in} denotes incident voltage at the beginning of the line, V_r denotes a reflected voltage wave caused by a fault.

3 Result and discussion

Consider the short circuit fault on a single phase at the transmission line end (point A) when the phase voltage is at the peak value. The Maximum values of the sending-end faulted phase current for different line lengths are given in Table 2. The simulation result shows that the maximum magnitude of the sending end currents increases as the line length increases. Also, the observed ripples along the line attenuate as the line length increases. The faulted phase sending-end currents during fault are computed for various line lengths and plotted to obtain faulted phase current waveform as shown in Fig. 4a and 4b, respectively.

Table 2. Table captions should be placed above the tables.

Distance between fault point and the first sending-end of the line (km)	Maximum magnitude of the first sending-end current (A)
20	249.42
40	353.39
60	397.19
80	408.02

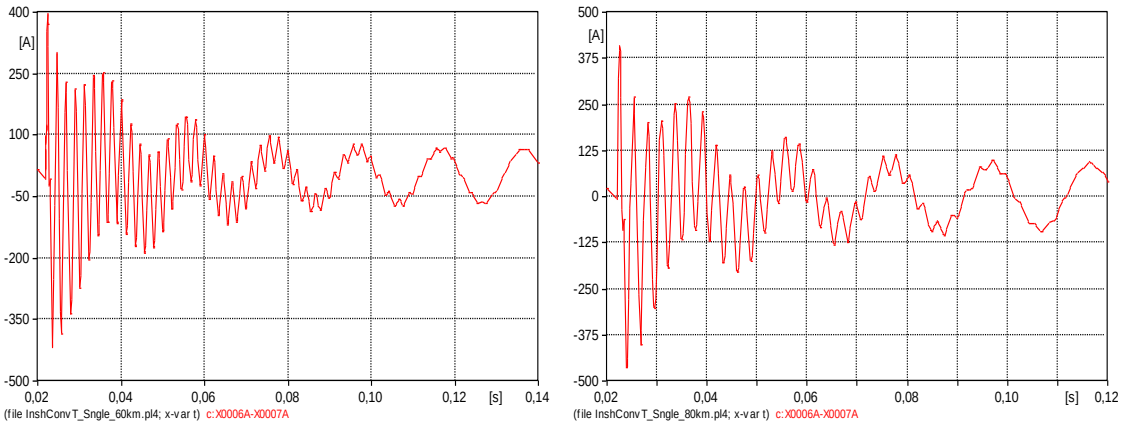


Fig. 4. Sending-end faulted phase current on the line at (a) 60km, (b) 80km.

The sending-end unfaulted phase voltages waveform is shown in Fig. 5a and 5b for 40 and 100km, respectively. It is observed from the result that as the line length increases, the unfaulted phase voltages decrease, and likewise, the distortion also decreases.

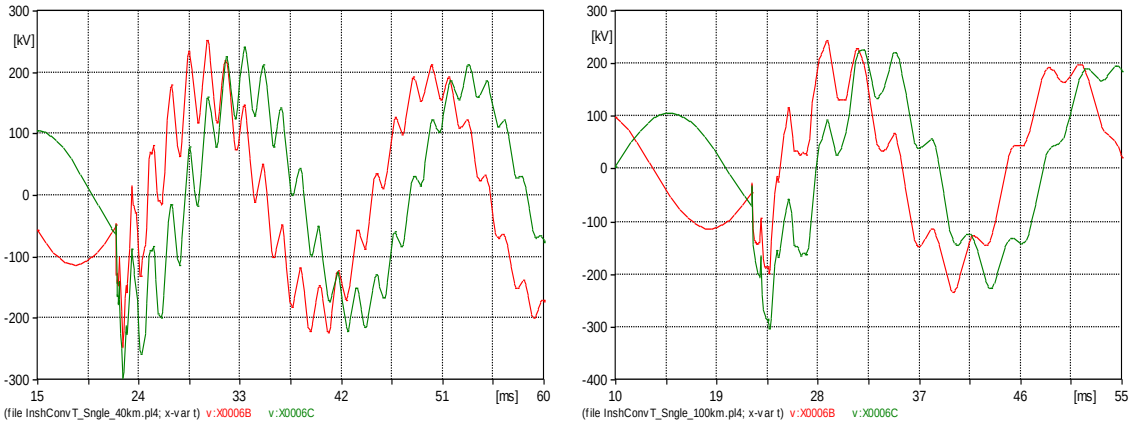


Fig. 5. Sending-end unfaulted phase voltages for the line at (a) 40 km, (b) 100km.

A single-phase to-earth fault is considered to occur at the receiving end of the line during fault resistance, as shown in Fig 6. The earth fault is assumed to occur when the voltage of the faulted phase is at its peak value. When an earth fault happens, it often causes a sudden increase in current flow through the grounding system. Detecting and addressing earth faults promptly is crucial because they can lead to equipment damage, electrical fires, or even pose a risk to human safety. One common method used to identify earth faults is by monitoring the voltage of the faulted phase.

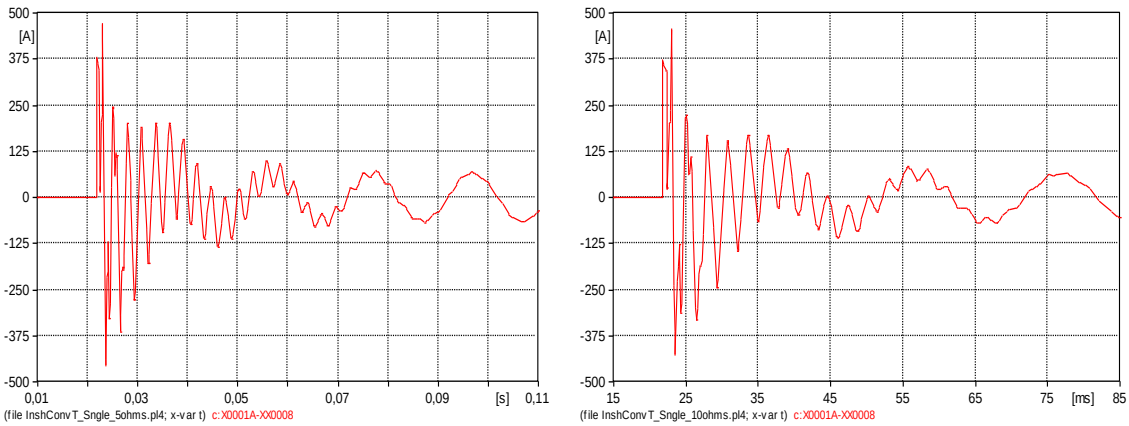


Fig. 6. Fault current at the fault location fault resistance (a) 5 ohms, (b) 10 ohms.

Variation of maximum fault currents at the sending end and the fault location for different fault resistances is given in Table 3. The maximum magnitude of fault currents at the sending-end and fault location decreases as the fault resistance increases. The distortion in the fault current waveform is higher at a lower value of the fault resistance as compared to that of a higher value.

Table 3. Variation of maximum sending-end faulted phase current and maximum magnitude fault current at fault location against fault resistance.

Fault resistance (ohms)	Maximum magnitude of first sending-end current (A)	Maximum magnitude fault current at fault location (A)
1	406.59	485.22
5	400.97	472.33
10	394.16	457.10
20	381.17	429.28
50	346.94	362.64

Double-phase to-earth and three-phase to-earth faults are considered. The fault occurs at the receiving end of the line on phases B and C in the case of a double-phase fault. The maximum magnitude of the fault current at the fault location is recorded. Similarly, in the case of three-phase-to-earth fault simulation, currents and voltages computed were also taken at the fault and sending-end points, respectively. For a double phase-to-earth fault, waveforms of faulted phase currents at the sending end are given in Fig. 7a. Similarly, Fig. 7b depicts the faulted phase current during a three-phase fault at the sending end. However, the three-phase faulted waveforms for the faulted phases A, B, and C voltage at the sending end, and the faulted phase currents at the fault location are given in Fig. 8a and 8b, respectively. This information aids in the design and setting of protective devices such as circuit

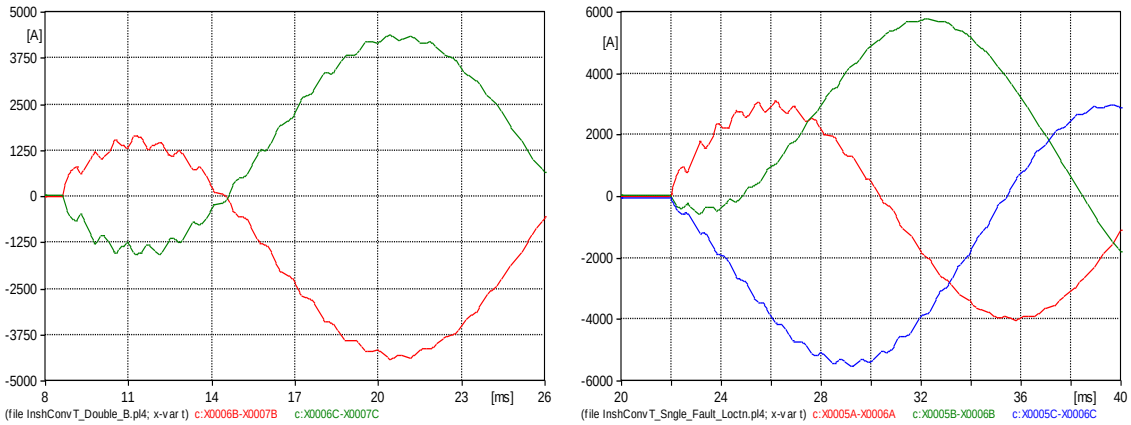


Fig. 7. Faulted phase currents at the sending-end (a) Double phase (b) Three phase.

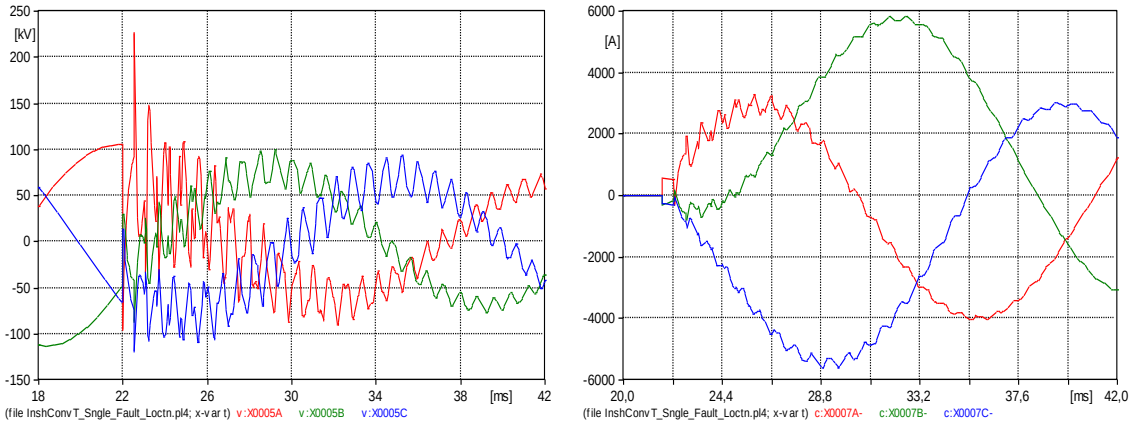


Fig. 8. Faulted phases (a) voltages at the sending-end, (b) currents at the fault location

breakers and relays. Understanding the variation of fault currents against fault resistance helps in the selection of appropriate protection settings to isolate the faulty section quickly, preventing extensive damage to the equipment.

This study investigates transient voltage and over-current responses arising from various fault conditions within a power system. The findings confirm that the severity of fault transients in the examined power system is contingent upon several factors, including fault type, line length, fault location, and the system voltage magnitude at the moment of the fault occurrence. These variables influence the amplitudes and shapes of current and voltage waveforms along the transmission system. The analysis of the waveforms reveals that an increase in line length or fault resistance correlates with the distortion reduction within the current waveforms. Moreover, voltage waveforms exhibit higher amplitude and frequency oscillations than the current waveforms. During a three-phase fault to ground occurring at the line's end, voltage waveforms display substantial instability characterized by high amplitudes, distinguishing them from other fault types. Similarly, transient fault currents recorded at the fault location surpass those at any other point within the transmission system.

4 Conclusion

The analysis conducted in this study plays a fundamental role in the strategic planning, design, and operation of hybrid power systems. Voltage and current data collected during various fault scenarios serve as crucial inputs for devising the protective framework, comprising protective relays, switch gears, and circuit breakers. Notably, this research focuses explicitly on assessing the impact of short circuit faults on hybrid power systems.

A distinctive feature of this study lies in its explicit focus on the short circuit faults assessment within hybrid power systems. Through rigorous analysis and meticulous experimentation, the research sheds light on the intricate dynamics of these faults, unraveling their impact on the stability and reliability of hybrid power setups. This insight is invaluable, guiding future endeavors in the field and providing a solid foundation for advanced protective strategies. In essence, this study not only contributes to the academic discourse but also holds immense practical implications for the broader energy landscape. By continually refining our understanding of hybrid power system behavior, we move closer to a future where clean and reliable energy is readily accessible, paving the way for a more sustainable world.

References

[1] Zhuang, S., Miao, X., Lin, Y., and Liu, Q. (2024). The early detection of short-circuit fault in the active low-voltage AC system. Int. J. Electr. Power Energy Syst., 155: 109476.

[2] Taheri, B., Salehimehr, S., and Sedighizadeh, M. (2022). A novel strategy for fault location in shunt-compensated double circuit transmission lines equipped by wind farms based on long short-term memory. Cleaner Eng. Technol., 6: 100406.

[3] Pascoalato, T. F. G., de Araújo, A. R. J., Kurokawa, S., and Filho, J. P. (2023). Alternative method to include the frequency-effect on transmission line parameters via state-space representation.

Int. J. Electr. Power Energy Syst., x: 109375.
[4] Topolanek, D., Krcal, V., Foltyn, L., Praks, P., Vysocky, J., Praksova, R., Prettico, G., and Fulli, G. (2023). Optimization method for short circuit current reduction in extensive meshed LV network. Int. J. Electr. Power Energy Syst., 152: 109203.
[5] Zheng, Z., Li, Q., Li, X., Zheng, P., Wang, K., and Cui, P. (2022). Analysis and fault-tolerant control of inter-turn short-circuit fault for five-phase permanent-magnet synchronous machine. Energy Rep., 8: 7360–7373.
[6] Xiao, F., Xia, Y., Zhang, K., Zhang, Z., and Yin, X. (2022). Short-circuit model of the DFIG considering coordinated control strategy of grid- and rotor-side converters. Energy Rep., 8: 1046–105.
[7] Yin, J. (2021). Influence of reactive power support control strategy on short-circuit current calculation and fault analysis method of DFIG. Energy Rep., 7: 5933–5942.
[8] Murzintseva, A., Korolev, A., Zhgun, K., and Baembitov, R. (2020). Short-circuit Current reduction in auxiliary network of traction substation. Transp. Res. Procedia., 54: 346–354.
[9] Lacerda, V. A., Araujo, E. P., Chea-Mañe, M., and Gomis-Bellmunt, O. (2023). Phasor and EMT models of grid-following and grid-forming converters for short-circuit simulations. Electric Power Syst. Res., 223: 109662.
[10] Mishra, S. K., Tripathy, L. N., and Swain, S. C. (2019). DWT approach based differential relaying scheme for single circuit and double circuit transmission line protection including STATCOM. Ain Shams Eng. J., 10: 93-102.
[11] Amin, A., Abdelaziz, A. Y., Attia, M. A., and Kamh, M. Z. (2023). Optimal reconfiguration for Extra high voltage transmission networks using an enhanced Brute-Force algorithm. Ain Shams Eng. J., X: 102246
[12] Teng, Z., Chen, W., Zhaoa, J., Zhang, J., Gan, Z., and Li, K. (2022). Measurement of electromagnetic environment of hybrid DC circuit breaker during bipolar short circuit fault. Energy Rep., 8: 1328–1335.
[13] Abdulkareem, Adesanya, A., Agbetuyi, A. F., and Alayande, A. S. (2021). Novel approach to determine unbalanced current circuit on Nigerian 330kV transmission grid for reliability and security enhancement. Heliyon, 7: e07563.
[14] Ding, C., Tian, X., Nie, T., and Yuan, Z. (2020). Influence of capacitor-buffered hybrid DC circuit breaker on bipolar short circuit fault of three-terminal MMC-HVDC transmission system. Energy Rep., 6: 1276–1282.
[15] Daisy, M., Aliabadi, M. H., Javadi, S., and Naimi, H. M. (2023). A robust transient and sustainable faults location approach for AC microgrid based on voltage and current difference measurements. Int. J. Electr. Power Energy Syst., 153: 109343.
[16] Song X., Feng T., Han, L., Smith, T. M., Dong, X., Liu, W., and Zhang, R. (2018). Analysis on the fault characteristics of three-phase short-circuit for half-wavelength AC transmission lines. Glob. Energy Intercon., 1: 115-121.
[17] Pinchukov, P. and Makasheva, S. (2023). Harmonic Monitoring in Normal and Short-Circuit Modes of AC Traction Network. Transport. Res. Procedia 68: 980–986.
[18] Liu, Y., Lu, D., Vasilev, S., Wang, B., Lu, D., and Terzija, V. (2023). Model-based transmission line fault location methods: A review. Int. J. Electr. Power Energy Syst., 153:109321.
[19] Zhang, Y., Zhanga, Y., Pan, X., Zhao, B., He, J., Han, Y., Zhang, J., Wang, X., Yu, Z., Bu, G., and Ye, J. (2022). Equivalent modeling method of induction motor contribution to short-circuit current. Energy Rep., 8:1202–1210.
[20] Qi, S., Chang, S., and Cao, L. (2021). Transient discharge characteristics of insulator short-circuit

under high voltage. Alex. Eng. J. 60: 5175-5181.
[21] Zhang, T., and Wang, N. (2023). Transmission line fault classification based on spatiotemporal characteristic analysis with global and local discriminant analysis. Eng. Sci. Technol. Int. J., 45: 101476.
[22] Treider, T. and Høidalen, H. K. (2023). Estimating distance to transient and restriking earth faults in high-impedance grounded, ring-operated distribution networks using current ratios. Electric Power Syst. Res., 224: 109765.
[23] E. Muljadi, N. Samaan, V. Gevorgian,; J. Li; S. Pasupulati, "Short Circuit Current Contribution for Different Wind Turbine generator Types" Proc. IEEE PES Gen. Meeting, 1-8.
[24] Khalilnezhad, H., Popov, M., van der Sluis, L., Bos, J. A., and Ametani, A. (2018). Statistical analysis of energization overvoltages in EHV hybrid OHL–cable systems, IEEE Trans. Power Del., 33: 2765–2775.
[25] Høidalen, H. K., Mork, B. A., Gonzalez, F., Ishchenko, D., and Chiesa, N. (2007) "Implementation and verification of the Hybrid Transformer model in ATPDraw" IPST., 4-7.

An Investment Model for a DC Pension System with Refund Clause under Quadratic Utility

K.N.C. Njoku*

Abstract

Following the Nigerian pension reform act of 2004, there is a clause mandating the pension fund administrators (PFAs) in the defined contributory pension scheme to make a refund to their retirement savings account (RSA) holder's family who died during the accumulation phase. As good as this clause is to RSA holders; it posed a serious challenge to PFAs on the investment strategy to be used under this condition. In this paper, the optimal investment strategy (OIS) is studied for defined contributory pension with return of premium clause under quadratic utility function. The charge on balance by pension fund administrators and the mortality risk of members of the scheme during the accumulation period by introducing return of premium clause is considered. To achieve this, a portfolio consisting of a risk free and a risky asset with charge on balance by pension fund administrators is considered and the Abraham De Moivre force function is used to establish the mortality rate of members during accumulation. Furthermore, we obtained an optimization problem using dynamic programming approach. Using Legendre transformation and Dual theory, the value function, OIS with return clause is obtained under quadratic utility function. Finally, numerical simulations of the effect of some sensitive parameters on the OIS were obtained and analyzed.

Keywords and phrases: quadratic utility; optimal investment strategy; return clause of premium; charge on balance; Abraham De Moivre force function; Legendre transformation method.

1 Introduction

In a DC pension scheme, there exist two crucial phases; one the accumulation phase [1-9] followed by the distribution phase [10]. During the accumulation phase, members contribute a certain percentage of their income into their retirement savings account (RSA) which is managed by the pension fund administrator (PFA) by investing the accumulated funds for the purpose of maximizing his members' wealth toward actualizing a better retirement package [11]. During the accumulation phase, members were only supposed to contribute and wait till after retirement for distribution. However, in recent years, this has not been the case since PFAs will have to make sum refunds during the accumulation phase due to some conditions such as loss of job, dead of members or even for the mortgage. This has

*Department of Mathematics, Imo State University, Owerri, Nigeria.

somehow affected the dynamics of the investment strategies already in existence. Hence this has led to the study of optimal investment strategies with return of premium clauses under different assumptions.

In [12], the optimal investment strategy with return of premium clause was studied under mean variance utility function. In their research work, they considered a PFA who invested in one risk free asset and a risky asset where the risky asset followed the geometric Brownian motion (GBM). [13] studied the OIS for a DC pension scheme with return of premium when the risky asset followed the Heston volatility model; they also determine the efficient frontier of the investor. The OIS with return of premium was also studied by [14]. In their work, they considered a portfolio which comprised of one risk free asset and two risky assets bond modeled by geometric Brownian motion (GBM) and stock modeled by constant elasticity of variance and obtained the OIS under mean variance utility. In [15] the authors studied the OIS with return of premium clause where the price process of the risky asset followed the jump diffusion process. [16], investigated investment in one risk free asset, stock and inflation index bond where the stock market price was modeled by Heston's volatility model and proceed to obtain OIS with return clause for both the inflation index bond and the stock market price. The mean variance optimization of portfolio with return of premium clause in a DC plan with multiple contributors under CEV model was studied in [17] by extending the work of [14]. [18], further extended the work of [12] by studying the OIS with return of premium for a portfolio consisting of assets invested in fixed deposit, stock and loan. Furthermore, the explicit solution of an investment strategy with voluntary contribution and return clause was studied under logarithm utility by [19]. However, in all the literature mentioned above, they assumed the returned funds are without interest from the invested funds but in [20-21], they studied the OIS for a DC scheme with return of premium clause where the return of premium was with predetermined interest. In their work, they assumed the refund premiums are with predetermined interest from investment on risk free asset. In each of the above, they used the Abraham De Moivre model as their mortality force function.

Very recently, some authors have modelled their mortality rate using the Weibull force function as their mortality force function and proceed to obtain the OIS for a DC pension scheme using different utility functions.In [22-23], they studied OIS with return clause with proportional administrative charges; in their work, they used the Weibull force function to model the mortality rate of a DC pension scheme and obtained the OIS under exponential and mean variance utilities respectively.

So far in the literature, we observed that several utility functions have been used to determine the OIS with return of premium which include mean variance, exponential, power and logarithm. All through the literature and to the best of my knowledge, the OIS have not yet been studied with return of premium clause using quadratic utility function under any condition. In this paper, we used the quadratic utility in [2] to study the OIS with return of premium and charge on balance. The Abraham De Moivre model is used as the mortality force function to model the death rate of members.

2 Methodology/model formulation

Let $K_t(t)$ represents the price of the risk free asset and its price process is similar to the one in [12] and [20] given by

$$\begin{cases} dK_t(t) = rK_t(t)dt \\ K_0(0) = k_0 > 0 \end{cases}, \tag{2.1}$$

where $r > 0$ is the predetermined interest rate of the risk free asset.

Similarly, the pension fund administrator may also be willing to invest in a risky asset (stock) modeled by the geometric Brownian motion whose price process is given as follows as in [12] and [20]

$$\begin{cases} dL_t(t) = L_t(t)(\mu dt + \sigma dN_t) \\ L_t(0) = 1 \end{cases}, \tag{2.2}$$

where μ is the expected appreciation rate of $L_t(t)$, σ is the volatility of the stock market price and N_t is the Brownian motion generating the available information in the market generated represented by $\mathcal{F}_t$ called the filtration in a complete probability space $(\Omega, \mathcal{F}_t, \mathcal{P})$, where Ω, is a real space and $\mathcal{P}$ a probability measure.

Next, we consider $I(t)$ to be the fraction of the accumulated wealth to be invested in risky asset and $1 - I(t)$, the fraction to be invested in a risk free asset.
Let a be the monthly contributions at a given time by the pension member, u_0 the initial age during the accumulation phase, T the accumulation phase period, and $u_0 + T$ is the terminal age of the member. $W_{\frac{1}{q},u_0+t}$is the mortality rate from time $t$to $t+\frac{1}{q}$, ta is the accumulated contributions at time t, $mtaW_{\frac{1}{q},u_0+t}$ is the returned contributions to the death members' families within the accumulation period. Also, let α be the charge on balance which is determined based on the value by the pension fund administrators [8].

From the work of [12-23], if we consider the accumulation period $[t, t+\frac{1}{q}]$ and the investment strategy for the risky asset, the differential form of the fund sizeis given as:

$$V\left(t+\frac{1}{q}\right) = \left[\begin{array}{c} V(t)\left(\left(1-I(t)\right)\frac{K_{t+\frac{1}{q}}}{K_t} + I(t)\frac{K_{t+\frac{1}{q}}}{K_t} - \alpha\frac{1}{q}\right) \\ +a\frac{1}{q} - mtaW_{\frac{1}{q},u_0+t} \end{array}\right]\left(\frac{1}{1-W_{\frac{1}{q},u_0+t}}\right) \tag{2.3}$$

$$V\left(t+\frac{1}{z}\right) - V(t) = \left[\begin{array}{c} V(t)\left(\begin{array}{c} \left(1-I(t)\right)\left(\frac{K_{t+\frac{1}{z}}}{K} - \frac{K_t}{K_t}\right) \\ +\pi(t)\left(\frac{L_{t+\frac{1}{z}}}{L_t} - \frac{L_t}{L_t}\right) - \alpha\frac{1}{q} \end{array}\right) \\ +a\frac{1}{q} - mtaW_{\frac{1}{q},u_0+t} \end{array}\right]\left(1+\frac{W_{\frac{1}{q},u_0+t}}{1-W_{\frac{1}{q},u_0+t}}\right) \tag{2.4}$$

From the work of [12], we have

$$\begin{cases} \frac{1}{q} \to 0, W_{\frac{1}{q},u_0+t} = A(u_0+t)dt, \frac{W_{\frac{1}{q},u_0+t}}{1-W_{\frac{1}{q},u_0+t}} = A(u_0+t)dt, a\frac{1}{q} \to adt, \\ \alpha\frac{1}{q} \to \alpha dt, \frac{K_{t+\frac{1}{q}}}{K} - \frac{K_t}{K_t} \to \frac{dK_t(t)}{K_t(t)}, \frac{L_{t+\frac{1}{q}}}{L_t} - \frac{L_t}{L_t} \to \frac{dL_t(t)}{L_t(t)} \end{cases} \tag{2.5}$$

Substituting (2.5) into (2.4) we have

$$dV(t) = \begin{bmatrix} V(t)\left(I(t)\frac{dL_t(t)}{L_t(t)} + \left(1 - I(t)\right)\frac{dK_t(t)}{K_t(t)} - \alpha dt\right) \\ +a(1 - mtA(u_0 + t)dt \end{bmatrix}(1 + A(u_0 + t)dt) \qquad (2.6)$$

where $A(t)$ is given as the De Moivre force function and u is the maximal age of the life table. According to [25], $A(t)$ and u are related thus

$$A(t) = \frac{1}{u-t} \;\; 0 \leq t < u$$

This implies that

$$A(u_0 + t) = \frac{1}{u-u_0-t} \qquad (2.7)$$

Substituting (2.1), (2.2) and (2.7) into (2.6), we have

$$dV(t) = \begin{bmatrix} \left\{ V(t)\begin{pmatrix} I(t)(\mu - r) + (r - \alpha) \\ +\frac{1}{u-u_0-t} \\ +\left(\frac{u-u_0-(1+m)t}{u-u_0-t}\right)a \end{pmatrix} \right\} dt + V(t)I(t)\sigma dN_t \\ V(0) = v_0 \end{bmatrix} \qquad (2.8)$$

2.1 The Value Function and HJB Equation

Let $I(t)$ be the optimal investment strategy and we define the utility attained by the investor from a given state v at time t as

$$M_{I(t)}(t, v) = E_{I(t)}\left[U\big(V(T)\big) \mid V(t) = v \right], \qquad (2.9)$$

where t is the time and v is the wealth. The objective here is to determine the optimal investment strategy and the optimal value function of the investor given as

$$I(t)^* \text{and } M(t, v) = \sup_{I(t)} M_{I(t)}(t, v) \qquad (2.10)$$

Respectively such that

$$M_{I(t)^*}(t, v) = M(t, v). \qquad (2.11)$$

Applying the Ito's lemma and maximum principle, the Hamilton Jacobi Bellman (HJB) equation which is a nonlinear PDE associated with (2.8) is obtained by maximizing $M_{I^*}(t, v)$ subject to the insurer's wealth as follows

$$\begin{pmatrix} M_t + \left(v\left(r-\alpha+\frac{1}{u-u_0-t}\right)+\left(\frac{u-u_0-(1+m)t}{u-u_0-t}\right)a\right)M_v \\ +\sup_{I(t)}\left\{I(t)(\mu-r)M_v+\frac{1}{2}v^2I^2\sigma^2M_{vv}\right\} \end{pmatrix} = 0 \tag{2.12}$$

Differentiating (2.12) with respect to $I(t)$, we obtain the first order maximizing condition for equation (2.12) as

$$I(t)^* = -\frac{(\mu-r)}{v\sigma^2}\frac{M_v}{M_{vv}} \tag{2.13}$$

Substituting (2.13) into (2.12), we have

$$\begin{Bmatrix} M_t + \left(v\left(r-\alpha+\frac{1}{u-u_0-t}\right)+\left(\frac{u-u_0-(1+m)t}{u-u_0-t}\right)a\right)M_v \\ -\frac{1}{2}\frac{(\mu-r)^2}{\sigma^2}\frac{M_v^2}{M_{vv}} \end{Bmatrix} = 0 \tag{2.14}$$

2.2 Legendre Transformation and Dual theory

The differential equation in (2.14) is a nonlinear partial differential equation and is difficult to solve with direct method. In this section, we introduce the Legendre transformation and dual theory it to transform the nonlinear partial differential equation to a linear partial differential equation.

Theorem 2.1: Let $g: \mathcal{R}^n \to \mathcal{R}$ be a convex function for $z > 0$, define the Legendre transform

$$G(z) = \max_v\{g(v) - zv\}, \tag{2.15}$$

where $G(z)$ is the Legendre dual of $g(v)$.

Since $g(v)$ is convex, from theorem 2.1 and [26-27], the Legendre transform for the value function $M(t,v)$ can be defined as follows

$$\widehat{M}(t,z) = \sup\{M(t,v) - zv \mid 0 < v < \infty\}\ 0 < t < T \tag{2.16}$$

where $\widehat{M}$ is the dual of M and $z > 0$ is the dual variable of v.

The value of v where this optimum is achieved is represented by $g(t,z)$, such that

$$g(t,z) = \inf\{v \mid M \geq zv + \widehat{M}(t,z)\}\ 0 < t < T. \tag{2.17}$$

From (2.17), the function g and $\widehat{M}$ are very much related and can be refers to as the dual of M and are related thus

$$\widehat{M}(t,z) = M(t,g) - zg. \tag{2.18}$$

where

$$g(t,z) = v, M_v = z,\ g_{\cdot} = -\widehat{M}_{z.} \tag{2.19}$$

Differentiating (2.18) with respect to $t, and v$

$$\left\{M_t = \widehat{M}_t,\ \ M_v = z, M_{vv} = \frac{-1}{\widehat{M}_{zz}}\right. \tag{2.20}$$

At terminal time T, we define the dual utility in terms of the original utility function $U(v)$ as

$$\widehat{U}(z) = sup\{\, U(v) - zv \mid 0 < v < \infty\},$$

and

$$G(z) = sup\,\{v \mid U(x) \geq zv + \widehat{U}(z).$$

As a result $\widehat{M}(t,z) = M(t,g) - zg.$

$$G(z) = (U^{'})^{-1}(z), \tag{2.21}$$

Where G is the inverse of the marginal utility U and note that $M(T,v) = U(v)$

At terminal time T, we can define

$$g(T,z) = \underset{v>0}{inf}\left\{\, v \mid U(v) \geq zv + \widehat{M}(t,z)\,\right\} and\ \widehat{M}(t,z) = \underset{v>0}{sup}\{\, U(v) - zv\}$$

so that

$$g(T,z) = (U^{'})^{-1}(z). \tag{2.22}$$

Substituting (2.20) into (2.13) and (2.14), we have

$$\left\{\widehat{M}_t + \left[\begin{matrix} g\left(r - \alpha + \frac{1}{u-u_0-t}\right) \\ +\left(\frac{u-u_0-(1+m)t}{u-u-t}\right)a \end{matrix}\right] z - \frac{1}{2}\left(\frac{(\mu-r)^2}{\sigma^2}\right) z^2 \widehat{M}_{zz}\right\} = 0 \tag{2.23}$$

$$I(t)^* = -\left[\frac{(\mu-r) z \widehat{M}_{zz}}{v\sigma^2}\right] \tag{2.24}$$

From equation (2.19), differentiating (2.23) and (2.24) with respect to z, we have

$$\left\{\begin{matrix} g_t - \left[\begin{matrix} g\left(r - \alpha + \frac{1}{u-u_0-t}\right) \\ +\left(\frac{u-u_0-(1+m)t}{u-u-t}\right)a \end{matrix}\right] - z g_z \left(r - \alpha + \frac{1}{u-u_0-t}\right) \\ +z g_z \frac{(\mu-r)^2}{\sigma^2} + \frac{1}{2}\left(\frac{(\mu-r)^2}{\sigma^2}\right) z^2 g_{zz} \end{matrix}\right\} = 0 \tag{2.25}$$

$$I(t)^* = -\left[\frac{(\mu-r)}{v\sigma^2} z g_z\right] \tag{2.26}$$

where, $M(T,z) = U(z)$ and $U(z)$ is the marginal utility of the investor. Next, we proceed to solve (2.25) for g considering an investor with quadratic utility, then substitute the solution into (2.26) for the OIS using change of variable approach.

3 Analysis of the model

3.1 Investor's OIS under Quadratic Utility Function

In this section, we follow the work of [2] and define the quadratic utility function as follows

$$U(v) = (v-c)^2, \tag{3.1}$$

where v is the investor's wealth and c is a constant coefficient.

Our interest is to solve (2.25) for g considering a pension fund manager with quadratic utility, then substitute the solution into (2.26) for the OIS using change of variable approach.

From (2.22) and (3.1), the boundary condition is given as

$$g(T,z) = \frac{1}{2}z + c \tag{3.2}$$

Lemma 3.1: The optimal investment plan for a DC plan with refund clause under quadratic utility is by

$$I(t)^* = \frac{c(\mu-r)}{\sigma^2}\left[1 - \frac{1}{v}\left[\left[\frac{u-u_0-T}{u-u_0-t}\right] EXP[(r-\alpha)(t-T)]\right]\right]$$

Proof

Next, we formulate a solution to (2.25) similar to [21] as follows:

$$\begin{cases} g(t,z) = zd(t) + e(t) \\ d(T) = \frac{1}{2},\ e(T) = c, \end{cases} \tag{3.3}$$

Differentiating (3.3), we have

$$\{g_t = zd_t + e_t,\ g_z = d,\quad g_{zz} = 0 \tag{3.4}$$

Substituting (3.4) into (2.25), we have

$$\left\{\begin{array}{c} \left[e_t - \left(r - \alpha + \frac{1}{u-u_0-t}\right)e\right] \\ +z\left[d_t - 2\left(r-\alpha+\frac{1}{u-u_0-t}\right)d + \frac{(\mu-r)^2}{\sigma^2}d - \left(\frac{u-u_0-(1+m)t}{u-u_0-t}\right)ad\right] \end{array}\right\} = 0 \tag{3.5}$$

Splitting (3.5), we have

$$\begin{cases} e_t - \left(r - \alpha + \frac{1}{u-u_0-t}\right)e = 0 \\ e(T) = c \end{cases} \tag{3.6}$$

$$\begin{cases} d_t - \left[2\left(r-\alpha+\frac{1}{u-u-t}\right) - \frac{(\mu-r)^2}{\sigma^2} - \left(\frac{u-u_0-(1+m)t}{u-u_0-t}\right)a\right]d = 0 \\ d(T) = \frac{1}{2} \end{cases} \tag{3.7}$$

Solving equation (4.6) and (4.7), we obtain

$$d(t) = \frac{1}{2}\left[\frac{u-u_0-T}{u-u_0-t}\right]^{\left(2+a(1+m)(u-u_0)\right)} EXP\left[\left[2(r-\alpha) - \frac{(\mu-r)^2}{\sigma^2} + (m-1)a\right](t-T)\right] \tag{3.8}$$

$$g(t) = c\left[\left[\left[\frac{u-u_0-T}{u-u_0-t}\right]\right] EXP[(r-\alpha)(t-T)]\right] \tag{3.9}$$

Substituting (3.7) and (3.8) into (3.3) and (3.4), we obtain

$$g(t,z) = \left[\begin{array}{c} z\frac{1}{2}\left[\frac{u-u_0-T}{u-u_0-t}\right]^{\left(2+a(1+m)(u-u_0)\right)} EXP\left[\left[\begin{array}{c} 2(r-\alpha) \\ -\frac{(\mu-r)^2}{\sigma^2} + (m-1)a \end{array}\right](t-T)\right] \\ +c\left[\left[\frac{u-u_0-T}{u-u_0-t}\right] EXP[(r-\alpha)(t-T)]\right] \end{array}\right] \tag{3.10}$$

$$g_z = \frac{1}{2}\left[\frac{u-u_0-T}{u-u_0-t}\right]^{\left(2+a(1+m)(u-u_0)\right)} EXP\left[\left[\begin{array}{c} 2(r-\alpha) \\ -\frac{(\mu-r)^2}{\sigma^2} + (m-1)a \end{array}\right](t-T)\right] \tag{3.11}$$

Simplify (4.10) for z, we have

$$z = \left[\begin{array}{c} 2\left[g - c\left[\left[\frac{u-u_0-T}{u-u_0-t}\right] EXP[(r-\alpha)(t-T)]\right]\right]\left[\frac{u-u_0-T}{u-u_0-t}\right]^{\left(2+a(1+m)(u-u_0)\right)} \\ \times EXP\left[\left[2(r-\alpha) - \frac{(\mu-r)^2}{\sigma^2} + (m-1)a\right](T-t)\right] \end{array}\right] \tag{3.12}$$

$$g = v$$

Substituting (3.10), (3.11) and (3.12) into (2.26), we have

$$I(t)^* = \frac{c(\mu-r)}{\sigma^2}\left[1 - \frac{1}{v}\left[\left[\frac{u-u_0-T}{u-u_0-t}\right] EXP[(r-\alpha)(t-T)]\right]\right], \tag{3.13}$$

which completes the proof

4 Numerical simulations/sensitivity analysis

In this section, some numerical simulations showing the relationship between the OIS and some sensitive parameters are presented and we will discuss the effect of the parameters on OIS as it affects the PFAs behaviour toward investment under quadratic utility function using (4.13). To achieve this, the following data are used similar to [12,24] unless otherwise stated: $\mu = 0.5, c = 0.01, r = 0.3, , v = 1, \alpha = 0.1, \sigma = 0.1, \ , u = 100, u_0 = 20, T = 20$.

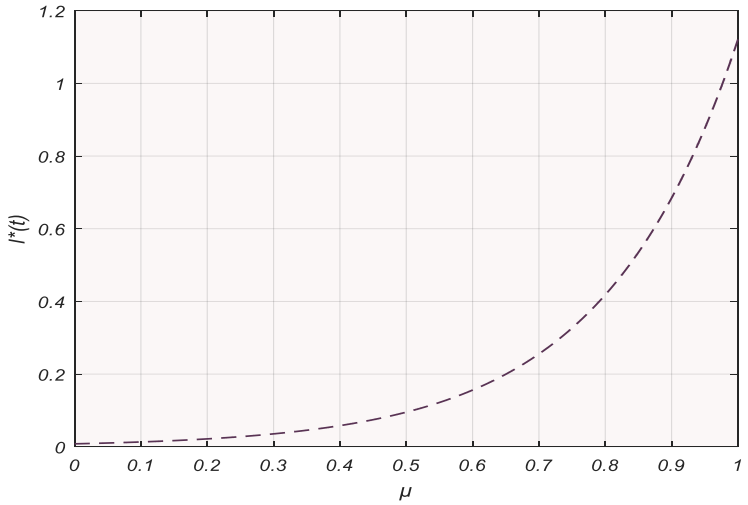


Fig. 1: OIS with appreciation rate of the risky asset

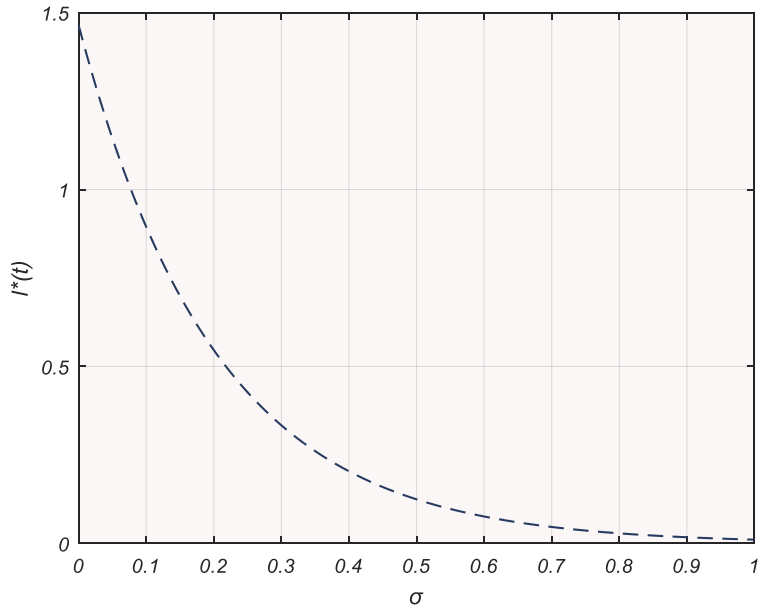


Fig. 2: OIS with instantaneous volatility of the risky asset

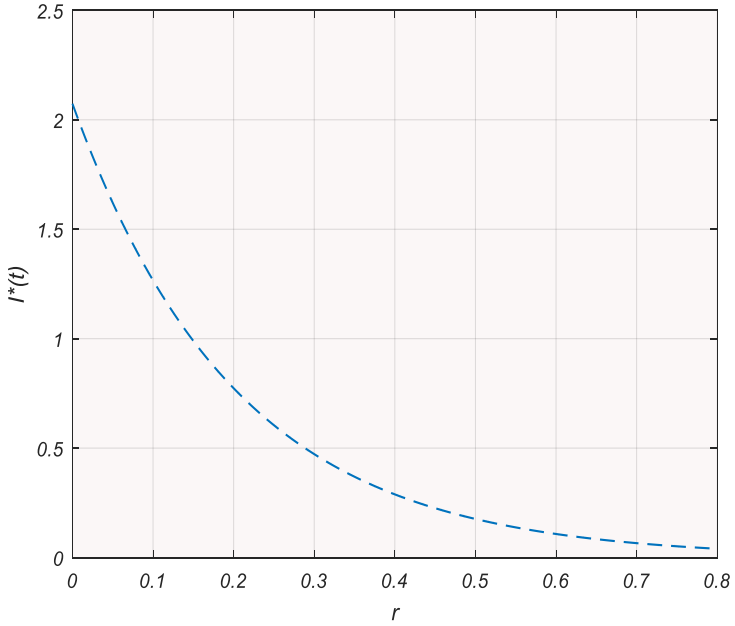


Fig. 3 OIS with predetermined interest rate

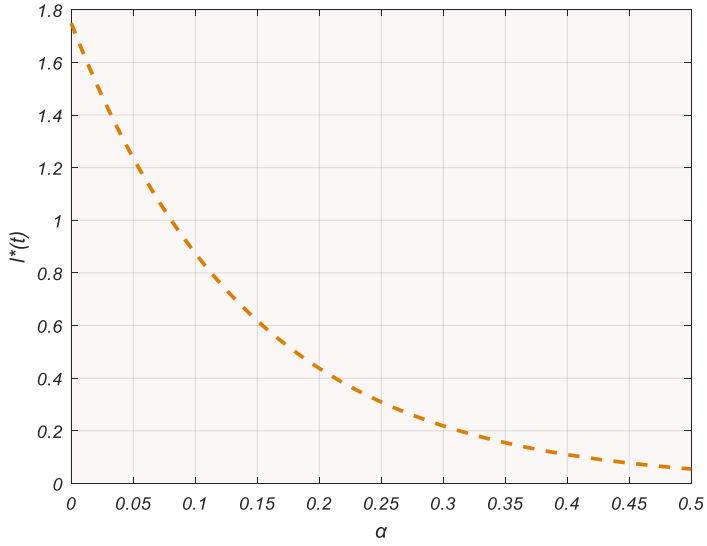


Fig. 4 OIS with charge on balance

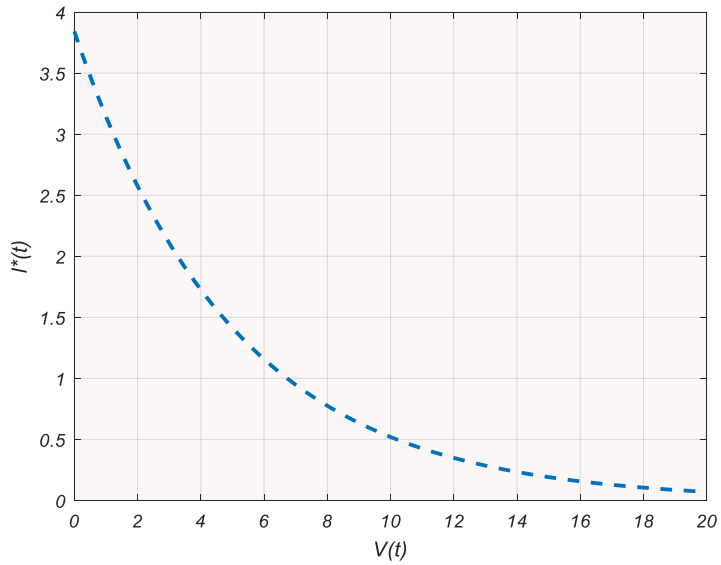


Fig. 5 OIS with wealth of the investor

5 Discussions and conclusion

In fig. 1, the graph of the optimal portfolio distribution against the appreciation rate of the risky asset is presented; the graph shows that the optimal portfolio distribution is an increasing function of the appreciation rate of the risky asset. The implication of the graph is that any asset with higher appreciation rate will naturally be appealing and attractive to an investor; hence the investor may be willing to commit more of his resources into such asset with the expectation of more returns and vice versa.

In fig. 2, the graph of optimal portfolio distribution against the instantaneous volatility is presented; the graph shows that the optimal portfolio distribution is inversely proportional to the instantaneous volatility of the risky asset. This implies that the higher the instantaneous volatility of the risky asset, the higher the risk involved in the investment in such asset. Hence this may create more fears in the mind of the investor toward investing in the risky asset, furthermore reduce the proportion of the investor's wealth in risky asset.

In fig. 3, the graph of the optimal portfolio distribution with the predetermined interest rate is presented; the graph shows that the optimal portfolio distribution is a decreasing function of the predetermined interest rate. The implication of the graph is that a member with large funds prefers to invest where there is lesser risk since they may not want to lose what they have gathered already.

In Fig. 4, the graph of optimal portfolio distribution for the risky asset with tax on invested fund size is presented; the graph shows that, optimal portfolio distribution for the risky asset decreases with increase on tax on the invested fund. The implication of this graph is that members may be discouraged from investment on highly taxed investment and vice versa.

In fig. 5, the graph of optimal portfolio distribution for the risky asset with the investor's wealth is presented. We observed that the optimal portfolio distribution is a decreasing function of the wealth function. This implies that an investor will invest more in the risky assets if their wealth is small and vice versa.

In conclusion, this research work investigated the study of OIS with return of premium clause under quadratic utility function and its application to portfolio optimization and risk management. Also, a portfolio made of a risk free asset and a risky asset which follows the GBM was considered. We took into consideration charge on balance by the PFA. We used the Ito's lemma to obtain an optimization problem in the form of Hamilton Jacobi Bellman equation and investment strategy. These problems are functions of the value function which is dependent on the utility of the investor at the expiration of such investment. Also, the Legendre transformation method and quadratic utility function were used in solving for the OIS. Furthermore, some numerical simulations were also presented to study the effect of some sensitive parameters on the OIS and were observed that OIS under quadratic utility function is an increasing function of appreciation rate of the risky asset, and a decreasing function of charge on balance, instantaneous volatility, member's wealth and predetermined interest rate.

References

[1] Gao, J. (2008). Stochastic optimal control of DC pension funds, Insurance Math. Econom. 42 (3) 1159–1164.

[2] Li, D. Rong, X. and Zhao, H. (2013). Optimal investment problem with taxes, dividends and transaction costs under the constant elasticity of variance model. Transaction on Mathematics, 12(3), 243-255.

[3] Egbe, G. A. Awogbemi, C. A. and Osu, B. O. (2013). Portfolio optimization of pension fund contribution in Nigeria. Mathematical theory and modelling, 3(8), 42-52.

[4] Zhang C and Rong X. Optimal investment strategies for DC pension with astochastic salary under affine interest rate model. Hindawi Publishing Corporation; 2013. Available:http://dx.doi.org/10.1155/2013/297875

[5] Njoku, K.N. C, Osu, B. O., Akpanibah, E. E. and Ujumadu, R. N. (2017). Effect of Extra Contribution on Stochastic Optimal Investment Strategies for DC Pension with Stochastic Salary under the Affine Interest Rate Model. Journal of Mathematical Finance, 7, 821-833.

[6] Akpanibah, E. E. and Samaila**,** S. K. (2017). Stochastic strategies for optimal investment in a defined contribution (DC) pension fund. International Journal of Applied Science and Mathematical Theory, 3(3) 48-55.

[7] Osu, B. O., Akpanibah, E. E. and Njoku, K.N.C. (2017). On the Effect of Stochastic Extra Contribution on Optimal Investment Strategies for Stochastic Salary under the Affine Interest Rate Model in a DC Pension Fund, General Letters in Mathematics, 2(3), 138-149.

[8] Njoku, K. N. C. and Osu, B. O., (2019). On the Modified Optimal Investment Strategy for Annuity Contracts under the Constant elasticity of Variance (CEV) model. *Earthline Journal of Mathematical Sciences*, 1. 169:90.

[9] Njoku, K. N. C., Osu, B. O and Philip, U. U, (2019). On the Investment Approach in a DC Pension Scheme for Default Fund Phase IV under the Constant Elasticity of Variance (CEV) model, *International Journal of Advances in Mathematics*, 2018, 3. 65-76.

[10] Gao J., (2008) Stochastic optimal control of DC pension plan under a CEV model" Insurance: Mathematics and Economics 44, 479-490.
[11] Antolin, P., Payet, S. and Yermo, J. (2010). Accessing default investment strategies in DC pension plan. Financial Market Trends*,* 2010 (1).
[12] He L. and Liang. Z. (2013). The optimal investment strategy for the DC plan with the return of premiums clauses in a mean-variance framework, *Insurance*, **53**, 643-649.
[13] Sheng, D. and Rong, X. (2014). Optimal time consistent investment strategy for a DC pension with the return of premiums clauses and annuity contracts, Hindawi Publishing Corporation vol**2014**http://dx.doi.org/10.1155/2014/862694. 1-13.
[14] Li, D. Rong, X. Zhao, H. and Yi, B. (2017). Equilibrium investment strategy for DC pension plan with default risk and return of premiums clauses under CEV model, *Insurance*:**72,** 6-20.
[15] Chai, Z.P., Rong, X.M. and Zhao, H. (2017). Optimal investment strategy for the DC plan with return of premium. System Engineering- Theory & Practice 37, 1688–1696, (2017).
[16] Wang, Y. Fan, S and Chang, H. (2018). DC Pension Plan with the Return of Premium Clauses under Inflation Risk and Volatility Risk, J. Sys. Sci. & Math. Scis., 38(4), 423-437.
[17] Osu B. O., Akpanibah E. E and Olunkwa O (2018). Mean-Variance Optimization of portfolios with return of premium clauses in a DC pension plan with multiple contributors under constant elasticity of variance model, International journal of mathematical and computational sciences pure and applied researches, 12(5):85-90.
[18] Azor P. A., Avievie I and Esabai M. A. (2023). Explicit solution of an investment plan for a DC pension scheme with voluntary contributions and return clause under logarithm utility. International journal of physical and Mathematical sciences, 17(8), 115-121.
[19] Akpanibah, E. E., Osu, B. O. Oruh, B. I. and Obi, C. N. (2019). Strategic optimal portfolio management for a DC pension scheme with return of premium clauses. *Transaction of the Nigerian association of mathematical physics*, 8(1): 121-130.
[20] Akpanibah E. E. and Osu B. O. (2018). Optimal Portfolio Selection for a Defined Contribution Pension Fund with Return Clauses of Premium with Predetermined Interest Rate under Mean variance Utility. *Asian Journal of Mathematical Sciences.* **2**(2), 19 –29.
[21] Akpanibah, E. E., Osu, B. O. and Ihedioha, S. A. (2020). On the optimal asset allocation strategy for a defined contribution pension system with refund clause of premium with predetermined interest under Heston's volatility model. *J. Nonlinear Sci. A ppl.* **13**(1),:53–64.
[22] Lai C., Liu, S. and Wu, Y. (2021). Optimal portfolio selection for a defined contribution plan under two administrative fees and return of premium clauses. Journal of Computational and Applied Mathematics 398, 1-20.
[23] Njoku K.N. C and Akpanibah, E. E. Modelling and optimization of portfolio in a dc scheme with return of contributions and tax using weibull force function. Asian Journal of Probability and Statistics 16(3): 1-12, 2022.
[24] Chávez-Bedoya, L. (2016). Determining equivalent charges on flow and balance in individual account pension systems, J. Econ. Finance Adm. Sci. 21 (40), 2–7.
[25] Kohler, P.-H. and Kohler, I., (2000). Frailty modeling for adult and old age mortality: the application of a modified De Moivre Hazard function to sex differentials in mortality. Demographic Research 3(8).
[26] Jonsson M. and Sircar, R. (2002). Optimal investment problems and volatility homogenization approximations", Modern Methods in Scientific Computing and Applications 75 255.
[27] Xiao, J. Hong, Z. and Qin, C. (2007). The constant elasticity of variance(CEV) model and the Legendre transform-dual solution for annuity contracts, Insurance, 40(2), 302–31.

Stability analysis of an HIV/AIDS model with saturated incidence

O.A. Odebiyi*† and J.K. Oladejo‡

Abstract

Human Immunodeficiency Virus – Acquired Immune Deficiency Syndrome HIV/AIDS stands as one of the most prevalent sexually transmitted disease globally and is regarded as one of the deadliest epidemic in human history. This study presents a mathematical model for understanding the dynamics of HIV/AIDS transmission, incorporating a saturated incidence rate. The model employs a system of ordinary differential equations, comprising various group of individuals including susceptible $S(t)$, asymptomatic infective $I_1(t)$, symptomatic infective $I_2(t)$, treated $T(t)$ and AIDS $A(t)$ class. The validity of the solution states affirms that the model is well-defined and holds epidemiological significance. The disease-free and endemic equilibrium states are identified, and their stability is analyzed using Routh Hurwitz criteria and Descartes rule of signs. Sensitivity analysis was carried out using normalized forward sensitivity index and result showed that the contact rate β_1 is the most sensitive parameter. Existence of backward bifurcation analysis is equally carried out. More so, it is observed from the numerical simulation that screening and treatment of the infective play a significant role in reducing the transmission of the disease. The outcome of the stability analysis for both disease-free and endemics equilibrium states indicates the potential for HIV/AIDS control.

Keywords and phrases: basic reproduction number; bifurcation analysis; saturated incidence; stability, sensitivity analysis;

1 Introduction

HIV/AIDS is seen as a chronic disease nowadays, because HIV-positive people can live with infection for many years provided their immune systems are checked. It gradually destroys the immune system until it is unable to fight infections that would normally have been prevented. With deterioration of the immune system, the body develops opportunistic diseases that lead to AIDS [1].

*Corresponding Author; E-mail: oaodebiyi@lautech.edu.ng
†Department of Pure and Applied Mathematics Sciences, Ladoke Akintola University of Technology, PMB 4000, Ogomoso, Oyo State, Nigeria.
‡Department of Pure and Applied Mathematics Sciences, Ladoke Akintola University of Technology, PMB 4000, Ogomoso, Oyo State, Nigeria.. E-mail: jkoladejo@lautech.edu.ng

As the immune system becomes compromised, the HIV opportunistic diseases such as meningitis, Cancers and Tuberculosis do easily attack the body [2].

In 2022, approximately 39million people died from AIDS worldwide, about 740 children became infected with HIV and approximately 274 children died from AIDS related causes every day [3]. More so, in the countries hardest hit, AIDS has sapped the population of young men and women who form the foundation of the labor force. Most die while in the peak of their reproductive years. Moreover, the epidemic has overwhelmed health care systems, increases the number of orphans, and caused life expectancy rates to plummet. It therefore constitutes a serious threat to future development in Africa.

At the end of 2022, approximately 39.0 million (33.1million-45.7million) people were living with HIV globally. 1.3million [1million-1.7million] people became newly infected with HIV while 630000 [480000-880000] people died from AIDS-related illnesses. 1.5 million (1.2-2.1million) children were living with HIV (0-14 years old) [4]. More so, according to HIV/AIDS prevalence estimates between 2023-2024, African countries with HIV/AIDS adult prevalence rates among adults in various countries according to CIA world fact book are Eswatini with 28.30%, Lesotho 24.10%, Botswana 22.60% and Zimbabwe 22.10% and outside Africa, Bahamas has the highest prevalence rate [5].

Transmission of HIV/AIDS causing virus occurs most commonly through sexual intercourse. HIV can also be transmitted through transfusions of HIV-contaminated blood or by using a contaminated needle or syringe to inject drugs into the blood stream. Infection with HIV does not necessarily mean that a person has AIDS. Some people who have HIV infection may not develop any of the clinical illnesses that define the full-blown disease of AIDS for ten years or more. Physicians prefer to use the term AIDS for cases where a person has reached the final, life-threatening stage of HIV infection [6]. In a person infected with HIV, the virus steadily destroys $CD4^{+}T$ cells over a period of years, diminishing the cells protective ability and weakening the immune system. HIV infects some other cells and wrecks the largest part of the $CD4^{+}T$ cells and this causes the $CD4^{+}T$ cells destruction and decline, hence reducing the confrontation of the susceptible system [7, 8].

Screening is the process of performing the HIV-antibody test to all individuals within a defined population. Routine screening of unaware infective has now become an integral part of programs in low and middle income countries. People can get HIV tests done at a health clinic, at special HIV voluntary counseling and testing (VCT) sites [9]. Antiretroviral medication has made it possible for many individuals who have been very sick with HIV/AIDS to become fully functioning again, with a low or even undetectable viral load. Without antiretroviral therapy, someone who has AIDS typically dies within a year [10]. Transmission of the disease and influence of the infection can be curbed by taking adequate treatment and administering suitable vaccine to infected class [11-14].

In the context of mathematical modeling of HIV/AIDS dynamics, Saturation incidence refers to a situation where the rate of new infections reaches a plateau, indicating that the epidemic has stable and under control and therefore no longer growing exponentially. This simply means that the number of new infections is roughly balanced by the number of individuals recovering or dying from the infection.

Various mathematical models were formulated for developing strategies to control the outbreak of disease and thereby making a trade-offs in choosing a best possible treatment for curbing and controlling the infection. Ross Ronald derived a threshold quantity called basic reproduction number. This helps the planners such as medical and health practitioners to determine and conclude when infection will fade out in a system. Incidence rate play a vital and significance role in discussing nature of a disease in epidemiology. In early, bilinear incidence rate in the form βxy and standard incidence rate in the form $\frac{\beta xy}{N}$ are usually used in epidemic model where β is the transmission of the disease per contact. x and y are the number of susceptible population and infected population respectively. N is the total number of population [15]. Many authors studied nonlinear types of incidence rate. Few among them are [15-18, 20]. [20] introduced saturated types of infection rate in the form $\frac{\beta xy}{(1+\alpha y)}$ where βy denotes force of infection and $\frac{\beta xy}{(1+\alpha y)}$ measures inhibition factors due to crowding effect of infected class and also an appropriate social awareness given by the population. α is the coefficient of inhibition. Later, a non-monotone type of infection rate in the form $\frac{\beta xy}{(1+\alpha y^2)}$ was also introduced to include the population psychological [11, 20]. [21] also introduced Saturated incidence rate $\frac{\beta SI}{(1+\alpha I)}$, tends to a saturation level when it gets large, where βI measures the infection force when the disease is entering a fully susceptible population and $\frac{1}{(1+\alpha I)}$ measures the inhibition effect from the behavioral change of susceptible. The saturated incidence rate of the form $\frac{1}{(1+\alpha_1 S)}$ where α_1 is a positive constant. Here, the effect of saturation factor α_1 stems from epidemic control taking appropriate percussive measures. The function forms for disease incidence with the susceptible population in the denominator of the saturating function is simply to know when the population become saturated and affected with the virus. The saturated incidence function of the form $\frac{1}{(1+\alpha_2 I)}$, where α_2 is a positive constant. Here, the number of effective contacts between infective individuals or due to the protective measures by the susceptible individuals.

From an epidemiological standpoint, saturation incidence suggests that the epidemic has reached a steady state, with the disease prevalence remaining relatively constant over time. This could simply be due to various factors such as behavioral changes, implementation of prevention strategies, availability of treatment, or natural progression of the epidemic within a population. Understanding saturation incidence therefore helps public health officials and policy makers assess the effectiveness of interventions and plan future strategies for controlling the spread of the menace.

Researchers such as [19, 22-23] among others have worked on the transmission and prevention of HIV/AIDS incorporating various stages of HIV infection and AIDS, screening and treatment of HIV/AIDS, vaccination and saturated incidence rate. Although no cure has been found for AIDS

[14], new drugs are available that can prolong the life span and improve the quality of life of infected people [12, 22,38].

2 Model formulation

In this research, the susceptible and infectious epidemic model (SI) is considered as presented by [19, 24]. A population size of $N(t)$ was partitioned into 5 subclasses of individuals which are; susceptible, asymptomatic infective, symptomatic infective, treated infective, and AIDS with sizes denoted by $S(t), I_1(t), I_2(t), T(t),$ and $A(t)$, respectively such that $N = S + I_1 + I_2 + T + A,$ as shown in figure 1.

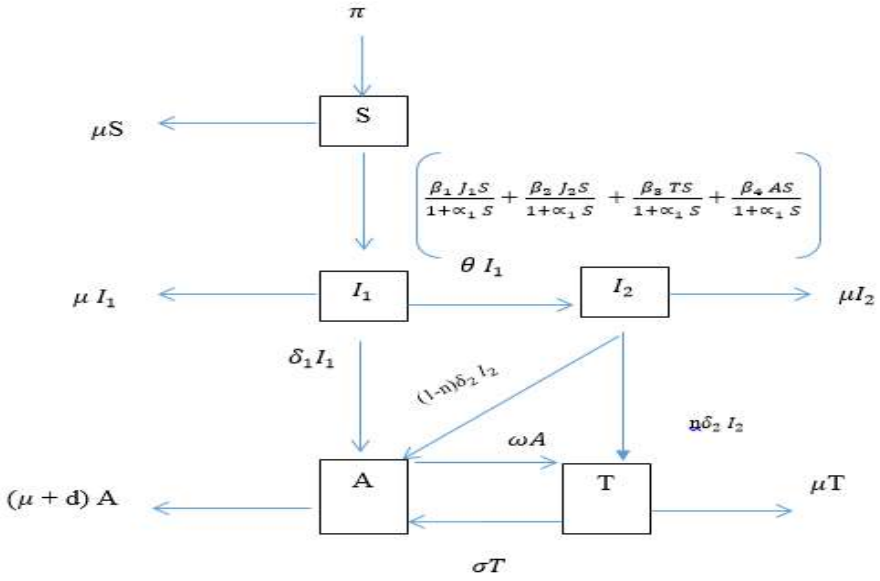


Figure 1: Transmission diagram for susceptible, infected model with the saturation term to the susceptible $(1+\alpha_1 S)$

Following the transmission diagram, in Figure 1, which incorporates the saturation term to the susceptible, asymptomatic infective, symptomatic infective, treated infective and AIDS individual. The following assumptions are taken into consideration in formulating our proposed model:

People are recruited into the Susceptible population by birth . All parameters are positive. Asymptomatic infective class (I_1) can move to symptomatic class (I_2) and full blown AIDS and asymptomatic infective population can be screened at a rate θ and progress to symptomatic class. Asymptomatic infective, Symptomatic infective, Treated class (T) and full blown AIDS can infect Susceptible class at different rates $\beta_1, \beta_2, \beta_3$ and β_4 respectively. Asymptomatic infective, Symptomatic infective, Treated class (T) will move to full blown AIDS at different rates $\delta_1, \delta_2,$ and σ respectively . Infective can be treated with ARV therapy (i.e can move to treated class) at rate ω . Considering all the assumptions made, the following system of ordinary differential equations of the proposed model is therefore considered.:

$$\left.\begin{aligned}
\frac{dS}{dt} &= \pi - \frac{\beta_1 I_1 S}{(1+\alpha_1 S)} - \frac{\beta_2 I_2 S}{(1+\alpha_1 S)} - \frac{\beta_3 TS}{(1+\alpha_1 S)} - \frac{\beta_4 AS}{(1+\alpha_1 S)} - \mu S \\
\frac{dI_1}{dt} &= \frac{\beta_1 I_1 S}{(1+\alpha_1 S)} + \frac{\beta_2 I_2 S}{(1+\alpha_1 S)} + \frac{\beta_3 TS}{(1+\alpha_1 S)} + \frac{\beta_4 AS}{(1+\alpha_1 S)} - (\theta + \mu + \delta_1) I_1 \\
\frac{dI_2}{dt} &= \theta I_1 - (\mu + \delta_2) I_2 \\
\frac{dT}{dt} &= n\delta_2 I_2 - (\sigma + \mu) T + \omega A \\
\frac{dA}{dt} &= (1-n)\delta_2 I_2 + \delta_1 I_1 - (\mu + d + \omega) A + \sigma T
\end{aligned}\right\} \quad (1)$$

As initial condition, we choose

$$S(0) = S_0, I_1(0) = I_{1_0}, I_2(0) = I_{2_0}, T(0) = T_0, A(0) = A_0$$

The model parameters are defined as follows

$\pi > 0$ is the constant number of recruitment of susceptible, $\beta_1, \beta_2, \beta_3, \beta_4$ are the transmission rates for susceptible individuals with asymptomatic infective, susceptible individuals with symptomatic infective, susceptible individuals with treated infective, and susceptible individuals with AIDS respectively, α is the Saturation term to the susceptible individual. μ is the natural mortality rate unrelated to AIDS, σ is rate at which treated individual develops to full blown AIDS, ω is the rate at which AIDS patients get treatment, δ_1 is rate of movement from asymptomatic class I_1 (t) to full blown AIDS A (t). δ_2 is rate of movement from symptomatic class I_2 (t) to treated and AIDS class respectively, n is the fraction of symptomatic infective that moved to treated class, d is the AIDS related death rate/Disease related death rate and θ is the screening rate.

2.1 Positivity and Boundedness of Solutions of the Model

We can show from model (1) that the state variables are non-negative and the solutions remain positive for all time $t \geq 0$. Here, the parameters in the model are assumed to be positive. We equally show that the feasible solutions are bounded in a region $\Omega: \Omega = \left\{ (S, I_1, I_2, T, A) \in \Omega_+^5 : N(t) \leq \frac{\pi}{\mu} \right\}$ at any time corresponding to the system (1)

Theorem 2.1: Let the initial values of the state variables be such that

$$\left\{ (S(0) \geq 0, I_1(0) \geq 0, I_2(0) \geq 0, T(0) \geq 0, A(0) \geq 0) \in \Omega_+^5 \right\}$$

then, the set $\{S(t), I_1(t), I_2(t), T(t), A(t), \quad and \quad N(t)\}$ is non-negative in Ω for all time $t \geq 0$.

Proof: Considering the first equation of system (1) are considered for the positivity of the state variables as follows;

Using the approach of [25, 26], we let

$$\lambda = \frac{\beta_1 I_1 S}{(1+\alpha_1 S)} + \frac{\beta_2 I_2 S}{(1+\alpha_1 S)} + \frac{\beta_3 TS}{(1+\alpha_1 S)} + \frac{\beta_4 AS}{(1+\alpha_1 S)} \tag{2}$$

Then,

$$\frac{dS}{dt} \geq -(\lambda + \mu)S$$

$$\int \frac{1}{S} dS \geq -\int (\lambda + \mu) dt$$

$$S \geq S_0 e^{-(\lambda+\mu)t} \geq 0$$

Hence, $S \geq 0$ (3)

Also considering the second equation in (1)

$$\frac{dI_1}{dt} = \frac{\beta_1 I_1 S}{(1+\alpha_1 S)} + \frac{\beta_2 I_2 S}{(1+\alpha_1 S)} + \frac{\beta_3 TS}{(1+\alpha_1 S)} + \frac{\beta_4 AS}{(1+\alpha_1 S)} - (\theta + \mu + \delta_1) I_1$$

$$\frac{dI_1}{dt} \geq -(\theta + \mu + \delta_1) I_1$$

$$\int \frac{1}{I_1} dI_1 \geq \int -(\theta + \mu + \delta_1) dt$$

$$I_1 \geq I_{1_0} e^{-(\theta+\mu+\delta_1)t} \geq 0$$

Hence, $I_1 \geq I_{1_0}$ (4)

We can proceed in a similar approach to proof the rest of the positivity of solutions of other state variables of I_2, T, A.

Theorem 2.2: Every solution in the region

$\Omega = \left\{(S(t), I_1(t), I_2(t), T(t), A(t) \in \Re_+^5, : S(t) + I_1(t) + I_2(t) + T(t) + A(t) \leq N(t)\right\}$ is positively invariant with respect to the HIV/AIDS model (1) in population. The solutions for the system in (1) are contained and remain in the region Ω for all time $t \geq 0$.

Proof: Considering the equation of the model (1), and taking the derivative with respect to time t of N we obtained

$$\frac{dN(t)}{dt} = \pi - \mu N(t) - dA$$

$$\Rightarrow \frac{dN}{dt} \leq \pi - \mu N(t)$$

$$\Rightarrow N \leq \frac{\pi}{\mu} + \left(N_0 - \frac{\pi}{\mu} \right) e^{-\mu t}$$

where N_0 is the initial size of the population,

$$\text{Therefore, } \lim_{t \to \infty} N(t) \leq \frac{\pi}{\mu} \tag{5}$$

Using this result together with theorem 1 and model (1), we have $0 \leq N(t) \leq \frac{\pi}{\mu}$. This result implies that HIV/AIDS model (1) has non-negative and bounded solutions in the region Ω and all the solutions starting in Ω approach, enter or stay in Ω. Hence, it is sufficient to conclude that the model is epidemiologically well posed.

3 Mathematical Analysis of the Model

3.1 Disease free equilibrium point

This is the equilibrium point at which population remains in the absence of disease. In this case, no strain of the disease is present in the entire population.

At the equilibrium,

$$\frac{dS}{dt} = \frac{dI_1}{dt} = \frac{dI_2}{dt} = \frac{dT}{dt} = \frac{dA}{dt} = 0 \tag{6}$$

Equation (1) becomes

$$\pi - \frac{\beta_1 I_1 S}{(1+\alpha_1 S)} - \frac{\beta_2 I_2 S}{(1+\alpha_1 S)} - \frac{\beta_3 T S}{(1+\alpha_1 S)} - \frac{\beta_4 A S}{(1+\alpha_1 S)} - \mu S = 0 \tag{7}$$

$$\frac{\beta_1 I_1 S}{(1+\alpha_1 S)} + \frac{\beta_2 I_2 S}{(1+\alpha_1 S)} + \frac{\beta_3 T S}{(1+\alpha_1 S)} + \frac{\beta_4 A S}{(1+\alpha_1 S)} - (\theta + \mu + \delta_1) I_1 = 0 \tag{8}$$

$$\theta I_1 - (\mu + \delta_2) I_2 = 0 \tag{9}$$

$$n\delta_2 I_2 - (\sigma + \mu) T + \omega A = 0 \tag{10}$$

$$(1-n)\delta_2 I_2 + \delta_1 I_1 + \sigma T - (\mu + d + \omega) A = 0 \tag{11}$$

At disease free,

$S \neq 0, I_1 = I_2 = T = A = 0$ Substituting these to equations (7), (8), (9), (10) and (11), and solving gives the infection – free equilibrium as:

$$E^0 = \left(S^0, I_1^0, I_2^0, T^0, A^0 \right) = \left(\frac{\pi}{\mu}, 0, 0, 0, 0 \right)$$

3.2 Endemic equilibrium point

The endemic equilibrium state is the state where the disease cannot be totally eradicated but remains in the population. For the endemic equilibrium, $S \neq 0, I_1 \neq 0, I_2 \neq 0, T \neq 0, A \neq 0$

Solving equations (7)-(11) simultaneously when $S \neq 0, I_1 \neq 0, I_2 \neq 0, T \neq 0, A \neq 0$, we have the endemic equilibrium points respectively as;

$$E^* = \left(S^*, I_1^*, I_2^*, T^*, A^*\right) = \left\{ \begin{array}{l} \dfrac{\pi}{R_0 I_1 + \mu} \\ \dfrac{\pi R_0 - \mu K_1}{K_1 R_0}, \\ \dfrac{\theta I_1}{K_2}, \\ \dfrac{\left(\delta_2\theta\left(\eta\left(\mu K_4 + \sigma(\mu + d)\right) + \omega\left((1-n)+\sigma\right)\right) + \omega K_2 K_3 \delta_1\right) I_1}{K_2\left(\mu K_4 + \sigma(\mu + d)\right)}, \\ \dfrac{\left(\delta_2\theta\left((1-n)+\sigma\right) + K_2 K_3 \delta_1\right) I_1}{K_2\left(\mu G_4 + \sigma(\mu + d)\right)} \end{array} \right\} \tag{12}$$

respectively, where,

$K_1 = (\theta + \mu + \delta), K_2 = (\mu + \delta_2), K_3 = (\sigma + \mu), K_4 = (\mu + d + \omega)$

3.3 Derivation of Basic Reproduction Number, R_0

The computation of the basic reproduction number is essential. The basic reproduction number R_0 is defined as the effective number of secondary infections caused by infected individual during his entire period of infectiousness [26]. To determine the next generation matrix for the model, the following are considered:

1. The number of ways that new infections can arise or be created;
2. The number of ways that infections can be transferred between compartments. Thus, the I_1, I_2, T, A compartment of system (1).

Then F_i and V_i are computed as follows using the approach of [21]:

$$F_i = \begin{pmatrix} \dfrac{\beta_1 S I_1}{(1+\alpha_1 S)} + \dfrac{\beta_2 S I_2}{(1+\alpha_1 S)} + \dfrac{\beta_3 S T}{(1+\alpha_1 S)} + \dfrac{\beta_4 S A}{(1+\alpha_1 S)} \\ 0 \\ 0 \\ 0 \end{pmatrix}, \; V_i = \begin{pmatrix} (\theta + \mu + \delta_1) I_1 \\ -\theta I_1 + (\mu + \delta_2) I_2 \\ -n\delta_2 I_2 + (\sigma + \mu) T - \omega A \\ -(1-n)\delta_2 I_2 - \delta_1 I_1 - \sigma T + (\mu + d + \omega) A \end{pmatrix} \tag{13}$$

Let G be the next generation matrix. It comprises of two parts F and V^{-1} where

$$F = \left[\frac{\partial F_i(x_0)}{\partial x_j}\right] = \begin{pmatrix} \dfrac{\beta_1\pi}{(\mu+\alpha_1\pi)} & \dfrac{\beta_2\pi}{(\mu+\alpha_1\pi)} & \dfrac{\beta_3\pi}{(\mu+\alpha_1\pi)} & \dfrac{\beta_4\pi}{(\mu+\alpha_1\pi)} \\ 0 & 0 & 0 & 0 \\ 0 & 0 & 0 & 0 \\ 0 & 0 & 0 & 0 \end{pmatrix} \tag{14}$$

$$V = \left[\frac{\partial V_1(x_0)}{\partial x_j}\right] = \begin{pmatrix} \theta+\mu+\delta_1 & 0 & 0 & 0 \\ -\theta & (\mu+\delta_2) & 0 & 0 \\ 0 & -n\delta_2 & \sigma+\mu & -\omega \\ -\delta_1 & -(1-n)\delta_2 & -\sigma & \mu+d+\omega \end{pmatrix} \quad (15)$$

The basic reproduction number, which is the dominant eigenvalue of the product FV^{-1}, is therefore obtained as:

$$R_0 = \frac{\pi\left(\left(\beta_1 K_2 + \theta\beta_2\right)\left(\mu K_4 + \sigma\left(\mu+d\right)\right) + \beta_3\left(\delta_2\theta\left(\omega + n\left(\mu+d\right)\right) + \omega\delta_1 K_2\right) + \beta_4\left(\delta_2\theta\left(\sigma + \mu\left(1-n\right)\right) + \delta_1 K_2 K_3\right)\right)}{K_1 K_2\left(\mu K_4 + \sigma\left(\mu+d\right)\right)} \quad (16)$$

3.4 Computing Numerical Sensitivity

The [26,37] normalized forward sensitivity index approach which defines a variable "P" that depends on a differentiable parameter "q" is defined as

$$X_q^p := \frac{\partial p}{\partial q} * \frac{q}{p} \quad (17)$$

As we have an explicit formula for R_0 in equation (17), we derive an analytical expression for the sensitivity of R_0, as $X_q^p := \frac{\partial p}{\partial q} * \frac{q}{p}$ with respect to each of the parameters involved in R_0 as follows:

Table 3.1: Numerical values of sensitivity indices of R_0

Parameter	Value
β_1	+ 0.847905341
θ	+ 0.0102753420
μ	- 0.4949636613
ω	+0.0768207412
α_1	--0.7142857144
δ_1	-0.7712241608
σ	-0.0037923097
d	-0.08936914870

β_2	+0.0049296821
β_3	+0.0088462045
β_4	+ 0.0143357909
π	+0.2857142856
d	-0.0893691487
θ	+0.0102753420
δ_2	-0.2692217346

3.4.1 Interpretation of Sensitivity Indices

The Table 3.1 represents the sensitivity index for the base line parameter values and it shows that when the parameters $\beta_1, \pi, \omega, \beta_4, \theta, \beta_3$ and β_2 increase while the other parameters remain constant, the value of R_0 will also increase implying that they increase the endemicity of the disease as they have positive indices and should be targeted by intervention strategies.

More so, when the parameters $\delta_1, \alpha_1, \mu, \delta_2, d,$ and σ increase while keeping other parameters constant, the value of R_0 will decrease, implying that they decrease the endemicity of the disease as they have negative indices and should equally be targeted by intervention strategies. From the table, it was revealed that the most sensitive parameter is the transmission rates for the susceptible individuals with asymptomatic infective (β_1) followed by rate of movement from asymptomatic class to AIDS class (δ_1) when we take absolute values of the sensitivity index. For instance, $X_{\beta_1}^{R_0} = +0.8479053410$ means that increasing or decreasing β_1 by 10% increases or (decreases) R_0 by 8.479053410% while $X_{\delta_2}^{R_0} = -0.2692217346$ means that increasing or (decreasing) δ_2 by 10% decreases (or increases) R_0 by 2.692217346%. we can easily check for the other parameters following similar trend.

3.5 Stability analysis of the disease free equilibrium

3.5.1 Local Stability

The Nonlinear equation (1) needs to be linearized to obtain a simpler description that approximates the true system near the equilibrium point. The following conditions are said to be strictly adhered to when linearizing.

(1) The constant terms and the product term must be neglected (Nonlinear Terms)
(2) The higher order terms must as well be neglected

The system of equation (1) was linearized about ($S^0, I_1^0, I_2^0, T^0, A^0$), by setting

$$\left.\begin{aligned} S &= S^0 + x \\ I_1 &= I_1^0 + y \\ I_2 &= I_2^0 + z \\ T &= T^0 + m \\ A &= A^0 + p \end{aligned}\right\} \tag{18}$$

where at DFE we have $S^0, I_1^0, I_2^0, T^0, A^0$.

Then,

$$\left.\frac{dx}{dt} = \frac{dS}{dt}, \frac{dy}{dt} = \frac{dI_1}{dt}, \frac{dz}{dt} = \frac{dI_2}{dt}, \frac{dm}{dt} = \frac{dT}{dt}, \frac{dp}{dt} = \frac{dA}{dt}\right\} \tag{19}$$

Substituting (18) and (19) into system (1) yields

$$\begin{aligned} \frac{dx}{dt} &= \pi - \frac{\beta_1(I_1^0 + y)(S^0 + x)}{1 + \alpha_1(S^0 + x)} - \frac{\beta_2(I_2^0 + z)(S^0 + x)}{1 + \alpha_1(S^0 + x)} - \frac{\beta_3(T^0 + m)(S^0 + x)}{1 + \alpha_1(S^0 + x)} - \frac{\beta_4(A^0 + p)(S^0 + x)}{1 + \alpha_1(S^0 + x)} \\ &- \mu(S^0 + x) \\ \frac{dy}{dt} &= \frac{\beta_1(I_1^0 + y)(S^0 + x)}{1 + \alpha_1(S^0 + x)} + \frac{\beta_2(I_2^0 + z)(S^0 + x)}{1 + \alpha_1(S^0 + x)} + \frac{\beta_3(T^0 + m)(S^0 + x)}{1 + \alpha_1(S^0 + x)} + \frac{\beta_1(A^0 + p)(S^0 + x)}{1 + \alpha_1(S^0 + x)} \\ &- (\theta + \mu + \delta_1)(I_1^0 + y) \\ \frac{dz}{dt} &= \theta(I_1^0 + y) - (\mu + \delta_2)(I_2^0 + z) \\ \frac{dm}{dt} &= n\delta_2(I_2^0 + z) - (\sigma + \mu)(T^0 + m) + \omega(A^0 + p) \\ \frac{dp}{dt} &= (1 - n)\delta_2(I_2^0 + z) + \delta_1(I_1^0 + y) - (\mu + d + \omega)(A^0 + p) + \sigma(T^0 + m) \end{aligned} \tag{20}$$

we expand and separate the linear terms and neglect the higher order terms and other nonlinear to obtain,

$$\left.\begin{aligned}
\frac{dx}{dt} &= \left(\begin{matrix} 2\beta_1 I_1^0 S^0\alpha_1 - \beta_1 I_1^0 + 2\beta_2 I_2^0 S^0\alpha_1 - \beta_2 I_2^0 + 2\beta_3 T^0 S^0\alpha_1 - \beta_3 T^0 + 2\beta_4 T^0 S^0\alpha_1 \\ -\beta_4 A^0 - \mu \end{matrix}\right)x - \\
&\left(\beta_1 S^0\right)y - \left(\beta_2 S^0\right)z - \left(\beta_3 S^0\right)m - \left(\beta_4 S^0\right)p + Nonlinear terms \\
\frac{dy}{dt} &= \left(\begin{matrix} \beta_1 I_1^0 - 2\beta_1 I_1^0 S^0\alpha_1 - 2\beta_2 I_2^0\alpha_1 S^0 + \beta_2 I_2^0 + \beta_3 T^0 S^0\alpha_1 + \beta_3 T^0 - \beta_3 T^0 S^0\alpha_1 - \beta_4 A^0 S^0\alpha_1 + \\ \beta_4 A^0 - \beta_4 A^0 S^0\alpha_1 \end{matrix}\right)x + \\
&\left(\beta_1 S^0 - (\theta+\mu+\delta_1)\right)y + \left(\beta_2 S^0\right)z + \left(\beta_3 S^0\right)m + \left(\beta_4 S^0\right)p + Nonlinear terms \\
\frac{dz}{dt} &= \theta y - (\mu+\delta_2)z \\
\frac{dm}{dt} &= n\delta_2 z - (\sigma+\mu)m + \omega p \\
\frac{dp}{dt} &= \delta_1 y + ((1-n)\delta_2)z + \sigma m - (\mu+d+\omega)p
\end{aligned}\right\} \quad (21)$$

Theorem 3.1

Let $(K_1+K_2+K_3+K_4) > \dfrac{\beta_1\pi}{\mu}$,

$$\left(K_3(K_1+K_2+K_4) + K_4(K_1+K_2) + K_2K_1\right) > \left(\frac{\beta_1(K_2+K_3+K_4)+\beta_2\theta}{\mu}\right),$$

$$\left(K_4(K_1+K_2)+K_1K_2)K_3 + K_4K_2K_1\right)\mu > \frac{\pi}{\mu}\left[\begin{matrix}\beta_1\left((K_2+K_4)K_3 + K_2K_4\right) + \beta_2\theta(K_3+K_4) + \\ \delta_2\theta\left(\beta_4(1-n)+\beta_3 n\right)\end{matrix}\right],$$

$$K_4K_3K_2K_1\left(1-R_0\right) > 0$$

Then the disease free equilibrium is locally asymptotically stable.

Proof:

The Jacobian matrix of the above linearized equation (21) at the disease free equilibrium $\left(\dfrac{\pi}{\mu},0,0,0,0\right)$ is

$$E^0 = \begin{pmatrix} -\mu & -\beta_1 q & -\beta_2 q & -\beta_3 q & -\beta_4 q \\ 0 & \beta_1 q - K_1 & \beta_2 q & \beta_3 q & \beta_4 q \\ 0 & \theta & -K_2 & 0 & 0 \\ 0 & 0 & n\delta_2 & -K_3 & 0 \\ 0 & 0 & (1-n)\delta_2 & \sigma & -K_4 \end{pmatrix} \quad (22)$$

where,

$$q = \frac{\pi}{(\mu+\alpha_1\pi)}$$
$$K_1 = (\theta+\mu+\delta_1)$$
$$K_2 = (\mu+\delta_2)$$

$$K_3 = (\sigma + \mu)$$
$$K_4 = (\mu + d + \omega)$$

The characteristic equation is obtained as

$$(\lambda + \mu)\left(P_0\lambda^4 + P_1\lambda^3 + P_2\lambda^2 + P_3\lambda + P_4\right) = 0 \tag{23}$$

Clearly, $\lambda = -\mu$

and,

$$P_0 = 1,$$

$$P_1 = (K_1 + K_2 + K_3 + K_4) - \frac{\beta_1\pi}{\mu},$$

$$P_2 = \left(K_3(K_1 + K_2 + K_4) + K_4(K_1 + K_2) + K_2K_1\right) - \left(\frac{\beta_1(K_2 + K_3 + K_4) + \beta_2\theta}{\mu}\right),$$

$$P_3 = \left(K_4(K_1 + K_2) + K_1K_2)K_3 + K_4K_2K_1\right) - \frac{\pi}{\mu}\left[\begin{array}{l}\beta_1\left((K_2 + K_4)K_3 + K_2K_4\right) + \\ \beta_2\theta(K_3 + K_4) + \delta_2\theta\left(\beta_4(1-n) + \beta_3 n\right)\end{array}\right]$$

$$P_4 = K_4K_3K_2K_1\left(1 - R_0\right) > 0$$

$$P_0 > 0, P_1 > 0, P_2 > 0, P_3 > 0, P_4 > 0 \Rightarrow R_0 > 1,$$

Then by Routh Hurwitz criteria, the remaining four eigen values are negative. Hence, the disease free equilibrium is locally asymptotically stable.

3.5.2 Stability of the Endemic equilibrium

The stability of the endemic equilibrium was carried out by linearizing (1) about $\left(S^*, I_1^*, I_2^*, T^*, A^*\right)$ Keeping in mind the conditions guiding linearization

Let

$$\left.\begin{array}{l} S = S^* + w \\ I_1 = I_1^* + f \\ I_2 = I_2^* + g \\ T = T^* + h \\ A = A^* + q \end{array}\right\} \tag{24}$$

where $S^*, I_1^*, I_2^*, T^*, A^*$ are the endemic equilibrium

$$\left.\frac{dS}{dt} = \frac{dw}{dt}, \frac{dI_1}{dt} = \frac{df}{dt}, \frac{dI_2}{dt} = \frac{dg}{dt}, \frac{dT}{dt} = \frac{dh}{dt}, \frac{dA}{dt} = \frac{dq}{dt}\right\} \tag{25}$$

Substituting (24) and (25) into (1) gives

$$\frac{dw}{dt}=\pi-\frac{\beta_1(f+I_1^*)(w+S^*)}{1+\alpha_1(w+S^*)}-\frac{\beta_2(g+I_2)(w+S^*)}{1+\alpha_1(w+S^*)}-\frac{\beta_3(h+T^*)(w+S^*)}{1+\alpha_1(w+S^*)}-\frac{\beta_4(q+A^*)(w+S^*)}{1+\alpha_1(w+S^*)}$$

$$-\mu(w+S^*)$$

$$\Rightarrow\frac{dw}{dt}=\pi-\beta_1(f+I_1^*)(w+S^*)\left[1+\alpha_1(w+S^*)\right]^{-1}-\beta_2(g+I_2^*)(w+S^*)\left[1+\alpha_1(w+S^*)\right]^{-1}$$

$$-\beta_3(h+T^*)(w+S^*)\left[1+\alpha_1(w+S^*)\right]^{-1}-\beta_4(q+A^*)(w+s^*)\left[1+\alpha_1((w+S^*)\right]^{-1}-\mu(w+S^*)$$

Following binomial expansion and neglecting all higher order terms and nonlinear terms to obtain

$$\frac{dw}{dt}=\begin{pmatrix}\beta_1I_1^*\alpha_1S^*+\beta_1I_1^*S^*\alpha_1-\beta_2I_2^*+2\beta_2I_2^*\alpha_1S^*-\beta_1I_1^*+\beta_3T^*\alpha_1S^*-\\ \beta_3T^*+\beta_3T^*S^*\alpha_1-\beta_4A^*+2\beta_4A^*\alpha_1S^*-\mu\end{pmatrix}w+ \tag{26}$$

$$\left(-\beta_1S^*\right)f+\left(-\beta_2S^*\right)g+\left(-\beta_3S^*\right)h-\left(\beta_4S^*\right)q+Nonlinearterms$$

And also,

$$\frac{df}{dt}=\begin{pmatrix}\beta_1I_1^*-\beta_1I_1^*\alpha_1S^*+\beta_4A^*-2\beta_4A^*\alpha_1S^*+\beta_2I_2^*-2\beta_2I_2^*\alpha_1S^*\\ +\beta_3T^*-\beta_3T^*\alpha_1S^*-2\beta_3T^*\alpha_1S^*\end{pmatrix}w+ \tag{27}$$

$$\left(\beta_1S^*-(\theta+\mu+\delta_1)\right)f+\left(\beta_2S^*\right)g+\left(\beta_3S^*\right)h+\left(\beta_4S^*\right)q+\text{Nonlinear Terms}$$

Also,

$$\frac{dg}{dt}=\theta f-(\mu+\delta_2)g \tag{28}$$

Also,

$$\frac{dh}{dt}=n\delta_2g-(\sigma+\mu)h+\omega q \tag{29}$$

Likewise,

$$\frac{dq}{dt}=\delta_1f+((1-n)\delta_2)g+\sigma h-(\mu+d+\omega)q \tag{30}$$

Therefore, the linearized equations are:

$$\frac{dw}{dt}=\begin{pmatrix}\beta_1I_1^*\alpha_1S^*+\beta_1I_1^*S^*\alpha_1-\beta_2I_2^*+2\beta_2I_2^*\alpha_1S^*-\beta_1I_1^*+\beta_3T^*\alpha_1S^*-\\ \beta_3T^*+\beta_3T^*S^*\alpha_1-\beta_4A^*+2\beta_4A^*\alpha_1S^*-\mu\end{pmatrix}w+ \tag{31}$$

$$\left(-\beta_1S^*\right)f+\left(-\beta_2S^*\right)g+\left(-\beta_3S^*\right)h-\left(\beta_4S^*\right)q+Nonlinearterms$$

$$\frac{df}{dt}=\left(\beta_1I_1^*-\beta_1I_1^*\alpha_1S^*+\beta_4A^*-2\beta_4A^*\alpha_1S^*+\beta_2I_2^*-2\beta_2I_2^*\alpha_1S^*+\beta_3T^*-\beta_3T^*\alpha_1S^*-2\beta_3T^*\alpha_1S^*\right)w \tag{32}$$

$$+\left(\beta_1S^*-(\theta+\mu+\delta_1)\right)f+\left(\beta_2S^*\right)g+\left(\beta_3S^*\right)h+\left(\beta_4S^*\right)q+\text{Nonlinear Terms}$$

$$\frac{dg}{dt}=\theta f-(\mu+\delta_2)g \tag{33}$$

$$\frac{dh}{dt}=n\delta_2g-(\sigma+\mu)h+\omega q \tag{34}$$

$$\frac{dq}{dt} = \delta_1 f + \left((1-n)\delta_2\right) g + \sigma h - (\mu + d + \omega) q \tag{35}$$

Theorem 3.2: Let $K_1 + K_2 + K_3 + K_4 + A > \beta_1 S$,

$$(K_1 + K_2)(A + K_3 + K_4) + A(K_4 + K_3)K_1K_2 + \mu K_4 + \sigma(\mu + d) + \beta SB > \beta S(A + K_4 + K_3 + K_2)$$

$$\begin{pmatrix} B\beta_2\theta + (K_4 + K_3)((K_1 + K_2)A + K_1K_2 + \beta_1 B) + (\mu K_4 + \sigma(\mu + d))(A + (K_1 + K_2)) \\ + AK_1K_2 \end{pmatrix} >$$

$$S\begin{pmatrix} \beta_1(\mu K_4 + \sigma(\mu + d)) + BK_2 + (\beta_1 A + \beta_2\theta + K_2)(K_3 + K_4) + (\beta_2\theta + K_2)A + \\ \delta_2\theta(\beta_3 n + \beta_4(1-n)) \end{pmatrix}$$

$$\begin{pmatrix} (\mu K_4 + \sigma(\mu + d))((K_1 + K_2)A + K_1K_2)AK_1K_2(K_3 + K_4) + \\ BS((\beta_1 + \beta_2\theta)K_2(K_3 + K_4) + \beta_1(\mu K_4 + \sigma(\mu + d)) + +(\beta_3 n + \beta_4(1-n))\delta_2\theta) \end{pmatrix} >$$

$$S\begin{Bmatrix} \beta_1[(\mu K_4 + \sigma(\mu + d))(K_2 + A) + K_2(K_3 + K_4)A] \\ \beta_2\theta((K_3 + K_4)(A) + (\mu K_4 + \sigma(\mu + d))) + \beta_3(n(A + K_4) + (1-n)\omega)\theta\delta_2 + \\ \beta_4((1-n)A + \delta_2\theta[(1-n)K_3 + n\theta]) \end{Bmatrix} \quad \text{and}$$

$$K_1K_2(\mu K_4 + \sigma(\mu + d))(A + R_0 B)S + \beta_3 B(1-n)\omega\theta S > (K_1K_2(\mu K_4 + \sigma(\mu + d))R_0 + \beta_3(1-n)\omega\theta)AS$$

Then the endemic equilibrium point $\left(S^*, I_1^*, I_2^*, T^*, A^*\right)$ is locally asymptotically stable.

Proof:

Equations (31)-(35) can be expressed in matrix form as

$$\begin{pmatrix} w' \\ f' \\ g' \\ h' \\ q' \end{pmatrix} = \begin{pmatrix} A & -\beta_1 S^* & -\beta_2 S^* & -\beta_3 S^* & -\beta_4 S^* \\ B & -\beta_1 S^* - (\theta + \mu + \delta_1) & \beta_2 S^* & \beta_3 S^* & \beta_4 S^* \\ 0 & \theta & -(\mu + \delta_2) & 0 & 0 \\ 0 & 0 & n\delta_2 & -(\sigma + \mu) & \omega \\ 0 & \delta_1 & (1-n)\delta_2 & \sigma & -(\mu + d + \omega) \end{pmatrix} \begin{pmatrix} w \\ f \\ g \\ g \\ q \end{pmatrix} + Nonlinearterms \tag{36}$$

where,

$$A = \begin{pmatrix} \beta_1 I_1^* \alpha_1 S^* + \beta_1 I_1^* S^* \alpha_1 - \beta_2 I_2^* + 2\beta_2 I_2^* \alpha_1 S^* - \beta_1 I_1^* + \beta_3 T^* \alpha_1 S^* - \beta_3 T^* + \beta_3 T^* S^* \alpha_1 \\ -\beta_4 A^* + 2\beta_4 A^* \alpha_1 S^* - \mu \end{pmatrix}$$

$$B = \left(\beta_1 I_1^* - \beta_1 I_1^* \alpha_1 S^* + \beta_4 A^* - 2\beta_4 A^* \alpha_1 S^* + \beta_2 I_2^* - 2\beta_2 I_2^* \alpha_1 S^* + \beta_3 T^* - \beta_3 T^* \alpha_1 S^* - 2\beta_3 T^* \alpha_1 S^*\right)$$

The Jacobian matrix of the equation (31)-(35), at endemic equilibrium point $\left(S^*, I_1^*, I_2^*, T^*, A^*\right)$

Let $C^* = \begin{pmatrix} A & -\beta_1 S^* & \left(-\beta_2 S^*\right) & -\beta_3 S^* & -\beta_4 S^* \\ B & \left(\beta_1 S^* - (\theta + \mu + \delta_1)\right) & \beta_2 S^* & \beta_3 S^* & \beta_4 S^* \\ 0 & \theta & -(\mu + \delta_2) & 0 & 0 \\ 0 & 0 & n\delta_2 & -(\sigma + \mu) & \omega \\ 0 & \delta_1 & \left((1-n)\delta_2\right) & \sigma & -(\mu + d + \omega) \end{pmatrix}$ (37)

Therefore the characteristic equation, $\left|C^* - \lambda I\right| = 0 \Rightarrow$

$$\begin{vmatrix} A-\lambda & -\beta_1 S^* & -\beta_2 S^* & -\beta_3 S^* & -\beta_4 S^* \\ 0 & \left(\beta_1 S^* - (\theta+\mu+\delta_1)\right)-\lambda & \beta_2 S^* & \beta_3 S^* & \beta_4 S^* \\ 0 & \theta & -(\mu+\delta_2)-\lambda & 0 & 0 \\ 0 & 0 & n\delta_2 & -(\sigma+\mu)-\lambda & \omega \\ 0 & \delta_1 & (1-n)\delta_2 & \sigma & -(\mu+d+\omega)-\lambda \end{vmatrix} \quad (38)$$

Evaluating for λ in (38) yields the characteristic equation

$$\lambda^3 + a_1\lambda^4 + a_2\lambda^3 + a_3\lambda^2 + a_4\lambda + a_5 = 0 \quad (39)$$

where.

$$a_0 = 1$$

$$a_1 = K_1 + K_2 + K_3 + K_4 + A - \beta_1 S$$

$$a_2 = (K_1+K_2)(A+K_3+K_4) + A^*(K_4+K_3)K_1K_2 + \mu K_4 + \sigma(\mu+d) - \beta S(A+K_4+K_3+K_2-B)$$

$$a_3 = \beta_1\left[\{-(K_3+K_4+K_2)A - (K_4-B+K_2)K_3 + (K_2-B)K_4 - BK_2 - \sigma\omega\}\right]S$$
$$-\beta_2\{\theta[(A-B)+K_3+K_4]\} - \beta_3 n\delta_2\theta S - \beta_4\delta\theta(1-n)S + (K_4+K_3)[(K_1+K_2)A + K_1K_2]$$
$$+(\mu K_4 + \mu(\mu+d))[A+(K_1+K_2)]K_1K_2A$$

$$a_4 = (\mu K_4 + \sigma(\mu+d))((K_1+K_2)A + K_1K_2)AK_1K_2(K_3+K_4) + BS\begin{pmatrix}(\beta_1+\beta_2\theta)K_2(K_3+K_4)+\\ \beta_1(\mu K_4+\sigma(\mu+d))+\\ +(\beta_3 n+\beta_4(1-n))\delta_2\theta\end{pmatrix}$$

$$-S\begin{Bmatrix}\beta_1[(\mu K_4+\sigma(\mu+d))(K_2+A)+K_2(K_3+K_4)A]\\ \beta_2\theta((K_3+K_4)(A)+(\mu K_4+\sigma(\mu+d)))+\beta_3(n(A+K_4)+(1-n)\omega)\theta\delta_2+\\ \beta_4((1-n)A+\delta_2\theta[(1-n)K_3+n\theta])\end{Bmatrix}$$

$$a_5 = K_1K_2(\mu K_4+\sigma(\mu+d))(A+R_0B)S + \beta_3 B(1-n)\omega\theta S -$$
$$(K_1K_2(\mu K_4+\sigma(\mu+d))R_0 + \beta_3(1-n)\omega\theta)AS$$

Then the endemic equilibrium point $\left(S^*, I_1^*, I_2^*, T^*, A^*\right)$ is locally asymptotically stable, it follows from Descartes rule of signs, that equation (39) have no change in sign meaning there are no positive roots. Therefore, since all eigenvalues are negative then the endemic or disease equilibrium is locally asymptotically stable. Then the endemic equilibrium point $\left(S^*, I_1^*, I_2^*, T^*, A^*\right)$ is locally asymptotically stable.

3.6 Existence of backward bifurcation

The existence of backward bifurcation is explored using the centre manifold made popular by [28]. This has widely been used in the study of some epidemiological models [27,29-32,34-36].

For understanding and convenience, we consider the following change of variables

Let $S = x_1, I_1 = x_2, I_3 = x_3, T = x_4,$ and $A = x_4$ Also, Let $x = (x_1, x_2, x_3, x_4, x_5)^T$, so the system (2) can be re-written in the form $\frac{dx}{dt} = F(x),$ where $F = (f_1, f_2, f_3, f_4, f_5)^T$, as follows, then the model equations becomes

$$\begin{aligned}
\frac{dx_1}{dt} &= \pi - \frac{\beta_1 x_2 x_1}{(1+\alpha_1 x_1)} - \frac{\beta_2 x_3 x_1}{(1+\alpha_1 x_1)} - \frac{\beta_3 x_4 x_1}{(1+\alpha_1 x_1)} - \frac{\beta_3 x_5 x_1}{(1+\alpha_1 x_1)} - \mu x_1 = 0 \\
\frac{dx_2}{dt} &= \frac{\beta_1 x_2 x_1}{(1+\alpha_1 x_1)} + \frac{\beta_2 x_3 x_1}{(1+\alpha_1 x_1)} + \frac{\beta_3 x_4 x_1}{(1+\alpha_1 x_1)} + \frac{\beta_4 x_5 x_1}{(1+\alpha_1 x_1)} - (\theta + \mu + \delta_1) x_2 = 0 \\
\frac{dx_3}{dt} &= \theta x_2 - (\mu + \delta_2) x_3 = 0 \\
\frac{dx_4}{dt} &= n\delta_2 x_3 - (\sigma + \mu) x_4 + \omega x_5 = 0 \\
\frac{dx_5}{dt} &= (1-n)\delta_2 x_3 + \delta_1 x_2 + \sigma x_4 - (\mu + d + \omega) x_5 = 0
\end{aligned} \tag{40}$$

Taking $\beta_1 = \beta_1^*$, where β_1^* is the chosen bifurcation parameter and the case when $R_0 = 1.$ Then,

$$\beta_1^* = \frac{(K_1 K_2 + \pi\theta\beta_2)(\mu K_4 + \sigma(\mu + d)) - \pi(\beta_3(\delta_2\theta(\omega + n(\mu + d)) + \omega\delta_1 K_2) + \beta_4(\delta_2\theta(\sigma + \mu(1-n)) + \delta_1 K_2 K_3))}{\pi K_2(\mu K_4 + \sigma(\mu + d))}$$

The Jacobian of system (40), evaluated at the disease free equilibrium E_0, and β_1^* is given by

$$J(E_0, \beta_1^*) = \begin{pmatrix} -\mu & -\beta_1 q & -\beta_2 q & -\beta_3 q & -\beta_4 q \\ 0 & \beta_1 q - K_1 & \beta_2 q & \beta_3 q & \beta_4 q \\ 0 & \theta & -K_2 & 0 & 0 \\ 0 & 0 & n\delta_2 & -K_3 & 0 \\ 0 & 0 & (1-n)\delta_2 & \sigma & -K_4 \end{pmatrix} \tag{41}$$

The characteristic equation of the Jacobian matrix

$$(\lambda + \mu)(P_0\lambda^4 + P_1\lambda^3 + P_2\lambda^2 + P_3\lambda + P_4) = 0 \tag{42}$$

where $P_i; i = 0,1,..4 > 0$.

The polynomial equation (41) has a zero eigenvalue when $P_4 = 0$, that is when $(R_0 = 1)$.

$$\lambda(P_0\lambda^3 + P_1\lambda^2 + P_2\lambda^1 + P_3) = 0 \tag{43}$$

such that $\lambda = 0$ is a zero eigenvalue and

$$P_0\lambda^3 + P_1\lambda^2 + P_2\lambda^1 + P_3 = 0 \tag{44}$$

So that all the eigenvalues in (44) will have negative real parts indicating that there exist bifurcation at $R_0 = 1$. Hence, the need for the centre manifold theorem [28], the associated right eigenvector w corresponding to the zero eigenvalue, where $w = (w_1, w_2, w_3, w_4, w_5)^T$, can be obtained from $J(E_0, \beta_1^*)w = 0$. Hence, we have

$$\begin{cases} w_1 = -q\left\{\dfrac{(\beta_1 K_2 + \beta_3\theta)(K_4 - \sigma w) + \delta_1 K_2(\beta_3 w + \beta_4) + \theta\delta_2(n + (1-n)(1-\sigma))(1+\omega)}{\theta(K_4 - \sigma\omega)}\right\}w_3 \\ w_2 = \dfrac{K_2 w_3}{\theta} \\ w_3 = w_3 > 0 \\ w_4 = \dfrac{\theta\delta_2(n + w(1-n+\sigma n) + w\delta_1 K_2)w_3}{K_3\theta(k_4 - \sigma w)} \\ w_5 = \dfrac{(\delta_1 K_2 + \theta\delta_2((1-n)+\sigma n))w_3}{\theta(K_4 - \sigma\omega)} \end{cases}$$

Similarly, the Jacobian, $J(E_0, \beta_1^*)$, has a left eigenvector $v = (v_1, v_2, v_3, v_4, v_5)$ satisfying $v.w = 1$, where

$$\begin{cases} v_1 = 0 \\ v_2 = \dfrac{(K_4 - \sigma\omega)v_5}{q\beta_3(K_3 + \omega)} \\ v_3 = \dfrac{\{(K_4 - \sigma)(n\delta_2\beta_3 - \omega\beta_2) + (K_3 + \omega)(\beta_2 K_4 + \beta_3(1-n)\delta_2)\}v_5}{K_2\beta_3(K_3 + \omega)} \\ v_4 = \dfrac{(k_3(K_4 - \sigma) + \sigma(K_3 + \omega))v_5}{(K_3 + \omega)} \\ v_5 = v_5 > 0 \end{cases}$$

3.6.1 Computation of a and b

The coefficients a and b as defined by Castillo-Chavez and Song [34] are given by:

$a = \sum_{i,j,k=1}^{\infty} v_k w_i w_j \dfrac{\partial^2 f_k(E_0, \beta^*)}{\partial x_i \partial x_j}$ and $b = \sum_{k,i,j=1}^{\infty} v_k w_i \dfrac{\partial^2 f_k(E_0, \beta^*)}{\partial x_i \partial \beta^*}$; and are algebraically computed as follows, considering only the nonzero components $f_i : k = 2,3,4,5.$ With these definitions, the following were obtained:

$$\Rightarrow v_2 w_1 \left\{-2\left(\frac{w_2\beta_1^* + w_3\beta_2 + w_4\beta_3 + w_5\beta_5}{(1+\alpha_1 x_2)^2}\right)\right\}$$

w_1 is non positive, while $(w_2, w_3, w_4, w_5) > 0$, and $v_2 > 0$

On substituting of necessary quantities and simplifying,

$$\Rightarrow a = \left\{ \frac{\begin{array}{c} 2qw_3v_5\left(w_2\beta_1^* + w_3\beta_2 + w_4\beta_3 + w_5\beta_5\right)\left(K_3\left(K_4 - \sigma\right) + \sigma(K_3 + \omega)\right) \\ \left(\beta_1 K_2 + \beta_3\theta\right)\left(K_4 - \sigma\omega\right) + \delta_1 K_2(\beta_3\omega + \beta_4) + \theta\delta_2\left(n + \left(1-n\right)\left(1-\sigma\right)\right)(1+\omega) \end{array}}{q\beta_3\theta\left(K_4 - \sigma\omega\right)\left(K_3 + \omega\right)\left(1 + \alpha_1\frac{\pi}{\mu}\right)} \right\} \quad (45)$$

$$b = qw_3v_5\pi\left(\frac{\begin{array}{c} \left(\beta_1 K_2 + \beta_3\theta\right)\left(K_4 - \sigma\omega\right) + \delta_1 K_2\left(\beta_3\omega + \beta_4\right) + \theta\delta_2(n + (1 - n(1-\sigma))(1+\omega) \\ \left(K_3(K_4 - \sigma) + \sigma(K_3 + \omega)\right) \end{array}}{q\beta_3\theta\left(\mu + \pi\alpha_1\right)\left(K_3 + \omega\right)\left(K_5 - \sigma\omega\right)} \right) \quad (46)$$

Clearly, from (43) and (44), $a > 0, b > 0,$ then the model exhibits a backward bifurcation around $R_0 = 1$, that is there exists bi-stability of equilibrium point (one stable disease free and stable endemic equilibrium for $R_0 < 1.$ This is implying that the disease free is not globally stable. The implication, from epidemiological view point of the existence of backward bifurcation is that the classical necessary requirement of $R_0 < 1$ is insufficient to control the spread of HIV in the population.

4 Numerical simulations and discussion

This section presents the numerical simulation results for the HIV/AIDS model.

The parameters in the model (1) shown in table 4.1 were obtained from literatures published by different researchers and referenced accordingly.

Table 4.1: **parameters, values and source used in the model**

d	1.0	[24]
θ	0.01	[33]
μ	0.02	Assumed
ω	0.1	[33]
n	0.2	Assumed
α_1	0.1	Assumed

δ_1	0.2	[19]
δ_2	0.01	[19]
σ	0.001	[19]
β_1	0.86	[19]
β_2	0.15	[19]
β_3	0.10	[19]
β_4	0.08	Assumed

4.1 Numerical simulation

Simulation of the model was performed for better understanding of dynamical spread of transmission of HIV/AIDS infection using Maple 18 software. The results of the model equations are presented below in form of graphs and are discussed in the figure below to illustrate the changes in the compartments. The screening rate, treatment rate and the saturation terms were checked in order to observe their impact on the numerical spread of the disease using a set of reasonable parameters.

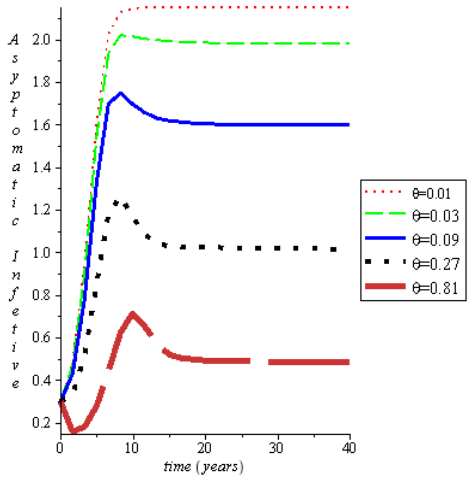


Fig.1 (a)

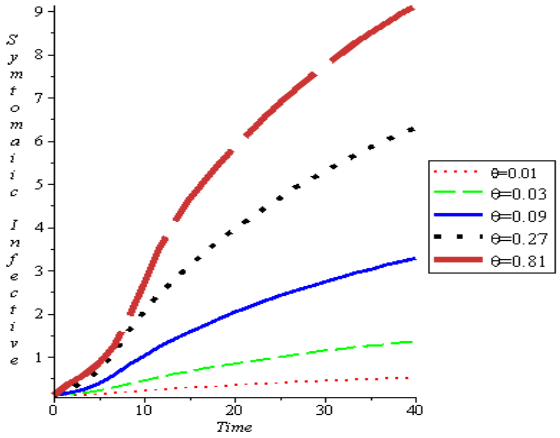


Fig. 1 (b)

Figures 1(a)-1(b) depicts the effect of screening rates (θ) on asymptomatic infective population $I_1(t)$ against time (t) and symptomatic infective $I_2(t)$ population. As the asymptomatic HIV infective population become aware of their status, there is a decrease in the population of asymptomatic infective population which ultimately bring about an increase in the population of

symptomatic infective population as seen in **Figure 1(b)**. It was observed here that there is an increase in the population of symptomatic infective as the screening rate increases. This is simply due to the population of asymptomatic infective that migrated to the symptomatic infective compartment as a result of the awareness gotten.

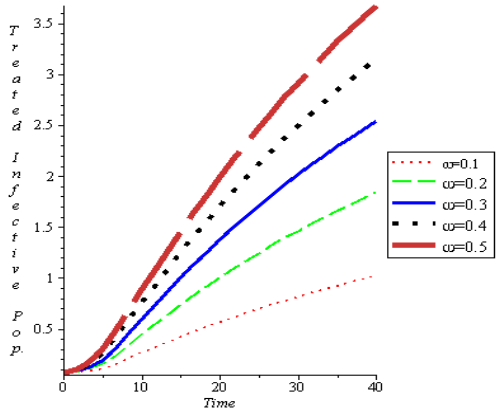


Fig.2 (a)

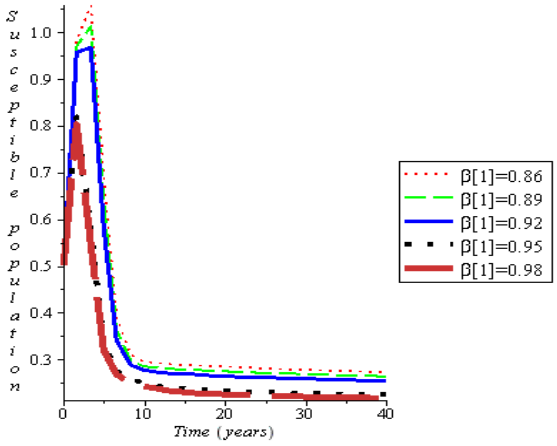


Fig.2 (b)

Figure 2(a) depicts the graph of Treated infective population $T(t)$ against Time (t) for different values of treatment rate and **Figure 2(b)** depicts the graph of susceptible Population against time (t) for different values of transmission rate for susceptible individuals with asymptomatic infective (β_1) The symptomatic infective undergo and submit to treatment with antiretroviral therapy which as a result leads to an increase in the proportion of symptomatic infective population. This therefore result to an increase in the proportion of treated infective populations as shown in **Figure (2a)** while **Figure (2b)** shows that as transmission rate increase, the susceptible population decrease significantly. It is clearly seen that as the transmission parameter values increase in the population, the number of susceptible population also reduce. As long as susceptible population continue to interact with the infective without taking any preventive measures at any of the infective stages, there is going to be a continuous reduction in the susceptible population.

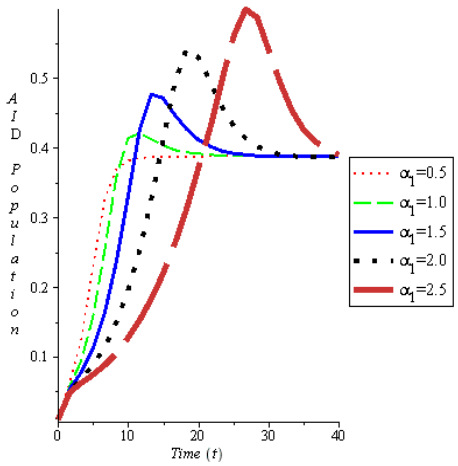


Fig.3 (a)

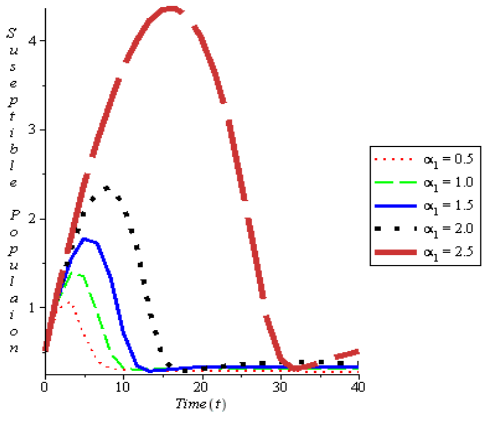


Fig.3 (b)

Fig. (3a) This depicts the graph of Aids population A(t) against time (t) for different values of saturation term (α_1) while **Fig. (3b).** depicts the graph of susceptible population against time for various values of saturation term (α_1). This shows that as the saturation term α_1 increases, the AIDS population decreases. This is simply due to the crowding effects of AIDS individual and other infective as seen in **Figure (3a)** while also, as the saturation term α_1 increases in **Figure (3b)**, the susceptible population increases. This is simply due to the precautionary measures taken by susceptible individual.

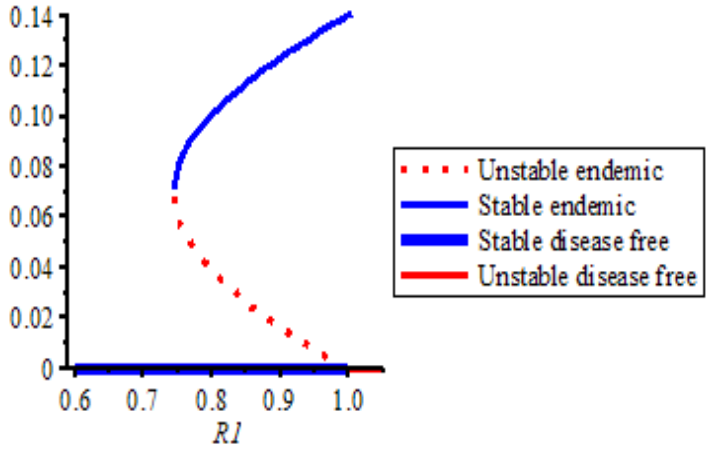


Fig.4. Backward Bifurcation Diagram

The phenomenon of Figure 7 shows that the HIV/AIDS model have multiple endemic equilibrium whenever $R_0 < 1$. In this case, the classical requirement of having $R_0 < 1$, is necessary but no longer sufficient for effective disease elimination.

5 Conclusion

In this paper, we formulated and presented a mathematical model for HIV/AIDS transmission, which incorporated saturated incidence term. It was shown that the system of equation represents a useful mathematical model of a physical system by carrying out a classical qualitative proof of the positivity of solution of the governing system of model equations. More so, the existence of both the disease-free and endemic equilibria were established and analyzed for stability, and it was shown that both equilibria were locally asymptotically stable. This implies that whenever the said conditions are satisfied, the HIV/AIDS infection can be controlled. The result of the sensitivity analysis showed the transmission rates for susceptible individuals with asymptomatic infective β_1, as the most sensitive parameter. The result of the bifurcation analysis showed that the model exhibit a backward bifurcation which indicates that $R_0 < 1$ is no longer sufficient for effective disease control. However, screening and treatment of the infective have a significant effect in reducing the transmission of the disease. Susceptible population also reduce when infective carelessly interact with other infective and also susceptible population increase as saturation increase due to the precautionary measures taken.

Acknowledgments

The authors of this paper wish to thank the editor and the anonymous reviewers for their constructive comments and suggestions that greatly improved this paper. Author also declare that there is no conflict of interest.

References

[1] Mbabazi, D. (2016). Mathematical Modelling of the Spread of HIV/AIDS by Markov Chain Process. American Journal of Applied Mathematics,; 4(5):235-246.

[2] Lamptey, P., Wigley, M., D. Carr, and Y. Collymore , (2003). "Facing the HIV/AIDS Pandemic" Publication of the Population References Bureau (PRB), population bulleting Washinton DC, 57(1):1-43

[3] Global and Regional Trend (2023)- Unicef data. Aidsinfo.unaids.org

[4] UNAIDS/WHO estimates (2023). Global HIV/AIDS Statistics-Fact sheet

[5] CIA world factbook (2023). www.cia.gov/the-world-factbook/

[6] HIV/AIDS facts (2004).Pediatric HIV Infection and AIDS: Point of View

[7] A.M. Arafa., S.Z.Rida, and M.Khalili. A Fractional- Order Model of HIV Infection with Drug Therapy Effect. Journal of the Egyptian Mathematical society, 22 (3):538-543.

[8] Odebiyi, O.A. and R.O.Ayeni, Modelling (2012). and Simulation of HIV infection of $CD4^+$ T cells with past and current History of the disease. Journal of Nigerian Association of Mathematical Physics (NAMP), 22:495-502.

[9] UNAIDS/WHO (2002). Pediatric HIV infection and AIDS: Point of view

[10] Morgan, D. , C.Mabe, B.Mayanla, J.M.Okongo, R.Lubega, and J.A.Whitworth, (2002). "HIV- 1 infection in rural Africa: is there a difference in median time to AIDS and survival compared with that in industrialized countries?",AIDS 16 (4): 597-632

[11] Pritam Saha and Uttam Ghosh. (2023). Complex dynamics and conflict analysis of an epidemic-model with non-monotone incidence and saturated treatment. International journal of dynamics and control G 11:301-323.

[12] Oladejo J.K, Oluyo T.O (2022). Effect of Prep on HIV/AIDS dynamics with Immigration of Infective.IJMAN,vol.5,issue2(2022). https://tnsmb.org/journal/index.php/ijman/article/view/54

[13] Cox N.S., Wu.L, Wittenaver, R.,Clark S. (2024). Impact of HIV self-testing of oral pre-exposure prophylaxis scale-up on drug resistance and HIV outcomes in Kenya; a modeling study. The Lancet vol 11, issues 3, 167-175.

[14] Udoo, I.J.M., R.A. Kimbir, and R.M. Odekunle, (2015). Existence and Uniqueness of Solution of an HIV/AIDS Model Considering Counselling, Vaccination and Antiretroviral Therapy. Math. Theory and Modelling, vol. 15, No. 11.

[15] Wang J, Zhang J (2010). Analysis of an SIR Model with bilinear incidence rate, Nonlinear anal RWA 11:2390-2402.

[16] Jin Y, Wang W, Xiao S. (2007). An SIR model with a non-linear incidence rate. *Chaos* Solitions Fractails 34: 1482-1497.

[17] Jana S, Nandi SK, Kar TK. (2015). Complex dynamics of an SIR epidemic model with saturated incidence rate and treatment. Acta Biotheor 64:65-84.

[18] Dubey P, Dubey B, Dubey US (2016). Dynamics of a SIR model with nonlinear incidence rate and treatment rate. Nonlinear Appl. Maths. 10:718-737.

[19] Ratera Safiel., Estomih,S.Massawe and Daniel,O.Makinde (2012). Modelling the Effect of Screening and Treatment on Transmission of HIV/AIDS Infection in a Population. American journal of Mathematics and Statistics, 2(4):75-88

[20] Pritam Saha and Uttam Ghosh. (2021). Global dynamics and control strategies of an epidemic model having logistic growth, non-monotone incidence with the impact of limited hospital beds. Nonlinear Dyn. (2021):971-996. https//doi.org/10.1007/s11071-021-06607-9.

[21] Zhang, J.Z., Z.Jin, Q.X. Liu, and Z.Y, Zang (2008). Analysis of a delayed SIR model with non-linear incidence rate. Discrete dyn, nat, soc. Doi: 10.1155/2008/636153. PP 1-16.

[22] Huo, H.F, Chen, R. and Wang, X.Y. (2016). Modelling and Stability of HIV/AIDS Epidemic Model with Treatment. Appl. Math. Model. 40, 6550-6559.

[23] Oladejo J.K, Oluyo T.O. Effect of Prep on HIV/AIDS dynamics with immigration of infectives. IJMAN, vol. 5, issue 2 (2022).

[24] Odebiyi, O.A., (2019). Modelling the effects of Screening and Treatment on human immunodeficiency Virus/Acquired Immune-Deficiency Syndrome Transmission with Saturated Incidence Rate, Ph.D thesis LAUTECH Ogbomoso, Nigeria.

[25] Diekmann, O., J.A. Heesterbeek, andJ.A.J. Metz, (1990). On the definition and the computation of the basic reproduction ratio R_0 in models for infectious diseases in heterogeneous population. J.maths. *Bio.*28:265-382

[26] Chitnis N, Cushing J,M and Hyman M (2008). Determining Important parameters in the spread of Malaria: Through the sensitivity analysis of Mathematical model. Bulleting of Mathematical Biology, 70:1272-1296

[27] Hu Zy, Chang L.L, Teng ZD, Chen X. (2016). Bifurcation analysis of a discrete SIRS epidemic model with standard incidence, Adv Differ Equ. 155:1-22.

[28] Castillo-Chavez and B. Song.(2024) Dynamical Models of Tuberculosis and their Applications, Math.Biosci. Eng. 1(2) (2004), pp.361-404.

[29] Egonmwan, A.O., and D. Okuonghae, (2012). Analysis of a Mathematical Model for Tuberculosis with Diagnosis. J. Appl. Comput. 59, pp.129-162 doi:10.1007/s12190-018-12190-018-1172-1

[30] Malik, T.M. , A.A. Alsaleh, A.B. Gumeel and M.A. Safi, Optimal strategies for controlling the MERS coronavirus during a mass gathering, Global J. pure Appl. Math. (11), pp. 4831-4865

[31] Okosun, K.O., M.A. Khan, E. Bonyah and S.T. Ogunlade, (2017). On the dynamics of HI-AIDS and Cryptosporidiosis. Eur. Phys. J. plus. 132, p.363.doi:101140/epjp/:i2017-11625-3

[32] Srivastav, A.K.., N.K. Goswami, M. Ghosh and X.Z, Li. (2018), Modeling and optimal control analysis of zika virus with media impact, Int. J. Dyn. Control. 6(2018), pp.1673-1689. Doi:10.1007//s40435-018-0416-0

[33] Abdallah. W., Massawe E.S. and Makinde O.D. (2012): Mathematical Modelling of HIV/AIDS dynamics with treatment and vertical transmission: Applied Mathematics (3) pp77-89.

[34] Ong'ala Jacob Otieno, Mugisha Joseph and Odahiambo John (2012). Mathematical Model forPneumonia Dynamics among Children. Africa Mathematical Sciences Association Conference (SAMSA 2012) 26th -29th Nov.2012.

[35] Olaniyi, S., K.O. Okosun, S.O. Adesanya and R.S. Lebelo. (2020) Modelling malaria dynamics with partial immunity and protected travelers: Optimal control and cost effectiveness analysis. Journal of Biological Dynamics, vol. 14, No. 1, 90-115. http://doi.org/10.1080/17513758.2020.1722265

[36] Adeyemi, M.O., and T.O. Oluyo; (2023). Mathematical Modeling for the Control of Fly Borne Mastitis Disease in Cattle. Frontiers in applied mathematics and statistics. June, 2023 DOI: 10.3389/fams.2023.1171157

[37] Marsudi, Marjono, A. Andari, Sensitivity Analysis of Effect of Screening and HIV Therapy on the Dynamics of Spread of HIV, Applied Mathematical Sciences, vol.8,no.155,pp.7749-7763, 2014. DOI: https://doi.org/10.12988/ams.2014.49737.

[38] Stoddart, C.A., and R.A. Reyes.(2006). Models of HIV-1 disease: A Review Status, Drug Discovery Today Disease models 3(1):113-119 .

Revealing some of the hidden mathematical models of educational theories

C.V. Obasi*†, E.N. Didigwu‡, and I.G. Ezugorie†§

Abstract

This paper delves into the intersection of mathematical modeling and educational theory, exploring how mathematical frameworks have been instrumental in advancing our understanding of educational processes and pedagogical practices. This paper focused on such educational theories as information memory-processing theory, dynamic equilibrium theory, cooperative learning theory, Maslow motivation theory, Lewin's field theory and social learning theory. By employing mathematical models, researchers have been able to dissect complex educational phenomena, elucidate underlying mechanisms, and predict outcomes with a level of precision that traditional qualitative approaches often struggle to achieve.

Keywords and phrases: mathematical modeling; education; theories; educational theory

1 Introduction

Education as a field of study is interdisciplinary, drawing on insights and methodologies from multiple disciplines to address complex educational challenges and advance knowledge, policy, and practice. It plays a critical role in shaping individual opportunities, social mobility, economic development, and societal well-being by fostering intellectual growth, critical thinking, creativity, and citizenship. Educational theory encompasses a broad range of perspectives, principles, and frameworks that aim to understand and improve the process of teaching and learning [1]. It draws upon insights from various disciplines, including psychology, sociology, philosophy, and anthropology, to examine how individuals acquire knowledge, develop skills, and engage in educational experiences. It goes to show that educational theory informs the development of educational policies, practices, and interventions aimed at promoting equitable access to quality education and fostering lifelong learning [2]. By understanding the underlying principles and dynamics of teaching and learning, educators can adapt their approaches to meet the diverse needs of learners and create supportive learning environments that facilitate academic achievement, personal growth, and social development through mathematical modeling.

*Corresponding Author; E-mail: chinedu.obasi@alvanikoku.edu.ng
†Department of Mathematics, Alvan Ikoku Federal University of Education, Owerri, Nigeria.
‡Department of Industrial Mathematics/Applied Statistics, ESUT, Enugu, Nigeria. E-mail: edith.didiegwu@esut.edu.ng
† E-mail: ikegodezugorie@esut.edu.ng

Mathematical modeling is a method used to represent, analyze, and understand real-world phenomena or systems using mathematical structures and techniques. It involves creating mathematical descriptions of these systems based on observations, data, and theoretical principles. Mathematical modeling plays a crucial role in the field of education by providing a systematic framework for understanding, analyzing, and improving various aspects of teaching, learning, and educational systems. Advancing educational theories through mathematical modeling can be a powerful approach to understanding and improving learning processes. Mathematical modeling provides a systematic framework for studying educational theories, identifying factors that influence learning outcomes, and developing evidence-based practices for improving education. Advancing educational theories through mathematical modeling offers several significant benefits and opportunities. By mathematically formalizing educational theories, researchers can identify underlying patterns, predict outcomes, and test hypotheses with a higher degree of precision and clarity. Mathematical modeling allows researchers to simulate these complex systems, uncover emergent properties, and explore how various factors interact to influence educational outcomes [3]. By capturing the dynamic nature of education systems, mathematical models can provide insights into the underlying mechanisms driving learning, teaching, and educational change.

Mathematical models can be used to predict the outcomes of different educational interventions, policies, and practices, allowing policymakers, educators, and stakeholders to make informed decisions based on evidence and data. Advancing educational theories through mathematical modeling often involves interdisciplinary collaboration between researchers from diverse fields, including mathematics, computer science, psychology, sociology, and education. By bringing together expertise from multiple disciplines, interdisciplinary research teams can develop innovative modeling approaches, integrate insights from different domains, and address complex educational challenges from a holistic perspective [1, 4]. Interdisciplinary collaboration fosters cross-fertilization of ideas, methodologies, and best practices, leading to more robust and impactful research outcomes. Thus, advancing educational theories through mathematical modeling offers a powerful means of understanding, analyzing, and improving educational processes and outcomes. By harnessing the analytical power of mathematical modeling, researchers can contribute to the development of evidence-based educational theories, practices, and policies that promote student success, equity, and lifelong learning. This paper focused on such educational theories as information memory-processing theory, dynamic equilibrium theory, cooperative learning theory, Maslow motivation theory, Lewin's field theory and social learning theory.

2 Information memory-processing theory

The cognitive revolution of the 1950s and 1960s gave rise to the multi-store model of memory, or MSM. According to the theory put forth by Atkinson and Shiffrin in 1968 [5], environmental stimuli first arrive in sensory memory, where they can be registered for very short times before deteriorating or moving on to short-term memory (STM). The minimal amount of information that is truly in use at any given time is all that is contained in STM. At this point, verbal information is encoded in terms of sounds. According to Atkinson and Shiffrin, if memory traces in STM are not repeated (rehearsed), they can vanish in as little as 30 seconds. Practiced material is transferred to the long-term store, where it can stay indefinitely, albeit it may be lost there due to interference or deterioration. In view of the foregoing, we formulated a mathematical model of the information-memory processing approach as

envisaged by Atkinson and Shiffrin. The mathematical model is based on the schematic diagram shown in Fig. 1 and the list of variables is given in Table 1.

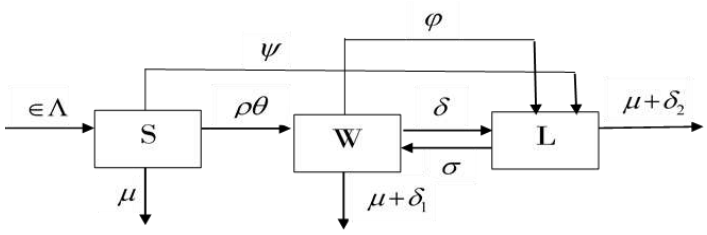


Fig. 1: Mathematical model flow diagram

Table 1: Model symbols and descriptions

Symbols	Description
S	Information in the sensory memory at time, t
W	Information in the short-term/working memory at time, t
L	Information in the long-term memory at time, t
Λ	Outside stimuli rate
θ	Initial processing rate
μ	Rate of forgetting, lost or interference
δ	Rate of transfer/progression/elaboration and organization into the LTM
σ	Rate of retrieval/reconstruction
ρ	Fraction of attention rate
ϵ	Fraction of outside stimuli rate
ψ	Attention rate
φ	Rehearsal rate
δ_1	Information loss rate due to displacement
δ_2	Information loss rate due to interference

Thus, putting the above formulations and assumptions together gives the following information memory-processing model, given by system of ordinary differential equations below:

$$\begin{cases} \dfrac{dS(t)}{dt} = \in \Lambda - \rho\theta S(t) - \psi S(t) - \mu S(t) \\ \dfrac{dW(t)}{dt} = (1-\rho)\theta S(t) - \sigma L(t) - (\delta + \delta_1 + \varphi + \mu) W(t) \\ \dfrac{dL(t)}{dt} = (\delta + \varphi) W(t) + \psi S(t) - (\sigma + \delta_2 + \mu) L(t) \end{cases} \tag{1.1}$$

For model (1.1) to be psychologically meaningful, it is important to prove that all its state variables are non-negative for all time (t). In other words, the solutions of model (1.1) with positive initial data will remain positive for all $t \geq 0$. Since model (1.1) monitors the human memory processing, all the

state variables and parameters of the model are non-negative. Consider the psychologically feasible region

$$D=\left\{S,W,L\in\mathbb{R}_{+}^{3}:N\leq\frac{\in\Lambda}{\mu}\right\}. \tag{1.2}$$

It can be shown that the set D is a positively invariant set and a global attractor of this system. That is, any phase trajectory initiated anywhere in the non-negative region $\mathbb{R}_{+}^{3}$ of the phase space eventually enters the region D and remains in D thereafter. The region D is positively invariant for model (1.1). It follows from the first equation of the system (1.1), that

$$\begin{cases}\dfrac{dS(t)}{dt}=\in\Lambda-\rho\theta S(t)-\psi S(t)-\mu S(t)\\ \dfrac{d}{dt}\left\{S(t)\exp\left[(\rho\theta+\psi+\mu)t\right]\right\}=(\in\Lambda)\exp\left[(\rho\theta+\psi+\mu)t\right]\\ S(t_1)\exp\left[(\rho\theta+\psi+\mu)t\right]-S(0)=\int_0^{t_1}(\in\Lambda)\exp\left[(\rho\theta+\psi+\mu)\,p\right]dp\\ S(t_1)=S(0)\exp\left[-(\rho\theta+\psi+\mu)t_1\right]+\exp\left[-(\rho\theta+\psi+\mu)t_1\right]\\ \times\int_0^{t_1}(\in\Lambda)\exp\left[(\rho\theta+\psi+\mu)\,p\right]dp>0\end{cases}$$

It can similarly be shown that $W>0$ and $L>0$ for all $t>0$. Now, the rate of change of the total memory ($N=S+W+L$) is given by

$$\frac{dN(t)}{dt}=\in\Lambda-(2\rho-1)\theta S(t)-\delta_1 W(t)-\delta_2 L(t)-\mu N(t) \tag{1.3}$$

Since the right-hand side of (1.3) is bounded $\in\Lambda-\mu N(t)$, a standard comparison theorem can be used to show that

$$N(t)\leq N(0)e^{-\mu t}+\frac{\in\Lambda}{\mu}\left(1-e^{-\mu t}\right). \tag{1.4}$$

In particular, if $N(0)\leq\mu$, then $N(t)\leq\mu$. Thus, D is positively invariant. Hence, no solution path leaves through any boundary of D and it is sufficient to consider the dynamics of model (1.1) in D. In this region, the model can be considered as being mathematically and psychologically well posed. Equilibrium analysis gives the fixed points, or equilibrium solutions, the values of state variables for which the system (1.1) will no longer change. At that time the rate of change are equated to zero. On the other hand, local stability analysis helps us to determine the dynamics of different memory stages near the equilibrium solutions. To achieve this, we compute the linearization of the system (1.1), which we obtained from the Jacobian matrix of the system (1.1). The Jacobian of the system (1.1) is given as:

$$J=\begin{pmatrix}-(\rho\theta+\psi+\mu) & 0 & 0\\ (1-\rho)\theta & -(\delta+\delta_1+\varphi+\mu) & \sigma\\ \psi & (\delta+\varphi) & -(\sigma+\delta_2+\mu)\end{pmatrix} \tag{1.5}$$

A memory becomes information-free at the point $(S_0,T_0,L_0)=\left(\frac{\epsilon\Lambda}{\mu},0,0\right)$. We refer to this point as the information-free equilibrium (IFE). There is neither outside stimuli (information) in the STM nor LTM. The expected information size at this state will simply be the solution of $\frac{dS(t)}{dt}=\epsilon\Lambda-\mu S$. Solving the equation gives $S(t)=\frac{\epsilon\Lambda}{\mu}+\left(S_0-\frac{\epsilon\Lambda}{\mu}\right)e^{-\mu t}$, where S_0 is the initial information in the sensory register. It is easy to see that as $t\to\infty, S(t)\to\frac{\epsilon\Lambda}{\mu}$, which is the asymptotic information size. Hence, the entire information is wholly in the sensory register. Now, what happen if the

information that enters into the memory is not recognized and attended or organized? Will the information-free state be achieved? Therefore, we carry out the stability analysis for the steady state. Again, we compute the Jacobian matrix of the system at IFE to obtain:

$$J_0 = \begin{pmatrix} -(\rho\theta+\psi+\mu) & 0 & 0 \\ (1-\rho)\theta & -(\delta+\delta_1+\varphi+\mu) & \sigma \\ \psi & (\delta+\varphi) & -(\sigma+\delta_2+\mu) \end{pmatrix}$$

On the roots of the characteristic equation:

$$\begin{aligned}\lambda^3+\mu^3-\left(-\rho\theta-\psi-3\mu-\delta-2\delta_1-\varphi-\sigma\right)\lambda^2-\Big(&-2\delta\mu-\delta\psi-2\delta\sigma-\delta\rho\theta-\delta\delta_1\\&-3\mu^2-2\mu\psi-2\mu\sigma-2\mu\rho\theta-2\mu\varphi-4\mu\delta_1-\psi\sigma-\psi\varphi-2\psi\delta_1-\sigma\rho\theta-2\sigma\varphi\\&-\sigma\delta_1-\rho\theta\varphi-2\rho\theta\delta_1-\varphi\delta_1-\delta_1^2\Big)\lambda+\delta\mu^2+\mu^2\psi+\mu^2\sigma+\mu^2\rho\theta+\mu^2\varphi+2\mu^2\delta_1\\&+\mu\delta_1^2+\psi\delta_1^2+\rho\theta\delta_1^2+\delta\mu\psi+2\delta\mu\sigma+\delta\mu\rho\theta+\delta\mu\delta_1+2\delta\psi\sigma+\delta\psi\delta_1+2\delta\sigma\rho\theta\\&+\delta\rho\theta\delta_1+\mu\psi\sigma+\mu\psi\varphi+2\mu\psi\delta_1+\mu\sigma\rho\theta+2\mu\sigma\varphi+\mu\sigma\delta_1+\mu\rho\theta\varphi+2\mu\rho\theta\delta_1\\&+\mu\varphi\delta_1+2\psi\sigma\varphi+\psi\sigma\delta_1+\psi\varphi\delta_1+2\sigma\rho\theta\varphi+\sigma\rho\theta\delta_1+\rho\theta\varphi\delta_1\end{aligned}$$

The eigenvalues are obtained as:

$$\lambda_1 = -(\rho\theta+\psi+\mu)$$

$$\lambda_{2,3} = \frac{1}{2}\left[-(\delta+\delta_1+\varphi+\mu)\pm\sqrt{(\delta+\delta_1+\varphi+\mu)^2-4\big((\delta+\delta_1+\varphi+\mu)(\sigma+\delta_2+\mu)-\sigma(\delta+\varphi)\big)}\right]$$

$$\lambda_2 = \frac{1}{2}\left[-(\delta+\delta_1+\varphi+\mu)-\sqrt{(\delta+\delta_1+\varphi+\mu)^2-4\big((\delta+\delta_1+\varphi+\mu)(\sigma+\delta_2+\mu)-\sigma(\delta+\varphi)\big)}\right]$$

For λ_2 to be negative, this implies that

$$\big((\delta+\delta_1+\varphi+\mu)(\sigma+\delta_2+\mu)-\sigma(\delta+\varphi)\big)<0$$

$$\Rightarrow \frac{(\delta+\delta_1+\varphi+\mu)(\sigma+\delta_2+\mu)}{\sigma(\delta+\varphi)}<1$$

where

$$\frac{(\delta+\delta_1+\varphi+\mu)(\sigma+\delta_2+\mu)}{\sigma(\delta+\varphi)} = I_0 \qquad (1.6)$$

This implies that $I_0-1<0$ or $I_0<1$, I_0 is called the basic information-processing number. This number is yet to be defined in the context of memory-processing but serves as a threshold. Hence, if $I_0<1$, the information-free equilibrium (IFE) is asymptotically stable. Therefore, information dies out with time, i.e., memory decay. This goes to show that, if the rate at which people are exposed to information and the rate of elaboration, organization and retrieval in memory are not enhanced, information size becomes asymptotically stable. In other words, if the quantity representing I_0 is less than unity, the information in the memory dies out with time; thereby, providing evidence to support the theory of memory decay.

To understand system dynamics, exact model solution is determined. Note that exact solutions provide insights into the interactions and dependencies between variables within the system. They reveal how changes in one variable affect others and help uncover patterns and behaviours that might not be immediately obvious. Exact solutions enable accurate predictions of the future behaviour of the system or the state of the variables at any given time within the domain. This predictive ability is especially useful for making informed decisions and planning. Thus, the equation (4.15) are first-order linear ODEs, which can be solved via the IF technique. We obtain

$$
\begin{cases}
S(t)=\dfrac{\in\Lambda}{\rho\theta+\psi+\mu}+\left(S_0-\dfrac{\in\Lambda}{\rho\theta+\psi+\mu}\right)e^{-(\rho\theta+\psi+\mu)t} \ \ as\ t\to\infty,\ S(t)\to\dfrac{\in\Lambda}{\rho\theta+\psi+\mu} \\
W(t)=\left(\dfrac{\in\Lambda}{(\rho\theta+\psi+\mu)^2}e^{-(\rho\theta+\psi+\mu)t}+\left(S_0-\dfrac{\in\Lambda}{\rho\theta+\psi+\mu}\right)t\right)(1-\rho)\theta e^{-(\rho\theta+\psi+\mu)t} \\
-\sigma H(t)e^{-(\rho\theta+\psi+\mu)t}+ke^{-(\rho\theta+\psi+\mu)t} \ \ as\ t\to\infty,\ W(t)\to 0 \\
L(t)=(\delta+\varphi)\left[\dfrac{-\in\Lambda}{a^2(2a-b)}e^{-(2a-b)t}-\dfrac{(1-\rho)\theta}{a-b}(S_0-k_1)\left(t+\dfrac{1}{a-b}\right)e^{-(a-b)t}-G(t)-\dfrac{c_1}{a-b}e^{-(a-b)t}\right]e^{-bt} \\
+\psi\left(\dfrac{k_1}{b}e^{-bt}-\dfrac{S_0-k_1}{a-b}e^{-(a-b)t}\right)+c_2 \\
where\ \ a=\delta+\delta_1+\varphi+\mu;b=\sigma+\delta_2+\mu;k_1=\dfrac{\in\Lambda}{a};H(t)=\int L(t)e^{at}dt;G(t)=\sigma\int H(t)e^{-(a-b)t}dt \\
as\ t\to\infty,\ L(t)\to\infty\ \ provided\ \ b>a
\end{cases}
$$

As a result, the precise solutions of the differential equations system (1.1) provide a thorough and rigorous mathematical explanation of the interactions and behaviours of the system's variables. It is an effective instrument for understanding, theoretical investigation, and prediction in a variety of scientific, engineering, and mathematical domains. In actuality, though, memories can deteriorate and fade over time for a variety of reasons, such as interference, a lack of reinforcement, and the forgetting process itself. Not all of the data kept in long-term memory will always be available or undamaged over time. Although the theoretical notion that information stored in long-term memory may eventually reach infinity as time tends to infinity is thought-provoking, the above-mentioned practical constraints and limitations imply that this claim is not directly applicable in the real world. Rather, a variety of elements that interact with one another and with the passage of time affect memory capacity and retention. In conclusion, it is critical to understand the practical constraints and complexity of human memory and cognition, even though there are theoretical scenarios in which information in long-term memory could possibly accumulate as time approaches infinite. There are several facets and practical limitations to the link between time, memory, and information.

3 The dynamic equilibrium theory

The dynamic equilibrium theory of learning as envisaged by [28] states that the total information gain (say, N) is partly constant and partly decreases with N. That is, learning is as a result of dynamic equilibrium between information acquisition and loss. Mathematically, it is written as:

$$\frac{dN(t)}{dt}=p-qN(t) \qquad (2.1)$$

The equation gives the total information gain (N) at a point in time (t), where p and q are constants for a particular individual in a given learning situation. The constant p is a measure of the individual's aptitude for learning. The constant q is a measure of the probability of information being forgotten, and there is evidence that this is independent of the individual's aptitude [28]. Solving equation (2.1) using separation of variable method, we have the following analytical solution

$$N(t)=\frac{p}{q}+\left(N_0-\frac{p}{q}\right)e^{-qt} \qquad (2.2)$$

Now, as $t\to 0,\ N(t)\to N_0$ and as $t\to\infty,\ N(t)\to\frac{p}{q}$.

Equation (2.2) describes information gain dynamics. It tells us that the amount of information gain approaches the equilibrium value $\frac{p}{q}$. This is an indication that, an individual is capable of learning

a limited amount of information. That is, if one learned over an infinite amount of time, this individual would have approached his or her upper limit N_∞. This number is referred to as the capacity of a student to learn. However, an individual is capable of learning a very large amount of information and is difficult to determine the capacity of the person to learn [6]. Therefore, the major limitation of Hicklin's model is its disagreement with neurological findings and a set of experimental data due to forgetting function. A more realistic model is presented below. In our model, we modify equation (2.1) by proposing the probability of information being forgotten as a function of time and not a constant as envisaged by Hicklin. A study on a large set of experimental data found that long-term memory retention can be described by several mathematical functions that are in a good correlation with experimental data [7, 8]. Considering the properties of the functions and the analysis carried out in [7], the following function is chosen for the description of the forgetting process:

$$q(t) = ae^{-bt} + w(t) \tag{2.3}$$

where a is a constant associated with the quantity of information forgotten, the exponential term depicts the decaying form of forgetting in the memory as time progresses and b is the forgetting rate. This equation (2.3) shows that the effect of the acquisition tails off to (t) after some time, but not to zero or constant. In the present study, a modified dynamic equilibrium model of learning as envisaged by Hecklin is presented, as it takes into account one of the most important features of this theory-its exponential forgetting character. Thus, this model modification could be termed Hecklin-Obasi model of learning. The model equation due to Obasi [1] is given in (2.4) below:

$$\frac{dN(t)}{dt} = \alpha - \left(ae^{-bt} + w(t)\right)N(t) \tag{2.4}$$

where

$$w(t) = \begin{cases} \beta t + \gamma, \ function\ of\ time \\ w_0, otherwise \end{cases}$$

Solving equation (2.4) gives the integrating factor as:

$$IF = \exp\left(-\frac{a}{b}e^{-bt} + \frac{1}{2}\beta t^2 + \gamma t\right)$$

$$N(t)IF = \int \alpha IF dt$$

$$N(t)\exp\left(-\frac{a}{b}e^{-bt} + \frac{1}{2}\beta t^2 + \gamma t\right) = \int \alpha \exp\left(-\frac{a}{b}e^{-bt} + \frac{1}{2}\beta t^2 + \gamma t\right)dt \tag{2.5}$$

$$N(t) = \frac{\alpha t}{ae^{-bt} + \beta t + \gamma} + \left(N_0 - \frac{\alpha}{a+\gamma}\right)\exp(-1)\left(\frac{1}{2}\beta t^2 + \gamma t - \frac{a}{b}e^{-bt}\right)$$

$$as\ \ t \to \infty, N(t) \to \infty$$

All other things being equal, it appears that the solution to the model equation (2.4) validates the theory that a person can acquire a significant quantity of knowledge (taking into account the control of extraneous variables). This suggests that it becomes challenging to assess a person's learning capacity if they learnt over an endless period of time. Limits and the theoretical concept of infinite learning are related to the idea that if a person learns over an unlimited amount of time, it becomes difficult to determine their capacity to learn. This idea entails investigating what occurs when learning is prolonged indefinitely and how it affects our comprehension of human potential. The idea of a limit is used in analysis and mathematics to characterize how a function behaves as its input gets closer to a particular value, like infinity. Comparably, thinking about what would happen if someone learned over an endless period of time has intriguing implications for the field of learning. If an individual were to learn indefinitely, it suggests that they would have the opportunity to continually acquire new knowledge and skills. This implies an unlimited potential for learning and personal growth. Over an

infinite time span, the person would have the chance to accumulate an immense amount of knowledge. This accumulation could cover a vast array of subjects, from basic to highly specialized topics. Thus, the notion that determining an individual's capacity to learn becomes difficult over an infinite amount of time reflects the intricate interplay between the potential for lifelong learning and the limitations posed by factors such as diminishing returns, memory, specialization, and the finite nature of human existence. While infinite learning is an interesting theoretical concept, it's important to consider the practical implications and constraints that shape human learning and knowledge acquisition.

4 Cooperative learning theory

Cooperative learning theory is an educational approach that emphasizes collaborative and interactive learning among students. It is based on the idea that students working together in small groups can achieve better learning outcomes than when working individually. The theory draws on social interdependence and the positive interplay between individual and group goals [9]. Cooperative learning theory has roots in the work of several theorists, and it has evolved over time. One of the key figures associated with the development and popularization of cooperative learning is Dr. David W. Johnson and Dr. Roger T. Johnson, a husband-and-wife team of educational psychologists [10]. They have conducted extensive research on cooperative learning and are known for their contributions to the field. Cooperative learning is widely used in classrooms across various educational levels and disciplines. Its success relies on effective implementation, careful task design, and a supportive learning environment that encourages positive interdependence and individual accountability [11].

For the field of learning research to progress, the concept of quantifying and assessing knowledge, learning, etc., is crucial. Within education, this is a current problem. According to a quote from Lord Kelvin, educational psychology and pedagogy do not have to be imprecise fields of study [3]. Mathematical models, including differential equations, can be used to describe the dynamics of learning within a cooperative group. These models may consider factors such as the rate of knowledge transfer, individual learning rates, and the impact of collaboration on learning outcomes. The combination of mathematical models with insights from educational psychology provides a more comprehensive understanding of the dynamics within cooperative learning environments. Thus, cooperative learning is seen as a system of linear differential equation which relates a knowledge function to its derivatives. This brings us to a mathematical model for cooperative learning; let us take the example of three students, each of whose knowledge G, K, and R is quantified in terms of the estimated number of connected and unlinked ideas for a given lesson. $G(t)$, $K(t)$, and $R(t)$ are assumed to be functions of time expressed in weeks. Based on previous observations and experiences, the following assumptions are made by our cooperative learning model [3]:

i. The knowledge of each learner will increase at a rate that is proportional to the knowledge of the other learners;
ii. The knowledge of each learner may decrease at a rate that is proportional to its own amount of knowledge;
iii. The rate of change of knowledge for a learner has a constant component that measures the level of amiability (i.e., trust and friendliness) of that learner toward the others.

These assumptions lead to the system of linear differential equation (3.1) below:

$$\begin{cases} \dfrac{dG(t)}{dt} = \alpha K + \delta R - \rho G + r(s,h) \\ \dfrac{dK(t)}{dt} = \beta G + \eta R - \varphi K + s(r,h) \\ \dfrac{dR(t)}{dt} = \sigma K + \tau G - \upsilon R + h(r,s) \end{cases} \tag{3.1}$$

The variables and parameters of the model are described in Table 2 below.

Table 2: Description of variables and parameters of the model

Variable	Description
$G(t)$	Knowledge of first student at a time
$K(t)$	Knowledge of second student at a time
$R(t)$	Knowledge of third student at a time
α	Openness of first student to learning from second student
δ	Openness of first student to learning from third student
ρ	Learning decay rate of first student
β	Openness of second student to learning from first student
η	Openness of second student to learning from third student
φ	Learning decay rate of second student
σ	Openness of third student to learning from second student
τ	Openness of third student to learning from first student
υ	Learning decay rate of third student
r	First student's level of cordiality towards second & third students
s	Second student's level of cordiality towards first & third students
h	Third student's level of cordiality towards first & second students

The constants $\alpha, \delta, \rho, \beta, \eta, \varphi, \sigma, \tau, and\ \upsilon$ are non-negative but the numbers $r, s\ and\ h$ have any value: positive values for attitudes of trust for the other, and negative values for antagonism and aversion. In matrix notation, the case may be written as:

$$X' = AX + B$$

$$\begin{pmatrix} G'(t) \\ K'(t) \\ R'(t) \end{pmatrix} = \begin{pmatrix} -\rho & \alpha & \delta \\ \beta & -\varphi & \eta \\ \tau & \sigma & -\upsilon \end{pmatrix} \begin{pmatrix} G \\ K \\ R \end{pmatrix} + \begin{pmatrix} r \\ s \\ h \end{pmatrix}, A = \begin{pmatrix} -\rho & \alpha & \delta \\ \beta & -\varphi & \eta \\ \tau & \sigma & -\upsilon \end{pmatrix} \tag{3.2}$$

We see that the nature of the solutions of the system will depend on the eigenvalues of the matrix A. The determinant, $det(A)$ and trace, $tr(A)$ of this matrix play a crucial role in determining the stability of the solutions. If $det(A) > 0$ and $tr(A) < 0$, the system is stable. These criteria are derived from the fact that the signs of the eigenvalues influence the stability of the system [12, 1]. Positive real parts of eigenvalues are associated with instability, while negative real parts suggest stability. The determinant and trace help in identifying these signs and making predictions about the system's behaviour. On the roots of the characteristic equation:

$$\lambda^3 + (\upsilon + \varphi + \rho)\lambda^2 + \big((\rho + \upsilon)\varphi - \sigma\eta + \upsilon\rho - \tau\delta - \beta\alpha\big)\lambda + (\rho\upsilon - \delta\tau)\varphi - \eta\rho\sigma - \alpha\eta\tau - \alpha\beta\upsilon - \beta\delta\sigma = 0 \tag{3.3}$$

with the determinant and trace of matrix A obtained as:

$$\begin{cases} \det(A) = \sigma(\beta\delta + \eta\rho) + (\alpha\beta - \rho\varphi)\upsilon + \tau(\alpha\eta + \delta\varphi) \\ tr(A) = -(\upsilon + \varphi + \rho) \end{cases} \tag{3.4}$$

It can easily be seen from (3.4) that $tr(A) < 0$, but if $\alpha\beta - \rho\varphi > 0$ then $det(A) > 0$, which implies stability. That is, if both learners mildly like each other ($r > 0, s > 0 \; and \; h > 0$) and if the product of their knowledge decay indices is less than the product of their receptivity to learning from each other, there will be joint increased learning. However, if $\alpha\beta - \rho\varphi < 0$, and ($r < 0, s < 0 \; and \; h < 0$) there will be retrogression. That is, first student and second student do not like each other and if the product of their knowledge decay indices is greater than the product of the indices of their receptivity to each other's learning, it will lead to retrogression. Their unpracticed or unutilized knowledge will decay.

In the context of cooperative learning, stability often refers to the ability of the system to reach and maintain a desirable state, such as a state where all individuals in the group have acquired and retained knowledge or skills. Consider a simple cooperative learning scenario where individuals positively influence each other's learning, and the matrix A has eigenvalues with negative real parts. In this case, the cooperative learning system is stable, and the group is likely to converge to a state where all individuals have acquired the desired knowledge or skills. Note that stability suggests that the learning trajectories of individuals within the group are predictable and do not exhibit erratic behaviour. Predictability is desirable in educational settings to ensure a steady and effective learning process [3]. Cooperative learning often involves individual accountability and positive interdependence, where the success of one individual benefits the entire group. Systems that promote positive interdependence and individual accountability are more likely to be stable. Stability implies a balance in the interactions between individuals in the cooperative learning group. If the interactions are too competitive or too cooperative, it may lead to instability. It should be noted that stable systems tend to converge to an equilibrium state where learning is balanced and individuals have acquired the desired knowledge or skills. To further understanding system dynamics, exact model solution is determined. Thus, the system of equations (3.1) are first-order linear ODEs, which can be solved via the matrix method. We have that

$$\begin{cases} X = e^{At}X(0), \;\; X(0) = \begin{pmatrix} G_0 \\ K_0 \\ R_0 \end{pmatrix} \\ \dfrac{dX(t)}{dt} = AX(t) = \begin{pmatrix} -\rho & \alpha & \delta \\ \beta & -\varphi & \eta \\ \tau & \sigma & -\upsilon \end{pmatrix} \begin{pmatrix} G(t) \\ K(t) \\ R(t) \end{pmatrix}, \;\; X(t) = e^{At} \begin{pmatrix} G_0 \\ K_0 \\ R_0 \end{pmatrix}, \; but \\ e^{At} = 1 + At + \dfrac{A^2}{2!}t^2 + \dfrac{A^3}{3!}t^3 + \ldots \end{cases}$$

$$\therefore e^{At} = \begin{pmatrix} 1 & 0 & 0 \\ 0 & 1 & 0 \\ 0 & 0 & 1 \end{pmatrix} + \begin{pmatrix} -\rho & \alpha & \delta \\ \beta & -\varphi & \eta \\ \tau & \sigma & -\upsilon \end{pmatrix} t + \frac{1}{2!}\begin{pmatrix} -\rho & \alpha & \delta \\ \beta & -\varphi & \eta \\ \tau & \sigma & -\upsilon \end{pmatrix}^2 t^2 + \frac{1}{3!}\begin{pmatrix} -\rho & \alpha & \delta \\ \beta & -\varphi & \eta \\ \tau & \sigma & -\upsilon \end{pmatrix}^3 t^3 + \ldots$$

$$= \begin{pmatrix} (1-\rho)t + \frac{1}{2}(\alpha\beta + \delta\tau + \rho^2)t^2 & \alpha t - \frac{1}{2}(\alpha\rho + \alpha\varphi + \delta\alpha)t^2 & \delta t + \frac{1}{2}(\alpha\eta - \delta\rho + \delta\upsilon)t^2 \\ \beta t + \frac{1}{2}(\eta\tau - \beta\rho - \beta\varphi)t^2 & (1-\varphi)t + \frac{1}{2}(\alpha\beta + \eta\sigma + \varphi^2)t^2 & \eta t + \frac{1}{2}(\beta\delta - \eta\upsilon - \eta\varphi)t^2 \\ \tau t + \frac{1}{2}(\beta\sigma - \rho\tau - \tau\upsilon)t^2 & \sigma t + \frac{1}{2}(\alpha\tau - \sigma\upsilon - \sigma\varphi)t^2 & (1-\upsilon)t + \frac{1}{2}(\delta\eta + \eta\sigma + \upsilon^2)t^2 \end{pmatrix}$$

$$\begin{cases} X = \begin{pmatrix} (1-\rho)t+\frac{1}{2}(\alpha\beta+\delta\tau+\rho^2)t^2 & \alpha t-\frac{1}{2}(\alpha\rho+\alpha\varphi+\delta\alpha)t^2 & \delta t+\frac{1}{2}(\alpha\eta-\delta\rho+\delta\upsilon)t^2 \\ \beta t+\frac{1}{2}(\eta\tau-\beta\rho-\beta\varphi)t^2 & (1-\varphi)t+\frac{1}{2}(\alpha\beta+\eta\sigma+\varphi^2)t^2 & \eta t+\frac{1}{2}(\beta\delta-\eta\upsilon-\eta\varphi)t^2 \\ \tau t+\frac{1}{2}(\beta\sigma-\rho\tau-\tau\upsilon)t^2 & \sigma t+\frac{1}{2}(\alpha\tau-\sigma\upsilon-\sigma\varphi)t^2 & (1-\upsilon)t+\frac{1}{2}(\delta\eta+\eta\sigma+\upsilon^2)t^2 \end{pmatrix} \begin{pmatrix} G_0 \\ K_0 \\ R_0 \end{pmatrix} \\ X(t) \equiv (G(t),K(t),R(t)) = \begin{pmatrix} G_0(1-\rho)t+\frac{1}{2}G_0(\alpha\beta+\delta\tau+\rho^2)t^2+K_0\alpha t-\frac{1}{2}K_0(\alpha\rho+\alpha\varphi+\delta\alpha)t^2+R_0\delta t+\frac{1}{2}R_0(\alpha\eta-\delta\rho+\delta\upsilon)t^2 \\ G_0\beta t+\frac{1}{2}G_0(\eta\tau-\beta\rho-\beta\varphi)t^2+K_0(1-\varphi)t+\frac{1}{2}K_0(\alpha\beta+\eta\sigma+\varphi^2)t^2+R_0\eta t+\frac{1}{2}R_0(\beta\delta-\eta\upsilon-\eta\varphi)t^2 \\ G_0\tau t+\frac{1}{2}G_0(\beta\sigma-\rho\tau-\tau\upsilon)t^2+K_0\sigma t+\frac{1}{2}K_0(\alpha\tau-\sigma\upsilon-\sigma\varphi)t^2+R_0(1-\upsilon)t+\frac{1}{2}R_0(\delta\eta+\eta\sigma+\upsilon^2)t^2 \end{pmatrix} \end{cases}$$

Therefore, the solution of the system of equations (1) is obtained as:

$$\begin{cases} G(t) = G_0(1-\rho)t+\frac{1}{2}G_0(\alpha\beta+\delta\tau+\rho^2)t^2+K_0\alpha t-\frac{1}{2}K_0(\alpha\rho+\alpha\varphi+\delta\alpha)t^2+R_0\delta t+\frac{1}{2}R_0(\alpha\eta-\delta\rho+\delta\upsilon)t^2+\mathrm{O}(t^3) \\ K(t) = G_0\beta t+\frac{1}{2}G_0(\eta\tau-\beta\rho-\beta\varphi)t^2+K_0(1-\varphi)t+\frac{1}{2}K_0(\alpha\beta+\eta\sigma+\varphi^2)t^2+R_0\eta t+\frac{1}{2}R_0(\beta\delta-\eta\upsilon-\eta\varphi)t^2+\mathrm{O}(t^3) \\ R(t) = G_0\tau t+\frac{1}{2}G_0(\beta\sigma-\rho\tau-\tau\upsilon)t^2+K_0\sigma t+\frac{1}{2}K_0(\alpha\tau-\sigma\upsilon-\sigma\varphi)t^2+R_0(1-\upsilon)t+\frac{1}{2}R_0(\delta\eta+\eta\sigma+\upsilon^2)t^2+\mathrm{O}(t^3) \end{cases}$$

$as\ t\to\infty, G(t)\to\infty, K(t)\to\infty, R(t)\to\infty$

The exact solutions above show the idea that knowledge of students in cooperative learning could theoretically approach infinity as time tends to infinity. This indicates that there is a situation or condition described as "unbounded in time" which leads to a consequence of "unleashed" increased learning for the learners. This means a growth or enhancement in the process of acquiring knowledge or skills. Thus, the result of a situation being "unbounded in time" is that it allows for a significant and unrestrained increase in learning for the individuals involved. This might imply that without time constraints or limitations, learners are able to explore, absorb, and acquire knowledge in a more effective or accelerated manner. The use of "unleashed" suggests a kind of freedom or release that enables a fuller and more extensive learning experience.

Therefore, the mathematical formulation provides a theoretical framework for exploring the cooperative theory of learning in a controlled and abstract manner. The study indicates that the mathematical model proposed for the cooperative theory of learning demonstrates a high degree of accuracy in predicting learning outcomes within cooperative learning environments. The model has successfully captured the complex interactions and dynamics involved in collaborative learning settings. The mathematical formulations have allowed for a deeper understanding of the dynamics between individual and group learning. The study highlights how individual contributions impact the overall group learning process and vice versa, providing a nuanced perspective on the interplay between individual and collective knowledge acquisition. The mathematical model and findings from this paper have direct implications for educational practices. Educators can use the insights to design and implement cooperative learning activities that are not only pedagogically sound but also backed by quantitative evidence supporting their effectiveness.

5 Abraham Maslow's motivation theory

Abraham Maslow's motivation theory, often represented as Maslow's Hierarchy of Needs, outlines a hierarchical model of human needs, with each level building upon the previous one. Abraham Maslow proposed a hierarchical model of human needs, arranged in a pyramid. According to [13], individuals are motivated to fulfill basic physiological needs (such as food and shelter) before progressing to higher-level needs like safety, belongingness, esteem, and self-actualization. This theory, introduced by Maslow in the mid-20th century, is not specifically focused on learning but provides a framework for understanding human motivation, including aspects related to education and learning [14]. Maslow's Hierarchy of Needs has since become a foundational concept in psychology and education, influencing discussions on motivation, human development, and the design of effective learning environments [15]. While Maslow did not specifically focus on education in his original works, educators and psychologists have applied and adapted his theory to better understand and address the motivational aspects of the learning process [16]. We can attempt to create a simplified mathematical model inspired by the theory. Let us consider a system of differential equations that represent the dynamics of the hierarchy of needs:

$$\begin{cases} \frac{dP(t)}{dt} = -\alpha P(t) \\ \frac{dS(t)}{dt} = \beta P(t) - \delta S(t) \\ \frac{dB(t)}{dt} = \phi S(t) - \rho B(t) \\ \frac{dE(t)}{dt} = \varphi B(t) - \eta E(t) \\ \frac{dA(t)}{dt} = \sigma E(t) \end{cases} \tag{4.1}$$

The first equation represents the rate of change of physiological needs (P), indicating a natural decrease over time without external inputs. The second equation represents the dynamics of safety needs. Safety needs (S) increase when physiological needs (P) are satisfied but decrease naturally over time without further inputs. The third equation describes Belongingness and love needs (B) which increase when safety needs (S) are satisfied but decrease naturally over time without further inputs. In the fourth equation, esteem needs (E) increase when belongingness and love needs (B) are satisfied but decrease naturally over time without further inputs. The fifth equation represents the dynamics of Self-actualization (A) which increases when esteem needs (E) are satisfied. In these equations: $P(t), S(t), B(t), E(t), and\ A(t)$ represent the levels of physiological needs, safety needs, belongingness and love needs, esteem needs, and self-actualization, respectively. The values of $\alpha, \beta, \delta, \phi, \rho, \varphi, \eta, \sigma$ are positive constants representing the impact of one need level on the rate of change of the next. These equations attempt to capture the idea that the satisfaction of one level of need contributes positively to the next level while recognizing that needs naturally decrease over time if not continuously satisfied. In matrix notation, the case may be written as:

$$X'(t) = AX(t)$$

$$\begin{pmatrix} P'(t) \\ S'(t) \\ B'(t) \\ E'(t) \\ A'(t) \end{pmatrix} = \begin{pmatrix} -\alpha & 0 & 0 & 0 & 0 \\ \beta & -\delta & 0 & 0 & 0 \\ 0 & \phi & -\rho & 0 & 0 \\ 0 & 0 & \varphi & -\eta & 0 \\ 0 & 0 & 0 & \sigma & 0 \end{pmatrix} \begin{pmatrix} P(t) \\ S(t) \\ B(t) \\ E(t) \\ A(t) \end{pmatrix}, A = \begin{pmatrix} -\alpha & 0 & 0 & 0 & 0 \\ \beta & -\delta & 0 & 0 & 0 \\ 0 & \phi & -\rho & 0 & 0 \\ 0 & 0 & \varphi & -\eta & 0 \\ 0 & 0 & 0 & \sigma & 0 \end{pmatrix} \tag{4.2}$$

We see that the nature of the solutions of the system will depend on the eigenvalues of the matrix A. On the roots of the characteristic equation:

$$\lambda^5+(\alpha+\delta+\rho+\eta)\lambda^4+(\alpha\delta+\alpha\eta+\alpha\rho+\delta\eta+\delta\rho+\eta\rho)\lambda^3 +(\alpha\delta\eta+\alpha\delta\rho+\alpha\eta\rho+\delta\eta\rho)\lambda^2+\eta\rho\delta\alpha\lambda=0 \tag{4.3}$$

with eigenvalues obtained as:

$$\lambda_{i,i=1,2,3,4,5}=\begin{pmatrix}0\\-\rho\\-\eta\\-\delta\\-\alpha\end{pmatrix} \tag{4.4}$$

It can easily be seen from (4.4) that all the eigenvalues are negative except one which is zero. The zero eigenvalue can lead to different stability scenarios depending on the nature of the accompanying eigenvalues. If all other eigenvalues have negative real parts, the equilibrium is a stable center [1]. The negative eigenvalues indicate that small perturbations from the equilibrium will decay over time, and the system will return to the balanced state. In the context of the hierarchy of needs, negative eigenvalues would imply that, when the physiological, safety, and love and belonging needs are at an equilibrium point, any deviations from this point are dampened, and the individual tends to return to a balanced state in terms of these needs. This suggests a stable and adaptive psychological state where the person's needs are generally met and maintained over time. In practical terms, this means that individuals are inclined to return to a balanced state where their physiological, safety, and social needs are met.

Stability in the system implies that when an individual's needs are satisfied at a certain level, they are more likely to maintain a state of well-being. The negative eigenvalues reflect a tendency for individuals to maintain a balanced and satisfied state in terms of their needs, fostering psychological well-being. Negative eigenvalues suggest that the system is adaptive and resilient to perturbations. In the face of external or internal challenges, individuals tend to return to a stable state. This aligns with Maslow's idea that individuals have an inherent drive for self-actualization and growth, and negative eigenvalues indicate a capacity to adapt and recover from disruptions. The hierarchy of needs is characterized by the transition from lower-level needs to higher-level needs as lower-level needs are satisfied. Individuals, having satisfied lower-level needs, are more likely to progress to addressing higher-level needs, such as esteem and self-actualization, in a stable manner. To further understand the system dynamics, exact model solution is determined. Thus, the system of equations (4.1) are first-order linear ODEs, which can be solved via the integrating factor method. Therefore, the exact solutions of the system of equations (4.1) is obtained as:

$$
\begin{cases}
P(t) = P_0 e^{-\alpha t},\ as\ t \to \infty,\ P(t) \to 0 \\
S(t) = \dfrac{P_0\beta}{\delta-\alpha} e^{(\delta-\alpha)t} + \left(S_0 + \dfrac{P_0\beta}{\delta-\alpha}\right) e^{-\delta t},\ as\ t \to \infty,\ \boldsymbol{S}(t) \to 0, \delta < \alpha \\
B(t) = \phi e^{-\beta t}\left[\dfrac{P_0\beta}{(\delta-\alpha)(\delta-\alpha+\beta)} e^{(\delta-\alpha+\beta)t} + \dfrac{1}{\beta-\delta}\left(S_0 + \dfrac{P_0\beta}{\delta-\alpha}\right) e^{(\beta-\delta)t}\right] + \left[B_0 - \phi\left(\dfrac{P_0\beta}{(\delta-\alpha)(\delta-\alpha+\beta)} + \dfrac{1}{\beta-\delta}\left(S_0 + \dfrac{P_0\beta}{\delta-\alpha}\right)\right)\right] e^{-\beta t},\ as\ t \to \infty,\ \boldsymbol{B}(t) \to 0 \\
E(t) = \varphi\phi\left[\dfrac{P_0\beta}{(\delta-\alpha)(\delta-\alpha+\beta)(\delta-\alpha+\eta)} e^{(\delta-\alpha+\eta)t} - \dfrac{1}{(\beta-\delta)(\delta-\eta)}\left(S_0 + \dfrac{P_0\beta}{\delta-\alpha}\right) e^{(\delta-\eta)t} - \dfrac{B_0}{\beta-\eta} e^{-(\beta-\eta)t} - \dfrac{\phi}{2\beta-\eta}\left(\dfrac{P_0\beta}{(\delta-\alpha)(\delta-\alpha+\beta)} + \dfrac{1}{\beta-\delta}\left(S_0 + \dfrac{P_0\beta}{\delta-\alpha}\right)\right) e^{-(2\beta-\eta)t}\right] \\
\quad + \left[E_0 - \varphi\phi\left(\dfrac{P_0\beta}{(\delta-\alpha)(\delta-\alpha+\beta)(\delta-\alpha+\eta)} - \dfrac{1}{(\beta-\delta)(\delta-\eta)}\left(S_0 + \dfrac{P_0\beta}{\delta-\alpha}\right) - \dfrac{B_0}{\beta-\eta} - \dfrac{\phi}{2\beta-\eta}\left(\dfrac{P_0\beta}{(\delta-\alpha)(\delta-\alpha+\beta)} + \dfrac{1}{\beta-\delta}\left(S_0 + \dfrac{P_0\beta}{\delta-\alpha}\right)\right)\right)\right] \\
as\ t \to \infty,\ \boldsymbol{E}(t) \to E^*,\ provided\ \delta-\alpha+\eta<0, \delta-\eta<0, \beta-\eta>0, 2\beta-\eta>0, \\
where \\
E^* = E_0 - \varphi\phi\left(\dfrac{P_0\beta}{(\delta-\alpha)(\delta-\alpha+\beta)(\delta-\alpha+\eta)} - \dfrac{1}{(\beta-\delta)(\delta-\eta)}\left(S_0 + \dfrac{P_0\beta}{\delta-\alpha}\right) - \dfrac{B_0}{\beta-\eta} - \dfrac{\phi}{2\beta-\eta}\left(\dfrac{P_0\beta}{(\delta-\alpha)(\delta-\alpha+\beta)} + \dfrac{1}{\beta-\delta}\left(S_0 + \dfrac{P_0\beta}{\delta-\alpha}\right)\right)\right) \\
A(t) = \sigma\varphi\phi\left[\dfrac{P_0\beta}{(\delta-\alpha)(\delta-\alpha+\beta)(\delta-\alpha+\eta)^2} e^{(\delta-\alpha+\eta)t} - \dfrac{1}{(\beta-\delta)(\delta-\eta)^2}\left(S_0 + \dfrac{P_0\beta}{\delta-\alpha}\right) e^{(\delta-\eta)t} + \dfrac{B_0}{(\beta-\eta)^2} e^{-(\beta-\eta)t} + \dfrac{\phi}{(2\beta-\eta)^2}\left(\dfrac{P_0\beta}{(\delta-\alpha)(\delta-\alpha+\beta)} + \dfrac{1}{\beta-\delta}\left(S_0 + \dfrac{P_0\beta}{\delta-\alpha}\right)\right) e^{-(2\beta-\eta)t}\right] \\
\quad + \left[E_0 - \varphi\phi\left(\dfrac{P_0\beta}{(\delta-\alpha)(\delta-\alpha+\beta)(\delta-\alpha+\eta)} - \dfrac{1}{(\beta-\delta)(\delta-\eta)}\left(S_0 + \dfrac{P_0\beta}{\delta-\alpha}\right) - \dfrac{B_0}{\beta-\eta} - \dfrac{\phi}{2\beta-\eta}\left(\dfrac{P_0\beta}{(\delta-\alpha)(\delta-\alpha+\beta)} + \dfrac{1}{\beta-\delta}\left(S_0 + \dfrac{P_0\beta}{\delta-\alpha}\right)\right)\right)\right] t \\
\quad + A_0 - \sigma\varphi\phi\left[\dfrac{P_0\beta}{(\delta-\alpha)(\delta-\alpha+\beta)(\delta-\alpha+\eta)^2} - \dfrac{1}{(\beta-\delta)(\delta-\eta)^2}\left(S_0 + \dfrac{P_0\beta}{\delta-\alpha}\right) + \dfrac{B_0}{(\beta-\eta)^2} + \dfrac{\phi}{(2\beta-\eta)^2}\left(\dfrac{P_0\beta}{(\delta-\alpha)(\delta-\alpha+\beta)} + \dfrac{1}{\beta-\delta}\left(S_0 + \dfrac{P_0\beta}{\delta-\alpha}\right)\right)\right] \\
as\ t \to \infty,\ \boldsymbol{A}(t) \to A^*,\ provided\ \delta-\alpha+\eta<0, \delta-\eta<0, \beta-\eta>0, 2\beta-\eta>0, \\
where \\
A^* = A_0 - \sigma\varphi\phi\left[\dfrac{P_0\beta}{(\delta-\alpha)(\delta-\alpha+\beta)(\delta-\alpha+\eta)^2} - \dfrac{1}{(\beta-\delta)(\delta-\eta)^2}\left(S_0 + \dfrac{P_0\beta}{\delta-\alpha}\right) + \dfrac{B_0}{(\beta-\eta)^2} + \dfrac{\phi}{(2\beta-\eta)^2}\left(\dfrac{P_0\beta}{(\delta-\alpha)(\delta-\alpha+\beta)} + \dfrac{1}{\beta-\delta}\left(S_0 + \dfrac{P_0\beta}{\delta-\alpha}\right)\right)\right]
\end{cases}
$$

From the exact solutions, the tendency of physiological, safety, belongingness and love, esteem, and self-actualization needs to approach zero or equilibrium values indicates a long-term stability in the system. Individuals in the model reach a balanced state where their various needs, spanning from basic survival to higher-level self-fulfillment, are either completely satisfied or in a state of sustained equilibrium. The result suggests that, over time, individuals progress through Maslow's hierarchy of needs and eventually reach a state where the pursuit of these needs becomes less dominant. Basic physiological and safety needs tend to zero, indicating that individuals achieve a stable state of physical well-being and security. Meanwhile, higher-level needs like belongingness, esteem, and self-actualization tend to equilibrium values, suggesting a sustained and balanced pursuit of social connection, recognition, and personal growth.

The findings imply that individuals in the model adapt to their environments and find satisfaction in the fulfillment of their diverse needs. As basic needs are met, the focus shifts to higher-level needs, leading to a dynamic and evolving psychological state. The tendency of self-actualization needs to approach equilibrium values indicates that individuals, even in a state of equilibrium, continue to experience personal growth and pursue self-fulfillment. This aligns with Maslow's concept of self-actualization as an ongoing process of realizing one's potential. This goes to show that individuals have a natural inclination to maintain a stable and satisfied state, adapting to changing circumstances while progressing through the hierarchy of needs. This stability aligns with the notion that individuals strive for fulfillment and self-actualization in a resilient and balanced manner. The result suggests a long-term stability and adaptation in the modeled hierarchy of needs. Individuals reach a balanced state where basic needs are satisfied, and higher-level needs are pursued in a sustainable and evolving manner. The exact solutions highlight the dynamic and continuous nature of human motivation and well-being as individuals progress through the hierarchy over an extended period.

6 Lewin's Field Theory

Lewin's Field Theory, developed by the psychologist Kurt Lewin [17], is a psychological framework that emphasizes the importance of considering the totality of influences on an individual's behaviour. Lewin's Field Theory is particularly relevant to social psychology and understanding the dynamics of social environments. This theory was influential in shaping the way psychologists and researchers approach the study of human behaviour [18]. Key concepts and principles of Lewin's Field Theory include: life space, psychological field, force field analysis, equilibrium and change. Lewin introduced the concept of "life space," which refers to the internal psychological environment of an individual. It encompasses all the psychological influences and experiences that shape a person's thoughts, feelings, and behaviours. The psychological field is the totality of influences acting on an individual at a given time. It includes both the external environment and the individual's internal psychological state. According to [17], behaviour is a function of the psychological field.

$$B = f(P, E) \tag{5.1}$$

One of the fundamental equations associated with Lewin's Field Theory is equation (5.1), where B represents behaviour, P represents the person's psychological state, and E represents the external environment. This equation highlights that behaviour is a function of both the person and the environment. Lewin introduced the concept of force field analysis to describe the driving and restraining forces that influence behaviour. Driving forces propel an individual towards a particular behaviour, while restraining forces act as barriers or obstacles. Behaviour is seen as the result of the dynamic interplay between these opposing forces [19]. Lewin argued that individuals seek a state of equilibrium, where driving and restraining forces are balanced. Changes in behaviour occur when there is an imbalance in the force field, leading to a shift in the equilibrium. Lewin referred to the process of achieving change as "unfreezing" the existing equilibrium, making the desired change, and then "freezing" the new equilibrium [20]. Lewin's ideas influenced the development of action research, an approach that integrates research and practical action to address social issues. Action research involves collaboration between researchers and participants to understand and change social systems.

Lewin's Field Theory has had a lasting impact on the field of social psychology and organizational development. It provides a framework for understanding the complex interactions between individuals and their social environments, emphasizing the need to consider both internal and external factors when studying behaviour and implementing interventions [21]. The researcher can create a simplified mathematical representation inspired by the key concepts of Lewin's Field Theory. Let: $B(t)$ be behaviour at time t, $P(t)$ is psychological state at time t, and $E(t)$ is external environment at time t. The dynamics of Lewin's Field Theory are represented using a simple differential equation in (5.2) below:

$$\begin{cases} \dfrac{dP(t)}{dt} = \alpha\left(E(t) - P(t)\right) \\ \dfrac{dB(t)}{dt} = \beta P(t) \\ \dfrac{dE(t)}{dt} = 0 \end{cases} \tag{5.2}$$

Here, the first equation describes how the psychological state changes over time. The rate of change is proportional to the difference between the external environment and the current psychological state, α is a parameter that captures the influence of the external environment on the psychological state. $(E - P)$ represents the difference between the external environment and the

psychological state, indicating the driving or restraining forces. This equation suggests that the rate of change in an individual's psychological state is proportional to the difference between the external environment and the current psychological state. It reflects Lewin's idea that behaviour is influenced by both internal and external factors, and the psychological state seeks equilibrium with the environment [22]. The second equation models how behaviour changes over time. The rate of change is proportional to the psychological state. This suggests that behaviour is influenced by the current psychological state, with β determining the strength of this influence. The third equation assumes a constant external environment, implying that it does not change over time in this simple model. In matrix notation, the case may be written as:

$$X'(t) = AX(t)$$

$$\begin{pmatrix} P'(t) \\ B'(t) \\ E'(t) \end{pmatrix} = \begin{pmatrix} -\alpha & 0 & \alpha \\ \beta & 0 & 0 \\ 0 & 0 & 0 \end{pmatrix} \begin{pmatrix} P(t) \\ B(t) \\ E(t) \end{pmatrix} \tag{5.3}$$

On the roots of the characteristic equation:

$$\lambda^3 + \alpha\lambda^2 = 0 \Rightarrow \lambda = 0\,(twice),\ \lambda = -\alpha \tag{5.4}$$

Obtaining zero and negative eigenvalues in the system of equations describing Lewin's Field Theory carries significant implications for the stability and dynamics of the psychological system. Zero eigenvalues typically indicate that there are dimensions or directions in the psychological field where there is no change or movement. In the context of Lewin's Field Theory, this might suggest the presence of stable or unchanging aspects within the psychological system. These could represent elements that remain constant or have a long-term influence, contributing to a sense of stability or continuity in certain aspects of behaviour or mental processes. The negative eigenvalues would suggest that the psychological system is inherently stable. This stability could represent a tendency for individuals or groups to return to a certain psychological equilibrium over time, even when perturbed by external or internal factors.

To further understand the system dynamics, exact model solution is determined. An exact solution means that you can precisely determine the values of the variables over time or in a given state. It provides a comprehensive understanding of how the psychological field evolves and how individuals or groups respond to different influences [21]. They reveal how changes in one variable affect others and help uncover patterns and behaviours that might not be immediately obvious. An exact solution in the mathematical model of Lewin's Field Theory implies a clear and precise understanding of the system dynamics. Thus, the system of equations (5.2) are first-order linear ODEs, which can be solved via the integrating factor method. The exact solutions of the equation are given as:

$$\begin{cases} P(t) = k + (P_0 - k)e^{-\alpha t};\ as\ t \to \infty,\ P(t) \to k \\ B(t) = \beta\left(kt - \dfrac{1}{\alpha}(P_0 - k)e^{-\alpha t}\right) + B_0 + \dfrac{\beta}{\alpha}(P_0 - k);\ as\ t \to \infty,\ \boldsymbol{B}(t) \to \infty \\ E(t) = k,\ k\ is\ cons\tan t;\ as\ t \to \infty,\ \boldsymbol{E}(t) \to k \end{cases} \tag{5.5}$$

So, the implication of an exact solution is that it provides a solid foundation for understanding and manipulating the psychological dynamics described by Lewin's Field Theory, offering a more precise and actionable framework for studying and influencing human behaviour. The exact solution reflects the idea that behaviour and the external environment tend to reach a stable or equilibrium state over time, while the psychological state may not necessarily converge to a fixed value and can potentially become more complex or diverse as time progresses. The result that behaviour and external environment reaching a certain value suggests that, with time, individuals or groups tend to settle into specific patterns of behaviour and adapt to their external surroundings. It aligns with the notion of

psychological equilibrium or stability, where certain behavioural patterns become established and predictable over time [22]. On the other hand, the psychological state not converging to a certain value implies that the internal psychological dynamics may not settle into a stable equilibrium. Instead, the psychological state might continue to evolve, change, or diversify over time. This could be due to the complexity of internal factors, emotions, and cognitive processes that may not have a fixed endpoint. In essence, this observation underscores the dynamic and evolving nature of the psychological state in Lewin's Field Theory. It suggests that while external behaviours and environmental interactions may stabilize, the internal psychological landscape remains open-ended and may continuously unfold in various ways. This dynamic perspective aligns with Lewin's emphasis on understanding behaviour within a changing and interactive psychological field, highlighting the ongoing nature of personal and group development [23]. Thus, the mathematical results from Lewin's Field Theory suggest a system characterized by a balance of stability and dynamism, while stability is observed in behaviour and the external environment, the internal psychological landscape remains open-ended, continually evolving and possibly influenced by a variety of factors. Therefore, researchers and practitioners in psychology should consider the dynamic and evolving nature of the psychological state. Interventions and strategies may need to account for the potential for ongoing change and adaptation.

7 Social learning theory

Social learning theory (SLT), developed by psychologist Albert Bandura [24], is a comprehensive theory that emphasizes the importance of social interactions in learning. It proposes that individuals learn not only through direct experiences but also by observing others and modeling their behaviours, attitudes, and emotional reactions. Bandura's work expanded traditional behaviourist theories by integrating cognitive and social aspects into the learning process. The key concepts of social learning theory include: observational learning, modeling, reinforcement, attention, retention, reproduction, motivation, and self-efficacy [25]. Observational learning also known as modeling or vicarious learning occurs when individuals observe the actions and outcomes of others and incorporate this information into their own behaviours. Bandura's famous Bobo doll experiment demonstrated how children learned aggressive behaviours by observing adults. Modeling involves imitating the behaviours of role models or significant others. Individuals are more likely to emulate behaviours they perceive as rewarding or socially acceptable. For example, children may imitate the behaviours of parents, teachers, or peers. While traditional behaviourist theories emphasize external reinforcement, SLT suggests that reinforcement can be vicarious [26]. Individuals are motivated to imitate behaviours that result in positive outcomes for others. Conversely, observing negative consequences for certain behaviours may inhibit imitation. Bandura proposed a four-step process involved in observational learning. Individuals must pay attention to the model's behaviour and its consequences. They must remember the observed behaviour. Individuals must have the ability to reproduce the observed behaviour. Finally, individuals are more likely to imitate behaviours if they are motivated to do so, either through intrinsic or extrinsic factors. Central to social learning theory is the concept of self-efficacy, which refers to an individual's belief in their own ability to succeed in specific situations or accomplish tasks [27]. Bandura argued that self-efficacy influences motivation, behaviour, and resilience in the face of challenges.

Representing social learning theory using mathematics offers several advantages. Mathematical models provide a systematic framework for quantitatively analyzing the dynamics of social learning. By expressing SLT concepts in mathematical terms, researchers can conduct rigorous analyses, perform simulations, and make predictions about learning outcomes. Mathematics enables clear and precise formulation of SLT concepts, making them easier to understand and communicate.

Mathematical models can formalize complex relationships between variables, parameters, and processes involved in social learning. Mathematical modeling allows researchers to dissect and understand the underlying mechanisms driving social learning. By representing SLT in mathematical terms, researchers can identify key factors influencing learning outcomes and explore how they interact. Well-constructed mathematical models of SLT can yield predictive insights into learning behaviours and outcomes. Researchers can use simulations to explore hypothetical scenarios and assess the potential impact of interventions or changes in social contexts. In the words of [3], mathematics serves as a common language across disciplines, facilitating interdisciplinary integration of SLT with fields such as psychology, sociology, education, and computer science. Mathematical modeling encourages collaboration and exchange of ideas among researchers from diverse backgrounds. Mathematical models of SLT can inform the design of educational interventions and instructional strategies. By understanding the underlying mechanisms of social learning, educators can develop more effective approaches to teaching and fostering collaborative learning environments.

By leveraging mathematical tools and techniques, learning theorists can develop precise models, formulate hypotheses, conduct empirical studies, and derive insights into the mechanisms underlying learning processes and behaviour. Mathematics provides a rigorous framework for studying and understanding the complexities of learning theory, facilitating advancements in educational research and practice [3]. Therefore, representing social learning theory using mathematics enhances our understanding of the complex interplay between social interactions, cognitive processes, and learning outcomes. Mathematical modeling provides a powerful tool for exploring, analyzing, and advancing our knowledge of social learning phenomena. To develop a system of differential equations describing social learning theory, we need to consider the key components of this theory, which emphasize learning through observation, modeling, and social interaction. The model variables and parameters are defined in Table 3.

Table 3: Model variable and parameter descriptions

Variables	Descriptions
$\boldsymbol{L(t)}$	Level of learning or knowledge at time
$\boldsymbol{I(t)}$	Intensity of exposure to social interactions or observational learning at time.
Parameters	
$\boldsymbol{\alpha}$	Rate at which learning occurs through observation.
$\boldsymbol{\beta}$	Rate at which learning occurs through direct experience or instruction.
$\boldsymbol{\gamma}$	Rate at which forgetting occurs.
$\boldsymbol{\delta}$	Influence of reinforcement or feedback.

Based on these variables and parameters, we can formulate a system of differential equations describing the social learning theory as developed Albert Bandura:

$$\frac{dL(t)}{dt} = \alpha I(t) - \beta L(t) - \gamma L(t) \qquad (6.1)$$

This equation describes how the level of learning ($L(t)$) changes over time. Learning increases based on the intensity of exposure to social interactions ($I(t)$) with a rate proportional to α. Learning also decreases over time due to forgetting ($\gamma L(t)$) and through direct experience or instruction ($\beta L(t)$). Additionally, we can introduce a differential equation to model the intensity of exposure to social interactions ($I(t)$):

$$\frac{dI(t)}{dt} = \delta\big(L(t) - I(t)\big) \qquad (6.2)$$

This equation describes how the intensity of exposure to social interactions changes over time. It depends on the difference between the level of learning ($L(t)$) and the current intensity of exposure to social interactions ($I(t)$), with a rate proportional to δ. Thus, putting the two equations together we have

$$\begin{cases} \dfrac{dL(t)}{dt} = \alpha I(t) - \beta L(t) - \gamma L(t) \\ \dfrac{dI(t)}{dt} = \delta\left(L(t) - I(t)\right) \end{cases} \tag{6.3}$$

This system of differential equations captures the essence of social learning theory by modeling how learning evolves over time through observation, direct experience, forgetting, and feedback from social interactions. Adjustments and refinements can be made to this model to account for specific contexts and factors influencing social learning. In matrix notation, the case may be written as:

$$\begin{aligned} X'(t) &= AX(t) \\ \begin{pmatrix} L'(t) \\ I'(t) \end{pmatrix} &= \begin{pmatrix} -(\beta+\gamma) & \alpha \\ \delta & -\delta \end{pmatrix} \begin{pmatrix} L(t) \\ I(t) \end{pmatrix} \end{aligned} \tag{6.4}$$

We see that the nature of the solutions of the system will depend on the eigenvalues of the matrix A. The determinant, $det(A)$ and trace, $tr(A)$ of this matrix play a crucial role in determining the stability of the solutions. If $det(A) > 0$ and $tr(A) < 0$, the system is stable. These criteria are derived from the fact that the signs of the eigenvalues influence the stability of the system [12, 1]. Positive real parts of eigenvalues are associated with instability, while negative real parts suggest stability. The determinant and trace help in identifying these signs and making predictions about the system's behaviour. On the roots of the characteristic equation:

$$\lambda^2 + (\delta + \beta + \gamma)\lambda - \delta\alpha + \delta\beta + \delta\gamma = 0 \tag{6.5}$$

with the determinant and trace of matrix A obtained as:

$$\begin{cases} \det(A) = -\delta\alpha + \delta\beta + \delta\gamma \\ tr(A) = -(\delta + \beta + \gamma) \end{cases} \tag{6.6}$$

It can easily be seen from (6.6) that $tr(A) < 0$, but if $\beta + \gamma > \alpha$ then $det(A) > 0$, which implies stability. That is, if the sum of rate at which learning occurs through direct experience or instruction and the rate at which forgetting occurs is greater than the rate at which learning occurs through observation, there will be increased learning. In the context of social learning theory, stability in the system of differential equations implies that the behaviours or patterns modeled by the equations tend to settle down or remain consistent over time. When the system is stable, it suggests that the dynamics of learning and behaviour tend to reach an equilibrium or a steady state. In other words, the behaviours modeled by the equations do not wildly fluctuate or diverge from each other over time. Instead, they converge towards certain patterns or norms, reflecting the stability of the social learning process within the theoretical framework being studied. This finding suggests that the effectiveness of learning can be enhanced when the combined rate of learning from direct experience or instruction, along with the rate of forgetting, surpasses the rate of learning through observation. This underscores the importance of active learning approaches, such as hands-on practice, interactive instruction, and spaced repetition, in promoting deep understanding and long-term retention of knowledge and skills. By balancing direct experience with effective instructional techniques and reinforcement strategies, educators and learners can optimize the learning process and enhance educational outcomes.

The stability of social learning theory in the context of learning has several important implications. Stable social learning processes imply that individuals are likely to consistently adopt and exhibit behaviours that are learned from observing others in their social environment. This consistency can lead to the establishment and maintenance of social norms and cultural practices within a group or society. When social learning processes are stable, it becomes easier to predict how individuals will respond to different social cues or stimuli. This predictability can be valuable for educators, policymakers, and social scientists who seek to understand and influence behaviour within various social contexts. It facilitates the transmission of knowledge, skills, and cultural traditions across generations. When individuals reliably learn from their social environment, valuable information and practices can be passed down from one generation to the next, contributing to the continuity and evolution of society. More so, it can contribute to social cohesion by promoting shared values, beliefs, and behaviours within a group or community.

When individuals consistently learn from and imitate each other, it fosters a sense of belonging and solidarity, which can strengthen social bonds and cooperation. While stability implies consistency, it does not necessarily mean rigidity. Social learning processes can also be adaptive, allowing individuals and societies to respond to changing circumstances and environments. Stable social learning frameworks provide a foundation upon which new behaviours and innovations can be integrated and disseminated. A stable social learning system can enhance the resilience of individuals and communities by providing a reliable mechanism for acquiring knowledge and coping strategies in the face of challenges or adversity. Consistent learning from others can help individuals navigate uncertain or unfamiliar situations more effectively. Thus, the stability of social learning theory in learning underscores its significance as a fundamental mechanism through which individuals acquire knowledge, skills, and social behaviours within their cultural and social contexts. To further understand the system dynamics, exact model solution is determined. The system of equations (6.3) are first-order linear ODEs, which can be solved via the matrix method. We have that

$$X = e^{At}X(0),\ X(0) = \begin{pmatrix} L_0 \\ I_0 \end{pmatrix}$$

$$\begin{cases} \dfrac{dX(t)}{dt} = AX(t) = \begin{pmatrix} -(\beta+\gamma) & \alpha \\ \delta & -\delta \end{pmatrix}\begin{pmatrix} L(t) \\ I(t) \end{pmatrix},\ X(t) = e^{At}\begin{pmatrix} L_0 \\ I_0 \end{pmatrix},\ \textit{but} \\ e^{At} = 1 + At + \dfrac{A^2}{2!}t^2 + \dfrac{A^3}{3!}t^3 + \ldots \\ \therefore\ e^{At} = \begin{pmatrix} 1 & 0 \\ 0 & 1 \end{pmatrix} + \begin{pmatrix} -(\beta+\gamma) & \alpha \\ \delta & -\delta \end{pmatrix}t + \dfrac{1}{2!}\begin{pmatrix} -(\beta+\gamma) & \alpha \\ \delta & -\delta \end{pmatrix}^2 t^2 + \dfrac{1}{3!}\begin{pmatrix} -(\beta+\gamma) & \alpha \\ \delta & -\delta \end{pmatrix}^3 t^3 + \ldots \\ = \begin{pmatrix} 1-(\beta+\lambda)t + \dfrac{1}{2}\left((\beta+\gamma)^2 + \delta\alpha\right)t^2 & \alpha t - \dfrac{1}{2}(\beta+\gamma-\delta)\alpha t^2 \\ \delta t - \dfrac{1}{2}(\beta+\gamma-\delta)\delta t^2 & 1-\delta t + \dfrac{1}{2}(\alpha+\delta)\delta t^2 \end{pmatrix} \end{cases}$$

$$\begin{cases} X = \begin{pmatrix} 1-(\beta+\lambda)t+\frac{1}{2}\left((\beta+\gamma)^2+\delta\alpha\right)t^2 & \alpha t-\frac{1}{2}(\beta+\gamma-\delta)\alpha t^2 \\ \delta t-\frac{1}{2}(\beta+\gamma-\delta)\delta t^2 & 1-\delta t+\frac{1}{2}(\alpha+\delta)\delta t^2 \end{pmatrix}\begin{pmatrix} L_0 \\ I_0 \end{pmatrix} \\ X(t)\equiv(L(t),I(t)) = \begin{pmatrix} L_0-(\beta+\lambda)L_0 t+\frac{1}{2}L_0\left((\beta+\gamma)^2+\delta\alpha\right)t^2+I_0\alpha t-\frac{1}{2}I_0(\beta+\gamma-\delta)\alpha t^2 \\ L_0\delta t-\frac{1}{2}L_0(\beta+\gamma-\delta)\delta t^2+I_0(1-\delta t)+\frac{1}{2}I_0(\alpha+\delta)\delta t^2 \end{pmatrix} \end{cases}$$

Therefore, the solution of the system of equations (6.3) is obtained as:

$$\begin{cases} L(t) = L_0-(\beta+\lambda)L_0 t+\frac{1}{2}L_0\left((\beta+\gamma)^2+\delta\alpha\right)t^2+I_0\alpha t-\frac{1}{2}I_0(\beta+\gamma-\delta)\alpha t^2+\mathrm{O}(t^3) \\ I(t) = L_0\delta t-\frac{1}{2}L_0(\beta+\gamma-\delta)\delta t^2+I_0(1-\delta t)+\frac{1}{2}I_0(\alpha+\delta)\delta t^2+\mathrm{O}(t^3) \end{cases} \tag{6.7}$$

$as\ t\to\infty, \boldsymbol{L}(t)\to\infty, \boldsymbol{I}(t)\to\infty$

The exact solutions (6.7) above show the idea that level of learning or knowledge and the intensity of exposure to social interactions or observational learning could theoretically approach infinity as time tends to infinity. This suggests that, theoretically, there is no upper limit to the level of learning or knowledge that individuals can attain, nor to the intensity of exposure to social interactions or observational learning, given an infinite amount of time. Level of learning or knowledge refers to the depth and breadth of understanding that individuals can achieve in various domains, such as academic subjects, skills, or personal development. The finding suggests that as individuals engage in learning activities over an extended period, their level of knowledge can continue to grow indefinitely. This implies that there is always more to learn, discover, and understand, and that the process of learning is potentially limitless. It goes to show that social interactions and observational learning play crucial roles in the learning process. Through interactions with others, individuals can exchange ideas, perspectives, and information, which can enrich their understanding and stimulate further learning. Observational learning, where individuals learn by observing and imitating others, also contributes significantly to the acquisition of new skills and behaviours. The finding suggests that as individuals engage in more social interactions and observational learning experiences over time, the potential for learning increases without bounds.

Therefore, given an infinite amount of time, there is no limit to how much individuals can learn or how intensively they can engage in social interactions or observational learning. In other words, as time goes on indefinitely, the potential for learning and exposure to learning opportunities continues to grow without constraint. However, it is essential to note that while this finding provides an intriguing theoretical perspective on the potential for lifelong learning and continuous personal growth, it is practically impossible for individuals to have infinite time or resources for learning. In reality, people have finite lifespans, limited resources, and various constraints that affect their learning opportunities. Nonetheless, the idea that learning and exposure to learning experiences can continue to expand without limit underscores the importance of fostering a lifelong learning mindset and seeking out opportunities for growth and development throughout one's life.

8 Concluding remarks

This paper delves into the intersection of mathematical modeling and educational theory, exploring how mathematical frameworks have been instrumental in advancing our understanding of educational processes and pedagogical practices. Advancing educational theories through mathematical modeling offers several significant benefits and opportunities. This is because mathematical models provide a

precise and systematic framework for representing complex educational phenomena, allowing researchers to formalize theoretical concepts, relationships, and mechanisms in a clear and rigorous manner. This paper focused on such educational theories as information memory-processing theory, dynamic equilibrium theory, cooperative learning theory, Maslow motivation theory, Lewin's field theory and social learning theory. By employing mathematical models, researchers have been able to dissect complex educational phenomena, elucidate underlying mechanisms, and predict outcomes with a level of precision that traditional qualitative approaches often struggle to achieve.

References

[1] Obasi, C. (2023). Mathematical modeling of issues in educational research based on the theory of differential equations. Doctoral Thesis, Ignatius Ajuru University of Education, Port Harcourt.
[2] Ormrod, J.E. (2012). Human learning (6th ed.). Boston: Pearson.
[3] Fadul, J.A. (2006). Mathematical formulations of learning based on ten learning principles. International Journal of Learning, 13(6), 140-151.
[4] Klang, N., Karlsson, N., Kilborn, W., Eriksson, P. & Karlberg, M. (2021). Mathematical problem-solving through cooperative learning: The importance of peer acceptance and friendships. Front. Educ. 6:710296. doi: 10.3389/feduc.2021.710296
[5] Atkinson, R.C. & Shiffrin, R.M. (1968). Human memory: A proposed system and its control processes. In K.W. Spence & J.T. Spence (Eds.), the psychology of learning and motivation: Advances in research and theory. New York: Academic Press.
[6] Carson, B (2015). You have a brain: A teen's guide to think big. Michigan: Zondervan.
[7] Rubin, D.C & Wenzel, A.E (1996). One hundred years of forgetting: A quantitative description of retention. Psychological Review, 103(4), 743-760.
[8] Altmann, E. M. & Gray, W. D. (2002). Forgetting to remember: The functional relationship of decay and interference. Psychological Science, 13(1), 27-33.
[9] Davidson, N. & Major, C. H. (2014). Boundary crossings: Cooperative learning, collaborative learning, and problem-based learning. J. Excell. Coll. Teach. 25 (3-4), 7.
[10] Johnson, D. W., Johnson, R. T., & Johnson Holubec, E. (1993). Cooperation in the classroom. Gurgaon: Interaction Book Company.
[11] Klang, N., Olsson, I., Wilder, J., Lindqvist, G., Fohlin, N., & Nilholm, C. (2020). A cooperative learning intervention to promote social inclusion in heterogeneous classrooms. Front. Psychol. 11, 586489. doi:10.3389/fpsyg.2020.586489
[12] Obasi, C. & Mbah, G.C.E (2019). On the stability analysis of a mathematical model of Lassa fever disease dynamics. Journal of the Nigerian Society for Mathematical Biology (JNSMB), 2(1), 135-144.
[13] Maslow, A. H. (1943). A theory of human motivation. Psychological Review, 50, 370-396.
[14] Maslow, A. H. (1968). Toward a psychology of being. New York, NY: D. Van Nostrand Company.
[15] Young, P. T. (1936). Motivation of behaviour. New York: John Wiley & Sons.
[16] Tay, L., & Diener, E. (2011). Needs and subjective well-being around the world. Journal of Personality and Social Psychology, 101(2), 354-365.
[17] Lewin, K. (1935). A dynamic theory of personality: Selected papers. New York, NY: McGraw-Hill.
[18] Lewin, K. (1936). Principles of topological psychology. New York, NY: McGraw-Hill.
[19] Deutsch, M. (1968). Field theory in social psychology. In Lindzey G., Aronson E. (Eds.), The handbook of social psychology (Vol. 1, 2nd ed., pp. 412-487). Reading, MA: Addison-Wesley.

[20] Cummings, S., Bridgman, T. & Brown, K. G. (2016). Unfreezing change as three steps: Rethinking Kurt Lewin's legacy for change management. Human Relations, 69, 33-60.
[21] Burnes, B. & Cooke, B. (2013). Kurt Lewin's field theory: A review and re-evaluation. *International* Journal of Management Reviews, 15, 408-425.
[22] Bartunek, J. M. & Woodman, R. W. (2015). Beyond Lewin: Toward a temporal approximation of organization development and change. In Morgeson F. P., Aguinis H., Ashford S. J. (Eds.), Annual review of organizational psychology and organizational behaviour (Vol. 2, pp. 157-182). Palo Alto, CA: Annual Reviews.
[23] Burnes, B. (2017). Managing change (7th ed.). Harlow, England: Pearson.
[24] Bandura, A. (1977). Social learning theory. Prentice Hall.
[25] Bandura, A. (1986). Social foundations of thought and action: A social cognitive theory. Prentice Hall.
[26] Bandura, A., & Walters, R. H. (1977). Social learning theory. Prentice-Hall.
[27] Bandura, A. (2001). Social cognitive theory: An agentic perspective. Annual Review of Psychology, 52(1), 1-26.
[28] Hicklin, W.J (1976). A model for mastering learning based on dynamic equilibrium theory. Journal of Mathematical Psychology, 13(1), 79-88.

.

Optimal control and sensitivity analysis of age-structured mathematical model of Diphtheria infection

E.S. Udofia*, J.I. Uwakwe†, and H.S. Thomas‡

Abstract

The work presented an age-structured deterministic model of a system of ordinary differential equations of diphtheria infection transmission dynamics. Optimal control theory was used to study the impact of personal protection, vaccination and treatment as effective control measures against the epidemics and established necessary conditions for the optimal control of the system. The application of time-dependent controls can reduce the total number of infected (symptomatic and asymptomatic) individuals in the population To determine the most influential parameters of the model that greatly influence the prevalence of diphtheria, sensitivity analysis was carried out on R_b using the normalised forward sensitivity index of R_b that depends differentially on basic reproduction ration parameters. From the sensitivity analysis is was discovered that, the most influential parameters of the model that greatly influence the prevalence of diphtheria are effective rate of transmission, rate of progression from the latent state to the infected state, fraction of new infection that are both symptomatic and asymptomatic, detection rate, natural and infection death rate. The numerical simulations show that there is a significant effect of vaccination (u_2) and isolation (u_1) for susceptible individuals. The number of susceptible infants (S_1) reduces and drops to zero when each of the controls are applied with time. The use of treatment / drug inhibition control could significantly reduce the number of both asymptomatic and symptomatic infected individuals

Keywords and phrases: Diphtheria; Optimal Control; Sensitivity; Asymptomatic; Symptomatic;

1 Introduction

Diphtheria is a highly contagious vaccine-preventable bacterial infection caused by *Corynebacterium diphtheriae* that primarily infects the throat (pharynx and tonsils) and nose. The bacterium has an

* Corresponding Author. Department of Mathematics, Akwa Ibom State University, Ikot Akpaden, Akwa Ibom State, Nigeria ekereudofia@yahoo.com

† Department of Mathematics, Alvan Ikoku University of Education, Owerri, Imo State, Nigeria jiuwakwe.aicedu@gmail.com

‡Department of Mathematics, Akwa Ibom State University, Ikot Akpaden, Akwa Ibom State, Nigeria ekereudofia@yahoo.com

estimated basic reproduction number of 1.7–4.3 [1,2]. Although diphtheria is treatable if detected early, it can lead to severe complications such as respiratory failure, heart problems and even deaths (case-fatality ratio among untreated, never vaccinated cases 28.8–29.2%) [1]. It remains a health problem in low-resource countries, particularly where vaccination uptake and coverage are low and where sanitation conditions remain poor [3].

On December 1, 2022, the Nigeria Centre for Disease Control (NCDC) was notified of suspected diphtheria outbreaks in two of the largest states in Nigeria, Lagos, and Kano, with a combined population of over 30 million. On January 20, 2023, the Director General of the NCDC issued an advisory confirming the outbreaks in Lagos and Kano and the development in two other states, Yobe and Osun, is being monitored. As of February 3, 2023, 216 confirmed cases and 40 persons have died (case fatality rate of 18.5%) from the infection in the current outbreak in Nigeria [4]. This ongoing outbreak mainly occurred in children aged 2 to 14 years (85.2%) and in Kano state (97.7%). It is worth mentioning that only a fraction, 27 (12.5%) of the confirmed cases, were fully vaccinated with diphtheria-tetanus-pertussis (DTP3)—a three-dose vaccine [4]. The Nigerian outbreak has underscored the importance of vaccination and herd immunity, impact of vaccination coverage and sensitisation (media coverage) and effect of complacency in controlling the spread of infectious disease, as emphasized by [5,6,7], blaming it on low vaccination uptake occasioned by COVID-19 in many low-resource countries and consequent opportunistic outbreaks. In Nigeria, case fatality rate among untreated and unvaccinated population is 28.8- 28.2%. because health problem in low resource areas where vaccination uptake and coverage is low and which sanitation conditions remain poor. Diphtheria vaccination coverage estimate in Nigeria have been in the decline. The vaccination rate dropped from 86% in 2019 to 81% in 2021. The overall vaccination coverage of 56% in Nigeria is suboptimal, this is as a result of unavailability of vaccines [4].

Nigeria is currently facing a second wave of diphtheria outbreak. There is an increase in the affected population with a rise in the number of confirmed cases and related death. This is due to the low national vaccination coverage of 56% while vaccination coverage of 80-86% must be maintained to ensure community protection [8].

The control of diphtheria is based on primary prevention of disease by ensuring high population immunity through vaccination. Secondary prevention spread by the rapid investigation of close contacts to ensure prompt treatment of those infected. To effectively contend the spread of Diphtheria, Government has been implementing different control measures, such as isolation of patient, maintenance of one meter between patients, keeping patient care areas well ventilated, the use medical mask and cover any wound/lesions on patient's body by patient who may have to move out of the isolation areas, high risk population such as young children under five years of age, school children, elderly close contact with diphtheria cases and health workers should be vaccinated on a priority basis, epidemiological surveillance ensuring early detection of diphtheria outbreak, administering antitoxin to neutralize the toxin and antibiotics to kill the bacteria, reducing complication and mortality [8].

Mathematical models over the years have become a veritable tool in the hand of mathematicians and epidemiologist in studying, understanding, describing and analysing the dynamics of infectious diseases [9, 10, 11, 12, 13, 14,15, 16, 28, 29, 30,31]. Some mathematical models such as [17, 18] has been formulated for the transmission dynamics of diphtheria, which correctly describe the decreasing

trend of diphtheria cases and predicted the diphtheria outbreak patterns that may occur in the near future. Finds parameters that gives contribution endemic and non-endemic condition

In [17] the SIR mathematical of diphtheria transmission is discussed, simplifying the assumptions and find parameters that give contribution to endemic and nonendemic condition. The model assumes that infected humans can heal by itself. The Basic Reproduction Number was used to analyse the endemic equilibrium.

The work in [18] presented a mathematical model, describing diphtheria transmission in Thailand. Based on the course of diphtheria infection, the population was divided into 8 epidemiological classes, namely, susceptible, symptomatic infectious, asymptomatic infectious, carrier with full natural-acquired immunity, carrier with partial natural-acquired immunity, individual with full vaccine-induced immunity, and individual with partial vaccine-induced immunity.

In this work, the S V E I R age -structured model of diphtheria infection dynamics is presented. Since People who are most susceptible to infection are those who are not completely immunized or have low antitoxin antibody levels and have been exposed to a carrier or diseased individual [26, 27]. The work assumes that those that have been completely vaccinated have no or negligible fatality.
Previous works by other researchers had not taken into consideration age sensitivity in diphtheria infection. This work has successfully structured the susceptible class into two groups: S_1 − Susceptible infant at time t (0-1 year), S_2 − Susceptible school children population at time t (1-15 years) which are the categories that is mostly affected by the infection.

2 Methodology/model formulation

2.1 Assumptions

- The control of diphtheria is based on primary prevention of disease by ensuring high population immunity of the infant ((0-1 year) and school children by vaccination
- Isolation of detected cases (that is confirmed cases are not allowed to interact with the population freely.
- Epidemiological surveillance ensuring early detection through contact tracing is carried out
- Secondary prevention spread by the rapid investigation of close contacts to ensure prompt treatment of those infected

The total population of human at time t under consideration denoted by N_h is split into mutually exclusive sub-population of S_1 Susceptible infant at time t (0-1years), S_2 , Susceptible school children population at time t, V, Vaccination population at time t, E, Exposed population at time t , I_1, Asymptomatic infection population at time t, I_2., Symptomatic infection population at time t, R., Recovered population at time t. I_D., Detected infectious humans at time t (Asymptomatic and symptomatic) population through testing,

$$N_h = S_1 + S_2 + V + E + I_1 + I_2 + R + I_D$$

2.2 State variables

N_h −The total population of human at time t under consideration
S_1 − Susceptible infant at time t (0-1years),
S_2 − Susceptible school children population at time t, (1-15years)
V −Vaccination population at time t,
E − Exposed population at time t , (the exposed are the unvaccinated individuals in S_1 and S_2 who are in contact with the infected individuals)
I_1. − Asymptomatic infection population at time t,
I_2. − Symptomatic infection population at time t,
R − Recovered population at time t.
I_D. − Detected infectious humans at time t (Asymptomatic and symptomatic) population through testing,
Note: It is assume that the age bracket in the classes I_1, I_2, I_D, V and R may range from 0 -15 and above depending on their progression in each of the stages.

2.3 Parameters

σ_1 − progress rate from exposed to I_1, Asymptomatic infection population
σ_2 − progress rate efrom exposed to I_2, symptomatic infection population
δ − fraction of new infection that are I_1, Asymptomatic
$1-\delta$ − fraction of new infection that are I_2, symptomatic
β_1 − effective transmission rate from S_1
β_2 − effective transmission rate from S_2
τ_1 − vaccination coverage for S_1
τ_2 − vaccination coverage for S_2
ε − vaccine efficacy
ρ − maturity rate from S_1 to S_2
b − per capita birth rate of humans
$\varepsilon\tau_1$ − immunization rate in S_1
$\varepsilon\tau_2$ − immunization rate in S_2
θ_1 − detection rate (via contact tracing) for S_1
θ_2 − detection rate (via contact tracing) for S_2
η − death due to infection
α − natural death rate

$$\lambda_1(t) = \frac{\beta_1(\sigma_1 I_1 + \sigma_2 I_2)}{N_h - I_D}$$

$$\lambda_2(t) = \frac{\beta_2(\sigma_1 I_1 + \sigma_2 I_2)}{N_h - I_D}$$

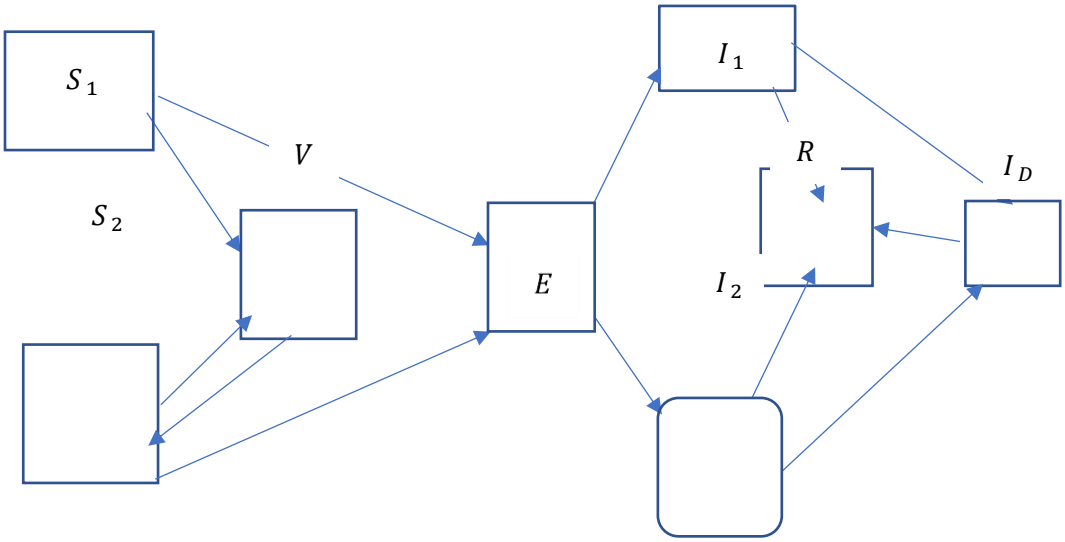


Figure 1: FLOWCHART OF AGE-STRUCTURED DIPHTHERIA DYNAMICS

2.4 Model equations

Using the above-described state variables and parameters together with the schematic diagram in figure 1, the model of the diphtheria infection transmission dynamics results in the following system of deterministic non-linear first order differential equations

$$\frac{dS_1}{dt} = bN_h - \frac{\beta_1(\sigma_1 I_1 + \sigma_2 I_2)}{N_h - I_D} S_1 - \varepsilon\tau_1 S_1 - \rho S_1 - \alpha S_1 \quad (2.1)$$

$$\frac{dS_2}{dt} = \rho S_1 - \frac{\beta_2(\sigma_1 I_1 + \sigma_2 I_2)}{N_h - I_D} S_2 - \varepsilon\tau_2 S_2 - \alpha S_2 \quad (2.2)$$

$$\frac{dV}{dt} = \varepsilon\tau_1 S_1 + \varepsilon\tau_2 S_2 - \alpha V \quad (2.3)$$

$$\frac{dE}{dt} = \frac{\beta_1(\sigma_1 I_1 + \sigma_2 I_2)}{N_h - I_D} S_1 + \frac{\beta_2(\sigma_1 I_1 + \sigma_2 I_2)}{N_h - I_D} S_2 - \sigma_1\delta E - \sigma_2(1-\delta)E - \alpha E \quad (2.4)$$

$$\frac{dI_1}{dt} = \sigma_1\delta E - \gamma_1 I_1 - \theta_1 I_1 - \alpha I_1 - \eta I_1 \quad (2.5)$$

$$\frac{dI_2}{dt} = \sigma_2(1-\delta)E - \gamma_2 I_2 - \theta_2 I_2 - \alpha I_2 - \eta I_2 \quad (2.6)$$

$$\frac{dR}{dt} = \gamma_1 I_1 + \gamma_2 I_2 + \gamma_3 I_D - \alpha R \quad (2.7)$$

$$\frac{dI_D}{dt} = \theta_1 I_1 + \theta_2 I_2 - \gamma_3 I_D - \alpha I_D - \eta I_D \quad (2.8)$$

3 Analysis of the model

This section seeks to study qualitatively the dynamical properties of the Diphtheria model (2.1) – (2.8).

3.1 Basic properties of the model

Before the model (2.1) – (2.8) is epidemiologically meaningful, it is important to show that all its state variables are positive (non-negative) at all time $t > 0$ in the domain $\wp$, and that the domain $\wp$ is indeed bounded. This shall be done through the following theorems and proves.

Theorem 3.1 Let the initial data of the model (2.1) – (2.8) be given as $S_1(0) \geq 0$, $S_2(0) \geq 0, V(0) \geq 0, E(0) \geq 0$, $I_1(0) \geq 0$, $I_2(0) \geq 0$, $R(0) \geq 0$, $I_D(0) \geq 0$. Then the solutions S_1, S_2, V, E, I_1, I_2, R, I_D of the model (2.1) – (2.8) are non-negative $\forall\ t > 0$

Proof: Let $t_1 = sup\{t > 0: S_1 > 0$, $S_2 > 0, V > 0, E > 0$, $I_1 > 0$, $I_2 > 0$, $R > 0$, $I_D > 0 \in [0, t]\}$. Thus, $t_1 > 0$.

We have from (2.1)

$$\frac{dS_1}{dt} = bN_h - \frac{\beta_1(\sigma_1 I_1 + \sigma_2 I_2)}{N_h - I_D} S_1 - \varepsilon\tau_1 S_1 - \rho S_1 - \alpha S_1$$

$$\frac{dS_1}{dt} = bN_h - (\lambda S_1 + \varepsilon\tau_1 + \rho + \alpha) S_1 \qquad where\ \lambda_1(t) = \frac{\beta_1(\sigma_1 I_1 + \sigma_2 I_2)}{N_h - I_D}$$

which can be re-written as

$$\frac{dS_1}{dt} + (\lambda S_1 + \varepsilon\tau_1 + \rho + \alpha) S_1 = bN_h$$

So that $S_1(t) = e^{-(\lambda S_1 + \varepsilon\tau_1 + \rho + \alpha)t} \int_0^t bN_h\, e^{-(\lambda S_1 + \varepsilon\tau_1 + \rho + \alpha)s} ds > 0$

Similarly, it can be shown that: $S_2 > 0, V > 0, E > 0$, $I_1 > 0$, $I_2 > 0$, $R > 0$, $I_D > 0$

Theorem 3.2 : The domain $\wp = \{(S_1, S_2, V, E, I_1, I_2, R, I_D) \in \Re_+^8 : N_h \leq N_h(0)\}$ is positively-invariant for the model (2.1)- (2.8) and attracts all positive solutions of the model.

Proof: adding all the equation of the model (2.1) – (2.8), we have

$$\frac{dN_h}{dt} = bN_h - \alpha S_1 - \alpha S_2 - \alpha V - \alpha E - \alpha I_1 - \eta I_1 - \alpha I_2 - \eta I_2 - \alpha I_D - \eta I_D - \alpha R$$

$$\varphi = \text{Max}\{\alpha, \eta\}$$

$$\frac{dN_h}{dt} \leq bN_h - \varphi N_h = \vartheta N_h,\ \vartheta = b - \varphi$$

$$\frac{dN_h}{dt} \leq \vartheta N_h,$$

$$\int \frac{dN_h}{N_h} \leq \int \vartheta dt$$

$$N_h(t) = N_h(0) e^{\vartheta t}$$

$$N_h(t)\ approaches\ N_h(0)\ as\ t \to \infty\ \forall\ b < \varphi$$

3.2 The basic reproductive ratio

The basic reproductive ratio R_b of the model (2.1) – (2.8) can be established by the use of next generation matrix method on the system (2.1) – (2.8) using the methods in [5,6,19, 20]. Hence, the

transmission matrix F and the transition matrix of the system (2.1) – (2.8) is given respectively as follows:

$$F(E, I_1, I_2, I_D) = \begin{pmatrix} 0 & \sigma_1(\beta_1+\beta_2) & \sigma_2(\beta_1+\beta_2) & 0 \\ 0 & 0 & 0 & 0 \\ 0 & 0 & 0 & 0 \\ 0 & 0 & 0 & 0 \end{pmatrix}$$

$$V(E, I_1, I_2, I_D) = \begin{pmatrix} \sigma_1\delta + \sigma_2(1-\delta) + \alpha & 0 & 0 & 0 \\ -\sigma_1\delta & \gamma_1 + \theta_1 + \alpha + \eta & 0 & 0 \\ -\sigma_2(1-\delta) & 0 & \gamma_2 + \theta_2 + \alpha + \eta & 0 \\ 0 & -\theta_1 & -\theta_2 & \gamma_1 + \alpha + \eta \end{pmatrix}$$

From [5,6,19, 20,28, 29], it follows that the basic reproduction number denoted by R_b

ss obtained as $R_b = \frac{\sigma_1^2\delta(\beta_1+\beta_2)}{((\sigma_1\delta+\sigma_2(1-\delta)+\alpha)(\theta_1+\gamma_1+\alpha+\eta)} + \frac{\sigma_2^2(1-\delta)(\beta_1+\beta_2)}{((\sigma_1\delta+\sigma_2(1-\delta)+\alpha)(\theta_2+\gamma_2+\alpha+\eta)}$ or

$$R_b = (\beta_1+\beta_2)\left\{\frac{\sigma_1^2\delta}{((\sigma_1\delta+\sigma_2(1-\delta)+\alpha)(\theta_1+\gamma_1+\alpha+\eta)} + \frac{\sigma_2^2(1-\delta)}{((\sigma_1\delta+\sigma_2(1-\delta)+\alpha)(\theta_2+\gamma_2+\alpha+\eta)}\right\}$$

3.3 Formulation of the optimal control problem for Diphtheria

Given the initial population size $S_1(0), S_2(0), V(0), E(0), I_1(0), I_2(0), I_D(0), R(0)$. of all the eight classes of model (2.1) – (2.8), the aim of this section is to find the best control strategy that would minimize the number of individuals that die as a result of the disease, at the same time minimizing the cost of the strategy.

Introducing the controls strategies $u_1(t)\ u_2(t), u_3(t)$,and $u_4(t)$ representing the efficiency of isolation/prevention, efficiency of the vaccine therapy in preventing new diphtheria infection, the efficiency of testing the exposed, the efficiency of drug in inhibiting the virus strain and effort on infected human to increase the number of recovered individuals respectively, the model (2.1) – (2.8) becomes Eq. (3.1) – (3.8). $u_1(t)$ is defined to be the prevention/isolation control, minimizing the contact among the healthy and infected individuals. $u_2(t)$, is the vaccination control, it represents the effort in the possible vaccination of all the individuals in order to reduce the further spread of diphtheria, thereby reducing the infection in the system. Control u_3 denotes the effort in testing individuals in the exposed stage, to identify the symptomatic and asymptomatic individuals. The control u_4 represents the treatment effort on the $I_1.-$ Asymptomatic infection population $I_2.-$ Symptomatic infection population $I_D.-$ Detected infectious humans (Asymptomatic and symptomatic) population through testing. r_1, r_2, r_D represent the rate of treatment of $I_1.-$ Asymptomatic infection population $I_2.-$ Symptomatic infection population $I_D.-$ Detected infectious humans (Asymptomatic and symptomatic) population through testing respectively. ξ_1, ξ_2

represent the rate of the effect of the control u_2 on the S_1 and S_2 respectively. ξ_3 represent the rate of the effect of control u_3 on E. ρ_1 is the proportion of the effect of control u_3 on E that move to I_1 class. The above illustrations and parameters leads to the following optimal control problem for diphtheria infection.

$$\frac{dS_1}{dt} = bN_h - \frac{\beta_1(\sigma_1 I_1 + \sigma_2 I_2)}{N_h - I_D}(1-u_1)S_1 - \varepsilon\tau_1 S_1 - \rho S_1 - (\alpha + \xi_1 u_2)S_1 \quad (3.1)$$

$$\frac{dS_2}{dt} = \rho S_1 - \frac{\beta_2(\sigma_1 I_1 + \sigma_2 I_2)}{N_h - I_D}(1-u_1)S_2 - \varepsilon\tau_2 S_2 - (\alpha + \xi_2 u_2)S_2 \quad (3.2)$$

$$\frac{dV}{dt} = u_2\xi_1 S_1 + u_2\xi_2 S_2 + \varepsilon\tau_1 S_1 + \varepsilon\tau_2 S_2 - \alpha V \quad (3.3)$$

$$\frac{dE}{dt} = \frac{\beta_1(\sigma_1 I_1 + \sigma_2 I_2)}{N_h - I_D}(1-u_1)S_1 + \frac{\beta_2(\sigma_1 I_1 + \sigma_2 I_2)}{N_h - I_D}(1-u_1)S_2 - \sigma_1\delta E - \sigma_2(1-\delta)E - \alpha E - (1-u_3)\xi_3 E \quad (3.4)$$

$$\frac{dI_1}{dt} = \rho_1 u_3 \xi_3 E + \sigma_1 \delta E - \gamma_1 I_1 - \theta_1 I_1 - \alpha I_1 - \eta I_1 - r_1 u_4 I_2 \quad (3.5)$$

$$\frac{dI_2}{dt} = (1-\rho_1)u_3\xi_3 E + \sigma_2(1-\delta)E - \gamma_2 I_2 - \theta_2 I_2 - \alpha I_2 - \eta I_2 - r_2 u_4 I_2 \quad (3.6)$$

$$\frac{dI_D}{dt} = \theta_1 I_1 + \theta_2 I_2 - \gamma_3 I_D - \alpha I_D - \eta I_D - r_D u_4 I_D \quad (3.7)$$

$$\frac{dR}{dt} = \gamma_1 I_1 + \gamma_2 I_2 + \gamma_3 I_D - \alpha R \quad (3.8)$$

The control functions $u_1(t)\ u_2(t), u_3(t)$,and $u_4(t)$ are bounded lebesgue integrable functions. The control $u_1(t)$ is the time dependent effort on prevention/isolation control, minimizing the contact among the healthy and infected individuals, practiced on the time interval $[0, t_f]$ to reduce the number of individuals that may become fully infected.

The control $u_2(t)$ is the time dependent effort on the efficiency of the vaccine therapy in preventing new diphtheria infection, practiced on the time interval $[0, t_f]$ to reduce the number of individuals that may become fully infected.

The control $u_3(t)$ is the time dependent effort on the efficiency of testing individuals in the exposed stage, to identify the symptomatic and asymptomatic individuals, practiced on the time interval $[0, t_f]$ to reduce the number of individuals that may become fully infected.

The control $u_4(t)$ is the time dependent effort on the treatment effort on the actively infected individuals ($I_1.\ I_2.\ I_D$), practiced on the time interval $[0, t_f]$ to increase the number of recovered individuals.

The optimal control problem in this work, involves that in which the number of vaccinated, exposed and active diphtheria infections and the cost of treatment controls $u_1(t)\ u_2(t), u_3(t), u_4(t)$, are minimized subject to the differential Equations $(3.1) - (3.8)$. This involves the number of individuals with active and latent diphtheria infection respectively as well as the cost of applying the

vaccine therapy in preventing new diphtheria infection, the efficiency of drug in inhibiting the virus strain and effort on infected human to increase the number of recovered individuals
The objective functional is defined as

$$J = \int_0^{t_f} \{A_1E + A_2I_1 + A_3I_2 + A_4I_D + \frac{A_5}{2}u_1^2 + \frac{A_6}{2}u_2^2 + \frac{A_7}{2}u_3^2 + \frac{A_8}{2}u_4^2\}dt \quad \ldots\ldots\ldots\ldots\ldots\ldots (3.9)$$

where t_f is the final time and the coefficient $A_1 > 0$, $A_2 > 0$, $A_3 > 0, A_4 > 0, A_5 > 0$, $A_6 > 0$, $A_7 > 0, A_8 > 0$ are the balancing cost factors.

We seek the minimize the objective functional

$$J = \int_0^{t_f} \{A_1E + A_2I_1 + A_3I_2 + A_4I_D + \frac{A_5}{2}u_1^2 + \frac{A_6}{2}u_2^2 + \frac{A_7}{2}u_3^2 + \frac{A_8}{2}u_4^2\}dt$$

subject to the optimal control system (3,1) –(3.8)

Hence minimizing the number of infected individuals but keeping the cost of vaccination, treatment/drugs low. That is, to find the optimal control $u_1^0, u_2^0, u_3^0, u_4^0$ such that $J(u_1^0, u_2^0, u_3^0, u_4^0) = Min[J(u_1(t)\ u_2(t), u_3(t), u_4(t),)\ /u_1(t)\ u_2(t), u_3(t), u_4(t), u_5(t)\ \epsilon\Omega]$
where $\Omega = \{(u_1(t)\ u_2(t), u_3(t), u_4(t)\ )\ /\ u_1(t)\ u_2(t), u_3(t), u_4(t)$ are measurable$\}$
$a_i < u_1(t)\ \ u_2(t),\ \ u_3(t), u_4(t)\ < b_i, i = 1,2,3,4\ \ t\ \epsilon[0, t_f]$ is the control set. Also $a_i. and\ b_i\ are\ constant\ in\ [0,\ 1]$.

We use the quadratic control functions in this problem because the controls cost of intervention is nonlinear. It means that there is no linear relationship among the cost of intervention among infected individuals and the cost of intervention.

3.4 Characterization of an optimal control

We shall apply the Pontryagin's Maximum Principle [12,21,22,23], to convert the system (3.1) – (3.8) and (3.9) to a problem of minimizing a pointwise a Hamiltonian functional with respect to the controls u_i . And also establish necessary conditions for the optimal control of the system.
We take λ_k, $\forall\ k = S_1, S_2, V, E,\ I_1,\ I_2,\ I_D,\ R$ to be the adjoint variable associated with the state variable $S_1, S_2, V, E,\ I_1,\ I_2,\ I_D,\ R$.

Theorem 3.3: Given the optimal control u_j^0 and solutions $S_1^0,\ S_2^0,\ V^0,\ E^0,\ I_1^0,\ I_2^0,\ I_D^0, R^0$ of the control system (3.1) – (3.8) that minimizes $J(u_j^0)\ over\ \Omega$. Then there exist adjoint variables λ_k satisfying

$$\frac{\partial \lambda_k}{\partial t} = -\frac{\partial H}{\partial i} \quad \ldots\ldots\ldots\ldots\ldots (3.11)$$

with transversality conditions

$$\lambda_k(t_f) = 0, where\ k = S_1, S_2, V, E,\ I_1,\ I_2,\ I_D,\ R \quad \ldots. (3.12)$$

The optimality condition is given by

$$\frac{\partial H}{\partial u_j} = 0, \forall j = 1, 2, 3, 4 \qquad (3.13)$$

with controls $u_1^0 = min\left\{1,\ max\left[0,\ \frac{\left[\left(\lambda_E^*-\lambda_{S_1}^*\right)\beta_1 S_1^0+\ \left(\lambda_E^*-\lambda_{S_2}^*\right)\beta_2 S_2^0\right]\frac{\left(\sigma_1 I_1^0+\sigma_2 I_2^0\right)}{\left(N_h^0-I_D^0\right)}}{A_5}\right]\right\}$

$$u_2^0 = min\left\{1,\quad max\left[0,\quad \frac{\left[\left(\lambda_{S_1}^*-\xi_1\lambda_V^*\right)S_1^0+\ \left(\lambda_{S_2}^*-\xi_2\lambda_V^*\right)S_2^0\right]}{A_6}\right]\right\}$$

$$u_3^0 = min\left\{1,\quad max\left[0,\quad \frac{\lambda_{I_2}^*(\rho_1-1)\xi_3E^0-\lambda_E^*\xi_3E^0-\lambda_{I_1}^*\rho_1\xi_3E^0}{A_7}\right]\right\}$$

$$u_4^0 = min\left\{1,\quad max\left[0,\quad \frac{\lambda_{I_1}^* r_1 I_1^0+\lambda_{I_2}^* r_2 I_2^0+\lambda_{I_D}^* r_D I_D^0}{A_8}\right]\right\}$$

Proof:

Since we have eight state variables, $S_1, S_2, V, E,\ I_1,\ I_2,\ I_D,\ R$, we shall have eight corresponding adjoint variables $\lambda_1, \lambda_2, \lambda_3, \lambda_4, \lambda_5, \lambda_6, \lambda_7, \lambda_8$. Then we obtain the Hamiltonian functional:

$$\begin{aligned}
H\ =\ & A_1E + A_2I_1 + A_3I_2 + A_4I_D\ + \frac{A_5}{2}u_1^2 + \frac{A_6}{2}u_2^2 + \frac{A_7}{2}u_3^2 + \frac{A_8}{2}u_4^2 \\
& + \lambda_1\left\{bN_h - \frac{\beta_1(\sigma_1I_1+\sigma_2I_2)}{N_h-I_D}(1-u_1)S_1 - \varepsilon\tau_1S_1 - \rho S_1 - (\alpha+\xi_1u_2)S_1\right\} \\
& + \lambda_2\left\{\rho S_1 - \frac{\beta_2(\sigma_1I_1+\sigma_2I_2)}{N_h-I_D}(1-u_1)S_2 - \varepsilon\tau_2S_2 - (\alpha+\xi_2u_2)S_2\right\} \\
& + \lambda_3\{u_2\xi_1S_1 + u_2\xi_2S_2 + \varepsilon\tau_1S_1 + \varepsilon\tau_2S_2 - \alpha V\} \\
& + \lambda_4\left\{\frac{\beta_1(\sigma_1I_1+\sigma_2I_2)}{N_h-I_D}(1-u_1)S_1 + \frac{\beta_2(\sigma_1I_1+\sigma_2I_2)}{N_h-I_D}(1-u_1)S_2 - \sigma_1\delta E\right. \\
& \left. - \sigma_2(1-\delta)E - \alpha E - (1-u_3)\xi_3E\right\} \\
& + \lambda_5\{\rho_1u_3\xi_3E + \sigma_1\delta E - \gamma_1I_1 - \theta_1I_1 - \alpha I_1 - \eta I_1 - r_1u_4I_1\} \\
& + \lambda_6\{(1-\rho_1)u_3\xi_3E + \sigma_2(1-\delta)E - \gamma_2I_2 - \theta_2I_2 - \alpha I_2 - \eta I_2 - r_2u_4I_2\} \\
& + \lambda_7\{\theta_1I_1 + \theta_2I_2 - \gamma_3I_D - \alpha I_D - \eta I_D - r_Du_4I_D\} \\
& + \lambda_8\{\gamma_1I_1 + \gamma_2I_2 + \gamma_3I_D - \alpha R\} \ldots\ldots\ldots\ldots\ldots\ldots\ldots\ldots (3.10)
\end{aligned}$$

The system of adjoint equation is obtained by taking the appropriate partial derivative of H with respect to the respective state variables.

$$\begin{aligned}
\frac{\partial\lambda_{S_1}}{\partial t}\ &= -\frac{\partial H}{\partial S_1} \\
&= \left(\lambda_{S_1}-\lambda_E\right)\frac{\beta_1(\sigma_1I_1+\sigma_2I_2)}{N_h-I_D}(1-u_1) + \left(\lambda_{S_1}-\lambda_V\right)\varepsilon\tau_1 + \left(\lambda_{S_1}-\lambda_V\right)\xi_1u_2 \\
&+ \left(\lambda_{S_1}-\lambda_{S_2}\right)\rho + \alpha\lambda_{S_1} \\
&\lambda_{S_1}(t_f)\ = 0
\end{aligned}$$

$$\frac{\partial \lambda_{S_2}}{\partial t} = -\frac{\partial H}{\partial S_2}$$

$$= \left(\lambda_{S_2} - \lambda_E\right)\frac{\beta_2(\sigma_1 I_1 + \sigma_2 I_2)}{N_h - I_D}(1-u_1) + \left(\lambda_{S_2} - \lambda_V\right)\varepsilon\tau_2 + \left(\lambda_{S_2} - \lambda_V\right)u_2\xi_2 + \alpha\lambda_{S_2}$$

$$\lambda_{S_2}(t_f) = 0$$

$$\frac{\partial \lambda_V}{\partial t} = -\frac{\partial H}{\partial V} = \lambda_V \alpha V$$

$$\lambda_{S_V}(t_f) = 0$$

$$\frac{\partial \lambda_E}{\partial t} = -\frac{\partial H}{\partial E}$$

$$= \left(\lambda_E - \lambda_{I_1}\right)\sigma_1\delta + \left(\lambda_E - \lambda_{I_2}\right)\sigma_2(1-\delta) - \left(\lambda_E + \lambda_{I_2}\right)u_3\xi_3 + \left(\lambda_{I_2} - \lambda_{I_1}\right)\rho_1 u_3\xi_3 + (\alpha + \xi_3)\,\lambda_E - A_1$$

$$\lambda_E(t_f) = 0$$

$$\frac{\partial \lambda_{I_1}}{\partial t} = -\frac{\partial H}{\partial I_1} = (\lambda_{I_1} - \lambda_R)\gamma_1 + (\lambda_{I_1} - \lambda_{I_D})\theta_1 + (\alpha + \eta + r_1 u_4)\lambda_{I_1} - A_2$$

$$\lambda_{I_1}(t_f) = 0$$

$$\frac{\partial \lambda_{I_2}}{\partial t} = -\frac{\partial H}{\partial I_2} = \left(\lambda_{I_2} - \lambda_R\right)\gamma_2 + \left(\lambda_{I_2} - \lambda_{I_D}\right)\theta_2 + (\alpha + \eta + r_2 u_4)\lambda_{I_2} - A_3$$

$$\lambda_{I_2}(t_f) = 0$$

$$\frac{\partial \lambda_{I_D}}{\partial t} = -\frac{\partial H}{\partial I_D} = (\lambda_{I_D} - \lambda_R)\gamma_3 + (\alpha + \eta + r_D u_4)\,\lambda_{I_D} - A_4$$

$$\lambda_{I_D}(t_f) = 0$$

$$\frac{\partial \lambda_R}{\partial t} = -\frac{\partial H}{\partial R} = \alpha\lambda_R$$

$$\lambda_R(t_f) = 0$$

The optimal control $u_1^0, u_2^0, u_3^0\, u_4^0$ can be solved from optimality conditions

$$\frac{\partial H}{\partial u_1} = A_5 u_1 + \frac{\beta_1(\sigma_1 I_1 + \sigma_2 I_2)}{N_h - I_D} S_1\lambda_1 + \frac{\beta_2(\sigma_1 I_1 + \sigma_2 I_2)}{N_h - I_D} S_2\lambda_2 - \frac{\beta_1(\sigma_1 I_1 + \sigma_2 I_2)}{N_h - I_D} S_1\lambda_4 - \frac{\beta_2(\sigma_1 I_1 + \sigma_2 I_2)}{N_h - I_D} S_2\lambda_4 = 0$$

$A_5 u_1^0 + \left(\{\beta_1 S_1^0 \lambda_{S_1}^* + \beta_2 S_2 \lambda_{S_2}^*\} - \{\beta_1 S_1^0 \lambda_E^* + \beta_2 S_1^0 \lambda_E^*\}\right) \frac{(\sigma_1 I_1^0 + \sigma_2 I_2^0)}{(N_h^0 - I_D^0)} = 0$. Hence $u_1^0 = \frac{\left[\left(\lambda_E^* - \lambda_{S_1}^*\right)\beta_1 S_1^0 + \left(\lambda_E^* - \lambda_{S_2}^*\right)\beta_2 S_2^0\right]\frac{(\sigma_1 I_1^0 + \sigma_2 I_2^0)}{(N_h^0 - I_D^0)}}{A_5}$

$$\frac{\partial H}{\partial u_2} = A_6 u_2 - \lambda_{S_1} S_1 - \lambda_{S_2} S_2 + \lambda_V(\xi_1 S_1 + \xi_2 S_2) = A_6 u_2 - \left[\left(\lambda_{S_1} - \xi_1\lambda_V\right)S_1 + \left(\lambda_{S_2} - \xi_2\lambda_V\right)S_2\right] = 0$$

$A_6 u_2 - \left[\left(\lambda_{S_1}^* - \lambda_V^*\right)S_1^0 + \left(\lambda_{S_2}^* - \lambda_V^*\right)S_2^0\right] = 0 \Rightarrow u_2^0 = \frac{\left[\left(\lambda_{S_1}^* - \xi_1\lambda_V^*\right)S_1^0 + \left(\lambda_{S_2}^* - \xi_2\lambda_V^*\right)S_2^0\right]}{A_6}$

$\frac{\partial H}{\partial u_3} = A_7 u_3 + \lambda_E \xi_3 E + \lambda_{I_1}\rho_1\xi_3 E + \lambda_{I_2}(1-\rho_1)\xi_3 E = A_7 u_3 + \lambda_E\xi_3 E + \lambda_{I_1}\rho_1\xi_3 E - \lambda_{I_2}(\rho_1 - 1)\xi_3 E = 0$

$A_7 u_3 = \lambda_{I_2}^*(\rho_1 - 1)\xi_3 E^0 - \lambda_E^*\xi_3 E^0 - \lambda_{I_1}^*\rho_1\xi_3 E^0 \quad u_3^0 = \frac{\lambda_{I_2}^*(\rho_1-1)\xi_3 E^0 - \lambda_E^*\xi_3 E^0 - \lambda_{I_1}^*\rho_1\xi_3 E^0}{A_7}$

$\frac{\partial H}{\partial u_4} = A_8 u_4 - \lambda_5 r_1 I_1 - \lambda_6 r_2 I_2 - \lambda_7 r_D I_D = 0 \quad u_4^0 = \frac{\lambda_{I_1}^* r_1 I_1 + \lambda_{I_2}^* r_2 I_2 + \lambda_{I_D}^* r_D I_D}{A_8}$

4 Numerical simulations/sensitivity analysis

4.1 Numerical simulations

The numerical simulation was carried out using Matlab 15 to show the effect of the controls on the spread of diphtheria. The parameter values used are shown in the table below

Table 1 Model Parameters and Values

Parameters	Values	Source
B	0.15448/dy	Rahmi &Pratama (2023)
α	0.0000194	Rahmi & Pratama (2023)
r_1, r_2, r_D	0.5, 0.6, 0.7	Assumed
$\varepsilon_1, \varepsilon_2, \varepsilon_3$	0.7,0.7,0.3	Assumed
θ_1, θ_2	0.3, 0.4	Assumed
β_1, β_2	0.57	Izzati & Andriani (2021)
ϵ	0.6	Assumed
ρ	0.7	Assumed
σ_1, σ_2	0.143, 0.140	Rahmi & Pratama (2023)
γ	0.5	Rahmi & Pratama (2023)
δ	0.2	Assumed
τ_1, τ_2	0.5, 0.4	Rahmi & Pratama (2023)

The initial conditions for the variables are; $S_1(0) = 500$, $S_2(0) = 500$, $V(0) = 200$, $E(0) = 700$, $I_1(0) = 100$, $I_2(0) = 200$, $I_D(0) = 400$

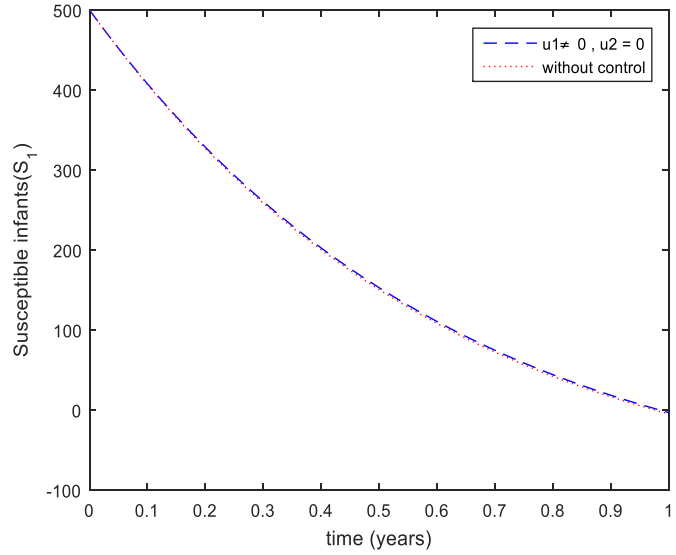


Fig 2. Effect of isolation on S_1

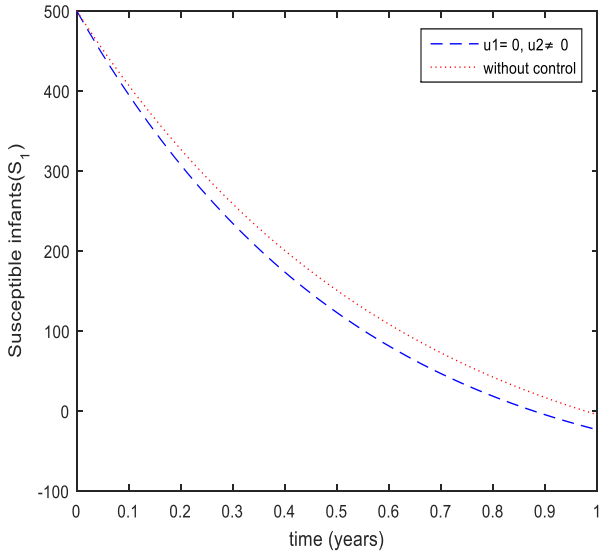


Fig 3. Effect of vaccination on S_1

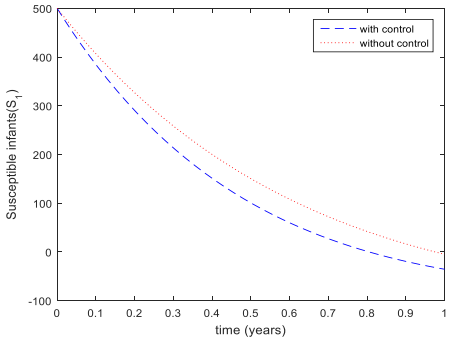


Fig. 4. Effect of vaccination and isolation on S_1

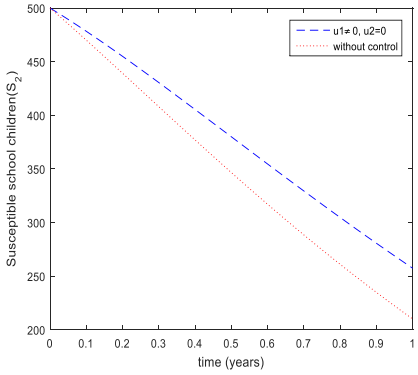


Fig. 5. Effect of isolation on S_2

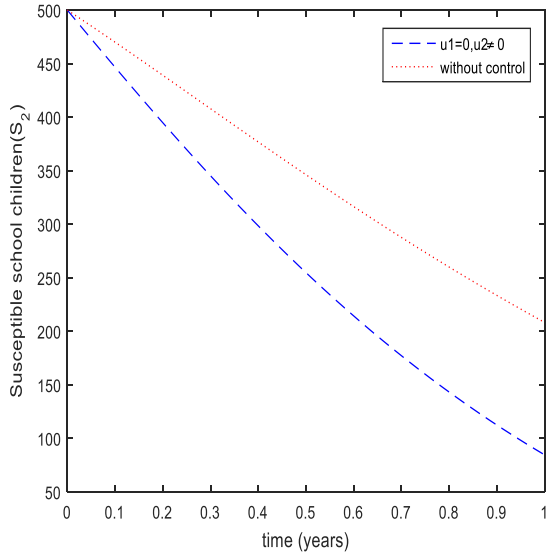


Fig. 6. Effect of vaccination onS_2

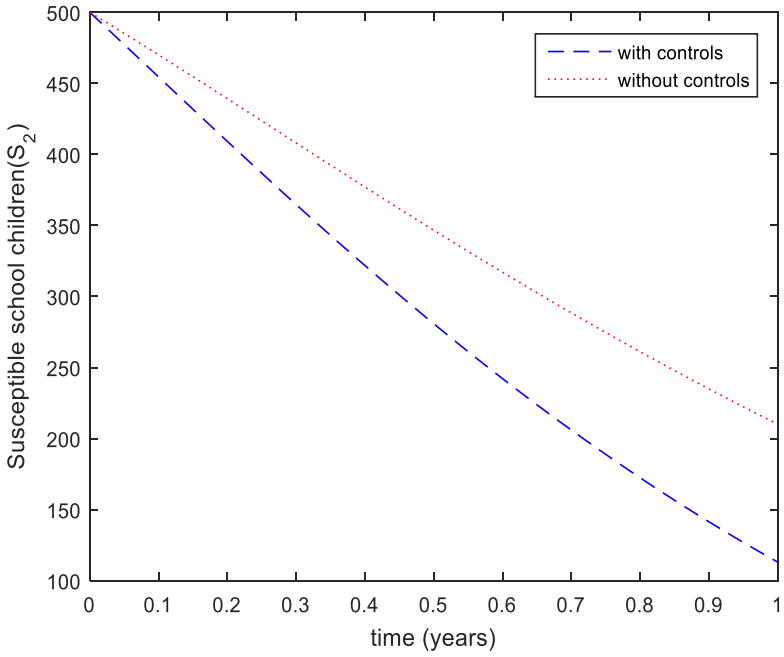


Fig.7. Effect of isolation and vaccination on S_2

The numerical simulations show that there is a significant effect of vaccination (u_2) and isolation (u_1) for susceptible individuals. The number of susceptible infants (S_1) reduces and drops to zero when each of the controls are applied with time as shown in fig 2. However, from Fig. 5 and 6, vaccination (u_2) tends to significantly reduce the number of susceptible school children population (S_2) with time compared to applying only isolation control (u_1).

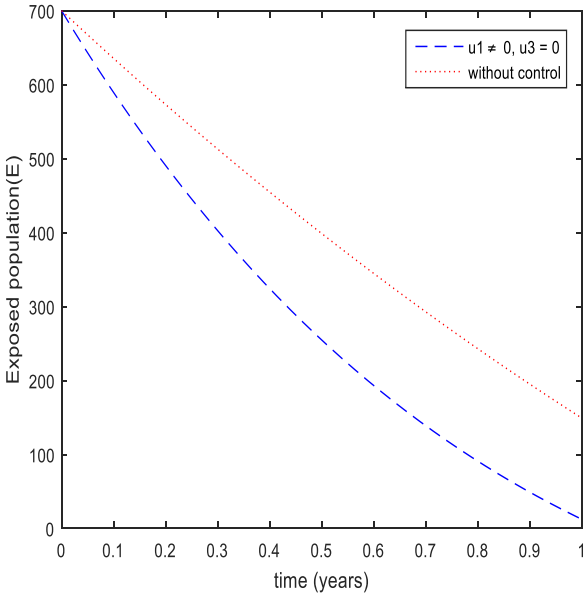


Fig. 8. Effect of Isolation on Exposed population

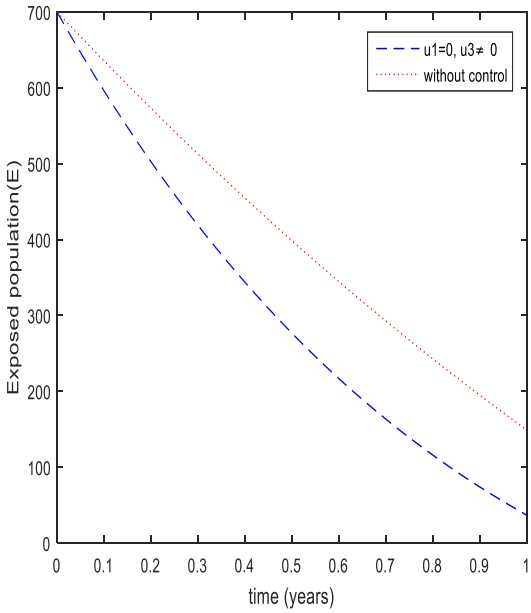


Fig. 9. Effect of testing on Exposed population

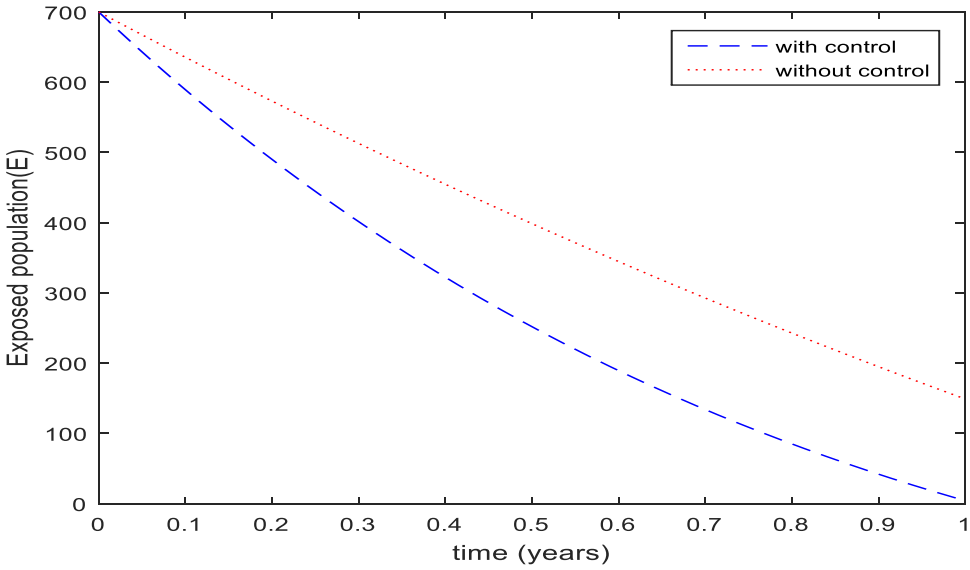


Fig. 10. Effect of Isolation and testing on Exposed population

We can see from Fig. 10 that the isolation of exposed individuals could reduce the number of exposed population to almost zero with time but the combination of isolation (u_1) and testing (u_3) brings the number of exposed individuals to zero after 9years.

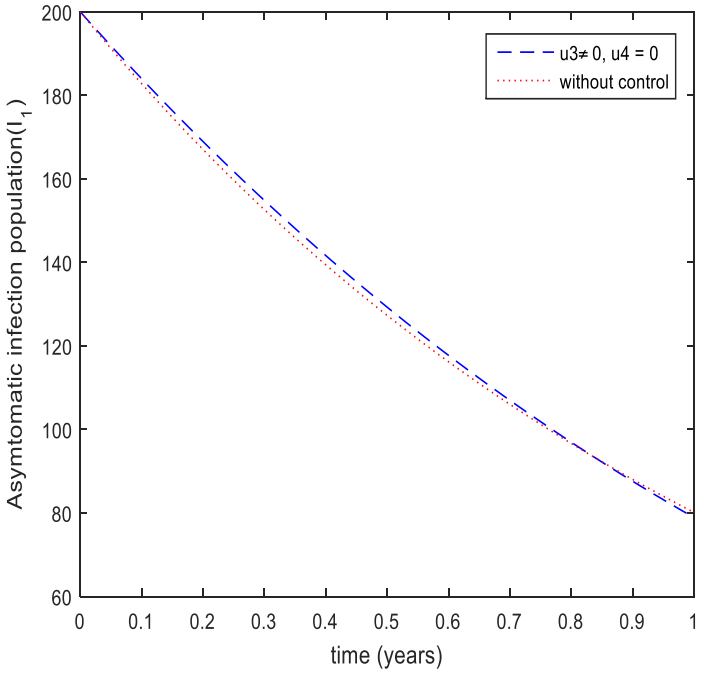


Fig. 11. Effect of testing on I_1

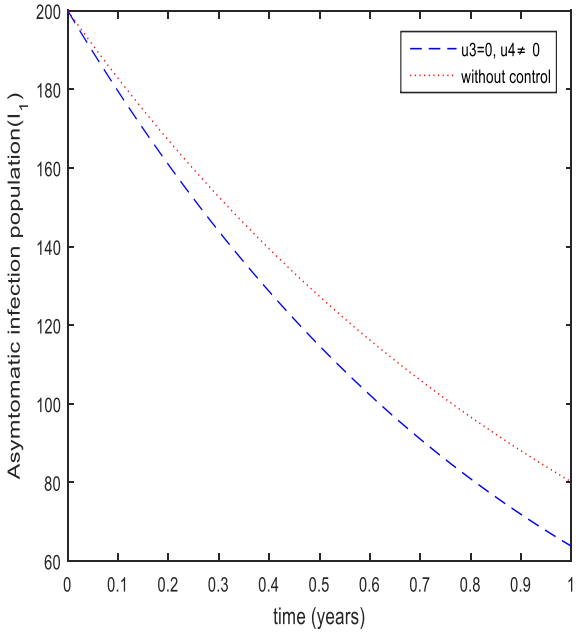


Fig. 12. Effect of treatment on I_1

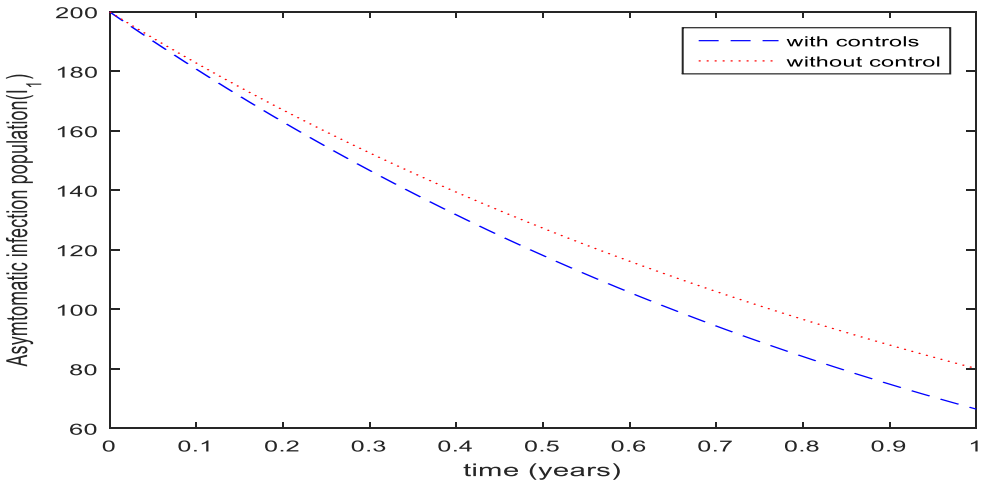


Fig. 13. Effect of testing and treatment on I_1

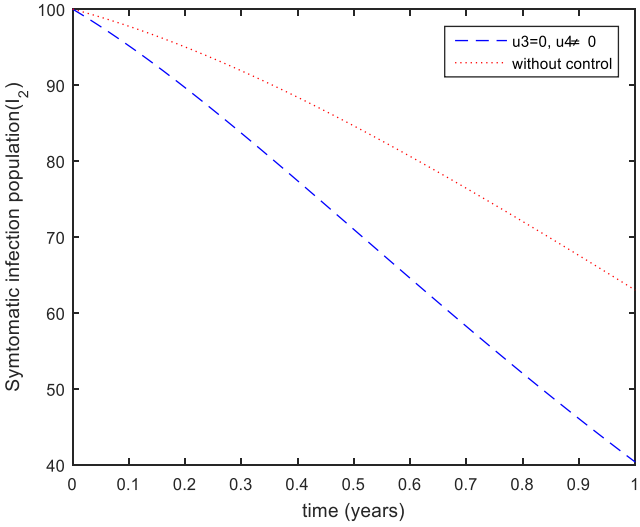


Fig.14. Effect of testing on I_2

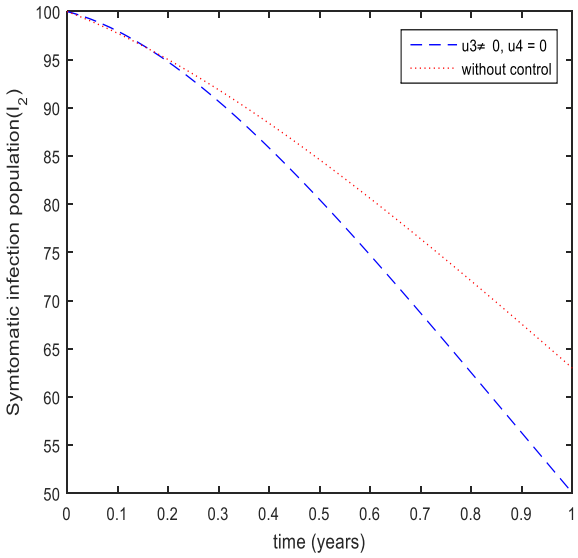


Fig. 15. Effect of treatment on I_2

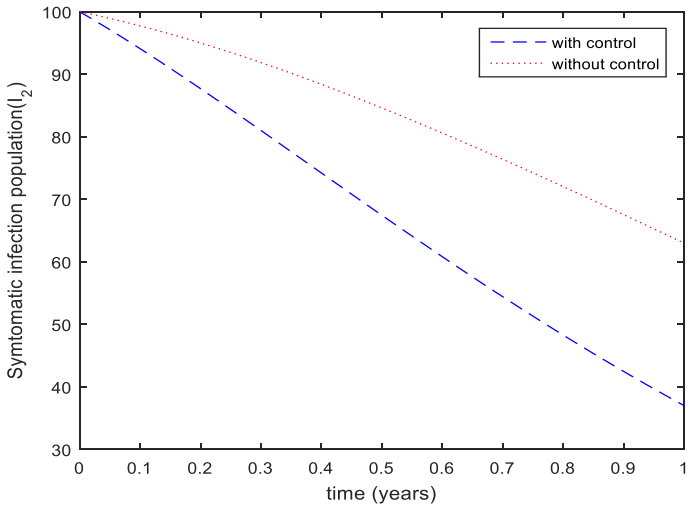


Fig. 16. Effect of treatment and testing on Symptomatic infected population (I_2)

The effect of treatment (u_4) and testing (u_3) of infected individuals can be observed in Figs 11, 12, 13, 14, 15, and 16. The use of treatment / drug inhibition control could significantly reduce the number of both asymptomatic and symptomatic infected individuals as shown in Figs 12 and 15. However the combination of testing and treatment controls could be more effective in reducing the number of symptomatic infected individuals as shown in Fig 16.

4.2 Sensitivity analysis on $\mathbf{R_b}$

A sensitivity analysis is done to determine the parameters most responsible for the transmission and spread of diphtheria and to measure the effect of changes in the dominant factors of the model. Sensitivity analysis of the basic reproductive number is employed to design an intervention strategy to curtail the spread of the infection by reducing R_b. With the basic reproductive number one can discover the parameters that have high impact on the values of R_b, that is the most influential parameters of the model that greatly influence the prevalence of infection. These parameters are then targeted as a means of reducing the value of R_b.

The normalised forward sensitivity index of R_b that depends differentially on a parameter p is defined by

$r_t^{R_b} = \left(\frac{\partial R_b}{\partial t}\right)\left(\frac{t}{R_b}\right)$ $where\ t = \beta_1, \beta_2, \sigma_1, \sigma_2, \delta, \theta_1, \theta_2, \gamma_1, \alpha, \eta)$ is used to compute the sensitivity analysis on the R_b of the system.

In particular, sensitivity indices of the basic reproduction number, R_b, with respect to the model parameters are computed as follows:

$$\left(\frac{\partial R_b}{\partial \beta_1}\right)\left(\frac{\beta_1}{R_b}\right) = \frac{\beta_1}{\beta_1 + \beta_2}$$

$$\left(\frac{\partial R_b}{\partial \beta_2}\right)\left(\frac{\beta_2}{R_b}\right) = \frac{\beta_2}{\beta_1 + \beta_2}$$

$$\left(\frac{\partial R_b}{\partial \sigma_1}\right)\left(\frac{\sigma_1}{R_b}\right) = (\theta_1 + \gamma_1 + \alpha + \eta)(\theta_2 + \gamma_2 + \alpha + \eta)\left\{\frac{2\sigma_1^2\delta((\sigma_1\delta + \sigma_2(1-\delta) + \alpha)}{\sigma_1^2\delta + \sigma_2^2(1-\delta)} - \sigma_1\delta\right\}$$

$$\left(\frac{\partial R_b}{\partial \sigma_1}\right)\left(\frac{\sigma_1}{R_b}\right) = \frac{\sigma_1^3\delta^2 + 2\sigma_1^2\delta(\sigma_2 + \alpha) - \sigma_2^2\sigma_1\delta(1-\delta) - 2\sigma_2\sigma_1\delta^2}{\left((\sigma_1\delta + \sigma_2(1-\delta) + \alpha)\right)\left(\sigma_1^2\delta + \sigma_2^2(1-\delta)\right)}$$

$$\left(\frac{\partial R_b}{\partial \sigma_2}\right)\left(\frac{\sigma_2}{R_b}\right) = \frac{(1-\delta)\sigma_2\{2\sigma_2\sigma_1\delta + \sigma_2^2(1-\delta) + 2\sigma_2\alpha - \sigma_1^2\delta}{\left((\sigma_1\delta + \sigma_2(1-\delta) + \alpha)\right)\left(\sigma_1^2\delta + \sigma_2^2(1-\delta)\right)}$$

$$\left(\frac{\partial R_b}{\partial \delta}\right)\left(\frac{\delta}{R_b}\right)$$

$$= \frac{\delta\left((\sigma_1\delta + \sigma_2(1-\delta) + \alpha)\right)(\theta_1 + \gamma_1 + \alpha + \eta)(\theta_2 + \gamma_2 + \alpha + \eta)\{(\sigma_2 + \alpha)\sigma_1^2 - (\sigma_1 + \alpha)\sigma_2^2 - \sigma_2^3\}}{\left(\sigma_1^2\delta + \sigma_2^2(1-\delta)\right)}$$

$$\left(\frac{\partial R_b}{\partial \alpha}\right)\left(\frac{\alpha}{R_b}\right) = \frac{-\{(\theta_1 + \gamma_1 + \alpha + \eta)(\theta_2 + \gamma_2 + \alpha + \eta) + (\theta_1 + \theta_2 + \gamma_1 + \gamma_2 + 2\alpha + 2\eta)\}}{(\theta_1 + \gamma_1 + \alpha + \eta)(\theta_2 + \gamma_2 + \alpha + \eta\ )}\alpha$$

$$\left(\frac{\partial R_b}{\partial \theta_1}\right)\left(\frac{\theta_1}{R_b}\right) = -\frac{\theta_1}{(\theta_1 + \gamma_1 + \alpha + \eta)}$$

$$\left(\frac{\partial R_b}{\partial \theta_2}\right)\left(\frac{\theta_2}{R_b}\right) = -\frac{\theta_2}{(\theta_2 + \gamma_2 + \alpha + \eta)}$$

$$\left(\frac{\partial R_b}{\partial \eta}\right)\left(\frac{\eta}{R_b}\right) = \frac{-[(\theta_1+\gamma_1+\alpha+\eta)+(\theta_2+\gamma_2+\alpha+\eta)]}{(\theta_1+\gamma_1+\alpha+\eta)(\theta_2+\gamma_2+\alpha+\eta)}\eta$$

The sensitivity index of the basic reproduction number to the model parameters indicates that an increase (or decrease) in value of the following parameters $\beta_1, \beta_2, \sigma_1, \sigma_2, \delta,$ will lead to an increase (or decrease) in the basic reproduction number. On the other hand, an increase (or decrease) in the death rates (α, η) and detection rate, (θ_1, θ_2) leads to a corresponding decrease (or increase) in the basic reproduction number of the disease.

The most influential parameters of the model that greatly influence the prevalence of diphtheria are effective rate of transmission, rate of progression from the latent state to the infected state, fraction of new infection that are both symptomatic and asymptomatic, detection rate, natural and infection death rate.

5 Discussions and conclusion

We summarize some of the main theoretical and epidemiological findings of this study as follows: the work presented an age-structured deterministic model of a system of ordinary differential equations of diphtheria infection transmission dynamics. It was established that the model is epidemiologically meaningful, with theorem and proof that shows that all its state variables are positive (non-negative) at all-time $t > 0$ in the domain $\wp$, and that the domain $\wp$ is indeed bounded.

The basic reproductive ratio R_b of the model (2.1) – (2.8) was established as

$$R_b = (\beta_1+\beta_2)\left\{\frac{\sigma_1^2\delta}{((\sigma_1\delta+\sigma_2(1-\delta)+\alpha)(\theta_1+\gamma_1+\alpha+\eta)} + \frac{\sigma_2^2(1-\delta)}{((\sigma_1\delta+\sigma_2(1-\delta)+\alpha)(\theta_2+\gamma_2+\alpha+\eta)}\right\}$$

by the use of next generation matrix method on the system (2.1) – (2.8) using the methods in [5,6,19, 20,30,31]. To determine the most influential parameters of the model that greatly influence the prevalence of diphtheria, sensitivity analysis was carried out on R_b using the normalised forward sensitivity index of R_b that depends differentially on basic reproduction ration parameters. From the sensitivity analysis is was discovered that, the most influential parameters of the model that greatly influence the prevalence of diphtheria are effective rate of transmission, rate of progression from the latent state to the infected state, fraction of new infection that are both symptomatic and asymptomatic, detection rate, natural and infection death rate.

Optimal control theory was used to study the impact of personal protection, vaccination and treatment as effective control measures against the epidemics. And establish necessary conditions for the optimal control of the system. The application of time-dependent controls can reduce the total number of infected (symptomatic and asymptomatic) individuals in the population.

The numerical simulations show that there is a significant effect of vaccination (u_2) and isolation (u_1) for susceptible individuals. The number of susceptible infants (S_1) reduces and drops to zero when each of the controls are applied with time as shown in fig 2. However, from Fig. 5 and 6, vaccination (u_2) tends to significantly reduce the number of susceptible school children population (S_2) with time compared to applying only isolation control (u_1).

As seen from Fig. 10, the isolation of exposed individuals could reduce the number of exposed population to almost zero with time but the combination of isolation (u_1) and testing (u_3) brings the number of exposed individuals to zero after 9years. The effect of treatment (u_4) and testing (u_3) of infected individuals can be observed in Figs 11, 12, 13, 14, 15, and 16. The use of treatment / drug inhibition control could significantly reduce the number of both asymptomatic and symptomatic infected individuals as shown in Figs 12 and 15. However the combination of testing and treatment controls could be more effective in reducing the number of symptomatic infected individuals as shown in Fig 16.

References

[1] Truelove SA, Keegan LT, Moss WJ, et al. (2020). Clinical and epidemiological aspects of diphtheria: a systematic review and pooled analysis. Clin Infect Dis 2020; 71: 89–97.

[2] Oyelola A. Adegboye, Faith O. Alele, Anton Pak, Maria E. Castellanos, Malachy I. Okeke, Mohammed A.S., Theophilus I. Emeto, Emma S. McBryde (2023). A resurgence and re-emergence of diphtheria in Nigeria. Ther Adv Infect Dis., 10: 20499361231161936.

[3] Al-Dar AA, Al-Qassimi M, Ezzadeen FH, et al. (2020). Diphtheria resurgence in Sada'a-Yemen, 2017–2020. BMC Infect Dis., 22: 46.

[4] Nigeria Centre for Disease Control Prevention (NCDC). Diphtheria situation report. Serial number 02, https://ncdc.gov.ng/diseases/sitreps/?cat=18&name=An%20Update%20of%20Diphtheria%20Outbreak%20in%20Nigeria (accessed 3 February 2023).

[5] Udofia E.S., Udoh K.J., and Inyama S.C. (2016) The impact of media coverage on the transmission dynamics of fowl pox in poultry. International J. of Math. Sci. & Engg. Appls., 10(1): 103-114.

[6] Udofia E.S. and Inyama S.C. (2011) Mathematical model of the impact of vaccination on the transmission dynamics of fowl pox in poultry. Journal of Modern Mathematics and Statistics 5 (5-6): 102-105.

[7] Udofia, E.S., Sampson, M.I. (2014). Mathematical model of the effect of complacency in hiv/aids preventions IOSR Journal of Mathematics, 10(6):30-33.

[8] World Health Organization (27 April 2023). Disease Outbreak News; Diphtheria – Nigeria. Available at https://www.who.int/emergencies/disease-outbreak-news/item/2023-DON452

[9] Onuoha J.I., Inyama S.C., Udofia E.S., and Omame A. (2015) Mathematical model of the transmission dynamics of swine flu with the vaccination of non newborns. International J. of Math. Sci. & Engg. Appls., 9(1):1-17.

[10] Udofia S.E. (2023), Mathematical model of male circumcision in hiv/aids preventions, International Journal of Innovative Science and Research Technology, Volume 8, Issue 8, August – 2023 ISSN No: -2456-2165 www.ijisrt.com

[11] Onuoha J.I., Inyama S.C., Udofia E.S. (2014) Mathematical model of the transmission dynamics of swine flu with the vaccination of newborns. International J. of Math. Sci. & Engg. Appls. (IJMSEA) ISSN 0973-9424, Vol. 8 No. V (September, 2014), pp. 217-229

[12] Udofia Ekere Sunday and Inyama Simeon Chioma (2012) Application of optimal control to the epidemiology of fowl pox transmission dynamics in poultry. Journal of Mathematics and Statistics 8 (2): 248-252

[13] Udofia, Ekere Sunday and Inyama, Simeon Chioma (2013). Mathematical model of structural strategy (delayed first intercoure) in hivaids prevention. Journal of the Nigerian Association of

Mathematical Physics Volume 24 (July, 2013) pp 257-260 © J. of NAMP
[14] Udofia, Ekere Sunday, Sampson, Marshal Imeh (2014) Mathematical model for the epidemiology of fowl pox infection transmission that incorporates discrete delay, IOSR Journal of Mathematics (IOSR-JM) e-ISSN: 2278-5728, p-ISSN: 2319-765X. Volume 10, Issue 4 Ver. V (July - Aug. 2014), PP 08-16 **www.iosrjournals.org**
[15] IA Agwu, SC Inyama, RA Umana, A Omame, N Ukanwoke, A Ofomata, HI Mbachu, ES Udofia, JI Uwakwe (2018) Determining the impact of variation of harvesting effort on the qualitative behaviour of a coexistence steady state solution and its stability in prey-predator fishery model, Academic Journal of Applied Mathematical Sciences Vol. 4 Issue 10 Pages 119-128, 2018
[16] D. Okuonghae and A. Omame (2020). Analysis of a mathematical model for COVID-19 population dynamics in Lagos, Nigeria. Chaos, Solitons and Fractals, 139.
[17] K an Sornbundit, Wannapong Triampo, Charin Modchang (2017) Mathematical modelling of Diphtheria Transmission innThailand, Computers in Biology and Medicine Vol. 87 1 August 2017 pages 162-168 **https://doi.org/10.1016/j.copbiomed.201705.31**
[18] H.S. Husain (2019) An SIR Mathematical model for diphtheria disease, J. Phys. Conf. Ser.1280 Doi.10.1088/1742-6596/1280/2/022051
[19] Van den Driessche P , Watmough J . (2002). Reproduction numbers and sub-threshold endemic equilibria for compartmental models of disease transmission. Math Biosci., 180:29–48.
[20] Udofia Ekere Sunda and Inyama Simeon Chioma (2011), Mathematical modeling of the transmission dynamics of fowl pox in poultry. Journal of Modern Mathematics and Statistics, 5(5-6): 106-111.
[21] Pontryagin Lev Semenovich. Mathematical theory of optimal processes. CRC Press; 1987.
[22] Kirschner D, Lenhart S, Serbin S (1997). Optimal Control of the Chemotherapy of HIV. J. Math. Biol. 35:775-792.
[23] Fleming Wendell H, Rishel Raymond W. Deterministic and stochastic optimal control. Vol. 1. Springer Science & Business Media; 2012.
[24] Izzati, N. and Andriani A. (2021). Dynamical Analysis of diptheteria epidemic model with natural immunity, Journal of Physics: conference series. doi: 10.1088/1742-6596/1869/1/01211
[25] Rahmi, N. and Pratama, I. (2023). Model analysis of diphtheria disease transmission with vaccination, quarantine and hand-washing behaviour, Jurnal Tearl an Apilkasi Matematika (JTAM), 7(2), 462-474 .
[26] Jennifer L Liang, Tejpratap Tiwari, Pedro Moro, Nancy E Messonnier, Arthur Reingold, Mark Sawyer, Thomas A Clark (2018) Prevention of Pertussis, Tetanus, and Diphtheria with Vaccines in the United States: Recommendations of the Advisory Committee on Immunization Practices (ACIP).MMWR. Recommendations and Reports : Morbidity and Mortality Weekly Report. Recommendations and Reports 2018 April 28
[27] Ekere Sunday Udofia, Ubong Dominic Akpan, Joy Ijeoma Uwakwe and Henry Sylvester Thomas, Age structured deterministic model of diphtheria infection. Earthline Journal of Mathematical Sciences, Volume 14, Number 3, 2024, Pages 391-404 .
[28] Ekere Sunday Udofia, Ubong Dominic Akpan, Joy Ijeoma Uwakwe and Henry Sylvester Thomas, Mathematical modeling of bird harvesting in intensive poultry system. Asian Journal of Probability and Statistics, Volume 26, Issue 2, Page 76-83, 2024; Article no.AJPAS.112594 ISSN: 2582-0230 DOI: 10.9734/AJPAS/2024/v26i2593.
[29] Udofia, Ekere Sunday, Thomas Henry Sylvester (2023) Lyapunov stability of male circumcision in hiv/aids preventions. The Transaction of the Nigerian Association of Mathematical Physics, Volume 19, pages 1-16

[30] Udofia, Ekere Sunday, Thomas Henry Sylveste, Uwakwe Joy Ijeoma (2023) Discrete delay on the impact of media coverage in the transmission dynamics of fowl pox infection. The Transaction of the Nigerian Association of Mathematical Physics, Volume 19, pages 111-124

Algorithm for semigroup bases I

M.I. Sampson[*†], Z. Lipcsey[‡], E.O. Akak[†§], F.A. Efiong[†] and M.A. Essien[†††]**

Abstract

The study of generating sets and bases in semigroup theory started with the experience in the topics in vector spaces, and so with comparison, theorems on independent generating sets of Semigroup that vary from those about independent generating sets in vector spaces due to some differences in their structures are given. The paper shows that there may exist a maximal independent set of elements in a semigroup which does not form a generating set. It reveals that there may exists independent set in a semigroup which cannot be expanded to a generating set, and that adding an element independent from an independent set may make the independent set dependent in a semigroup. Also, given is an important condition fulfilled by a Basis in a semigroup. The paper gives an interesting property that serves as a relevant test tool for independent generating sets in the developed algorithms for determining the basis of any given semigroup. The resulting algorithm works for determining the basis any semigroup including classes of semigroups.

Keywords and phrases: Basis, Independent, generating set, Minimal, maximal, Vector spaces

1 Introduction

The characterization of an algebraic structure has as one of its popular tasks, the problem of solving for an independent generator of the algebraic structure. Such independent generators are called the bases. So many papers have been written on independent generating sets or bases of semigroups. Some recent ones are [1], [2], [3] and [4]. The paper [2], gives universal solution algorithm for the bases problem of semigroups. The paper [1] discusses certain semigroups in which the number of independent elements is larger than the basis, hence being just independent alone does not guarantee it being the basis of a semigroup. A later paper by [4] improved upon this algorithm which this paper further advances with more theorems that serve as easier tools for implementing the algorithm.,

[*]Corresponding Author; E-mail: **marshalsampson@aksu.edu.ng**
[†]Department of Mathematics, Akwa Ibom State University, Ikot Akpaden, AKS, Nigeria.
[‡]Department of Mathematics, University of Calabar, Calabar, CRS, Nigeria. E-mail: lipzsoltt@gmail.com
[§]Department of Mathematics, Akwa Ibom State University, Ikot Akpaden, AKS, Nigeria. E-mail: eyoakak3@gmail.com
[**]Department of Mathematics, University of Uyo, Nigeria E-mail: felixefiong@uniuyo.edu.ng
[††]Department of Mathematics, Akwa Ibom State University, Ikot Akpaden, AKS, Nigeria. E-mail: **essienmfon4real@gmail.com**

It is a common practice to study individual classes of semigroup as part of the numerous efforts to characterize semigroup in general. The approach, II. (in figure 1) which summarizes the solution approach used in this paper for determining the independent generator of semigroups is different from what is often found in most literatures that utilize the Greens equivalences. The green points $t_i, i \in N,$ in figure 1 which represent classes of semigroups are likened to trees of the forest (forming the whole semigroup) while the central spots in each of figures I and II respectively represent the researcher trying to study desired structure of the 'forest of semigroups. The researcher in I analyses from within the 'forest' while that in II. analyses from outside the 'forest' with a clearer view of the entire 'forest structure' but not afforded a detailed understanding of the individual properties of the trees as I. would be more privileged to.

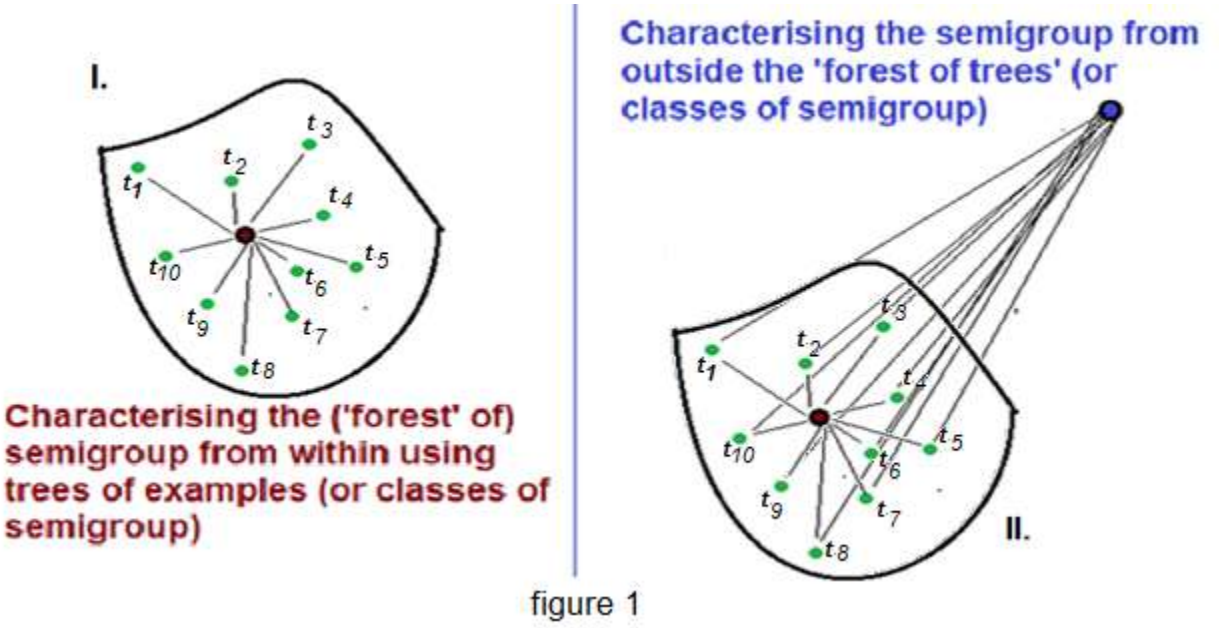


figure 1

The dots $t_i, i \in N$ represent Classes of Semigroups while the central spots represent the researcher I and II respectively.

This work will for now centre on constructing the algorithm for determining the bases of any semigroup. In a later paper, we will present the utilization of the ideas raised here in determining the Basis of classes of semigroup.

Definition 1.1. Let the set $P(W)$ be the power-set of the non-empty set W. A set $A \in P(W)$ with a property pr is maximal (minimal) if $\nexists U \in P(W)$ with the property pr such that $A \subset U$ $(U \subset A)$ and $A \neq U$.

Definition 1.2. The set $H \subset V$ is a generating set if $L(H) =: < H > = V$.

Definition 1.3. Let $\emptyset \neq H \subset V$ then $x \in V$ is independent from H if $x \notin L(H)$.

Definition 1.4. The set $H \subset V$ is an independent set if $x \notin L(H \setminus \{x\}) = < H \setminus \{x\}) >, \forall\, x \in H$.

Definition 1.5. An independent generating set $B \subset V$ is called a basis.

Let $\{V, +, *\}$ be a vector space over a field F and let $H \subset V$. The statements of the following theorem are popularly known to be true.

Theorem 1.1

1. A maximal independent set $B \subset V$ is a basis.

2. A minimal generating set $B \subset V$ is a basis i.e. it is independent;

3. If $H \subset V$ is an independent set and $v \in V$ is independent from H then $H \cup \{v\}$ is an independent set. Equivalently any independent set has an extension to a basis.

4. In a vector space $\{V, +, *\}$ over a field F the cardinality of all maximal independent sets is the same, which is the dimension of a vector space.

Proof. We prove them one after the other in the order they are given:

Proof of 1. Readers can also look up detailed explanations and proof in sections 1.3.1 – 1.3.2 of [6]. A slightly similar proof is also given by Sampson et. Al in [2] and [7].

Proof of 2. We show first as given in [2] that a generating set G being minimal $\Rightarrow$ G is independent: Let $x \in G$ be any element. We assume that G is dependent $\Longrightarrow \exists x \in \langle G \backslash \{x\} \rangle$ then

$$(G \setminus \{x\}) \cup \{x\}) \subset \langle G \backslash \{x\} \rangle \Longrightarrow V = \langle G \rangle = \langle (G \backslash \{x\}) \cup \{x\}) \rangle \subset \langle \langle G \setminus \{x\} \rangle \rangle$$

Which contradicts with the minimality of G. Hence G is rather independent, and also being a generating set implies that it is a basis. This completes the proof of 2.

Proof of 3.

See lemma 22 of [6] for the proof of 3.

Remark 1.6.1 (About proof of 4)**.** The proof of 4 is directly implied from the Steinitz Exchange (Replacement) Lemma (see theorem 31 of [6]) about exchange of elements of bases of a set. It states that if there are two bases of a set, then taking one basis, each element of it can be replaced by one element of the other basis. Hence the second basis has at least as many elements as the first one has. Next, the roles of the bases are exchanged. Repeating the process for more bases justifies the equality of the dimension of all the bases of the set.

Example 1.1.1 (Example 2.9 of [2]). Let $\{p_i\}_{i=1}^{m}$, $n = \prod_{i=1}^{m} p_i$ and $\{Z, +\}$ a group. Let

$$G_m := \left\{\frac{n}{p_i} | 1 \leq i \leq m\right\}$$

Let $\frac{n}{p_i} \in G_m$ be selected:

$$\frac{n}{p_i} = p_1 \times p_2 \times \ldots \times p_{i-1} \times p_{i+1} \times \cdots \times p_m.$$

Since p_i is not in the product, p_i is not its factor.

Consider $G_m \backslash \left\{\frac{n}{p_i}\right\}$. Then $\forall z \in G_m \backslash \left\{\frac{n}{p_i}\right\}$, $p_i / z \Longrightarrow \forall u \in \langle G_m \backslash \left\{\frac{n}{p_i}\right\}\rangle$, $p_i | u$ while $p_i \nmid \frac{n}{p_i}$

In summary, $\frac{n}{p_i} \notin \langle G_m \backslash \left\{\frac{n}{p_i}\right\}\rangle$ meaning that $\left\{\frac{n}{p_i}\right\}$ is independent from $G_m \backslash \left\{\frac{n}{p_i}\right\}$.

Remark 1.1.1 It can be shown with examples (see Example 1.8) that handling generating sets and independence including construction of bases in semigroup theory requires a technique different from the technique used in vector spaces. Important conclusions are the deviations from the properties discussed in Theorem 1.6 about vector spaces stated in theorem 1.10 about semigroups.

1. Independence: There may exist maximal independent set of elements in a semigroup which does not form a generating set.

2. There may exists independent set in a semigroup which cannot be expanded to a generating set.

3. Adding an element independent from an independent set may make the independent set dependent in a semigroup.

1.2 Construction of generating sets and bases in semigroups.

We will first analyze the basis construction in vector spaces.

1.2.1. Basis in Vector Spaces.

The algorithm to select a basis in vector spaces is based on the properties of independence.

Let $\{V, +, *\}$ be a vector space over a field F and let $B \subset V$ hold the selected basis elements, let $B = \emptyset$ for starting. Let $G \subset V$ be the starting system of vectors. Then

(a) If $G \neq \emptyset$ then $\exists x \in G$ otherwise [exit];

(b) If $x \notin L(B)$ then $B = B \cup \{x\}$ and $G = G \backslash L(B)$ otherwise $G = G \backslash \{x\}$.

(c) goto (a).

This algorithm collects a basis in B by the Theorem 1.6 (1) and (3). Since these ((1) and (3)) are not necessarily true in semigroups, this cannot be adopted to semigroups. One most important consideration is that a maximal independent subset of a semigroup may not be a generating set and a basis must be a generating set. Since a generating set may not be reached from an independent set, we will work from starting with a generating set and we will sustain it throughout the process. Note that if $\{S,*\}$ is a semigroup then $S \subset S =< S >$ is a generating set. Therefore $G = S$ always can serve as a starting generating set.

Example 1.8. Consider the following semigroup $\{S,*\}$ where S := {a, b, c}, and the operation

is defined by the operation table (Table 1.):

$*$	a	b	c
a	a	c	c
b	c	b	c
c	c	c	c

Table 1: The operation table of {S, $*$}.

Theorem 1.2 The structure {S, $*$} is a semigroup, the operation is associative.

Proof. It suffices to check that associativity holds for $*$ in $(S,*)$:

$a * (b * \mathrm{c}) = (a * \mathrm{b}) * \mathrm{c} = c,$ $\quad$ $a * (c * \mathrm{b}) = (a * \mathrm{c}) * \mathrm{b} = c,$

$b * (a * c) = (b * a) * c = c,$ $\quad$ $b * (c * a) = (b * c) * a = c,$

$c * (b * \mathrm{a}) = (c * \mathrm{b}) * \mathrm{a} = c,$ $\quad$ $c * (a * b) = (c * a) * b = c.$

Clearly $\forall x, y, z \in S, x * (y * \mathrm{z}) = (x * \mathrm{y}) * \mathrm{z}$, so {S, $*$} is a semigroup

Theorem 1.3 In the semigroup $\{S,*\}$ given in Example 1.8, the following are true.

1. The subset $\{b, c\} \subset S$ is a subsemigroup of S. The members of $\{b, c\}$ are independent: $\{b, c\} \setminus \{b\} = \{c\}$ and $b \notin < \{c\} >= \{c\}$. Similarly, $\{b, c\} \backslash \{c\} = \{b\}$ and $c \notin < \{b\} >= \{b\}$.

2. The subset $\{a, b\} \subset S$ is a generating set of S and a and b are independent hence it is a basis and

$a \in S$ is independent from $\{b, c\} \subset S$ since this set is a sub semigroup of S and a is not in it.

3. Since $\{b, c\} \subset S$ is an independent subsemigroup, there is only one element in S which is independent from this set, it is $a \in S$ and adding a to $\{b, c\}$ forms a dependent set:

$$\{a, b, c\} \setminus \{c\} = \{a, b\} \subset S \; gives \; < \{a, b\} >= S \ni c.$$

Proof. We proved the statements of the theorem in the theorem so this does not require a separate proof.

1.2. Remarks. The example shows that handling generating sets and independence including construction of bases in semigroup theory requires a technique different from the technique used in vector spaces. Important conclusions are the deviations from the properties discussed in Theorem 1.6 about vector spaces now stated in theorem 1.0 about semigroups.

1. Independence: There may exist maximal independent set of elements in a semigroup which does not form a generating set.

2. There may exists independent set in a semigroup which cannot be expanded to a generating set.

3. Adding an element independent from an independent set may make the independent set dependent in a semigroup.

2 Bases of Semigroups: The Algorithm.

The following is the first presented algorithmic for obtaining the bases set of any semigroup. We present some below.

Let $\{S,*\}$ be a semigroup and let $\emptyset \neq G \subset S$ be a generating set. Let $S \supset B = \emptyset$.

(a) If $G \neq \emptyset$ then $\exists x \in G$ and $G_{test} = G \setminus \{x\}$ otherwise [exit];

(b) If $x \notin L(G_{test} \cup B)$ then $B = B \cup \{x\} \; and \; G = G \setminus L(B)$ otherwise $G = G_{test}$;

(c) goto (a).

Remark 2.1.

(1). At starting $G \cup B = G$ is a generating set.

(2). In step (a) $G_{test} = G \setminus \{x\}$ removes x from G hence the test $x \notin L(G_{test} \cup B)$ in (b) checks for $x \notin L((G \cup B)\setminus\{x\})$ which checks if x is independent from the generating set $G \cup B$.

Observe that in the case of vector spaces we check for the independence from B only.

(3). In step (b) we change B to a new value $B_{new} = B \cup \{x\}$ and $G_{new} = G \setminus L(B_{new})$ if

the independence of x holds otherwise $G_{new} = G_{test}\ and\ B_{new} = B$. The set $G_{new} \cup B_{new}$ is

a generating set in the step (c): At step (a) $(G \cup B)$ was a generating set at starting since

$B = \emptyset$ and G was a generating set.

After selecting $x \in G$ we have two options:

i). $x \notin L(G_{test} \cup B)$: Then $x \in B_{new}(= B \cup \{x\})$ and $G_{new} = G_{test}$ hence $x \in G$ moves from

G into $B \subset S$. The final value of G is $G_{new,f} = G_{new} \setminus L(B_{new})$.

The set $G_{new,f} \cup B_{new}$ is a generating set: $L(G_{new,f} \cup B_{new}) \supset G_{new,f} \cup L(B_{new}) \supset G_{new} \cup B_{new}$. Then $G_{new} = G \setminus \{x\}$ and $B_{new} = B \cup \{x\} \Rightarrow G_{new} \cup B_{new} = G \cup B$. Since $G \cup B$ was a generating set and $L(G_{new,f} \cup B_{new}) \supset G \cup B$, $G_{new,f} \cup B_{new}$ is a generating set.

ii). $x \in L(G_{test} \cup B)$: Then $G_{new} = G_{test}$ and $B_{new} = B$.

Since in this case $x \in L(G_{test} \cup B)$ holds, $L(G_{test} \cup B) \supset G_{test} \cup B \cup \{x\} = G \cup B$. Hence $G_{new} \cup B_{new}$ is a generating set.

(4). $G \cup B \supset G_{new,f} \cup B_{new}$ and $G = G_{new,f}$ moreover if $x \in G$ is selected in step (a) then

$x \notin G_{new} \supset G_{new,f}$ hence or otherwise, any x can be selected only once. Therefore, if we select basis vectors $x_1, x_2, \ldots, x_k, \ldots$ one after the other then

$G_0 := G, B_0 := B = \emptyset,\quad G_1 := G_{new,f}\ ,\ B_1 := B_{new}, \ldots,\quad G_k := (G_{k-1})_{new,f}\ , B_k := (B_{k-1})_{new}, \ldots$.

Then the system of sets $\{G_S, B_S\}_{1 \le s' < \infty}$ and the selected points $\{x_S\}_{1 \le s \le \infty}$ fulfil:

$$(G_k \cup B_k) \supset (G_{k+1} \cup B_{k+1});\ G_k \supset G_{k+1}\ and\ G_k \neq G_{k+1}\ \forall\ 0 \le k < \infty$$

$$x_j \in B_j \ \forall\, 1 \leq j < k, \ B_k = \{x_j \mid 1 \leq j \leq k\}, \ \forall\, k \in N\,. \qquad (11)$$

Theorem 2.1.
The set $B_k \subset S$ is independent $\forall 1 \leq k < \infty$.

Proof. The proof is a direct implication of Remarks 2.1 (1) – (4), populating the set B_k is done with independent elements at each stage, giving rise to a set in which each element is not in the subsemigroup generated by the remaining elements up to the last set B_k. Hence B_k is independent.

Theorem 2.2.
In any semigroup $\{S,*\}$ there exists an independent generating set B ⊂ S (basis). If in the semigroup $S\ \exists x, y, z \in S$ such that $x * y = z$ and $z \notin \{x, y\}$, then there exists a basis $B \subset S, B \neq S$ (B is a proper subset of S).

Proof. The existence follows from our reasoning above. If there exists x, y, z ∈ S as stated in the theorem then let us select $z \in G = S$ as the first choice. Then $S\backslash\{z\} \supset \{x, y\} \Rightarrow x * y = z \in \langle\{x, y\}\rangle \subset \langle G\backslash\{z\}\rangle$ hence z is not independent from $G\backslash\{z\}$ hence z is not a selected basis element. Therefore, the selected basis B is a proper subset of S.

3 Discussions and Conclusion

In any semigroup there exists a maximal independent subset that is a generating set hence that is a basis. With the example of the semigroup of integers in [7] and [4], we proved that there are bases in a semigroup which can have different numbers of elements. With the example we showed that in a semigroup there may exists a maximal independent set of elements which is not a generating set.

The idea of the algorithm is as follows: When we select the next candidate to be a basis element from the current generating set then we assure that it is independent from all the previously selected basis elements (this is B) and it is independent from all possible future selections (this is the current G). This puts $x \notin (G \cup B) \setminus \{x\}$ into the selection condition.

4 Recommendation

This work has for now been focused on constructing the algorithm for determining the bases of any semigroup. In a later paper soon, we will present the utilization of the ideas raised here in determining the Basis of some classes of semigroup. This will take us off the need to rely on the popular green's equivalences that have been the tools in several articles over the years. It will be an interesting exercise to compare results starting with bases in Abundant Semigroups, Superabundant semigroup, Orthogroup, the Cyber Group and the Brandt Semigroup as given in [8], [9], [3], [5], [10] and [11].

The characterizations in [11] are used for presenting an algorithm in [7] for generators of the Additive Semigroup of Integers.

References

[1] Sampson M.I. (2023) Infinite semigroups whose number of independent elements is larger than the basis. IJRTI | Volume 8, Issue 7 | ISSN: 2456-3315.

[2] Sampson M.I., L. Zsolt, Achuobi J.O., Igiri C.F., Effiong L.E. (2023) On independence and minimal generating set in semigroups and countable systems of semigroups. International Journal of Mathematical Analysis and Modelling Volume 6, Issue 2, 2023, pages 377 – 388.

[3] X.M. Ren, K.P. Shum (2007). On superabundant semigroups whose set of idempotents forms a subsemigroup. Semantic Scholar. DOI:10.1142/S1005386707000223Corpus ID: 122226849.

[4] Zsolt, Lipcsey and Sampson M.I. (2023). On existence of minimal generating sets and maximal independent sets in groups and the additive semigroup of integers. IOSR Journal of Mathematics (IOSR-JM). e-ISSN: 2278-5728, p-ISSN: 2319-765X. Volume 19, Issue 4 Ser. 1 (July. – August. 2023), PP 57-64 www.iosrjournals.org.

[5] Udoaka O.G, and Sampson, Marshal I. (2018). Direct product of brandt semigroup and its rank as a class of algebra

[6] Lior Silberman (2022). Linear Algebra Lecture Notes. https://personal.math.ubc.ca/~lior/teaching/2122/223_W22/223-notes.pdf

[7] Sampson, M.I. Generating Systems of Semigroups and Independence. PhD Thesis. University of Calabar, CRS, Nigeria.

[8] Abdulsalam El-Qallali (1990). On the construction of a class of abundant semigroups. Acta Mathematica Hungarica 56, 1990.

[9] Abdulsalam El-Qallali (1991) Left regular bands of groups of left quotients. Glasgow Math. J. 33, 29-40.

[10] Michael N. J., Sampson M.I., C. F. Igiri, O.G. Udoaka, L.E. Effiong, Jackson A. (2024). A study on the relationship between minimal generating sets and independence in semigroups. International Journal of Computer Science and Mathematical Theory (IJCSMT) E-ISSN 2545-5699 P-ISSN 2695-1924 Vol 10. No.1 2024 www.iiardjournals.org.

[11] Sampson M.I., Zsolt Lipcsey(2019). rank of semigroup: generating sets and independent sets conference: International Conference on Mathematics, Istanbul, Fatih Sultan Mehmet University, Istanbul, Turkey.

Utility maximization and portfolio management with administrative fee and dividend

E.E. Akpanibah[*†], **L.E. George**[†], and **W.V. German**[†]

Abstract

The study of utility maximization cannot be over emphasized in the study of portfolio management as it plays crucial role in the determination of investor's strategy over any investment. In this research work, we investigate some utility functions and their applications to portfolio optimization and risk management. Also, a portfolio consisting of one risk free asset and a risky asset which follows the geometric Brownian motion was considered. We took into consideration transaction cost, dividend and tax on invested funds. By applying Ito's lemma and maximum principle, we obtained an optimization problem which comprise of a nonlinear PDE (Hamilton Jacobi Bellman equation) and a control problem (optimal investment strategy). These problems are functions of the value function which is dependent on the utility of the investor at the expiration of such investment. Furthermore, the exponential and logarithm utility were used in solving for the optimal investment strategies and some numerical results also presented. It was observed for both cases that the optimal investment strategies (OIS) were directly proportional to appreciation rate, dividend and inversely proportional to the administrative charges, instantaneous volatility, tax and risk averse coefficient. Also, the OIS under logarithmic utility does not depend on the risk averse coefficient and tax while the optimal investment strategy under exponential utility does not depend on wealth.

Keywords and phrases: portfolio management; utility maximization; ito's lemma; geometric brownian motion; financial market.

1 Introduction

1.1 Background of the study

The study of Investment strategy and portfolio optimization has become increasingly of important in managing financial resources of individual investors and financial institutions for purpose of achieving optimal returns for both the investors and the fund managers. In years past, many authors such as [1] - [6] have spent time in developing robust investment plans and strategies to investment decision making. In developing investment strategies, one crucial aspect to be considered is the utility functions which evaluate or quantify investor's preferences and risk tolerance [7].

The idea of utility is rooted in the area of study involving economics; more specifically, the theory of consumer behaviour established by Daniel Bernoulli in the 18^{th} century which later evolves into expected utility theory by John von Neumann and Oskar Morgenstern in the mid-20^{th}century. According to [8], utility is a subjective psychological feeling or a trade off response of an investor to the anticipated gains (satisfaction) or losses (dissatisfaction) of specific risk events. It helps to measure investors' attitude and courage toward investments.

It serves as a mathematical illustration of an investor's satisfaction he or she derived from different investment outcomes [9]. By integrating utility functions into the investment decision making process, investors can align their investment choices with their distinct risk preferences, financial goals and attitude toward wealth. The utility functions help investors to make an informed investment decisions

*Corresponding Author; E-mail: edemae@fuotuoke.edu.ng

†Department of Mathematics and Statistic, Federal University Otuoke, Bayelsa, Nigeria.

by carefully examining the risk-reward trade off and choosing investment combinations that maximize their expected utility. Utility functions can be linear, exponential, quadratic, logarithm, power, and other functional forms captures different aspect of investor preferences and risk aversion [10].
There are mainly two types of widely used utility goals in the study of optimal investment. one which maximizes the accumulated amount at the end of investment and the other is to balance the expected return and the risk .The first goal is made up of three types of utility function which include utility functions which exhibits Constant Relative Risk Aversion (CRRA) and example include logarithm utility [11] - [14] and power utility [15] - [18]. Also, utility functions which exhibits Constant Absolute Risk Aversion (CARA) and example which include exponential utility [19] - [23] and the quadratic loss function [24] - [27] While the second goals is made up of Value-at-risk (VAR) utility [28] and mean-variance utility [29] - [34].
As earlier stated, utility functions are tools which enable investor's decisions or investment choices. However, in solving optimal investment problems, some challenges exist owed to uncertainty in the market, behavioural indifference, volatility of the stock market prices, parameter determination, inadequate information and change in market structure, etc. It is of importance to be familiar with these challenges while choosing utility functions to solve optimal investments problems and to consider them together with other techniques in investment decision making process. The application of utility function to portfolio optimization has become very important as it helps investors to make informed investment decision. Hence in this research, we will be studying two classes of utility functions: one which exhibits constant absolute risk averse (CARA) and that which exhibits constant relative risk averse (CRRA), use it to maximize a given portfolio involving transaction cost, dividend and tax and use it to discuss the effect of some these parameters on the OIS and also compare the OIS for the two cases.

2 Methodology and financial market model

2.1 Methodology

In this section, we shall discuss the Itô process since it is the essential tool required in solving stochastic differential equations. Also, we will also formulate and modeled our required problem. So we begin with some definitions which will be of important to our study in this section.

Definition 2.1. *Let* $\mathrm{B_t}$ *be a one-dimensional Brownian motion on* $(\Omega, \mathrm{F}, \mathrm{p})$*. A (one-dimensional) Itô process (or stochastic integral) is a stochastic process* $X(t)$ *on* $(\Omega, \mathrm{F}, \mathrm{p})$ *of the form*

$$X\left(t\right) = X\left(0\right) + \int_S^T \alpha\left(s,\ \omega\right)ds + \int_S^T \sigma\left(s,\ \omega\right)dW(t) \tag{2.1}$$

where $\sigma \in \mathrm{W_H}$ *so that*

$$\mathrm{p}\left[\int_S^T \alpha\left(s,\ \omega\right)^2 ds < 8,\ \forall\, t = 0\right] = 1. \tag{2.2}$$

We also assume that u *is* $H(t)-$*adapted, where* $H(t)$ *is an increasing family of* σ*-algebras,* $\{H\left(t\right)\}\ t = 0$ *, such that* $\mathrm{B_t}$ *is a martingale with respect to* $H(t)$*, and*

$$\mathrm{p}\left[\int_S^T |\sigma\left(s,\ \omega\right)|ds < 8,\ \forall\, t = 0\right] = 1.$$

Assuming $X(t)$ *is an Itô process in the of form* (2.1)*, the differential form of* (1) *is given as*

$$dX(t) = \alpha dt + \sigma dW(t) \tag{2.3}$$

Where α *is the drift and* σ*, the standard deviation representing the instantaneous volatility.*

Remark 2.2. Let $X(t)$ be an Itô process given by (2.3)
Let $g(t,\ x)\ \in\ C^2([0,8)\ \times\ \Re)$. Then $Y\ (t)\ =\ g(t,X(t))$ is again an Itô process, and

$$dY\ \ (t)=\frac{\partial g}{\partial t}\left(t,X\left(t\right)\right)dt\ +\frac{\partial g}{\partial x}\left(t,X\left(t\right)\right)dX\left(t\right)+\frac{1}{2}\frac{\partial^2 g}{\partial w^2}(t,X(t))(dX(t))^2, \tag{2.4}$$

Remark 2.3. For Ito processes $U(t)$ and $V\ (t)$ in $\Re$, Itô's product rule gives

$$d(U(t)V\ (t))\ =\ U(t)dV(t)\ +\ V\ (t)dU(t)\ +\ dU(t)dV(t).$$

where $(dX(t))^2=\ dX(t)dX(t)$ is computed according to the rules

$$dtdt\ =\ dtdW(t)\ =\ dW(t)dt\ =\ 0;;\ dW(t)dW(t)\ =\ dt.$$

(2.4) can also be written as

$$dg(t,X(t))\ \ (t)=\frac{\partial g}{\partial t}\left(t,X\left(t\right)\right)dt\ +\frac{\partial g}{\partial x}\left(t,X\left(t\right)\right)dX\left(t\right)+\frac{1}{2}\frac{\partial^2 g}{\partial w^2}(t,X(t))(dX(t))^2, \tag{2.5}$$

2.2 Financial market model and formulation

Let us consider a portfolio which is made up of a risk free asset and a risky asset which follows the geometric Brownian motion in a financial market which is continuously open for a given period of time $t\ \in\ [0,\ T]$ where T is the expiration date of the investment. Let $\{W\left(t\right):t=\ 0\}$ be standard Brownian motion defined on a complete probability space (Ω,F,p) where Ω is a real space and p is a probability measure and F is the filtration which represents the information generated by the three Brownian motions.

$$\frac{dA}{A}=rdt\quad A(0)=1 \tag{2.6}$$

The price process is described in [2, 4, 35]

$$\frac{ds}{s}=\omega dt\ +kdW(t) \tag{2.7}$$

Where ω is the appreciation rate of the risky asset and r is is the interest rate of the risk free asset, W(t) is the standard Brownian motion defined on a complete probability space $(\Omega,\ f,p)$.
Let π, be the amount an investor is allowed to invest in the risky asset. Hence the amount to be invested in the risk asset is given as $X-\pi$. where X is the wealth process of the investor.
Let $\tau,\kappa and\zeta$ represent the rate of taxes in the financial market, dividend income and transaction cost comprising of fees and stamp duties [24].
Also, we assume that $\omega+\kappa-\zeta-r\ >\ o$ the wealth process $X\ (t)$ corresponding to the investment strategy and the initial wealth of the investor $X_{O,}$ is given as

$$dX=\pi\frac{ds}{s}+\left(X-\pi\right)\frac{dA}{A}-\tau X\left(t\right)dt \tag{2.8}$$

Substitute (2.6) and (2.7) in (2.8), we have

$$\begin{aligned}dX&=\pi\left[\omega dt+kdW\right]+\left(X-\pi\right)rdt-\tau Xdt\\&=\pi\omega dt+\pi kdW+rXdt-\pi rdt-\tau Xdt\\&=\left[\pi\left(\omega-r\right)+\left(r-\tau\right)X\right]dt+\pi kdW\end{aligned} \tag{2.9}$$

Considering the dividend and transaction cost, then (2.9) becomes

$$dX=\left[\pi\left(\omega+\kappa-\zeta-r\right)+\left(r-\tau\right)X\right]dt+\pi kdW \tag{2.10}$$

Next, we defined the value function of the investor's utility at the expiration of his or her investment as follows

$$G(T,x) = Max\ E\left[U\left(X\left(t\right)\right)/X = x\right] \tag{2.11}$$

From Ito's lemma Taylor series expansion, and maximum principle can obtain the (HJB) equation as follows

$$dG = G_t\ dt + G_x\ dx + \frac{1}{2}G_{xx}\left(dx\right)^2 = \begin{bmatrix} G_t\ dt + G_x\left[\left[\pi\left(\omega+\kappa-\zeta-r\right)+\left(r-\tau\right)X\right]dt+\pi k dW\right] \\ +\frac{1}{2}G_{xx}\left[\left[\pi\left(\omega+\kappa-\zeta-r\right)+\left(r-\tau\right)X\right]+\pi k dW\right]^2 \end{bmatrix} = G_t\ dt + G_x\ [$$

According to Ito's lemma $dwdt = dtdt = 0,\ \left(dw\right)^2 = dt$

$$\frac{dG}{dt\to 0} = G_t + G_x\left[\pi\left(\omega+\kappa-\zeta-r\right)+\left(r-\tau\right)X\right] + \frac{1}{2}\pi^2 k^2 G_{xx} = 0$$

$$G_t + \left(r-\tau\right)X\,G_x + Sup\left\{\frac{1}{2}\pi^2 k^2 G_{xx} + \pi\left(\omega+\kappa-\zeta-r\right)G_x\right\} = 0$$

$$G(T,x) = U(x) \tag{2.12}$$

Where $G_t,\ G_x\ and\ G_{xx}$ are partial derivatives of the first and second order w.r.t time, and wealth. Differentiating (2.12) with respect to π, we have

$$\pi = \frac{-\left(\omega+\kappa-\zeta-r\right)G_x}{k^2 G_{xx}} \tag{2.13}$$

Substituting (2.13) into (2.12), we have,

$$G_t + \left(r-\tau\right)xG_x + \frac{1}{2}k^2\left(\frac{\left(\omega+\kappa-\zeta-r\right)}{k^2}\frac{G_x}{G_{xx}}\right)^2 xG_{xx} - \frac{\left(\omega+\kappa-\zeta-r\right)G_x}{k^2 G_{xx}}x\left(\omega+\kappa-\zeta-r\right)G_x = 0$$

$$\begin{bmatrix} G_t + \left(r-\tau\right)xG_x - \frac{1}{2}\left(\frac{\omega+\kappa-\zeta-r}{k}\right)^2\frac{G_x^2}{G_{xx}} = 0 \\ G\left(T,x\right) = U\left(x\right) \end{bmatrix} \tag{2.14}$$

Next we will proceed to solve the nonlinear PDE in (2.14) for $G\left(T,x\right)$ under exponential utility, and logarithmic utility functions.

3 Analysis of the model

In this section we will be solving for the value function $G\left(T,x\right)$ from the HJB equation in (2.14) and the solution obtained will be used to obtain our investment strategies under exponential and logarithmic utility functions.
To achieve this, we will use the power transformation method similar to the used in [24].

3.1 Optimal investment strategy under logarithm utility function

The logarithmic utility function is given as

$$u\left(x\right) = \ln x \tag{3.1}$$

Next we conjecture a solution to (3.1) as follows

$$\begin{cases} G(t,x) = a(t)\ln x + b(t) \\ a(T)=1,\ b(t)=0 \end{cases} \tag{3.2}$$

Differentiating (3.2), we have

$$G_t = a'\left(t\right)\ln x + b'\left(t\right), G_x = \frac{a_t}{x}, G_{xx} = \frac{-a_t}{x^2} \tag{3.3}$$

Substituting (3.3) into (2.14), we have

$$a'(t)\ln x + b'(t) + (r-\tau)x\left(\frac{a(t)}{x}\right) - \frac{1}{2}\left(\frac{\omega+\kappa-\zeta-r}{k^2}\right)\left(\frac{a(t)}{x}\right)^2 \div \left(\frac{-a(t)}{x}\right) = 0$$

$$a'(t)\ln x + b'(t) + (r-\tau)a(t) + \frac{1}{2}\left(\frac{\omega+\kappa-\zeta-r}{k^2}\right)\frac{(a(t))^2}{a(t)} = 0$$

$$a'(t)\ln x + b'(t) + (r-\tau)a(t) + \frac{1}{2}\left(\frac{\omega+\kappa-\zeta-r}{k^2}\right)a(t) = 0 \tag{3.4}$$

Splitting

$$\begin{cases} a'(t)=0 \\ a(T)=1 \end{cases} \tag{3.5}$$

$$\begin{cases} b'(t)+(r-\tau)a(t)+\frac{1}{2}\left(\frac{\omega+\kappa-\zeta-r}{k^2}\right)a(t)=0 \\ b(T)=0 \end{cases} \tag{3.6}$$

Solving (3.5), we have

$$a(t) = 1 \tag{3.7}$$

Substituting (3.7) into (3.6)

$$b'(t) + (r-\tau) + \frac{1}{2}\left(\frac{\omega+\kappa-\zeta-r}{k^2}\right) = 0 \tag{3.8}$$

Solving (3.8), we have

$$b(t) = \left[(r-\tau) + \frac{1}{2}(\omega+\kappa-\zeta-r)\right](T-t) \tag{3.9}$$

Hence from (3.7) and (3.9) the value function in (3.2) becomes

$$G(t,x) = \ln x + \left[(r-\tau) + \frac{1}{2}(\omega+\kappa-\zeta-r)\right](T-t) \tag{3.10}$$

Also from (3.3)

$$G_x = \frac{a(t)}{x} = \frac{1}{x} \tag{3.11}$$

$$G_{xx} = \frac{-a(t)}{x^2} = \frac{-1}{x^2} \tag{3.12}$$

From equ (3.11) and (3.12), equation (2.13)

$$\pi = \frac{-(\omega+\kappa-\zeta-r)}{k^2}\left(\frac{1}{x} \div \frac{-1}{x^2}\right)$$

$$= \frac{(\omega+\kappa-\zeta-r)}{k^2}\left(\frac{1}{x} \times \frac{x^2}{1}\right)$$

Hence the optimal investment strategy under logarithmic utility is given as

$$\pi^* = \frac{x(\omega+\kappa-\zeta-r)}{k^2} \tag{3.13}$$

3.2 Optimal investment strategy under exponential utility function

The exponential utility function is given by

$$U(x) = \frac{-1}{q} e^{-qx},\ q > 0 \tag{3.14}$$

Where q is the risk averse coefficient of the member and x is the investor's wealth
Next, we conjecture a solution to (3.14) as follows

$$G(x,t) = \frac{-1}{q} \exp\{-q[a(t)(x - d(t)) + g(t)]\} \tag{3.15}$$

$$a(T) = 1,\ d(T) = 0,\ g(T) = 0$$

Differentiating (3.15), we have

$$G_t = -q[q_t(x-d) - d_t a + g_t]G, G_x = -qag,\ G_{xx} = q^2a^2G \tag{3.16}$$

Substituting (3.16) into (2.14), we have

$$-qG\left\{[a_t + (r-\tau)a]x - \left(d_t + \frac{a_t}{a}d\right)a + \left[g_t - \frac{1}{2}\frac{(\omega+\kappa-\zeta-r)}{qk^2}\right]\right\} = 0 \tag{3.17}$$

Splitting (3.17), we have

$$\begin{cases} a_t + (r-\tau)a = 0 \\ a(T) = 1 \end{cases} \tag{3.18}$$

$$\begin{cases} d_t + \frac{a_t}{a}d_t = 0 \\ d(T) = 0 \end{cases} \tag{3.19}$$

$$\begin{cases} g_t - \frac{1}{2}\left(\frac{\omega+\kappa-\zeta-r}{qk^2}\right) = 0 \\ g(T) = 0 \end{cases} \tag{3.20}$$

From (3.18), we have

$$\frac{a_t}{a} = -(r-\tau) \tag{3.21}$$

Substituting (3.21) into (3.19), we have

$$\begin{cases} d_t - (r-\tau)d(t) = 0 \\ d(T) = 0 \end{cases} \tag{3.22}$$

Next, we solve (3.18) to obtain

$$a(t) = e^{(r-\tau)(T-t)} \tag{3.23}$$

Similarly, if we solve (3.22), we have

$$d(t) = 0 \tag{3.24}$$

Finally, we solve (3.20) for $g(t)$as follows

$$g(t) = \left(\frac{\omega+\kappa-\zeta-r}{2qk^2}\right)(t-T) \tag{3.25}$$

Substituting (3.23), (3.24) and (3.25) into (3.15) we obtain our value function as follows

$$G(t,x) = \frac{-1}{q} Exp\left[-q\left(xe^{(r-\tau)(T-t)}\right) + \left(\frac{\omega+\kappa-\zeta-r}{2qk^2}\right)(t-T)\right] \tag{3.26}$$

From (3.16),

$$\frac{G_x}{G_{xx}} = \frac{-qaG}{q^2a^2G} = \frac{-1}{qa} \tag{3.27}$$

Substitute (3.23) into (3.27), we have

$$\frac{G_x}{G_{xx}} = \frac{-1}{qe^{(r-\tau)(T-t)}} = \frac{-1}{q}e^{(r-\tau)(t-T)} \tag{3.28}$$

Therefore, (2.13) now becomes

$$\pi* = \frac{-(\omega+\kappa-\zeta-r)}{k^2}\left(\frac{-1}{q}e^{(r-\tau)(t-T)}\right)$$

$$\pi* = \frac{(\omega+\kappa-\zeta-r)}{qk^2}e^{(r-\tau)(t-T)} \tag{3.29}$$

Hence the optimal investment strategy under exponential utility is given in (3.29)

4 Numerical simulations/sensitivity analysis

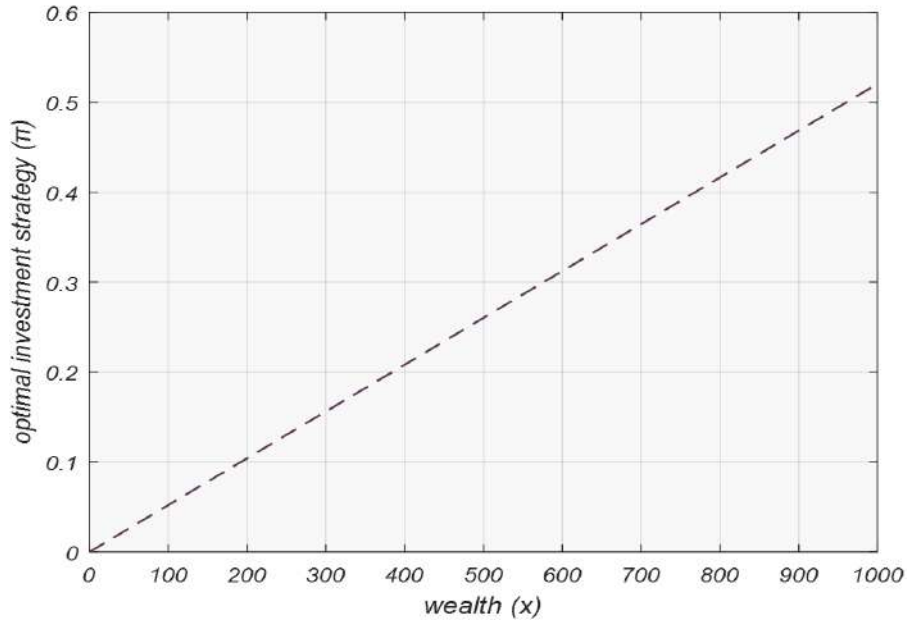


Figure 1: The variation of the optimal investment strategy with investor's wealth.

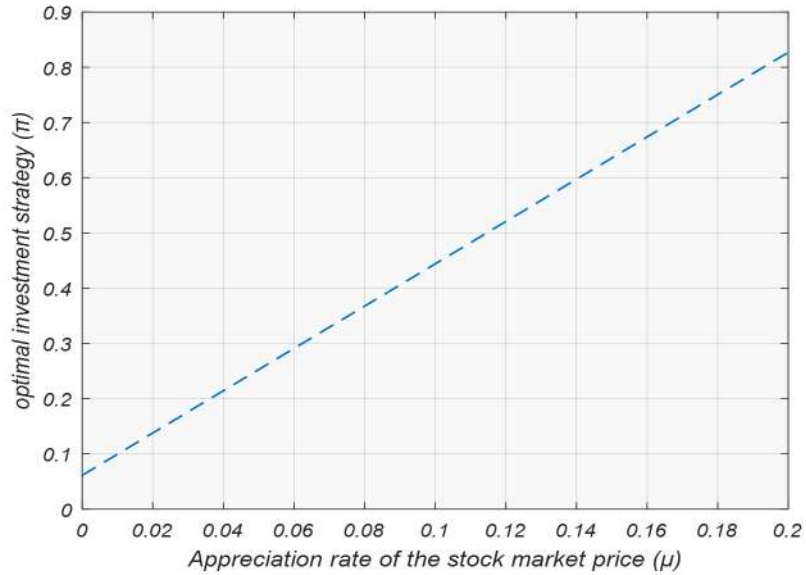


Figure 2: The variation of the optimal investment strategy with appreciation.

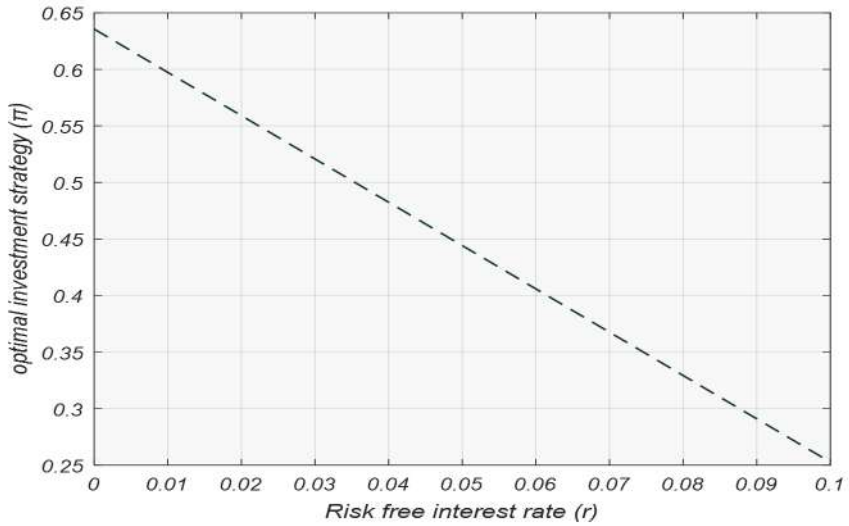


Figure 3: The variation of the optimal investment strategy with risk free interest rate.

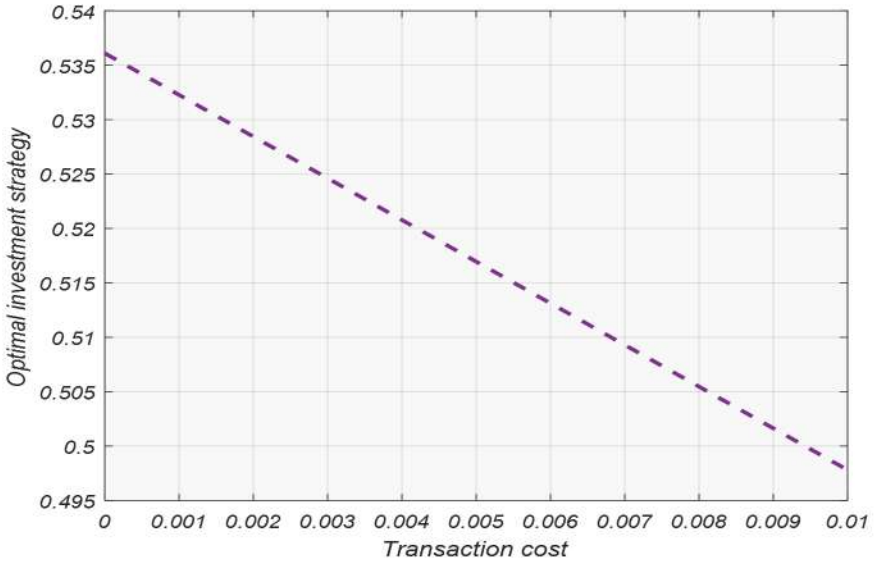


Figure 4: The variation of the optimal investment strategy with transaction cost.

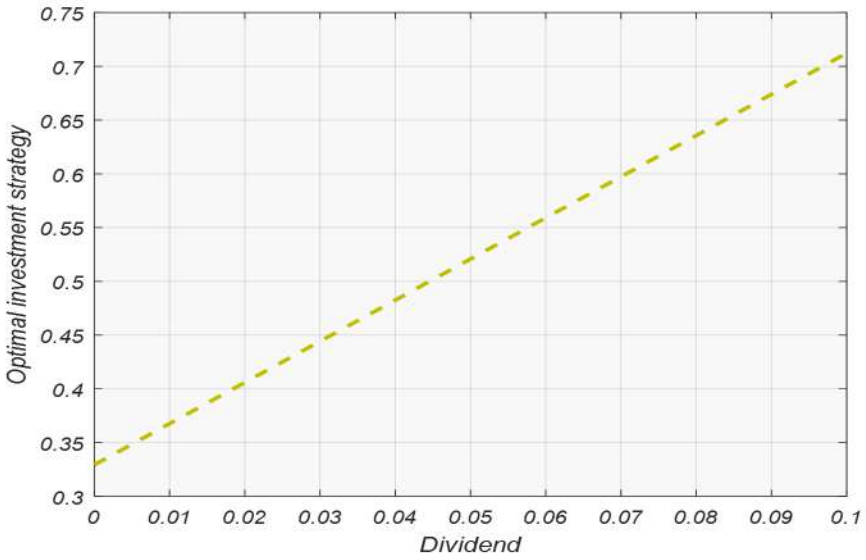


Figure 5: The variation of the optimal investment strategy with dividend.

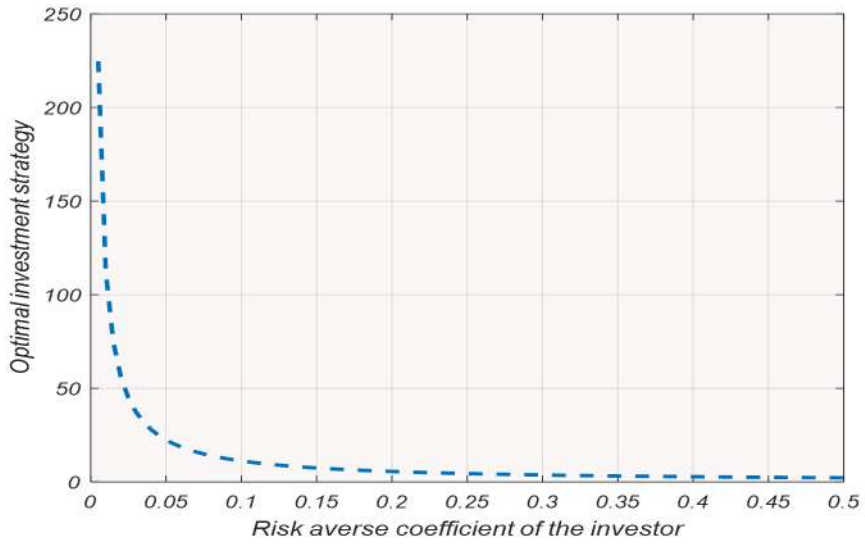


Figure 6: The variation of the optimal investment strategy with risk averse coefficient.

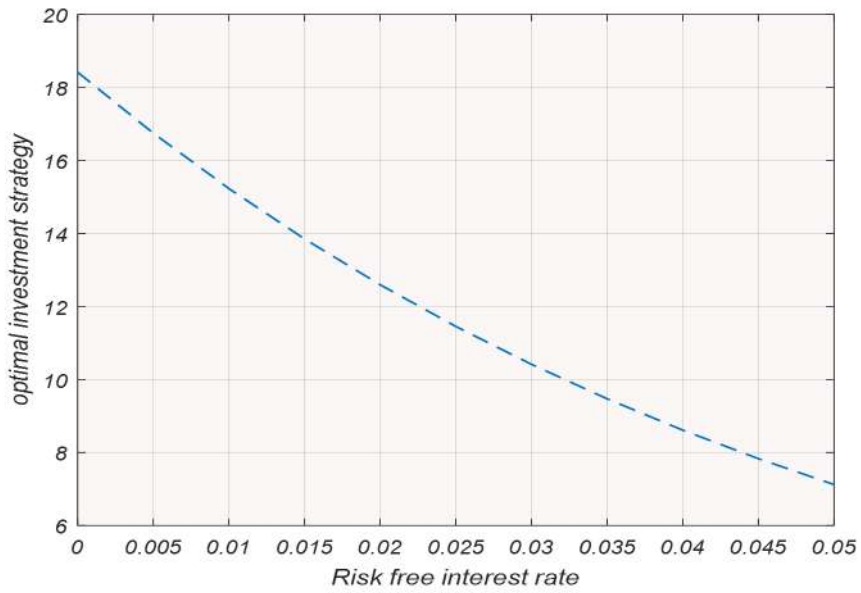


Figure 7: The variation of the optimal investment strategy with risk free interest.

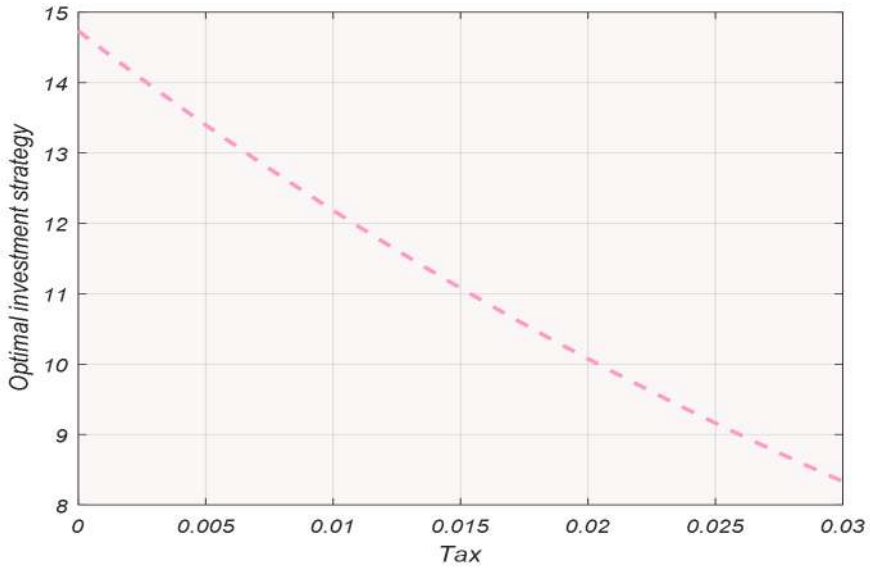


Figure 8: The variation of the optimal investment strategy with tax.

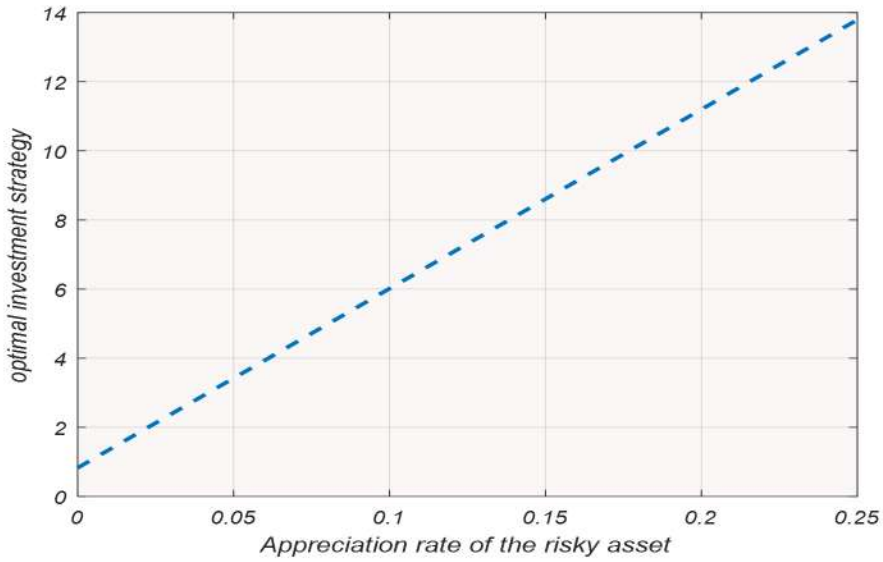


Figure 9: The variation of the optimal investment strategy with appreciation rate.

5 Discussions and conclusion

From (3.13), it is observed that the optimal investment strategy for an investor with logarithmic utility is a function of the wealth function, appreciation rate, dividend, transaction cost, risk free interest rate and instantaneous volatility. Also from fig 1, we observe that the investment strategy, is an increasing function of the wealth function. This implies that an investor will invest more when the wealth is more.

Figs. 2 and 5 show that the investment strategy is an increasing function of the appreciation rate; this is so, because the investor will be more interested in any asset with high expected rate of returns. Also,

if the dividend from any given investment is attractive at the expiration of such investment year, the investor will be more interested in such asset and may be willing to increase the size of fund for such investment.

From (3.13), figs. 3 and 4, it can clearly be seen that the optimal investment strategy is a decreasing function of the transaction cost, risk free interest rate and instantaneous volatility. This is so because any business that attract high cost of operation, usually discourage the investor hence the reduction in funds allocated for such asset. Similarly, higher instantaneous volatility indicate the presence of higher risk and most investors get scared and worried over taking risk hence, this may lead to such investor reducing the funds allocation into such investment. This is also the reason why investors go for risk free assets more than risky assets when the interest of the risk free asset is high and attractive.

Furthermore, we observed the investment with strategy under logarithmic utility does not depend on the risk averse coefficient and tax.

From (3.29), it is observed that the optimal investment strategy for an investor with exponential utility is a function of the appreciation rate, dividend, transaction cost, risk free interest rate, tax and risk averse coefficient and instantaneous velocity of the risky asset. It is observed that the optimal investment strategy is an increasing function of the appreciation rate, and dividend but a decreasing function of transaction cost, risk free interest rate, tax on investment, risk averse coefficient and instantaneous volatility.

Fig. 6, discuss the effect of the risk aversion coefficient on the optimal investment strategy of the investor and we observed that the optimal control strategy for the risky asset, is inversely proportional to the risk aversion coefficient parameter. What we deduced from the graph in figure 4 is that an investor with higher risk aversion coefficient may invest a lesser percentage of their wealth in the risky asset (stock) while members with lower risk aversion coefficient may invest higher percentage of their wealth in the risky assets while reducing investment in the risk free asset. Fig. 7, shows that the optimal investment strategy decreases as the risk free interest rate increases and increases when the risk free interest rate decreases. This simply indicates that members will likely want to invest in risky asset when the interest rate from the risk free asset is not attractive. However, if the risk free interest rate is attractive enough, the investor may be advised by their fund administrators to invest more in the risk free asset, thereby reducing their investment in the risky asset. From fig. 8 and (3.29), the relationship between the optimal investment strategy, dividend and tax is established. We observed that the optimal investment strategy of the investor is an increasing function of the dividend and a decreasing function of tax. The consequence of (3.29) is that if the dividend from the risky asset is attractive, the investor may be tempted to invest more in risky asset and will invest less if the dividend from such investment is not attractive. Also, from figure 8, we observed that as the proportion of tax increases, the investor may tend to invest less in risky asset in other to balance his or wealth before retirement. This shows that higher tax rate could expose an investor to higher risk during investment planning and decision making. Also, we observed that the optimal investment strategy is a decreasing function of the administrative cost. The consequence of (3.29) is that if the administrative charges on investment of the risky asset is relatively low, the investor may be encouraged to invest more in risky asset and may invest less if otherwise.

From (3.29), the optimal investment strategy is a decreasing function of the instantaneous volatility. Since the instantaneous volatility represents the risk coefficient of the risky asset, risk averse members with high instantaneous volatility will be scared of investing much in the risky asset, thereby investing more in the risk free asset and vice versa.

Fig. 9, presents the graph of the optimal investment strategy against appreciation rate of the risky asset. It was observed that the investment strategy is an increasing function of the appreciation rate. This is so, because the investor will be more interested in any asset with high expected rate of returns. This is similar to the case under logarithm utility. Finally, we observed that the investment strategy does not depend on wealth.

In conclusion, this research presents the study of utility and its application to portfolio optimization and risk management. We discussed different utility functions such as, exponential and logarithm util-

ities. Also, a portfolio consisting of one risk free asset and a risky asset which follows the geometric Brownian motion was considered. We took into consideration transaction cost, dividend and tax on invested funds. Applying Ito's lemma and maximum principle, we obtained an optimization problem which comprise of a nonlinear PDE (Hamilton Jacobi Bellman equation) and a control problem (optimal investment strategy). These problems are functions of the value function which is dependent on the utility of the investor at the expiration of such investment. Furthermore, the exponential and logarithm utility were used in solving for the optimal investment strategies and some numerical results also presented. It was observed that the optimal investment strategy under logarithmic utility does not depend on the risk averse coefficient and tax while the optimal investment strategy under exponential utility does not depend on wealth.

Conflict of Interests

The authors declare that there is no conflict of interests regarding this paper.

Acknowledgments

The authors are very grateful to anonymous referees for their careful reading of the paper and helpful suggestions. This research has not received any sponsorship.

References

[1] Gao, J. (2008). Stochastic optimal control of DC pension funds, Insurance Math. Econom. 42 (**3**) 1159 - 1164.

[2] Gao, J. (2009). Optimal portfolios for DC pension plan under a CEV model, Insurance Mathematics and Economics: **44**, 479-490.

[3] Akpanibah, E.E. and Ini U.O. (2020). Portfolio strategy for an investor with logarithm utility and stochastic interest rate under constant elasticity of variance model, Journal of the Nigerian Society of Physical Sciences, 2 (**3**) , 186-196.

[4] He, L. and Liang, Z. (2013). The optimal investment strategy for the DC plan with the return of premiums clauses in a mean-variance framework, Insurance, **53**, 643-649.

[5] Sheng, D. and Rong, X. (2014). Optimal time consistent investment strategy for a DC pension with the return of premiums clauses and annuity contracts, Hindawi Publishing Corporation vol**2014**http://dx.doi.org/10.1155/2014/862694. 1-13.

[6] Akpanibah, E.E. and Samaila, S.K. (2017). Stochastic strategies for optimal investment in a defined contribution (DC) pension fund. International Journal of Applied Science and Mathematical Theory, 3, 3, 48-55.

[7] Gao, F. and Li, X. (2016). A utility-based asset liability management model for insurance companies under Solvency II. Journal of Risk and Financial Management, 9 (**3**) , 13.

[8] Gong, X., Brazil, I.A., Chang L.J. and Sanfey, A.G. (2019). Psychopathic traits are related to diminished guilt aversion and reduced trustworthiness during social decision making Scientific Report, 9, 7307.

[9] Smith, J. and Johnson, A. (2022). Utility functions and their role in optimal investment strategy: A comprehensive review. Journal of Finance and Economics, 45 (**3**) , 127-150.

[10] Majumder, D., Ray, A., and Banerjee, S. (2021). A comprehensive review on utility functions in financial decision making.

[11] Harel, A., Francis, J.C., and Harpaz, G. (2018). Alternative utility functions: review, analysis, and comparison. Review of Quantitative Finance and Accounting, 51, 785–811. https://doi.org/10.1007/s11156-017-0688-z

[12] Viscusi, W.K. (2020). Pricing the global health risks of the COVID-19 pandemic. Journal of Risk and Uncertainty, 61, 101–128. https://doi.org/10.1007/s11166-020-09337-2

[13] Akpanibah, E.E., Osu, B.O. and Ihedioha, S.A. (2020). On the optimal asset allocation strategy for a defined contribution pension system with refund clause of premium with predetermined interest under Heston's volatility model. J. Nonlinear Sci. Appl. 13 (**1**), : 53 - 64.

[14] Azor, P.A., Igodo, A and Ase, E.M. (2023). Explicit Solution of an Investment Plan for a DC Pension Scheme with voluntary contributions and return clause under Logarithm utility. International Journal of physical and mathematical sciences, 17(**8**) , 115-121

[15] Fan, P.Z., and Ke, S.J. (2010). The Optimal Enterprise R & D Investment Strategy Based on CRRA Utility function. 3rd International Conference on Information Management, Innovation Management and Industrial Engineering 388-392. https://doi.org/10.1109/ICIII.2010.258

[16] Wakker, P.P. (2008). Explaining the characteristics of the power (CRRA) utility family. Health Economics, 17, 1329-1344. https://doi.org/10.1002/hec.1331

[17] Miao, Y., and Zhang, Q. (2023). Optimal Investment and Consumption Strategies with General and Linear Transaction Costs under CRRA Utility.

[18] Cairns, A.J.G., Blake, D. and Dowd, K. (2006). Stochastic lifestyling: optimal dynamic asset allocation for defined contribution pension plans, Journal of Economic Dynamics and Control, 30, 843-877.

[19] Devolder, P., Bosch, M., and Dominguez, I. (2003). Stochastic optimal control of annuity contracts. Insurance, Mathematics and Economics, 33: 227–238.

[20] Battocchio, P. and Menoncin, F. (2004) Optimal Pension Management in a Stochastic Framework. Insurance , 34, 79-95.

[21] Osu, B.O., Akpanibah, E.E. and Njoku, K.N.C. (2017). On the Effect of Stochastic Extra Contribution on Optimal Investment Strategies for Stochastic Salary under the Affine Interest Rate Model in a DC Pension Fund, General Letters in Mathematics, 2 (**3**) , 138-149.

[22] Ma, G. and Zhu, S.P. (2022). Revisiting the Merton Problem: from HARA to CARA Utility. Computational Economics, 59, 651–686. https://doi.org/10.1007/s10614-021-10102-z

[23] Liang, Z. and Ma, M. (2020). Robust consumption-investment problem under CRRA and CARA utilities with time-varying confidence sets. Mathematical Finance, 30, 1035–1072. https://doi.org/10.1111/mafi.12217

[24] Li, D., Rong, X. and Zhao, H. (2013). Optimal investment problem with taxes, dividends and transaction costs under the constant elasticity of variance model, Transaction on Mathematics, **12**, 243-255.

[25] Salehi, Z., Chen, Y., Ratnam, E., Petersen, I. R., and Shi, G. (2021). Social Shaping of Linear Quadratic Multi-Agent Systems. Australian and New Zealand Control Conference (ANZCC) 232-237. Gold Coast, Australia. https://doi.org/10.1109/ANZCC53563.2021.9628389

[26] Carli, R. and Dotoli, M. (2020). A Dynamic Programming Approach for the Decentralized Control of Discrete Optimizers with Quadratic Utilities and Shared Constraint. 28th Mediterranean Conference on Control and Automation (MED) pp. 611-616. Saint-Raphaël, France. https://doi.org/10.1109/MED48518.2020.9183012

[27] Chubing, Z. and Ru-jing, H. (2011). Optimal Portfolios for DC Pension under the Quadratic Utility Function. International Conference of Information Technology, Computer Engineering and Management Sciences, 297-300. Nanjing, China. https://doi.org/10.1109/ICM.2011.385

[28] Li, Z.F., Ng, K.W., and Deng, X.T. (2007). Continuous-time optimal portfolio selection using mean-VaR models. Nonlinear Dynamics and Systems Theory 7, 83–97.

[29] Richardson, H. (1989). A minimum variance result in continuous trading portfolio optimization. Management Science 35: 1045–1055.

[30] Zhu J. and Li S. (2020). Time-consistent investment and reinsurance strategies for mean-variance insurers under stochastic interest rate and stochastic volatility, *Mathematics*, 8, pp. 2162-2183.

[31] Björk T. and Murgoci. A. (2010). A general theory of Markovian time inconsistent stochastic control problems. Working Paper. Stockholm School of Economics. http://ssrn.com/abstract=1694759.

[32] Björk T., Murgoci. A., and Xunyu Z. (2012). Mean-variance portfolio optimization with state dependent risk aversion. Mathematical Finance, 24(**1**) : 1–24.

[33] Li, D. Rong, X. Zhao, H., and Yi, B. Equilibrium investment strategy for DC pension plan with default risk and return of premiums clauses under CEV model, *Insurance:***72**, 6-20.

[34] Akpanibah, E.E., Osu, B.O. Oruh, B.I. and Obi, C.N. (2019). Strategic optimal portfolio management for a DC pension scheme with return of premium clauses. Transaction of the Nigerian association of mathematical physics, 8(**1**), 121-130.

[35] Akpanibah E.E. and Osu B.O. (2017). Portfolio strategy for an investor with stochastic premium under exponential utility via Legendre transform and dual theory. International Journal of Advances in Mathematics, (**6**), 27-35.

The influence of aquatic mosquitoes on Lymphatic Filariasis transmission dynamics: mathematical model approach

A. Abokwara*†and C.E. Madubueze‡

Abstract

The disease burden of lymphatic filariasis (LF) is a concern worldwide as it is one of the leading causes of permanent disability. In this study, a mathematical model of lymphatic filariasis is formulated with interest in the aquatic mosquito population (egg, larva and pupa) on the metamorphosis of the mosquito life cycle. The existence of the disease-free and the endemic equilibrium states and the basic reproduction number are established. In addition, the sensitivity indices indicate that the biting rate of mosquitoes, the recruitment rate of the aquatic mosquito population, the probability of transmitting infection during contact between humans and mosquitoes and the mortality rate of mosquitoes are the sensitive parameters in the disease dynamics. Through numerical simulations, it is observed that the sensitive parameters have an effect in reducing the burden of lymphatic filariasis in the population. Thus, public health education and the usage of larvicides should be encouraged as these would cause a drastic reduction in the maturation rate of mosquitoes, especially in communities where stagnant waters are endemic.

Keywords: Lymphatic Filariasis; aquatic mosquitoes; basic reproduction number; sensitivity analysis

1 Introduction

Lymphatic filariasis (LF), also called elephantiasis, is a neglected tropical disease whose causative agent are filaria worms, and it infects the lymphatic system [1]. LF is categorised into acute and chronic stages, and about 1.4 billion persons worldwide are at risk of infection [2]. The disease is transmitted via mosquitoes from one person to another, and infected persons can suffer from elephantiasis [3]. Lymphatic filariasis is a public health challenge in developing countries, even though the knowledge of drug usage is high. The relationship between lymphatic filariasis and humans depends on the filaria worms, external conditions and mosquitoes [4], [5]. One of the ways to control diseases caused by mosquitoes is to control the mosquito population. Thus, understanding the mosquito life cycle dynamics is important [6]. An important parameter affecting the mosquito population's size is the availability of breeding sites as it influences its life cycle [7]. The life cycle of a mosquito is categorised into four clearly different stages of progression: egg, larva, pupa and adult in its lifetime. They are completely distinct, even in habitation and ecology. After sucking blood from its victims, non-aquatic female mosquitoes lay a large amount of eggs in stagnant or slow-moving water. In less than seven days, larvae emerge from the egg, breathing through tubes that protrude above the water surface. They feed on floating organic matter and practise cannibalism. The larvae shed part of their bodies four times in the growth process and metamorphosed into pupae. The habitat of the pupa is close to the water's surface, and respiration occurs through the siphons on their back. The pupae stage of the life cycle does not feed until the skin splits and an adult mosquito emerges. The egg, larva and pupa stages are aquatic stages. In contrast, the adult stage is the non-aquatic stage in the metamorphosis of mosquitoes, and each has different responses to the environment and regulating factors to the population [8], [9] and [6]. Thus,

*Corresponding Author; E-mail: agathamicheal@gmail.com
†Department of Statistics, Nigerian Army College of Environmental Science and Technology, Makurdi, Nigeria.
‡Department of Mathematics, Joseph Sarwuan Tarka University, Makurdi, Nigeria; E-mail: ce.madubueze@gmail.com

to improve our understanding of the dynamics of lymphatic filariasis concerning the mosquito vector, we need to include the age structure to determine the appropriate mosquito population targeted for control strategies.

Several mathematical models that analyse the dynamics of lymphatic filariasis abound. Even though some have limitations, none of them has considered the influence of the aquatic mosquito on lymphatic filariasis disease. For instance, Mwamtobe *et al.* [10] considered quarantine of infected individuals as a strategy for reducing the transmission of lymphatic filariasis while Oguntolu *et al.* [11] considered treatment as a control measure for lymphatic filariasis. Simelane *et al.* [12] examined the application of indoor residual spraying to non-aquatic or adult mosquitoes while Salonga *et al.* [13], Rychta and Taylor [14] introduced mass drug administration for persons so that the disease could be eliminated. In addition, Stephano *et al.* [15] suggested that the recruitment rate of mosquitoes positively influences the spread of lymphatic filariasis. Hence, the aquatic mosquito compartment (eggs, larvae and pupa stages), which influences the rate of recruitment of the non-aquatic mosquito population (adult stage), is introduced in this study since ecological interactions among aquatic mosquitoes are crucial because they influence egg hatching, competition and population density [16].

The remaining part considers the formulation of the model in Section 2, qualitative analysis of the model in Section 3, while Numerical simulations with discussion and conclusion are presented in Section 4.

2 Model formulation

The total human population, N_h, at any time t, is subdivided into susceptible human, S_h, exposed human, E_h, asymptomatic infected human, I_{1h}, and symptomatic infected human, I_{2h}. The population of susceptible humans is generated by recruitment or birth at a constant rate of Λ_h and treatment of individuals in the asymptomatic human class at a rate, α. Proportion of this individuals acquires filariasis infection following effective contact with infectious mosquitoes, I_m, at the rate of λ_h where $\lambda_h = \frac{\beta\theta_1 I_m}{N_h}$, is the force of infection with β as mosquito biting rate and θ_1 as the probability that a bite from infected mosquito results in an infection. Humans exit this class due to natural death rate, μ_h; this is given by

$$\frac{dS_h}{dt} = \Lambda_h - \lambda_h S_h - \mu_h S_h + \alpha I_{1h}.$$

Humans in the exposed class, E_h, are recruited from the susceptible human class with contact with an infected mosquito. Exposed humans exit the class at a rate, τ, to the asymptomatic human class when the contact results in an infection or due to a natural death rate, μ_h. The rate of change of the exposed humans is given by

$$\frac{dE_h}{dt} = \lambda_h S_h - (\tau + \mu_h)E_h.$$

Members of the asymptomatic infected human class, I_{1h}, are recruited from the E_h class at a rate τ and exit this class to the susceptible human class due to treatment at a rate, α, or via natural death rate, μ_h. Some proceeds to the symptomatic human class due to lack of treatment at a rate, η. This yields

$$\frac{dI_{1h}}{dt} = \tau E_h - (\alpha + \mu_h + \eta)I_{1h}.$$

The symptomatic human class comprises humans who do not pay attention to health instructions, and they are recruited from the asymptomatic human class, I_{1h}, at a rate, η. They exit the class as a result of natural death rate, μ_h, or disease-induced death rate, δ. Thus,

$$\frac{dI_{2h}}{dt} = \pi I_{1h} - (\delta + \mu_h)I_{2h}.$$

The mosquito population comprises aquatic and non-aquatic mosquitoes. The population of aquatic mosquitoes is divided into eggs, larvae, and pupae, while the non-aquatic mosquito population is divided into susceptible mosquitoes, S_m, and infected mosquitoes, I_m. The aquatic mosquito population

increases through oviposition by reproductive mosquitoes at the rate, Λ, and they exit this class through maturation at a rate, ϕ, or by death rate, μ_l. This yields

$$\frac{dL}{dt} = \Lambda - (\phi + \mu_l)L.$$

The susceptible mosquitoes are recruited from the aquatic mosquito class due to maturation, and they exit this class due to death rate, μ_m, or as a result of infection when they come in contact with infected humans. The dynamics of this class are given by

$$\frac{dS_m}{dt} = \phi L - \lambda_m S_m - \mu_m S_m,$$

with $\lambda_m = \frac{\beta\theta_2(I_{1h}k+I_{2h})}{N_h}$, where θ_2 is the probability that a contact with an infected human result in an infection and k accounts for the reduced adult microfilariae due to treatment.

Finally, the population of infectious mosquitoes, I_m, is generated by the progression of mosquitoes from the susceptible mosquito class when they come in contact with infected humans at a rate, λ_m, and they exit this class as a result of death rate, μ_m. Thus,

$$\frac{dI_m}{dt} = \lambda_m S_m - \mu_m I_m.$$

It is assumed that the mosquito does not die of the disease.
Using the above information and the model schematic diagram, the non-linear system of equations is derived as below.

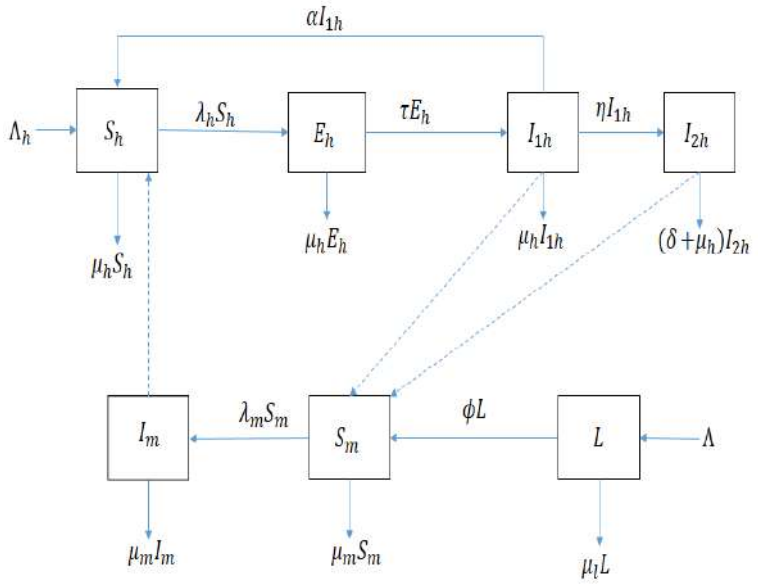


Figure 1: Schematic diagram of the lymphatic filariasis model

$$\left.\begin{aligned}
\frac{dS_h}{dt} &= \Lambda_h - \lambda_h S_h - \mu_h S_h + \alpha I_{1h}, \\
\frac{dE_h}{dt} &= \lambda_h S_h - (\tau + \mu_h) E_h, \\
\frac{dI_{1h}}{dt} &= \tau E_h - (\alpha + \mu_h + \eta) I_{1h}, \\
\frac{dI_{2h}}{dt} &= \eta I_{1h} - (\delta + \mu_h) I_{2h}, \\
\frac{dL}{dt} &= \Lambda - (\phi + \mu_l) L, \\
\frac{S_m}{dt} &= \phi L - \lambda_m S_m - \mu_m S_m, \\
\frac{dI_m}{dt} &= \lambda_m S_m - \mu_m I_m,
\end{aligned}\right\} \tag{1}$$

subject to initial conditions $S_h(0) > 0$, $E_h(0) \geq 0$, $I_{1h}(0) \geq 0$, $I_{2h}(0) \geq 0$, $L > 0$, $S_m(0) > 0$, $I_m(0) \geq 0$ where $\lambda_h = \frac{\beta\theta_1 I_m}{N_h}$ and $\lambda_m = \frac{\beta\theta_2(kI_{1h}+I_{2h})}{N_h}$. The system (1) is assumed to have positive model parameters.

The following Table 1 shows the parameter values of the lymphatic filariasis model.

Table 1: Values of parameters used in simulation.

Parameter	Symbol	Value	Source
Human recruitment rate	Λ_h	2500	[10]
Human mortality rate	μ_h	0.039	[10]
Human disease-induced death rate	δ	0.1	Assumed
Treatment rate for I_{1h} class	α	0.619	[13]
Movement rate from the E_h to the I_{1h} class	τ	0.25	[12]
Movement rate from the I_{1h} to the I_{2h} class	η	0.35	[12]
Aquatic mosquito maturity rate	ϕ	0.6	Assumed
Non-aquatic mosquito mortality rate	0.166	μ_m	[1]
Aquatic mosquito recruitment rate	Λ	40000	Assumed
Aquatic mosquito mortality rate	μ_l	0.019	[17]
Reduction parameter for I_{1h} due to treatment	k	0.055	[10]
Mosquito biting rate	β	0.3	[1]
Transmission rate for interaction between S_h and I_m class	θ_1	0.64	[17]
Transmission rate for interaction between S_m and I_{1h}, I_{2h} class	θ_2	0.64	[17]

3 Analysis of the model

3.1 Invariant region

The model parameters are assumed to be non-negative with non-negative initial conditions, implying that the model is biologically meaningful. The system of equations (1) will be analysed in a suitable feasible region, obtained as follows.

Let the total human population, $N_h(t) = S_h(t) + E_h(t) + I_{1h}(t) + I_{2h}(t)$, the aquatic mosquito population, $L(t)$, and the total non aquatic mosquito population $N_m(t) = S_m(t) + I_m(t)$, at time $t > 0$ have initial conditions $N_h(0)$= N_{h0}, $L(0)$ = L_0, and $N_m(0) = N_{m0}$ respectively. We state the following lemma.

Lemma 3.1. *All feasible solutions are uniformly bounded in a proper subset*

$$\varphi = \varphi_h \times \varphi_l \times \varphi_m$$

where

$$\varphi_h = \left\{(S_h, E_h, I_{1h}, I_{2h}) \in \Re_+^4 : N_h(t) \leq \frac{\Lambda_h}{\mu_h}\right\},\ \varphi_l = \left\{L\epsilon\Re_+ : L(t) \leq \frac{\Lambda}{\phi + \mu_l}\right\}$$

and

$$\varphi_m = \left\{(S_m, I_m)\epsilon\Re_+^2 : N_m(t) \leq \frac{\phi\Lambda}{\mu_m(\phi + \mu_l)}\right\}$$

are subsets for human, aquatic mosquitoes and non-aquatic mosquito populations, respectively.

Proof. It is assumed without loss of generality that disease-induced death rate, δ, in the human class in Equation (1) is negligible; that is, adding all human sub-populations to get

$$\frac{dN_h}{dt} = \Lambda_h - \mu_h N_h - \delta I_{2h} \ \leq \ \Lambda_h - \mu_h N_h. \tag{2}$$

Applying Birkhoff and Rota [18] theorem on differential inequality and integrating both sides of (2), we have after simplifying that

$$N_h \leq \frac{\Lambda_h}{\mu_h} - \left[\frac{\Lambda_h - \mu_h N_{h0}}{\mu_h}\right] e^{-\mu_h t}. \tag{3}$$

As $t \longrightarrow \infty$ in (3), the human population size, $N_h \longrightarrow \frac{\Lambda_h}{\mu_h}$. Therefore, all feasible regions of the human populations, S_h, E_h, I_{1h}, and I_{2h} enter the region

$$\varphi_h = \left\{(S_h, E_h, I_{1h}, I_{2h}) \in \Re_+^4 : N_h(t) \leq \frac{\Lambda_h}{\mu_h}\right\}.$$

For the aquatic mosquito population, we have

$$\frac{dL}{dt} = \Lambda - (\phi + \mu_l)L. \tag{4}$$

Applying Birkhoff and Rota [18] theorem of differential inequality and integrating both sides of (4) using the initial condition, $L(0) = L_0$ results to

$$L \leq \frac{\Lambda}{\mu_l + \phi} - \left[\frac{\Lambda - (\mu_l + \phi)L_0}{\mu_l + \phi}\right] e^{(-\mu_l + \phi)t}. \tag{5}$$

As $t \longrightarrow \infty$ in (5), the aquatic mosquito population size, L approaches $\frac{\Lambda}{\mu_l + \phi}$. Thus, the feasible regions of the aquatic mosquito populations, L, will enter the region

$$\varphi_l = \left\{L\epsilon\Re_+ : L(t) \leq \frac{\Lambda}{\phi + \mu_l}\right\}.$$

Since the non-aquatic mosquito population, $N_m(t)$, does not suffer from disease-induced death, we have

$$\frac{dN_m}{dt} = \phi L - \mu_m N_m. \tag{6}$$

Applying Birkhoff and Rota [18] theorem on differential inequality and integrating both sides of (6) with $L(t) \leq \frac{\Lambda}{\phi + \mu_l}$, we have

$$N_m \leq \frac{\phi\Lambda}{\mu_m(\mu_l + \phi)} - \left[\frac{\phi\Lambda - \mu_m(\mu_l + \phi)N_{m0}}{\mu_m(\mu_l + \phi)}\right] e^{-(\frac{\phi\Lambda}{\mu_m(\mu_l + \phi)})t}. \tag{7}$$

As $t \longrightarrow \infty$ in (7), the non-aquatic mosquito population size, $N_m \longrightarrow \frac{\phi\Lambda}{\mu_m(\mu_l + \phi)}$. Therefore, all feasible regions of the non-aquatic mosquito populations, S_m and I_m, enter the region

$$\varphi_m = \left\{(S_m, I_m) \in \Re_+^2 : N_m(t) \leq \frac{\phi\Lambda}{\mu_m(\mu_l + \phi)}\right\}.$$

This implies that every solution with an initial condition in $\Re_+^6$ remains in that region for $t > 0$, which is a positively invariant set under the flow induced by the model (1). Thus, the system (1) is epidemiologically meaningful and mathematically well-posed in the domain's interior, φ. Therefore, in this domain, it is sufficient to consider the dynamics of the flow generated by the model (1).

3.2 Positivity of solutions

Since φ is a positive invariant set, we now show that for $t > 0$, every solution of the model is positive and remains in the region.

Theorem 3.2. *The closed set*

$$D = \Big\{ \Big(S_h(t), E_h(t), I_{1h}(t), I_{2h}(t), L(t), S_m(t), I_m(t) \Big) \in \mathbb{R}^7_+ : N_h(t) \leq \frac{\Lambda_h}{\mu_h}, L(t) \leq \frac{\Lambda}{\phi + \mu_l}, \\ N_m(t) \leq \frac{\phi\Lambda}{\mu_m(\mu_l + \phi)} \Big\}$$

is positively invariant and attracts all positive solutions of the model (1) where $N_h(t)$ is the human population size, L(t) is the aquatic mosquito population and $N_m(t)$ is the non-aquatic mosquito population at any time t, respectively.

Proof. Let $\tau = sup\{t > 0 : S_h(0) > 0, I_{1h}(0) > 0, I_{2h}(0) > 0, L(0) > 0, S_m(0) > 0, I_m(0) > 0\}\epsilon[0, t]$.

From the first Equation in (1), we have

$$\frac{dS_h}{dt} = \Lambda_h - \lambda_h S_h - \mu_h S_h + \alpha I_{1h} \geq -(\lambda_h + \mu_h)S_h.$$

This implies by integration with initial condition, $S_h(0)$, that

$$S_h \geq S_h(0) exp\{-(\mu_h + \int_0^t \lambda_h(u))t\} > 0.$$

This shows that S_h is always positive for $t > 0$.

In similar way for $t > 0$,

$$E_h(t) \geq E_h(0) \exp -(\tau + \mu_h)t > 0, \;\; I_{1h}(t) \geq I_{1h}(0) \exp -(\alpha + \eta + \mu_h)t > 0,$$

$$I_{2h}(t) \geq I_{2h}(0) \exp -(\mu_h + \delta)t > 0, \;\; L(t) \leq L(0) \exp -(\phi + \mu_l) > 0,$$

$$S_m(t) \geq S_m(0) exp\{-\int_0^t (\lambda_m + \mu_m) du\} > 0, \;\; I_m(t) \geq I_m(0) \exp(-\mu_m)t > 0.$$

Therefore, we can conclude that the solutions

$$(S_h(t), E_h(t), I_{1h}(t), I_{2h}(t), L(t), S_m(t), I_m(t))$$

of model Equation (1) are non-negative for $t > 0$. This implies the model is well-positioned and makes biological meaning because we cannot have negative sub-populations for living organisms.

3.3 Disease-free equilibrium state and basic reproduction number

The disease-free equilibrium (DFE) is the steady-state solution of the system of equations (1) obtained in the absence of disease, that is, $E_h = I_{1h} = I_{2h} = I_m = 0$. Thus, the disease-free equilibrium state E_0, is given by

$$E_0 = \Big(S_h^0, 0, 0, 0, L^0, S_m^0, 0 \Big) = \Big(\frac{\Lambda_h}{\mu_h}, 0, 0, 0, \frac{\Lambda}{\phi + \mu_l}, \frac{\phi\Lambda}{\mu_m(\phi + \mu_l)}, 0 \Big). \tag{8}$$

3.3.1 Basic reproduction number

The basic reproduction number, R_0, is the number of new cases reproduced in a wholly susceptible population when an infective individual is introduced into the population (Van den Driessche and Watmough, [19]). We apply the next-generation approach by Van den Driessche and Watmough, [19], [20]. The next generation matrix comprises two parts: F and V, where $F = \frac{\partial f_i(E_0)}{\partial x_j}$ and $V = \frac{\partial v_i(E_0)}{\partial x_j}$. Also, the f_i are the new infections while the v_i are transfers of infections from one compartment to another with E_0 as a disease-free equilibrium state. R_0 is the the spectral radius of the matrix FV^{-1} with the associated matrix F and matrix V as Jacobian matrices of f_i and v_i at disease-free equilibrium state, E_0.

The Jacobian matrix F and V and the inverse of matrix V are given as

$$F = \begin{pmatrix} 0 & 0 & 0 & \beta\theta_1 \\ 0 & 0 & 0 & 0 \\ 0 & 0 & 0 & 0 \\ 0 & k\beta\theta_2 a_4 & \beta\theta_2 a_4 & 0 \end{pmatrix}, V = \begin{pmatrix} a_1 & 0 & 0 & 0 \\ -\tau & a_2 & 0 & 0 \\ 0 & -\eta & a_3 & 0 \\ 0 & 0 & 0 & \mu_m \end{pmatrix} \text{ and } V^{-1} = \begin{pmatrix} \frac{1}{a_1} & 0 & 0 & 0 \\ \frac{\tau}{a_1 a_2} & \frac{1}{a_2} & 0 & 0 \\ \frac{\eta\tau}{a_1 a_2 a_3} & \frac{\eta}{a_2 a_3} & \frac{1}{a_3} & 0 \\ 0 & 0 & 0 & \frac{1}{\mu_m} \end{pmatrix}$$

where

$$a_1 = \tau + \mu_h, a_2 = \alpha + \eta + \mu_h, a_3 = \delta + \mu_h, a_4 = \frac{S_m^0}{N_h^0} = \frac{\Lambda\phi\mu_h}{\Lambda_h\mu_m(\phi + \mu_l)}, a_6 = \phi + \mu_l. \quad (9)$$

The spectral radius (dominant eigenvalue) of FV^{-1},which is the basic reproduction number R_0 is given by

$$R_0 = \rho(FV^{-1}) = \sqrt{\frac{\beta^2 a_4\theta_1\theta_2\tau(a_3k + \eta)}{a_1a_2a_3\mu_m}}.$$

With the definition in Equation in (9), we have

$$R_0 = \sqrt{\frac{\beta^2\theta_1\theta_2\tau\Lambda\phi\mu_h(k(\delta + \mu_h) + \eta)}{(\tau + \mu_h)(\alpha + \eta + \mu_h)(\delta + \mu_h)\mu_m^2\Lambda_h(\phi + \mu_l)}}. \quad (10)$$

Interpretation of the basic reproduction number

The biological interpretation of the basic reproduction number, R_0, is as follows:

- $\frac{\tau}{\tau+\mu_h}$ is the probability of survival of the individuals from the exposed state to the infectious state,
- $\frac{\theta_1\beta}{\mu_m^2}$ is the number of humans that one mosquito infects during the duration of the infectious period, provided all humans are susceptible,
- $\frac{\theta_2\beta}{(\alpha+\eta+\mu_h)(\delta+\mu_h)}$ is the number of mosquitoes that a human infects during the duration of the infectious period, provided all mosquitoes are susceptible,
- $\frac{\beta\theta_2\Lambda\phi}{\mu_m^2(\phi+\mu_l)}$ is the contribution of the mosquito population when humans are infected,
- $\frac{\beta\theta_1\tau(k(\delta+\mu_h)+\eta)}{(\tau+\mu_h)(\alpha+\eta+\mu_h)(\delta+\mu_h)\Lambda_h)}$ is the contribution of the human population when mosquitoes are infected.

The square root is the geometric mean of the average number of new infections produced by one mosquito and the average number of new infections produced by a human. Thus, R_0 could be written as

$$R_0 = \sqrt{(R_{1h} + R_{2h})R_m}, \quad (11)$$

where

$R_m = \frac{\beta\theta_1}{\mu_m}$ is the reproduction number resulting from the interaction of susceptible humans and infected mosquitoes,

$R_{1h} = \frac{\beta\theta_2\tau\Lambda\phi\mu_h k(\delta+\mu_h)}{(\tau+\mu_h)(\alpha+\eta+\mu_h)(\delta+\mu_h)\mu_m\Lambda_h(\phi+\mu_l)}$ is the reproduction number resulting from the interaction of asymptomatic infected humans and susceptible mosquitoes,

$R_{2h} = \frac{\beta\theta_2\tau\Lambda\phi\mu_h\eta}{(\tau+\mu_h)(\alpha+\eta+\mu_h)(\delta+\mu_h)\mu_m\Lambda_h(\phi+\mu_l)}$ is the the basic reproduction number resulting from the interaction of symptomatic infected humans and susceptible mosquitoes.

3.4 Stability of the disease-free equilibrium state

3.4.1 Local stability of the disease-free equilibrium state

The local stability of the DFE depends on the basic reproduction number, R_0, as proved by Van den Driessche and Watmough [19]. The linearization method at the equilibrium state is used to establish the local stability of the DFE. We state and prove the following theorem.

Theorem 3.3. *If E_0 is the DFE of the model, then E_0 is locally asymptotically stable if $R_0 < 1$, but unstable if $R_0 > 1$.*

Proof. The Jacobian matrix of the model (1) at DFE, E_0, is given by

$$J(E_0) = \begin{pmatrix} -\mu_h & \alpha & 0 & 0 & 0 & 0 & -\beta\theta_1 \\ 0 & -a_1 & 0 & 0 & 0 & 0 & \beta\theta_1 \\ 0 & \tau & -a_2 & 0 & 0 & 0 & 0 \\ 0 & 0 & \eta & -a_3 & 0 & 0 & 0 \\ 0 & 0 & 0 & 0 & -a_6 & 0 & 0 \\ 0 & 0 & -\beta\theta_2 k a_4 & -\beta\theta_2 a_4 & \phi & -\mu_m & 0 \\ 0 & 0 & \beta\theta_2 k a_4 & \beta\theta_2 a_4 & 0 & 0 & -\mu_m \end{pmatrix}.$$

The eigenvalues of the Jacobian matrix, $J(E_0)$, are $-\mu_h$, $-\mu_m$, $-a_6$ and the roots of the polynomial

$$\lambda^4 + A_3\lambda^3 + A_2\lambda^2 + A_1\lambda + A_0 = 0,$$

where

$$\begin{aligned} A_3 &= \mu_m + a_3 + a_2 + a_1, \\ A_2 &= a_1a_2 + a_1a_3 + a_1\mu_m + a_2a_3 + a_2\mu_m + a_3\mu_m, \\ A_1 &= a_1a_2a_3 + a_1a_3\mu_m + a_2a_3\mu_m + a_1a_2\mu_m\left(1 - \frac{\beta^2 k\tau\theta_1\theta_2 a_4 a_5}{a_1a_2\mu_m}\right), \\ A_0 &= a_1a_2a_3\mu_m\left(1 - \frac{\beta^2\theta_1\theta_2\tau a_4a_5(ka_3+\eta)}{a_1a_2a_3\mu_m}\right). \end{aligned}$$

Writing the coefficients of the polynomial in terms of the basic reproduction number yields

$$A_1 = a_1a_2a_3 + a_1a_3\mu_m + a_2a_3\mu_m + a_1a_2\mu_m(1 - R_{1h}),\ A_0 = a_1a_2a_3\mu_m\left(1 - R_0^2\right).$$

Thus, the stability of the disease-free equilibrium of the model (1) is determined solely by the sign of the constant term of the characteristic equation where all parameters are non-negative. Also, A_1, A_2, A_3 has the property that $A_0, A_1, A_2, A_3 > 0$. Hence, we can conclude that the eigenvalues of the system have negative real parts if $R_0 < 1$, therefore, the DFE, E_0, is locally asymptotically stable if $R_0 < 1$.

3.4.2 Global stability of the disease-free equilibrium state

The global stability of disease-free equilibrium is established using the Comparison theorem by Castillo-Chavez *et al.* [21]. We state the following theorem for the global stability of the DFE E_0.

Theorem 3.4. *The DFE E_0 of the model equations (1) is globally asymptotically stable if $R_0 \leq 1$ and unstable if $R_0 > 1$.*

Proof. The first condition is to define new variables and rewrite the system into subsystems.

Let X_1 and Y_1 represent susceptible and infectious classes, respectively. The subsystems of the model equations (1) gives $X_1 = (S_h, L, S_m)$ and $Y_1 = (E_h, I_{1h}, I_{2h}, I_m)$ which could be represented as

$$\left.\begin{aligned} \frac{dX_1}{dt} &= F(X_1, Y_1), \\ \frac{dY_1}{dt} &= G(X_1, Y_1), \end{aligned}\right\} \tag{12}$$

with $X_1 \in \mathbb{R}^3_+, Y_1 \in \mathbb{R}^4_+$. The two vector value functions are

$$\left.\begin{aligned} F(X_1, Y_1) &= (\Lambda_h - \lambda_h S_h - \mu_h S_h + \alpha I_{1h},\ \Lambda - (\phi + \mu_l)L,\ \phi L - \lambda_m S_m - \mu_m S_m)^T, \\ G(X_1, Y_1) &= (\lambda_h S_h - (t + \mu_h)E_h,\ \tau E_h - (\alpha + \mu_h + \eta)I_{1h},\ \eta I_{1h} - (\delta + \mu_h)I_{2h},\ \lambda_m S_m - \mu_m I_m)^T, \end{aligned}\right\}$$

where T is the transpose, $\lambda_h = \frac{\beta\theta_1 I_m}{N_h}$, and $\lambda_m = \frac{\beta\theta_2(I_{1h}k + I_{2h})}{N_h}$.

The reduced system, $\frac{dX_1}{dt}F(X_1, 0)$, in the absence of disease is given as

$$\left.\begin{aligned} \frac{dS_h}{d_t} &= \Lambda_h - \mu_h S_h, \\ \frac{dL}{dt} &= \Lambda - (\phi + \mu_l)L, \\ \frac{dS_m}{d_t} &= \phi L - \mu_m S_m. \end{aligned}\right\} \tag{13}$$

with the Jacobian matrix $\begin{pmatrix} -\mu_h & 0 & 0 \\ 0 & -a_6 & 0 \\ 0 & \phi & -\mu_m \end{pmatrix}$.

The Jacobian matrix has the eigenvalues $-\mu_h, -a_6$ and $-\mu_m$. The equilibrium state of the $\frac{dX_1}{dt}F(X_1, 0)$, in the absence of disease is $X^* = (S_h^*, L^*, S_m^*) = (\frac{\Lambda_h}{\mu_h}, \frac{\Lambda}{\phi + \mu_l}, \frac{\phi\Lambda}{\mu_m(\phi + \mu_l)})$ and it is globally asymptotically stable, which implies that the reduced system does not dependent on the initial conditions in $\mathbb{R}^7_+$.

Condition 2 states that $G(X_1, Y_1) = AY - G^*(X_1, Y_1)$, where $G(X_1, Y_1) \geq 0$ for $X_1, Y_1 \in \varphi$ and $A = D_Y G(X^*, 0)$ is an M-matrix. Form the model system (1),

$$A = D_Y G(X_1, 0) = \begin{pmatrix} -a_1 & 0 & 0 & \beta\theta_1 \\ \tau & -a_2 & 0 & 0 \\ 0 & \eta & -a_3 & 0 \\ 0 & \beta k\theta_2 a_4 & \beta\theta_2 a_4 & -\mu_m \end{pmatrix} \text{ and } G^*(X_1, Y_1) = \begin{pmatrix} \beta\theta_1 I_m \left(\frac{S_h^0}{N_h^0} - \frac{S_h}{N_h}\right) \\ 0 \\ 0 \\ \beta\theta_2 I_{2h} \left(\frac{S_m^0}{N_h^0} - \frac{S_m}{N_h}\right) \end{pmatrix},$$

where $G(X_1, Y_1)$ satisfies $G(X_1, 0) = 0$. We observed that $G(X_1, Y_1) = A^* Y_1 - G^*(X_1, Y_1)$, and $G^*(X_1, Y_1) \geq 0$ since $\frac{S_h^0}{N_h^0} \geq \frac{S_h}{N_h}$, $\frac{S_m^0}{N_h^0} \geq \frac{S_m}{N_h}$. Therefore by Castillo-Chavez *et al.* [21], X^* is a globally asymptotically stable state of the model equations (1) of which $R_0 < 1$ makes matrix A an M-matrix.

3.5 Endemic equilibrium state

The endemic equilibrium (EE) is an equilibrium state in the presence of the disease. At the endemic equilibrium state, E_e, the infected compartments are not equal to zero implying that $\lambda_h \neq 0$ and

$\lambda_m \neq 0$. Solving the model equations (1) in terms of the force of infection, λ_h and λ_m gives

$$\left.\begin{aligned} S_h^e &= \frac{a_2\Lambda_h - (a_1a_2 - \alpha\tau)E_h^e}{a_1\mu_h},\ E_h^e = \frac{\Lambda_h a_2\lambda_h^e}{\mu_h a_1 a_2 + (a_1a_2 - \alpha\tau)\lambda_h^e},\ I_{1h}^e = \frac{\tau E_h^e}{a_2}, \\ I_{2h}^e &= \frac{\eta I_{1h}^e}{a_3},\ L^e = \frac{\Lambda}{a_6},\ S_m^e = \frac{\phi L^e}{\lambda_m^e + \mu_m},\ I_m^e = \frac{\lambda_m^e S_m^e}{\mu_m},\ N_h^e = \frac{\Lambda_h - \delta I_{2h}^e}{\mu_h}. \end{aligned}\right\} \tag{14}$$

Substituting (14) into $\lambda_m^e = \frac{\beta\theta_2(kI_{1h}^e + I_{2h}^e)}{N_h^e}$ and $\lambda_h^e = \frac{\beta\theta_1 I_m^e}{N_h^e}$ and solve simultaneously to get

$$\lambda_m^e = \frac{C\lambda_h^e}{B\lambda_h^e + D}$$

and λ_h^e as the solution of the polynomial

$$\lambda_h^e(M_2\lambda_h^{e2} + M_1\lambda_h^e + M_0) = 0 \tag{15}$$

where

$$M_2 = \mu_m a_6\Lambda_h B(\mu_m B + C),\ M_1 = \mu_m a_6\Lambda_h D(\mu_m B + C - \mu_m\delta\eta\tau + \mu_m a_3 A(1 - R_0^2)),$$
$$M_0 = \mu_h\mu_m^2 D a_1a_2a_3a_6\Lambda_h(1 - R_0^2),$$

with

$$A = a_1a_2 - \alpha\tau > 0,\ B = a_3A - \delta\eta\tau > 0,\ C = \tau\beta\theta_1\mu_h(ka_3 + \eta),\ D = \mu_h a_1a_2a_3.$$

From the polynomial (15), it is either

$$\lambda_h^e = 0 \tag{16}$$

or

$$M_2\lambda_h^{e2} + M_1\lambda_h^e + M_0 = 0. \tag{17}$$

Equation (16) corresponds to the disease-free equilibrium (DFE) while we determine the existence of the possible number of endemic state(s) of the polynomial (17). Using Descartes's rule of signs with regards to the value of R_0, the result of the number of positive endemic state(s) are summarised in Table 2.

Table 2: Number of positive endemic states

M_2	M_1	M_0	Range of R_0	Number of possible positive real roots
+	+	-	$R_0 > 1$	1
+	-	-	$R_0 > 1$	1
+	+	+	$R_0 < 1$	0
+	+	+	$R_0 < 1$	2

From Table 2, we have $R_0 > 1$ for the existence of a unique positive endemic state. Meanwhile, $R_0 < 1$ may create no endemic state or two endemic states that will co-exist with the disease-free equilibrium, E_0 leading to a backward bifurcation at $R_0 = 1$. Plotting the polynomial in Equation (17) yields a forward bifurcation plot in Figure 2, which implies the existence of a unique endemic equilibrium that is stable when $R_0 > 1$.

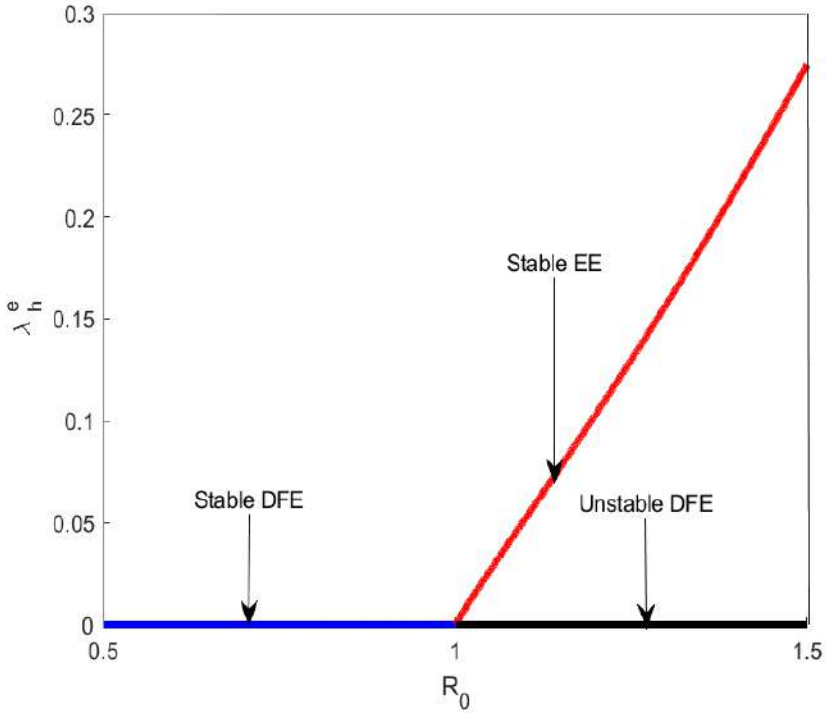


Figure 2: Plot for forward bifurcation of the Lymphatic Filariasis model at basic reproduction number R_0 using the parameter values in Table 1.

4 Numerical simulations/sensitivity analysis

4.1 Sensitivity Analysis

To determine the parameters to be targeted for intervention strategies to reduce the spread of LF disease, we need to understand the influence of the model parameters in the system concerning the flow of infection. Thus, we would conduct the sensitivity analysis on the basic reproduction number. This is carried out using the normalised forward sensitivity indices given by

$$\Gamma_p^{R_0} = \frac{\partial R_0}{\partial p} \times \frac{p}{R_0}, \tag{18}$$

where p is any parameter of the R_0 [22]. The sensitivity indices of parameters of the basic reproduction number, R_0, are shown in Figure 2.

The sensitivity indices of the influence of the model parameters on the basic reproduction number show that mortality rate for non-aquatic mosquito population, μ_m, recruitment rate for aquatic mosquito population, Λ, mosquito biting rate, β, probability that interaction with an infected mosquito result in disease transmission, θ_1, and probability that contact with infected human results in LF disease transmission, θ_2, are sensitive parameters implying that they have an impact on the value of the basic reproduction number, R_0. In particular, mosquito biting rate, β, and mortality rate for non-aquatic mosquitoes, μ_m, are the most sensitive parameters with sensitivity indices of $+1$ and -1 respectively. It follows that β, μ_m, θ_1, θ_2 and Λ should be targeted for intervention strategies.

The 3D plots for the most sensitivity parameters are shown in Figure 4. It could be observed from the contour plots that the influence of the non-aquatic mosquito death rate, μ_m, with the mosquito biting rate, β, the recruitment rate for aquatic mosquitoes, Λ, the disease transmission rate, θ_1, and the maturity rate of mosquitoes, ϕ, on the basic reproduction number increases irrespective of the mortality rate of the non-aquatic mosquito population, μ_m. Thus, this supports the usage of larvicides to be paramount in reducing the maturity rate of mosquitoes, leading to a reduction in the mosquito

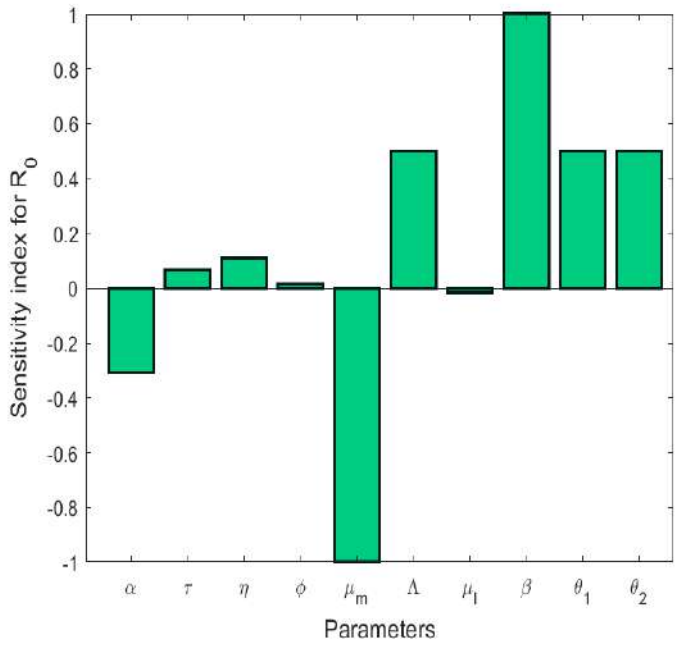


Figure 3: Sensitivity index plot of the parameters of the basic production number, R_0, using the parameter values in Table 1.

biting rate, probability of transmission and recruitment of aquatic mosquitoes.

5 Numerical Simulations

Numerical simulations of the model are carried out to investigate the behaviour of the sensitive parameters arising from the sensitivity analysis result. The parameter values in Table 1 are used for the simulations. The model is simulated by introducing one infected mosquito at the DFE of the system based on the definition of R_0.

Figure 5 shows the effect of increasing the aquatic mosquito recruitment rate, Λ. It illustrates that an increase in Λ causes an increase in infected humans and aquatic mosquito populations, contributing to the burden of LF disease in the community. In Figure 6, we observe a sharp increase in the infected human and mosquito populations when there is an increase in mosquito biting rate, β, which would cause an increase in the basic reproduction number, R_0. Furthermore, there are effects of the human transmission rate, θ_1, mosquito transmission rate, θ_2 and mosquito mortality rate, μ_m, on the spread of the LF disease in Figures 7, 8 and 9, respectively. It could be seen that an increase in θ_1 and θ_2 increases the LF burden while an increase in μ_m reduces the burden of LF in the population.

6 Discussions and Conclusion

In Figure 5 for recruitment rate for aquatic mosquitoes, $\Lambda = 60000$, there is a sharp increase in the infected human and mosquito populations in less than day 200 of the simulation as compared to $\Lambda = 40000$ and $\Lambda = 20000$ respectively. It implies that control measures like larvicide application in the environment, especially stagnant waters, should be encouraged to mitigate the maturation of aquatic mosquitoes. For Figure 6, we notice an increase in the biting rate of mosquitoes causes an increase in the number of infected humans and mosquitoes in the first 100 days of disease invasion in the population while at a reduced biting rate, say $\beta = 0.3$, it takes a longer time. The implication is that interventions such as public enlightenment campaigns on using larvicides in the environment should be encouraged to reduce the maturation of aquatic mosquitoes. It is known that the fewer mature mosquitoes in the

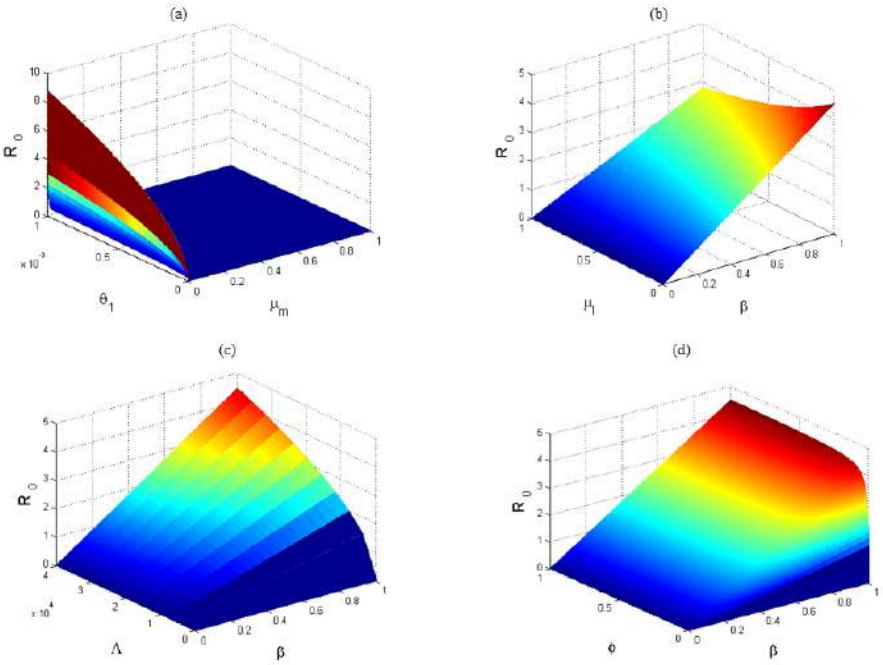


Figure 4: Contour plots showing the influence the non-aquatic mosquito death rate (μ_m), with mosquito biting rate (β), recruitment rate for aquatic mosquitoes, (Λ) disease transmission rate, (θ_1), death rate for aquatic mosquitoes, (μ_l), and maturity rate for aquatic mosquitoes, (ϕ).

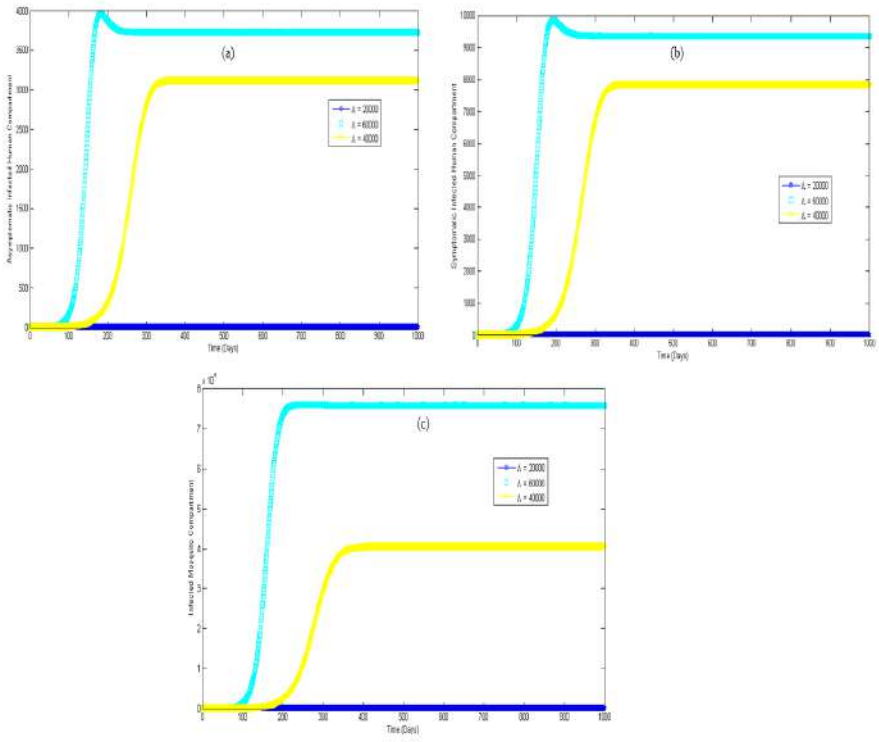


Figure 5: The influence of varying the aquatic mosquito recruitment rate (Λ) on the infective humans $(I_{1h}(t) + I_{2h}(t))$, the aquatic mosquito $(L(t))$ and the infected mosquito $(I_m(t))$ populations.

environment, the lower the biting rate of mosquitoes will lead to fewer mosquitoes in the community. Figures 7 and 8 show a geometric increase in the infected human and mosquito populations in the first 200 days when θ_1, $\theta_2 \geq 0.64$, respectively. Meanwhile, for θ_1 θ_2 equal to $= 0.44$, an increase in the

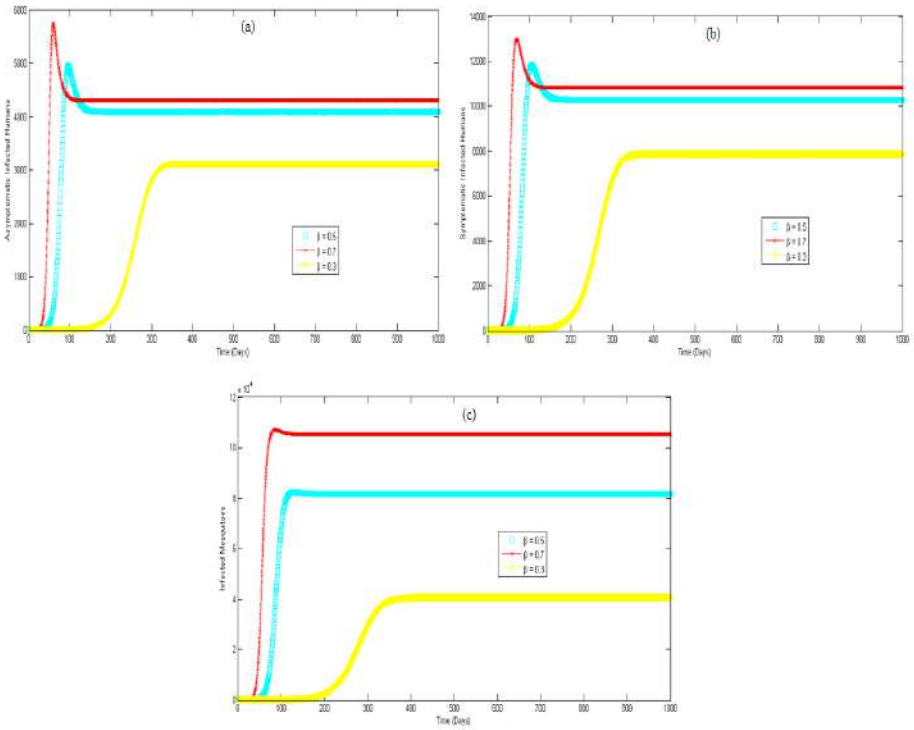


Figure 6: The influence of varying the biting rate of the non-aquatic infected mosquito (β) on the infective humans $(I_{1h}(t) + I_{2h}(t))$, the aquatic mosquito $(L(t))$ and the infected mosquito $(I_m(t))$ populations.

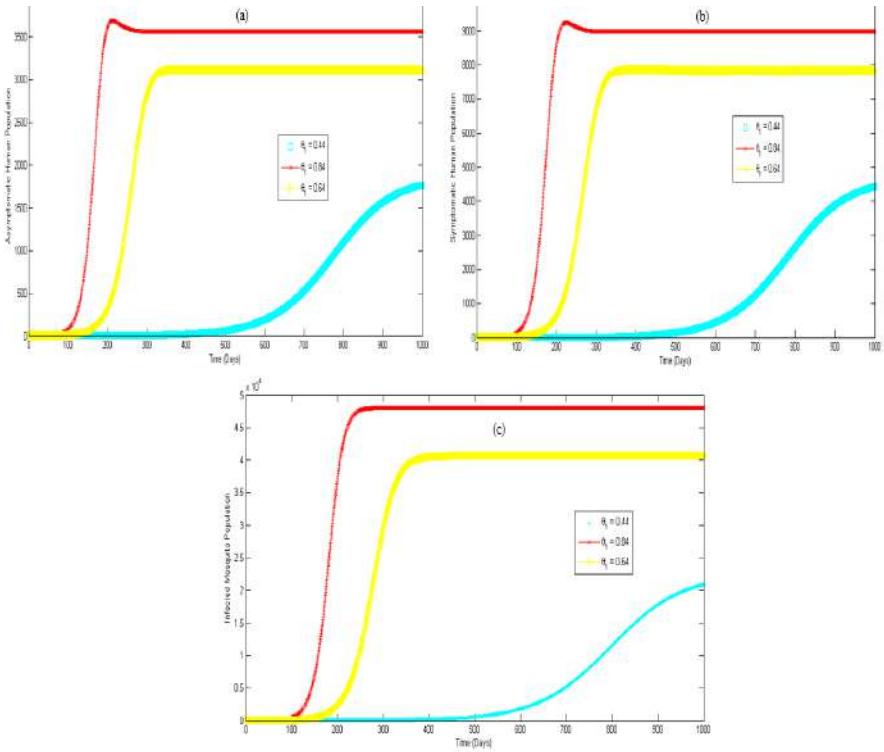


Figure 7: The influence of varying the human transmission rate (θ_1) on the infective humans $(I_{1h}(t) + I_{2h}(t))$, the aquatic mosquito $(L(t))$ and the infected mosquito $(I_m(t))$ populations.

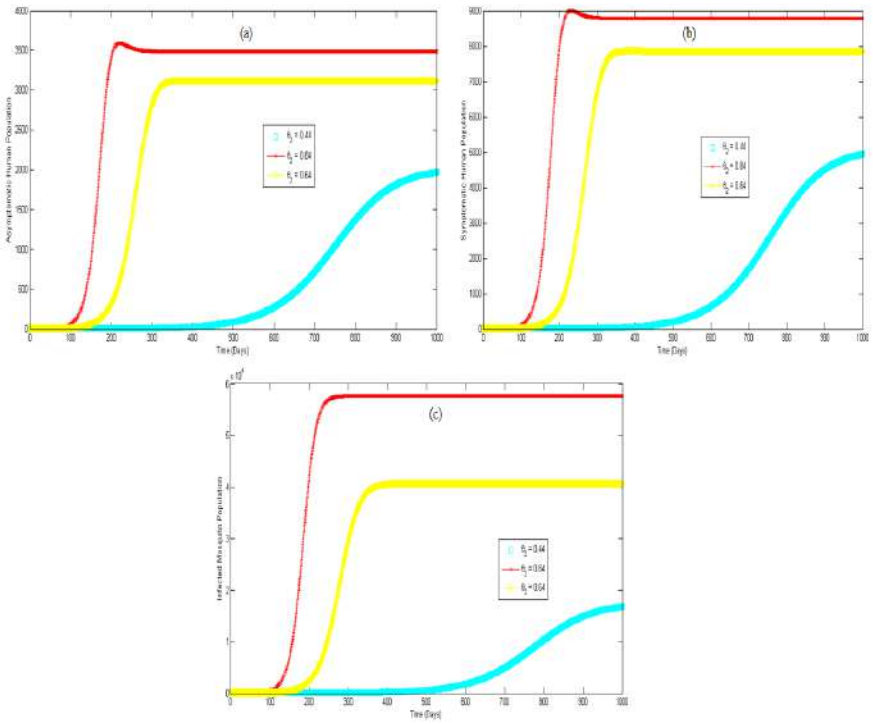


Figure 8: The influence of varying the mosquito transmission rate (θ_2) on the infective humans $(I_{1h}(t)+I_{2h}(t))$, the aquatic mosquito $(L(t))$ and the non-aquatic infected mosquito $(I_m(t))$ populations.

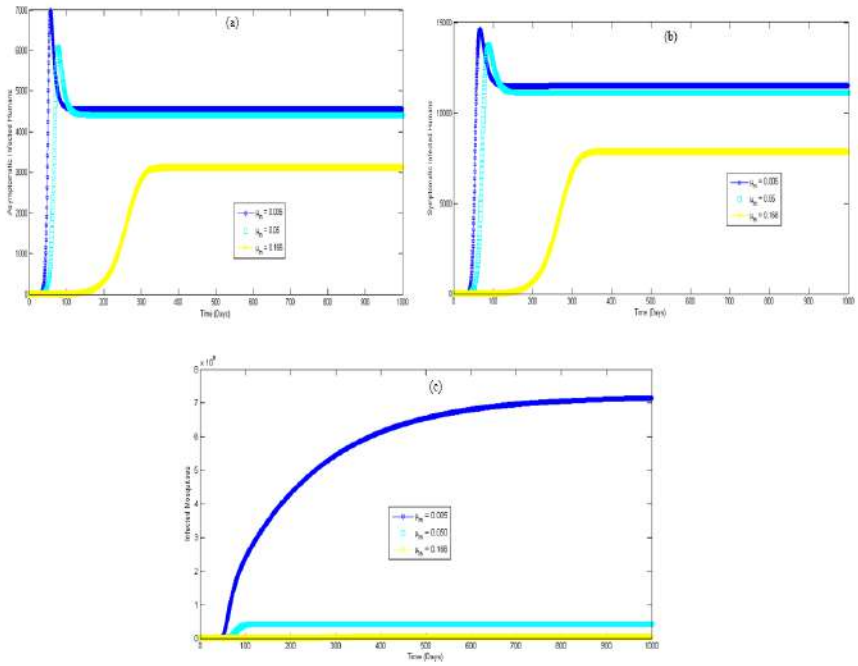


Figure 9: The influence of varying the aquatic mosquito death rate (μ_l) on the infective humans $(I_{1h}(t) + I_{2h}(t))$, the aquatic mosquito $(L(t))$ and the non-aquatic infected mosquito $(I_m(t))$ populations.

infected compartments begins in about day 600 of LF invasion. This implies that using larvicides to prevent the maturation of mosquitoes is an essential tool to reduce the probability of contact between humans and mosquitoes as it would reduce the number of mature mosquitoes in the environment. Figure 9 shows a reduction in the mortality rate of mosquitoes, causing a sharp increase in the infected human and the infected mosquito populations in less than day 100 of LF invasion. This poses a great danger to the lives of humans as the disease burden is on the rise. Thus, control measures such as public health education on the use of larvicides to eliminate the aquatic mosquito population, indoor residual spraying, and insecticide-treated bed nets are encouraged to promote the mortality rate of mosquitoes.

In conclusion, the impact of aquatic mosquitoes on the transmission dynamics of LF is studied. This involves formulating a mathematical model of LF with aquatic mosquito sub-population and conducting quantitative analysis such as computation of R_0, existence of equilibrium states and stability of disease-free equilibrium state. Furthermore, the sensitivity analysis and numerical simulations are examined in the study. Based on the result, public enlightenment campaigns should be set in motion in communities where lymphatic filariasis is endemic so that sensitisation of individuals on the usage of larvicides, insecticides-treated bed nets, indoor residual spraying as well as treatment of infected individuals should be emphasized to avoid symptomatic human cases that promote poor self-esteem among victims. Further studies could focus on modifying or extending this work to cater for individuals migrating from non-endemic areas to endemic areas and the influence of seasonality conditions to advance the understanding of the dynamics of lymphatic filariasis.

Acknowledgements

We especially acknowledge the Nigerian Tertiary Education Trust Fund (TETfund) for sponsoring this research and Nigerian Army College of Environmental Science and Technology, Makurdi, for giving us the opportunity to access this research grant.

References

[1] Irvine, M.A., Reimer, L.J., Njenga, S.M., Gunawarden, S., Kelly-Hope, L., Bockarie, M. and Hollingsworth, D. (2015). Modelling Strategies to Break Transmission of Lymphatic Filariasis - Aggregation, Adherence and Vector Competence Greatly Alter Elimination. Parasites and Vectors 8(1), 1-19.

[2] Alshehri A., Shah, Z. and Jan, R. (2023).Mathematical Study of the Dynamics of Lymphatic Filariasis Infection via Fractional-Calculus. The European Physical Journal Plus. 279-293.

[3] Nwadibia, A.I., Eze,F., Inyama, S.C. Nse, C.A. Omaine, A. and Mbachu, H.I. (2018). Mathematical Model of the Transmission Dynamics of Genital Elephantiasis (Lymphatic Filariasis). *Mathematical Theory and Modelling* 8(4), 71-115.

[4] Murdock, C.C., Sternberg, E.D. and Thomas, M. B. (2016). Malaria transmission Potential Could be Reduced with Current and Future Climate Change. *Sci. Rep.* 6: 27771.

[5] Parham, E., Waldock, J., Christophides, G. K., Hemming, D., Agusto, F., Evans, K.J., Fefferman, N. Gaff, H., Gumel, A., LaDeau, S. and Lenhart, S. (2015). Climate, Environmental and Socio-Economic Change: Weighing up the Balance in Vector-Borne Disease Transmission. Philo. Trans. R. Soc. B 370: 20130551.

[6] Lu, J. and Li, J. (2011). Dynamics of Stage-Structure Discrete Mosquito Population Models. *Journal of Applied Analysis and Computation.* 1:(1) 53-67.

[7] Shaman, J. Spiegelman, M. cane, M. and Stieglitz, M. (2006). A Hydrologically Driven Model of Swamp Water Mosquito Population Dynamics. *Ecological Modelling.* 194, 395–404.

[8] Becker, N. (2003). Mosquitoes and Their Control, Kluwer Academic/Plenum, New York.

[9] Ruiz, D., Poveda, G., Velez, I. D., Quinones, M. L. Rua,G.L., Velasquesz, L.E. and Zuluaga, J.S. (2006). Modelling Entomological-Climatic Interactions of Plasmodium Falciparum Malaria Transmission in two Colombian Endemic-Regions: Contributions to a National Malaria Early Warning System, Malaria Journal , 5:66.

[10] Mwamtobe, P.M., Simelane, S.M., Abelman, S. and Tchuenche, J.M. (2017) Mathematical Analysis of a Lymphatic Filariasis Model with Quarantine and Treatment. BMC Public Health. 17:265-278.

[11] Oguntolu, F.A., Bolarin, G. Peter, J.O, Enagi, A.I. and Oshinubi, K.(2021). Mathematical Model for the Control of Lymphatic Filariasis Transmission Dynamics. Communications in Mathematical Biology and Neuroscience. 2021, 17-45.

[12] Simelane, S.M., Mwamtobe, P.M., Abelonam, S., and Tchuenche, J.M. (2019). A Mathematical Model for the Transmission Dynamics of Lymphatic Filariasis and Intervention Strategies. Acta Biotheorica. https://doi.org/10.1007/s10441-019-09370-y

[13] Salonga, P.K.N., Mendoza, V.M.P., Mendoza, R.G. and Belizario Jr., V.Y. (2021). A Mathematical Model of the Dynamics of Lymphatic Filariasis in Caraga Region, the Philippines. R. Soc Open Sci.8,1-24.

[14] Rychta J. and Taylor, D. (2022). A Game-theoretic Model of Lymphatic Filariasis Prevention. Neglected Tropical Diseases 16(9), 1-18.

[15] Stephano, M.A., Mayengo, M.M., Irunde, J.I. and Kuznetsov D. (2023). Sensitivity Analysis of Parameter Estimation for the Transmission of Lymphatic Filariasis. Hellyon. 9(2023), 1-14.

[16] Ukubuiwe, A.C. Ojianwuna, C.C., Olayemi, I.K., Arimoro, F.O., Omalu, I.C.J., Ukubuiwe, C.C. and Baba, B.M. (2020). Quantifying the Influence of Larval Density on Disease Transmission Indices in Culex quinquefasciatus, the Major African Vector of Filariasis. International Journal of Insect Science. 11(1),

[17] Garba, S.M. and Danbaba, U.A. (2020). Modelling the Effect of Temperature Variability on Malaria Control Strategies. Mathematical Modelling of Natural Phenomena. https://doc.org/10.1051/mmnpl2020044.

[18] Birkhoff, G. and Rota, C. (1998). Ordinary Differential Equations. 4th edn. John Wiley and Sons, New York.

[19] Van den Driessche P. and Watmough J. (2002). Reproduction Numbers and Sub-threshold Endemic Equilibria for Compartmental Models of Disease Transmission. Mathematical Biosciences. 180, 29-48.

[20] Van den Driessche, P. (2017). Reproduction Numbers of Infectious Disease Models. Infectious Disease Models. 2(3), 288-303.

[21] Castillo-Chavez, C. Feng Z. and Huang, W. (2014). On the Computation of R_0 and its Role in Global Stability. *https: www.researchgate.net/publication/228915276.*

[22] Marsudi, Hidayat, N. and Wibowo, R.B.E. (2021). Optimal Control and Sensitivity Analysis of HIV Model with Public Health Education Campaign and Antiretroviral Therapy, : AIP Conference Proceedings 2021, 060033 (2018); https://doi.org/10.1063/1.5062797

Approximate common solution of variational inequality and fixed point problems for family of nonexpansive semigroup

A.H. Ugwu*, I.G. Ezugorie†, E.C. Agbo‡, and E.U. Ofoedu§

Abstract

In this paper, we prove a path convergence theorem and introduce a new iterative scheme for approximation of common element of fixed point sets of family of nonexpansive semigroup and the set of solutions of variational inequality problem for an α-inverse strongly accretive mapping in strictly convex q-uniformly smooth real Banach space. As an application, solution is given to the problem of finding a common element of fixed point sets of family of nonexpansive semigroup and the set of zeros of an α-inverse strongly accretive operator. The result obtained augment and generalize several existing results.

Keywords and phrases: Modulus of smoothness; Modulus of convexity; generalized duality maps; α-inverse strongly accretive operators; k-strictly pseudocontractive mappings.

1 Introduction

Let E be a real normed linear space. The modulus of convexity of E is the function $\delta_E : [0,2] \to [0,1]$ defined by

$$\delta_E(\epsilon) = inf\Big\{1 - \frac{\|x+y\|}{2} : \|x\| = \|y\| = 1,\ \epsilon = \|x-y\|\Big\}.$$

The space E is said to be uniformly convex if and only if $\delta_E(\epsilon) > 0\ \forall\ \epsilon \in (0,2]$. E is said to be *strictly convex* if for all $x, y \in E$ such that $\|x\| = \|y\| = 1$ and for all $\lambda \in (0,1)$ we have $\|\lambda x + (1-\lambda)y\| < 1$. It is well known that every uniformly convex Banach space is strictly convex.

Let $S := \{x \in E : \|x\| = 1\}$. The space E is said to have a *Gâteaux differentiable* norm if the limit

$$\lim_{t\to 0} \frac{\|x+ty\| - \|x\|}{t}$$

exists for each $x, y \in S$. When this limit exists, we say that E is smooth. E is said to have a *uniformly Gâteaux differentiable* norm if for each $y \in S$ the limit is attained uniformly for $x \in S$. Furthermore, E is said to be uniformly smooth if the limit exists uniformly for $(x,y) \in S \times S$. It is well known that every uniformly smooth real Banach space is a reflexive real Banach space (see e.g., [13]).

*E-mail: albertugwu5@gmail.com; Department of Industrial Mathematics/Applied Statistics, Enugu State University of Science and Technology, Enugu, Nigeria

†E-mail: ikegodezugorie@esut.edu.ng; Department of Industrial Mathematics/Applied Statistics, Enugu State University of Science and Technology, Enugu, Nigeria

‡E-mail: agk.ejike@gmail.com; Department of Industrial Mathematics/Applied Statistics, Enugu State University of Science and Technology, Enugu, Nigeria

§Corresponding Author; Department of Mathematics, Nnamdi Azikiwe University, P.M.B. 5025, Awka, Anambra State, Nigeria. E-mail: euofoedu@yahoo.com; eu.ofoedu@unizik.edu.ng

Let E be a real normed linear space with dimension, $dim(E) \geq 2$. The *modulus of smoothness* of E is the function $\rho_E : [0, \infty) \to [0, \infty)$ defined by

$$\rho_E(t) = \sup\Big\{\frac{\|x+y\| + \|x-y\|}{2} - 1 : \|x\| = 1, \|y\| = t\Big\}.$$

In terms of the modulus of smoothness, the space E is called uniformly smooth if and only if $\lim_{t\to 0^+} \frac{\rho_E(t)}{t} = 0$. E is called *q-uniformly smooth* if there exists a constant $c > 0$ such that $\rho_E(t) \leq ct^q,\ t > 0$. It is easy to see that for $1 < q < +\infty$, every q-uniformly smooth Banach space is uniformly smooth; and thus has a uniformly Gâteaux differentiable norm.

Let E be a real normed linear space with dual E^*. We denote by J_q *the generalized duality mapping* from E to 2^{E^*} defined by

$$J_q x := \{f^* \in E^* : \langle x, f^*\rangle = \|x\|^q, \|f^*\| = \|x\|^{q-1}\},$$

where $\langle ., .\rangle$ denotes the generalized duality pairing between members of E and members of E^*. For $q = 2$, the mapping $J = J_2$ of E to 2^{E^*} is called *the normalized duality mapping*. It is well known that if E is uniformly smooth or E^* is strictly convex, then duality mapping is single-valued; and if E has a uniformly Gâteaux differentiable norm then the duality mapping is norm-to-weak* uniformly continuous on bounded subsets of E. If $E = H$ is a Hilbert space then the duality mapping becomes the identity map of H (see e.g., [50]). In the sequel, we shall denote the single-valued generalized duality mapping by j_q and the single valued normalized duality mapping by j.

Let K be a closed convex nonempty subset of a real normed space. One parameter family $\Psi := \{T(t) : t \in \mathbb{R}^+\}$, where $\mathbb{R}^+$ denotes the set of nonnegative real numbers, is said to be a (continuous) Lipschitzian semigroup (see e.g. [47]) of mappings from K to K if the following conditions are satisfied:

1. $T(0)x = x\ \forall\ x \in K$;
2. $T(s+t)x = T(s)T(t)x\ \forall\ s, t \in \mathbb{R}^+,\ x \in K$;
3. for each $t > 0$, there exists a bounded measurable function $L_t : [0, +\infty) \to [0, +\infty)$ such that $\|T(t)x - T(t)y\| \leq L_t\|x - y\|\ \forall\ x, y \in K$;
4. for each $x \in K$, the mapping $T(.)x$ from $\mathbb{R}^+$ into K is continuous.

A Lipschitzian semigroup is called nonexpansive if $L_t = 1$ for all $t > 0$ and asymptotically nonexpansive if $\limsup_{t\to\infty} L_t \leq 1$. We shall denote by $F(\Psi)$ the set of common fixed points of the semigroup Ψ, that is

$$F(\Psi) = \{x \in K : T(t)x = x,\ \forall\ t \in \mathbb{R}^+\} = \bigcap_{t\in\mathbb{R}^+} F(T(t)).$$

As a motivation for study of semigroup of operators, consider the Cauchy problem

$$\begin{cases} u'(t) = Au(t), t \geq 0, \\ u(0) = x, \end{cases} \tag{1}$$

where $A = (a_{ij})$ is an $n \times n$ matrix with $a_{ij} \in \mathbb{C}$ for $i, j = 1, 2, ..., n$, and x is a given vector in $\mathbb{C}^n$. It is well-known that the above Cauchy problem has a unique solution given by

$$u(t) = e^t Ax,\ t \geq 0,$$

where e^tA represents the fundamental matrix of the linear differential system $u'(t) = Au(t)$; and equals I for $t = 0$. We have

$$e^tA = \sum_{k=1}^{\infty} \frac{t^k}{k!} A_k,$$

valid for all $t \in \mathbb{R}$. Here, A and e^tA can be interpreted as linear operators, $A \in L(X)$, $e^tA \in L(X)$, where $X = \mathbb{C}^n$, equipped with any of its equivalent norms.

Note that the family of matrices (operators) $\{T(t) = e^tA, t \geq 0\}$ is a (uniformly continuous) semigroup on $X = \mathbb{C}^n$. Even more, $\{T(t) : t \geq 0\}$ extends to a group of linear operators, $\{e^tA : t \in \mathbb{R}\}$. The representation of the solution $u(t)$ as

$$u(t) = T(t)x, t \geq 0, \tag{2}$$

allows the derivation of some properties of the solution from the properties of the family $\{T(t) : t \geq 0\}$. This idea extends easily to the case in which X is a general Banach space and A is a bounded linear operator, $A \in L(X)$.

If A is a linear unbounded operator, $A : D(A) \subseteq X \to X$, with some additional conditions, then one can associate with A a so-called C_0-semigroup of linear opera- tors $\{T(t) \in L(X) : t \geq 0\}$, such that the solution of the Cauchy problem is again represented by the above formula (2). In this way one can solve various linear Partial Diferencial Equations (PDEs), where A represents linear unbounded differential operator with respect to the spacial variables, defined on convenient function spaces.It is worth mentioning that the connection between A and the corresponding semigroup $\{T(t) : t \geq 0\} \subset L(X)$ is established by the well-known Hille-Yosida theorem.

Linear semigroup theory received considerable attention in the 1930s as a new approach in the study of linear parabolic and hyperbolic partial differential equations. Note that the linear semigroup theory has later developed as an independent theory, with applications in some other fields, such as ergodic theory, the theory of Markov processes, and so on. It is well known that importance of the system (1) in modeling the dynamism of evolution system in Mathematical Biology cannot be over emphasized.

Iterative approximation of fixed points and zeros of nonlinear operators have been studied extensively by many authors to solve nonlinear operator equations as well as variational inequality problems (see e.g., [1], [6], [7], [8], [14], [15], [18], [25]-[29], [12], [20], [21], [31], [43], [32]-[36], [47], [51]). Construction of fixed points of nonexpansive semigroups is an important subject in nonlinear operator theory and its applications, in particular, in image recovery and signal processing (see e.g., [9, 30, 49]). Most published results on family of nonexpansive semigroup centered on the iterative approximation of common fixed points of the family. Shioji and Takahashi (1998) introduced the following implicit iteration process for approximation of common fixed point of family of nonexpansive semigroup

$$x_n = \alpha_n u + (1 - \alpha_n)\sigma_{t_n}(x_n), \ n \geq 1, \tag{3}$$

where $\{\alpha_n\}_{n\geq 1}$ is a sequence in $(0, 1)$ and $\{t_n\}_{n\geq 1}$ is a sequence of positive real numbers such that $\lim_{n\to\infty} t_n = +\infty$; and for $t > 0$, σ_t is given by $\sigma_t(x) = \frac{1}{t}\int_0^1 T(s)xds$. Under suitable conditions on the sequence $\{\alpha_n\}_{n\geq 1}$, Shioji and Takahashi [37] proved the convergence of (3) to an element of $F(\Psi)$.

Chen and Song [11] introduced the following implicit and explicit viscosity iteration processes

$$x_n = \alpha_n f(x_n) + (1 - \alpha_n)\sigma_{t_n}x_n, \ n \geq 1 \tag{4}$$

$$x_{n+1} = \alpha_n f(x_n) + (1 - \alpha_n)\sigma_{t_n}x_n, \ n \geq 1 \tag{5}$$

and proved that these sequences converge to some element of $F(\Psi)$ in uniformly convex Banach space with uniformly Gâteaux differentiable norm.

Suziki [40] proved the convegence of the iteration scheme

$$x_n = \alpha_n u + (1-\alpha_n)T(t_n)x_n,\ n \geq 1 \tag{6}$$

to a common fixed point of family of nonexpansive semigroup in Hilbert space.

In 2002, Benavides *et al.* [4] proved in uniformly smooth Banach space that if Ψ satisfies some asymptotic regularity condition and $\{\alpha_n\}_{n\geq 1}$ satisfies some mild conditions, then the implicit scheme (6) and the explicit scheme

$$x_{n+1} = \alpha_n u + (1-\alpha_n)T(t_n)x_n,\ n \geq 1 \tag{7}$$

converges strongly to an element of $F(\Psi)$.

In [48], Xu studied the strong convergence of the implicit iteration processes (3) and (6) in uniformly convex Banach space which admits a weakly sequential continuous duality mapping.

Recently, Song and Xu [39], studied the convergence of the following implicit and explicit viscosity iteration processes in strictly convex reflexive real Banach space with uniformly Gâteaux differentiable norm

$$x_n = \alpha_n f(x_n) + (1-\alpha_n)T(t_n)x_n,\ n \geq 1$$

$$x_{n+1} = \alpha_n f(x_n) + (1-\alpha_n)T(t_n)x_n,\ n \geq 1$$

They improved and generalized the corresponding results of Chen and Song [11], Aleyner and Censor [2] and Aleyner and Reich [?], Benavides *et al.* [4].

In this paper, it is our purpose to prove a path convergence theorem and construct a new iterative scheme for approximation of common element of fixed point sets of family of nonexpansive semigroup and the set of solution of variational inequality problem for an α-inverse strongly accretive mapping in q-uniformly smooth real Banach space. As an application, solution is given to the problem of finding a common element of fixed point sets of family of nonexpansive semigroup and the set of zeros of an α-inverse strongly accretive operator. Our iteration schemes, corollaries and method of proof are of independent interest.

2 Methodology/Model formulation

We shall now discuss various tools which we shall make use of in this paper; some of them will be stated as lemmas and propositions.

Let H be a real Hilbert space, a mapping $A : H \to H$ is said to be monotone if

$$\langle Ax - Ay, x - y\rangle \geq 0\ \forall\ x, y \in D(A).$$

The mapping $A : H \to H$ is called α-inverse strongly monotone if there exists a positive real number α such that

$$\langle Ax - Ay, x - y\rangle \geq \alpha\|Ax - Ay\|^2\ \forall\ x, y \in D(A).$$

A mapping $T : H \to H$ is said to be k-strictly pseudocontractive if there exists a constant $k \in [0, 1)$ such that

$$\|Tx - Ty\|^2 \leq \|x - y\|^2 + k\|(I - T)x - (I - T)y\|^2 \ \forall \ x, y \in D(T).$$

Observe that if $k = 0$, then the mapping T is nonexpansive. Observe also that if T is a k-strictly pseudocontractive mapping and we put $A = I - T$, where I is the identity operator of H, then we have that

$$\|(I - A)x - (I - A)y\|^2 \leq \|x - y\|^2 + k\|Ax - Ay\|^2 \ \forall \ x, y \in D(A)$$

and since H is a real Hilbert space, we have that

$$\|(I - A)x - (I - A)y\|^2 = \|x - y\|^2 + \|Ax - Ay\|^2 - 2\langle x - y, Ax - Ay\rangle,$$

so that

$$\langle x - y, Ax - Ay\rangle \geq \frac{1 - k}{2}\|Ax - Ay\|^2.$$

Thus, if T is k-strictly pseudocontractive mapping, then $A = I - T$ is α-inverse strongly monotone operator with $\alpha = \frac{1-k}{2}$.

Let K be a closed convex subset of a real Hilbert space H. A variational inequality problem is to find $x^* \in K$ such that

$$\langle Ax^*, y - x^*\rangle \geq 0 \ \forall \ y \in K,$$

where A is a monotone mapping of K to E (see e.g., [22, 24, 42, 29]).

In the sequel, we shall denote the set of solutions of variational inequality problems by $VI(K, A)$.

Let H be a real Hilbert space with inner product $\langle ., .\rangle$ and norm $\|.\|$; and let K be a closed convex subset of H. For any point $u \in H$, there exists a unique $P_K u \in K$ such that

$$\|u - P_K u\| \leq \|u - y\| \ \forall \ y \in K.$$

P_K is called the *metric projection* of H onto K. It is well known that P_K is a nonexpansive mapping of H onto K. It is also known that P_K satisfies

$$\langle x - y, P_K x - P_K y\rangle \geq \|P_K x - P_K y\|^2 \ \forall \ x, y \in H.$$

Furthermore, $P_K x$ is characterized by the properties $P_K x \in K$ and $\langle x - P_K x, P_K x - y\rangle \geq 0 \ \forall \ y \in K$. In the context of variational inequality problem, this implies that

$$u \in VI(K, A) \Leftrightarrow u = P_K(u - \lambda Au) \ \forall \ \lambda > 0.$$

A monotone operator A is said to be *maximal* if the graph, $G(A)$, of A is not properly contained in the graph of any other monotone operator, where $G(A) = \{(x, y) \in H \times H : y = Ax\}$. It is also known that A is maximal monotone if and only if for $(x, f) \in H \times H$, $\langle f - Ay, x - y\rangle \geq 0$ for every $(y, Ay) \in G(A)$ implies $f = Ax$. Let A be an α-inverse strongly monotone mapping defined from K into H and $N_K v$ be a normal cone to K at $v \in K$, that is $N_K v = \{w \in H : \langle w, v - u\rangle \geq 0, \ \forall \ u \in K\}$. Define a map M by

$$Mv = \begin{cases} Av + N_K v, & v \in K, \\ \emptyset, & v \notin K. \end{cases} \tag{8}$$

Then, M is maximal monotone and $u \in M^{-1}(0) \ \Leftrightarrow \ u \in VI(K, A)$, (see e.g., [34]).

We now turn to the generalized concept of variational inequality problem. Let E be a real Banach space. A mapping $A : D(A) \subset E \to E$ is said to be *accretive* if for all $x, y \in D(A)$ there exists $j_q(x-y) \in J_q(x-y)$ such that

$$\langle Ax - Ay, j_q(x-y)\rangle \geq 0$$

The mapping A is called an α-*inverse strongly accretive* if there exists a positive real number α such that $\forall\, x, y \in D(A)$ there exists $j_q(x-y) \in J_q(x-y)$ such that

$$\langle Ax - Ay, j_q(x-y)\rangle \geq \alpha \|Ax - Ay\|^q.$$

Observe that an α-inverse strongly accretive mapping is $\frac{1}{\alpha^{\frac{1}{q-1}}}$-Lipschitz.

Let K be a closed, convex and nonempty subset of E, Let $A : K \to E$ be an accretive mapping. A variational inequality problem is to find $x^* \in K$ such that for some $j_q(x-x^*) \in J_q(x-x^*)$,

$$\langle Ax^*, j_q(x-x^*)\rangle \geq 0 \;\forall\, x \in K.$$

We observe that the concept of monotonicity and accretivity coincide if and only if the underlying space is a real Hilbert space.

Let Q be a mapping of E onto K; Q is said to be *sunny* if $Q\big(Qx + t(x - Qx)\big) = Qx$ for all $x \in E$ and $t \geq 0$. A mapping Q of E into E is said to be a retraction if $Q^2 = Q$. If a mapping Q is a retraction, then $Qz = z$ for every $z \in R(Q)$, the range of Q. A subset K is said to be sunny nonexpansive retract of E if there exists a sunny nonexpansive retraction of E onto K. A retraction Q is said to be orthogonal if for each $x \in E,\ x - Q(x)$ is normal to K in the sense of R. C. James [19].

In [10], Bruck established the following:

1. A nonexpansive projection is necessarily an orthogonal retraction; and if E is smooth, then the converse is also true.

2. If E is smooth, then there can exist at most one nonexpansive projection of K onto a given subset C of K.

3. If E is uniformly smooth and there exists a nonexpansive retraction of K onto C, then there exists a nonexpansive projection of K onto C. The proximity mapping is nonexpansive projection in a Hilbert space, but not in a general Banach space.

It is well known (see e.g., [10]) that if E is a smooth real Banach space, then Q is an orthogonal retraction of E onto K if and only if $Q(x) \in K$ and

$$\langle Q(x) - x, j_q(Q(x) - y)\rangle \leq 0 \;\forall\, y \in K. \tag{9}$$

It then follows that for $x, y \in K$, we have $\langle Q(x) - x, j_q(Q(x) - Q(y))\rangle \leq 0$ and $\langle Q(y) - y, j_q(Q(y) - Q(x))\rangle \leq 0$ which implies that

$$\|Q(x) - Q(y)\|^2 \leq \langle x - y, j_q(Q(x) - Q(y))\rangle. \tag{10}$$

In the context of variational inequality problem, (9) implies that

$$u \in VI(K, A) \Leftrightarrow u = Q(u - \lambda Au) \;\forall\, \lambda > 0,$$

where in this case the mapping $A : K \to E$ is an accretive mapping.

An accretive mapping A is said to be *maximal accretive* if its graph, $G(A)$, is not contained in the graph of any other accretive mapping. Equivalently, A is maximal accretive if for every $(x, f) \in E \times E$ such that $\langle f - Ay, j_q(x-y)\rangle \geq 0$ holds for all $(y, Ay) \in G(A)$ implies $f = Ax$.

Proposition 2.1. *Let K be a closed convex nonepmty subset of a Banach space E. Let $A : K \to E$ be an α-inverse strongly accretive mapping. Let M be defined by*

$$Mv = \begin{cases} Av + N_K v, \ v \in K, \\ \emptyset, \ v \notin K. \end{cases} \tag{11}$$

where $N_K v = \{w \in E : \langle w, j_q(v-u)\rangle \geq 0, \ \forall \ u \in K\}$, then M is maximal accretive and $u \in M^{-1}(0) \Leftrightarrow u \in VI(K, A)$.

Proof. Let $v_0, w_0 \in E$ such that $\langle w - w_0, j_q(v - v_0)\rangle \geq 0$ holds for all $w \in Mv = Av + N_K v$. Then since $0 \in N_K v$, we have that

$$\langle Av - w_0, j_q(v - v_0)\rangle \geq 0 \ \forall \ v \in K.$$

Let $w_0 = Av_0 + w_1$, then $\langle Av - Av_0, j_q(v - v_0)\rangle \geq \langle w_1, j_q(v - v_0)\rangle$. For $\varepsilon \in (0, 1)$, let $v_\varepsilon = \varepsilon(v - v_0) + v_0$, then by convexity of K we have that $v_\varepsilon \in K$; and so,

$$\langle Av_\varepsilon - Av_0, j_q(v_\varepsilon - v_0)\rangle \geq \langle w_1, j_q(v_\varepsilon - v_0)\rangle.$$

Thus, we have the following estimate,

$$\begin{aligned} \varepsilon^{q-1}\langle w_1, j_q(v - v_0)\rangle &= \langle w_1, j_q(v_\varepsilon - v_0)\rangle \leq \langle Av_\varepsilon - Av_0, j_q(v_\varepsilon - v_0)\rangle \\ &\leq \|Av_\varepsilon - Av_0\| \|j_q(\varepsilon(v - v_0))\| \\ &\leq \varepsilon^{q-1}\frac{1}{\alpha^{q-1}}\|v_\varepsilon - v_0\| \|v - v_0\|^{q-1} \\ &= \varepsilon^q \frac{1}{\alpha^{q-1}}\|v - v_0\|^q. \end{aligned}$$

Thus, $\langle w_1, j_q(v - v_0)\rangle \leq \varepsilon\frac{1}{\alpha^{q-1}}\|v - v_0\|^q$, so that as $\varepsilon \to 0$, we have

$$\langle w_1, j_q(v_0 - v)\rangle \geq 0 \ \forall \ v \in K.$$

Hence, $w_1 \in N_K v_0$ and $w_0 \in Mv_0$, that is M is maximal accretive. It is therefore obvious that $u \in M^{-1}(0) \Leftrightarrow u \in VI(K, A)$. □

Let μ be a bounded linear functional defined on ℓ_∞ satisfying $\|\mu\| = 1 = \mu(1)$. It is known that μ is a mean on $\mathbb{N}$ if and only if

$$\inf\{a_n : n \in \mathbb{N}\} \leq \mu(a_n) \leq \sup\{a_n : n \in \mathbb{N}\}$$

for every $a = (a_1, a_2, a_3, ...) \in \ell_\infty$. In the sequel, we shall use $\mu_n(a_n)$ instead of $\mu(a)$. A mean μ on $\mathbb{N}$ is called *a Banach limt* if $\mu_n(a_n) = \mu_n(a_{n+1})$ for every $a = (a_1, a_2, a_3, ...) \in \ell_\infty$. It is well known that if μ is a Banach limit, then

$$\liminf_{n\to\infty} a_n \leq \mu_n a_n \leq \limsup_{n\to\infty} a_n$$

for all $a = (a_1, a_2, a_3, ...) \in \ell_\infty$. Furthermore, if $a = (a_1, a_2, ...), \ b = (b_1, b_2, ...) \in \ell_\infty$ and $\lim_{n\to\infty} a_n = a^* \left(\lim_{n\to\infty}(a_n - b_n) = 0\right)$, then $\mu_n(a_n) = a^* \left(\text{repectively, } \mu_n(a_n) = \mu_n(b_n)\right)$.

In the sequel, we shall make use of the following Lemmas:

Lemma 2.2. *Let E be a real normed linear space, then for $1 < q < +\infty$, the following inequality holds:*

$$\|x + y\|^q \leq \|x\|^q + q\langle y, j_q(x + y)\rangle \ \forall \ x, y \in E, \ \forall \ j_q(x + y) \in J_q(x + y).$$

In particular, for $q = 2$,

$$\|x + y\|^2 \leq \|x\|^2 + 2\langle y, j(x + y)\rangle \ \forall \ x, y \in E, \ \forall \ j(x + y) \in J(x + y).$$

Lemma 2.3. *(See e.g., [5, 44, 45]) Let $\{\lambda_n\}_{n\geq 1}$ be a sequence of nonnegative real numbers satisfying the condition*

$$\lambda_{n+1} \leq (1-\alpha_n)\lambda_n + \sigma_n,\ n \geq 0,$$

where $\{\alpha_n\}_{n\geq 0}$ and $\{\sigma_n\}_{n\geq 0}$ are sequences of real numbers such that $\{\alpha_n\}_{n\geq 1} \subset [0,1]$, $\sum_{n=1}^{\infty} \alpha_n = +\infty$. Suppose that $\sigma_n = o(\alpha_n),\ n \geq 0$ (i.e., $\lim_{n\to\infty} \frac{\sigma_n}{\alpha_n} = 0$) or $\sum_{n=1}^{\infty} |\sigma_n| < +\infty$ or $\limsup_{n\to\infty} \frac{\sigma_n}{\alpha_n} \leq 0$, then $\lambda_n \to 0$ as $n \to \infty$.

Lemma 2.4. *(See e.g. [41]) Let $\{x_n\}_{n\geq 1}$ and $\{y_n\}_{n\geq 1}$ be bounded sequences in a real Banach space E and let $\{\gamma_n\}_{n\geq 1}$ be a sequence in $[0,1]$ with $0 < \liminf \gamma_n \leq \limsup_{n\to\infty} \gamma_n < 1$. Suppose that $x_{n+1} = \gamma_n y_n + (1-\gamma_n)x_n$ for all integers $n \geq 0$ and $\limsup_{n\to\infty}(\|y_{n+1}-y_n\| - \|x_{n+1}-x_n\|) \leq 0$, then $\lim_{n\to\infty} \|x_n - y_n\| = 0$.*

Lemma 2.5. *(See e.g. [46]) Let E be a q-uniformly smooth real Banach space for some $q > 1$, then there exists some positive constant d_q such that*

$$\|x+y\|^q \leq \|x\|^q + q\langle y, j_q(x)\rangle + d_q\|y\|^q \ \forall\ x,y \in E,\ \forall\ j_q(x) \in J_q(x). \tag{12}$$

If E is L_q (or ℓ_q) space, the constant d_q in (12) has been calculated. This is shown in the following lemma.

Lemma 2.6. *(See e.g. [23]) Let E be L_q (or ℓ_q) space $(1 < q < +\infty)$ and $x, y \in E$,*

1. *if $1 < q < 2$, then*

$$\|x+y\|^q \leq \|x\|^q + q\langle y, j_q(x)\rangle + d_q\|y\|^q \ \forall\ x,y \in E,\ \forall\ j_q(x) \in J_q(x),$$

where $d_q = \frac{1+b_q^{q-1}}{(1+b_q)^{q-1}}$, and b_q is the unique solution of the equation $(q-2)b^{q-1} + (q-1)b^{q-2} - 1 = 0, 0 < b < 1$.

2. *if $2 \leq q < +\infty$, then*

$$\|x+y\|^2 \leq \|x\|^2 + 2\langle y, j(x)\rangle + (q-1)\|y\|^2 \ \forall\ x,y \in E,\ \forall\ j(x) \in J(x).$$

Now, let E be a q-uniformly smooth real Banach space. Let $A : K \to E$ be an α-inverse strongly accretive mapping. Then for the map $(I-\lambda A) : K \to E$ (where I is the identity map of K and $\lambda > 0$), we have the following estimates:

$$\begin{aligned}
\|(I-\lambda A)x - (I-\lambda A)y\|^q &= \|x-y-\lambda(Ax-Ay)\|^q \\
&\leq \|x-y\|^q - q\lambda\langle Ax-Ay, j_q(x-y)\rangle \\
&\quad + d_q\lambda^q\|Ax-Ay\|^q \\
&\leq \|x-y\|^q - \lambda(q\alpha - d_q\lambda^{q-1})\|Ax-Ay\|^q.
\end{aligned}$$

If λ is such that $0 < \lambda < \left(\frac{q\alpha}{d_q}\right)^{\frac{1}{q-1}}$, we have that $(I-\lambda A)$ is a nonexpansive mapping of K into E.

For L_q (or ℓ_q) spaces, $(2 \leq q < +\infty)$ we have the following:

$$\begin{aligned}
\|(I-\lambda A)x - (I-\lambda A)y\|^2 &= \|x-y-\lambda(Ax-Ay)\|^2 \\
&\leq \|x-y\|^2 - 2\lambda\langle Ax-Ay, j_q(x-y)\rangle \\
&\quad + (q-1)\lambda^2\|Ax-Ay\|^2 \\
&\leq \|x-y\|^2 - \lambda(2\alpha - (q-1)\lambda)\|Ax-Ay\|^q \\
&\leq \|x-y\|^2,
\end{aligned}$$

provided $\lambda \in \left(0, \frac{2\alpha}{q-1}\right)$. In particular, if $E = H$ is a Hilbert space and we choose $\lambda \in (0, 2\alpha)$, then $(I - \lambda A)$ is nonexpansive.

We now present the concept of uniformly asymptotic regular semigroup (see e.g [2]-[4], [39]). Let K be a nonempty closed convex subset of a Banach space E, $\Psi := \{T(t) : t \in \mathbb{R}^+\}$ a continuous operator semigroup on K. Then Ψ is said to be uniformly asymptotic regular on K if for all $h \in \mathbb{R}^+$ and any bounded subset C of K,

$$\lim_{t\to\infty} \sup_{x\in C} \|T(h)(T(t)x) - T(t)x\| = 0.$$

The nonexpansive semigroup $\{\sigma_t : t > 0\}$ defined by the following lemma is an example of uniformly asymptotic regular semigroup of mappings.

Lemma 2.7. *(See [11] Lemma 2.7, [39] lemma 2.2) Let K be a nonempty closed convex subset of a uniformly convex Banach space E, and D a bounded closed convex subset of K, and $\Psi := \{T(t) : t \in \mathbb{R}^+\}$ a nonexpansive semigroup on K such that $F(\Psi) \neq \emptyset$. For each $x \in K$, define $\sigma_t(x) := \frac{1}{t}\int_0^t T(s)xds$, then*

$$\lim_{t\to\infty} \sup_{x\in D} \|T(h)(\sigma_t x) - \sigma_t x\| = 0.$$

Other examples of uniformly asymptotic regular semigroup of mappings can be found in Examples 17 and 18 of [2].

3 Analysis of the model

Proposition 3.1. *Let K be a nonempty closed convex subset of a reflexive strictly convex real Banach space E. Let $\Psi = \{T(t) : t \in \mathbb{R}^+\}$ be a family of nonexpansive semigroup from K into itself. Let $\{x_n\}_{n\geq 1}$, a bounded sequence in K, be an approximate fixed point sequence of Ψ, that is, $\lim_{n\to\infty} \|x_n - T(t)x_n\| = 0 \ \forall\ t \in \mathbb{R}^+$. Let*

$$\Omega := \left\{x \in K \bigcap B : \mu_n\|x_n - x\|^2 = \min_{y\in K} \mu_n\|x_n - y\|^2\right\},$$

for some bounded closed convex nonempty subset, B, of E such that $x_n \in B \ \forall\ n \in \mathbb{N}$. If $F(\Psi) \neq \emptyset$, then $\Omega \bigcap F(\Psi) \neq \emptyset$.

Proof. Fix $x^* \in F(\Psi)$, then since $\{x_n\}_{n\geq 1}$ is bounded, there exists $R > 0$ sufficiently large such that $x_n \in B = \overline{B_R(x^*)}$ for all $n \in \mathbb{N}$. Furthermore, $K \bigcap B$ is a bounded closed convex and nonempty subset of E. Define a map $\phi : E \to \mathbb{R}$ by

$$\phi(y) = \mu_n\|x_n - y\|^2,$$

then ϕ is continuous, convex and coersive (that is $\phi(y) \to \infty$ as $\|y\| \to \infty$). Thus, since E is a reflexive Banach space, there exists $x_0 \in K \bigcap B$ such that

$$\phi(x_0) = \min_{y\in K\bigcap B} \mu_n\|x_n - y\|^2.$$

So, the set

$$\Omega := \left\{x \in K \bigcap B : \mu_n\|x_n - x\|^2 = \min_{y\in K\bigcap B} \mu_n\|x_n - y\|^2\right\} \neq \emptyset.$$

Ω is also bounded, closed and convex. We now show that $\Omega \bigcap F(\Psi) \neq \emptyset$. Let $z \in \Omega$, then since $\lim_{n\to\infty} \|x_n - T(t)x_n\| = 0$ for all $t \in \mathbb{R}^+$, we obtain that for all $t \in \mathbb{R}^+$,

$$\phi\big(T(t)z\big) = \mu_n\|x_n - T(t)z\|^2 \leq \mu_n\|T(t)x_n - T(t)z\|^2 \leq \mu_n\|x_n - z\|^2.$$

This implies that

$$\phi\big(T(t)z\big) \leq \phi(z) \ \forall \ t \in \mathbb{R}^+,$$

so that as $t \to \infty$, using that fact that ϕ is continuous, we obtain that

$$\phi\big(\lim_{t\to\infty} T(t)z\big) \leq \phi(z).$$

Hence, $\lim_{t\to\infty} T(t)z \in \Omega$. Let $p \in F(\Psi)$, then since every closed convex and nonempty subset of a reflexive strictly convex real Banach space E is a Chebyshev set (see e.g. [26], corollary 5.1.19), there exists a uniqe $u^* \in \Omega$ such that $\|p - u^*\| = \inf_{x\in\Omega} \|p - x\|$. Since $\lim_{t\to\infty} T(t)p = p$ and $\lim_{t\to\infty} T(t)u^* \in \Omega$, we have that

$$\|p - \lim_{t\to\infty} T(t)u^*\| = \|\lim_{t\to\infty} T(t)p - \lim_{t\to\infty} T(t)u^*\| = \lim_{t\to\infty} \|T(t)p - T(t)u^*\| \leq \|p - u^*\|.$$

Thus, $\lim_{t\to\infty} T(t)u^* = u^*$. Now, since $T(h+t)x = T(h)T(t)x \ \forall \ h, t \in \mathbb{R}^+, \ x \in \Omega$, then we have that $u^* = \lim_{t\to\infty} T(t)u^* = \lim_{t\to\infty} T(t+h)u^* = \lim_{t\to\infty} T(t)T(h)u^* = T(h)\lim_{t\to\infty} T(t)u^* = T(h)u^* \ \forall \ h \in \mathbb{R}^+$. Hence, $u^* \in F(\Psi)$. This completes the proof. □

Remark 3.2. *In what follows, the real sequences* $\{\alpha_n\}_{n\geq 1}$ *and* $\{\sigma_{i,n}\}_{n\geq 1}, \ i \in \mathbb{N}$ *in* $(0,1)$ *are such that* $\sum_{i=1}^{\infty} \sigma_{i,n} = 1 - \alpha_n$ *and* $\lim_{n\to\infty} \frac{\alpha_n}{\sigma_{i,n}} = 0, \ i = 1, 2, ...;$ $\{t_i\}_{i\geq 1}$ *is a sequence in* $\mathbb{R}^+$ *such that* $\lim_{i\to\infty} t_i = +\infty;$ $\delta \in (0,1)$ and $\lambda \in \left(0, \left(\frac{q\alpha}{d_q}\right)^{\frac{1}{q-1}}\right)$ *are fixed.* $\Psi := \{T(t) : t \in \mathbb{R}^+\}$, $FV := F(\Psi) \bigcap VI(K, A) \neq \emptyset$ *and* $F(S) := \{x \in D(S) : Sx = x\}$.

We state without proof the following proposition whose proof is immediate.

Proposition 3.3. *Let* K *be a nonempty closed and convex nonexpansive retract of a* q*-uniformly smooth real Banach space* E *with nonexpansive retraction* Q*. Let* $A : K \to E$ *be an* α*-inverse strongly accretive mapping and* Ψ *be a family of nonexpansive semigroup from* K *into itself. Define a map* $G_n : K \to K$ *by*

$$G_n x = \alpha_n u + (1-\delta)(1-\alpha_n)x + \delta \sum_{i\geq 1} \sigma_{i,n} T(t_i) Q(x - \lambda A x), \ \forall \ x \in K,$$

where $u \in K$ *is arbitrary. Then,* G_n *is a strict contraction and thus, for each* $n \in \mathbb{N}$ *there exists a unique* $z_n \in K$ *such that*

$$z_n = \alpha_n u + (1-\delta)(1-\alpha_n)z_n + \delta \sum_{i\geq 1} \sigma_{i,n} T(t_i) Q(z_n - \lambda A z_n). \tag{13}$$

Lemma 3.4. *Let* K *be a nonempty closed and convex nonexpansive retract of a* q*-uniformly smooth real Banach space* E *with nonexpansive retraction* Q*. Let* $\{z_n\}_{n\geq 1}$ *be a sequence satisfying (13), then* $\{z_n\}$ *is bounded.*

Proof. Let $p \in FV$, then using (13), we have

$$\begin{aligned}
\|z_n - p\|^2 &= \big\langle \alpha_n(u-p) + (1-\delta)(1-\alpha_n)(z_n - p) \\
&\quad + \delta \sum_{i\geq 1} \sigma_{i,n}\Big(T(t_i)Q(z_n - \lambda A z_n) - p\Big), j(z_n - p)\big\rangle \\
&\leq \alpha_n \big\langle u - p, j(z_n - p)\big\rangle + (1-\alpha_n)(1-\delta)\|z_n - p\|^2 \\
&\quad + \delta \sum_{i\geq 1} \sigma_{i,n} \|z_n - p\|^2 \\
&= \alpha_n \big\langle u - p, j(z_n - p)\big\rangle + (1-\alpha_n)\|z_n - p\|^2.
\end{aligned}$$

This implies that

$$\|z_n - p\| \leq \|u - p\| \ \forall \ n \in \mathbb{N}.$$

Hence, $\{z_n\}$ is bounded. □

Lemma 3.5. *Let K be a nonempty closed and convex nonexpansive retract of a q-uniformly smooth real Banach space E with nonexpansive retraction Q such that $q \geq 1+d_q$. Let $\Psi = \{T(t) : t \in \mathbb{R}^+\}$ be a family of uniformly asymptotic regular nonexpansive semigroup from K into itself and let $A : K \to E$ be an α-inverse strongly accretive mapping. Let $\{z_n\}_{n\geq 1}$ be a sequence satisfying (13), then $\lim_{n\to\infty} \|z_n - T(t)z_n\| = 0 \ \forall \ t \in \mathbb{R}^+$.*

Proof. Let $i \in \mathbb{N}$ and $p \in FV$, then using the hypothesis that $q \geq 1 + d_q$, we obtain from Lemma 2.5 that

$$\begin{aligned}
\|T(t_i)Q(z_n - \lambda Az_n) - z_n\|^q &= \|T(t_i)Q(z_n - \lambda Az_n) - p + p - z_n\|^q \\
&\leq \|p - z_n\|^q + q\big\langle T(t_i)Q(z_n - \lambda Az_n) - p, j_q(p - z_n)\big\rangle \\
&\quad + d_q\|T(t_i)Q(z_n - \lambda Az_n) - p\|^q \\
&\leq (1 + d_q)\|z_n - p\|^q \\
&\quad + q\big\langle T(t_i)Q(z_n - \lambda Az_n) - p, j_q(p - z_n)\big\rangle \\
&= (1 + d_q - q)\|z_n - p\|^q \\
&\quad + q\big\langle T(t_i)Q(z_n - \lambda Az_n) - z_n, j_q(p - z_n)\big\rangle \\
&\leq q\big\langle z_n - T(t_i)Q(z_n - \lambda Az_n), j_q(z_n - p)\big\rangle. \qquad (14)
\end{aligned}$$

Using (13), we obtain

$$\begin{aligned}
\big\langle z_n - p, j_q(z_n - p)\big\rangle &= \alpha_n\big\langle u - p, j_q(z_n - p)\big\rangle \\
&\quad + (1 - \alpha_n)(1 - \delta)\big\langle z_n - p, j_q(z_n - p)\big\rangle \\
&\quad + \delta\sum_{i\geq 1}\sigma_{i,n}\big\langle T(t_i)Q(z_n - \lambda Az_n) - z_n + z_n - p, j_q(z_n - p)\big\rangle \\
&= \alpha_n\big\langle u - p, j_q(z_n - p)\big\rangle + (1 - \alpha_n)\big\langle z_n - p, j_q(z_n - p)\big\rangle \\
&\quad + \delta\sum_{i\geq 1}\sigma_{i,n}\big\langle T(t_i)Q(z_n - \lambda Az_n) - z_n, j_q(z_n - p)\big\rangle.
\end{aligned}$$

This implies that

$$\delta\sum_{i\geq 1}\sigma_{i,n}\big\langle z_n - T(t_i)Q(z_n - \lambda Az_n), j_q(z_n - p)\big\rangle = \alpha_n\big\langle u - z_n, j_q(z_n - p)\big\rangle. \qquad (15)$$

Using (14) and (15), we obtain

$$\frac{\delta}{q}\sum_{i\geq 1}\sigma_{i,n}\|T(t_i)Q(z_n - \lambda Az_n) - z_{t_n}\|^q \leq \alpha_n\big\langle u - z_n, j_q(z_n - p)\big\rangle.$$

Thus, since $\sigma_{i,n}$ is positive for each $i,\ n \in \mathbb{N}$ and by Lemma 3.4 $\{z_n\}$ is bounded, we have that

$$\begin{aligned}
\frac{\delta}{q}\sigma_{i,n}\|T(t_i)Q(z_n - \lambda Az_n) - z_n\|^q &\leq \frac{\delta}{q}\sum_{i\geq 1}\sigma_{i,n}\|T(t_i)Q(z_n - \lambda Az_n) - z_n\|^q \\
&\leq \alpha_n\big\langle u - z_n, j_q(z_n - p)\big\rangle \leq \alpha_n R, \ \forall \ i, \ n \in \mathbb{N}
\end{aligned}$$

and for some real constant $R > 0$. So,

$$\|T(t_i)Q(z_n - \lambda Az_n) - z_n\|^q \leq \frac{qR}{\delta}\Big(\frac{\alpha_n}{\sigma_{i,n}}\Big).$$

Hence,

$$\lim_{n\to\infty} \|T(t_i)Q(z_n - \lambda A z_n) - z_n\| = 0 \ \forall\ i \in \mathbb{N}. \tag{16}$$

Since $\{z_n\}_{n\geq 1}$ is bounded, we have that $Q(z_n - \lambda A z_n)$ is also bounded. Thus, for all $t \in \mathbb{R}^+$,

$$\Big\|T(t)\Big(T(t_i)Q(z_n - \lambda A z_n)\Big) - T(t_i)Q(z_n - \lambda A z_n)\Big\| \leq \sup_{x\in C}\Big\|T(t)(T(t_i)x) - T(t_i)x\Big\|,$$

where C is any bounded subset of K containing $Q(z_n - \lambda A z_n)$. Furthermore, since $\lim_{i\to\infty} t_i = +\infty$ and the family Ψ is uniformly asymptotic regular, we have that

$$\lim_{i\to\infty}\sup_{x\in C}\Big\|T(t)(T(t_i)x) - T(t_i)x\Big\| = 0.$$

Thus, for all $t \in \mathbb{R}^+$, we have that

$$\begin{aligned}
\|z_n - T(t)z_n\| &\leq \|z_n - T(t_i)Q(z_n - \lambda A z_n)\| \\
&\quad + \Big\|T(t_i)Q(z_n - \lambda A z_n) - T(t)\Big(T(t_i)Q(z_n - \lambda A z_n)\Big)\Big\| \\
&\quad + \Big\|T(t)\Big(T(t_i)Q(z_n - \lambda A z_n)\Big) - T(t)z_n\Big\| \\
&\leq 2\|z_n - T(t_i)Q(z_n - \lambda A z_n)\| \\
&\quad + \Big\|T(t)\Big(T(t_i)Q(z_n - \lambda A z_n)\Big) - T(t_i)Q(z_n - \lambda A z_n)\Big\| \\
&\leq 2\|z_n - T(t_i)Q(z_n - \lambda A z_n)\| \\
&\quad + \sup_{x\in C}\Big\|T(t)(T(t_i)x) - T(t_i)x\Big\|.
\end{aligned}$$

So,

$$\limsup_{n\to\infty} \|z_n - T(t)z_n\| \leq \sup_{x\in C}\Big\|T(t)(T(t_i)x) - T(t_i)x\Big\|$$

and taking limit as $i \to \infty$ on both sides of this inequality, we obtain

$$\limsup_{n\to\infty} \|z_n - T(t)z_n\| \leq \lim_{i\to\infty}\sup_{x\in C}\Big\|T(t)(T(t_i)x) - T(t_i)x\Big\| = 0.$$

Hence, $\lim_{n\to\infty} \|z_n - T(t)z_n\| = 0 \ \forall\ t > 0$. This completes the proof. □

Theorem 3.6. *Let K be a nonempty closed and convex nonexpansive retract of a strictly convex q-uniformly smooth real Banach space E with nonexpansive retraction Q and such that $q \geq 1 + d_q$. Let Ψ be a family of uniformly asymptotic regular nonexpansive semigroup from K into itself and let $A : K \to E$ be an α-inverse strongly accretive mapping. Let $\{z_n\}$ be a sequence satisfying (13), then $\{z_n\}$ converges strongly to an element of FV.*

Proof. Let $p^* \in FV$, then since the sequence $\{z_n\}_{n\geq 1}$ is bounded, there exists $R > 0$ sufficiently large such that $u, z_n \in B^* := \overline{B_R(p^*)}$ for all $n \in \mathbb{N}$. Define the set

$$K_{min} = \Big\{x \in K \bigcap B^* : \mu_n\|z_n - x\|^2 = \min_{y\in K\bigcap B^*} \|z_n - y\|\Big\}.$$

Then, since $\lim_{n\to\infty} \|z_n - T(t)z_n\| = 0 \ \forall\ t \in \mathbb{R}^+$, we have by Proposition 3.1 that there exists a unique $u^* \in K_{min}$ such that $u^* = T(t)u^* \ \forall\ t \in \mathbb{R}^+$, i.e., $u^* \in F(\Psi)$. Let $\gamma \in (0, 1)$. Then, by convexity of $K \bigcap B^*$, we have that $(1-\gamma)u^* + \gamma u \in K \bigcap B^*$. So, $\mu_n\|z_n - u^*\|^2 \leq \mu_n\|z_n - \big((1-\gamma)u^* + \gamma u\big)\|^2$. By Lemma 2.2, we have that

$$\|z_n - u^* - \gamma(u - u^*)\|^2 \leq \|z_n - u^*\|^2 - 2\gamma\big\langle u - u^*, j\big(z_n - u^* - \gamma(u - u^*)\big)\big\rangle.$$

So,

$$\mu_n\|z_n - u^* - \gamma(u-u^*)\|^2 \leq \mu_n\|z_n - u^*\|^2 - 2\gamma\mu_n\langle u-u^*, j\big(z_n - u^* - \gamma(u-u^*)\big)\rangle.$$

This implies that $\mu_n\langle u-u^*, j\big(z_n - u^* - \gamma(u-u^*)\big)\rangle \leq 0$. Furthermore, since the normalized duality mapping j is norm-to-weak* uniformly continuous on bounded subsets of E, we obtain that

$$\lim_{\gamma\to 0}\Big(\langle u-u^*, j(z_n-u^*)\rangle - \langle u-u^*, j\big(z_n-u^*-\gamma(u-u^*)\big)\rangle\Big) = 0$$

Thus, for all $\epsilon > 0$, there exists $\eta_\epsilon > 0$ such that for all $\gamma \in (0, \eta_\epsilon)$ and for all $n \in \mathbb{N}$,

$$\langle u-u^*, j(z_n-u^*)\rangle - \langle u-u^*, j\big(z_n-u^*-\gamma(u-u^*)\big)\rangle < \epsilon.$$

Therefore, for all $\gamma \in (0, \eta_\epsilon)$,

$$\mu_n\langle u-u^*, j(z_n-u^*)\rangle - \mu_n\langle u-u^*, j\big(z_n-u^*-\gamma(u-u^*)\big)\rangle \leq \epsilon,$$

so that as $\epsilon \to 0$, we obtain that $\mu_n\langle u-u^*, j(z_n-u^*)\rangle \leq 0$. Using (13), we obtain that

$$\begin{aligned}\|z_n-u^*\|^2 &= \Big\langle \alpha_n(u-u^*) + (1-\alpha_n)(1-\delta)(z_n-u^*) \\ &\quad +\delta\sum_{i\geq 1}\sigma_{i,n}\Big(T(t_i)Q(z_n-\lambda Az_n)-u^*\Big), j(z_n-u^*)\Big\rangle \\ &\leq \alpha_n\langle u-u^*, j(z_n-u^*)\rangle + (1-\alpha_n)\|z_n-u^*\|^2. \end{aligned} \tag{17}$$

This implies that

$$\|z_n-u^*\|^2 \leq \langle u-u^*, j(z_n-u^*)\rangle.$$

Thus, $\mu_n\|z_n-u^*\|^2 \leq \mu_n\langle u-u^*, j(z_n-u^*)\rangle \leq 0$. So $\mu_n\|z_n-u^*\|^2 = 0$. Thus, there exists a subsequence $\{z_{n_k}\}_{k\geq 1}$ of $\{z_n\}_{n\geq 1}$ such that $z_{n_k} \to u^*$ as $k \to \infty$.

Claim. $z_n \to u^*$ as $n \to \infty$.

Proof of claim. Suppose $\{z_{n_m}\}_{m\geq 1}$ is another subsequence of $\{z_n\}_{n\geq 1}$ which converges strongly to q^*. Then, it is clear that $q^* \in F(\Psi)$ since $T(t)$ is continuous and $\lim_{m\to\infty}\|T(t)z_{n_m} - z_{n_m}\| = 0 \ \forall\ t \in \mathbb{R}^+$. Furthermore, since $\lim_{m\to\infty}\|T(t_i)Q(z_{n_m}-\lambda Az_{n_m})\| = 0 \ \forall\ i \in \mathbb{N}$ (see (16)), we have by continuity of $T(t_i)Q(I-\lambda A)$ that $T(t_i)Q(q^*-\lambda Aq^*) = q^* \ \forall\ i \in \mathbb{N}$. We now show that $q^* = u^*$. Suppose for contradiction the $q^* \neq u^*$. Then using (13),

$$\begin{aligned}\|z_{n_k}-q^*\|^2 &= \Big\langle \alpha_{n_k}(u-q^*) + (1-\delta)(1-\alpha_{n_k})(z_{n_k}-q^*) \\ &\quad +\delta\sum_{i\geq 1}\sigma_{i,n_k}\Big(T(t_i)Q(z_{n_k}-\lambda Az_{n_k}\Big)-q^*), j(z_{n_k}-q^*)\Big\rangle \\ &= \alpha_{n_k}\langle u-u^*, j(z_{n_k}-q^*)\rangle + \alpha_{n_k}\langle u^*-z_{n_k}, j(z_{n_k}-q^*)\rangle \\ &\quad +\alpha_{n_k}\|z_{n_k}-q^*\|^2 + (1-\delta)(1-\alpha_{n_k})\|z_{n_k}-q^*\|^2 \\ &\quad +\delta\sum_{i\geq 1}\sigma_{i,n_k}\Big\langle\Big(T(t_i)Q(z_{n_k}-\lambda Az_{n_k})-q^*\Big), j(z_{n_k}-q^*)\Big\rangle \\ &\leq \alpha_{n_k}\langle u-u^*, j(z_{n_k}-q^*)\rangle + \alpha_{n_k}\langle u^*-z_{n_k}, j(z_{n_k}-q^*)\rangle \\ &\quad +\alpha_{n_k}\|z_{n_k}-q^*\|^2 + (1-\delta)(1-\alpha_{n_k})\|z_{n_k}-q^*\|^2 \\ &\quad +\delta(1-\alpha_{n_k})\|z_{n_k}-q^*\|^2 \\ &= \alpha_{n_k}\langle u-u^*, j(z_{n_k}-q^*)\rangle + \alpha_{n_k}\langle u^*-z_{n_k}, j(z_{n_k}-q^*)\rangle \\ &\quad +\|z_{n_k}-q^*\|^2, \end{aligned}$$

so that

$$\langle u-u^*, j(q^*-z_{n_k})\rangle \leq M\|z_{n_k}-u^*\| \tag{18}$$

for some $M>0$. Since the duality mapping j is norm-to-weak* uniformly continuous on bounded subsets of E, we have that

$$\langle u-u^*, j(q^*-z_{n_k})\rangle \to \langle u-u^*, j(q^*-u^*)\rangle.$$

Thus, we obtain from (18) that

$$\langle u-u^*, j(q^*-u^*)\rangle \leq 0. \tag{19}$$

Following the same line of argument, we also obtain that $\langle u-q^*, j(u^*-q^*)\rangle \leq 0$, which implies that

$$\langle q^*-u, j(q^*-u^*)\rangle \leq 0. \tag{20}$$

Adding (19) and (20) we obtain that $\langle q^*-u^*, j(q^*-u^*)\rangle \leq 0$, that is, $\|q^*-u^*\|\leq 0$, a contradiction. So, $q^*=u^*$. Hence, $\{z_n\}_{n\geq 1}$ converges strongly to $u^*\in F(\Psi)$.

Next, we show that $u^*\in VI(K,A)$. Let $x^*\in FV$ and $y_n=Q(z_n-\lambda Az_n)$. Then,

$$\begin{aligned}\|y_n-x^*\|^q &= \|Q(z_n-\lambda Az_n)-Q(x^*-\lambda Ax^*)\|^q\\ &\leq \|z_n-x^*-\lambda(Az_n-Ax^*)\|^q\\ &\leq \|z_n-x^*\|^q+\lambda(d_q\lambda^{q-1}-q\alpha)\|Az_n-Ax^*\|^q.\end{aligned}$$

Again, using (13) and the convexity of $\|.\|^q$, we have that

$$\begin{aligned}\|z_n-x^*\|^q &= \|\alpha_n(u-x^*)+(1-\alpha_n)(1-\delta)(z_n-x^*)+\delta\sum_{i\geq 1}\sigma_{i,n}(T(t_i)y_n-x^*)\|^q\\ &\leq \alpha_n\|u-x^*\|^q+(1-\alpha_n)(1-\delta)\|z_n-x^*\|^q+(1-\alpha_n)\delta\|y_n-x^*\|^q\\ &\leq \alpha_n\|u-x^*\|^q+(1-\alpha_n)(1-\delta)\|z_n-x^*\|^q\\ &\quad +(1-\alpha_n)\delta\Big[\|z_n-x^*\|^q+\lambda(d_q\lambda^{q-1}-q\alpha)\|Az_n-Ax^*\|^q\Big]\\ &\leq \alpha_n\|u-x^*\|^q+\|z_n-x^*\|^q+(1-\alpha_n)\delta\lambda(d_q\lambda^{q-1}-q\alpha)\|Az_n-Ax^*\|^q.\end{aligned}$$

This implies that

$$(1-\alpha_n)\delta\lambda(q\alpha-d_q\lambda^{q-1})\|Az_n-Ax^*\|^q \leq \alpha_n\|u-x^*\|^q$$

Thus, since $\{z_n\}_{n\geq 1}$ is bounded, $\alpha_n\to 0$ as $n\to\infty$, we have that $\lim_{n\to\infty}\|Az_n-Ax^*\|=0$. Besides, by property (10) of Q and Lemma 2.5, we obtain

$$\begin{aligned}\|y_n-x^*\|^q &= \|Q(z_n-\lambda Az_n)-Q(x^*-\lambda Ax^*)\|^q\\ &\leq \big\langle (z_n-\lambda Az_n)-(x^*-\lambda Ax^*), j_q(y_n-x^*)\big\rangle\\ &= \big\langle z_n-x^*, j_q(y_n-x^*)\big\rangle-\lambda\big\langle Az_n-Ax^*, j_q(y_n-x^*)\big\rangle\\ &\leq \frac{1}{q}\Big(\|y_n-x^*\|^q+d_q\|z_n-x^*\|^q-\|y_n-z_n\|^q\Big)\\ &\quad -\lambda\big\langle Az_n-Ax^*, j_q(y_n-x^*)\big\rangle,\end{aligned}$$

so that

$$\|y_n-x^*\|^q\leq\frac{d_q}{q-1}\|z_n-x^*\|^q-\frac{1}{q-1}\|y_n-z_n\|^q-\frac{q\lambda}{q-1}\big\langle Az_n-Ax^*, j_q(y_n-x^*)\big\rangle.$$

Thus, we have

$$\begin{aligned}
\|z_n - x^*\|^q &= \|\alpha_n(u-x^*) + (1-\alpha_n)(1-\delta)(z_n - x^*) + \delta\sum_{i\geq 1}\sigma_{i,n}(T(t_i)y_n - x^*)\|^q \\
&\leq \alpha_n\|u-x^*\|^q + (1-\alpha_n)(1-\delta)\|z_n - x^*\|^q + (1-\alpha_n)\delta\|y_n - x^*\|^q \\
&\leq \alpha_n\|u-x^*\|^q + (1-\alpha_n)(1-\delta)\|z_n - x^*\|^q \\
&\quad +(1-\alpha_n)\delta\Big[\frac{d_q}{q-1}\|z_n - x^*\|^q - \frac{1}{q-1}\|y_n - z_n\|^q \\
&\quad -\frac{q\lambda}{q-1}\big\langle Az_n - Ax^*, j_q(y_n - x^*)\big\rangle\Big] \\
&= \alpha_n\|u-x^*\|^q + (1-\alpha_n)\Big[1-\delta\Big(1-\frac{d_q}{q-1}\Big)\Big]\|z_n - x^*\|^q \\
&\quad -\frac{\delta(1-\alpha_n)}{q-1}\|y_n - z_n\|^q - \frac{q\delta\lambda(1-\alpha_n)}{q-1}\big\langle Az_n - Ax^*, j_q(y_n - x^*)\big\rangle.
\end{aligned}$$

But $q \geq 1 + d_q$. Thus,

$$\frac{\delta(1-\alpha_n)}{q-1}\|y_n - z_n\|^q \leq \alpha_n\|u-x^*\|^q - \frac{q\delta\lambda(1-\alpha_n)}{q-1}\big\langle Az_n - Ax^*, j_q(y_n - x^*)\big\rangle.$$

Using the fact that $\alpha_n \to 0$ and $\|Az_n - Ax^*\| \to 0$ as $n \to \infty$, we obtain that

$$\lim_{n\to\infty}\|y_n - z_n\| = 0 \text{ and thus, } y_n \to u^* \text{ as } n \to \infty.$$

Let

$$Mv = \begin{cases} Av + N_K v, \ v \in K, \\ \emptyset, \ v \notin K. \end{cases}$$

Then, M is maximal accretive. Let $G(M)$ denote the graph of M. Let $(v,w) \in G(M)$. Since $w - Av \in N_K v$ and $y_n \in K$, we have (by definition of $N_K v$) that $\langle w - Av, j_q(v - y_n)\rangle \geq 0$. Also by the definition of y_n, $n \in \mathbb{N}$ and property (9) of Q, we have that

$$\big\langle y_n - (z_n - \lambda Az_n), j_q(v - y_n)\big\rangle \geq 0.$$

Hence,

$$\big\langle \frac{y_n - z_n}{\lambda} + Az_n, j_q(v - y_n)\big\rangle \geq 0.$$

Using this, we obtain the following estimate:

$$\begin{aligned}
\big\langle w, j_q(v - y_n)\big\rangle &\geq \big\langle Av, j_q(v - y_n)\big\rangle \\
&\geq \big\langle Av, j_q(v - y_n)\big\rangle - \big\langle \frac{y_n - z_n}{\lambda} + Az_n), j_q(v - y_n)\big\rangle \\
&= \big\langle Av - \frac{y_n - z_n}{\lambda} - Az_n, j_q(v - y_n)\big\rangle \\
&= \big\langle Av - Ay_n, j_q(v - y_n)\big\rangle + \big\langle Ay_n - Az_n, j_q(v - y_n)\big\rangle \\
&\quad -\big\langle \frac{y_n - z_n}{\lambda}, j_q(v - y_n)\big\rangle \\
&\geq \alpha\|Av - Ay_n\| + \big\langle Ay_n - Az_n, j_q(v - y_n)\big\rangle \\
&\quad -\big\langle \frac{y_n - z_n}{\lambda}, j_q(v - y_n)\big\rangle \\
&\geq \big\langle Ay_n - Az_n, j_q(v - y_n)\big\rangle - \big\langle \frac{y_n - z_n}{\lambda}, j_q(v - y_n)\big\rangle
\end{aligned}$$

so that as $n \to \infty$ (using the fact that A is uniformly continuous and the fact that E has uniformly Gâteaux differentiable norm), we have that

$$\langle w, j_q(v - u^*)\rangle \geq 0,$$

and since M is maximal accretive, we obtain that $u^* \in M^{-1}(0)$. So, by Proposition 2.1 $u^* \in VI(K, A)$ or equivalently $u^* = Q(I - \lambda A)u^*$. Hence, $\{z_n\}_{n\geq 1}$ converges strongly to $u^* \in FV$. □

Remark 3.7. *If E is real L_q (or ℓ_q) space, $2 \leq q < +\infty$, then we have from (2) of Lemma 2.6 that $d_q = q - 1$ so that $1 + d_q = q$. Hence, Theorem 3.6 holds in L_q (or ℓ_q) space, $2 \leq q < +\infty$, In particular, Theorem 3.6 holds in real Hilbert spaces. Thus, we have the following corollaries.*

Corollary 3.8. *Let H be a real Hilbert space. Let $K,\ A,\ \{z_n\}$ and $\{T(t) : t \in \mathbb{R}^+\}$ be as in Theorem 3.6 and $Q = P_K$. Then $\{z_n\}$ converges strongly to an element of FV.*

Corollary 3.9. *Let E be real L_q (or ℓ_q) space, $2 \leq q < +\infty$,. Let $K,\ A,\ \{z_n\}$ and $\{T(t) : t \in \mathbb{R}^+\}$ be as in Theorem 3.6. Then $\{z_n\}$ converges strongly to an element of FV.*

Remark 3.10. *We note that if $1 < q < 2$, then by (1) of Lemma 2.6, $d_q = \frac{1+b_q^{q-1}}{(1+b_q)^{q-1}}$, where b_q is the unique solution of the equation $(q-2)b^{q-1} + (q-1)b^{q-2} - 1 = 0,\ 0 < b < 1$. It therefore follows that $1 + b_q^{q-1} = (q-1)(b_q+1)b_q^{q-2}$. Hence,*

$$\begin{aligned} d_q = \frac{1 + b_q^{q-1}}{(1+b_q)^{q-1}} &= \frac{(q-1)(b_q+1)b_q^{q-2}}{(1+b_q)^{q-1}} \\ &= (q-1)\Big(\frac{b_q}{1+b_q}\Big)^{q-2} = (q-1)\Big(\frac{1+b_q}{b_q}\Big)^{2-q} > q-1 \end{aligned}$$

(since $1 < q < 2$). Thus, $q < 1 + d_q$. So Theorem 3.6 is not applicable in L_q (or ℓ_q) spaces when $1 < q < 2$.

4 Applications.

We now construct an explicit iterative algorithm for approximation of a common element of fixed point set of family of uniformly asymptotic regular nonexpansive semigroup and the set of solutions of variational inequality problem for an α-inverse strongly accretive operator.

Theorem 4.1. *Let K be a nonempty closed, convex nonepansive retract of a strictly convex q-uniformly smooth real Banach space E with nonexpansive retraction Q and such that $q \geq 1 + d_q$. Let Ψ be a family of uniformly asymptotic regular nonexpansive semigroup from K into itself. Let $A : K \to E$ be an α-inverse strongly accretive mapping. For some real numbers $\delta \in (0,1)$ and $\lambda \in \Big(0, \Big(\frac{q\alpha}{d_q}\Big)^{\frac{1}{q-1}}\Big)$ and for arbitrary $x_1, u \in K$, define a sequence $\{x_n\}_{n=1}^{\infty}$ by*

$$x_{n+1} = \alpha_n u + (1-\delta)(1-\alpha_n)x_n + \delta \sum_{i\geq 1} \sigma_{i,n} T(t_i) Q(x_n - \lambda A x_n),\ n \geq 1. \tag{21}$$

Suppose that $\lim_{n\to\infty} \sum_{i\geq 1} |\sigma_{i,n+1} - \sigma_{i,n}| = 0$, then $\{x_n\}_{n\geq 1}$ converges strongly to some element of FV.

Proof. We first show that $\{x_n\}_{n\geq 1}$ is bounded. Let $x^* \in FV$. We have the following claim.

Claim. $\|x_n - x^*\| \leq \max\{\|u - x^*\|,\ \|x_1 - x^*\|\}\ \forall\ n \geq 1$.

Proof of Claim. We do this by induction. Observe that for $n = 1$, the claim clear holds. Suppose that for some $k \in \mathbb{N}\backslash\{1\}$, the claim is true for $n = k$. We show that it is also true for $n = k + 1$. Now, we have from equation 21 that

$$\begin{aligned}\|x_{k+1} - x^*\| &\leq \alpha_k\|u - x^*\| + (1 - \alpha_k)(1 - \delta)\|x_k - x^*\| \\ &\quad +\delta\sum_{i\geq 1}\sigma_{i,k}\|T(t_i)Q(x_k - \lambda Ax_k) - x^*\| \\ &\leq \alpha_k\|u - x^*\| + (1 - \alpha_k)\|x_k - x^*\| \\ &\leq \max\{\|u - x^*\|,\ \|x_1 - x^*\|\}.\end{aligned}$$

So, the claim is true for $n = k+1$. Hence, $\{x_n\}_{n\geq 1}$ is bounded. It is now easy to see that $\{T(t_i)Q(x_n - \lambda Ax_n)\}_{n\geq 1}$, $\{Ax_n\}_{n\geq 1}$ and $\{T(t_i)x_n\}_{n\geq 1}$, $i = 1, 2, ...$ are all bounded. Now, define the sequences $\{\gamma_n\}_{n\geq 1}$ and $\{u_n\}_{n\geq 1}$ by $\gamma_n = (1 - \delta)\alpha_n + \delta$ and $u_n = \frac{x_{n+1} - x_n + \gamma_n x_n}{\gamma_n}$. Then

$$u_n = \frac{\alpha_n u + \delta\sum_{i\geq 1}\sigma_{i,n}T(t_i)Q(x_n - \lambda Ax_n)}{\gamma_n}.$$

Observe that $\{u_n\}_{n\geq 1}$ is bounded and that

$$\begin{aligned}\|u_{n+1} - u_n\| - \|x_{n+1} - x_n\| &\leq \left|\frac{\alpha_{n+1}}{\gamma_{n+1}} - \frac{\alpha_n}{\gamma_n}\right|\|u\| + \left|\frac{\delta(1 - \alpha_{n+1})}{\gamma_{n+1}} - 1\right|\|x_{n+1} - x_n\| \\ &\quad +\frac{\delta M_0}{\gamma_{n+1}\gamma_n}\Big(\sum_{i\geq 1}|\sigma_{i,n+1} - \sigma_{i,n}| + |\gamma_{n+1} - \gamma_n|\Big),\end{aligned}$$

for some real constant $M_0 > 0$. This implies that

$$\limsup_{n\to\infty}(\|u_{n+1} - u_n\| - \|x_{n+1} - x_n\|) \leq 0.$$

So, by lemma 2.4, $\lim_{n\to 0}\|u_n - x_n\| = 0$. But,

$$\|x_{n+1} - x_n\| = \gamma_n\|u_n - x_n\|.$$

Thus,

$$\lim_{n\to\infty}\|x_{n+1} - x_n\| = 0.$$

Moreover, from the recursion formula (21) we have that

$$x_{n+1} - x_n = \alpha_n(u - x_n) + \delta\sum_{i\geq 1}\sigma_{i,n}(T(t_i)Q(x_n - \lambda Ax_n) - x_n).$$

This implies that

$$\delta\Big\|\sum_{i\geq 1}\sigma_{i,n}(T(t_i)Q(x_n - \lambda Ax_n) - x_n)\Big\| \leq \|x_{n+1} - x_n\| + \alpha_n\|u - x_n\|.$$

Thus,

$$\lim_{n\to\infty}\Big\|\sum_{i\geq 1}\sigma_{i,n}(T(t_i)Q(x_n - \lambda Ax_n) - x_n)\Big\| = 0.$$

Let $\{\alpha_n\}_{n\geq 1}$ in Remark 3.2 also satisfy the following condition:

$$\lim_{n\to\infty}\frac{\|\sum_{i\geq 1}\sigma_{i,n}(T(t_i)Q(x_n - \lambda Ax_n) - x_n)\|}{\alpha_n} = 0.$$

For each $n \in \mathbb{N}$, let $z_n \in K$ be the unique fixed point satifying (13). Then, by Theorem 3.6, we have that $z_n \to u^* \in FV$ as $n \to \infty$. Using (13) and Lemma 2.2 we obtain that

$$\begin{aligned}
\|z_n - x_n\|^2 &\leq \|(1-\delta)(1-\alpha_n)(z_n - x_n) + \delta \sum_{i\geq 1} \sigma_{i,n}\Big(T(t_i)Q(z_n - \lambda A z_n) \\
&\quad -T(t_i)Q(x_n - \lambda A x_n) + T(t_i)Q(x_n - \lambda A x_n) - x_n\Big)\|^2 \\
&\quad +2\alpha_n\big\langle u - x_n, j(z_n - x_n)\big\rangle \\
&\leq \Big[(1-\delta)(1-\alpha_n)\|z_n - x_n\| + \delta(1-\alpha_n)\|z_n - x_n\| \\
&\quad +\|\delta \sum_{i\geq 1} \sigma_{i,n}\Big(T(t_i)Q(x_n - \lambda A x_n) - x_n\Big)\|\Big]^2 \\
&\quad +2\alpha_n\big\langle u - x_n, j(z_n - x_n)\big\rangle \\
&= \Big[(1-\alpha_n)\|z_n - x_n\| + \delta\|\sum_{i\geq 1} \sigma_{i,n}\Big(T(t_i)Q(x_n - \lambda A x_n) - x_n\Big)\|\Big]^2 \\
&\quad +2\alpha_n\big\langle u - x_n, j(z_n - x_n)\big\rangle.
\end{aligned}$$

This implies that

$$\begin{aligned}
&\big\langle u - x_n, j(x_n - z_n)\big\rangle \leq \frac{\alpha_n}{2}\|z_n - x_n\|^2 \\
&+\delta(1-\alpha_n)\|z_n - x_n\|\Big(\frac{\|\sum_{i\geq 1}\sigma_{i,n}(T(t_i)Q_(x_n - \lambda A x_n) - x_n)\|}{\alpha_n}\Big) \\
&+\frac{\delta^2\|\sum_{i\geq 1}\sigma_{i,n}(T(t_i)Q(x_n - \lambda A x_n) - x_n)\|^2}{2\alpha_n}.
\end{aligned}$$

Hence,

$$\limsup_{n\to\infty} \big\langle u - x_n, j(x_n - z_n)\big\rangle \leq 0.$$

Furthermore,

$$\begin{aligned}
\big\langle u - x_n, j(x_n - z_n)\big\rangle &= \big\langle u - u^*, j(x_n - u^*)\big\rangle \\
&\quad +\big\langle u - u^*, j(x_n - z_n) - j(x_n - u^*)\big\rangle \\
&\quad +\big\langle u^* - z_n, j(x_n - z_n)\big\rangle.
\end{aligned}$$

Again, using the fact that E has uniformly Gâteaux differentiable norm we have that

$$\limsup_{n\to\infty} \big\langle u - u^*, j(x_n - u^*)\big\rangle \leq 0.$$

Set

$$\omega_n = \max\{0,\ \big\langle u - u^*, j(x_n - u^*)\big\rangle\}.$$

Then, $0 \leq \omega_n\ \forall\ n \geq 1$. Also, if $\varepsilon > 0$ is given, then there exists $n_\varepsilon \in \mathbb{N}$ such that $\big\langle u - u^*, j(x_n - u^*)\big\rangle < \varepsilon\ \forall\ n \geq n_\varepsilon$. This implies that $0 \leq \omega_n < \varepsilon\ \forall\ n \geq n_\varepsilon$. Thus, $\lim_{n\to\infty} \omega_n = 0$. Moreover, we have from the recursion formula (21) and Lemma 2.2 that

$$\begin{aligned}
\|x_{n+1} - u^*\|^2 &= \|\alpha_n(u - u^*) + (1-\alpha_n)(1-\delta)(x_n - u^*) \\
&\quad +\delta\sum_{i\geq 1}\sigma_{i,n}(T(t_i)Q(x_n - \lambda A x_n) - u^*)\|^2 \\
&\leq \|(1-\alpha_n)(1-\delta)(x_n - u^*) \\
&\quad +\delta\sum_{i\geq 1}\sigma_{i,n}(T(t_i)Q(x_n - \lambda A x_n) - u^*)\|^2 \\
&\quad +2\alpha_n\big\langle u - u^*, j(x_{n+1} - u^*)\big\rangle \\
&\leq (1-\alpha_n)\|x_n - u^*\|^2 + 2\alpha_n\omega_{n+1}.
\end{aligned}$$

Hence, by Lemma 2.3, we have that $\{x_n\}_{n\geq 1}$ converges strongly to $u^* \in FV$. This completes the proof. □

Corollary 4.2. *Let E be a strictly convex q-uniformly smooth real Banach space such that $q \geq 1 + d_q$. Let $A : E \to E$ be an α-inverse strongly accretive mapping. Let Ψ be a family of uniformly asymptotic regular nonexpansive semigroup from E into itself such that $F(\Psi) \bigcap A^{-1}(0) \neq \emptyset$. For fixed $u \in E$, let $\{x_n\}_{n\geq 1}$ be a sequence generated from arbitrary $x_1 \in E$ by*

$$x_{n+1} = \alpha_n u + (1-\delta)(1-\alpha_n)x_n + \delta \sum_{i\geq 1} \sigma_{i,n} T(t_i)(x_n - \lambda A x_n),\ n \geq 1, \tag{22}$$

where $\{\alpha_n\}_{n\geq 1}$ and $\{\sigma_{i,n}\}_{n\geq 1},\ i = 1, 2, \ldots$ are as in Theorem 4.1. Then, $\{x_n\}_{n\geq 1}$ converges strongly to an element of $F(\Psi) \bigcap A^{-1}(0)$.

Proof. Here, $A^{-1}(0) = VI(E, A)$, $FV := F(\Psi) \bigcap A^{-1}(0)$ and $Q = I$, where I is the identity operator defined on E. The rest follows as in the proof of Theorem 4.1. □

Corollary 4.3. *Let H be a real Hilbert space. Let $A : H \to H$ be an α-inverse strongly monotone mapping. Let Ψ be a family of uniformly asymptotic regular nonexpansive semigroup from H into itself such that $F(\Psi) \bigcap A^{-1}(0) \neq \emptyset$. For fixed $u \in H$, let $\{x_n\}_{n\geq 1}$ be a sequence generated from arbitrary $x_1 \in H$ by 22. Then, $\{x_n\}_{n\geq 1}$ converges strongly to an element of $F(\Psi) \bigcap A^{-1}(0)$.*

Proof. Here, $A^{-1}(0) = VI(H, A)$, $FV := F(\Psi) \bigcap A^{-1}(0)$ and $Q = P_H = I$, where I is the identity operator defined on H. The rest follows as in Theorem 4.1. □

Corollary 4.4. *Let K be a nonempty closed convex subset of a real Hilbert space. Let $S : K \to K$ be a k-strictly pseudocontractive mapping. Let Ψ be a family of uniformly asymptotic regular nonexpansive semigroup from K into itself such that $F(\Psi) \bigcap F(S) \neq \emptyset$. For fixed $u \in K$, let $\{x_n\}_{n\geq 1}$ be a sequence generated from arbitrary $x_1 \in K$ by*

$$x_{n+1} = \alpha_n u + (1-\delta)(1-\alpha_n)x_n + \delta \sum_{i\geq 1} \sigma_{i,n} T(t_i)\Big((1-\lambda)x_n + \lambda S x_n\Big),\ n \geq 1,$$

where $\{\alpha_n\}_{n\geq 1}$ and $\{\sigma_{i,n}\}_{n\geq 1},\ i = 1, 2, \ldots$ are as in Theorem 4.1. Then, $\{x_n\}_{n\geq 1}$ converges strongly to an element of $F(\Psi) \bigcap F(S)$.

Proof. Put $A = I - S$, where I is the identity operator defined on K. Then A is α-inverse strongly monotone with $\alpha = \frac{1-k}{2}$. Moreover $F(S) = VI(K, A)$, $Q = P_K$ and $P_K(x_n - \lambda A x_n) = (1-\lambda)x_n + \lambda S x_n$. So, by Theorem 4.1, the result follows. □

5 Numerical simulations/sensitivity analysis

Remark 5.1. *Prototypes for our iteration parameters $\{\alpha_n\}_{n\geq 1}$ and $\{\sigma_{i,n}\}_{n\geq 1},\ i = 1, 2, \ldots$ are*

$$\alpha_n = \frac{1}{n+1},\ \sigma_{i,n} = \frac{n}{2^i(n+1)},\ i,\ n \in \mathbb{N}.$$

Remark 5.2. *The addition of bounded error terms in any of the recursion formulas leads to no further generalization.*

Remark 5.3. *If $f : K \to K$ is a contraction map and we replace u by $f(x_n)$ in the recursion formulas of our theorems, we obtain what some authors now call* viscosity *iteration process. We observe that all our theorems in this paper carry over trivially to the so-called viscosity process. One simply replaces u by $f(x_n)$, repeats the argument of this paper, using the fact that f is a contraction map.*

6 Discussions and Conclusion

The theorems obtained in this paper extend, improve and generalize many recently announced results.

References

[1] M. O. Aibinu and J. K. Kim, Convergence analysis of viscosity implicit rules of nonexpansive mappings in Banach spaces, *Nonlinear Functional Analysis and Applications* **24** (2019) no. 4, 691-713.

[2] A. Aleyner and Y. Censor, Best approximation to common fixed points of a semigroup of nonexpansive operators, *J. Nonlinear Convex Anal.* **6**(1) (2005), 137-151.

[3] A. Aleyner and S. Reich, An explicit construction of sunny nonexpansive retractions in Banach spaces, *Fixed Point Theory Appl.* **2005** (3) (2005), 295-305.

[4] T. D. Benavides, G. L. Acedo and H. K. Xu, Construction of sunny nonexpansive retracions in Banach spaces, *Bull. Austral. Math. Soc.* **66** (1) (2002), 9-16.

[5] V. Berinde, Iterative approximation of fixed points, *Editura Efemeride Baia Mare,* 2002.

[6] V. Berinde, Approximating fixed points of enriched nonexpansive mappings by Krasnoseskij iteration in Hilbert spaces, *Carpathian J. Math.* **35** (2019) no.3, 293-304.

[7] V. Berinde, Approximating fixed point of enriched nonexpansive mappings in Banach spaces by using a retraction-displacement condition, *Carpathian J. Math.* **36** (2020) no.1, 27-34.

[8] X. Bian, S. Shahzeen, M. Abbas, M. S. Ahmad and B. Zhang, The generalized implicit iterative process for approximating fixed points of nonexpansive mappings in CAT(0) spaces, *IEEE Access* (2019), Doi 10.1109/Access 2019.2963024.

[9] C. Byrne, A unified treatment of some iterative algorithms in signal processing and image construction, *Inverse problems* **20** (2004) 103-120.

[10] R. E. Bruck; Jr. Nonexpansive projections on subsets of Banach space, *Pacific J. Math.* **47** (1973), 341-355.

[11] R. Chen and Y. Song, Convergence to common fixed point of nonexpansive semigroup, *J. Comput. Appl. Math.* **200** (2007), 566-575.

[12] L. C. Ceng and M. Shang, Hybrid inertial subgradient extragradient methods for variational inequalities and fixed point problems involving asymptotically nonexpansive mappings, *Optimization*, 70:4, (2021),715-740, DOI: 10.1080/02331934.2019.1647203

[13] C. E. Chidume, Geometric properties of Banach spaces and nonlinear iterations, *Springer Verlag Series:* Lecture Notes in Mathematics, Vol. 1965 (2009), ISBN 978-1-84882-189-7.

[14] C. E. Chidume and E. U. Ofoedu, A new iteration process for finite families of generalized Lipschitz pseudo-contractive and generalized Lipschitz accretive mappings, *Nonlinear Analysis; TMA.*, In press, accepted manuscript, available online 27 June 2007.

[15] C. E. Chidume and E. U. Ofoedu, Approximation of common fixed points for finite families of total asymptotically nonexpansive mappings, *J. Math. Anal. Appl.,* **333**(1) (2007), 128-141.

[16] K. Goebel and W. A. Kirk, A fixed point theorem for asymptotically nonexpansive mappings, *Proc. Amer. Math. Soc.* **35** (1972) 171-174.

[17] H. Iiduka and W. Takahashi, Strong convergence theorems for nonexpansive mappings and inverse-strongly monotone mappings, *Nonlinear Anal.* **61** (2005), 341-350.

[18] S. Ishikawa, Fixed point by a new iteration method, *Proc. Amer. Math. Soc.* **44** (1974), 147-150.

[19] R. C. James, Orthogonal and linear functionals in normed linear spaces, *Trans. Amer. Math. Soc.* **61** (1947), 265-292.

[20] A. Kalsoom, N. Saleem, H. Isik, T. M. Al-Shami, A. Bibi and H. Khan, Fixed point approximation of monotone nonexpansive mappings in hyperbolic spaces, *Journal of Function Spaces*, vol. 2021, Article ID 3243020, 14 pages, (2021). https://doi.org/10.1155/2021/3243020

[21] S. Khatoon, I. Uddin, J. Ali and R. George, Common fixed points of two G-Nonexpansive mappings via a faster iteration procedure, *Journal of Function Spaces*, vol. 2021, Article ID 9913540, 8 pages, (2021). https://doi.org/10.1155/2021/9913540

[22] D. Kinderlebrer, and G. Stampacchia, An introduction to variational inequalitites and their applications, *Academic press, Inc. 1980.*

[23] T. C. Lim, H. K. Xu and Z. B. Xu, Some L_P inequalities and their applications to fixed point theory and approximation theory, *in progress in Approximation theory (P. Nevai and A. Pinkus, Eds.)*, pp. 609-624, Academic press, 1991.

[24] J. L. Lions and G. Stampacchia, Variational inequalities, *Comm. Pure Appl. Math.* **20** (1967), 493-517.

[25] W. R. Mann, Mean value methods in iteration, *Proc. Amer. Math. Soc.* **4** (1953) 506-510.

[26] R. E. Megginson, An introduction to Banach space theory, *Springer-Verlag*, New York, Inc., 1998.

[27] E. U. Ofoedu, Iterative approximation of a common zero of a countably infinite family of m-accretive operators in Banach spaces, *Hindawi-Fixed point theory and applications, doi:10.1155/2008/325792.*

[28] E. U. Ofoedu and Y. Shehu, Iterative construction of a common fixed point of finite families of nonlinear mappings, *in press, to appear in Vol. 16 No 1 of Journal of Applied Analysis (2010).*

[29] E. U. Ofoedu, Y. Shehu and J. N. Ezeora, Solution by iteration of nonlinear variational inequalities involving finite family of asymptotically nonexpansive mappings and monotone mappings, *PanAmer. Math. J.* **18** (2008) (4), 61-75.

[30] C. I. Polilchuk and R. J. Mammone, Image recovery by convex projections using a least-square constraint, *J. Opt. Soc. Amer.* **A7** (1990) 517-521.

[31] V. Pragadeeswarar and R. Gopi, Iterative approximation to common best proximity points of proximally mean nonexpansive mappings in Banach spaces, *Afrika Matematika* **32** (2021), 289-300.

[32] S. Reich, Weak convergence theorems for nonexpansive mappings in Banach spaces, *J. Math. Anal. Appl.* **67** (1979), 274-276.

[33] B. E. Rhoades, Fixed point iterations for certain nonlinear mappings, *J Math. Anal. Appl.* **183** (1994) 118-120.

[34] R. T. Rockefellar, Monotone operators and proximal point algorithm, SIAM, *J. Control Optim.* **14** (1976), 877-898.

[35] J. Schu, Iterative construction of fixed points of asymptotically nonexpansive mappings, *J. Math. Anal. Appl.* **158** (1991), 407-413.

[36] J. Schu, Weak and strong convergence of fiexd points of asymptotically nonexpansive mappings, *Bull. Austral. Math. Soc.* **43** (1991), 153-159.

[37] N. Shioji and W. Takahashi, Strong convergence theorems for asymptotically nonexpansive mappings in Hilbert spaces, *Nonlinear Anal.* **34** (1998), 87-99.

[38] N. Shrama, L. N. Mishra, V. N. Mishra and H. Almusewa, Endpoint approximation of standard three-step multi-valued iteration algorithm for nonexpansive mappings, *Appl. Math. Inf. Sci.* **15** (2021) no. 1, 78-81.

[39] Y. Song and S. Xu, Strong convergence theorems for nonexpansive semigroup in Banach spaces, *J. Math. Anal. Appl.* **338** (2008), 152-161.

[40] T. Suzuki, On the convergence to common fixed points of nonexpansive semigroup in Hilbert spaces, *Proc. Amer. Math. Soc.* **131** (2002), 2133-2136.

[41] T. Suzuki, Strong convergence of Krasnoselskii and Mann's type sequences for one-parameter nonexpansive semigroups without Bouchner integrals, *J. Math. Anal. Appl.* **305** (2005) 227-239.

[42] W. Takahashi, Nonlinear complementary problem and systems of convex inequalities, *J. Optim. Theory Appl.* **24** (1978), 493-508.

[43] X. Wu, Fixed point problems for nonexpansive mappings in bounded sets of Banach spaces, *Advances in Mathematical Physics*, vol. 2020, Article ID 9182016, 6 pages, (2020). https://doi.org/10.1155/2020/9182016

[44] H. K. Xu, Iterative algorithms for nonlinear operators, *J. London Math. Soc.* **66** (2002) 240-256.

[45] H. K. Xu, An iterative approach to quadratic optimization, *Journal of Optimization Theory and Applications,* **116** (2003) no.3, 659-678.

[46] H. K. Xu, Inequality in Banach spaces with applications, *Nonlinear Anal.* **16** (1991), 1127-1138, *London Math. Soc.*, **66** (2) (2002), 240-256.

[47] H. K. Xu, Strong asymptotic behavior of almost orbits of nonlinear semigroups, *Nonlinear Anal.* **46** (2001), 135-151.

[48] H. K. Xu, A strong convergence theorem for contraction semigroup in Banach spaces, *Bull. Austral. Math. Soc.* **72** (2005) 371-379.

[49] D. Youla, On deterministic convergence of iterations of related projection operators, *J. Vis. Commun. Image Represent* **1** (1990), 12-20.

[50] W. Takahashi, Nonlinear Functional Analysis, *Yokohama publishers, Yokohama,* 2000.

[51] L. Zhao, S. Chang, L. Wang and G. Wang, Viscosity approximation methods for the implicit midpoint rule of nonexpansive mappings in CAT(0) spaces, *J. Nonlinear Sci. Appl.* **10** (2017), 386-394.

Numerical solution approximation of nonlinear functional integral by Homotopy perturbation method

C.E. Chika*

Abstract

A numerical method for solving nonlinear functional integral is presented. Numerical examples are presented to show the validity of the numerical algorithm developed using Homotopy Perturbation Method (HPM). This method is simple to implement and gives good approximation at first iteration.

Keywords and phrases: Homotopy perturbation method; Nonlinear integral equations; Functional integral, Numerical Method.

1 Introduction

Finding solution to integral equations has been studied by scientists and engineers over the years; this is due to their immense applications in the field of sciences and engineering. These applications appear in the arrears of chaos, solitons, fractals, as well as scattering like the one encountered by Chika and Hooshyar [1].

Most of the methods developed work for specific assumptions, hence the need to develop more methods that include other cases that are not yet covered in the assumptions or the methods that may be simpler or easier to implement. Some of these methods solve linear functional integrals like the one presented by Abbasbandy [2] and [3] as well as other literatures. After the introduction of Homotopy Perturbation Method (HPM) by He in [4]; it has been used to solve many linear and nonlinear problems. This method has been applied also to linear functional integral equations and specific integral equations like Fredholm and Volterra [5, 6, 7, 8, 9] . In this work, the objective is to apply Homotopy Perturbation Method in solving a class of nonlinear functional integral.
In section 2, numerical algorithm for solving nonlinear functional integral is presented; in section 3, examples are presented to show the validity of the method. Finally, conclusion and further works are presented in section 4.

2 Numerical Algorithm

Functional integral can be written in two types: the Fredholm type as in Eq(1) and the Voltera type shown in Eq(2)

$$y(x) + w(x)y(h(x)) + \lambda \int_a^b K(x,t)(y(t))^m dt = g(x) \tag{1}$$

$$y(x) + w(x)y(h(x)) + \lambda \int_a^x K(x,t)(y(t))^m dt = g(x) \tag{2}$$

$x, t \in [a, b]$, $w(x)$, $y(h(x))$, $K(x,t)$ and $g(x)$ known

*E-mail: charles.chika@unn.edu.ng; Department of Mathematics, University of Nigeria, Nsukka, Enugu State, Nigeria

We form the homotopy equation using the Fredholm type

$$H(y,p) = (1-p)F(y) + pL(y) \tag{3}$$

where $p \in [0,1]$

$$L(y) = y(x) + w(x)y(h(x)) + \lambda \int_a^b K(x,t)(y(t))^m dt - g(x)$$

from Eq(3) $H(y,0) = F(y)$ and $H(y,1) = L(y)$, therefore, the solution to Eq(1) is traced when p increases from 0 to 1 by setting $H(y,p) = 0$.
Let $y(x) = \sum_{n=0}^{\infty} p^n y_n(x)$, and $F(y) = y(x) - y_0(x)$, Eq(3) becomes;

$$(1-p)\left(\sum_{n=0}^{\infty} p^n y_n(x) - y_0(x)\right) + p\left[\sum_{n=0}^{\infty} p^n y_n(x) + w(x)q(x) + \lambda \int_a^b K(x,t)(\sum_{n=0}^{\infty} p^n y_n(x))^m dt - g(x)\right] = 0 \tag{4}$$

where $q(x) = y(h(x))$
Expanding and equating like powers of p in Eq(4), we obtain
$p^0 : y_0(x) - y_0(x) = 0$
$p^1 : y_1(x) + y_0(x) + w(x)q(x) - g(x) - \lambda \int_a^b K(x,t)(y_0(t))^m dt = 0$

$$p^2 : \begin{cases} y_2(x) + \lambda \int_a^b K(x,t)(2y_0(t)y_1(t))dt = 0, & \text{if } m = 2 \\ y_2(x) + \lambda \int_a^b K(x,t)(3((y_0(t))^2 y_1(t))dt = 0, & \text{if } m = 3 \\ y_2(x) + \lambda \int_a^b K(x,t)(4(y_0(t))^3 y_1(t))dt = 0, & \text{if } m = 4 \\ y_2(x) + \lambda \int_a^b K(x,t)(5(y_0(t))^4 y_1(t))dt = 0, & \text{if } m = 5 \\ . \\ . \\ . \end{cases}$$

.
.
.

It follows that

$$p^n : \begin{cases} y_n(x) + \lambda \int_a^b K(x,t) \sum_{k=0}^{n-1} (y_k(t) y_{n-k-1}(t))dt = 0, & \text{if } m = 2 \\ y_n(x) + \lambda \int_a^b K(x,t) \sum_{i=0}^{n-1} \sum_{k=0}^{n-i-1} (y_i(t) y_k(t) y_{n-k-i-1}(t))dt = 0, & \text{if } m = 3 \\ y_n(x) + \lambda \int_a^b K(x,t) \sum_{i=0}^{n-1} \sum_{k=0}^{n-i-1} \sum_{l=0}^{n-i-k-1} (y_i(t) y_k(t) y_l(t) y_{n-l-k-i-1}(t))dt = 0, & \text{if } m = 4 \\ . \\ . \\ . \end{cases}$$

.
.
.

Therefore, the algorithm for Fredholm type can be written as follows:
$y_0(x) = g(x) - w(x)y(h(x))$, since $q(x) = y(h(x))$
for $n > 0$

$$y_n(x) = \begin{cases} -\lambda \int_a^b K(x,t) \sum_{k=0}^{n-1} (y_k(t) y_{n-k-1}(t))dt, & \text{if } m = 2 \\ -\lambda \int_a^b K(x,t) \sum_{i=0}^{n-1} \sum_{k=0}^{n-i-1} (y_i(t) y_k(t) y_{n-k-i-1}(t))dt, & \text{if } m = 3 \\ -\lambda \int_a^b K(x,t) \sum_{i=0}^{n-1} \sum_{k=0}^{n-i-1} \sum_{l=0}^{n-i-k-1} (y_i(t) y_k(x) u_l(t) y_{n-l-k-i-1}(t))dt, & \text{if } m = 4 \\ . \\ . \\ . \end{cases}$$

.
.
.

Similarly, the algorithm for Volterra type is

$y_0(x) = g(x) - w(x)y(h(x))$, since $q(x) = y(h(x))$

for $n > 0$

$$y_n(x) = \begin{cases} -\lambda \int_a^x K(x,t) \sum_{k=0}^{n-1} (y_k(t) y_{n-k-1}(t)) dt, & \text{if } m = 2 \\ -\lambda \int_a^x K(x,t) \sum_{i=0}^{n-1} \sum_{k=0}^{n-i-1} (y_i(t) y_k(t) y_{n-k-i-1}(t)) dt, & \text{if } m = 3 \\ -\lambda \int_a^x K(x,t) \sum_{i=0}^{n-1} \sum_{k=0}^{n-i-1} \sum_{l=0}^{n-i-k-1} (y_i(t) y_k(x) u_l(t) y_{n-l-k-i-1}(t)) dt, & \text{if } m = 4 \\ . \\ . \\ . \end{cases}$$

.
.
.

Since, the solution is traced as p increases from 0 to 1 $\Rightarrow y(x) = \lim_{p \to 1^-} \sum_{n=1}^{\infty} p^n y_n(x)$, so we take $y(x) = \sum_{n=1}^{\infty} y_n(x)$

3 Examples

Here we present examples to validate the algorithms stated above.

Example 1: Solve for $y(x)$ in the equation

$$y(x) + e^{-x}(1 - \cos^2 x) + \frac{1}{10} \int_0^{\frac{1}{2}} xt(y(t))^2 = (1 - x^2) + e^{-x}(1 - \cos^2 x) + \frac{37}{3840} x$$

Solution:
The equation in example 1 is of Fredholm type with $w(x) = e^{-x}$, $y(h(x)) = 1 - \cos^2 x$ and $g(x) = (1 - x^2) + e^{-x}(1 - \cos^2 x) + \frac{37}{3840} x$
Therefore,
$y_0(x) = (1 - x^2) + \frac{37}{3840} x$
for $n > 1$

$$y_n(x) = -\frac{1}{10} \int_0^{\frac{1}{2}} xt \sum_{k=0}^{n-1} (y_k(t) y_{n-k-1}(t)) dt$$

The exact solution is $1 - x^2$
Using Matlab to compute and compare the solutions show that the exact and approximate solution have good agreement by just taking the first partial sum for the approximate solution. This can be seen in Figure 1 and Table 1.

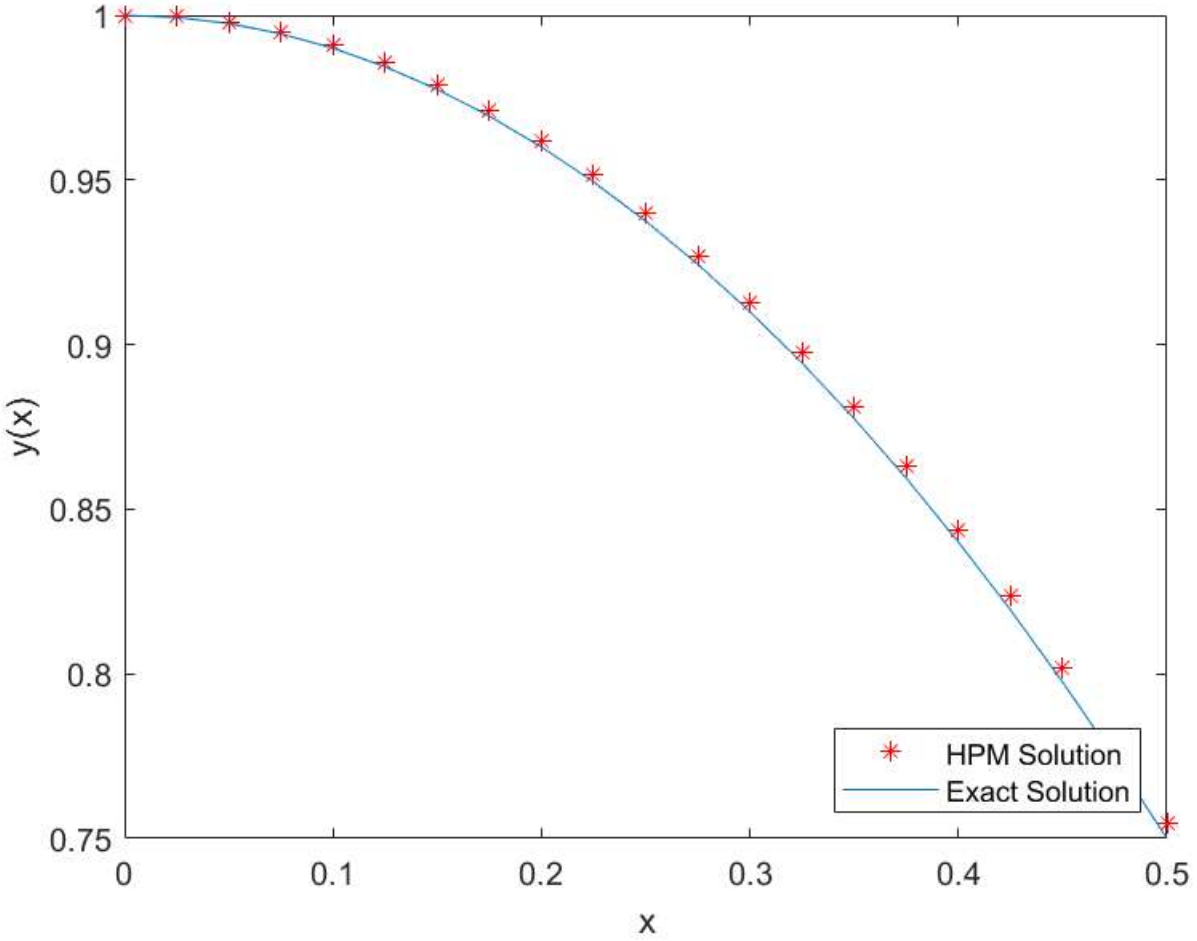


Figure 1: The graph of exact and HPM solution in Example 1

Table 1: Numerical values for example 1

x_i	Approximate $y(x_i)$	Exact $y(x_i)$	Relative error (%)
0	1.0000	1.0000	0
0.0500	0.9980	0.9975	0.0483
0.1000	0.9910	0.9900	0.0973
0.1500	0.9789	0.9775	0.1479
0.2000	0.9619	0.9600	0.2007
0.2500	0.9399	0.9375	0.2569
0.3000	0.9129	0.9100	0.3177
0.3500	0.8809	0.8775	0.3843
0.4000	0.8439	0.8400	0.4588
0.4500	0.8018	0.7975	0.5437
0.5000	0.7548	0.7500	0.6424

Example 2: Solve for y(x) such that
$y(x) + xe^{-3x} + \frac{1}{100}\int_0^x x(y(t))^3 dt = x(e^{-3x} + \frac{1}{300}) + e^x(1 - \frac{1}{300}e^{2x})$, $x \in [0, \frac{1}{2}]$

Solution: The equation in example 2 is of Volterra type with $w(x) = x$, $y(h(x)) = e^{-3x}$ and

$g(x) = x(e^{-3x} + \frac{1}{300}) + e^x(1 - \frac{1}{300}e^{2x})$
$y_0 = x(e^{-3x} + \frac{1}{300}) + e^x(1 - \frac{1}{300}e^{2x}) - xe^{-3x}$
for $n > 0$
$y_n = -\frac{1}{100}\int_0^x x \sum_{i=0}^{n-1} \sum_{k=0}^{n-i-1}(y_i(t)y_k(t)y_{n-k-i-1}(t))dt$
The exact solution to this problem is $y(x) = e^x$.
Figure 2 shows the exact and approximate solution plotted and Table 2 displays their errors for different values of x, as can be seen, there is a good agreement between the exact and approximate solution.

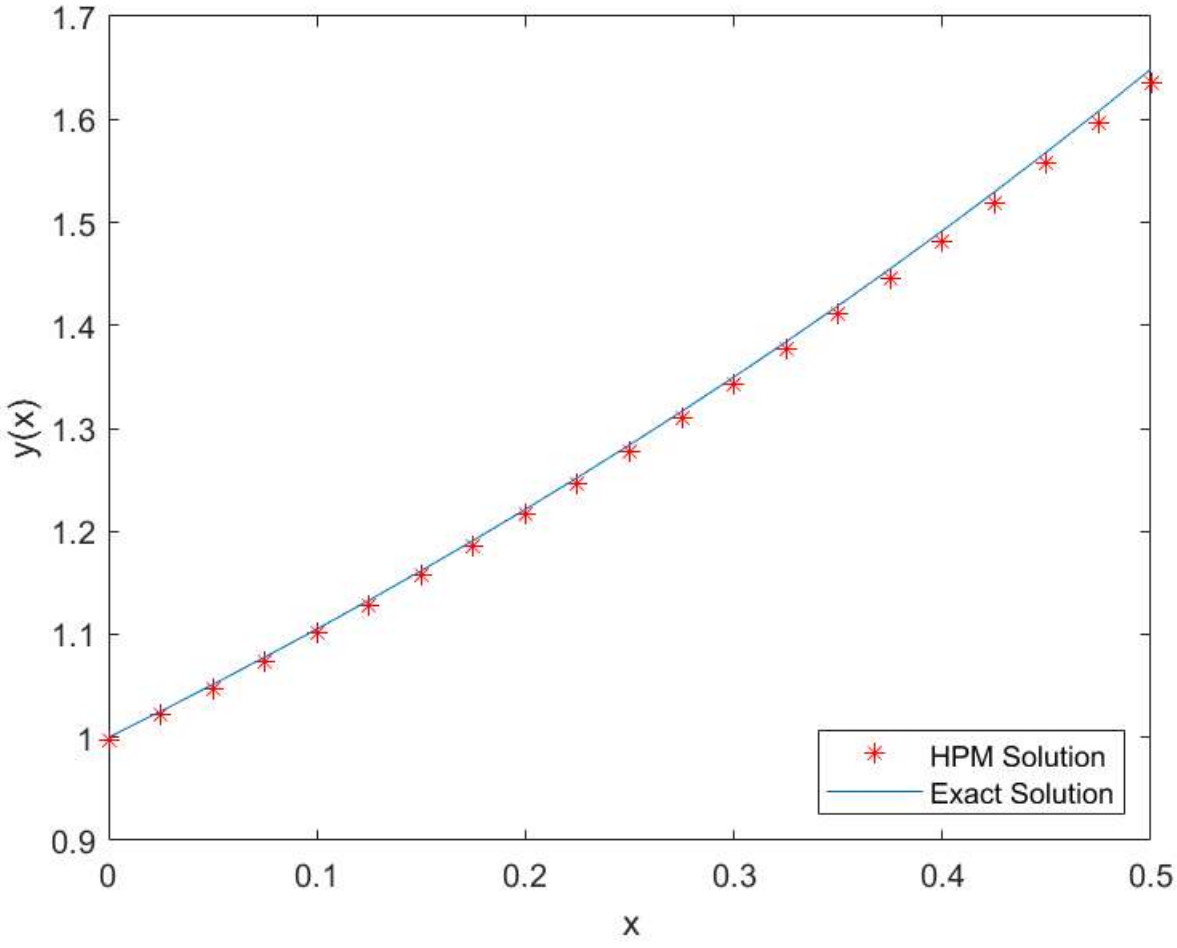


Figure 2: The graph of exact and HPM solutions in Example 2

Table 2: Numerical values for example 2

x_i	Approximate $y(x_i)$	Exact $y(x_i)$	Relative error (%)
0	0.9967	1.0000	0.3333
0.0500	1.0476	1.0513	0.3525
0.1000	1.1010	1.1052	0.3770
0.1500	1.1571	1.1618	0.4069
0.2000	1.2160	1.2214	0.4427
0.2500	1.2778	1.2840	0.4847
0.3000	1.3427	1.3499	0.5333
0.3500	1.4107	1.4191	0.5890
0.4000	1.4821	1.4918	0.6525
0.4500	1.5570	1.5683	0.7242
0.5000	1.6354	1.6487	0.8050

4 Conclusion

The numerical method works well according to the shown examples, only first partial sum is needed to get good agreement with the exact result. The maximum relative error for example 1 and 2 are 0.64% and 0.805% respectively; this further confirms how good the numerical solution approximates exact solution. Since this gives good agreement, we intend carrying out further analysis on the method to explain some of its numerical behavior and convergence.

References

[1] Chika CE, Hooshyar MA. , "An electromagnetic inverse scattering problem for dielectrics that depend on two spatial variables via Eikonal approximation," Microw Opt Technol Lett., 2019;1–7. https://doi.org/10.1002/mop.31752

[2] S. Abbasbandy, "Application of He's homotopy perturbation method to functional integral equations," Chaos, Solitons and Fractals, 31 (2007) 1243-1247.

[3] Abdul-Majid Wazwaz , " *Linear and Nonlinear Integral Equations,*" Higher Education Press; Springer, Beijing (2011).

[4] J.H. He, "Homotopy perturbation Technique," Computer Methods in Applied Mechanics and Engineering, 178 (1999) 257-262.

[5] J. Biazar, H. Ghazvini , "Numerical solution for special non-linear Fredholm integral equation by HPM," Appl. Math. Comput. 195 (2008) 681-687.

[6] Edyta Hetmaniok, Damian Slota, Roman Witula , "Convergence and error estimation of homotopy perturbation method for Fredholm and Volterra integral equations," Appl. Math. Comput. 218 (2012) 10717-10725.

[7] Behzad Ghanbari, "On the Convergence of the Homotopy Analysis Method for Solving Fredholm Integral Equations," Walailak J Sci & Tech, 2013; 10(4):395–403.

[8] S. Abbasbandy, "Numerical solutions of the integral equations: Homotopy perturbation method and Adomain's decomposition method," Applied Mathematics and Computation, 173 (2006) 493-500.

[9] Charles Ekene Chika, Chinedu Junior Okere, "Iterative Solution and Convergence of Nonlinear Volterra Integral Equations of The Second Second Kind Using HPM," International Journal of Engineering Research and Technology (IJERT) Volume 09, Issue 09 (2020).

A theoretical investigation of the impact of a 2-dose vaccination strategy on Monkeypox transmission dynamics at population level

I.I. Ako*

Abstract

In order to qualitatively evaluate the influence of a two-dose monkeypox (MPV) vaccination strategy when decreased human-to-human infection is accounted for, a new deterministic model for MPV is created and implemented. The backward bifurcation phenomena is demonstrated to occur in the model as a result of the parameter that describes how quickly susceptible individuals receive their first dose of the MPV vaccination. Additionally, a distinct cutoff point for the rate at which vulnerable individuals receive the first dose of the MPV vaccination was discovered An example of the model demonstrated that, in the absence of the rate at which susceptible individuals receive the first dose of the MPV vaccine, the disease-free equilibrium was globally asymptotically stable. The endemic equilibrium point of the distinguished case was also shown to globally asymptotically stable.

Keywords and phrases: Monkeypox virus; Backward bifurcation; Vaccination; Equilibria

1 Introduction

With a clinically-reduced severity than smallpox, monkeypox virus illness (MPV) is zoonotic with accompanying symptoms reminiscent of those seen in previous smallpox cases [1]. MPV tops the chart in terms of the significance of orthopoxviruses on public health since the eradication of smallpox and the resultant annulment of its corresponding vaccine circa 1980 [1]. Central Africa and West Africa regions are the basic habitatas for MPV due to the proximity to the tropical rainforests in the tropics, and has been reported to be more common in cities in this environment [1]. Assorted rodent species cum animal primates are examples of animal hosts [1].

The premier case of human MPV on record was in DR Congo in 1970. Since then, several cases have been reported with the majority of such infections arising from rural communities in the rainforests domiciled in the Congo Basin especially in the DR Congo [1].

Eleven African nations, Nigeria inclusive, have documented human cases of MPV since 1970 [1]. There has been a significant outbreak in Nigeria beginning from 2017, which accounts for ≥ 500 suspected cases, ≥ 200 confirmed cases, and a CFR of approximately 3%. Infections are still being reported as of right now [1].

Due to its widespread distribution throughout the world, MPV is a disease of worldwide public health significance [1]. It is not limited to nations in western and central Africa. According to [1], MPV cases have been reported in nations outside Africa, namely: in the USA since 2003 (and also in 2021),in Israel (in 2018), in the UK (2018, 2019, 2021 and 2022) and in Singapore in 2019 [1]. Numerous cases of monkeypox were reported in May 2022 in a number of non-endemic nations. Research is presently being conducted to gain additional insight into the epidemiology, infection origins, and transmission patterns [1].

Although the most likely natural reservoir for monkeypox is rats, this has not yet been determined [1].

*E-mail: ignatius.ako@uniben.edu; Department of Mathematics, University of Benin, Benin City, Nigeria

The consumption of meat and other products not properly prepared from contaminated animals is a major risk factor [1]. Living in or close to forested regions can expose people to sick animals indirectly or at a low level [1].
Close contact with bodily secretions, injuries of an infected case, or just contaminated materials result in human-to-human infection [1]. Health professionals, family members, and other close contacts of active patients are more at risk of contracting the disease since droplet respiratory particles typically require prolonged face-to-face contact for transmission. Nevertheless, from six to nine consecutive person-to-person infections, the longest known chain of transmission in a community has increased recently [1]. This might be a result of smallpox vaccinations ending in all areas, which is causing immunity to decline [1]. In addition, congenital monkeypox can be transmitted through the placenta from mother to fetus or through intimate contact both during and after delivery [1]. Despite the fact that intimate physical contact is a well-established risk factor for transmission, it is currently unknown whether sexual contact is a specific means of transmission for monkeypox. To fully comprehend this risk, more research is required [1].
The typical course of monkeypox is self-limited, with symptoms lasting two to four weeks [1]. Severe cases are more common in youngsters and are associated with factors such as the degree of viral exposure, the patient's health, and the type of sequelae. Poorer results could result from underlying immunological deficits [1]. Although smallpox vaccination was protective in the past, people under the age of 40 to 50 (depending on the country) may now be more vulnerable to monkeypox due to the worldwide discontinuation of smallpox vaccine campaigns following the disease's elimination [1]. Secondary infections, bronchopneumonia, sepsis, encephalitis, and corneal infection leading to visual loss are among the complications associated with monkeypox [1]. It is unknown how much an asymptomatic infection can spread [1]. Monkeypox has historically had a case fatality ratio in the general population ranging from 0 to 11%, with a greater rate among young children. The case fatality ratio has been approximately 3-6% in the recent past [1].
Other rash illnesses like chickenpox, measles, bacterial skin infections, scabies, syphilis, and medication-associated allergies are among the clinical differential diagnosis that need to be taken into account [1]. A clinical characteristic that can be used to differentiate smallpox or chickenpox from monkeypox is lymphadenopathy during the prodromal stage of the illness [1]. Antigen and antibody detection techniques do not yield monkeypox-specific confirmation because orthopoxviruses are serologically cross-reactive [1]. Therefore, in situations when resources are scarce, serology and antigen detection techniques are not advised for diagnosis or case investigation. Furthermore, false positive results may result from recent or distant immunization with a vaccinia-based vaccine (e.g., anyone immunized before to smallpox eradication, or more recently vaccinated due to heightened risk, such as orthopoxvirus laboratory personnel) [1].
The literature has been enhanced by the development of mathematical models by multiple authors addressing various topics related to the dynamics of MPV illness [2, 3, 4, 5, 6]. As the above makes clear, many mathematical models have been created to analyze the monkeypox virus disease. However, to the best of the authors' awareness, none of these models have taken into account the potential influence of a two-dose vaccination strategy on the disease burden in the population in the presence of decreased infection for human to human infection transmission on the population dynamics for monkeypox virus disease burden transmission.
In Section 2 of this paper, a mathematical model is developed to examine how a 2-dose monkeypox vaccination method affects the disease burden in the community in the context of a lower population-level infection rate for human-to-human MPV illness. Important thresholds regulating the dynamics of the disease are found in Section 3, along with the local and global asymptotic stabilities of equilibria and the paper's conclusion is provided in Section 4.

2 Methodology/Model formulation

The model accounts for the total animal population responsible for the disease at time t into mutually exclusive classes of susceptible to infections $(S_a(t))$, infectious $(I_a(t))$ and recovered $(R_a(t))$ given by

$$N_a(t) = S_a(t) + I_a(t) + R_a(t).$$

At any given time t, let $N_h(t)$ denote the the total number of human beings in the environment which is decomposed into classes that are exclusive mutually, represented by: individuals susceptible to infection $(S_h(t))$, vaccinated with the first dose of monkeypox vaccine $(V_{h1}(t))$, vaccinated with the second (and final) dose of monkeypox vaccine $(V_{h2}(t))$, exposed to MPV $(E_h(t))$, infected with MPV $(I_a(t))$, and infectious humans recovered from MPV $(R_h(t))$, individuals so that

$$N_h(t) = S_h(t) + V_{h1}(t) + V_{h2}(t) + E_h(t) + I_h(t) + R_h(t).$$

The susceptible animal class, $S_a(t)$, is created by the influx of animals (assumed wholly susceptible) into the population at a rate Λ_a. The population of susceptible animals is reduced due to MPV infection at the rate λ_a. The class is further reduced by natural mortality at a rate μ_a. Thus

$$S_a' = \Lambda_a - \lambda_a S_a - \mu_a S_a. \tag{1}$$

The infected animal population, $I_a(t)$, is generated by the influx of individuals from the susceptible animals class that are infected with the MPV at the rate λ_a. The class of infectious animals declines in size as they recover from infection arising from MPV at the rate r_a and infection-induced mortality d_a. This particular class is further shrunken in size by natural mortality at a rate μ_a. Thus

$$I_a' = \lambda_a S_a - (\mu_a + r_a + d_a) I_a. \tag{2}$$

The recovered animal population, $R_a(t)$, is generated by the influx of infectious individuals who recover from MPV at the rate r_a. The population of recovered animals is reduced by natural mortality at a rate μ_a. Thus

$$R_a' = r_a I_a - \mu_a R_a. \tag{3}$$

The wholly susceptible human population, $S_h(t)$, is generated by the recruitment of individuals (assumed susceptible) into the population at a rate Λ_h. The population of susceptible individuals is reduced due to MPV infection at the rate λ_h. The population is further reduced by natural mortality at a rate μ_h. Thus

$$S_h' = \Lambda_h - \lambda_h S_h - (\mu_h + \eta_v) S_h. \tag{4}$$

The population of humans vaccinated with the first dose for mpox V_{h1} is generated by at the rate η_v. This class is depleted by vaccinated individuals who relatively at risk of breakthrough infection with MPV at the rate $(1-\epsilon)\lambda_h$. The class is also depleted by humans who receive the second mandatory dose thus entering the class V_{h2} at the rate η_v. Furthermore, this class is reduced by the natural death rate μ_h. Thus

$$V_{h1}' = \eta_v S_h - (1-\epsilon)\lambda_h V_{h1} - (\mu_h + n_0) V_{h1}. \tag{5}$$

The population of humans vaccinated with the second mandatory dose for mpox V_{h2} is generated by at the rate n_0. This class is depleted by vaccinated individuals who are relatively at reduced risk of breakthrough infection with MPV at the rate $\psi(1-\epsilon)\lambda_h$. The class is reduced by the natural death rate μ_h. Thus

$$V'_{h2} = n_0 V_{h1} - \psi(1-\epsilon)\lambda_h V_{h2} - \mu_h V_{h2}. \tag{6}$$

The exposed human population, $E_h(t)$, is populated by the movement of individuals from susceptible individuals infected with MPV infection at the rate λ_h. The population is further populated by vaccinated individuals who are relatively at risk of breakthrough infection with MPV at the rates of $(1-\epsilon)\lambda_h$ and $\psi(1-\epsilon)\lambda_h$, from classes V_{h1} and V_{h2} respectively. The population is further reduced by individuals who become infectious at the rate π. The population is further reduced by the natural death rate μ_h. Thus

$$E'_h = \lambda_h S_h + (1-\epsilon)\lambda_h V_{h1} + \psi(1-\epsilon)\lambda_h V_{h2} - (\mu_h + \pi)E_h. \tag{7}$$

The infected human population, $I_h(t)$, is populated by the movement of individuals from the exposed class at the rate π. The population is depleted by individuals who recover from MPV infection at the rate r_h. The population is further reduced by individuals who suffer disease-induced mortality at the rate d_h and natural death rate μ_h. Thus

$$I'_h = \pi E_h - (\mu_h + r_h + d_h)I_h. \tag{8}$$

The recovered human population, $R_h(t)$, is populated by the movement of the population of infected individuals who recovered from MPV infection at the rate r_h. The recovered human population is reduced by individuals who succumb to natural death at the rate μ_h. Thus

$$R'_h = r_h I_h - \mu_h R_h. \tag{9}$$

On the basis of the foregoing, the MPV model is the following deterministic system of nine non-linear ordinary differential equations (the schematics of the model is shown Figure 1, and the state variables and parameters of the model are tabulated in Table 1 and Table 2 respectively):

$$\begin{aligned}
S'_a &= \Lambda_a - \lambda_a S_a - \mu_a S_a,\\
I'_a &= \lambda_a S_a - (\mu_a + r_a + d_a)I_a,\\
R'_a &= r_a I_a - \mu_a R_a,\\
S'_h &= \Lambda_h - \lambda_h S_h - (\mu_h + \eta_v)S_h,\\
V'_{h1} &= \eta_v S_h - (1-\epsilon)\lambda_h V_{h1} - (\mu_h + n_0)V_{h1},\\
V'_{h2} &= n_0 V_{h1} - \psi(1-\epsilon)\lambda_h V_{h2} - \mu_h V_{h2},\\
E'_h &= \lambda_h S_h + (1-\epsilon)\lambda_h V_{h1} + \psi(1-\epsilon)\lambda_h V_{h2} - (\mu_h + \pi)E_h,\\
I'_h &= \pi E_h - (\mu_h + r_h + d_h)I_h,\\
R'_h &= r_h I_h - \mu_h R_h,
\end{aligned} \tag{10}$$

where the force of infection associated with MPV animal to animal transmission is given below:

$$\lambda_a = \frac{\beta_{a0} I_a}{N_a}. \tag{11}$$

The corresponding infection force associated with MPV animal to human and human to human transmission, respectively, is given below:

$$\lambda_h = \frac{\beta_{a1} I_a}{N_a} + \frac{(1-\alpha)(1-\rho)\theta_0 \beta_h I_h}{N_h} \tag{12}$$

where

$$\frac{\beta_{a1}}{N_a}$$

is the animal to human contribution to the force of infection associated with MPV while

$$\frac{(1-\alpha)(1-\rho)\theta_0 \beta_h}{N_h}$$

is the human to human contribution to the force of infection associated with MPV.
Model flow diagram is seen in Figure 1:

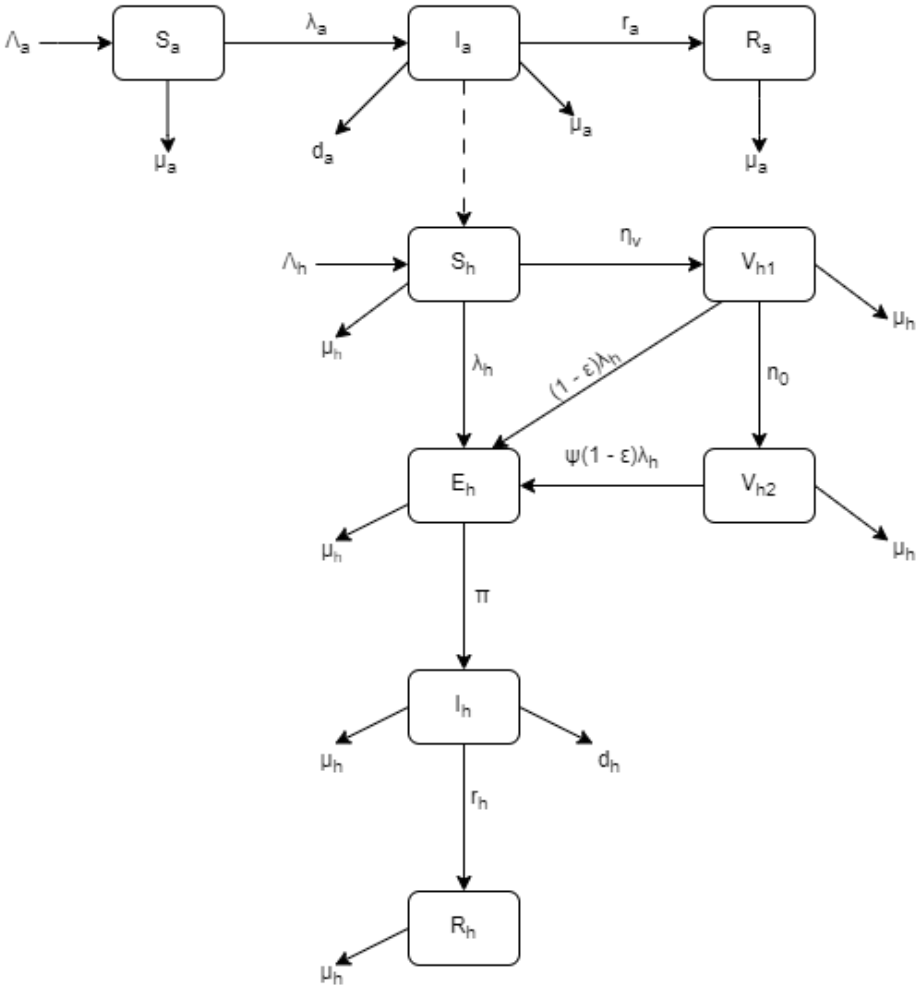


Figure 1: Schematic diagram for the MPV transmission dynamics model (10).

2.1 Description of State variables and Parameters

2.1.1 Description of State variables

The following Table 1 gives a summary of the state variables used herein:

Table 1: Description of state variables of the model (10)

Variables	Description
S_a	Susceptible animal population
I_a	Infected animal population
R_a	Recovered animal population
S_h	Susceptible human population
V_{h1}	Human population vaccinated (with the initial dose) against MPV
V_{h2}	Human population vaccinated (with the second and final dose) against MPV
E_h	Humans beings exposed to MPV
I_h	Humans beings infected with MPV
R_h	Humans beings recovered from MPV

2.1.2 Description of Parameters

The following Table 2 gives a summary of the parameters used herein:

Table 2: Description of parameters of the model (10)

Parameter	Description
Λ_a	Animal recruitment rate
μ_a	Natural death rate of animals
d_a	Infection-induced mortality rate for animals
r_a	Recovery rate for animals
β_{a0}	Animal to animal transmission rate
β_{a1}	Animal to human transmission rate
Λ_h	Human recruitment rate
μ_h	Natural death rate of humans
d_h	Infection-induced mortality rate for humans
r_h	Recovery rate for humans
β_h	Human to human transmission rate
θ_0	Modification parameter which accounts for reduced rate of infection of human to human transmission, with $0 < \theta_0 \leq 1$
η_v	Rate at which susceptible humans are inoculated with the first dose of the MPV vaccine
n_0	Rate at which humans vaccinated with the first dose are inoculated with the second and final dose of the MPV vaccine
π	Rate at which the exposed class progresses to the infectious class
ψ	Modification parameter which accounts for reduced rate of infection for humans vaccinated with the mandatory second dose of the MPV vaccine, with $0 < \psi \leq 1$
α	Proportion of humans maintaining the use of hand sanitizers, with $0 \leq \alpha < 1$
ρ	Proportion of humans using personal protection equipment, with $0 \leq \rho < 1$
ϵ	Relative risk of a human vaccinated with MPV vaccine experiencing a breakthrough infection, with $0 < \epsilon \leq 1$

2.2 Positivity and Boundedness of Solutions

Theorem 2.1. *Permit the initial data for the monkeypox virus transmission model (10) be given as* $S_a(0) > 0, I_a(0) > 0, R_a(0) > 0, S_h(0) > 0, V_{h1}(0) > 0, V_{h2}(0) > 0, E_h(0) > 0, I_h(0) > 0$ *and* $R_h(0) > 0$. *Therefore the solutions* $\big(S_a(t), I_a(t), R_a(t), S_h(t), V_{h1}(t), V_{h2}(t), E_h(t), I_h(t)$ *and* $R_h(t)\big)$ *of the model with initial conditions that are positive, will remain positive for every time* $t > 0$.

Proof: Permit $t_1 = \sup\{t > 0 : S_a(0) > 0, I_a(0) > 0,\ R_a(0) > 0,\ S_h(0) > 0,\ V_{h1}(0) > 0,\ V_{h2}(0) > 0,\ E_h(0) > 0,\ I_h(0) > 0,\ R_h(0) > 0\}$.
Looking at the premier equation of model (10), represented as

$$\frac{dS_a(t)}{dt} = \Lambda_a - (\lambda_a + \mu_a)S_a(t), \tag{13}$$

which can be re-expressed as

$$\frac{d}{dt}\Big[S_a(t)\exp\Big\{\mu_a t + \int_0^t \lambda_a(\tau)d\tau\Big\}\Big] \tag{14}$$

$$= \Lambda_a \exp\Big\{\mu_a t + \int_0^t \lambda_a(\tau)d\tau\Big\}. \tag{15}$$

$$S_a(t_1)\exp\Big\{\mu_a t_1+\int_0^{t_1}\lambda_a(\tau)d\tau\Big\}-S_a(0) \\ =\int_0^{t_1}\Lambda_a\Big[\exp\Big\{\mu_a y+\int_0^{y}\lambda_a(\tau)d\tau\Big\}\Big]dy, \tag{16}$$

So that,

$$S_a(t_1)=S_a(0)\exp\Big[-\mu_a t_1-\int_0^{t_1}\lambda_a(\tau)d\tau\Big] \\ +\Big[\exp\Big\{-\mu_a t_1-\int_0^{t_1}\lambda_a(\tau)d\tau\Big\}\Big] \\ \times\int_0^{t_1}\Lambda_a\Big[\exp\Big\{\mu_a y+\int_0^{y}\lambda_a(\tau)d\tau\Big\}\Big]dy>0. \tag{17}$$

Therefore $S_a(t)>0,\ \forall\, t>0$.
Correspondingly, other state variables in (10) can be shown to be positive, i.e., $I_a(t)>0,\ R_a(t)>0,\ S_h(t)>0,\ V_{h1}(t)>0,\ V_{h2}(t)>0,\ E_h(t)>0,\ I_h(t)>0,\ R_h(t)>0,\ \forall\, t>0$.
Hence, we have shown that all state variables in model (10) are positive always.

We proceed to establish the boundedness of solutions to the model (10).

Theorem 2.2. *Allow* $\big(S_a(t),I_a(t),R_h(t),S_h(t),V_{h1}(t),V_{h2}(t),E_h(t),I_h(t),R_h(t)\big)$ *to be flows of the system* (10) *with initial conditions cum the biological feasible region given by the set* $\mathcal{D}_o=\mathcal{D}_a\times\mathcal{D}_h\times\subset\mathbb{R}^3_+\times\mathbb{R}^6_+$, *where:*

$$\mathcal{D}_a=\{(S_a,I_a,R_a)\in\mathbb{R}^3_+:N_a\le\frac{\Lambda_a}{\mu_a}\}$$
$$\mathcal{D}_h=\{(S_h,V_{h1},V_{h2},E_h,I_h,R_h)\in\mathbb{R}^6_+:N_h\le\frac{\Lambda_h}{\mu_h}\}$$

is invariant positively, attracting every positive solutions of the model (10).

Proof: Summing up the first three equations on the right flank of the vector field representing the animal populace in (10), leads to

$$\frac{dN_h}{dt}=\Lambda_a-\mu_a N_a-d_a I_a. \tag{18}$$

From (18), it ensues that $\frac{dN_a}{dt}\le\Lambda_a-\mu_a N_a$. Hence, $\frac{dN_a}{dt}\le 0$ if $N_a(t)\ge\frac{\Lambda_a}{\mu_a}$. Employing [7] comparison theorem, we reveal that $N_a(t)\le N_a(0)e^{-\mu_a t}+\frac{\Lambda_a}{\mu_a}(1-e^{-\mu_a t})$. Specifically, if $N_a(0)\le\frac{\Lambda_a}{\mu_a}$, thus $N_a(t)\le\frac{\Lambda_a}{\mu_a}$ for every $t>0$. Hence, the set $\mathcal{D}_a$ is invariant positively. Moreover, if $N_a(0)>\frac{\Lambda_a}{\mu_a}$, then either the orbits penetrate the set $\mathcal{D}_a$ in fixed time or $N_a(t)$ asymptotically tends in the direction of $\frac{\Lambda_a}{\mu_a}$ as $t\to\infty$. Thus, the set $\mathcal{D}_a$ attracts every trajectory in $\mathbb{R}^3_+$.

Similarly, adding up the right flank of last five equations of the vector field representing the human population in (10), yields

$$\frac{dN_h}{dt}=\Lambda_h-\mu_h N_h-d_h I_h. \tag{19}$$

From (19), it ensues that $\frac{dN_h}{dt}\le\Lambda_h-\mu_h N_h$. Hence, $\frac{dN_h}{dt}\le 0$ if $N_h(t)\ge\frac{\Lambda_h}{\mu_h}$. Employing [7] comparison theorem, we reveal that $N_h(t)\le N_h(0)e^{-\mu_h t}+\frac{\Lambda_h}{\mu_h}(1-e^{-\mu_h t})$. Specifically, if $N_h(0)\le\frac{\Lambda_h}{\mu_h}$,

thus $N_h(t) \leq \frac{\Lambda_h}{\mu_h}$ for all $t > 0$. Therefore, the set $\mathcal{D}_h$ is invariant positively. Furthermore, suppose that $N_h(0) > \frac{\Lambda_h}{\mu_h}$, then either the solutions penetrate the set $\mathcal{D}_h$ in fixed time or $N_h(t)$ asymptotically tends in the direction of $\frac{\Lambda_h}{\mu_h}$ as $t \to \infty$. Thus, the set $\mathcal{D}_h$ attracts every flow in $\mathbb{R}^6_+$.
Thus, it is enough to investigate the dynamics of the flows generated by the system (10) in $\mathcal{D}_o$. We come to the conclusion, thus, that the model (10) is altogether mathematically and epidemiologically well-posed.

3 Analysis of the model

3.1 Local Asymptotic Stability (LAS) of the Disease-free Equilibrium (DFE)

The disease-free equilibrium (DFE) of the system (10) is represented by

$$\begin{aligned}\mathcal{E}_0 &= (S_a^*, I_a^*, R_a^*, S_h^*, V_{h1}^*, V_{h2}^*, E_h^*, I_h^*, R_h^*) \\ &= (\frac{\Lambda_a}{\mu_a}, 0, 0, \frac{\Lambda_h}{\mu_h + \eta_v}, \frac{\eta_v \Lambda_h}{(\mu_h + \eta_v)(\mu_h + n_0)}, \frac{n_0 \eta_v \Lambda_h}{\mu_h(\mu_h + \eta_v)(\mu_h + n_0)}, 0, 0, 0)\end{aligned} \tag{20}$$

The linear stability of $\mathcal{E}_0$ is shown by employing the next-generation operator method on the system (10) [8]. Using the original notations given in [8], it ensues that matrices F and V, respectively, for the fresh infection terms and the other transition terms, are given by

$$F = \begin{bmatrix} \beta_{a0} & 0 & 0 \\ \frac{\Lambda_h \mu_a \beta_{a1}}{\Lambda_a \mu_h}\left(\frac{\mu_h(\mu_h+n_0)+(1-\epsilon)\eta_v(\mu_h+\psi n_0)}{(\mu_h+\eta_v)(\mu_h+n_0)}\right) & 0 & (1-\alpha)(1-\rho)\theta_0\beta_h\left(\frac{\mu_h(\mu_h+n_0)+(1-\epsilon)\eta_v(\mu_h+\psi n_0)}{(\mu_h+\eta_v)(\mu_h+n_0)}\right) \\ 0 & 0 & 0 \end{bmatrix}$$

and

$$G = \begin{bmatrix} (\mu_a + r_a + d_a) & 0 & 0 \\ 0 & (\mu_h + \pi) & 0 \\ 0 & -\pi & (\mu_h + r_h + d_h) \end{bmatrix}.$$

It ensues that the *effective reproduction number*, denoted by $\mathcal{R}_m = \rho\left(FG^{-1}\right)$, where $\rho\left(FG^{-1}\right)$ is the spectral radius belonging to the matrix FG^{-1}, is denoted by

$$\mathcal{R}_m = max\{\mathcal{R}_{ma}, \mathcal{R}_{mh}\} \tag{21}$$

where

$$\mathcal{R}_{ma} = \frac{\beta_{a0}}{\mu_a + r_a + d_a} \tag{22}$$

where $\mathcal{R}_{ma}$ represents the MPV transmission dynamics amongst the animal population. While

$$\begin{aligned}\mathcal{R}_{mh} &= \frac{(1-\alpha)(1-\rho)\pi\theta_0\beta_h}{(\mu_h+\pi)(\mu_h+r_h+d_h)}\left(\frac{\mu_h(\mu_h+n_0)+(1-\epsilon)\eta_v(\mu_h+\psi n_0)}{(\mu_h+\eta_v)(\mu_h+n_0)}\right) \\ &= \mathcal{R}_{0h}\left(\frac{\mu_h(\mu_h+n_0)+(1-\epsilon)\eta_v(\mu_h+\psi n_0)}{(\mu_h+\eta_v)(\mu_h+n_0)}\right) \\ &= \mathcal{R}_{0h}\left((1-\epsilon).\frac{\eta_v}{\mu_h+\eta_v}.\frac{\mu_h+\psi n_0}{\mu_h+n_0} + \frac{\mu_h}{\mu_h+\eta_v}\right)\end{aligned} \tag{23}$$

represents the control reproduction number of the MPV transmission dynamics amongst the human population [9]. Now, the quantity $\mathcal{R}_{mh} \geq 0$, since $\frac{\eta_v}{\mu_h+\eta_v} \leq 1$, $\frac{\mu_h+\psi n_0}{\mu_h+n_0} \leq 1$ and $\frac{\mu_h}{\mu_h+\eta_v} \leq 1$ and $0 < \psi, \epsilon \leq 1$ (hence, $1-\epsilon \geq 0$). The quantity $\mathcal{R}_{0h} = \frac{(1-\alpha)(1-\rho)\pi\theta_0\beta_h}{(\mu_h+\pi)(\mu_h+r_h+d_h)}$ represents the basic reproduction

number of the MPV transmission amongst humans in the absence of intervention (which is vaccination, in this case).
Therefore, the consequent result arises from the deductions of Theorem 2 in [8].

Lemma 3.1. *The DFE $\mathcal{E}_0$ of (10) is locally asymptotically stable given that $\mathcal{R}_m < 1$ and unstable given condition that $\mathcal{R}_m > 1$.*

The critical quantity, $\mathcal{R}_m$, is the basic reproduction ratio of the malady [8] . It represents the measure of the average number of secondary monkeypox virus infections generated by a typical infectious human in an entirely susceptible populace or at the DFE [8]. The epidemiological consequence of Lemma 3.1 implies that whenever $\mathcal{R}_{m<1}$, monkeypox virus infections can be extricated from the population if the initial sizes of the components of the system are in the basin of attraction of the DFE, $\mathcal{E}_0$. Hence, a small inflow of monkeypox virus-infected persons into the populace will not provoke large monkeypox virus outbreaks, leading to the gradual decline of the disease time goes on.

3.2 Endemic Equilibrium Point (EEP)

We define the endemic equilibrium point, $\mathcal{E}_M^*$, of the system (10) by

$$\mathcal{E}_m^* = \left(S_a^{**},\ I_a^{**},\ R_a^{**}, S_h^{**},\ V_{h1}^{**},\ V_{h2}^{**},\ E_h^{**},\ I_h^{**},\ R_h^{**}\right) \tag{24}$$

where

$$\begin{aligned}
S_a^{**} &= \frac{\Lambda_a(\beta_{a0} - d_a\mathcal{R}_{ma})}{\mu_a(\beta_{a0} - d_a)\mathcal{R}_{ma}},\\
I_a^{**} &= \frac{\Lambda_a}{\beta_{a0} - d_a}(\mathcal{R}_{ma} - 1),\\
R_a^{**} &= \frac{\Lambda_a r_a}{\mu_a(\beta_{a0} - d_a)}(\mathcal{R}_{ma} - 1),\\
S_h^{**} &= \frac{\Lambda_h}{\lambda_h^{**} + \mu_h + \eta_v},\\
V_{h1}^{**} &= \frac{\Lambda_h\eta_v}{(\lambda_h^{**} + \mu_h + \eta_v)((1-\epsilon)\lambda_h^{**} + \mu_h + n_0)},\\
V_{h2}^{**} &= \frac{\Lambda_h n_0\eta_v}{(\lambda_h^{**} + \mu_h + \eta_v)((1-\epsilon)\lambda_h^{**} + \mu_h + n_0)(\psi(1-\epsilon)\lambda_h^{**} + \mu_h)},\\
E_h^{**} &= \frac{\lambda_h^{**}S_h^{**} + (1-\epsilon)\lambda_h^{**}V_{h1}^{**} + \psi(1-\epsilon)\lambda_h^{**}V_{h2}^{**}}{\mu_h + \pi},\\
I_h^{**} &= \frac{\pi E_h^{**}}{\mu_h + r_h + d_h},\\
R_h^{**} &= \frac{r_h}{\mu_h}I_h^{**}.
\end{aligned} \tag{25}$$

The forces of infection are:

$$\lambda_a^{**} = \frac{\beta_{a0}I_a^{**}}{N_a^{**}}, \tag{26}$$

and

$$\lambda_h^{**} = \frac{\beta_{a1}I_a^{**}}{N_a^{**}} + \frac{\theta_0(1-\alpha)(1-\rho)\beta_h I_h^{**}}{N_h^{**}} \tag{27}$$

Substituting both (26) and (27) in (25), after multiple calculations, we have that the EEP connected with the system (10) satisfies the polynomial (in terms of λ_h^{**})

$$\mathcal{M}_1(\lambda_h^{**})^2 + (\mathcal{M}_2 + \mathcal{M}_3)(\lambda_h^{**}) + \mathcal{M}_4 = 0. \tag{28}$$

where,

$$\begin{aligned}
\mathcal{M}_1 &= \Lambda_h\mu_h(1-\epsilon)^2\psi(\mu_h+\pi)(\mu_h+r_h+d_h)(1-\mathcal{R}_{0h})\\
&\quad+\Lambda_h(1-\epsilon)^2\psi\frac{\beta_{a1}\mu_a}{\mathcal{R}_{ma}}(1-\mathcal{R}_{ma}),\\
\mathcal{M}_2 &= \Lambda_h\Big(\mu_h(\mu_h+r_h+d_h+\pi)+r_h)+\mu_h(\mu_h+\pi)(\mu_h+r_h+d_h)(1-\epsilon)\psi\eta_v\epsilon\Big),\\
\mathcal{M}_3 &= \Lambda_h\mu_h(1-\epsilon)\big(\mu_h+\psi(\mu_h+n_0)+(1-\epsilon)\psi\eta_v\big)(\mu_h+\pi)(\mu_h+r_h+d_h)(1-\mathcal{R}_{0h})\\
&\quad+\Lambda_h\Big(\mu_h(\mu_h+\pi)(\mu_h+r_h+d_h)\psi(1-\epsilon)^2\\
&\qquad+(1-\epsilon)(\mu_h+(\mu_h+n_0)\psi)+\psi(1-\epsilon)^2\eta_v\Big)\frac{\beta_{a1}\mu_a}{\mathcal{R}_{ma}}(1-\mathcal{R}_{ma}),\\
\mathcal{M}_4 &= \Lambda_h\mu_h(\mu_h+\eta_v)(\mu_h+n_0)(\mu_h+\pi)(\mu_h+r_h+d_h)(1-\mathcal{R}_{mh})\\
&\quad+\Lambda_h\big(\mu_h(\mu_h+n_0)+(1-\epsilon)\eta_v(\mu_h+\psi n_0)\big)\frac{\beta_{a1}\mu_a}{\mathcal{R}_{ma}}(1-\mathcal{R}_{ma}).
\end{aligned} \tag{29}$$

We summarize the results obtained above in the following theorem expressed below.

Theorem 3.2. *The model system (10) has:*

1. *two endemic equilibria given that $\mathcal{M}_1<0,\ \mathcal{M}_2>\mathcal{M}_3,\ \mathcal{M}_4<0$ or $\mathcal{M}_1>0,\ \mathcal{M}_2<\mathcal{M}_3,\ \mathcal{M}_4>0$ and $\mathcal{R}_m>1$,*

2. *one unique endemic equilibrium given that $\mathcal{M}_1>0,\ \mathcal{M}_2<\mathcal{M}_3,\ \mathcal{M}_4<0$ or $\mathcal{M}_1<0,\ \mathcal{M}_2>\mathcal{M}_3,\ \mathcal{M}_4>0$,*

3. *nil endemic steady state otherwise, whenever $\mathcal{R}_m<1$.*

It is crucial to state right here, that the first item (1) of Theorem 3.1 is reveals the existence of the backward bifurcation in (10). The backward bifurcation phenomenon, defined as the simultaneous existence of a DFE and EEP that both exhibit stability whenever $\mathcal{R}_m<1$. The implication of this is that the recognized and accepted requirement for the control of MPV disease ($\mathcal{R}_m<1$) is no longer sufficient but necessary criterion. In this situation, successful strategies for MPV control will now depend on the initial conditions of various components of the system under scrutiny [10]. It is seen that the model (10)'s EEP subject to $\mathcal{R}_m>1$ (and does not exist given that $\mathcal{R}_m<1$), and thus, no likelihood of backward bifurcation given that $\mathcal{R}_m<1$).

3.2.1 Backward Bifurcation Analysis

Theorem 3.3. *The model (10) experiences backward bifurcation at $\mathcal{R}_m=1$ whenever $\eta_v>\eta_v^c$, with η_v^c defined as*

$$\eta_v^c=\frac{(\mu_h+n_0)}{\beta_h\theta_h\Lambda_h}\frac{\Omega_2}{\Omega_1}>0, \tag{30}$$

Proof: We employ the ensuing alteration of variables. Let $S_a=x_1$, $I_a=x_2$, $R_a=x_3$, $S_h=x_4$, $V_{h1}=x_5$, $V_{h2}=x_6$, $E_h=x_7$, $I_h=x_8$ and $R_h=x_9$, so that $N_a=x_1+x_2+x_3$ and $N_h=$

$x_4 + x_5 + x_6 + x_7 + x_8 + x_9$ and; therefore, model (10) is re-expressed as

$$\begin{aligned}
\dot{x}_1 &\equiv f_1 = \Lambda_a - \Big(\frac{\beta_{a0} x_1 x_2}{x_1 + x_2 + x_3}\Big) - \mu_a x_1,\\
\dot{x}_2 &\equiv f_2 = \Big(\frac{\beta_{a0} x_1 x_2}{x_1 + x_2 + x_3}\Big) - (\mu_a + r_a + d_a) x_2,\\
\dot{x}_3 &\equiv f_3 = r_a x_2 - \mu_a x_3,\\
\dot{x}_4 &\equiv f_4 = \Lambda_h - \Big(\frac{\beta_{a1} x_2}{x_1 + x_2 + x_3} + \frac{\theta_h \beta_h x_8}{x_4 + x_5 + x_6 + x_7 + x_8 + x_9}\Big) x_4 - (\mu_h + \eta_v) x_4,\\
\dot{x}_5 &\equiv f_5 = \eta_v x_4 - (1-\epsilon)\Big(\frac{\beta_{a1} x_2}{x_1 + x_2 + x_3} + \frac{\theta_h \beta_h x_8}{x_4 + x_5 + x_6 + x_7 + x_8 + x_9}\Big) x_5 - (\mu_h + n_0) x_5,\\
\dot{x}_6 &\equiv f_6 = n_0 x_5 - (1-\epsilon)\psi\Big(\frac{\beta_{a1} x_2}{x_1 + x_2 + x_3} + \frac{\theta_h \beta_h x_8}{x_4 + x_5 + x_6 + x_7 + x_8 + x_9}\Big) x_6 - \mu_h x_6,\\
\dot{x}_7 &\equiv f_7 = (x_4 + (1-\epsilon)(x_5 + \psi x_6))\Big(\frac{\beta_{a1} x_2}{x_1 + x_2 + x_3} + \frac{\theta_h \beta_h x_8}{x_4 + x_5 + x_6 + x_7 + x_8 + x_9}\Big) - (\mu_h + \pi) x_7,\\
\dot{x}_8 &\equiv f_8 = \pi - (\mu_h + r_h + d_h) x_8,\\
\dot{x}_9 &\equiv f_9 = r_h x_8 - \mu_h x_9.
\end{aligned} \tag{31}$$

The Jacobian for the system (31) at the DFE is given by

$$J_{\beta_h^*} = \begin{bmatrix}
-\mu_a & -\beta_{a0} & 0 & 0 & 0 & 0 & 0 & 0 & 0\\
0 & -(\mu_a + r_a + d_a) + \beta_{a0} & 0 & 0 & 0 & 0 & 0 & 0 & 0\\
0 & r_a & -\mu_a & 0 & 0 & 0 & 0 & 0 & 0\\
0 & -\frac{\beta_{a1}\Lambda_h \mu_a}{\Lambda_a(\mu_h+\eta_v)} & 0 & -(\mu_h+\eta_v) & 0 & 0 & 0 & -\frac{\beta_h \theta_h \mu_h}{\mu_h+\eta_v} & 0\\
0 & -\frac{(1-\epsilon)\beta_{a1}\eta_v \Lambda_h \mu_a}{\Lambda_a(\mu_h+\eta_v)(\mu_h+n_0)} & 0 & \eta_v & -(\mu_h+n_0) & 0 & 0 & -\frac{(1-\epsilon)\beta_h \theta_h \eta_v \mu_h}{(\mu+\eta_v)(\mu_h+n_0)} & 0\\
0 & -\frac{(1-\epsilon)\psi\beta_{a1} n_0 \eta_v \mu_a}{\Lambda_a \mu_h(\mu+\eta_v)(\mu_h+n_0)} & 0 & 0 & n_0 & -\mu_h & 0 & -\frac{(1-\epsilon)\psi\beta_{a1} n_0 \eta_v}{(\mu+\eta_v)(\mu_h+n_0)} & 0\\
0 & B_0 & 0 & 0 & 0 & 0 & -(\mu_h+\pi) & B_1 & 0\\
-\mu_a & 0 & 0 & 0 & 0 & 0 & 0 & 0 & 0
\end{bmatrix} \tag{32}$$

where $B_0 = \frac{\beta_{a1}\Lambda_h \mu_a \big(\mu_h(\mu_h+n_0)+(1-\epsilon)\eta_v(\mu_h+\psi n_0)\big)}{\Lambda_a \mu_a(\mu+\eta_v)(\mu_h+n_0)}$ and $B_1 = \frac{\beta_h \beta_h \big(\mu_h(\mu_h+n_0)+(1-\epsilon)\eta_v(\mu_h+\psi n_0)\big)}{(\mu+\eta_v)(\mu_h+n_0)}$.

Observing the particular situation when $\mathcal{R}_{mh} = 1$. Calculating the value for $\beta_h = \beta_h^*$ from $\mathcal{R}_{mh} = 1$ gives

$$\beta_h = \beta_h^* = \frac{(\mu_h + \pi)(\mu_h + \eta_v)(\mu_h + n_0)(\mu_h + r_h + d_h)}{\mu_h\big(\beta_h(\mu_h + n_0) + (1-\epsilon)\eta_v(\mu_h + \psi n_0)\big)} \tag{33}$$

Matrix $J_{\beta_h^*}$ possesses a right eigenvector given by $\mathbf{w} = (\omega_1, \omega_2, ..., \omega_9)^T$, such that

$$\begin{aligned}
\omega_1 &= \omega_2 = \omega_3 = 0,\\
\omega_4 &= -\frac{\beta_h \theta_h \mu_h^2}{r_h(\mu_h+\eta_v)^2}\omega_9,\\
\omega_5 &= -\frac{\beta_h \theta_h \eta_v \mu_h^2\big((1-\epsilon)(\mu_h+\eta_v) + (\mu_h+n_0)\big)}{r_h(\mu_h+\eta_v)^2(\mu_h+n_0)^2}\omega_9,\\
\omega_6 &= -\frac{\beta_h \theta_h n_0 \eta_v\big((1-\epsilon)(\mu_h+\eta_v)(\psi\Lambda_h(\mu_h+n_0)+\mu_h) + \mu_h(\mu_h+n_0)\big)}{r_h(\mu_h+\eta_v)^2(\mu_h+n_0)^2}\omega_9,\\
\omega_7 &= \frac{\mu_h(\mu_h+r_h+d_h)}{\pi r_h}\omega_9,\\
\omega_8 &= \frac{\mu_h}{r_h}\omega_9,\\
\omega_9 &= \omega_9 > 0.
\end{aligned} \tag{34}$$

In addition, $J_{\beta_h^*}$ possesses a left eigenvector $\mathbf{v} = (\nu_1, \nu_2, ..., \nu_9)$ satisfying **v.w = 1**, with

$$\begin{aligned}
&\nu_1 = 0,\\
&\nu_2 = -\frac{\beta_{a1}\Lambda_h\mu_a\big(\mu_h(\mu_h+n_0)+(1-\epsilon)\eta_v(\psi n_0+\mu_h)\big)}{\Lambda_a\mu_h(\beta_{a0}-(\mu_a+r_a+d_h))(\mu_h+n_0)(\mu_h+\eta_v)}\nu_7,\\
&\nu_3 = \nu_4 = \nu_5 = \nu_6 = 0,\\
&\nu_7 = \nu_7 > 0, \nu_8 > 0,\\
&\nu_9 = 0
\end{aligned} \tag{35}$$

The application of the *Center Manifold Theory* given by [11], deriving the connected non-zero partial derivatives of the right sides of the changed system (31), *(without infection with $\beta_h = \beta_h^*$)* we have that the associated bifurcation coefficients, a and b, are represented by

$$a = \sum_{k,i,j=1}^{n} v_k w_i w_j \frac{\partial^2 f_k}{\partial x_i \partial x_j}(0,0), \qquad \text{and} \qquad b = \sum_{k,i=1}^{n} v_k w_i \frac{\partial^2 f_k}{\partial x_i \partial \beta^*}(0,0), \tag{36}$$

The bifurcation coefficient a for the model system (10) (or (31)) (after several algebraic calculations), is:

$$\begin{aligned}
a &= v_7 \sum_{i,j=1}^{9} w_i w_j \frac{\partial^2 f_7}{\partial x_i \partial x_j}\\
&= \frac{2\beta_h\theta_h\mu_h^2}{r_h^2(\mu_h+\eta_v)(\mu_h+n_0)^2}\Big(-\frac{\Omega_2}{\Lambda_h}+\frac{\theta_h\beta_h\eta_v\Omega_1}{\mu_h+n_0}\Big)\nu_7\omega_9^2.
\end{aligned} \tag{37}$$

where

$$\begin{aligned}
\Omega_1 &= \big((1-\epsilon)(\mu_h+\eta_v)+(\mu_h+n_0)+n_0((1-\epsilon)(\mu_h+\eta_v)(\psi\Lambda_h(\mu_h+n_0)+\mu_h)+\mu_h(\mu_h+n_0))\big),\\
\Omega_2 &= \big((\mu_h(\mu_h+n_0)+(1-\epsilon)\eta_v(\mu_h+\psi n_0))+((\mu_h+r_h)(\mu_h+\eta_v)^2(\mu_h+n_0)\\
&\quad+\beta_h\theta_h\Lambda_h(\mu_h(\mu_h+n_0)+\eta_v(\mu_h+n_0))\\
&\quad+\beta_h\theta_h n_0\eta_v\Lambda_h(1-\epsilon)\psi(\mu_h+\eta_v)((1-\epsilon)(\mu_h+\eta_v)(\psi\Lambda_h(\mu_h+n_0)+\mu_h)+\mu_h(\mu_h+n_0))\big)
\end{aligned} \tag{38}$$

Thus, $a > 0$ if and only if

$$\eta_v^c = \eta_v > \frac{(\mu_h+n_0)}{\beta_h\theta_h\Lambda_h}\frac{\Omega_2}{\Omega_1}. \tag{39}$$

The bifurcation coefficient b for the model system (10) (or (31)) is:

$$\begin{aligned}
b &= v_7 \sum_{i=1}^{9} w_i \frac{\partial^2 f_7}{\partial x_i \partial \beta_h^*},\\
&= \frac{\theta_h\mu_h\big(\mu_h(\mu_h+n_0)+(1-\epsilon)\eta_v(\mu_h+\psi n_0)\big)}{r_h(\mu+\eta_v)(\mu_h+n_0)}\nu_7\omega_9.
\end{aligned} \tag{40}$$

Obviously $b > 0$ for every biologically reasonable parameter values. Therefore, backward bifurcation appears if and only if the rate at which susceptible humans are inoculated with the first dose of the MPV vaccine (η_v), is large enough such that $a > 0$. Therefore, the implication is that if the rate at which susceptible humans are inoculated with the first dose of the MPV vaccine is less than the quantity, (η_v^c),

the effective reproduction ratio then becomes a necessary and sufficient tool for facilitating control measures that will culminate in the eradication of MPV disease. □

As a derivative of the results from Theorem 3.2, we declare this result.

Theorem 3.4. *(Non-existence of backward bifurcation) The model (10) (or (31)) does not manifest backward bifurcation in the direction $\mathcal{R}_m = 1$, on the condition that $\eta_v = 0$.*

Proof: Looking at the special case of (10) where the rate at which susceptible humans are inoculated with the first dose of the MPV vaccine is negligible (i.e., $\eta_v = 0$). Therefore, the backward bifurcation coefficient, a, in (37) shrinks to:

$$a = -\frac{2\beta_h\theta_h\mu_h^2\Omega_2}{\Lambda_h r_h^2(\mu_h+\eta_v)(\mu_h+n_0)^2}\nu_7\omega_9^2 < 0. \tag{41}$$

Consequently, this study proved that the presence of the rate at which susceptible humans are inoculated with the first dose of the MPV vaccine causes backward bifurcation in the epidemic dynamics of MPV disease. □

3.2.2 Global Asymptotic Stability (GAS) of DFE

Looking at the situation of model (10) with the condition that $\eta_v = 0$ (i.e., eliminating the parameter responsible backward bifurcation as stated earlier). Under this condition, the model shrinks to

$$\begin{aligned}
S_a' &= \Lambda_a - \lambda_a S_a - \mu_a S_a,\\
I_a' &= \lambda_a S_a - (\mu_a + r_a + d_a)I_a,\\
R_a' &= r_a I_a - \mu_a R_a,\\
S_h' &= \Lambda_h - \lambda_h S_h - \mu_h S_h,\\
E_h' &= \lambda_h S_h - (\mu_h + \pi)E_h,\\
I_h' &= \pi E_h - (\mu_h + r_h + d_h)I_h,\\
R_h' &= r_h I_h - \mu_h R_h.
\end{aligned} \tag{42}$$

The following result holds.

Theorem 3.5. *The DFE of the model (42), without the rate at which susceptible humans are inoculated with the first dose of the MPV vaccine (i.e., $\eta_v = 0$) is GAS in $\mathcal{D}_o$ if $\mathcal{R}_m \leq 1$ and unstable on the condition that $\mathcal{R}_m > 1$.*

Proof: Looking at the peculiar Lyapunov function below

$$\mathcal{V} = \mathcal{K}_1 I_a + \mathcal{K}_2 E_h + \mathcal{K}_3 I_h, \tag{43}$$

where

$$\mathcal{K}_1 = 1, \quad \mathcal{K}_2 = \pi, \quad \mathcal{K}_3 = \mu_h + \pi, \tag{44}$$

alongside Lyapunov derivatives (in this case, the time derivative is represented by a dot)

$$\dot{\mathcal{V}} = \mathcal{K}_1 \dot{I}_a + K_2 \dot{E}_h + \mathcal{K}_3 \dot{I}_h. \tag{45}$$

Transferring the right hand side of (42) to (45) leads to

$$\begin{aligned}\dot{\mathcal{V}} &= \mathcal{K}_1\lambda_a S_a \\ &\quad - \big[\mathcal{K}_1(\mu_a + r_a + d_a)\big] I_a \\ &\quad + \mathcal{K}_2\lambda_h S_h \\ &\quad - \big[\mathcal{K}_2(\mu_h + \pi) - \mathcal{K}_3\pi\big] E_h \\ &\quad - \big[\mathcal{K}_3(\mu_h + r_h + d_h)\big] I_h, \\ &= (\mu_a + r_a + d_a) I_a \Big[\frac{S_a}{N_a}.\frac{\beta_{a0}}{\mu_a + r_a + d_a} - 1\Big] \\ &\quad + (\mu_h + \pi)(\mu_h + r_h + d_h) I_h \Big[\frac{S_h}{N_h}.\frac{(1-\alpha)(1-\rho)\theta_0\beta\pi}{(\mu_h + \pi)(\mu_h + r_h + d_h)} - 1\Big] \\ &\quad + \beta_{a1}\pi.\frac{S_a}{N_a} I_a.\end{aligned} \tag{46}$$

Substituting $(N_a - S_a)$ for I_a in (46), we obtain

$$\begin{aligned}\dot{\mathcal{V}} &= (\mu_a + r_a + d_a) I_a \Big[\frac{S_a}{N_a}.\frac{\beta_{a0}}{\mu_a + r_a + d_a} - 1\Big] \\ &\quad + (\mu_h + \pi)(\mu_h + r_h + d_h) I_h \Big[\frac{S_h}{N_h}.\frac{(1-\alpha)(1-\rho)\theta_0\beta\pi}{(\mu_h + \pi)(\mu_h + r_h + d_h)} - 1\Big] \\ &\quad + \beta_{a1}\pi.\frac{S_a}{N_a}(N_a - S_a).\end{aligned} \tag{47}$$

At DFE, $S_h \leq \Lambda_h/\mu_h$ and $S_a \leq N_a$. Hence

$$\begin{aligned}\therefore \dot{\mathcal{V}} &\leq (\mu_a + r_a + d_a) I_a \big(\mathcal{R}_{ma} - 1\big) \\ &\quad + (\mu_h + \pi)(\mu_h + r_h + d_h) I_h \big(\mathcal{R}_{mh} - 1\big).\end{aligned} \tag{48}$$

Hence, $\dot{\mathcal{V}} \leq 0$ whenever $\mathcal{R}_{ma} \leq 1$ and $\mathcal{R}_{mh} \leq 1$ with $\dot{\mathcal{V}} = 0$ if and only if $I_a = I_h = 0$. Therefore, $\mathcal{V}$ satisfies the condition for a Lyapunov function in $\mathcal{D}_o$. Hence, it is established from *LaSalle's Invariance Principle* [12] that:

$$(I_a(t), E_h(t), I_h(t)) \to (0, 0, 0) \quad \text{as} \quad t \to \infty.$$

As a consequence, every flow of the equations of the model (42), with the condition that $\eta_v = 0$, advances in the direction of the DFE of the model (42), as $t \to \infty$ for $\mathcal{R}_{ma} \leq 1$ and $\mathcal{R}_{mh} \leq 1$.
This outcome reveals that in an environment that accommodates both *recovery from and medical intervention for MPV cases*, predicated on the premise we have a negligible that there is negligible rate at which susceptible humans are inoculated with the first dose of the MPV vaccine , that is, $\eta_v = 0$, the DFE will be GAS on the condition that $\mathcal{R}_m \leq 1$. Therefore, MPV disease can be eradicated from the populace on the condition that $\mathcal{R}_m \leq 1$, regardless of the initial sizes of the sub-populations.

3.2.3 Global Asymptotic Stability (GAS) of EEP

The stable manifold of the DFE of the system (42) is assumed to be

$$\mathcal{D}_0 = \{(S_a, I_a, R_a, S_h, E_h, I_h, R_h) \in \mathcal{D}_1 : S_a = I_a = R_a = S_h = E_h = I_h = R_h = 0\}. \tag{49}$$

The following result is established.

Theorem 3.6. *The unique EEP, $\mathcal{E}_L^*$, of model (42) with $\eta_v = 0$ is globally asymptotically stable in $\mathcal{D}_1 \backslash \mathcal{D}_0$ at any time $\mathcal{R}_m > 1$.*

Proof: Again, looking at the non-linear Lyapunov function

$$\begin{aligned}\mathcal{L} &= S_a - S_a^{**}\ln\Big(\frac{S_a}{S_a^{**}}\Big) + A_1\Big(I_a - I_a^{**}\ln\frac{I_a}{I_a^{**}}\Big) + A_2\Big(R_a - R_a^{**}\ln\frac{R_a}{R_a^{**}}\Big)\\ &+ S_h - S_h^{**}\ln\Big(\frac{S_h}{S_h^{**}}\Big) + A_3\big(E_h - E_h^{**}\ln\frac{E_h}{E_h^{**}}\big) + A_4\Big(I_h - I_h^{**}\ln\frac{I_h}{I_h^{**}}\Big)\\ &+ A_5\Big(R_h - R_h^{**}\ln\frac{R_h}{R_h{}^{`**}}\Big),\end{aligned} \tag{50}$$

where

$$\begin{aligned}A_1 = 0, \quad A_2 = \frac{\mu_h+\pi}{\pi}, \quad A_3 = 0\\ \mu_a + r_a + d_a = \tilde{\beta}_{a0}S_a^{**} + \tilde{\beta}_{a1}S_h^{**}\\ ,\mu_h + r_h + d_h = \frac{\pi\theta_h\tilde{\beta}_h S_h^{**}}{\mu_h+\pi}\end{aligned} \tag{51}$$

$\mathcal{L}$ has Lyapunov derivatives, given as

$$\begin{aligned}\dot{\mathcal{L}} = \Big(1-\frac{S_a^{**}}{S_a}\Big)\dot{S}_a + \Big(1-\frac{I_a^{**}}{I_a}\Big)\dot{I}_a + A_1\Big(1-\frac{R_a^{**}}{R_a}\Big)\dot{R}_a + \Big(1-\frac{S_h^{**}}{S_h}\Big)\dot{S}_h\\ + \Big(1-\frac{E_h^{**}}{E_h}\Big)\dot{E}_h + A_2\Big(1-\frac{I_h^{**}}{I_h}\Big)\dot{I}_h + A_3\Big(1-\frac{R_h^{**}}{R_h}\Big)\dot{R}_h.\end{aligned} \tag{52}$$

Substituting the right right hand sides of the equations in model (42) corresponding to $\dot{S}_h$, $\dot{E}_h$, $\dot{I}_a$, $\dot{I}_s$, $\dot{R}_h$, $\dot{S}_r$, $\dot{I}_r$, and (51) into (52), and after several algebraic calculations gives:

$$\begin{aligned}\dot{\mathcal{L}} &= \mu_a S_a^{**}\Big(2 - \frac{S_a^{**}}{S_a} - \frac{S_a}{S_a^{**}}\Big)\\ &+ \tilde{\beta}_{a0}S_a^{**}I_a^{**}\Big(2 - \frac{S_a}{S_a^{**}} - \frac{S_a^{**}}{S_a}\Big)\\ &+ \tilde{\beta}_{a1}S_h^{**}I_a^{**}\Big(3 - \frac{S_h^{**}}{S_h} - \frac{E_h}{E_h^{**}}\frac{I_a^{**}}{I_a} - \frac{S_h}{S_h^{**}}\frac{E_h^{**}}{E_h}\frac{I_a}{I_a^{**}}\Big)\\ &+ \mu_h S_h^{**}\Big(2 - \frac{S_h^{**}}{S_h} - \frac{S_h}{S_h^{**}}\Big)\\ &+ \theta_h\tilde{\beta}_h S_h^{**}I_h^{**}\Big(3 - \frac{S_h^{**}}{S_h} - \frac{E_h}{E_h^{**}}\frac{I_h^{**}}{I_h} - \frac{S_h}{S_h^{**}}\frac{E_h^{**}}{E_h}\frac{I_h}{I_h^{**}}\Big).\end{aligned} \tag{53}$$

In the situation that the *arithmetic mean is greater than the geometric mean*, the following inequalities hold

$$\begin{aligned}&2 - \frac{S_a^{**}}{S_a} - \frac{S_a}{S_a^{**}} \le 0, \quad 2 - \frac{S_a}{S_a^{**}} - \frac{S_a^{**}}{S_a} \le 0, \quad 3 - \frac{S_h^{**}}{S_h} - \frac{E_h}{E_h^{**}}\frac{I_a^{**}}{I_a} - \frac{S_h}{S_h^{**}}\frac{E_h^{**}}{E_h}\frac{I_a}{I_a^{**}} \le 0,\\ &2 - \frac{S_h^{**}}{S_h} - \frac{S_h}{S_h^{**}} \le 0, \quad 3 - \frac{S_h^{**}}{S_h} - \frac{E_h}{E_h^{**}}\frac{I_h^{**}}{I_h} - \frac{S_h}{S_h^{**}}\frac{E_h^{**}}{E_h}\frac{I_h}{I_h^{**}}.\end{aligned} \tag{54}$$

Thus, $\dot{\mathcal{L}} \le 0$ whenever $\mathcal{R}_m > 1$.

As far as the important variables in the equations of I_a and I_h respectively are at the endemic equilibrium, substituting them into the equations are represent I_a and I_h, respectively, in (42) such that

$$I_a(t) \to I_a^{**}, \quad I_h(t) \to I_h^{**} \quad \text{as} \quad t \to \infty. \tag{55}$$

Therefore, $\mathcal{L}$ represents a Lyapunov function in $\mathcal{D}_1 \setminus \mathcal{D}_0$. □

This result shows that in MPV population, if $\eta_v = 0$, the EEP will be GAS on the condition that $\mathcal{R}_m > 1$. Hence, MPV will persist in the human community regardless of the initial sizes of the sub-populations on the condition that $\mathcal{R}_m > 1$.

4 Discussions and Conclusion

In order to qualitatively evaluate the impact of a 2-dose monkeypox vaccination strategy on the disease burden in the population in the presence of reduced infection for human to human infection transmission for the disease, a deterministic model for the transmission dynamics of the monkeypox virus (MPV) malady was specifically developed and used theoretically. It was demonstrated that the existence of the parameter that describes the rate at which susceptible persons receive the first dose of the MPV vaccine causes the model to experience the backward bifurcation concept. It was also possible to determine a significant threshold for the rate at which susceptible individuals receive their first dose of the MPV vaccination. When vulnerable humans are vaccinated against MPV at a minimal rate, the DFE is globally asymptotically stable (GAS), according to a particular case study of the model. It was also demonstrated that the endemic equilibrium point of the model system's special case is globally asymptotically stable.

References

[1] World Health Organization (WHO) (2022). Monkeypox Factsheet 2022. *World Health Organization Press; Geneva*, Switzerland.

[2] Bhunu, C. P. and Mushayabasa, S. (2011). Modelling the Transmission Dynamics of Pox-like Infections, *IAENG International Journal of Applied Mathematics*, 41:2.

[3] Emeka, P. C., Onuorah, M. O., Eguda, F. Y., and Babangida, B. G. (2018). Mathematical Model for Monkeypox Virus Transmission Dynamics. *Epidemiology (Sunnyvale)*; 8(3):1-7.

[4] Ngungu, M., Addai E., Adeniji, A., Adam , U. M., and Oshinubi, K. (2023). Mathematical epidemiological modeling and analysis of monkeypox dynamism with non-pharmaceutical intervention using real data from United Kingdom, *Front. Public Health*. 11:1101436, doi.10.3389/fpubh.2023.1101436.

[5] Okyere, S. and Ackora-Prah, J. (2023). Modelling and analysis of monkeypox disease using fractional derivatives. *Results in Engineering* 17:100786.

[6] Peter, O. J., Kumar, S., Kumari, N., Oguntolu, F. A., Oshinubi, K., and Musa, R. (2022). Transmission dynamics of Monkeypox virus: a mathematical modelling approach. *Modeling Earth Systems and Environment*, 8: 3423–3434. http://doi.org/10.1007/s40808-021-01313-2

[7] Lakshmikantham, V., Leela, S., and Martynyuk, A.A. (1991). Stability analysis of nonlinear systems, *SIAM Review* 33(1): 152–154.

[8] van den Driessche, P. and Watmough, J. (2002). Reproduction numbers and sub-threshold endemic equilibria for compartmental models of disease transmission, *Mathematical Biosciences* 180: 29–48.

[9] Elbasha, E. H., Podder, C. N., Gumel, A.B. (2011). Analyzing the dynamics of an SIRS vaccination model with waning natural and vaccine-induced immunity. *Nonlinear Analysis: Real World Applications*; 12 :2692–2705. ;139(3):398-404.

[10] Gumel, A. B. (2012). Causes of backward bifurcations in some epidemiological models, *J. Math. Anal. Appl.*, 395 (2012), pp. 355–365 DOI: 10.1016/j.jmaa.2012.04.077

[11] Castillo-Chavez, C. and Song, B. (2004). Dynamical Models of Tuberculosis and their Applications, *Mathematical Biosciences and Engineering*, Volume 1, Number 2, pp. 361-404.

[12] LaSalle, J. P. and Lefschetz, S. (1976). The stability of dynamical systems, *SIAM, Philadelphia*.

Complex Ebola Virus Disease fractional order model in the Caputo sense with Laplace Adomian Decomposition Method model solution

Q.O. Ahman [*], R.O. Aja[††], W. Atokolo [‡§], D. Omale[¶], N.E. Didigwu[‖], C.S. Ugwu[**]
A.L. Ozioko[††], S.O. Joseph[‡‡], V.I. Ezaegu[*], R.V. Paul[†], and G.C.E. Mbah[‡]

Abstract

Ebola Virus Disease is a life-threatening disease that is transmitted between humans and animals. The aim of this study is to develop a fractional order Ebola Virus Disease model for the dynamics of Ebola considering the control measures;quarantine,isolation,treatment, vaccine and protection (condom use) with a view to study the effects of these control measures on the spread of Ebola in a given population of humans and animals in the Caputo Sense. The fractional order Ebola Virus Disease model in the Caputo sense to control the spread of the disease with eighteen compartments is considered in this paper.This model considered vaccination, condom use, quarantine, use of treatment drugs and isolation as control measures combined together. We analyzed the model where the validity of the model was proven by establishing a region of invariance and the positivity of solutions. We also established the model disease-free equilibrium (DFE)and endemic equilibrium (EE). The reproduction number (a threshold value) (B) was obtained using the next generation matrix. The result of the study produced an expression for B, where if the reproduction number B, is less than 1 then the model DFE point is stable, so the Ebola virus disease dies out. If the reproduction number B is greater than 1, then the model DFE point is unstable, so the Ebola Virus disease persists in the populations.We also analysed the local stability of the DFE point and found out it will be stable when the reproduction number $B < 1$. The novel application of the Laplace–Adomian decomposition method to the model obtained a result of the complex fractional model in an infinite series form which converges further to its exact value. Comparing the solutions of the fractional Ebola virus disease model with that of the classical case using simulation plots we found out that the case of fractional order has more degree of freedom in such a way that can be varied as the fraction (α) could be varied to get different results. We proved convergence of the Laplace Adomian Decomposition method using the Cauchy-Kovalevskaya theorem for differential equations with analytic vector fields and then obtained a new result on the convergence rate of the Laplace Adomian Decomposition Method.

Keywords and phrases: Ebola virus Disease; Laplace–Adomian decomposition method; Fractional order model; Mathematical model; Approximate (Analytical) Solution

[*]Department of Mathematics/Statistics, Confluence University of Science and Technology, Osara, Nigeria
[†]Department of Mathematics, Micheal Okpara University of Agriculture, Umudike, Nigeria
[‡]Corresponding Author; E-mail: williamsatokolo@gmail.com
[§]Department of Mathematics, Kogi State University, Anyigba, Nigeria
[¶]Department of Mathematics, Kogi State University, Anyigba, Nigeria
[‖]Department of Industrial Mathematics, Enugu State University of Science and Technology, Enugu, Nigeria
[**]Department of Mathematics, Enugu State University of Medical and Applied Sciences, Igbo-Ano, Nigeria
[††]Department of Mathematics, Federal University Lokoja, Lokoja, Nigeria
[‡‡]Department of Mathematics/Statistics, Confluence University of Science and Technology, Osara, Nigeria
[*]Department of Mathematics, Ebonyi State University, Abakiliki Nigeria
[†]Department of Mathematics, Kogi State University Anyigba, Nigeria
[‡]Department of Mathematics, University of Nigeria, Nsukka, Nigeria

1 Introduction

Ebola Virus Disease (EVD) is a disease that is also called Ebola haemorrhagic fever which is deadly in nature[1]. The disease was discovered near Ebola River in The Democratic Republic of Congo in 1976 [2, 3]. The disease infects and affects human and non – human pirates. Five species of the virus namely; Bundibugyo Ebola Virus, Tai Forest Ebola Virus, Reston Ebola Virus, Su-dan Ebola Virus, and Zaire Ebola Virus have been identified [4]. Since the birthing and naming of the disease so many outbreaks of the disease have been witnessed in Africa including the 2014 Ebola outbreak in West Africa which in history was called the largest of its kind because it affected many countries at the same time. A group of viruses known as orthoebolaviruses causes Ebola virus disease. This virus is formally known as ebolavirus. The disease has an incubation period of 2 to 21 days after first contact with the symptoms that may include fever, aches, pains, fatigue diarrhea, vomiting, and unexplained bleeding[3, 5]. Scientists believe that human can initially get infected with Ebola virus disease through effective contact with an infected animal which may be fruit bat or non human primate. Research shows that hosts of Ebola Virus may be bats, arthropods and rodents [6].

Ebola virus disease can infect human beings through direct contact with body fluids or blood an Ebola Virus infectious or sick person, infected object and surfaces and dead person. Vaccine drugs and treatment drugs for Ebola Virus disease against the virus are now in use such that those dying from the disease are far less than those recovering from the disease. These drugs include rVSV- EBOV which is 70% to 100% effective to protect against the virus [7, 8]. Some cases have been traced to sexual transmission due to virus residual being persistent in the sperm of men that recovered from the disease[9, 10] . In applied sciences Frac-tional Calculus has so many applications hence in mathematical modelling. From many studies we have seen that fractional calculus can develop the process of some Phenomena in natural science [11, 12] . Fractional-order differential systems have been found to have the advantage of sample modelling, clear parameter meaning and accurate description of some materials and processes with memory and genetic characteristics [13]. Now within the circle of researchers there is a high growing interest into the role of fractional calculus in many areas of modelling real- world problems like Ebola Virus Disease outbreaks particularly in Africa [14, 15].

Laplace–Adomian decomposition method (LADM) is a technique that requires the combination of the Laplace Transforms and the Adomian decomposition method (ADM) [16]. Adomian's is a good effective technique for the solutions of an Ebola virus disease model or a disease model system of ordinary differential equations. On the other hand, Laplace transform is a perfect method applied in applied sciences and engineering. The Laplace–Adomian decomposition method (LADM) is the combination of these two methods. LADM has been applied to so many problems in physics, engineering, biology and applied mathematics [17]. The main idea of the method is to assume an infinite solution of the form: $Z = \sum_{n=0}^{\infty} Z_n$ then apply Laplace transformation to the differential equation. The non-linear terms of the model equation are then decomposed in terms of the Adomian polynomials, and then an iterative procedure is formulated for the determination of the (Z_n) in a recursive form. This method can be used for a system of linear and non-linear ordinary and partial differential equations of the classical and fractional order model. This method does not require any perturbation and also has no need for a predefined step size. This method is an effective method for explicit and numerical solutions of a system of differential equations representing all kinds of physical problems [17].

The Laplace Adomian Decomposition Method has been used by many to obtain the approximate solution of frac-tional order models, The approximate solution of a model for HIV infection was obtained using the Laplace–Adomian decomposition method by Ongun [11]. Adejoh and Mbah [17] in their work also obtained the approximate and numerical solution of their fractional order cancer disease model using Laplace–Adomian decomposition method. The numerical solution of a fractional order smoking model was obtained via the Laplace–Adomian decomposition method by Fazal et al. [5]. Fazal et al. [5] also determined the numerical solution of a fractional order epidemic model of a childhood disease using the Laplace–Adomian decomposition method. Recent studies have employed the Laplace-Adomian decomposition method (LADM) to solve fractional-order models of Ebola virus dynamics.Atokolo et al [18] considered fractional mathematical model of Lassa Fever where Adams

Bashforth-Moultan method was used to investigate the model approximate solution. In 2020, Akeem Olarewaju Yunus and Morufu Oyedunsi Olayiwola utilized LADM to analyze a co-dynamic Ebola and malaria transmission model with Caputo fractional-order [19]. Similarly, Queeneth Ojoma Ahman et al. applied LADM to approximate the solution of a large fractional-order Ebola virus disease model with control measures [20].

The LADM has also been used to solve various nonlinear fractional differential equations. Shah et al. (2020) employed a new analytical technique to analyze the fractional view of third-order Kortewege–De Vries equations [21]. Ganji and Jafari (2020) developed a new approach using LADM to solve nonlinear Volterra integro-differential equations with Mittag-Leffler kernel [22]. Furthermore, Shah et al. (2020) utilized LADM to solve the family of Kuramoto–Sivashinsky equations semi-analytically [23]. Additionally, Shah et al. (2019) proposed a novel method using LADM to obtain the analytical solution of fractional Zakharov–Kuznetsov equations [24]. These studies demonstrate the effectiveness and efficiency of LADM in solving fractional-order models and nonlinear differential equations, highlighting its potential as a valuable tool for researchers in the field. The Laplace–Adomian decomposition method unlike other numerical methods requires no linearization and discretization and as such the results obtained from it are more realistic and effective[25, 26, 27]. Un-like the classical integer model that describes only the local properties of a system, The fractional order model provides a better description of the whole space of a model system; it also provides a better explanation of a real-life system with memory effects [28, 12, 29, 30, 31, 32, 33] The Riemann–Liouville derivative and the Caputo derivative are regarded as sin-gular kernels fractional derivative relative to biological problems, Others that are also non singular are; Mittag-Lefler and the Atangana–Baleanu operators [31]. The classical order and fractional order derivatives have been used in studying transmission dynamics of Ebola disease models [25, 26, 27] and the likes, but to the best of our knowledge it has not been adopted and applied in a large eighteen equation compartmental Ebola model. Also, an eighteen equation Ebola Virus model solution has not been determined using the LADM. To the best of our knowledge, no author has presented an Ebola model that has up to eighteen (18) compartments to study the transmission dynamics of Ebola. Above all we considered a non-integer Ebola model which has more degree of freedom and as such can be varied to obtain more preferred responses which also to the best of our knowledge has not been given adequate attention by researchers. Thus, in this work, we considered a system of eighteen equation compartmental fractional order Ebola model (using the Caputo derivative) for the control of Ebola disease presented with analysis and the analytical solution would be obtained using the Laplace–Adomian decomposition method (LADM).

2 Methodology/Model formulation

We consider two communities of human and animal interacting with each other. The human population is divided into sixteen compartments of Susceptible human population $(S(t))$,Vaccinated human population $(S_v(t))$, unvaccinated human population $(S_u(t))$, vaccinated condom using human population $(S_{vc}(t))$, vaccinated non using condom human population $(S_{vn}(t))$, unvaccinated condom using human population $(S_{uc}(t))$, unvaccinated non using condom human population $(S_{un}(t))$, Exposed human population$(E(t))$, Exposed quarantined human population $(E_Q(t))$, Exposed treated human population $(E_T(t))$,Infectious human population $(I(t))$, Infectious treated human population$(I_T(t))$, Infectious isolated human population $(I_i(t))$, Infectious not treated human population $(I_N(t))$, Recovered human population $(R(t))$ and Dead unburied human population $(D_u(t))$ while the animal population is divided into three compartments of susceptible animal population $(S_r(t))$, Exposed animal population $(E_r(t))$ and Infectious animal population $(I_r(t))$. The animal population is recruited into the animal susceptible population at the rate (Λ) while the animal susceptible population is reduced through exposure to the disease at the rate (ω) and entering the animal exposed population and animal natural death at the rate (μ_r),the exposed animal population reduces by becoming infectious and entering the animal infectious population at the rate (ϕ) and animal natural death at the rate (μ_r) and the infectious population reduces due to animal natural death at the rate (μ_r) and animal disease

death at the rate (δ_4). The human population is recruited into the human susceptible population at the rate (P) while the human susceptible population reduces due to human natural death at the rate (μ), through those going for vaccination at the proportion (r) and those not going for vaccination at the proportion ($X = 1 - r$) with its modification parameter (K_1). The human susceptible vaccinated population reduces due to human natural death at the rate (μ), through those using condom at the proportion (λ) and those not using condom at the proportion ($Z = 1 - \lambda$) with its parameter modification (K_2).The human susceptible unvaccinated population reduces due to human natural death at the rate (μ), through those using condom at the proportion (σ) and those not using condom at the proportion ($Y = 1 - \sigma$) with its parameter modification (K_3). The human susceptible vaccinated condom using population reduces due to human natural death at the rate (μ) and through exposure to the disease at the rate (β_1) and entering the human exposed population.The human susceptible vaccinated not using condom population reduces due to human natural death at the rate (μ) and through exposure to the disease at the rate (β_2) and entering the human exposed population. The human susceptible unvaccinated condom using population reduces due to human natural death at the rate (μ) and through exposure to the disease at the rate (β_3) and entering the human exposed population.The human susceptible unvaccinated not using condom population reduces due to human natural death at the rate (μ) and through exposure to the disease at the rate (β_4) and entering the human exposed population. The exposed human population reduces due to human natural death at the rate (μ) and through those exposed going into quarantine at the rate (α_1) and those exposed going for treatment after exposure at the rate (α_2). The exposed quarantined human population reduces due to human natural death at the rate (μ) and by becoming infectious and entering the human infectious population at the rate (θ_1). The exposed treated human population reduces due to human natural death at the rate (μ) and by becoming infectious and entering the human infectious population at the rate (θ_2) with those recovered entering the recovered population at the rate (ρ). The infectious human population reduces due to human natural death at the rate (μ) and through those infectious going for treatment at the rate (S_1) and those infectious going into isolation at the rate (S_2) with those not going for any form of treatment or isolation at the rate (S_3). The infectious treated human population reduces due to human natural death at the rate (μ), by those recovering from the disease and are entering the recovered population at the rate (J_2) and through those that die from the disease and are entering the dead unburied population at the rate (δ_1).The infectious isolated human population reduces due to human natural death at the rate (μ), by those recovering from the disease and are entering the recovered population at the rate (J_1) and through those that die from the disease and are entering the dead unburied population at the rate (δ_2).The infectious not treated human population reduces due to human natural death at the rate (μ) and through those that die from the disease and are entering the dead unburied population at the rate (δ_3).The recovered human population reduces due to human natural death at the rate (μ) and through those that are losing their temporal immunity and becoming susceptible to the disease again at the rate (τ). The dead unburied human population reduces due to proper burial of the corps at the rate (q).

2.1 The assumptions of the model

(1) There is no vertical transmission of the infection i.e. there is no infection from mother to unborn baby.

(2) There is no herd immunity in the population.

(3) The population is not constant and there is no inherent immunity in the population.

(4) The infectious compartment is a transition point i.e. Infected and infectious individuals do not stay long before joining isolated, treated or not treated compartments.

(5) The disease recovered individuals are still infectious through semen.

(6) Quarantined and isolated individuals are under close surveillance and do not contribute to the transmission of the disease.

(7) Death resulting from the disease only takes place in the infectious compartments.

(8) Ebola infected and infectious animals in the population have interactions with the susceptible human population.

(9) The animals do not recover from the disease.

The schematic diagram of the Ebola Mathematical model is shown in Figure 1 below.

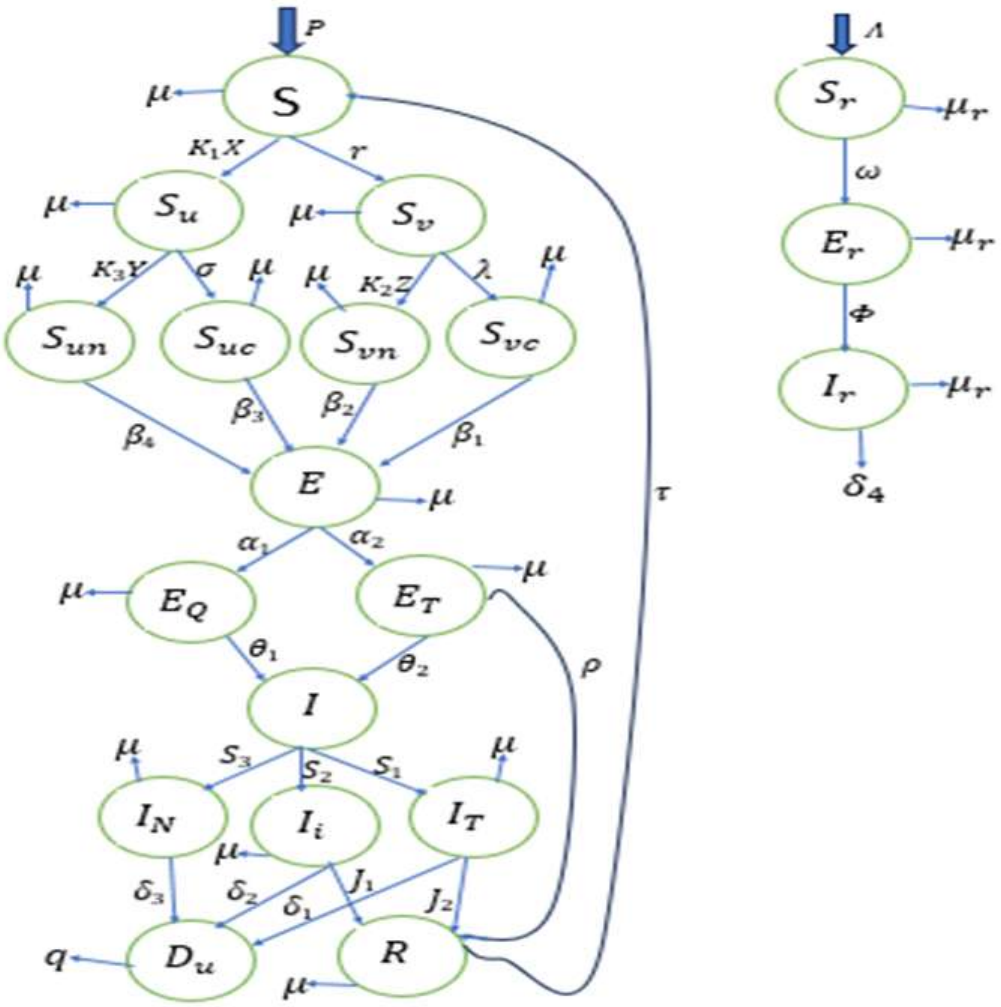


Figure 1: THE EBOLA VIRUS DISEASE FLOW DIAGRAM

2.2 Ebola mathematical model equations

incorporating the above assumptions, formulations and Figure 1 we produce the mathematical model equations as follows:

$$
\left.\begin{aligned}
(1)\frac{dS}{dt} &= P\breve{}\,(\mu + r + K_1X)S + \tau R\\
(2)\frac{dS_v}{dt} &= rS\breve{}(\mu + \lambda + K_2Z)S_v\\
(3)\frac{dS_u}{dt} &= K_1XS\breve{}(\mu + \sigma + K_3Y)S_u\\
(4)\frac{dS_{vc}}{dt} &= \lambda S_v - (\mu + \beta_1)S_{vc}\\
(5)\frac{dS_{vn}}{dt} &= K_2ZS_v - (\mu + \beta_2)S_{vn}\\
(6)\frac{dS_{uc}}{dt} &= \sigma S_u - (\mu + \beta_3)S_{uc}\\
(7)\frac{dS_{un}}{dt} &= K_3YS_u - (\mu + \beta_4)S_{un}\\
(8)\frac{dE}{dt} &= \beta_1S_{vc} + \beta_2S_{vn} +\\
&\quad \beta_3S_{uc} + \beta_4S_{un} - (\mu + \alpha_1 + \alpha_2)E\\
(9)\frac{dE_Q}{dt} &= \alpha_1E - (\mu + \theta_1)E_Q\\
(10)\frac{dE_T}{dt} &= \alpha_2E - (\mu + \theta_2 + \rho)E_T\\
(11)\frac{dI_T}{dt} &= \theta_1S_1E_Q + \theta_2S_1E_T - (\mu + \delta_1 + J_2)I_T\\
(12)\frac{dI_i}{dt} &= \theta_1S_2E_Q + \theta_2S_2E_T - (\mu + \delta_2 + J_1)I_i\\
(13)\frac{dI_N}{dt} &= \theta_1S_3E_Q + \theta_2S_3E_T - (\mu + \delta_3)I_N\\
(14)\frac{dR}{dt} &= J_1I_i + J_2I_T + \rho E_T\breve{}(\mu + \tau)R\\
(15)\frac{dD_u}{dt} &= \delta_3I_N + \delta_2I_i + \delta_1I_T - qD_u\\
(16)\frac{dS_r}{dt} &= \Lambda - (\mu_r + \omega)S_r\\
(17)\frac{dE_r}{dt} &= \omega S_r - (\mu_r + \phi)E_r\\
(18)\frac{dI_r}{dt} &= \phi E_r - (\mu_r + \delta_4)I_r
\end{aligned}\right\} \tag{1}
$$

With initial conditions given as follows;

$$
\left.\begin{aligned}
S(0) = g_1 \geq 0, S_v(0) = g_2 \geq 0, S_u(0) = g_3 \geq 0,\\
S_{vc}(0) = g_4 \geq 0, S_{vn}(0) = g_5 \geq 0, S_{uc}(0) = g_6 \geq 0,\\
S_{un}(0) = g_7 \geq 0, E(0) = g_8 \geq 0, E_Q(0) = g_9 \geq 0, E_T(0) = g_{10} \geq 0,\\
I_T(0) = g_{11} \geq 0, I_i(0) = g_{12} \geq 0, I_N(0) = g_{13} \geq 0, R(0) = g_{14} \geq 0,\\
D_u(0) = g_{15} \geq 0, S_r(0) = g_{16} \geq 0, E_r(0) = g_{17} \geq 0 \; and \; I_r(0) = g_{18} \geq 0.
\end{aligned}\right\} \tag{2}
$$

where;

$$\left.\begin{aligned}\beta_1 &= \frac{m_1 I_N + m_2 I_T + m_3 I_r + m_4 D_u}{N}\\ \beta_2 &= \frac{n_1 I_N + n_2 I_T + n_3 I_r + n_4 D_u}{N}\\ \beta_3 &= \frac{e_1 I_N + e_2 I_T + e_3 I_r + e_4 D_u}{N}\\ \beta_4 &= \frac{t_1 I_N + t_2 I_T + t_3 I_r + t_4 D_u}{N}\\ T_s(t) &= S + S_v + S_u + S_{vc} + S_{vn} + S_{uc} + S_{un} +\\ &\quad E + E_Q + E_T + I_T + I_i + I_N + R + D_u\\ T_r(t) &= S_r + E_r + I_r\\ N(t) &= T_s + T_r\end{aligned}\right\} \tag{3}$$

Applying assumption (4) the model equation became 18 instead of 19 as the compartments are 19 but the infectious compartment is a transition point such that no one stays there for long. The model variables and parameters descriptions are presented in Table 1 and Table 2 respectively.

2.3 Fractional order Ebola Virus Disease model

In this model the Caputo derivative is considered as a differential operator.When using the Caputo fractional initial value problem, we can express the initial condition with an initial integer order with physical interpretation that is very easy for real life interpretation, and thus is suitable for the Ebola Virus Disease model. In this section, we now present some well known definitions and results that will be used throughout this paper.

Definition 1

The Caputo fractional order derivative of a function (f) on the interval $[0, T]$ is defined as follows:

$$[{}^cD_0^\alpha f(t)] = \frac{1}{\Gamma(n-\alpha)} \int_0^t (t-s)^{n-\alpha-1} f^n(s) ds \tag{4}$$

where $n = [\alpha] + 1 \; and \; [\alpha]$ represents the integer part of α. In particular, for $0 < \alpha < 1$ the Caputo derivative becomes;

$$[{}^cD_0^\alpha f(t)] = \frac{1}{\Gamma(n-\alpha)} \int_0^t \frac{f(s)}{(t-s)^\alpha} ds \tag{5}$$

Definition 2

The Laplace transform of Caputo derivatives is defined as follows:

$$\mathcal{L}[{}^cD^\alpha v(t)] = M^\alpha h(M) \sum\nolimits_{k=0}^{n} M^{\alpha-i-1} x^k(0), n-1 < \alpha < n, n \in N \tag{6}$$

for arbitrary $b_i \in R, i = 0, 1, 2, ..., n-1$ where $n = [\alpha] + 1 \; and \; [\alpha]$ represents the non - integer part of α.

Lemma 1.1

The following result stands for fractional differential equations;

$$I^\alpha [{}^cD^\alpha r(t)] = r(t) + \sum\nolimits_{i=0}^{n-1} \frac{r^{(i)}(0)}{i!} t^i \tag{7}$$

for arbitrary $\alpha > 0, i = 0, 1, 2, ..., n-1$ where $n = [\alpha] + 1 \; and \; [\alpha]$ represents the integer parts of α. Introducing the fractional order and substituting equation (3) into the model (1), we have a new set of model equation which is described by the following set of fractional differential equations of order

(α) *for* $0 < \alpha < 1$.

$$
\left.
\begin{aligned}
(1)D^{\alpha}S(t) &= P - (\mu + r + K_1X)S + \tau R \\
(2)D^{\alpha}S_v(t) &= rS - (\mu + \lambda + K_2Z)S_v \\
(3)D^{\alpha}S_u(t) &= K_1XS - (\mu + \sigma + K_3Y)S_u \\
(4)D^{\alpha}S_{vc}(t) &= \lambda S_v - [\mu S_{vc} + 1/N(m_1I_NS_{vc}+ \\
&\quad m_2I_TS_{vc} + m_3I_rS_{vc} + m_4D_uS_{vc})] \\
(5)D^{\alpha}S_{vn}(t) &= K_2ZS_v - [\mu S_{vn} + 1/N(n_1I_NS_{vn}+ \\
&\quad n_2I_TS_{vn} + n_3I_rS_{vn} + n_4D_uS_{vn})] \\
(6)D^{\alpha}S_{uc}(t) &= \sigma S_u - [\mu S_{uc} + 1/N(e_1I_NS_{uc}+ \\
&\quad e_2I_TS_{uc} + e_3I_rS_{uc} + e_4D_uS_{uc})] \\
(7)D^{\alpha}S_{un}(t) &= K_3YS_u - [\mu S_{un} + 1/N(t_1I_NS_{un}+ \\
&\quad t_2I_TS_{un} + t_3I_rS_{un} + t_4D_uS_{un})] \\
(8)D^{\alpha}E(t) &= 1/N[m_1I_NS_{vc} + m_2I_TS_{vc}+ \\
&\quad m_3I_rS_{vc} + m_4D_uS_{vc} + n_1I_NS_{vn}+ \\
&\quad n_2I_TS_{vn} + n_3I_rS_{vn} + n_4D_uS_{vn}+ \\
&\quad e_1I_NS_{uc} + e_2I_TS_{uc} + e_3I_rS_{uc}+ \\
&\quad e_4D_uS_{uc} + t_1I_NS_{un} + t_2I_TS_{un}+ \\
&\quad t_3I_rS_{un} + t_4D_uS_{un}] - (\mu + \alpha_1 + \alpha_2)E \\
(9)D^{\alpha}E_Q(t) &= \alpha_1E - (\mu + \theta_1)E_Q \\
(10)D^{\alpha}E_T(t) &= \alpha_2E - (\mu + \theta_2 + \rho)E_T \\
(11)D^{\alpha}I_T(t) &= \theta_1S_1E_Q + \theta_2S_1E_T - (\mu + \delta_1 + J_2)I_T \\
(12)D^{\alpha}I_i(t) &= \theta_1S_2E_Q + \theta_2S_2E_T - (\mu + \delta_2 + J_1)I_i \\
(13)D^{\alpha}I_N(t) &= \theta_1S_3E_Q + \theta_2S_3E_T - (\mu + \delta_3)I_N \\
(14)D^{\alpha}R(t) &= J_1I_i + J_2I_T + \rho E_T - (\mu + \tau)R \\
(15)D^{\alpha}D_u(t) &= \delta_3I_N + \delta_2I_i + \delta_1I_T - q \\
(16)D^{\alpha}S_r(t) &= \Lambda - (\mu_r + \omega)S_r \\
(17)D^{\alpha}E_r(t) &= \omega S_r - (\mu_r + \phi)E_r \\
(18)D^{\alpha}I_r(t) &= \phi E_r - (\mu_r + \delta_4)I_r
\end{aligned}
\right\} \tag{8}
$$

The Table 1 gives a description summary of the Variables used herein:
The Table 2 gives a description summary of the Parameters used herein:

3 Analysis of the model

In this section, we herein analyse the system of fractional Ebola model(8) as follows;

3.1 Positively invariant Region

In this section we show that the closed set $\Omega = \{(S, S_v, S_u, S_{vc}, S_{vn}, S_{uc}, S_{un}, E, E_Q, E_T, I_T, I_i, I_N, R, D_u, S_r, E_r, I_r) \in R_+^{18} : 0 \leq N\}$ provides the Fractional Ebola Virus model system (8) positively invariant feasible region.

Lemma 3.1

The solutions of the Fractional Ebola Virus model system (8) are non-negative and bounded if they start in Ω.

Proof

Table 1: **Ebola model variables and descriptions**

Variables	Descriptions
$S(t)$	Ebola Susceptible Population
$S_v(t)$	Ebola Susceptible Vaccinated Population
$S_u(t)$	Ebola Susceptible Unaccinated Population
$S_{vc}(t)$	Ebola Susceptible Vaccinated Condom using Population
$S_{vn}(t)$	Ebola Susceptible Vaccinated not using Condom Population
$S_{uc}(t)$	Ebola Susceptible Unaccinated Condom using Population
$S_{un}(t)$	Ebola Susceptible Unaccinated not using Condom Population
$E(t)$	Ebola Exposed Population
$E_Q(t)$	Ebola Exposed Quarantined Population
$E_T(t)$	Ebola Exposed Treated Population
$I(t)$	Ebola Infectious Population
$I_T(t)$	Ebola Infectious Treated Population
$I_i(t)$	Ebola Infectious Isolated Population
$I_N(t)$	Ebola Infectious no Treatment Population
$R(t)$	Ebola Recovered Population
$D_u(t)$	Ebola Disease Dead Unburied Population
$S_r(t)$	Ebola Susceptible Animal Population
$E_r(t)$	Ebola Exposed Animal Population
$I_r(t)$	Ebola Susceptible Animal Population
$T_s(t)$	Total Human Population
$T_r(t)$	Total Animal Population
$N(t)$	Total Human and Animal Population

Table 2: **Ebola model parameters and descriptions**

Parameters	Descriptions
P	Human rate of recruitment
μ	Human rate of natural death
r	Human rate of Vaccination
K_1	Human vaccination modification parameter
λ	Human Vaccinated rate of condom use
K_2	Human Vaccinated condom use modification parameter
σ	Human Unaccinated rate of condom use
K_3	Human Unaccinated condom use modification parameter
β_1	Human Vaccinated condom using population force of infection
β_2	Human Vaccinated non condom using population force of infection
β_3	Human Unaccinated condom using population force of infection
β_4	Human Unvaccinated non condom using population force of infection
α_1	Human exposed rate of quarantine
α_2	Human exposed rate of treatment
θ_1	Human exposed quarantined rate of becoming infectious
θ_2	Human exposed treated rate of becoming infectious
ρ	Human exposed treated rate of recovery
S_1	Human infectious rate of treatment
S_2	Human infectious rate of isolation
S_3	Human infectious rate of no treatment or isolation
J_1	Human infectious isolated rate of recovery
J_2	Human infectious treatment rate of recovery
δ_1	Human infectious treated disease death rate
δ_2	Human infectious isolated disease death rate
δ_3	Human infectious no treatment disease death rate
τ	Human Recovered rate of immunity loss
q	Disease dead unburied rate of proper burial
Λ	Animal Population recruitment rate
μ_r	Animal Population natural death rate
ω	Animal Population rate of exposure to disease
ϕ	Animal Population rate of becoming infectious
δ_4	Animal Population disease death rate

from (8) we obtain the following;

$$\left.\begin{aligned}
D^\alpha S(t)|_{s=0} = P - \tau R \geq 0 \\
D^\alpha S_v(t)|_{S_v=0} = rS \geq 0 \\
D^\alpha S_u(t)|_{S_u=0} = K_1 XS \geq 0 \\
D^\alpha S_{vc}(t)|_{S_{vc}=0} = \lambda S_v \geq 0 \\
D^\alpha S_{vn}(t)|_{S_{vn}=0} = K_2 ZS_v \geq 0 \\
D^\alpha S_{uc}(t)|_{S_{uc}=0} = \sigma S_u \geq 0 \\
D^\alpha S_{un}(t)|_{S_{un}=0} = K_3 YS_u \geq 0 \\
D^\alpha E(t)|_{E=0} = \beta_1 S_{vc} + \beta_2 S_{vn} + \beta_3 S_{uc} + \beta_4 S_{un} \geq 0 \\
D^\alpha E_Q(t)|_{E_Q=0} = \alpha_1 E \geq 0 \\
D^\alpha E_T(t)|_{E_T=0} = \alpha_2 E \geq 0 \\
D^\alpha I_T(t)|_{I_T=0} = \theta_1 s_1 E_Q + \theta_2 s_1 E_T \geq 0 \\
D^\alpha I_i(t)|_{I_i=0} = \theta_1 s_2 E_Q + \theta_2 s_2 E_T \geq 0 \\
D^\alpha I_N(t)|_{I_N=0} = \theta_1 s_3 E_Q + \theta_2 s_3 E_T \geq 0 \\
D^\alpha R(t)|_{R=0} = J_1 I_i + J_2 I_T + \rho E_T \geq 0 \\
D^\alpha D_u(t)|_{D_u=0} = \delta_3 I_N + \delta_2 I_i + \delta_1 I_T \geq 0 \\
D^\alpha S_r(t)|_{S_r=0} = \Lambda \geq 0 \\
D^\alpha E_r(t)|_{E_r=0} = \omega S_r \geq 0 \\
D^\alpha I_r(t)|_{I_r=0} = \phi E_r \geq 0
\end{aligned}\right\} \tag{9}$$

Hence, the sub-populations $S, S_v, S_u, S_{vc}, S_{vn}, S_{uc}, S_{un}, E, E_Q, E_T, I_T, I_i, I_N, R, D_u,$
$S_r, E_r \; and \; I_r$ are non-negative. Also, as $N = T_s + T_r$ wherever N is considered to be constant each of the sub-population will lie in $[0, N]$. Thus, the sub-populations $S, S_v, S_u, S_{vc}, S_{vn}, S_{uc}, S_{un}, E, E_Q, E_T, I_T, I_i, I_N, R,$ $D_u, S_r, E_r \; and \; I_r$ are also bounded.

3.2 Fractional Ebola Virus model equilibrium points and basic reproduction number

At equilibrium;

$$\left.\begin{aligned}
D^\alpha S = D^\alpha S_v = D^\alpha S_u = D^\alpha S_{vc} = D^\alpha S_{vn} = D^\alpha S_{uc} = D^\alpha S_{un} = 0 \\
D^\alpha E = D^\alpha E_Q = D^\alpha E_T = D^\alpha I_T = D^\alpha I_i = D^\alpha I_N = 0 \\
D^\alpha R = D^\alpha D_u = D^\alpha S_r = D^\alpha E_r = D^\alpha I_r = 0
\end{aligned}\right\} \tag{10}$$

The Fractional Ebola Virus Disease free equilibrium $(C^f) = \{S^f, S_v^f, S_u^f, S_{vc}^f, S_{vn}^f, S_{uc}^f, S_{un}^f, E^f, E_Q^f, E_T^f, I_T^f, I_i^f, I_N^f,$
$R^f, D_u^f, S_r^f, E_r^f, I_r^f\} = \{\frac{P}{(\mu+r+K_1X)}, \frac{rS^f}{(\mu+\lambda+K_2Z)},$
$\frac{K_1XS^f}{(\mu+\sigma+K_3Y)}, \frac{\lambda S_v^f}{\mu}, \frac{K_2ZS_v^f}{\mu}, \frac{\sigma S_u^f}{\mu},$
$\frac{K_3YS_u^f}{\mu}, 0, 0, 0, 0, 0, 0, 0, 0, \frac{\Lambda}{\mu_r}, 0, 0\}.$
while
The Fractional Ebola Virus Disease endemic equilibrium $(C^h) = \{S^h, S_v^h, S_u^h, S_{vc}^h, S_{vn}^h, S_{uc}^h, S_{un}^h, E^h, E_Q^h, E_T^h, I_T^h,$
$I_i^h, I_N^h, R^h, D_u^h, S_r^h, E_r^h, I_r^h\}$
$= \{A_1, A_2, A_3, A_4, A_5, A_6, A_7, A_8, A_9,$
$A_{10}, A_{11}, A_{12}, A_{13}, A_{14}, A_{15}, A_{16}, A_{17}, A_{18}\}.$

where

$$\left.\begin{aligned}
A_1 &= \frac{P+\tau R^h}{(\mu+r+K_1X)},\\
A_2 &= \frac{rS^h}{(\mu+\lambda+K_2Z)},\\
A_3 &= \frac{K_1XS^h}{(\mu+\sigma+K_3Y)},\\
A_4 &= \frac{\lambda rS^h}{(\mu+\lambda+K_2Z)(\mu+\beta_1)},\\
A_5 &= \frac{K_2ZrS^h}{(\mu+\lambda+K_2Z)(\mu+\beta_2)},\\
A_6 &= \frac{\sigma K_1XS^h}{(\mu+\sigma+K_3Y)(\mu+\beta_3)},\\
A_7 &= \frac{K_3YK_1XS^h}{(\mu+\sigma+K_3Y)(\mu+\beta_4)},\\
A_8 &= \frac{\beta_1S^f_{vc}+\beta_2S^f_{vn}+\beta_3S^f_{uc}+\beta_4S^f_{un}}{(\mu+\alpha_1+\alpha_2)},\\
A_9 &= \frac{\alpha_1E^h}{(\mu+\theta_1)},\\
A_{10} &= \frac{\alpha_2E^h}{(\mu+\theta_2+\rho)},\\
A_{11} &= \frac{\theta_1s_1E^h_Q+\theta_2s_1E^h_T}{(\mu+\delta_1+J_2)}, A_{12} = \frac{\theta_1s_2E^h_Q+\theta_2s_3E^h_T}{(\mu+\delta_3)},\\
A_{13} &= \frac{\theta_1s_3E^h_Q+\theta_2s_1E^h_T}{(\mu+\delta_1+J_2)}, A_{14} = \frac{J_1I^h_i+J_2I^h_T+\rho E^h_T}{(\mu+\tau)},\\
A_{15} &= \frac{\delta_3I^h_N+\delta_2I^h_i+\delta_1I^h_T}{q},\\
A_{16} &= \frac{\Lambda}{(\mu_r)+\omega},\\
A_{17} &= \frac{\omega S^h_r}{(\mu_r+\phi)}, A_{18} = \frac{\phi E^h_r}{(\mu_r+\delta_4)}
\end{aligned}\right\} \tag{11}$$

The basic reproduction number B can be computed for the model using the next-generation matrix method as described in [28], we calculate B as follows; considering the newly occurring infections $E, E_Q, E_T, I_T, I_i, I_N, R, D_u, S_r, E_r \; and \; I_r$ we calculate the corresponding Jacobian matrices F and V

at the Ebola model disease-free equilibrium point C_f

$$\left.\begin{aligned} F = &\begin{bmatrix} 0 & 0 & 0 & a_1 & 0 & a_2 & 0 & a_3 & 0 & a_4 \\ 0 & 0 & 0 & 0 & 0 & 0 & 0 & 0 & 0 & 0 \\ 0 & 0 & 0 & 0 & 0 & 0 & 0 & 0 & 0 & 0 \\ 0 & 0 & 0 & 0 & 0 & 0 & 0 & 0 & 0 & 0 \\ 0 & 0 & 0 & 0 & 0 & 0 & 0 & 0 & 0 & 0 \\ 0 & 0 & 0 & 0 & 0 & 0 & 0 & 0 & 0 & 0 \\ 0 & 0 & 0 & 0 & 0 & 0 & 0 & 0 & 0 & 0 \\ 0 & 0 & 0 & 0 & 0 & 0 & 0 & 0 & 0 & 0 \\ 0 & 0 & 0 & 0 & 0 & 0 & 0 & 0 & 0 & 0 \\ 0 & 0 & 0 & 0 & 0 & 0 & 0 & 0 & 0 & 0 \end{bmatrix} \\ V = &\begin{bmatrix} b_1 & 0 & 0 & 0 & 0 & 0 & 0 & 0 & 0 & 0 \\ -a & b_2 & 0 & 0 & 0 & 0 & 0 & 0 & 0 & 0 \\ -b & 0 & b_3 & 0 & 0 & 0 & 0 & 0 & 0 & 0 \\ 0 & -c & -d & b_4 & 0 & 0 & 0 & 0 & 0 & 0 \\ 0 & -e & -f & 0 & b_5 & 0 & 0 & 0 & 0 & 0 \\ 0 & -g & -h & 0 & 0 & b_6 & 0 & 0 & 0 & 0 \\ 0 & 0 & -w & -k & -x & 0 & b_7 & 0 & 0 & 0 \\ 0 & 0 & 0 & -m & -n & -p & 0 & b_8 & 0 & 0 \\ 0 & 0 & 0 & 0 & 0 & 0 & 0 & 0 & b_9 & 0 \\ 0 & 0 & 0 & 0 & 0 & 0 & 0 & 0 & -y & b_{10} \end{bmatrix} \end{aligned}\right\} \tag{12}$$

where;

$$\left.\begin{aligned} a_1 &= \frac{m_2 S^e_{vc} + n_2 S^e_{vn} + e_2 S^e_{uc} + t_2 S^e_{un}}{N} \\ a_2 &= \frac{m_1 S^e_{vc} + n_1 S^e_{vn} + e_1 S^e_{uc} + t_1 S^e_{un}}{N} \\ a_3 &= \frac{m_4 S^e_{vc} + n_4 S^e_{vn} + e_4 S^e_{uc} + t_4 S^e_{un}}{N} \\ a_4 &= \frac{m_3 S^e_{vc} + n_3 S^e_{vn} + e_3 S^e_{uc} + t_3 S^e_{un}}{N} \end{aligned}\right\} \tag{13}$$

and

$$\left.\begin{aligned} a_1 &= \frac{P\left[\frac{r(m_2\lambda + n_2 K_2 Z)}{(\mu+\lambda+K_2 Z)} + \frac{K_1 X(e_2\sigma + t_2 K_3 Y)}{(\mu+\sigma+K_3 Y)}\right]}{\mu N(\mu + r + K_1 X)} \\ a_2 &= \frac{P\left[\frac{r(m_1\lambda + n_1 K_2 Z)}{(\mu+\lambda+K_2 Z)} + \frac{K_1 X(e_1\sigma + t_1 K_3 Y)}{(\mu+\sigma+K_3 Y)}\right]}{\mu N(\mu + r + K_1 X)} \\ a_3 &= \frac{P\left[\frac{r(m_4\lambda + n_4 K_2 Z)}{(\mu+\lambda+K_2 Z)} + \frac{K_1 X(e_4\sigma + t_4 K_3 Y)}{(\mu+\sigma+K_3 Y)}\right]}{\mu N(\mu + r + K_1 X)} \\ a_4 &= \frac{P\left[\frac{r(m_3\lambda + n_3 K_2 Z)}{(\mu+\lambda+K_2 Z)} + \frac{K_1 X(e_3\sigma + t_3 K_3 Y)}{(\mu+\sigma+K_3 Y)}\right]}{\mu N(\mu + r + K_1 X)} \\ b_1 &= (\mu + \alpha_1 + \alpha_2), b_2 = (\mu + \theta_1), \\ b_3 &= (\mu + \theta_2 + \rho), b_4 = (\mu + \delta_1 + J_2), \\ b_5 &= (\mu + \delta_2 + J_1), b_6 = (\mu + \delta_3), \\ b_7 &= (\mu + \tau), b_8 = q, b_9 = (\mu_r + \phi), \\ b_{10} &= (\mu_r + \delta_4), a = \alpha_1, b = \alpha_2, c = \theta_2 s_1, \\ d &= \theta_1 s_1, e = \theta_1 s_2, f = \theta_2 s_2, g = \theta_1 s_3, \\ h &= \theta_2 s_3, w = \rho, k = J_2, x = J_1, m = \delta_1, \\ n &= \delta_2, p = \delta_3, y = \phi. \end{aligned}\right\} \tag{14}$$

With,

$$eig(FV^{-1}) = \begin{bmatrix} 0 \\ 0 \\ 0 \\ 0 \\ 0 \\ 0 \\ 0 \\ 0 \\ 0 \\ 0 \\ \frac{1}{b_1b_2b_3b_4b_5b_6b_8}[b_8b_5(a_1b_6(dbb_2+cab_3)+a_2b_4(hbb_2+gab_3))+ \\ a_3(b_2b_5b(phb_4+mdb_6)+b_4(nfbb_2b_6+pgab_3b_5)+ \\ b_3b_6a(neb_4+mcb_5)] \end{bmatrix} \tag{15}$$

Thus, the basic reproduction number of our Ebola Virus model which is given as the largest eigenvalue $\rho(FV^{-1})$ is given as follows;
$\rho(FV^{-1}) = \frac{1}{b_1b_2b_3b_4b_5b_6b_8}[b_8b_5(a_1b_6(dbb_2+cab_3)+a_2b_4(hbb_2+gab_3))+a_3(b_2b_5b(phb_4+mdb_6)+b_4(nfbb_2b_6+pgab_3b_5)+b_3b_6a(neb_4+mcb_5)]$
$\Rightarrow B = \frac{1}{b_1b_2b_3b_4b_5b_6b_8}[b_8b_5(a_1b_6(dbb_2+cab_3)+a_2b_4(hbb_2+gab_3))+a_3(b_2b_5b(phb_4+mdb_6)+b_4(nfbb_2b_6+pgab_3b_5)+$
$b_3b_6a(neb_4+mcb_5)]$

$$\left.\begin{aligned} \therefore B \\ = \frac{P}{\mu N(\mu+r+K_1X)(\mu+\alpha_1+\alpha_2)(\mu+\theta_1)(\mu+\theta_2+\rho)(\mu+\delta_1+J_2)(\mu+\delta_2+J_1)(\mu+\delta_3)q} \\ [q(\mu+\delta_2+J_1)(\frac{r(m_2\lambda+n_2K_2Z)}{(\mu+\lambda+K_2Z)}+\frac{K_1X(e_2\sigma+t_2K_3Y)}{(\mu+\sigma+K_3Y)}) \\ (\mu+\delta_3)(\theta_1s_1\alpha_2(\mu+\theta_1)+\theta_2s_1\alpha_1(\mu+\theta_2+\rho))+(\frac{r(m_1\lambda+n_1K_2Z)}{(\mu+\lambda+K_2Z)}+\frac{K_1X(e_1\sigma+t_1K_3Y)}{(\mu+\sigma+K_3Y)}) \\ (\mu+\delta_1+J_2)(\theta_2s_3\alpha_2(\mu+\theta_1)+\theta_1s_3\alpha_1(\mu+\theta_2+\rho))) \\ +(\frac{r(m_4\lambda+n_4K_2Z)}{(\mu+\lambda+K_2Z)}+\frac{K_1X(e_4\sigma+t_4K_3Y)}{(\mu+\sigma+K_3Y)})((\mu+\theta_1)(\mu+\delta_2+J_1)\alpha_2 \\ (\delta_3\theta_2s_3(\mu+\delta_1+J_2)+\delta_1\theta_1s_1(\mu+\delta_3))+(\mu+\delta_1+J_2)(\delta_2\theta_2s_2\alpha_2(\mu+\theta_1) \\ (\mu+\delta_3)+\delta_3\theta_1s_3\alpha_1(\mu+\theta_2+\rho)(\mu+\delta_2+J_1))+(\mu+\theta_2+\rho)(\mu+\delta_3)\alpha_1 \\ (\delta_2\theta_1s_2(\mu+\delta_1+J_2)+\delta_1\theta_2s_1(\mu+\delta_2+J_1))] \end{aligned}\right\} \tag{16}$$

$B = \frac{(a_1b_6(dbb_2+cab_3)+a_2b_4(hbb_2+gab_3))}{b_1b_2b_3b_4b_6} + \frac{a_3(b_2b_5b(phb_4+mdb_6)+b_4(nfbb_2b_6+pgab_3b_5)+b_3b_6a(neb_4+mcb_5)}{b_1b_2b_3b_4b_5b_6b_8}$
$B = B_r + B_i$
where
$B_r = \frac{(a_1b_6(dbb_2+cab_3)+a_2b_4(hbb_2+gab_3))}{b_1b_2b_3b_4b_6}$
$B_r = B_{r1} + B_{r2}$
$B_{r1} = \frac{(a_1(dbb_2+cab_3)}{b_1b_2b_3b_4}$,
$B_{r2} = \frac{a_2(hbb_2+gab_3)}{b_1b_2b_3b_6}$
and
$B_i = \frac{a_3(b_2b_5b(phb_4+mdb_6)+b_4(nfbb_2b_6+pgab_3b_5)+b_3b_6a(neb_4+mcb_5)}{b_1b_2b_3b_4b_5b_6b_8}$

with
$B_r = \frac{a_1b_6dbb_2}{b_1b_2b_3b_4b_6} + \frac{a_1b_6cab_3}{b_1b_2b_3b_4b_6} +$
$\frac{a_2b_4hbb_2}{b_1b_2b_3b_4b_6} + \frac{a_2b_4gab_3}{b_1b_2b_3b_4b_6}$

$B_r = B_{r1a} + B_{r1b} + B_{r2a} + B_{r2b}$
$B_{r1a} = \frac{a_1 b_6 dbb_2}{b_1 b_2 b_3 b_4 b_6} = \frac{a_1 b_6 db}{b_1 b_3 b_4 b_6} = \frac{a_1 db}{b_1 b_3 b_4}$
$B_{r1b} = \frac{a_1 b_6 cab_3}{b_1 b_2 b_3 b_4 b_6} = \frac{a_1 b_6 ca}{b_1 b_2 b_4 b_6} = \frac{a_1 ca}{b_1 b_2 b_4}$
$B_{r2a} = \frac{a_2 b_4 hbb_2}{b_1 b_2 b_3 b_4 b_6} = \frac{a_2 b_4 hb}{b_1 b_3 b_4 b_6} = \frac{a_2 hb}{b_1 b_3 b_6}$
$B_{r2b} = \frac{a_2 b_4 gab_3}{b_1 b_2 b_3 b_4 b_6} = \frac{a_2 b_4 ga}{b_1 b_2 b_4 b_6} = \frac{a_2 ga}{b_1 b_2 b_6}$

The basic reproductive number B is a crucial tool that helps in evaluating Ebola infectious disease transmission potential in a given susceptible population free of the disease at the time. It helps to quantify the mean number of the secondary Ebola disease infections generated by a single Ebola infected individual in the population that is wholly susceptible to Ebola disease. If the Basic reproduction number $B < 1$, the Ebola Virus infection quickly come to an end as the disease will not spread. However, the disease will spread through the population if $B > 1$.

3.3 Local stability analysis of the model DFE (C^f)

Here, we analyze local stability of the model DFE points (C^f) and show its local stability by showing that all the eigenvalues of the Jacobian matrix obtained from the linearization of the model system (8) and evaluated at C^f are negative. This is stated as a theorem and proven as follows;

Theorem 2

The DFE of the Fractional bola Model system (8) is locally asymptotically stable in Ω, if $B < 1$ and unstable $B > 1$.

Proof

The Jacobian matrix J of the model at the DFE point is obtained as follows:

$$J = \begin{bmatrix}
-h_1 & 0 & 0 & 0 & 0 & 0 & 0 & 0 & 0 & 0 & 0 & 0 & 0 & \tau & 0 & 0 & 0 & 0 \\
r & -h_2 & 0 & 0 & 0 & 0 & 0 & 0 & 0 & 0 & 0 & 0 & 0 & 0 & 0 & 0 & 0 & 0 \\
K_1 X & 0 & -h_3 & 0 & 0 & 0 & 0 & 0 & 0 & 0 & 0 & 0 & 0 & 0 & 0 & 0 & 0 & 0 \\
0 & \lambda & 0 & -\mu & 0 & 0 & 0 & 0 & 0 & 0 & -y_1 & 0 & -y_2 & 0 & -y_3 & 0 & 0 & -y_4 \\
0 & K_2 Z & 0 & 0 & -\mu & 0 & 0 & 0 & 0 & 0 & -x_1 & 0 & -x_2 & 0 & -x_3 & 0 & 0 & -x_4 \\
0 & 0 & \sigma & 0 & 0 & -\mu & 0 & 0 & 0 & 0 & -c_1 & 0 & -c_2 & 0 & -c_3 & 0 & 0 & -c_4 \\
0 & 0 & K_3 Y & 0 & 0 & 0 & -\mu & 0 & 0 & 0 & -d_1 & 0 & -d_2 & 0 & -d_3 & 0 & 0 & -d_4 \\
0 & 0 & 0 & 0 & 0 & 0 & 0 & -b_1 & 0 & 0 & a_1 & 0 & a_2 & 0 & a_3 & 0 & 0 & a_4 \\
0 & 0 & 0 & 0 & 0 & 0 & 0 & a & -b_2 & 0 & 0 & 0 & 0 & 0 & 0 & 0 & 0 & 0 \\
0 & 0 & 0 & 0 & 0 & 0 & 0 & b & 0 & -b_3 & 0 & 0 & 0 & 0 & 0 & 0 & 0 & 0 \\
0 & 0 & 0 & 0 & 0 & 0 & 0 & 0 & c & d & -b_4 & 0 & 0 & 0 & 0 & 0 & 0 & 0 \\
0 & 0 & 0 & 0 & 0 & 0 & 0 & 0 & e & f & 0 & -b_5 & 0 & 0 & 0 & 0 & 0 & 0 \\
0 & 0 & 0 & 0 & 0 & 0 & 0 & 0 & g & h & 0 & 0 & -b_6 & 0 & 0 & 0 & 0 & 0 \\
0 & 0 & 0 & 0 & 0 & 0 & 0 & 0 & 0 & w & k & x & 0 & -b_7 & 0 & 0 & 0 & 0 \\
0 & 0 & 0 & 0 & 0 & 0 & 0 & 0 & 0 & 0 & 0 & 0 & 0 & 0 & -b_8 & 0 & 0 & 0 \\
0 & 0 & 0 & 0 & 0 & 0 & 0 & 0 & 0 & 0 & 0 & 0 & 0 & 0 & 0 & -\mu_r & 0 & 0 \\
0 & 0 & 0 & 0 & 0 & 0 & 0 & 0 & 0 & 0 & 0 & 0 & 0 & 0 & 0 & 0 & -b_9 & 0 \\
0 & 0 & 0 & 0 & 0 & 0 & 0 & 0 & 0 & 0 & 0 & 0 & 0 & 0 & 0 & 0 & 0 & -b_{10}
\end{bmatrix} \tag{17}$$

where;

$$\left.\begin{aligned}
h_1 = (\mu + r + K_1 X), h_2 = (\mu + \lambda + K_2 Z), h_3 = (\mu + \sigma + K_3 Y), \\
y_1 = \frac{m_2 S^e_{vc}}{N}, y_2 = \frac{m_1 S^e_{vc}}{N}, y_3 = \frac{m_4 S^e_{vc}}{N}, y_4 = \frac{m_3 S^e_{vc}}{N} \\
x_1 = \frac{n_2 S^e_{vn}}{N}, x_2 = \frac{n_1 S^e_{vn}}{N}, x_3 = \frac{n_4 S^e_{vn}}{N}, x_4 = \frac{n_3 S^e_{vn}}{N} \\
c_1 = \frac{e_2 S^e_{uc}}{N}, c_2 = \frac{e_1 S^e_{uc}}{N}, c_3 = \frac{e_4 S^e_{uc}}{N}, c_4 = \frac{e_3 S^e_{uc}}{N} \\
d_1 = \frac{t_2 S^e_{un}}{N}, d_2 = \frac{t_1 S^e_{un}}{N}, d_3 = \frac{t_4 S^e_{un}}{N}, d_4 = \frac{t_3 S^e_{un}}{N}
\end{aligned}\right\} \tag{18}$$

with others as described in equations (13) and (14).

Applying matrix operations to (17) we obtain the following eigenvalues;

$$\left.\begin{aligned} \lambda_1 = -\mu, \lambda_2 = -\mu, \lambda_3 = -\mu, \lambda_4 = -\mu, \lambda_5 = -\mu_r, \\ \lambda_6 = -b_8, \lambda_7 = -b_9, \lambda_8 = -b_{10}, \lambda_9 = -h_2, \lambda_{10} = -h_3, \\ \lambda_{11} = -h_1, \lambda_{12} = -b_7 \; and \; \lambda_{13} = -b_5 \end{aligned}\right\} \tag{19}$$

which are all negative
With these obtained eigenvalues the matrix (17) reduces to;

$$J_e = \begin{bmatrix} -b_1 & 0 & 0 & a_1 & a_2 \\ a & -b_2 & 0 & 0 & 0 \\ 0 & 0 & -b_3 & 0 & 0 \\ 0 & c & d & -b_4 & 0 \\ 0 & g & h & 0 & -b_6 \end{bmatrix} \tag{20}$$

Using MATLAB software, we obtained the characteristic equation of (20) as follows;
$\lambda^5 + G_1\lambda^4 + G_2\lambda^3 + G_3\lambda^2 + G_4\lambda + G_5$
Where;
$G_1 = (b_1 + b_2 + b_3 + b_4 + b_6) > 0$
$G_2 = b_1(b_2 + b_3 + b_4 + b_6) + b_2(b_3 + b_4 + b_6)$
$+ b_3(b_4 + b_6) + b_4b_6 > 0$
$G_3 = b_1b_2b_3 + b_2b_3(b_4 + b_6) + b_4b_6(b_1 + b_2 + b_3) +$
$b_1b_2b_4(1 - B_{r1b}) + b_1b_2b_6(1 - B_{r2b}) +$
$b_1b_3b_4(1 - B_{r1a}) + b_1b_3b_6(1 - B_{r2a}) > 0 \; if \; B < 1$
$G_4 = b_2b_3b_4b_6 + b_1b_2b_3b_4(1 - B_{r1}) + b_1b_2b_3b_6(1 - B_{r2}) +$
$b_1b_3b_4b_6(1 - (B_{r1a} + B_{r2a})) +$
$b_1b_2b_4b_6(1 - (B_{r1b} + B_{r2b})) > 0 \;\; if \;\; B < 1)$
$G_5 = b_1b_2b_3b_4b_6(1 - Br) > 0 \;\; if \;\; B < 1$
By applying the Routh-Hurwitz criteria [34], the characteristic equation has a real root that is strictly negative if $G_1 > 0, G_2 > 0, G_3 > 0, G_4 > 0 \; and \; G_5 > 0$. Which we have shown that $G_1 > 0, G_2 > 0 \; with \; G_3, G_4 \; and \; G_5$ all greater than zero if $B < 1$.
Thus, we conclude that the fractional Ebola virus Model disease free-equilibrium point U^e of system (8) is locally asymptotically stable in Ω if $B < 1$.

4 Approximate solution of the Ebola Model applying Laplace-Adomian Decomposition Method(LADM)

In this section, we apply the Laplace - Adomian Decomposition Method (LADM) technique to the fractional order Ebola model (8)[20].

Applying Laplace transform to both sides of (8) we have;

$$
\left.\begin{aligned}
(1)S^{\alpha}\mathcal{L}\{S\} - S^{(\alpha-1)}S(0) &= \mathcal{L}\{P-(\mu+r+K_1X)S+\tau R\}\\
(2)S^{\alpha}\mathcal{L}\{S_v\} - S^{(\alpha-1)}S_v(0) &= \mathcal{L}\{rS-(\mu+\lambda+K_2Z)S_v\}\\
(3)S^{\alpha}\mathcal{L}\{S_u\} - S^{(\alpha-1)}S_u(0) &= \mathcal{L}\{K_1XS-(\mu+\sigma+K_3Y)S_u\}\\
(4)S^{\alpha}\mathcal{L}\{S_{vc}\} - S^{(\alpha-1)}S_{vc}(0) &= \mathcal{L}\{\lambda S_v-[\mu S_{vc}+1/N(m_1I_NS_{vc}+\\
&\quad m_2I_TS_{vc}+m_3I_rS_{vc}+m_4D_uS_{vc})]\}\\
(5)S^{\alpha}\mathcal{L}\{S_{vn}\} - S^{(\alpha-1)}S_{vn}(0) &= \mathcal{L}\{K_2ZS_v-[\mu S_{vn}+1/N(n_1I_NS_{vn}+\\
&\quad n_2I_TS_{vn}+n_3I_rS_{vn}+n_4D_uS_{vn})]\}\\
(6)S^{\alpha}\mathcal{L}\{S_{uc}\} - S^{(\alpha-1)}S_{uc}(0) &= \mathcal{L}\{\sigma S_u-[\mu S_{uc}+1/N(e_1I_NS_{uc}+\\
&\quad e_2I_TS_{uc}+e_3I_rS_{uc}+e_4D_uS_{uc})]\}\\
(7)S^{\alpha}\mathcal{L}\{S_{un}\} - S^{(\alpha-1)}S_{un}(0) &= \mathcal{L}\{K_3YS_u-[\mu S_{un}+1/N(t_1I_NS_{un}+\\
&\quad t_2I_TS_{un}+t_3I_rS_{un}+t_4D_uS_{un})]\}\\
(8)S^{\alpha}\mathcal{L}\{E\} - S^{(\alpha-1)}E(0) &= \mathcal{L}\{1/N[m_1I_NS_vc+m_2I_TS_vc+\\
&\quad m_3I_rS_vc+m_4D_uS_vc+n_1I_NS_vn+\\
&\quad n_2I_TS_vn+n_3I_rS_vn+n_4D_uS_vn+\\
&\quad e_1I_NS_uc+e_2I_TS_uc+e_3I_rS_uc+\\
&\quad e_4D_uS_uc+t_1I_NS_un+t_2I_TS_un+\\
&\quad t_3I_rS_un+t_4D_uS_un]-(\mu+\alpha_1+\alpha_2)E\}\\
(9)S^{\alpha}\mathcal{L}\{E_Q\} - S^{(\alpha-1)}E_Q(0) &= \mathcal{L}\{\alpha_1E-(\mu+\theta_1)E_Q\}\\
(10)S^{\alpha}\mathcal{L}\{E_T\} - S^{(\alpha-1)}E_T(0) &= \mathcal{L}\{\alpha_2E-(\mu+\theta_2+\rho)E_T\}\\
(11)S^{\alpha}\mathcal{L}\{I_T\} - S^{(\alpha-1)}I_T(0) &= \mathcal{L}\{\theta_1S_1E_Q+\theta_2S_1E_T-(\delta_1+J_2)I_T\}\\
(12)S^{\alpha}\mathcal{L}\{I_i\} - S^{(\alpha-1)}I_i(0) &= \mathcal{L}\{\theta_1S_2E_Q+\theta_2S_2E_T-(\delta_2+J_1)I_i\}\\
(13)S^{\alpha}\mathcal{L}\{I_N\} - S^{(\alpha-1)}I_N(0) &= \mathcal{L}\{\theta_1S_3E_Q+\theta_2S_3E_T-\delta_3I_N\}\\
(14)S^{\alpha}\mathcal{L}\{R\} - S^{(\alpha-1)}R(0) &= \mathcal{L}\{J_1I_i+J_2I_T+\rho E_T-\tau R\}\\
(15)S^{\alpha}\mathcal{L}\{D_u\} - S^{(\alpha-1)}D_u(0) &= \mathcal{L}\{\delta_3I_N+\delta_2I_i+\delta_1I_T\}\\
(16)S^{\alpha}\mathcal{L}\{S_r\} - S^{(\alpha-1)}S_r(0) &= \mathcal{L}\{\Lambda-\mu_rS_r\}\\
(17)S^{\alpha}\mathcal{L}\{E_r\} - S^{(\alpha-1)}E_r(0) &= \mathcal{L}\{\omega S_r-\mu_rE_r\}\\
(18)S^{\alpha}\mathcal{L}\{I_r\} - S^{(\alpha-1)}I_r(0) &= \mathcal{L}\{\phi E_r-(\mu_r+\delta_4)I_r\}
\end{aligned}\right\} \quad (21)
$$

Applying the initial conditions (2) to (8) and dividing by S^α gives the following;

$$\left.\begin{aligned}
(1)\mathcal{L}\{S\} &= \frac{g_1}{S} + \frac{1}{S^\alpha}[\mathcal{L}\{P-(\mu+r+K_1X)S+\tau R\}]\\
(2)\mathcal{L}\{S_v\} &= \frac{g_2}{S} + \frac{1}{S^\alpha}[\mathcal{L}\{rS-(\mu+\lambda+K_2Z)S_v\}]\\
(3)\mathcal{L}\{S_u\} &= \frac{g_3}{S} + \frac{1}{S^\alpha}[\mathcal{L}\{K_1XS-(\mu+\sigma+K_3Y)S_u\}]\\
(4)\mathcal{L}\{S_{vc}\} &= \frac{g_4}{S} + \frac{1}{S^\alpha}[\mathcal{L}\{\lambda S_v-[\mu S_{vc}+1/N(m_1I_NS_{vc}+\\
&\quad m_2I_TS_{vc}+m_3I_rS_{vc}+m_4D_uS_{vc})]\}]\\
(5)\mathcal{L}\{S_{vn}\} &= \frac{g_5}{S} + \frac{1}{S^\alpha}[\mathcal{L}\{K_2ZS_v-[\mu S_{vn}+1/N(n_1I_NS_{vn}+\\
&\quad n_2I_TS_{vn}+n_3I_rS_{vn}+n_4D_uS_{vn})]\}]\\
(6)\mathcal{L}\{S_{uc}\} &= \frac{g_6}{S} + \frac{1}{S^\alpha}[\mathcal{L}\{\sigma S_u-[\mu S_{uc}+1/N(e_1I_NS_{uc}+\\
&\quad e_2I_TS_{uc}+e_3I_rS_{uc}+e_4D_uS_{uc})]\}]\\
(7)\mathcal{L}\{S_{un}\} &= \frac{g_7}{S} + \frac{1}{S^\alpha}[\mathcal{L}\{K_3YS_u-[\mu S_{un}+1/N(t_1I_NS_{un}+\\
&\quad t_2I_TS_{un}+t_3I_rS_{un}+t_4D_uS_{un})]\}]\\
(8)\mathcal{L}\{E\} &= \frac{g_8}{S} + \frac{1}{S^\alpha}[\mathcal{L}\{1/N[m_1I_NS_vc+m_2I_TS_vc+\\
&\quad m_3I_rS_vc+m_4D_uS_vc+n_1I_NS_vn+\\
&\quad n_2I_TS_vn+n_3I_rS_vn+n_4D_uS_vn+\\
&\quad e_1I_NS_uc+e_2I_TS_uc+e_3I_rS_uc+\\
&\quad e_4D_uS_uc+t_1I_NS_un+t_2I_TS_un+\\
&\quad t_3I_rS_un+t_4D_uS_un]-(\mu+\alpha_1+\alpha_2)E\}]\\
(9)\mathcal{L}\{E_Q\} &= \frac{g_9}{S} + \frac{1}{S^\alpha}[\mathcal{L}\{\alpha_1E-(\mu+\theta_1)E_Q\}]\\
(10)\mathcal{L}\{E_T\} &= \frac{g_{10}}{S} + \frac{1}{S^\alpha}[\mathcal{L}\{\alpha_2E-(\mu+\theta_2+\rho)E_T\}]\\
(11)\mathcal{L}\{I_T\} &= \frac{g_{11}}{S} + \frac{1}{S^\alpha}[\mathcal{L}\{\theta_1S_1E_Q+\theta_2S_1E_T-(\delta_1+J_2)I_T\}]\\
(12)\mathcal{L}\{I_i\} &= \frac{g_{12}}{S} + \frac{1}{S^\alpha}[\mathcal{L}\{\theta_1S_2E_Q+\theta_2S_2E_T-(\delta_2+J_1)I_i\}]\\
(13)\mathcal{L}\{I_N\} &= \frac{g_{13}}{S} + \frac{1}{S^\alpha}[\mathcal{L}\{\theta_1S_3E_Q+\theta_2S_3E_T-\delta_3I_N\}]\\
(14)\mathcal{L}\{R\} &= \frac{g_{14}}{S} + \frac{1}{S^\alpha}[\mathcal{L}\{J_1I_i+J_2I_T+\rho E_T-\tau R\}]\\
(15)\mathcal{L}\{D_u\} &= \frac{g_{15}}{S} + \frac{1}{S^\alpha}[\mathcal{L}\{\delta_3I_N+\delta_2I_i+\delta_1I_T\}]\\
(16)\mathcal{L}\{S_r\} &= \frac{g_{16}}{S} + \frac{1}{S^\alpha}[\mathcal{L}\{\Lambda-\mu_rS_r\}]\\
(17)\mathcal{L}\{E_r\} &= \frac{g_{17}}{S} + \frac{1}{S^\alpha}[\mathcal{L}\{\omega S_r-\mu_rE_r\}]\\
(18)\mathcal{L}\{I_r\} &= \frac{g_{18}}{S} + \frac{1}{S^\alpha}[\mathcal{L}\{\phi E_r-(\mu_r+\delta_4)I_r\}]
\end{aligned}\right\} \quad (22)$$

Assuming that the solutions of
$S(t), S_v(t), S_u(t), S_{vc}(t), S_{vn}(t), S_{uc}(t), S_{un}(t), E(t), E_Q(t),$
$E_T(t), I_T(t), I_i(t), I_N(t), R(t), D_u(t), S_r(t), E_r(t), I_r(t)$

are in the form of infinite series given by;

$$\left.\begin{aligned} S(t)=\sum_{(n=0)}^{\infty}S_n, S_v(t)=\sum_{(n=0)}^{\infty}S_{v_n} \\ S_u(t)=\sum_{(n=0)}^{\infty}S_{u_n}, S_{vc}(t)=\sum_{(n=0)}^{\infty}S_{vc_n} \\ S_{vn}(t)=\sum_{(n=0)}^{\infty}S_{vn_n}, S_{uc}(t)=\sum_{(n=0)}^{\infty}S_{uc_n} \\ S_{un}(t)=\sum_{(n=0)}^{\infty}S_{un_n}, E(t)=\sum_{(n=0)}^{\infty}E_n \\ E_Q(t)=\sum_{(n=0)}^{\infty}E_{Q_n}, E_T(t)=\sum_{(n=0)}^{\infty}E_{T_n} \\ I_T(t)=\sum_{(n=0)}^{\infty}I_{T_n}, I_i(t)=\sum_{(n=0)}^{\infty}I_{i_n} \\ I_N(t)=\sum_{(n=0)}^{\infty}I_{N_n}, R(t)=\sum_{(n=0)}^{\infty}R_n \\ D_u(t)=\sum_{(n=0)}^{\infty}D_{u_n}, S_r(t)=\sum_{(n=0)}^{\infty}S_{r_n} \\ E_r(t)=\sum_{(n=0)}^{\infty}E_{r_n}, I_r(t)=\sum_{(n=0)}^{\infty}I_{r_n} \end{aligned}\right\} \tag{23}$$

We then decompose the nonlinear terms of the Ebola fractional order model (8) before we proceed as follows;

$$\left.\begin{aligned} I_N(t)S_{vc}(t)=\sum_{(n=0)}^{\infty}A_n \\ I_T(t)S_{vc}(t)=\sum_{(n=0)}^{\infty}B_n \\ I_r(t)S_{vc}(t)=\sum_{(n=0)}^{\infty}F_n \\ D_u(t)S_{vc}(t)=\sum_{(n=0)}^{\infty}G_n \\ I_N(t)S_{vn}(t)=\sum_{(n=0)}^{\infty}H_n \\ I_T(t)S_{vn}(t)=\sum_{(n=0)}^{\infty}L_n \\ I_r(t)S_{vn}(t)=\sum_{(n=0)}^{\infty}Q_n \\ D_u(t)S_{vn}(t)=\sum_{(n=0)}^{\infty}T_n \\ I_N(t)S_{uc}(t)=\sum_{(n=0)}^{\infty}U_n \\ I_T(t)S_{uc}(t)=\sum_{(n=0)}^{\infty}V_n \\ I_r(t)S_{uc}(t)=\sum_{(n=0)}^{\infty}W_n \\ D_u(t)S_{uc}(t)=\sum_{(n=0)}^{\infty}X_n \\ I_N(t)S_{un}(t)=\sum_{(n=0)}^{\infty}Y_n \\ I_T(t)S_{un}(t)=\sum_{(n=0)}^{\infty}Z_n \\ I_r(t)S_{un}(t)=\sum_{(n=0)}^{\infty}N_n \\ D_u(t)S_{un}(t)=\sum_{(n=0)}^{\infty}M_n \end{aligned}\right\} \tag{24}$$

Where the Adomian polynomials in (24) are defined as follows;

$$\left.\begin{aligned}
A_n &= \frac{1}{\Gamma(n+1)}\frac{d^n}{d\lambda^n}\{\sum_{(k=0)}^{n}\lambda^k I_{Nk}(t)\sum_{(k=0)}^{n}\lambda^k S_{vck}(t)\}|_{(\lambda=0)}\\
B_n &= \frac{1}{\Gamma(n+1)}\frac{d^n}{d\lambda^n}\{\sum_{(k=0)}^{n}\lambda^k I_{Tk}(t)\sum_{(k=0)}^{n}\lambda^k S_{vck}(t)\}|_{(\lambda=0)}\\
F_n &= \frac{1}{\Gamma(n+1)}\frac{d^n}{d\lambda^n}\{\sum_{(k=0)}^{n}\lambda^k I_{rk}(t)\sum_{(k=0)}^{n}\lambda^k S_{vck}(t)\}|_{(\lambda=0)}\\
G_n &= \frac{1}{\Gamma(n+1)}\frac{d^n}{d\lambda^n}\{\sum_{(k=0)}^{n}\lambda^k D_{uk}(t)\sum_{(k=0)}^{n}\lambda^k S_{vck}(t)\}|_{(\lambda=0)}\\
H_n &= \frac{1}{\Gamma(n+1)}\frac{d^n}{d\lambda^n}\{\sum_{(k=0)}^{n}\lambda^k I_{Nk}(t)\sum_{(k=0)}^{n}\lambda^k S_{vnk}(t)\}|_{(\lambda=0)}\\
L_n &= \frac{1}{\Gamma(n+1)}\frac{d^n}{d\lambda^n}\{\sum_{(k=0)}^{n}\lambda^k I_{Tk}(t)\sum_{(k=0)}^{n}\lambda^k S_{vnk}(t)\}|_{(\lambda=0)}\\
Q_n &= \frac{1}{\Gamma(n+1)}\frac{d^n}{d\lambda^n}\{\sum_{(k=0)}^{n}\lambda^k I_{rk}(t)\sum_{(k=0)}^{n}\lambda^k S_{vnk}(t)\}|_{(\lambda=0)}\\
T_n &= \frac{1}{\Gamma(n+1)}\frac{d^n}{d\lambda^n}\{\sum_{(k=0)}^{n}\lambda^k D_{uk}(t)\sum_{(k=0)}^{n}\lambda^k S_{vnk}(t)\}|_{(\lambda=0)}\\
U_n &= \frac{1}{\Gamma(n+1)}\frac{d^n}{d\lambda^n}\{\sum_{(k=0)}^{n}\lambda^k I_{Nk}(t)\sum_{(k=0)}^{n}\lambda^k S_{uck}(t)\}|_{(\lambda=0)}\\
V_n &= \frac{1}{\Gamma(n+1)}\frac{d^n}{d\lambda^n}\{\sum_{(k=0)}^{n}\lambda^k I_{Tk}(t)\sum_{(k=0)}^{n}\lambda^k S_{uck}(t)\}|_{(\lambda=0)}\\
W_n &= \frac{1}{\Gamma(n+1)}\frac{d^n}{d\lambda^n}\{\sum_{(k=0)}^{n}\lambda^k I_{rk}(t)\sum_{(k=0)}^{n}\lambda^k S_{uck}(t)\}|_{(\lambda=0)}\\
X_n &= \frac{1}{\Gamma(n+1)}\frac{d^n}{d\lambda^n}\{\sum_{(k=0)}^{n}\lambda^k D_{uk}(t)\sum_{(k=0)}^{n}\lambda^k S_{uck}(t)\}|_{(\lambda=0)}\\
Y_n &= \frac{1}{\Gamma(n+1)}\frac{d^n}{d\lambda^n}\{\sum_{(k=0)}^{n}\lambda^k I_{Nk}(t)\sum_{(k=0)}^{n}\lambda^k S_{unk}(t)\}|_{(\lambda=0)}\\
Z_n &= \frac{1}{\Gamma(n+1)}\frac{d^n}{d\lambda^n}\{\sum_{(k=0)}^{n}\lambda^k I_{Tk}(t)\sum_{(k=0)}^{n}\lambda^k S_{unk}(t)\}|_{(\lambda=0)}\\
N_n &= \frac{1}{\Gamma(n+1)}\frac{d^n}{d\lambda^n}\{\sum_{(k=0)}^{n}\lambda^k I_{rk}(t)\sum_{(k=0)}^{n}\lambda^k S_{unk}(t)\}|_{(\lambda=0)}\\
M_n &= \frac{1}{\Gamma(n+1)}\frac{d^n}{d\lambda^n}\{\sum_{(k=0)}^{n}\lambda^k D_{uk}(t)\sum_{(k=0)}^{n}\lambda^k S_{unk}(t)\}|_{(\lambda=0)}
\end{aligned}\right\} \quad (25)$$

From the definitions in (25) when $n = 0$ we have the following;

$$\left.\begin{aligned}
A_0 &= \frac{1}{\Gamma(1)}\frac{d^0}{d\lambda^0}[\lambda^0 I_{N0}][\lambda^0 S_{vc0}] = I_{N0}S_{vc0}\\
B_0 &= \frac{1}{\Gamma(1)}\frac{d^0}{d\lambda^0}[\lambda^0 I_{T0}][\lambda^0 S_{vc0}] = I_{T0}S_{vc0}\\
F_0 &= \frac{1}{\Gamma(1)}\frac{d^0}{d\lambda^0}[\lambda^0 I_{r0}][\lambda^0 S_{vc0}] = I_{r0}S_{vc0}\\
G_0 &= \frac{1}{\Gamma(1)}\frac{d^0}{d\lambda^0}[\lambda^0 D_{u0}][\lambda^0 S_{vc0}] = D_{u0}S_{vc0}\\
H_0 &= \frac{1}{\Gamma(1)}\frac{d^0}{d\lambda^0}[\lambda^0 I_{N0}][\lambda^0 S_{vn0}] = I_{N0}S_{vn0}\\
L_0 &= \frac{1}{\Gamma(1)}\frac{d^0}{d\lambda^0}[\lambda^0 I_{T0}][\lambda^0 S_{vn0}] = I_{T0}S_{vn0}\\
Q_0 &= \frac{1}{\Gamma(1)}\frac{d^0}{d\lambda^0}[\lambda^0 I_{r0}][\lambda^0 S_{vn0}] = I_{r0}S_{vn0}\\
T_0 &= \frac{1}{\Gamma(1)}\frac{d^0}{d\lambda^0}[\lambda^0 D_{u0}][\lambda^0 S_{vn0}] = D_{u0}S_{vn0}\\
U_0 &= \frac{1}{\Gamma(1)}\frac{d^0}{d\lambda^0}[\lambda^0 I_{N0}][\lambda^0 S_{uc0}] = I_{N0}S_{uc0}\\
V_0 &= \frac{1}{\Gamma(1)}\frac{d^0}{d\lambda^0}[\lambda^0 I_{T0}][\lambda^0 S_{uc0}] = I_{T0}S_{uc0}\\
W_0 &= \frac{1}{\Gamma(1)}\frac{d^0}{d\lambda^0}[\lambda^0 I_{r0}][\lambda^0 S_{uc0}] = I_{r0}S_{uc0}\\
X_0 &= \frac{1}{\Gamma(1)}\frac{d^0}{d\lambda^0}[\lambda^0 D_{u0}][\lambda^0 S_{uc0}] = D_{u0}S_{uc0}\\
Y_0 &= \frac{1}{\Gamma(1)}\frac{d^0}{d\lambda^0}[\lambda^0 I_{N0}][\lambda^0 S_{un0}] = I_{N0}S_{un0}\\
Z_0 &= \frac{1}{\Gamma(1)}\frac{d^0}{d\lambda^0}[\lambda^0 I_{T0}][\lambda^0 S_{un0}] = I_{T0}S_{un0}\\
N_0 &= \frac{1}{\Gamma(1)}\frac{d^0}{d\lambda^0}[\lambda^0 I_{r0}][\lambda^0 S_{un0}] = I_{r0}S_{un0}\\
M_0 &= \frac{1}{\Gamma(1)}\frac{d^0}{d\lambda^0}[\lambda^0 D_{u0}][\lambda^0 S_{un0}] = D_{u0}S_{un0}
\end{aligned}\right\} \tag{26}$$

Similarly, when $n = 1$ we have the following;

$$\left.\begin{aligned}
A_1 &= \frac{1}{\Gamma(2)}\frac{d}{d\lambda}[I_{N0}+\lambda I_{N1}][S_{vc0}+\lambda S_{vc1}]|_{(\lambda=0)} = I_{N0}S_{vc1}+I_{N1}S_{vc0}\\
B_1 &= \frac{1}{\Gamma(2)}\frac{d}{d\lambda}[I_{T0}+\lambda I_{T1}][S_{vc0}+\lambda S_{vc1}]|_{(\lambda=0)} = I_{T0}S_{vc1}+I_{T1}S_{vc0}\\
F_1 &= \frac{1}{\Gamma(2)}\frac{d}{d\lambda}[I_{r0}+\lambda I_{r1}][S_{vc0}+\lambda S_{vc1}]|_{(\lambda=0)} = I_{r0}S_{vc1}+I_{r1}S_{vc0}\\
G_1 &= \frac{1}{\Gamma(2)}\frac{d}{d\lambda}[D_{u0}+\lambda D_{u1}][S_{vc0}+\lambda S_{vc1}]|_{(\lambda=0)} = D_{u0}S_{vc1}+D_{u1}S_{vc0}\\
H_1 &= \frac{1}{\Gamma(2)}\frac{d}{d\lambda}[I_{N0}+\lambda I_{N1}][S_{vn0}+\lambda S_{vn1}]|_{(\lambda=0)} = I_{N0}S_{vn1}+I_{N1}S_{vn0}\\
L_1 &= \frac{1}{\Gamma(2)}\frac{d}{d\lambda}[I_{T0}+\lambda I_{T1}][S_{vn0}+\lambda S_{vn1}]|_{(\lambda=0)} = I_{T0}S_{vn1}+I_{T1}S_{vn0}\\
Q_1 &= \frac{1}{\Gamma(2)}\frac{d}{d\lambda}[I_{r0}+\lambda I_{r1}][S_{vn0}+\lambda S_{vn1}]|_{(\lambda=0)} = I_{r0}S_{vn1}+I_{r1}S_{vn0}\\
T_1 &= \frac{1}{\Gamma(2)}\frac{d}{d\lambda}[D_{u0}+\lambda D_{u1}][S_{vn0}+\lambda S_{vn1}]|_{(\lambda=0)} = D_{u0}S_{vn1}+D_{u1}S_{vn0}\\
U_1 &= \frac{1}{\Gamma(2)}\frac{d}{d\lambda}[I_{N0}+\lambda I_{N1}][S_{uc0}+\lambda S_{uc1}]|_{(\lambda=0)} = I_{N0}S_{uc1}+I_{N1}S_{uc0}\\
V_1 &= \frac{1}{\Gamma(2)}\frac{d}{d\lambda}[I_{T0}+\lambda I_{T1}][S_{uc0}+\lambda S_{uc1}]|_{(\lambda=0)} = I_{T0}S_{uc1}+I_{T1}S_{uc0}\\
W_1 &= \frac{1}{\Gamma(2)}\frac{d}{d\lambda}[I_{r0}+\lambda I_{r1}][S_{uc0}+\lambda S_{uc1}]|_{(\lambda=0)} = I_{r0}S_{uc1}+I_{r1}S_{uc0}\\
X_1 &= \frac{1}{\Gamma(2)}\frac{d}{d\lambda}[D_{u0}+\lambda D_{u1}][S_{uc0}+\lambda S_{uc1}]|_{(\lambda=0)} = D_{u0}S_{uc1}+D_{u1}S_{uc0}\\
Y_1 &= \frac{1}{\Gamma(2)}\frac{d}{d\lambda}[I_{N0}+\lambda I_{N1}][S_{un0}+\lambda S_{un1}]|_{(\lambda=0)} = I_{N0}S_{un1}+I_{N1}S_{un0}\\
Z_1 &= \frac{1}{\Gamma(2)}\frac{d}{d\lambda}[I_{T0}+\lambda I_{T1}][S_{un0}+\lambda S_{un1}]|_{(\lambda=0)} = I_{T0}S_{un1}+I_{T1}S_{un0}\\
N_1 &= \frac{1}{\Gamma(2)}\frac{d}{d\lambda}[I_{r0}+\lambda I_{r1}][S_{un0}+\lambda S_{un1}]|_{(\lambda=0)} = I_{r0}S_{un1}+I_{r1}S_{un0}\\
M_1 &= \frac{1}{\Gamma(2)}\frac{d}{d\lambda}[D_{u0}+\lambda D_{u1}][S_{un0}+\lambda S_{un1}]|_{(\lambda=0)} = D_{u0}S_{un1}+D_{u1}S_{un0}
\end{aligned}\right\} \tag{27}$$

We substitute (22) for $n = 0$ into (23) and (24) to have the following;

$$\left.\begin{aligned}
&\mathcal{L}\{S_0\} = \frac{g_1}{S}, \mathcal{L}\{S_{v0}\} = \frac{g_2}{S}, \mathcal{L}\{S_{u0}\} = \frac{g_3}{S}, \mathcal{L}\{S_{vc0}\} = \frac{g_4}{S}, \mathcal{L}\{S_{vn0}\} = \frac{g_5}{S}, \mathcal{L}\{S_{uc0}\} = \frac{g_6}{S},\\
&\mathcal{L}\{S_{un0}\} = \frac{g_7}{S}, \mathcal{L}\{E_0\} = \frac{g_8}{S}, \mathcal{L}\{E_{Q0}\} = \frac{g_9}{S}, \mathcal{L}\{E_{T0}\} = \frac{g_{10}}{S}, \mathcal{L}\{I_{T0}\} = \frac{g_{11}}{S}, \mathcal{L}\{I_{i0}\} = \frac{g_{12}}{S},\\
&\mathcal{L}\{I_{N0}\} = \frac{g_{13}}{S}, \mathcal{L}\{R_0\} = \frac{g_{14}}{S}, \mathcal{L}\{D_{u0}\} = \frac{g_{15}}{S}, \mathcal{L}\{S_{r0}\} = \frac{g_{16}}{S}, \mathcal{L}\{E_{r0}\} = \frac{g_{17}}{S}, \mathcal{L}\{I_{r0}\} = \frac{g_{18}}{S}
\end{aligned}\right\} \tag{28}$$

Similarly, for $n = 1\ to\ n = n + 1$, we obtain the following:

$$
\left.
\begin{aligned}
\mathcal{L}\{S_1\} &= \frac{1}{S^\alpha}[\mathcal{L}\{P^\smile(\mu + r + K_1X)S_0 + \tau R_0\}] \\
\mathcal{L}\{S_{v1}\} = \frac{1}{S^\alpha}[\mathcal{L}\{rS_0{}^\smile(\mu + \lambda + K_2Z)S_{v0}\}], \mathcal{L}\{S_{u1}\} &= \frac{1}{S^\alpha}[\mathcal{L}\{K_1XS_0{}^\smile(\mu + \sigma + K_3Y)S_{u0}\}] \\
\mathcal{L}\{S_{vc1}\} &= \frac{1}{S^\alpha}[\mathcal{L}\{\lambda S_{v0} - [\mu S_{vc0} + 1/N(m_1A_0 + m_2B_0 + m_3F_0 + m_4G_0)]\}] \\
\mathcal{L}\{S_{vn1}\} &= \frac{1}{S^\alpha}[\mathcal{L}\{K_2ZS_{v0} - [\mu S_{vn0} + 1/N(n_1H_0 + n_2L_0 + n_3Q_0 + n_4T_0)]\}] \\
\mathcal{L}\{S_{uc1}\} &= \frac{1}{S^\alpha}[\mathcal{L}\{\sigma S_{u0} - [\mu S_{uc0} + 1/N(e_1U_0 + e_2V_0 + e_3W_0 + e_4X_0)]\}] \\
\mathcal{L}\{S_{un1}\} &= \frac{1}{S^\alpha}[\mathcal{L}\{K_3YS_{u0} - [\mu S_{un0} + 1/N(t_1Y_0 + t_2Z_0 + t_3N_0 + t_4M_0)]\}] \\
\mathcal{L}\{E_1\} = \frac{1}{S^\alpha}[\mathcal{L}\{1/N[m_1A_0 + m_2B_0 + m_3F_0 + m_4G_0 + n_1H_0 + n_2L_0 + n_3Q_0 + n_4T_0 + e_1U_0 + e_2V_0 \\
+e_3W_0 + e_4X_0 + t_1Y_0 + t_2Z_0 + t_3N_0 + t_4M_0] - (\mu + \alpha_1 + \alpha_2)E_0\}] \\
\mathcal{L}\{E_{Q1}\} = \frac{1}{S^\alpha}[\mathcal{L}\{\alpha_1E_0{}^\smile(\mu + \theta_1)E_{Q0}\}], \mathcal{L}\{E_{T1}\} &= \frac{1}{S^\alpha}[\mathcal{L}\{\alpha_2E_0{}^\smile(\mu + \theta_2 + \rho)E_{T0}\}] \\
\mathcal{L}\{I_{T1}\} &= \frac{1}{S^\alpha}[\mathcal{L}\{\theta_1S_1E_{Q0} + \theta_2S_1E_{T0}{}^\smile(\mu + \delta_1 + J_2)I_{T0}\}] \\
\mathcal{L}\{I_{i1}\} &= \frac{1}{S^\alpha}[\mathcal{L}\{\theta_1S_2E_{Q0} + \theta_2S_2E_{T0}{}^\smile(\mu + \delta_2 + J_1)I_{i0}\}] \\
\mathcal{L}\{I_{N1}\} = \frac{1}{S^\alpha}[\mathcal{L}\{\theta_1S_3E_{Q0} + \theta_2S_3E_{T0}{}^\smile(\mu + \delta_3)I_{N0}\}], \mathcal{L}\{R_1\} &= \frac{1}{S^\alpha}[\mathcal{L}\{J_1I_{i0} + J_2I_{T0} + \rho E_{T0} - (\mu - \tau)R_0\}] \\
\mathcal{L}\{D_{u1}\} = \frac{1}{S^\alpha}[\mathcal{L}\{\delta_3I_{N0} + \delta_2I_{i0} + \delta_1I_{T0} - qD_{u0}\}], \mathcal{L}\{S_{r1}\} &= \frac{1}{S^\alpha}[\mathcal{L}\{\Lambda^\smile(\mu_r + \omega)S_{r0}\}] \\
\mathcal{L}\{E_{r1}\} = \frac{1}{S^\alpha}[\mathcal{L}\{\omega S_{r0}{}^\smile(\mu_r + \phi)E_{r0}\}], \mathcal{L}\{I_{r1}\} &= \frac{1}{S^\alpha}[\mathcal{L}\{\phi E_{r0}{}^\smile(\mu_r - \delta_4I_{r0}\}] \\
\ldots = \ldots, \mathcal{L}\{S_{(n+1)}\} &= \frac{1}{S^\alpha}[\mathcal{L}\{P^\smile(\mu + r + K_1X)S_n + \tau R_n\}] \\
\mathcal{L}\{S_{v(n+1)}\} = \frac{1}{S^\alpha}[\mathcal{L}\{rS_n{}^\smile(\mu + \lambda + K_2Z)S_{v_n}\}], \mathcal{L}\{S_{u(n+1)}\} &= \frac{1}{S^\alpha}[\mathcal{L}\{K_1XS_n{}^\smile(\mu + \sigma + K_3Y)S_{u_n}\}] \\
\mathcal{L}\{S_{vc(n+1)}\} &= \frac{1}{S^\alpha}[\mathcal{L}\{\lambda S_{v_n} - [\mu S_{vc_n} + 1/N(m_1A_n + m_2B_n + m_3F_n + m_4G_n)]\}] \\
\mathcal{L}\{S_{vn(n+1)}\} &= \frac{1}{S^\alpha}[\mathcal{L}\{K_2ZS_{v_n} - [\mu S_{vn_n} + 1/N(n_1H_n + n_2L_n + n_3Q_n + n_4T_n)]\}] \\
\mathcal{L}\{S_{uc(n+1)}\} &= \frac{1}{S^\alpha}[\mathcal{L}\{\sigma S_{u_n} - [\mu S_{uc_n} + 1/N(e_1U_n + e_2V_n + e_3W_n + e_4X_n)]\}] \\
\mathcal{L}\{S_{un(n+1)}\} &= \frac{1}{S^\alpha}[\mathcal{L}\{K_3YS_{u_n} - [\mu S_{un_n} + 1/N(t_1Y_n + t_2Z_n + t_3N_n + t_4M_n)]\}] \\
\mathcal{L}\{E_{(n+1)}\} = \frac{1}{S^\alpha}[\mathcal{L}\{1/N[m_1A_n + m_2B_n + m_3F_n + m_4G_n + n_1H_n + n_2L_n + n_3Q_n + n_4T_n + e_1U_n + e_2V_n \\
+e_3W_n + e_4X_n + t_1Y_n + t_2Z_n + t_3N_n + t_4M_n] - (\mu + \alpha_1 + \alpha_2)E_n\}] \\
\mathcal{L}\{E_{Q(n+1)}\} = \frac{1}{S^\alpha}[\mathcal{L}\{\alpha_1E_n{}^\smile(\mu + \theta_1)E_{Q_n}\}], \mathcal{L}\{E_{T(n+1)}\} &= \frac{1}{S^\alpha}[\mathcal{L}\{\alpha_2E_n{}^\smile(\alpha + \theta_2 + \rho)E_{T_n}\}] \\
\mathcal{L}\{I_{T(n+1)}\} &= \frac{1}{S^\alpha}[\mathcal{L}\{\theta_1S_1E_{Q_n} + \theta_2S_1E_{T_n}{}^\smile(\mu + \delta_1 + J_2)I_{T_n}\}] \\
\mathcal{L}\{I_{i(n+1)}\} &= \frac{1}{S^\alpha}[\mathcal{L}\{\theta_1S_2E_{Q_n} + \theta_2S_2E_{T_n}{}^\smile(\mu + \delta_2 + J_1)I_{i_n}\}] \\
\mathcal{L}\{I_{N(n+1)}\} = \frac{1}{S^\alpha}[\mathcal{L}\{\theta_1S_2E_{Q_n} + \theta_2S_3E_{T_n}{}^\smile(\mu + \delta_3)I_{N_n}\}], \mathcal{L}\{R_{(n+1)}\} &= \frac{1}{S^\alpha}[\mathcal{L}\{J_1I_{i_n} + J_2I_{T_n} + \rho E_{T_n} - \rho R_n\}] \\
\mathcal{L}\{D_{u(n+1)}\} = \frac{1}{S^\alpha}[\mathcal{L}\{\delta_3I_{N_n} + \delta_2I_{i_n} + \delta_1I_{T_n} - qD_n\}], \mathcal{L}\{S_{r(n+1)}\} &= \frac{1}{S^\alpha}[\mathcal{L}\{\Lambda^\smile(\mu_r + \omega)S_{r_n}\}] \\
\mathcal{L}\{E_{r(n+1)}\} = \frac{1}{S^\alpha}[\mathcal{L}\{\omega S_{r_n}{}^\smile(/mu_r + \phi)E_{r_n}\}], \mathcal{L}\{I_{r(n+1)}\} &= \frac{1}{S^\alpha}[\mathcal{L}\{\phi E_{r_n}{}^\smile(\mu + \delta_4)I_{r_n}\}]
\end{aligned}
\right\} \tag{29}
$$

Evaluating the Laplace transforms on the right hand side of (29) we have the following;

$$
\left.
\begin{aligned}
\mathcal{L}\{S_1\} &= \{P^{\smile}(\mu + r + K_1X)S_0 + \tau R_0\}\frac{1}{S^{\alpha+1}} \\
\mathcal{L}\{S_{v1}\} = \{rS_0{}^{\smile}(\mu + \lambda + K_2Z)S_{v0}\}\frac{1}{S^{\alpha+1}}, &\mathcal{L}\{S_{u1}\} = \{K_1XS_0{}^{\smile}(\mu + \sigma + K_3Y)S_{u0}\}\frac{1}{S^{\alpha+1}} \\
\mathcal{L}\{S_{vc1}\} &= \{\lambda S_{v0} - [\mu S_{vc0} + 1/N(m_1A_0 + m_2B_0 + m_3F_0 + m_4G_0)]\}\frac{1}{S^{\alpha+1}} \\
\mathcal{L}\{S_{vn1}\} &= \{K_2ZS_{v0} - [\mu S_{vn0} + 1/N(n_1H_0 + n_2L_0 + n_3Q_0 + n_4T_0)]\}\frac{1}{S^{\alpha+1}} \\
\mathcal{L}\{S_{uc1}\} &= \{\sigma S_{u0} - [\mu S_{uc0} + 1/N(e_1U_0 + e_2V_0 + e_3W_0 + e_4X_0)]\}\frac{1}{S^{\alpha+1}} \\
\mathcal{L}\{S_{un1}\} &= \{K_3YS_{u0} - [\mu S_{un0} + 1/N(t_1Y_0 + t_2Z_0 + t_3N_0 + t_4M_0)]\}\frac{1}{S^{\alpha+1}} \\
\mathcal{L}\{E_1\} = \{1/N[&m_1A_0 + m_2B_0 + m_3F_0 + m_4G_0 + n_1H_0 + n_2L_0 + n_3Q_0 + n_4T_0 + e_1U_0 + e_2V_0 \\
&+e_3W_0 + e_4X_0 + t_1Y_0 + t_2Z_0 + t_3N_0 + t_4M_0] - (\mu + \alpha_1 + \alpha_2)E_0\}\frac{1}{S^{\alpha+1}} \\
\mathcal{L}\{E_{Q1}\} = \{\alpha_1E_0{}^{\smile}(\mu + \theta_1)E_{Q0}\}\frac{1}{S^{\alpha+1}}, &\mathcal{L}\{E_{T1}\} = \{\alpha_2E_0{}^{\smile}(\mu + \theta_2 + \rho)E_{T0}\}\frac{1}{S^{\alpha+1}} \\
\mathcal{L}\{I_{T1}\} &= \{\theta_1S_1E_{Q0} + \theta_2S_1E_{T0}{}^{\smile}(\mu + \delta_1 + J_2)I_{T0}\}\frac{1}{S^{\alpha+1}} \\
\mathcal{L}\{I_{i1}\} &= \{\theta_1S_2E_{Q0} + \theta_2S_2E_{T0}{}^{\smile}(\mu + \delta_2 + J_1)I_{i0}\}\frac{1}{S^{\alpha+1}} \\
\mathcal{L}\{I_{N1}\} = \{\theta_1S_3E_{Q0} + \theta_2S_3E_{T0}{}^{\smile}(\mu + \delta_3)I_{N0}\}\frac{1}{S^{\alpha+1}}, &\mathcal{L}\{R_1\} = \{J_1I_{i0} + J_2I_{T0} + \rho E_{T0} - (\mu - \tau)R_0\}\frac{1}{S^{\alpha+1}} \\
\mathcal{L}\{D_{u1}\} = \{\delta_3I_{N0} + \delta_2I_{i0} + \delta_1I_{T0} - qD_{u0}\}\frac{1}{S^{\alpha+1}}, &\mathcal{L}\{S_{r1}\} = \{\Lambda^{\smile}(\mu_r + \omega)S_{r0}\}\frac{1}{S^{\alpha+1}} \\
\mathcal{L}\{E_{r1}\} = \{\omega S_{r0}{}^{\smile}(\mu_r + \phi)E_{r0}\}\frac{1}{S^{\alpha+1}}, &\mathcal{L}\{I_{r1}\} = \{\phi E_{r0}{}^{\smile}(\mu_r - \delta_4I_{r0}\}\frac{1}{S^{\alpha+1}} \\
\ldots = \ldots, &\mathcal{L}\{S_{(n+1)}\} = \{P^{\smile}(\mu + r + K_1X)S_n + \tau R_n\}\frac{1}{S^{\alpha+1}} \\
\mathcal{L}\{S_{v(n+1)}\} = \{rS_n{}^{\smile}(\mu + \lambda + K_2Z)S_{v_n}\}\frac{1}{S^{\alpha+1}}, &\mathcal{L}\{S_{u(n+1)}\} = \{K_1XS_n{}^{\smile}(\mu + \sigma + K_3Y)S_{u_n}\}\frac{1}{S^{\alpha+1}} \\
\mathcal{L}\{S_{vc(n+1)}\} &= \{\lambda S_{v_n} - [\mu S_{vc_n} + 1/N(m_1A_n + m_2B_n + m_3F_n + m_4G_n)]\}\frac{1}{S^{\alpha+1}} \\
\mathcal{L}\{S_{vn(n+1)}\} &= \{K_2ZS_{v_n} - [\mu S_{vn_n} + 1/N(n_1H_n + n_2L_n + n_3Q_n + n_4T_n)]\}\frac{1}{S^{\alpha+1}} \\
\mathcal{L}\{S_{uc(n+1)}\} &= \{\sigma S_{u_n} - [\mu S_{uc_n} + 1/N(e_1U_n + e_2V_n + e_3W_n + e_4X_n)]\}\frac{1}{S^{\alpha+1}} \\
\mathcal{L}\{S_{un(n+1)}\} &= \{K_3YS_{u_n} - [\mu S_{un_n} + 1/N(t_1Y_n + t_2Z_n + t_3N_n + t_4M_n)]\}\frac{1}{S^{\alpha+1}} \\
\mathcal{L}\{E_{(n+1)}\} = \{1/N[&m_1A_n + m_2B_n + m_3F_n + m_4G_n + n_1H_n + n_2L_n + n_3Q_n + n_4T_n + e_1U_n + e_2V_n + \\
&e_3W_n + e_4X_n + t_1Y_n + t_2Z_n + t_3N_n + t_4M_n] - (\mu + \alpha_1 + \alpha_2)E_n\}\frac{1}{S^{\alpha+1}} \\
\mathcal{L}\{E_{Q(n+1)}\} = \{\alpha_1E_n{}^{\smile}(\mu + \theta_1)E_{Q_n}\}\frac{1}{S^{\alpha+1}}, &\mathcal{L}\{E_{T(n+1)}\} = \{\alpha_2E_n{}^{\smile}(\alpha + \theta_2 + \rho)E_{T_n}\}\frac{1}{S^{\alpha+1}} \\
\mathcal{L}\{I_{T(n+1)}\} &= \{\theta_1S_1E_{Q_n} + \theta_2S_1E_{T_n}{}^{\smile}(\mu + \delta_1 + J_2)I_{T_n}\}\frac{1}{S^{\alpha+1}} \\
\mathcal{L}\{I_{i(n+1)}\} &= \{\theta_1S_2E_{Q_n} + \theta_2S_2E_{T_n}{}^{\smile}(\mu + \delta_2 + J_1)I_{i_n}\}\frac{1}{S^{\alpha+1}} \\
\mathcal{L}\{I_{N(n+1)}\} = \{\theta_1S_2E_{Q_n} + \theta_2S_3E_{T_n}{}^{\smile}(\mu + \delta_3)I_{N_n}\}\frac{1}{S^{\alpha+1}}, &\mathcal{L}\{R_{(n+1)}\} = \{J_1I_{i_n} + J_2I_{T_n} + \rho E_{T_n} - \rho R_n\}\frac{1}{S^{\alpha+1}} \\
\mathcal{L}\{D_{u(n+1)}\} = \{\delta_3I_{N_n} + \delta_2I_{i_n} + \delta_1I_{T_n} - qD_n\}\frac{1}{S^{\alpha+1}}, &\mathcal{L}\{S_{r(n+1)}\} = \{\Lambda^{\smile}(\mu_r + \omega)S_{r_n}\}\frac{1}{S^{\alpha+1}} \\
\mathcal{L}\{E_{r(n+1)}\} = \{\omega S_{r_n}{}^{\smile}(/mu_r + \phi)E_{r_n}\}\frac{1}{S^{\alpha+1}}, &\mathcal{L}\{I_{r(n+1)}\} = \{\phi E_{r_n}{}^{\smile}(\mu + \delta_4)I_{r_n}\}\frac{1}{S^{\alpha+1}}
\end{aligned}
\right\} \tag{30}
$$

Taking the Laplace inverse transform of (30) we have;

$$\left.\begin{aligned}
S_1 &= \{P^{\smile}(\mu + r + K_1X)S_0 + \tau R_0\}\frac{t^\alpha}{\Gamma(\alpha+1)} \\
S_{v1} &= \{rS_0{}^{\smile}(\mu + \lambda + K_2Z)S_{v0}\}\frac{t^\alpha}{\Gamma(\alpha+1)}, S_{u1} = \{K_1XS_0{}^{\smile}(\mu + \sigma + K_3Y)S_{u0}\}\frac{t^\alpha}{\Gamma(\alpha+1)} \\
S_{vc1} &= \{\lambda S_{v0} - [\mu S_{vc0} + 1/N(m_1A_0 + m_2B_0 + m_3F_0 + m_4G_0)]\}\frac{t^\alpha}{\Gamma(\alpha+1)} \\
S_{vn1} &= \{K_2ZS_{v0} - [\mu S_{vn0} + 1/N(n_1H_0 + n_2L_0 + n_3Q_0 + n_4T_0)]\}\frac{t^\alpha}{\Gamma(\alpha+1)} \\
S_{uc1} &= \{\sigma S_{u0} - [\mu S_{uc0} + 1/N(e_1U_0 + e_2V_0 + e_3W_0 + e_4X_0)]\}\frac{t^\alpha}{\Gamma(\alpha+1)} \\
S_{un1} &= \{K_3YS_{u0} - [\mu S_{un0} + 1/N(t_1Y_0 + t_2Z_0 + t_3N_0 + t_4M_0)]\}\frac{t^\alpha}{\Gamma(\alpha+1)} \\
E_1 &= \{1/N[m_1A_0 + m_2B_0 + m_3F_0 + m_4G_0 + n_1H_0 + n_2L_0 + n_3Q_0 + n_4T_0 + e_1U_0 + e_2V_0 \\
&\quad + e_3W_0 + e_4X_0 + t_1Y_0 + t_2Z_0 + t_3N_0 + t_4M_0] - (\mu + \alpha_1 + \alpha_2)E_0\}\frac{t^\alpha}{\Gamma(\alpha+1)} \\
E_{Q1} &= \{\alpha_1E_0{}^{\smile}(\mu + \theta_1)E_{Q0}\}\frac{t^\alpha}{\Gamma(\alpha+1)}, E_{T1} = \{\alpha_2E_0{}^{\smile}(\mu + \theta_2 + \rho)E_{T0}\}\frac{t^\alpha}{\Gamma(\alpha+1)} \\
I_{T1} &= \{\theta_1S_1E_{Q0} + \theta_2S_1E_{T0}{}^{\smile}(\mu + \delta_1 + J_2)I_{T0}\}\frac{t^\alpha}{\Gamma(\alpha+1)} \\
I_{i1} &= \{\theta_1S_2E_{Q0} + \theta_2S_2E_{T0}{}^{\smile}(\mu + \delta_2 + J_1)I_{i0}\}\frac{t^\alpha}{\Gamma(\alpha+1)} \\
I_{N1} &= \{\theta_1S_3E_{Q0} + \theta_2S_3E_{T0}{}^{\smile}(\mu + \delta_3)I_{N0}\}\frac{t^\alpha}{\Gamma(\alpha+1)}, R_1 = \{J_1I_{i0} + J_2I_{T0} + \rho E_{T0} - (\mu - \tau)R_0\}\frac{t^\alpha}{\Gamma(\alpha+1)} \\
D_{u1} &= \{\delta_3I_{N0} + \delta_2I_{i0} + \delta_1I_{T0} - qD_{u0}\}\frac{t^\alpha}{\Gamma(\alpha+1)}, S_{r1} = \{\Lambda^{\smile}(\mu_r + \omega)S_{r0}\}\frac{t^\alpha}{\Gamma(\alpha+1)} \\
E_{r1} &= \{\omega S_{r0}{}^{\smile}(\mu_r + \phi)E_{r0}\}\frac{t^\alpha}{\Gamma(\alpha+1)}, I_{r1} = \{\phi E_{r0}{}^{\smile}(\mu_r - \delta_4I_{r0}\}
\end{aligned}\right\}$$

$$\left.\begin{aligned}
\ldots &= \ldots, S_{(n+1)} = \{P^{\smile}(\mu + r + K_1X)S_n + \tau R_n\}\frac{t^\alpha}{\Gamma(\alpha+1)} S_{v(n+1)} = \{rS_n{}^{\smile}(\mu + \lambda + K_2Z)S_{v_n}\} \\
S_{u(n+1)} &= \{K_1XS_n{}^{\smile}(\mu + \sigma + K_3Y)S_{u_n}\}\frac{t^\alpha}{\Gamma(\alpha+1)} \\
S_{vc(n+1)} &= \{\lambda S_{v_n} - [\mu S_{vc_n} + 1/N(m_1A_n + m_2B_n + m_3F_n + m_4G_n)]\}\frac{t^\alpha}{\Gamma(\alpha+1)} \\
S_{vn(n+1)} &= \{K_2ZS_{v_n} - [\mu S_{vn_n} + 1/N(n_1H_n + n_2L_n + n_3Q_n + n_4T_n)]\}\frac{t^\alpha}{\Gamma(\alpha+1)} \\
S_{uc(n+1)} &= \{\sigma S_{u_n} - [\mu S_{uc_n} + 1/N(e_1U_n + e_2V_n + e_3W_n + e_4X_n)]\}\frac{t^\alpha}{\Gamma(\alpha+1)} \\
S_{un(n+1)} &= \{K_3YS_{u_n} - [\mu S_{un_n} + 1/N(t_1Y_n + t_2Z_n + t_3N_n + t_4M_n)]\}\frac{t^\alpha}{\Gamma(\alpha+1)} \\
E_{(n+1)} &= \{1/N[m_1A_n + m_2B_n + m_3F_n + m_4G_n + n_1H_n + n_2L_n + n_3Q_n + n_4T_n + e_1U_n + e_2V_n + e_3W_n \\
&\quad + e_4X_n + t_1Y_n + t_2Z_n + t_3N_n + t_4M_n] - (\mu + \alpha_1 + \alpha_2)E_n\}\frac{t^\alpha}{\Gamma(\alpha+1)}, E_{Q(n+1)} = \{\alpha_1E_n{}^{\smile}(\mu + \theta_1)E_{Q_n}\} \\
&\frac{t^\alpha}{\Gamma(\alpha+1)}, E_{T(n+1)} = \{\alpha_2E_n{}^{\smile}(\alpha + \theta_2 + \rho)E_{T_n}\}\frac{t^\alpha}{\Gamma(\alpha+1)}, I_{T(n+1)} = \{\theta_1S_1E_{Q_n} + \theta_2S_1E_{T_n}{}^{\smile}(\mu + \delta_1 + J_2)I_{T_n}\} \\
&\frac{t^\alpha}{\Gamma(\alpha+1)}, I_{i(n+1)} = \{\theta_1S_2E_{Q_n} + \theta_2S_2E_{T_n}{}^{\smile}(\mu + \delta_2 + J_1)I_{i_n}\}\frac{t^\alpha}{\Gamma(\alpha+1)}, I_{N(n+1)} = \\
&\{\theta_1S_2E_{Q_n} + \theta_2S_3E_{T_n}{}^{\smile}(\mu + \delta_3)I_{N_n}\}\frac{t^\alpha}{\Gamma(\alpha+1)}, R_{(n+1)} = \{J_1I_{i_n} + J_2I_{T_n} + \rho E_{T_n} - \rho R_n\}\frac{t^\alpha}{\Gamma(\alpha+1)} \\
D_{u(n+1)} &= \{\delta_3I_{N_n} + \delta_2I_{i_n} + \delta_1I_{T_n} - qD_n\}\frac{t^\alpha}{\Gamma(\alpha+1)}, S_{r(n+1)} = \{\Lambda^{\smile}(\mu_r + \omega)S_{r_n}\}\frac{t^\alpha}{\Gamma(\alpha+1)} \\
E_{r(n+1)} &= \{\omega S_{r_n}{}^{\smile}(/mu_r + \phi)E_{r_n}\}\frac{t^\alpha}{\Gamma(\alpha+1)}, I_{r(n+1)} = \{\phi E_{r_n}{}^{\smile}(\mu + \delta_4)I_{r_n}\}\frac{t^\alpha}{\Gamma(\alpha+1)}
\end{aligned}\right\} \quad (31)$$

Recalling and applying the initial conditions (2) we have the following;

$$\left.\begin{aligned} S_0 = g_1, S_{v0} = g_2, S_{u0} = g_3, S_{vc0} = g_4, \\ S_{vn0} = g_5, S_{uc0} = g_6, S_{un0} = g_7, E_0 = g_8, E_{Q0} = g_9, \\ E_{T0} = g_{10}, I_{T0} = g_{11}, I_{i0} = g_{12}, I_{N0} = g_{13}, R_0 = g_{14}, \\ D_{u0} = g_{15}, S_{r0} = g_{16}, E_{r0} = g_{17}, I_{r0} = g_{18}. \end{aligned}\right\} \tag{32}$$

Substituting all these conditions we finally obtain the Ebola fractional model solution in the form of infinite series (23)using LADM as follows;

$$\left.\begin{aligned} S(t) = S_0 + S_1 + S_2 + \dots \\ S(t) = g_1 + \{P^{\smile}(\mu + r + K_1 X)g_1 + \tau g_{14}\}\frac{t^\alpha}{\Gamma(\alpha+1)} \\ +\{P^{\smile}(\mu + r + K_1 X)S_1 + \tau R_1\}\frac{t^\alpha}{\Gamma(\alpha+1)} + \dots \end{aligned}\right\} \tag{33}$$

$$\left.\begin{aligned} S_v(t) = S_{v0} + S_{v1} + S_{v2} + \dots \\ S_v(t) = g_2 + \{r g_1{}^{\smile}(\mu + \lambda + K_2 Z)g_2\}\frac{t^\alpha}{\Gamma(\alpha+1)} \\ +\{r S_1{}^{\smile}(\mu + \lambda + K_2 Z)S_{v1}\}\frac{t^\alpha}{\Gamma(\alpha+1)} + \dots \end{aligned}\right\} \tag{34}$$

$$\left.\begin{aligned} S_u(t) = S_{u0} + S_{u1} + S_{u2} + \dots \\ S_u(t) = g_3 + \{K_1 X g_1{}^{\smile}(\mu + \sigma + K_3 Y)g_3\}\frac{t^\alpha}{\Gamma(\alpha+1)} \\ +\{K_1 X S_1{}^{\smile}(\mu + \sigma + K_3 Y)S_{u1}\}\frac{t^\alpha}{\Gamma(\alpha+1)} + \dots \end{aligned}\right\} \tag{35}$$

$$\left.\begin{aligned} S_{vc}(t) = S_{vc0} + S_{vc1} + S_{vc2} + \dots \\ S_{vc}(t) = g_4 + \\ \{\lambda g_2 - [\mu g_4 + 1/N(m_1 g_4 g_{13} + m_2 g_4 g_{11} + m_3 g_4 g_{18} + m_4 g_4 g_{15})]\}\frac{t^\alpha}{\Gamma(\alpha+1)} \\ +\{\lambda S_{v1} - [\mu S_{vc1} + 1/N(m_1 A_1 + m_2 B_1 + m_3 F_1 + m_4 G_1)]\}\frac{t^\alpha}{\Gamma(\alpha+1)} + \dots \end{aligned}\right\} \tag{36}$$

$$\left.\begin{aligned} S_{vn}(t) = S_{vn0} + S_{vn1} + S_{vn2} + \dots \\ S_{vn}(t) = g_5 + \\ \{K_2 Z g_2 - [\mu g_5 + 1/N(n_1 g_5 g_{13} + n_2 g_5 g_{11} + n_3 g_5 g_{18} + n_4 g_5 g_{15})]\}\frac{t^\alpha}{\Gamma(\alpha+1)} \\ +\{K_2 Z S_{v1} - [\mu S_{vn1} + 1/N(n_1 H_1 + n_2 L_1 + n_3 Q_1 + n_4 T_1)]\}\frac{t^\alpha}{\Gamma(\alpha+1)} + \dots \end{aligned}\right\} \tag{37}$$

$$\left.\begin{aligned} S_{uc}(t) = S_{uc0} + S_{uc1} + S_{uc2} + \dots \\ S_{uc}(t) = g_6 + \\ \{\sigma g_3 - [\mu g_6 + 1/N(e_1 g_6 g_{13} + e_2 g_6 g_{11} + e_3 g_6 g_{18} + e_4 g_6 g_{15})]\}\frac{t^\alpha}{\Gamma(\alpha+1)} \\ +\{\sigma S_{u1} - [\mu S_{uc1} + 1/N(e_1 U_1 + e_2 V_1 + e_3 W_1 + e_4 X_1)]\}\frac{t^\alpha}{\Gamma(\alpha+1)} + \dots \end{aligned}\right\} \tag{38}$$

$$\left.\begin{aligned} S_{un}(t) = S_{un0} + S_{un1} + S_{un2} + \dots \\ S_{un}(t) = g_7 + \\ \{K_3 Y g_3 - [\mu g_7 + 1/N(t_1 g_7 g_{13} + t_2 g_7 g_{11} + t_3 g_7 g_{18} + t_4 g_7 g_{15})]\}\frac{t^\alpha}{\Gamma(\alpha+1)} \\ + \{K_3 Y S_{u1} - [\mu S_{un1} + 1/N(t_1 Y_1 + t_2 Z_1 + t_3 N_1 + t_4 M_1)]\}\frac{t^\alpha}{\Gamma(\alpha+1)} + \dots \end{aligned}\right\} \tag{39}$$

$$\left.\begin{aligned} E(t) = E_0 + E_1 + E_2 + \dots \\ E(t) = g_8 + \{1/N[C_1 + C_2 + C_3 + C_4] - (\mu + \alpha_1 + \alpha_2) g_8\}\frac{t^\alpha}{\Gamma(\alpha+1)} \\ + \{1/N[C_5 + C_6 + C_7 + C_8] - (\mu + \alpha_1 + \alpha_2) E_1\}\frac{t^\alpha}{\Gamma(\alpha+1)} + \dots \end{aligned}\right\} \tag{40}$$

Where;

$$\left.\begin{aligned} C_1 = m_1 g_4 g_{13} + m_2 g_4 g_{11} + m_3 g_4 g_{18} + m_4 g_4 g_{15} \\ C_2 = n_1 g_5 g_{13} + n_2 g_5 g_{11} + n_3 g_5 g_{18} + n_4 g_5 g_{15} \\ C_3 = e_1 g_6 g_{13} + e_2 g_6 g_{11} + e_3 g_6 g_{18} + e_4 g_6 g_{15} \\ C_4 = t_1 g_7 g_{13} + t_2 g_7 g_{11} + t_3 g_6 g_{18} + t_4 g_7 g_{15} \\ C_5 = m_1 A_1 + m_2 B_1 + m_3 F_1 + m_4 G_1 \\ C_6 = n_1 H_1 + n_2 L_1 + n_3 Q_1 + n_4 T_1 \\ C_7 = e_1 U_1 + e_2 V_1 + e_3 W_1 + e_4 X_1 \\ C_8 = t_1 Y_1 + t_2 Z_1 + t_3 N_1 + t_4 M_1 \end{aligned}\right\} \tag{41}$$

$$\left.\begin{aligned} E_Q(t) = E_{Q0} + E_{Q1} + E_{Q2} + \dots \\ E_Q(t) = g_9 + \\ \{\alpha_1 g_8{}^{\smile}(\mu + \theta_1) g_9\}\frac{t^\alpha}{\Gamma(\alpha+1)} \\ + \alpha_1 E_1{}^{\smile}(\mu + \theta_1) E_{Q1}\frac{t^\alpha}{\Gamma(\alpha+1)} + \dots \end{aligned}\right\} \tag{42}$$

$$\left.\begin{aligned} E_T(t) = E_{T0} + E_{T1} + E_{T2} + \dots \\ E_T(t) = g_{10} + \\ \{\alpha_2 g_8{}^{\smile}(\mu + \theta_2 + \rho) g_{10}\}\frac{t^\alpha}{\Gamma(\alpha+1)} \\ + \{\alpha_2 E_1{}^{\smile}(\mu + \theta_2 + \rho) E_{T1}\}\frac{t^\alpha}{\Gamma(\alpha+1)} + \dots \end{aligned}\right\} \tag{43}$$

$$\left.\begin{aligned} I_T(t) = I_{T0} + I_{T1} + I_{T2} + \dots \\ I_T(t) = g_{11} + \\ \{\theta_1 S_1 g_9 + \theta_2 S_1 g_{10}{}^{\smile}(\mu + \delta_1 + J_2) g_{11}\}\frac{t^\alpha}{\Gamma(\alpha+1)} \\ + \{\theta_1 S_1 E_{Q1} + \theta_2 S_1 E_{T1}{}^{\smile}(\mu + \delta_1 + J_2) I_{T1}\}\frac{t^\alpha}{\Gamma(\alpha+1)} + \dots \end{aligned}\right\} \tag{44}$$

$$\left.\begin{aligned} I_i(t) = I_{i0} + I_{i1} + I_{i2} + \dots \\ I_i(t) = g_{12} + \\ \{\theta_1 S_2 g_9 + \theta_2 S_2 g_{10}{}^{\smile}(\mu + \delta_2 + J_1) g_{12}\}\frac{t^\alpha}{\Gamma(\alpha+1)} \\ + \{\theta_1 S_2 E_{Q1} + \theta_2 S_2 E_{T1}{}^{\smile}(\mu + \delta_2 + J_1) I_{i1}\}\frac{t^\alpha}{\Gamma(\alpha+1)} + \dots \end{aligned}\right\} \tag{45}$$

$$\left.\begin{aligned} I_N(t) = I_{N0} + I_{N1} + I_{N2} + \dots \\ I_N(t) = g_{13} + \\ \{\theta_1 S_3 g_9 + \theta_2 S_3 g_{10}\breve{}(\mu + \delta_3) g_{13}\}\frac{t^\alpha}{\Gamma(\alpha+1)} \\ +\{\theta_1 S_3 E_{Q1} + \theta_2 S_3 E_{T1}\breve{}(\mu + \delta_3) I_{N1}\}\frac{t^\alpha}{\Gamma(\alpha+1)} + \dots \end{aligned}\right\} \tag{46}$$

$$\left.\begin{aligned} R(t) = R_0 + R_1 + R_2 + \dots \\ R(t) = g_{14} + \\ \{J_1 g_{12} + J_2 g_{11} + \rho g_{10} - \tau g_{14}\}\frac{t^\alpha}{\Gamma(\alpha+1)} \\ +\{J_1 I_{i1} + J_2 I_{T1} + \rho E_{T1} - \tau R_1\}\frac{t^\alpha}{\Gamma(\alpha+1)} + \dots \end{aligned}\right\} \tag{47}$$

$$\left.\begin{aligned} D_u(t) = D_{u0} + D_{u1} + D_{u2} + \dots \\ D_u(t) = g_{15} + \\ \{\delta_3 g_{13} + \delta_2 g_{12} + \delta_1 g_{11} - q g 15\}\frac{t^\alpha}{\Gamma(\alpha+1)} \\ +\{\delta_3 I_{N1} + \delta_2 I_{i1} + \delta_1 I_{T1}\}\frac{t^\alpha}{\Gamma(\alpha+1)} + \dots \end{aligned}\right\} \tag{48}$$

$$\left.\begin{aligned} S_r(t) = S_{r0} + S_{r1} + S_{r2} + \dots \\ S_r(t) = g_{16} + \\ \{\Lambda\breve{}(\mu_r + \omega) g_{16}\}\frac{t^\alpha}{\Gamma(\alpha+1)} \\ +\{\Lambda\breve{}(\mu_r + \omega) S_{r1}\}\frac{t^\alpha}{\Gamma(\alpha+1)} + \dots \end{aligned}\right\} \tag{49}$$

$$\left.\begin{aligned} E_r(t) = E_{r0} + E_{r1} + E_{r2} + \dots \\ E_r(t) = g_{17} + \\ \{\omega g_{16}\breve{}(\mu_r + \phi) g_{17}\}\frac{t^\alpha}{\Gamma(\alpha+1)} \\ +\{\omega S_{r1}\breve{}(\mu_r + \phi) E_{r1}\}\frac{t^\alpha}{\Gamma(\alpha+1)} + \dots \end{aligned}\right\} \tag{50}$$

$$\left.\begin{aligned} I_r(t) = I_{r0} + I_{r1} + I_{r2} + \dots \\ I_r(t) = g_{18} + \\ \{\phi g_{17}\breve{}(\mu_r + \delta_4) g_{18}\}\frac{t^\alpha}{\Gamma(\alpha+1)} \\ +\{\phi E_{r1}\breve{}(\mu + \delta_4) I_{r1}\}\frac{t^\alpha}{\Gamma(\alpha+1)} + \dots \end{aligned}\right\} \tag{51}$$

Thus, the solution in series form is given as follows;

$$\left.\begin{aligned}
S(t) &= g_1 + \{P^{\smile}(\mu + r + K_1X)g_1 + \tau g_{14}\}\frac{t^\alpha}{\Gamma(\alpha+1)} + \{P^{\smile}(\mu + r + K_1X)S_1 + \tau R_1\}\frac{t^\alpha}{\Gamma(\alpha+1)} + \dots \\
S_v(t) &= g_2 + \{rg_1{}^{\smile}(\mu + \lambda + K_2Z)g_2\}\frac{t^\alpha}{\Gamma(\alpha+1)} + \{rS_1{}^{\smile}(\mu + \lambda + K_2Z)S_{v1}\}\frac{t^\alpha}{\Gamma(\alpha+1)} + \dots \\
S_u(t) &= g_3 + \{K_1Xg_1{}^{\smile}(\mu + \sigma + K_3Y)g_3\}\frac{t^\alpha}{\Gamma(\alpha+1)} + \{K_1XS_1{}^{\smile}(\mu + \sigma + K_3Y)S_{u1}\}\frac{t^\alpha}{\Gamma(\alpha+1)} + \dots \\
S_{vc}(t) &= g_4 + \{\lambda g_2 - [\mu g_4 + 1/N(m_1g_4g_{13} + m_2g_4g_{11} + m_3g_4g_{18} + m_4g_4g_{15})]\}\frac{t^\alpha}{\Gamma(\alpha+1)} \\
&\quad + \{\lambda S_{v1} - [\mu S_{vc1} + 1/N(m_1A_1 + m_2B_1 + m_3F_1 + m_4G_1)]\}\frac{t^\alpha}{\Gamma(\alpha+1)} + \dots \\
S_{vn}(t) &= g_5 + \{K_2Zg_2 - [\mu g_5 + 1/N(n_1g_5g_{13} + n_2g_5g_{11} + n_3g_5g_{18} + n_4g_5g_{15})]\}\frac{t^\alpha}{\Gamma(\alpha+1)} \\
&\quad + \{K_2ZS_{v1} - [\mu S_{vn1} + 1/N(n_1H_1 + n_2L_1 + n_3Q_1 + n_4T_1)]\}\frac{t^\alpha}{\Gamma(\alpha+1)} + \dots \\
S_{uc}(t) &= g_6 + \{\sigma g_3 - [\mu g_6 + 1/N(e_1g_6g_{13} + e_2g_6g_{11} + e_3g_6g_{18} + e_4g_6g_{15})]\}\frac{t^\alpha}{\Gamma(\alpha+1)} \\
&\quad + \{\sigma S_{u1} - [\mu S_{uc1} + 1/N(e_1U_1 + e_2V_1 + e_3W_1 + e_4X_1)]\}\frac{t^\alpha}{\Gamma(\alpha+1)} + \dots \\
S_{un}(t) &= g_7 + \{K_3Yg_3 - [\mu g_7 + 1/N(t_1g_7g_{13} + t_2g_7g_{11} + t_3g_7g_{18} + t_4g_7g_{15})]\}\frac{t^\alpha}{\Gamma(\alpha+1)} \\
&\quad + \{K_3YS_{u1} - [\mu S_{un1} + 1/N(t_1Y_1 + t_2Z_1 + t_3N_1 + t_4M_1)]\}\frac{t^\alpha}{\Gamma(\alpha+1)} + \dots \\
E(t) &= g_8 + \{1/N[C_1 + C_2 + C_3 + C_4] - (\mu + \alpha_1 + \alpha_2)g_8\}\frac{t^\alpha}{\Gamma(\alpha+1)} \\
&\quad + \{1/N[C_5 + C_6 + C_7 + C_8] - (\mu + \alpha_1 + \alpha_2)E_1\}\frac{t^\alpha}{\Gamma(\alpha+1)} + \dots \\
E_Q(t) &= g_9 + \{\alpha_1g_8{}^{\smile}(\mu + \theta_1)g_9\}\frac{t^\alpha}{\Gamma(\alpha+1)} + \alpha_1E_1{}^{\smile}(\mu + \theta_1)E_{Q1}\frac{t^\alpha}{\Gamma(\alpha+1)} + \dots \\
E_T(t) &= g_{10} + \{\alpha_2g_8{}^{\smile}(\mu + \theta_2 + \rho)g_{10}\}\frac{t^\alpha}{\Gamma(\alpha+1)} + \{\alpha_2E_1{}^{\smile}(\mu + \theta_2 + \rho)E_{T1}\}\frac{t^\alpha}{\Gamma(\alpha+1)} + \dots \\
I_T(t) &= g_{11} + \{\theta_1S_1g_9 + \theta_2S_1g_{10}{}^{\smile}(\mu + \delta_1 + J_2)g_{11}\}\frac{t^\alpha}{\Gamma(\alpha+1)} \\
&\quad + \{\theta_1S_1E_{Q1} + \theta_2S_1E_{T1}{}^{\smile}(\mu + \delta_1 + J_2)I_{T1}\}\frac{t^\alpha}{\Gamma(\alpha+1)} + \dots \\
I_i(t) &= g_{12} + \{\theta_1S_2g_9 + \theta_2S_2g_{10}{}^{\smile}(\mu + \delta_2 + J_1)g_{12}\}\frac{t^\alpha}{\Gamma(\alpha+1)} \\
&\quad + \{\theta_1S_2E_{Q1} + \theta_2S_2E_{T1}{}^{\smile}(\mu + \delta_2 + J_1)I_{i1}\}\frac{t^\alpha}{\Gamma(\alpha+1)} + \dots \\
I_N(t) &= g_{13} + \{\theta_1S_3g_9 + \theta_2S_3g_{10}{}^{\smile}(\mu + \delta_3)g_{13}\}\frac{t^\alpha}{\Gamma(\alpha+1)} + \{\theta_1S_3E_{Q1} + \theta_2S_3E_{T1}{}^{\smile}(\mu + \delta_3)I_{N1}\}\frac{t^\alpha}{\Gamma(\alpha+1)} + \dots \\
R(t) &= g_{14} + \{J_1g_{12} + J_2g_{11} + \rho g_{10} - \tau g_{14}\}\frac{t^\alpha}{\Gamma(\alpha+1)} + \{J_1I_{i1} + J_2I_{T1} + \rho E_{T1} - \tau R_1\}\frac{t^\alpha}{\Gamma(\alpha+1)} + \dots \\
D_u(t) &= g_{15} + \{\delta_3g_{13} + \delta_2g_{12} + \delta_1g_{11} - qg15\}\frac{t^\alpha}{\Gamma(\alpha+1)} + \{\delta_3I_{N1} + \delta_2I_{i1} + \delta_1I_{T1}\}\frac{t^\alpha}{\Gamma(\alpha+1)} + \dots \\
S_r(t) &= g_{16} + \{\Lambda^{\smile}(\mu_r + \omega)g_{16}\}\frac{t^\alpha}{\Gamma(\alpha+1)} + \{\Lambda^{\smile}(\mu_r + \omega)S_{r1}\}\frac{t^\alpha}{\Gamma(\alpha+1)} + \dots \\
E_r(t) &= g_{17} + \{\omega g_{16}{}^{\smile}(\mu_r + \phi)g_{17}\}\frac{t^\alpha}{\Gamma(\alpha+1)} + \{\omega S_{r1}{}^{\smile}(\mu_r + \phi)E_{r1}\}\frac{t^\alpha}{\Gamma(\alpha+1)} + \dots \\
I_r(t) &= g_{18} + \{\phi g_{17}{}^{\smile}(\mu_r + \delta_4)g_{18}\}\frac{t^\alpha}{\Gamma(\alpha+1)} + \{\phi E_{r1}{}^{\smile}(\mu + \delta_4)I_{r1}\}\frac{t^\alpha}{\Gamma(\alpha+1)} + \dots
\end{aligned}\right\} \tag{52}$$

The Laplace Adomian Decomposition method reduces a solution in form of an infinite series that further converges easily to the exact value. The method unlike other numerical techniques does not require any perturbation nor predefined step size. Also, the method does not require discretization and linearization and as such the results obtained from it are more effective and realistic.

5 Numerical simulations

In this section, we consider the numerical simulation of the Ebola fractional model. Using the initial values and the parameter values presented in Table 3 and Table 4 respectively which where also used in [2, 14, 15, 20]

Table 3: **Ebola Fractional Model Variable Initial Values**

Model Variables	Initial Values
S_0	4396521
S_{v0}	1758608
S_{u0}	2637913
S_{vc0}	527582
S_{vn0}	1231026
S_{uc0}	1582748
S_{un0}	1055165
E_0	0
E_{Q0}	74
E_{T0}	0
I_{T0}	500
I_{i0}	800
I_{N0}	400
R_0	0
D_{u0}	24
S_{r0}	6000
E_{r0}	100
I_{r0}	0

Table 4: **Ebola Fractional Model Variable Initial Values**

Parameters	Values	Parameters	Values
Λ	100	ω	0.8
ω	0.5	ϕ	0.6
μ_r	0.08	δ_4	0.3110
P	400	μ	0.0000246575
r	0.05	K_1	0.895
λ	0.02	K_2	0.765
σ	0.07	K_3	0.0886
S_1	0.2257	θ_1	0.08333
S_2	0.25	θ_2	0.014
S_3	0.148	δ_1	0.11386
J_1	0.105186	δ_2	0.0901
J_2	0.17	δ_3	0.2443
K_3	0.02	α_1	0.07143
ρ	0.0314862	α_2	0.02741
τ	0.06	q	0.5
m_1	0.03	m_2	0.00003
m_3	0.01	m_4	0.0003
m_5	0.003	n_1	0.04
n_2	0.00004	n_3	0.04
n_4	0.09	n_5	0.00009
e_1	0.07	e_2	0.00007
e_3	0.0001	e_4	0.0007
e_5	0.007	t_1	0.09
t_2	0.00009	t_3	0.0002
t_4	0.0009	t_5	0.009

6 Discussions and conclusion

Here, we discuss the numerical simulation of our Ebola fractional order model so as to compare with the classical order. All the variables of our Ebola fractional order model are presented in Figure 2, Figure 3, Figure 4, Figure 5, Figure 6 and Figure 7 with variation in the value of the model fractional

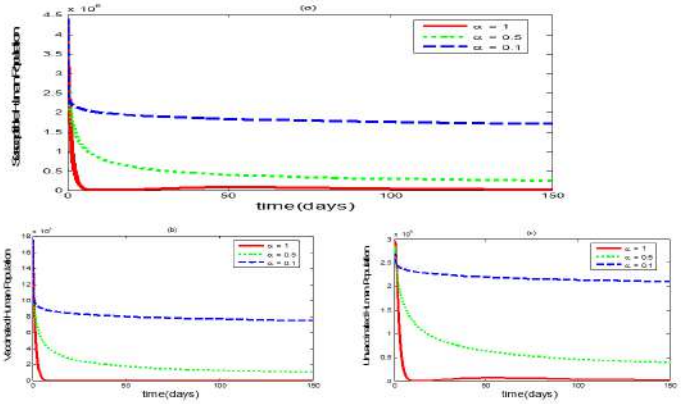


Figure 2: (a) Susceptible Human Population with Variation of α. (b) Vaccinated Human Population with Variation of α. (c) Unvaccinated Human Population with Variation of α.

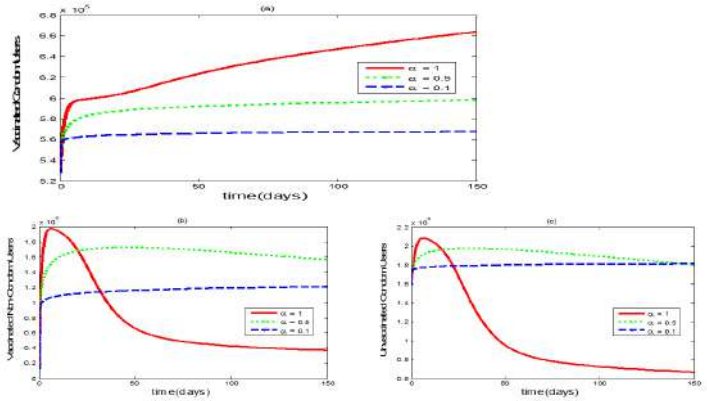


Figure 3: (a) Vaccinated Condom Users Population with Variation of α. (b) Vaccinated Non-Condom Users Population with Variation of α. (c) Unvaccinated Condom-Users Population with Variation of α.

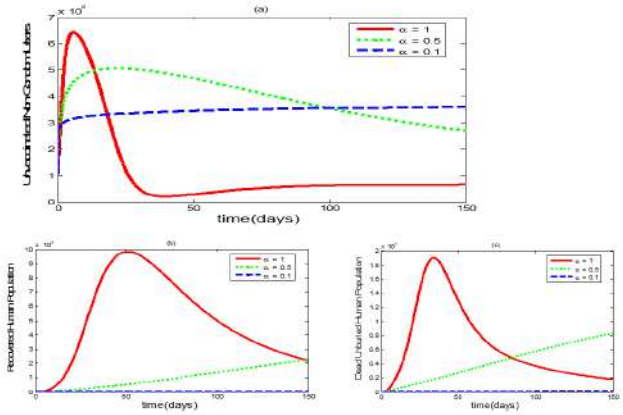


Figure 4: (a) Unvaccinated Non-Condom Users Population with Variation of α. (b) Recovered Human Population with Variation of α. (c) Dead Unburied Human Population with Variation of α.

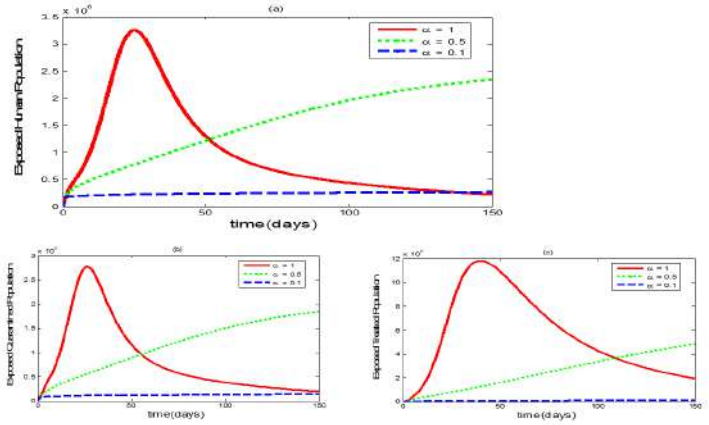


Figure 5: (a) Exposed Human Population with Variation of α. (b) Exposed Quarantined Human Population with Variation of α. (c) Exposed Treated Human Population with Variation of α.

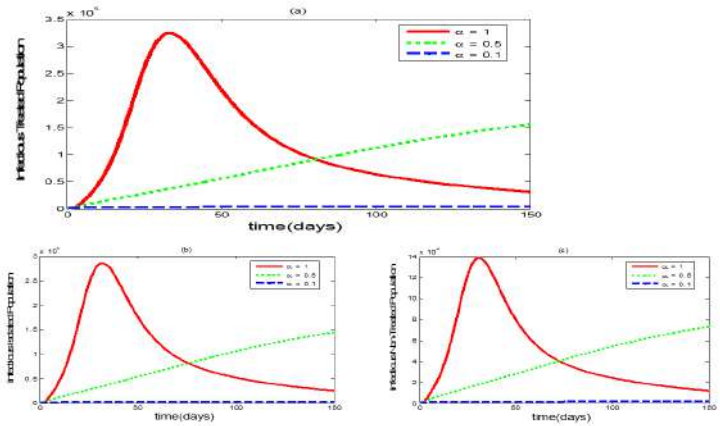


Figure 6: (a) Infectious Treated Human Population with Variation of α. (b) Infectious Isolated Human Population with Variation of α. (c) Infectious Non-Treated Human Population with Variation of α.

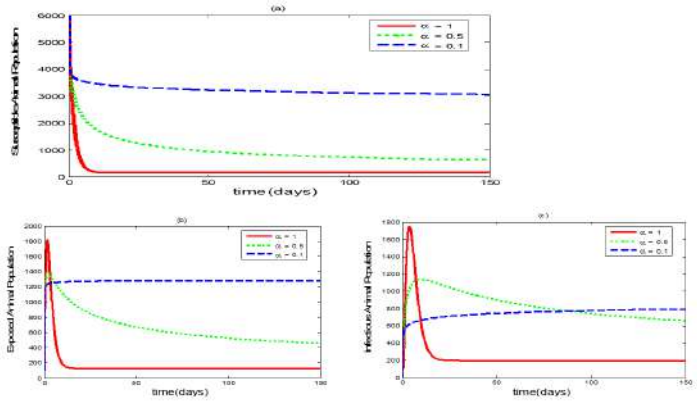


Figure 7: (a) Susceptible Animal Population with Variation of α. (b) Exposed Animal Population with Variation of α. (c) Infectious Animal Population with Variation of α.

order α. Figure 2 – Figure 7 shows that the Ebola fractional order model has more degrees of freedom as such the order α can then be varied in order to determine different degrees of responses of the different Variables that makes up the Ebola Fractional order model. This is seen when we compared the model fractional order (i.e.$\alpha = 0.5, 0.1$) with the model classical case where $\alpha = 1$. The graphs have shown the effect of α when $\alpha < 1$ and when $\alpha = 1$ which agrees with our earlier outcome that the Ebola fractional order model allows for determination of responses of α at different levels when compared with the Ebola classical order model. The Ebola fractional order model indeed assists us to obtain different outcomes in real time of the different classes of our Ebola fractional order model as shown in Figure 2 – Figure 7. We actually chose carefully our initial values and time to avoid obtaining negative population of human or animal which will not be meaningful biologically. The accuracy of a model numerical solution depends on the values of parameters and variables. To this end most of the parameter values employed in our analysis were not assumed but picked from existing literature on Ebola virus disease. Also, Since the main aim of this work is to determine the approximate solution of the formulated model, we did not boarder to calibrate to real data for Ebola virus. Secondly, getting real data for data fitting was challenging as the data was not always available on demand. So, we present in this work the approximate solution of the model using hypothetical data which the sources were acknowledged.

6.1 The Laplace–Adomian Decomposition Method (LADM) convergence analysis

The solution of (24) is expressed in form of infinite series as seen in equation (25) which converges uniformly to its exact solution. To verify the convergence of the series (24), we apply the method used in [25]. For sufficient conditions of convergence of the Laplace Adomian Decomposition Method, we present the following theorem:
Theorem 1 (see [33])
Let K be a Banach space and
$X :\to K$ be a constructive nonlinear operator such that for all
$(k), (k) \in K, \|X(k) - X(k')\| \leq m\|(k) - (k)'\|, 0 < m < 1$. Then, X has a unique point k such that $Xk = k$ where $k = (S, S_v, S_u, S_{vc}, S_{vn}, S_{uc}, S_{un}, E, E_Q, E_T, I_T, I_i,$
$I_N, R, D_u, S_r, E_r, I_r)$. The series can then be written by applying the Adomian decomposition method as follows:
$k_n = \sum_{i=1}^{n-1} k_i, n = 1, 2, 3 \ldots$
and assume that
$k_0 \in Z_r(k)$
where
$Z_r(k) = \{k' \in K : \|k' - k\| < r\}$
then we have as follows:
(i) $k_n \in Z_r(k)$
(ii) $\lim_{n\to\infty} k_n = k$
proof
To prove (i) we invoke mathematical induction
when $n = 1$ we have

$$\|k_0 - k\| = \|X(k_0) - X(k)\| \leq \|k_0 - k\| \tag{53}$$

if this is true for $y - 1$ then

$$\|k_0 - k\| \leq m^{y-1}\|k_0 - k\| \tag{54}$$

This gives the following

$$\|k_y - k\| = \|X(k_{y-1}) - X(k)\| \leq m\|k_{m-1} - k\| \leq m^n\|k_0 - k\| \tag{55}$$

Therefore,

$$\|k_m - k\| \leq m^n\|k_0 - k\| \leq m^n r < r \tag{56}$$

Which implies that $K_n \in Z_r(k)$.
Also, for condition (ii), we have that since

$$\|k_m - k\| \leq m^n \|k_0 - k\| \tag{57}$$

and

$$\lim_{n\to\infty} m^n = 0 \tag{58}$$

we can write

$$\lim_{n\to\infty} k_n = k \tag{59}$$

We thus prove convergence of the Laplace Adomian Decomposition method using the Cauchy-Kovalevskaya theorem for differential equations with analytic vector fields and then obtained a new result on the convergence rate of the Laplace Adomian Decomposition Method.

6.2 Conclusion

The Ebola Virus disease which is now preventable is still persisting and claiming the lives of many around some parts of the world. In this modified model, we studied the dynamics of Ebola transmission incorporating quarantine with contact tracing,Isolation, treatment, vaccine, and protection (condom use). We formulated an Ebola Virus fractional order mathematical model. through the analysis of the formulated model we found out that the disease (Ebola Virus) can go into extinction by maintaining the value of reproduction number (B) to be less than one through combined intervention of all our control measures put together. To solve the formulated model, we developed a numerical scheme that gives an approximate solution of our Ebola fractional order model using the Laplace–Adomian decomposition method. The solution obtained showed a good agreement with other numerical solutions. We also showed that approximate solution obtained converges to an exact solution.From our numerical simulation we finally, showed that the Ebola fractional order gives more degrees of freedom as the order can be varied to show responses by the different classes in real time. From the outcome it can also be seen that the reduction of the fractional order α gives a reduction in the population size of each of the considered classes, which by implication shows that the fractional order has a direct implication on our model . We herein have been able to show that the LADM can be used to solve an Ebola fractional order model with control measures of eighteen compartment after analysis which to the best of our knowledge has not been done before in literature. We also hope to compare our result with that of homotopy perturbation method and other methods in time for us to have a strong and better recommendation concerning the best method among them. We thus conclude that the Ebola fractional order model with eighteen equation set solved here using the Laplace–Adomian decomposition method gives a higher degree of freedom when compared to the Ebola classical order model. Therefore,linear and nonlinear ordinary and partial differential large equation set of fractional and classical orders can be solved using the Laplace–Adomian decomposition method.
From the result of our qualitative analysis, it was concluded that Ebola virus disease could be controlled provided the basic reproduction number could be maintained to a level below unity. The disease equilibrium points or state of the model was confirmed to be stable if the basic reproduction number is less than one, this epidemiologically implies that the disease will be eradicated from the population with respect to the initial population considered. It was further observed that Ebola virus disease would go into extinction through combined intervention of the control measures incorporated in our model. To this end, if all the control measures suggested in this research work were followed and implemented by medical health workers, the disease Ebola virus would be eradicated. To further understand the Ebola virus dynamics and return predictive accuracy, we recommend that both local and global sensitivity analysis should be carried out using the model basic reproduction number so as to know important parameters that should be targeted towards control intervention strategies. Secondly, real data could be fitted into the model so as to show real life scenario.

References

[1] Q.O. Ahman and G.C.E. Mbah, Modelling the Novel Coronavirus (Covid-19) With The Relevance Of Strict Movement Restriction In Italy, Academic Journal of Statistics and Mathematics (AJSM). (2020a) Vol.7 No.1.

[2] Q.O Ahman, D. Omale, C.C Asogwa, D.U Nnaji and G.C.E Mbah. Transmission Dynamics Of Ebola Virus Disease With Vaccine, Condom Use, Quarantine, Isolation And Treatment Drug. Afr., J. Infect. Dis.(2021) 15(1): 10-23. https://doi.org/10.21010/ajid v15i1.2

[3] Centers for Disease Control and Prevention, Why Ebola is not likely to become Airborne [PDF, 194KB].Atlanta, GA: CDC; 2014.

[4] Centers for Disease Control and Prevention (CDC). Ebola (Ebola virus disease) [Internet]. Available from: http://www.cdc.gov/vhf/ebola/symptoms/index.html

[5] H. Fazal, S. Kamal, U. R Ghaus, and S. Muhammed, "Numerical solution of fractional order smoking model via Laplace Adomian Decomposition Method," Alexandra Engineering Journal, vol. 57, pp. 1061–1069, 2017.

[6] World Health Organization Ebola Response Team (2014). Ebola Virus Disease in West Africa – The first 9 months of the epidemic and forward projections. New England Journal of Medicine.

[7] N. Sullivan, Z. Yang and G.J. Nabel (2003). Ebola Virus Pathogenesis; Implications for Vaccine and Therapies. Journal of Virology, 77(18): 9733-9737.

[8] N. O. Lasisi, N.I. Akinwande, R.O. Olayiwola and A.T. Cole, Mathematical Model for Ebola Virus Infection in Human with Effectiveness of Drug Usage. Journal of Applied Science Environment Management.Vol.22(7)1089-1095 July 2018. Doi: https:dx.doi.org/10.4314/jasem.v22i7.16.

[9] R.J. Fisher, S. Judson, K. Miazgowicz, Ebola Virus Persistence in Semen at vivo. Emerg Infect Dis 2016; 22- 289- 91.

[10] A. Thorson, P. Formenty, C. Lofthouse, Systematic Review of the Literature on Viral Persistence and Sexual Transmission from Recovered Ebola Survivors: Evidence and Recommendations. BMJ 2016; 6:e008859.

[11] M. Y. Ongun, "The Laplace Adomian decomposition method for solving a model for HIV infection of CD4+ T cells," Mathematical and Computer Modelling, vol.53, no. 5-6, pp. 597–603, 2011.

[12] E. K. Akg¨ul, A. Akg¨ul, and M. Yavuz, "New illustrative applications of integral transforms to financial models with different fractional derivatives," Chaos, Solitons and Fractals, vol. 146, Article ID 110877, 2021.

[13] J. Alidousti and M. Mostafavi Ghahfarokhi, "Dynamical behavior of a fractional three-species food chain model," Nonlinear Dynamics, vol. 95, no. 3, pp. 1841–1858, 2019.

[14] Q.O. Ahman, Application of Fractional Differential Calculus to the Study of the Dynamics of Ebola Virus Disease, Ph.D Thesis, University of Nigeria Nsukka, Nigeria (May 2021).

[15] Q.O. Ahman, D. Omale, W. Atokolo, D.U. Nnaji, S.C.Ugwu and G.C.E.Mbah. Application of Fractional Calculus to the Dynamics of Ebola Disease Combining Vaccine, Condom, Quarantine, Isolation and Treatment Drugs as Measures. Academic Journal of Statistics and Mathematics. (2020b), Vol.6 issue 11.

[16] F. Haq, M. Shahzad, S. Muhammad, H. A. Wahab, and G. ur Rahman, "Numerical analysis of fractional order epidemic model of childhood diseases," Discrete Dynamics in Nature and Society, vol 2017, pp. 1–7, 2017.

[17] P. Adejoh and G. C. E. Mbah, Application of Fractional Differential Equations in Studying the Dynamics of Cancer Disease with its Control, University of Nigeria, Nsukka, M. Sc, 2018.

[18] W.Atokolo, R.O.Aja,D.Omale,Q.O.Ahman,G.O.Acheneje and J. Amos, Fractional mathematical model for the transmission dynamics and control of Lassa fever.Franklin Open vol 7 (2024).

[19] A.O. Yunus, and M.O. Olayiwola, (2024). The Analysis of a Co-Dynamic Ebola and Malaria Transmission Model Using the Laplace Adomian Decomposition Method with Caputo Fractional-Order. Tanzania Journal of Science, 50(2), 204–243.

[20] Q.O. Ahman,C.S.Ugwu, I.V. Ezaegu, N.E.Didugwu,D.Omale,F.Adegboye and G.C.E. Mbah." Approximate Solution of a Large Fractional Order Ebola Virus Disease Model with Control Measures via Laplace-Adomian Decomposition Method," Medicon Microbiology, 2.3(2023):13-28.

[21] Shah R, Farooq U, Khan H, Baleanu D, Kumam P and Arif M (2020) Fractional View Analysis of Third Order Kortewege-De Vries Equations, Using a New Analytical Technique. Front. Phys. 7:244. doi: 10.3389/fphy.2019.00244

[22] R.M. Ganji, H. Jafari, S. Nemati, A new approach for solving integro-differential equations of variable order, Journal of Computational and Applied Mathematics, Volume 379, 2020, 112946,

[23] R. Shah, H. Khan, D. Baleanu, P. Kumam, and M. Arif, (2020). A semi-analytical method to solve family of Kuramoto–Sivashinsky equations. Journal of Taibah University for Science, 14(1), 402–411. https://doi.org/10.1080/16583655.2020.1741920

[24] R. Shah, H. Khan, D. Baleanu, P. Kumam, and M. Arif, (2019). A novel method for the analytical solution of fractional Zakharov–Kuznetsov equations. Adv. Differ. Equ., 517 (2019). https://doi.org/10.1186/s13662-019-2441-5

[25] I. Area, H. Batarfi, J. Losada, J. J. Nieto, W. Shammakh, and A. Torres, "On a fractional order Ebola epidemic model," Advances in Difference Equations, vol. 2015, no. 1, pp. 1–12, 2015.

[26] K. Muhammad Altaf and A. Atangana, "Dynamics of Ebola disease in the framework of different fractional derivatives," Entropy, vol. 21, no. 3, p. 303, 2019.

[27] H. Singh, "Analysis for fractional dynamics of Ebola virus model," Chaos, Solitons and Fractals, vol. 138, Article ID 109992, 2020.

[28] B. Das¸bas¸ı, "Stability analysis of an incommensurate fractional- order SIR model," Mathematical Modelling and Numerical Simulation with Applications, vol. 1, no. 1, pp. 44–55, 2021

[29] N. Sene, "Second-grade fluid with Newtonian heating under Caputo fractional derivative: analytical investigations via Laplace transforms," Mathematical Modelling and Numerical Simulation with Applications, vol. 2, no. 1, pp. 13–25, 2022.

[30] M. Yavuz and N. Ozdemir, "Numerical inverse Laplace homotopy technique for fractional heat equations," 9ermal Science, vol. 22, pp. 185–194, 2018.

[31] M. Yavuz and N. Sene, "Approximate solutions of the model describing fluid flow using generalized ρ-laplace transform method and heat balance integral method," Axioms, vol. 9, no. 4, p. 123, 2020.

[32] K. Shah, H. Khalil, and R. A. Khan, "Analytical solution of fractional order diffusion equations by natural transform method," Iranian Journal of Science and Technology, vol. 16, pp. 1–14, 2016.

[33] H. Fazal, S. Kamal, U.R. Ghaus, and S. Muhammed, "Numerical solution of fractional order smoking model via Laplace Adomian Decomposition Method," Alexandra Engineering Journal, vol. 57, pp. 1061–1069, 2017.

[34] L.B. Dano, K.P. Rao, T.D. Keno, and K.P. Rao, " Fractional order differential equations for chronic liver cirrhosis with frequent hospitalization," BMC Research Notes, vol. 15, no. 1, pp. 332–410, 2022

[35] P. Van den Driessche and J. Watmough, "Reproduction numbers and sub-threshold endemic equilibria for compartmental models of disease transmission," Mathematical Biosciences, vol. 180, no. 1-2, pp. 29–48, 2002.

Mathematical model for transmission dynamics of Malaria disease: impact of invasive alien plants

C.J. Alhassan*, D. Okuonghae†, and K.O. Achema‡

Abstract

A mathematical model to study the impact of invasive alien plants on the dynamics of malaria transmission and its analyses is studied in this work. The resulted model equations are divided into homogeneous and non-homogeneous equations. The homogeneous equations are solved to determine its disease free equilibrium (DFE) and their stabilities. A basic reproduction number was determined from the DFE. It was found that when $R_0 < 1$, the disease will die out, when $R_0 = 1$, the model undergoes a backward bifurcation, $R_0 = 0$, the model undergoes forward bifurcation and whenever $R_0 > 1$, the disease will persist in the population. At $R_0 > 1$, the global analysis of the model was carried out and it was found to be globally and asymptotically stable (GAS). A sensitivity analysis of the model parameters was also investigated to determine the parameters that are sensitive for malaria transmission. A travelling wave equations and solutions were also provided for possible understanding of the behaviour of mosquito's mobility in human environment.

Keywords and phrases: malaria; invasive alien plant; mathematical model; stability, wave equations

1 Introduction

Malaria is a life-threatening disease caused by plasmodium parasites. It is transmitted when an infected female anopheles mosquito bite a susceptible human [11, 12]. The parasite inform of a sporozoite is injected into the blood stream and that is where infection started, and can also be transmitted through blood transfusion and contaminated needles. Infections by malaria parasites may result in a wide variety of symptoms, mild symptoms are fever, chills and headache. Severe symptoms include fatigue, confusion, seizures, and difficulty breathing. In general, malaria is a curable disease if diagnosed and treated promptly and correctly [2]. 608,000 malaria deaths occurred in 2022, with 95% of them occurring in the African Region.

The African region carries the highest share of the global malaria burden, with 94% of malaria cases and 95% of malaria deaths in 2022. The Sub-Saharan Africa, with the highest transmission found near the equator, particularly in Nigeria, the Democratic Republic of the Congo, Uganda, and Mozambique. Estimated 233 million malaria cases was reported in African Region in 2022 [12]. Children under 5 years old accounted for 80% of all malaria deaths in the African Region in 2022. Nigeria accounted for 27% of the global malaria burden and 31% of estimated deaths was due to malaria in 2022.

Malaria control strategy agenda using Dichlorodiphenyltrichloroethane (DDT) that became the main tool for the World Health Organisation's (WHO) malaria eradication programme from 1956 – 1967 fell out because of its effects on environmental management. Since the failure of this campaign to sustainably eliminate malaria from the tropics, the effectiveness of environmental management has remained tragically under-exploited. The authors in [8] promised a modern way of vector control

*Corresponding Author; Department of Mathematics and Computer Science, Edo State University, Uzairue, Edo State, Nigeria; E-mail: charity.alhassan@edouniversity.edu.ng

†Department of Mathematics, University of Benin, Benin City, Nigeria; E-mail: daniel.okuonghae@uniben.edu

‡Department of Mathematics, College of Physical Sciences, Joseph Sarwuan Tarka University, Makurdi, Benue State, Nigeria; E-mail: achema.kenneth@uam.edu.ng

strategies such as: invasive plant control, vaccination, treatments, control of vectors, insecticide treated net (ITN). It is based on this tragic background that we wish to develop a sound spatial nonlinear mathematical model to investigate the effects of invasive plants that allow for vector proliferation and spatial dynamics of vectors on the dynamics of malaria within a given habitat.

Invasive alien plants have been shown to have significant impacts on malaria transmission in various ways. These plants can create suitable habitats for mosquito breeding, leading to increased mosquito populations and greater transmission of the malaria parasite. In addition, invasive plants can alter local ecosystems and disrupt the natural balance of predator-prey relationships, further contributing to increased mosquito populations. Some invasive plants also have medicinal properties that can affect malaria treatment and drug resistance [8].

Overall, the invasion of alien plants poses a serious threat to efforts to control and prevent malaria transmission. It is crucial for researchers and policymakers to consider the impact of invasive plants on malaria transmission when developing strategies for disease control and management. Additionally, more research is needed to better understand the specific mechanisms through which invasive plants influence malaria transmission and to develop effective interventions to mitigate their negative effects. Mathematical models have been used to study the effects of invasive alien plants on malaria transmission. These models typically involve a combination of ecological and epidemiological factors to simulate how the presence of invasive plants can impact mosquito populations, parasite transmission, and disease dynamics [13].

One key aspect of these models is the influence of invasive plant habitats on mosquito breeding and population dynamics. By incorporating data on mosquito behaviour, habitat preferences, and reproductive rates, researchers can assess how invasive plants create environments conducive to mosquito proliferation, leading to increased malaria transmission.

Additionally, mathematical models can examine how invasive plants alter local ecosystems and disrupt predator-prey relationships that may regulate mosquito populations. These models can help identify mechanisms through which invasive plants indirectly affect malaria transmission by altering the abundance of mosquito predators or competitors. Furthermore, some mathematical models have explored the impact of invasive plants on the efficacy of malaria control strategies, such as insecticide spraying and bed nets. By considering how invasive plants affect mosquito behaviour and distribution, researchers can evaluate the effectiveness of traditional control.

One mathematical model that has been used to study the effects of invasive plants on malaria transmission is the "Larval Habitat Model." This model focuses on the relationship between the abundance of mosquito larval habitats, which can be influenced by the presence of invasive plants, and the density of mosquito populations. By quantifying the impact of invasive plant habitats on mosquito breeding sites, researchers can predict changes in malaria transmission dynamics.

Another mathematical model is the "Vector-Host Model," which considers the interactions between mosquito vectors, human hosts, and invasive plant habitats. This model can help assess how invasive plants create environments that favour mosquito breeding, leading to increased transmission of the malaria parasite to human hosts. By incorporating data on mosquito feeding habits, parasite development, and human movement patterns, researchers can better understand the complex dynamics of invasive plants on malaria transmission. Additionally, the "Ecosystem Disruption Model" is a mathematical model that examines how the invasion of alien plants disrupts local ecosystems and influences malaria transmission. This model can The Larval Habitat Model uses a system of differential equations to describe the dynamics of mosquito larvae in response to changes in habitat availability. The basic equation for the larval habitat model is:

$$\frac{dL}{dt} = cE - mL$$

Where $\frac{dL}{dt}$ represents the rate of change in the number of mosquito larvae over time, L represents the number of mosquito larvae in the habitat, c represents the rate at which mosquito eggs hatch and develop into larvae in the habitat, E represents the availability of suitable habitat for mosquito larvae to breed, and m represents the mortality rate of mosquito larvae in the habitat. This equation captures

the balance between the hatching of mosquito eggs and the mortality of larvae in the habitat, which is influenced by the availability of suitable breeding sites (habitat quality) determined by the presence of invasive alien plants. By manipulating the variables in this equation, researchers can assess how changes in habitat availability due to invasive plants impact mosquito larval populations on malaria transmission dynamics.

2 Methodology/Model formulation

We shall begin our study of the mathematical dynamics of malaria motivated by invasive alien plants presence in this section.

2.1 Assumptions of the model equations

To begin the formulation, we briefly state some important assumptions of our proposed model as follows.

M_1 It is assumed that vegetation harbour mosquito population.

M_2 It is assumed that mosquitoes are in human environment without vegetation.

M_3 It is also assumed that mosquitoes migrate from vegetation in random motion.

M_4 we also assume that some recovered humans lost immunity and became susceptible.

M_5 It is assumed that mosquitoes rest in the Vegetation and not all of them leave the vegetation to human environment due to their reproduction cycle.

2.2 Model variables and parameters

Our proposed mathematical model is divided into eight (8) sub-population, and nineteen (19) parameters as shown below.

2.3 Model equations

$$\begin{aligned}
\frac{\partial S_h}{\partial t} &= \Lambda_h - \lambda_h S_h + \alpha_h R_h - \mu_h S_h \\
\frac{\partial E_h}{\partial t} &= \lambda_h S_h - (q_h + \mu_h) E_h \\
\frac{\partial I_h}{\partial t} &= q_h E_h - (\delta_h + \mu_h + v_h) I_h \\
\frac{\partial R_h}{\partial t} &= v_h I_h - (\mu_h + \alpha_h) R_h \\
\frac{\partial P}{\partial t} &= g(1 - \frac{P}{K_P})P - hP \\
\frac{\partial S_m}{\partial t} &= D\frac{\partial^2 S_m}{\partial x^2} - K\frac{\partial S_m}{\partial x} + \Lambda_m + \theta_m P - \lambda_m S_m - (\xi_m + \mu_m) S_m \\
\frac{\partial E_m}{\partial t} &= D\frac{\partial^2 E_m}{\partial x^2} - K\frac{\partial E_m}{\partial x} + \lambda_m S_m - (q_m + \xi_m + \mu_m) E_m \\
\frac{\partial I_m}{\partial t} &= D\frac{\partial^2 I_m}{\partial x^2} - K\frac{\partial I_m}{\partial x} + q_m E_m - (\xi_m + \mu_m) I_m
\end{aligned} \tag{1}$$

Where,

$$\lambda_h = (1 - \epsilon\gamma)\beta_{hm}\frac{bI_m}{N_h}, \lambda_m = (1 - \epsilon\gamma)\beta_{mh}\frac{bI_h}{N_h}$$

$$0 < \epsilon < 1, 0 < \gamma < 1$$

Table 1: Description of model variables and parameters

Variable/Parameter	Interpretation
$S_h(t)$	Number of susceptible human at time t
$E_h(t)$	Number of exposed humans at time t
$I_h(t)$	Number of infected humans at time t
$R_h(t)$	Number of recovered humans at time t
$P(t)$	Invasive Plants population
$S_m(t)$	Number of susceptible mosquitoes at time t
$E_m(t)$	Number of Exposed mosquitoes at time t
$I_m(t)$	Number of infected mosquitoes at time t
b	Number of bite per mosquito/vector
D	The coefficient of diffusion
K	The coefficient of advection
q_h	Rate at which exposed human population become infected
v_h	Recovered rate of infected individual
α_h	Recovery rate of human
h	Control rate of invasive plants
θ_m	recruitment rate of mosquitoes from the density of invasive plants into the general susceptible mosquito
μ_h	Natural death rate of humans
δ_h	Disease induced death rate
g	Growth rate of plant
K_p	Plant carrying capacity
μ_m	Natural death rate of mosquitoes
ξ_m	Death rate of mosquito due to insecticide spray
$\lambda_h(t)$	Force of infection for humans
$\lambda_m(t)$	Force of infection for vectors
β_{hv}	probability of malaria from infectious humans to susceptible mosquitoes
β_{mh}	probability of malaria from vectors to humans
ϵ	Availability of bed-nets
γ	Efficacy of bed-nets

The homogeneous part of system (1) is given by

$$\begin{aligned}
\frac{dS_h}{dt} &= \Lambda_h - \lambda_h S_h + \alpha_h R_h - \mu_h S_h \\
\frac{dE_h}{dt} &= \lambda_h S_h - (q_h + \mu_h) E_h \\
\frac{dI_h}{dt} &= q_h E_h - (\delta_h + \mu_h + v_h) I_h \\
\frac{dR_h}{dt} &= v_h I_h - (\mu_h + \alpha_h) R_h \\
\frac{dP}{dt} &= g(1 - \frac{P}{K_P})P - hP \\
\frac{dS_m}{dt} &= \Lambda_m + \theta_m P - \lambda_m S_m - (\xi_m + \mu_m) S_m \\
\frac{dE_m}{dt} &= \lambda_m S_m - (q_m + \xi_m + \mu_m) E_m \\
\frac{dI_m}{dt} &= q_m E_m - (\xi_m + \mu_m) I_m
\end{aligned} \tag{2}$$

from (1),we substituted $N = S_m + E_m + I_m$
or

$$\frac{\partial N}{\partial t} = \frac{\partial S_m}{\partial t} + \frac{\partial E_m}{\partial t} + \frac{\partial I_m}{\partial t}$$

Therefore, the non-homogeneous part of system (1) given as

$$D\frac{\partial^2 N}{\partial x^2} - K\frac{\partial N}{\partial x} \tag{3}$$

where D and K represent Diffusion and advection

Note: the constant K was introduced into the known parabolic partial differential equation to capture the behaviour of mosquito mobility. The resulted equation (3) can be solved with space in time and distance.We then omitted the solution since actual grid for its life application be determined explicitly.

3 Analysis of the model

We begin our analysis with the homogeneous model equations of system (2) as follows:
To find the disease free equilibrium (DFE), we equate the left hand sides of system (2) to zero, that is, $\frac{dS_h}{dt} = \frac{dE_h}{dt} = \frac{dI_h}{dt} = \frac{dR_h}{dt} = \frac{dP}{dt} = \frac{dS_m}{dt} = \frac{dE_m}{dt} = \frac{dI_m}{dt} = 0$. At the same time, the infected variables are equate to zero. We then solve for the rest of non-infected variables as follows. Hence, system (2) becomes

$$\begin{aligned}
0 &= \Lambda - \lambda_h S_h + \alpha_h R_h - \mu_h S_h \\
0 &= \lambda_h S_h - (q_h + \mu_h) E_h \\
0 &= q_h E_h - (\delta_h + \mu_h + v_h) I_h \\
0 &= v_h I_h - (\mu_h + \alpha_h) R_h \\
0 &= g(1 - \frac{P}{K_P})P - hP \\
0 &= \Lambda_m + \theta_m P - \lambda_m S_m - (\xi_m + \mu_m) S_m \\
0 &= \lambda_m S_m - (q_m + \xi_m + \mu_m) E_m \\
0 &= q_m E_m - (\xi_m + \mu_m) I_m
\end{aligned} \tag{4}$$

3.1 Case 1: Where there is plant

Also at DFE,we have $E_h = I_h = R_h = E_m = I_m = 0$, substituting these into (4), we have

$$\begin{aligned}
\Lambda_h - \mu_h S_h &= 0 \\
g(1 - \frac{P}{K_P})P - hP &= 0 \\
\Lambda_m + \theta_m p - (\xi_m + \mu_m) S_m &= 0
\end{aligned} \tag{5}$$

Solving equation (5) for S_h, P and S_m, we have

$$\begin{aligned}
S_h^* &= \frac{\Lambda_h}{\mu_h} \\
P^* &= \frac{K_p(g-h)}{g} \\
S_m^* &= \frac{V_h g + K_p \theta_m (g+h)}{g(\xi_m + \mu_m)}
\end{aligned} \tag{6}$$

Therefore, the Disease Free-equilibrium corresponding to the presence of invasive plants is given by

$$\begin{aligned} E_1 &= (S_h^*, E_h^*, I_h^*, R_h^*, P^*, S_m^*, E_m^*, I_m^*) \\ &= (S*_h, 0, 0, 0, P^*, S_m^*, 0, 0) \end{aligned}$$

where

$$\begin{aligned} S_h^* &= \frac{\Lambda}{\mu_h}, \\ P^* &= \frac{K_p(g-h)}{g}, g > h \\ S_m^* &= \frac{\Lambda_m g + K_p \theta_m (g-h)}{g(\xi_m + \mu_m)}, g > h \end{aligned}$$

3.1.1 Biological implication of E_1 equlibrium

The equilibrium, E_1 is the equilibrium state where there is plant in human environment with mosquito present.In this equilibrium there is a contact between human and mosquito population and breeding site for mosquito population to thrive.This may result to malaria in human population as time progresses.

3.2 Case II: When there is no invasive plant in human environment

In this case, we solve for the equilibrium where $P = 0$, that is, the plant population and obtain the second Disease Free equilibrium (DFE) as follows:

$$\begin{aligned} E_2 &= (S_h^+, E_h^+, I_h^+, R_h^+, P^+, S_m^+, E_m^+, I_m^+) \\ &= \Big(\frac{\Lambda}{\mu_h}, 0, 0, 0, 0, \frac{\Lambda_m}{\xi_m + \mu_m}, 0, 0\Big) \end{aligned} \tag{7}$$

3.3 Biological implication of E_2,equilibrium

The Equilibrium E_2 is a Disease Free Equilibrium at which there is no invasive plant in the host environment.The contact rate of mosquito and human is low as the mosquito do not have a resting place to reside around the human environment after bite.Malaria transmission is very low and it can easily be controlled by mere use of mosquito net.

3.4 Analysis of basic reproduction number (R_0)

To calculate the basic reproduction number, we divide system (2) into appearance of infection and transfer of infection as matrix $F_i(x)$ and $V_i(x)$ where $F_i(x)$ be the rate of appearance of new infections in compartment i and $V_i(x)$ be the difference between the transfer rate of individuals out of compartment i by all other means. Thus, the $F_i(x)$ and $V_i(x)$ of model (2) is shown below: Let x_0 be the DFE of model (2). Thus, we have the following partitioned derivatives,

$$DF(x_0) = \begin{pmatrix} F & 0 \\ 0 & 0 \end{pmatrix}$$

$$DV(x_o) = \begin{pmatrix} V & 0 \\ J_3 & J_4 \end{pmatrix}$$

Where F and V are MxN matrices defined by

$$F = \left(\frac{\partial F_i}{\partial x_j(x_o)}\right)$$

and

$$V = \left(\frac{\partial V_i}{\partial x_j(x_o)}\right)$$

$1 \leq 1, j \leq m$

Here,the partial derivatives of F_i and V_i are with respect to the infected classes only. The basic reproduction number is defined as

$$R_o = \rho(FV^{-1}) \tag{8}$$

Where ρ is the spectral radius of FV^{-1}(by spectral radius we mean the maximum eigenvalue of $FV-1$)

Theorem 1

Consider the disease transmission model (2) with $f(x)$ satisfying the stability conditions if x_0 is a DFE of the model,then x_o is locally asymptotically stable if $R_0 < 1$, but unstable if $R_0 > 1$, where R_0 is defined by (8).For the purpose of easy access and clarity, we shall rewrite model (2) as follows:

$$\begin{aligned}
S_h^{\cdot} &= \Lambda - \lambda_h S_h + \alpha_h R_h - \mu_h S_h \\
E_h^{\cdot} &= \lambda_h S_h - (q_h + \mu_h) E_h \\
I_h^{\cdot} &= q_h E_h - (\delta_h + \mu_h + v_h) I_h \\
R_h^{\cdot} &= v_h I_h - (\mu_h + \alpha_h) R_h \\
P^{\cdot} &= g(1 - \frac{P}{K_P})P - hP \\
S_m^{\cdot} &= \Lambda_m + \theta_m P - \lambda_m S_m - (\xi_m + \mu_m) S_m \\
E_m^{\cdot} &= \lambda_m S_m - (q_m + \xi_m + \mu_m) E_m \\
I_m^{\cdot} &= q_m E_m - (\xi_m + \mu_m) I_m
\end{aligned} \tag{9}$$

Where,

$$\lambda_h = (1 - \epsilon\gamma)\beta_{hv}\frac{bI_m}{N_h}, \lambda_m = (1 - \epsilon\gamma)\beta_{mh}\frac{bI_h}{N_h}$$

Thus, F and V are given as

$$F = \begin{pmatrix} (1 - \epsilon\gamma)\beta_h m\frac{bI_m}{N_h}S_h \\ 0 \\ (1 - \epsilon\gamma)\beta_m h\frac{bI_h}{N_h}S_m \\ 0 \end{pmatrix}$$

and

$$V = \begin{pmatrix} (q_h + \mu_h)E_h \\ (\delta_h + \mu_h + v_h)I_h - q_h E_h \\ (q_m + \xi_m + \mu_m)E_m \\ (\xi_m + \mu_m)I_m - q_m E_m \end{pmatrix} \tag{10}$$

Since we have only four infected classes, E_h, I_h, E_m and I_m, it follows that $m = 4$.
The DFE is $E_h^* = I_h^* = R_h^* = E_m^* = I_m^* = 0$ and

$$\begin{aligned}
S_h^* &= \frac{\Lambda}{\mu_h}, P^* = \frac{K_p(g-h)}{g} \\
S_m^* &= \frac{V_h g + K_p\theta_m(g-h)}{g(\xi_m + \mu_m)}
\end{aligned} \tag{11}$$

putting these into consideration, we have

$$F = \begin{pmatrix} 0 & 0 & 0 & (1-\epsilon\gamma)\beta_{hm}b \\ 0 & 0 & 0 & 0 \\ 0 & \frac{V_h g + K_p\theta_m(g-h)}{g(\xi_m+\mu_m)}(1-\epsilon\gamma)\beta_{hm}b\frac{\Lambda}{\mu_h} & 0 & 0 \\ 0 & 0 & 0 & 0 \end{pmatrix}, \tag{12}$$

$$V = \begin{pmatrix} q_h+\mu_h & 0 & 0 & 0 \\ -q_h & \delta_h+\mu_h+v_h & 0 & 0 \\ 0 & 0 & q_m+\xi_m+\mu_m & 0 \\ 0 & 0 & -q_m & \xi_m+\mu_m \end{pmatrix}$$

and

$$V^{-1} = \begin{pmatrix} \frac{1}{q_h+\mu_h} & 0 & 0 & 0 \\ \frac{q_h}{(q_h+\mu_h)(v_h+\delta_h+\mu_h)} & \frac{1}{\delta_h+\mu_h+v_h} & 0 & 0 \\ 0 & 0 & \frac{1}{q_m+\xi_m+\mu_m} & 0 \\ 0 & 0 & \frac{q_m}{(\mu_m+\xi_m)(q_m+\mu_m+\xi_m)} & \frac{1}{(\mu_m+\xi_m)} \end{pmatrix} \tag{13}$$

Therefore,

$$FV^{-1} = \begin{pmatrix} 0 & 0 & b(1-\epsilon\gamma)q_m\beta_{hm} & \frac{b(1-\epsilon\gamma)\beta_{hm}}{\mu_m+\xi_m} \\ 0 & 0 & 0 & 0 \\ \omega & \frac{b(1-\epsilon\gamma)q_m\beta_{hm}(gV_h+(g+h)K_p\theta_m)\Lambda_h}{g\mu_h(v_h+\delta_h+\mu_h)(\mu_m+\xi_m)} & 0 & 0 \\ 0 & 0 & 0 & 0 \end{pmatrix} \tag{14}$$

where $\omega = \frac{b(1-\epsilon\gamma)q_m\beta_{hm}(gV_h+(g+h)K_p\theta_m)\Lambda_h}{g\mu_h(q_h+\mu_h)(v_h+\delta_h+\mu_h)(\mu_m+\xi_m)}$

Thus, calculating the eigenvalues of equation (14), we have,

$\lambda_1 = 0, \lambda_2 = 0$

$\lambda_3 = -\frac{b(-1+\epsilon\gamma)\sqrt{q_h}\sqrt{q_m}\sqrt{\beta_{hm}}\sqrt{\beta_{mh}}\sqrt{gv_h+gK_p\theta_m+hK_p\theta_m}\sqrt{\Lambda_h}}{\sqrt{g}\sqrt{\mu_h}\sqrt{q_h+\mu_h}\sqrt{v_h+\delta_h+\mu_h}(\mu_m+\xi_m)\sqrt{q_m+\mu_m+\xi_m}}$

$\lambda_4 = \frac{b(-1+\epsilon\gamma)\sqrt{q_h}\sqrt{q_m}\sqrt{\beta_{hm}}\sqrt{\beta_{mh}}\sqrt{gv_h+gK_p\theta_m+hK_p\theta_m}\sqrt{\Lambda_h}}{\sqrt{g}\sqrt{\mu_h}\sqrt{q_h+\mu_h}\sqrt{v_h+\delta_h+\mu_h}(\mu_m+\xi_m)\sqrt{q_m+\mu_m+\xi_m}}$

More so, the dominant eigenvalue is the basic reproduction number. Therefore,

$$R_{01} = \lambda_4 = \frac{b(1-\epsilon\gamma)}{(\mu_m+\xi_m)}\sqrt{\frac{q_h q_m\beta_{hm}\beta_{mh}(gv_h+gk_p\theta_m+hk_p\theta_m)\Lambda_h}{g\mu_h(q_h+\mu_h)(v_h+\delta_h+\mu_h)(q_m+\mu_m+\xi_m)}}$$

3.5 Basic reproduction analysis in the absence of invasive plants

Here, we are interesting in calculating basic reproduction number of E_2 of the Disease Free Equilibrium where there are no invasive plant. Substituting the equilibrium, E_2 in (10) after its partial derivatives, and taking the inverse of V_2, where,

$$\begin{aligned} E_2 &= (S_h^+, E_h^+, I_h^+, R_h^+, P^+, S_m^+, E_m^+ I_m^+) \\ &= \Big(\frac{\Lambda_h}{\mu_h}, 0, 0, 0, 0, \frac{\Lambda_m}{(\xi_m+\mu_m)}, 0, 0\Big) \end{aligned}$$

Thus, the basic reproduction number of E_2 is computed as:

$$\bar{F_2} = DF_2(E2) = \begin{pmatrix} 0 & 0 & 0 & (1-\epsilon\gamma)\beta_{hm}b \\ 0 & 0 & 0 & 0 \\ 0 & \frac{(1-\epsilon\gamma)b\beta_{mh}\Lambda_h\Lambda_m}{\mu_h(\xi_m+\mu_m)} & 0 & 0 \\ 0 & 0 & 0 & 0 \end{pmatrix}$$

and

$$\bar{V_2}^{-1} = \begin{pmatrix} \frac{1}{q_h+\mu_h} & 0 & 0 & 0 \\ \frac{q_h}{(q_h+\mu_h)(v_h+\delta_h+\mu_h)} & \frac{1}{V_h+\delta_h+\mu_h} & 0 & 0 \\ 0 & 0 & \frac{1}{q_m+\mu_h+\xi_m} & 0 \\ 0 & 0 & \frac{\xi_m}{(\mu_m+\xi_m)(q_m+\mu_m+\xi_m)} & \frac{1}{\mu_m+\xi_m} \end{pmatrix}$$

Therefore,

$$\bar{F_2}\bar{V_2}^{-1} = \begin{pmatrix} 0 & 0 & \frac{b(1-\epsilon\gamma)q_m\beta_h m}{(\mu_m+\xi_m)(q_m+\mu_m+\xi_m)} & \frac{b(1-\epsilon\gamma)\beta_{hm}}{\mu_m+\xi_m} \\ 0 & 0 & 0 & 0 \\ \frac{b(1-\epsilon\gamma)q_h\beta_m h\Lambda_h\Lambda_m}{\mu_h(q_h+\mu_h)(v_h+\delta_h+\mu_h)(\mu_m+\xi_m)} & \frac{b(1-\epsilon\gamma)\beta_m h\Lambda_h\Lambda_m}{\mu_h(v_h+\delta_h+\mu_h)(\mu_m+\xi_m)} & 0 & 0 \\ 0 & 0 & 0 & 0 \end{pmatrix} \tag{15}$$

The eigenvalues corresponding to equation (15) are:

$$\lambda_1 = 0, \lambda_2 = 0$$

and

$$\lambda_3 = -\frac{b(1-\epsilon\gamma)\sqrt{q_h q_m \beta_{hm}\Lambda_h\Lambda_m}}{(\mu_m+\xi_m)\sqrt{\mu_h(q_h+\mu_h)(v_h+\delta_h+\mu_h)(q_m+\mu_m+\xi_m)}} g > h$$

$$\lambda_4 = \frac{b(1-\epsilon\gamma)\sqrt{q_h q_m \beta_{hm}\Lambda_h\Lambda_m}}{(\mu_m+\xi_m)\sqrt{\mu_h(q_h+\mu_h)(v_h+\delta_h+\mu_h)(q_m+\mu_m+\xi_m)}}$$

Therefore, we obtained the spectral radius $\rho(\bar{F_2}\bar{V_2}^{-1})$ as

$$R_{02} = \frac{b(1-\epsilon\gamma)}{(\mu_m+\xi_m)}\sqrt{\frac{q_h q_m \beta_{hm}\Lambda_h\Lambda_m}{\mu_h(q_h+\mu_h)(v_h+\delta_h+\mu_h)(q_m+\mu_m+\xi_m)}} \tag{16}$$

3.6 Biological implication $R_{01,02}$

As in the work of [9, 10], the epidemiological meaning of the square root value of the R_{01}, R_{02} are that, it takes two generation for infected host to produce new infected host. The biological implication of these R_{01}, R_{02} depends on its value: If $R_{01}, R_{02} < 1$ there will be no malaria in future but if R_{01}, $R_{02} > 1$ malaria will become endemic in the host population.

3.7 Local asymptotic stability (LAS) of E_1 equilibrium

Here, we investigate the local asymptotic stability of our model equations in the case where there are invasive plants in the human environment. To do this, we linearized the homogeneous part of our model equations with the corresponding equilibrium, E_1 and obtained the following:

$$J(E_1) = \begin{pmatrix} C_1 & 0 & 0 & \alpha_h & 0 & 0 & 0 & \frac{-b(1-\epsilon\gamma)\beta_{hm}}{S_h^*} \\ 0 & C_2 & 0 & 0 & 0 & 0 & 0 & \frac{b(1-\epsilon\gamma)\beta_{hm}}{S_h^*} \\ 0 & q_h & D_1 & 0 & 0 & 0 & 0 & 0 \\ 0 & 0 & v_h & -\lambda-\xi_m+\mu & 0 & 0 & 0 & 0 \\ 0 & 0 & 0 & 0 & G_2-\lambda & 0 & 0 & 0 \\ 0 & 0 & \frac{-b(1-\epsilon\gamma)\beta_{mh}}{S_h^*} & 0 & \theta_m & -\lambda+G_3 & 0 & 0 \\ 0 & 0 & D_2 & 0 & 0 & 0 & -\lambda-G_4 & 0 \\ 0 & 0 & 0 & 0 & 0 & 0 & q_m & D_3 \end{pmatrix} \tag{17}$$

where $C_1 = -\lambda - \mu_h, C_2 = -\lambda - G_1, D_1 = -\lambda - (\delta_h + \mu_h + v_h), D_2 = \frac{b(1-\epsilon\gamma)\beta_{mh}}{S_h^*}, D_3 = -\lambda - \xi_m + \mu_m$ where

$$G_1 = (q_h + mu_h), G_2 = \alpha_h + \mu_h, G_3 = g - \frac{2gP^*}{K_p} - h, G_4 = q_m + \xi_m + \mu_m$$

The characteristic polynomial corresponding to the matrix is given by

$$T_1\lambda^4 + T_2\lambda^3 + T_3\lambda^2 + T_4\lambda + T_5 = 0 \tag{18}$$

$T_1 = (S^*)_h^2$

$$T_2 = (S^*)_h^2 q_m + 2(S^*)_h^2 \mu_m + 2(S^*)_h^2 \xi_m + q_h (S^*)_h^2 + \delta_h (S^*)_h^2 + 2\mu_h (S^*)_h^2 + (S^*)_h^2 v_h$$

$$T_3 = \delta_h (S^*)_h^2 q_m + 2\mu_h (S^*)_h^2 q_m + 2q_h (S^*)_h^2 \mu_m + (S^*)_h^2 \mu_m q_m + 2q_h (S^*)_h^2 \xi_m + (S^*)_h^2 \xi_m q_m + (S^*)_h^2 v_h q_m + q_h (S^*)_h^2 q_m$$

$$T_4 = \delta_h\mu_h (S^*)_h^2 q_m + 2\delta_h q_h (S^*)_h^2 \mu_m + \delta_h (S^*)_h^2 \mu_m q_m + 2\delta_h q_h (S^*)_h^2 \xi_m + \delta_h (S^*)_h^2 \xi_m q_m + \delta_h q_h (S^*)_h^2 q_m + 2\mu_h q_h (S^*)_h^2 \xi_m + 2\mu_h (S^*)_h^2 \xi_m q_m + 2q_h (S^*)_h^2 \mu_m \xi_m + \mu_h^2 (S^*)_h^2 q_m + q_h (S^*)_h^2 \mu_m^2 + \mu_h q_h (S^*)_h^2 q_m + q_h (S^*)_h^2 \mu_m q_m + 2\mu_h q_h (S^*)_h^2 \mu_m + 2\mu_h (S^*)_h^2 \mu_m q_m + q_h (S^*)_h^2 \xi_m^2 + q_h (S^*)_h^2 \xi_m q_m + \mu_h (S^*)_h^2 v_h q_m + 2q_h (S^*)_h^2 v_h \mu_m + (S^*)_h^2 v_h \mu_m q_m + 2q_h (S^*)_h^2 v_h \xi_m + (S^*)_h^2 v_h \xi_m q_m + q_h (S^*)_h^2 v_h q_m + 2\delta_h\mu_h (S^*)_h^2 \xi_m + 2\delta_h (S^*)_h^2 \mu_m \xi_m + \delta_h (S^*)_h^2 \mu_m^2 + 2\delta_h\mu_h (S^*)_h^2 \mu_m + \delta_h (S^*)_h^2 \xi_m^2 + 2\mu_h (S^*)_h^2 \xi_m^2 + 2\mu_h^2 (S^*)_h^2 \xi_m + 4\mu_h (S^*)_h^2 \mu_m \xi_m + 2\mu_h (S^*)_h^2 \mu_m^2 + 2\mu_h^2 (S^*)_h^2 \mu_m + 2\mu_h (S^*)_h^2 v_h \xi_m + 2(S^*)_h^2 v_h \mu_m \xi_m + (S^*)_h^2 v_h \mu_m^2 + 2\mu_h (S^*)_h^2 v_h \mu_m + (S^*)_h^2 v_h \xi_m^2$$

$$T_5 = b^2 q_h \beta_{hm} q_m \beta_{mh} + 2b^2\gamma\epsilon q_h \beta_{hm} q_m \beta_{mh} + q_h (S^*)_h^2 v_h \mu_m q_m + \delta_h q_h (S^*)_h^2 \mu_m q_m + \mu_h q_h (S^*)_h^2 \mu_m q_m + \mu_h (S^*)_h^2 v_h \mu_m q_m + \delta_h\mu_h (S^*)_h^2 \mu_m q_m + \mu_h^2 (S^*)_h^2 \mu_m q_m + q_h (S^*)_h^2 v_h \mu_m^2 + \delta_h q_h (S^*)_h^2 \mu_m^2 + \mu_h q_h (S^*)_h^2 \mu_m^2 + \mu_h (S^*)_h^2 v_h \mu_m^2 + \delta_h\mu_h (S^*)_h^2 \mu_m^2 + \mu_h^2 (S^*)_h^2 \mu_m^2 + q_h (S^*)_h^2 v_h \xi_m q_m + \delta_h q_h (S^*)_h^2 \xi_m q_m + \mu_h q_h (S^*)_h^2 \xi_m q_m + \mu_h (S^*)_h^2 v_h \xi_m q_m + \delta_h\mu_h (S^*)_h^2 \xi_m q_m + \mu_h^2 (S^*)_h^2 \xi_m q_m + 2q_h (S^*)_h^2 v_h \mu_m \xi_m + 2\delta_h q_h (S^*)_h^2 \mu_m \xi_m + 2\mu_h q_h (S^*)_h^2 \mu_m \xi_m + 2\mu_h (S^*)_h^2 v_h \mu_m \xi_m + 2\delta_h\mu_h (S^*)_h^2 \mu_m \xi_m + 2\mu_h^2 (S^*)_h^2 \mu_m \xi_m + q_h (S^*)_h^2 v_h \xi_m^2 + \delta_h q_h (S^*)_h^2 \xi_m^2 + \mu_h q_h (S^*)_h^2 \xi_m^2 + \mu_h (S^*)_h^2 v_h \xi_m^2 + \delta_h\mu_h (S^*)_h^2 \xi_m^2 + \mu_h^2 (S^*)_h^2 \xi_m^2 (1 - R_{01}^2)$$

To show the local asymptotic stability (LAS) of the disease free equilibrium (DFE) where there are invasive plants in human environment, we establish the conditions that will make the polynomial (18) have negative roots. To do this, we simply apply the Routh-Hurwitz Criterion. The following theorem suffices the claim:

3.8 Theorem 2

The polynomial (18) have negative roots only when T_1, T_2, ..., $T_5 > 0$, $T_1T_2 > T_3$ and $T_1T_2T_3 > T_3^2 + T_1^2T_4$.

3.8.1 Remark

Clearly, T_1, T_2, ..., $T_4 > 0$ and $T_5 > 0$ provided that $R_{01} < 0$, thus, the DFE corresponding to the invasive plants in human environment is locally asymptotically stable (LAS).

3.9 Epidemiological implication of E_1 stability

The stability of E_1 implies that the host population is malaria free for a long time period provided that $R_{01} < 1$.

3.10 Local asymptotic stability (LAS) of E_2 equilibrium

We shall investigate the local asymptotic stability of our model equations in the case where there are no invasive plants in the human environment. Thus, we linearized the homogeneous part of our model equations with the corresponding equilibrium, E_2 and obtained the following:

$$J(E_2) = \begin{pmatrix} \mu_h - \lambda & 0 & 0 & \alpha_h & 0 & 0 & 0 & -B_1 \\ 0 & -\lambda - A_1 & 0 & 0 & 0 & 0 & 0 & B_1 \\ 0 & q_h & -\lambda - A_2 & 0 & 0 & 0 & 0 & 0 \\ 0 & 0 & v_h & -\lambda - A_3 & 0 & 0 & 0 & 0 \\ 0 & 0 & 0 & 0 & -\lambda - A_4 & 0 & 0 & 0 \\ 0 & 0 & -B_2 & 0 & \theta_m & -\lambda - A_5 & 0 & 0 \\ 0 & 0 & B_2 & 0 & 0 & 0 & -\lambda - A_6 & 0 \\ 0 & 0 & 0 & 0 & 0 & 0 & q_m & -\lambda - A_5 \end{pmatrix} \tag{19}$$

where

$$A_1 = q_h + \mu_h, A_2 = \delta_h + \mu_h + v_h, A_3 = \alpha_h + \mu_h, A_4 = -h + g$$
$$A_5 = \xi_m + \mu_m, A_6 = q_m + \xi_m + \mu_m, B_1 = b\frac{1 - \epsilon\gamma\beta_{hm}}{S_h^{**}}, B_2 = b\frac{1 - \epsilon\gamma\beta_{mh}}{S_h^{**}}$$

The characteristic polynomial corresponding to the matrix is given by

$$x^4 + c_1x^3 + c_2x^2 + c_3x + c4 = 0 \tag{20}$$

where

$$\begin{aligned} c_1 &= A_1 + A_2 + A_5 + A_6 \\ c_2 &= A_1A_2 + A_1A_5 + A_2A_5 + A_1A_6 + A_2A_6 + A_5A_6 \\ c_3 &= A_1A_2A_5 + A_1A_2A_6 + A_2A_5A_6 \\ c_4 &= A_1A_2A_5A_6 - B_1B_2q_hq_m \end{aligned}$$

or

$$a_4 = A_1A_2A_5A_6(1 - R_{02}^2) \tag{21}$$

3.10.1 Remark

Clearly, $c_1, c_2, c_3 > 0$ and $c_4 > 0$ provided that $R_{02} < 0$, thus, the DFE corresponding to where there are no invasive plants in human environment is locally asymptotically stable (LAS).

3.11 Epidemiological implication of E_2 stability

The stability of E_2 equilibrium is conditioned on the value of R_{02} being less than a unit.The stability of E_2 equilibrium implies a host population free of malaria.

3.12 Disease endemic equilibrium

In this section, we are investigating the existence of an endemic equilibrium, however, we term this equilibrium as E_3. Thus, the equilibrium, E_3 is computed by solving for each state variable of the model (2), we then have,

$$E_3 = (S_h^{**}, E_h^{**}, I_h^{**}, R_h^{**}, P^{**}, S_m^{**}, E_m^{**}, I_m^{**})$$

where,

$$\begin{aligned} S_h^{**} &= \frac{\Lambda_h a_1 a_2 a_3}{(a_1 a_2 a_3 - V_h q_h \lambda_h \alpha_h)\lambda_h^{**} + \mu_h a_1 a_2 a_3} \\ E_h^{**} &= \frac{\Lambda_h a_1, a_3 \lambda_h^{**}}{(a_1 a_2 a_3 - v_h q_h \alpha_h)\lambda_h^{**} + \mu_h a_1 a_2 a_3} \\ I_h^{**} &= \frac{q_h \lambda_h^{**} \Lambda_h a_2}{(a_1 a_2 a_3 - v_h q_h \alpha_h)\lambda_h^{**} + \mu_h a_1 a_2 a_3} \\ R_h^{**} &= \frac{\Lambda_h v_h q_h \lambda_h^{**}}{(a_1 a_2 a_3 - v_h q_h \alpha_h)\lambda_h^{**} + \mu_h a_1 a_2 a_3} \end{aligned} \tag{22}$$

$$\begin{aligned} P^{**} &= \frac{K_p(g-h)}{g}, g > h \\ S_m^{**} &= \frac{\Lambda_m g + \theta_m K_p(g-h)}{g\lambda_m^{**} + a_4}, g > h \\ E_m^{**} &= \frac{\lambda_m^{**}(\Lambda_m g + \theta_m K_p(g-h))}{(g\lambda_m^{**} + a_4)a_5}, g > h \\ I_m^{**} &= \frac{\lambda_m^{**}(\Lambda_m g + \theta_m K_p(g-h)}{(g\lambda_m^{**} + a_4)a_4 a_5}, g > h \\ N_h^{**} &= \frac{\Lambda_h(a_1 a_2 a_3 + \lambda_h^{**}(a_1 a_3 + a_2 q_h + q_h V_h))}{(a_1 a_2 a_3 - v_h q_h \alpha_h)\lambda_h^{**} + \mu_h a_1 a_2 a_3} \end{aligned} \tag{23}$$

where

$$\begin{aligned} a_1 = \delta_h + \mu_h + v_h, a_2 = q_h + \mu_h, a_3 = \mu_h + \alpha_h, \\ a_4 = \xi_m + \mu_m, a_5 = q_m + \xi_m + \mu_m \end{aligned}$$

and

$$\lambda_h^{**} = (1-\epsilon\gamma)\beta_{hm}\frac{bI_m^{**}}{N_h^{**}}, \lambda_m^{**} = (1-\epsilon\gamma)\beta_{mh}\frac{bI_h^{**}}{N_h^{**}} \tag{24}$$

substituting equations (24) in equations (22) show that the non-zero equilibrium of the model can be written in a compact form as:

$$Z_1\lambda_h^{**} + Z_2\lambda_h^{**} + Z_3 = 0 \tag{25}$$

where

$$\begin{aligned} Z_1 &= [(a_1a_3 + a_2q_h + q_hm_h)(1-\epsilon\gamma)\beta_{mh}q_ha_2\Lambda + (a_1a_3 + a_2q_h + q_hm_h)^2g(\xi_m+\mu_m)^2\Lambda_h] \\ Z_2 &= [\Lambda_h(1-\epsilon\gamma)\beta_{mh}bq_ha_1a_2^2a_3 + a_1a_2a_3g(\xi_m+\mu_m)^2(a_1a_3 + a_2q_h + q_hm_h)\Lambda + g(\xi_m+\mu_m)^2(a_1a_3 \\ &\quad + a_2q_h + q_hm_h)\Lambda_ha_1a_2a_3 - a_1a_2^2a_3(1-\epsilon)b)^2\beta_vh\beta_{hm}\theta_mK_p(g-h)q_h \\ &\quad + ((1-\epsilon\gamma)b)^2\beta_{mh}\beta_{hv}\theta_mK_p(g-h)q_h^2v_h\alpha_h] \\ Z_3 &= a_1^2a_2^2a_3^2\Lambda g(\xi_m+\mu_m)^2 - a_1a_2^2a_3((1-\epsilon\gamma)b)^2\beta_{mh}\beta_{hv}\theta_mK_p(g-h)q_h\mu_h \\ &= a_1^2a_2^2a_3^2\Lambda_h g(\xi_m+\mu_m)^2[1-R_{01}^2] \end{aligned} \tag{26}$$

The endemic equilibria of the homogeneous part of the model (2) can be obtained by solving for λ_h^{**} from (24), and substituting the positive values of λ_h^{**} in (25) can be analyzed for the possibility of endemic equilibria when $R_{01} < 1$. It is obvious that the coefficients, Z_1 and Z_2, of the equation (26) is always positive provided that $(a_1a_3 + a_2q_h + q_hm_h)(1-\epsilon\gamma)\beta_{mh}q_ha_2\Lambda > (a_1a_3 + a_2q_h + q_hm_h)^2g(\xi_m+\mu_m)^2\Lambda$ and $[\Lambda(1-\epsilon\gamma)\beta_{mh}bq_ha_1a_2^2a_3 + a_1a_2a_3g(\xi_m+\mu_m)^2(a_1a_3+a_2q_h+q_hm_h)\Lambda > g(\xi_m+\mu_m)^2(a_1a_3 + a_2q_h + q_hm_h)\Lambda a_1a_2a_3 - a_1a_2^2a_3(1-\epsilon)b)^2\beta_mh\beta_{hm}\theta_mK_p(g-h)q_h + ((1-\epsilon\gamma)b)^2\beta_{mh}\beta_{hm}\theta_mK_p(g-h)q_h^2v_h\alpha_h]$ respectively. Also, Z_3 is positive (negative) if $R_{01} < 1 (R_{01} > 1)$. Hence, the following claim is established:

Theorem 3

The homogeneous part of the model (2), has

1. a single endemic equilibrium solution if any of the following three conditions is satisfied: R_{02} or $Z_2 < 0$ and $Z_1 = 0$ or $Z_2 < 0$ and $Z_2^2 - 4Z_1Z_3 = 0$
2. two endemic equilibria solutions if $Z_1 > 0$,$Z_2 < 0$ and $Z_2^2 - 4Z_1Z_3 > 0$.
3. no endemic equilibrium solution if both conditions above are not satisfied.

3.13 Biological implication

Different endemic equilibrium state will be observed in the host population.The first condition known as single endemic equilibrium implies malaria in all area of human population.The two endemic equilibrium states implies different level of malaria endemicity in the host population.

3.14 Backward bifurcation phenomenon

Backward bifurcation may occur under certain conditions for R_{01}. In such a case, we must have $R_{01} < 1$. From the expression of R_{01}, we know that if the transmission rate of malaria from mosquito to human is too low, there is no backward bifurcation. The presence of backward bifurcation indicates that the necessary requirement of $R_{01} < 1$, is not sufficient for disease elimination. The Centre Manifold theory will be used to improve the conditions on existence of backward bifurcation. To investigate the existence of the backward bifurcation of model (2), we shall rewrite (2) in the vector form as:

$$\frac{dY}{dt} = H(y) \tag{27}$$

where

$$Y = (y_1, y_2, y_3, y_4, y_5, y_6, y_7, y_8)^T$$

and

$$H = (h_1, h_2, h_3, h_4, h_5, h_6, h_7, h_8)^T$$

so that

$$S_h = y_1, E_h = y_2, I_h = y_3, R_h = y_4, P = y_5, S_m = y_6, E_m = y_7, I_m = y_8$$

.
Thus, model (2) becomes

$$\begin{aligned}
\frac{dy_1}{dt} &= \Lambda_h - \lambda_h y_1 + \alpha_h y_4 - \mu_h y_1 = h_1 \\
\frac{dy_2}{dt} &= \lambda_h y_1 - (q_h + \mu_h) y_2 := h_2 \\
\frac{dy_3}{dt} &= q_h y_2 - (\delta_h + \mu_h + v_h) y_3 := h_3 \\
\frac{dy_4}{dt} &= v_h y_3 - (\mu_h + \alpha_h) y_4 := h_4 \\
\frac{dy_5}{dt} &= g(1 - \frac{P}{K_P})P - h y_5 := h_5 \\
\frac{dy_6}{dt} &= \Lambda_m + \theta_m y_5 - \lambda_m y_6 - (\xi_m + \mu_m) y_6 := h_6 \\
\frac{dy_7}{dt} &= \lambda_m y_6 - (q_m + \xi_m + \mu_m) y_7 := h_7 \\
\frac{dy_8}{dt} &= q_m y_7 - (\xi_m + \mu_m) y_8 := h_8
\end{aligned} \tag{28}$$

with

$$\lambda_h = \phi\beta_{mh}\frac{bI_m}{N_h}, \lambda_m = \phi\beta_{mh}\frac{bI_h}{N_h}, \phi = 1 - \epsilon\gamma$$

Choosing β_{mh} as the bifurcation parameter at $R_{01} = 1$, We have

$$\beta_{mh} = \beta^*_{mh} = \frac{(\mu_m + \xi_m)g\mu_h(q_h + \mu_h)(v_h + \delta_h + \mu_h)(q_m + \mu_m + \xi_m)}{b(1 - \epsilon\gamma)q_h q_m \beta_{mh}(gV_h + gK_p\theta_m + hK_p\theta_m)\Lambda_h} \tag{29}$$

so that the disease-free equilibrium,E_1,is locally stable when $\beta_{mh} < \beta^*_{mh}$,and is unstable when $\beta_{mh} > \beta^*_{mh}$. Thus, β^*_{mh} is a bifurcation parameter. Linearizing matrix of the system (2) around DFE, E_1 and evaluated at β^*_{mh}, we have the following.

$$J(E_1, \beta^*_{mh}) = \begin{pmatrix} -\mu_h & 0 & 0 & \alpha_h & 0 & 0 & 0 & K_1 \\ 0 & -(q_h + \mu_h) & 0 & 0 & 0 & 0 & 0 & K_2 \\ 0 & q_h & K_5 & 0 & 0 & 0 & 0 & 0 \\ 0 & 0 & v_h & -(\alpha_h + \mu) & 0 & 0 & 0 & 0 \\ 0 & 0 & 0 & 0 & -\frac{g-2gp^*}{K_p} & 0 & 0 & 0 \\ 0 & 0 & \frac{-b\phi\beta_{mh}}{S^*_h} & 0 & K_3 & 0 & 0 & \\ 0 & 0 & \frac{-b\phi\beta_{mh}}{S^*_h} & 0 & 0 & 0 & K_4 & 0 \\ 0 & 0 & 0 & 0 & 0 & 0 & q_m & K_6 \end{pmatrix} \tag{30}$$

where $K_1 = \frac{-b\phi\beta^*_{hm}}{S^*_h}, K_2 = \frac{b\phi\beta^*_{hm}}{S^*_h}, K_3 = \theta_m - (\xi_m + \mu_m), K_4 = -(q_m + \xi_m + \mu_m), K_5 = -(\delta_h + \mu_h + v_h), -\xi_m + \mu_m$

The eigenvalues of $J(E, \beta^*_{hm})$ given by (31) are the roots of the characteristic equation of the form:

$$P(\lambda) = (\lambda + \mu_h)(\lambda + \alpha_h + \mu_h)(\lambda + \mu_m + \xi_m)(\lambda + \frac{g(2p-1)}{K_p}), \tag{31}$$

where $P(\lambda)$ is a polynomial of degree four whose roots are real and negative except one zero eigenvalue. Thus, the right eigenvector, $w = (w_1, w_2, w_3, w_4, w_5, w_6, w_7, w_8)^T$, associated with the simple zero eigenvalue can be obtained from $J(E_1, \beta^*_{hm}).w = 0$. Thus, we get

$$\begin{aligned} w_1 &= \frac{\alpha_h w_4 - \frac{b\phi\beta^*_{hm}}{s^*_h}}{\mu_h}, w_2 = \frac{b\phi\beta^*_{hm}}{q_h + \mu_h}s^*_h w_8, \\ w_3 &= \frac{q_h w_2}{\delta_h + \mu_h + v_h}, w_4 = \frac{v_h w_3}{\alpha_h + \mu_h}, \\ w_5 &= 0, w_6 = -\frac{-b\phi\beta_{mh}}{\xi_m + \mu_m}S^*_h w_3, w_7 = -\frac{-b\phi\beta_{mh}}{q_m + \xi_m + \mu_m}S^*_h w_3 \\ w_8 &= \frac{q_m w_7}{\xi_m + \mu_m} \end{aligned} \tag{32}$$

More so, the left eigenvector, $v = (v_1, v_2, ..., v_8)$, corresponding to the simple zero eigenvalues of (30) is obtained from $V.J(E_1, \beta^*_{mh}) = 0$. Thus,

$$\begin{aligned} v_1 &= 0, v_2 = \frac{q_h v_3}{q_h + \mu_h}, v_3 = \frac{\frac{b\phi\beta_{mh}}{s^*_h}(v_7 - v_6) + v_h v_4}{\delta_h + \mu_h + v_h}, \\ v_4 &= \frac{\alpha_h v_1}{\alpha_h + \mu_h} = 0, v_5 = 0, v_6 = 0, v_7 = \frac{q_m v_8}{q_m + \xi_m + \mu_m}, \\ v_8 &= \frac{\frac{b\phi\beta^*_{hm}}{s^*_h}(w_2 - w_1}{\xi_m + \mu_m} \end{aligned} \tag{33}$$

Therefore, the second-order partial derivatives of h_i,$i = 1, 2, ..., 8$ from system (30) are zero at point (E_1, β^*_{mh}) except the following.

$$\begin{aligned}
\frac{\partial^2 h_2}{\partial y_1 \partial y_8} &= \frac{\phi\beta_{hm}\mu_h b}{\mu_h} - \frac{\phi\beta^*_{mh}\mu_h^2 b S^*_h}{\Lambda_h^2} \\
\frac{\partial^2 h_2}{\partial y_2 \partial \beta^*_{mh}} &= \frac{\phi b \mu_h S^*_h}{\Lambda_h} \\
\frac{\partial^2 h_2}{\partial y_2 \partial y_8} &= \frac{\partial^2 h_2}{\partial y_3 \partial y_8} = \frac{\partial^2 h_2}{\partial y_4 \partial y_8} = -\frac{\phi\beta^*_{mh} b \mu_h^2 S^*_h}{\Lambda_h^2} \\
\frac{\partial^2 h_7}{\partial y_3^2} &= \frac{-2\phi\beta_{hm} b \mu_h^2 S^*_m}{\Lambda_h^2} \\
\frac{\partial^2 h_7}{\partial y_3 \partial y_6} &= \frac{\phi\beta_{hm} b \mu_h}{\Lambda_h}
\end{aligned} \tag{34}$$

Theorem 4

The authors in [1] Consider a general system of ordinary differential equations with a parameter δ as follow:

$$\frac{dx}{dt} = f(x, \delta), f : R^n x R \implies R, \tag{35}$$

and

$$f \epsilon C^2(R^n x R)$$

without loss of generality, it is assumed that 0 is an equilibrium of the system for all values of the parameter δ, (that is $f(0, \delta) \equiv 0$).

Assume

1. A = $D_x h(0, 0) = (\frac{\partial h_i}{\partial x_j}, 0, 0)$ is the linearized matrix of the system around the equilibrium 0 with σ evaluated at 0. Zero is a simple eigenvalue of **A** and all other eigenvalues of **A** have negative real parts;

2. Matrix A have a non-negative right eigenvector, w and a left eigenvector, v corresponding to the zero eigenvalue. Let h_k be the $k - th$ component of h and

$$\begin{aligned}
a &= \sum_{k,i,j=1}^{n} v_k w_i w_j \frac{\partial^2 h_k}{\partial y_i \partial y_j}(0, 0), \\
b &= \sum_{k,j=1}^{n} v_k w_i \frac{\partial^2 h_k}{\partial y_i \partial \sigma}(0, 0).
\end{aligned} \tag{36}$$

The local dynamics of system (28) around 0 are totally determined by a and b

- $a > 0$, $b > 0$, when $\sigma < 0$ with $|\sigma| << 1$, 0 is locally asymptotically stable and there exists a positive unstable equilibrium; when $0 < \sigma << 1$, 0 is unstable and there exists a negative and locally asymptotically stable equilibrium;

- $a < 0$, $b < 0$, when $\sigma < 0$ with $|\sigma| << 1$,0 is unstable when $0 < \delta << 1$,0 is locally asymptotically stable,and there exists a positive unstable equilibrium;

- $a > 0$, $b < 0$, when $\sigma < 0$ with $|\sigma| << 1$,0 is unstable and there exists a locally asymptotically stable negative equilibrium; when $0 < \sigma << 1$,0 is stable and a positive unstable equilibrium appears;

- a < 0, $b > 0$. When σ changes from negative to positive, 0 changes its stability from stable to unstable. Correspondingly, a negative unstable equilibrium becomes positive and locally asymptotically stable.In particular, if $a > 0$ and $b > 0$, then a backward bifurcation occurs at $\sigma = 0$.

In order to assess the value of a and b, we substitute equations (32) - (34) in equations (36), we get

$$\begin{aligned} a &= v_7 w_3^2 \frac{\delta^2 h_7}{\delta y_3^2} + 2v_7 w_3 w_6 \frac{\delta^2 h_7}{\delta y_3 \delta y_6} \\ &= v_7 w_3^2 (\frac{-2\phi\beta_{hm} b\mu_h^2 S_m^*}{\Lambda_h^2}) + 2v_7 w_3 w_6 \frac{\phi_h m b \mu_h}{\Lambda_h} \\ &= -2[(\frac{q_m}{q_m + \xi_m + \mu_m})(\frac{q_h}{\delta_h + \mu_h + v_h})^2 (\frac{\theta\beta_h m b\mu_h^2 S_m^*}{\Lambda_h^2}) v_8 w_2^2 \\ &+ (\frac{q_m}{q_m + \xi_m + \mu_m})(\frac{q_h}{\delta_h + \mu_h + v_h})(\frac{\theta\beta_{hm}^2 b^2 \mu_h}{\Lambda_h(\xi_m + \mu_m) S_h^*}) v_8 w_2] \\ b &= v_2 w_2 \frac{q_h}{\delta_h + \mu_h + v_h} \frac{\phi b \mu_h S_h^*}{\Lambda_h} > 0 \end{aligned} \tag{37}$$

Remark: The coefficient b is always positive. Theorem 4 implies that system (2) will undergo backward bifurcation at $R_{01}(\beta_{mh}^*) = 1$ if $a > 0$. we recalled the fact that all the parameters of model (2) are positive and also the value of v_8 and w_2 are positive, it is easy to see that $a < 0$ and $b > 0$. Therefore, from Theorem 2 item (iv),the model (2) exhibit a forward (super-critical) bifurcation as R_{01} crosses the threshold, $R_{01} = 1$ (i.e; a locally asymptotically stable endemic equilibrium, $E_3 = (S_h^{**}, E_h^{**}, I_h^{**}, R_h^{**}, P^{**}, S_m^{**}, E_m^{**}, I_m^{**})$ representing the non-trivial positive steady-states of model (2) exists)

Biological implication

A host environment with free malaria can become malaria persistent environment when an individual previously affected by malaria transmit to other individuals with a given population.

3.15 Global stability of endemic equilibrium

The global stability of the Endemic Equilibrium E_3 of model (2) is very important in this study because both mosquito, vegetation and human co-exist. We will study this by considering the homogeneous

spatial model of system (2) given as:

$$\begin{aligned}
\frac{dS_h}{dt} &= \Lambda_h - \lambda_h S_h + \alpha_h R_h - \mu_h S_h \\
\frac{dE_h}{dt} &= \lambda_h S_h - (q_h + \mu_h) E_h \\
\frac{dI_h}{dt} &= q_h E_h - (\delta_h + \mu_h + v_h) I_h \\
\frac{dR_h}{dt} &= v_h I_h - (\mu_h + \alpha_h) R_h \\
\frac{dP}{dt} &= g(1 - \frac{P}{K_P})P - hP \\
\frac{dE_m}{dt} &= \phi\tilde{\beta_m} hb I_h S_m - (q_m + \xi_m + \mu_m) E_m \\
\frac{dS_m}{dt} &= \Lambda_m + \theta_m P - \lambda_m S_m - (\xi_m + \mu_m) S_m \\
\frac{dI_m}{dt} &= q_m E_m - (\xi_m + \mu_m) I_m
\end{aligned} \tag{38}$$

where

$$\lambda_h = (1 - \epsilon\gamma)\beta_{hm}\frac{bI_m}{N_h}, \lambda_m = (1 - \epsilon\gamma)\beta_{mh}\frac{bI_h}{N_h}$$

with

$$N = \frac{\Lambda_h}{\mu}$$

and

$$\phi = 1 - \epsilon\gamma,$$

we have

$$\lambda_h = \phi\beta_{hm}\frac{\mu b I_m}{\Lambda} = \phi\tilde{\beta}_h m b I_m$$

$$\lambda_m = \phi\tilde{\beta}_m h b I_h$$

We shall employ the method of Goh-Volterra type Lyapunov function to investigate the GAS of the EEP, E_3. Let

$$\begin{aligned}
W = (S_h - S_h^{**} - S_h^{**} ln\frac{S_h}{S_h^{**}}) + (E_h - E_h^{**} - E_h^{**} ln\frac{E_h}{E_h^{**}}) + C(I_h - I_h^{**} - I_h^{**} ln\frac{I_h}{I_h^{**}}) \\
+(S_m - S_m^{**} - S_m^{**} ln\frac{S_m}{S_m^{**}}) + (E_m - E_m^{**} - E_m^{**} ln\frac{E_m}{E_m^{**}}) + D(I_m - I_m^{**} - I_m^{**} ln\frac{I_m}{I_m^{**}})
\end{aligned} \tag{39}$$

be the Lyaponov function of the Goh-Voltera type. Taking the time derivative of equation (39), we have

$$\begin{aligned}
\dot{W} = (\dot{S_h} - \frac{S_h^{**}}{S_h}\dot{S_h}) + (\dot{E_h} - \frac{E_h^{**}}{E_h}\dot{E_h}) + C(\dot{I_h} - \frac{I_h^{**}}{I_h}\dot{I_h}) \\
+(\dot{S_m} - \frac{S_m^{**}}{S_m}\dot{S_m}) + (\dot{E_m} - \frac{E_m^{**}}{E_m}\dot{E_m}) + D(\dot{I_m} - \frac{I_m^{*}*}{I_m}\dot{I_m})
\end{aligned} \tag{40}$$

Substituting the right hand side of the equations (38) in (40)
we have

$$\begin{aligned}
\dot{W} &= \Lambda_h - \phi\tilde{\beta}_{hm}bI_mS_h + \alpha_hR_h - \mu_hS_h - \frac{S^**}{S}[\Lambda_h - \phi\tilde{\beta}_hmbS_h + \alpha_hR_h - \mu_hS_h] \\
&+ \phi\tilde{\beta}_hmbI_mS_h - (q_h + \mu_h)E_h - \frac{E_h^{**}}{E_h}[(\phi\tilde{\beta}_{hm}bI_mS_h - (q_h + \mu_h)E_h] \\
&+ C[q_hE_h - (\delta_h + \mu_h + v_h)I_h] - \frac{I_h^{**}}{I_h}[(q_hE_h - (\delta_h + \mu_h + v_h)I_h)] \\
&+ \Lambda_m + \theta_mp - [\phi\tilde{\beta_m}hbI_hS_m - (\xi_m + \mu_m)S_m] - \frac{S_m^{**}}{S_m}[\Lambda_m + \theta_mP - [\phi\tilde{\beta_m}hbI_hS_m - (\xi_m + \mu_m)S_m] \\
&+ \phi\tilde{\beta_m}hbI_hS_m - (q_m + \xi_m + \mu_m)E_m - \frac{E_m^{**}}{E_m}(\phi\tilde{\beta_m}hbI_hS_m - (q_m + \xi_m + \mu_m)E_m) \\
&+ D(q_mE_m - (\xi_m + \mu_m)I_m - \frac{I_m^{**}}{I_m}(q_m + (\xi_m + \mu_m)I_m))
\end{aligned} \tag{41}$$

At steady state, we observe that

$$\begin{aligned}
\Lambda_h &= \phi\tilde{\beta}_{hm}bI_m^{**}S_h^{**} + \mu_hS_h^{**} \\
\Lambda_m &= \phi\tilde{\beta}_{mh}bI_h^{**}S{*}{*}_m + (\xi_m + \mu_m)S_m^{**} - \theta_mP^{**}
\end{aligned} \tag{42}$$

Now, setting $\delta_h = 0$ and substituting (41) in (40), we have

$$\begin{aligned}
\dot{W} &= \phi\tilde{\beta}_{hm}bI_m^{**}S_h^{**} + \mu_hS_h^{**} - \phi\tilde{\beta}_{hm}bI_mS_h + \alpha_hR_h - \mu_hS_h \\
&- \phi\tilde{\beta}_{hm}bI_m^{**}\frac{S_h^{**2}}{S_h} - \frac{\mu S_h^{**2}}{S_h} + \phi\tilde{\beta}_{hm}bI_mS_h^{**} - \alpha_hR_h\frac{S_h^{**}}{S_h} \\
&+ \mu_hS_h^{**} + \phi\tilde{\beta}_{hm}bI_mS_h - (q_h + \mu_h)E_h - \phi\tilde{\beta}_{hm}bI_mS_h\frac{E_h^**}{E_h} \\
&+ (q_h + \mu_h)E_h^{**} + Cq_hE_h - C(v_h + \mu_h)I_h - Cq_hE_h\frac{I_h^**}{I_h} \\
&+ C(v_h + \mu_h)I_h^** \\
&+ \phi\tilde{\beta}_{hm}bI_h^{**}S_m^{**} + (\xi_m + \mu_h)S_m^{**} - \phi\tilde{\beta}_{mh}bI_hS_m \\
&+ \phi\tilde{\beta}_{mh}bI_h^{**}S_m^{**} + (\xi_m + \mu_h)S_m^{**} - \theta_mP + \theta_mP - \phi\tilde{\beta}_{mh}bI_hS_m - (\xi_m + \mu_h)S_m
\end{aligned}$$

$$\begin{aligned}
&- \frac{S_m^{**2}}{S_m}\phi\tilde{\beta}_{mh}bI_h^{**} - \frac{S_m^{**2}}{S_m}(\xi_m + \mu_m) + \frac{S_m^{**}}{S_m}\theta_mP - \theta_mP\frac{S_m^{**}}{S_m} + \phi\tilde{\beta}_{mh}bI_hS_m^{**} \\
&+ (\xi_m + \mu_m)S_m^{**} + \phi\tilde{\beta}_{mh}bI_hS_m - (q_m + \xi_m + \mu_m)E_m - \frac{E_m^{**}}{E_m}\phi\tilde{\beta}_{mh}bI_hS_m \\
&+ (q_m + \xi_m + \mu_m)E_m^{**} + Dq_mE_m - D(\xi_m + \mu_m)I_m - D\frac{I_m^{**}}{I_m}q_mE_m + D(\xi_m + \mu_m)I_m^{**}
\end{aligned}$$

Separating the infected classes without double stars on them (1.e E_h, I_h, I_m), we have

$$\begin{aligned}
\dot{W} &= \phi\tilde{\beta}_{hm}bI_m^{**}S_h^{**} + \mu_hS_h^{**} + \alpha_hR_h - \mu_hS_h \\
&- \phi\tilde{\beta}_{hm}bI_m^{**}\frac{S_h^{**2}}{S_h} - \frac{\mu S_h^{**2}}{S_h} + \phi\tilde{\beta}_{hm}bI_mS_h^{**} - \alpha_hR_h\frac{S_h^{**}}{S_h}
\end{aligned} \tag{43}$$

$$
\begin{aligned}
&+\mu_h S_h^{**} - (q_h+\mu_h)E_h - \phi\tilde{\beta}_{hm} b I_m S_h \frac{E_h^{**}}{E_h} \\
&+ (q_h+\mu_h)E_h^{*} * + C q_h E_h - C(\mu_h+v_h)I_h - C(q_h E_h \frac{I_h^{**}}{I_h}) + C(\mu_h+v_h)I_h^{**} \\
&+ \phi\tilde{\beta}_{hm} b I_h^{**} S_m^{**} + (\xi_m+\mu_h)S_m^{**} - \phi\tilde{\beta}_{mh} b I_h S_m \\
&- (\xi_m+\mu_h)S_m - \phi\tilde{\beta}_{mh} b I_h \frac{S_m^{**2}}{S_m} - (\xi_m+\mu_h)\frac{S_m^{**2}}{S_m} + \phi\tilde{\beta}_{mh} b I_h S_m^{**} \\
&+ (\xi_m+\mu_m)S_m^{**} - (q_m+\xi_m+\mu_m)E_m - \frac{E_m^{**}}{E_m}\phi\tilde{\beta}_{mh} b I_h S_m \\
&+ (q_m+\xi_m+\mu_m)E_m^{**} + D q_m E_m - D(\xi_m+\mu_m)I_m - D\frac{I_m^{**}}{I_m} - D(\xi_m+\mu_m)I_m^{**}
\end{aligned}
\tag{44}
$$

We then collect the terms without double stars on them together as

$$
\begin{aligned}
&\phi\tilde{\beta}_{hm} b I_m S_h^{**} - (q_h+\mu_h)E_h + C q_h E_h - C(\mu_h+v_h)I_h \\
&+ \phi\tilde{\beta}_{mh} b I_h S_m^{**} - (q_m+\xi_m+\mu_m)E_m + D q_m E_m - D(\xi_m+\mu_m)I_m = 0
\end{aligned}
\tag{45}
$$

Solving for C and D from (45) in terms of I_h and I_m, we have

$$
\begin{aligned}
I_h(\phi\tilde{\beta}_{mh} b I_h S_m^{**} - (\mu_h+v_h)) &= 0 \\
C &= \frac{\phi\tilde{\beta}_{mh} b S_m^{**}}{\mu_h+v_h}
\end{aligned}
$$

$$
\begin{aligned}
I_m(\phi\tilde{\beta}_{mh} b S_h^{**} - D(\xi_m+\mu_m)) &= 0 \\
D &= \frac{\phi\tilde{\beta}_{mh} b S_h^{**}}{(\xi_m+\mu_m)}
\end{aligned}
$$

Also, we have from (45) at steady state

$$
(q_h+\mu_h) = \frac{\phi\tilde{\beta}_{hm} b I_m^{**} S_h^{**}}{E_h^{**}}
$$

$$
q_h = \frac{(v_h+\mu_h)I_h^{**}}{E_h^{**}}
$$

$$
= \frac{\phi\tilde{\beta}_{mh} b I_h \frac{S_m^{**2}}{S_m} + \phi\tilde{\beta}_{mh} b S_m^{**}}{E_h^{*} *}
$$

$$
(q_m+\xi_m+\mu_m) = \frac{\phi\tilde{\beta}_{mh} b I_h^{**} S_m^{**}}{E_m^{**}}
$$

$$
q_m = \frac{(\xi_m+\mu_m)I_m^{**}}{E_m}
$$

Rewritten (44) without including terms with double stars on them, we have

$$\begin{aligned}\dot{W} &= \phi\tilde{\beta}_{hm}bI_m^{**}S_h^{**} + \mu_h S_h^{**} - \mu_h S_h - \phi\tilde{\beta}_{hm}bI_m^{**}\frac{S_h^{**2}}{S_h} \\ &- \frac{\mu_h S_h^{**}}{S_h} + \mu_h S_h^{**} - \phi\tilde{\beta}_{hm}bI_m S_h\frac{E_h^{*}*}{E_h} \\ &+ (q_h+\mu_h)E_h^{**} - C(q_h E_h\frac{I_h^{**}}{I_h}) + C(\mu_h+v_h)I_h^{**} \\ &+ \phi\tilde{\beta}_{hm}bI_h^{**}S_m^{**} + (\xi_m+\mu_m)S_m^{**} - (\xi_m+\mu_m)S_m \\ &- \frac{S_m^{**2}}{S_m}\phi\tilde{\beta_{mh}}bI_h^{**} - (\xi_m+\mu_h)\frac{S_m^{**2}}{S_m} \\ &+ (\xi_m+\mu_m)S_m^{**} + (\xi_m+\mu_m)S_m^{**} - \frac{E_m^{*}*}{E_m}\phi\tilde{\beta_{mh}}bS_m I_h + (q_m+\xi_m+\mu_m)E_m^{**} \\ &- D\frac{I_m^{**}}{I_m}q_m E_m + D(\xi_m+\mu_m)I_m^{**}\end{aligned} \tag{46}$$

Substituting for C, D and q_h, $(q_h+\mu_h)$ and $(q_m+\xi_m+\mu_m)$ and q_m into (46) we have

$$\begin{aligned}\dot{W} &= \phi\tilde{\beta}_{hm}bI_m^{**}S_h^{**} + \mu_h S_h^{**} - \mu_h S_h \\ &- \phi\tilde{\beta}_{mh}bI_m^{**}\frac{S_h^{**2}}{S_h} - \mu_h\frac{S_h^{**2}}{S_h} + \mu_h S_h^{**} - \phi\tilde{\beta}_{hm}bI_m S_h\frac{E_h^{**}}{E_h} \\ &+ \phi\tilde{\beta_{hm}}bI_m^{**}S_h^{**} - \phi\tilde{\beta}_{mh}bS_m^{**}\frac{I_h^{**2}}{I_h}\frac{E_h}{E_h^{**}} + \phi\tilde{\beta}_{mh}bI_h^{**}S_m^{**} \\ &+ \phi\tilde{\beta}_{mh}bI_h^{**}S_m^{**} + \xi_m S_m^{**} + \mu_m S_m^{**} - \xi_m S_m - \mu_m S_m - \frac{S_m^{**2}}{S_m}\phi\tilde{\beta}_{hm}bI_h^{**} - \frac{S_m^{**2}}{S_m}\xi_m \\ &- \mu_m\frac{S_m^{**2}}{S_m} + \xi_m S_m^{**} + \mu_m S_m** - \frac{E_m^{**}}{E_m}\phi\tilde{\beta}_{mh}I_h S_m \\ &+ \phi\tilde{\beta}_{mh}bI_h^{**}S_m^{**} - \phi\tilde{\beta}_{hm}S_h^{**}\frac{I_m^{**2}}{I_m}\frac{E_m}{E_m^{**}} + \phi\tilde{\beta}_{hm}bS_h^{**}I_m^{**}\end{aligned} \tag{47}$$

By gathering the terms with $\mu_h S_h, \mu_m S_m, \phi\tilde{\beta}_{hm}, \phi\tilde{\beta}_{mh}$ and factorizing (47), we have

$$\begin{aligned}\mu_h S_h^{**}(2 - \frac{S_h^{**}}{S_h} - \frac{S_h}{S_h^{**}}) \\ \mu_m S_m^{**}(2 - \frac{S_m}{S_m^{**}} - \frac{S_m^{**}}{S_m}) \\ \phi\tilde{\beta}_{hm}bI_m^{**}S_h^{**}(3 - \frac{S_h^{**}}{S_h} - \frac{S_h}{S}{}_h^{**}\frac{E_h^{**}}{E_h}\frac{I_m}{I_m^{**}} - \frac{I_m^{**}}{I_m}\frac{E_m}{E_m^{**}}) \\ \phi\tilde{\beta}_{mh}bI_h^{**}S_m^{**}(3 - \frac{S_h^{**}}{I_h}\frac{E_h}{E_h^{**}} - \frac{S_m^{**}}{S_m} - \frac{I_h}{I_h^{**}}\frac{E_m^{**}}{E_m})\end{aligned} \tag{48}$$

Finally, since the arithmetic mean exceeds the geometric mean, the following inequalities hold.

$$\mu_h S_h^{**}(2 - \frac{S_h^{**}}{S_h} - \frac{S_h}{S_h^{**}}) \leq 0$$

$$\mu_m S_m^{**}(2 - \frac{S_m}{S_m^{**}} - \frac{S_m^{**}}{S_m}) \leq 0$$

$$\phi\tilde{\beta}_{hm} b I_m^{**} S_h^{**}(3 - \frac{S_h^{**}}{S_h} - \frac{S_h}{S_h}^{**}\frac{E_h^{**}}{E_h}\frac{I_m}{I_m}^{**} - \frac{I_m^{**}}{I_m}\frac{E_m}{E_m^{**}}) \leq 0$$

$$\phi\tilde{\beta}_{mh} b I_h^{**} S_m^{**}(3 - \frac{S_h^{**}}{I_h}\frac{E_h}{E_h^{**}} - \frac{S_m^{**}}{S_m} - \frac{I_h}{I_h^{**}}\frac{E_m^{**}}{E_m}) \leq 0$$

Thus, we have $\dot{W} \leq 0$ for $R_{01} > 1$. Hence, W is a Lyaponov function and the equilibrium E_3 is globally asymptotically stable.

Biological implication

The disease will persist in the host environment provided that those that are infected with the disease keep on transmitting the disease.The less than or equal $(\leq)$ sign of the lyapunov function shows the decrease of the susceptible population.

3.16 Sensitivity analysis

In this section, we performed the sensitivity analysis in order to determine the relative importance of the model parameters on disease transmission. The analysis will enable us to find out parameters that have high impact on the basic reproduction number and which should be targeted for intervention strategies. We perform sensitivity analysis by calculating the sensitivity indices of the effective reproduction number R_{01} since our major emphasis is on the invasive plants in order to determine whether malaria fever can be controlled or not. These indices tell us how crucial each parameter is on the transmission of malaria fever. The sensitivity index of R_{01} to a parameter say τ, where τ is any of the parameters in Table 3 is given by

$$\Gamma_y^{R_{01}} = \frac{\partial R_{01}}{\partial y} \times \frac{y}{R_{01}} \tag{49}$$

Table (2) provides the indices of R_{01} to its parameters. From Table 2, it is obvious that the reproduction number, R_{01} is most sensitive to number of bite per mosquito (b), plants carrying capacity(K_p), recovered rate of humans(v_h), migration rate of mosquitoes from the vegetation (θ_m), disease induced death rate (δ_h), plants growth rate (g),deforestation rate (h) probability of transmission of malaria from infectious human to susceptible human (β_{hm}) and the probability of transferring malaria from vectors to human (β_{mh}) while the R_{02} is less sensitive to the recruitment rate of human population (Λ), rate at which exposed humans become infected (q_h), death rate of mosquitoes due to insecticides spray (ξ), availability of bed-nets and the efficacy of bed-nets (γ) [7].

The most sensitive parameter is number of bite per mosquito (b),followed by Λ_h recruitment rate of human population,Λ_m recruitment rate of mosquitoes δ_h disease induced death rate, natural death rate of humans (μ_h). Any increment in the values of the parameters with negative indices would reduce the value of the basic reproduction number, also any increment in the value of the parameters having positive indices will increase the endemicity of the disease. However Table 2 shows the relationship between the basic reproduction number and number of bite per mosquito, it shows that as number

of bite per mosquito increases, the basic Reproduction number increases. Also as the treatment of exposed class increases, the basic reproduction number reduces, this means that, with intensity control measure against mosquitoes and treatment of exposed class, we could eliminate malaria from the host environment. The basic reproduction number increases in all cases as all these parameters increases, which means that all these parameters have to be kept at minimal level to have a complete eradication of malaria.

Biological implication

The parameters with positive values have impact on the malaria transmission. Reducing them or decreasing them lead to the decrease of the basic reproduction number.

3.17 Travelling wave solution

In this section, we shall assess the spatial spread of malaria disease when some infected mosquitoes flies from the invasive plant to human environment. With this regard, we shall find the travelling wave linking the equilibrium points and to determine the conditions for the existence of the propagation speed of such wave[3, 9]. In our model, we assumed that the vector population takes both advection movement (k) which increase the wave speed and dispersal coefficient D which depend on the wave propagation speed, v.
Travelling wave solution with respect to our model equation are of the form:
$E_h(x,t) = e_h(z), I_h(x,t) = i_h(z), E_m(x,t) = e_m(z), I_m(x,t) = i_m(z)$, where $z = x - vt$ and v is the constant wave speed, which we shall determine. Replacing system (1) in wave equation form, we obtain the following system of ordinary differential equations:

$$\begin{aligned}
e_h + \frac{\tilde{\lambda_h}}{v}(1 - e_h - i_h - r_h) - (q_h + \mu_h)\frac{e_h}{v} = 0 \\
i_h + \frac{q_h}{v}eh - (\delta_h + \mu_h + v_h)\frac{i_h}{v} = 0 \\
r_h + \frac{v_h}{v}i_h - (\mu_h + \alpha_h)\frac{r_h}{v} = 0 \\
De_m^{''} - (k - v)e_m^{'} - \tilde{\lambda_m}(1 - e_m - i_m) + (\xi_m + \mu_m)e_m = 0 \\
Di_m^{''} - (k - v)i_m^{'} - q_m e_m + (\xi_m + \mu_m)i_m = 0
\end{aligned} \tag{50}$$

where the line denotes the derivative in relation to z. This system is equivalent to the following system of first-order differential equations:

$$\begin{aligned}
\frac{de_h}{dz} &= -\frac{\lambda_h}{v}(1 - e_h - i_h - r_h) + (q_h + \mu_h)\frac{e_h}{v} \\
\frac{di_h}{dz} &= -\frac{q_h}{v}eh + (\delta_h + \mu_h + v_h)\frac{i_h}{v} \\
\frac{dr_h}{dz} &= -\frac{v_h}{v}i_h + (\mu_h + \alpha_h)\frac{r_h}{v}
\end{aligned} \tag{51}$$

$$\begin{aligned}
\frac{de_m}{dz} &= u_1 \\
\frac{du_1}{dz} &= \frac{1}{D}(k - v)u_1 + \frac{\lambda_m}{D}(1 - e_m - i_m) - (\xi_m + \mu_m)\frac{e_m}{D} \\
\frac{di_m}{dz} &= u_2 \\
\frac{du_2}{dz} &= \frac{1}{D}(k - v)u_2 + \frac{1}{D}q_m e_m - (\xi_m + \mu_m)\frac{i_m}{D}
\end{aligned} \tag{52}$$

where

$$\frac{di_m}{dt} = i_m''(z), \frac{de_m}{dt} = e_m''(z)$$

There are two equilibrium point of the system above the first is $g_1 = (0,0,0,0,0,0,0)$ Which represents disease free equilibrium and the second, $g_2 = (E_h^o, I_h^o, R_h^o, E_m^o, I_m^o, 0, 0)$ which is the non trivial equilibrium that corresponds to infection The conditon for the existence of g_2 is $R_o > 1$ because $E_h^o, I_h^o, R_h^o, E_m^o, I_m^o$ are non-negative.We want to find the condition for a solution with a positive wave propagation speed v and with non-negative $E_h^o, I_h^o, R_h^o, E_m^o, I_m^o$ that the following boundary conditions holds.

$$\begin{gathered} e_h(-\infty) = E_h** \text{ and } e_h(+\infty) = 0 \\ i_h(-\infty) = I_h** \text{ and } i_h(-\infty) = 0 \\ e_m(-\infty) = E_m** \text{ and } e_m(-\infty) = 0 \\ i_m(-\infty) = I_m** \text{ and } i_m(-\infty) = 0 \\ u(-\infty) = 0 \text{and } u(+\infty) = 0 \end{gathered}$$

we searched for solutions in the positive region,such that $E_h^o > 0, I_h^o > 0, R_h^o > 0, E_m^o > 0, I_m^o > 0$ and the solution cannot oscillate near the origin. The eigen value of the Jacobian matrix must be real and non complex values otherwise $E_h^o < 0, I_h^o < 0, R_h^o < 0, E_m^o < 0, I_m^o < 0$ for some z
The Jacobian matrix at g^* is given by

$$Dg_1 = \begin{pmatrix} \frac{q_h+\mu_h}{v} - \psi & 0 & 0 & 0 & 0 & -\frac{b\phi\beta_{\text{hm}}}{v} & 0 \\ -\frac{q_h}{v} & \frac{v_h+\delta_h+\mu_h}{v} - \psi & 0 & 0 & 0 & 0 & 0 \\ 0 & -\frac{v_h}{v} & -\psi & 0 & 0 & 0 & 0 \\ 0 & 0 & 0 & -\psi & 1 & 0 & 0 \\ 0 & 0 & 0 & -\mu_m - \xi_m & \frac{k-v}{D} - \psi & 0 & 0 \\ 0 & 0 & 0 & 0 & 0 & 1-\psi & 0 \\ 0 & 0 & 0 & \frac{q_m}{D} & 0 & -\mu_m - \xi_m & \frac{k-v}{D} - \psi \end{pmatrix}, \quad (53)$$

The corresponding eigenvalues are the roots of the polynomial

$$p(\Psi) = \Psi^6 + b_0\Psi^5 + b_1\Psi^4 + b_2\Psi^3 + b_3\Psi^2 + b_4\Psi + b_5 \quad (54)$$

where

$b_0 = \frac{2k}{D} + \frac{2v}{D} - \frac{q_h}{v} - \frac{\delta_h}{v} + \frac{2\mu_h}{v} - \frac{v_h}{v} + 1$

$b_1 = \frac{k^2}{D^2} - \frac{2kv}{D^2} + \frac{v^2}{D^2} - \frac{2\delta_h}{D} + \frac{2kq_h}{Dv} + \frac{2k\delta_h}{Dv} + \frac{4k\mu_h}{Dv} + \frac{2kv_h}{Dv} - \frac{4\mu_h}{D} - \frac{2q_h}{D} - \frac{2v_h}{D} - \frac{2k}{D} - \frac{2v}{D} + \frac{\delta_h q_h}{v^2} + \frac{\mu_h q_h}{v^2} + \frac{q_h v_h}{v^2} + \frac{q_h}{v} + \frac{\delta_h \mu_h}{v^2} + \frac{\mu_h^2}{v^2} + \frac{\mu_h v_h}{v^2} + \frac{\delta_h}{v} + \frac{2\mu_h}{v} + \frac{v_h}{v} + \mu_m - \xi_m$

$b_2 = \frac{k^2 q_h}{D^2 v} - \frac{k^2\delta_h}{D^2 v} - \frac{2k^2\mu_h}{D^2 v} + \frac{k^2 v_h}{D^2 v} + \frac{2k\delta_h}{D^2} + \frac{4k\mu_h}{D^2} + \frac{2kq_h}{D^2} + \frac{2kv_h}{D^2} - \frac{vq_h}{D^2} - \frac{v\delta_h}{D^2} + \frac{2v\mu_h}{D^2} - \frac{vv_h}{D^2} - \frac{k^2}{D^2} + \frac{2kv}{D^2} - \frac{v^2}{D^2} + \frac{2\delta_h}{D} - \frac{2k\delta_h q_h}{Dv^2} - \frac{2k\mu_h q_h}{Dv^2} - \frac{2kq_h v_h}{Dv^2} - \frac{2kq_h}{Dv} - \frac{2k\delta_h\mu_h}{Dv^2} - \frac{2k\mu_h^2}{Dv^2} - \frac{2k\mu_h v_h}{Dv^2} - \frac{2k\delta_h}{Dv} - \frac{4k\mu_h}{Dv} - \frac{2kv_h}{Dv} + \frac{4\mu_h}{D} + \frac{2\delta_h q_h}{Dv} + \frac{2\mu_h q_h}{Dv} + \frac{2q_h v_h}{Dv} + \frac{2q_h}{D} + \frac{2\delta_h\mu_h}{Dv} + \frac{2\mu_h^2}{Dv} + \frac{2\mu_h v_h}{Dv} + \frac{2v_h}{D} - \frac{k\mu_m}{D} - \frac{k\xi_m}{D} + \frac{v\mu_m}{D} + \frac{v\xi_m}{D} - \frac{q_h\mu_m}{v} - \frac{q_h\xi_m}{v} - \frac{\delta_h\mu_m}{v} - \frac{\delta_h\xi_m}{v} - \frac{2\mu_h\xi_m}{v} - \frac{v_h\mu_m}{v} - \frac{2\mu_h\mu_m}{v} - \frac{v_h\xi_m}{v} - \frac{\delta_h q_h}{v^2} - \frac{\mu_h q_h}{v^2} - \frac{q_h v_h}{v^2} - \frac{\delta_h\mu_h}{v^2} - \frac{\mu_h^2}{v^2} - \frac{\mu_h v_h}{v^2} + \mu_m + \xi_m$

$b_3 = -\frac{q_h k^2}{D^2 v} - \frac{v_h k^2}{D^2 v} - \frac{\delta_h k^2}{D^2 v} - \frac{2\mu_h k^2}{D^2 v} - \frac{\mu_h^2 k^2}{D^2 v^2} - \frac{q_h v_h k^2}{D^2 v^2} - \frac{q_h\delta_h k^2}{D^2 v^2} - \frac{q_h\mu_h k^2}{D^2 v^2} - \frac{v_h\mu_h k^2}{D^2 v^2} - \frac{\delta_h\mu_h k^2}{D^2 v^2} + \frac{2\mu_h^2 k}{D^2 v} + \frac{2q_h k}{D^2} + \frac{2q_h v_h k}{D^2 v} + \frac{2v_h k}{D^2} + \frac{2q_h\delta_h k}{D^2 v} + \frac{2\delta_h k}{D^2} + \frac{2q_h\mu_h k}{D^2 v} + \frac{2v_h\mu_h k}{D^2 v} + \frac{2\delta_h\mu_h k}{D^2 v} + \frac{4\mu_h k}{D^2} - \frac{\mu_m k}{D} - \frac{\xi_m k}{D} - \frac{q_h\mu_m k}{Dv} - \frac{v_h\mu_m k}{Dv} - \frac{\delta_h\mu_m k}{Dv} - \frac{2\mu_h\mu_m k}{Dv} - \frac{q_h\xi_m k}{Dv} - \frac{v_h\xi_m k}{Dv} - \frac{\delta_h\xi_m k}{Dv} - \frac{2\mu_h\xi_m k}{Dv} - \frac{2\mu_h^2 k}{Dv^2} - \frac{2q_h v_h k}{Dv^2} - \frac{2q_h\delta_h k}{Dv^2} - \frac{2q_h\mu_h k}{Dv^2} - \frac{2v_h\mu_h k}{Dv^2} - \frac{2\delta_h\mu_h k}{Dv^2} + \frac{2\mu_h^2}{Dv} + \frac{2q_h v_h}{Dv} + \frac{2q_h\delta_h}{Dv} + \frac{2q_h\mu_h}{Dv} + \frac{2v_h\mu_h}{Dv} + \frac{2\delta_h\mu_h}{Dv} + \frac{v\mu_m}{D} + \frac{q_h\mu_m}{D} + \frac{v_h\mu_m}{D} + \frac{\delta_h\mu_m}{D} + \frac{2\mu_h\mu_m}{D} + \frac{v\xi_m}{D} + \frac{q_h\xi_m}{D} + \frac{v_h\xi_m}{D} + \frac{\delta_h\xi_m}{D} + \frac{2\mu_h\xi_m}{D} - \frac{\mu_h^2}{D^2} - \frac{vq_h}{D^2} - \frac{vv_h}{D^2} - \frac{q_h v_h}{D^2} - \frac{v\delta_h}{D^2} - \frac{q_h\delta_h}{D^2} - \frac{2v\mu_h}{D^2} - \frac{q_h\mu_h}{D^2} - \frac{v_h\mu_h}{D^2} - \frac{\delta_h\mu_h}{D^2} - \frac{q_h\mu_m}{v} - \frac{v_h\mu_m}{v} - \frac{\delta_h\mu_m}{v} - \frac{2\mu_h\mu_m}{v} - \frac{q_h\xi_m}{v} - \frac{v_h\xi_m}{v} - \frac{\delta_h\xi_m}{v} - \frac{2\mu_h\xi_m}{v} - \frac{\mu_h^2\mu_m}{v^2} - \frac{q_h v_h\mu_m}{v^2} - \frac{q_h\delta_h\mu_m}{v^2} - \frac{q_h\mu_h\mu_m}{v^2} - \frac{v_h\mu_h\mu_m}{v^2} - \frac{\delta_h\mu_h\mu_m}{v^2} - \frac{\mu_h^2\xi_m}{v^2} - \frac{q_h v_h\xi_m}{v^2} - \frac{q_h\delta_h\xi_m}{v^2} - \frac{q_h\mu_h\xi_m}{v^2} - \frac{v_h\mu_h\xi_m}{v^2} - \frac{\delta_h\mu_h\xi_m}{v^2}$

$b_4 = \frac{\mu_h^2 k^2}{D^2 v^2} + \frac{q_h v_h k^2}{D^2 v^2} + \frac{q_h\delta_h k^2}{D^2 v^2} + \frac{q_h\mu_h k^2}{D^2 v^2} + \frac{v_h\mu_h k^2}{D^2 v^2} + \frac{\delta_h\mu_h k^2}{D^2 v^2} + \frac{\mu_h^2\mu_m k}{Dv^2} + \frac{q_h\mu_m k}{Dv} + \frac{q_h v_h\mu_m k}{Dv^2} + \frac{v_h\mu_m k}{Dv} +$

$\frac{q_h\delta_h\mu_m k}{Dv^2} + \frac{\delta_h\mu_m k}{Dv} + \frac{q_h\mu_h\mu_m k}{Dv^2} + \frac{v_h\mu_h\mu_m k}{Dv^2} + \frac{\delta_h\mu_h\mu_m k}{Dv^2} + \frac{2\mu_h\mu_m k}{Dv} + \frac{\mu_h^2\xi_m k}{Dv^2}$

$b_5 = -\frac{k\delta_h q_h\mu_m}{Dv^2} - \frac{k\delta_h q_h\xi_m}{Dv^2} - \frac{k\mu_h q_h\xi_m}{Dv^2} - \frac{k\mu_h q_h\mu_m}{Dv^2} - \frac{kq_h v_h\mu_m}{Dv^2} - \frac{kq_h v_h\xi_m}{Dv^2} - \frac{k\delta_h\mu_h\xi_m}{Dv^2} - \frac{k\delta_h\mu_h\mu_m}{Dv^2} - \frac{k\mu_h^2\xi_m}{Dv^2} - \frac{k\mu_h v_h\xi_m}{Dv^2} - \frac{k\mu_h^2\mu_m}{Dv^2} - \frac{k\mu_h v_h\mu_m}{Dv^2} + \frac{\delta_h q_h\mu_m}{Dv} + \frac{\delta_h q_h\xi_m}{Dv} + \frac{\mu_h q_h\xi_m}{Dv} + \frac{\mu_h q_h\mu_m}{Dv} + \frac{q_h v_h\mu_m}{Dv} + \frac{q_h v_h\xi_m}{Dv} + \frac{\delta_h\mu_h\xi_m}{Dv} + \frac{\delta_h\mu_h\mu_m}{Dv} + \frac{\mu_h^2\xi_m}{Dv} + \frac{\mu_h v_h\xi_m}{Dv} + \frac{\mu_h^2\mu_m}{Dv} + \frac{\mu_h v_h\mu_m}{Dv}$

From Routh Hurwitz criterion, the root of the polynomial $g(x)$ are either negative or have a negative real part if and only if

1. $b_i(i = 1, 2, 3, 4, 5, 6)$

2. $b_1 b_2 > b_3$

3. $b_1 b_2 b_3 - b_1^2 b_4 > b_3^2 + b_1 b_5$

4. $b_3^2 b_4 + 2b_1 b_4 b_5 > b_1 b_5 b_2^2 + b_1 b_3 b_4 b_2 + b_3 b_5 b_2 + b_1^2 b_4^2 + b_5^2$

However, as $R_o > 1$, $\psi_5 > 0$, then $\lim_\Psi \longrightarrow \pm\infty$, $b(\Psi) = +\infty$. To provide the minimum wave propagation speed, the polynomial have 6 complex roots, 3 conjugated complex roots and 3 real roots. In equation (54), the trajectories must approach the disease -free equilibrium and they cannot oscillate because the positive region is invariant.Thus the polynomial must have negative real roots.

However, we consider the case without advection ($K = 0$). If $R_o 1 = 1$, then $p(0) = 0$, The polynomial $p(\Psi)$ always has a negative real root if the $\lim_\Psi \longrightarrow -\infty = +\infty$. Therefore,for $R_o 1 = 1$, we obtain that $v_{min} = 0$, and then, nonwave speed exists. For $R_o 1 > 1$,the existence of three real root depends on the value of v.For $v < v_{min}$,the roots are complex.For $v = v_m in$, we have a double negative real root and for $v > v_{min}$ three negative real roots. However,the minimal speed at the double root of the polynomial is $p(v_m in) = p'(v_m in) = 0$ Secondly, we consider the advection movement(i.e. $k \neq 0$), k appear adding the value of v, from the expression of the polynomial coefficients $b_0, b_1, b_2, b_3 and b_4$. Hence, advection increases the wave speed when it is in the same direction of the wave front and decreases it when it is in the opposite direction.

Remark The determination of the wave speed, v will be determine by estimating the fly speed of the mosquito per day which we term as diffusion (the D value). We will thereafter use appropriate curves for the explicit meaning of the wave speed and its epidemiological impact on the malaria transmission.

4 Numerical simulations/sensitivity analysis

The following Table 3 gives a summary of the parameter values used herein:

$$D = \frac{L^2}{2T}$$

where L is the average distance covered by mosquito in a day and T is the time taken to travel [10].

The following graphical representation of the formulated model are obtained from Table 2 parameters' values.

Table 2: Description of the model parameters' values

Parameter	Value	Sensitivity Index	Reference
μ_h	0.00004643/day	+0.500000	Kenya National Bureau of Statistics
β_{hm}	0.24/day	+0.230400	[5]
β_{mh}	0.14/day	+0.001000	[5]
q_h	0.083/day	+0.000300	[5]
α_h	0.000017/day	Not applicable	[4]
v_h	0.00265/day	-0.089600	[5]
K_p	1	+0.002100	Variable
ϵ	0.5	-0.015220	Variable
γ	0.6	+0.001000	Variable
δ_h	0.0003454/day	-0.489000	[4]
b	0.5	+1.000000	Variable
θ_m	0.343	+0.043210	[5]
q_m	0.091	+0.000500	[4]
g	1.84	+0.120000	[5]
μ_m	0.1041	-0.001600	[4]
h	0.05	Not applicable	Variable
D	3.125	Not applicable	Computed
k	4.5	Not applicable	[6]
L	2.5	Not applicable	[6]

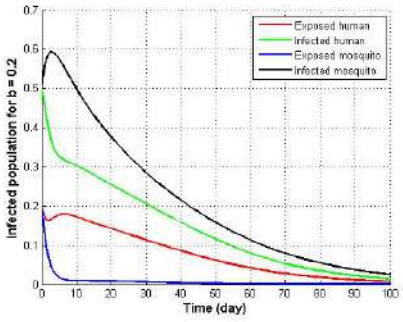


Figure 1: Plot of the infected population over time

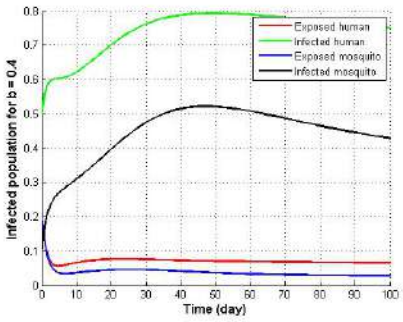


Figure 2: Plot of the infected population over time

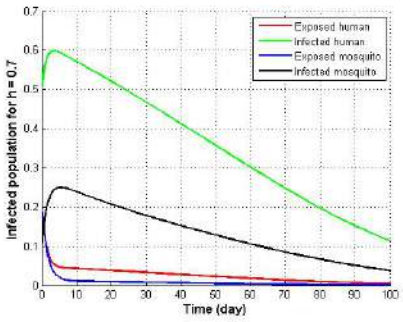


Figure 3: Plot of the infected population over time

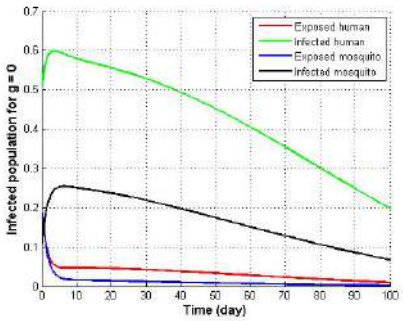


Figure 4: Plot of the infected population over time

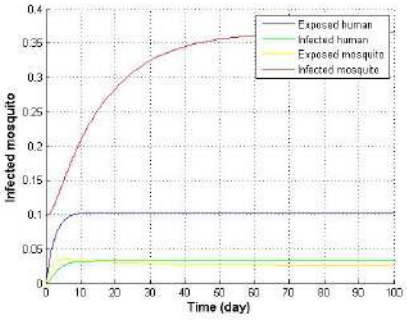


Figure 5: Plot of the infected compartment of Equations (4) with initial conditions $e_h(0) = 0, i_h(0) = 0, e_m(0) = 0$ and $i_m(0) = 0.1$

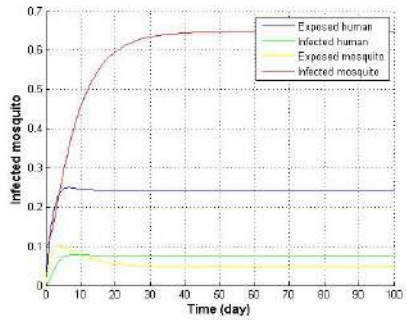


Figure 6: Plot of the infected compartment of Equations (4) with initial conditions $e_h(0) = 0, i_h(0) = 0, e_m(0) = 0$ and $i_m(0) = 0.3$

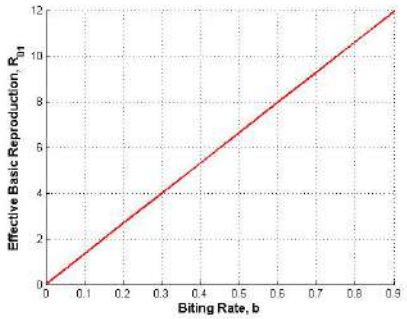


Figure 7: Plot of the effective reproduction number, R_{01} over the biting rate, b

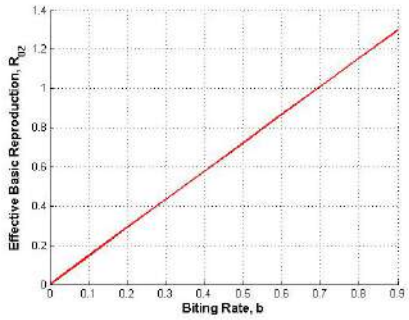


Figure 8: Plot of the effective reproduction number, R_{02} over the biting rate, b



Figure 9: Plot of the effective reproduction number, R_{01} over the disease induced death rate, δ_h

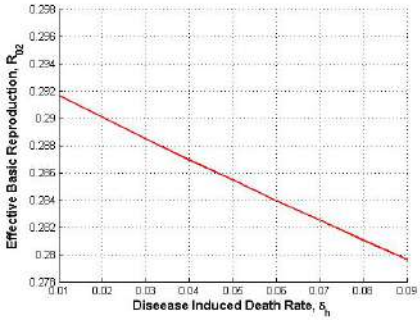


Figure 10: Plot of the effective reproduction number, R_{02} over the disease induced death rate, δ_h

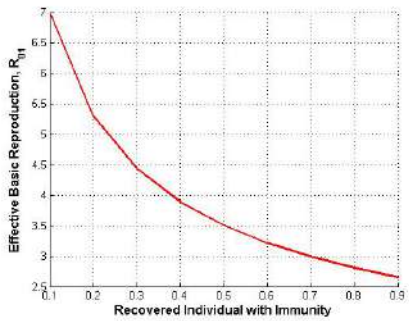


Figure 11: Plot of the effective reproduction number, R_{01} over the recovered individuals with immunity, v_h

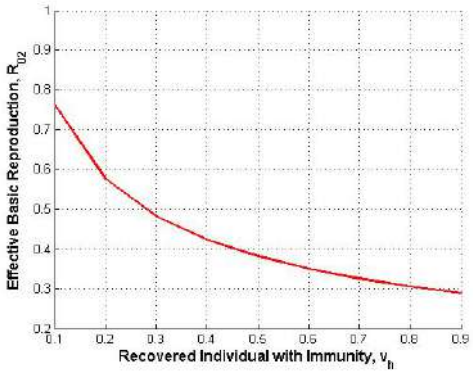


Figure 12: Plot of the effective reproduction number, R_{02} over the immune individuals, v_h

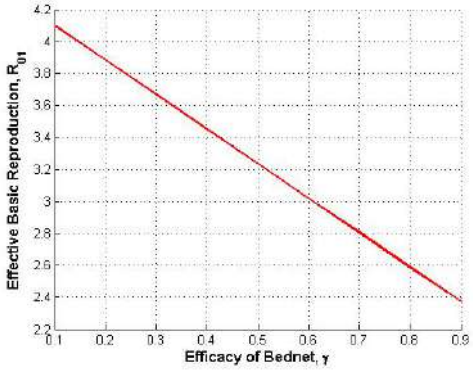


Figure 13: Plot of the effective reproductive number, R_{01} over the bed net efficacy, γ

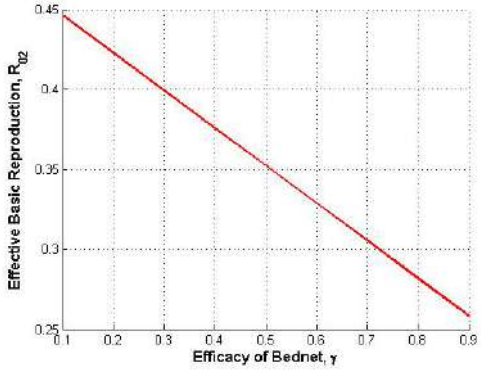


Figure 14: Plot of the effective reproductive number, R_{02} over the bed net efficacy, γ

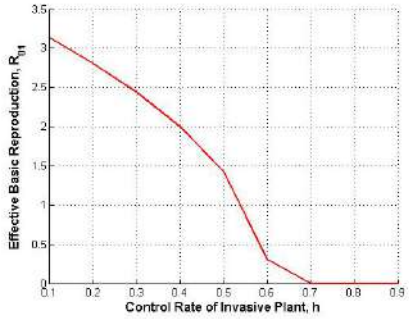


Figure 15: Plot of the effective reproductive number, R_{01} over the invasive plants control rate, h

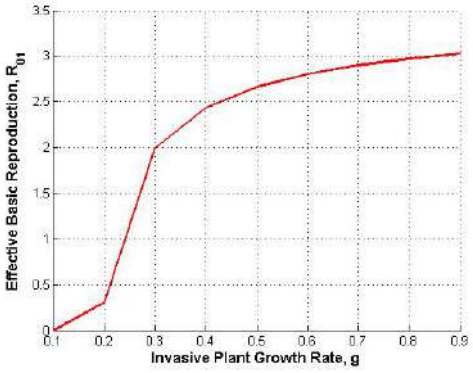


Figure 16: Plot of the effective reproductive number, R_{01} over the invasive plants growth rate, g

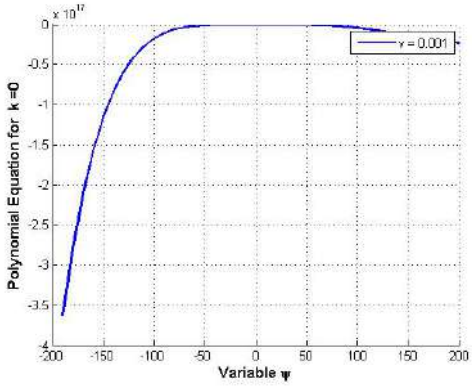


Figure 17: Graph of the polynomial $m(\psi)$ for the parameters outlined in Table 3

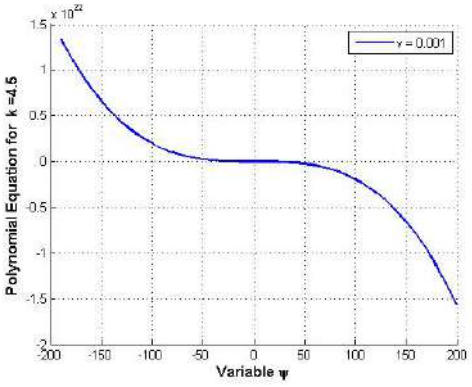


Figure 18: Graph of the polynomial $m(\psi)$ for the parameters outlined in Table 3

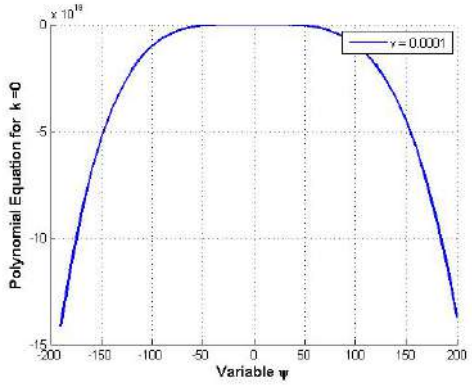


Figure 19: Graph of the polynomial $m(\psi)$ for the parameters outlined in Table 3

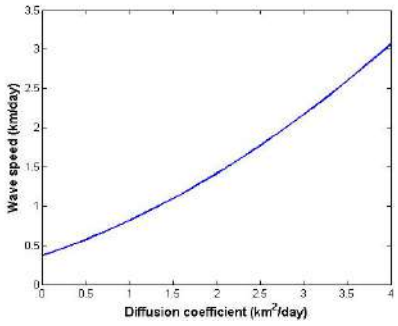


Figure 20: Graph of the propagation speed as a function of the diffusion coefficient D when $k = 0$. The values used for the other parameters are outlined in Table 3

5 Discussions and conclusion

The equilibrium,E_1 is the equilibrium state where there is plant in human environment with mosquito present.In this equilibrium there is a contact between human and mosquito population and breeding site for mosquito population to thrive. This may result to malaria in human population as time progresses. The Equilibrium E_2 is a Disease Free Equilibrium at which there is no invasive plant in the host environment.The contact rate of mosquito and human is low as the mosquito do not have a resting place to reside around the human environment after bite. Malaria transmission is very low and it can easily be controlled by mere use of mosquito net. The disease will persist in the host environment provided that those that are infected with the disease keep on transmitting the disease. The less than or equal $(\leq)$ sign of the lyapunov function shows the decrease of the susceptible population. The numerical analysis of the homogeneous model shows that the decrease in disease induced death rate, increase in bednet efficacy, and the control rate of alien invasive plant will drastically reduced malaria disease.

In conclusion, in this paper, we have presented a non-linear mathematical model that studies the impact of invasive alien plants on the dynamics of malaria transmission and its analyses. The non-linear homogeneous equations part of the model was analysed. The model had two basic reproduction numbers, R_{01} and R_{02} under two cases: where there is plant and where there is no plant respectively. Different analyses such as: equilibrium points, stabilities, backward bifurcation, travelling wave solutions were carried out in detailed for possible understanding of malaria transmission. Sensitivity analysis were carried out, and the result shows that it is quite sensitive to the biting rate, disease induced death rate, recovered rate and bed-net efficacy.

References

[1] Castilo-Chavez, C. and Song, B. (2004). Dynamical models of tuberculosis and their applications. Mathematical Biosciences and Engineering 1(2):361-404.

[2] CDC (2021). Malaria disease control and prevention. Available at http://www.cdc.gov/malaria/index.html.

[3] Murray, C.J., Rosenfeld, L.C., Lim, S.S., et al. (2012). Global malaria mortality between 1980 and 2010: a systematic analysis. Lancet 379, 413–431.

[4] Nwankwo, A., Okuonghae, D. (2019). A mathematical model for the population dynamics of malaria with a temperature dependent control. Foundation for Scientific Research and Technological Innovation, Springer, (2019), 1-30.

[5] Okuneye K., Gumel A.B. (2015). Analysis of temperature and rainfall dependent model for malaria transmission dynamics, Maths Bios., 1-12.

[6] Piet F.M.V., Anna A.B. (2014). Flight distance of mosquitoes (Culicdae): A metadata analysis to support the management of barrier zones around rewetted and newly constructed wetlands, Limnologica, 45:69-79.

[7] Samuel, B. and Bello, G. (2018). Global Sensitivity Analysis to study the impacts of Bed-Nets, Drug Treatment, and their efficacies on a two-strain Malaria model. Mathematical and computational Applications. 24:32.

[8] Stone, C.M., Arne B.R., Guillermo,C.W., Woodbridge,A.F.,and Sean,T.M.(2018). Would the control of Invasive Alien plant reduce malaria transmission?11:76.

[9] Van den Driessche, P., Watmough, J. (2008). Reproduction numbers and sub-threshold endemic equilibria for compartmental models of disease transmission. Math. Biosci. 180, 29–48

[10] Vanessa S, Norberto AM (2019). Modelling the Spatial Spread of Chagas Disease. Bulletin of Mathematical Biology, Springer, 1-44.

[11] World Health Organisation (2021). World Malaria Report. http://www.who.int/malaria/publications/world _malaria_report_2014/report/en/. Accessed 10 May 2021

[12] World Health Organisation (2022). World Malaria Report. http://www.who.int/malaria/publications/world _malaria_report_2021/report/en/. Accessed 13 June 2022.

[13] Alhassan, J.C., Achema, K.O. and Aondoaka, M.S. (2016). Modelling the Effect of Carriers and Treatment on the Transmission Dynamics of Typhoid Fever. Nigerian Mathematical Physics, 36:12-45.

On the nilpotents of the semigroup of partial contractions of a finite chain

M.M. Zubairu[*†] and **B. Ali**[†‡§]

Abstract

Let $[n] = \{1, 2, \ldots, n\}$ denote a finite chain. Consider the semigroups $\mathcal{P}_n$ and $\mathcal{OI}_n$, consisting of all partial, and all injective and order-preserving transformations on $[n]$, respectively. Furthermore, let $\mathcal{CP}_n = \{\alpha \in \mathcal{P}_n : |x\alpha - y\alpha| \leq |x - y| \ \ \forall\, x, y \in \text{ Dom } \alpha\}$ and $\mathcal{OCI}_n = \{\alpha \in \mathcal{OI}_n : |x\alpha - y\alpha| \leq |x - y| \ \ \forall\, x, y \in \text{ Dom } \alpha\}$. It follows that $\mathcal{CP}_n$ and $\mathcal{OCI}_n$ are subsemigroups of $\mathcal{P}_n$ and $\mathcal{OI}_n$, respectively. In this paper, we characterize the nilpotent elements in $\mathcal{CP}_n$, compute the number of nilpotents of height $(n-1)$ in $\mathcal{CP}_n$, and determine the number of nilpotents in $\mathcal{OCI}_n$ of a specific type.

Keywords and phrases: Transformations semigroup; Contraction maps; order preserving; nilpotent.

1 Introduction

Let $[n] = \{1, 2, \ldots, n\}$ denote a finite chain. A transformation of $[n]$ is considered *partial* if its domain is a subset of $[n]$ and *full* (or *total*) if its domain is $[n]$. When $\alpha \in S$ (where S is any transformation semigroup), we denote Dom α, Im α, $h(\alpha)$, and $b(\alpha)$ as the domain, image, height (denoted as |Im α|), and width or breadth (denoted as |Dom α|) of α, respectively. A transformation α is described as *order preserving* (or *order reversing*) if, for all $x, y \in$ Dom α, $x \leq y$ implies $x\alpha \leq y\alpha$ (or $x\alpha \geq y\alpha$). Denote $\mathcal{P}_n$, $\mathcal{T}_n$, and $\mathcal{OI}_n$ as the semigroups of partial, full, and one-one order-preserving transformations of $[n]$, respectively. A map $\alpha \in \mathcal{P}_n$ (resp., $\alpha \in \mathcal{T}_n$) is referred to as a *contraction* if $|x\alpha - y\alpha| \leq |x - y|$ for all x, y in Dom α (resp., x, y in $[n]$). Let

$$\mathcal{CP}_n = \{\alpha \in \mathcal{P}_n : |x\alpha - y\alpha| \leq |x - y| \ \ \forall\, x, y \in \text{Dom } \alpha\} \tag{1}$$

and

$$\mathcal{OCI}_n = \{\alpha \in \mathcal{OI}_n : |x\alpha - y\alpha| \leq |x - y| \ \ \forall\, x, y \in \text{Dom } \alpha\}. \tag{2}$$

It is well known that $\mathcal{CP}_n$ and $\mathcal{OCI}_n$ are subsemigroups of $\mathcal{P}_n$ and $\mathcal{OI}_n$, respectively. Denote

$$J_r = \{\alpha \in S : \ h(\alpha) = r\},$$

meaning that J_r contains elements of S with a height of r. For $\alpha, \beta \in S$, the composition of α and β is defined as $\alpha \circ \beta(x) = ((x)\alpha)\beta$ for any x in Dom α. Without ambiguity, we shall use the notation $\alpha\beta$ to denote $\alpha \circ \beta$. When $A = \{a_1, a_2, \ldots, a_n\} \subseteq [n]$ such that $a_1 < a_2 < \ldots < a_n$, the gap(A) is defined as

$$\text{gap}(A) = (|a_2 - a_1|, |a_3 - a_2|, \ldots, |a_n - a_{n-1}|)\,,$$

which yields an $(n-1)$-tuple of numbers. Similarly, the *reverse* gap of A is defined as

$$\text{gap}(A)^R = (|a_n - a_{n-1}|, |a_{n-1} - a_{n-2}|, \ldots, |a_3 - a_2|, |a_2 - a_1|) \text{ (see [1])}.$$

[*]Corresponding Author; E-mail: mmzubairu.mth@buk.edu.ng
[†]Department of Mathematical Sciences, Bayero University, Kano, Nigeria
[‡]E-mail: bali@nda.edu.ng
[§]Department of Mathematics, Nigeria Defence Academy, Kaduna, Nigeria

For a foundational understanding of semigroup theory, readers are encouraged to reference the works of Preston, Mazorchuk, and Howie. These are available in [2, 3, 4].

The algebraic study of the semigroup of contractions has attracted the interest of researchers recently. For example, Zho and Yang [5] characterized the regularity and Green's equivalences for the semigroup of order-preserving partial contractions, denoted as $\mathcal{OCP}_n$. In 2017, Garba et al. [6] investigated the algebraic properties of a certain semigroup of full contractions, providing a characterization of Green's and starred Green's equivalences of the semigroup $\mathcal{CT}_n$ (where $\mathcal{CT}_n$ denotes the semigroup of full contractions on $[n]$).

We also note that certain algebraic properties of some semigroups of contractions have been recorded recently. The concept of semigroups of contractions on chains has been studied by many authors in recent times, as seen in [5, 6, 7, 8, 9]. Combinatorial questions were recently explored by Zubairu and Ali [8] for the semigroups of partial and full contractions on chains. This paper attempts to address some of the questions raised in [8] for the semigroup of partial contractions.

Let S be a semigroup with a zero element. An element $a \in S$ is said to be a *nilpotent* if there exists a positive integer n such that $a^n = 0$. Gomes and Howie [10] demonstrated that $\mathcal{I}_n \setminus \mathcal{S}_n := \mathcal{SI}_n$ is nilpotent-generated if n is even, and they also characterized the nilpotent-generated subsemigroup for odd n. A similar result was obtained by Sullivan [11] for the semigroup $\mathcal{P}_n \setminus \mathcal{T}_n := \mathcal{SP}_n$. Furthermore, Laradji and Umar [12] characterized the nilpotent elements in $\mathcal{P}_n$ and computed the order of nilpotents in the semigroups $\mathcal{P}_n$ and $\mathcal{I}_n$. However, it appears that such characterizations for the semigroup of partial contractions is yet to be investigated, and the number of nilpotents in $\mathcal{CP}_n$ remains an open problem. Nevertheless, in this paper, we provide a characterization of nilpotents in $\mathcal{CP}_n$ and further compute the number of nilpotents of a specific type in $\mathcal{OCI}_n$.

We will now briefly describe the structure of the paper. Section one discusses some basic concepts and the background of the studies. In section two, we provide a certain characterization of nilpotents in $\mathcal{CP}_n$, which serves as a foundation for achieving some of the results in the subsequent sections. In section three, we compute the number of nilpotents in $\mathcal{CP}_n$ whose height is $(n-1)$. Finally, in section 4, we compute the number of nilpotents in $\mathcal{OCI}_n$ of a certain type.

2 Characterizations of nilpotent elements

In this section, we aim to characterize the nilpotent elements in $\mathcal{CP}_n$. Before we commence our investigation, we introduce the following lemma, attributed to Laradji and Umar [12].

Lemma 2.1 ([12]). *An element α in $\mathcal{P}_n$ is nilpotent if and only if there is no nonempty subset A of Dom (α) such that $A\alpha = A$.*

Remark 2.2. Notice that Lemma 2.1 implies that an element $\alpha \in \mathcal{P}_n$ is nilpotent if and only if it has no fixed point and does not form a *cycle*. A cycle occurs when there exist $x, y \in \text{Dom } \alpha$ such that $x\alpha = y$ and $y\alpha = x$. In other words, if α is of the form

$$\alpha = \begin{pmatrix} d_1 & d_2 & \dots & d_r & d_{r+1} & d_{r+2} \\ a_1 & a_2 & \dots & a_r & d_{r+2} & d_{r+1} \end{pmatrix},$$

then α has a cycle, represented by

$$\begin{pmatrix} d_{r+1} & d_{r+2} \\ d_{r+2} & d_{r+1} \end{pmatrix},$$

where $d_{r+1}\alpha = d_{r+2}$ and $d_{r+2}\alpha = d_{r+1}$.

Now, let $\alpha = \begin{pmatrix} d_1 & d_2 & \dots & d_r \\ a_1 & a_2 & \dots & a_r \end{pmatrix} \in \mathcal{CP}_n$, where $d_1 \leq d_2 \leq \dots \leq d_r$. We define the smallest element in the domain of α as $\min \text{Dom } (\alpha) = d_1$, referred to as the *first* element, and the largest element in the domain as $\max \text{Dom } (\alpha) = d_r$, denoted as the *last* element.

For the purpose of illustrations, consider $\alpha = \begin{pmatrix} 1 & 3 & 5 & 6 \\ 3 & 4 & 6 & 7 \end{pmatrix} \in \mathcal{CP}_7$. Then clearly 1 is the first element in the domain of α and 6 is the last element in the domain of α.

Next, let $\alpha \in \mathcal{CP}_n$ then Dom $\alpha \subseteq [n]$ and it is partitioned by the relation ker $\alpha = \{(x, y) \in \text{Dom } \alpha \times \text{Dom } \alpha : x\alpha = y\alpha\}$ into r blocks A_i $(1 \leq i \leq r)$. As such Dom $\alpha = A_1 \cup \cdots \cup A_r$ where $r \leq n$. As such every $\alpha \in \mathcal{CP}_n$ can be expressed as:

$$\begin{pmatrix} A_1 & A_2 & \dots & A_r \\ a_1 & a_2 & \dots & a_r \end{pmatrix},$$

where $r \leq n$ and $|a_i - a_j| \leq |x - y|$ for all $x \in A_i$ and $y \in A_j$ $(i, j \in \{1, 2, \dots, r\})$.

Let $N(\mathcal{CP}_n)$ be the set of all nilpotents in $\mathcal{CP}_n$. Then we have:

Lemma 2.3. *For $n \geq 2$, $N(\mathcal{CP}_n)$ is not a semigroup.*

Proof. Take $\alpha = \begin{pmatrix} 1 \\ 2 \end{pmatrix}, \beta = \begin{pmatrix} 2 \\ 1 \end{pmatrix} \in N(\mathcal{CP}_n)$. Then $\alpha\beta = \begin{pmatrix} 1 \\ 2 \end{pmatrix}\begin{pmatrix} 2 \\ 1 \end{pmatrix} = \begin{pmatrix} 1 \\ 1 \end{pmatrix} \notin N(\mathcal{CP}_n)$.

We now have the following lemma that characterizes nilpotent elements in $\mathcal{CP}_n$.

Lemma 2.4. *If α is a nilpotent in $\mathcal{CP}_n$, and i and j $(1 \leq i < j \leq n)$ are the first and last elements of the domain of α, then $\{i, j\} \nsubseteq Im(\alpha)$.*

Proof. Suppose, by way of contradiction, that $\alpha \in N(\mathcal{CP}_n)$ is a contraction with a domain containing i and j as the first and last elements, where $1 \leq i < j \leq n$. Assuming further, by way of contradiction, that $\{i, j\} \subseteq \text{Im}(\alpha)$ implies the existence of x and y in Dom (α) such that $x\alpha = i$ and $y\alpha = j$. However, as α is a nilpotent, Lemma 2.1 implies that $\{i, j\} = \{x\alpha, y\alpha\} = \{x, y\}\alpha \neq \{x, y\} \subseteq \text{Dom } (\alpha)$, i.e., $\{i, j\} \neq \{x, y\}$. We then consider three cases:

i $x = i$ and $y < j$,

ii $y = j$ and $x > i$, or

iii $i < x < j$ and $i < y < j$.

We shall demonstrate a contradiction for all the cases.

i Suppose $x = i$ and $y < j$ then $y\alpha - x\alpha = j - i > y - i = y - x$ which implies that $|y\alpha - x\alpha| > |y - x|$. This contradicts the fact that α is a contraction.

ii Suppose that $y = j$ and $x > i$ then $y\alpha - x\alpha = j - i > j - x = y - x$. Notice that $y\alpha - x\alpha$ and $y - x$ are positive, thus we have $|y\alpha - x\alpha| > |y - x|$, which contradicts the fact that α is a contraction.

iii Suppose that $i < x < j$ and $i < y < j$ then $y\alpha - x\alpha = j - i >= y - x$. Notice that $y\alpha - x\alpha$ and $y - x$ are positive, as such we have $|y\alpha - x\alpha| > |y - x|$. This also contradicts the fact that α is a contraction.

Hence $\{i, j\} \nsubseteq \text{Im } \alpha$.

For the purpose of illustrations we give the following example:

Example 2.5. Consider $\alpha = \begin{pmatrix} 1 & 3 & 5 & 6 \\ 3 & 4 & 6 & 7 \end{pmatrix} \in \mathcal{CP}_7$. Notice that 6 is the last element in Dom α and $6 \in \text{Im } \alpha$. However, it is easy to see that, replacing any element in Im $\alpha \setminus \{6\}$ with the first element 1, will render the new α not to be a contraction.

3 On the number of nilpotents in $\mathcal{CP}_n$

In this section, we aim to compute the number of nilpotents in $\mathcal{CP}_n$ with a height of $(n-1)$. Before commencing our investigation, we will first establish the following preliminaries. We denote J_{n-1} as the set of all elements in $\mathcal{CP}_n$ with a height of $(n-1)$, and $N(J_{n-1})$ denotes the set of all nilpotents in J_{n-1}. A subset B of $[n]$ is defined as *convex* if, whenever $x, y \in B$ with $x \leq y$ and $x \leq z \leq y$ for any $z \in [n]$, then $z \in B$. We will now present the following lemma describing the nilpotents in J_{n-1} with a convex domain.

Lemma 3.1. *Let $\alpha \in \mathcal{CP}_n$ and let $\alpha \in J_{n-1}$ be such that the domain of α is convex, of the form $\{1, \ldots, n-1\}$ or $\{2, \ldots, n\}$. Then $\alpha \in N(J_{n-1})$ if and only if α is equal to $\begin{pmatrix} 1 & 2 & \ldots & n-1 \\ 2 & 3 & \ldots & n \end{pmatrix}$ or α is equal to $\begin{pmatrix} 2 & 3 & \ldots & n \\ 1 & 2 & \ldots & n-1 \end{pmatrix}$.*

Proof. Let Dom $(\alpha) = \{1, \ldots, n-1\}$ or $\{2, \ldots, n\}$, where $\alpha \in J_{n-1}$. Suppose α is a nilpotent. Therefore, because Dom (α) is convex, it implies that the image of α must also be convex. It is noteworthy that the sets $\{2, 3, \ldots, n\}$ and $\{1, 2, \ldots, n-1\}$ are the only convex subsets of $[n]$ of order $n-1$. If we take Dom $(\alpha) = \{1, \ldots, n-1\}$, then all the possible contractions with the image $\{2, 3, \ldots, n\}$ or $\{1, 2, \ldots, n-1\}$ are:

$$\begin{pmatrix} 1 & 2 & \ldots & n-3 & n-2 & n-1 \\ 2 & 3 & \ldots & n-2 & n-1 & n \end{pmatrix}, \begin{pmatrix} 1 & 2 & \ldots & n-3 & n-2 & n-1 \\ n & n-1 & \ldots & 4 & 3 & 2 \end{pmatrix},$$

$$\begin{pmatrix} 1 & 2 & \ldots & n-3 & n-2 & n-1 \\ 1 & 2 & \ldots & n-3 & n-2 & n-1 \end{pmatrix}$$

and

$$\begin{pmatrix} 1 & 2 & \ldots & n-3 & n-2 & n-1 \\ n-1 & n-2 & \ldots & 3 & 2 & 1 \end{pmatrix}.$$

Notice that by Lemma 2.1, the first element $\begin{pmatrix} 1 & 2 & \ldots & n-3 & n-2 & n-1 \\ 2 & 3 & \ldots & n-2 & n-1 & n \end{pmatrix}$ is a nilpotent. However, by Lemma 2.1 the element $\begin{pmatrix} 1 & 2 & \ldots & n-3 & n-2 & n-1 \\ n & n-1 & \ldots & 4 & 3 & 2 \end{pmatrix}$ is not a nilpotent since it has a cycle $\begin{pmatrix} 2 & n-1 \\ n-1 & 2 \end{pmatrix}$.

Similarly, the elements

$$\begin{pmatrix} 1 & 2 & \ldots & n-3 & n-2 & n-1 \\ 1 & 2 & \ldots & n-3 & n-2 & n-1 \end{pmatrix} \text{ and } \begin{pmatrix} 1 & 2 & \ldots & n-3 & n-2 & n-1 \\ n-1 & n-2 & \ldots & 3 & 2 & 1 \end{pmatrix}$$

are not nilpotents since the first is a partial identity with $(n-1)$ fixed points and the second element has a cycle $\begin{pmatrix} 1 & n-1 \\ n-1 & 1 \end{pmatrix}$.

This shows that the only nilpotent $\alpha \in J_{n-1}$ with domain of the form $\{1, \ldots, n-1\}$ and image of the form $\{2, 3, \ldots, n\}$ or $\{1, 2, \ldots, n-1\}$ is

$$\begin{pmatrix} 1 & 2 & \ldots & n-3 & n-2 & n-1 \\ 2 & 3 & \ldots & n-2 & n-1 & n \end{pmatrix}.$$

One can show using similar argument that the only nilpotent in J_{n-1} with domain of the form $\{2, \ldots, n\}$ and image of the form $\{2, 3, \ldots, n\}$ or $\{1, 2, \ldots, n-1\}$ is

$$\begin{pmatrix} 2 & 3 & \ldots & n-2 & n-1 & n \\ 1 & 2 & \ldots & n-3 & n-2 & n-1 \end{pmatrix}.$$

Conversely, suppose $\alpha = \begin{pmatrix} 1 & 2 & \dots & n-1 \\ 2 & 3 & \dots & n \end{pmatrix}$ or $\alpha = \begin{pmatrix} 2 & 3 & \dots & n \\ 1 & 2 & \dots & n-1 \end{pmatrix}$. Then it is easy to see that by Lemma 2.1, both elements are nilpotents, each of height $n-1$.

Lemma 3.2. *Let $\alpha \in \mathcal{CP}_n$ ($n \geq 5$) be such that $\alpha \in J_{n-1}$. Suppose Dom $\alpha = \{1, \dots, n-2, n\}$ or $\{1, 3, \dots, n-1, n\}$ then α is not a nilpotent.*

Proof. Suppose Dom $(\alpha) = \{1, \dots, n-2, n\}$, and and suppose by way of contradiction that α is a nilpotent. Since the height of α is $n-1$ and the domain of α is a union of $\{1, \dots, n-2\}$ and $\{n\}$ (i.e., a union of two convex subsets of $[n]$), we observe from Lemma 2.4 that 1 and n cannot simultaneously belong to Im(α). This implies that Im(α) can be either $\{1, 2, \dots, n-2, n-1\}$ or $\{2, \dots, n-1, n\}$. Taking Im$(\alpha) = \{1, 2, \dots, n-2, n-1\}$ yields:

$$\alpha = \begin{pmatrix} 1 & 2 & \dots & n-3 & n-2 & n \\ 1 & 2 & \dots & n-3 & n-2 & n-1 \end{pmatrix}$$

which has at least one fixed point and, according to Lemma 2.1, is not a nilpotent. Alternatively, taking Im$(\alpha) = \{1, 2, \dots, n-2, n-1\}$ results in:

$$\alpha = \begin{pmatrix} 1 & 2 & \dots & n-3 & n-2 & n \\ n-1 & n-2 & \dots & 3 & 2 & 1 \end{pmatrix}$$

which includes a cycle $\begin{pmatrix} 2 & n-2 \\ n-2 & 2 \end{pmatrix}$ and, by Lemma 2.1, is not a nilpotent. This contradiction holds in each case, establishing the result. A similar argument demonstrates that α is not a nilpotent if Dom $(\alpha) = \{1, 3, \dots, n\}$. This completes the proof.

Lemma 3.3. *Let $\alpha \in J_{n-1}$ ($n \geq 5$) be such that Dom $(\alpha) = \{1, 2, \dots, i, i+2, i+3, \dots, n\}$ with gap(Dom (α)) $= (1, 1, \dots, 1, 2, 1, \cdots, 1)$ (an $(n-1)$-tuple of numbers) where 2 occupies the k^{th} position in the tuple ($2 \leq k \leq n-2$). Then, α is nilpotent if and only if $k = i$ (for n odd) or $k = i$ or $i+1$ (for n even) and Im $(\alpha) = \{2, \dots, n\}$ or $\{1, \dots, n-1\}$.*

Proof. Suppose, by way of contradiction, that α is a nilpotent and $k \neq i$ (for n odd) and $k \neq i$ and $k \neq i-1$ (for n even); or Im $(\alpha) \neq \{2, \dots, n\}$ and Im $(\alpha) \neq \{1, \dots, n-1\}$. This implies that if n is odd, then k can take any value, such as $i-l$ or $i+l$ for any $l \geq 1$. As α is a contraction, it falls into one of the following forms:

$$\alpha = \begin{pmatrix} 1 & 2 & \dots & i-1 & i & i+2 & i+3 & \dots & n \\ n & n-1 & \dots & i-l+1 & i-l & i-l-1 & i-l-2 & \dots & 2 \end{pmatrix}$$

or

$$\alpha = \begin{pmatrix} 1 & 2 & \dots & i-1 & i & i+2 & i+3 & \dots & n \\ n & n-1 & \dots & i+l & i+l-1 & i+l-2 & i+l-3 & \dots & 2 \end{pmatrix}$$

Notice that for all $1 \leq l \leq k$, the two maps above are contractions. Furthermore, if $l = 1$, the first map will exhibit the property $i-1 \mapsto i$ and $i \mapsto i-1$, demonstrating a cycle, while the second map will have $i \mapsto i$, signifying i as a fixed point, indicating that these maps are not nilpotent. This contradicts the assumption that they are nilpotent. A similar contradiction arises for even n.

If Im $(\alpha) \neq \{1, \dots, n-1\}$ and Im $(\alpha) \neq \{2, \dots, n\}$, then observe that the height of α is $n-1$. Therefore, if Im (α) is not convex, either $\{1, 2, \dots, i\}\alpha$ is not convex or $\{i+2, \dots, n\}\alpha$ is not convex, contradicting the fact that α is a contraction.

Conversely, suppose $k = i$ (for n odd) or $k = i$ or $i-1$ (for n even) and let Im $(\alpha) = \{2, \dots, n\}$ or Im $(\alpha) = \{1, \dots, n-1\}$.

For odd n, as α is a contraction and Dom (α) is the union of two convex sets (Dom $(\alpha) = \{1, \dots, n\} \cup \{i+2, \dots, n\}$), then (Dom $(\alpha))\alpha = (\{1, \dots, n\})\alpha \cup (\{i+2, \dots, n\})\alpha$ is a union of two convex sets. Hence,

$$\alpha = \begin{pmatrix} 1 & 2 & \dots & i-1 & i & i+2 & i+3 & \dots & n \\ n & n-1 & \dots & i+3 & i+2 & i+1 & i & \dots & 2 \end{pmatrix}$$

or

$$\alpha = \begin{pmatrix} 1 & 2 & \dots & i-1 & i & i+2 & i+3 & \dots & n \\ n-1 & n-2 & \dots & i+2 & i+1 & i & i-1 & \dots & 1 \end{pmatrix}$$

It is evident by Lemma 2.1 that both maps are nilpotent.

For even n,

$$\alpha = \begin{pmatrix} 1 & 2 & \dots & i-1 & i & i+2 & i+3 & \dots & n \\ n-1 & n & \dots & i+2 & i+1 & i & i-1 & \dots & 1 \end{pmatrix}$$

or

$$\alpha = \begin{pmatrix} 1 & 2 & \dots & i-1 & i & i+2 & i+3 & \dots & n \\ n & n-1 & \dots & i+2 & i+1 & i & i-1 & \dots & 2 \end{pmatrix}.$$

It easily follows from Lemma 2.1 that the two maps are nilpotents. This completes the proof.

We now complete the section with the main result.

Theorem 3.4. *Let $\mathcal{CP}_n$ $(n \geq 5)$ be as defined in (1), then $|N(J_{n-1})| = 4$.*

Proof. Notice that by Lemma 3.1, Lemma 3.2, and Lemma 3.3, the domain of a nilpotent α in J_{n-1} is of the form $\{1, \dots, n-1\}$ or $\{2, \dots, n\}$ or Dom $(\alpha) = \{1, 2, \dots, i, i+2, i+3, \dots, n\}$ with gap(Dom (α)) $= (1, 1, \cdots, 1, 2, 1, \cdots, 1)$ (an $n-1$ tuple of numbers) with 2 occupying the k^{th} position in the tuple $(2 \leq k \leq n-2)$. Thus, by Lemma 3.1, each of the domains $\{1, \dots, n-1\}$ or $\{2, \dots, n\}$ gives rise to only one nilpotent, and by Lemma 3.3, the domain Dom $(\alpha) = \{1, 2, \dots, i, i+2, i+3, \dots, n\}$ with gap (Dom (α)) $= (1, 1, \cdots, 1, 2, 1, \cdots, 1)$ gives rise to only two nilpotents. This completes the proof.

4 On the number of nilpotents in $\mathcal{OCI}_n$

In this section we compute the number of nilpotents in $\mathcal{OCI}_n$ whose domain is $\{1, 2, \dots, i\}$ and gap(Dom α) $= (1, 1, \dots, 1, k)$ of height equal $r = i - k + 1$, where $k \leq i \leq n$.

Let $S = \mathcal{IO}_n$ be the semigroup of one-to-one order-preserving partial transformations of $[n]$. The following lemma, attributed to Garba [13], characterizes nilpotent elements in $\mathcal{IO}_n$.

Lemma 4.1. *Let $\alpha \in \mathcal{IO}_n$ be such that $h(\alpha) < n$, then α is a nilpotent if and only if $x\alpha \neq x$ for every $x \in$ Dom α.*

Remark 4.2. Notice that since every nilpotent element of $\mathcal{OCI}_n$ is also a nilpotent element of $\mathcal{IO}_n$, then the above Lemma also holds in $\mathcal{OCI}_n$.

Let $P_r([n])$ be the collection of all subsets of $[n]$, each of order equal to r. For illustrative purposes, consider the cases when $n = 3$, i.e., $[3] = \{1, 2, 3\}$ and $r = 2$, we see that

$$P_2([3]) = \{\{1, 2\}, \{1, 3\}, \{2, 3\}\};$$

and when $[n] = \{1, 2, 3, 4\}$ and $r = 3$,

$$P_3([4]) = \{\{1, 2, 3\}, \{1, 2, 4\}, \{1, 3, 4\}, \{2, 3, 4\}\}.$$

Following the pattern in Section 1.2 of [14], we present the following lemma:

Lemma 4.3. *If $[n] = \{1, 2, \dots, n\}$ then $|P_r([n])| = \binom{n}{r}$.*

Corollary 4.4 (Problem 1.39, [14]). $\sum_{r=0}^{n} |P_r([n])| = 2^n$.

Recall that if $A = \{a_1, a_2, \ldots, a_n\} \subseteq [n]$ such that $a_1 < a_2 < \ldots < a_n$, then gap (A) is defined as

$$\text{gap}(A) = (|a_2 - a_1|, |a_3 - a_2|, \ldots, |a_n - a_{n-1}|),$$

which represents an $(n-1)$-tuple of numbers. Similarly, the reverse gap of A is defined as gap $(A)^R = (|a_n - a_{n-1}|, |a_{n-1} - a_{n-2}|, \ldots, |a_3 - a_2|, |a_2 - a_1|)$.

For example, if $A = \{1, 2, 4, 5, 8\}$, then gap $(A) = (1, 2, 1, 3)$ and $gap(A)^R = (3, 1, 2, 1)$.

Remark 4.5. (gap $(A)^R)^R =$ gap (A).

Define a relation $\sim$ on $P_r([n])$ as follows: for all A, B in $P_r([n])$, $A \sim B$ if and only if gap $(A) =$ gap (B) or gap $(A) =$ gap $(B)^R$. It is easy to see that the relation $\sim$ is an equivalence on $P_r([n])$.

Let $[A]$ denote the equivalence class of A under the relation $\sim$, then we have the following lemma:

Lemma 4.6. *Every equivalence class contains an element that includes 1*

Proof. Let $A \in P_r([n])$ and suppose $[A]$ is the equivalence class of A under the relation $\sim$. Now let B be an element in $[A]$, which means that $B \sim A$, i.e., $\text{gap}(B) = \text{gap}(A)$ or $\text{gap}(B) = \text{gap}(A)^R$. Without loss of generality, suppose $\text{gap}(B) = \text{gap}(A)$. This means that

$$(|b_2 - b_1|, |b_3 - b_2|, \ldots, |b_n - b_{n-1}|) = (|a_2 - a_1|, |a_3 - a_2|, \ldots, |a_n - a_{n-1}|),$$

where $a_i \in A$ and $b_i \in B$ for $1 \leq i \leq r$, which implies that $|b_{i+1} - b_i| = |a_{i+1} - a_i|$ for $1 \leq i \leq r$. Now suppose $|a_{i+1} - a_i| = k_i$ for $1 \leq i \leq r$, this implies that $|b_{i+1} - b_i| = k_i$ for $1 \leq i \leq r$. It is clear that $k_i \leq n - 1$ for any i, which means that $k_i + 1 \leq n$ for any i, implying that $k_i + 1 \in [n]$ for any i. As such, choosing $b_{i+1} = k_i + 1$ then $b_i = 1$ for any i, implies $1 \in B$. Similarly, choosing $\text{gap}(B) = \text{gap}(A)^R$ gives the same result. This completes the proof.

Lemma 4.7. $|[A]| = n - k - r + 2$, *where* $|A| = r$ *and gap* $(A) = (1, 1, \ldots, 1, k)$ *or* $gap(A)^R = (1, 1, \ldots, 1, k)$.

Proof. Let A be an element of $P_r([n])$, where $A = \{a_1, a_2, \ldots, a_{r-1}, a_r\}$ such that $|a_{i+1} - a_i| = 1$ for $1 \leq i \leq r-2$ and $|a_r - a_{r-1}| = k$. Now, by Lemma 2.4, there exists a B in the equivalence class of A which contains 1. Thus, $B = \{1, 2, 3, \ldots, r-1, r-1+k\}$. Then, by the definition of the relation $\sim$ and the fact that $k \leq n - 1$, we have:

$$[B] = \{\{1, 2, 3, \ldots, r-1, r-1+k\}, \{2, 3, \ldots, r, r+k\}, \{3, 4, \ldots, r+1, r+1+k\}, \ldots, \{n-k-r+2, n-k-r+3, \ldots, n\}\},$$

which implies that $|[B]| = n - k - r + 2$.

Now as a consequence of the above lemma, we already have the following (now) obvious result.

Corollary 4.8. *For any natural number* n *there are* $n - k - r + 2$ *possible subsets of* $[n]$ *of order* r *with gap of the form* $(1, 1, \ldots, 1, k)$, *which is an* $(r-1)$*-tuple of number(s).*

Lemma 4.9. *Let* $[i - k + 1] = \{1, 2, 3, \ldots, i - k - 1, i - k, i\}$, *then the number of nilpotents in* $\mathcal{OCI}_n$ *whose domain is* $[i - k + 1]$ *is* $\frac{(k-2)(k-1)}{2}$.

Proof. Let $[i - k + 1] = \{1, 2, 3, \ldots, i - k - 1, i - k, i\}$. Then $|[i - k + 1]| = i - k + 1$ and $k = |i - (i - k)|$, now let Dom $\alpha = [i - k + 1]$, then by Lemma 2.4, 1 and i cannot be in the image set of α, and notice that there are $k - 1$ jumps (by jumps here we are referring to missing elements between $i - k$ and i) between $i - k$ and i, then the image of α is of the form $\{2, 3, \ldots, i - k, i - k + 1, i - k + 2, \ldots, k - 2, k - 1\} = [k] \setminus \{1, k\}$, which gives a total of $k - 2$ elements.

Now we can define a one to one order preserving partial contraction map from Dom α to any subset of $\{2,3,\ldots,k-1\}$ of order i in $\binom{k-i}{k-i-1}$ ways $(2 \leq i \leq k-1)$, and summing over i, we have:

$$\begin{aligned}\sum_{i=2}^{k-1}\binom{k-i}{k-i-1} &= \binom{k-2}{k-3}+\binom{k-3}{k-4}+\ldots+\binom{k-(k-2)}{k-(k-2)-1}+\binom{k-(k-1)}{k-(k-1)-1}\\ &= \binom{k-2}{k-3}+\binom{k-3}{k-4}+\ldots+\binom{4}{3}+\binom{3}{2}+\binom{2}{1}+\binom{1}{0}\\ &= (k-2)+(k-3)+\cdots+4+3+2+1\\ &= \frac{(k-2)(k-1)}{2}.\end{aligned}$$

Corollary 4.10. *Let $S = \mathcal{OCI}_n$, then the number of nilpotents α in S whose domain is $\{1,2,3,\ldots,i-k,i\}$ and image a subset of $\{2,3,\ldots,k-1\}$ is $\frac{(k-2)(k-1)}{2}$.*

Lemma 4.11. *Let $[n] = \{1,2,\ldots,i-k-1,i-k,i-k+1,i-k+2,\ldots,i-k+k,i+1,i+2,\ldots,n\}$ and Dom $\alpha = \{1,2,\ldots,i-k-1,i-k,i\}$. Then the number of one to one order preserving partial contractions of height equal to $i-k+1$, whose image is a subset of $\{i-k+1,i-k+2,\ldots,i,i+1,i+2,\ldots,n\}$ (i.e., a set of order $n+k-r$) is $k(n-i)$.*

Proof. Notice that since 1 is in the domain of α, then 1 has the following possibilities: $1 \to i-k+1$ or $1 \to i-k+2$ or ... up to $1 \to i$ within the set $\{i-k+1,i-k+2,\ldots,i,i+1,i+2,\ldots,n\}$ of order $n+k-r$. This can be accomplished in a total of $i-(i-k+1)+1$ ways, which simplifies to k ways (i.e., since the last term is $i-k+k=i$).

In a similar fashion, we can do the same to the remaining elements in the domain in $n-k-m+1$ ways, where $m = h(\alpha) = i-k+1$, which is $(n-k-(i-k+1)+1) = (n-i)$ ways, hence applying product rule, we have a total of $k(n-i)$ ways.

Lemma 4.12. *Let $S = \mathcal{OCI}_n$. The number of nilpotents α in S whose domain is $\{1,2,\ldots,i\}$, gap (Dom α) $= (1,1,\ldots,k)$ and $h(\alpha) = i-k+1$ is $(n-k-i+2)\left(\frac{(k-2)(k-1)}{2}+k(n-i)\right) = (n-r+3)\left(\frac{(k-2)(k-1)}{2}+k(n-r-k+1)\right)$ where $r = i-k+1$ and $1 \leq k \leq n-1$.*

Proof. The proof follows directly from Lemma 4.7, Corollary 4.10 and Lemma 4.11.

Now as a consequence of the above Lemma 4.12 we now conclude this section with the main result.

Theorem 4.13. *Let $\mathcal{OCI}_n$ be as expressed in (2). Then the number of nilpotents in $\mathcal{OCI}_n$ whose domain is $\{1,2,\ldots,i\}$ and gap (Dom α) $= (1,1,\ldots,1,k)$ of height equal $r = i-k+1$, is $\sum_{k=1}^{n-1}(n-r+3)\left(\frac{(k-2)(k-1)}{2}+k(n-r-k+1)\right)$.*

Remark 4.14. The number of nilpotent elements in the semigroups $\mathcal{CP}_n$ and $\mathcal{OCI}_n$ has not been investigated.

5 Conclusion

We have successfully given a characterization of nilpotents in the semigroup of partial contractions of a finite chain. We also computed the order of nilpotents of height $n-1$ in $\mathcal{CP}_n$ and computed the order of certain one to one order preserving nilpotents contractions.

References

[1] Al-Kharousi, F., Kehinde, R. and Umar, A. (2016). On the Semigroup of Partial Isometries of a Finite Chain. Comm. Algebra. 44,

[2] Clifford, A. H. and Preston, G. B. The algebraic theory of semigroups, vol.1. Providence, R. I. American Mathematical Society. 639–647.

[3] Ganyushkin, O. and Mazorchuk, V.(2009) Classical Finite Transformation Semigroups. Springer—Verlag: London Limited.

[4] Howie, J. M. (1995). Fundamental of semigroup theory. London Mathematical Society, New series 12. The Clarendon Press, Oxford University Press.

[5] Zhao, P. and Yang, M. (2012) Regularity and Green's relations on semigroups of transformation preserving order and compression. Bull Korean Math Soc ; 5(49), 1015–1025.

[6] Garba, G. U., Ibrahim, M. J. and Imam, A. T. (2017). On certain semigroups of full contraction maps of a finite chain. Turk. J. Math., 41, 500–507.

[7] Ali, B., Umar, A. and Zubairu, M. M. (2023). Regularity and Green's relations for the semigroups of partial and full contractions of a finite chain. Scientific African, 21, p.e01890.

[8] Zubairu, M. M. and Ali, B. (2019). On certain combinatorial Problems of the semigroup of Partial and full contractions of a finite chain. Ba. J. Pure App. Sci ; 1(11), 377–380.

[9] Zubairu, M. M., Umar, A. and Aliyu, J. A. (2024). On certain semigroups of order decreasing full contraction mappings of a finite chain. Recent Developments in Algebra and Analysis: (Trend in Mathematics), Springer Int. Pub., **1**, 35–45.

[10] Gomes, G. M. S. and Howie, J. M. (1987). Nilpotents in finite symmetric inverse semigroups. Proc. Edinburgh. Math. Soc, 30, 383–395.

[11] Umar, A. (2014). Some combinatorial problems in the theory of partial transformation semigroups. J Algebra and Discr Math. 1(17), 110–134.

[12] Laradji, A. and Umar, A. (2004). On the number of nilpotents in the partial symmetric semigroup. Comm. Algebra. 32(8), 3017–3023.

[13] Garba, G. U. (1990). Nilpotents in partial one-to-one order-preserving transformations. Semigroup Forum, 116 A, 359–366.

[14] Balakrishnan, V. K. (1995). Theory and Problems of Combinatorics. Schaum's Outline, McGraw-Hill, Inc.

Detection and correction of heteroscedasticity and its effect on modelling of Nigerian economic data

E.O. Idowu[*†], E.M. Ikegwu[‡], A.A. Fadiji[†§] and M.U. Evro[†]**

Abstract

The study centred on detection and correction of heteroscedasticity and its effect on modelling of economic data. Data were collected from CBN Statistical bulletin on five economic variables namely; Gross Domestic Product (GDP), Inflation Rate, Exchange Rate (Exch_rate), Balance of Payment and Government Debt from 1987 - 2017. The data was analysed using the Ordinary Least Square method and variance stability techniques was used to correct heteroscedasticity using log transformation of the dependent variable while Breusch-Pagan, White and Harvey-Godfrey tests were used to detect the presence of heteroscedasticity in the variables at 5% level of significance with the aid of E-views 9. The regression model fitted to the data set was **GDP = 37242.63 - 256.7745 Inflr – 40.196 Exchr + 252.364 BoP + 3.147 GovD** and it showed that only inflation rate and Government debt were discovered to be significant predictors ($p < 0.05$) while and heteroscedasticity was detected. Result showed that after log transforming the variables, heteroscedasticity was eliminated as shown by Breusch-Pagan, White and Harvey-Godfrey test respectively. It is concluded therefore that transforming economic data helps correct and eliminate detected heteroscedasticity in modelled economic variables.

Keywords and phrases: Heteroscedasticity, GDP, Inflation Rate, Exchange rate, OLS

1 Introduction

Most linear model has as a basic assumption homoscedasticity which implies that the variance of the residual must be constant across the time interval or the explanatory variables. However, in most studies, this assumption is violated, and heteroscedasticity is observed. Heteroscedasticity represents a situation where the variance of the residuals varies across observations within a regression model, i.e. the disturbances (error) term does not have a constant or equal variance independent of time (t). Heteroscedasticity was viewed as the violation of constant variance assumption of ordinary least squares estimator [1, 2]. The violation of the assumption of homoscedasticity could increase Type I

[*]Corresponding Author; E-mail: godsbabe2002@gmail.com
[†]Department of Statistics, Yaba College of Technology, Yaba Lagos, Nigeria.
[‡]Department of Statistics, Yaba College of Technology, Yaba Lagos, Nigeria.
E-mail: emmanuel.ikegwu@yabatech.edu.ng
[§]E-mail: ademola.fadiji@yabatech.edu.ng
[**]E-mail: merit.evro@gmail.com

error, reduce statistical power, lead to inefficient estimation or incorrect inference [2 - 6] but does not affect the unbiasness of the model estimates.

Heteroscedasticity according to [7] is a common feature of cross - sectional data and correcting for it very vital for appropriate inference with the estimated model. This study explored consistent lack of fit tests to assess the presence of heteroscedasticity in linear regression models and hence correct for same as expounded by other studies [4, 8].

Economic growth is usually exponential in nature according to [9] and so modelling such always requires transformation using appropriate procedures like the Box – Cox transformation. This study attempted the detection and correction of heteroscedasticity in economic data and also evaluated its effect in economic models. The outcome will not only contribute to literatures on the concept of heteroscedasticity but also enable governmental agencies and policy makers as it deals with correcting its effects on models of economic growth.

1.1 Detection

It is always necessary to assess the assumption of the linear model and one of such is the assumption of homoscedasticity (equal variance) of the residual over the period. Graphical diagnostic procedures, such as plotting the residuals versus the time period or the fitted value, often provide useful visual aid [10, 11, 12]. Other formal tests are also employed to evaluate whether the patterns observed are due to random fluctuations [13]. Some of the formal tests include white's test, Gold Quandt (GQ) test, Harvey test, Breusch – Pagan – Godfrey test [14, 1, 15]. However, the White test procedure has become popular for detecting heteroscedasticity and is included in most software.

1.2 Correction

[7] used WLS to correct the presence of heteroscedasticity which led to an efficient and significant result. [4] managed the problem of heteroscedasticity by transforming the response variable. However, [16] dealt with the problem of non – constant variance by transforming both the predictor and response variables.

2 Methodology

This study used five (5) economic variables namely: Gross Domestic Product (GDP), Inflation Rate, Exchange Rate, Balance of Payment and Government Debt for a 31 years period spanning 1987 - 2017 obtained from the Central Bank of Nigeria statistical Bulletin to model economic growth in Nigeria.

With the major objectives of detection and correction of heteroscedasticity in economic data and also evaluating its effect on models of economic growth, the OLS model was fitted and the presence of heteroscedasticity examined. The log transformation was employed in the OLS model to obtain the estimates and examine the resultant effects on heteroscedasticity. However, because it has been shown that heteroscedasticity in longitudinal time series data was not as impactful as in cross – sectional data

2.1 The OLS Model Specification

The functional model in this study is given as:

$$GDP = \beta_0 + \beta_1 * Inflr + \beta_2 * Exchr + \beta_3 * BoP + \beta_4 * GovD + \varepsilon_i \qquad (1)$$

where

GDP = Gross Domestic Product (a proxy for measuring economic growth)

Inflr = Inflation Rate; Exchr = Exchange Rate; BoP = Balance of Payment;

GovD = Government Debt; ε_i = Stochastic error term

β_i's = Regression parameters (i = 0, 1, …, 4)

2.2 Detecting Heteroskedasticity

2.2.1. White's General Heteroscedasticity Test

White's test estimates the parameters of an auxiliary regression model with OLS residual U_i as the dependent variable in the form below:

$$U_i^2 = \beta_0 + \beta_1 X_1 + \cdots + v_i \quad (2)$$

The new coefficient of determination (R^2) is used to test the null hypothesis that there is no heteroscedasticity and the test statistics is

$$n.R^2 \sim x_{df}^2 \quad (3)$$

where df is the number of parameters in the auxiliary regression model without intercept [17].

2.2.2. The Breusch – Pagan - Godfrey LM Test

In the Breusch – Pagan – Godfrey test, the OLS model yields the residuals and the auxiliary regression is obtained as follows:

$$P_i^2 = \beta_0 + \beta_1 X_1 + \cdots + v_i \quad (4)$$

$$P_i^2 = \sum \left({u_i^2}/{\sigma^2} \right) \quad (5)$$

With u_i^2 and σ^2 were estimated from the initial OLS model. Then, $\Theta = {1}/{2}\,(ESS)$ where ESS is the explained sum of square from the auxiliary regression and $\Theta \sim \chi_{m-1}^2$ [8].

2.3 Correcting/ Resolving Heteroscedasticity

The variance stabilising technique of correcting heteroscedasticity was adopted using log transformation of the dependent variable (GDP) in line with literature [4].

The transformed model using log transformation is:

$$\text{Log_GDP} = \beta 0 + \beta_1 \text{INFLR} + \beta_2 \text{EXCHR} + \beta_3 \text{BOP} + \beta_4 \text{GovD} + \varepsilon_t \quad (6)$$

The data was analysed using Statistical package for Social Sciences (SPSS 25.0).

3 Results

The result of the analysis of the economic variables are presented and interpreted and includes the test for the presence or otherwise of heteroscedasticity.

Table 1. Descriptive statistics for individual variables

Statistic	GDP	Inflr	Exchr	BoP	GovD	Residual
Mean	38796.5	20.63	111.847	-0.489	3644.99	1.13e-11
Median	25647.30	12.880	91.500	-1.247	1166.001	-545.230
Maximum	135277.2	72.840	305.800	10.000	40640.40	13468.230
Minimum	15242.60	5.380	49.780	-9.700	36.789	-15555.54
Std. dev	25548.47	18.646	62.249	4.775	7490.089	9067.091
Skewness	1.864	1.526	1.863	0.654	4.092	-0.0834
Kurtosis	7.435	3.916	5.648	3.359	20.568	1.823
Probability	0.000	0.001	0.000	0.304	0.000	0.402
Observations	31	31	31	31	31	31

Table 1 reveals that the mean (std deviation) of GDP is 38796.5 (25548.47), Inflation rate 20.63 (18.65), Exchange rate 111.85, (62.249), Balance of payment -0.489, (4.775) and Government debt 3644.99 (7490.089). It also showed that the residual is normally distributed ($p > 0.05$) is almost symmetrical conforming with OLS normality assumption.

Table 2. Estimation coefficients and model significance

	Actual data			Log transformed data		
Regressors	**B**	**t**	**p-value**	**B**	**t**	**p-value**
Constant	37242.63	8.478826	0.0000	10.548	68.629	0.0000
Inflation Rate	-256.7748	-2.605731	0.0150*	-0.0097	-2.8066	0.0094*
Exchange Rate	-40.19632	-1.144763	0.2627	-0.0013	-1.0814	0.2894
Balance of payment	252.3637	0.647752	0.5228	0.0108	0.7937	0.4345
Government Debt	3.146929	10.62749	0.0000*	0.0000564	5.4397	0.0000*
$R^2 = 0.874$; Adj. $R^2 = 0.855$; $p(F_{4,26}) < 0.001$; DW = 0.452				$R^2 = 0.683$; Adj. $R^2 = 0.635$; $p(F_{4,26}) < 0.001$; DW = 0.498		

The OLS model fitted is given as:

$$\boldsymbol{GDP = 37242.63 - 256.775 * Inflr - 40.196 * Exchr + 252.364 * BoP + 3.147 * GovD} \quad (7)$$

From the relative statistics, we discover that two (2) variables Inflation Rate and Government debt are statistically significant ($p < 0.05$) while Exchange Rate and Balance of payment are not statistically significant ($p > 0.05$)

The inflation rate ($\beta_{Inflr} = -256.775$) has the greatest effect on GDP as a unit change in inflation rate decreases GDP by 256.775 units. Also, BOP ($\beta_{BoP} = 252.36$) which mean a unit change in BOP increases GDP by 252.3. in addition, a unit increase in exchange rate ($\beta_{Exchr} = -40.196$) decreases GDP by 40.196 and Government Debt ($\beta_{GovD} = 3.15$) imply that a unit change in Govt Debt increases GDP by 3.15.

The $p(F_{4,26}) < 0.001$ implies that the dependent variables combined significantly contributed to GDP while the Adjusted R^2 of 0.855 shows that Inflation rate, Exchange rate, Balance of Payment and Government Debt collectively explained 85.5% of the total variability in GDP over the years modelled. Lastly, the Durbin Watson obtained was 0.452 which shows that there is negative serial correlation among the dependent variable.

The OLS model of the fitted log transformed data is given as:

$$\boldsymbol{Log_GDP = 10.548 - 0.0097 * Inflr - 0.0013 * Exchr + 0.0108 * BoP + 0.0000564 * GovD} \quad (8)$$

From the relative statistics, two (2) variables also, Inflation Rate and Government debt are statistically significant ($p < 0.05$) while Exchange Rate and Balance of payment are not statistically significant ($p > 0.05$) (see table 2)

The result shows that as a unit change in inflation rate ($\beta_{Inflr} = -.0097$) decreases GDP by about 0.1%, a unit change in exchange rate ($\beta_{Exchr} = -.0013$) reduces GDP by 0.13%, a unit increase BOP in ($\beta_{BoP} = 0.0108$) increases GDP by 1.1% and a unit change in Govt Debt ($\beta_{GovD} = 5.64E\text{-}05$) increases GDP by 0.006%.

The $p(F_{4,26}) < 0.001$ implies that the dependent variables combined significantly contributed to Log_GDP while the Adjusted R^2 of 0.635 shows that Inflation rate, Exchange rate, Balance of Payment and Government Debt collectively explained 63.5% of the total variability in Log_GDP over the years modelled. Lastly, the Durbin Watson obtained was 0.498 which shows that there is negative serial correlation among the dependent variable.

3.1 Heteroscedasticity Test

H_0: There is no heteroscedasticity vs H_1: There is heteroscedasticity

Table 3: Test of heteroscedasticity

	a. Actual data		b. Log transformed data	
Test	**p -value**	**Decision**	**p - value**	**Decision**
Breusch – Pagan – Godfrey	0.0089*	heteroscedasticity	0.0997	No Heteroscedasticity
White	0.0305*	heteroscedasticity	0.1097	No Heteroscedasticity
Harvey	0.0093*	heteroscedasticity	0.0492	Heteroscedasticity

The three tests in table 3(a) show that heteroscedasticity was a problem as they are all significant ($p < 0.05$) and it is concluded that there is presence of heteroscedasticity (i.e. unequal variance).

3.2 Correction of Heteroscedasticity

The adopted correction for this study using log transformation to transform the dependent variable (GDP) is presented also in table 2.

The Breusch - Pagan – Godfrey and White tests above show that heteroscedasticity was no longer problem as they are not significant ($p > 0.05$) and it is concluded that there is absence of heteroscedasticity (i.e. unequal variance) but the Harvey was slightly different (see table 3 (b)).

5 Discussions and Conclusion

The result of the study showed that heteroscedasticity was present in the time series economic data because they are exponentially distributed agreeing other studies [14, 9]. The observed problem was detected using the traditional tests and corrected for using the Cox transformation by log transforming the dependent variable and the residuals were homoscedastic agreeing with other researchers [18, 4]. From our analysis, we have been able to detect heteroscedasticity in the residual of the modelled economic data and correction was made using log transformation. The log transformed data show no presence of heteroscedasticity. Unequal variance (heteroscedasticity) affects efficiency therefore making the OLS estimate no longer BLUE, even though the unbiasedness property holds. To eliminate the chances of heteroscedasticity, more observations and more explanatory variables should be used for analysis for efficient estimate (result). Other methods for detection and correction of heteroscedasticity should be explored

References

[1] Rehal, V. (2023, February 10). White Test for Heteroscedasticity. Retrieved June 24, 2024, from https://spureconomics.com/white-test-for-heteroscedasticity/#google_vignette
[2] Obomeghie, M. A. (2008). Applied Econometrics. An Introductory Text. Benin City: Isa - Mini Printers.
[3] Rehal, V. (2023, February 08). Heteroscedasticity: Causes and Consequences. Retrieved June 24, 2024, from https://spureconomics.com: https://spureconomics.com/heteroscedasticity-causes-and-consequences/
[4] Rosopa, P. J., Schaffer, M. M., & Schroeder, A. N. (2013). Managing Heteroscedasticity in General Linear Models. Psychological Methods, 18(3), 335 - 351.
[5] Ruppert, D., Wand, M. P., & Carroll, R. J. (2009). Semiparametric regression during 2003 - 2007. Electronic Journal of Statistics, 3, 1193 – 1256.
[6] Greens, W. H. (2000). Econometric Analysis, 4th ed. (4th ed.). Upper Saddle River, New Jersey: Prentice Hall.
[7] Agunbiade, D. A., & Adeboye, N. O. (2012). Estimation of Heteroscedasticity Effects in a Classical Linear Regression Model of a Cross - Sectional Data. Progress in Applied Mathematics, 4(2), 18 – 28.
[8] Gujarati, D. N. (2013). Basic Econometrics (5th ed.). Glasgow: Bell & Bain Ltd.
[9] Jones, C. I. (2016). The Facts of Economic Growth. In C. I. Jones, Handbook of Macroeconomics 2A: 3 - 69. online: Elsevier B.V. doi:10.1016/bs.hesmac.2016.03.002.
[10] Tan, F., Jiang, X., Guo, X., & Zhu, L. (2021). Testing Heteroscedasticity for Regression Models based on Projections on JSTOR. Statistica Sinica, 31(2), 625-646. doi:27008056.
[11] Feng, S., Li, G., Tong, T., & Luo, S. (2019). Testing for heteroskedasticity in two-way fixed effects panel data models. Journal of Applied Statistics, 1634682. doi:10.1080/02664763.2019.1634682.
[12] Cohen, P., West, S. G., & Aiken, L. S. (2007). Applied multiple regression/correlation analysis for the behavioral sciences. Erlbaum: Mahwah.
[13] Qian, L., & Wang, S. (2001). Bias-corrected heteroscedasticity robust covariance matrix (sandwich) estimators. Journal of Statistical Computation and Simulation, 70, 161 – 174.
[14] Romeo, G., Buonaccorsi, J. P., & Thoresen, M. (2023). Detecting and correcting for heteroscedasticity in the presence of measurement error. Communications in Statistics - Simulation and Computation, 2190061. doi:10.1080/03610918.2023.2190061.
[15] Berenguer-Rico, V., & Wilms, I. (2021). Heteroscedasticity testing after outlier removal. Econometric Reviews, 40(1), 51 - 58. doi:10.1080/07474938.2020.1735749.
[16] Van Keilegom, I., & Wang, L. (2010). Semiparametric modeling and estimation of heteroscedasticity in regression analysis of cross-sectional data. Electronic Journal of Statistics, 4, 133 – 160.
[17] White, H. (1980). A Heteroskedasticity-Consistent Covariance Matrix and a Direct Test for Heteroskedasticity. Econometrica, 48, 817 – 838.
[18] Astivia, O. L., & Zumbo, B. D. (2019). Heteroskedasticity in Multiple Regression Analysis: What it is, How to Detect it and How to Solve it with Applications in R and SPSS. Practical Assessment, Research & Evaluation, 24(1), 1 - 16.

Options pricing using combination of Brownian motion with a random time component

C.A. Onyegbuchulem*†, B.O. Onyegbuchulem‡, and U. Alwell†

Abstract

This paper provides an efficient option pricing technique for European call options. The technique is a process that combines Geometric Brownian motion with random time component. The additional parameter to the Geometric Brownian motion is the volatility of the time change. This additional parameter provides control over the skewness and kurtosis of the return distribution. Partial integro-differential equation (PIDE) for pricing options under the proposed process was derived. Its values were priced numerically and the pricing performance of the new model is compared on option data sourced from Bloomberg on 28th April, 2023 with the Geometric Brownian motion. The result revealed that the additional parameter was able to address the pricing biases of the Geometric Brownian motion. Recommendation was made that more work should be done in the advancement of quick and effective procedures for calculating PIDE's having in view to calibrating stochastic processes to a surface of option prices.

Keywords and phrases: Extended Brownian motion; Geometric Brownian motion; Lévy processes

1 Introduction

Geometric Brownian Motion (GBM) is a mathematical technique used to model the unpredictable movement of stock prices. It is widely used for stock price forecasting. This paper develops an efficient technique for valuing options when the basic asset price has dynamics given by a pure jump infinity activity Lévy process. The proposed technique is a process that combines Geometric Brownian motion with a random time component, governed by a gamma process. This approach allows for flexible modelling of economic time periods, where each unit of time has a variable length, described by a gamma distribution with unit mean and positive variance. The process yields normally distributed returns over a unit period, conditional on the random time realization, which follows a gamma distribution. This framework provides a strong three-parameter model, extending the existing Geometric Brownian motion model by incorporating additional parameter that controls kurtosis and skewness in the return distribution. We termed the proposed technique Extended Geometric

* Corresponding Author; E-mail: ochialuka@yahoo.com
† Department of Mathematics, Alvan Ikoku Federal University of Education, Owerri, Imo State, Nigeria
‡ Department of Statistics, Imo State Polytechnic, Omuma, Imo State, Nigeria

Brownian Motion model (EGBM). The process has finite moments, distinguishing it from many Lévy processes. There is no diffusion component in the new process and it is thus a pure jump process.

The motivation for this study is to address the pricing biases of the Geometric Brownian motion of assuming constant volatility, which is not realistic as volatility changes over time and assuming a log-normal distribution of asset prices, which may not capture extreme events making it less sensitive to changes in underlying variables and less suitable for modelling assets with volatile prices. The fact that the price change of the asset is often influenced by the suddenly incoming and highly important price-making information, which results rather in the significant price jump makes it necessary to develop an efficient technique for valuing options and a model that could more accurately, express the empirical leptokurtic distributions of logarithmic returns in financial assets. Models that are incorporated with jumps offer better mathematical tool as described in [1], [2], [3], [4], [5], [6], [7]. We used three studies to demonstrate the effectiveness of Geometric Brownian motion in this paper. [8] tested the Geometric Brownian motion model for predicting stock prices in Nigeria. The model worked well for short-term predictions but was less accurate for long-term prediction. [9] used GBM to predict short-term stock prices for 24 Malaysian stocks, achieving accurate results for up to two weeks. [10] simulated 50 Australian stock prices using GBM and the Capital Asset Pricing Model (CAPM), finding that the model's predictions matched actual price movements around 50% of the time, across various timeframes. These suggest that GBM is a reliable tool for short-term stock price forecasting, with moderate accuracy over different time horizons. However, GBM does not predict extreme market events or crashes. It assumes constant volatility and continuous trading, which may not accurately reflect real-world market conditions. GBM also assumes continuous price movements, but in reality, prices can exhibit sudden jumps. We derived a form of partial integro-differential equation (PIDE) particularly suited to our proposed numerical implementation. This result is followed by developing a numerical method that will compute an approximate solution to the PIDE. However, we claim that the method is consistent, stable, and converging. This claim is built on the observation that the numerical values for European options converge to the closed form solutions presented in [11]. We calibrated the observed values of the market for European options prices sourced from Bloomberg on 28th April, 2023.

2 Methodology/Model formulation

This section presents the methods adopted in this paper.

2.1 Geometric Brownian Motion (GBM)

Given $\theta, \sigma > 0$ and $x_0 > 0$. The GBM is the continuous time process, X_t that solves the SDE

$$dS_t = \theta S_t dt + \sigma S_t dW_t \tag{1}$$

Here, S is the stock price, θ and σ are constants, t is time, and W follows a stochastic process called Wiener process, under which $dW = \varepsilon\sqrt{dt}$, where ε is a random draw from the standardized normal distribution. (1) is commonly known as Geometric Brownian motion (GBM), with θ and σ called the drift parameter and the volatility parameter, respectively. The solution is given by

$$d\ln S = \left(\theta - \frac{\sigma^2}{2}\right)dt + \sigma dW \tag{2}$$

The stochastic process as characterized by (2) indicates that $\ln S$ is normally distributed. Equivalently, S is lognormally distributed. With S_0 and S_T denoted as the stock prices at time 0 and time T, respectively, (2) leads to

$$S_T = S_0 exp\left[\left(\theta - \frac{\sigma^2}{2}\right)T + \sigma\varepsilon\sqrt{T}\right] \tag{3}$$

Further, the expected value and the variance of S_T are

$$E\left(S_T\right) = S_0 \exp\left(\theta T\right) \tag{4}$$

and

$$Var\left(S_T\right) = S_0^2\left[\exp\left(2\theta T\right)\right]\left[\exp\left(\sigma^2 T\right) - 1\right] = \left[E\left(S_T\right)\right]^2\left[\exp\left(\sigma^2 T\right) - 1\right] \tag{5}$$

2.2 The Extended Geometric Brownian Motion Model (EGBM)

The EGBM process $X\left(t;\sigma,\nu,\theta\right)$ is derived by approximating a Brownian motion $W\left(t\right)$ with drift $b\left(t;\theta,\nu\right) = \theta t + \sigma W\left(t\right)$ at a random time given by a gamma process with unit mean rate, $\gamma\left(t;1,\nu\right)$,

$$X\left(t;\sigma,\nu,\theta\right) = b\left(\gamma\left(t;1,\nu\right);\theta,\sigma\right). \tag{6}$$

The (EGBM) process consist of three parameters: first is the volatility σ of the Brownian motion, followed by the drift θ of the Brownian motion, then the volatility ν of the time change which is the new parameter added to the existing Geometric Brownian Motion.
The EGBM process has its characteristic function as:

$$\phi X\left(t\right)^{(u)} = \mathrm{E}\left(e^{iuX(t)}\right) = \left(\frac{1}{1 - iu\theta\nu + \sigma^2 u^2/2}\right)^{\frac{t}{\nu}} \tag{7}$$

This characteristic function is infinitely divisible with a zero continuous martingale component and a Lévy measure denoted by

$$k\left(x\right)dx = \frac{\theta x/\sigma^2}{\nu/x}\,\mathrm{esp}\left(\frac{\sqrt{2/\nu + \theta^2/\sigma^2}}{\sigma}\left|x\right|\right)dx \tag{8}$$

2.3 The Extended Brownian Motion Model European Option Pricing Formulas

Let $S\left(t\right)$ be the stock price at time t. The EGBM risk neutral process for the stock price is denoted by

$$S\left(t\right) = S\left(0\right)e^{(r-q)t + X(t) + \omega t} \tag{9}$$

where the normalization factor $e^{\omega t}$ ensuring that $\mathrm{E}\left[S\left(t\right)\right] = S\left(0\right)e^{(r-q)t}$, requires that $\omega = \frac{1}{\nu}\ln\left(1 - \sigma^2\nu/2 - \theta\nu\right).$

The price of a European call option with strike K and maturity T following the risk neutrality is given as

$$c\left(S(0);K,t\right)=e^{-rt}\mathrm{E}_t\left(\left(S(t)-K(\ )\right)^+\right) \tag{10}$$

The Derivation of the Partial Integro-Differential Equation (PIDE)

The partial integro-differential equation was derived following the work of [12]

Suppose, $Y(t)=\log\left(S(t)\right)$. This follows from (9) that

$$Y(t)=Y(0)+(r-q+\omega)t+X(t;\sigma,\nu,\theta).$$

Note, that $X(t;\sigma,\nu,\theta)$ is a jump process that may be written as the sum of all its jumps we may write the explicit semi-martingale decomposition for $Y(t)$ as follows.

Let μ be the value of the random measure associated with the jumps of the process $X(t;\sigma,\nu,\theta)$ and let ν denotes the predictable compensator. Considering the specific case of EGBM we have that

$$\nu(dx,dt)=k(x)dxdt$$

$$k(x)=\frac{e^{-\lambda px}}{\nu x}1_{x>0}+\frac{e^{-\lambda_n|x|}}{\nu|x|}1_{x<0}$$

$$\lambda_p=\left(\frac{\theta^2}{\sigma^4}+\frac{2}{\sigma^2\nu}\right)^{\frac{1}{2}}-\frac{\theta}{\sigma^2}$$

$$\lambda_n=\left(\frac{\theta^2}{\sigma^4}+\frac{2}{\sigma^2\nu}\right)^{\frac{1}{2}}+\frac{\theta}{\sigma^2}$$

The semi-martingale decomposition for $Y(t)$ is given by

$$Y(t)=Y(0)+(r-q+\omega)t+x*\nu t+x*(\mu-\nu)t$$

where the operation $*$ signifies a double integration with respect to $x,\ t$ in the domain $\mathbb{R}\times[0,t]$, and $\mathbb{R}$ denotes the real line.

The infinitesimal generator for the Markov process $Y(t)$ applies to functions *f(Y, t)* $f(Y,t)$ and given by

$$\Gamma f=\left[\frac{\partial}{\partial t}+\left(r-q+\omega+\int_{-\infty}^{\infty}xk(x)dx\right)\frac{\partial}{\partial Y}\right]f+\int_{-\infty}^{\infty}\left[f(Y+x,t)-f(Y,t)-x\frac{\partial}{\partial Y}f\right]k(x)dx \tag{11}$$

We deduce and prove that the option pricing PIDE in the Lévy models is of the form:

$$\frac{\partial \omega}{\partial \tau}(x,\tau)-(r-q+\omega)\frac{\partial \omega}{\partial x}(x,\tau)+r\omega(x,\tau)$$
$$-\int_{-\infty}^{+\infty}\left[\omega(x+y,\tau)-\omega(x,\tau)\right]k(y)dy \qquad (12)$$
$$-1_{x<x(\tau)}\left\{rK-qe^{x}-\int_{x(\tau)-x}^{\infty}\left[\omega(x+y,\tau)-\left(K-e^{x+y}\right)\right]k(y)dy\right\}=0$$

This PIDE must be solved subject to initial condition

$$\omega(x,0)=\left(K-e^{x}\right)^{+}, \qquad (13)$$

and boundary conditions

$$\frac{\partial^{2}\omega}{\partial x^{2}}(-\infty,\tau)-\frac{\partial \omega}{\partial x}(-\infty,\tau)=0\ \forall\tau \qquad (14)$$

$$\frac{\partial^{2}\omega}{\partial x^{2}}(+\infty,\tau)-\frac{\partial \omega}{\partial x}(+\infty,\tau)=0\ \forall\tau \qquad (15)$$

3 Analysis of the model

3.1 Discretization

To compute the numerical solution, we employed the finite difference discretization scheme developed and analyzed by [13]. This scheme utilizes a uniform spatial discretization with a step size of $\Delta x = 0.01$ and implicit time discretization with a step size of $\Delta t = 0.005$. We selected $N = 400$ spatial discretization steps and $M = 200$-time discretization steps. The spatial computational domain was limited to $x \in [-L, L]$, where $L = 4$. The rationale behind choosing this scheme is its computational efficiency, as it requires less computational resources and time compared to other methods.

4 Numerical simulations/sensitivity analysis

In this section comparisons are made between the value of a European call option under the assumption that price movements follow Extended Geometric Brownian motion and the corresponding Geometric Brownian motion.

4.1 Calibration of Extended Geometric Brownian Motion Model to Real Market Prices

Here, we calibrate EGBM to data obtained from real market. The data used was extracted from Bloomberg. The data consists of option market data observed on NASDAQ (National Association of Securities Dealers Automated Quotations) index Call Option Price Quotations on 28th April,2023. We calibrated EGBM parameters for each maturity separately resulting to parameters in Table 1.

Table 1: Calibrated EGBM Parameters

T	S_0	r	q	σ	ν	θ
0.3397	268.74	0.0423	0.021	0.2687	0.2317	-0.4064
0.4164	268.74	0.0426	0.022	0.2650	0.4240	-0.3883
0.5547	268.74	0.0429	0.021	0.2707	0.6908	-0.3811

0.6316	268.74	0.0421	0.022	0.2872	0.7025	-0.3288

Note from Table 1 that as maturity T gets higher, the annualized kurtosis parameter ν gets larger and annualized skewness θ reduces. The increase in ν is slower than the increase in maturity T and this is stable with an approach to normality, though at a rate slower than would be the case if ν were constant. The decrease in θ is also stable with the approach to normality.

Table 2: Early Exercise Premiums for EGBM and GBM

Maturity	$T_1 = 0.3397$		$T_2 = 0.4164$		$T_3 = 0.5547$		$T_4 = 0.6316$	
Strike	**GBM**	**EGBM**	**GBM**	**EGBM**	**GBM**	**EGBM**	**GBM**	**EGBM**
100	0.0412	0.0422	0.0324	0.0520	0.353	0.429	0.656	1.032
120	0.0317	0.0361	0.1333	0.1320	0.745	0.776	0.861	1.250
140	0.0120	0.1317	0.1365	0.1910	0.569	0.835	1.131	1.489
160	0.0565	0.1559	0.0381	0.2530	0.918	0.997	1.192	1.742
180	0.1313	0.1396	0.2351	0.2440	0.856	1.185	1.483	2.023
200	0.1564	0.1239	0.3359	0.2400	1.298	1.388	1.756	2.339
220	0.2531	0.1328	0.8853	0.2956	1.318	1.681	1.966	2.741
240	0.3528	0.6108	0.5365	0.4791	1.856	2.008	2.462	3.178
260	0.5462	0.8169	0.6745	1.0780	1.999	2.392	2.686	3.687
280	0.630	1.1103	1.0669	1.3740	2.664	2.795	3.400	4.241
300	1.066	1.4183	1.4375	1.6780	3.112	3.291	3.771	4.861

Table 2 gives the early exercise premiums for pricing options under the Extended Geometric Brownian motion model and Geometric Brownian motion dynamics respectively. Note that for all strikes and maturities, the EGBM early exercise premiums dominate those from Geometric Brownian motion. The differences are significant, for example when strike price is 220 with maturity 0.4164, it is about a 1/3 of the option value under Geometric Brownian motion. This drove us into concluding that the pricing of options under the underlying dynamics may be difficult but more efficient, it is important from the viewpoint of accounting for the values of these instruments correctly. The Extended Brownian motion model does not require unrealistic assumptions and is more consistent with the financial theory.

4.2 Simulated Price Path Comparisons for the EGBM and GBM

This section gives a comparison of stock price paths for the EGBM and GBM. To give a meaningful comparison, we have ensured that the same random numbers and time are used to generate all the paths. The simulated price paths of EGBM and GBM models are shown in Figure 1.

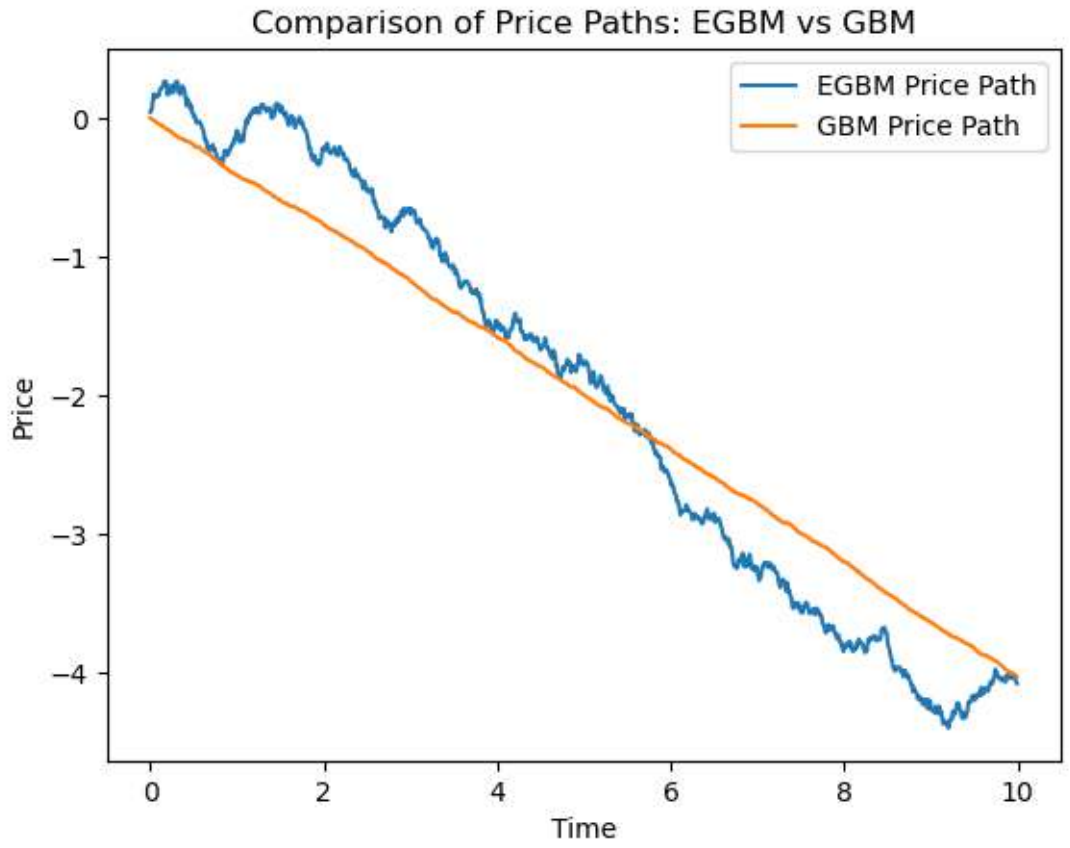


Figure 1: Simulated Price Paths of EGBM and GBM Models

It could be observed that the EGBM price path exhibits more volatility and randomness compared to the GBM price path, which is consistent with the EGBM model's stochastic volatility and jump components. It could also be noticed that the EGBM price path has a more irregular and unpredictable behavior, with sudden jumps and changes in direction, reflecting the model's ability to capture extreme events and volatility clustering. The GBM price path on the other hand, appears smoother and more predictable, with a more consistent and gradual change in price over time, reflecting the model's constant volatility and lack of jumps. The negative drift parameter θ **= -0.4064** in both models causes the price paths to decline over time, but the EGBM price paths declines more rapidly and unpredictably due to its stochastic volatility and jump component. The EGBM variance coefficient ν = 0.2317 introduces additional randomness and variability making the EGBM price path more sensitive to changes in the underlying variables. The figure 1 demonstrates the EGBM ability to capture more complex and realistic market dynamics. However, the EGBM model is more capable of producing stock price returns distributions with fat tails and which exhibit skewness.

4.3 Volatility Paths of EGBM Model Compared with Volatility Paths of GB

This section shows the simulated volatility paths of EGBM and GBM models which are demonstrated in Figure 2

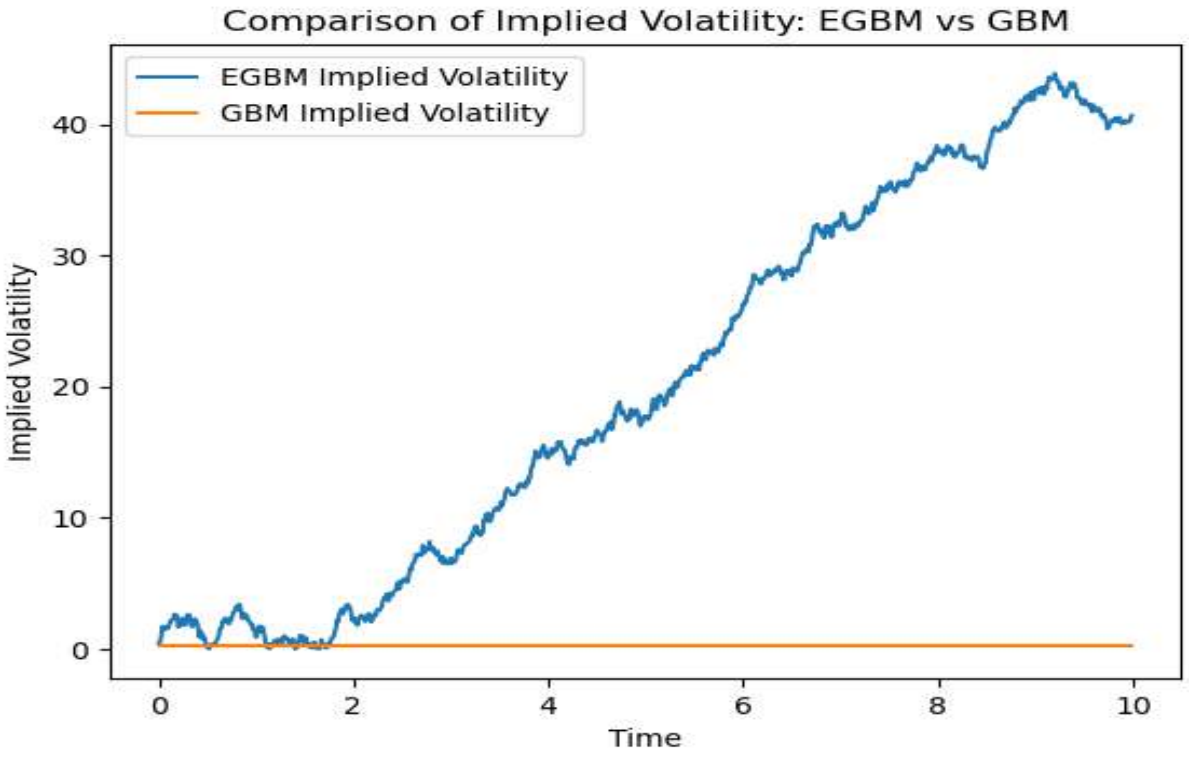


Figure 2: Volatility Paths of EGBM Model Compared with Volatility Paths of GBM Model

The EGBM model exhibits higher implied volatility than GBM indicating higher uncertainty or risk. The GBM model's constant implied volatility indicates a constant level of uncertainty or risk, whereas the EGBM model's time-varying implied volatility suggests a changing risk profile. Note that the implied volatility is a measure of the market's expected volatility, and the EGBM implied volatility is more volatile and unpredictable indicating a greater uncertainty in the market's expectations, hence demonstrating the EGBM ability to capture more unrealistic market dynamics.

5 Discussions and conclusion

We propose a model that combines Geometric Brownian motion with random time component. The proposed model is termed the Extended Geometric Brownian motion. Partial integro-differential equation (PIDE) for pricing options under the proposed process was derived and its values were estimated numerically. The pricing performance of the new model is compared on option data sourced from Bloomberg on 28th April, 2023 with the Geometric Brownian motion (GBM). The result revealed that the additional parameter was able to address the pricing biases of the Geometric Brownian motion. The approach developed here would consequently be applicable to a varied class of problems. However, more work is required in developing fast and efficient procedures for solving PIDE's with a view to calibrating stochastic processes to a surface of option prices.

References

[1] Fiorani, F. (2009). Option pricing under the variance gamma process. VDM Verlag Dr. Müller.
[2] Atiase, D.D., Boiquaye, P.A. & Doku-Amponsah, K. (2021). Derivation of European option pricing formula when the asset is geometric mean reverting. Science and Development 5, (1), 47-46
[3] Cont, R., & Tankov, P. (2004). Financial modelling with jump processes. Chapman & Hall/CRC.
[4] Nwobi, F. N., Inyama, S. C., & Onyegbuchulem, C. A. (2019). Option pricing within Heston's stochastic and stochastic-jump models. Communications in Mathematical Finance, 8(1), 79-91.
[5] Onyegbuchulem, C. A., Nwobi, F. N., & Onyegbuchulem, B. O. (2020). Valuation of agricultural commodity in an unstructured Nigerian market using Black-Scholes' model. Asian Journal of Probability and Statistics, 9(2), 43-50.
[6] Onyegbuchulem, C. A., Onyegbuchulem, B. O., & Imoh, J. C. (2020). Index options under Heston's stochastic volatility model: A characteristic function approach. Academic Journal of Statistics and Mathematics, 6(9), 1-11.
[7] Onyegbuchulem, C. A., Onyegbuchulem, B. O., & Achugamuonu, P. C. (2021).). Valuation of Nigerian crude oil using Heston's stochastic-jump model. Royal Statistical Society-Nigeria Local Group Annual Conference Proceedings. 20 - 24
[8] Agbam, A. S. (2021). Stock prices prediction using Geometric Brownian motion: Analysis of the Nigerian stock exchange. Journal of Engineering and Applied Scientific Research 13(1), 2384-6569
[9] Abidin, S. & Jaffar, M.M. (2012). A review on Geometric Brownian motion in forecastingthe share prices in Bursa Malaysia. World Applied Sciences Journal, 17, 87-93.
[10] Reddy, K. & Clinton V. (2016). Simulating stock prices using Geometric Brownian motion: Evidence from Australian companies, Australasian Accounting, Business and Finance Journal,10(3),23-47.
[11] Madan, D. B., Carr, P., & Chang, E. C. (1998). The variance gamma process and option pricing. European Finance Review, 2, 79-105.
[12] Phewchean, N., & Wu, Y. (2022). Solution of partial integro-differential equations. Global Journal of Pure and Applied Mathematics.13(8), 260- 286
[13] Cruz, J., & Ševčovič, D. (2018). Option pricing in illiquid markets with jumps. Applied Mathematics in Finance, 25(4), 389-409.
.

An effective new one-step block integrator for the numerical solution of system of first order differential equation arising from epidemiology models

M.I. Modebei*†, O.O. Olaiya†‡, O.E. Faniyi§, and O.F. Anorue¶

Abstract

This paper proposes an effective new one-step block integrator for the solution of system of first-order ordinary differential equation that arise from models in epidemiology in life science. Showing the performance of this method, SIR, SEIR and more compartmental models are solve numerically and thus comparing with the classical Runge-Kutta to reveal its accuracy. The numerical results obtained clearly shows that the proposed method is more efficient and robust for obtaining the numerical solution of mathematical models in epidemiology.

1 Introduction

Its not contentious that first order differential equation are models of many physical phenomenons. In science and engineering, usually mathematical models are developed to help in the understanding of physical phenomena. These models especially in economics, medicine, chemical, electrical, and mechanical engineering, physics, and mathematical biology, often yields equations of first order with certain initial condition. In mathematical biology especially in the study of spread of diseases in epidemiology, mathematical models formulated form system of first-order ordinary differential equations (ODEs) with prescribed initial conditions. Motivated by this life applications, the following initial value problem (IVP) is considered in this work:

$$\frac{\bar{y}}{dx} = \bar{f}(\bar{x}, \bar{y}), \quad \bar{y}(a) = \bar{y_0} \quad a \leq x \leq b, \tag{1}$$

where $\bar{y} = (y_1, y_2, \ldots, y_n)^T$, $\bar{f} = (f_1, f_2, \ldots, f_n)^T$, and $\bar{x} = (x_1, x_2, \ldots, x_n)^T$, with $\bar{y}$ being unknown vectors or real vector functions which are at least one time differentiable in $\mathbf{R}$, $F \in \mathbf{R^n} \times \mathbf{R}^m$ and $a,\ b$ are real constants. It is assumed that f_i, $i = 1, \ldots, n$ are continuous and each f_i satisfies the following Lipschitz conditions:

$$|f_i(x, y_{j_1}) - f_i(x, y_{j_2})| \leq \gamma |y_{j_1} - y_{j_2}| \tag{2}$$

for some positive γ thus guaranteeing the existence and uniqueness of solution of the system (1) in $\mathbf{R}$.

In literature, there are diverse numerical methods for solving scalar form of (1). There are numerous numerical method for the numerical solution of the system in (1). One available approach is the Runge-Kutta method. This method has a very wide range of applicability in terms of nature of problems being solved ranging from oscillatory to stiff problem and thus obtaining good good approximation of solution with appreciable absolute and relative errors [1, 2]. In many cases, some of the system may

*Corresponding Author; E-mail: gmarc.ify@gmail.com
†Mathematics Programme, National Mathematical Centre, Abuja, Nigeria
‡E-mail: oolaiya.o@gmail.com
§Department of Mathematics, Anchor University, Lagos, Nigeria; E-mail: ofaniyi@aul.edu.ng
¶Department of Mathematics, Michael Okpara University of Agriculture, Umudike, Abia State, Nigeria; E-mail: onyinyechianorue@gmail.com

be stiff, that is, the solution varies rapidly over a short time. In this case, Runge-Kutta methods are mostly inappropriate for dealing with such differential systems. Other numerical approaches for solving (1) includes the Differential Transform Method (DTM) as seen in [3, 4, 5], Adomian Decomposition Method (ADM) have been used in [6, 7, 8], Homotopy Perturbation Method (HPM) applied in [9]. There exists other methods are in the literature for the numerical solution of (1). In this paper, Linear Multistep Block method based on collocation techniques is applied. In this approach a one-step block method is derived. This method has the advantage of being self-starting, i.e, they do not require a staring value to kick-start their implementation. They also have the advantage of producing smaller global errors (at the end of the range of integration) than those produced by the step-by-step methods due to the presence of accumulated errors at each step in the step-by-step method. This paper is structured as follows: Section 2 explains the derivation of the method and section 3 presets the characteristics of the derived method. the implementation of the derived method with epidemiological model in literature is presented in section 4, and section 5 summarizes and concludes the work.

2 Derivation of the Method

The derivation of a continuous implicit three off-step hybrid block method is described in this section. Consider an approximate solution $y(x)$ of (1) over the integration subinterval $[x_n, x_{n+1}]$ with the polynomial given as

$$y(x) \approx T(x) = \sum_{k=0}^{7} \rho_k x^k \tag{3}$$

with the first derivative

$$f(x)y'(x) \approx T'(x) = \sum_{k=1}^{7} \rho_k k x^{k-1} = f(x) \tag{4}$$

where ρ_k. $k = 0(1)7$ are unknown parameters to be determined with the method of collocation/interpolation. Considering a one-step method in the interval $[x_n, x_{n+1}]$, the p_i, $i = 1(1)5$ off-grid points in the interval $[0, 1]$ such that $0 < p_1 < p_2 < p_3 < p_4 < p_5 < 1$ with x_n and x_{n+1} being the points of interpolations while the points of interpolation are x_n, x_{n+p_i}, $i = 1(1)5$ and x_{n+1}. , thereby obtaining the following system of equations $T(x_n) = y_n$; $T(x_{n+p_i}) = y_{n+p_1}$; $T'(x_n) = f_n$; $T'(x_{n+p_i}) = f_{n+p_i}$, $i = 1(1)5$; $T'(x_{n+1}) = f_{n+1}$, where $y_{n+p_i} \simeq y(x_{n+p_i})$, $f_{n+p_i} \simeq f(x_{n+p_i}, y(x_{n+p_i}))$.
Solving the above system using a computer algebraic system (cas) in Mathematica we obtain the values of the coefficients ρ_k $k = 0(1)7$ (not included here). Substituting these values of ρ_k's into the polynomial (3), the following is obtained:

$$T(x_n + th) = y_n + h\left(\beta_0 f_n + \beta_{p_1} f_{n+p_1} + \beta_{p_2} f_{n+p_2} + \beta_{p_3} f_{n+p_3} + \beta_{p_4} f_{n+p_4} + \beta_{p_5} f_{n+p_5} + \beta_1 f_{n+1}\right) \tag{5}$$

where $p_1 = \frac{1}{10}, p_2 = \frac{1}{4}, p_3 = \frac{1}{2}, p_4 = \frac{13}{20}, p_5 = \frac{9}{10}$. Evaluating (5) at the points $t = \frac{1}{10}, \frac{1}{4}, \frac{1}{2}, \frac{13}{20}, \frac{9}{10}, 1$ and after simplifying, the following formulas are obtained

$$\begin{aligned}
y_{n+p_1} &= y_n + h\left(\tfrac{4484209}{122850000} f_n + \tfrac{97247}{1247400} f_{n+p_1} - \tfrac{307313}{15356250} f_{n+p_2} + \tfrac{68659}{6300000} f_{n+p_3} - \tfrac{103193}{15765750} f_{n+p_4} + \tfrac{18247}{9828000} f_{n+p_5} - \tfrac{130681}{198450000} f_{n+1}\right),\\
y_{n+p_2} &= y_n + h\left(\tfrac{18383}{628992} f_n + \tfrac{1972625}{12773376} f_{n+p_1} + \tfrac{111131}{157248} f_{n+p_2} - \tfrac{473}{64512} f_{n+p_3} + \tfrac{13675}{4036032} f_{n+p_4} - \tfrac{3775}{5031936} f_{n+p_5} + \tfrac{253}{1016064} f_{n+1}\right),\\
y_{n+p_3} &= y_n + h\left(\tfrac{55}{1456} f_n + \tfrac{5875}{49896} f_{n+p_1} + \tfrac{1075}{4914} f_{n+p_2} + \tfrac{109}{672} f_{n+p_3} - \tfrac{1775}{42042} f_{n+p_4} + \tfrac{25}{2912} f_{n+p_5} - \tfrac{181}{63504} f_{n+1}\right),\\
y_{n+p_4} &= y_n + h\left(\tfrac{202501}{5600000} f_n + \tfrac{39521833}{319334400} f_{n+p_1} + \tfrac{7835347}{37800000} f_{n+p_2} + \tfrac{16690609}{67200000} f_{n+p_3} + \tfrac{412009}{12936000} f_{n+p_4} + \tfrac{7267}{1792000} f_{n+p_5} - \tfrac{4716959}{3175200000} f_{n+1}\right),\\
y_{n+p_5} &= y_n + h\left(\tfrac{198243}{4550000} f_n + \tfrac{1503}{15400} f_{n+p_1} + \tfrac{142749}{568750} f_{n+p_2} + \tfrac{101979}{700000} f_{n+p_3} + \tfrac{450927}{1751750} f_{n+p_4} + \tfrac{45189}{364000} f_{n+p_5} - \tfrac{47529}{2450000} f_{n+1}\right),\\
y_{n+1} &= y_n + h\left(\tfrac{205}{4914} f_n + \tfrac{10375}{99792} f_{n+p_1} + \tfrac{592}{2457} f_{n+p_2} + \tfrac{83}{504} f_{n+p_3} + \tfrac{14800}{63063} f_{n+p_4} + \tfrac{7675}{39312} f_{n+p_5} + \tfrac{149}{7938} f_{n+1}\right)
\end{aligned} \tag{6}$$

The above formulas together constitute the required block integrator for the direct approximation of the (1).

3 Analysis of the Block Integrator

For any numerical scheme, It is very important to know the order of accuracy and the nature of the local error in the implementation of the scheme. We thus introduce the difference operator corresponding

to each of the formula in (6) as

$$\mathcal{L}[y(x);h] = y(x) - h\left(\beta_0 y'(x_n) + \beta_1 y'(x_{n+1}) + \sum_{j=1}^{5} \beta_j y'(x_{n+p_j})\right) \tag{7}$$

where $y'(x_{n+p_j}) = f(x_{n+p_j})$ and $y(x) \in C[a,b]$. Expanding (6) in Taylor series about x_n, and after collecting all the terms in h the following local truncation errors (LTEs) are obtained

$$\left(\frac{1247969y^{(8)}(x_n)h^8}{846720000000000}, -\frac{9799y^{(8)}(x_n)h^8}{34681651200000}, \frac{383y^{(8)}(x_n)h^8}{90316800000},\right.$$

$$\left.\frac{104583791y^{(8)}(x_n)h^8}{36126720000000000}, \frac{354483y^{(8)}(x_n)h^8}{31360000000000}, \frac{37y^{(8)}(x_n)h^8}{4233600000}\right)^T$$

The block method in (6) takes the matrix form

$$A_1 Y_{n+p} = A_0 Y_n + h(B_0 F_n + B_1 F_{n+p}) \tag{8}$$

where

$$Y_{n+p} = (y_{n+p_1}, y_{n+p_2}, y_{n+p_3}, y_{n+p_4}, y_{n+p_5}, y_{n+1})^T$$
$$Y_n = (y_n, y_{n-p_1}, y_{n-p_2}, y_{n-p_3}, y_{n-p_4}, y_{n+p_5})^T$$
$$F_{n+p} = (f_{n+p_1}, y_{n+p_2}, y_{n+p_3}, y_{n+p_4}, y_{n+p_5}, y_{n+1})^T$$
$$F_n = (f_n, f_{n-p_1}, f_{n-p_2}, f_{n-p_3}, f_{n-p_4}, f_{n+p_5})^T$$

The zero-stability refers to stability of the difference system in (7) as $h \to 0$. As such, if $h \to 0$ in (7) and by extension the the matrix representation in (8), we obtain

$$A_1 Y_{n+p} = A_0 Y_n \tag{9}$$

where A_1 is $I_{6\times 6}$ identity matrix and $A_0 = \begin{pmatrix} 1 & 0 & 0 & 0 & 0 & 0 \\ 1 & 0 & 0 & 0 & 0 & 0 \\ 1 & 0 & 0 & 0 & 0 & 0 \\ 1 & 0 & 0 & 0 & 0 & 0 \\ 1 & 0 & 0 & 0 & 0 & 0 \\ 1 & 0 & 0 & 0 & 0 & 0 \end{pmatrix}$ The characteristic equation of (9) is given as $\lambda^5(\lambda - 1)$, which yields $\lambda_r = 0$, for $r = 1, 2, \ldots, 5$ and $\lambda_6 = 1$. The block method (6) is 0-stable since the root of the first characteristic polynomial in (9), that is $p(\lambda) = 0$ satisfies the strict root condition, i.e, all its roots lie inside the unit circle, $|r| < 1$ and with those on the boundary being simple, see [2].

The block method in (6) has the property of consistency since it has accuracy greater than one as seen in its LTEs and it satisfies zero stability. Then, the method is concluded to be convergent.

3.1 Linear stability

For the linear stability of the NOSBI, the following test prob;em is adopted

$$y'(x) = -\xi y(x) \tag{10}$$

where $\xi \in \mathbf{C}$. It can be easily seen that (10) has a bounded solution for $\xi \geq 0$ as $x \to \infty$. Substituting (10) into (5) and (6), we obtain

$$\bar{Y}_{n+\tau} = \Omega(\omega)\bar{Y}_n \tag{11}$$

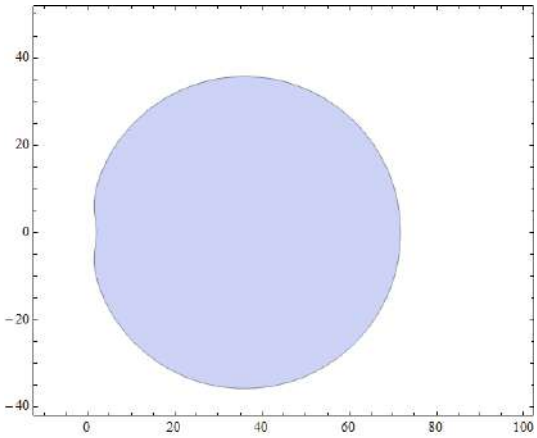


Figure 1: Region of absolute stability of the NOSBI

where $\omega = \xi h$ and the matrix $\Omega(\omega)$ is the amplification matrix or the stability matrix defined as

$$\Omega(\omega) = (A_0 + \omega B)^{-1}(A_1 + \omega C) \tag{12}$$

with

$$A_0 = \begin{pmatrix} 1 & 0 & 0 & 0 & 0 & 0 \\ 0 & 1 & 0 & 0 & 0 & 0 \\ 0 & 0 & 1 & 0 & 0 & 0 \\ 0 & 0 & 0 & 1 & 0 & 0 \\ 0 & 0 & 0 & 0 & 1 & 0 \\ 0 & 0 & 0 & 0 & 0 & 1 \end{pmatrix}; \quad A_1 = \begin{pmatrix} 0 & 0 & 0 & 0 & 0 & 1 \\ 0 & 0 & 0 & 0 & 0 & 1 \\ 0 & 0 & 0 & 0 & 0 & 1 \\ 0 & 0 & 0 & 0 & 0 & 1 \\ 0 & 0 & 0 & 0 & 0 & 1 \\ 0 & 0 & 0 & 0 & 0 & 1 \end{pmatrix}$$

$$B = \begin{pmatrix} 0 & 0 & 0 & 0 & 0 & \frac{4484209}{122850000} \\ 0 & 0 & 0 & 0 & 0 & \frac{18383}{628992} \\ 0 & 0 & 0 & 0 & 0 & \frac{55}{1456} \\ 0 & 0 & 0 & 0 & 0 & \frac{202501}{5600000} \\ 0 & 0 & 0 & 0 & 0 & \frac{198243}{4550000} \\ 0 & 0 & 0 & 0 & 0 & \frac{205}{4914} \end{pmatrix}$$

$$C = \begin{pmatrix} \frac{97247}{1247400} & -\frac{307313}{15356250} & \frac{68659}{6300000} & -\frac{103193}{15765750} & \frac{18247}{9828000} & -\frac{130681}{198450000} \\ \frac{1972625}{12773376} & \frac{11131}{157248} & -\frac{473}{64512} & \frac{13675}{4036032} & -\frac{3775}{5031936} & \frac{253}{1016064} \\ \frac{5875}{49896} & \frac{1075}{4914} & \frac{109}{672} & -\frac{1775}{42042} & \frac{25}{2912} & -\frac{181}{63504} \\ \frac{16690609}{67200000} & \frac{7835347}{37800000} & \frac{16690609}{67200000} & \frac{412009}{12936000} & \frac{7267}{1792000} & -\frac{4716959}{3175200000} \\ \frac{1503}{15400} & \frac{142749}{568750} & \frac{101979}{700000} & \frac{450927}{1751750} & \frac{45189}{364000} & -\frac{47529}{2450000} \\ \frac{10375}{99792} & \frac{592}{2457} & \frac{83}{504} & \frac{14800}{63063} & \frac{7675}{39312} & \frac{149}{7938} \end{pmatrix}$$

Hence obtaining the the following eigenvalues

$$\Omega(\omega) = \left(0, 0, 0, 0, 0, \frac{3(26880000 + 138240\omega - 3265600\omega^2 + 459552\omega^3)}{8064000 - 391680\omega + 8644800\omega^2 + 1122144\omega^3}\right); \tag{13}$$

The values in (13) shows the stability of the NOSBI entirely described by the amplification matrix $\Omega(\omega)$, whose region of absolute stability is is given as by $|\xi\Omega(\omega)| \leq 1$.The stability interval is thus (0, 71.795). The region of absolute stability is thus given in Figure 1

4 Computational procedure

The proposed method is implemented in a fixed step-size block mode in such that, on the each block interval of the form $[x_n, x_{n+1}]$, $n = 0, 1, N-1$, where N is the number of subinterval of the integration

interval $[a, b]$. Applying the proposed method to system of m first order ODEs, we have the following procedure

$$Y' = F(X, Y^T), \quad Y(a) = Y_0, \quad [X_0, X_N]$$

where

$$Y = (y_1, y_2, \ldots, y_m)^T,$$
$$F(X, Y^T) = (f_1(x, Y^T), f_2(x, Y^T), \ldots, f_m(x, Y^T))^T$$

and

$$Y_0 = (y_{1,0}, y_{2,0}, \ldots, y_{m,0})^T, \quad)^T.$$

The method is applied to each of the scalar equations in the differential system so that a total of $6 \times m$ are obtained. This is solved using the Newton's method.

5 Numerical experiments

In this section, the implementation of the proposed method is performed on modeled problems rising from diseases in human population. The comparison of the proposed method is done with the classical fourth-order Runge-Kutta (RK) method.

Model Problem 1. Consider a three compartmental model of a disease epidemic discussed in [3]

$$\begin{aligned} \frac{dS}{dt} &= \beta - \alpha SI - (\rho + \mu)S + \sigma R \\ \frac{dI}{dt} &= \alpha SI - (\gamma + \delta + \mu)I \\ \frac{dR}{dt} &= \gamma I - (\mu + \sigma)R + \rho S \end{aligned} \tag{14}$$

where the state variables S, I and R are susceptible, infected nd recovered population with their respective initial state given as $S(0) = 300$, $I(0) = 200$ and $R(0) = 100$. Here, α, β, γ, δ, μ, ρ and σ are parameters which describes how human migrates from one compartment to another. The following values are obtained in [3]: $\alpha = 0.0011$, $\beta = 10^8$, $\gamma = 0.01$, $\delta = 0.013$, $\mu = 0.02$, $\rho = 0.33$ and $\sigma = 0.44$. Solving (14) with the developed NOSBI and the classical Runge-Kutta method,, the following figure shows how efficient and accurate the new method performed.

In Figure 2, the continuous line indicates solution using the classical Runge-Kutta method while the dots show the solution obtained using the NOSBI. These two methods agree which indicate he suitability of NOSBI for solving similar epidemiological models.

Model Problem 2. Consider the solution for a mathematical model of the SEIR COVID-19 outbreak that includes partially and fully vaccinated individual discussed in [6].

$$\begin{aligned} \frac{dS}{dt} &= A - \alpha SI - \mu S - V_p S - V_f S \\ \frac{dE}{dt} &= \alpha SI - \mu E - \delta E + V_p S \\ \frac{dI}{dt} &= \delta E - \mu I - \mu_1 I - \gamma I \\ \frac{dR}{dt} &= V_f S + \gamma I - \mu R \end{aligned} \tag{15}$$

with the following descriptions with respect to [6]:
A($= 33.595$)- recruitment rate; $\alpha(= 10^-5)$- rate of interaction between susceptible and infected population; $\mu(= 0.143)$- death rate; $V_p(= 0.2522)$- partially vaccinated population; $V_f(= 0.1517)$- fully

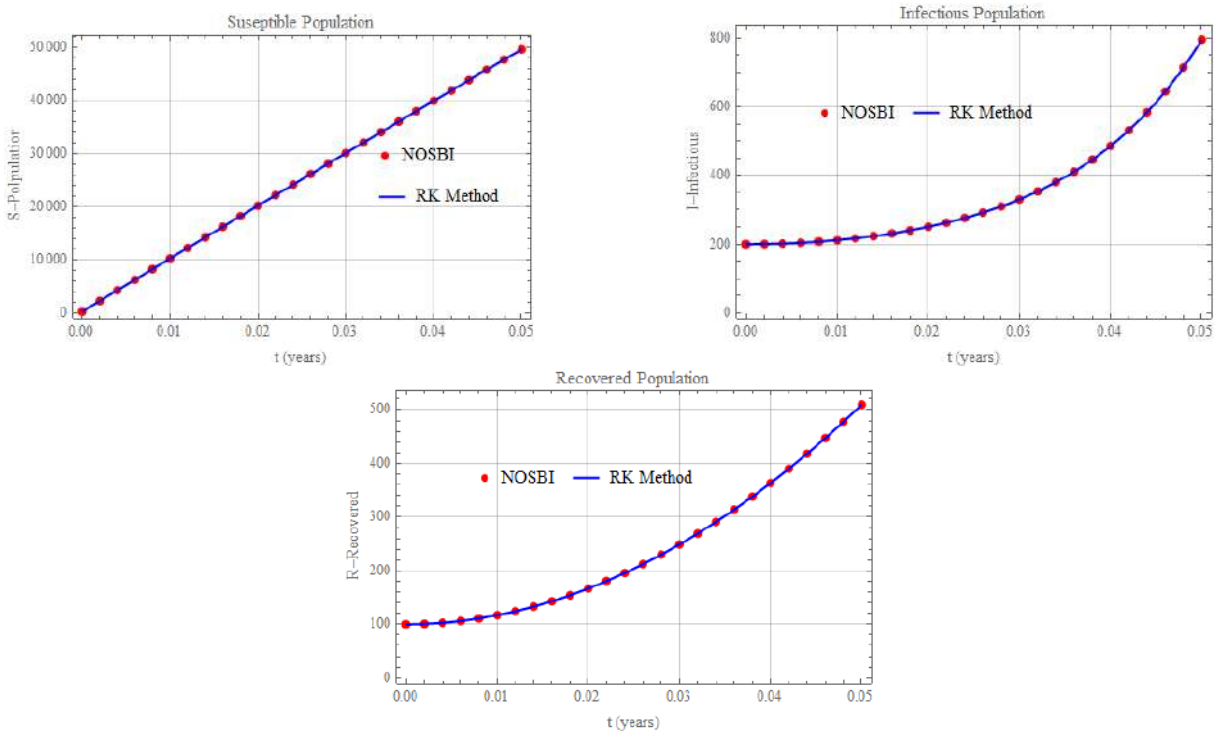


Figure 2: Both NOSBI and the classical Runge-Kutta numerical method

vaccinated population; $\delta(= 1.01)$- rate of infection by exposed population; $\mu_1(= 0.1595)$- disease-related rate; $\gamma(= 0.9)$- rate of recovery. The state variables at time $t_0 = 0$ (in days) are as follows: $S(t_0) = 1,661,987$; $E(t_0) = 1,661$; $I(t_0) = 481$; $R(t_0) = 487$. The developed NOSBI and the classical fourth-order Runge-Kutta method was used to solve 14 numerically. The table below shows curves of the solutions of $S(t)$, $E(t)$, $I(t)$, $R(t)$.

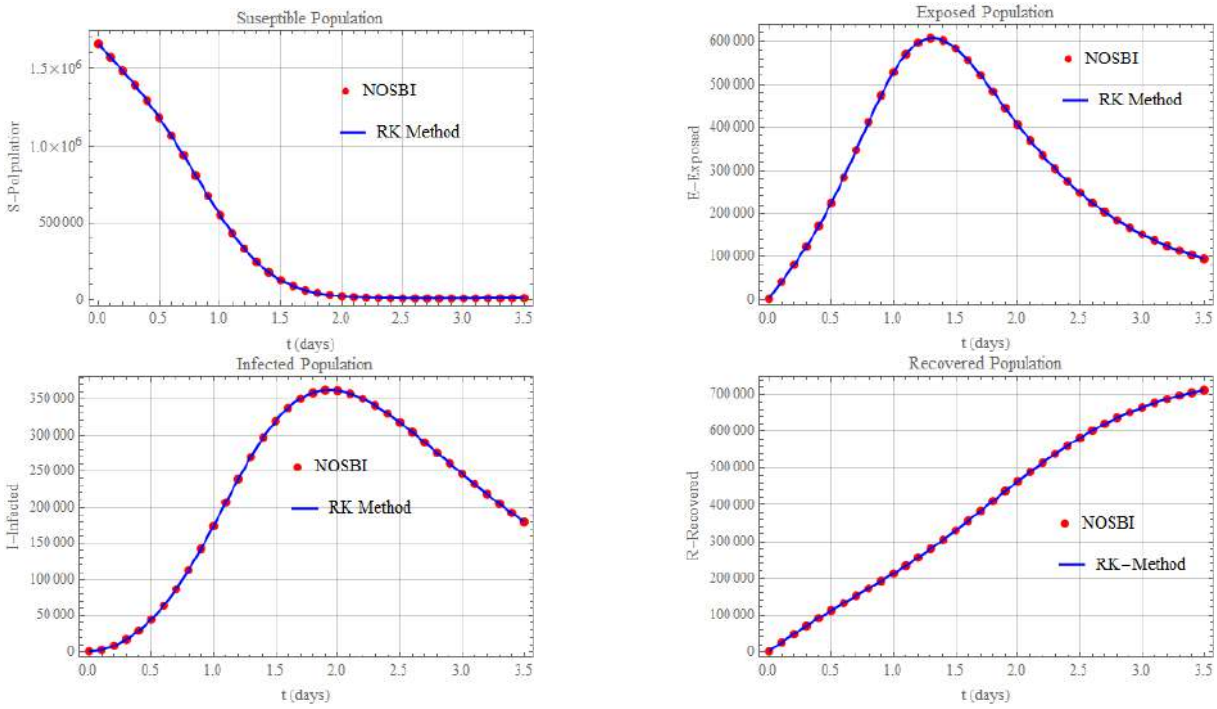


Figure 3: NOSBI and the classical Runge-Kutta numerical method

Model Problem 3. In this experiment, a nonlinear malaria transmission epidemic model discussed in [10] is considered.

$$\begin{aligned} \frac{dS}{dt} &= \Omega - \tau SI - \phi S \\ \frac{dE}{dt} &= \tau SI - (\sigma_1 + \phi)E \\ \frac{dI}{dt} &= \sigma_1 E - (\sigma_2 + \phi + \theta)I \\ \frac{dR}{dt} &= \sigma_2 I - \phi R \end{aligned} \tag{16}$$

where the state variables are Susceptible (S), Exposed (E), Infected (I), and Removed (R). Here, Ω is susceptible recruitment rate, τ is infection rate (effective infection rate), σ_1 is the increasing rate of exposed (human) being infectious, σ_2 is human recovery rate (removal rate), ϕ is natural mortality rate and θ is the Increase in death rate.

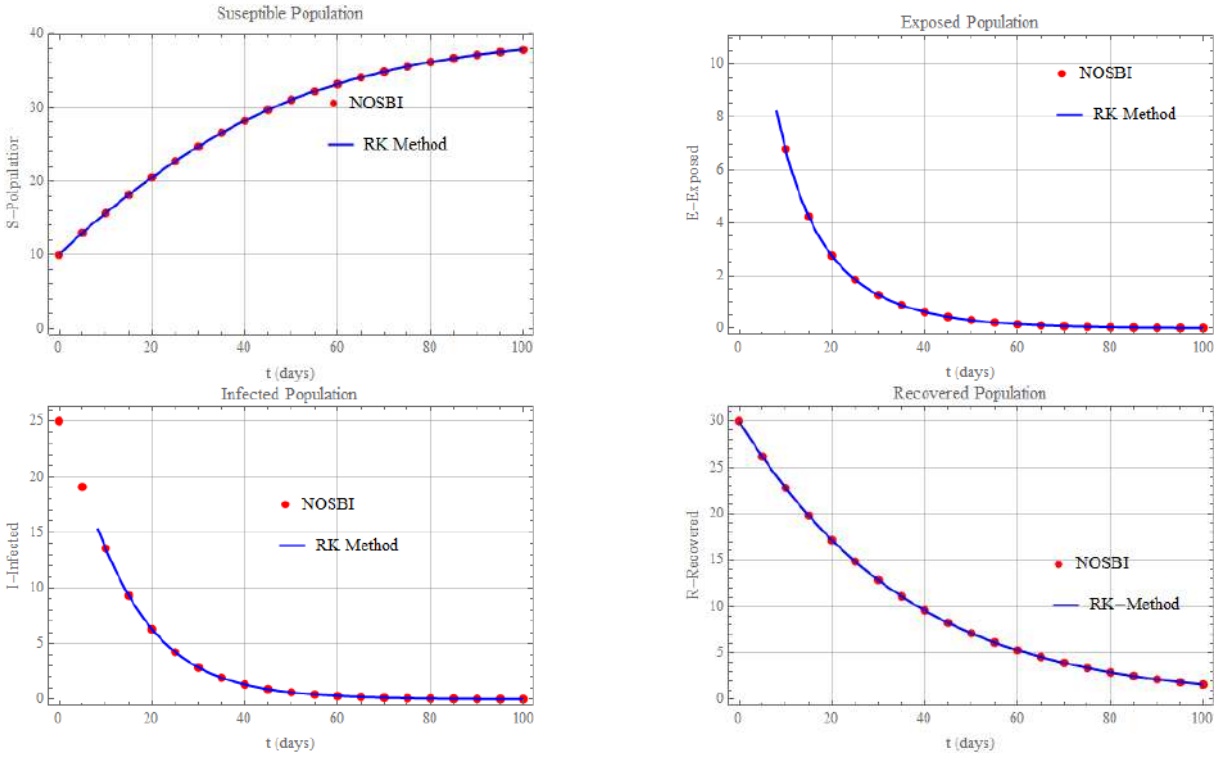


Figure 4: NOSBI and the classical Runge-Kutta numerical method

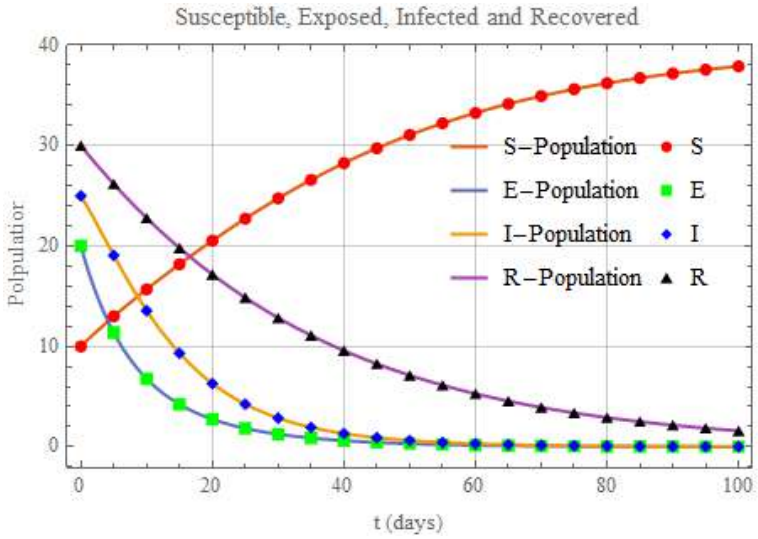


Figure 5: NOSBI and the classical Runge-Kutta numerical method

The following parameter values and initial conditions are used for this experiment. $S(0) = 10$, $E(0) = 20$, $I(0) = 25$, $R(0) = 30$, with $\Omega = 1.2$, $\tau = 0.001$, $\phi = 0.03$, $\sigma_1 = 0.1$, $\sigma_2 = 0.0035$, $\theta = 0.089$.

Generally, it can be clearly seen that, apart from the Runge-Kutta method, this method proves better approximation of the solution of the model so far presented. The effectiveness of the NOSBI is seen in the highly nonlinear model that follows.

Model Problem 4. In this experiment, a mathematical model to cholera transmission with vaccination strategy discussed in [10] is considered.

$$\begin{aligned}
\frac{dS}{dt} &= \Lambda - (1-\omega)\left(\frac{\beta_e B}{B+k} + \beta_h I\right) S - \mu S - \psi S \\
\frac{dV}{dt} &= \psi S - p(1-\omega)\left(\frac{\beta_e B}{B+k} + \beta_h I\right) V - \mu V \\
\frac{dI}{dt} &= (1-\omega)\left(\frac{\beta_e B}{B+k} + \beta_h I\right) S + p\left(\frac{\beta_e B}{B+k} + \beta_h I\right)(1-\omega)V - I(\delta + \mu + \epsilon) \\
\frac{dQ}{dt} &= \varepsilon I - Q(\delta + \eta + \mu) \\
\frac{dR}{dt} &= \eta Q - \mu R \\
\frac{dB}{dt} &= \alpha(1-\omega)I - \sigma B
\end{aligned} \tag{17}$$

Here the physical meaning of the parameters and state values for (17) as stated in [10] are as follows:

$S(t)$-susceptible population, $V(t)$-vaccinated population, $I(t)$-infected population, $Q(t)$-quarantined population and $R(t)$-Recovered population and $B(t)$-is the vibrio cholerae.

Λ: Rate of human Population recruited in susceptible compartment with the value 15.1854/day;

$1/\mu$: Average life expectancy with value 60 years;

δ: Death rate from cholera infection with value 0.015/day;

β_e: Human-to–human interaction rate with value 0.2143/day;

β_h: Vibrios ingestion rate from the Surroundings with value 0.0040963/day;

ω: Measure of education campaign and treatment efficacy with value 0.39;

k: Concentration of the bacterium Vibrio cholerae with value 10^9cells/L;

ε: Quarantine rate of cholera patients with value 0.00331428/day;

η: Rate of quarantine individual recover through treatment with value 0.003/day

α: Contribution rate of infected persons to Vibrio cholerae amount in the environment with value 10

cells/ml-day;
σ: Decay rate of Vibrio cholerae from the atmosphere with value 0.00174478/day;
ψ: The rate at which Susceptible class is Vaccinated 0.07/day;
p: Modification Parameter with value 0.0186821.

The following initial conditions are considered: $S(0) = 15$, $V(0) = 20$, $I(0) = 50$, $Q(0) = 75$, $R(0) = 30$, $B(0) = 0$.

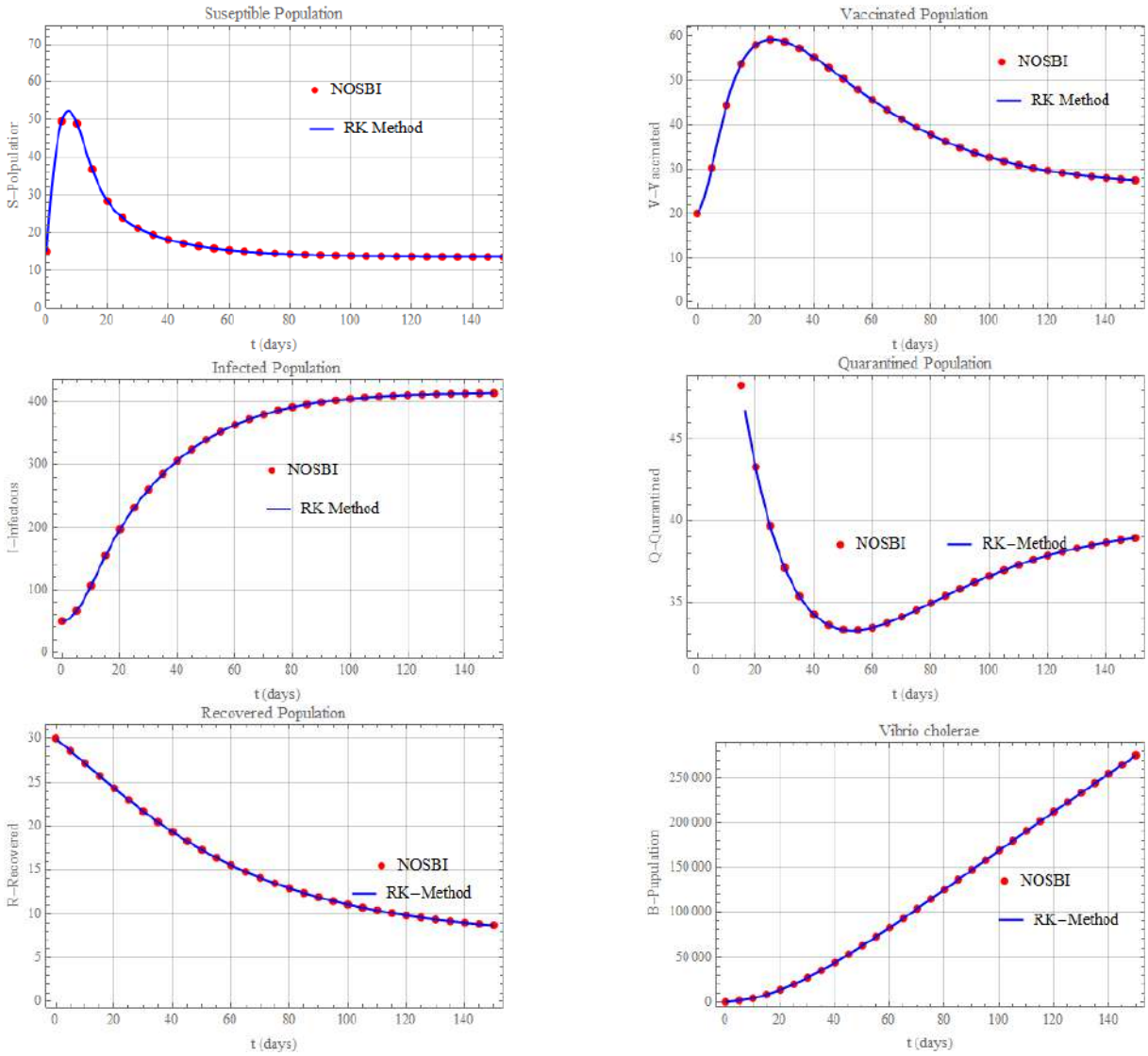


Figure 6: NOSBI and the classical Runge-Kutta numerical method

The applicability of the NOSBI to epidemiological models can not be over emphasized as can be see in the numerical solution of model problem (17) shown by the graph in Figure 6. It clearly agrees with the RK-4 method and invariable with other methods as described in literatures. The numerical experiments shown in the Figures above demonstrate the robustness of the derived NOSBI.

6 Conclusion

Linear multistep method has been shown in several literature to have a good performance in obtaining the numerical solutions of a very large range of problems both scalar and in the case of this work, system of ordinary differential equation. The key advantages of the NOSBI are demonstrated its ease of derivation and implementation. The theoretical properties of the developed scheme shows the robust-

ness in real application to epidemiological dynamics even with large time step sizes. This is a significant implementation and computational advantage.

References

[1] Lambert, J.D. (1991). Numerical Methods for Ordinary Differential Systems. The Initial Value Problem, first, John Wiley, New York.

[2] Henrici, P. (1962). Discrete Variable Methods in Ordinary Differential Equations, John Wiley & Sons, New York, NY, USA.

[3] Adebisi, A.F, Peter, O.J, Ayoola, T.A, Ayoade, A.A, Faniyi, O.E, and Ganiyu, A.B. (2019). Semi analytic method for solving infectious disease model. Science World Journal 14(1): 1-4.

[4] Abioye, A.I., Ibrahim, M.O., Peter, O.J., Amadiegwu, S., and Oguntolu, F.A. (2018). Differential transform method for solving mathematical model of SEIR and SEI spread of Malaria. International Journal of Sciences: Basic and Applied Research (IJSBAR) 40(1), 197-219

[5] Msmali, A.H., Alotaibi, A.M., El-Moneam, M.A., Badr, B.S., and Ahmadini, A.A.H. (2021). A general scheme for solving systems of linear first-order differential equations based on the differential transform method. Hindawi Journal of Mathematics, Article ID 8839201, 9 pages https://doi.org/10.1155/2021/8839201

[6] Blanco-Cocom L. (2024). The multi-step adomian decomposition method applied to an SEIR COVID-19 mathematical model with a vaccinated population. Journal of Hunan University (Natural Sciences), 51(5), 98-106.

[7] Adebisi, A.F., Uwaheren, O.A., Abolarin, O.E., Raji, M.T., Adedeji, J.A., and Peter, O.J. (2021). Solution Of Typhoid Fever model by adomian decomposition method, Math. Comput. Sci. 11(2), 1242-1255. https://doi.org/10.28919/jmcs/5288

[8] Mulenga, J. and Phiri, P.A. (2024). Application of the modified adomian decomposition method on a mathematical model of COVID-19, American Journal of Computational and Applied Mathematics, 14(1), 1-14.

[9] Sotonwa, O.E. and Obabiyi, O.S. (2021). Application of homotopy analysis method for solving the Onchocerciasis (Riverblindness). Global Journal of Pure and Applied Mathematics, 17(2), 371-387. http://www.ripublication.com/gjpam.htm

[10] Jun J.H., Aljohani, A., Mustafa, S., Shokri, A., Khalsaraei, M.M., and Mukalazi, H. (2024). Stability analysis of a nonlinear malaria transmission epidemic model using an effective numerical scheme, Scientific Reports-Springer Nature. 14:17413 https://doi.org/10.1038/s41598-024-66503-1

Mathematical model showing preventive measure as a key to reducing Coronavirus disease (COVID-19) spread

C. Okoye*†, M.B. Okofu†‡, N.K. Nubila§, C.L. Ejikeme ¶, and D.F. Agbebaku‖

Abstract

A set of non-linear Mathematical equations of COVID-19 model, presented in a flow diagram was proposed to study and ascertain the impact of preventive measures (self isolation and social distancing) to curtailing the spread of the disease. To this effect, we computed the threshold quantity R_{eff} (Effective Reproduction Number), carried out the stability analysis on the equilibrium points obtained using Jacobian technique (Eigenvalue approach), Castilo-Chavez method and a suitable Lyapunov function. We discovered that the Disease Free equilibrium point failed the long term test whereas the Endemic Equilibrium was globally asymptotically stable, thus implying that the COVID-19 spread could be curtailed or curbed in the presence of preventive measures (self isolation and social distancing) as advocated.

Keywords and phrases: COVID-19; preventive measures; effective reproduction number; equilibrium point; stability

1 Introduction

At the moment, the world is seized, hanged on a serious lockdown, with capitulating economy and heralded in panic. Coronavirus disease-19 often referred to as "COVID-19" is a viral infectious disease. The outbreak started in late 2019 and became a global pandemic by March 2020. The World health organization labelled it a "pandemic" due to its global network of spread, infact the first pandemic caused by a Coronavirus [1].

As at the time of this writing, the number of confirmed cases, deaths and recovery stood at 553, 244; 25, 034; and 126,630 respectively spanning about 176 countries of the world [2]. Other viral infections such as Ebola and Lassa Fever have models already proposed for them with possible treatment but this could not suffice for COVID-19 as a result of its peculiar mode of spread. The virus spreads through person to person, between people who are in close contact with one another (within about 5 feet or 3 metres) and through respiratory droplets produced when an infected person coughs or sneezes. These droplets can land on mouth, nose or eyes which are openings into the human system. The virus can stay on stainless steel, plastic and cardboard close to $48, 72$ and 24 hours respectively [3] . The symptoms include; sore throat, dry cough, fever, fatigue, diarrhea (mild/moderate cases), difficulty in breathing (severe case) [4]. There is an already developed screening test for identifying and confirming cases. The more diagnosis are made, the more control on the level of exposure [5].

Most pathetic, there are two exposure periods. The first case, an individual shows no sign until after 5 days and the second level is the full blown COVID 19 which shows up $6-7$ days later from the first

*E-mail: chukwudi.okoye@unn.edu.ng
†Department of Mathematics, University of Nigeria, Nsukka, Nigeria
‡Corresponding Author; E-mail: mary.okofu@unn.edu.ng
§Department of Pharmacology and Therapeutics, University of Nigeria, Nsukka, Nigeria; E-mail: nkoyo.nubila@unn.edu.ng
¶Department of Mathematics, University of Nigeria, Nsukka, Nigeria; E-mail: chioma.ejikeme@unn.edu.ng
‖Department of Mathematics, University of Nigeria, Nsukka, Nigeria; E-mail: dennis.agbebaku@unn.edu.ng

exposure. If the infection is not COVID-19, the individual recovers with treatment after a few days of incubation, otherwise he/she becomes infectious and needs to be quarantined to avoid further spread . The quarantined stays under serious surveillance and likely recovers afterwards if a mild infection.

COVID-19 if not confirmed early or managed as soon as confirmed could lead to breakdown in respiration, chronic pneumonia, failure of vital organs and eventual death. The global death rate is 4.4% though Nationality death rate varies [6].

It has been proposed that self isolation and social distancing as preventive measures could cut down on the spread of COVID-19 outbreak [7]. Other necessary measures include; washing of hands with sanitizer, wearing a face mask and keeping the immune system strong with proper diet [8].

In this paper, we employed the mathematical modelling tool in order to ascertain the effectiveness of the preventive measures to curtailing the pandemic.

The threshold quantity known as the effective reproduction number (R_{eff}) was computed [9] and the equilibrium points obtained. The impact of the preventive measures were studied on the short and long run (local and global stability) using the approaches by Castilo- Chavez [10] and Lyapunov method [11].

2 Methodology/Model formulation

We present a flow diagram to illustrate the pattern of dynamism associated with COVID-19. The total population is denoted by $N(t)$ since population is time dependent. Hence

$$N(t) = S_p(t) + S(t) + E(t) + E_T(t) + I(t) + Q(t) + R(t) \tag{1}$$

S is the Susceptible population; S_p the population guarded via self isolation and social distancing; E is the exposed individuals; E_T the exposed but treated individuals; I the infective/infectious individuals; Q the Quarantined individuals and R the Recovered individuals.
$(I-\phi)\Lambda$ is the recruitment rate into the population susceptible to COVID-19; $\phi\Lambda$ is the recruitment rate of individuals prevented /protected /guarded against COVID-19 ; μ is the Natural death/mortality rate; β is the exposure rate of susceptible individuals to COVID-19; α is the rate of treatment of the exposed; $\lambda = 1-\alpha$ is the rate at which the untreated exposed (those that are actual carriers-under incubation period) becomes infectious (tests positive/confirmed cases); η is the rate at which the infectious individuals become quarantined; τ_1 and τ_2 are the rates at which the quarantined and exposed treated recovers respectively; δ_1 is the COVID-19 induced death rate.
All variables and parameters are positive for all time $t > 0$ in the feasible region Ω where $S_p(t)$, $S(t)$, $E(t)$, $E_T(t)$, $I(t)$, $Q(t)$, $R(t) \in \Omega \subset \Re^7_+$
The solution of each equation are bounded in Ω , $\forall\, t > 0$ such that $0 \leq N \leq \frac{(1-\phi)\Lambda}{\mu}$.
It follows that the Model is Epidemiologically and Biologically well posed in the region. Model flow diagram is seen in Figure 1:

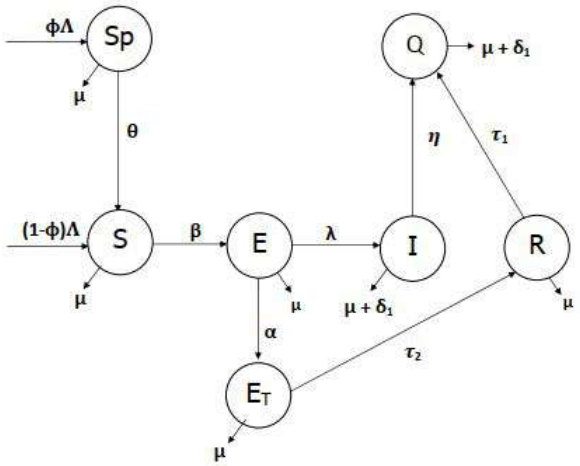


Figure 1

3 Analysis of the model

The Governing equation

$$\begin{aligned}
\frac{dS_p}{dt} &= \phi\Lambda - (\theta+\mu)S_p \\
\frac{dS}{dt} &= (1-\phi)\Lambda + \theta S_p - \beta SE - \mu S \\
\frac{dE}{dt} &= \beta SE - \lambda E - \alpha E - \mu E \\
\frac{dE_T}{dt} &= \alpha E - (\tau_2+\mu)E_T \\
\frac{dI}{dt} &= \lambda E - (\mu+\delta_1+\eta)I \\
\frac{dQ}{dt} &= \eta I - (\tau_1+\mu+\delta_1)Q \\
\frac{dR}{dt} &= \tau_1 Q + \tau_2 E_T - \mu R
\end{aligned} \tag{2}$$

The force of infection is given by

$$\beta E = \frac{\gamma\varepsilon(1-\xi)E}{N} \tag{3}$$

where γ is the probability rate of contracting COVID-19; ε is the infection contact rate; and ξ denotes the chance of success of preventive measures (self isolating and social distancing) against COVID-19; and hence the effective reproductive number (R_{eff})is given as

$$R_{eff} = \frac{\beta S^{\circ}}{(\lambda+\alpha+\mu)} = \frac{\gamma\varepsilon(1-\xi)}{(\lambda+\alpha+\mu)}. \tag{4}$$

Note:

- S° is the COVID-19 free equilibrium point obtained as $\frac{(1-\phi)\Lambda}{\mu} \geq N$.
- R_{eff} is the average number of secondary infection per infectious case in a population made up of both susceptible and non-susceptible (protected/prevented) population [9].

The disease free equilibrium point DFE is given by solving (2).

$$E_\circ = (S_p^\circ, S, E^\circ, E_T^\circ, I^\circ, Q^\circ, R^\circ) = (0, \frac{(1-\phi)\Lambda}{\mu}, 0, 0, 0, 0, 0)$$

where

$$S_p^\circ = E^\circ = E_T^\circ = I^\circ = Q^\circ = R^\circ = 0 \text{ and } S^\circ > 0$$

and the endemic equilibrium point

$$E_* = (S_p^*, S^*, E^*, E_T^*, I^*, Q^*, R^*)$$

where

$$S_p^* \neq 0,\ S^* \neq 0,\ E^* \neq 0,\ E_T^* \neq 0,\ I^* \neq 0,\ Q^* \neq 0,\ R^* \neq 0.$$

$$S_p^* = \frac{\phi\Lambda}{\theta+\mu}\ ;\ S^* = \frac{\lambda+\alpha+\mu}{\beta} = \frac{1}{R_{eff}} > 0 \text{ iff } R_{eff} > 1.$$

Thus less susceptible individuals get exposed.

$$\begin{aligned} E^* &= \frac{(1-\phi)\Lambda + \theta S_p^* - \mu S^*}{\beta S^*} \\ &= \frac{(1-\phi)\Lambda}{(\lambda+\alpha+\mu)} + \frac{\phi\theta\Lambda}{(\lambda+\alpha+\mu)(\theta+\mu)} - \frac{\mu}{\beta} \\ &= \frac{\mu}{\beta}\Big[\frac{(1-\phi)\Lambda(\theta+\mu)+\phi\theta\Lambda}{(\theta+\mu)(\lambda+\alpha+\mu)}.\frac{\beta}{\mu} - 1\Big] \\ &= \frac{\mu}{\beta}\Big[\frac{(1-\phi)\Lambda(\theta+\mu)+\phi\theta\Lambda}{\mu(\theta+\mu)}.R_{eff} - 1\Big] \end{aligned}$$

$$E^* > 0 \text{ provided that } R_{eff} > 1 \text{ and } \frac{\phi\theta\Lambda}{\mu(\theta+\mu)} > \frac{(1-\phi)\Lambda}{\mu} \text{ and } \frac{\mu}{\beta} > 0$$

(since all parameters are positive), this implies that exposure to COVID$-$19 reduces with an increase in preventive measures (self isolation and social distancing).

$$I^* = \frac{\lambda E^*}{\mu+\delta_1+\eta} = \frac{\mu\lambda}{\beta(\mu+\delta_1+\eta)}\Big[\frac{(1-\phi)\Lambda(\theta+\mu)+\phi\theta\Lambda}{\mu(\theta+\mu)}.R_{eff} - 1\Big]$$

$$I^* > 0 \text{ if and only if } R_{eff} > 1 \text{ and } \frac{\phi\theta\Lambda}{\mu(\theta+\mu)} > \frac{(1-\phi)\Lambda}{\mu} \text{ with } \frac{\mu\lambda}{\beta(\mu+\delta_1+\eta)} > 0$$

This suggests that infection from COVID$-$19 decreases due to a decrease in exposure level resulting from increased preventive measures.

$$E_T^* = \frac{\alpha E^*}{\tau_2+\mu}\ ;\ Q^* = \frac{\eta I^*}{\tau_1+\mu+\delta_1}\ ;\ R^* = \frac{\tau_1 Q^* + \tau_2 E_T^*}{\mu}$$

3.1 Local stability of DFE and Endemic equilibrium points

Theorem 3.1. *The COVID−19 free and endemic equilibrium points are locally asymptotically stable (LAS), if* $R_{eff} < 1$ *and* $\det(J) > 0,\ Tr(J) < 0$.

Proof:
We obtain Jacobian of (2) evaluated at DFE and EEP and check if $\det(J) > 0$, and $Tr(J) < 0$

$$|J - \lambda I| = \begin{bmatrix} A & 0 & 0 & 0 & 0 & 0 & 0 \\ \theta & B & -\beta S & 0 & 0 & 0 & 0 \\ 0 & \beta E & C & 0 & 0 & 0 & 0 \\ 0 & 0 & \alpha & D & 0 & 0 & 0 \\ 0 & 0 & \lambda & 0 & F & 0 & 0 \\ 0 & 0 & 0 & 0 & 0 & G & 0 \\ 0 & 0 & 0 & \tau_2 & 0 & \tau_1 & -\mu - \lambda \end{bmatrix}$$

where $A = -(\theta + \mu) - \lambda$, $B = -(\beta E + \mu) - \lambda$, $C\beta S - (\lambda + \alpha + \mu) - \lambda\ D = -(\tau_2 + \mu) - \lambda$, $F = -(\mu + \delta_1 + \eta) - \lambda$, $G = \eta - (\tau_1 + \mu + \delta_1) - \lambda$.

$$\lambda_1 = -(\theta + \mu)\ ;\ \lambda_2 = -\mu\ ;\ \lambda_3 = -(\tau_1 + \mu + \delta_1)\ ;\ \lambda_4 = -(\mu + \delta_1 + \eta)\ ;\ \lambda_5 = -(\tau_2 + \mu)$$

The Jacobian reduces to

$$\begin{pmatrix} -(\beta E + \mu) - \lambda_6 & -\beta S \\ \beta E & \beta S - (\lambda + \alpha + \mu) - \lambda_7 \end{pmatrix}$$

Let $a = \beta E + \mu\ ;\ b = \beta S\ ;\ c = \beta E\ \ d = \lambda + \alpha + \mu = \frac{\beta}{R_{eff}}$

$$\begin{aligned} &\Rightarrow \quad (-a - \lambda)(b - d - \lambda) + bc = 0 \\ &\Rightarrow \quad \lambda^2 + \lambda(a + d - b) + ad + bc - ab = 0. \end{aligned}$$

If $a+d > b$ then $a+d-b > 0$; also if $ad+bc > ab$, then, $ad+bc-ab > 0$. Hence by Routh-Hurwitz Criterion $\lambda_6, \lambda_7 < 0$. Since $\lambda_i's,\ i = 1, 2, ...7$, are < 0 if $R_{eff} < 1$, and clearly $\det(J) > 0$ and $Tr(J) > 0$ then DFE and EEP are Locally asymptotically stable (LAS)

3.2 Global stability of Disease free equilibrium

Lemma 3.2. *Consider a Model System written in the form*

$$\begin{aligned} \frac{dz_1}{dt} &= F(z_1, z_2) \\ \frac{dz_2}{dt} &= G(z_1, z_2),\ \ G(z_1, 0) \end{aligned}$$

where $z_1 \in \Re^m$ *and* $z_2 \in \Re^n$ *and* $z_0 = (z_1, 0)$ *is an equilibrium point of the system. Assume that*
$(H1)$: *for* $\frac{dz_1}{dt} = F(z_1, 0),\ z_1^*$ *is GAS*
$(H2) : G(z_1, z_2) = Az_2 - \hat{G}(z_1, z_2),\ \ G(z_1, z_2) \geq 0$ *For* $z_1,\ z_2 \in \Omega$, *where the Jacobian* $A = \frac{\partial G}{\partial z_2}(z_1, 0)$ *is an* $M - matrix$ *(the off diagonal elements of A are non-negative) the model makes biological sense. Hence* z_0 *is GAS provided* $R_{eff} < 1$

We need to show that both $(H1)$ and $(H2)$ hold for $R_{eff} < 1$.
Let $z_1 = (S_p, S, E_T, Q, R)\ ,\ z_2 = (E, I)$ and $z_1^* = (S_p^\circ, S^\circ, E_T^\circ, Q^\circ, R^\circ)$. $G(z_1, z_2)$ is given by

$$G(z_1, z_2) = \begin{pmatrix} \beta SE & -(\lambda + \alpha + \mu)E \\ \lambda E & -(\mu + \delta_1 + \eta)I \end{pmatrix}$$

This can be rewritten as $Az_2 - \hat{G}(z_1, z_2)$

$$A = \begin{pmatrix} \beta S^{\circ} - (\lambda + \alpha + \mu) & 0 \\ \lambda & -(\mu + \delta_1 + \eta) \end{pmatrix}$$

$\hat{G} = (z_1, z_2) = \beta E(S^{\circ} - S)$ then $\hat{G}(z_1, z_2) = \beta E S^{\circ} > 0$ it is obvious that $S^{\circ} > S$, $AZ = 0$, hence $G(z_1, z_2) = -\beta E S^{\circ} = -\gamma\varepsilon\frac{(1-\xi)}{N} E.S^{\circ}$.
Since $G(z_1, z_2) < 0$, it follows that condition $(H2)$ fails.
The DFE, E_0 is not globally asymptotically stable, this implies a continuous outbreak is imminent if condition that gives rise to it are not properly handled. This encourages compulsory enlightenment on self isolation and social distancing.

3.3 Global Stability of the Endermic Equilibrium

We seek this by means of Lyapunov direct method and Lasalle's invariant principle.
We assume the non-linear Lyapunov function

$$L : \{(S_p, S, E, E_T, I, Q, R) \in \Omega \subset \Re_+^7 : S_p(t), S(t), E(t), E_T(t), I(t), Q(t), R(t) > 0\}$$

Then

$$\begin{aligned} L : (S_p, S, E, E_T, I, Q, R) &= \beta(S - S^* - S^* \log \frac{S}{S^*}) + \beta(S_p - S_p^* - S_p^* \log \frac{S_p}{S_p^*}) \\ &\quad +\beta(E - E^* - E^* \log \frac{E}{E^*}) \\ &\quad +\beta(E_T - E_T^* - E_T^* \log \frac{E_T}{E_T^*}) \\ &\quad +\beta(I - I^* - I^* \log \frac{I}{I^*}) \\ &\quad +\beta(Q - Q^* - Q^* \log \frac{Q}{Q^*}) \\ &\quad +\beta(R - R^* - R^* \log \frac{R}{R^*}), \end{aligned}$$

where L is C' in the region of Ω, L on Ω has a global minimum E_* and $L : (S_p, S, E, E_T, I, Q, R) = 0$.
Thus

$$\begin{aligned} \frac{dL}{dt} = \dot{L} &= \beta(1 - \frac{S^*}{S})\frac{dS}{dt} + \beta(1 - \frac{S_p^*}{S_p})\frac{dS_p}{dt} + \beta(1 - \frac{E^*}{E})\frac{dE}{dt} + \beta(1 - \frac{E_T^*}{E_T})\frac{dE_T}{dt} \\ &+ \beta(1 - \frac{I^*}{I})\frac{dI}{dt} + \beta(1 - \frac{Q^*}{Q})\frac{dQ}{dt} + \beta(1 - \frac{R^*}{R})\frac{dR}{dt} \\ &= \beta(\frac{S - S^*}{S})\frac{dS}{dt} + \beta(\frac{S_p - S_p^*}{S_p})\frac{dS_p}{dt} + \beta(\frac{E - E^*}{E})\frac{dE}{dt} + \beta(\frac{E_T - E_T^*}{E_T})\frac{dE_T}{dt} \\ &+ \beta(\frac{I - I^*}{I})\frac{dI}{dt} + \beta(\frac{Q - Q^*}{Q})\frac{dQ}{dt} + \beta(\frac{R - R^*}{R})\frac{dR}{dt}. \end{aligned}$$

Clearly, we see that $\dot{L} = 0$ provided $S = S^*,\ S_p = S_p^*,\ E = E^*,\ E_T = E_T^*, I = I^*,\ Q = Q^*$ and $R = R^*$.
Hence E_* is globally asymptotically stable within the region Ω. We have succeeded in showing Mathematically that in the long run that active and constant preventive approach yields expected results as regards outbreak intervention with special reference to COVID-19 being considered.

4 Discussions and conclusion

The Mathematical analysis shows that the DFE, E_0 is not globally asymptotically stable meaning the spread continues unless there be an enforcement of self isolation and social distancing across the infected regions and even uninfected, as these reduces the exacerbation of COVID−19 spread.

The spread of COVID−19 can be effectively and efficiently controlled over a given population with time, if the individuals take responsibility through preventive measures (self isolation and social distancing for the carriers and non-carriers) as encouraged.

Exposure to spread decreases with a suitable increase in preventive/protective measures resulting in subsequent lowering in number of new cases/infection.

Acknowledgment

This research is sponsored by TETFUND Nigeria under the IBR funding with
project number:TETFUND/DR&D/CE/UNI/NSUKKA/RP/VOL.I

References

[1] World Health Organization (WHO) https://www.who.int/europe/emergencies/situations/covid-19 last accessed 27/9/2024

[2] John Hopkins COVID−19 Resource Center, John Hopkins University of Medicine, https://github.com/CSSEGISandData/COVID-19/tree/master/csse_covid_19_data last accessed 27/9/2024.

[3] John Hopkins University (JHU) HUB, https://hub.jhu.edu/search/?q=coronavirus, last accessed 27/9/2024

[4] Adhikari, S. P., Meng, S., Wu, Y. J., Mao, Y. P., Ye, R. X., Wang, Q. Z., & Zhou, H. (2020). Epidemiology, causes, clinical manifestation and diagnosis, prevention and control of coronavirus disease (COVID-19) during the early outbreak period: a scoping review. Infectious diseases of poverty, 9, 1-12.

[5] http: // www.who.int>docs.

[6] https: // doi.org /10.1186/540249.020.00646.

[7] https : // Coronavirus.jhu.edu.

[8] http://www.fda.gov/

[9] Hethcote, H. W. (2000). The mathematics of infectious diseases. SIAM review, 42(4), 599-653.

[10] Castillo-Chavez, C., Feng, Z. and Huang, W. (2002) On the Computation of RO and Its Role on Global Stability. In: Castillo-Chavez, P.C., Blower, S., Driessche, P., Kirschner, D. and Yakubu, A.-A., Eds., Mathematical Approaches for Emerging and Reemerging Infectious Diseases: An Introduction, Springer, Berlin, 229. https://doi.org/10.1007/978-1-4757-3667-0_13

[11] Korobeinikov, A., & Wake, G. C. (2002). Lyapunov functions and global stability for SIR, SIRS, and SIS epidemiological models. Applied Mathematics Letters, 15(8), 955-960.

On the vector Lyapunov functions and eventual stability of nonlinear impulsive differential equations

J.E. Ante[*†], A.B. Inyang[‡], E.J. Oduobuk[†§], and U.P. Akai[**]

Abstract

In this paper, the eventual stability of nonlinear impulsive differential equations with fixed moments of impulse is examined using the vector Lyapunov functions which is generalized by a class of piecewise continuous functions. The novelty in the use of the vector form of the Lypunov function lies in the fact that the "restrictions" encountered via the use of scalar Lyapunov function is safely handled especially for large scale dynamical systems, since it involves splitting the Lyapunov functions into components so that each of the components can easily describe the behaviour of the solution state Together with comparison results, sufficient conditions for eventual stability are presented. Results obtained are extensions and improvements on existing results.

Keywords and phrases: eventual stability; impulsive differential equation; vector Lyapunov functions.

1 Introduction

One of the main properties of interest in the qualitative theory of differential equations is the stability of solutions. Stability enables us to compare the behaviour of solutions starting at different points [1].

Now, the stability of solutions of differential equations via Lyapunov method has been intensively investigated in the past, and in many real cases, it is obligatory to study the stability of such sets, which are invariant with respect to a given system of differential equation. This immediately excludes the stability in the sense of Lyapunov [23]. To allay the problem that will arise subsequently, [14] introduced a new concept called eventual stability, maintaining that, the set under consideration, despite not being invariant in the usual sense, is invariant in the asymptotic sense (See also [25]).

[*]Corresponding Author; E-mail: jackson.ante@topfaith.edu.ng
[†]Department of Mathematics, Topfaith University, Mkpatak, Nigeria.
[‡]Department of Business Administration, Topfaith University, Mkpatak, Nigeria E-mail: ab.inyang@topfaith.edu.ng
[§]Department of Physics, Topfaith University, Mkpatak, Nigeria.E-mail: ej.oduobuk@topfaith.edu.ng
[**]Department of Mathematics, Topfaith University, Mkpatak, Nigeria E-mail: up.akai@topfaith.edu.ng

The theory of impulsive differential equation (IDE) is richer than the corresponding theory of differential equations [11], as they constitute very important models for describing the true state of several real life processes and phenomena.

Of course, many evolution processes are characterized by the fact that at certain moments of time they undergo a change of state abruptly. These processes are subject to short term perturbations whose duration is negligible in comparison with the duration of the process. Consequently, it is natural to assume that these perturbations act instantaneously, that is, in the form of impulses. It is known, for example, that many biological phenomena involving thresholds, bursting rhythm models in medicine and biology, optimal control models in economics, pharmacokinetics and frequency modulated systems, do exhibit impulsive effects [11].

Now, the efficient applications of impulsive differential system require the finding of criteria for stability of their solutions [21], and one of the most versatile methods in the study of the stability properties of impulsive systems is the method of Lyapunov functions.

There are several approaches in the literature in the study of the stability of solutions, one of which is the Lyapunov's second method. The novelty of the method over other methods of examining stability properties like the Razumikhin technique, the use of matrix inequality, variational method, Banach fixed point theory, monotone iteration method, etc. stems from the fact that the method allows us to examine the stability of solutions without first solving the given differential system. It involves seeking an appropriate continuous Lyapunov function that is positive definite and whose time derivative along the solution path is negative semidefinite. The stability of the trivial solution of impulsive differential equations has been extensively studied in [3, 6, 20].

In this paper, eventual stability of the system of nonlinear impulsive differential equation is examined. By employing the vector Lyapunov functions, generalized by a class of piecewise continuous Lyapunov functions together with the comparison results, sufficient conditions for the eventual stability of the solution is established with illustrative example.

2 Preliminaries, Notations and Definitions

Let R^n be the n-dimensional Euclidean space with norm $\|.\|$. Let Ω be a domain in R^n containing the origin; $R_+ = [0,\infty)$, $R = (-\infty,\infty)$, $t_0 \in R_+$, $t > 0$.

Let $J \subset R_+$. Define the following class of functions is a piecewise continuous function with points of discontinuity $t_k \in J$ at which $\alpha(t)$ exists.

Consider the impulsive differential system

$$\begin{aligned} x' &= f(t,x), t \neq t_k,\ t \geq t_0 \\ \Delta x &= I_k(x),\ t = t_k, k \in N \\ x(t_0^+) &= x_0 \end{aligned} \tag{2.1}$$

under the following assumptions:

A_0 (i) $0 < t_1 < t_2 < ... < t_k < ...,$ and $t_k \to \infty$ $k \to \infty$;

(ii) $f : R_+ \times R^n \to R^n$ is continuous in $(t_{k-1,}\ t_k] \times R^N$ and for each $x \in R^n$, $k = 1,2,...,$

$$\lim_{(t,y)\to(t_k^+,x)} f(t,y) = f(t_k^+, x) \text{ exists;}$$

(iii) $I_k : R^n \to R^n$

In this paper, we assume that the function f is Lipschitz continuous with respect to its second argument, and $f(t,0) \equiv 0, I_k(0) \equiv 0$ for all k, so that we have the trivial solution for (2.1), and the points $t_k, k = 1,2,...$ are fixed such that $0 < t_1 < t_2 < ... and \lim_{k\to\infty} t_k = \infty.$ The system (2.1) with initial condition $x(t_0) = x_0$ is assumed to have a solution $x(t;t_0,x_0) \in PC([t_0,\infty), R^N).$ Note that some sufficient conditions for the existence and uniqueness of the global solutions to (2.1) are considered in [9, 15-16, 18, 26].

Remark 2.1.

The second equation in (2.1) is called the impulsive condition, and the function $I_k(x(t_k))$ gives the amount of jump of the solution at the point t_k.

Let $V : R_+ \times R^N, R_+^N$. Then V is said to belong to class L if,

(i) V is continuous in $(t_{k-1,}\ t_k] \times R^N$ and for each $x \in R^N$, $k = 1,2,...,$ and $\lim_{(t,y)\to(t_k^+,x)} V(t,y) = V(t_k^+, x)$ exists;

(ii) V is locally Lipschitz with respect to its second argument x. For $(t_{k-1,}\ t_k] \times R^N$, we define the upper right Dini derivative of V with respect to (2.1) as,

$$D^+V(t,x) = \limsup_{h\to 0^+} \tfrac{1}{h}[V(t+h, x+hf(t,x)) - V(t,x)] \qquad (2.2)$$

Note that in (2.1), $D^+V(t,x)$ is a functional whereas V is a function.

Definition 2.1.

A function $g(t,u)$ is said to be quasimonotone nondecreasing in u, if $u \le v$ and $u_i = v_i$ for $1 \le i \le N$ implies $g_i(t,u) \le g_i(t,v)$ for all i.

Definition 2.2.

The set $x(t)$ of the trivial solution $x=0$ of (2.1) is said to be

(ES$_1$) eventually stable if for every $\varepsilon>0$ *and* $t_0 \in R_+$ there exist $\delta=\delta(\varepsilon,t_0)>0$ such that for any $x_0 \in R^n$ the inequality $\|x_0\|<\delta$ implies $\|x(t,t_0,x_0)\|<\varepsilon$ *for* $t \geq t_0$;

(ES$_2$) uniformly eventually stable if for every $\in>0$ *and* $t_0 \in R_+$ there exist $\delta=\delta(\in)>0$ such that for any $x_0 \in R^n$, the inequality $\|x_0\|<\delta$ implies $\|x(t,t_0,x_0)\|<\varepsilon$ *for* $t \geq t_0$;

(ES$_3$) asymptotically eventually stable if it is stable and if for each $\varepsilon>0$ *and* $t_0 \in R_+$ there exist positive numbers $\delta_0=\delta_0(t_0)>0$ and $T=T(t_0,\varepsilon)$ such that for $t \geq t_0+T$ and $\|x_0\| \leq \delta$ we have $\|x(t,t_0,x_0)\|<\varepsilon$.

(ES$_4$) uniformly asymptotically eventually stable if it is uniformly stable and $\delta_0=\delta_0(\in)$ and $T=T(\varepsilon)$ such that for $t \geq t_0+T$, the inequality $\|x_0\| \leq \delta$ implies $\|x(t,t_0,x_0)\|<\varepsilon$.

Definition 2.3.

A function $a(r)$ is said to belong to the class K if $a \in C[[0,\rho),R_+], a(0)=0,$ *and* $a(r)$ is strictly monotone increasing in r.

In this paper, we define the following sets:

$$\bar{S}_\psi = \{x \in R^N : \|x\| \leq \psi\}$$

$$S_\psi = \{x \in R^N : \|x\| < \psi\}$$

Remark 2.2.

The inequalities between vectors are understood to be component-wise inequalities.

Definition 2.4.

A function $b(r)$ is said to belong to a class L if $b \in C[J,R_+], b(t)$ is monotone decreasing in t *and* $b(t) \to 0$ *as* $t \to \infty$.

Definition 2.5.

A function $a(t,r)$ is said to belong to the class KK if $a \in C[[0,\rho),R_+]$, $a \in K$ for each $t \in J$, and a is monotone increasing in t for each $r>0$ and $a(t,r) \to \infty$ *as* $t \to \infty$ for each $r>0$.

Definition 2.6.

A function $V(t,x)$ with $V(t,0)=0$ is said to be positive definite if there exists a function $a \in K$ such that the relation $V(t,x) \geq a(\|x\|)$ is satisfied for $(t,x) \in J \times S_\rho$.

Definition 2.7.

A function $V(t,x)$ with $V(t,0)=0$ is said to be negative definite if there exists a function $a \in K$ such that the relation $V(t,x) \leq -a(\|x\|)$ is satisfied for $(t,x) \in J \times S_\rho$.

Definition 2.8.

A function $V(t,x) \geq 0$ is said to be decrescent if there exists a function $a \in K$ such that the relation $V(t,x) \leq a(\|x\|)$ is satisfied for $(t,x) \in J \times S_\rho$.

Alongside (2.1), we shall consider a comparison system of the form

$$\begin{aligned} u' &= g(t,u), t \neq t_k,\ t \geq t_0, k = 1,2,... \\ \Delta u &= \psi_k(u(t_k)),\ t = t_k, \\ u(t_0^+) &= u_0 \end{aligned} \tag{2.3}$$

existing for $t \geq t_0$, where $u \in R^n$, elation $V(t,x) \leq a(\|x\|)$ is satisfied for $(t,x) \in J \times S_\rho$. existing for $t \geq t_0$, $u \in R^n$, $R_+ = [t_0, \infty)$, $g : R_+ \times R_+^n \to R^n$, $g(t,0) \equiv 0$, where g is the continuous mapping of $R_+ \times R_+^n$ into R^n. The function $g \in PC[R_+ \times R_+^n, R^n]$ is such that for any initial data $(t_0, u_0) \in R_+ \times R^n$, the system (2.3) with initial condition $u(t_0) = u_0$ is assumed to have a solution $u(t, t_0, u_0) \in PC([t_0, \infty), R^n)$. Note that some sufficient conditions for the existence of solution of (2.3) has been examined in [9,18, 24, 26].

Lemma 2.2. Assume that the hypotheses $A_0(i), (ii), (iii)$ hold, and that $f(t,0) \equiv 0$ and that $I_k(0) \equiv 0$. Then the interval J can be extended to the maximal interval of existence $[t_0, \infty)$.

Proof. Since the conditions $A_0(i), (ii), (iii)$ hold, and that $f(t,0) \equiv 0$ and that $I_k(0) \equiv 0$, then from the existence theorem for the equation $x' = f(t, x(t))$ [18] with impulses, it follows that the solution $x(t) = x(t, t_0, x_0)$ of the IVP (2.1) is defined on each of the intervals $(t_{k-1}, t_k]$, $k = 1,2,...$ Again, since $0 < t_1 < t_2 < ... and \lim_{k \to \infty} t_k = \infty$, then we conclude that the interval J can be continued to $[t_0, \infty)$ for t_0.

3 Main results

In this section we begin by proving the comparison results, then proceed to established the necessary conditions for the eventual stability of the set $x=0$ of the impulsive differential systems with fixed moments of impulse.

Using (2.3), Definition 2.2 can be analogously defined as follows:

Definition 3.1.
The set $u(t)$ of the trivial solution $u=0$ of (2.3) is said to be

(ES_1^*) eventually stable if for every $\varepsilon>0 \; and \; t_0 \in R_+$ there exist $\delta=\delta(\varepsilon,t_0)>0$ such that for any $x_0 \in R^n$ the inequality $\|u_0\|<\delta$ implies $\|u(t,t_0,u_0)\|<\varepsilon \;\; for \; t \geq t_0;$

(ES_2^*) uniformly eventually stable if the δ in (ES_1^*) above is independent of t_0 i.e. for every $\varepsilon>0 \; and \; t_0 \in R_+$ there exist $\delta=\delta(\varepsilon)>0$ such that the inequality $\|u_0\|<\delta$ implies $\|u(t,t_0,u_0)\|<\varepsilon \;\; for \; t \geq t_0;$

(ES_3^*) equiasymptotically eventually stable if ES_1^* is satisfied and given $\varepsilon>0 \; and \; t_0 \in R_+$ there exist positive numbers $\delta_0=\delta_0(t_0)>0$ and $T=T(t_0,\varepsilon)>0$ such that for $t \geq t_0+T$ and $\|u_0\| \leq \delta$ we have $\|u(t,t_0,u_0)\|<\varepsilon, \; t \geq t_0+T.$

(ES_4^*) uniformly asymptotically eventually stable if (ES_2^*) is satisfied and (ES_3^*) is independent of t_0.

THEOREM 3.1. (Comparison results) Assume that:

(i) $g \in C[J \times R_+^n, R^n], \; g(t,0) \equiv 0, \; and \; g(t,u)$ is quasimonotone nondecreasing in u for each $u \in R^n$ and $\lim\limits_{(t,y)\to(t_k^+,u)} g(t,u)=g(t_k^+,u)$ exists;

(ii) $r(t)=r(t,t_0,u_0) \in PC([t_0,T),R^n)$ is the maximal solution of (2.3) existing for $t \geq t_0$.

(iii) $V \in C[J \times S_\psi, R_+^N], \; V \in L$ such that for $(t,x) \in J \times S_\psi$

$$D^+V(t,x) \leq g(t,V(t,x)), \; t \neq t_k$$

and

$V(t, x + I_k(x(t_k)) \le \rho_k(V(t,x)), t = t_k,\ x \in S_\psi$ and the function $\rho_k : R_+^N \to R_+^N$ is nondecreasing for $k = 1,2,...$

(iv) $x(t) = x(t, t_0, x_0) \in PC([t_0, T], R^N)$ is a solution of (2.1) such that

$$V(t_0, x_0) \le u_0 \tag{3.1}$$

existing for $t \ge t_0$. Then

$$V(t, x(t)) \le r(t) \tag{3.2}$$

Proof.

Let $x(t) = x(t, t_0, x_0)$ be any solution of (2.1) existing for $t \ge t_0$, such that $V(t_0, x_0) \le u_0$.

Set $m(t) = V(t, x(t))$ for $t \ne t_k$ so that for small $h > 0$, using (2.2) we have

$$m(t+h) - m(t) = V(t+h, x(t+h)) - V(t+h, x(t) + hf(t, x(t)) + V(t+h, x(t) + hf(t, x(t)) - V(t, x)$$

Since $V(t, x)$ is locally Lipschitzian in x for $t \in [t_0, \infty)$, we have

$$m(t+h) - m(t) \le k\|x(t+h) - (x(t) + hf(t, x(t)))\| + V(t+h, x(t) + hf(t, x(t)) - V(t, x)$$

Dividing through by $h > 0$, and taking the $\limsup$ as $h \to 0^+$ we have

$$\limsup_{h\to 0^+} \tfrac{1}{h}[m(t+h) - m(t)] \le \limsup_{h\to 0^+} \tfrac{i}{h}\left[k\|x(t+h) - x(t) - hf(t, x(t)\|e\right] + \limsup_{h\to 0^+} \tfrac{1}{h}[V(t+h, x(t) + hf(t, x(t)) - V(t, x)]$$

where k is the local Lipschitz constant and $e = (1,1,...,1)^T$

It follows that

$$D^+ m(t) = D^+ V(t, x(t)) \le g(t, m(t))$$

and using condition (ii) of Theorem 3.1 we arrive at

$$V(t, x(t)) \le r(t)$$

provided

$$V(t_0, x_0) \le u_0$$

Also,

$$m(t_k^+) = V(t_k^+, x(t_k) + I_k(x(t_k^+)) \leq \psi_k(m(t_k^+))$$

Hence, by Cor. 1.7.1 in [13], we obtain the desired estimate of (3.1).

Corollary 3.2. Assume that:

(i) $g \in C[J \times R_+^n, R^n]$, $g(t,0) \equiv 0$, *and* $g(t,u)$ is quasimonotone nondecreasing in u for each $u \in R^n$ and $\lim_{(t,y)\to(t_k^+,u)} g(t,u) = g(t_k^+,u)$ exists;

(ii) $p(t) = p(t,t_0,u_0) \in PC([t_0,T),R^n)$ is the minimal solution of (2.3) existing for $t \geq t_0$.

(iii) $V \in C[J \times S_\psi, R_+^N]$, $V \in L$ such that for $(t,x) \in J \times S_\psi$

$$D^+V(t,x) \geq g(t,V(t,x)),\ t \neq t_k$$

and

$V(t,x+I_k(x(t_k))) \geq \rho_k(V(t,x)),\ t = t_k,\ x \in S_\psi$ and the function $\rho_k : R_+^N \to R_+^N$ is nondecreasing for $k = 1,2,...$

(iv) $x(t) = x(t,t_0,x_0) \in PC([t_0,T],R^N)$ is a solution of (2.1) such that

$$V(t_0,x_0) \geq u_0 \tag{3.3}$$

existing for $t \geq t_0$. Then

$$V(t,x(t)) \geq p(t) \tag{3.4}$$

Proof.

Let $x(t) = x(t,t_0,x_0)$ be any solution of (2.1) existing for $t \geq t_0$, such that $V(t_0,x_0) \geq u_0$.

Set $m(t) = V(t,x(t))$ for $t \neq t_k$ so that for small $h > 0$, using (2.2) we have

$$m(t+h) - m(t) = V(t+h, x(t+h)) - V(t+h, x(t) + hf(t,x(t))) + V(t+h, x(t) + hf(t,x(t))) - V(t,x)$$

Since $V(t,x)$ is locally Lipschitzian in x for $t \in [t_{0,} \infty)$, we have

$$m(t+h) - m(t) \geq k\|x(t+h) - (x(t) + hf(t,x(t))\| + V(t+h, x(t) + hf(t,x(t)) - V(t,x)$$

Dividing through by $h > 0,$ and taking the $\limsup$ as $h \to 0^+$ we have

$$\limsup_{h\to 0^+} \tfrac{1}{h}[m(t+h) - m(t)] \geq \limsup_{h\to 0^+} \tfrac{i}{h}\left[k\|x(t+h) - x(t) - hf(t,x(t)\|\right]e + \limsup_{h\to 0^+} \tfrac{1}{h}[V(t+h, x(t) + hf(t,x(t)) - V(t,x)]$$

where k is the local Lipschitz constant and $e = (1,1,...,1)^T$

It follows from condition (ii) of Cor 3.2 we arrive atat the estimate

$$D^+ m(t) = D^+ V(t,x(t)) \geq g(t,m(t)), t \neq t_k,\ m(t_0^+) \geq u_0 \tag{3.5}$$

Also,

$$m(t_k^+) = V(t_k^+, x(t_k) + I_k(x(t_k^+)) \geq \psi_k(m(t_k^+)) \tag{3.6}$$

Hence, by Cor. 1.7.1 in [13], we obtain the desired estimate of (3.5).

In what follows, we shall obtain sufficient conditions for the eventual stability of the system (2.3).

THEOREM 3.2. Assume that:

(i) $g \in C[J \times R_+^n, R^n],\ g(t,0) \equiv 0,\ and\ g(t,u)$ is quasimonotone nondecreasing in u for fixed $t \in J.$

(ii) $V \in C[J \times S_\rho, R_+^n],\ V(t,x)$ is locally Lipschitzian in x and $\sum_{i=1}^{N} V(t,x) \to 0\ as\ \|x\| \to 0$ for each t and $(t,x) \in J \times S_\rho,$

$$D^+ V(t,x) \leq g(t, V(t,x)) \tag{3.7}$$

(iii) $for\ (t,x) \in J \times S_\rho,$

$$b(\|x\|) \leq \sum_{i=1}^{N} V_i(t,x) \leq a(t, \|x\|) \tag{3.8}$$

where $b \in K, a(t,.) \in K$ whence $a \in C[J \times S_\rho, R_+]$

Then the eventual stability of the set of trivial solution $u = 0$ of the system (2.3) implies the eventual stability of the set of trivial solution $x = 0$ of the system (2.1).

Proof.

Let $0 < \varepsilon < \rho$ and $t_0 \in R_+$ be given.

Assume that the solution (2.3) is eventually stable. Then given $b(\varepsilon) > 0$ and $t_0 \in R_+$, there exists a positive function $\delta = \delta(t_o, \varepsilon) > 0$ which is continuous in t_0 for each $\in$ such that

$$\sum_{i=1}^{N} u_{i0} \leq \delta \text{ implies } \sum_{i=1}^{N} u_i(t, t_0, u_0) < b(\in), t \geq t_0 \tag{3.9}$$

Since $V(t,x)$ is continuous and mildly unbounded i.e. $V(t,0) \to 0 \; as \; \|x\| \to 0,$ then by the property of continuity, given $\varepsilon > 0$ there exists a positive function $\delta_1 = \delta_1(t_o, \varepsilon) > 0$ that is continuous in t_o for each $\in$ such that the inequalities

$$\|x_0\| < \delta_1 \;\; and \;\; V(t_0, x_0) < \delta \tag{3.10}$$

are satisfied simultaneously.

We claim that if $\|x_0\| < \delta_1$ then $\|x(t, t_0, x_0)\| <\in$ by the stability of $x(t)$.

Now suppose this claim is false, the there would exists a point $t_1 \in [t_0, t)$ and the solution $x(t, t_0, x_0)$ with $\|x_0\| < \delta_1$ such that

$$\|x(t_1)\| = \varepsilon \;\; and \;\; \|x(t)\| < \varepsilon \text{ for } t \in [t_0, t_1) \tag{3.11}$$

So that using equation (3.11); (3.8) reduces to the form

$$b(\|x(t_1)\|) \leq \sum_{i=1}^{N} V_i(t_1, x(t_1)), \text{ implying}$$

$$b(\varepsilon) \leq \sum_{i=1}^{N} V_i(t_1, x(t_1)) \tag{3.12}$$

This implies that $x(t) \in S_\psi$ for $t \in [t_0, t_1)$ and from Theorem 3.1,

$$V(t,x(t)) \le r(t,t_0,u_0), \tag{3.13}$$

where $r(t,t_0,u_0)$ is the maximal solution of (2.3).

Then using (3.8), (3.11), (3.12) and (3.13) we arrive at the estimate

$$b(\varepsilon) \le V_0(t_1,x(t_1)) \le \sum_{i=1}^{N} r_i(t,t_0,u_0) < b(\varepsilon)$$

which leads to a contradiction.

Hence, the eventual stability of the set of trivial solution $u=0$ of (2.3) implies the eventual stability of the set of trivial solution $x=0$ of (2.1).

4 Application

Consider the system of fractional differential equations

$$\begin{aligned} x_1'(t) &= -6x_1 + x_2\cos x_1 + x_1\sin x_2 + x_2\tan x_1,\ t \ne t_k \\ x_2'(t) &= 3x_1 - 2x_2\sin x_1 + x_2\sec x_1 + x_1\cos x_2,\ \ t \ne t_k \\ \Delta x_1 &= c_k(x(t_k)), t = t_k \\ \Delta x_2 &= d_k(x(t_k)),\ t = t_k,\ k = 1,2,... \end{aligned} \tag{4.1}$$

for $t \ge t_0,$ with initial conditions

$$x_1(t_0^+) = \gamma_{10}\ and\, x_2(t_0^+) = \gamma_{20}$$

where $x_1, x_2 \in R^N$ are arbitrary functions.

Equation (4.1) is equivalent to (2.3) and $f = (f_1 f_2),$ where $f_1(t,x_1) = -6x_1 + x_2\cos x_1 + x_1\sin x_2 + x_2\tan x$ and $f_2(t,x_2) = 3x_1 - 2x_2\sin x_1 - x_2\sec x_1 - x_1\cos x_2$

Consider a vector Lyapunov function of the form $V = (V_1,V_2)^T,$ where

$V_1(t,x_1,x_2) = |x_1|\ and\ V_2(t,x_1,x_2) = |x_2|$

So that $V = (V_1,V_2)^T$ with $x = (x_1,x_2) \in R^2,$ so t its associated norm defined by $\|x\| = |x_1| + |x_2|.$ Now,

$$\sum_{i=1}^{2} V_i(t,x_1,x_2) = |x_1| + |x_2|$$

So that, the assumption,

$b(\|x\|) \le \sum_{i=1}^{n} V_i(x,y) \le a(t,\|x\|)$ reduces to

$$\sqrt{x_1^{\,2} + x_2^{\,2}} \le x_1^{\,2} + x_2^{\,2} \le 2\left(\sqrt{x_1^{\,2} + x_2^{\,2}}\right)^2$$

with the proviso that $b(r) = r, and\ a(r) = 2r^2$.

Furthermore, we deduce that using equation (3.4) and $V_1(t, x_1, x_2) = |x_1|$

$$D^+V(t,x) = \limsup_{h\to 0^+} \tfrac{1}{h}\{V(t+h, x+hf(t,x) - V(t,x)\}, t \ge t_0$$

$$D^+V_1(t,x_1) = \limsup_{h\to 0^+} \tfrac{1}{h}\{|x_1 + hf_1(t,x_1)| - |x_1|\}$$

$$= \limsup_{h\to 0^+} \tfrac{1}{h}\{hf_1(t,x_1)\}$$

$$\le f_1(t,x_1) \tag{4.2}$$

$$D^+V_1(t,x_1) = -6x_2 - x_2\cos x_1 + x_1\sin x_2 + x_2\tan x_1$$

$$D^+V_1(t,x_1) = x_1(-6+\sin x_2) + x_2(\cos x_1 + \tan x_1)$$

$$= x_1(-6+\sin x_2) + x_2(\cos x_1 + \frac{\sin x_1}{\cos x_1})$$

$$\le |x_1|(-6+|\sin x_2|) + |x_2|(|co)sx_1| + \frac{|\sin x_1|}{|\cos x_1|})$$

$$\le |x_1|(-6+1) + |x_2|(1+\frac{1}{1})$$

$$\therefore D^+V_1(t,x_1) \le -5V_1 + 2V_2 \tag{4.3}$$

Also for $x_0 \in S_\psi,\ for\ t = t_k, k = 1,2,...$ we have

$$V(t, x(t) + c_k) = |c_k + x(t)| \le V(t, x(t))$$

Again for $V_2(t, x_1, x_2) = |x_2|$ and deducing from (4.2)e we have

$$D^+V_2(t,x_1) \le f_2(t,x_2)$$

$$D^+V_2(t,x_2) = 3x_1 - 2x_2\sin x_1 - x_2\sec x_1 - x_1\cos x_2$$

$$= x_1(3-\cos x_2) + x_2(-2\sin x_1 - \sec x_2)$$
$$\leq |x_1|(3-|\cos x_2|) + |x_2|(-2|\sin x_1| - \frac{1}{|\cos x_1|})$$
$$\leq |x_1|(3-1) + |x_2|(-2-1)$$

$$\therefore D^+V_2(t,x_1) \leq 2V_1 - 3V_2 \tag{4.4}$$

Also for $x_0 \in S_\psi$, $for\ t = t_k, k = 1,2,...$ we have

$$V(t, x(t) + d_k) = |d_k + x(t)| \leq V(t, x(t))$$

Combining (4.3) and (4.4) gives

$$D^+V \leq \begin{pmatrix} -5 & 2 \\ 2 & -3 \end{pmatrix} \begin{pmatrix} V_1 \\ V_2 \end{pmatrix} = g(t,V) \tag{4.5}$$

$$u' = g(t,u) = Au$$

where $A = \begin{pmatrix} -5 & 2 \\ 2 & -3 \end{pmatrix}$.

Thus, the vectorial inequality (4.5) and all other conditions of Theorem 3.2 are satisfied since the eigenvalues of A are all negative real parts. Hence, the system (4.1) is eventually stable. Therefore, the set $x(t) = 0$ is eventually stable.

5 Conclusion

This research examined the eventual stability of nonlinear impulsive differential equations using the auxiliary Lyapunov functions which are analogues of vector Lyapunov functions. By splitting the Lyapunov function into components, each of the solution states or the solution vectors can be inserted into each of the components of the Lyapunov function rather than in the whole Lyapunov function. This way, it becomes easier for the Lyapunov function to adequately predicts the behavior of the solution vectors so that the "restrictions and difficulties" imposed on the Lyapunov function which is occasioned by the use of the scalar Lyapunov function is reduced. Together with the comparison results, sufficient conditions for the eventual stability of the impulsive differential systems are presented with an illustrative example.

References

[1] R. Agarwal, D. O'Regan, & S. Hristova, (2015). Stability of Caputo fractional differential equations by Lyapunov functions. Applications of Mathematics, 60, 653-676.

[2] R. Agarwal, S. Hristova and D. O'Regan, (2016). Stability of Solutions of Impulsive Caputo Fractional Differential Equations. Electronic Journal of Differential Equations, Vol. 2016, No. 58, pp. 1-22.

[3] Akpan, E. P. & O. Akinyele, (1992). On the ϕ_0 stability of comparison differential systems. Journal of Mathematical Analysis and applications}, 164(2), 307-324.

[4] L. Arnold, and B. Schmalfuss, (2001). Lyapunov's Second Method for Random Dynamical systems. Journal of differential equations, 177 (1), 235-265.

[5] D. Băleanu, D. & O. G. Mustafa, (2010). On the Global Existence of Solutions to a Class of Fractional Differential Equations. Computers & Mathematics with Applications, 59(5), 1835-1841.

[6] V. J. Devi, F. A. Mc Rae & Z. Drici. (2012). Variational Lyapunov method for Fractional Differential Equations. Computers & Mathematics with Applications, {64(10), 2982-2989.

[7] J. Hale. (1977). Theory of Functional Differential Equations. Springer-Verlag, New York, Heidelberg, Berlin.

[8] D. K. Igobi and M. P. Ineh, (2024). Results on Existence and Uniqueness of Solutions of Dynamic Equation on Time Scale via Generalized Ordinary Differential Equations. International Journal of Applied Mathematics, 37, No. 1, 1-20,

[9] D. K. Igobi and J. E. Ante, (2018). Results on Existence and Uniqueness of Solutions of Impulsive Neutral Integro-Differential System". Journal of Mathematics Research, Vol 10, No. 4. http://doi:10.5539/jmr.v10n4p165.

[10] V. Lakshmikantham, (1974). On the Method of vector Lyapunov Functions. Technical report No. 16.

[11] V. Lakshmikantham, D. D. Bainov and P. S. Simeonov, (1989). The Theory of Impulsive Differential Equations. Series in Modern Applied Mathematics, No. 6, 1989, World Scientific Publishing C. Pte, Ltd.

[12] V. Lakshmikantham and A. S. Vatsala. (2008). Basic Theory of Impulsive Differential Equations. Nonlinear Analysis: Theory, Methods & Applications, 69(8), 2677-2682.

[13] V. Lakshmikantham and S. Leela, Differential and Integral Inequalities, Theory and Application, Vol. 1. Academic Press, Inc. New York and London, 1969.

[14] V. Lakshmikantham, S. Leela and A. S. Martynyuk (1990. Practical Stability Analysis of nonlinear Systems, World Scientific, Singapore, New Jersey, London, Hong Kong.

[15] V. Lakshmikantham, S. Leela and J. V. Devi (2009). Theory of Fractional Dynamic Systems. Cambridge Scientific Publishers.

[16] V. Lakshmikantham and A. S. Vatsala, (2007). General Uniqueness and Monotone Iterative Technique for Fractional Differential Equations," Applied Mathematics Letters 21, 828-834.

[17] V. Lakshmikantham, S. Sivasundaram ((991) On Vector Lyapunov Functions and Stability Analysis of Nonlinear Systems. Springer Science-Business Media Dordrecht.

[18] Z. Lipscey, J. A. Ugboh, I. M. Esuabana and I. O. Isaac, (2020). Existence Theorem for Impulsive Differential Equations with Measurable Right Side for Handling Delay Problems. Hindawi Journal of Mathematics, Vol. 2020, Article ID 7089313, 17 pages.

[19] A. Ludwig, B. Pustal, D. M. Herlach, (2001). General Concept for a Stability Analysis of a Planar Interface under Rapid Solidification Conditions in Multi-Component Alloy Systems. Material Science and Engineering: A, 304, 277-280.

[20] V. D. Milman and A. D. Myshkis, (1960). On Motion Stability with Shocks, Sibirsk. Mat Zh. 1 233-237, [in Russian].

[21] Z. Qunli, (2014). A Class of Vector Lyapunov Functions for Stability Analysis of Nonlinear Impulsive Differential System, Hindawi Publishing Corporation. Mathematical Problems in Engineering, Article ID 649012, 9pages.

[22] S. K. Srivastava, K. Amanpreet, (2009). A New Approach to Stability of Impulsive Differential Equations. Int. Journal of Math. Analysis, Vol. 3, no. 4, 179-185.

[23] I. Stamova, (2011). Eventual Stability and Eventual Boundedness for Impulsive Differential Equations with "Supremum". Mathematical Modelling and Analysis. Vol. 16, No. 2, 304-314.

[24] J. A. Ugboh and I. M. Esuabana, (2018). Existence and Uniqueness Result for a Class of Impulsive Delay Differential Equations. International Journal ofChemistry, Mathematics and Physics, Vol. 2, Issue 4.

[25] T. Yoshizawa, (1966). Stability Theory by Lyapunov's Second Method. The Mathematical Soiety of Japan.

[26] C. Wu, (2020). A General Comparison Principle for Caputo Fractional-Order Ordinary Differential Equations, Fractals, 28(04), 2050070.

Effect of thermal radiation and chemical reaction on unsteady MHD plane – Poiseuille flow of fourth-grade fluid in horizontal parallel plates

K.M. Joseph[*†], E.A. Andi[‡], E.J. Adoyi[†§], C.O. Akusu[†], and C. Onwubuoua[††],**

Abstract

A fourth-grade fluid is an important subclass of differential type that is capable of describing shear thinning and shear thickening effects (examples are ketchup, blood, paint, cream, nail polish, etc.). This sort of model is used to explain the flow behaviour of non-Newtonian fluids which are considered vital and applicable in many industrial production processes such as in the drilling of oil and gas wells, polymer extrusion from dye, glass fibre, paper production and draining of plastics films, etc. There is a dearth of knowledge in this area, therefore, this study investigated the thermal radiation and chemical reaction effects on unsteady magnetohydrodynamics plane – poiseuille flow of fourth-grade fluid in horizontal parallel plates channel. The equations that governed the flow were the momentum equation; which is a coupled nonlinear differential equation, the energy equation and concentration equation. The partial differential equations were solved using He – Laplace method which is a combination of Homotopy perturbation method and Laplace transformation method. The findings of the study revealed that: (i) Velocity and temperature fields rise due to the increment of thermal radiation parameter. (ii) For upsurging data of chemical reaction, velocity and concentration fields diminish. (iii) Velocity profile goes up when third and fourth-grade parameters get to raise; Velocity and skin friction fields decline due to the increment of magnetic parameter. (iv) Increasing Prandtl number tend to diminish the velocity and temperature profiles. (v) Strong values of Schmidt number decrease the boundary layer of the Sherwood number field. The results of this work are applicable to industrial processes such polymer extrusion of dye, draining of plastic films etc.

Keywords and phrases: thermal radiation; chemical reaction; Plane-Poiseuille flow; fourth-grade fluid; He-Laplace Scheme

[*]Corresponding Author; E-mail: kpop.moses@kasu.edu.ng
[†]Department of Mathematical Sciences, Kaduna State University, Kaduna, Nigeria.
[‡]Department of Mathematical Sciences, Nigerian Defence Academy, Kaduna, Nigeria. E-mail: **eaandi@nda.edu.ng**
[§]Department of Physics, Nigeria Defence Academy, Kaduna, Nigeria. E-mail: **jeadoyi@nda.edu.ng**
[**]Department of Physics, Nigerian Defence Academy, Kaduna, Nigeria. E-mail: cakusu@nda.edu.ng
[††]Department of Computer Science/Mathematics, Novena University, Ogume, Nigeria.
E-mail: onwubuoyacletus@novenauniversity.edu.ng

1 Introduction

The study of thermal radiation and chemical reaction is of most realistic significance to engineers and scientists because of its universal incidence in many branches of science and engineering. This phenomenon plays a significant role in chemical industry, power and cooling industry for dying, evaporation, energy transfer in cooling tower and flow in s desert cooler, etc. [1].

Thermal radiation is the process by which energy in the form of electromagnetic radiation, is emitted by a heated surface in all directions and travels directly to its point of absorption at the speed of light. While, Chemical reaction is a process that involves rearrangement of the molecular or ionic structure of a substance, as distinct from a change in physical form or nuclear reaction. There are two types of such reactions namely homogeneous reaction which occurs uniformly throughout a given phase of a flow and heterogeneous reaction which takes place in a particular region or within the boundary of a phase [2]. And Magneto hydrodynamics (MHD) is the study of the magnetic properties and behaviour of electrically conducting fluids. Example of such magneto fluids include plasma, liquid metals, salt water and electrolytes. The fundamental concept of MHD is that magnetic fields can induce currents in a moving conductive fluid, which in turn polarizes the fluid and reciprocally changes the magnetic field itself. And, couette flow is the flow of a viscous fluid in the space between two surfaces, one of which is moving tangentially relative to the other. The configuration often takes the form of two parallel plates.

The fourth-grade fluid flow model is an exceptional model which is being used to explain the flow attitude of non-Newtonian fluids, which are considered vital and applicable in many industrial producing processes such in the drilling of oil and gas wells, polymer extrusion from dye, glass fibre, paper production and draining of plastics films etc.

A vast analysis of non-Newtonian fluids problems has been done by many researches, amongst whom are [3 – 14]. Researchers that considered the effects of thermal radiation and chemical reaction include [15], who investigated the unsteady flow of an electrically conducting incompressible non-Newtonian viscoelastic fluid through a porous medium filled in a vertical porous channel in the presence of transverse magnetic field. The fluid and the channel rotate as a solid body with constant angular velocity about an axis perpendicular to the planes of the plates. The effects of thermal radiation and chemical reaction are taken into account embedded with slip boundary condition. The closed-form analytical solutions are obtained for momentum, energy and concentration equations. The influences of the various parameters entering into the problem in the velocity, temperature and concentration field are discussed with the help of graphs. Also, numerical values of physical quantities, such as skin friction coefficient, Nusselt number and Sherwood number are presented in tabular form. [16], who presented an analytical solution to the problem of plane Poiseuille flow in a channel filled with a porous medium. [17], who analysed heat and mass transfer characteristics of naturally corrective hydro-magnetic flows of fourth grade radiative fluid resulting from vertical porous plate. They considered non-linear order chemical reaction and heat generation with thermal diffusion. The complete fundamental equations were transformed into dimensionless equations by implementing finite difference scheme explicitly.

Others and recent investigations were made by [18], who carried out an analysis for unsteady magnetohydrodynamic (MHD) flow of a generalized third grade fluid between two parallel plates. The fluid flow was as a result of the plate oscillating, moving and pressure gradient. Three flow problems were investigated, namely: Couette, Poiseuille and Couette-Poiseuille flows and a number of nonlinear partial differential equations were obtained which were solved using the He-Laplace method. Expressions for the velocity field, temperature and concentration fields were given for each case and finally, effects of physical parameters on the fluid motion, temperature and concentration were plotted and discussed. They found that an increase in the thermal radiation parameter increases the temperature of the fluid and hence reduces the viscosity of the fluid while the concentration of the fluid reduces as the chemical reaction parameter increases. [19] presented an analysis to explore analytical treatment for the computation of Poiseuille flow of a micropolar fluid in a channel placed in between two horizontal parallel plates. Both the plates were placed at constant wall temperatures. Therefore, the flow region was portioned into two different zones named zone I and zone II. Eringen's micropolar fluid flow phenomena took place by assuming no-slip conditions at the interface. Suitable nondimensional variables were imposed for the transformation of governing equations. Analytical treatment was carried out by employing the in-house symbolic command using the MAPLE software. The behavior of several contributing parameters such as material parameters, the couple stresses for both the zones on the velocity, and microrotation profiles were investigated and presented via graphs. The volume flow rate was also calculated and presented in tabular form. The major outcomes of the results were presented as the higher the Reynolds number, the rate increases significantly. The profile was tiled near the central region with a pick starting from the lower plate region to the central region in zone I and retards from the central region to the upper plate in the zone II, and the profiles of angular momentum seem to be symmetric in nature about the central region that was shown in both the zones. And, [20] investigated the unsteady MHD flow of fourth-grade fluid in horizontal parallel plates channel. The upper plate was oscillating and moving while the bottom plate remained stationary. Solutions for momentum, energy and concentration equation were obtained by the He-Laplace scheme. The effect of various flow parameters controlling the physical situation is discussed with the aid of graphs. Significant results from this study, showed that velocity and temperature fields increase with the increase in thermal radiation parameter, while the velocity and concentric fields decrease with increase in chemical reaction parameter. Furthermore, velocity, temperature and concentric fields decrease with the increase in suction parameter.

However, in the above aforementioned investigations, the effect of thermal radiation and chemical reaction on the unsteady MHD plane – poiseuille flow of fourth-grade fluid in a horizontal parallel plates have not been paid attention. We shall therefore, consider this where both the lower plate and the upper plate are fixed.

2 Methodology/Model formulation

We consider an unsteady flow of an electrically incompressible fourth grade fluid between two parallel plates distance h apart and subjected to a uniform transverse magnetic field B_0. Here, both plates are fixed (stationary) and with constant fluid speed u. The thermally radiative and chemically reactive flow is heading x – direction along infinite porous plate with heat generation.

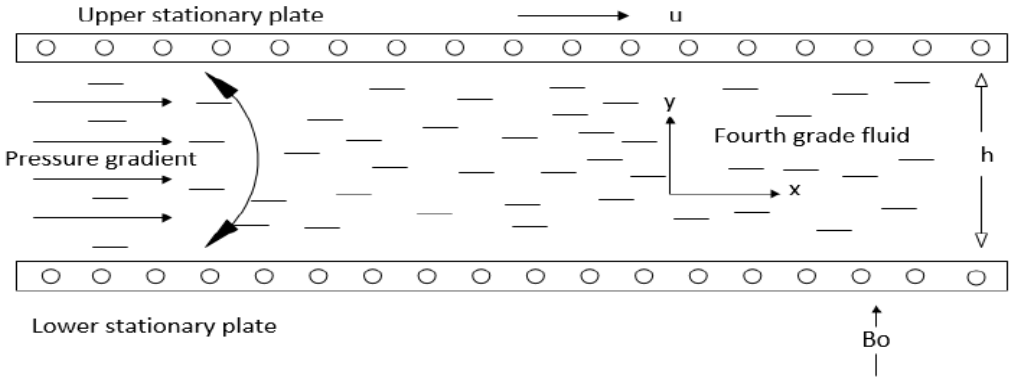


Figure 1: Physical Configuration of the Flow

The state of this fluid is determined by the history of the deformation gradient without a preferred reference configuration. Its constitute equation can be written as

$$T(x,t) = -PI + f_{s=0}^{\infty}\left(F_t^t(s)\right) \tag{2.1}$$

Where PI is the undetermined part of the stress – tensor, F is the deformation gradient and f is the functional.

[21] prescribed different sorts of incompressible fluid category n as viscous fluid agreeing on [22 – 23]. Incompressible fluid of differential type of grade n is the simple fluid obeying the constitutive equation

$$T = -PI + \sum_{j=1}^{n} S_j \tag{2.2}$$

obtained by asymptotic expansion of the functional in equation (2.1) through a retardation parameter α. For $n = 4$ as elucidate by [22], [23] and [17], the first four (4) tensors S_j are given by

$$S_1 = \mu A_1 \tag{2.3}$$

$$S_2 = \alpha_1 A_2 + \alpha_2 A_1^2 \tag{2.4}$$

$$S_3 = \beta_1 A_3 + \beta_2 (A_1 A_2 + A_2 A_1) + \beta_3 (tr A_1^2) A_1 \tag{2.5}$$

$$S_4 = \gamma_1 A_4 + \gamma_2 (A_3 A_1 + A_1 A_3) + \gamma_3 A_2^2 + \gamma_4 (A_2 A_1^2 + A_1^2 A_2) + \gamma_5 (tr A_2) A_2 + \gamma_6 (tr A_2) A_1^2 + [\gamma_7 tr A_3 + \gamma_8 tr(A_2 A_1)] A_1 \tag{2.6}$$

Where, μ is the coefficient of shear viscosity, $\alpha_i (i = 1,2)$, $\beta_i (i = 1,2,3)$ and $\gamma_i (i = 1(1)8)$ are material constants. The A_n are the Rivlin – Ericksen tensors defined by the recursion relation

$$A_n = \frac{d}{dt}A_{n-1} + A_{n-1}L + L^T A_{n-1}, \quad n>1 \tag{2.7}$$

$$A_1 = L + L^T \tag{2.8}$$

where $L = \nabla V$, $\frac{d}{dt}$ is the material time derivative and $V$is the velocity.

The thermally radiative and chemically reactive flow is heading x – direction along infinite porous plate with heat generation. Here, U_0 is the uniform velocity, T_∞ and C_∞ are the fluid temperature and concentration.

Under the above consideration, the equations that described the physical circumstances are

(I) The Momentum equation:

$$\frac{\partial u}{\partial t} = -\frac{\partial p}{\partial x} + \nu\frac{\partial^2 u}{\partial y^2} - \frac{\partial u}{\partial y} + \frac{\alpha_1\nu}{\rho}\frac{\partial^3 u}{\partial y^2\partial t} + \frac{\beta_1\nu^2}{\rho}\frac{\partial^4 u}{\partial y^2\partial t^2} + \frac{6(\beta_2+\beta_3)}{\rho}\left(\frac{\partial u}{\partial y}\right)^2\frac{\partial^2 u}{\partial y^2} + \frac{\gamma_1\nu^3}{\rho}\frac{\partial^5 u}{\partial y^2\partial t^3} + \frac{2\nu(3\gamma_2+\gamma_3+\gamma_4+\gamma_5+\gamma_7+\gamma_8)}{\rho C_p}\left[2\frac{\partial u}{\partial y}\frac{\partial^2 u}{\partial y^2}\frac{\partial^2 u}{\partial t\partial y} + \left(\frac{\partial u}{\partial y}\right)^2\frac{\partial^3 u}{\partial y^2\partial t}\right] - \frac{\sigma B_0^2}{\rho C_p}u + g\beta_T(T-T_\infty) + g\beta_C(C-C_\infty) - \frac{\nu}{k}u \tag{2.9}$$

(II) The Energy equation:

$$\frac{\partial T}{\partial t} = \frac{k}{\rho C_p}\frac{\partial^2 T}{\partial y^2} + \frac{\nu}{k}\left(\frac{\partial u}{\partial y}\right)^2 - \frac{1}{\rho C_p}\frac{\partial q_r}{\partial y} \tag{2.10}$$

And,

(III) The Concentration equation:

$$\frac{\partial C}{\partial t} = D\frac{\partial^2 C}{\partial y^2} - K_c(C-C_\infty) \tag{2.11}$$

Where u is the fluid velocity, T is the temperature, C is the species concentration equationFrom equation (2.10), q_r is the radiative heat flux define as

$$\frac{\partial q_r}{\partial y} = 4\alpha^2(T_w - T_\infty) \tag{2.11i}$$

We note that, when $\gamma_i = 0$, the fourth grade model reduces to the third grade model. When $\beta_i = 0$, the third grade model reduces to second grade model. When $\alpha_i = 0$, $\beta_i = 0$ and $\gamma_i = 0$ then the model reduces to classical Navier – Stoke equation.

The initial and boundary conditions (Idowu and Sani (2019)) are

$$u(y,t) = h + h\cos(\omega y), \theta(y,t) = h + h\cos(\omega y), C(y,t) = h + h\cos(\omega y) \ at\ y > 0, t = 0$$
$$u(y,t) = 1, \theta(y,t) = 1, C(y,t) = 1\ at\ y = 0\ and\ t \geq 0$$
$$u(y,t) \to \infty, \theta(y,t) \to \infty, C(y,t) \to \infty\ as\ y \to \infty\ at\ t > 0 \tag{2.12}$$

Where u is the fluid velocity, T is the temperature and C is the species concentration equation, q_r is the radiative heat flux, ρ is the density of the fluid, C_p is the heat capacity, B_0 is the external magnetic field.

In order to transform equations (2.10) – (2.13), we use the following dimensionless parameters

$$u^* = \frac{u}{U_0},\ p^* = \frac{p}{\mu U_0^2}, t^* = \frac{tU_0^2}{\nu}, G_r = \frac{g\beta_T(T_w - T_\infty)\nu}{U_0^3}, G_c = \frac{g\beta_C(C_w - C_\infty)\nu}{U_0^3}, Ha^2 = \frac{\sigma B_0^2 \nu}{\rho U_0^2}, Da = \frac{KU_0^2}{h^2}, S_c = \frac{D}{\nu}, y^* = \frac{yU_0}{\nu}, x^* = \frac{x}{h}, h = \frac{U_0}{\nu}\ P_r = \frac{kU_0^2}{\nu^2},, \theta = \frac{T - T_0}{T_w - T_\infty}, C^* = \frac{C - C_0}{C_w - C_\infty}, \delta = \frac{4\alpha^2 U_0^2}{\rho c_p \nu}, \alpha = \frac{\alpha_1 U_0^2}{\rho\nu^2}, \beta_a = \frac{\beta_1 U_0^4}{\rho\nu^3}, \beta_b = \frac{(\beta_2 + \beta_3)U_0^4}{\rho\nu^3}, \gamma_a = \frac{\gamma_1 U_0^6}{\rho\nu^3}, \gamma_b = \frac{2(3\gamma_2 + \gamma_3 + \gamma_4 + \gamma_5 + 3\gamma_7 + \gamma_8)U_0^6}{\rho\nu^4}, Da = \frac{kU_0^2}{\nu^2}, K_r = \frac{K_c\nu}{U_0^2} \tag{2.13}$$

Substituting equation (2.13) into equations (2.9) – (2.12) and by dropping the asterisks, we have the following:

$$\frac{\partial u}{\partial t} = -\frac{\partial p}{\partial x} + \frac{\partial^2 u}{\partial y^2} + \alpha\frac{\partial^3 u}{\partial y^2 \partial t} + \beta_a\frac{\partial^4 u}{\partial y^2 \partial t^2} + \beta_b\left(\frac{\partial u}{\partial y}\right)^2\frac{\partial^2 u}{\partial y^2} + \gamma_a\frac{\partial^5 u}{\partial y^2 \partial t^3} + \gamma_b\left[2\frac{\partial u}{\partial y}\frac{\partial^2 u}{\partial y^2}\frac{\partial^2 u}{\partial t \partial y} + \left(\frac{\partial u}{\partial y}\right)^2\frac{\partial^3 u}{\partial y^2 \partial t}\right] - \left(Ha + \frac{1}{Da}\right)u + G_r\theta + G_c C \tag{2.14}$$

$$\frac{\partial \theta}{\partial t} = \frac{1}{P_r}\frac{\partial^2 \theta}{\partial y^2} + \delta\theta \tag{2.15}$$

$$\frac{\partial C}{\partial t} = \frac{1}{S_c}\frac{\partial^2 C}{\partial y^2} - K_r C \tag{2.16}$$

While, the initial and boundary conditions become

$$\left.\begin{array}{c} u(y,t) = 1 + \cos\omega y, \theta(y,t) = 1 + \cos\omega y, C(y,t) = 1 + \cos\omega y\ at\ t = 0\ for\ 0 \leq y \geq 1 \\ u(y,t) = 1, \theta(y,t) = 1, C(y,t) = 1\ at\ y = 0\ for\ t \geq 0 \\ u(y,t) \to \infty, T(y,t) \to \infty, C(y,t) \to \infty\ as\ y \to \infty\ for\ t > 0 \end{array}\right\} \tag{2.17}$$

3 Analysis of the model

In this section we employ the He – Laplace scheme to solve equations (2.14) to (2.16) subjects to the initial and boundary conditions (2.17).
Since equation (2.16) is a coupled non – linear partial differential equation, we have to solve equations (2.15) and (2.16) first.

Now applying Laplace transform on equation (2.16), we have;

$$L\left\{\frac{\partial C}{\partial t}\right\} = \frac{1}{S_c} L\left\{\frac{\partial^2 C}{\partial y^2}\right\} - L\{K_r C\} \tag{3.1}$$

Applying the initial condition and dividing through by s and rearranging, we obtain;

$$L\{C(y,t)\} = \frac{1+\cos(\omega y)}{s} + \frac{1}{s}\left\{\frac{1}{S_c} L\left\{\frac{\partial^2 C}{\partial y^2}\right\} - L\{K_r C\}\right\} \tag{3.2}$$

Taking the inverse Laplace transform of both sides of equation (3.2), gives;

$$C(y,t) = 1 + \cos(\omega y) + L^{-1}\left[\frac{1}{s}\left\{\frac{1}{S_c} L\left\{\frac{\partial^2 C}{\partial y^2}\right\} - L\{K_r C\}\right\}\right] \tag{3.3}$$

Applying the Homotopy perturbation technique, equation (3.3) yields

$$\sum_{n=0}^{\infty} P^n C_n(y,t) = e^{-y} + P\left[L^{-1}\left\{\frac{1}{s}\left\{\frac{1}{S_c} L\left\{\frac{\partial^2 C}{\partial y^2}\right\} - L\{K_r C\}\right\}\right\}\right] \tag{3.4}$$

Comparing the coefficients of the like powers of $'P'$, the following approximations were obtained;

$$P^0 : C_0(y,t) = 1 + \cos(\omega y) \tag{3.5}$$

$$P^1 : C_1(y,t) = L^{-1}\left[\frac{1}{s}\left\{\frac{1}{S_c} L\left\{\frac{\partial^2 C_0}{\partial y^2}\right\} - L\{K_r C_0\}\right\}\right] = L^{-1}\left\{\frac{1}{S_c}\left(\frac{\omega^2 \cos(\omega y)}{s^2}\right) - K_r\left(\frac{1+\cos(\omega y)}{s^2}\right)\right\} = \left(\frac{-\omega^2}{S_c}\cos(\omega y) - K_r(1+\cos(\omega y))\right) t \tag{3.6}$$

$$P^2 : C_2(y,t) = L^{-1}\left[\frac{1}{s}\left\{\frac{1}{S_c} L\left\{\frac{\partial^2 C_1}{\partial y^2}\right\} - L\{K_r C_1\}\right\}\right] =$$

$$L^{-1}\left[\frac{1}{s}\left\{\frac{1}{S_c} L\left\{\left(\frac{\omega^4}{S_c}\cos(\omega y) + \omega^2 K_r \cos(\omega y)\right) t\right\} + L\left\{K_r\left(\frac{\omega^2}{S_c}\cos(\omega y) +\right.\right.\right.$$

$$K_r^2(1+\cos(\omega y))\,t\Big\}\Big\}\Big] = \Big(\frac{\omega^4}{S_c^2}\cos(\omega y) + \frac{2Se^{-y}}{S_c} - \frac{2K_r\omega^2}{S_c}\cos(wy) + K_r^2\cos(\omega y) + K_r^2\Big)\frac{t^2}{2!} \tag{3.7}$$

$$P^3: C_3(y,t) = L^{-1}\left[\frac{1}{s}\left\{\frac{1}{S_c}L\left\{\frac{\partial^2 C_2}{\partial y^2}\right\} - L\{K_rC_2\}\right\}\right] =$$

$$L^{-1}\left[\frac{1}{s}\left\{L\left\{\Big(\frac{-\omega^6}{S_c^3}\cos(\omega y) - \frac{3K_r\omega^4}{S_c}\cos(\omega y) - \frac{3K_r^2\omega^2}{S_c}\cos(\omega y) - K_r^3\cos(\omega y) - K_r^3\Big)\frac{t^2}{2!}\right\}\right\}\right] = \Big(\frac{-\omega^6}{S_c^3}\cos(\omega y) - \frac{3K_r\omega^4}{S_c}\cos(\omega y) - \frac{3K_r^2\omega^2}{S_c}\cos(\omega y) - K_r^3\cos(\omega y) - K_r^3\Big)\frac{t^3}{3!} \tag{3.8}$$

$$P^4: C_4(y,t) = L^{-1}\left[\frac{1}{s}\left\{\frac{1}{S_c}L\left\{\frac{\partial^2 C_3}{\partial y^2}\right\} - L\{K_rC_3\}\right\}\right] =$$

$$L^{-1}\left[\frac{1}{s}\left\{L\left\{\Big(\frac{\omega^8}{S_c^4}\cos(\omega y) + \frac{4K_r\omega^6}{S_c^3}\cos(\omega y) + \frac{4K_r^2\omega^4}{S_c^2}\cos(\omega y) + \frac{4K_r\omega^2}{S_c}\cos(\omega y) + K_r^4\cos(\omega y) + K_r^4\Big)\frac{t^3}{3!}\right\}\right\}\right] = \Big(\frac{\omega^8}{S_c^4}\cos(\omega y) + \frac{4K_r\omega^6}{S_c^3}\cos(\omega y) + \frac{4K_r^2\omega^4}{S_c^2}\cos(\omega y) + \frac{4K_r\omega^2}{S_c}\cos(\omega y) + K_r^4\cos(\omega y) + K_r^4\Big)\frac{t^4}{4!} \tag{3.9}$$

Therefore, in view of equations (3.5), (3.6), (3.7), (3.8) and (3.9) the solution to equation (2.16) is,

$$C(y,t) = C_0(y,t) + C_1(y,t) + C_2(y,t) + C_3(y,t) + C_4(y,t)\cdots \tag{3.10}$$

$$C(y,t) = 1 + \cos(\omega y) + \Big(\frac{-\omega^2}{S_c}\cos(\omega y) - K_r(1+\cos(\omega y))\Big)t + \Big(\frac{\omega^4}{S_c^2}\cos(\omega y) + \frac{2Se^{-y}}{S_c} - \frac{2K_r\omega^2}{S_c}\cos(wy) + K_r^2\cos(\omega y) + K_r^2\Big)\frac{t^2}{2!} + \Big(\frac{-\omega^6}{S_c^3}\cos(\omega y) - \frac{3K_r\omega^4}{S_c}\cos(\omega y) - \frac{3K_r^2\omega^2}{S_c}\cos(\omega y) - K_r^3\cos(\omega y) - K_r^3\Big)\frac{t^3}{3!} + \Big(\frac{\omega^8}{S_c^4}\cos(\omega y) + \frac{4K_r\omega^6}{S_c^3}\cos(\omega y) + \frac{4K_r^2\omega^4}{S_c^2}\cos(\omega y) + \frac{4K_r\omega^2}{S_c}\cos(\omega y) + K_r^4\cos(\omega y) + K_r^4\Big)\frac{t^4}{4!} + \cdots \tag{3.11}$$

Next, we consider equation (2.15), which is reaaranged to give;

$$\frac{\partial\theta}{\partial t} = \frac{1}{P_r}\frac{\partial^2\theta}{\partial y^2} + \delta\theta \tag{3.11i}$$

Now applying Laplace transform on equation (3.11i).), we get,

$$L\left\{\frac{\partial\theta}{\partial t}\right\} = \frac{1}{P_r}L\left\{\frac{\partial^2\theta}{\partial y^2}\right\} + L\{\delta\theta\} \tag{3.12}$$

Applying the initial condition and dividing through by s and rearranging we obtain;

$$L\{\theta(y,t)\} = \frac{1+\cos(\omega y)}{s} + \frac{1}{s}\left\{\frac{1}{P_r}L\left\{\frac{\partial^2\theta}{\partial y^2}\right\} + L\{\delta\theta\}\right\} \tag{3.13}$$

Taking the inverse Laplace transform of both sides of equation (3.13) gives,

$$\theta(y,t) = 1 + \cos(\omega y) + L^{-1}\left[\frac{1}{s}\left\{\frac{1}{P_r}L\left\{\frac{\partial^2\theta}{\partial y^2}\right\} + +L\{\delta\theta\}\right\}\right] \tag{3.14}$$

Applying the Homotopy perturbation technique on equation (3.14), yields

$$\sum_{n=0}^{\infty} P^n\theta_n(y,t) = e^{-y} + P\left[L^{-1}\left\{\frac{1}{s}\left\{\frac{1}{P_r}L\left\{\frac{\partial^2\theta}{\partial y^2}\right\} + L\{\delta\theta\}\right\}\right\}\right] \tag{3.15}$$

Comparing the coefficients of the like powers of $'P'$in equation (3.14), the following approximations are obtained;

$$P^0: \theta_0(y,t) = 1 + \cos(\omega y) \tag{3.16}$$

$$P^1: \theta_1(y,t) = L^{-1}\left[\frac{1}{s}\left\{\frac{1}{P_r}L\left\{\frac{\partial^2\theta_0}{\partial y^2}\right\} + L\{\delta\theta_0\}\right\}\right] = L^{-1}\left\{\frac{1}{s^2P_r}(-\omega^2\cos(\omega y)) + \frac{\delta}{s^2}(1+\cos(\omega y))\right\} = \left(\frac{-\omega^2}{P_r}\cos(\omega y) + \delta(1+\cos(\omega y))\right)t \tag{3.17}$$

$$P^2: \theta_2(y,t) = L^{-1}\left[\frac{1}{s}\left\{\frac{1}{P_r}L\left\{\frac{\partial^2\theta_1}{\partial y^2}\right\} + L\{\delta\theta_1\}\right\}\right] = L^{-1}\left[\frac{1}{s}\left\{\frac{1}{P_r}L\left\{\left(\frac{\omega^4}{P_r}\cos(\omega y) - \delta\omega^2\cos(\omega y)\right)t\right\} + \delta L\left\{\left(\frac{-\omega^2}{P_r}\cos(\omega y) + \delta(1+\cos(\omega y))\right)t\right\}\right\}\right] = \left(\frac{\omega^4}{P_r}\cos(\omega y) - \frac{2\delta\omega^2}{P_r}\cos(\omega y) + \delta^2\cos(\omega y) + \delta^2\right)\frac{t^2}{2!} \tag{3.18}$$

$$P^3: \theta_3(y,t) = L^{-1}\left[\frac{1}{s}\left\{\frac{1}{P_r}L\left\{\frac{\partial^2\theta_2}{\partial y^2}\right\} + SL\left\{\frac{\partial\theta_2}{\partial y}\right\} + L\{\delta\theta_2\}\right\}\right] = L^{-1}\left[\frac{1}{s}\left\{\frac{1}{P_r}L\left\{\left(\frac{-\omega^6}{P_r^2}\cos(\omega y) + \frac{2\delta\omega^4}{P_r}\cos(\omega y) - \delta^2\omega^2\cos(\omega y)\right)\frac{t^2}{2!}\right\} + \delta L\left\{\left(\frac{\omega^4}{P_r}\cos(\omega y) - \frac{2\delta\omega^4}{P_r}\cos(\omega y) + \delta^2\cos(\omega y) + \delta^2\right)\right\}\frac{t^2}{2!}\right\}\right] = \left(\frac{-\omega^6}{P_r^3}\cos(\omega y) + \frac{3\delta\omega^4}{P_r^2}\cos(\omega y) - \frac{3\delta^2\omega^2}{P_r}\cos(\omega y) + \delta^3\cos(\omega y) + \delta^3\right)\frac{t^3}{3!} \tag{3.19}$$

$$P^4: \theta_4(y,t) = L^{-1}\left[\frac{1}{s}\left\{\frac{1}{P_r}L\left\{\frac{\partial^2\theta_3}{\partial y^2}\right\} + L\{\delta\theta_2\}\right\}\right] = L^{-1}\left[\frac{1}{s}\left\{\frac{1}{P_r}L\left\{\left(\frac{\omega^8}{P_r^3}\cos(\omega y) - \frac{3\delta\omega^4}{P_r^2}\cos(\omega y) + \frac{3\delta^2\omega^4}{P_r^2}\cos(\omega y) - \delta^3\omega^2\cos(\omega y)\right)\frac{t^2}{3!}\right\} + \delta L\left\{\left(\frac{-\omega^6}{P_r^3}\cos(\omega y) + \frac{3\delta\omega^4}{P_r^2}\cos(\omega y) - \frac{3\delta^2\omega^2}{P_r}\cos(\omega y) + \delta^3\cos(\omega y) + \delta^3\right)\right\}\frac{t^2}{3!}\right\}\right] = \left(\frac{\omega^8}{P_r^4}\cos(\omega y) - \frac{4\delta\omega^4}{P_r^3}\cos(\omega y) + \frac{6\delta^2\omega^4}{P_r^2}\cos(\omega y) - \frac{4\delta^2\omega^2}{P_r}\cos(\omega y) - \delta^4\cos(\omega y) + \delta^4\right)\frac{t^4}{4!} \quad (3.20)$$

Therefore, in view of equations (3.16), (3.17), (3.18), (3.19) and (3.20), the solution to (2.15) is,

$$\theta(y,t) = \theta_0(y,t) + \theta_1(y,t) + \theta_2(y,t) + \theta_3(y,t)\cdots$$

$$\theta(y,t) = 1 + \cos(\omega y) + \left(\frac{-\omega^2}{P_r}\cos(\omega y) + \delta(1+\cos(\omega y)\right)t + \left(\frac{\omega^4}{P_r}\cos(\omega y) - \frac{2\delta\omega^2}{P_r}\cos(\omega y) + \delta^2\cos(\omega y) + \delta^2\right)\frac{t^2}{2!} + \left(\frac{-\omega^6}{P_r^3}\cos(\omega y) + \frac{3\delta\omega^4}{P_r^2}\cos(\omega y) - \frac{3\delta^2\omega^2}{P_r}\cos(\omega y) + \delta^3\cos(\omega y) + \delta^3\right)\frac{t^3}{3!} + \left(\frac{\omega^8}{P_r^4}\cos(\omega y) - \frac{4\delta\omega^4}{P_r^3}\cos(\omega y) + \frac{6\delta^2\omega^4}{P_r^2}\cos(\omega y) - \frac{4\delta^2\omega^2}{P_r}\cos(\omega y) - \delta^4\cos(\omega y) + \delta^4\right)\frac{t^4}{4!} + \cdots \quad (3.21)$$

Finally, we now solve equation (2.14), which is rearranged to give

$$\frac{\partial u}{\partial t} = -\frac{\partial p}{\partial x} + \frac{\partial^2 u}{\partial y^2} + \alpha\frac{\partial^3 u}{\partial y^2\partial t} + \beta_a\frac{\partial^4 u}{\partial y^2\partial t^2} + \beta_b\left(\frac{\partial u}{\partial y}\right)^2\frac{\partial^2 u}{\partial y^2} + \gamma_a\frac{\partial^5 u}{\partial y^2\partial t^3} + \gamma_b\left[2\frac{\partial u}{\partial y}\frac{\partial^2 u}{\partial y^2}\frac{\partial^2 u}{\partial t\partial y} + \left(\frac{\partial u}{\partial y}\right)^2\frac{\partial^3 u}{\partial y^2\partial t}\right] - l_2 u + G_r\theta + G_c C \text{ where, } Ha + \frac{1}{Da} = l_2 \quad (3.22)$$

Applying the Laplace transform on both sides of equation (3.22) gives

$$L\left\{\frac{\partial u}{\partial t}\right\} = L\left\{-\frac{\partial p}{\partial x} + \frac{\partial^2 u}{\partial y^2} + \alpha\frac{\partial^3 u}{\partial y^2\partial t} + \beta_a\frac{\partial^4 u}{\partial y^2\partial t^2} + \beta_b\left(\frac{\partial u}{\partial y}\right)^2\frac{\partial^2 u}{\partial y^2} + \gamma_a\frac{\partial^5 u}{\partial y^2\partial t^3} + \gamma_b\left[2\frac{\partial u}{\partial y}\frac{\partial^2 u}{\partial y^2}\frac{\partial^2 u}{\partial t\partial y} + \left(\frac{\partial u}{\partial y}\right)^2\frac{\partial^3 u}{\partial y^2\partial t}\right] - l_2 u + G_r\theta + G_c C\right\} \quad (3.23)$$

$$\text{But, } L\left\{\frac{\partial u}{\partial t}\right\} = sL\{u(y,t)\} - u(y,0) \quad (3.24)$$

Hence,

$$L\{u(y,t)\} = \frac{u(y,0)}{s} + \frac{1}{s}\, L\left\{-\frac{\partial p}{\partial x} + \frac{\partial^2 u}{\partial y^2} + \alpha\frac{\partial^3 u}{\partial y^2 \partial t} + \beta_a \frac{\partial^4 u}{\partial y^2 \partial t^2} + \beta_b \left(\frac{\partial u}{\partial y}\right)^2 \frac{\partial^2 u}{\partial y^2} + \gamma_a \frac{\partial^5 u}{\partial y^2 \partial t^3} + \gamma_b \left[2\frac{\partial u}{\partial y}\frac{\partial^2 u}{\partial y^2}\frac{\partial^2 u}{\partial t \partial y} + \left(\frac{\partial u}{\partial y}\right)^2 \frac{\partial^3 u}{\partial y^2 \partial t}\right] - l_2 u + G_r\theta + G_c C\right\} \quad (3.25)$$

Taking the inverse Laplace transform of both sides of equation (3.25), we have;

$$L^{-1}\{L\{u(y,t)\}\} = L^{-1}\left\{\frac{u(y,0)}{s} - \frac{\partial p}{\partial x} + \frac{1}{s}\, L\left\{\frac{\partial^2 u}{\partial y^2} + \alpha\frac{\partial^3 u}{\partial y^2 \partial t} + \beta_a \frac{\partial^4 u}{\partial y^2 \partial t^2} + \beta_b \left(\frac{\partial u}{\partial y}\right)^2 \frac{\partial^2 u}{\partial y^2} + \gamma_a \frac{\partial^5 u}{\partial y^2 \partial t^3} + \gamma_b \left[2\frac{\partial u}{\partial y}\frac{\partial^2 u}{\partial y^2}\frac{\partial^2 u}{\partial t \partial y} + \left(\frac{\partial u}{\partial y}\right)^2 \frac{\partial^3 u}{\partial y^2 \partial t}\right] - l_2 u + \frac{G_r}{s}\left(1 + \cos(\omega y) + \left(\frac{-\omega^2}{S_c}\cos(\omega y) - K_r(1 + \cos(\omega y))\right)t + \left(\frac{\omega^4}{S_c^2}\cos(\omega y) + \frac{2Se^{-y}}{S_c} - \frac{2K_r\omega^2}{S_c}\cos(wy) + K_r^2\cos(\omega y) + K_r^2\right)\frac{t^2}{2!} + \left(\frac{-\omega^6}{S_c^3}\cos(\omega y) - \frac{3K_r\omega^4}{S_c}\cos(\omega y) - \frac{3K_r^2\omega^2}{S_c}\cos(\omega y) - K_r^3\cos(\omega y) - K_r^3\right)\frac{t^3}{3!} + \left(\frac{\omega^8}{S_c^4}\cos(\omega y) + \frac{4K_r\omega^6}{S_c^3}\cos(\omega y) + \frac{4K_r^2\omega^4}{S_c^2}\cos(\omega y) + \frac{4K_r\omega^2}{S_c}\cos(\omega y) + K_r^4\cos(\omega y) + K_r^4\right)\frac{t^4}{4!}\right) + \frac{G_c}{s}\left(1 + \cos(\omega y) + \left(\frac{-\omega^2}{P_r}\cos(\omega y) + \delta(1 + \cos(\omega y)\right)t + \left(\frac{\omega^4}{P_r}\cos(\omega y) - \frac{2\delta\omega^2}{P_r}\cos(\omega y) + \delta^2\cos(\omega y) + \delta^2\right)\frac{t^2}{2!} + \left(\frac{-\omega^6}{P_r^3}\cos(\omega y) + \frac{3\delta\omega^4}{P_r^2}\cos(\omega y) - \frac{3\delta^2\omega^2}{P_r}\cos(\omega y) + \delta^3\cos(\omega y) + \delta^3\right)\frac{t^3}{3!} + \left(\frac{\omega^8}{P_r^4}\cos(\omega y) - \frac{4\delta\omega^4}{P_r^3}\cos(\omega y) + \frac{6\delta^2\omega^4}{P_r^2}\cos(\omega y) - \frac{4\delta^2\omega^2}{P_r}\cos(\omega y) - \delta^4\cos(\omega y) + \delta^4\right)\frac{t^4}{4!}\right)\right\}\right\} \quad (3.26)$$

or,

$$u(y,t) = 1 + \lambda + \cos(\omega y) + G_c(1 + \cos(\omega y)) + G_r(1 + \cos(\omega y)) + \left(\frac{-\omega^2}{P_r}\cos(\omega y) + \delta(1 + \cos(\omega y) - \frac{\omega^2}{S_c}\cos(\omega y) - K_r(1 + \cos(\omega y))\right)t + \left(\frac{\omega^4}{P_r}\cos(\omega y) - \frac{2\delta\omega^2}{P_r}\cos(\omega y) + \delta^2\cos(\omega y) + \delta^2 + \frac{\omega^4}{S_c^2}\cos(\omega y) + \frac{2Se^{-y}}{S_c} - \frac{2K_r\omega^2}{S_c}\cos(wy) + K_r^2\cos(\omega y) + K_r^2\right)\frac{t^2}{2!} + \left(\frac{-\omega^6}{P_r^3}\cos(\omega y) + \frac{3\delta\omega^4}{P_r^2}\cos(\omega y) - \frac{3\delta^2\omega^2}{P_r}\cos(\omega y) + \delta^3\cos(\omega y) + \delta^3 - \frac{\omega^6}{S_c^3}\cos(\omega y) - \frac{3K_r\omega^4}{S_c}\cos(\omega y) - \frac{3K_r^2\omega^2}{S_c}\cos(\omega y) - K_r^3\cos(\omega y) - K_r^3\right)\frac{t^3}{3!} + \left(\frac{\omega^8}{P_r^4}\cos(\omega y) - \frac{4\delta\omega^4}{P_r^3}\cos(\omega y) + \frac{6\delta^2\omega^4}{P_r^2}\cos(\omega y) - \frac{4\delta^2\omega^2}{P_r}\cos(\omega y) - \delta^4\cos(\omega y) + \delta^4 + \frac{\omega^8}{S_c^4}\cos(\omega y) + \frac{4K_r\omega^6}{S_c^3}\cos(\omega y) + \frac{4K_r^2\omega^4}{S_c^2}\cos(\omega y) + \frac{4K_r\omega^2}{S_c}\cos(\omega y) + K_r^4\cos(\omega y) + K_r^4\right)\frac{t^4}{4!} + L^{-1}\left\{\frac{1}{s}\, L\left\{\frac{\partial^2 u}{\partial y^2} + \alpha\frac{\partial^3 u}{\partial y^2 \partial t} + \beta_a \frac{\partial^4 u}{\partial y^2 \partial t^2} + \beta_b \left(\frac{\partial u}{\partial y}\right)^2 \frac{\partial^2 u}{\partial y^2} + \gamma_a \frac{\partial^5 u}{\partial y^2 \partial t^3} + \gamma_b \left[2\frac{\partial u}{\partial y}\frac{\partial^2 u}{\partial y^2}\frac{\partial^2 u}{\partial t \partial y} + \left(\frac{\partial u}{\partial y}\right)^2 \frac{\partial^3 u}{\partial y^2 \partial t}\right] - l_2 u\right\}\right\} \quad (3.27)$$

Applying the Homotopy perturbation method to equation (3.27), gives

$$\sum_{n=0}^{\infty} P^n u_n(y,t) = 1 + \lambda + \cos(\omega y) + G_c(1 + \cos(\omega y)) + G_r(1 + \cos(\omega y)) + \left(\frac{-\omega^2}{P_r}\cos(\omega y) + \delta(1 + \cos(\omega y) - \frac{\omega^2}{S_c}\cos(\omega y) - K_r(1 + \cos(\omega y))\right) t + \left(\frac{\omega^4}{P_r}\cos(\omega y) - \frac{2\delta\omega^2}{P_r}\cos(\omega y) + \delta^2\cos(\omega y) + \delta^2 + \frac{\omega^4}{S_c^2}\cos(\omega y) + \frac{2Se^{-y}}{S_c} - \frac{2K_r\omega^2}{S_c}\cos(wy) + K_r^2\cos(\omega y) + K_r^2\right)\frac{t^2}{2!} + \left(\frac{-\omega^6}{P_r^3}\cos(\omega y) + \frac{3\delta\omega^4}{P_r^2}\cos(\omega y) - \frac{3\delta^2\omega^2}{P_r}\cos(\omega y) + \delta^3\cos(\omega y) + \delta^3 - \frac{\omega^6}{S_c^3}\cos(\omega y) - \frac{3K_r\omega^4}{S_c}\cos(\omega y) - \frac{3K_r^2\omega^2}{S_c}\cos(\omega y) - K_r^3\cos(\omega y) - K_r^3\right)\frac{t^3}{3!} + \left(\frac{\omega^8}{P_r^4}\cos(\omega y) - \frac{4\delta\omega^4}{P_r^3}\cos(\omega y) + \frac{6\delta^2\omega^4}{P_r^2}\cos(\omega y) - \frac{4\delta^2\omega^2}{P_r}\cos(\omega y) - \delta^4\cos(\omega y) + \delta^4 + \frac{\omega^8}{S_c^4}\cos(\omega y) + \frac{4K_r\omega^6}{S_c^3}\cos(\omega y) + \frac{4K_r^2\omega^4}{S_c^2}\cos(\omega y) + \frac{4K_r\omega^2}{S_c}\cos(\omega y) + K_r^4\cos(\omega y) + K_r^4\right)\frac{t^4}{4!} + P\left(L^{-1}\left\{\frac{1}{s}L\left\{S\frac{\partial u}{\partial y} + \frac{\partial^2 u}{\partial y^2} + \alpha\frac{\partial^3 u}{\partial y^2\partial t} + \beta_a\frac{\partial^4 u}{\partial y^2\partial t^2} + \beta_b H_a(u_n) + \gamma_1\frac{\partial^5 u}{\partial y^2\partial t^3} + \gamma_b\left[2H_b(u_n) + H_c(u_n)\frac{\partial u}{\partial y}\frac{\partial^2 u}{\partial y^2}\frac{\partial^2 u}{\partial t\partial y} + \left(\frac{\partial u}{\partial y}\right)^2\frac{\partial^3 u}{\partial y^2\partial t}\right] - l_2 u\right\}\right\}\right) \tag{3.28}$$

Where, $H_a(u_n), H_b(u_n)$ and $H_c(u_n)$ are the He's polynomials for $\left(\frac{\partial u}{\partial y}\right)^2$, $\frac{\partial u}{\partial y}\frac{\partial^2 u}{\partial y^2}\frac{\partial^2 u}{\partial t\partial y}$ and $\left(\frac{\partial u}{\partial y}\right)^2\frac{\partial^3 u}{\partial y^2\partial t}$ respectively.

The He's polynomials for $\left(\frac{\partial u}{\partial y}\right)^2$ are as follows

$$\begin{cases} H_0(u) = (u_0')^2 \\ H_1(u) = 2u_0'u_1' \\ H_2(u) = 2u_0'u_2' + (u_1')^2 \\ H_3(u) = 2u_1'u_2' \\ \vdots \end{cases} \tag{3.29}$$

The He's polynomials for $\frac{\partial u}{\partial y}\frac{\partial^2 u}{\partial y^2}\frac{\partial^2 u}{\partial t\partial y}$ are as follows

$$\begin{cases} H_0(u) = u_0'''u''_{0t} \\ H_1(u) = u_0'''u''_{1t} + u_1'''u''_{1t} \\ H_2(u) = u_0'''u''_{2t} + u_1'''u''_{1t} + u_2'''u''_{0t} \\ H_3(u) = u_1'''u''_{2t} + u_2'''u''_{1t} \\ \vdots \end{cases} \tag{3.30}$$

The He's polynomials for $\left(\frac{\partial u}{\partial y}\right)^2 \frac{\partial^3 u}{\partial y^2 \partial t}$ are as follows

$$\begin{cases} H_0(u) = (u_0')^2(u_0''u_{0t}') \\ H_1(u) = (u_0')^2(u_0''u_{1t}') + (u_0')^2(u_1''u_{0t}') + 2u_0'u_1'(u_0''u_{0t}') \\ H_2(u) = (u_0')^2(u_0''u_{2t}') + (u_0')^2(u_1''u_{1t}') + (u_0')^2(u_2''u_{0t}') + 2u_0'u_1'(u_0''u_{1t}') + 2u_0'u_1'(u_1''u_{0t}') + 2u_0'u_2'(u_0''u_{0t}') \\ \vdots \end{cases} \tag{3.31}$$

Now, comparing the like powers of P in equation (3.28) and equating their coefficients gives

$$P^0; u_0(y,t) = 1 + \lambda + \cos(\omega y) + G_c(1 + \cos(\omega y)) + G_r(1 + \cos(\omega y)) + \left(\frac{-\omega^2}{P_r}\cos(\omega y) + \delta(1 + \cos(\omega y) - \frac{\omega^2}{S_c}\cos(\omega y) - K_r(1 + \cos(\omega y))\right)t + \left(\frac{\omega^4}{P_r}\cos(\omega y) - \frac{2\delta\omega^2}{P_r}\cos(\omega y) + \delta^2\cos(\omega y) + \delta^2 + \frac{\omega^4}{S_c^2}\cos(\omega y) + \frac{2Se^{-y}}{S_c} - \frac{2K_r\omega^2}{S_c}\cos(wy) + K_r^2\cos(\omega y) + K_r^2\right)\frac{t^2}{2!} + \left(\frac{-\omega^6}{P_r^3}\cos(\omega y) + \frac{3\delta\omega^4}{P_r^2}\cos(\omega y) - \frac{3\delta^2\omega^2}{P_r}\cos(\omega y) + \delta^3\cos(\omega y) + \delta^3 - \frac{\omega^6}{S_c^3}\cos(\omega y) - \frac{3K_r\omega^4}{S_c}\cos(\omega y) - \frac{3K_r^2\omega^2}{S_c}\cos(\omega y) - K_r^3\cos(\omega y) - K_r^3\right)\frac{t^3}{3!} + \left(\frac{\omega^8}{P_r^4}\cos(\omega y) - \frac{4\delta\omega^4}{P_r^3}\cos(\omega y) + \frac{6\delta^2\omega^4}{P_r^2}\cos(\omega y) - \frac{4\delta^2\omega^2}{P_r}\cos(\omega y) - \delta^4\cos(\omega y) + \delta^4 + \frac{\omega^8}{S_c^4}\cos(\omega y) + \frac{4K_r\omega^6}{S_c^3}\cos(\omega y) + \frac{4K_r^2\omega^4}{S_c^2}\cos(\omega y) + \frac{4K_r\omega^2}{S_c}\cos(\omega y) + K_r^4\cos(\omega y) + K_r^4\right)\frac{t^4}{4!} \tag{3.32}$$

$$P^1; u_1(y,t) = L^{-1}\left\{\frac{1}{s}L\left\{S\frac{\partial u_0}{\partial y} + \frac{\partial^2 u_0}{\partial y^2} + \alpha\frac{\partial^3 u_0}{\partial y^2\partial t} + \beta_a\frac{\partial^4 u_0}{\partial y^2\partial t^2} + \beta_b(u_0')^2(u_0'') + \gamma_a\frac{\partial^5 u_0}{\partial y^2\partial t^3} + \gamma_b[2u_0'''u''_{0t} + (u_0')^2(u_0''u_{0t}')] - l_2u_0\right\}\right\} \tag{3.33}$$

Or,

$$u_1(y,t) = (A_{11} + \alpha A_{18} + \beta_b A_{11} + 2\gamma_b A_{15}A_{16} + A_{11}A_{13}A_{17} - l_2A_{19})t + (A_{12} + \beta_b A_{12}A_{13} + \beta_b A_{11}A_{14} + 2\gamma_b A_{16}^2 + A_{13}A_{14}A_{17} - l_2A_{10})\frac{t^2}{2!} + (2\beta_b A_{12}A_{14} + 2A_{11}A_{14}^2 - l_2A_{21})\frac{t^3}{3!} - l_2A_{22}\frac{t^4}{4!} - l_2A_{23}\frac{t^5}{5!} \tag{3.34}$$

Therefore, the solution to equation (2.14) is;

$$u(y,t) = u_0(y,t) + u_1(y,t) + u_2(y,t)\cdots \tag{3.35}$$

$$u(y,t) = A_{19} + (A_{10} + A_{11} + \alpha A_{18} + \beta_b A_{11} + 2\gamma_b A_{15}A_{16} + A_{11}A_{13}A_{17} - l_2A_{19})t + (A_{12} + A_{21} + \beta_b A_{12}A_{13} + \beta_b A_{11}A_{14} + 2\gamma_b A_{16}^2 + A_{13}A_{14}A_{17} - l_2A_{10})\frac{t^2}{2!} + (A_{22} + 2\beta_b A_{12}A_{14} + 2A_{11}A_{14}^2 - l_2A_{21})\frac{t^3}{3!} + \left(A_{23} - l_2A_{22}\frac{t^4}{4!}\right) - l_2A_{23}\frac{t^5}{5!} + \cdots \tag{3.36}$$

where,

$$A_{10} = \frac{-\omega^2}{P_r}\cos(\omega y) + \delta(1 + \cos(\omega y) - \frac{\omega^2}{S_c}\cos(\omega y) - K_r(1 + \cos(\omega y))$$

$$A_{11} = -\omega^2 \cos(\omega y) - G_c\omega^2 \cos(\omega y) - G_r\omega^2 \cos(\omega y)$$

$$A_{12} = G_cK_r\omega^2 \cos(\omega y) - \delta G_r\omega^2 \cos(\omega y) + \frac{G_c\omega^4 \cos(\omega y)}{S_c} + \frac{G_r\omega^4 \cos(\omega y)}{P_r}$$

$$A_{13} = \omega^2 \sin^2(\omega y) + 2G_c\omega^2 \sin^2(\omega y) + 2G_r\omega^2 \sin^2(\omega y) + 2G_cG_r\omega^2 \sin^2(\omega y) + G_c^2 \sin^2(\omega y) + G_r^2 \sin^2(\omega y)$$

$$A_{14} = \frac{-2G_r\omega^4}{P_r}\sin^2(\omega y) + 2\delta G_r\omega^2 \sin^2(\omega y) - \frac{2G_c\omega^4}{S_c}\sin^2(\omega y) - \frac{2G_r\omega^4}{P_r}\sin^2(\omega y) - 2\delta G_r^2\omega^2 \sin^2(\omega y) - \frac{4G_cG_r\omega^4}{S_c}\sin^2(\omega y) - 2G_cG_r\omega^2 \sin^2(\omega y) - \frac{G_cG_r\omega^2}{P_r}\sin^2(\omega y) - \frac{G_c^2\omega^4}{S_c}\sin^2(\omega y) - K_rG_c^2\omega^2 \sin^2(\omega y) + \frac{G_r^2\omega^6}{P_r^2}\sin^2(\omega y) - \frac{2\delta G_r^2\omega^4}{P_r}\sin^2(\omega y) + \frac{2G_cG_r\omega^6}{P_rS_c}\sin^2(\omega y) + \frac{2K_rG_cG_r\omega^4}{P_r}\sin^2(\omega y) + \delta^2G_r^2\omega^2 \sin^2(\omega y) + \frac{G_c^2\omega^6}{S_c^2}\sin^2(\omega y) + \frac{2K_rG_c^2\omega^4}{S_c}\sin^2(\omega y) + G_c^2K_r^2\omega^2 \sin^2(\omega y)$$

$$A_{15} = \omega^3 \sin^2(\omega y) + G_c\omega^3 \sin^2(\omega y) + G_r\omega^3 \sin^2(\omega y)$$

$$A_{16} = -\frac{G_c\omega^5}{S_c}\sin(\omega y) - \frac{G_r\omega^5}{P_r}\sin(\omega y) - G_cK_r\omega^2 \sin(\omega y) - \delta G_r\omega^3 \sin(\omega y)$$

$$A_{17} = G_cK_r\omega \sin(\omega y) - \delta G_r\omega \sin(\omega y) + \frac{G_c\omega^3}{S_c}\sin(\omega y) + \frac{G_r\omega^3}{P_r}\sin(\omega y)$$

$$A_{18} = \alpha G_cK_r\omega^2 \cos(\omega y) - \alpha\delta G_r\omega^2 \cos(\omega y) + \frac{\alpha G_c\omega^2 \cos(\omega y)}{S_c} + \frac{\alpha G_r\omega^2 \cos(\omega y)}{P_r}$$

$$A_{19} = 1 + \lambda + \cos(\omega y) + G_c(1 + \cos(\omega y)) + G_r(1 + \cos(\omega y))$$

$$A_{21} = \frac{\omega^4}{P_r}\cos(\omega y) - \frac{2\delta\omega^2}{P_r}\cos(\omega y) + \delta^2 \cos(\omega y) + \delta^2 + \frac{\omega^4}{S_c^2}\cos(\omega y) + \frac{2Se^{-y}}{S_c} - \frac{2K_r\omega^2}{S_c}\cos(wy) + K_r^2 \cos(\omega y) + K_r^2$$

$$A_{22} = \frac{-\omega^6}{P_r^3}\cos(\omega y) + \frac{3\delta\omega^4}{P_r^2}\cos(\omega y) - \frac{3\delta^2\omega^2}{P_r}\cos(\omega y) + \delta^3 \cos(\omega y) + \delta^3 - \frac{\omega^6}{S_c^3}\cos(\omega y) - \frac{3K_r\omega^4}{S_c}\cos(\omega y) - \frac{3K_r^2\omega^2}{S_c}\cos(\omega y) - K_r^3 \cos(\omega y) - K_r^3$$

$$A_{23} = \frac{\omega^8}{P_r^4}\cos(\omega y) - \frac{4\delta\omega^4}{P_r^3}\cos(\omega y) + \frac{6\delta^2\omega^4}{P_r^2}\cos(\omega y) - \frac{4\delta^2\omega^2}{P_r}\cos(\omega y) - \delta^4\cos(\omega y) + \delta^4 + \frac{\omega^8}{S_c^4}\cos(\omega y) + \frac{4K_r\omega^6}{S_c^3}\cos(\omega y) + \frac{4K_r^2\omega^4}{S_c^2}\cos(\omega y) + \frac{4K_r\omega^2}{S_c}\cos(\omega y) + K_r^4\cos(\omega y) + K_r^4 .$$

4 Numerical simulations/sensitivity analysis

Theoretical work on unsteady MHD Poiseuille flow of fourth-grade fluid in horizontal parallel plates channel with thermal radiation and chemical reaction effects has been analyzed and discussed in details. The impact of thermal radiation, chemical reaction, third and fourth-grade parameters along with other pertinent flow parameters are plotted graphically on different flow fields. The default values for the pertinent flow parameters are taken as [20];

$$\lambda = 0.30, \alpha = 0.20, \beta_a = 0.05, \beta_b = 0.05,\ \gamma_a = 0.05, \gamma_b = 0.05,\ S_c = 0.50, G_r = 5, G_c = 5, P_r = 0.71, Ha = 0.30, \delta = 0.05, Da = 1.00, K_r = 0.50.$$

To validate this present work, a numerical comparison is provided in Table 1.

Table 1. Validation of present study against [20] for velocity profile, when the suction parameter $S = 0$

δ	Velocity u (Present work)	Velocity u [20]	Difference
0.05	9.2474	9.2474	0.0001
0.10	9.2675	9.2678	0.0003
0.15	9.2874	9.2885	0.0011
0.20	9.3091	9.3094	0.0003

From Table 1, it can be seen there is no significant difference.

Figs 2 and **3** depict the velocity and temperature fields for increment of thermal radiation parameter δ $(1.00 \leq \delta \geq 4.00)$. Thermal radiation is known as electromagnetic radiation or the conversion of thermal energy which generates the thermal motion of particles in matter. Thermal radiation could be attributed due to thermal excitation. It is observed that both velocity and temperature fields are affected significantly with increase in thermal radiation parameter (δ). Thermal radiation for a medium which contains it inevitably has pressure and density gradients, and the treatment requires the use of hydrodynamics.

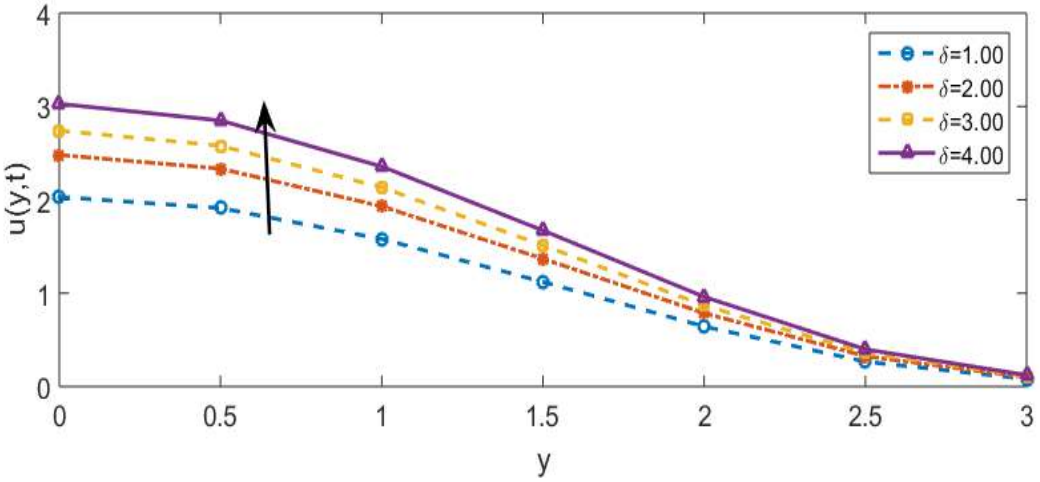


Fig. 2. Effect of thermal radiation parameter δ on Velocity profile u

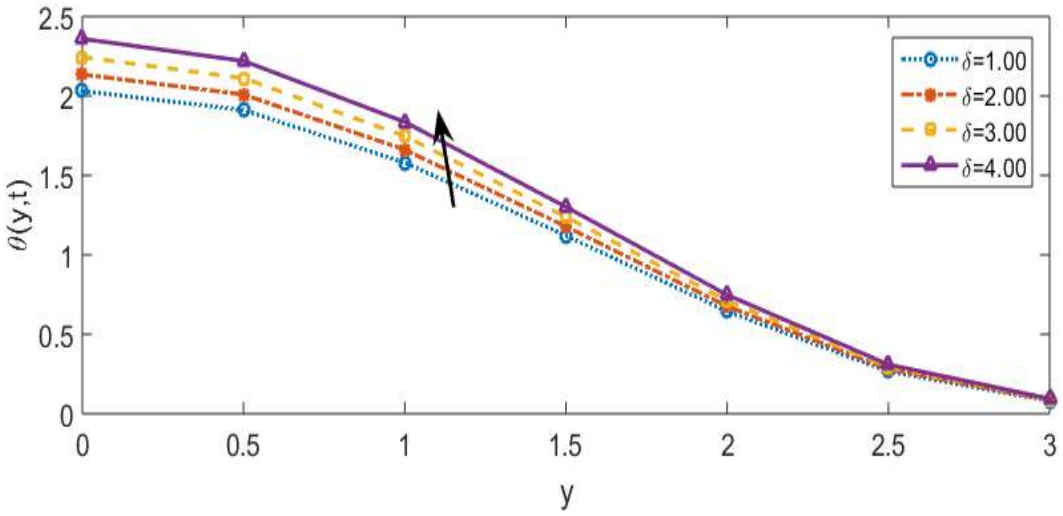


Fig. 3. Effect of thermal radiation parameter δ on temperature distribution θ

The effect of chemical reaction parameter (K_r) on velocity and concentration profiles are depicted in **Figs 4** and **5** respectively. Due to the rise of chemical reaction (K_r) from $1.00 \leq K_r \geq 4.00$, the velocity field decreases, and the concentration field also decreases. Physically, chemical reaction occurs with more disturbance which develops the molecular motion and upsurges the heat transport phenomena and as a result retards the velocity of the flow.

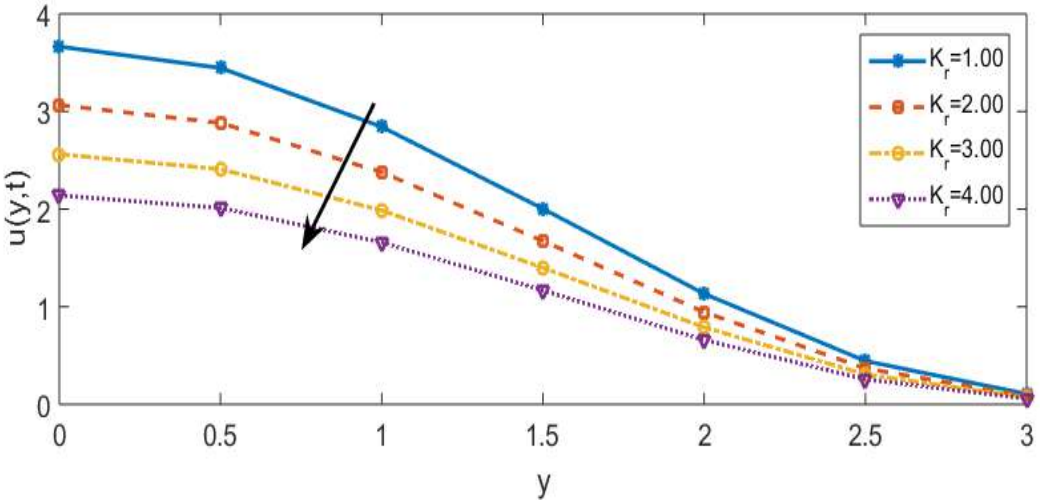


Fig. 4. Effect of chemical reaction parameter K_r on Velocity profile u

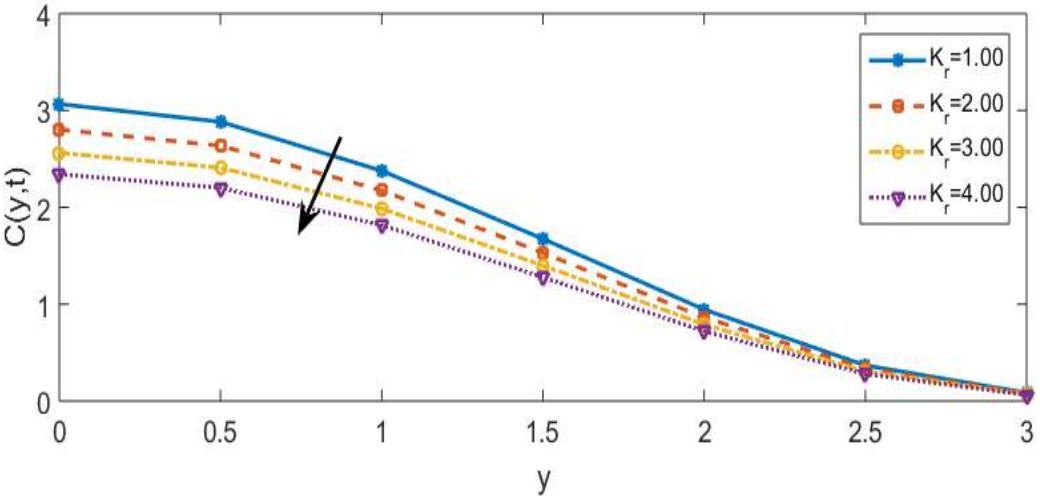


Fig. 5. Effect of chemical reaction parameter K_r on Concentration distribution C

Fig. 6 illustrates the drag force effect on fluid flow. The velocity profile decreases with the increment of Hartmann number $(1.00 \leq Ha \geq 4.00)$. The role of Hartmann number which is the magnetic parameter is to suppress turbulence. Physically, when magnetic field is applied to any fluid, the apparent viscosity of the fluid increases to the point of becoming viscous elastic solid. It is of great interest that yield stress of the fluid can be controlled very accurately through variation of the magnetic field intensity. The result is that the ability of the fluid to transmit force can be controlled with help of electromagnet which give rise to many possible control – based applications, including MHD power generation, electromagnetic casting of metals, MHD propulsion etc.

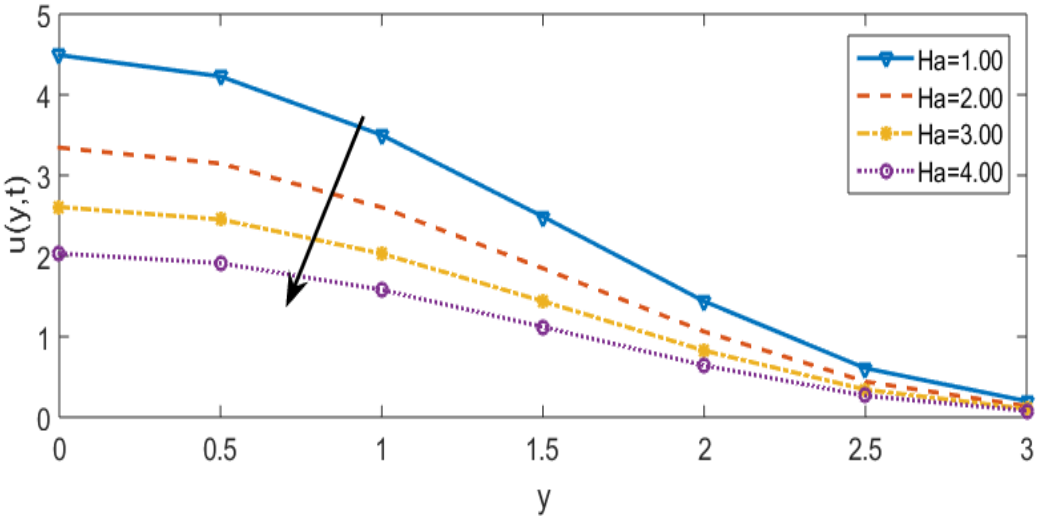


Fig. 6. Effect of Hartmann number Ha on Velocity profile u

The impression of third – grade and fourth – grade parameters on velocity profiles are respectively illustrated in **Figs 7** and **8**. It is observed that the velocity profile develops with the increase in both third – grade $(1.00 \leq (\beta_a = \beta_b) \geq 4.00)$ and fourth – grade $(1.00 \leq (\gamma_a = \gamma_b) \geq 4.00)$ parameters.

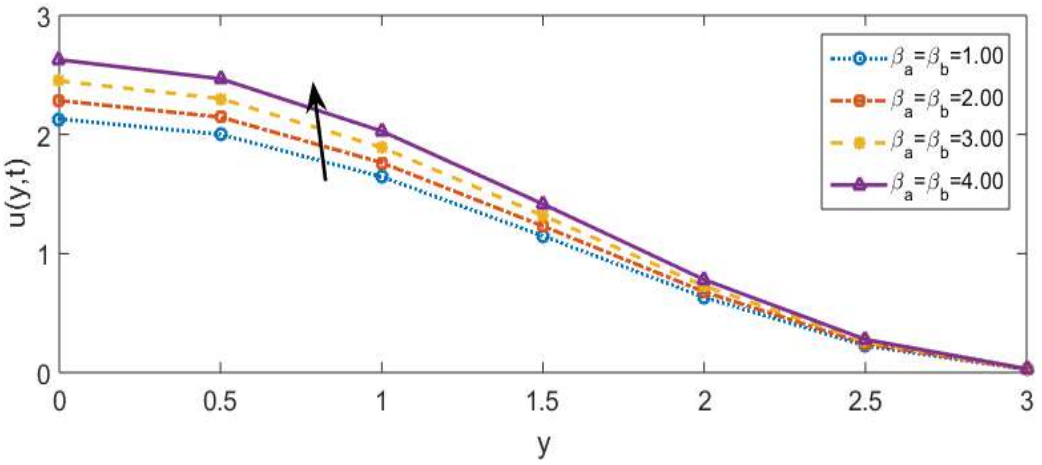


Fig. 7. Effect of β_a and β_b on Velocity profile u

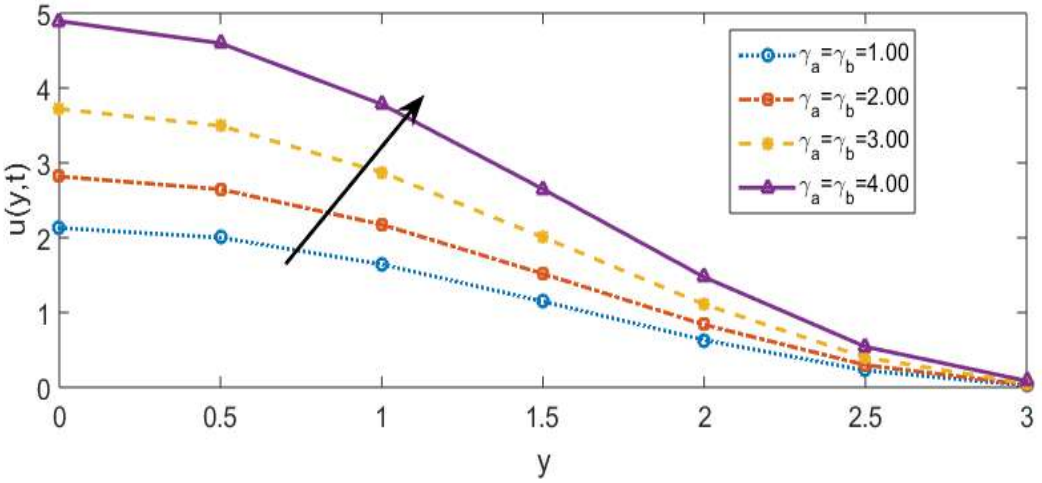


Fig. 8. Effect of γ_a and γ_b on Velocity profile u

Figs 9 and **10** show the impression of Prandtl number (P_r) on velocity and temperatures profiles respectively. The parameter (P_r) is the proportion of kinematic viscosity and thermal diffusivity which changes physically with temperature. For example, water $P_r = 7.0$ (at 20^0C) and Ammonia $P_r = 1.38$ decline more rapidly than air $P_r = 0.71$. However, increase in P_r depict the domination of thermal and momentum diffusivity respectively. Prandtl number is used to determine whether heat transport occurs with either conduction or convection process. Since, Prandtl number is inversely proportional to thermal diffusivity so that increasing P_r led to the decrease in velocity and temperature profiles.

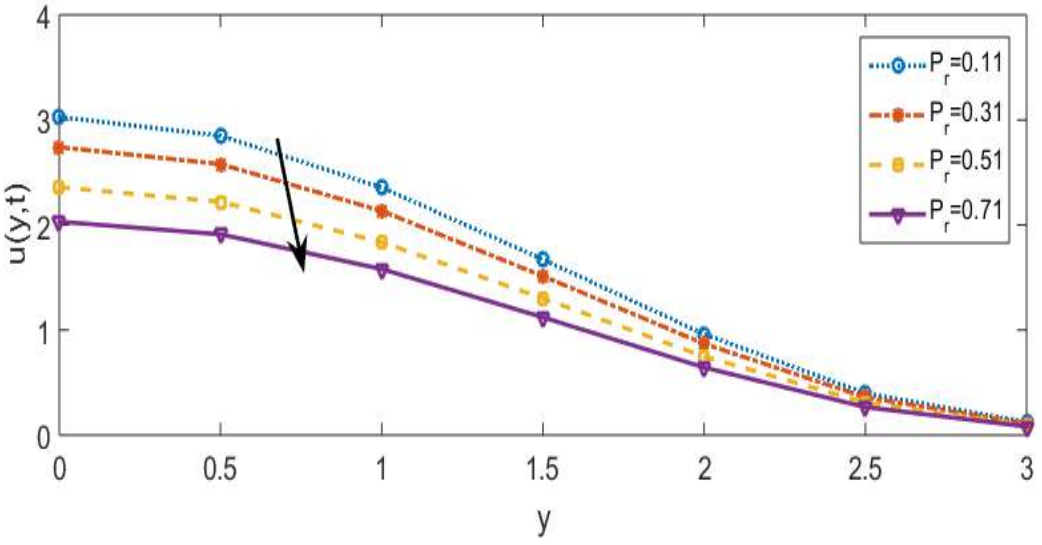


Fig. 9. Effect of Prandtl number P_r on Velocity profile u

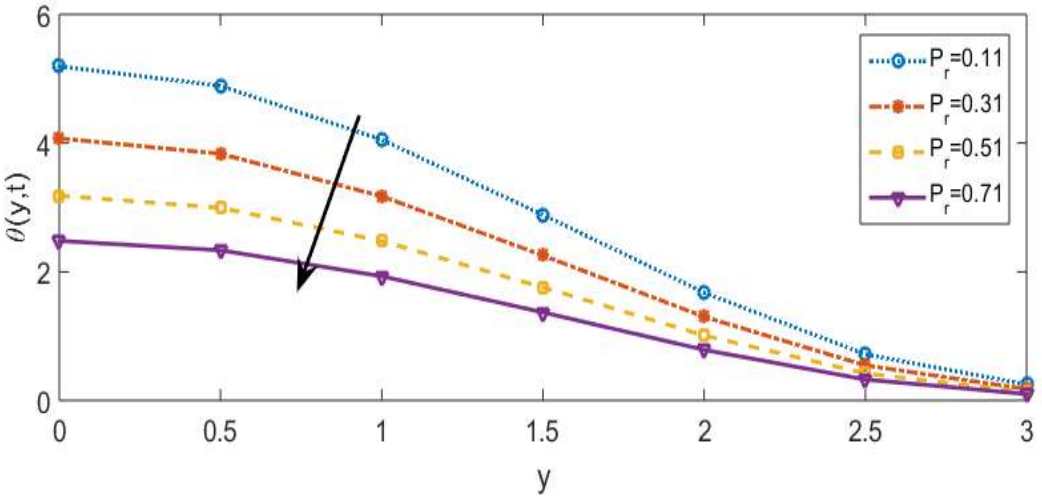


Fig. 10. Effect of Prandtl number P_r on Temperature distribution θ

Figs 11 and **12** display the velocity and concentration profiles respectively for the increment of Schmidt number $(1.00 \leq S_c \geq 4.00)$. Both the velocity and concentration profiles decrease with increase of Schmidt number (S_c). Physically, Schmidt number (S_c) helps to develop fluid concentration and concentration buoyancy force. Furthermore, it can also be used to improve the visualization of fluid fields.

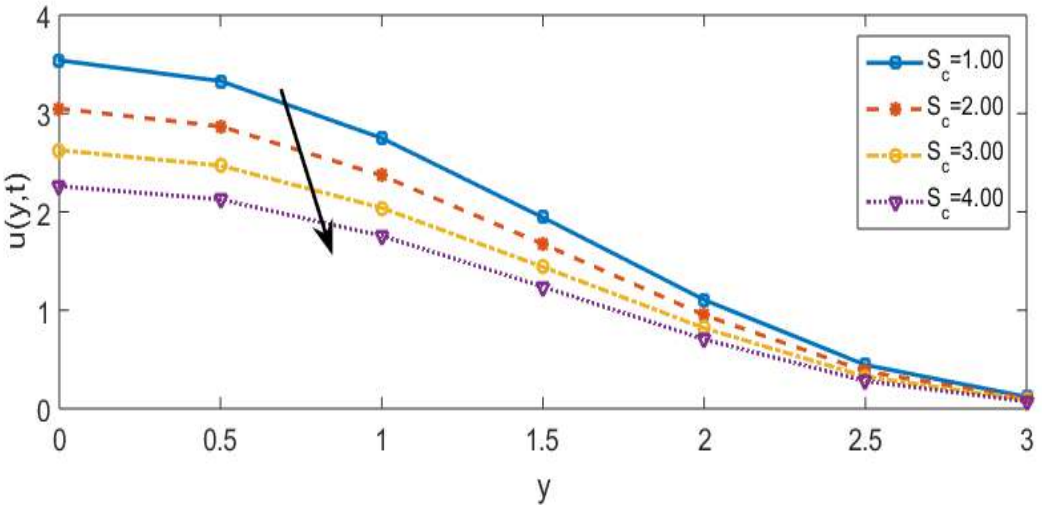


Fig. 11. Effect of Schmidt number S_c on Velocity profile u

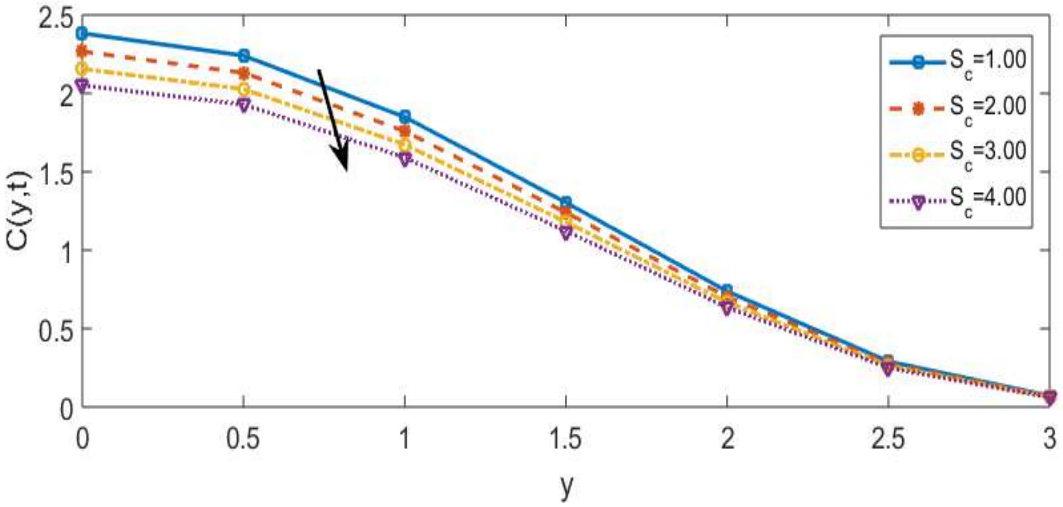


Fig. 12. Effect of Schmidt number S_c on Concentration distribution C

Since, the flow is driven by an externally imposed pressure gradient without motion of either plate, Negative and positive pressure gradients increase and decrease the flow rate, respectively. This is illustrated in **Fig. 13**. It is seen that increase in pressure gradient λ enhances the flow significantly. Pressure Gradient is a physical quantity that describes which direction and at what rate the pressure changes the most rapidly around a particular location.

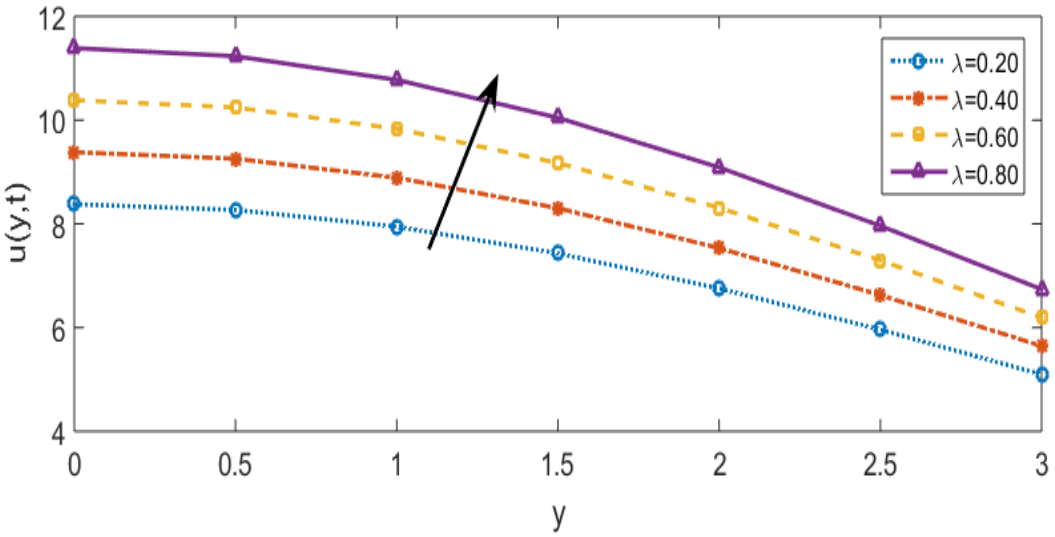


Fig. 13: Effect of Pressure gradient λ on Velocity profile u

5 Conclusion

The effect of thermal radiation and chemical reaction on unsteady MHD flow of fourth-grade fluid in horizontal parallel plates channel has been investigated. The solution for the nonlinear partial differential equations were obtained by the He-Laplace scheme. The effects of flow parameters on velocity, temperature and concentration profiles were depicted in figures and discussed. From the results obtained, the following conclusions are made:

(i) Velocity and temperature fields rise due to the increment of thermal radiation parameter.
(ii) For upsurging data of chemical reaction, velocity and concentration fields diminish.
(iii) Velocity, temperature and concentration fields diminish due to the increment of suction parameter.
(iv) Velocity profile goes up when third and fourth-grade parameters get to raise.
(v) Increasing Prandtl number tend to diminish the velocity and temperature profiles.
(vi) Strong values of Schmidt number decrease the magnitude of velocity and concentration distribution.
(vii) Velocity increases with increase in pressure gradient.

The results of this work are applicable in many industrial producing processes such in the drilling of oil and gas wells, polymer extrusion from dye, glass fibre, paper production and draining of plastics films etc.

References

[1] Umavathi, J.C., Liu, I.C. and Meera, S. (2010). Unsteady flow and heat transfer of porous media sandwiched between viscous fluids. Applied Mathematics and Mechanics 31(12), 1497 – 1516.

[2] Satya, P.V., Venkateswarlu, B., and Devika B. (2015). Chemical reaction and heat source effect on MHD oscillatory flow in an irregular channel. Ain Shams Engineering Journal 7(4), 1 – 10.

[3] Rehan, A.S., Islam, S., and Siddiqui, A.M. (2010). Couette and poiseuille flows for fourth-grade fluids using optimal homotopy asymptotic method. World Applied Science Journal 9(1), 1228 – 1236.

[4] Islam, S., Bano, Z., Siddique, I., and Siddiqui, A.M. (2011). The optimal solutions for the flow of a fourth-grade fluid with partial slip. Computer and Mathematics with Application 6, 1507 – 1516.

[5] Shehzad, N., Zeeshan, A., and Ellahi, R. (2018). Electroosmotic flow of MHD power law Al2O3-PVC nanofluid in a horizontal channel: couette-poiseuille flow model. Commun. Theor. Phys. 6(6), 655 – 666.

[6] Zeeshan, K., Ilyas, K., Murad, U., and Tlili, I. (2018). Effect of thermal radiation and chemical reaction on non-newtonian fluid through a vertically stretching porous plate with suction. Results in Physics 9, 1086 – 1095.

[7] Santhosa, B., Younus S., Kamala G., and Ramana Murthy, MV. (2017). Radiation and chemical effects on MHD free convective heat and mass transfer flow of a viscoelastic fluid past a porous Plate with Heat Generation/Absorption. Int J Chem Sci.15(3), 1 – 16.

[8] Mohan RamiReddy, A., Ramana Reddy, J.V., Sandeep N., and Sugunamma, V., (2017). Effect of nonlinear thermal radiation on MHD chemically reacting Maxwell fluid flow past a linearly stretching sheet. Applications and Applied Mathematics: An International Journal 12(1), 259 – 274.
[9] Opanuga, A.A., Okagbue, H.I., and Agboola, O.O. (2017). Irreversibility analysis of a radiative MHD Poiseuille flow through porous medium with slip condition. Proceedings of the World Congress on Engineering 2017 Vol I WCE 2017, July 5-7, 2017, London, U.K.
[10] Sumathia, K., Arunachalamb, T., and Kavithac, R. (2017). Effect of thermal radiation and chemical reaction on three dimensional MHD fluid flow in porous medium – a numerical study. International Journal of Control Theory and Applications 10(32), 9 – 19.
[11] Hayat, T., Ellahi R., and Mahomed, F.M. (2007). Exact solutions for couette and poiseuille flows for fourth grade Fluids. Acta Mechanica 188, 69 – 78.
[12] Ambreen A.K., Syeda, R.B., Marin, M., Rahmat, E. (2019). Effects of chemical reaction on third-grade mhd fluid flow under the influence of heat and mass transfer with variable reactive index. Journals Heat Transfer Research 50, 1061 – 1080.
[13] Sajid, R., Taza, G., Waris, K., Aamir K., and Zeeshan, K. (2022). Effects of chemical reaction, viscosity, thermal conductivity, heat source, radiation/absorption, on MHD mixed convection nano-fluids flow over an unsteady stretching sheet by HAM and numerical method. Advances in Mechanical Engineering 14(1), 1–20.
[14] Famakinwa, O.A., Koriko, O.K., Adegbie, K.S. and Omowaye, O.J. (2022)*:* Effects of viscous variation, thermal radiation, and Arrhenius reaction: The case of MHD nanofluid flow containing gyrotactic microorganisms over a convectively heated surface. Partial Differential Equations in Applied Mathematics 5, 1 – 7.
[15] Aarti, M., and Gorla, M.G. (2012). The effects of thermal radiation, chemical reaction and rotation on unsteady mhd viscoelastic slip flow. Global Journal of Science Frontier Research Mathematics and Decision Sciences 12(14), 1 – 15.
[16] Joshi, A. (2018). Exact Solution of Plane Poiseuille Fflow in a Channel Filled with a Porous Medium. Fluid Mech Res Int. 2(3), 131–136.
[17] Arifuzzaman, S.M, Shakhaoth, K.Md., Al-Mamum, A., Reza- E-Rabbi S.K, Biswas P., and Karim, I. (2018). Hydrodynamic stability and heat and mass transfer flow analysis of mhd radiative fourth-grade fluid through porous plate with chemical reaction. Journal of King Saud University 31(4), 1388 – 1398.
[18] Idowu, A.S. and Sani, U. (2019). Thermal radiation and chemical reaction effects on unsteady magnetohydrodynamic third-grade fluid flow between stationary and oscillating plates. Int. J. of Applied Mechanics and Engineering 24, 269 – 293.
[19] Priya, M., Mishra, S. R., Mahesh, B., Suthar, D. L., and Purohit, S. D. (2021). Computational behavior of second law poiseuille flow of micropolar fluids in a channel: analytical treatment. Journal of Mathematics, Hindawi 2021, 1 – 13.
[20] Joseph, K.M., Ayankop-Andi, E. and Mohammed, S.U. (2021). Unsteady MHD plane couette-poiseuille flow of fourth-grade fluid with thermal radiation, chemical reaction and suction effects. International Journal of Applied Mechanics and Engineering 26(4), 77 – 98.

[21] Coleman, B.D. and Noll, W. (1960). An approximation theorem for functionals with applications in continuum mechanics. Arch. Ration. Mech. Analy. 6, 355 – 370.
[22] Hayat, T., Wang, Y. and Hutter, K. (2002): Flow of a fourth-grade fluid. Math. Models Methods Appl. Sci. 12, 797 – 811.
[23] Hayat, T., Khan, M., Ayub, M., and Siddiqui, A.M. (2005): The Unsteady Couette Flow of a Second Grade Fluid in a Layer of Porous Medium. Archives of Mechanics 57, 405 – 416.

APPENDIX

Nomenclature

B_0 – external magnetic field
T – temperature of the fluid
C – species concentration
q_r – radiative heat flux
u – fluid velocity
C_p – specific heat capacity
Ha – Hartmann number
P_r – Prandtl number
G_r – Grashof number due to heat transfer
G_c – Grashof number due to mass transfer
K_r – chemical reaction parameter
S_c – Schmidt number
T_w – temperature at the surface
T_∞ – ambient temperature as $y \to \infty$
C_w – concentration at the surface
C_∞ – concentration as $y \to \infty$
x, y – cartesian coordinates

Greek Symbols
μ – coefficient of shear viscosity
α – second grade parameter
β_a, β_b – third grade parameters
γ_a, γ_b – fourth grade parameters
β – thermal expansion coefficient
β_c – concentration expan\sion coefficient
δ – thermal radiation parameter
σ – Stefan – Boltzmann constant
ρ – density of the fluid
ν – kinematic viscosity
λ - pressure gradient

Fractional order model of dynamical behavior and qualitative analysis of Anthrax with infected vector and saturation

A.C. Loyinmi*† and A.L. Ijaola‡

Abstract

We present a fractional order model to capture the transmission dynamics of anthrax infection with a nonlinear force of infection and its long-term impacts. An analysis with the standard Caputo–Fabrizio approach established that the model is well posed, and for the investigation on the stability of the model, an anthrax-free equilibrium as connected to the basic reproduction number $R_0 < 1$ and other important conditions that consolidate epidemiological feasibility of the model were established. Using a normalized forward sensitivity index, we conducted the sensitivity analysis of important variables, the contact rates, and the recruitment rate of the vectors to examine the effects of their variation on the dynamics of anthrax. These allow us to identify the most sensitive parameters that healthcare professionals need to pay attention to. The results from simulations also demonstrated that the presence of saturation instantly causes the system to approach an anthrax-free equilibrium (DFE), and our findings from the qualitative analysis compel us to recommend maximum hygiene practices for humans and domestic animals, early intervention, and the treatment of anthrax with a vaccine (as well as all other medical interventions) on the infected and periodic evaluation of these practices in households and the community at large to achieve a disease-free community.

Keywords and phrases: fractional model; incidence rate; anthrax; stability; sensitivity

1 Introduction

Bacillus anthracis is the bacteria that causes the infectious disease called anthrax. Both domestic and wild animals are affected by the disease. When vulnerable individuals come into touch with diseased animals or eat contaminated dairy and animal products, they can contract the anthrax virus. A zoonotic disease called anthrax is naturally occurring in soil and affects populations of humans and animals globally. People can become sick from tainted animal products or by having close contact with animals [1 - 4]. Infected animals, especially livestock, may die suddenly and unexpectedly from it, and it can occasionally be dangerous to people. Anthrax may generally be spread to animals in two ways: either by consuming a significant amount of spores found in soil or on plants or by stable insects called Stomoxys calcitrans, which feed on contaminated blood that leaks from the remains of animals that

*Corresponding Author; E-mail: loyinmiac@tasued.edu.ng
†Department of Mathematics, Tai Solarin University of Education, Ijagun, Ijebu –Ode, Ogun State, Nigeria.
‡Department of Mathematics, Federal University of Agriculture, Abeokuta, Ogun State, Nigeria.

have contracted the disease [5 - 6]. Applying immunizations before exposure is the only effective way to control anthrax and is advisable to do so between 2–4 weeks prior to the anticipated endemic season [5]. Anthrax spores may survive for up to two centuries because of their remarkable resilience to temperature fluctuations, desiccation, heat, and a range of chemical agents [7]. Furthermore, in cattle, anthrax infections frequently worsen without showing any signs (symptoms) [5]. The time frame in such a scenario could be critical for averting anthrax outbreaks.

In addition to herbivorous animals, predators that eat the contaminated carcasses of anthrax-infected prey are also at risk from anthrax. However, compared to herbivores, carnivores often have lower infection and death rates. According to the World Health Organization (WHO), the World Anthrax Data Site has recorded anthrax outbreaks in animals from around 200 nations, especially in areas with large populations of both humans and animals. For example, the exact reason of the anthrax deaths of a variety of animals in Etosha National Park, including ostriches and elephants, was still unclear. Three captive cheetahs were reported dead in November 2004 at the Jwana Game Reserve in Jwanen, Botswana. Meat from deceased red hartebeest infected with anthrax had been given to them [8 -9]. Africa, the Middle East, and Asia have relatively high rates of anthrax infection in wild animals and livestock, with periodic outbreaks and epizootics [10]. Anthrax is quite widespread in Bangladesh and India, two nations in southern Asia; outbreaks and diseases in both humans and animals are often reported [11 -12]. If treatment measures are not taken, the most common cutaneous type of anthrax infection can have a morbidity (fatality) rate of up to 20%; however, with appropriate treatment, it can drop to less than 1% [13].

Both natural phenomena and the dynamics of infectious disease transmission may be explained by mathematical models. In epidemiology, these models are essential for controlling infectious diseases. These models are able to clearly describe the dynamics and mechanisms of disease transmission [14 - 15]. Lotka and Volterra introduced the field of prey–predator ecosystem in mathematical research, which was termed the Lotka–Volterra model [16 - 17]. In mathematical modeling, Kermack and Kendrick coined the term "epidemiology" and investigated an SEIRS compartment model [18 - 19]. For a while now, there have been proposals and research done on complex models for the transmission dynamics of diseases, including periodic orbits, Hoff bifurcations, and multiple equilibria. They provide a clear qualitative depiction of the dynamics of the disease, together with improved analysis and consequences for disease forecasting [20 - 21]. The authors of [1] examined how a continuous vaccine affected an anthrax model, but they never took into account the consequences of the best possible control. Based on their studies, theoretical findings under continuous vaccination, the disease model's transmission resembles dynamics in the absence of vaccination. Additionally, [22] created a model by taking the influence of vaccines into account and came to a conclusion for the ideal vaccination coverage threshold needed for disease elimination. On the other hand, [23] employed optimum control while examining a nonlinear SIR epidemic model that included a vaccination plan.

No nation can really declare itself free of anthrax since the disease's spores may survive for a very long period in the soil. Nonetheless, anthrax epidemics tend to occur more often in developing nations.

Furniss and Hahn conducted groundbreaking research on anthrax modeling from a mathematical modeling standpoint when they examined an anthrax epizootic in South Africa's Kruger National Park [24]. The same researchers put up a different deterministic model with some threshold findings in 1983 [25]. Friedman and Yakubu added elements such as as migration, growth, and the host's natural death [26] to the model put forward in [24], adding a predetermined time delay. Mushayabasa suggested a fresh approach that was based on the model of Hahn and Furniss [25]. The function of human labor (as a control mechanism) in cleaning up contaminated carcasses, including the soil or surrounding region, is also included in their model [27]. Two distinct models investigating the spread and management of anthrax infection within two frameworks were provided in [28]. They investigated the effects of the incubation time and carcass clearance in the first framework. They looked at how the vector population affected the transmission and management of anthrax in the second approach. Using vaccination as a control, Kimathi and Wainaina [29] looked at the dynamics of anthrax spread in animal populations. The co-dynamics of anthrax and listeriosis infections were investigated, and the qualitative and quantitative link between them within preventative and treatment strategies was researched in [30]. According to their research, anthrax infection may raise the chance of listeriosis, but the listeriosis disease itself is not linked to an increased risk of anthrax. Their results show that while listeriosis infection is not linked to an increased risk of anthrax infection, anthrax infection is associated with a higher likelihood of listeriosis infection. A novel fractional ordered model in the sense of the Caputo–Fabrizio fractional derivative was suggested in [31]. This work was inspired by the work of [29]. They examined the asymptotic stability of the equilibrium states that are endemic and disease-free in order to calculate the fundamental reproduction number R0 of the fractional system.

Researchers' interest in disease modeling, particularly the modeling of diseases such as HIV and cancer, has increased recently. The SARS-CoV-2 virus is the source of the COVID-19 pandemic, which has lately garnered a lot of attention, with over 21 million confirmed cases and 758,000 fatalities recorded. During the COVID-19 epidemic, mathematical models were essential in predicting different waves, and research in this field is still ongoing [4, 32].

Our examination of the literature indicates that, compared to diseases such as cancer or HIV, modeling the anthrax disease has received comparatively less attention from researchers. The ongoing threat that anthrax poses in developing nations (Africans and the likes) is a strong incentive for us to investigate the mathematical modeling of anthrax in this research work.

1.1 Epidemiology of Anthrax in Nigeria

Following the discovery of widespread death resulting from the pathognomonic signs of the disease in a multi-species farm in Gajiri Village, Suleja, Niger State, Nigeria's index anthrax case was confirmed by the Nigerian Center for Disease Control (NCDC). About 100 cows (49 foreign and 51 native varieties), 73 sheep (a breed of fat-tailed sheep from Sudan), and 19 goats were present on the property where the index case was located. On 27 June 2023, the circumstances that led to the verified anthrax epidemic began. Thirteen cattle and ten sheep were among the

thirty-five instances (twenty cattle and fifteen sheep) that had been reported as of 13 July 2023, the day the samples were collected. The national reference laboratory made a confirmation diagnosis of anthrax on 16 July 2023 (Nigerian Veterinary Research Institute). In VOM, Plateau State, although animals are driven to graze on natural grass, the majority of the cows were grown in large production systems. On 19 July 2023, the global disease notice was transmitted to the World Animal Health Information system, and an urgent notification was issued to the World Organization for Animal Health on 17 July 2023.

In addition, more research is being done to determine the infection's origin and how it spread to other farms and people. Although reports of human exposure exist, no human symptoms or deaths have been documented yet. To identify, isolate, and monitor all affected individuals, the FMARD and the Nigeria Centre for Disease Control and Prevention (NCDC) are presently collaborating closely with the Ministries of Agriculture and Health of Niger State. The incident manager has been designated by the NCDC to ensure efficient response coordination, and the incident management system (IMS) has been activated at level two (2). The probability of an epidemic and its possible effects on humans were rated as HIGH in the risk assessment carried out by the human health sector (NCDC).

1.2 Treatment of Anthrax

Adequate immunization of vulnerable vector populations lowers the likelihood of it spreading to humans because the disease is zoonotic and preventable with the recommended vaccine. Therefore, minimizing contact with diseased vectors and managing vectors with anthrax effectively removes the danger to humans. Annual preventative vaccination is the main method of controlling animal anthrax, but if an epidemic starts, other methods of controlling the disease might also be effective, including ring vaccination, the correct disposal of carcasses, and the separation of newly acquired or infected vectors (animals) [33]. For vectors in the red zone as well as other vectors around the nation, ring vaccination is recommended. Research has indicated that immunization with either the non-living anthrax vaccine prototypes or the Sterne live anthrax spore vaccine, which is a non-pathogenic, non-encapsulated strain of ***Bacillus anthracis***, has produced an immune response to the disease [34]. Health commissions must warn that simultaneous antibiotic treatment might significantly reduce the efficiency of the live-attenuated vaccine because animal producers, out of fear, may give antibiotics to animals in order to avoid anthrax. Therefore, field personnel need to make sure that animals on antibiotic programs are vaccinated again [33, 35]. Another crucial element of prevention in humans is the prescription of antibiotics as post-exposure interventions. Post-exposure interventions should be administered to danger groups, such as veterinarians, animal health professionals, and anyone engaged in the removal of carcasses, and personal protective equipment (PPE) must be worn [36].

1.3. Forces of Infections and Incidences

Various researchers have utilized some incidence functions, which include the bilinear incidence rate βSI, where β is a positive constant S is the susceptible individual in the population and I is infected people in the population.

Similarly, some researcher's also make use of $\frac{\beta SI}{1+PS}$ and $\frac{\beta SI}{1+PI}$, where p>0 is the saturated incidence rate.

Most studies employ the bilinear rate of incidence βSI and the conventional rates βSI/N; there has been less focus on applying the incident rate of saturation in epidemiological models. This served as inspiration for this study.

1.4. The Sensitivity Analysis Theory

Because anthrax is so widespread, it is imperative that control measures be designed, assessed, and put into action in order to eradicate the virus's ever-present nature. In this instance, this means testing and examining the dynamics of the disease to identify the sensitive parameters causing the outbreak; this requires performing a sensitive analysis on the behavioral changes of the disease's transmission.

An analysis of the sensitivity examines how changes in the inputs might affect a model's outputs. A sensitivity analysis basically identifies the parameters and starting circumstances (inputs) that have the greatest impact on the model's outputs or quantities of interest. This study is significant in the first place because it indicates to the scientist (researchers) which parameters require the greatest amount of arithmetical consideration [34-35].

1.4. Preliminary and Definitions

This section includes some notations, definitions, and established results that are required for the sequel. This study uses Liouville–Caputo's fractional derivative.

Definition 1. Let U be a real function in the range $C_\chi, where \chi \in R, t > 0$, $\exists$ a $n > \chi$, which is real, then

$$U(t) = t^n k(t), \tag{1}$$

and for k∈ C [0,∞], it is said to be in the range C_χ^m if and only if $U^{(m)} \in C_\chi, m \in M$.

Definition 2. The Transformation of Laplace is given by

$$F(s) = L\{F(t)\}(s) = \int_0^\infty e^{-st} F(t)dt \quad , \tag{2}$$

where F(t) is a valued function of t.

Definition 3. The fractional integrating operator of order $\alpha \geq 0$ of the Riemann Liouville of function $U \in L^1(a,b)$ *is defined as*

$$I^\alpha U(t) = \frac{1}{\Gamma(\alpha)} \int_0^t (t-\tau)^{\alpha-1} U(\tau)d\tau, \quad t > 0, \alpha > 0 \tag{3}$$

where Γ is the function of gamma and $I^0 U(t) = f(t).$

Definition 4. The fractional derivative in the sense of Liouville–Caputo is given by [35, 39].

$$D^\alpha U(t) = I^{n-\alpha} D^n U(t) = \frac{1}{\Gamma(n-\alpha)} \int_0^t (t-\tau)^{n-\alpha-1} U^{(n)}(\tau)d\tau, \tag{4}$$

Where $n \in N$ and $n-1 \prec \alpha \leq n$ for $t \succ 0.$

Definition 5. The Mittag–Lefller generalized function, also known as two parameter Mittag–Leffler function, is given by

$$E_{\alpha,\beta}(z) = \sum_{k=0}^{\infty} \frac{z^k}{\Gamma(\alpha k + \beta)} \ , \ \mathrm{Re}(\alpha) > 0 \, , \, \beta, Z \in \mathbb{C} \tag{5}$$

When β = 1, the Mittag–Leffler function with one parameter is derived as a particular instance of this function and is denoted as

$$E_{\alpha,\beta}(Z) = E_{\alpha,1}(z) = \sum_{k=0}^{\infty} \frac{Z^k}{\Gamma(\alpha k + 1)} \, , \ \mathrm{Re}(\alpha) > 0 \ \text{ for, } Z \in \mathbb{C} \tag{6}$$

α and β can as well take any form of different values in other to show that the Mittag–Leffler function can represent important special cases.

Lemma 1. [36]. For $\mu > 0$ and $0 < \alpha \leq 1$, the function $E_{\alpha,\beta}(-\mu z^\alpha)$, $\alpha \leq \beta$ is monotonically decreasing positive function of $z > 0$.

Definition 6. For the Caputo's derivative, its Laplace transform is given by

$$L\{D^{\alpha}N(t)(s)\} = S^{\alpha}N(s) + \sum_{k=0}^{n-1} S^{n-k-1}N^{k}(0),\ \mathrm{Re}(\alpha) > 0,\ n-1 < \alpha \le n. \tag{7}$$

Lemma 2. Putting into consideration the two parameters of Mittag–Leffler function, we then have the Laplace transform formula as

$$L\{x^{\beta-1}E_{\alpha,\beta}(\mu^{*}t^{\alpha})\}(s) = \frac{s^{\alpha-\beta}}{s^{\alpha}-\mu^{*}},\ \mathrm{Re}(z) > 0 \tag{8}$$

where $\alpha, \beta, \mu^{*} \in \mathbb{C},\ \mathrm{Re}(\beta) > 0,\ \mathrm{Re}(\alpha) > 0$

Lemma 3. Let $\Psi \in C[a,b]$ and $D^{\alpha}\Psi \in (0,b]$, and let $0 < \alpha \le 1,$; therefore, we have $U(t) = U(\alpha) + \frac{1}{\Gamma(\alpha)} D^{\alpha}U(\chi)(t-a)^{\alpha}$ for $0 \le \chi \le t$ and for $t \in (a, b]$.

The above lemma is mean value theorem, which is the generalized one.

Lemma 4. For $U \in C[a,b]$ and $D^{\alpha}U \in (a,b]$, let $0 < \alpha \le 1$; hence, we have the following:

(a) For $D^{\alpha}U(t) \ge 0,\ \forall\ t \in (0,b)$, the function u is increasing.

(b) For $D^{\alpha}U(t) \le 0$, $\forall\ t \in (0,b)$, the function u is decreasing.

2 Model formulation

According to the proposed model, the whole system (population) is represented by the letter "N" and has been split into two primary parts: "N_v" and "N_h" for vectors and humans, respectively. The susceptible, exposed, infected, and recovered human sub-populations (S_h, E_h, I_h, and R_h) are present in 'N_h', respectively, from this subdivision; similarly, for the vector sub-population, N_v, we have susceptible, infected, and recovered (S_v, I_v, and R_v), assuming that the domestic animals can recover from the disease with appropriate control techniques.

Additionally, the recruitment/immigration of humans and vectors into the population in question occurs through birth or immigration at rates of Λ_h and Λ_v, respectively. Humans and vectors contract the anthrax virus through contact with diseased animals or the consumption of tainted dairy and animal products containing *Bacillus anthracis* at forced or saturated rates of infection, Φ_1 and Φ_2.

$$\Phi_1 = \frac{\beta_1 I_H}{1+a_H I_H} + \frac{\beta_2 I_v}{1+a_v I_v} \tag{8}$$

$$\Phi_2 = \frac{\beta_3 I_v}{1+a_v I_v} \tag{9}$$

where a_H is the saturation factor for humans and a_v is the saturation force for vectors.

The effective contact rates that can result in infection and saturation factors are represented by β_1, β_2, β_3, and a_H, a_v, respectively.

The results of this study show that the saturation rates and infection forces in (9) and (10) above predict the behavioral change in the model when I_h and I_v grow very big in the system as well as their repressive effects when simulated. This is the reason this model has taken into account the specific saturation incidence rate.

In this model, we have also taken into account the possibility that individuals may lose their immunity, making them susceptible to infection again at the rate ϱ after receiving treatment, with a recovery rate of η. However, in severe cases of anthrax sickness, people may pass away at a rate of δ because of the virus's virulence.

2.1 The Anthrax model's equations

The set of time fractional differential equations designed to describe the dynamics of the disease is basically on the descriptions and assumptions of the above model (Figure 1).

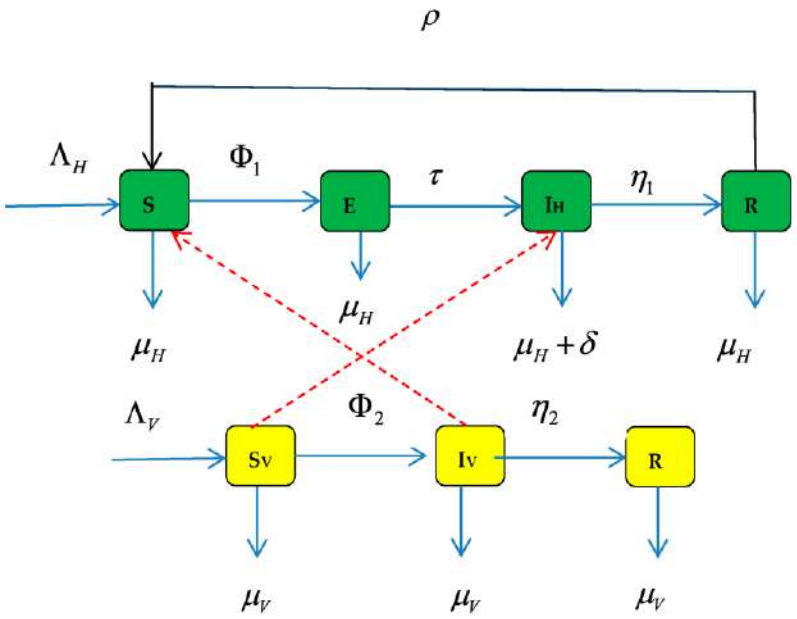


Figure 1. Schematic flow of the anthrax model.

$$\left.\begin{aligned}
D^{\alpha}S_H(t) &= \Lambda_H - \mu_H S_H - \Phi_1 S_H + \rho R_H \\
D^{\alpha}E_H(t) &= \Phi_1 S_H - \mu_H E_H - \tau E_H \\
D^{\alpha}I_H(t) &= \tau E_H - \mu_H I_H - \delta I_H - \eta_1 I_H \\
D^{\alpha}R_H(t) &= \eta_1 I_H - \mu_H R_H - \rho R_H \\
D^{\alpha}S_v(t) &= \Lambda_V - \mu_V S_V - \Phi_2 S_V \\
D^{\alpha}I_v(t) &= \Phi_2 S_V - \mu_V I_V - \eta_2 I_V \\
D^{\alpha}R_v(t) &= \eta_2 I_V - \mu_V R_V
\end{aligned}\right\} \tag{10}$$

Here $D^{\alpha} = \dfrac{d^{\alpha}}{dt^{\alpha}}$, for $0 < a \leq 1$ in the sense of the Caputo fractional derivative of order a

Table 1. Parameters and Descriptions

Parameters	Description
S_H	Human Susceptible
E_H	Human Exposed
I_H	Human Infected
R_H	Human Recover
S_V	Vector Susceptible
I_V	Infected vector
R_V	Recovered vector
Λ_H	Immigration/recruitment rate for human
Λ_V	Immigration/recruitment rate for vector
Φ_1	Force of infection for human
Φ_2	Force of infection for vector
ρ	Loss of immunity human
μ_H	Natural death rate for human
μ_V	Natural death rate for vector
τ	Rate of Progression from exposed to infected class of human
η_1	Rate of Progression from infected to recovery class of human
η_2	Rate of Progression from infected to recovery class of vector
β_1	The rate of effective contact between for humans
β_2	Rate of effective contact between domestic vector and *Bacillus anthracis*
β_3	Rate of contact leading to infection for the vector

δ	Disease-induced death
a_H	Saturation factor for human
a_V	Saturation factor for vector

3 Analysis of the model

3.1 Existence and Uniqueness of the Model Solution

To demonstrate the uniqueness and existence of solutions to the system (11), Lemma 4 as it has been given above, is required, which is given as follows: For $U \in C[a, b]$ and $D^{\alpha}U \in (0, b]$, let $0 < a \leq 1$. Hence, we have the following:

(a) For $D^{\alpha}U(t) \geq 0$, $\forall\, t \in (0, b)$, the function u is increasing.

(b) For $D^{\alpha}U(t) \leq 0$, $\forall\, t \in (0, b)$, the function u is decreasing.

The proof of the above lemma is a direct consequence of Lemma 3, which is the generalized mean value theorem.

3.2. Boundedness and Positivity of the Model

In this section, we verify and ascertain if our proposed model is epidemically and mathematically accurate. Moreover, each compartment's solutions are non-negative (positive). The whole vector population is represented by $N_V = S_V + I_V + R_V$, while the total human system is represented by $N_H = S_H + E_H + I_H + R_H$.
Therefore,

$$N_H = S_H + E_H + I_H + R_H$$

$$N_V = S_V + I_V + R_V$$

which yields

$$\left.\begin{aligned} D^{\alpha}N_H(t) &= D^{\alpha}S_H(t) + D^{\alpha}E_H(t) + D^{\alpha}I_H(t) + D^{\alpha}R_H(t) \\ D^{\alpha}N_V(t) &= D^{\alpha}S_V(t) + D^{\alpha}I_V(t) + D^{\alpha}R_V(t) \end{aligned}\right\} \tag{11}$$

From (12), we can conclude that for both the human and vector compartment, we have

$$\left.\begin{aligned} D^{\alpha}N_H(t) &= \Lambda_H - \mu_H N_H \\ D^{\alpha}N_V(t) &= \Lambda_V - \mu_V N_V \end{aligned}\right\} \tag{12}$$

with $\delta = 0$ for both the human and vector compartment, i.e., the disease-induced death in order to achieve (13).

Theorem 1. Let (S_H, E_H, I_H, R_H) and (S_V, I_V, R_V) be the solution to the anthrax fractional model equation (11) in an epidemiologically viable area Γ, where

$$\left.\begin{aligned} \Gamma &= (S_H, E_H, I_H, R_H) \in R_+^{\,4} : N_H \le \frac{\Lambda_H}{\mu_H} \\ \Gamma &= (S_V, I_V, R_V) \in R_+^{\,3} : N_V \le \frac{\Lambda_V}{\mu_V} \end{aligned}\right\} \tag{13}$$

Proof. With the Laplace transform applied on both sides of (13) (for both humans and vectors) and using the Definition 6, we have

$$\left.\begin{aligned} S^{\alpha}N_H(s) + S^{\alpha-1}N(0) &= \frac{\Lambda_H}{s} - \mu_H N_H(s) \\ S^{\alpha}N_V(s) + S^{\alpha-1}N(0) &= \frac{\Lambda_V}{s} - \mu_V N_V(s) \end{aligned}\right\} \tag{14}$$

After little modifications and rearrangement on (15), we have

$$\left.\begin{aligned} N_H(s) &= \frac{\Lambda_H}{s(s^{\alpha} + \mu_H)} + \frac{s^{\alpha-1}}{s^{\alpha} + \mu_H} N(0) \\ N_V(s) &= \frac{\Lambda_V}{s(s^{\alpha} + \mu_V)} + \frac{s^{\alpha-1}}{s^{\alpha} + \mu_V} N(0) \end{aligned}\right\} \tag{15}$$

After considerable simplification and application of the Laplace inverse transform and (Lemma 2), as given earlier on (16), the following was derived:

$$\left.\begin{aligned} N_H(t) &= N(0)E_{\alpha}(-\mu_H t^{\alpha}) + \frac{\Lambda_H}{\mu_H}[1 - E_{\alpha}(-\mu_H t^{\alpha})] \\ N_V(t) &= N(0)E_{\alpha}(-\mu_V t^{\alpha}) + \frac{\Lambda_V}{\mu_V}[1 - E_{\alpha}(-\mu_V t^{\alpha})] \end{aligned}\right\} \tag{16}$$

Applying (17) with Lemma 1, as *t* tends to ∞, the following are obtained:

$$\left.\begin{aligned} N_H(t) &\le \frac{\Lambda_H}{\mu_H} \\ N_V(t) &\le \frac{\Lambda_V}{\mu_V} \end{aligned}\right\} \tag{17}$$

Thus, every solution for system (11) is included inside the set Γ; hence, Γ is bounded for both the human and vector population.

Hence, from Equations (13)–(18), we have been able to verify that the solutions for the various compartments are bounded and that the model is well posed both mathematically and epidemiologically.

This ends the proof.

3.3 Positivity

For all time t > 0, the fractional order model's solution in system (11) with positive initial conditions will continue to be positive and non-negative.

Proof

Using the Mittag–Leffter function, also known as two parameter function (5) and (6), we derive

$$E_{\alpha,\beta} = \sum_{k=0}^{\infty} \frac{(Z)^k}{\Gamma \alpha k + \beta}$$

Replacing Z with our population $N_H(t)$ and $N_V(t)$, respectively and separately, where $k = 0,1,2,\ldots$ and $\alpha = \beta = 1$, we derive

$$\left.\begin{aligned} E_{1,1} &= \sum_{k=0}^{\infty} \frac{(N_H(t))^k}{\Gamma \alpha k + \beta} = \frac{(N_H(t))^0}{\Gamma(0+1)} + \frac{(N_H(t))^1}{\Gamma(1+1)} + \ldots \\ E_{1,1} &= \sum_{k=0}^{\infty} \frac{(N_V(t))^k}{\Gamma \alpha k + \beta} = \frac{(N_V(t))^0}{\Gamma(0+1)} + \frac{(N_V(t))^1}{\Gamma(1+1)} + \ldots \end{aligned}\right\} \tag{18}$$

Neglecting the higher terms, we derive

$$\left.\begin{aligned} E_{1,1} &= \sum_{k=0}^{\infty} \frac{\left(N_H(t)\right)^k}{\Gamma \alpha k + \beta} \approx \frac{1}{\Gamma(1)} + \frac{\left(N_H(t)\right)^1}{\Gamma(2)} \\ E_{1,1} &= \sum_{k=0}^{\infty} \frac{\left(N_V(t)\right)^k}{\Gamma \alpha k + \beta} \approx \frac{1}{\Gamma(1)} + \frac{\left(N_V(t)\right)^1}{\Gamma(2)} \end{aligned}\right\} \tag{19}$$

$\Gamma(1) = 1$

$$\left.\begin{aligned} E_{1,1} &= \frac{\left(N_H(t)\right)}{\Gamma \alpha k + \beta} \approx 1 \\ E_{1,1} &= \frac{\left(N_V(t)\right)}{\Gamma \alpha k + \beta} \approx 1 \end{aligned}\right\} \tag{20}$$

We have also been able to verify that the model is positive for time (t) based on equations of model (11)

This ends the proof.

3.4. Presence of the disease-free equilibrium points

The term "disease-free system (equilibrium) (DFE) points" refers to stable-state solutions when the population as a whole becomes immune to anthrax infection.

We have

$$S_H{}^0 \neq 0, \;\; S_V{}^0 \neq 0,$$

$$\text{for} \left.\begin{aligned} &S_H{}^0 \neq 0, E_H{}^0 = 0, I_H{}^0 = 0, R_H{}^0 = 0 \\ &S_V{}^0 \neq 0, I_H{}^0 = 0, R_H{}^0 = 0 \end{aligned}\right\} \tag{21}$$

Hence, system (18) becomes

$$\left.\begin{aligned} \Lambda_H - \mu_H S_H{}^0 &= 0 \\ \Lambda_V - \mu_V S_V{}^0 &= 0 \end{aligned}\right\} \tag{22}$$

This yields

$$\left.\begin{aligned} S_H^0 &= \frac{\Lambda_H}{\mu_H} \\ S_V^0 &= \frac{\Lambda_V}{\mu_V} \end{aligned}\right\} \tag{23}$$

Therefore, the disease-free equilibrium point for both the human and vector population is

$$E^0 = (S_H^0, E_H^0, I_H^0, R_H^0, S_V^0, I_V^0, R_V^0) = \left(\frac{\Lambda_H}{\mu_H}, 0, 0, 0, \frac{\Lambda_V}{\mu_V}, 0, 0\right) \tag{24}$$

Equation (25) is the DFE point for the system.

3.5. Computation of the R_0 (reproduction number) of the human–vector model

In an epidemic model, the R_0 is an essential concept. This figure indicates the typical number of later infections in the exposed section of the population among all individuals in a population that is fully susceptible and infected by an infectious person already in the infected compartment. Similarly, R_0 is a crucial metric that tells us whether or not a disease will spread over the population. The "next generation matrix method" will be used in order to calculate it.

Using system (11), the model's fundamental reproduction number is obtained using $R_0 = \Delta(FV^{-1})$, where Δ is the dominant eigenvalue of FV^{-1}, which yields R_{HV}; here, R_{HV} is the combination of both compartments (human and vector). **V** is the linear system of additional transfer terms with infection, and F is the linear system matrix of the new infection. Consequently, for simplicity, we calculate separately the human reproduction number, R_H, and vector reproduction number, R_v, and then obtain the product.

Proof. We implement the next generation matrix [41 - 44] on the human compartment, that is

$$\begin{aligned} D^\alpha S_H(t) &= \Lambda_H - \mu_H S_H - \Phi_1 S_H + \rho R_H \\ D^\alpha E_H(t) &= \Phi_1 S_H - \mu_H E_H - \tau E_H \\ D^\alpha I_H(t) &= \tau E_H - \mu_H I_H - \delta I_H - \eta_1 I_H \\ D^\alpha R_H(t) &= \eta_1 I_H - \mu_H R_H - \rho R_H \end{aligned} \tag{25}$$

and $\Phi_1 = (\frac{\beta_1 I_h}{1+a_h I_h} + \frac{\beta_2 I_v}{1+a_v I_v}) S_H$; here, $a_H = a_v = \frac{\beta_2 I_V}{1+a_v I_V} = 0$ since the assumption is that the infection is more dominant in the exposed and the infected class of the human population.

$$F_H = \begin{bmatrix} \Phi_1 S_h \\ 0 \end{bmatrix} = \begin{bmatrix} \frac{\partial F_1}{\partial E_H} & \frac{\partial F_1}{\partial I_H} \\ \frac{\partial F_2}{\partial E_H} & \frac{\partial F_2}{\partial I_H} \end{bmatrix} = \begin{bmatrix} 0 & \beta_1 S_H \\ 0 & 0 \end{bmatrix} \tag{26}$$

Similarly, $V_H = \begin{bmatrix} -\mu_H E_H - \tau E_H \\ \tau E_H - \mu_H I_H - \delta I_H - \eta_1 I_H \end{bmatrix} = \begin{bmatrix} \frac{\partial V_1}{\partial E_H} & \frac{\partial V_1}{\partial I_H} \\ \frac{\partial V_2}{\partial E_H} & \frac{\partial V_2}{\partial I_H} \end{bmatrix} = \begin{bmatrix} -(\mu_H + \tau) & 0 \\ \tau & -(\mu_H + \delta + \eta_1) \end{bmatrix}$ (27)

$$V_H^{-1} = \frac{Adj(V)}{|V|},$$

using $R_{0H} = \Delta(F_H V_H^{-1})$.

We have

$$F_H V_H^{-1} = \begin{bmatrix} \frac{\tau\beta_1 S_H}{(\mu_H + \delta + \eta_1)(\mu_H + \tau)} & \frac{\beta_1 S_H}{(\mu_H + \delta + \eta_1)} \\ 0 & 0 \end{bmatrix}$$

$$| F_H V_H^{-1} - \lambda I | = \left| \begin{bmatrix} \frac{\tau\beta_1 S_H}{(\mu_H + \delta + \eta_1)(\mu_H + \tau)} - \lambda & \frac{\beta_1 S_H}{(\mu_H + \delta + \eta_1)} \\ 0 & 0 - \lambda \end{bmatrix} \right|$$

The most dominant eigenvalue was utilized, which is the spectral radius; therefore,

$R_{0H} = \frac{\tau\beta_1 S_h}{(\mu_H + \delta + \eta_1)(\mu_H + \tau)}$. Recall that $S_H \le \frac{\Lambda_H}{\mu_H}$; hence,

$$R_{0H} = \frac{\tau\beta_1 \Lambda_H}{(\mu_H + \delta + \eta_1)(\mu_H + \tau)\mu_H} \tag{28}$$

It is obvious that the effective contact rate of the human population β_1 will contribute to the reproduction number in the human population.

In the same vein, we calculate the reproduction number for the vector population R_v

Considering the vector compartment,

$$
\begin{aligned}
D^{\alpha} S_{v}(t) &= \Lambda_V - \mu_V S_V - \Phi_2 S_V \\
D^{\alpha} I_{v}(t) &= \Phi_2 S_V - \mu_V I_V - \eta_2 I_V \\
D^{\alpha} R_{v}(t) &= \eta_2 I_V - \mu_V R_V
\end{aligned} \tag{29}
$$

and

$\Phi_2 = (\frac{\beta_3 I_v}{1+a_v I_v}) S_V$. Note that $a_v = 0$

$$
F_V = \begin{bmatrix} \Phi_2 S_V \\ 0 \end{bmatrix} = \qquad \begin{bmatrix} \frac{\partial F_1}{\partial E_V} & \frac{\partial F_1}{\partial I_V} \\ \frac{\partial F_2}{\partial E_V} & \frac{\partial F_2}{\partial I_V} \end{bmatrix} = \begin{bmatrix} 0 & \beta_1 S_V \\ 0 & 0 \end{bmatrix} \tag{30}
$$

$$
V_V = -(\mu_V + \eta_2) I_V \,,\ \frac{\partial V_V}{\partial I_V} = -(\mu_V + \eta_2)
$$

Using $R_{0v} = \Delta(F_v V_v^{-1}) and \mid F_V V_V^{-1} - \lambda I \mid$,

$R_{0v} = \frac{\beta_3 S_V}{(\mu_V + \eta_2)}$. Recall that $S_V \le \frac{\Lambda_V}{\mu_V}$; therefore,

$$
R_{0v} = \frac{\beta_3 \Lambda_V}{(\mu_V + \eta_2)\mu_V} \tag{31}
$$

It is also obvious that the infection rate of the vector population β_3 will influence the reproduction number in the vector population.

The product of the reproduction number for both human and vector compartments is given as

$$
\begin{aligned}
R_{0HV} &= R_{0V} x R_{0H} = R_{0HV}^2 \\
R_{0HV} &= \sqrt{\frac{\beta_1 \beta_3 \Lambda_V \Lambda_H \tau}{\mu_V \mu_H (\mu_V + \eta_2)(\mu_H + \delta + \eta_1)(\mu_H + \tau)}}
\end{aligned} \tag{32}
$$

The possibility that a human will survive the exposed stage before becoming infectious is $\frac{\tau}{(\mu_H + \tau)}$.

Similarly, $\frac{1}{(\mu_V + \eta_2)}$ is the possibility that vector population might also endure the exposed stage before becoming infectious, where $\frac{1}{(\mu_H + \delta + \eta_1)}$ is the median duration of the infectious time in the human population.

This ends the proof. □

3.6. Local stability analysis of Anthrax at (DFE)

After establishing the existence of a disease-free equilibrium for our proposed model, we will now conduct stability analyses on the system to infer its long-term effects regarding whether or not it is stable.

Theorem 2: If all the population's Jacobian eigenvalues are non-positive (negative) real values, then our system's DFE is locally asymptotically stable If $R_{HV} < 1$.

Proof. In order to establish the theorem above, we calculate the Jacobian of the model's system (11) at its disease-free equilibrium (DFE) E^0.

$$\left.\begin{aligned} F_1 &= \Lambda_H - \mu_H S_H - \Phi_1 S_H + \rho R_H \\ F_2 &= \Phi_1 S_H - \mu_H E_H - \tau E_H \\ F_3 &= \tau E_H - \mu_H I_H - \delta I_H - \eta_1 I_H \\ F_4 &= \eta_1 I_H - \mu_H R_H - \rho R_H \\ F_5 &= \Lambda_V - \mu_V S_V - \Phi_2 S_V \\ F_6 &= \Phi_2 S_V - \mu_V I_V - \eta_2 I_V \\ F_7 &= \eta_2 I_V - \mu_V R_V \end{aligned}\right\} \tag{33}$$

The Jacobian computation is thus

$$J(S_H, E_H, I_H, R_H, S_V, I_V, R_V) \tag{34}$$

$$J=\begin{bmatrix} \frac{\partial F_1}{\partial S_H} & \frac{\partial F_1}{\partial E_H} & \frac{\partial F_1}{\partial I_H} & \frac{\partial F_1}{\partial R_H} & \frac{\partial F_1}{\partial S_V} & \frac{\partial F_1}{\partial I_V} & \frac{\partial F_1}{\partial R_V} \\ . & . & . & . & . & . & . \\ . & . & . & . & . & . & . \\ . & . & . & . & . & . & . \\ \frac{\partial F_7}{\partial S_H} & \frac{\partial F_7}{\partial E_H} & \frac{\partial F_7}{\partial I_H} & \frac{\partial F_7}{\partial R_H} & \frac{\partial F_7}{\partial S_V} & \frac{\partial F_7}{\partial I_V} & \frac{\partial F_7}{\partial R_V} \end{bmatrix} \tag{35}$$

$$J=\begin{bmatrix} -(\mu_H+\Phi_1) & 0 & \frac{\beta_1 S_H}{(1+aI_H)^2} & \rho & 0 & \frac{\beta_2 S_H}{(1+aI_V)^2} & 0 \\ \Phi_1 & -(\mu_H+\tau) & \frac{\beta_1 S_H}{(1+aI_H)^2} & 0 & 0 & \frac{\beta_2 S_H}{(1+aI_V)^2} & 0 \\ 0 & \tau & -(\mu_H+\delta+\eta_1) & 0 & 0 & 0 & 0 \\ 0 & 0 & \eta_1 & -(\mu_H+\rho) & 0 & 0 & 0 \\ 0 & 0 & 0 & 0 & -(\mu_V+\Phi_2) & \frac{\beta_3 S_V}{(1+aI_V)^2} & 0 \\ 0 & 0 & 0 & 0 & \frac{\beta_3 S_V}{(1+aI_V)^2} & -(\mu_V+\eta_2) & 0 \\ 0 & 0 & 0 & 0 & 0 & \eta_2 & -\mu_V \end{bmatrix} \tag{36}$$

Now, at a disease-free equilibrium and introducing our 7 by 7 identity matrix, we have

$$|J-\lambda I|=\begin{bmatrix} -\mu_H-\lambda & 0 & \frac{\beta_1\Lambda_H}{\mu_H} & \rho & 0 & \frac{\beta_2\Lambda_H}{\mu_H} & 0 \\ 0 & -(\mu_H+\tau)-\lambda & \frac{\beta_1\Lambda_H}{\mu_H} & 0 & 0 & \frac{\beta_2\Lambda_H}{\mu_H} & 0 \\ 0 & \tau & -(\mu_H+\delta+\eta_1)-\lambda & 0 & 0 & 0 & 0 \\ 0 & 0 & \eta_1 & -(\mu_H+\rho)-\lambda & 0 & 0 & 0 \\ 0 & 0 & 0 & 0 & -\mu_V-\lambda & \frac{\beta_3\Lambda_V}{\mu_V} & 0 \\ 0 & 0 & 0 & 0 & \frac{\beta_3\Lambda_V}{\mu_V} & -(\mu_V+\eta_2)-\lambda & 0 \\ 0 & 0 & 0 & 0 & 0 & \eta_2 & -\mu_V-\lambda \end{bmatrix} \tag{37}$$

After solving and necessary simplifications of the 7 by 7 Jacobian matrix, we obtain the following eigenvalues:

$$\lambda_1=-\mu_H, \lambda_2=-\mu_V, \lambda_3=-(\mu_H+\rho), \lambda_4=-(\mu_H+\tau), \lambda_5=-((\mu_H+\delta+\eta_1)-\frac{\tau\beta_1\Lambda_H}{(\mu_H+\tau)\mu_H})$$

$$\lambda_6=-(\mu_V+\eta_2) \text{ and } \lambda_7=-\frac{\beta_3\Lambda_V}{\mu_V(\mu_V+\eta_2)}$$

Note that $\lambda_5 = -((\mu_H + \delta + \eta_1) - \frac{\tau\beta_1\Lambda_H}{(\mu_H + \tau)\mu_H})$ can be re-written as

$$\lambda_5 = -(\mu_H + \delta + \eta_1)(1 - \frac{\tau\beta_1\Lambda_H}{\mu_H(\mu_H + \delta + \eta_1)(\mu_H + \tau)})$$

$$\lambda_5 \leq -(\mu_H + \delta + \eta_1)(1 - R_{OH})$$

Similarly, from $\lambda_7 = -\frac{\beta_3\Lambda_V}{\mu_V(\mu_V + \eta_2)} < 1$, the stability holds from λ_5 and λ_7, which shows that $R_{OH} < 1$ *and* $R_{OV} < 1$. Therefore, $R_{HV} < 1$, which substantiates Theorem 1; therefore, the local asymptotical stability holds.

Every eigenvalue of the 7 by 7 dimensional systems is negative (λ1, λ2, λ3, λ4,..., λ7 < 0), indicating that the local stability of the system DFE exists. □

3.7. Global stability (GAS) of the Anthrax model at DFE

Theorem 3. If $R_{HV} < 1$, then model (11) is globally asymptotically stable (GAS) and unstable otherwise.

$$\left.\begin{aligned}
D^\alpha S_H(t) &= \Lambda_H - \mu_H S_H - \Phi_1 S_H + \rho R_H \\
D^\alpha E_H(t) &= \Phi_1 S_H - \mu_H E_H - \tau E_H \\
D^\alpha I_H(t) &= \tau E_H - \mu_H I_H - \delta I_H - \eta_1 I_H \\
D^\alpha R_H(t) &= \eta_1 I_H - \mu_H R_H - \rho R_H \\
D^\alpha S_v(t) &= \Lambda_V - \mu_V S_V - \Phi_2 S_V \\
D^\alpha I_v(t) &= \Phi_2 S_V - \mu_V I_V - \eta_2 I_V \\
D^\alpha R_v(t) &= \eta_2 I_V - \mu_V R_V
\end{aligned}\right\} \quad (38)$$

We start by implementing the method in [35, 45], dividing the system into two distinct parts and also declaring some new variables to verify Theorem 2.

In addition, $E^0 = (S_H^0, E_H^0, I_H^0, R_H^0, S_V^0, I_V^0, R_V^0) = \left(\frac{\Lambda_H}{\mu_H}, 0, 0, 0, \frac{\Lambda_V}{\mu_V}, 0, 0\right)$ is a necessary condition for anthrax-free equilibrium.

Dividing the system, we have

$$F(K,J)=\begin{bmatrix}\Lambda_H-\mu_H S_H-\Phi_1 S_H+\rho R_H\\ \eta_1 I_H-\mu_H R_H-\rho R_H\\ \Lambda_V-\mu_V S_V-\Phi_2 S_V\\ \eta_2 I_V-\mu_V R_V\end{bmatrix},\ G(K,J)=\begin{bmatrix}\Phi_1 S_H-\mu_H E_H-\tau E_H\\ \tau E_H-\mu_H I_H-\delta I_H-\eta_1 I_H\\ \eta_2 I_V-\mu_V R_V\end{bmatrix} \tag{39}$$

where $K=(S_H,R_H,S_V,R_v,)\in R_+^4$ and $J=(E_H,I_H,I_V,)\in R_+^3$, K denoting the set of uninfected and J denoting the set of infected. We say that the point $E^0=(K^*,0)$ is globally asymptotically stable (GAS) if $R_{HG}<1$, $K^*=\left(\frac{\Lambda_H}{\mu_H},0,\frac{\Lambda_V}{\mu_V},0\right)$, denoting the disease-free equilibrium of the subpopulation.

The subsequent conditions hold the following:

$\frac{d^\alpha K}{dt^\alpha}=F(K,0)$, then E^0 is GAS; here, $0<\alpha\le 1$, which is the integer order of our fractional model, and we assume for simplicity that $\alpha=1$

There exist $G(K,J)=BC-G^0(K,J)$ such that $G^0(K,J)\ge 0$, for every $(K,J)\in R_+^7$

Proof. Proof of the first conditions is as follows:

$\frac{dK}{dt}=(K,0)$, for $J=0$, so we have that the infection does not exist in this instance. Remember, J denotes the infected classes, and the system is reduced to

$$F(K,0)=\left.\begin{matrix}\Lambda_H-\mu_H S_H+\rho R_H\\ -\mu_H R_H-\rho R_H\\ \Lambda_V-\mu_V S_V\\ -\mu_V R_V\end{matrix}\right\} \tag{40}$$

It is evident that the first condition holds because this has been obtained earlier while proving the positivity of the model (using Mittag–Leffler); however, the below proof also suffices.

Mini-proof.

$$\frac{dS}{dt}=(\Lambda_H+\rho R_H)-\mu_H S_H, \text{ using the method of } I.F=e^{\int \mu dt}$$

$$\frac{d(S_H e^{\mu_H t})}{dt}=(\Lambda_H+\rho R_H)e^{\mu_H t}$$

$S_H = \frac{\Lambda_H}{\mu_H} + \frac{1}{e^{\mu_H t}} \int \rho R_H e^{\mu_H t} dt$, and as $t \to \infty$, we have that $S_H(t) \to \frac{\Lambda_H}{\mu_H}$. This also goes for the vector population:

$S_V(t) \to \frac{\Lambda_V}{\mu_V}$ as $t \to \infty$, showing that both populations are bounded.

The reduced system for the GAS equilibrium point is $K^* = \left(\frac{\Lambda_H}{\mu_H}, 0, \frac{\Lambda_V}{\mu_V}, 0 \right) = (S_H, R_H, S_V, R_H,)$

Conveying the global convergence and global stability on our model, $F(K,0) \in R_+^7$

This completes the mini-proof. □

Proof. Proof of the second condition.

We need to show that for every $G^0(K, J) \geq 0$, $(K, J) \in R_+^7$, $G(K, J) = BC - G^0(k, J)$.

We have

$$G(K, J) = \frac{dY}{dt}$$

$$G(K, J) = \left.\begin{array}{c} \Phi_1 S_H - \mu_H E_H - \tau E_H \\ \tau E_H - \mu_H I_H - \delta I_H - \eta_1 I_H \\ \Phi_2 S_V - \mu_V I_V - \eta_2 I_V \end{array}\right\} \tag{41}$$

which yields

$$\mathrm{B} = \begin{bmatrix} -(\mu_H + \tau) & 0 & 0 \\ \tau & -(\mu_H + \delta + \eta_1) & 0 \\ 0 & 0 & -(\mu_V + \eta_2) \end{bmatrix} \tag{42}$$

Clearly, all diagonal entries of B are less than unity (i.e., 1) after differentiating with respect to variables in matrix C.

$C = \begin{bmatrix} E_H \\ I_H \\ I_V \end{bmatrix}$, where $G(K, J) = G^0(K, J)$ is the stable state matrix, which establishes the second condition of the GAS.

$$BC = \begin{bmatrix} -(\mu_H + \tau) & 0 & 0 \\ \tau & -(\mu_H + \delta + \eta_1) & 0 \\ 0 & 0 & -(\mu_V + \eta_2) \end{bmatrix} \begin{bmatrix} E_H \\ I_H \\ I_V \end{bmatrix} \tag{43}$$

$$G^0(K, J) = \begin{bmatrix} \Phi_1(\frac{\Lambda_H}{\mu_H} - S_H) \\ 0 \\ \Phi_2(\frac{\Lambda_V}{\mu_V} - S_V) \end{bmatrix} \tag{44}$$

which demonstrate the boundedness of our model, which also substantiate Theorem 2.

This completes the proof. □

3.8. Analysis of the sensitivity of parameters of the Anthrax–Vector model

The main goal of the sensitivity analysis is to ascertain how each variable affects the rate of reproduction. This aids in determining the parameters that have a significant influence on R_{HV}. In order to determine whether or not immunization, mortality, and infection treatments could help in the management or eradication of the disease in the system, the basic reproduction rate is often examined [46]. This technique is widely employed to test the resilience of model assumptions to variable values. The examination of the model's reproduction number R_{HV}, which looks for variance and the impact of changing a parameter on R_{HV}, will be carried out.

Definition 7. *The normalized forward sensitivity index of a variable a is given by*

$$M_b^a = \frac{\partial a}{\partial b} x \frac{b}{a} \tag{45}$$

which depends on the differentiability of parameter *b*.

We would now have to carry out the analysis of the fundamental reproduction number specifically on some key parameters that make up the reproduction number R_{0HV} and with regard to parameters that make up our model.

The sensitivity index for $\beta_1, \beta_2, \beta_3, ...$ and every other parameter will be computed for as follows:

$$R_{0HV} = \sqrt{\frac{\beta_1 \beta_3 \Lambda_V \Lambda_H \tau}{\mu_V \mu_H (\mu_V + \eta_2)(\mu_H + \delta + \eta_1)(\mu_H + \tau)}} \tag{46}$$

Analyzing the derivatives in Equation (47) gives

$$M_{\beta_1}^{R_{HV}} = \frac{\partial R_{HV}}{\partial \beta_1}.\frac{\beta_1}{R_{HV}}, \ \frac{\partial R_{HV}}{\partial \beta_1} = 0.5\frac{R_{HV}}{\beta_1}, \text{ hence}$$

$$M_{\beta_1}^{R_{HV}} = \frac{\partial R_{HV}}{\partial \beta_1}.\frac{\beta_1}{R_{HV}} = 0.5\frac{R_{HV}}{\beta_1}.\frac{\beta_1}{R_{HV}}$$

Conclusively,

$$M_{\beta_1}^{R_{HV}} = +0.5$$

With this, we obtain the sensitivity index for β_1.

In the same vein, we will use this method for all other parameters that make up the reproduction number to obtain their sensitivity index, though not all the parameters have positive values according to Table 2.

Table 2. Parameters and their sensitivity indices (SI).

Parameters	**Sensitivity Indices (S.I)**
Λ_H	+ve
Λ_V	+ve
μ_H	-ve
μ_V	-ve
β_1	+ve
β_3	+ve
β_2	+ve
η	-ve
δ	-ve
τ	+ve

3.9 Interpretation of R_{HV} sensitivity indices

The value of R_{HV} in epidemiological models indicates how easily a disease may spread throughout the community. By calculating the sensitivity indices of R_{HV} with regard to the model's parameter values, we will be able to calculate the decrease in infections caused by the diseases. The contribution of each parameter to the dynamics of the diseases is determined by the sensitivity indices. We determine the sensitivity of R_{HV} to each parameter in model (11), taking into account all of the system's properties.

Table 2 lists the sensitivity indices of R_{HV} for each system parameter in model (11).

A thorough sensitivity analysis of R_{HV} revealed that a rise in η would result in a reduction in R_{HV}. Furthermore, if η were to decrease, R_{0HV} would rise. Moreover, a rise in R_{0HV} implies that there is an increase in the values of $\Lambda_H, \Lambda_V, \beta_1, \beta_2, and \beta_3,$, and a fall in R_{0HV} would result from a decrease in those values, respectively.

4 Numerical simulations

We have reviewed, investigated, and evaluated the analytical/simulated outcomes of the anthrax–vector interactive model in this section. This is completed to confirm the results of our sensitivity analysis, to validate our theoretical conclusions, and to investigate, evaluate, and elucidate the dynamic behavior of the infection in the proposed population. We have simulated the full model and individual compartments using the MATLAB program, taking into account the initial circumstances (state variable values) and changing a few significant model parameters. Tables 3 and 4 present the values and origins of these parameters. Furthermore, the extended Adams–Bashforth–Moulton-type predictor–corrector technique is used to obtain approximate solutions for our fractional ordered model using MATLAB [47]. Time series solutions of system (11) with varying values of *a* are produced using the same parameters given in Table 4 for the population (6000, 1750, 700, 150) for the human population and (100, 70, 0) for the vector population (refer to Figures 14–20) for the simulated results.

Table 3. State variables values and their sources used in simulations.

State Variable	Values	Source
S_H	6000	Assumed
E_H	1750	Assumed
I_H	700	Assumed
R_H	150	Assumed
S_V	100	Assumed
I_V	70	Assumed
R_V	0	Assumed

Table 4. Parameter values and their sources used in simulation.

Parameter	**Values**	**Source**
Λ_H	0.2	[25]
Λ_V	0.005	[25]
μ_H	0.0003466	Assumed
μ_v	0.00261076	Assumed
δ	0.01710615	Assumed
β_1	0.04	Assumed
β_2	0.04	Assumed
β_3	0.005	Assumed
Φ_1	0.091193	Assumed
Φ_2	0.1	Assumed

ρ	0.0090	Assumed
η_1	0.30	Assumed
η_2	0.1	[26]
τ	0.057	[26]
a_H	0.95	Assumed
a_V	0.95	Assumed

While some of these parameters were based on reasonable estimations and assumptions, the majority of them were clinical facts that were taken from reputable studies.

The above tables were derived from Table 1.

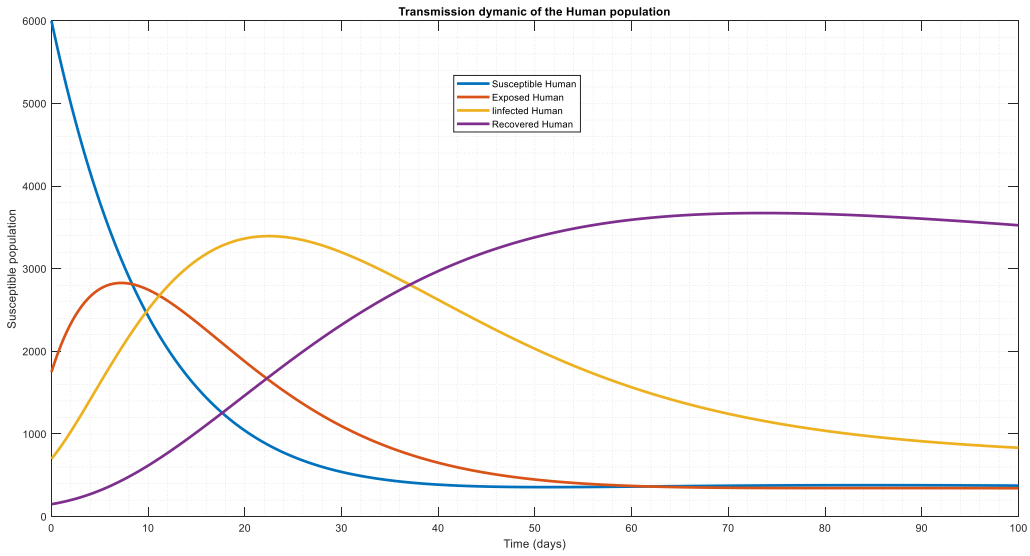


Figure 2. Solution trajectories of the susceptible human population.

The human population dynamical behavior with $\Lambda_H = 0.2$, $\Phi_1 = 0.091193$, $\mu_H = 0.0003466$, $\rho = 0.0085$, $\tau = 0.10$, $\delta = 0.01710615$, and $\eta_1 = 0.30$ demonstrate the coexistence of the compartment and drive the system's tendency toward an endemic condition.

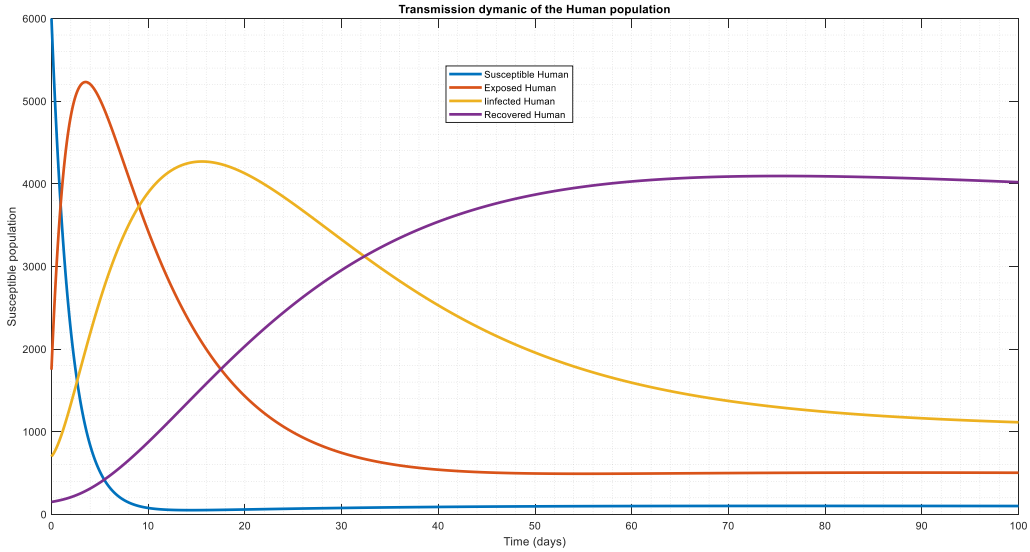


Figure 3. Solution trajectories of the susceptible human population with variations of a few parameters.

Here, the recruitment was increased $\Lambda_H = 12$ and the force of infection $\Phi_1 = 0.5$, while other parameters remain the same, which also shows that all compartments co-exist, causing the population to approach an endemic state, but one thing that is noticeable here is that the susceptible population shows a sharp decline compared to Figure 2.

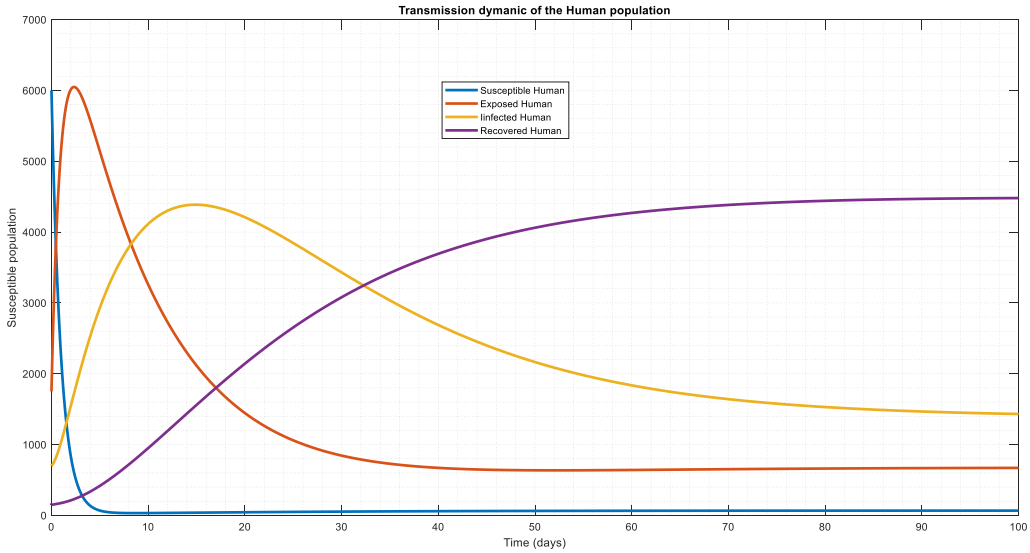


Figure 4. Solution trajectories of the susceptible human population with variations of a few parameters.

Similarly, the recruitment rate was increased a third time, i.e., $\Lambda_H = 25, \Phi_1 = 1$, and again, we notice a sharp decline in the susceptible region, which will hence affect the exposed and the infected, causing the whole population to tend to toward an endemic state.

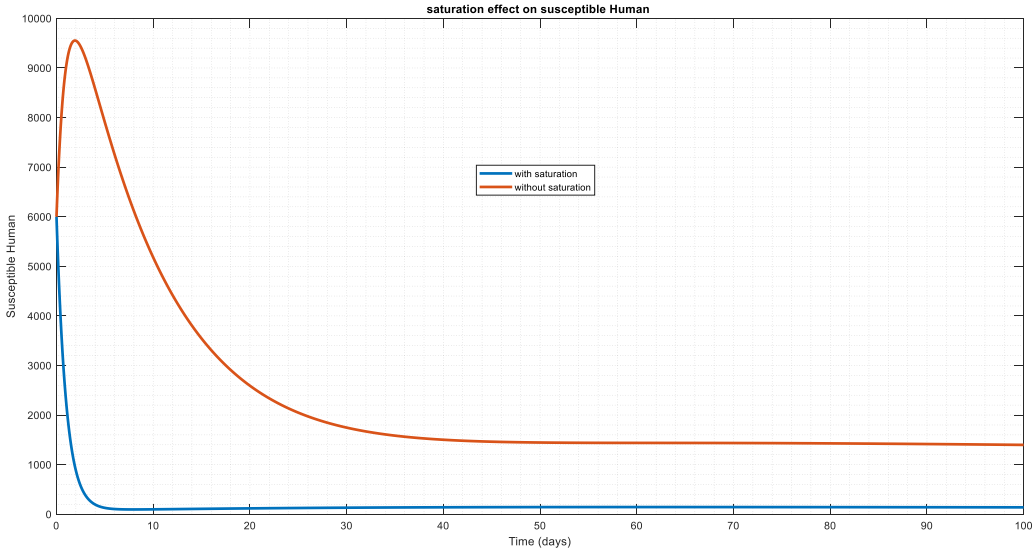


Figure 5. Solution trajectories of the susceptible human population with(out) the saturation factor.

The susceptible humans' changing effects, both with and without the "saturation factor", indicate that the introduction of saturation lowers the incidence of human vulnerability to anthrax.

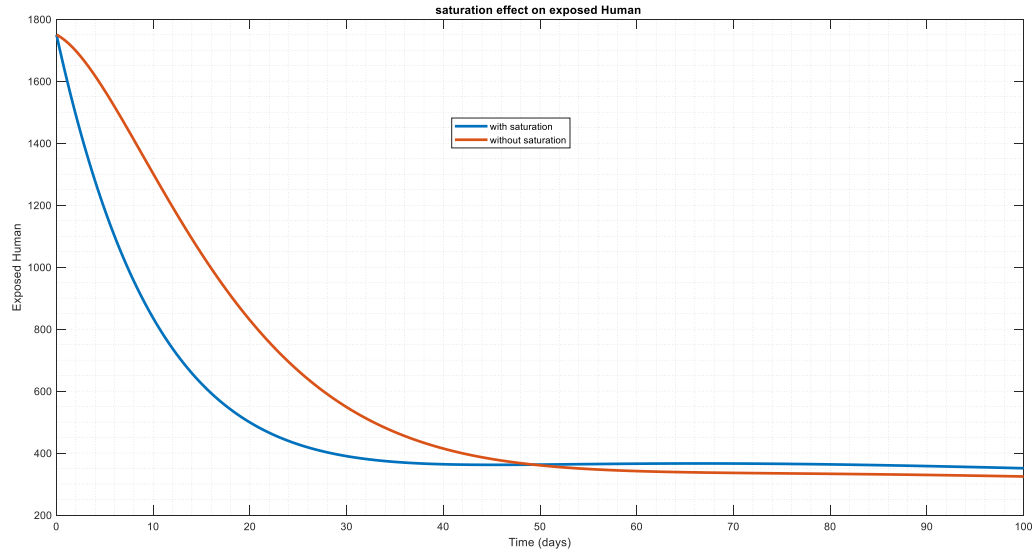


Figure 6. Solution trajectories of the exposed human population with(out) the saturation factor.

The exposed humans' changing effects, both with and without the "saturation factor", indicate that the introduction of saturation lowers the incidence of exposed compartments to anthrax.

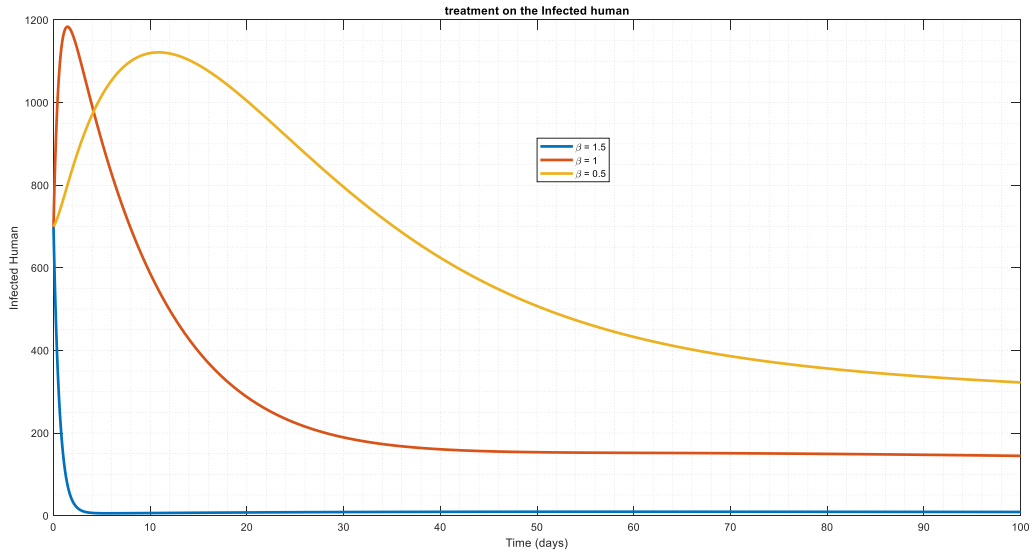


Figure 7. Solution trajectories of the infected human population with proper treatment by doubling and tripling the effect.

The effect of increasing the rate of treatment for infected individuals using vaccination administration (along with other essential treatments) demonstrates how early antiviral medication administration and implementation may significantly reduce the population of the infected in the infected human compartment.

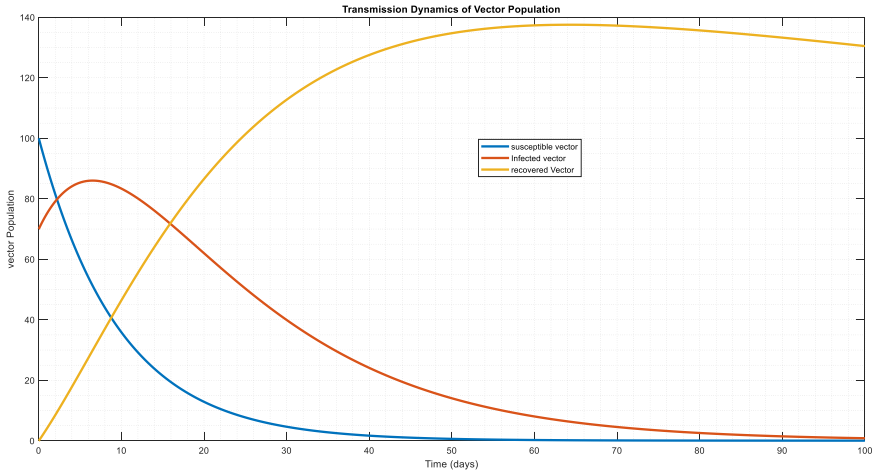


Figure 8. Solution trajectories of the susceptible vector.

The dynamical behavior of the vector population with $\Lambda_V = 0.005$, $\Phi_2 = 0.1$, $\delta = 0.00261076$, $\eta_2 = 0.057$ shows how the compartments co-exist, in which, in essence, the vector population tends towards an endemic state.

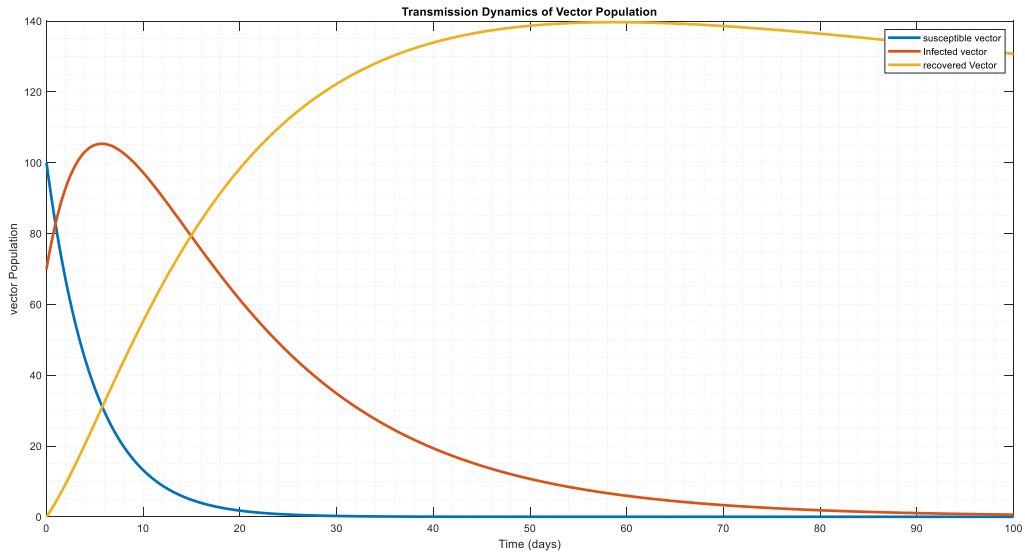


Figure 9. Solution trajectories of the susceptible vector while doubling the force of infection.

In the above figure, $\Phi_2 = 0.2$, we doubled the force of infection; while other parameters remain the same, we notice a sharp decline in the susceptible class, which changes the behavior of the population as a whole.

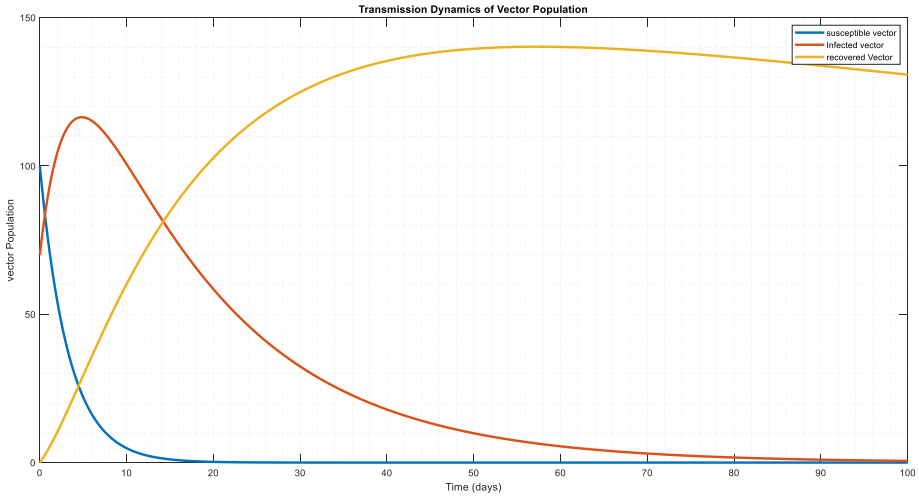


Figure 10. Solution trajectories of the susceptible vector while tripling the force of infection.

In the above figure, $\Phi_2 = 0.3$ to see how the population behaves; while other parameters remain same, we notice a sharp decline in the susceptible class, which changes the behavior of the population as a whole.

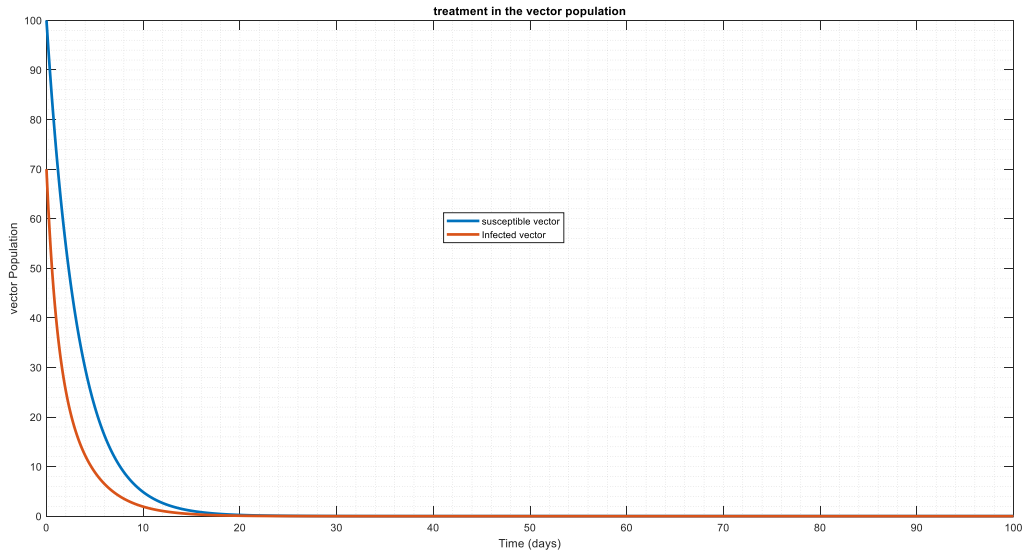


Figure 11. Solution trajectories of the susceptible and the infected vector while implementing the control plan.

Here, we try to introduce an effective control plan to the vector population (domestic), with $\Lambda_V = 0.005$, $\Phi_2 = 0.3$. The figure above shows that the vector population can approach a disease-free equilibrium (DFE), especially the susceptible and infected populations.

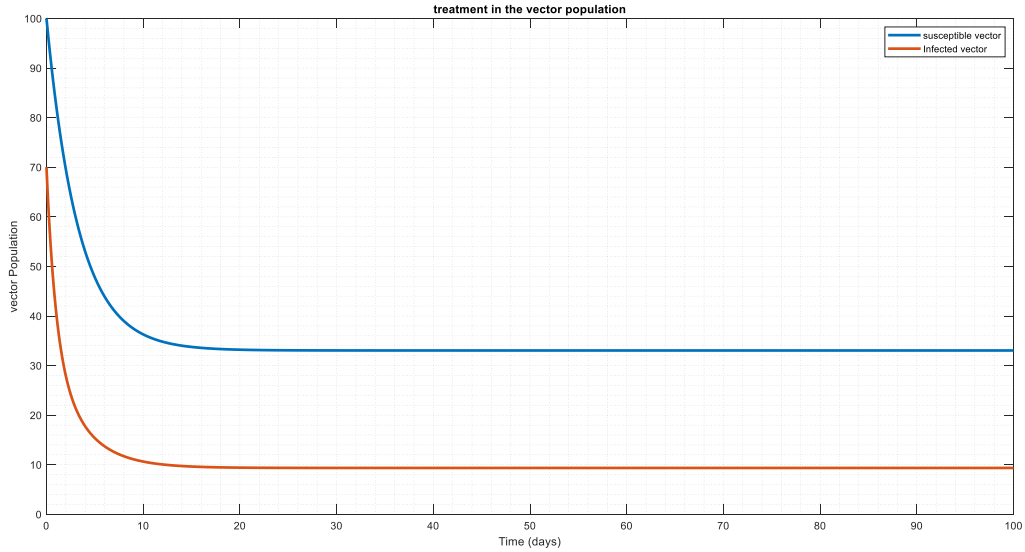


Figure 12. Solution trajectories of the susceptible and the infected vector while implementing a control plan by increasing the recruitment rate.

In the figure above, the vector recruitment rate was increased to $\Lambda_V = 10$; while other parameters remain the same, we noticed that, irrespective of the susceptible number to the system, with effective control strategies, the vector population will still attain a DFE.

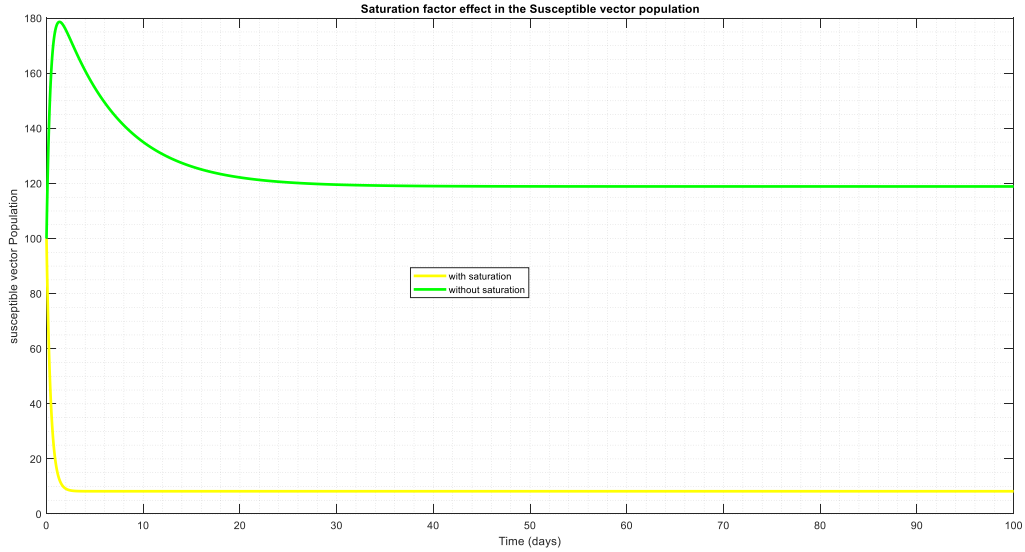


Figure 13. Solution trajectories of susceptible vector population with(out) saturation.

The susceptible vector changing effects, both with and without the "saturation factor", indicate that the introduction of saturation lowers the incidence of vector vulnerability to anthrax.

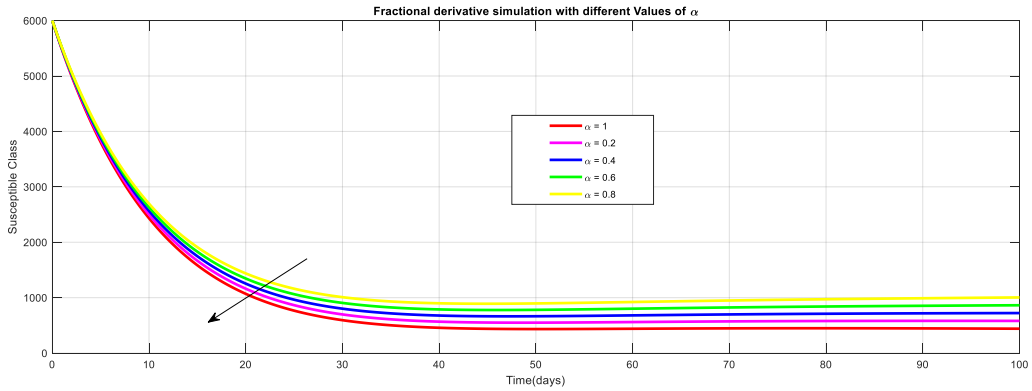


Figure 14. The fractional derivative variation simulation on susceptible human populations.

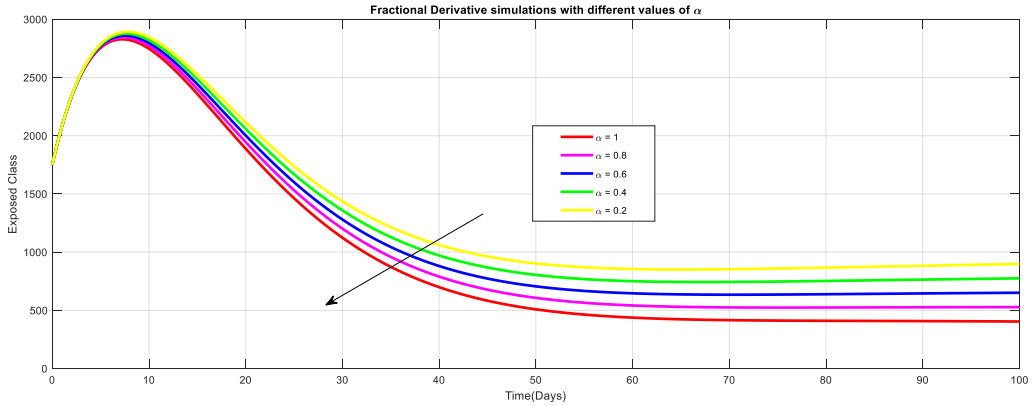


Figure 15. The fractional derivative variation simulation on exposed human populations.

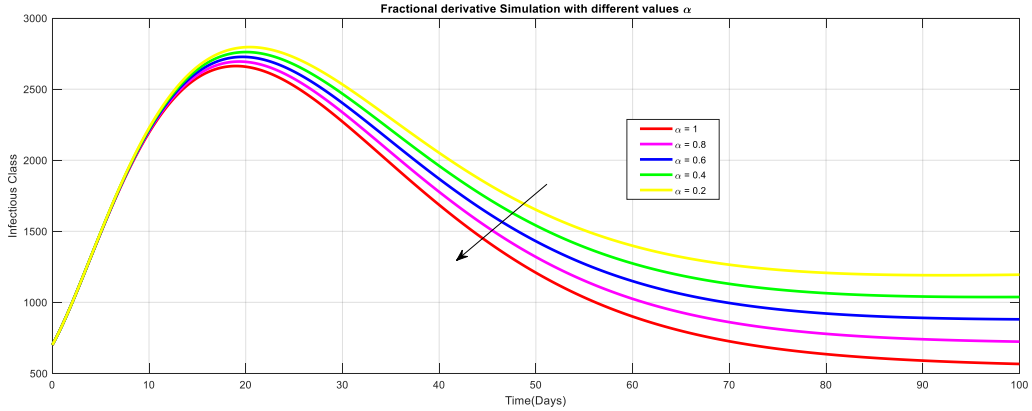


Figure 16. The fractional derivative variation simulation on infected human populations.

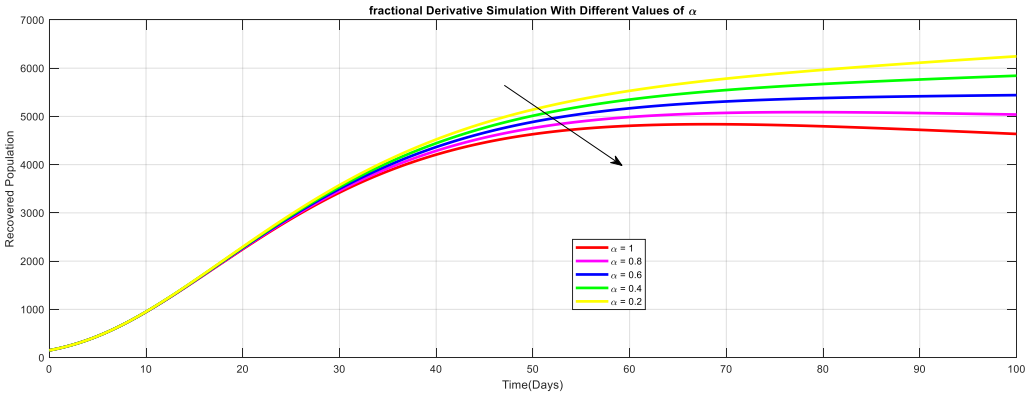


Figure 17. The fractional derivative variation simulation on recovered human populations.

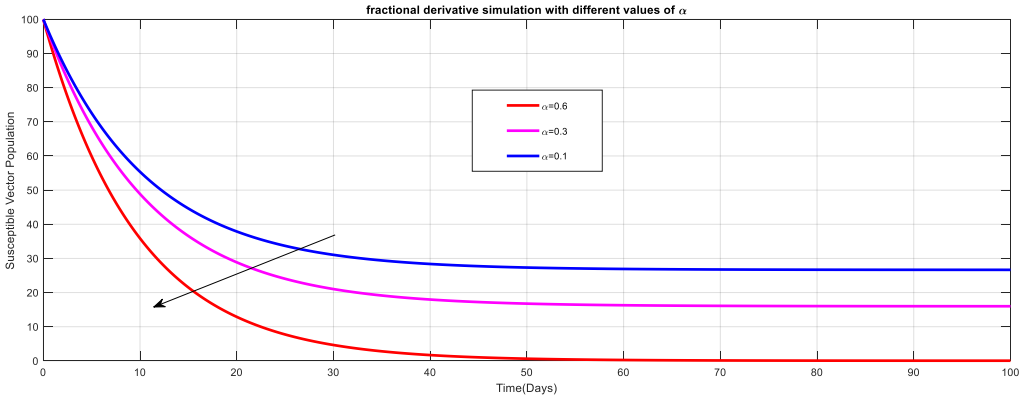


Figure 18. The fractional derivative variation simulation on susceptible vector populations.

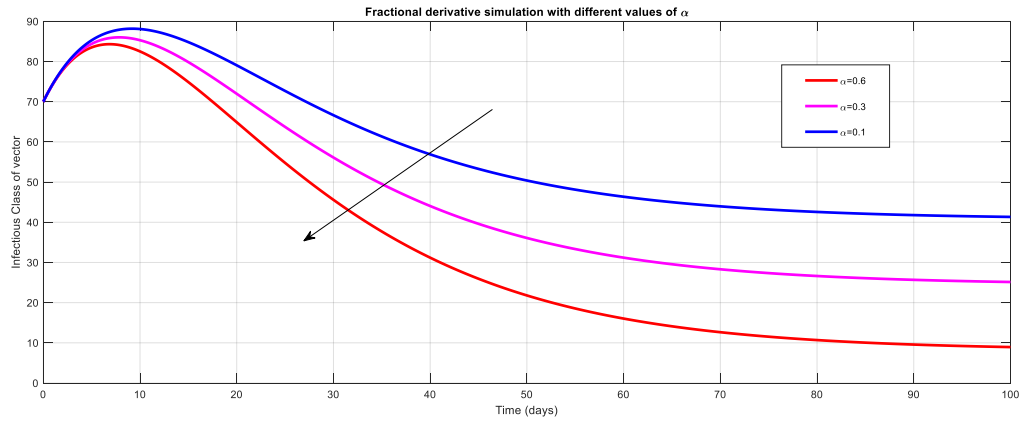


Figure 19. The fractional derivative variation simulation on infected vector populations.

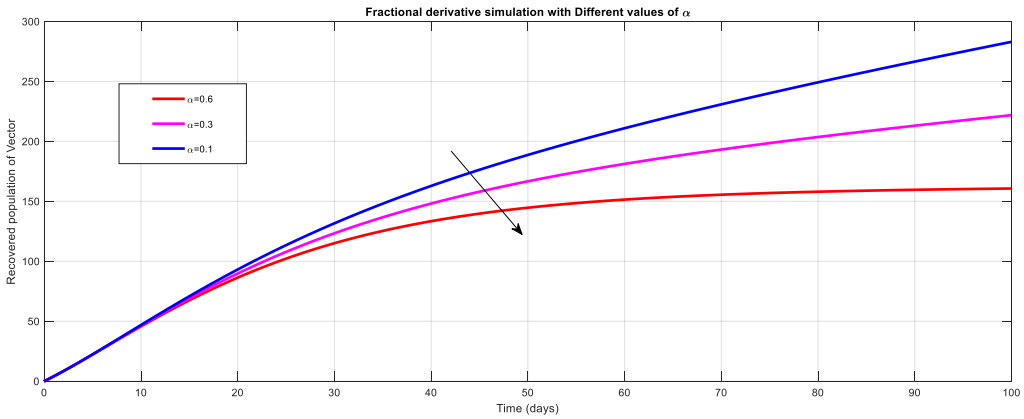


Figure 20. The fractional derivative variation simulation on recovered vector populations.

5. Discussions and conclusion

Using the values on Tables 3 and 4 alongside the parameters, we have simulated the model. We now must adjust a few of these factors on the above table in order to see the changes (behavior) in our model.

Using the initial conditions and parameter values from Tables 3 and 4, the merged graphs of the whole human population are shown in Figure 1. The section of exposed and infected humans increases during the starting phase (instantaneous time); however, over time, both the exposed and the infected reach a stable state as a result of the system's dynamic behavior, as shown in Figure 1. The human population begins to recover after a while; however, during the early phase, the whole system tends to be vulnerable, demonstrating the mathematical epidemiology of our model (which tends towards endemic conditions).

The dynamic behavior of each human compartment is depicted in Figure 3 when the infection force Φ_1 and the human immigration rate Λ_H are varied. By changing these parameters, we found that people become increasingly exposed to the virus and become sick; the population of susceptible people declines dramatically and abruptly in less than ten (10) days compared to Figure 1, although people generally recover within ninety days. These all demonstrate how the system is approaching an endemic condition since every compartment coexists in it.

The system's behavior when the immigration rate is raised and the infection force is $\Phi_1 = 1$ is unity, as seen in Figure 4. The human system is exposed very quickly at one point in time, again demonstrating the mathematical epidemiology of our model, and after a month (30 days), the infected human population likewise grows at a steady rate, leading to a sharp decline in the susceptible population below 10 days.

In Figures 5 and 6, the dynamic of the exposed and susceptible humans reveals that when "saturation" occurs, the populations of these humans are drastically reduced, leading the system to approach stability (DFE). This could be caused by various control measures, such as hunting wild animals with the infection in the instance of the vector population, as seen in Figure 13;

immune responses to the infection; or the early management of medications, such as vaccination (and other necessary interventions) in both populations.

For the vector system's dynamic behavior in Figures 8–10, in relation to the starting conditions and parameter figures on Tables 3 and 4, we double and triple the infection force for Figures 9 and 10, respectively. This indicates that the vector tends to be exposed at a single moment, resulting in infection in lesser periods of 30, 20, and 10 days apart; however, the population of the infected eventually reaches a stable state, and the population of the susceptible disappear over time, leaving only the population of the infected in the system.

Figure 7 presents a control strategy that aims to flatten the spread of disease among the infected human population. The therapy is modified by doubling and tripling its effect over time; hence, the system tends towards a DFE state. That is a disease-free system.

Since vectors are the carriers of the disease, we aim to minimize the rate at which humans will contract it by introducing an effective control plan in susceptible vector and infected vector populations (Figures 11 and 12). Additionally, Figure 12 illustrates that, regardless of the number of susceptible vector populations, an effective control plan will eventually cause the population to reach a disease-free system.

Figures 14–20 illustrates the constantly changing complexity of the fractional ordinary differential equations, highlighting their enhanced capability as descriptors for biological phenomena in comparison to the ordinary differential equation models. Additionally, the model's solutions, which depend on the continuously changing time-fractional derivative, consistently converge to equilibrium points, which in turn aid the stability in each simulated compartment.

5.1 Conclusion

The present study examines an unprecedented interactive anthrax–vector model, constructed on a seven-dimensional nonlinear system of fractional differential equations, with the aim of characterizing and capturing the dynamics of the anthrax infection's propagation. Stability, boundedness, positivity, and sensitivity analyses have been provided for this model. Importantly, we have used clinical, approximated, and assumed data from the well-known literature to run the model.

We draw the conclusion from our data and research that the system approaches an anthrax-free equilibrium instantaneously when "saturation" occurs (which may be caused by treatments or control measures impeding the virus's spread in a vulnerable population). In other words, the mass elimination of the disease would be greatly aided by the execution of a suitable management strategy (treatment and other medical interventions).

Furthermore, based on the stability and sensitivity study, the vector recruitment rate Λ_V and the effective contact rates ($\beta 1$, β_2, $\beta 3$) that result in anthrax infection are the most sensitive parameters that need to be addressed by the control organization (health officials). Because of this, the regulated basic reproduction number would continue to be less than unity (1).

Additionally, we recommend that early intervention and prompt treatment with a "recommended diagnosis" be used to increase the effectiveness and expand the capacity of

treatment in order to instantly eradicate the disease. People should also make every effort to maintain maximum hygiene and a clean environment in order to avoid providing a breeding ground for *Bacillus anthracis* within homes and among animal populations (domestic); this could be accomplished through public awareness campaigns and sensitization to the anthrax infection.

References

[1] Osman, S.; and Makinde, O.D. (2018). A Mathematical Model for Co-Infection of Listeriosis and Anthrax Diseases. Int. J. Math. Math. Sci., 1725671. https://doi.org/10.1155/2018/1725671.

[2] Samad; M.A. (2013). Public Health Threat Caused by Zoonotic Diseases in Bangladesh. Bangladesh J. Vet. Med. 9, 95–120. https://doi.org/10.3329/bjvm.v9i2.13451.

[3] Agbomola J O., and Loyinmi A C. (2022). Modelling the impact of some control strategies on the transmission dynamics of Ebola virus in human-bat population: An optimal control analysis. Heliyon, 8:e12121. https://doi.org/10.1016/j.heliyon.2022.e12121.

[4] Idowu O K., and Loyinmi A C. (2023). Qualitative analysis of the transmission dynamics and optimal control of covid-19. EDUCATUM Journal of Science, Mathematics and Technology 10(1), 54-70. https://doi.org/10.37134/ejsmt.vol10.1.7.2023.

[5] Survely, A.N., Kvasnicka, B., and Torell, R. (2001). Anthrax:a Guide for Livestock Producers. Western Beef Resource Committee. Available online: https://extension.colostate.edu/docs/pubs/ag/anthraxguide.pdf (accessed on 20 February 2024).

[6] Baldacchino, F., Muenworn, V., Desquesnes, M., Desoli, F., Charoenviriyaphap, T., and Duvallet, G. (2013). Transmission of pathogens by Stomoxys flies (Diptera, Muscidae): A review. Parasite *20*, 26. https://doi.org/10.1051/parasite/2013026.

[7] Lewerin, S.S., Elvander, M., Westermark, T., Hartzell, L.N., Norstrom, A.K., Ehrs, S., Knutsson, R., Englund, S., Andersson, A. C., and Granberg, M. (2010). Anthrax outbreak in a Swedish beef cattle herd-1st case in 27years: Case report. Acta Vet. Scand. *52*, 7. https://doi.org/10.1186/1751-0147-52-7

[8] Good, K.M., Marobela, C., and Houser, A.M. (2005). A report of anthrax in cheetahs (Acinonyx jubatus) in Botswana. J. S. Afr. Vet. Assoc. 76, 186. https://doi.org/10.10520/EJC99644.

[9] Lembo, T., Hampson, K., Auty, H., Beesley, C.A., Bessell, P., Packer, C., Halliday, J., Fyumagwa, R., Hoare, R., and Ernest, E. (2011) Serologic surveillance of anthrax in the Serengeti ecosystem, Tanzania, 1996–2009. Emerg. Infect. Dis. 17, 387–394. https://doi.org/10.3201/eid1703.101290.

[10] World Health Organization. Food and Agriculture Organization of the United Nations & World Organisation for Animal Health. In *Anthrax in Humans and Animals*, 4th ed.; World Health Organization: Geneva, Switzerland, 2008. Available online: https://apps.who.int/iris/handle/10665/97503 (accessed on 20 February 2024).

[11] Thapa, N.K., Tenzin, W.K., Dorji, T., Migma, D.J., Marston, C.K., and Hoffmaster, A.R. (2014). Investigation and control of anthrax outbreak at the human-animal interface, Bhutan, 2010. Emerg. Infect. Dis. 20, 1524–1526. https://doi.org/10.3201/eid2009.140181.

[12] Ahmed, B., Sultana, Y., Fatema, D.S.M., Ara, K., Begum, N., Mostanzid, S.M., and Jubayer, S. (2010). Anthrax: An emerging zoonotic disease in Bangladesh. Bangladesh J. Med. Microbiol. *4*, 4650. https://doi.org/10.3329/bjmm.v4i1.8470.

[13] Nayak, P., Sodha, S.V., Laserson, K.F., Padhi, A.K., Swain, B.K., Hossain, S.S., Shrivastava, A., Khasnobis, P., Venkatesh, S.R., and Patnaik, B. (2019). A cutaneous Anthrax outbreak in Koraput district of OdishaIndia 2015. BMC Public Health 19, 470. https://doi.org/10.1186/s12889-019-6787-0.

[14] Eustace, K.A.., Osman, S. and Wainaina, M. (2018). Mathematical Modelling and Analysis of the Dynamics of Cholera. Glob. J. Pure Appl. Maths. 14, 1259–1275.

[15] Muia, D.W., Osman, S. and Wainaina, M.(2018). Modelling and Analysis of Trypanosomiasis Transmission Mechanism. Glob. J. Pure Appl. Maths. 14, 1311–1331.

[16] Lotka, A.J. (1925). Elements of Physical Biology; Williams & Wilkins: Baltimore, MD, USA.

[17] Volterra, V. (1928). Variations and fluctuations of a number of individuals in animal species living together. ICES J. Mar. Sci. 3, 3–51. https://doi.org/10.1093/icesjms/3.1.3.

[18] Loyinmi, A C, Akinfe T K. and Ojo A A, (2021). Qualitative analysis and dynamical behavior of a Lassa haemorrhagic fever model with exposed rodents and saturated incidence rate. Sci. African, 14 e01028. https://doi.org/10.1016/j.sciaf.2021.e01028.

[19] Kermack, W.O. and McKendrick, A.G. (1927). A contribution to the mathematical theory of epidemics. Proc. R. Soc. Lond. 115, 700–721. https://doi.org/10.1098/rspa.1927.0118.

[20] Osman, S., Musyoki, E.A. and Ndungu, R.M. (2019). A Mathematical Model for the transmission of Measles with passive Immunity. Int. J. Res. Math. Stat. Sci. 6, 1–8.

[21] Karunditu, J.W., Kimathi, G. and Osman, S. (2019). Mathematical Modeling of Typhoid Fever Disease Incorporating Unprotected Humans in the Spread Dynamics. J. Adv. Math. Comput. Sci. 32, 1–11. https://doi.org/10.9734/jamcs/2019/v32i330144.

[22] Gumel; A.B. and Moghadas, S.M. (2003). A Qualitative Study of a Vaccination Model with Non-Linear Incidence. Appl. Math. Comput. 143, 409–419. https://doi.org/10.1016/S0096-3003(02)00372-7.

[23] Kar; T.K. and Batabyal. (2011). A. Stability Analysis and Optimal Control of an SIR Epidemic Model with Vaccination. Biosystems 104, 127–135. https://doi.org/10.1016/j.biosystems.2011.02.001.

[24] Hahn, B.D. and Furniss, P.R. (1981). A mathematical model of anthrax epizootic in the Kruger National Park. Appl. Math. Model. 5, 130–136. https://doi.org/10.1016/0307-904X(81)90034-2.

[25] Hahn, B.D. and Furniss, P.R. (1983). A deterministic model of anthrax epizootic: Threshold results. Ecol. Model. 20, 233–241. https://doi.org/10.1016/0304-3800(83)90009-1.

[26] Friedman, A. and Yakubu, A.A. (2013). Anthrax epizootic and migration: Persistence or extinction. Math. Biosci. 241, 137–144. https://doi.org/10.1016/j.mbs.2012.10.004.

[27] Mushayabasa, S. (2015). Global stability of an anthrax model with environmental decontamination and time delay. Discret. Dyn. Nat. Soc. 573146. https://doi.org/10.1155/2015/573146.

[28] Mushayabasa, S., Marijani, T. and Masocha, M. Dynamical analysis and control strategies in modeling anthrax. *Comput. Appl. Math.* **2017**, *36*, 1333–1348. https://doi.org/10.1007/s40314-015-0297-1.

[29] Kimathi, G. and Wainaina, M. (2019). Analysis of transmission dynamics of anthrax in animals: A modeling approach. J. Sci. Res. Rep. 23, 1–9. https://doi.org/10.9734/jsrr/2019/v23i130111.

[30] Osman, S., Otoo, D., Sebil, C. and Makinde, O.D. (2020). Bifurcation, sensitivity and optimal control analysis of modelling anthrax-listeriosis co-dynamics. Commun. Math. Biol. Neurosci. 98. https://doi.org/10.28919/cmbn/5161.

[31] Rezapour, S., Etemad, S. and Mohammadi, H. (2020). Mathematical analysis of a system of Caputo-Fabrizio fractional differential equations for the anthrax disease modeling animals. Adv. Differ. Equations, 481. https://doi.org/10.1186/s13662-020-02937x.

[32] Khan, M.A. and Atangana, A. (2020). Modeling the dynamics of novel coronavirus (2019-nCov) with fractional derivative. Alex. Eng. J. 59, 2379–2389. https://doi.org/10.1016/j.aej.2020.02.033.

[33] World Health Organization. (2008). Anthrax in Humans and Animals. https://www.who.int/publications-detail-redirect/9789241547536 (accessed on 4 February 2024).

[34] Jauro, S., Ndumnego, O.C., Ellis, C., Buys, A., Beyer, W. and Van Heerden, H.V. (2020). Immunogenicity and protective efficacy of a non-living anthrax vaccine versus a live spore vaccine with simultaneous penicillin-G treatment in cattle. Vaccines *8*, 595. https://doi.org/10.3390/vaccines8040595.

[35] Loyinmi, A. C. (2024). A fractional order model for zika virus transmission dynamics: analysis, control strategies, and simulation insights. *F*NAS Journal of Scientific Innovations 6(1), 84-108.

[36] Sidwa, T., Salzer, J.S., Traxler, R., Swaney, E., Sims, M.L., Bradshaw, P., O'Sullivan, B.J., Parker, K., Waldrup, K.A. and Bower, W.A. (2020). Control and prevention of anthrax, Texas, USA, 2019. Emerg Infect Dis. *26*, 2815–2824. https://doi.org/10.3201/eid2612.200470.

[37] Hendricks, K.A., Wright, M.E., Shadomy, S.V., Bradley, J.S., Morrow, M.G., Pavia, A.T., Rubinstein, E., Holty, J.-E.C., Messonnier, N.E. and Smith, T.L. (2014). Centers for Disease Control and Prevention expert panel meetings on prevention and treatment of anthrax in adults. Emerg. Infect. Dis. 20, e130687. https://doi.org/10.3201/eid2002.130687.

[38] Mikucki, M.A. (2012). Sensitivity Analysis of the Basic Reproduction Number and other Quantities for Infectious Disease Models. Master's Thesis, Department of Mathematics, Colorado State University, Fort Collins, CO, USA.

[39] Podlubny, I. (1999). Fractional Differential Equations. In Volume 198 of Mathematics in Science and Engineering; Academic Press: San Diego, CA, USA.

[40] Furati; K.M., Iyiola; O.S. and Mustapha, K. (2017). An inverse source problem for a twoparameter anomalous diffusion with local time datum. Comput. Math. Appl. 73, 1008–1015.
[41] Castillo-Chavez, C., Feng, Z. and Huang, W. (2001). On the computation of Ro and its role on global stability. Biom. Unit Tech. Rep.**6**, 1–18.
[42] Leroy, E.M., Kumulungui, B., Pourrut, X., Rouquet, P., Hassanin, A., Yaba, P., Délicat, A., Paweska, J.T., Gonzalez, J.-P. and Swanepoel, R. (2005). Fruit bats as reservoirs of Ebola virus. Nature 438, 575–576.
[43] Diekmann, O., Heesterbeek, J.A.P. and Metz, J.A.J. (1990). On the definition and the computation of the basic reproduction ratio R_0 in models for infectious diseases in heterogeneous populations. J. Math. Biol. 28, 365–382. https://doi.org/10.1007/BF00178324.
[44] Driessche, P.V. and Watmough, J. (2002). Reproduction numbers and sub-threshold endemic equilibria for Compartmental models of disease transmission. Math. Biosci. 180, 29–48.
[45] Baloba, E.B. and Seidu, B. (2022). A mathematical model of anthrax epidemic with behavioral change. J. Math. Model. Control *2*, 243–256. https://doi.org/10.3934/mmc.2022023.
[46] Osman, S., Makinde, O.D. and Theuri, D.M. (2018). Stability Analysis and Modelling of Listeriosis Dynamics in Human and Animal Populations. Glob. J. Pure Appl. Maths. 14, 115–137.
[47] Garrappa, R. (2018). Numerical solution of fractional differential equations: A survey and a software tutorial. Mathematics 6, 16. https://doi.org/10.3390/math6020016.

An infection-age-structured modelling for Monkey-Pox disease dynamics incorporating control measures

N.O. Lasisi [*†], O.J. Ejiwole [‡], E. Azuaba[†§], and A. A. Ibrahim[†]**

Abstract

Monkey-pox is known as pathogens affecting livestock animals and humans and belongs to the orthopox virus. The pathogen causes lymph nodes to swell and increasing transmission risk associated with factors involving introduction of virus to the oral mucosa. In this paper, we developed an Age-Structured model for Monkey-pox disease in a population with vital dynamics, incorporating standard incidence rate and vaccination. We showed the existence and uniqueness of the solution of the model. We obtained the Disease-Free Equilibrium state and shown the effective reproduction number of the model. We proved the conditions for Local and Global Stability of the Disease-Free Equilibrium (DFE) State and we found that the disease free equilibrium state is locally asymptotically stable if $G(0) < 1$ ($R_E < 1$) and Globally Asymptotically Stable (GAS) in Ω if $R_E \leq 1$ while unstable if $R_E \geq 1$.

Keywords: disease-free equilibrium; mathematical modeling; Monkey Pox disease

1 Introduction

Monkey pox, Small pox and Cow pox diseases belong to the family of orthopox viruses cause infection in humans and primates [1]. Monkey pox causes lymph nodes to swell up. The symptoms are fever, headache, muscle aches, backache, swollen lymph nodes, a feeling of discomfort and exhaustion. The virus spread to humans from an infected animal (rodents) through direct contact, animal bite and eating infected animal meats without proper done or cook. The virus spread from infected human to human, less infectious than small pox virus, transmitted by direct contact with body fluids of an infected person, contaminated objects and sexual intercourse. The risk factors for transmission include sharing a bed, room, or using the same utensils as an infected patient. Increased

[*]Corresponding Author; E-mail: *nurudeenlasisi2009@yahoo.com*
[†]Department of Statistics, Federal Polytechnic, Kaura Namoda, Nigeria.
[††] Department of Statistics, Federal Polytechnic, Kaura Namoda, Nigeria
[‡‡] Department of Mathematical Sciences, Bingham University, Karu, Nasarawa State, Nigeria.
[##] enitioluwafe2012@gmail.com
[†§] emmanuel.azuaba@binghamuni.edu..ng
[†**] Department of Statistics, Federal Polytechnic, Kaura Namoda, Nigeria E-mail: ibrahimabdukareema@fedponam.edu.ng.com

transmission risk associated with factors involving introduction of virus to the oral mucosa. [2]. Presently, there are no vaccines for monkey pox, however evidence showed that small pox vaccine reduced the risk of monkey pox among previously vaccinated persons in Africa [3]. The incubation period is 7–14 days, the illness lasted for 2 to 4 weeks [1] and the fatality ratio is 1% to 10%. [4]. Therefore, there is non-numerous work on mathematical modeling of monkey pox. This paper reviewed the work of [5]. The organization of paper is as follows, in the next section; the formulation of monkey pox model is presented, Existence and Uniqueness of Solution of the Model, Effective Reproduction Number, Local Stability of the Disease Free Equilibrium (DFE) State, Global Stability of the DFE State are presented and analyzed.

2 Model formulation

We formulate a model for the spread of Monkey-pox disease in human and Monkey population. This study reviewed the work of [6] on a model the dynamics of monkey-pox by incorporating the Age-of-Infection to the dynamic of monkey-pox disease. The populations are compartmentalized into epidemiological classes. The total human population is divided into four subgroups that is the Susceptible, $S_h(t)$, the Vaccinated, $V_h(t)$, the Infected, $I_h(t)$, and the Recovery with permanent immunity, $R_h(t)$. The total Monkey population model is divided into the Susceptible, $S_p(t)$, the Vaccinated, $V_p(t)$, the Infected primates, $I_p(t)$, and the recovery with permanent immunity, $R_p(t)$. As shown in the model, people enter Susceptible class through birth and immigration, (Π_h), where a proportion of vaccinated human immigrants (f) enter to the vaccinated class and proportion of unvaccinated immigrants (1-f) enter to the susceptible class. We do not consider the immigration of infection person, because we assume that people who are coming from monkey-pox endemic zones have to be vaccinated. The susceptible human individuals vaccinated at the rate $\gamma_h$and loss the vaccination at the rate ω_h. Susceptible human, S_h are exposed to monkey-pox infection at the rate α_h and are infected at the rate β_h, with natural death μ_h and die due to the infection at the rate δ_h and recovery with permanent immunity at a rate ρ_h. The Susceptible primates, S_p class is generated from the daily recruitment of individuals through birth and immigration at the Π_p and natural death rate μ_p. The susceptible primate individuals vaccinated at the rate $\gamma_p$and loss the vaccination at the rate ω_p and leave the class to infected class at the rate β_p. Individual primate infected die due to the infection at the rate δ_p and recovery with the permanent immunity at the rate ρ_p. Base on the assumptions and explanation, the model for transmission dynamics of Monkey-pox infection in human and primates (Monkey) is described by a system of both Ordinary and Partial Differential Equations (ODE/PDE) and nonlinear integro-partial differential equations given below:

$$\frac{dS_h}{dt} = (1-f)\Pi_h + \omega_h V_h - \gamma_h S_h - [\frac{\sigma_p I_p}{N_p} + \frac{\sigma_h I_h}{N_h}]S_h - \mu_h S_h \tag{1}$$

$$\frac{\partial i_h(t,\tau)}{\partial t} + \frac{\partial i_h(t,\tau)}{\partial \tau} + (\mu_h + \delta_h + e_h)i_h(t,\tau) = 0 \tag{2}$$

$$\frac{dV_h}{dt} = f\Pi_h + \gamma_h S_h - \omega_h V_h - \mu_h V_h \tag{3}$$

$$\frac{dR_h}{dt} = e_h I_h - \mu_h R_h \tag{4}$$

$$\frac{dS_p}{dt} = (1-g)\Pi_p + \omega_p V_p - \gamma_p S_p - \frac{\sigma_p I_p}{N_p} S_p - \mu_p S_p \tag{5}$$

$$\frac{\partial i_p(t,\tau)}{\partial t} + \frac{\partial i_p(t,\tau)}{\partial \tau} + (\mu_p + \delta_p + e_p) i_p(t,\tau) = 0 \tag{6}$$

$$\frac{dV_p}{dt} = g\Pi_p + \gamma_p S_p - \omega_p V_p - \mu_p V_p \tag{7}$$

$$\frac{dR_p}{dt} = e_p I_p - \mu_p R_p \tag{8}$$

with boundary conditions

$$B_h = i_h(t,0) = \frac{\sigma_p I_p S_h}{N_p} + \frac{\sigma_h I_h S_h}{N_h} \;\; \& \;\; B_p = i_p(t,0) = \frac{\sigma_p I_p S_p}{N_p} \tag{9}$$

and initial condition

$$i_h(0,\tau) = i_h(\tau) = \psi_h \;\; \& \;\; i_p(0,\tau) = i_p(\tau) = \psi_p \tag{10}$$

where, $I_h = \int_0^T i_h(t,\tau)d\tau$ and $I_p = \int_0^T i_p(t,\tau)d\tau$ (11)

T is the maximum infection age and if $\tau = T$ the infected person die, then implies

$i_h(t,T) = 0$ and $i_p(t,T) = 0$. (12)

Integration of (2) over τ give,

$$\frac{dI_h}{dt} = \frac{\sigma_p I_p S_h}{N_p} + \frac{\sigma_h I_h S_h}{N_h} - (\mu_h + \delta_h + e_h) I_h \tag{13}$$

Similarly, integrating (6) over τ

$$\int_0^T \left(\frac{\partial i_p(t,\tau)}{\partial t} + \frac{\partial i_p(t,\tau)}{\partial \tau}\right) d\tau + \int_0^T (\mu_p + \delta_p + e_p) i_p(t,\tau) d\tau = 0 \tag{14}$$

Implies, $\frac{dI_p}{dt} = \frac{\sigma_p I_p S_p}{N_p} - (\mu_p + \delta_p + e_p) I_p$. (15)

3 Analysis of the model

3.1 Existence and Uniqueness of Solution for the Model

We prove the existence and uniqueness of the solution of the problems (2), (6), (9) and (10). We show that solutions of problems (2), (6), (9) and (10) dependently continuously on the initial age of infection. We define the partial derivative part of (2) and (6) give,

$$\frac{\partial i_h(t,\tau)}{\partial t}+\frac{\partial i_h(t,\tau)}{\partial \tau}=\lim_{h\to 0}\frac{i_h(t+h,\tau+h)-i_h(t,\tau)}{h} \tag{16}$$

Let, $f(h)=i_h(t_0+h,\tau_0+h)$ (17)

The ordinary differential equation

$$\frac{df_1(h)}{dt}+(\mu_h+\delta_h+e_h)f_1(h)=0 \tag{18}$$

Equation (18) has a unique solution as follows

$$f_1(h)=f(0)e^{-\int_0^h(\mu_h+\delta_h+e_h)ds} \tag{19}$$

Substitute (17) into (19), we have

$$i_h(t_0+h,\tau_0+h)=i_h(t_0,\tau_0)e^{-\int_0^h(\mu_h+\delta_h+e_h)ds} \tag{20}$$

This gives the value of i_h at all points on the characteristics passing through the point $i_h(t_0,\tau_0)$

When $i_h(t_0,\tau_0)=(0,t-\tau);h=t$, we have that

$$i_h(t,\tau)=\psi_h(\tau-t)e^{-\int_0^\tau(\mu_h+\delta_h+e_h)ds};t\le\tau \tag{21}$$

Also, when $i_h(t_0,\tau_0)=(t-\tau,0);h=\tau$, gives

$$i_h(t,\tau)=B_h(t-\tau)e^{-\int_0^\tau(\mu_h+\delta_h+e_h)ds};t>\tau \tag{22}$$

Then equations (21) and (22) give the solution of $i_h(t,\tau)$ in the positive quadrant $t\ge 0;\tau\ge 0$. Thus, problem (2), (6), (9), (10) and (11) - (12) has the following unique solution that exists for all time

$$i_h(t,\tau)=\begin{cases}B_h(t-\tau)\pi_h(\tau);t>\tau\\ \psi_h(\tau-t)\dfrac{\pi_h(\tau)}{\pi_h(\tau-t)};t<\tau\end{cases} \tag{23}$$

and

$$i_p(t,\tau)=\begin{cases}B_p(t-\tau)\pi_p(\tau);t>\tau\\ \psi_p(\tau-t)\dfrac{\pi_p(\tau)}{\pi_p(\tau-t)};t<\tau\end{cases} \tag{24}$$

where, $\pi_h(\tau)=e^{-\int_0^{\tau}(\mu_h+\delta_h+e_h)ds}$ and $\pi_p(\tau)=e^{-\int_0^{\tau}(\mu_p+\delta_p+e_p)ds}$ (25)

Equation (25) denotes the survival probability i.e the probability for an individual to survive to age τ ; thus, it must be $\pi(\tau)=0\ni(\pi_h,\pi_p\in\pi)$ and more over according to [7]. The function

$$K_h(\tau)=\psi_h(\tau)\pi_h(\tau);\tau\in[0,T] \tag{26}$$

Gives an infection function of newly infected individuals, it is related to the parameter:

$$\Gamma=\int_0^T\psi_h(\tau)\pi_h(\tau)d\tau \tag{27}$$

Equation (27) presents the total infection rate which is the newly infected population that an infected individual is expected to infect during the infected period we now consider the expected life of an infected individual given below

$$\bar{\pi}_h=\int_0^T\pi_h(\tau)d\tau \tag{28}$$

Equation (28) gives the mean value of the life of an infected individual; actually (28) is better understood if we note that $(\mu_h+\delta_h+e_h)\pi_h(\tau)d\tau$ is the probability for an infected individual to survive to age τ and then dies in $[\tau,\tau+d\tau]$; thus

$$\begin{aligned}\bar{\pi}_h&=\int_0^T\tau(\mu_h+\delta_h+e_h)\pi_h(\tau)d\tau=-\int_0^T\tau\frac{d}{d\tau}\pi(\tau)d\tau=-\int_0^T\tau d[\pi(\tau)]\\&=-\tau\pi(\tau)\Big|_0^T+\int_0^T\pi(\tau)d\tau=\int_0^T\pi(\tau)d\tau\end{aligned} \tag{29}$$

We list some of the assumptions that equation (2), (9) and (10) are supposed to fulfil in order to show that (2), (9) and (10) depend continuously on the initial age of infection and are biologically significant or mathematically well posed.

$\psi_h(\cdot)$ is non-negative and belong to $L^T(0,\tau)$ (30)

$(\cdot)$ is non-negative and belong to $L^1{}_{loc}([0,\tau))$ (31)

$$\int_0^{\tau}(\mu_h+\delta_h(s)+e_h(s))ds=T \tag{32}$$

$$\psi_h \in L^1(0,\tau), \psi_h(\tau) \geq 0 \text{ a.e in } [0,\tau] \tag{33}$$

We rewritten (9) in the form

$$B(t) = B_h + B_p = i_h(t,0) + i_p(t,0) = \frac{\sigma_p I_p S_h}{N_p} + \frac{\sigma_h I_h S_h}{N_h} + \frac{\sigma_p I_p S_p}{N_p}$$

$$B(t) = B_h + B_p = \int_0^T M_1(\tau) i_p(t,\tau) d\tau + \int_0^T M_2(\tau) i_h(t,\tau) d\tau + \int_0^T M_3(\tau) i_p(t,\tau) d\tau \tag{34}$$

where, $M_1 = \frac{\sigma_p S_h}{N_p}; M_2 = \frac{\sigma_h S_h}{N_h}; M_3 = \frac{\sigma_p S_p}{N_p}$ (35)

Equation (35) is also non-negative and belongs to $L^T(0,\tau)$ substitute (23) - (24) into (34), we obtain B(t) as,

$$B(t) = \int_0^T M_1(\tau) B_p(t-\tau)\pi_p(\tau) d\tau + \int_0^T M_1(\tau)\psi_p(\tau-t)\frac{\pi_p(\tau)}{\pi_p(\tau-t)} d\tau + \int_0^T M_2(\tau) B_h(t-\tau)\pi_h(\tau) d\tau$$
$$+ \int_0^T M_2(\tau)\psi_h(\tau-t)\frac{\pi_h(\tau)}{\pi_h(\tau-t)} d\tau + \int_0^T M_3(\tau) B_p(t-\tau)\pi_p(\tau) d\tau + \int_0^T M_3(\tau)\psi_p(\tau-t)\frac{\pi_p(\tau)}{\pi_p(\tau-t)} d\tau \tag{36}$$

Thus, B(t) satisfied the following Volterra Integral equation of the second kind.

$$B(t) = F_1(t) + \int_0^t M_1(\tau) B_p(t-\tau)\pi_p(\tau) d\tau + F_2(t) + \int_0^t M_2(\tau) B_h(t-\tau)\pi_h(\tau) d\tau$$
$$+ F_3(t) + \int_0^t M_3(\tau) B_p(t-\tau)\pi_p(\tau) d\tau \tag{37}$$

with, $F_1(t) = \int_0^T M_1(\tau)\psi_p(\tau-t)\frac{\pi_p(\tau)}{\pi_p(\tau-t)} d\tau = \int_0^T M_1(\tau+t)\psi_p(\tau)\frac{\pi_p(\tau+t)}{\pi_p(\tau)} d\tau$ (38)

$$F_2 = \int_0^T M_2(\tau)\psi_h(\tau-t)\frac{\pi_h(\tau)}{\pi_h(\tau-t)} d\tau = \int_0^T M_2(\tau+t)\psi_h(\tau)\frac{\pi_h(\tau+t)}{\pi_h(\tau)} d\tau \tag{39}$$

$$F_3 = \int_0^T M_3(\tau)\psi_p(\tau-t)\frac{\pi_p(\tau)}{\pi_p(\tau-t)} d\tau = \int_0^T M_3(\tau+t)\psi_p(\tau)\frac{\pi_p(\tau+t)}{\pi_p(\tau)} d\tau \tag{40}$$

and, $K_1(t) = M_1(t)\pi_p(t), K_2(t) = M_2(t)\pi_h(t), K_3(t) = M_3(t)\pi_p(t)$ (41)

implies, $B(t) = F_1(t) + \int_0^T K_1(t-s) B_p(s) ds$

$$+ F_2(t) + \int_0^T K_2(t-s)B_h(s)ds + F_3(t) + \int_0^T K_3(t-s)B_p(s)ds \tag{42}$$

When $t \geq 0$ and the functions $M_1, M_2, M_3, \psi_h, \psi_p$ are extended by zero outside the interval [0.T]. equation (37) is known as the renewal equation and also as the Lokta equation, we observed that the Kernal $K_1(t), K_2(t)$ and $K_3(t)$ is an infectious function of newly infected individuals of both human and primate defined in (26). Equation (42) is equivalent to (2), (9), (10) and (11); actually (42) is the main tool to investigate the existence of (2), (9), (10), and (12), the connection being provided by (38), (39), (40) - (41) and (23)-(24) respectively. The following Lemma states some properties on the basis of the assumptions (30) - (33).

Lemma 1: Let (38) - (41) be satisfied then,

$$K_1(t) \text{ a.e } K_1(t) = 0 \text{ for } t > \tau \text{ , } K_1 \in L^1(\Re_+) \bigcap L^T(\Re_+) \tag{43}$$

$$F_1(t) \geq 0, F_2(t) \geq 0, K_1(t) = 0 \text{ for } t > \tau \text{ , } F(F_1, F_2, F_3) \in C(\Re_+) \tag{44}$$

According to [12]

$$\psi((\psi_h, \psi_p) \in W^{1,1}(0,\tau) \text{and } (\mu_h + \delta_h + e_h)\psi_h(\cdot) \in L^1(0,\tau), \&(\mu_p + \delta_p + e_p)\psi_p(\cdot) \in L^1(0,\tau)$$

$$\text{then } F \in W^{1,T}(\Re_+) \tag{45}$$

Proof: Equation (43) and the first part of (44) are obvious. To show that, $F \in C(\Re_+)$, we take $t \geq 0$ then we have

$$F_1(t) = \int_t^T M_1(\tau)\psi_p((\tau - t) - (\tau - t_0))\frac{\pi_p(\tau)}{\pi_p(\tau - t)}d\tau + \int_t^T M_1(\tau)\psi_p(\tau - t_0)\frac{\pi_p(\tau)}{\pi_p(\tau - t)}d\tau \tag{46}$$

$$F_2(t) = \int_t^T M_2(\tau)\psi_h((\tau - t) - (\tau - t_0))\frac{\pi_h(\tau)}{\pi_h(\tau - t)}d\tau + \int_t^T M_2(\tau)\psi_h(\tau - t_0)\frac{\pi_h(\tau)}{\pi_h(\tau - t)}d\tau \tag{47}$$

$$F_3(t) = \int_t^T M_3(\tau)\psi_p((\tau - t) - (\tau - t_0))\frac{\pi_p(\tau)}{\pi_p(\tau - t)}d\tau + \int_t^T M_3(\tau)\psi_p(\tau - t_0)\frac{\pi_p(\tau)}{\pi_p(\tau - t)}d\tau \tag{48}$$

Since, $\psi_p \in L^1(\Re), \psi_h \in L^1(\Re)$

$$\left|\int_t^T M_1(\tau)\frac{\pi_p(\tau)}{\pi_p(\tau - t)}\psi_p((\tau - t) - (\tau - t_0))d\tau\right| \leq |M_1|_{L^T}\int_0^T |\psi_p(\tau - t) - \psi_p(\tau - t_0)|d\tau \to 0 \tag{49}$$

As $t \to t_0$

so that, $$\lim_{t \to t_0} F_1(t) = \int_{t_0}^T M_1(\tau)\frac{\pi_h(\tau)}{\pi_h(\tau - t_0)}\psi_h(\tau - t_0)d\tau = F_1(t_0) \tag{50}$$

$$\left|\int_t^T M_2(\tau)\frac{\pi_h(\tau)}{\pi_h(\tau - t)}\psi_h((\tau - t) - (\tau - t_0))d\tau\right| \leq |M_2|_{L^T}\int_0^T |\psi_h(\tau - t) - \psi_h(\tau - t_0)|d\tau \to 0, t \to t_0 \tag{51}$$

$$\lim_{t\to t_0} F_2(t) = \int_{t_0}^{T} M_2(\tau)\frac{\pi_p(\tau)}{\pi_p(\tau-t_0)}\psi_p(\tau-t_0)d\tau = F_2(t_0) \tag{52}$$

$$\left|\int_{t}^{T} M_3(\tau)\frac{\pi_p(\tau)}{\pi_p(\tau-t)}\psi_p((\tau-t)-(\tau-t_0))d\tau\right| \le \left|M_3\right|_{L^T}\int_{0}^{T}\left|\psi_p(\tau-t)-\psi_p(\tau-t_0)\right|d\tau \to 0, t\to t_0 \tag{53}$$

$$\lim_{t\to t_0} F_3(t) = \int_{t_0}^{T} M_3(\tau)\psi_p(\tau-t_0)\frac{\pi_p(\tau)}{\pi_p(\tau-t_0)}d\tau = F_3(t_0) \tag{54}$$

Therefore, equations (38), (39), (40) implies $F \in W^{1,T}(\Re_+)$. This completes the proof of the lemma 1. In the next theorem, we establish the existence and uniqueness of (2), (9), (10) and (12) by considering (37) - (41). Since the function Fs is continuous, for the purpose of this section it is sufficient to study (37) in the class of continuous functions. Thus, we introduced the following definition of a solution.

Definition 1: A Solution to (37) is a function $B(B_h, B_p) \in C(\Re_+, \Re)$ satisfying (37), firstly, we have the following theorem, which is standard in the theory of Volterra Equations. We provide a proof here for the sake of completeness.

Theorem 1: Let (30) - (33) be satisfied, then equation (37) - (41) has a unique solution $B(B_h, B_p) \in C(\Re_+, \Re)$ such that $B(t) \ge 0$ for all t in addition if $\psi(\psi_h, \psi_p)$ satisfied (45), then $B \in W_{loc}^{1,T}(\Re_+)$ and

$$\begin{aligned} B^1(t) &= F_1^1(t) + K_1(t)B_p(0) + \int_0^t K_1(t-s)B_p^1(s)ds + F_2^1(t) + K_2(t)B_h(0) \\ &+ \int_0^t K_2(t-s)B_h^1(s)ds + F_3^1(t) + K_3(t)B_p(0) + \int_0^t K_3(t-s)B_p^1(s)ds \end{aligned} \tag{55}$$

Proof: Firstly, we assume that

$$\left|K\right|_{L^1(\Re_+)} = \int_0^T K(s)ds < 1 \qquad (K_1 + K_2 + K_3) \in K \tag{56}$$

The solution of (37) – (42) is obtained using the standard Picard iteration defined, for $t \ge 0$ by

$$B^{k+1}(t) = F_1(t) + \int_0^t K_1(s)B_p^k(t-s)ds + F_2(t) + \int_0^t K_2(s)B_h^k(t-s)ds + F_3(t) + \int_0^t K_3(s)B_p^k(t-s)ds \tag{57}$$

And initialized by $B^0(t) = 0$ on IR, therefore,

$$\begin{cases} B^0(t) = F(t) \\ B^{k+1}(t) = F_1(t) + \int_0^t K_1(s)B_p^k(t-s)ds + F_2(t) + \int_0^t K_2(s)B_h^k(t-s)ds + F_3(t) + \int_0^t K_3(s)B_p^k(t-s)ds \end{cases} \tag{58}$$

If we take any $T > 0$, then by (43) - (44) we obtained $B^k \in ([0,T])$ and $B^k(T) \geq 0$, moreover

$$\begin{aligned} \left|B^{k+1}(t) - B^k(t)\right| &\leq \int_0^t K_1(t-s)\left|B_p^k(s) - B_p^{k-1}(s)\right|ds + \int_0^t K_2(t-s)\left|B_h^k(s) - B_h^{k-1}(s)\right|ds \\ &+ \int_0^t K_3(t-s)\left|B_p^k(s) - B_p^{k-1}(s)\right|ds \end{aligned} \tag{59}$$

And,

$$\left|B^{k+1} - B^k\right|_{C([0,T])} \leq \left|K_1\right|_{L^1(\Re_+)}\left|B_p^k - B_p^{k-1}\right|_{C([0,T])} + \left|K_2\right|_{L^1(\Re_+)}\left|B_h^k - B_h^{k-1}\right| + \left|K_3\right|_{L^1(\Re_+)}\left|B_p^k - B_p^{k-1}\right|_{C([0,T])} \tag{60}$$

Thus, by (56) the sequence $B^k(t)$ converges uniformly on $[0,T]$ to a solution of (37) – (42) ∋ $B \in C([0,T])$ and $B(t) \geq 0$. Concerning Uniqueness of this solution of the model, we set B(t) and $\bar{B}$(t) to be the two solutions of (37) - (42), so that

$$\left|B - \bar{B}\right|_{C([0,T])} \leq \left|K\right|_{L^1(\Re_+)}\left|B - \bar{B}\right|_{C([0,T])} \tag{61}$$

This implies that by equation (56), $B(t) = \bar{B}(t)$.

In addition, if ψ satisfies (45) then by theorem J and (58), we have $B^k \in W^{1,T}(\Re_+)$ and setting $V^k(t) = \frac{d}{dt}B^k(t)$ a.e we have $V^k \in L^T(\Re_+)$ and

$$\begin{aligned} V^{k+1}(t) &= F_1^1(t) + K_1(t)V_p(0) + \int_0^t K_1(t-s)V_p^k(s)ds + F_2^1(t) + K_2(t)V_h(0) \\ &+ \int_0^t K_2(t-s)V_h^k(s)ds + F_3^1(t) + K_3(t)V_p(0) + \int_0^t K_3(t-s)V_p^k(s)ds \end{aligned} \tag{62}$$

This yield, $\left|V^{k+1} - V^k\right|_{L^T(\Re_+)} \leq \left|K\right|_{L^1(\Re_+)}\left|V^k - V^{k-1}\right|_{L^T(\Re_+)}$ (63)

Thus, again by (56) the sequence V^k converges in $L^T(\Re_+)$ to $V(t) = \frac{d}{dt}B(t)$ are therefore (55) following from (62). In addition to (57), to make valid argument, we take α ∋

$$\int_0^T e^{-\alpha t} K(t)dt < 1$$

Setting, $\overline{B}_h = e^{-\alpha t} B_h(t), \overline{B}_p = e^{-\alpha t} B_p(t), \overline{F}_1 = e^{-\alpha t} F_1(t), \overline{F}_2 = e^{-\alpha t} F_2(t), \overline{F}_3 = e^{-\alpha t} F_3(t),$
$\overline{K}_h = e^{-\alpha t} K_h(t), \overline{K}_p = e^{-\alpha t} K_p(t)$

in equation (37) - (42) is transformed into an equation below

$$B(t) = \overline{F_1}(t) + \int_0^t \overline{K_1}(t-s)\overline{B_p}(s)ds + \overline{F_2}(t) + \int_0^T \overline{K_2}(t-s)\overline{B_h}(s)ds + \overline{F_3}(t) + \int_0^T \overline{K_3}(t-s)\overline{B_p}(s)ds \tag{64}$$

And since (64) satisfies (56), this is similar with equation (63). The next theorem allows us to state results for problem (2), (9) and (10) through (23) - (24).

Theorem 2: let (30) - (33) and (45) be satisfied. And we also assume that

$$\psi_h(0) = \int_0^T M_1(\tau)\psi_h(\tau), \psi_p(0) = \int_0^T M_2(\tau)\psi_p(\tau) \,\&\, \psi_p(0) = \int_0^T M_3(\tau)\psi_p(\tau) \tag{65}$$

And let $i(t,\tau)$ be defined by (23) - (24) where B(t) is the solution of (37) - (42). Then

$$i \in ([0,\tau]\times\Re_+), i(t,\tau) \geq 0, \ (\mu+\delta+e)i(t,\cdot) \in L^1(0,\tau)\forall t > 0 \tag{66}$$

$$\frac{\partial i(t,\tau)}{\partial t} + \frac{\partial i(t,\tau)}{\partial \tau} \text{ exist a.e in } [0,\tau]\times[0,T] \tag{67}$$

And problem (2), (9) and (10) is satisfied. Moreover according to Webb (1985), $i(t,\tau)$ is the only solution in the sense of (57) and (67).

Proof:

The proof of (66) - (67) is quite straightforward and follows from the properties of B(t) which is stated in theorem 1. We only note the following inequality concerning the last part of (66).

$$\begin{aligned}
&\int_0^\tau (\mu_h+\delta_h+e_h)i_h(t,\tau)d\tau + \int_0^\tau (\mu_p+\delta_p+e_p)i_p(t,\tau)d\tau = \int_0^{t\wedge\tau} (\mu_h+\delta_h+e_h)B_h(t-\tau)\pi_h(\tau)d\tau \\
&+ \int_{t\wedge\tau}^\tau (\mu_h+\delta_h+e_h)\psi_h(\tau-t)\frac{\pi_h(\tau)}{\pi_h(\tau-t)}d\tau + \int_0^{t\wedge\tau} (\mu_p+\delta_p+e_p)B_p(t-\tau)\pi_p(\tau)d\tau \\
&+ \int_{t\wedge\tau}^\tau (\mu_p+\delta_p+e_p)\psi_p(\tau-t)\frac{\pi_p(\tau)}{\pi_p(\tau-t)}d\tau
\end{aligned} \tag{68}$$

$$\begin{aligned}
&\leq \underset{S_h\in[0,t]}{Max}\left|B_h(t)\right| \int_0^{t\wedge\tau} (\mu_h+\delta_h+e_h)\pi_h(\tau)d\tau + e^{\int_0^{(t\vee\tau)-t}(\mu_h+\delta_h+e_h)ds}\left|\psi_h\right|_{C(|0,\tau|)} \int_{t\wedge\tau}^\tau (\mu_h+\delta_h+e_h)\pi_h(\tau)ds + \\
&\underset{S_p\in[0,t]}{Max}\left|B_p(t)\right| \int_0^{t\wedge\tau} (\mu_p+\delta_p+e_p)\pi_p(\tau)d\tau + e^{\int_0^{(t\vee\tau)-t}(\mu_p+\delta_p+e_p)ds}\left|\psi_p\right|_{C(|0,\tau|)} \int_{t\wedge\tau}^\tau (\mu_p+\delta_p+e_p)\pi_p(\tau)ds
\end{aligned} \tag{69}$$

$$\leq \underset{S_h\in[0,t]}{Max}\left|B_h(t)\right| + e^{\int_0^{(t\vee\tau)-t}\mu_h+\delta_h+e_h)ds}\left|\psi_h\right|_{C(|0,\tau|)} + \underset{S_p\in[0,t]}{Max}\left|B_p(t)\right| + e^{\int_0^{(t\vee\tau)-t}\mu_p+\delta_p+e_p)ds}\left|\psi_p\right|_{C(|0,\tau|)} \tag{70}$$

Equation (70) provides the fact that (65) is intended to guarantee the continuity of $i(t,\tau)$ through the line $\tau = t$; so that

$$B_h(0) = \int_0^T M_1(\tau)\psi_h(\tau)d\tau = \psi_h(0) \,\&\, B_p(0) = \int_0^T (M_2 + M_3)(\tau)\psi_h(\tau)d\tau = \psi_p(0) \tag{71}$$

We note that the solution of problem (2), (9) and (10) must be in the form of (23) - (24) with B(t) satisfying (37) - (42) such that equation (23) - (24) and (45) are enough to provide a classical solution in the next following theorem.

Theorem 3: Let (30) - (33) be satisfied, then $i(t,\tau)$ defined by (23) - (24) has the following properties;

$$i(t,\cdot) \in C([0,T]; L^1(0,\tau)), i(t,\tau) \geq 0 \ni (i_h + i_p \in i) \text{ a.e in } [0,\tau]\times\Re_+ \tag{72}$$

$$\left|i(t,\cdot)\right|_{L^1} \leq e^{t|M|_{L^T}} \left|\psi\right|_{L^1} \ni (M_1 + M_2 + M_3) \in M, (\psi_h + \psi_p) \in \psi \tag{73}$$

$$i(t,\tau) \text{ is continuous for } \tau < t \text{ and satisfies (9) for } t > 0 \tag{74}$$

$$\lim_{h\to 0}\frac{1}{h}[i(t+h,\tau+h) - i(t,\tau)] = -(\mu + \delta + e)i(t,\tau) \text{ a.e in } [0,\tau]\times\Re_+ \tag{75}$$

Proof: let us prove (73) first. From (38) - (42), we have

$$\begin{aligned} &F_1(t) \leq \left|M_1\right|_{L^T}\left|\psi_p\right|_{L^1}, K_1(t) \leq \left|M_1\right|_{L^T}; F_2(t) \leq \left|M_2\right|_{L^T}\left|\psi_h\right|_{L^1}, K_2(t) \leq \left|M_2\right|_{L^T}; \\ &F_3(t) \leq \left|M_3\right|_{L^T}\left|\psi_p\right|_{L^1}, K_3(t) \leq \left|M_3\right|_{L^T} \end{aligned} \tag{76}$$

Then, from (37) - (42)

$$\begin{aligned} B(t) &\leq \left|M_1\right|_{L^T}\left|\psi_p\right|_{L^1} + \left|M_1\right|_{L^T}\int_0^t B_p(s)ds + \left|M_2\right|_{L^T}\left|\psi_h\right|_{L^1} + \left|M_2\right|_{L^T}\int_0^t B_h(s)ds \\ &+ \left|M_3\right|_{L^T}\left|\psi_p\right|_{L^1} + \left|M_3\right|_{L^T}\int_0^t B_h(s)ds \end{aligned} \tag{77}$$

Thus, by classical Gronwall's inequality

$$B(t) \leq \left|M_1\right|_{L^T} e^{t|M_1|_{L^T}}\left|\psi_p\right|_{L^1} + \left|M_2\right|_{L^T} e^{t|M_2|_{L^T}}\left|\psi_h\right|_{L^1} + \left|M_3\right|_{L^T} e^{t|M_3|_{L^T}}\left|\psi_p\right|_{L^1} \tag{78}$$

From this estimate, equation (23) - (24) yields;

$$\begin{aligned} \left|i(t,\cdot)\right|_{L^1} &= \int_0^t B_p(t-\tau)\pi_p(\tau)d\tau + \int_0^t \psi_p(\tau)\frac{\pi_p(\tau+t)}{\pi_p(\tau)}d\tau + \int_0^t B_h(t-\tau)\pi_h(\tau)d\tau + \int_0^t \psi_h(\tau)\frac{\pi_h(\tau+t)}{\pi_h(\tau)}d\tau \\ &+ \int_0^t B_p(t-\tau)\pi_p(\tau)d\tau + \int_0^t \psi_p(\tau)\frac{\pi_p(\tau+t)}{\pi_p(\tau)}d\tau \\ &\leq (\left|M_1\right|_{L^T}\int_0^t e^{(t-\tau)|M_1|_{L^T}}d\tau + 1)\left|\psi_p\right|_{L^1} + (\left|M_2\right|_{L^T}\int_0^t e^{(t-\tau)|M_2|_{L^T}}d\tau + 1)\left|\psi_h\right|_{L^1} + (\left|M_3\right|_{L^T}\int_0^t e^{(t-\tau)|M_3|_{L^T}}d\tau + 1)\left|\psi_p\right|_{L^1} \\ &= e^{t|M_1|_{L^T}}\left|\psi_p\right|_{L^1} + e^{t|M_2|_{L^T}}\left|\psi_h\right|_{L^1} + e^{t|M_3|_{L^T}}\left|\psi_p\right|_{L^1} \end{aligned} \tag{79}$$

Equation (72) follows easily from (75). Now, for a given $\psi \in L^1(0,\tau)$, let ψ^n be a sequence such that ψ^n satisfy (51) and (65)

$$\lim_{n\to T}\left|\psi_h^n - \psi_h\right|_{L^1} = 0 \text{ and } \lim_{n\to T}\left|\psi_p^n - \psi_p\right|_{L^1} = 0 \tag{80}$$

And let i^n be the solution of (2), (9), (10) and (12) corresponding to ψ^n. Thus $i^n \in C([0,T];L^1(0,\tau))$ and by (73) and linearity, we have

$$\left|i^n(t,\cdot) - i(t,\cdot)\right|_{L^1} \le e^{t|M|_{L^T}}\left|\psi^n - \psi\right|_{L^1}$$

$$\text{Or}\left|i_h^n(t,\cdot) - i_h(t,\cdot)\right|_{L^1} + \left|i_p^n(t,\cdot) - i_p(t,\cdot)\right|_{L^1} \le e^{t|M_1|_{L^T}}\left|\psi_p^n - \psi_p\right|_{L^1} + e^{t|M_2|_{L^T}}\left|\psi_h^n - \psi_h\right|_{L^1} + e^{t|M_3|_{L^T}}\left|\psi_p^n - \psi_p\right|_{L^1} \tag{81}$$

So that i is the limit of the sequence i^n in the space $C([0,T];L^1(0,\tau))$ i.e (72) is true. Finally, equations (74) - (75) are straightforward and that completes the proof. This shows that even when the initial age of infection ψ is not regular, the solution $i(t,\tau)$ still has some regularity. We also note that the estimate (73) provides continuity of the solution i with respect initial age of infection ψ. Hence, model (2), (9) and (10) exist and are unique and well posed mathematically. In the norm of the space $L^1(0,\tau)$: this illustrates the existence and uniqueness of model (2), (9) and (10) which is in agreement with the biological meaning of the infection age density $i(t,\tau)$ for the model.

In the next theorem, we used a similar approach to the work of [8] to prove the existence and uniqueness of solution for the model equations (1)-(8).

Theorem 4: The exists of a unique solution of (1) - (8) for $|t-t_0| \le a, |S_h - S_{h0}| \le b$

$$,|I_h - I_{h0}| \le c, |V_h - V_{h0}| \le d, |R_h - R_{h0}| \le e, |S_p - S_{p0}| \le f, |I_p - I_{p0}| \le g, |V_p - V_{p0}| \le j, |R_p - R_{p0}| \le l$$

Proof: To show this, from (1)-(8) yields the following

$$\left|\frac{\partial f_1}{\partial S_h}\right| = \left|+(\gamma_h + \mu_h + \frac{\sigma_p I_p}{N_p} + \frac{\sigma_h I_h}{N_h})\right|, \left|\frac{\partial f_1}{\partial I_h}\right| = \left|\frac{\sigma_h S_h}{N_h}\right|, \left|\frac{\partial f_1}{\partial V_h}\right| = |\omega_h|, \left|\frac{\partial f_1}{\partial I_p}\right| = \left|\frac{\sigma_p S_h}{N_p}\right|, \left|\frac{\partial f_1}{\partial R_p}\right| = |0|$$

$$\left|\frac{\partial f_2}{\partial S_h}\right| = \left|\frac{\sigma_p I_p}{N_p} + \frac{\sigma_h I_h}{N_h}\right|, \left|\frac{\partial f_2}{\partial I_h}\right| = \left|\frac{\sigma_h S_h}{N_h} - (\mu_h + \delta_h + e_h)\right|, \left|\frac{\partial f_2}{\partial I_p}\right| = \left|\frac{\sigma_p S_h}{N_p}\right|, \left|\frac{\partial f_2}{\partial V_p}\right| = |0|, \left|\frac{\partial f_2}{\partial R_p}\right| = |0|$$

$$\left|\frac{\partial f_3}{\partial S_h}\right| = |\gamma_h|, \left|\frac{\partial f_3}{\partial I_h}\right| = |0|, \left|\frac{\partial f_3}{\partial V_h}\right| = |\omega_h + \mu_h|, \left|\frac{\partial f_3}{\partial R_h}\right| = |0|, \left|\frac{\partial f_3}{\partial S_p}\right| = |0|, \left|\frac{\partial f_3}{\partial R_p}\right| = |0|$$

$$\left|\frac{\partial f_4}{\partial S_h}\right| = |0|, \left|\frac{\partial f_4}{\partial I_h}\right| = |e_h|, \left|\frac{\partial f_4}{\partial V_h}\right| = |0|, \left|\frac{\partial f_4}{\partial R_h}\right| = |\mu_h|, \left|\frac{\partial f_4}{\partial S_p}\right| = |0|, \left|\frac{\partial f_4}{\partial I_p}\right| = |0|, \left|\frac{\partial f_4}{\partial V_p}\right| = |0|, \left|\frac{\partial f_4}{\partial R_p}\right| = |0|$$

$$\left|\frac{\partial f_5}{\partial S_h}\right| = |0|, \left|\frac{\partial f_5}{\partial S_p}\right| = \left|+(\gamma_p + \mu + \frac{\sigma_p I_p}{N_p})\right|, \left|\frac{\partial f_5}{\partial I_p}\right| = \left|\frac{\sigma_p S_p}{N_p}\right|, \left|\frac{\partial f_5}{\partial V_p}\right| = |\omega_p|, \left|\frac{\partial f_5}{\partial R_p}\right| = |0|$$

$$\left|\frac{\partial f_6}{\partial S_h}\right| = |0|, \left|\frac{\partial f_6}{\partial R_h}\right| = |0|, \left|\frac{\partial f_6}{\partial S_p}\right| = \left|\frac{\sigma_p I_p}{N_p}\right|, \left|\frac{\partial f_6}{\partial I_p}\right| = \left|\frac{\sigma_p S_p}{N_p} - (\mu_p + \delta_p + e_p)\right|, \left|\frac{\partial f_6}{\partial V_p}\right| = |0|, \left|\frac{\partial f_6}{\partial R_p}\right| = |0|$$

$$\left|\frac{\partial f_7}{\partial S_h}\right| = |0|, \left|\frac{\partial f_7}{\partial I_h}\right| = |0|, \left|\frac{\partial f_7}{\partial V_h}\right| = |0|, \left|\frac{\partial f_7}{\partial R_h}\right| = |0|, \left|\frac{\partial f_7}{\partial S_p}\right| = |\gamma_p|, \left|\frac{\partial f_7}{\partial I_p}\right| = |0|, \left|\frac{\partial f_7}{\partial V_p}\right| = |+\omega_p + \mu_p|, \left|\frac{\partial f_7}{\partial R_p}\right| = |0|$$

$$\left|\frac{\partial f_8}{\partial S_h}\right| = |0|, \left|\frac{\partial f_8}{\partial I_h}\right| = |0|, \left|\frac{\partial f_8}{\partial V_h}\right| = |0|, \left|\frac{\partial f_8}{\partial R_h}\right| = 0, \left|\frac{\partial f_8}{\partial S_p}\right| = |0|, \left|\frac{\partial f_8}{\partial I_p}\right| = |e_p|, \left|\frac{\partial f_8}{\partial V_p}\right| = |0|, \left|\frac{\partial f_8}{\partial R_p}\right| = |\mu_p| \tag{82}$$

This implies that $\left|\frac{\partial f_i}{\partial x_j}\right|, i = 1,2,3,4,5,6,7,8 \Rightarrow j = S_h, I_h, \mathrm{V_h}, R_h, S_p, I_p, \mathrm{V_p}, R_p$ are bounded. Hence, there exists a unique solution of the model (1) - (8).

3.2 The existence of equilibrium state

The existence of equilibrium state was done by rewrite equations (1) - (8) as follows;

$$(1-f)\Pi_h + \omega_h V_h - A_1 S_h - [\frac{\sigma_p \int_0^T i_p(t,\tau)d\tau}{N_p} + \frac{\sigma_h \int_0^T i_h(t,\tau)d\tau}{N_h}]S_h = 0 \tag{83}$$

$$\frac{\partial i_h(t,\tau)}{\partial t} + \frac{\partial i_h(t,\tau)}{\partial \tau} + A_2 i_h(t,\tau) = 0 \tag{84}$$

$$f\Pi_h + \gamma_h S_h - A_3 V_h = 0 \tag{85}$$

$$\int_0^T e_h i_h(t,\tau)d\tau - \mu_h R_h = 0 \tag{86}$$

$$(1-g)\Pi_p + \omega_p V_p - B_1 S_p - \frac{\sigma_p \int_0^T i_p(t,\tau)d\tau}{N_p} S_p = 0 \tag{87}$$

$$\frac{\partial i_p(t,\tau)}{\partial t} + \frac{\partial i_p(t,\tau)}{\partial \tau} + B_2 i_p(t,\tau) = 0 \tag{88}$$

$$g\Pi_p + \gamma_p S_p - B_3 V_p = 0 \tag{89}$$

$$\int_0^T e_p i_p(t,\tau)d\tau - \mu_p R_p = 0 \tag{90}$$

$$B_h = i_h(t,0) = \frac{\sigma_p I_p S_h}{N_p} + \frac{\sigma_h I_h S_h}{N_h} \tag{91}$$

$$B_p = i_p(t,0) = \frac{\sigma_p I_p S_p}{N_p} \tag{92}$$

where,

$A_1 = \gamma_h + \mu_h; A_2 = \mu_h + \delta_h + e_h; A_3 = \omega_h + \mu_h; B_1 = \gamma_p + \mu_p; B_2 = \mu_p + \delta_p + e_p; B_3 = \omega_p + \mu_p$

and $S_h(0) = S_{h0}, I_h(0) = I_{h0}, V_h(0) = V_{h0}, R_h(0) = R_{h0}, S_p(0) = S_{p0}, I_h(0) = I_{p0},$

$V_p(0) = V_{p0}, R_p(0) = R_{p0}, i_h(0,\tau) = \psi_h, i_p(0,\tau) = \psi_p, N_h{}^0 = S_h^0 + V_h^0, N_p{}^0 = S_p^0 + V_p^0$ (93)

Solving the system of equations (1) – (8) simultaneously, at the disease free equilibrium state, we have the following points,

$$E^0 = (S_h^0, I_h^0, V_h^0, R_h^0, S_p^0, I_p^0, V_p^0, R_p^0) =$$
$$\left(\frac{(1-f)\Pi_h A_3 + \omega_h f\Pi_h}{(A_1 A_3 - \omega_h \gamma_h)}, 0, \frac{f\Pi_h A_1 + \gamma_h (1-f)\Pi_h}{(A_1 A_3 - \omega_h \gamma_h)}, 0, \right.$$
$$\left. \frac{(1-g)\Pi_p B_3 + \omega_p g\Pi_p}{(B_1 B_3 - \omega_p \gamma_p)}, 0, \frac{g\Pi_p B_1 + \gamma_p (1-g)\Pi_p}{(B_1 B_3 - \omega_p \gamma_p)}, 0 \right) \tag{94}$$

3.3 Effective reproduction number

Infection age and age-Structured models, the effective or basic reproduction number are often expressed as the sum of the infectivity of each infected compartment [9, 10]. For a single infected compartment, the basic reproduction number is simply the product of the infection rate and the mean duration of the infection. In view of the above explanation, the effective reproduction number of the model becomes;

$$R_E = R_h + R_p$$

$$R_E = \frac{\sigma_p(B_1B_3 - \omega_p\gamma_p)\{(1-f)\Pi_h A_3 + \omega_h f\Pi_h\}}{(A_1A_3 - \omega_h\gamma_h)\{(1-g)\Pi_p B_3 + \omega_p g\Pi_p + g\Pi_p B_1 + \gamma_p(1-g)\Pi_p\}}\int_0^T \pi_p(\tau)d\tau$$
$$+\frac{\sigma_h\{(1-f)\Pi_h A_3 + \omega_h f\Pi_h\}}{(1-f)\Pi_h A_3 + \omega_h f\Pi_h + f\Pi_h A_1 + \gamma_h(1-f)\Pi_h}\int_0^T \pi_h(\tau)d\tau \quad (95)$$
$$+\frac{\sigma_p((1-g)\Pi_p B_3 + \omega_p g\Pi_p)}{(1-g)\Pi_p B_3 + \omega_p g\Pi_p + g\Pi_p B_1 + \gamma_p(1-g)\Pi_p}\int_0^T \pi_p(\tau)d\tau$$

3.4 Local stability of the disease-free equilibrium (DFE) State

Theorem 5: The DFE state E^0 is locally asymptotically stable if $R_E < 1$ and unstable if $R_E > 1$.
Proof: we consider the local stability of DFE state given by (94) and we have the following results,

$$\bar{z}(0) = \frac{\sigma_p(B_1B_3 - \omega_p\gamma_p)[(1-f)\Pi_h A_3 + \omega_h f\Pi_h]}{[(1-g)\Pi_p B_3 + \omega_p g\Pi_p + g\Pi_p B_1 + \gamma_p(1-g)\Pi_p](A_1A_3 - \omega_h\gamma_h)}\int_0^T \bar{z}_p(0)e^{-\lambda\tau}\pi_p(\tau)d\tau$$
$$+\frac{\sigma_h[(1-f)\Pi_h A_3 + \omega_h f\Pi_h]}{(1-f)\Pi_h A_3 + \omega_h f\Pi_h + f\Pi_h A_1 + \gamma_h(1-f)\Pi_h}\int_0^T \bar{z}_h(0)e^{-\lambda\tau}\pi_h(\tau)d\tau \quad (96)$$
$$+\frac{\sigma_p[(1-g)\Pi_p B_3 + \omega_p g\Pi_p]}{(1-g)\Pi_p B_3 + \omega_p g\Pi_p + g\Pi_p B_1 + \gamma_p(1-g)\Pi_p}\int_0^T \bar{z}_p(0)e^{-\lambda\tau}\pi_p(\tau)d\tau$$

From (96), we divide both sides by $\bar{z}(0)$, yields

$$1 = \frac{\sigma_p(B_1B_3 - \omega_p\gamma_p)[(1-f)\Pi_h A_3 + \omega_h f\Pi_h]Q_1(0)}{[(1-g)\Pi_p B_3 + \omega_p g\Pi_p + g\Pi_p B_1 + \gamma_p(1-g)\Pi_p](A_1A_3 - \omega_h\gamma_h)}\int_0^T e^{-\lambda\tau}\pi_p(\tau)d\tau$$
$$+\frac{\sigma_h[(1-f)\Pi_h A_3 + \omega_h f\Pi_h]Q_2(0)}{(1-f)\Pi_h A_3 + \omega_h f\Pi_h + f\Pi_h A_1 + \gamma_h(1-f)\Pi_h}\int_0^T e^{-\lambda\tau}\pi_h(\tau)d\tau \quad (97)$$
$$+\frac{\sigma_p[(1-g)\Pi_p B_3 + \omega_p g\Pi_p]Q_1(0)}{(1-g)\Pi_p B_3 + \omega_p g\Pi_p + g\Pi_p B_1 + \gamma_p(1-g)\Pi_p}\int_0^T e^{-\lambda\tau}\pi_p(\tau)d\tau$$

Where, $Q_1(0) = \bar{z}_p(0)/\bar{z}(0) \,\&\, Q_2(0) = \bar{z}_h(0)/\bar{z}(0)$ (98)

We define a function $G(\lambda)$ to be the right hand side in (97), obviously, $G(\lambda)$ is continuously differentiable function with $\lim_{\lambda\to\infty} G(\lambda) = 0$. By direct computation, it can be shown that $G^1(\lambda) < 0$ and therefore, $G(\lambda)$ is a decreasing functions. Hence, any real solution of equation (97) is negative if $G(0) < 1$ and positive if $G(0) > 1$ thus, if $G(0) > 1$, then DFE state is unstable .

Next, we show that equation (97) has no complex solution with non-negative real part if $G(0) < 1$. In fact, we set

$$H_1(\tau) = \frac{\sigma_p(B_1B_3 - \omega_p\gamma_p)[(1-f)\Pi_h A_3 + \omega_h f\Pi_h]Q_1(0)\pi_p(\tau)}{[(1-g)\Pi_p B_3 + \omega_p g\Pi_p + g\Pi_p B_1 + \gamma_p(1-g)\Pi_p](A_1A_3 - \omega_h\gamma_h)}$$

$$H_2(\tau) = \frac{\sigma_h[(1-f)\Pi_h A_3 + \omega_h f\Pi_h]Q_2(0)\pi_h(\tau)}{(1-f)\Pi_h A_3 + \omega_h f\Pi_h + f\Pi_h A_1 + \gamma_h(1-f)\Pi_h}$$

$$H_3(\tau) = \frac{\sigma_p[(1-g)\Pi_p B_3 + \omega_p g\Pi_p]Q_1(0)\pi_p(\tau)}{(1-g)\Pi_p B_3 + \omega_p g\Pi_p + g\Pi_p B_1 + \gamma_p(1-g)\Pi_p} \tag{99}$$

$$G(\lambda) = \int_0^T H_1(\tau)e^{-\lambda\tau}d\tau + \int_0^T H_2(\tau)e^{-\lambda\tau}d\tau + \int_0^T H_3(\tau)e^{-\lambda\tau}d\tau \tag{100}$$

Suppose $G(0) < 0$. Assume that $\lambda = a_1 + ib$ is a complex solution of equation (100) with $a_1 \geq 0$ [10]. Then,

$$|G(\lambda)| = \left|\int_0^T H_1(\tau)e^{-\lambda\tau}d\tau + \int_0^T H_2(\tau)e^{-\lambda\tau}d\tau + \int_0^T H_3(\tau)e^{-\lambda\tau}d\tau\right|$$

$$\leq \left|\int_0^T H_1(\tau)e^{-(a_1+ib)\tau}d\tau\right| + \left|\int_0^T H_2(\tau)e^{-(a_1+ib)\tau}d\tau\right| + \left|\int_0^T H_3(\tau)e^{-(a_1+ib)\tau}d\tau\right|$$

$$G(\lambda) \leq \int_0^T \left|e^{-(a_1+ib)\tau}\right| H_1(\tau)d\tau + \int_0^T \left|e^{-(a_1+ib)\tau}\right| H_2(\tau)d\tau + \int_0^T \left|e^{-(a_1+ib)\tau}\right| H_3(\tau)d\tau$$

$$\leq \int_0^T e^{-a_1\tau}H_1(\tau)d\tau + \int_0^T e^{-a_1\tau}H_2(\tau)d\tau + \int_0^T e^{-a_1\tau}H_3(\tau)d\tau \tag{101}$$

$$= G(a_1) \leq G(0) < 1 \tag{102}$$

3.5 Global stability of the DFE state

Theorem 6: The DFE state E_0 of the model equation (1) - (5) is Globally Asymptotically Stable (GAS) in Ω if $R_E \leq 1$ while unstable if $R_E \geq 1$

Proof: The approach of [9] and [11-14] are used to construct a suitable lyapunov function,

$$L(t) = (x - x^0 - x^0 \ln\frac{x}{x^0}) + (y - y^0 - y^0 \ln\frac{y}{y^0}) + \int_0^T r(\tau)\frac{i_h(t,\tau)}{\pi_h(\tau)}d\tau$$
$$+ (m - m^0 - m^0 \ln\frac{m}{m^0}) + (j - j^0 - j^0 \ln\frac{j}{j^0}) + \int_0^T q(\tau)\frac{i_p(t,\tau)}{\pi_p(\tau)}d\tau \quad (103)$$

Using (23) - (24) in (103) and solving at DFE, we have the following results,

$$\frac{dL(t)}{dt} = -\frac{A_1}{x}(x - x^0)^2 - \frac{A_3}{y}(y - y^0)^2 - \frac{B_1}{m}(m - m^0)^2 - \frac{B_3}{j}(j - j^0)^2$$
$$- i_h(t,0)(1 - R_h) - i_p(t,0)(1 - R_P) \le 0, if, R_h \le 1, R_p \le 1 \quad (104)$$

The equality $\frac{dL}{dt} = 0$ holds if and only if $x = x^0, y = y^0, m = m^0, j = j^0, i_h(t,0) = 0 \,\&\, i_p(t,0) = 0$. Thus, from the solution (23) – (24) for the model equation (2), (6), (9) along the characteristics lines, we have $i_h(t,0) = 0$ and $i_p(t,0) = 0$ for all $t > \tau$. Hence, $i(t,0) \to 0$ as $t \to \infty$. It can be verified that $\{E^0\}$ is the maximal compact invariant set. Therefore, from the Lassalle invariant principle, we conclude that the disease-free equilibrium E^0 is globally asymptomatically stable if $R_E \le 1$

4 Conclusion

In this paper, an infection-age-structured model was developed to study the Monkey-pox disease in a population with vital dynamics, incorporating standard incidence rate and vaccination and we analyzed the model by showed the existence and uniqueness of the solution of the model. Meanwhile, we obtained the Disease Free Equilibrium state and shown the effective reproduction number of the model. We showed the conditions for Local and Global Stability of the Disease Free Equilibrium (DFE) State, where we found that the disease free equilibrium state is locally asymptotically stable if $G(0) < 1$ ($\mathrm{R_E} < 1$) and Globally Asymptotically Stable (GAS) if $\mathrm{R_E} \le 1$ while unstable if $\mathrm{R_E} \ge 1$

References

[1] Essbauer, S., Pfeffer, M. Meyer, H. (2009). Zoonotic poxviruses. Vet. Microbiol. doi:10.1016/j.vetmic.

[2] Kantele, A. Chickering, K., Vapalahti, O., and Rimoin, A.W. (2016). Emerging diseases— the monkey pox epidemic in the Democratic Republic of the Congo, *Clinical Microbiology and Infection.* 22(8), 658–659.

[3] Centres for Disease Control (2003). Morbidity and Mortality Weekly Report, Atlanta Georgia, (MMWR). 52(27), 642-646.

[4] Rimoin, A.W., Kisalu, N., Kebela-Ilungam, B., Mukaba, T., Wright, L.L., Formenty, P., Wolfe, N.D., Shongo, R.L., Tshioko, F., Okitolonda, E., Muyembe, J.J., Ryder, R.W., and Meyer, H. (2007). Endemic human monkey pox, Democratic Republic of Congo, 2001-2004. *Emerg. Infect. Dis.* 13(6), 934 - 936.

[5] Lasisi, N.O., Akinwande, N.I., Olayiwola, R.O., et al. (2018). Mathematical Model for Ebola Virus Infection In Human With Effectiveness of Drug Usage. J. Appl. Sci. Environ. Manage, Vol. 22(7), 1089 – 1095. DOI: https://dx.doi.org/10.4314/jasem.v22i7.16. http://ww.bioline.org.br/ja or https://www.ajol.info/index.php/jasem
[6] Lasisi, N.O., Akinwande, N.I., and Oguntolu, F.A., (2020). Development and exploration of a Mathematical Model for Transmission of Monkey-Pox in Humans. *Journal of Mathematical Models in Engineering*. 6(1) 23-33. https://doi.org/10.21595/mme.2019.21234
[7] Mimmo Iannelli, and Fabio Milner (2010). The Basic Approach to Age-Structured Population Dynamics. Retrieved from www.springer.com/series/10049
[8] Ashezua, T. T. (2016). An Infection-age-structured Mathematical Model for Tuberculosis Disease Dynamics Incorporating Control Measures, PhD Thesisi. Federal University of Technology, Minna. Nigeria.
[9] Shuai, Z, and Van Den Driessche, P. (2013). Global stability of infectious disease models using Lyapunov functions, *SIAM Journal on Applied Mathematics*. 73, 1513-1532.
[10] Wang, J., and Zhang, T. (2016). Mathematical Analysis for An age-structured Hiv Infection Model with Saturation Infection Rate, *Electronic Journal of Differential Equations*. 33, 1-19. http://www.ejde.math.unt.eduftpejde.math.txstate.edu.
[11] Huang, G., Liu, X. and Takeuchi, Y. (2012). Lyapunov functions and global stability for age structured HIV infection model, *SIAM. Journal Applied Mathematics*. 72(1), 25-38
[12] Sebastian Anita (2000). Analysis and Control of Age-Dependent Population Dynamics, Kluwer Academic Publishers-Dordrecht/Boston/London. ISBN 0-7923-6639-5.
[13] Lasisi, N. O. (2020). Effect of public awareness, behaviours and treatment on infection-age-structured of mathematical model for HIV/AIDS dynamics. *Journal of Mathematical Models in Engineering*, Vol. 6, Issue 2, p. 103-121.*DOI https://doi.org/10.21595/mme.2020.21249*
[14] Lasisi, N. O., Akinwande, N. I., Abdulrahaman, S. (2020). Optimal Control and Effect of Poor Sanitation on Modeling the Acute Diarrhea Infection. *Journal of Complexity in Health Sciences*, 3(1), 91-103. *DOI https://doi.org/10.21595/chs.2020.21409*

.

An equivalence in a selected family of cyclic subsemigroups and algorithm for generating systems of semigroup

M.I. Sampson[*†], C. F. Igiri [‡], J.O. Achuobi[†§], C.T. Madubuike[†], and L.E. Effiong[†††]**

Abstract

This paper focuses on generators of cyclic subsets of semigroups which determines the whole semigroup through algebraic closure. We call a generating set minimal if it does not have a proper generating subset. A set is independent if no element of the set can be generated by the remaining members of the set. Independent subsystems of cyclic semigroups are intersected to obtain the generating set of cyclic semigroups. From intersecting subsystems of cyclic semigroups, a certain equivalence relation on the set of all cyclic Subsemigroups are obtained. The paper also shows how such equivalence relation is a tool for partitioning cyclic subsemigroups into generating subsystems. Algorithm to find the minimal generating set of a semigroups is given.

Keywords and phrases: Semigroup, Cyclic, Independent, Minimal, Generating sets

1 Introduction: somethings about cyclic semigroups

In this section, we investigate some behaviour of cyclic semigroups and discuss about the problem of intersecting semigroups/groups. We show some connections between members in such intersection and also show how some selected family of connected cyclic semigroups can be embedded into a cyclic semigroup. These provide tools for obtaining algorithms for finding generating sets. We can also determine minimal generating sets as we can intersect independent subsystems to obtain the generating set of such semigroups. We begin with definitions of Semigroups, Subsemigroups, Cosets and other relevant terminologies. Where they are not defined, the reader can read up the definitions in [1], [2], [3], [5], [6], [8], [11]. and [12].

Definition 1.1 (Semigroup). Let S be a set with a mapping $*: S \times S \Longrightarrow S$. Then S forms a semigroup $(S,*)$ if $\forall\, a,b,c \in S \Longrightarrow\ (a*b)*c = a*(b*c)$ holds.

[*]Corresponding Author; E-mail: marshalsampson@aksu.edu.ng
*†Department of Mathematics, Akwa Ibom State University, Ikot Akpaden, Nigeria.
‡Department of Mathematics, University of Calabar, Calabar, Nigeria. E-mail: jonasogarachuobi@yahoo.com
†§ Department of Mathematics, University of Calabar, Calabar, Nigeria. E-mail: chrixigiri@unical.edu.ng
†**Department of Mathematics, Abia State Polytechnic, Aba. E-mail: vinc56@yahoo.com
††† Department of Mathematics, Abia State Polytechnic, Aba. E-mail: louisn66@yahoo.com

Definition 1.2 (Subsemigroup). Let $(S, *)$ be a semigroup. If a subset $H \subset S$ forms a semigroup for the same operation $* : H \times H \to H$ as in S, then H is a subsemigroup of S.
Definition 1.3 (Monoid). Let $(S, *)$ be as semigroup. If there is a neutral element $\mathrm{e} \in \mathrm{S}$, such that $e * a = a * e = a, \ \forall a \in S$, then S is a Monoid.

Lemma 1.4 [5]. Let $(S,*)$ be a semigroup. If S is not a monoid, if there exists a set $M_S := S \cup \{e\}$ and an operation $\circ$ such that $e \circ e = e; \ e \circ a = a \circ e = a, \ \forall a \in S$ and $a \circ b := a * b, \forall a, b \in S$. Then $\{M_S, \circ\}$ is a monoid.
Proof. If S is not a monoid, adjoining an identity e to S produces $M_S := S \cup \{e\}$. If multiplication in M_S is defined as given: $e \circ e = e; \ e \circ a = a \circ e = a, \forall a \in S$, then replacing $\circ$ by $*$ accords $\{M_S, \circ\}$ the properties of $(S, *)$ in definition 1.3. Hence $\{M_S, \circ\}$ is a monoid.

Remarks 1.5. There is no essential difference between a monoid and a semigroup. A monoid $\{M,*\}$ with a neutral element $e \in M$ represents a semigroup if $M \backslash \{e\} =: S$, is a subsemigroup of M. In other words, $S \subset M$ is a subsemigroup of M if S is an invariant subset of M for the semigroup operation, which means S does not have any invertible element. Any semigroup is a subsemigroup of a monoid by the lemma 1.4.

Theorem 1.6. Let $\{S,*\}$ be a semigroup. Let $H_\alpha \subset S$ be a subsemigroup $\forall \alpha \in A \neq \emptyset$, then

$$\emptyset \neq H = \bigcap_{\alpha \in A} H_\alpha$$

is a subsemigroup of S.
Proof. Let $u, v \in H$. Then $u, v \in H_\alpha, \forall \alpha \in A \implies$

$$u * v \in H_\alpha, \forall \alpha \in A \implies u * v \in H = \bigcap_{\alpha \in A} H_\alpha$$

Definition 1.7. (Commutative Semigroup). Let $(S, \cdot)$ be a semigroup. $(S, \cdot)$ is called a Commutative Semigroup, if $\forall x, y \in S : x \cdot y = y \cdot x$.

Definition 1.8. (Cosets). Let S be a semigroup containing the subsemigroup U, and let $c_i \in S$, then by the Left (right) Coset, $c_i U$ $(U c_i)$ of U, we mean the set of elements obtained by multiplying c_i on the right (left) by each element of U. A left coset of U that is also a right coset is simply called a Coset.

2 Intersections of subsemigroups

We now define a fundamental subsemigroup called cyclic subsemigroup.

Definition 2.1. (Cyclic Subsemigroup). Let $\{S,*\}$ be a semigroup with a neutral element $e \in S$. Let $a \in S$. Then $\{\theta^j \mid 0 \leq j \leq \infty, \ e = \theta^0\} =: \langle a \rangle$ is called a cyclic subsemigroup.

Remark 2.2. The subset $\{\theta^j \mid j \in N\} =: \langle\theta\rangle \subset S$ is a commutative subsemigroup (see **Definition 1.7.** for definition of commutative semigroup):

$$\forall\, u, v \in \langle\theta\rangle \implies u = \theta^p, \qquad v = a^q$$

$\implies u * v = \theta^p * \theta^q = \theta^{p+q} = \theta^{q+p} = \theta^q * \theta^p = v * u \in \langle\theta\rangle$ by $p + q \in N$.

Definition 2.3. **(**Connected Family of Subsemigroups). Let $H := \{H_\alpha\}_{\alpha\in A}$ be a family of subsemigroups of S. Then H is a connected family of subsemigroups if $(H_\alpha \cap H_\beta)\backslash\{e\} \neq \emptyset$, $\forall\alpha, \beta \in A$, where $e \in S$ is the neutral element of S (Existence of a neutral element may always be assumed by lemma of section 1.4).

Lemma 2.4. Let S be a semigroup, let $H_1, H_2 \subset S$ be subsemigroups such that $H_1, H_2 \notin \{\emptyset, \{e\}\}$. Let H_1, H_2 be related by $H_1 \bowtie H_2$ if $H_1 \cap H_2 \notin \{\emptyset, \{e\}\}$.Then the relation $\bowtie$ is reflexive and symmetric but not necessarily transitive.

Proof. 1. Reflexivity**:** If the subsemigroup $H \subset S$ fulfils $H\backslash\{e\} \neq \emptyset$; then $H \cap H = H \notin \{\emptyset, \{e\}\}$, hence $H \bowtie H$ is true.

2. Symmetry**:** Let $\emptyset \neq H_1, H_2 \subset S$ fulfill $H_1 \bowtie H_2$ then $H_1 \bowtie H_2 \implies H_1 \cap H_2 \notin \{\emptyset, \{e\}\} \implies H_2 \cap H_1 \notin \{\emptyset, \{e\}\} \implies H_2 \bowtie H_1$ that proves the symmetry.

3. Transitivity**:** We give an example that the transitivity does not necessarily hold. Let $S \subset R^2$ be an open convex cone with addition of vectors as its operation. To make it concrete, let the cone be $S := \{(x, y) \mid y > 0\}$. Let

$H_1 := \{(x, y) \mid 0 < y < \frac{\sqrt{3}}{2}(-x),\ -\infty < x < 0\} \subset S$

$H_2 := \{(x, y) \mid y > \frac{\sqrt{2}}{2}|x|,\ x \in R\} \subset S$

$H_3 := \{(x, y) \mid 0 < y < \frac{\sqrt{3}}{2}x,\ \infty > x > 0\} \subset S$

The upper borders of H_1 *and* H_3 are segments of straight lines enclosing 120^0 and 60^0 angles respectively with the first (x) axes. The border of H_2 consists of two segments of straight lines enclosing 135^0 and 45^0 angles with the first axes.

$H_1 \cap H_2 = \{(s, t) \mid \frac{\sqrt{2}}{2}|s| < t < \frac{\sqrt{3}}{2}|x|,\ -\infty < x < 0\} \notin \{\emptyset, \{e\}\} \implies H_1 \bowtie H_2$ holds.

$H_2 \cap H_3 = \{(s, t) \mid \frac{\sqrt{2}}{2}|s| < y < \frac{\sqrt{3}}{2}|s|,\ \infty > x > 0\} \notin \{\emptyset, \{e\}\} \implies H_2 \bowtie H_3$ holds.

$H_1 \cap H_3 = \{(s, t) | 0 < y < \frac{\sqrt{3}}{2}|x|,\ -\infty < x < 0\} \cap \{(s, t) \mid 0 < y < \frac{\sqrt{3}}{2}|s|,\ \infty > x > 0\} = \emptyset \implies$ the relation $H_1 \bowtie H_3$ is not true. Hence the relation $\bowtie$ is not transitive.

2.1 Intersecting cyclic subsemigroups - their equivalence relation

We now do a quick study of the structure of cyclic subsemigroups as graphs first with infinite cyclic subsemigroups as intersecting chains where the intersection of any two infinite cyclic semigroups is an infinite cyclic subsemigroup of the two intersecting infinite cyclic semigroups. In our graph the nodes will be semigroup elements, and the edges connecting the a^k elements of the cycle to the consecutive a^{k+1} element. In this graph we do not consider multiplications between elements coming from two different chains. The graph structure is available in the original semigroup also and the smallest semigroup containing original cyclic semigroups can be mapped into the free semigroups.

Lemma 2.6. Let $\{S,*\}$ be a semigroup, let $C_1 = \langle a\rangle,\ C_2 = \langle b\rangle \subset S$ be two cyclic semigroups, $a \notin C_2$ and $b \notin C_1$. If $C_1 \cap C_2 \neq \{\emptyset\}$ and $C_1 \cap C_2 \neq \{e\}$; then there exists a free cyclic semigroup $F_{a,b} = \langle s\rangle$ and an isomorphism $i: \langle a\rangle \cup \langle b\rangle \to F = \langle s\rangle$. In other words, $C_1\ and\ C_2$ can be embedded into one cyclic group.

Proof. Let the first common element $c \in C_1 \cap C_2$ (c is the generator element of the cyclic semigroup: $C_1 \cap C_2 = \langle s\rangle$). Then $\langle a\rangle \ni a^p = c = b^q \in \langle b\rangle$. Then there is a free semigroup $\langle s\rangle$ in which $a = s^q$ and $b = s^p$ thus $a^p = s^{q*p} = s^{p*q} = b^q = c$ holds hence the cyclic group $\langle s\rangle$ contains the image of $C_1,\ C_2$ and $C_1 \cap C_2 \subset S$ by the mapping $i(a^t) \coloneqq s^{pt}$ and $i(b^t) \coloneqq s^{qt},\ \forall t \in N\backslash\{0\}$ which is an isomorphism. ■

Remark 2.7. The isomorphism here does not map from $\langle a, b\rangle \to \langle c\rangle$. It maps from the $\langle a\rangle \bigcup \langle b\rangle \to \langle c\rangle$ where $\langle a\rangle \bigcup \langle b\rangle \subset \langle a, b\rangle$ using the operations of $\langle a, b\rangle$ along the cyclic groups $\langle a\rangle$ and $\langle b\rangle$. This mapping however, truly represents the intersections between the two subsemigroups.

Remark 2.8. Note that $s \in F$ is determined by $a \in \langle a\rangle$, $b \in \langle b\rangle$ and $c \in \langle a\rangle \cap \langle b\rangle$ which is the generator $\langle c\rangle = \langle a\rangle \cap \langle b\rangle$ of the intersection, the minimal power appearing in the intersection from both $\langle a\rangle$ and $\langle b\rangle$. It can be proved then that the mapping stated in the lemma 2.6 is a unique isomorphism, in other words, the relative positions of the three semigroups are fully determined in the free group.

Lemma 2.9. (Equivalence Relation on the Set of all Cyclic Subsemigroups)

Let S be a semigroup and let $S_C \coloneqq \{\langle x\rangle \mid x \in S\}$ be the set of all cyclic subsemigroups. Then the relation $\langle a\rangle \asymp \langle \theta\rangle \Leftrightarrow \langle a\rangle \bigcap \langle \theta\rangle \neq \{\emptyset\}$ and $\langle a\rangle \bigcap \langle \theta\rangle \neq \{e\}$ is an equivalence relation $\forall\ \langle \alpha\rangle, \langle \theta\rangle \in S_C$.

Proof. (i) The relation is reflexive:

$\forall \langle a\rangle \in S_C,\ \langle \alpha\rangle \bigcap \langle \alpha\rangle = \langle \alpha\rangle \neq \langle \alpha\rangle \bigcap \langle b\rangle \neq \{\emptyset\}$ and $\langle \alpha\rangle \bigcap \langle b\rangle \neq \{e\} \Rightarrow \langle \alpha\rangle \asymp \langle a\rangle$.

Note that $a \in S$ is an existing element hence $\langle \alpha\rangle \neq \langle a\rangle \bigcap \langle \alpha\rangle \neq \{\emptyset\}$ and $\langle \alpha\rangle \bigcap \langle \alpha\rangle \neq \{e\}$.

(ii) The relation is symmetric:

$\forall \langle \alpha\rangle, \langle \alpha\rangle \in S_C, \langle \alpha\rangle \asymp \langle b\rangle \Leftrightarrow \langle \alpha\rangle \bigcap \langle \theta\rangle \neq \emptyset \Leftrightarrow \langle \alpha\rangle \bigcap \langle \theta\rangle \neq \langle \alpha\rangle \bigcap \langle \theta\rangle \neq \{\emptyset\}$ and $\langle \alpha\rangle \bigcap \langle \theta\rangle \neq \{e\} \Leftrightarrow \langle \theta\rangle \asymp \langle \alpha\rangle$ completes the proof of the symmetry.

(iii) Let $\langle \alpha\rangle, \langle \theta\rangle\ and\ \langle c\rangle \in S_C$. Let $\langle \alpha\rangle \asymp \langle \theta\rangle$ and $\langle \theta\rangle \asymp \langle c\rangle$ hold.

By $\langle \alpha\rangle \asymp \langle \theta\rangle \Longrightarrow \langle \alpha\rangle \bigcap \langle \theta\rangle \neq \{\emptyset\}$ and $\langle \alpha\rangle \bigcap \langle \theta\rangle \neq \{e\} \Longrightarrow \exists p_1, p_2 > 0$ such that

$$\langle \alpha\rangle \ni \alpha^{p_1} = b^{p_2} \in \langle b\rangle$$

Similarly, $\langle \theta\rangle \asymp \langle \omega\rangle \Longrightarrow \langle \alpha\rangle \bigcap \langle \theta\rangle \neq \{\emptyset\}$ and $\langle \alpha\rangle \bigcap \langle \theta\rangle \neq \{e\} \Longrightarrow \exists p_3, p_4 \in N$ such that

$$\langle b\rangle \ni \theta^{p_3} = \omega^{p_4} \in \langle c\rangle$$

Then raising both sides of $\alpha^{p_1} = \theta^{p_2}$ to the power p_3 results in $\alpha^{p_1 p_3} = \theta^{p_2 p_3}$ and raising both sides of $b^{p_3} = c^{p_4}$ to the power p_2 results in $\theta^{p_3 p_2} = \theta^{p_4 p_2}$

Therefore $a^{p_1 p_3} = \theta^{p_2 p_3} = \theta^{p_3 p_2} = \theta^{p_4 p_2} =: h$ fulfills

$$h \in \langle \alpha\rangle \bigcap \langle \theta\rangle \neq \{\emptyset\} \text{ and } \langle \alpha\rangle \bigcap \langle \theta\rangle \neq \{e\}$$

Therefore $\langle \alpha\rangle \asymp \langle \omega\rangle$ holds hence the transitivity holds. ■

3 Partitioning of cyclic semigroup

The equivalence relation of Lemma 2.9 partitions a cyclic semigroup into subsemigroups that are independent generators of its oversemigroup. In [6], they obtain a result that relate both concepts (minimal generating set and maximal independent set). There is analogue of this result in group theory. This needs a suitable equivalence relation and we determined one $S/\asymp$.

Corollary 3.2 (Partitioning Semigroup). Let $\{S,*\}$ be a semigroup. Then the system S_C of cyclic subsemigroups of S can be partitioned into a set of pairwise disjoint equivalence classes $S/\asymp \coloneqq \{\hat{C} \mid C \in S_C\}$ where $\hat{C}$ is the equivalence class of cyclic subsemigroups containing the subsemigroup $C \in S_C$.

Proof. S_C be a set and an equivalence class (in this case $S/\asymp$) in S_C divides S_C into pairwise disjoint

Remarks 3.3. The system of all cyclic subsemigroups is $S_C \coloneqq \{\langle a\rangle | a \in S\}$ (see the lemma 2.9). This means that the partitioning splits up the whole original semigroup S into the union of pairwise disjoint components

$$S = \bigcup_{a\in S} \widehat{\langle a\rangle}$$

Each such component contains a maximal set of equivalent sub-cyclic semigroups generated by the points of the component. Let $\hat{S}_C = S/\asymp$ be the set of equivalence classes with respect to the connectedness relation. Then let $\forall a, b \in S, \langle a\rangle \in \hat{a}, \langle b\rangle \in \hat{b}$.

Remarks 3.4. (On Cosets of Cyclic Semigroups). The definition of cosets given in section 1.8. serves as a very useful tool for partitioning sets especially where there is a single operation on the set. In the next section we will use the same concept but specialised for Cyclic Semigroups to present an analogue of the Normal Subgroup for semigroup.

Definition 3.5. (Cosets). Let S be a semigroup and let $S_C = \{\langle a\rangle \mid a \in S\}$ be the set of its cyclic semigroups. Let $c \in S_C,\ C \coloneqq \langle c\rangle$ be a cyclic semigroup and let $b \in S$. Then
$\theta C \coloneqq b * C = \theta \langle c\rangle = \{\theta * c^k \mid k \in \mathbb{N}\}$ is a left coset formed by θ and C. Similarly
$C\theta \coloneqq C * \theta = \langle c\rangle\theta = \{c^k\theta \mid k \in \mathbb{N}\}$ is a right coset formed by θ and C.

Theorem 3.6. (An Analogue of Normal Subgroup [5]). Let S be a semigroup with a neutral element and let $C \subset S$ be subsemigroups with neutral element. Then the following hold:

1. $C * C = \{\beta * \gamma \mid \beta, \gamma \in C\} = C;$
2. Let $C \subset H \subset S$ where H, C are cyclic subsemigroups, $C = \langle\tau\rangle, \tau \in H$. Then the cosets fulfill $\beta * C = C * \beta,\ \forall \beta \in H$. In other words, using terminology of group theory, C is a normal subsemigroup of H.
3. Let $C = \langle\tau\rangle, \tau \in H$. Let $C_k \coloneqq \{(\tau^k)^s = \tau^{k*s} \mid 0 \le s < \infty\} \subset C$. Then
$$(\tau^p * C) \cap (\tau^q * C) = \emptyset\ ;\ \forall\ 0 \le p,\ q < k, p \ne q.$$

Proof. (i). Since $e \in C,\ C = e * C \subset \{a * b \mid a, b \in C\} = C * C \subset C \Longrightarrow C * C = C$.

(ii). Since H is a cyclic subsemigroup of S, it is a commutative semigroup. A subsemigroup

$C \subset H$ is then a commutative subsemigroup of H also. Then the left cosets are equal to the right ones: $a * C = C * \beta,\ \forall\ \beta \in H$ by the commutativity of H.

(iii). Let $C = \langle \tau \rangle = \{\tau^p \mid 0 \leq p < \infty\}, t \in H$. Let

$$C_k := \{(\tau^k)^s = \tau^{k*s} \mid 0 \leq s < \infty\} \subset C.$$

The congruence relation of $mod\ k$ equivalence is an equivalence relation. It partitions the natural numbers into k pairwise disjoint equivalence classes

$$N_{k,q} := \{p \mid q \equiv p\ (mod\ k)\}, 0 \leq q < k.$$

Accordingly, the cosets

$\{\tau^p C_k = \{\tau^p(\tau^k)^s \mid \tau^p(\tau^k)^s = \tau^{p+ks}, 0 \leq s < \infty\} = \{\tau^\alpha \mid \alpha \in N_{k,p}\},\ 0 \leq p < k.$

Hence let $\tau^p * C_k = \{\tau^\alpha \mid \alpha \in N_{k,p}\}$, and $\tau^q * C_k = \{\tau^\alpha \mid \alpha \in N_{k,q}\}, \forall 0 \leq p,\ q < k, p \neq q.$

Then

$$N_{k,p} \cap N_{k,q} = \emptyset \Longrightarrow (\tau^p * C_k) \cap (\tau^q * C_k) = \emptyset\ ;\ \forall 0 \leq p,\ q < k,\ p \neq q. \qquad \blacksquare$$

3.1 Intersections of subsemigroups with cyclic semigroups

The cyclic subsemigroups were defined in section 2.1 and their commutative property explained in section 2.2. This together with the existence of an explicit formula for its elements extends the study of independence/generating sets to $N - modulus's$.

Lemma 3.8. Let S be a semigroup and let $\emptyset \neq H, C \subset S$ be subsemigroups, let $C = \langle a \rangle$ be a cyclic subsemigroup. Then $T := H \cap C$ is a commutative subsemigroup of S with connected cyclic subsemigroups.

Proof. It was proved in theorem 1.6 that non-empty intersections of subsemigroups are subsemigroups hence T is a subsemigroup of C. Since C is commutative, then the intersection T of H and C is a commutative subsemigroup of $H, a\ subset\ of\ S$. Let $\lambda, \mu \in T \Longrightarrow \lambda = a^p,\ v = a^q$. Then $\lambda^q = a^{p*q} = a^{q*p} = \mu^p$ proves that $\langle \lambda \rangle \cap \langle \mu \rangle \neq \{\emptyset\}$ and $\langle \lambda \rangle \cap \langle \mu \rangle \neq \{e\}$.

Hence the cyclic subsemigroups of T form a connected system. $\blacksquare$

Remark 3.9. It was mentioned in the Remark 2.7, that the connected families (see definition 2.3) form the equivalence classes as stated in the lemma 2.9, each equivalence class is represented by a free cyclic group. Therefore, in these classes we have a free semigroup operation instead of the original semigroup operation. The case discussed in (the lemma of) 2.13 is different: here we have truly commutative subsemigroups of the original semigroup *S*.

Theorem 3.10. *Let* $\{S,*\}$ be a semigroup. Let $H, C \subset S,\ H \cap C \neq \{\emptyset\}$ and $H \cap C \neq \{e\}$ be subsemigroups and let $C := \langle s \rangle,\ s \in S$ be a cyclic subsemigroup. Then $\emptyset \neq T := H \cap C$ fulfills the following:

1. $\forall \tau \in T,\ \exists! p \in N$ (there exists ***a unique*** $p\ in\ N$) such that $\tau = \alpha^p$.
2. $\forall (\emptyset \neq A) \subset T\ ,\ \exists p_{min}\ (A) := min\{p \mid \alpha^p \in A\}$;

Proof. 1. C is a cyclic subsemigroup, so $\forall a \in C, \exists p \in N$ such that $\tau = \alpha^p$. Hence $\forall \tau \in T := H \cap C \subset C,\ \exists p \in N$ such that $\tau = \alpha^p$.

2. Since $\emptyset \neq A \subset T,\ \emptyset \neq \tilde{A} := \{p \mid \alpha^p \in A\} \subset N$. Since the set of natural numbers is a well ordered set with its natural ordering, any of its non-empty subset has a minimum. Hence $\tilde{A}$ has a minimum. ■

4 Algorithm for generating systems of semigroup

We have formed enough tools in the previous section for creating algorithms for generating set of semigroups. We conclude with one algorithm for the minimal generating set of a semigroup.

4.1. **Important Corollary** (Algorithm for Minimal Generating Set).
Let S, H, C and T be semigroups as defined in definition 3.7. Let M be initialized as $M \subset N$ and Let $M = \emptyset$; Let $N \subset T$ and let N be initialized as $N = \emptyset$; Let $\Gamma \subset C$ and let $\Gamma = T$. Let $n \in \mathbb{N}$ be the counter, set to $n = 0$ for starting. Then let us consider the following algorithm:
Step 1. If $\Gamma \neq \emptyset$; then goto Step 2 else [exit].
Step 2. Let $n = n + 1$, $k_n = p_{min}(\Gamma)$, $M = M \cup \{k_n\}$ and $N = N \cup \{s^{k_n}\}$ goto step 3.
Step 3. $\Gamma = \Gamma \backslash \langle N \rangle$ goto Step 1.
If this algorithm stops after finite steps then we get a set of powers which are independent

$$\forall p \in M, s^p \notin \langle \{s^t | t \in M, t < p\} \rangle$$

The value of n, $1 \leq n \leq \infty$ gives the total number of minimums recorded. Let a set $A \subset C$ be given. Then the ascending sequence M defined by the algorithm with $\Gamma = A$ is unique.
Proof. 1. Let $P := \{t \mid s^t \in T\} \subset \mathbb{N}, P \neq \emptyset$. Since the set of natural numbers is well ordered with its natural order relation, P has a minimum $m_j \in P$ in the $j - th$ loop of the algorithm. If the minimum is removed from P, $P = P \backslash \langle N \rangle$ and $P \neq \emptyset$, then the new set P has a new minimum $m_{j+1} \in P, m_{j+1} > m_j$. Hence the algorithm will produce a finite or infinite strictly ascending sequence of natural numbers.
2. Let $0 < j \leq n$ be selected. Then let $M_j := \{k_t | \ k_t \in M, 1 \leq t \leq j\} \subset M$ and $N_j := \{s^{k_t} \mid s^{k_t} \in N, 1 \leq t \leq j\} \subset N$. M_j carry the sequence of collected minimum exponent values and N_j carry the set of corresponding sequence of members of T. The sub-semiring $\langle N_j \rangle \supset N_j$ is generated by N_j.

$$\langle N_j \rangle = \left\{ \prod_{t=1}^{j} (s^{p_t})^{\propto_{p_t}} | p_t \in M_j, \propto_{p_t} \in N \right\} = \left\{ \prod_{t=1}^{j} s^{p_t \propto_{p_t}} | p_t \in M_j, \propto_{p_t} \in N \right\}$$

$$= \left\{ s^{\eta} | \ \eta := \sum_{\substack{p \in M_j \\ \alpha_p \in N}} p \times \alpha_p \right\}$$

This shows that the semi-ring $\langle N_j \rangle$ is isomorphic to a positive cone of a sub-module of Z-module over the ring of Z:

Definition 4.1.1. (Positive Cone in the Z −module over Z). Let $M \subset \mathbb{N} \subset Z$ be a countable set of positive coprime numbers (as defined in [8]). Then

$$M_M := \left\{ s^{\eta} | \eta := \sum_{\substack{p \in M_j \\ \alpha_p \in N}} p \times \alpha_p \right\}$$

is a positive cone in the Z −module over Z.

3. Let a set $A \subset C$ be a subsemigroup. The ascending sequence $M := \{k_j\}$ defined by the algorithm in corollary of section 4.1 is unique. We prove this by mathematical induction.

Let $\{a_u\}_{u=1}^{n}$ and $\{b_v\}_{v=1}^{m}$be two sequences such that with $P = A$, $a_1 = b_1 := min\{p \mid s^p \in P\}$. Then $\langle\{a_1\}\rangle = \langle\{b_1\}\rangle \Longrightarrow P \setminus \langle\{a_1\}\rangle = P \setminus \langle\{b_1\}\rangle = P$ hence $a_2 = min\{p \mid s^p \in P\} = b_2$.

Assume that we proved that $a_t = b_t$, $\forall 1 \leq t \leq q$. Then $\langle\{a_t\}_{t=1}^{q}\rangle = \langle\{b_t\}_{t=1}^{q}\rangle$

Hence $P\setminus\{a_t\}_{t=1}^{q} = P\setminus\{b_t\}_{t=1}^{q} \Longrightarrow a_{q+1} = b_{q+1} = min\{p \mid s^p \in P\}$. Hence $a_q = b_q, \forall t$ until $P = \emptyset$.

This happens at the same subscript n since $P\setminus\{a_t\}_{t=1}^{q} = P\setminus\{b_t\}_{t=1}^{q}$, $1 \leq p \leq n$. Hence, we proved the statement.

4. When the algorithm stops, then $A\setminus\langle\{s^{a_t} \mid 1 \leq t \leq n\}\rangle = \emptyset$;
   Hence $A = \langle\{s^{a_t} \mid 1 \leq t \leq n\}\rangle$ holds.

5. If $\bigcap_{p=1}^{n}(C\setminus\langle\{s^{a_t} \mid 1 \leq t \leq n\}\rangle) = \emptyset$ then $T = C \Leftrightarrow C = H$

This follows from the complementation of the intersection with respect to C:

$$\emptyset' = C = \left(\bigcap_{p=1}^{n}(C\setminus\langle\{s^{a_t} \mid 1 \leq t \leq n\}\rangle)\right)' = \bigcup_{p=1}^{n}(C\setminus\langle\{s^{a_t} \mid 1 \leq t \leq n\}\rangle)'$$

$$\bigcup_{p=1}^{n}\langle\{s^{a_t} \mid 1 \leq t \leq n\}\rangle = \langle\{s^{a_t} \mid 1 \leq t \leq n\}\rangle = T$$

■

Remark 4.1.2. As a direct consequence of the statements of the theorem about $M_j \subset M$ and $N_j \subset N$, $1 \leq j \leq n$ and their definition in corollary 4.1, we have the following theorem.

Theorem 4.2. Let S be a semigroup with a neutral element $e \in S$. Let $H, C \subset S$ be subsemigroups, and let C be a cyclic subsemigroup. Let $T := H \cap C =: T \notin \{\emptyset, \{e\}\}$. Let $M \subset \mathbb{N}, N \subset T$ be sequences produced by the algorithm in corollary of section 4.1. Let $n \in \mathbb{N}$ be the number of sequence elements in M *or* N and let $M_j \subset M$, $N_j \subset N$, $1 \leq j \leq n$ be as defined in the point 2 of proof of the corollary 4.1. Then the following hold.

1. $\bigcup_{j=1}^{n}\langle N_j\rangle = \langle N\rangle = T$

2. $\bigcap_{j=1}^{n}\langle N_j\rangle' = \emptyset \Leftrightarrow C = T \subset H$, hence C is dependent on H

Proof. Set $M_j := \{k_t | k_t \in M, 1 \leq t \leq j\} \subset M$ and $N_j := \{s^{k_t} | s^{k_t} \in N, 1 \leq t \leq j\} \subset N, 1 \leq j \leq n$ as defined in corollary 4.1. The proofs of 1 and 2 follow from the concluding part of the proof of corollary 4.1.

■

5 Conclusion and recommendation

The algorithmic approach for determining minimal generating set discussed here is being improved upon with alternative characterizations to handle the bases (Independent generating set) problem of semigroups. This circumvents the task in utilizing equivalences for partitioning set into generating subsystems as given in section 3 which is also what the use of the popular green's equivalences aims at achieving. In [11], algorithmic approach has been used for the basis of Additive Semigroup of Integers while [3] is about Countable systems of semigroup and [4] about Infinite Semigroups. A newer and interesting characterization in [12] can be applied to Classes of Semigroups. We shall dwell on bases of classes of semigroups in later articles.

References

[1] Howie, J. M. 1995. Fundamentals of semigroup theory. Academic Press [Harcourt Brace Jovanovich Publishers], London, L.M.S. Monographs, No. 7.

[2] Sampson M.I. (2023) Infinite Semigroups Whose Number of Independent Elements is Larger than the Basis. IJRTI, Volume 8, Issue 7, ISSN: 2456-3315.

[3] Sampson M.I., L. Zsolt, Achuobi J.O., Igiri C.F., Effiong L.E. (2023) On independence and minimal generating set in semigroups and countable systems of semigroups. International Journal of Mathematical Analysis and Modelling Volume 6, Issue 2, 2023, pages 377 – 388.

[4] Eke, N., Effiong, L. E., Madubuike, C. T., Otobong J. T., Sampson, M. I. (2023). Independent Elements and Minimal Generating Sets in Infinite Semigroups. International Journal of Scientific Research and Engineering Development-– Volume 6 Issue 4, July- Aug 2023

[5] Sampson, M. I. (2022). Generating Systems of Semigroups and Independence. Ph.D. thesis, Department of Mathematics, University of Calabar, Calabar, Nigeria.

[6] Sampson, M. I. 2023. Infinite Semigroups whose Number of Independent Elements is Larger than the Basis", International Journal of Science & Engineering Development Research (www.ijrti.org), ISSN:2455-2631, Vol.8, Issue 7, page no.1001 - 1005, http://www.ijrti.org/papers/IJRTI2307145.pdf

[7] Sampson, M.I. (2019). Generating Systems of Semigroups and Independent Set. Paper Presented at 3rd International Conference on Mathematics "An Istanbul Meeting for World Mathematicians" July 3 – 5, 2019, Istanbul, Turkey.

[8] Sampson M.I., Jackson Ante, Nduka Wonu (2020). On divisibility of Sum of Coprimes of Integers by Integers and Primes. IOSR Journal of Mathematics (IOSR-JM) e-ISSN: 2278-5728, p-ISSN: 2319-765X. Volume 17, Issue 1 Ser. III, PP 39-49. www.iosrjournals.org.

[9] Udoaka O.G, and Sampson, Marshal I. (2018). Direct Product of Brandt Semigroup and Its Rank as A Class of Algebra.

[10] Zsolt, Lipcsey, Sampson M.I. (2023). On Existence of Minimal Generating Sets and Maximal Independent Sets in Groups and The Additive Semigroup of Integers. IOSR Journal of Mathematics (IOSR-JM). e-ISSN: 2278-5728, p-ISSN: 2319-765X. Volume 19, Issue 4 Ser. 1 (July. – August. 2023), PP 57-64. www.iosrjournals.org.

[11] Sampson M. I, Zsolt Lipcsey, Akak Eyo Offiong, Mfon Augustine Essien (2024). Algorithms for Semigroup Bases I. International Journal of Mathematical Analysis and Modelling, Volume 7, Issue 1, 2024. https://tnsmb.org/jurnal/

[12] Weaver, M. W. 2010. Cosets in a semi-group. *Mathematics Magazine*, 25(3). Taylor & Francis, Ltd. on behalf of the Mathematical Association of America. https://www.jstor.org/stable/3029444.

Application of Jensen's integral formulae on polynomials with entire functions of positive real parts and Gauss mean value theorem

G.N. Emenogu [*†], I.C. Yemisi [‡], E.I. Edugbe [†§], C. Chigozie [†], and B.O. Osu [†††]**

Abstract

In this study, new theorems with proofs for new inequalities on polynomials which are of the importance in the theory of transcendental numbers, the product of polynomials and their associated roots were developed. Jensen's integral formula was applied to obtain new results about the bounds on the poles and roots of complex functions with positive real parts and Gauss Mean Value Theorem through the relationship between the coefficients and zeros of polynomials. It was shown that if the k-polynomials have $n_i\ roots, i = 1,2,3, \dots, k$, then their products $f_1(z)f_2(z)\dots f_{k-1}(z)f_k(z)$ have distinct roots of $n_1 + n_2 + n_3 \dots + n_{k-1} + n_k$.

Keywords and phrases: Jensen's formulae; polynomials; complex variable; meromorphic functions; zeros and roots of multiplicity

1 Introduction

Polynomials are a natural type of function to consider: a generalization of linear, quadratic and cubic functions. They can sometimes be solved exactly. They graphs can be sketched. Many quantities in the real world are related by polynomial functions. Importantly, any smooth function can be approximated by polynomials. So proficiency in dealing with polynomial is also important. In [1, 2, 3], a polynomial of degree 'n' is a function of the form $f(x) = a_n x^n + a_{n-1}x^{n-1} +$

†††Corresponding Author; E-mail: Osu.bright@abiastateuniversity.edu.ng (https://orcid.org/0000-0003-2463-430X)
†††Department of Mathematics, Abia State University, Uturu, Nigeria.
*†Department of of Mathematics, Michael Okpara University of Agriculture, Umudike, Nigeria.
*†E-mail: ng.emenogi@mouau.edu.ng
‡Department of Mathematics, National Open University, Nigeria
§E-mail: cishola@noun.edu.ng
†§Department of Mathematics, Abia State University, Uturu, Nigeria
E-mail: iedugbe01@gmail.com
†** Department of Insurance, University of Jos, Jos, Nigeria
†E-mail: chigoziec@unijos.edu.ng (https://orcid.org/0000- 0002-3174-7751)

$\cdots + a_2x^2 + a_1x + a_0$ where the *a*'s are real numbers (sometimes called the coefficient of the polynomial and n is an integer). The degree of a polynomial is the highest of x in its expression. Polynomial of degree 1, 2, 3, 4, 5 are respectively are called linear, quadratic, cubic, quartic and quintic. A degree zero polynomial is just a constant function. A root or a zero polynomial *f(x)* is a number r such that *f(r) =0*. According to [4, 5], a polynomial function is a function such as a quadratic, a cubic etc involving only non-negative-integer power of x. The highest degree term a_nx^n is called the leading term and its coefficient a_n is called the leading coefficient. If the leading coefficient is 1, the polynomial is called Monic. The term a_0 is called the constant term. However, the leading coefficient is always non-zero as it is the coefficient of the highest power of *x* which actually appears. Jensen's formula has been applied by many scholars to study roots and poles of meromorphic function which is only analytic everywhere in the finite plane. [6,7,8,9,10] applied Jensen's formula in geometry of the zeros of the derivative of a polynomial a central role is taken by luca's theorem in which the derivative lie in the smallest convex polygon containing the zeros of the original polynomial under certain conditions. [11,12,13] studied multivariate polynomial with complex coefficients with concerns in plurisubharmonic functions with very small order to determine area of the intersection of the analytic set and inequality similarly to the case of p complex variable and where the unit disk in C is replaced by the unit ball of C^P. [14, 15, 16,] used theory of transcendental number to obtain an inequality for a pair of relatively prime polynomials.

These researchers encountered a setback in the generalization of its inequality which involves several numbers and weights of measure theory in probability form. In order to overcome this setback, this research aims at applying Jensen's Integral formula on meromorphic function which is not only analytic everywhere in the finite plane but also at a finite number of poles and applying it to polynomials of entire function with positive real parts and Gauss Mean Value Theorem to determine the relationship between the coefficients and zeros of polynomials and give theorems about the product polynomials and their associated roots. Entire function is a function that is analytic everywhere in the finite plane except at ∞. To achieve the aim of this research, this paper focuses on functions of one complex variable z, $Q(z)$ which are regular inside and on the circle$|z| = r$; when $Q(0) \neq 0$ and all the zeros of $Q(z)$ satisfying $|a_k| \leq r$ where multiple zeros are counted as many times as their multiplicity with $Q(z)$ having the exact degree of $d(Q) = n$ to obtain new proofs, new results about the number of roots of the product of polynomial and new results on functions with positive real parts for new inequalities on polynomials through the application of Jensen's integral formula developed by [17]

2 Methodology/Model formulation

In [18], Jensen's integral formula was adapted and presented below

$$\frac{1}{2\pi}\int_0^{2\pi} ln\left|Q(pe^{i\theta})\right| d\theta = ln|Q(0)| + \sum_{k=1}^{N} ln\frac{p}{|a_k|} \quad (1)$$

Let $\Omega \subseteq \mathbb{C}$ be a region (connected open set). A a function U: $\Omega \to R$ is said to be harmonic if u$\in C^2(\Omega)$ and $\Delta u(z) = 0$ for all z $\in \Omega$. Here,

$$\Delta u(z) = u_{x,x}(z) + v_{y,y}(z); z = x + iy \quad (2)$$

2.1 Basic Properties of Meromorphic or harmonic Function [19, 20, 21]

i). Mean value property: let u$\in C^2(\Omega)$. Then u is harmonic if and only if it has the mean value property (MVP). Recall that u is said to have MVP if

$$u(z) = \frac{1}{2\pi}\int_0^{2\pi} u(z + re^{i\theta})d\theta \quad (3)$$

for all z $\in \Omega$ and $r > 0$ such that

$\overline{D}$(z, r) $\subseteq$ Ω. Hence we have averaged u over a circle centered at z. one can also average over disk. In the other words, MVP is equivalent to saying

$$u(z) = \frac{1}{\pi r^2}\int_{D(z,r)} u(w)dm(w) \quad (4)$$

for all z $\in \Omega$ and $r > 0$ such that $\overline{D}$(z, r) $\subseteq$ Ω.

ii). Maximum principle: let Ω be a bounded region, $u \in C(\bar{\Omega})$ and $\Delta u = 0$ in Ω. Then $\max_{\bar{\Omega}} u = \max_{\partial\Omega} u$. Further, if $u(z) = \max_{\bar{\Omega}} u$ for some z $\in \Omega$, then the u must be constant. Since $-u$ is harmonic whenever u is the same holds for the minimum too.

iii). (relationship analytic function): If $f: \Omega \to c$ is holomorphic, then $u = Re\ f$ is harmonic in Ω. The converse is true if Ω is a disk.

i.e. if Ω is a disk and u is a harmonic on Ω, then there is a holomorphic function on Ω whose real part is equal to u. An algebra is of the form;

$$P(z) = a_n z^n + a_{n-1}z^{n-1} + a_1 z + a_0 = 0 \quad (5)$$

where a_i is the complex number and the degree of the equation is $n(if\ a_n \neq 0)$.

2.2.1 Zeroes and Roots

A number r is a zero of multiplicity m of a polynomial $P(z)$ if there is a polynomial $Q(z)$ with $Q(r) \neq 0$ such that $P(z) = (z - r)^m Q(z)$. Also, r is a root of multiplicity m of the equation $P(z)$ =0. If r is a root of multiplicity $m(m \geq 1)$ of the equation $P(z)$ =0, then r is a root of multiplicity $m - 1$of the equation $P'(z) = 0$.

2.2.2 The Factor Theorem

$P(z)$ contains the factor $z - r \leftrightarrow P(r) = 0$

$P(z)$ contains the factor $(z - r)^m \leftrightarrow P(r) = P'(r) = P^{(m-1)}(r) = 0$

2.2.3 The Fundamental Theorem of Algebra

An algebra equation $P(z) = 0$ of degree n has exactly n roots (including multiplicity) in $C.$ if the roots are $r_1, \dots, r_n,$ then

$$P(z) = a_n(z - r_1), \dots, (z - r_n) \tag{6}$$

2.2.4 Relationship between Roots and Coefficients

If $r_1, \dots, r_n,$ are the roots (4), then

$$\begin{cases} r_1 + r_2, \dots, +r_n = -\frac{a_{n-1}}{a_n} \\ r_1r_2 + r_1r_3 + \cdots + r_{n-1}r_n = \sum_{i<j} r_ir_j = \frac{a_{n-2}}{a_n} \\ \dots \\ r_1r_2 \dots r_n = (-1)^n \frac{a_0}{a_n} \end{cases} \tag{7}$$

3 Discussions and conclusion

In this work new proofs are obtained for new inequalities on polynomials following Jensen's Integral formula which are of importance in the theory of transcendental numbers different from the initial results carried-out by other researchers which are not fully connected to the basic properties of meromorphic or harmonic function, we shall deduce the new proofs of inequalities on polynomials from the same source, viz from Jensens integral formula in the theory of analytic functions.

Link between Coefficient and Roots of Polynomials

Theorem 1

Let $a_1, a_2, \dots, a_n$ be all the zeroes of the nth degree polynomial

$$Q_n(z) = \alpha_0 z^n + \alpha_1 z^{n-1} + \cdots + \alpha_{n-2} z^2 + \alpha_{n-1} z + \alpha_n \tag{8}$$

Where $\alpha_k, k = 0,1,2, \dots, n$ are arbitrary real or complex coefficients. With $\alpha_n \neq 0$ and $\alpha_0 \neq 0$ then

(i) $Q_n(o) = (-1)^n, a_1.a_2.a_3 \dots a_{n-3}.a_{n-2}.a_{n-1}.a_n$ (8a)

$(ii) Q_n(z)$ has exact degree $d(Q_n(z) = n$ and does not vanish for $z = 0$. (8b)

Proof

Let $a_1, a_2, \dots, a_n$ be the only zeroes of $Q_n(z)$, these are all different from 0.

Since $Q_n(z)$ is of exact degree n, the fundamental theorem of algebra affirms that $Q_n(z)$ has exactly n zeroes $a_1, a_2, a_3 \dots a_{n-2}a_{n-1}, a_n$ and can be written as

$$Q_n(z) = (z-a_1)(z-a_2)(z-a_3)\dots(z-a_{n-2})(z-a_{n-1})(z-a_n)$$

$$= a_1\left(\frac{z}{a_1}-1\right)a_2\left(\frac{z}{a_2}-1\right)a_3\dots a_{n-2}\left(\frac{z}{a_2}-1\right)a_{n-1}\left(\frac{z}{a_1}-1\right)\ a_n\left(\frac{z}{a_n}-1\right)$$

$$= (-1)^n a_1a_2a_3\dots a_{n-2}a_{n-1}a_n\prod_{k=1}^{n}\left(1-\frac{z}{a_k}\right) \quad (9)$$

In the form (9) $Q_n(z)$ is expressed in an finite product and we need not bother about its convergence from (8) it follows that

$$|Q_n(o)| = |a_1||a_2||a_3|\dots|a_{n-2}||a_{n-1}||a_n| \quad (10)$$

From (10)

$$|Q_n(z)| = |a_1||a_2||a_3|\dots|a_{n-2}||a_{n-1}||a_n|\ \prod_{k=1}^{n}\left|\left(1-\frac{z}{a_k}\right)\right|$$

$$|Q_n(o)|\prod_{k=1}^{n}\left|\left(1-\frac{z}{a_k}\right)\right| \quad (11)$$

It will be convenient to order the zeroes so that

$$|a_1| \le |a_2| \le |a_3| \le \dots \le |a_N| \le 1 \le |a_{N+1}| \le |a_{N+2}| \le \dots \le |a_n|.$$

Let $Q(z)$ be a function of a complex variable z, which is regular inside and on the circle $|z| = r$, let $Q(0) \neq 0$ and let $a_1, a_2, \dots, a_N$ be all the zeroes of Q(z) satisfying $|a_k| \le r$ where the multiple zeroes are counted as many times as their multiplicity.

A polynomial of degree n is written as

$$Q_n(z) = \alpha_0 z^n + \alpha_1 z^{n-1} + \dots + \alpha_{n-2}z^2 + \alpha_{n-1}z + \alpha_n \quad (12)$$

where

$\alpha_k, k = 0,1,2, \dots, n$ are arbitrary real or complex coefficients. We shall assume that

$\alpha_0 \neq 0$, $\alpha_n \neq 0$. so that $Q(z)$is of exact degree n there is no restriction in assuming that the zeroes have been numbered so that some are less than 1 and others greater than 1.That is:

$$|a_1| \leq |a_2| \leq \cdots \leq |a_N| \leq 1 < |a_{N+1}| \leq |a_{N+2}| \leq \cdots \leq |a_n| \tag{13}$$

Suppose $r = 1$ in Jensen's integral formula developed by [18], then

$$\frac{1}{2\pi}\int_0^{2\pi} ln\left|Q(e^{i\theta})\right| d\theta = ln|Q(0)| + \sum_{k=1}^{N} ln\frac{1}{|a_k|} \tag{14}$$

It follows then that

$$\frac{1}{2\pi}\int_0^{2\pi} ln\left|Q(e^{i\theta})\right| d\theta = ln|a_n| + \sum_{v=1}^{N} ln\frac{1}{|a_k|} = ln\left|\frac{\alpha_0 a_1 a_2 a_3 \dots a_N a_{N+1} a_{N+2} \dots a_n}{a_1 a_2 a_3 \dots a_N}\right| \tag{15}$$

Thus (15) may also be written as

$$\frac{1}{2\pi}\int_0^{2\pi} ln\left|Q(e^{i\theta})\right| d\theta = ln|\alpha_0 a_{N+1} a_{N+2} \dots a_n| \tag{16}$$

Let

$i_1, i_2 \dots i_m$ be an arbitrary set of not more than n distinct suffixes 1, 2, … n; neither of the cases when $m = 0, \ and \ m = n$ is excluded. From the numbering of the zeros, it is obvious that

$$\left|\alpha_0 a_{i_1} a_{i_2} \dots a_{i_m}\right| \leq |\alpha_0 a_{N+1} a_{N+2} \dots a_n|$$

Hence, the identity (16) implies the inequality

$$ln\left|\alpha_0 a_{i_1} a_{i_2} \dots a_{i_m}\right| \leq \frac{1}{2\pi}\int_0^{2\pi} ln\left|Q(e^{i\theta})\right| d\theta \tag{17}$$

Apart from a factor ± 1, each coefficient α_m of $Q(z)$ is a sum of $\binom{n}{m}$ terms of same form

$$\alpha_0 a_{i_1} a_{i_2} \dots a_{i_m}$$

From (17)

$$|\alpha_0| + |\alpha_1| + \cdots + |\alpha_n| \leq \sum\left|\alpha_0 a_{i_1} a_{i_2} \dots a_{i_m}\right|$$

where the summation extends over all possible sets of suffixes

$i_1, i_2 \dots i_m$ since m can have the value 0,1,…,n, the sum has $\binom{n}{0} + \binom{n}{1} + \cdots + \binom{n}{n} = 2^n$ terms

More ever, each term satisfies the inequality (16), we have

$$\ln (|\alpha_0| + |\alpha_1| + \cdots + |\alpha_n|) \leq d(Q) ln2 + \frac{1}{2\pi}\int_0^{2\pi} ln\left|Q(e^{i\theta})\right| d\theta \qquad (18)$$

The upper estimate for the integral

$$\left|Q(e^{i\theta})\right| \leq |\alpha_0| + |\alpha_1| + \cdots + |\alpha_n| \; for \; 0 \leq \theta \leq 2\pi$$

So also

$$\frac{1}{2\pi}\int_0^{2\pi} ln\left|Q(e^{i\theta})\right| d\theta \leq ln|\alpha_0| + |\alpha_1| + \cdots + |\alpha_n| \qquad (19)$$

From Feldman and Gelfond inequalities, we have by combining (12) and (14), we find that

$$\left|\alpha_0 a_{i_1} a_{i_2} \dots a_{i_m}\right| \leq |\alpha_0| + |\alpha_1| + \cdots + |\alpha_n| \qquad (20)$$

Then the strengthened form of Feldman's inequality, let $Q(z)$ be written as a product of polynomials

$$Q(z) = \prod_{\sigma=1}^{s} Q_\sigma (z)$$

We use the abbreviation

$$S(Q) = |\alpha_0| + |\alpha_1| + \cdots + |\alpha_n| \qquad (21)$$

(21) implies therefore the s relation

$$S(Q_\sigma) = d(Q_\sigma) ln2 + \frac{1}{2\pi}\int_0^{2\pi} ln\left|Q(e^{i\theta})\right| d\theta \quad (\sigma = 1,2, \dots ,5) \qquad (22)$$

where

$$\sum_\sigma^s d(Q_\sigma) = d(Q)$$

Hence, adding these inequalities

$$ln \prod_{\sigma=1}^{s} S(Q_\sigma) \leq d(Q) ln\, 2 + \frac{1}{2\pi}\int_0^{2\pi} ln\left|Q(e^{i\theta})\right| d\theta$$

Hence, it follows from (17) that Gelfond's inequality is;

$$\prod_{\sigma=1}^{s} S(Q_\sigma) \leq 2^{d(Q)} S(Q). \qquad (23)$$

Application of Jensens's integral formula to entire functions with positive real part

order axioms of set positive numbers

Let R be the set of real numbers, then R is a ring and three exits a subset IR^+ of IR whose elements are called positive real numbers, such that the following statements are true.

Axioms (a) (close of IR^+): If $a\ and\ b$are positive real numbers, then so are $a+b$ and ab (juxtapositions means ordinary multiplication).

Axioms (b) (Trichotomy axiom of IR^+): if a is a real number then one and only one of the following three statement is true: $a\epsilon IR^+, -a\epsilon IR^+, or\ a=0$

Axioms (c) (cancellation law of IR^+): if $a>b$ then $a+c>b+c$ for any a,b in $IR^+$and $c\ in\ IR$.

Lemma 1

If a, b, c, and d are in IR^+ and $a<b$ and $c<d$, then

$(i)\ \ a+c<b+d$

$(ii)\ \ ac<bd$

Proof

If $a<b$ then $b-a>0$ i.e $b-a\epsilon IR^+$.

If $c<d$ then $d-c>0$ i.e $d-c\epsilon IR^+$

By the closure property of IR^+

$(b-a)+(d-c)>0$ hence,

$$(b+d)-(a+c)>0$$

Or

$$a+c<b+d$$

(ii). $(b-a)c>0$ and $b(d-c)>0$

Or

$$(bc-ac)>0 \text{ and } (bd-bc)>0$$

or

$$ac < bc \text{ and } bc < bd$$

Hence,

$$ac < bd$$

Lemma 2

If $0 < A < B < C$ then

(i).$e^A < e^B < e^C$

(ii) $InA < InB < InC$

Proof

(i). the positive number axiom for this expression is: if $\varphi > 0$ then $e^{\varphi} > 1$

Therefore,

$$A < B \text{ implies } B - A > 0$$

So,

$$e^{B-A} > 1$$

Or

$$e^B e^{-A} > 1$$

That is,

$$e^B > e^A \tag{24}$$

Similarly,

$$B < C \text{ implies } C - B > 0$$

Then,

$$e^{C-B} > 1$$

Or

$$e^C e^{-B} > 1$$

That is

$$e^C > e^B \tag{25}$$

Then equation (24) and (25) lead to

$$e^A < e^B \text{ and } e^B < e^C$$

Or,

$$e^A < e^B < e^C$$

(ii). The IR^+ axiom for this case is if $\emptyset > 1$ then, $In\emptyset > 0$,

Now, if $A < B \; then \; \frac{B}{A} > 1$

and by the axiom

$$In\frac{B}{A} > 0 \text{ or } InB - InA > 0$$

That is

$$InA < InB \tag{26}$$

On the other hand, if $B < C$ then, $\frac{C}{B} > 1$ and by the axiom

$$In\frac{C}{B} > 0 \text{ or } InC - InB > 0$$

that is

$$InB < InC \tag{27}$$

By equation (26) and (27)

$$InA < InB < InC \tag{28}$$

Definition 1

The set $Q = \{f(z): z \in E\}$ is called a set of functions with positive real parts if its members satisfying the following conditions,

(i). $f(z) = 1 + q_1 z + q_2 z^1 + \cdots + q_n z^n + \cdots = + \sum_{n=1}^{\infty} q_n z^n$ (29a)

that are regular in E= $\{z: |z| < 1\}$ and such that for $z \; in \; E$

(ii). $Re(f(z)) > 0$ (29b)

Examples following Definition 1

i). $e^z = 1 + z + \frac{z^2}{2!} + \frac{z^3}{3!} + \cdots + \frac{z^n}{n!} + \cdots |z| < \infty$ (30)

(ii). $\frac{\sin z}{z} = \frac{1}{z}\left\{z - \frac{z^3}{3!} + \frac{z^5}{5!} - \frac{z^7}{7!} + \cdots\right\} = 1 - \frac{z^2}{3!} + \frac{z^4}{5!} - \frac{z^6}{7!} + \cdots$ (31)

(iii). $\frac{\sin^{-1} z}{z} = 1 + \frac{1}{z}\frac{z^2}{3} + \frac{1.3}{2.4}\frac{z^4}{5} + \frac{1.3.5}{2.4.6}\frac{z^6}{7} + \cdots + F\left(\frac{1}{2}, \frac{1}{2}, \frac{3}{2}; z^2\right)$ (32)

(iv). $(1+z)^p = 1 + pz + \frac{p(p-1)}{2!}z^2 + \cdots + \frac{p(p-1)\ldots(p-n+1)}{n!}z^n + \cdots |z| < 1$ (33)

(v). $\frac{\tan^{-1} z}{z} = 1 - \frac{z^2}{2} + \frac{z^4}{4} - \cdots (-1)^{n-1}\frac{z^{2n-1}}{2n-1} + \cdots |z| < 1$ (34)

Any function in Q is called a function with positive real part in E.

Thus $f(z) = 1 + z^n$ is in Q for any integer $n \geq 0$. it is clear that with sufficient labour, any theorem about the class Q can be transformed into a suitable theorem about a fraction $g(z)$ that carries E into some prescribed half plane.

The mobius function

$$L_0(z) = \frac{1+z}{1-z} = 1 + 2z + 2z^2 + \cdots = 1 + 2\sum_{n=1}^{\infty} z^n \quad (35)$$

Plays a central role in the class Q, it is regular in E, and maps E onto the half-plane H^+, and maximizes $|q_n|$ in the Q.

Some operations that carry functions in Q into function in Q are given (33).

Definition 2

Let $f(z)$ and $F(z)$ be given by the power series

$f(z) = \sum_{n=0}^{\infty} a_n z^n$ (36)

and $F(z) = \sum_{n=0}^{\infty} A_n Z^n$ (37)

Convergent in some disk $E_R: |z| < R, R > 0$. e say that $f(z)$ is dominated by $F(z)$ or $F(z)$ dominates $f(z)$, and we write $f(z) \ll F(z)$ if for each integer $n \geq 0$.

$|a_n| \leq A_n$ (38)

Theorem 2

Suppose that $f(z) \ll F(z)$. then $A_n \geq 0, n = 0,1,2, \ldots$

$$|f(z)| \leq F(r), 0 \leq |z| \equiv r < R \tag{39}$$

$$f'(z) \ll F'(z)$$

$$\int_0^z f(\zeta)d\zeta \ll \int_0^z F(\zeta)d\zeta$$

$$e^{f(z)} \ll e^{F(z)}$$

And if $|F(z)| < 1$ in some disk Ethen in that disk $-In\big(-f(z)\big) \ll -In(1-F(z))$

Further, if $|b| \leq B$ and $k \geq 0$ is any integer, then $bz^k f(z) \ll BZ^k F(z)$

and $[f(z)]^k \ll [F(z)]^k$

Finally, if $f(z) \ll F(z)$ and $g(z) \ll G(z)$, then $f(z) + g(z) \ll F(z) + G(z)$

And $f(z)g(z) \ll F(z)G(z)$

Theorem 3

Suppose that $f(z)$ is in Q, then the function $g(z)$ is in Q, where,

$$g(z) = f(e^{i\alpha}z), \alpha\ real. \tag{40}$$

$$g(z) = [f(z)]^t, org(z) = f(tz) \qquad -1 < t < 1 \tag{41}$$

$$g(z) = \frac{1}{f(z)} \tag{42}$$

Theorem 4

Let $N \geq 1$ be a fixed integer. If $f(z)$, given by (4.4.4(a)) is in Q, then

$$|q_n| \leq 2 \tag{43}$$

This inequality is sharp, if $\eta = e^{\frac{2\pi i}{N}}$ and

$$f(z) = \sum_{k=1}^{N} \mu_k \frac{1+\eta^k z}{1-\eta^k z} = 1 + \sum_{n=1}^{\infty} q_n z^n \tag{44}$$

where $\mu_k \geq 0\ for\ k = 1, 2, \ldots, N$ and

$$\sum_{k=1}^{N} \mu_k = 1 \tag{45}$$

Then, $f(z)$ is in Q and qN=2

Theorem 5

If $f(z)$ is in Q and $z = re^{i\theta}$, then

$$\frac{1-r}{1+r} \leq |f(z)| \leq \frac{1+r}{1-r} \tag{46}$$

$$|f'(z)| \leq \frac{2}{(1-r)^2} \tag{47}$$

Theorem 6

If $f(z)$ is in Q and $z = re^{i\theta}, r < 1$ then

$$\frac{1-r}{1+r} \leq \prod_{i=1}^{m} \frac{r^m}{|a_i|} - \prod_{j=1}^{n} \frac{r^n}{|b_j|} \leq \frac{1+r}{1-r}$$

where $a_{\mathrm{i}}, b_{\mathrm{j}}$, $\mathrm{i} = 1,2,3 \ldots, \mathrm{m}$ and $\mathrm{j} = 1,2,3, \ldots, \mathrm{n}$ are the roots and poles respectively of $f(z)$ and $f(z)$ has neither zeros nor poles on $|\mathrm{z}| = 1$

Proof

(i) From lemma 1

$$ln\frac{1-r}{1+r} \leq ln|f(z)| \leq ln\frac{1+r}{1-r}$$

Taking the integral

$$\frac{1}{2\pi}\int_0^{2\pi} ln\frac{1-r}{1+r}d\theta \leq \frac{1}{2\pi}\int_0^{2\pi} ln\,|f(z)|d\theta \leq \frac{1}{2\pi}\int_0^{2\pi} ln\frac{1+r}{1-r}d\theta$$

$$ln\frac{1-r}{1+r} \leq \frac{1}{2\pi}\int_0^{2\pi} ln\,|f(z)|d\theta \leq ln\frac{1+r}{1-r}$$

By lemma 2

$$ln\frac{1-r}{1+r} \leq ln|f(0)| + \sum_{i=1}^{m} ln\frac{r}{|a_i|} - \sum_{j=1}^{n} ln\frac{r}{|b_j|} \leq ln\frac{1+r}{1-r}$$

$$\exp\,(ln\frac{1-r}{1+r}) \leq \exp\,(ln|f(0)|) + \exp\,(\sum_{i=1}^{m} ln\frac{r}{|a_i|}) - \exp\,(\sum_{j=1}^{n} ln\frac{r}{|b_j|}) \leq \exp\,(ln\frac{1+r}{1-r})$$

$$\frac{1-r}{1+r} \leq e^{(ln\frac{r}{|a_1|}+\frac{r}{|a_2|}\ldots+\frac{r}{a_m})} - e^{(ln\frac{r}{|b_1|}+\frac{r}{|b_2|}\ldots+\frac{r}{|b_n|})} \leq \frac{1+r}{1-r}$$

$$\frac{1-r}{1+r} \leq \prod_{i=1}^{m} \frac{r^m}{|a_i|} - \prod_{j=1}^{n} \frac{r^n}{|b_j|} \leq \frac{1+r}{1-r}$$

Theorem 7

If $f(z)$ is in Q and $z = re^{i\theta}, r < 1$ then

$$N - P \leq \frac{2r(1+r)}{(1-r)^3}$$

Proof

If $|f'(z)| \leq \frac{2}{(1-r)^2}$ then

$$\frac{1}{|f(z)|} \leq \frac{1+r}{1-r}$$

By lemma 2

$$\left|\frac{f'(z)}{f(z)}\right| \leq \frac{2(1+r)}{(1-r)^3}$$

$$\int_0^{2\pi} \left|\frac{f'(z)}{f(z)}\right| dz \leq \int_0^{2\pi} \frac{2(1+r)}{(1-r)^3} dz$$

But

$$\int_0^{2\pi} \left|\frac{f'(z)}{f(z)}\right| dz = \int_0^{2\pi} \left|\frac{f'(z)}{f(z)}\right| rd\theta$$

Since

$$|dz| = rd\theta$$

$$\int_c \left|\frac{f'(z)}{f(z)}\right| rd\theta \leq \int_0^{2\pi} \frac{2(1+r)}{(1-r)^3} rd\theta$$

But from 18

$$\frac{1}{2\pi i} \int_c \left|\frac{f'(z)}{f(z)}\right| dz = N - P$$

Then

$$N - P \leq \frac{2r(1+r)}{(1-r)^3}$$

Theorem 8

If $f(z) and\ g(z)$ are polynomials of degree n and m respectively then the number of roots of fg is the number of roots of f plus the number of roots of g.

Proof

$$(fg)' = f'g + fg'$$

Hence

$$\frac{(fg)'}{fg} = \frac{f'g}{fg} + \frac{fg'}{fg}$$

$$= \frac{f'}{f} + \frac{g'}{g}$$

So

$$\frac{1}{2\pi i}\oint \frac{(fg)'}{fg}dz = \frac{1}{2\pi i}\oint \frac{f'}{f}dz + \frac{1}{2\pi i}\oint \frac{g'}{g}dz$$

$$N_{fg} = N_f + N_g$$

Theorem 9

The number of the roots of the product of k- polynomials is the sum of the number of the roots of each of the polynomials in the product

Proof

$$(f_1(z)\, f_2 \dots f_{k-1}(z)f_k(z))' = f'_1(z)f_2(z) \dots f_{k-1}(z)f_k(z) + f_1(z)\, f'_2(z) \dots f_{k-1}(z)f_k(z) + \cdots . + f_1(z)\, f_2 \dots f_{k-1}(z)f'_k(z)$$

$$\frac{(f_1(z)\, f_2 \dots f_{k-1}(z)f_k(z))'}{(f_1(z)\, f_2 \dots f_{k-1}(z)f_k(z))} = \frac{f'_1(z)f_2(z) \dots f_{k-1}(z)f_k(z)}{f_1(z)\, f_2 \dots f_{k-1}(z)f_k(z)} + \frac{f_1(z)\, f'_2(z) \dots f_{k-1}(z)f_k(z)}{f_1(z)f_2(z) \dots f_{k-1}(z)f_k(z)} + \cdots + \frac{f_1(z)\, f_2 \dots f_{k-1}(z)f'_k(z)}{f_1(z)\, f_2 \dots f_{k-1}(z)f_k(z)}$$

$$\frac{1}{2\pi i}\oint \frac{(f_1(\mathrm{z})\, f_2 \ldots f_{k-1}(z) f_k(z))'}{(f_1(\mathrm{z})\, f_2 \ldots f_{k-1}(z) f_k(z))}dz$$
$$= \frac{1}{2\pi i}\oint \frac{f'_1(z)}{f_1(\mathrm{z})}dz + \frac{1}{2\pi i}\oint \frac{f'_2(z)}{f_2(z)}dz + \cdots + \frac{1}{2\pi i}\oint \frac{f'_k(z)}{f_k(z)}dz$$

$$N_{f_1(\mathrm{z})\, f_2 \ldots f_k(z)} = N_{f_1} + N_{f_2} + \ldots + N_{f_K}$$

Application of Jensens's Integral Formula to Gauss Mean Value Theorem

Theorem 10

Suppose $f(z)$ is analytic inside and on circle C with center at a and radius r. Then $f(a)$is the mean of the value of $f(z)$ on C for

$$|z-a| < r,\ z = a + re^{i\theta}|a| < r\ and$$
$$f(a) = \frac{1}{2\pi}\int_0^{2\pi} f(a + re^{i\theta})d\theta. \quad (48)$$

Lemma 3

Harmonicity of $ln|f(z)|$

If $f(z)$ is analytic and non-zero for $|z| \le R$. Then ln$|f(z)|$ is harmonic for

$$|z| \le R. \quad (49$$

Proof

If $f(z) \neq 0, |z| \le R$.

There exists an analytic function $g(z)$ for which

$$f(z) = e^{g(z)}$$

Let

$$g(z) = u(z) + iv(z)$$

Then

$$f(z) = e^{u(z)+iv(z)}$$
$$= e^{u(z)}e^{iv(z)}$$

So

$$|f(z)| = e^{u(z)}$$

Therefore

$$ln|f(z)| = lne^{u(z)} = u(z)$$

Hence

$ln|f(z)|$ is a harmonic function for $|z| \leq R$

Lemma 4

MVP for $ln|h(z)|$

If $h(z)$ is analytic and non-zero for all z such that$|z| \leq R$, then.

$$ln|h(z)| = \frac{1}{2\pi}\int_0^{2\pi} ln\left|h\left(z + Re^{i\theta}\right)\right| d\theta \quad (50)$$

Proof

$$ln|h(a)| = \frac{1}{2\pi}\int_c ln\left|\frac{h(z)}{z-a}\right| dz$$

Let $z - a = Re^{i\theta}$ then $dz = iRe^{i\theta}, 0 \leq \theta \leq 2\pi$

So

$$ln|h(a)| = \frac{1}{2\pi}\int_0^{2\pi} \frac{ln|h(a+Re^{i\theta})|}{Re^{i\theta}} iRe^{i\theta} d\theta$$

$$ln|h(a)| = \frac{1}{2\pi}\int_0^{2\pi} ln\left|h\left(a + Re^{i\theta}\right)\right| d\theta$$

Hence

$$ln|h(z)| = \frac{1}{2\pi}\int_0^{2\pi} ln\left|h\left(z + Re^{i\theta}\right)\right| d\theta$$

Corollary 1

If $h(z)$ is analytic and non-zero for all z such that $|z| \leq R$

Then

$$ln|h(0)| = \frac{1}{2\pi}\int_0^{2\pi} ln\left|h\left(Re^{i\theta}\right)\right| d\theta \quad (51)$$

Proof

Let $z = 0$ in equation (50) from lemma 4

Then

$$ln|h(0)| = \frac{1}{2\pi}\int_0^{2\pi} ln\left|h\left(Re^{i\theta}\right)\right| d\theta$$

Theorem 11

Let f(z) be analytic inside and on a simple closed curve C except for a pole $z = \alpha$

of order (multiplicity) p inside C. suppose also that inside C, f(z) has only one zero $z = \beta$

of order (multiplicity) n and no zero on C then

$$\frac{1}{2\pi i}\oint_C \frac{f'(z)}{f(z)}\, dz = n - p. \tag{52}$$

Proof

If f(z) has a pole at $z = \alpha$ of order p and a zero at $z = \beta$ of order n

Let c_1 and Γ_1 be non-overlapping circles lying inside C and enclosing $z = \alpha$ and

$z = \beta$ respectively as shown below

Then

$$\frac{1}{2\pi i}\int \frac{f'(z)}{f(z)} dz = \frac{1}{2\pi i}\int_{c_1} \frac{f'(z)}{f(z)} dz + \frac{1}{2\pi i}\int_{c_2} \frac{f'(z)}{f(z)} dz \tag{53}$$

Now

Since f(z) has a pole of order P at $z = \alpha$ we have

$$f(z) = \frac{f(z)}{(z-\alpha)^p} \tag{54}$$

Upon differentiation

$$f'(z) = \frac{f'(z)}{(z-\alpha)^p} - \frac{pf(z)}{(z-\alpha)}$$

Dividing through by equation (54)

$$\frac{f'(z)}{f(z)} = \frac{f'(z)}{(z-\alpha)^p}\cdot\frac{(z-\alpha)^p}{f(z)} - \frac{pf(z)}{(z-\alpha)^{p+1}}\cdot\frac{(z-\alpha)^p}{f(z)}$$

$$\frac{f'(z)}{f(z)} = \frac{f'(z)}{f(z)} - \frac{p}{(z-\alpha)}$$

Upon integration we have

$$\frac{1}{2\pi i}\int_{c_1} \frac{f'(z)}{f(z)}dz = \frac{1}{2\pi i}\int \frac{f'(z)}{f(z)}dz - \frac{p}{2\pi i}\int \frac{dz}{(z-\alpha)}$$

By CIF

$$\frac{1}{2\pi i}\int \frac{f'(z)}{f(z)}dz = -p$$

If $f(z)$ has a zero of multiple n at $z = \beta$ we have

$$f(z) = (z-\beta)^n g(z), g(\beta) \neq 0 \tag{55}$$

Differentiating equation (55)

$$f'(z) = g'(z)(z-\beta)^n + ng(z)(z-\beta)^{n-1} \tag{56}$$

Dividing through by equation (54) we have

$$\frac{f'(z)}{f(z)} = \frac{g'(z)(z-\beta)^n}{g(z)(z-\beta)^n} + \frac{ng(z)(z-\beta)^{n-1}}{g(z)(z-\beta)^n}$$

$$\frac{f'(z)}{f(z)} = \frac{g'(z)}{g(z)} + \frac{n}{(z-\beta)}$$

Upon integration

$$\int_{c_2} \frac{f'(z)}{f(z)}dz = \frac{1}{2\pi i}\int \frac{g'(z)}{(z)}dz + \frac{n}{2\pi i}\int \frac{dz}{z-\beta}dz$$

By CIF

$$\frac{1}{2\pi i}\int_{c_2} \frac{f'(z)}{f(z)}dz = n \tag{57}$$

Adding equation (53) and (54) and from (55) give

$$\frac{1}{2\pi i}\int_{c_1} \frac{f'(z)}{f(z)}dz + \frac{1}{2\pi i}\int_{c_2} \frac{f'(z)}{f(z)} = n - p$$

Lemma 5

For all $z \in C$ and any $r > 0$

$$\frac{1}{2\pi}\int_0^{2\pi} ln\left|z - re^{i\theta}\right| d\theta = \begin{cases} ln|z| \; if \; |z| < r \\ lnr \; if \; |z| = r \\ -ln|z| \; if |z| > r \end{cases}$$

Proof

$$\text{If } |z| < r$$

$$z - re^{i\theta} = -(re^{i\theta} - z)$$

$$= -e^{i\theta}\left(r - \frac{z}{e^{i\theta}}\right)$$

$$= -e^{i\theta}\left(\frac{rz}{z} - \frac{rz}{re^{i\theta}}\right)$$

$$= -e^{i\theta} z\left(\frac{1}{z} - \frac{1}{re^{i\theta}}\right)$$

Hence

$$\left|z - re^{i\theta}\right| = |r||z|\left|\frac{1}{z} - \frac{1}{re^{i\theta}}\right|$$

and

$$ln\left|z - re^{i\theta}\right| = ln|z| + lnr + ln\left|\frac{1}{z} - \frac{1}{r}e^{-i\theta}\right|$$

So integrating over θ from $\theta = 0 \; to \; \theta = 2\pi$

$$\int_0^{2\pi} ln\left|z - re^{i\theta}\right| d\theta = \int_0^{2\pi} ln|z| d\theta + \int_0^{2\pi} lnr d\theta + \int_0^{2\pi} ln\left|\frac{1}{z} - \frac{1}{re^{i\theta}}\right| d\theta$$

So that

$$\frac{1}{2\pi}\int_0^{2\pi} ln\left|z - re^{i\theta}\right| d\theta = ln|z| + lnr + \int_0^{2\pi} ln\left|\frac{1}{z} - \frac{1}{re^{i\theta}}\right| d\theta$$

Set

$$ln\left|\frac{1}{z} - \frac{1}{r}e^{-i\theta}\right| = ln\left|Z - Re^{i\emptyset}\right|, \; Z = \frac{1}{z}, \; R = \frac{1}{r}, \; \emptyset = -\theta, \; d\theta = -d\emptyset$$

Then

$$\frac{1}{2\pi}\int_0^{2\pi} ln\left|\frac{1}{z} - \frac{1}{r}e^{-i\theta}\right| d\theta = \frac{1}{2\pi}\int_{-2\pi}^{0} ln\left|Z - Re^{i\emptyset}\right| d\emptyset$$

$$= \frac{1}{2\pi}\int_0^{2\pi} ln\left|Z - Re^{i\emptyset}\right| d\emptyset = ln|Z|$$

Since

$Z = \frac{1}{z},\ R = \frac{1}{r}$, and

$|Z| < R. then\ \left|\frac{1}{z}\right| < \frac{1}{r}$

Hence if $|z| > r$

$\frac{1}{2\pi}\int_0^{2\pi} ln\left|z - re^{i\theta}\right| d\theta = ln\frac{1}{|z|} = -ln|z|$

Now, suppose

$|z| < r$

$\frac{1}{2\pi}\int_0^{2\pi} ln\left|z - re^{i\theta}\right| d\theta = lnr$

Proof

Set

$|z| < r$

We have that

$$z - re^{i\theta} = -(re^{i\theta} - z)$$

$$= -e^{i\theta}(r - \frac{z}{e^{i\theta}})$$

$$= -e^{i\theta}\left(\frac{rz}{z} - \frac{rz}{re^{i\theta}}\right)$$

$$= -e^{i\theta}z\left(\frac{1}{z} - \frac{1}{re^{i\theta}}\right)$$

Hence

$$\left|z - re^{i\theta}\right| = |r||z|\left|\frac{1}{z} - \frac{1}{re^{i\theta}}\right|$$

and

$$ln\left|z - re^{i\theta}\right| = ln|z| + lnr + ln\left|\frac{1}{z} - \frac{1}{r}e^{-i\theta}\right|$$

Integrating over θ

$$\int_0^{2\pi} ln\left|z - re^{i\theta}\right|d\theta = \int_0^{2\pi} ln|z|d\theta + \int_0^{2\pi} lnrd\theta + \int_0^{2\pi} ln\left|\frac{1}{z} - \frac{1}{re^{i\theta}}\right| d\theta$$

$$2\pi\, ln|z| + 2\pi lnr + \int_0^{2\pi} lnr d\theta + \int_0^{2\pi} ln\left|\frac{1}{z} - \frac{1}{re^{i\theta}}\right| d\theta$$

So

$$\frac{1}{2\pi}\int_0^{2\pi} ln\left|z - re^{i\theta}\right| d\theta = ln|z| + lnr + \int_0^{2\pi} ln\left|\frac{1}{z} - \frac{1}{re^{i\theta}}\right| d\theta$$

The last integral, $ln\left|\frac{1}{z}\right|$. Adding the first five terms we have

$$\frac{1}{2\pi}\int_0^{2\pi} ln\left|z - re^{i\theta}\right| d\theta = \frac{1}{|z|} < \frac{1}{r}$$

If $|z| < r$

Then

$$\frac{1}{2\pi}\int_0^{2\pi} ln\left|z - re^{i\theta}\right| d\theta = ln\mathrm{r}$$

Lemma 6 (Jensen's Lemma)

Let *f* be a meromorphic function on the whole plane. If $f(0) \neq 0, \infty$ then , for any $r > 0$ we have

$$\frac{1}{2\pi}\int_0^{2\pi} ln\left|f(re^{i\theta})\right| d\theta = ln|f(0)| + \sum_{i=1}^{m} ln\frac{r}{|a_i|} - \sum_{j=1}^{n} ln\frac{r}{|b_j|} \quad (58)$$

where $a_i \ldots a_m$ are the zeros of *f* in $|z| \leq r$ and $b_1 \ldots b_n$ are the poles of *f* in $|z| \leq r$.

Proof

Let

$$f(z) = g(z)\prod_{i=1}^{m}(z - a_i)\left[\prod_{j=1}^{n}(z - b_j)\right]^{-1}$$

where $g(z)$ is an analytic function on the whole plane that has no zeros or poles in $|z| \leq r$. Then

$$|f(z)| = \left|g(z)\frac{(z-a_1)(z-a_2)\ldots(z-a_m)}{(z-b_1)(z-b_2)\ldots(z-b_n)}\right|$$

$$|f(0)| = |g(0)|\left|\frac{(-a_1)(-a_2)\ldots(-a_m)}{(-b_1)(-b_2)\ldots(-b_n)}\right|$$

and

$$ln|f(z)| = ln\left|g(z)\frac{(z-a_1)(z-a_2)\ldots(z-a_m)}{(z-b_1)(z-b_2)\ldots(z-b_n)}\right|$$

Thus

$$ln|f(z)| = ln|g(z)| + ln\{|z-a_1||z-a_2|\dots|z-a_m|\}$$
$$-ln\{|z-b_1||z-b_2|\dots|z-b_n|\}$$

Or

$$ln|f(z)| = ln|g(z)| + \sum_{i=1}^{m} ln\,|z-a_i| - \sum_{j=1}^{n} ln|z-b_j|$$

and

$$ln|f(0)| = ln|g(0)| + \sum_{i=1}^{m} ln\,|a_i| - \sum_{j=1}^{n} ln|b_j| \quad (59)$$

Upon integration for $|z| = r$, we get

$$\frac{1}{2\pi}\int_0^{2\pi} ln|f(z)|d\theta = \frac{1}{2\pi}\int_0^{2\pi} ln|g(z)|d\theta + \frac{1}{2\pi}\int_0^{2\pi}\sum_{i=1}^{m} ln|z-a_i|d\theta$$
$$-\frac{1}{2\pi}\int_0^{2\pi}\sum_{j=1}^{n} ln|z-b_j|d\theta$$
$$\frac{1}{2\pi}\int_0^{2\pi} ln|f(re^{i\theta}|d\theta = \frac{1}{2\pi}\int_0^{2\pi} ln|g(re^{i\theta}|d\theta + \frac{1}{2\pi}\int_0^{2\pi} ln|re^{i\theta}-a_i|d\theta$$
$$-\frac{1}{2\pi}\int_0^{2\pi} ln|re^{i\theta}-b_j|d\theta$$

But by lemma 4 and equation (50)

$$\frac{1}{2\pi}\int_0^{2\pi} ln|f(re^{i\theta}|d\theta = ln|g(0)| + mlnr - nlnr$$

By application of equation (57), this become

$$\frac{1}{2\pi}\int_0^{2\pi} ln|f(re^{i\theta}|d\theta = ln|f(0)| - \sum_{i=1}^{m} ln\,|a_i| + \sum_{j=1}^{n} ln|b_j| + mlnr - nlnr$$
$$ln|f(0)| + lnr + lnr + \cdots + lnr - (ln|a_1| + ln|a_2| + \cdots + ln|a_m|)$$
$$-lnr - lnr - \cdots - lnr + (ln|b_1| + ln|b_2| + \cdots ln|b_n|)$$

Then

$$\frac{1}{2\pi}\int_0^{2\pi} ln|f(re^{i\theta}|d\theta = ln|f(0)| + ln\frac{r}{|a_1|} + ln\frac{r}{|a_2|} + \cdots + ln\frac{r}{|a_m|}$$
$$-(ln\frac{r}{|b_1|} + ln\frac{r}{|b_2|} + \cdots + ln\frac{r}{|b_n|})$$

Then

$$\frac{1}{2\pi}\int_0^{2\pi} ln\left|f(re^{i\theta}\right|d\theta = ln|f(0)| + \sum_{i=1}^{m} ln\frac{r}{|a_i|} - \sum_{j=1}^{n} ln\frac{r}{|b_j|}$$

Hence,

$$ln|f(0)| = \frac{1}{2\pi}\int_0^{2\pi} ln\left|f(re^{i\theta}\right|d\theta - \sum_{i=1}^{m} ln\frac{r}{|a_i|} + \sum_{j=1}^{n} ln\frac{r}{|b_j|}$$

Theorem 12

Let $f(z)$and $g(z)$ be analytic inside and on simple closed curve C except that $f(z)$ has

zero at $a_1, a_2, \dots a_m$ and poles at $b_1, b_2, \dots . b_n$ of orders (multiplicity) $p_1, p_2, \dots p_m$

and $q_1, q_2, \dots q_n$ respectively. Then

$$\frac{1}{2\pi i}\oint_c g(z)\frac{f'(z)}{f(z)}dz = \sum_{k=1}^{m} p_k g(a_k) - \sum_{k=1}^{n} q_k g(b_k)$$

Theorem 13

Suppose $f(z)$ is analytic inside and on the $|z| = R$ except for zeros at $a_1, a_2, \dots, a_m$

of multiplicities $\alpha_1, \alpha_2, \dots, \alpha_m$ and poles at $b_1, b_2, \dots, b_n$ of multiplicities $\beta_1, \beta_2, \dots, \beta_n$ respectively and suppose $f(0)$ is finite and different from zero. Then

$$\frac{1}{2\pi}\int_0^{2\pi} ln\left|f(Re^{i\theta})\right|d\theta = ln|f(0)| + \sum_{k=1}^{m} \alpha_k ln\left(\frac{R}{|a_k|}\right) - \sum_{k=1}^{n} \beta_k ln\left(\frac{R}{|b_k|}\right)$$

Proof

Let

$$f(z) = g(z)\prod_{i=1}^{m}(z-a_m)^{\alpha_m}\left[\prod_{j=1}^{n}(z-b_n)^{\beta_n}\right]^{-1}$$

$$f(z) = g(z)\frac{(z-a_1)^{\alpha_1}(z-a_2)^{\alpha_2}\dots(z-a_m)^{\alpha_m}}{(z-b_1)^{\beta_1}(z-b_2)^{\beta_2}\dots(z-b_n)^{\beta_n}}$$

Where $g(z)$ is analytic and has no zero on $|z| \le R$

and

$$ln|f(0)| = |g(0)|\left|\frac{(-a_1)^{\alpha_1}(-a_2)^{\alpha_2}\dots(-a_m)^{\alpha_m}}{(-b_1)^{\beta_1}(-b_2)^{\beta_2}\dots(-b_n)^{\beta_n}}\right|$$

$$ln|f(z)| = ln\left|g(z)\frac{(z-a_1)^{\alpha_1}(z-a_2)^{\alpha_2}\dots(z-a_m)^{\alpha_m}}{(z-b_1)^{\beta_1}(z-b_2)^{\beta_2}\dots(z-b_n)^{\beta_n}}\right|$$

$$ln|f(z)| = ln|g(z)| + ln|(z-a_1)^{\alpha_1}(z-a_2)^{\alpha_2}\dots(z-a_m)^{\alpha_m}|$$

$$-ln\left|(z-b_1)^{\beta_1}(z-b_2)^{\beta_2}\dots(z-b_n)^{\beta_n}\right|$$

$$ln|f(z)| = ln|g(z)| + \alpha_1 ln|z-a_1| + \alpha_2 ln|z-a_2| + \cdots + \alpha_m ln|z-a_m|$$

$$-(\beta_1 ln|z-b_1| + \beta_2 ln|z-b_2| + \cdots + \beta_n ln|z-b_n|)$$

$$ln|f(z)| = ln|g(z)| + \sum_{k=1}^{m} \alpha_k ln\,|z-a_k| - \sum_{k=1}^{n} \beta_k ln\,|z-b_k|$$

and

$$ln|f(0)| = |g(0)| + \sum_{k=1}^{m} \alpha_k ln\,|a_k| - \sum_{k=1}^{n} \beta_k ln\,|b_k| \tag{60}$$

Upon integration for $z = R$ we get

$$\frac{1}{2\pi}\int_0^{2\pi} ln|f(z)|d\theta = \frac{1}{2\pi}\int_0^{2\pi} ln\,|g(z)|d\theta + \sum_{k=1}^{m}\frac{1}{2\pi}\int_0^{2\pi} \alpha_k ln|z-a_k|d\theta$$

$$-\sum_{k=1}^{n}\frac{1}{2\pi}\int_0^{2\pi} \beta_k ln|z-b_k|d\theta$$

$$\frac{1}{2\pi}\int_0^{2\pi} ln|f(z)|d\theta = \frac{1}{2\pi}\int_0^{2\pi} ln\left|g(Re^{i\theta})\right|d\theta + \sum_{k=1}^{m}\frac{1}{2\pi}\int_0^{2\pi} \alpha_k ln\left|Re^{i\theta}-a_k\right|d\theta$$

$$-\sum_{k=1}^{n}\frac{1}{2\pi}\int_0^{2\pi} \beta_k ln\left|Re^{i\theta}-b_k\right|d\theta$$

$$\frac{1}{2\pi}\int_0^{2\pi} \alpha_1 \ln|z-a_m|\,d\theta + \frac{1}{2\pi}\int_0^{2\pi} \alpha_2 ln|z-a_2|d\theta + \cdots + \frac{1}{2\pi}\int_0^{2\pi} \alpha_m ln|z-a_m|d\theta$$

$$-(\frac{1}{2\pi}\int_0^{2\pi} \beta_1 \ln|z-b_1|\,d\theta + \frac{1}{2\pi}\int_0^{2\pi} \beta_2 ln|z-b_2|d\theta + \cdots + \frac{1}{2\pi}\int_0^{2\pi} \beta_n ln|z-b_n|d\theta$$

$$= \alpha_1 lnR + \alpha_2 lnR + \cdots + \alpha_m lnR - (\beta_1 lnR + \beta_2 lnR + \cdots + \beta_n lnR)$$

But by lemma 6 and equation (57)

$$\frac{1}{2\pi}\int_0^{2\pi} ln\left|f(Re^{i\theta})\right|d\theta = ln|g(0)| + \sum_{k=1}^{m} \alpha_k lnR - \sum_{k=1}^{n} \beta_k lnR$$

Thus, using equation (58) to eliminate $ln|g(0)|$, we have

$$\frac{1}{2\pi}\int_0^{2\pi} ln\left|f\left(Re^{i\theta}\right)\right|d\theta = ln|f(0)| - \sum_{k=1}^{m} \alpha_k ln\,|a_k|$$

$$+\sum_{k=1}^{n} \beta_k ln\left|b_j\right| + \sum_{k=1}^{m} \alpha_k lnR - \sum_{k=1}^{n} \beta_k lnR$$

$$\frac{1}{2\pi}\int_0^{2\pi} ln\left|f\left(Re^{i\theta}\right)\right|d\theta = ln|f(0)| + \alpha_k[lnR + lnR + \cdots -$$

$$\begin{pmatrix} lnR + ln|a_1| + ln|a_2| + \cdots + ln|a_k|) \\ -\beta_k[(lnR + lnR + \cdots + lnR \end{pmatrix} + (ln|b_1| + ln|b_2| + \cdots + ln|b_k|)]$$

$$\frac{1}{2\pi}\int_0^{2\pi} ln\left|f(Re^{i\theta})\right|d\theta = ln|f(0)| + \alpha_k(ln\frac{R}{|a_1|} + ln\frac{R}{|a_2|} + \cdots + ln\frac{R}{|a_k|})$$

$$-\beta_k(ln\frac{R}{|b_1|} + ln\frac{R}{|b_2|} + \cdots + ln\frac{R}{|b_k|})$$

Hence

$$\frac{1}{2\pi}\int_0^{2\pi} ln\left|f(Re^{i\theta})\right|d\theta = ln|f(0)| + \sum_{k=1}^{m}\alpha_k \ln\left(\frac{R}{|a_i|}\right) - \sum_{k=1}^{n}\beta_k \ln\left(\frac{R}{|b_k|}\right)$$

Theorem 14

Let a complex variable be given by $z = re^{i\theta}$, then

(i) The function $f(z)$ is analytical in the region $|z| \leq R$

(ii) $f(z)$ has no zeroes on $|z| = R$, and

(iii) $f(0) = 1$ then

$$\frac{1}{2\pi}\int_0^{2\pi} ln\left|f(Re^{i\theta})\right|dr = \int_0^R \frac{n(r)}{r}dr \tag{61}$$

Where the function $n(r)$ is the number of zeroes of $f(z)$ inside the disc $|z| = r$.

Proof

Let

$$z = re^{i\theta}\ for\ |z| \leq R, 0 \leq r \leq R,$$

Since $f(z)$ has no zero on the circumference of the circle of radius R, we have that a function $y(z)$ exist such that

$$f(z) = e^{y(z)}$$

that is

$$y(z) = lnf(z)$$

Then

$$\frac{dy}{dz} = \frac{d}{dz}lnf(z)$$

$$= \frac{d}{df(z)} lnf(z). \frac{df(z)}{dz}$$

$$= \frac{1}{f(z)} \frac{df(z)}{d(z)} = \frac{f'(z)}{f(z)}$$

That is, on the circumference of the circle, $0 \leq r \leq R$

$$\frac{d}{dz} lnf(z) = \frac{f'(z)}{f(z)}$$

Integrating with respect to r

$$\int_0^R dlnf\left(re^{i\theta}\right) = \int_0^R \frac{f'(re^{i\theta})}{f(z)} dz = \int_0^R \frac{f'(re^{i\theta})}{f(re^{i\theta})} e^{i\theta} dr$$

$$lnf\left(re^{i\theta}\right)/_{r=0}^{r=R} = \int_0^R \frac{f'(z)}{f(z)} dz$$

or

$$lnf\left(re^{i\theta}\right) - \ln f(0) = \int_0^R \frac{f'(z)}{f(z)} dz$$

Hence, considering the pole, θ from 0 to 2π, we integrate with respect to θ we get

$$\int_0^{2\pi} lnf\left(Re^{i\theta}\right) d\theta - \int_0^{2\pi} lnf(o) d\theta = \int_0^{2\pi} \int_0^R \frac{f'(z)}{f(z)} dz$$

$$\ln f(0) = 0. \; If \; f(0) = 1$$

So,

$$\int_0^{2\pi} lnf\left(Re^{i\theta}\right) d\theta = \frac{1}{2\pi} \int_0^{2\pi} \left(\int_0^R \frac{f'(z)}{f(z)} dz \right) d\theta$$

Now, if $z = re^{i\theta}$, then since $r < R$, we consider points in the interior of the circle of circumference $2\pi R$. Then

$$dz = e^{i\theta} dr \text{ and } dz = rie^{i\theta} d\theta$$

So, the polar and radial variable are connected through

$$e^{i\theta} dr = rie^{i\theta} d\theta$$

$$\frac{rie^{i\theta}}{ri} dr = rie^{i\theta} d\theta$$

Implies,

$$\frac{dr}{ir} = d\theta$$

Hence,

$$\frac{1}{2\pi}\int_0^{2\pi} lnf\left(Re^{i\theta}\right)d\theta = \frac{1}{2\pi}\int_0^{2\pi}\left(\int_0^R \frac{f'(z)}{f(z)}dz\right)\frac{dr}{ir}$$

Since, $\frac{f'(z)}{f(z)}$ is continous on (0,R) we can interchange the double integrals to get

$$\frac{1}{2\pi}\int_0^{2\pi} lnf\left(Re^{i\theta}\right)d\theta = \int_0^R\left\{\frac{1}{2\pi ir}\int_0^{2\pi}\frac{f'(z)}{f(z)}dz\right\}dr$$

$$= \int_0^R\left\{\frac{1}{2\pi ir}\int_{|z|=r}\frac{f'(z)}{f(z)}dz\right\}dr$$

But $$\frac{1}{2\pi ir}\int_{|z|=R}\frac{f'(z)}{f(z)}dz = n(r),$$

where n(r) is the number of zeroes of $f(z)$ in the circle of radius r.

Hence

$$\frac{1}{2\pi}\int_0^{2\pi} ln\left|f(Re^{i\theta})\right|d\theta = \int_0^R \frac{n(r)}{r}dr$$

Thus,

$$\int_0^R \frac{n(r)}{r}dr = \left(\int_0^{r_1} + \int_{r_1}^{r_2} + \int_{r_2}^{r_3} + \cdots + \int_{r_{n-1}}^{r_n} + \int_{r_n}^{R}\right)\frac{n(r)}{r}dr$$

Suppose that the zeros of the function $f(z)$ are at the points $z_1, z_2, z_3, \ldots, z_n$. These zeroes are isolated .Let

$z_i \in (r_i, r_{i+1})$ $\quad i = 1,2,\ldots,n$ without any zero in $(0, r_i)$ or$z_0 \in (r_0, r_1)$ and n(z_i) $= i$

Then

$$\int_0^R \frac{n(r)}{r}dr = \left(\int_0^{r_1}\frac{n(r)}{r}dr\int_0^{r_2}\frac{n(r)}{r}dr\int_0^{r_3}\frac{n(r)}{r}dr + \cdots + \int_{r_{n-1}}^{r_n}\frac{n(r)}{r}dr + \int_{r_n}^{R}\frac{n(r)}{r}dr\right)$$

$$= \int_0^{r_1}\frac{0}{r}dr\int_{r_1}^{r_2}\frac{1}{r}dr\int_2^{r_3}\frac{2}{r}dr + \cdots + \int_{r_{n-1}}^{r_n}\frac{n-1}{r}dr + \int_{r_n}^{R}\frac{n}{r}dr$$

$$= 0 + lnr|_{r_1}^{r_2} + 2lnr|_{r_2}^{r_3} + \cdots + n-1lnr|_{r_{n-1}}^{r_n} + nlnr|_{r_n}^{R}$$

$$= lnr_2 - lnr_1 + 2(lnr_3 - lnr_2) + 3(lnr_4 - lnr_3) + \cdots + n - 1(lnr_n - lnr_{n-1}) + n(lnR - lnr_{n-1})$$

$$= lnr_2 - lnr_1 + 2lnr_3 - 2lnr_2 + 3lnr_4 - 3lnr_3 + \cdots + (n - 1lnr_n) - (n - 1lnr_{n-1} + nlnR - lnr_n$$

$$= -lnr_1 - lnr_2 - lnr_3 - lnr_4 + \cdots nlnR - lnr_n$$

$$= nlnR - (lnr_1 + lnr_2 + lnr_3 + lnr_4 + \cdots + lnr_n$$

But

$$nlnR = \left(\frac{1+1+1+\cdots+1+1}{n-times}\right) lnR$$

Then

$$= -lnr_1 + lnR - lnr_2 + lnR - \cdots - lnr_n + lnR$$

$$= -ln\frac{r_1}{R} - ln\frac{r_2}{R} - \cdots - ln\frac{r_n}{R}$$

$$= ln\frac{R}{r_1} + ln\frac{R}{r_2} + \cdots + ln\frac{R}{r_n}$$

$$= ln\left|\frac{R}{r_1}\right| + ln\left|\frac{R}{r_2}\right| + \cdots + ln\left|\frac{R}{r_n}\right|$$

$$= ln\frac{R^n}{|r_1 r_2 r_3 \ldots r_n|}$$

From our analysis $In|Q(z)|$ is harmonic in any region in which $Q(z)$ does not vanish, in particular when $Q(z)$ is analytic and non zero for $|z| \leq R$ and the Jensen's formulae tells us that the average value of $In|Q(z)|$ on the circumference of the circle $|Z| = R$ is increased by the presence of zeros $Q(z)$ within the circle, the closer these zeros are to the origin, the more this average value is increased. Also the larger the number of zeros within the circle $|Z| = R$, the more rapidly the average value of $In|Q(z)|$ on the circumference of the circle grows as R increases. Also Q(z) which is analytic inside and on the circle of center r attains its mean value at the evaluation of Q(z) at z = r which is regular inside and on the circle $|z| = r, Q(0) \neq 0$ and $a_1, a_2, \ldots, a_N$ are zeros of $Q(z)$ satisfying $|a_k| \leq r$ with multiple zeros counted as times as their multiplicity. Also the new inequalities on polynomials are obtained using Jensen's Integral formula and are of the fundamental importance in the theory of transcendental numbers different from the initial results carried-out by other researchers which are not fully connected to the basic properties of meromorphic or harmonic function.

References

[1] Mahler, K. (1961). On the zeros of the derivative of a polynomial, Mathematics Department, University of Manchester. Royal Society London.

[2] Trudgian, T. (2009). Jensens Theorem and a Simple Application. Mathematical Institute Oxford. London Mathematical Society, London.

[3] Oxford University Press (1939).Theory of Functions (2nd Edition).280.London

[4] www.mathcentre.ac.uk (2009). A guide for teachers, Functions: Module 10,Australian Mathematical Science Institute.

[5] Xiangdong, Y., Calfeng YI, Jin Tu.(2011). A note on the number of zeros of polynomials in an annulus: Annales polonici mathematici 100.1.

[6] Kreyszig, E.(2012). Advanced Engineering Mathematics (10th Edition). Wiley, Inc.

[7] Hayman, W.K. (1964). Meromorphic Functions, Oxford University Press.

[8] Gelfond, A.O. (1960). Transcendal and Algebraic numbers, Dover New York.

[9] Walsh, J.L. (1961). A new generalization of Jensen's theorem on the zeros of the derivative of a polynomial. Mathematical Science Directorate, Air force office of scientific research, Washington 25. DC

[10] Goldman, A.W. (1983). Univalent Functions, Vol. 1, mariner pusblishing Inc. University of South florida.

[11] Churchchill, R.V. (1960). Complex variable and Applications, McGrawHill, New York.

[12] Mahler, K. (1960). Mathematika 7, 98-100. Mathematics Department, University of Manchester.3wweplex Variable; Introduction and Application. 2nd ed. Cambridge University Press, 647.

[13] Nehari, Z. (1952) . Conformal Mapping; New York: Dover.

[14] Boyd, D.W. (1992). Two sharp Inequalities for the norm of a factor polynomial, mathematika 39, 341-349.

[15] Spiegel M.R, Seymour L, John J, Dennis S. (2009). Schaum's Outline Series McGrawHill, New york.

[16] Mahler, K. (1964). An inequality for a pair of polynomials that are relatively prime. Mathematics Department, IAS. Australian National University.

[17] Jensen, A. (2008). Note On Polynomials. Department of Mathematical Sciences Aalborg University,Denmark.

[18] Gelfond, A.O, Feldman N.I.(1950). On the measure of relative transcendentality of certain numbers, Izv. Akad. Nauk SSSR Ser. Mat 14(Russian) MR 12,493-500

[19] Conway, J.B. (1978). Functions of Complex Variable Chp.11,Springer Verlag, Newyork Heidelbeg Berln.

[20] Gamelin, T.W. (2001). Complex Analysis. Spinger Verlag New yoke Inc., 478.

[21] Rudin, W. (1974). Real and Complex Analysis, McGrawHill.Inc. New York.

.

A generalize Picard's successive iteration method for the nth order initial valued problem

A.K. Bello[a], A.M. Ayinde[*b], A.A. Ishaq[c], M.T. Raji[d] and A.E. Adenipekun[e]

Abstract

This research extends Picard's successive iteration method from solving first-order initial value problems to a generalized approach for nth-order problems. A recursive formula is introduced, eliminating the need for linearization and discretization by leveraging previous point values for subsequent iterations. The method's convergence is rigorously established and validated through numerous tests and examples. Notably, as the order of the problem approaches infinity, the iterations consistently converge to the exact solution, demonstrating the method's scalability and efficacy. This advancement offers a robust and accurate approach for solving higher-order initial value problems.

Keywords and phrases: discretization; linearization; ordinary differential equation; Picard's successive iteration method; initial value problem

1 Introduction

Differential equations form a significant and vital branch of mathematics, marked by extensive theoretical exploration and practical utility, a relevance that persists to this day. This prominence naturally raises several inquiries: What exactly is a differential equation, and what does it represent? Where do these equations come from, and how are they applied? When faced with a differential equation, what steps should one take, and what outcomes can be expected? These questions underscore three key facets of the subject: theory, methodology, and application. This chapter aims to familiarize readers with the fundamental aspects of differential equations while providing a concise overview of these three dimensions. Through this discussion, we will uncover insights into these queries, insights that will gain deeper significance as we delve into the study of differential equations in subsequent sections. Differential equations take the form $y^{(n)} = f(t, y, y', \dots, y^{(n-1)}), n \geq 1$ and f is not necessarily linear in its arguments, representing various physical phenomena. For instance, these

[*]Corresponding author: ayinde.abdullahi@uniabuja.edu.ng
[a]Department of Mathematics, University of Ilorin, Ilorin, Kwara, Nigeria. bello.ak@unilorin.edu.ng
[b]Department of Mathematics, University of Abuja, Abuja, Nigeria. ayinde.abdullahi@uniabuja.edu.ng
[c]Department of Physical Sciences, Al-Hikmah University, Ilorin, Kwara, Nigeria. aaishaq@alhikmah.edu.ng
[d]Department of Mathematics, Federal University of Agriculture, Abeokuta, Nigeria. rajimt@funaab.edu.ng
[e]Department of Mathematics, Federal Polytechnic, Edo, Osun, Nigeria. waltolxy@yahoo.com

equations describe free oscillations of positively damped systems, nonlinear systems under harmonic excitations, and the motion of a particle on a rotating parabola.

Over time, initial value problems (IVPs) have remained a focal point in literature due to their significant relevance in modeling real-life problems from physics, engineering, and biology. Although closed-form solutions for these IVPs are often elusive, researchers have strived to find closed-form, semi-analytical, or series solutions. Well-known methods for computing power series or semi-analytic solutions of IVPs include the Adomian Decomposition Method (ADM) [3], Variational Iteration Method (VIM) [4], Homotopy Perturbation Method (HPM) [5], and their various modifications. These methods have been effectively employed for finding series solutions of differential equations in general [6, 7, 8].

However, applying these methods can be challenging, often requiring additional effort. Furthermore, numerical solutions for linear boundary value problems (BVPs) have been described using a combination of superposition and orthonormalization. Recently, many methods for the numerical solutions of linear BVPs of different orders, have been developed [10, 11], splines [12, 14], parametric splines [15, 16], among others. This paper explores initial value problems (IVPs) of arbitrary order, providing certain existence results and introducing linearly convergent numerical schemes. These schemes are designed to find approximate solutions for IVPs associated with nth-order equations of the form mentioned earlier.

2 Preliminaries

2.1 Picard's theorem I:

Suppose $f\ (t, \mu)$ and $\frac{\partial F(t,\ \mu)}{\partial \mu}$ are both continuous on the rectangle$R\ = \{(t, \mu): t_0\ \leq\ t\ \leq\ t_0\ +\ a, \mu_0\ -\ b\ \leq\ \mu\ \leq\ \mu_0\ +\ b\}$, where a and b are positive constants. Let M be the maximum value of $|f\ (t, \mu)|$ on R and let α be the minimum of a and b. Then the initial-value problem $\frac{\partial \mu}{\partial t} = f(t, \mu), \mu(t_o) = y_0$, has a unique solution $\mu(t)$ defined on the interval$[t_0, t_0 + a]$.

2.2 The Existence and uniqueness theorem

Consider the differential equation

$$\mu^{(n)}(x) = f\big(x, \mu(x), \mu'(x), \dots, \mu^{(n-1)}(x)\big). \tag{1}$$

Suppose x_0 is a given "initial point" $x = x_0$, and suppose $a_0, a_1, \dots, a_{n-1}$ are given constants. Then there is exactly one solution to the differential equation (1) which satisfies the initial conditions.

$$\mu(x_0) = a_0, \mu'(x_0) = a_1, \mu''(x_0) = a_2, \dots \mu^{(n-1)}(x_0) = a_{n-1} \tag{2}$$

Note that for an n^{th} order equation we can prescribe exactly n initial values.

2.3 Differential technique

Here we present techniques

Let $U(x)$ b continuous function on the interval of discussion, and we consider the transformation:

$$\mu^{(n)}(x) = u(x). \tag{3}$$

Integrating both side with respect to x gives

$$\mu^{(n-1)}(x) = c_{n-1} + \int_0^x u(t)dt \tag{4}$$

Integrating again both side with respect to x yields

$$\mu^{(n-2)}(x) = c_{n-2} + c_{n-1}x + \iint_0^x u(t)dtdt = c_{n-2} + c_{n-1}x + \int_0^x (x-t)u(t)dt\,, \tag{5}$$

Obtained by reducing the double integral to a single integral. Processing as before we find

$$\mu^{(n-3)}(x) = c_{n-3} + c_{n-2}x + \frac{1}{2}c_{n-1}x^2 + \frac{1}{2}\int_0^x (x-t)^2 u(t)dt \tag{6}$$

Continuing the integration process leads to

$$\mu(x) = \sum_{k=0}^{n-1} \frac{c_k x^i}{k!} + \frac{1}{(n-1)!}\int_0^x (x-t)^{n-1}u(t)dt \tag{7}$$

2.4 Reducing multiple integral to simple integral

It will be seen later that we can convert initial value problems and other problems to integral equations. It is normal to outline the formula that will reduce multiple integral to single integrals. Using integration by parts

$$\int udv = uv - \int vdu\,, \tag{8}$$

$$u(x_1) = \int_0^{x_1} F(t)dt, \tag{9}$$

Then we find

$$\int_0^x \int_0^{x_1} F(t)dtdx_1 = x_1 \int_0^{x_1} F(t)dt\Big|_0^x - \int_0^x x_1 F(x_1)dx_1$$

$$= x\int_0^x F(t)dt - \int_0^x x_1 F(x_1)dx_1 1$$

$$= \int_0^x (x-t)F(t)dt \tag{10}$$

Obtained upon setting $x_1 = t$.

The general formula that converts multiple integrals to single integral is given by

$$\int_0^x \int_0^{x_1} \dots \int_0^{x_{n-1}} u(x_n) dx_n dx_{n-1} \dots dx_1 = \frac{1}{(n-1)!} \int_0^x (x-t)^{(n-1)} u(t) dt. \quad (11)$$

This formula will be used to convert initial value problem to Volterra integral equation.

2.5 Principle of Induction

In mathematics, we use a form of complete induction called mathematical induction to ascertain the validity of an assertion. The simplest and most common form of mathematical induction infers that a statement involving a natural number (that is, an integer or 1) holds for all values of the proof. The principle of mathematical induction is outlined as thus:

Suppose there is a given statement $P(n)$ involving the natural number n such that

(i) The statement is true for $n = 1$, i.e., $P(1)$ is true, and
(ii) If the statement is true for $n = k$ (where k is some positive integer),

then the statement is also true for $n = k + 1$, i.e., truth of P(k) implies the truth of $P(k + 1)$. Then, $P(n)$ is true for all natural numbers$n$.

3 Methodology

We consider $\frac{d^n \mu}{dx^n} = f(x, \mu, \mu^i, \dots \mu^{(n-1)}),\ x_0 < x < 1 \quad (12)$

$$\mathrm{x}\,(0) = x_0, \mu(0) = \mu_0, \mu'(0) = \mu'_0, \dots, \mu^{n-1}(0) = \mu_0^{(n-1)} \quad (13)$$

Integrating equation (13)

$$\mu^{(n-1)}(x) = \mu^{(n-1)}(x_0) + \int_{x_0}^x f\left(t, \mu(t), \mu'(t) \dots \mu^{(n-1)}(t)\right) dt \quad (14)$$

Integrating (14) with respect to x,

$$\mu^{(n-2)}(x) = \mu^{(n-2)}(x_0) + \int_{x_0}^x \mu^{n-1}(x_0) dx + \int_{x_0}^x (x-t) f\left(t, \mu(t), \mu'(t) \dots \mu^{(n-1)}(t)\right) dt \quad (15)$$

$$\mu^{(n-2)}(x) = \mu^{(n-2)}(x_0) + (x - x_0)\mu^{(n-1)}(x_0) + \int_{x_0}^x (x-t) f\left(t, \mu(t), \mu'(t) \dots \mu^{(n-1)}(t)\right) dt\, dt \quad (16)$$

Integrating (16) with respect to x,

$$\mu^{(n-3)}(x) = \mu^{(n-3)}(x_0) + (x - x_0)\mu^{(n-2)}(x_0) + \left(\frac{x^2}{2} - x x_0\right) \mu^{(n-1)}(x_0) + \frac{1}{2!} \int_{x_0}^x (x - t)^2 f\left(t, \mu(t), y'(t) \dots \mu^{(n-1)}(t)\right) dt\, dt dt \quad (17)$$

Integrating (17) with respect to x yield:

$$\mu^{(n-4)}(x) = \mu^{(n-4)}(x_0) + (x - x_0)\mu^{(n-3)}(x_0) + (\frac{x^2}{2} - xx_0)\mu^{(n-2)}(x_0) + \left(\frac{x^3}{6} - \frac{x^2}{2}x_0\right)\mu^{(n-1)}(x_0) + \quad \frac{1}{3!}\int_{x_0}^{x}(x-t)^3 f\left(t, \mu(t), \mu'(t) \dots \mu^{(n-1)}(t)\right)dt \tag{18}$$

Integrating (18) with respect to x gives:

$$\mu^{(n-5)}(x) = \mu^{(n-5)}(x_0) + (x - x_0)\mu^{(n-4)}(x_0) + (\frac{x^2}{2} - xx_0)\mu^{(n-3)}(x_0) + \left(\frac{x^3}{6} - \frac{x^2}{2}x_0\right)\mu^{(n-2)}(x_0) + (\frac{x^4 - 4x^3}{24}x_0)\mu^{(n-1)}(x_0) + \quad \frac{1}{4!}\int_{x_0}^{x}(x-t)^4 f\left(t, \mu(t), \mu'(t) \dots \mu^{(n-1)}(t)\right)dt \tag{19}$$

The continues integration process leads to

$$\mu(x) = \sum_{i=0}^{n-1}\frac{x^{i-1}}{i!}(x - ix_0)\mu_{(0)}^{i} + \frac{1}{(n-1)!}\int_{x_0}^{x}(x-t)^{n-1} f\left(t, \mu_{(t),}\mu^{!}(t) \dots \mu^{(n-1)}(t)\right)dt \tag{20}$$

For $n \geq 1$

For $x_0 = 0$ we have

$$\mu(x) = \sum_{i=0}^{n-1}\frac{x^{i}}{i!}\mu_{(0)}^{i} + \frac{1}{(n-1)!}\int_{0}^{x}(x-t)^{n-1} f\left(t, \mu_{(t),}\mu^{!}(t) \dots \mu^{(n-1)}(t)\right)dt \tag{21}$$

For generalized solution

$$\mu_{m+1}(x) = \sum_{i=0}^{n-1}\frac{x^{i-1}}{i!}(x - ix_0)\mu_{(0)}^{i} + \frac{1}{(n-1)!}\int_{0}^{x}(x-t)^{n-1} f\left(t, \mu_{m(t),}\mu_{m(t)}^{!} \dots \mu_{m}^{(n-1)}(t)\right)dt \tag{22}$$

Proof

Here we prove (20) by mathematical induction

$$\mu(x) = \sum_{i=0}^{n-1}\frac{x^{i-1}}{i!}(x - kx_0)\mu_{(0)}^{i} + \frac{1}{(n-1)!}\int_{x_0}^{x}(x-t)^{n-1} f\left(t, \mu(t), \mu'(t) \dots \mu^{(n-1)}(t)\right)dt \tag{23}$$

For $n = 1$ equation (12) becomes

$$\frac{d^1\mu}{dx^1} = f(x, \mu, \mu^{i}, \dots \mu^{(1-1)}), \tag{24}$$

i.e, $\frac{d\mu}{dx} = f(x, \mu)$ and thus equation (23) becomes

$$x\,(0) = x_0, \qquad \mu(0) = \mu_0,$$

$$\mu(x) = \sum_{i=0}^{1-1} \frac{x^{i-1}}{i!}(x - ix_0)\,\mu_{(0)}^{(0)} + \frac{1}{(1-1)!}\int_{x_0}^{x}(x-t)^{1-1} f\left(t,\ \mu_{(t),}\ \mu^{!}(t) \ldots\ \mu^{(1-1)}(t)\right) dt \tag{25}$$

Which is the solution to equation (12), $for\ m = k$ equation (12) becomes

$$\frac{d^k \mu}{dx^k} = f(x, \mu,\ \mu', \ldots\ \mu^{(k-1)}),\ x_0 < x < 1 \tag{26}$$

$$x\,(0) = x_0,\ \ \mu(0) =\ \mu_0,\ \ \mu'(0) =\ \mu'_0, \ldots,\ \mu^{k-1}(0) =\ \mu_0^{(k-1)} \tag{27}$$

The solution becomes

$$\mu(x) = \sum_{i=0}^{k-1} \frac{x^{i-1}}{i!}(x - ix_0)\,\mu_{(0)}^{i} + \frac{1}{(k-1)!}\int (x-t)^{k-1} f\left(t,\ \mu_{(t),}\ \mu^{!}(t) \ldots\ \mu^{(k-1)}(t)\right) dt \tag{28}$$

$form = k + 1$, we have

$$\frac{d^{k+1} \mu}{dx^{k+1}} = f(x, \mu,\ \mu', \ldots\ \mu^{(k-1)}, \mu^{(k)})\ x_0 < x < 1\ , \tag{29}$$

$$x\,(0) = x_0, \mu(0) =\ \mu_0,\ \mu'(0) =\ \mu'_0, \ldots,\ \mu^{k-1}(0) =\ \mu_0^{(k-1)},\ \mu^{k}(0) =\ \mu^{k}{}_0, \ldots,\ \mu^{k-1}(0) \tag{30}$$

Integration (29) together with (30)

$$\mu^k(x) =\ \mu^k(x_0) + \int_{x_0}^{x} f(x, \mu,\ \mu', \ldots\ \mu^{(k-1)}, \mu^{(k)})dt \tag{31}$$

Integrating (31) we have

$$\mu^{k-1}(x) =\ \mu^{k-1}(x_0) + (x - x_0)\,\mu^k(x_0) + \int_{x_0}^{x}(x-t) f(x,\ \mu,\ \mu', \ldots\ \mu^{(k-1)}, \mu^{(k)})dt \tag{32}$$

Integrating (32) yields

$$\mu^{k-2}(x) =\ \mu^{k-2}(x_0) + (x - x_0)\,\mu^{k-1}(x_0) + (\frac{x^2}{2} - xx_0)\,\mu^k(x_0) + \frac{1}{2!}\int_{x_0}^{x}(x-t)^2 f(x, \mu,\ \mu', \ldots\ \mu^{(k-1)}, \mu^{(k)})dt \tag{33}$$

Integrating (33)

$$\mu^{k-3}(x) = \mu^{k-3}(x_0) + (x - x_0)\,\mu^{k-2}(x_0) + (\frac{x^2}{2} - xx_0)\,\mu^{k-1}(x_0) + (\frac{x^3}{6} - \frac{x^2}{2}x_0)\,\mu^{k}(x_0) + \frac{1}{3!}\int_{x_0}^{x}(x-t)^3 f(x,\ \mu,\ \mu', \ldots\ \mu^{(k-1)}, \mu^{(k)})dt \quad (34)$$

Subsequent integration of the above equation gives

$$\mu(x) = \sum_{i=0}^{k} \frac{x^{i-1}}{i!}(x - ix_0)\,\mu_{(0)}^{(i)} + \frac{1}{(k)!}\int (x-t)^k f\left(t,\ \mu_{(t),}\ \mu^{!}(t) \ldots\ \mu^{(k)}(t)\right) dt \quad (35)$$

when $x_0 = 0$, (35) becomes

$$\mu(x) = \sum_{i=0}^{k} \frac{x^{i}}{i!}\,\mu_{(0)}^{(i)} + \frac{1}{(k)!}\int (x-t)^k f\left(t,\ \mu_{(t),}\ \mu^{!}(t) \ldots\ \mu^{(k)}(t)\right) dt \quad (36)$$

$for\ k \geq 0$, Hence, it is true for $m = K + 1$.

Since the Given statement is true for m$= 1, m = k, and m = k + 1$, hence it is true for all positive integer. Therefore, the derived equation can be used to solve differential equation of any order

4. Numerical Examples

Example 1

Consider the Second order differential equation

$$\mu'' + \mu = 0\,, \quad (37)$$

Together with the initial conditions

$$\mu(0) = 0,\ \ \mu'(0) = 1 \quad (38)$$

Exact solution

$$\mu(x) = \sin x \quad (39)$$

$$\mu'' + \mu = 0 \implies \mu'' = -\mu \quad (40)$$

$$\mu_{m+1} = \mu_o + x\,\mu_o' + \int_{x_o}^{x}(x-t)f(t,\ \mu_m(t),\ \mu_m'(t))dt \quad (41)$$

When $m = 0$

$$\mu_1 = \mu_o + x\,\mu_o' + \int_{x_o}^{x}(x-t)f(t,\ \mu_0(t),\ \mu_0'(t))dt \quad (42)$$

$$\mu_1 = \mu_o + x\,\mu_o' + \int_{x_o}^{x}(x-t)(0)dt \quad (43)$$

$$\mu_1 = x \quad (44)$$

When $m = 1$

$$\mu_2 = \mu_o + x\,\mu_o' + \int_{x_o}^{x}(x-t)f(t,\,\mu_1(t),\,\mu_1'(t))dt \tag{45}$$

$$\mu_2 = x - \int_{x_o}^{x}(x-t)tdt \tag{46}$$

$$\mu_2 = x - \left[\frac{x^3}{6}\right] \tag{47}$$

$$\mu_2 = x - \frac{x^3}{6} \tag{48}$$

When m=2

$$\mu_3 = \mu_o + x\,\mu_o' + \int_{x_o}^{x}(x-t)f(t,\,\mu_2(t),\,\mu_2'(t))dt \tag{49}$$

$$\mu_3 = x - \int_{x_o}^{x}(x-t)\left(x - \frac{t^3}{6}\right)dt \tag{50}$$

$$\mu_3 = x - \left[\frac{x^3}{6} - \frac{x^5}{5!}\right] \tag{51}$$

$$\mu_3 = x - \frac{x^3}{3!} + \frac{x^5}{5!} \tag{52}$$

Subsequently, $\mu_4 = x - \frac{x^3}{3!} + \frac{x^5}{5!} - \frac{x^7}{7!}$ (53)

$$\mu_5 = \mu_4 = x - \frac{x^3}{3!} + \frac{x^5}{5!} - \frac{x^7}{7!} + \frac{x^9}{9!} \tag{54}$$

Conclusively therefore, for $m = k-1$, we have the series in the form

$$\mu_{k-1} = \sum_{m=0}^{m=\infty}\frac{(-1)^m}{(2m+1)!}x^{2m+1} \tag{55}$$

which gives as $m \to \infty$, it will converge to

$$\mu = sinx \tag{56}$$

which is the exact solution.

Example 2

Consider the third order differential equation

$$\mu''' + \mu = 0\,, \tag{57}$$

Together with the initial conditions

$$\mu(0) = 1,\ \ \mu'(0) = -1,\ \mu''(0) = -1 \tag{58}$$

Exact solution

$$\mu(x) = e^{-t} \tag{59}$$

$$\mu''' + \mu = 0 \implies \mu''' = -\mu \tag{60}$$

$$\mu_{m+1} = \mu_o + x\,\mu_o' + \frac{x}{2!}x\,\mu_o'' + \frac{1}{2!}\int_{x_o}^{x}(x-t)^2) f(t,\ \mu_m(t),\ \mu_m'(t),\ \mu_m''(t))dt \tag{61}$$

When $m = 0$

$$\mu_1 = 1 - x + \frac{x^2}{2} + \frac{1}{2!}\int_{x_o}^{x}(x-t)^2\ \ (-1)dt \tag{62}$$

$$\mu_1 = 1 - x + \frac{x^2}{2} - \frac{x^3}{6} \tag{63}$$

When $m = 1$

$$\mu_2 = 1 - x + \frac{x^2}{2} + \frac{1}{2!}\int_{x_o}^{x}(x-t)^2\ \ (1 - t + \frac{t^2}{2} - \frac{t^3}{6})dt$$

$$\mu_2 = 1 - x + \frac{x^2}{2} - \frac{x^3}{6} + \frac{x^4}{4!} - \frac{x^5}{5!} + \frac{x^6}{6} \tag{64}$$

When $m = 2$

$$\mu_2 = 1 - x + \frac{x^2}{2} + \frac{1}{2!}\int_{x_o}^{x}(x-t)^2\ \ (1 - x + \frac{t^2}{2} - \frac{t^3}{6} + \frac{t^4}{4!} - \frac{t^5}{5!} + \frac{t^6}{6}\ )dt$$

$$\mu_3 = 1 - x + \frac{x^2}{2} - \frac{x^3}{6} + \frac{x^4}{4!} - \frac{x^5}{5!} + \frac{x^6}{6} - \frac{x^7}{7!} - \frac{x^8}{8!} + \frac{x^9}{9} \tag{65}$$

Conclusively therefore, as$m \to \infty$, we have the series in the form

$$\mu(x) \sim \sum_{m=0}^{k=\infty} \frac{(-1)^m}{m!}x^m \tag{66}$$

Thus the solution of (66) becomes

$$\mu = e^{-x} \tag{67}$$

which is the exact solution.

Example 3

Consider the fourth order differential equation

$$\mu'^{v} + x = 0\,, \tag{68}$$

Together with the initial conditions

$$\mu(0) = 0,\ \ \mu' = -1,\ \mu''(0) = 0,\ \mu'''(0) = 0 \tag{69}$$

Exact solution

$$y(x) = x + \frac{x^5}{120} \tag{70}$$

Solution

we write (68) as

$$\mu'^{v} = -x \tag{71}$$

Recall

$$\mu_{m+1} = \ \mu_o + (x - x_o)\,\mu_o' + \frac{x}{2!}(x - 2x_o)\,\mu_o'' \ \ + \frac{x^2}{3!}(x - 3x_o)\,\mu_o'' + \frac{1}{3!}\int_{x_o}^{x}(x - t)^3) f\big(t,\ \mu_m(t),\ \mu_m'(t),\ \mu_m''(t),\ \mu_m'''(t)\big)dt \tag{72}$$

$$\mu_1 = 0 + x + \frac{x}{2!}(x - 2x_o)0 \ \ + \frac{x^2}{3!}(x - 3x_o)0 + \frac{1}{3!}\int_0^x (x - t)^3 t dt \tag{73}$$

$$\mu_1 = x + \frac{1}{3!}\int_0^x (x - t)^3 t dt \tag{74}$$

$$\mu_1(x) = x + \frac{x^5}{120} \tag{75}$$

which is the exact solution.

5 Conclusion

In conclusion, this research successfully extends Picard's successive iteration method to provide a generalized solution for nth order initial value problems. By deriving a recursive formula that bypasses the need for linearization and discretization, the method demonstrates robustness and efficiency. The established convergence and validated accuracy through various tests and examples underscore its reliability. Notably, as n tends to infinity, the iterations converge towards the exact solution, highlighting the scalability and effectiveness of the proposed approach. This contribution opens avenues for further exploration and application in solving complex initial value problems across various domains.

References

[1] Nayfeh, A. H. (1985). Problems in Perturbations, Wiley, New York

[2] Akindeinde, S. O. (2016). A new approach for finding closed form solution of nth order initial value problems. Journal of the Nigerian Mathematical Society, 35: 546-559

[3] Adomian, G. (1994). Solving frontier problems of physics: the decomposition method, Kluwer Academic Publishers

[4] He, J. (1999).Variational iteration method - a kind of nonlinear analytical technique, International Journal of Non-Linear Mechanics, 34(4): 699-708

[5] He, J. (1999). Homotopy perturbation technique. Computer Methods in Applied Mechanics and Engineering, 178(3-4): 257-262.

[6] Hassan, I. A. (2004). Differential transformation technique for solving higher-order initial value problems, Applied Mathematics and Computation, 154(2): 299-311.

[7] He, J. and Wu, X. (2007).Variational iteration method: new development and applications, Computers & Mathematics with Applications, 54(7-8): 881-894.

[8] Akindeinde, S. O. (2015). Homotopy Perturbation Method for the Strongly Nonlinear Darcy-Forscheimer Model, Mathematical Theory and Modeling, 5(9): 78-84.

[9] Scott, M. R. and Wattts, H.A. (1976). A systematized collection of codes for solving two-point BVPs, Numerical Methods for Differential Systems, Academic Press

[10] Li, C. (2008). A kind of multistep finite difference methods for arbitrary order linear boundary value problems, Applied Mathematics and Computation, 196: 858-865.

[11] Kanth, A. and Reddy, Y. (2004). Higher order finite difference method for a class of singular boundary value problems, Applied Mathematics and Computation, 155: 249- 258.

[12] Siddiqi, S. S. and Twizell, E.H. (1997). Spline solutions of linear twelfth-order boundary value problems, Applied Mathematics and Computation, 68: 371-390.

[13] Siddiqi, S. S. and G. Akram, (2008). Solutions of 12th order boundary value problems using non-polynomial spline technique, Applied Mathematics and Computation, 199: 559-571.

[14] Siddiqi, S. S., Akram, G. and Elahi, A. (2008). Quartic spline solution of linear fifth order boundary value problems, Applied Mathematics and Computation, 196: 214-220.

[15] Khan, A. (2004). Parametric cubic spline solution of two point boundary value problems, Applied Mathematics and Computation, 154: 175-182.

[16] Rashidinia, J., Mahmoodi, Z., Ghasemi, M. (2007). Parametric spline method for a class of singular two-point boundary value problems, Applied Mathematics and Computation 188: 58-63.

Mathematical model of the transmission dynamics of Anthrax disease

C. Omeh [*†], G.C.E. Mbah[†‡], D. Nnaji[§], I.G. Ezema[¶], A.Y. Danjuma[‖], and E.O. Oshilim[**]

Abstract

Anthrax is a deadly disease,that occurs in ruminant animals such as sheep,cattle and others.The human can also contract anthrax when one comes in contact with infected animal or their product like hide,wool and so on.In this paper a system of non-linear differential equation is formulated to describe the transmission dynamics of the disease in human.The model was well formulated and epidemiologically meaningful by showing the positivity of the variables and obtaining the invariant region of the various compartment of the model.The equilibrium analysis[EEP] were also carried out and stability analysis based on the equilibrium points were also carried out. Finally, Numerical simulation was done using MATLAB which helped us to show in one of the graphs that with early treatment,the disease may eventually may be controlled

Keywords and phrases: Anthrax; mathematical model;endemic equilibrium point(EEP); numerical simulation

1 Introduction

Bacillus anthracis (anthrax) refers to the black,coal-like leision that is frequently seen on infected people's skin and also derived from Greek word anthracite which means coal [1].Anthrax was first mentioned in 1491 B.C in Mesopotamian writting and Book of Geenesis.The $5th$ and$6th$ Egyptian plagues shows the symptoms of anthrax.The disease is a spore-forming bacterium,a rare but serious illness which primarily affects livestock and game. Human become infected through either first hand or second hand interaction with sick animals [1].

The signs and symptoms are headache,Bulging of sore lymph glands surrounding it,swollen neck,shortness of breath,meningitis and spinal cord inflammation,failure of multiple organ and shock e.t.c

The mode of transmission are as follows; Cutaneous anthrax is gotten through skin wound or cut as the infection enters the body. It's the least dangerous because, with proper care, cutaneous anthrax seldom results in death. Secondly,Gastrointestinal anthrax is the type of anthrax infection,caused by consuming raw meat of an infected animal.Thirdly is the Pulmonary anthrax which happens when anthrax spores are inhaled.It is the most dangerous way to get the disease, and even with treatment, it is frequently fatal.Finally Injection anthrax which is the most recent method of anthrax infection that has been discovered. It is acquired through drug injection and has only been documented thus far in Europe.

[*]Corresponding Author; E-mail: chinenye.omeh@unn.edu.ng
[†]Department of Mathematics, University of Nigeria, Nsukka
[‡]E-mail: godwin.mbah@unn.edu.ng
[§]Department of Mathematics, University of Nigeria, Nsukka; E-mail:daniel.nnaji@unn.edu.ng
[¶]Department of Mathematics, State University of Medical and Applied Sciences, Igbo-Eno, Nsukka; E-mail: izuchukwu.ezema@sumas.edu.ng
[‖]Department of Actuarial Science, Confluence University of Science and Technology, Osara, Nigeria; E-mail: : danjumaay@custech.edu.ng
[**]Department of Mathematics, University of Nigeria, Nsukka, Nigeria. E-mail: emoshilim@gmail.com

There are some risk factors for those who works in a laboratory, for example the veterinary especially for those that deal with livestock, Handles or dress game animals ,Inject illegal drugs like heroin and Handle animal by-product, examples wools, skins from areas with a high incidence of Anthrax and also in military especially those that are in the the area with high risk of anthrax exposure.

2 Prevention and control

The control measure as shown in Figure [1] above which is by breaking the infection cycle. The following procedure must be strictly followed:

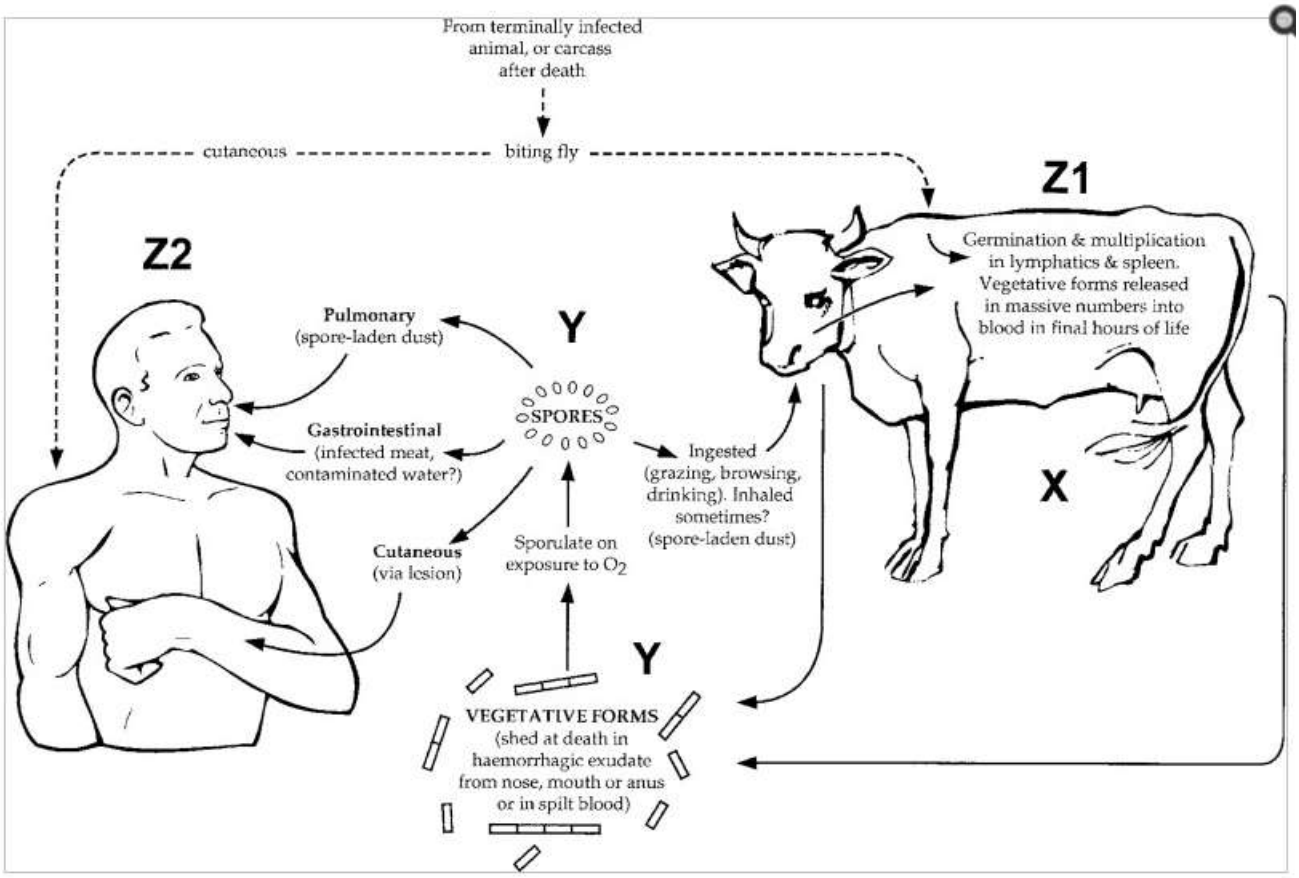


Figure 1: Breaking the cycle of infection

2.1 Disposal of anthrax (animal) carcasses

- Principles involved:Sporulation of anthrax does not occur inside an enclosed carcass. Most countries' policies do not involve postmortem examination of animals when anthrax is suspected. Without that, all vegetative B. anthracis cells in the carcass are killed in a few days by a putrefactive process(decay). The actual length of time after which no feasible B. anthracis remains in a carcass is unpredictable but depends immensely on the condition of the climate that is temperature.

- incineration: Incineration must be carried out with appropriate care to ensure complete burning from beneath. Usually, this involves raising the carcass off the ground before the process is started.

- Rendering:The sterilization of staple(raw materials) of animal rootage by heating method or treatment such that parts of carcasses are used later for commercial designs.

This procedure involves accurate performance at each of three stages: the collection stage, transport stage, and treatment stage of the carcass [5, 6].

2.2 Disinfection and decontamination by fumigation (formaldehyde or ethylene oxide)

Disinfection, decontamination, and proper disposal of infected/contaminated material are critical in preventing long-distance and international anthrax transmission, in addition to assisting in breaking the cycle of anthrax infection locally.

2.3 Infection control for human

1 If reasonable precautions are taken, Human-to-human communication poses no significant risk. For example, during the first $24-48$ hours post operative , cutaneous anthrax lesions should be dressed; and disposing of test samples or sterilizing equipment. Postmortem examinations should be discouraged in fatal cases; cremation is preferable for burial where local custom allows.

2 Antibiotics are advised to be used by anyone who has been exposed to spores. The Food and Drug Administration has approved ciprofloxacin (Cipro), doxycycline (Monodox, Vibramycin, and others), and levofloxacin (Levaquin) for the avoidance of diease in human.[2]

3 Visitors should wear protective clothing and footwear that can be sanitized or packaged for burning before entering infected properties.[2]

The study of Anthrax was based on the hypothesis that the disease is primarily spread by environmental contamination where the generation multiplication rate is defined as the number of new cases arising from a single isolated case.The effects of anthrax transmission via carcass ingestion,carcass-induced environmental contamination and migration rates leads to disease infection on animal population which may be persistence or lead to extinction.The basic reproduction number R_0 for the anthrax epizootic model was calculated with animal migration.It was observed that the removal of remains in the game reserves brings about a decrease in the level of carcass ingestion.As a result of that, the increase in level of carcass induced environmental contamination rate in an enzootic anthrax region can lead to the extinction of a persistent animal population[Friedman etall 2012].The researcher[Zerihun et al 2016] formulated a model of four compartment and studied the effectiveness of clinical signs on the infected animals.In 2018,Osman et al carried out a review study on the mathematcal modelling of transmission dynamics of anthrax in human and animal population indicating the quantitative and qualitative analyses of the model.Elijah et al. (2020) conducted a mathematical analysis of the Effects of Controls on the Anthrax Transmission Dynamics in ruminant and non-ruminant animals. The study proposed a nonlinear differential equation model to investigate the impact of vaccination on the dynamics of anthrax disease transmission in livestock and human populations. The model is shown to have only two equilibria, the disease-free and the endemic equilibrium points, both of which are locally stable if the Basic reproduction number (R0) is less than unity and greater than unity, respectively. According to local sensitivity analysis, the infection rate, pathogen-shedding rate, and vaccination rate of livestock are the parameters with the greatest positive impact on disease spread. The rate of disinfection, followed by the rate of vaccination, has the greatest negative impact on disease transmission. The numerical simulation demonstrated that implementing all control measures (vaccination, education, disinfection, and treatment) is the most effective strategy for preventing disease spread.Firstly, we considered the presence of Bacillius Anthracis in the environment through Air(aerosol).Secondly, an exposed treated class was included in the human compartment to checkmate the bacteria. Lastly, the model accommodated the class of infectious vectors without treatment in the animal compartment.

3 Methodology/model formulation

In this Section, we developed a Mathematical model describing the transmission dynamics of Anthrax. The definitions and representations of the model parameters and variables declaration are highlighted,

flow diagram describing the dynamics of the disease was shown, basic assumptions are all clearly stated.

3.1 Assumptions of the model

In this study, the following assumptions were made;

1. There is adquate contact of a susceptible individual with an infected individual,carcasses and spores in air,so that transmission may occur,and the susceptible individual may join the exposed class at the rate $\beta = (\alpha_1 C + \alpha_2()I_H + I_V) + \alpha_3(e^{\theta} - 1)$
2. We assumed in vector compartment that the infectious population,I_V is classified into 2 stages as the one undergoing treatment I_{VT} at the rate sigma (σ) and the second stage is the infectious vector without treatment,I_{VN} and recover at the rate rho (ρ) due to immunity.
3. In the infectious human class,there is inhalation i.e spores in air at the rate of Ae^{θ}. Due to this there may be no disease free equilibrium (DFE)and therefore, the Basic reproduction number R_0 is not calculated.
4. We also assumed that recovered human and vector are permanently immuned to the disease.

Model flow diagram is seen in Figure ??:

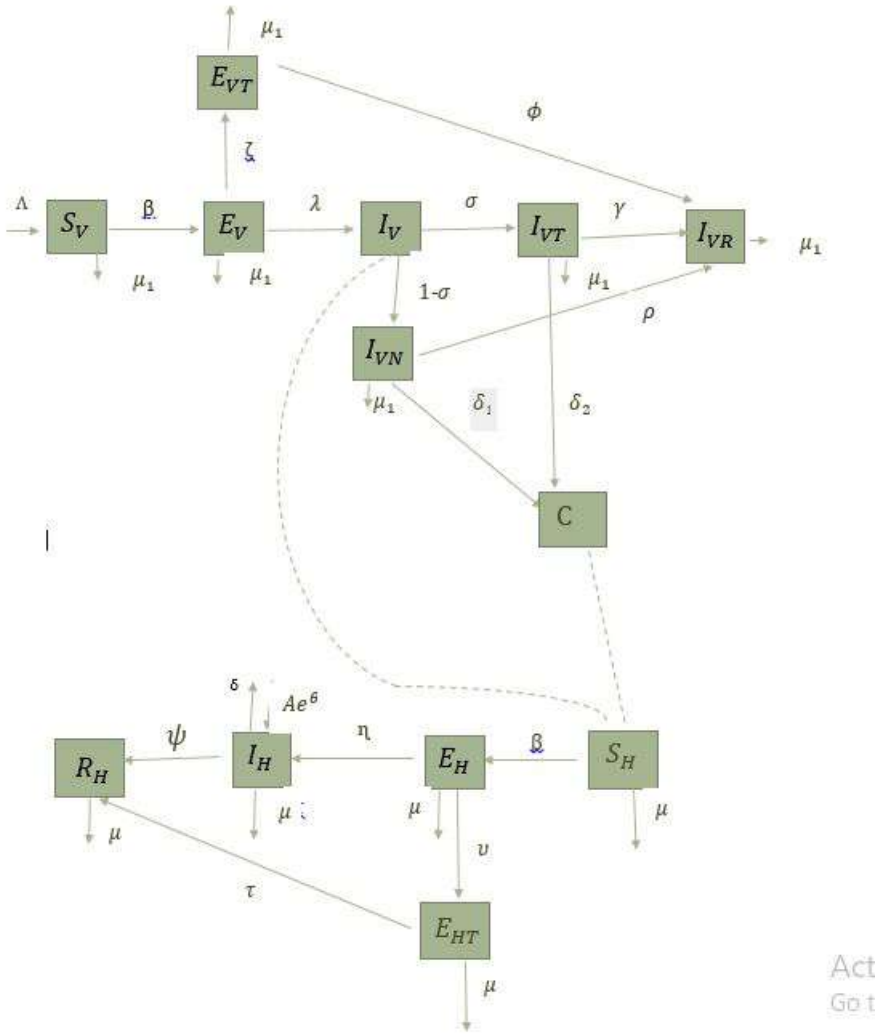


Figure 2: Flow diagram for transmission dynamics of Anthrax model.

Table 1: Variable declaration

Variable	Description
S_V	Total number of susceptible vectors at time t
E_v	The number of Exposed vectors at time t
E_{vT}	The number of Exposed vectors undergoing treatment at time t
I_v	The number of infectious vectors
I_{vT}	The number of infectious vectors undergoing treatment at time,t
I_{vN}	The number of infectious vectors without treatment at time,t
I_{vR}	The number of recovered vectors at time,t
C	The number of infected / infectious Carcasses at time,t
S_H	The number of Susceptible humans at time,t
E_H	The number of Exposed humans at time, t
E_{HT}	The number of Exposed humans undergoing treatment at time,t
I_v	The number of infectious humans at time ,t
R_H	The number of recovered humans at time,t

Table 2: Parameter declaration

parameter	Description
Λ	recruitment level of the vectors
β	force of infection , $\beta = \alpha_1 C + \alpha_2(I_H + I_v) + \alpha_3(e^{\theta} - 1)$
β_1	force of infection , $\beta_1 = \alpha_{11} C + \alpha_{21}(I_v) + \alpha_{31}(e^{\theta} - 1)$
ζ	progression from exposed to exposed undergoing treatment
λ	progression rate from exposed to infectious
σ	rate at which the infectious go for treatment
1-σ	rate of recovery without treatment
ϕ	progression rate from exposed treated to recovered
γ	rate of recovery from infectious vector that are treated
ρ	rate of recovery from infectious vectors without treatment
δ_1, δ_2	death rate due to disease
η	progression rate from exposed humans to infectious humans
υ	rate at which exposed human go for treatment
θ	density of the particles in the Air
τ	recovery rate of treated exposed humans
Ψ	recovery rate of treated infectious humans
ϵ	recovery rate of infectious humans without treatment
μ	natural death unrelated to the disease

3.1.1 Subsubsection

4 Analysis of the model

Endemic Equilibrium Point

The endemic equilibrium point (EEP) E^* i.e where $R_0 > 1$ is a steady state solution,where the disease persists in the population.The existence and uniqueness of endemic equilibrium point E^* should satisfy the conditions: $E^* = (S_V^*, E_V^*, E_{VT}^*, I_{VT}^*, I_{VN}^*, I_{VR}^*, S_H^*, E_H^* E_{HT}^*, I_H^*, R_H^*)$ and
$E^* = (S_V^*, E_V^*, E_{VT}^*, I_{VT}^*, I_{VN}^*, I_{VR}^*, S_H^*, E_H^* E_{HT}^*, I_H^*, R_H^*, C^*) \neq 0$.It is now needed to find the endemic equilibrium point of the system (4.1) -(4.12)and setting right hand to zero gives

$$\begin{aligned}
\Lambda_v - \beta_1 S_v - \mu_1 S_v &= 0 && (1)\\
\beta_1 S_v - (\zeta + \lambda + \mu_1) E_v &= 0 && (2)\\
\zeta E_v - \Phi E_{VT} - \mu_1 E_{vT} &= 0 && (3)\\
\lambda\sigma E_v - (\gamma + \delta_2) I_{VT} &= 0 && (4)\\
\lambda(1-\sigma) E_v - (\rho + \delta_1) I_N &= 0 && (5)\\
\Phi E_{vT} + \gamma I_{vT} + \rho I_{vN} - \mu_1 I_{VR} &= 0 && (6)\\
\Lambda_H - \beta S_H - \mu S_H &= 0 && (7)\\
\beta S_H - (\eta + \upsilon + \mu) E_H &= 0 && (8)\\
\upsilon E_H - (\tau + \mu) E_{HT} &= 0 && (9)\\
\eta E_H - (\Psi + \mu) I_H + (e^{\theta} - 1) S_H &= 0 && (10)\\
\Psi I_H + \tau E_{HT} - \mu R_H &= 0 && (11)\\
\delta_1 I_{VN} + \delta_2 I_{VT} &= 0 && (12)
\end{aligned}$$

On solving (1) -(12), the variables were obtained as
$C^* = \frac{\Lambda_V - \alpha_2 S_V (I_H + I_V - \alpha_3 (e^{\theta}-1) - \mu S_V}{\alpha_1 S_V}, E_H^* = \frac{\beta \Lambda_H}{(\beta+\mu)(\eta+\upsilon+\mu)}, E_{HT}^* = \frac{\upsilon \beta \Lambda_H}{(\beta+\mu)(\tau+\mu)(\eta+\upsilon+\mu)}, E_V = \frac{\beta S_V}{(\beta+\mu)(\eta+\lambda+\mu)}, E_{VT}^* = \frac{\eta \beta \Lambda_V}{(\phi+\mu)(\beta+\mu)(\eta+\lambda+\mu)}, I_H^* = \frac{\eta \beta \Lambda_H}{(\beta+\mu)(\tau+\mu)(\eta+\upsilon+\mu) - a(e^{\theta}-1)}, I_{VN} = \frac{\lambda(1-\sigma)\beta \Lambda_V}{(\rho+\delta_1+\mu)(\beta+\mu)(\zeta+\lambda+\mu)}, I_{VT} = \frac{\lambda\sigma)\beta \Lambda_V}{(\gamma+\delta_2+\mu)(\beta+\mu)(\zeta+\lambda+\mu)}, I_{VR}^* = \frac{\phi Q_1 + \gamma Q_2 + \rho Q_3}{\mu}, R_H^* = \frac{\psi Q_5 + \tau Q_4}{\mu}, S_H^* = \frac{\Lambda_H}{\beta+\mu}, S_V^* = \frac{\Lambda_V}{\beta_1+\mu_1}$

4.0.1 Invariant region and positivity of solution

For the Anthrax transmission dynamics model(??)-(??) to be epidemiological meaningful,it is necessary to prove that all solutions with non-negative initial data will remain non-negative or positive for all time and therefore is mathematically well posed.

4.0.2 Positivity of solution

Here now it is to be shown that all state variables remain non-negative since they represent human population and the presence of the disease in the population.
The invariant set
For $\Omega = \Omega_H + \Omega_V$
Let$\Omega_H = (S_H, E_H, E_{HT}, I_H, R_H) and$
$\Omega_V = (S_V, E_V, E_{VT}, I_{VN}, I_{VT}, I_{VR})$
Then let $\Omega = (S_H, E_H, E_{HT}, I_H, R_H, S_V, E_V, E_{VT}, I_{VN}, I_{VT}, I_{VR}) \in \Re_+^{11}$
So at initial time $S_H(0) > 0, E_H(0) > 0, E_{HT}(0) > 0, I_H(0) > 0, R_H(0) > 0, S_V(0) > 0, E_V(0) > 0, E_{VT}(0) > 0, I_{VN}(0) > 0, I_{VT}(0) > 0, I_{VR}(0) > 0$.This is because at the initial time of study of the disease transmission,there is the presence of the disease in the population and so each compartment of the disease population is non negative.

the equation (??)

$$\begin{aligned}
\frac{dS_V}{dt} &= \Lambda_V - \beta_1 S_V - \mu_1 S_V \\
\frac{dS_V}{dt} &\geq -\mu_1 S_V \\
\int \frac{dS_V}{S_V} &\geq -\mu_1 \int dt \\
lnS_V &\geq -\mu_1 t + C \\
e^{lnS_V} &\geq e^{-\mu_1 t} * e^c \\
S_V(t) &\geq Ae^{-\mu_1 t} \quad where \qquad A = e^C \qquad (13) \\
at \quad t = 0 & \\
S_V(0) &= S_{V_0} \geq A \qquad (14)
\end{aligned}$$

Substitute equation (14) into (13) we have

$$S_V(t) \geq S_{V_0} e^{-\mu t}$$

as $t \to \infty$,

$$S_V(t) \to 0$$

from equation (??)

$$\begin{aligned}
\frac{dE_V}{dt} &= \beta_1 S_V - (\zeta + \lambda + \mu_1 + \lambda + \mu) E_V \\
\frac{dE_V}{dt} &\geq -(\zeta + \lambda + \mu_1) E_V \\
\int \frac{dE_V}{E_V} &\geq -\int (\zeta + \lambda + \mu_1) dt \\
lnE_V &\geq -(\zeta + \lambda + \mu_1)t + c \\
e^{lnE_V} &\geq e^(\zeta + \lambda + \mu_1)t * e^c \\
E_V(t) &\geq Be^{(\zeta+\lambda+\mu_1)t} \qquad where \qquad B = e^C \qquad (15)
\end{aligned}$$

at t = 0

$$E_V(0) = E_{V_0} \geq B \qquad (16)$$

Put equation (16) into (15)

$$E_V(t) = E_{V_0} e^{-[\zeta+\lambda+\mu_1]t} \qquad (17)$$

as $t \to \infty$, $E_V(t) \to 0$
Similarly, the same argument holds for the remain variables.

4.1 Invariant Region

The total population size for human and animal are

$$N = N_H + N_V \qquad (18)$$

$$\text{let} N_H = S_H + E_H + E_{HT} + I_H + R_H \qquad (19)$$

$$\Rightarrow \frac{dN_H}{dt} = \frac{dS_H}{dt} + \frac{dE_H}{dt} + \frac{dE_{Ht}}{dt} + \frac{dI_H}{dt} + \frac{dR_H}{dt} \qquad (20)$$

$$\frac{dN_H}{dt} = \Lambda_H - \beta S_H - \mu S_H + \beta S_H - \eta E_H - \upsilon E_H - \mu E_H + \upsilon E_E H \tag{21}$$

$$-\tau E_{HT} - \mu E_{HT} + \eta E_H - \Psi I_H - \mu I_H + a(e^{\theta} - 1) + \Psi I_H + \tau E_{HT} - \mu R_H \tag{22}$$

$$\frac{dN_H}{dt} = \Lambda_H - (S_H + E_H + E_{HT} + I_H + R_H)\mu + a(e^{\theta - 1}) \tag{23}$$

$$\frac{dN_H}{dt} = \Lambda_H - N_H\mu + a(e^{\theta} - 1) \tag{24}$$

$$\rightarrow \frac{dN_H}{dt} + \mu N_H = \Lambda_H + a(e^{\theta} - 1) \tag{25}$$

$\rightarrow (I.F) = e^{\int \mu dt} = e^{\mu t}$
we integrate

$$N_H(t)e^{\mu}t = \int (\Lambda_H + a(e^{\theta} - 1))e^{\mu t}dt + C \tag{26}$$

$$= (\frac{\Lambda_H + a(e^{\theta} - 1)}{\mu})e^{\mu t} + C \tag{27}$$

$$\rightarrow N_H(t) = \frac{\Lambda_H + a(e^{\theta} - 1)}{\mu} + Ce^{-\mu t} \tag{28}$$

$$\tag{29}$$

at $t = 0, N_H = N_H(0) = N_{H0}$

$$\rightarrow N_{H0}(t) = \frac{\Lambda_H + a(e^{\theta} - 1)}{\mu} + C \tag{30}$$

$$\rightarrow C = N_{H_0} - \frac{\Lambda_H + a(e^{\theta} - 1)}{\mu} \tag{31}$$

$\Rightarrow$

$$N_H(t) = \Lambda_H + a(e^{\theta} - 1) + \left[N_{H_0} - \frac{\Lambda_H + a(e^{\theta} - 1)}{\mu}\right] e^{-\mu t} \tag{32}$$

$$= \frac{\Lambda_H + a(e^{\theta} - 1)}{\mu} \left[1 - e^{-\mu t}\right] + N_{H_0}e^{-\mu t} \tag{33}$$

As $t \longrightarrow \infty, e^{-\mu t} \longrightarrow 0$ and so we have

$$N_H(t) = \frac{\Lambda_H}{\mu} \tag{34}$$

when $e^{\theta} = e^0 = 1$ so that $a(e^0 - 1) = 0$

The total population size of animal

$$N_V = S_V + E_V + E_{VT} + I_{VT} + I_{VN} + I_{VR} \tag{35}$$

$$\Rightarrow \frac{dN_V}{dt} = \frac{S_V}{dt} + \frac{E_V}{dt} + \frac{E_{VT}}{dt} + \frac{I_{VT}}{dt} + \frac{I_{VN}}{dt} + \frac{I_{VR}}{dt} + \frac{C}{dt} \tag{36}$$

$$\frac{N_V}{dt} = \Lambda_V - \beta S_V - \mu S_V + \beta S_V - \zeta E_V - \lambda E_V - \mu E_V \zeta E_V - \phi E_{VT} - \mu_1 E_{VT} + \lambda\sigma E_V - \gamma I_{VT} - \delta_2 I_{VT} \tag{37}$$

$$\lambda E_V - \lambda\sigma E_V - \rho I_{VN} - \delta_1 I_{VN} + \phi E_{VT} + \gamma I_{VT} + \rho I_{VN} - \mu_1 I_{VR} + \delta_1 I_{VN} + \delta_2 I_{VT} + \mu_1 I_{VN} \tag{38}$$

$$\frac{dN_V}{dt} = \Lambda_V - (S_V + E_V + E_{VT} + I_{VN} + I_{VT} + I_{VR})mu_1 \tag{39}$$

In the absence of the disease (Anthrax) we are left with

$$\frac{N_V}{dt} = \Lambda_V - N_V\mu_1 \tag{40}$$

$$\text{integrating factor (I.F)} = e^{\int \mu_1 dt} = e^{\mu_1 t} \tag{41}$$

$$\frac{dN_V}{dt} + \mu_1 N_V e^{\mu_1 t} = \Lambda_V e^{\mu_1 t} \tag{42}$$

$$dN_V(t)e^{\mu_1}(t) = \Lambda_V e^{\mu_1 t} \tag{43}$$

we integrate

$$N_V(t)e^{\mu} t = \frac{1}{\mu}\Lambda_V e^{\mu} t + C \tag{44}$$

$$N_V(t) = \frac{\Lambda_V}{\mu} + \frac{C}{e^{\mu} t} \tag{45}$$

$$N_V(t) = \frac{\Lambda_V}{\mu} + Ce^{\mu_1} t \tag{46}$$

At the initial condition $N_V(0) = N_{H_0}$ for $t = 0$

$$N_{V_0} = \frac{\Lambda}{\mu_1} + C \tag{47}$$

$$C = N_{V_0} - \frac{\Lambda_V}{\mu_1} \tag{48}$$

substitute equation (48) into equation (46)

$$\Rightarrow N_V(t) = \frac{\Lambda_V}{\mu_1} + e^{-\mu_1 t}(N_{V_0} - \frac{\Lambda_V}{\mu_1}) \tag{49}$$

$$\Rightarrow N_V(t) \leq \frac{\Lambda_V}{\mu} + N_{V_0}e^{-\mu t} - \frac{\Lambda_V}{\mu_1}e^{-\mu_1 t} \tag{50}$$

At t $\longrightarrow \infty, N_V(t) \longrightarrow \frac{\Lambda}{\mu_1}$

Thus,the feasible set for the model system (??)-(??) is given by

$$\left\{ \begin{bmatrix} S_H \\ E_H \\ E_{HT} \\ I_H \\ R_H \\ S_V \\ E_V \\ E_{VT} \\ I_V \\ I_{VT} \\ I_{VN} \\ I_{VR} \end{bmatrix} \in R_+^{12} \middle| \begin{array}{l} S_H \geq 0 \\ E_H \geq 0 \\ E_{HT} \geq 0 \\ I_H \geq 0 \\ R_H \geq 0 \\ S_V \geq 0 \\ E_V \geq 0 \\ E_{VT} \geq 0 \\ I_V \geq 0 \\ I_{VT} \geq 0 \\ I_{VN} \geq 0 \\ I_{VR} \geq 0 \\ N_H \leq 0 \\ N_V \leq 0 \end{array} \right\}$$

It implies that model equations are positively invariant.Hence the model is mathematically well posed and biologically meaningful (Gumel & Niger 2008).

5 Numerical simulations/sensitivity analysis

In this section, the numerical simulation of the model equations is conducted to find out the dynamics of the disease in the human population and afterwards the animal population.The simulations were conducted using MATLAB.

S/N	Parameter	Values	Source
1	Λ_H	1000	O.Sharomi et al,2007
2	Λ_V	2000	O.Sharomi et al,2007
3	α_1	0.0033	Pantha Buddhi Raj,2016
4	α_1	0.0022	Assumed
5	α_1	0.02	Assumed
6	λ	0.001	Pantha Buddhi Raj,2016
7	σ	0.45	O.Sharomi et al,2007
8	γ	0.0034	O.Sharomi et al,2007
9	δ_1	0.0043	O.Sharomi et al,2007
9	δ_2	0.0036	O.Sharomi et al,2007
10	ρ	0.003	O.Sharomi et al,2007
11	ϵ	0.03	Assumed
12	μ	0.0005	Pantha Buddhi Raj,2016
13	ϕ	0.05	Assumed
14	υ	1	Assumed
15	τ	0.065	Pantha Buddhi Raj,2016
16	Ψ	0.045	Assumed
17	e	0.23	Estimated
18	a	0.2	Estimated

Variable @ initial condition	Value
S_V	1000
E_V	800
E_{VT}	700
I_{VT}	690
I_{VN}	650
I_{VR}	600
S_H	2000
E_H	400
E_{HT}	300
I_H	150
R_H	130

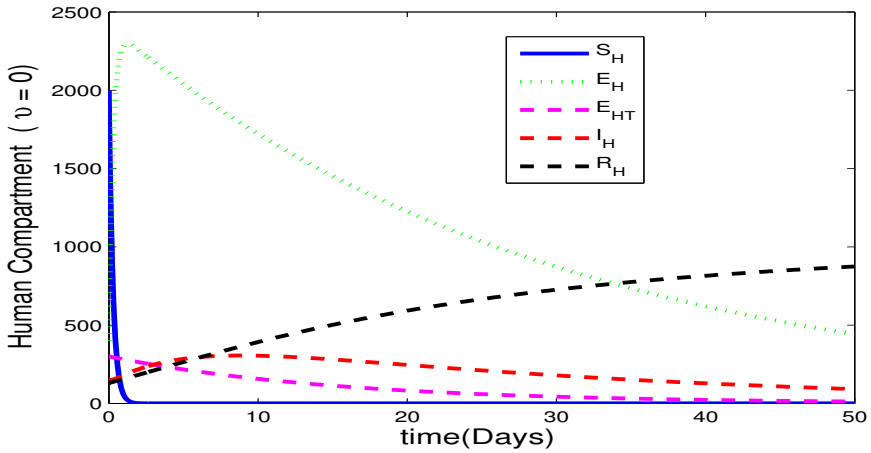


Figure 3: Graph of the dynamic of Human population when $\upsilon = 0$

It is shown in the above graph that after some time,all the people in susceptible class will become infected.Since there is no treatment the infected population E_H continues to develop infectious fully and thus reduces the population of the exposed class.The only few people that recovered is due to strong immune system.

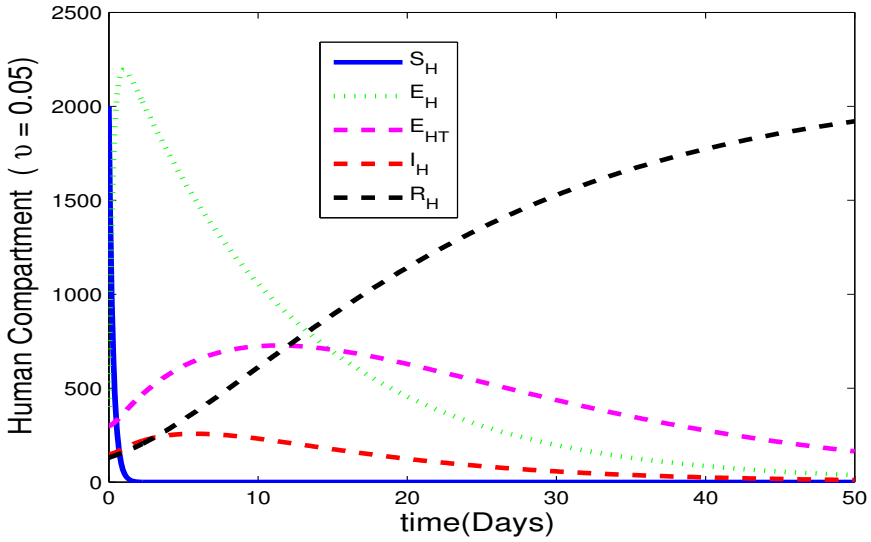


Figure 4: Effect of when $\upsilon = 0.05$ on the human population

The graph above showed the effect of prophylaxis as we can see the sharp drop in the curve of exposed Human and sharp increase in recovered class

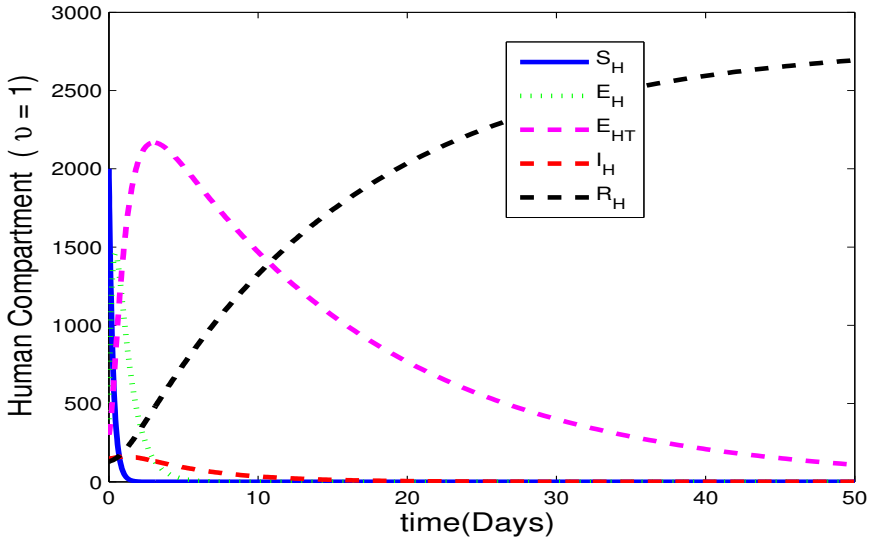


Figure 5: Effect of $\upsilon = 1$ on the human population

In this figure,the exposed and infectious population reduce drastically leading to large increase in recovered population due to treatment and can be seen also all the susceptible population became infected and thus exposed due lack of treatment at the initial time.

6 Discussions and conclusion

We have derived and analyzed a mathematical model for the transmission and control of Anthrax.A flow diagram was drawn showing the transmission,stratagies for control and treatment.The basic reproduction number R_0 and disease free equilibrium point (DFE) is not computered due to the presence of the (inhalation ,Ae^0) Bacillus anthracis spore in the air.Then, we perform the stability analysis of the model and showed that the endemic equilibrium is stable.

The Numerical Stimulation was carried out using MATLAB and we analyzed that $fig4.1$ and $fig4.4$ shows no effect of treatment on both human and vector population. $fig4.2$ and $fig4.5$ shows that Human and vector exposed to the disease are being treated and more human and vector enter the recovering class while $fig4.6$ and $fig4.7$ depicts the rate at which exposed Human and vector population decreases at the increase in treatment .

References

[1] Koch R. The etiology of anthrax, based on the life history of Bacillus anthracis. Beitrage zer Biologie der Ppanzen 1876;2.2:277-310. Available from the American Society for Microbiology. [PubMed]

[2] Mayo Foundation for Medical Education and Research (MFMER)(1998-2019).

[3] Shaibu Osman, Oluwole Daniel Makinde and David Mwangi Theuri "Mathematical Modelling of Transmission Dynamics of Anthrax in Human and Animal Population",vol.8 no.6,2018

[4] Centers for Disease Control and Prevention, National Center for Emerging and Zoonotic Infectious Diseases (NCEZID), http : //www:cdc:gov/ncezid/dw-index.html, 2016.

[5] Riedinger O, Strauch D, Böhm R (1975). [The destruction of pathogenic and non-pathogenic spore-formers by heat sterilization of slaughterhouse waste]. Zentralblatt für Veterinarmedizin Medizin Reihe B, 22:860–865. (In German, summary in English.)

[6] Riedinger O (1980). [Computation for the sterilization process in rendering plants]. Zentralblatt für Bakteriologie i Abt Originale B Hygiene, 170:287–296. (In German, summary in English.)

[7] A. Friedman and A. A. Yakubu, "Anthrax epizootic and migration:persistence or extinction," Mathematical Biosciences, vol.241, no. 1, pp. 137–144, 2013.

[8] Shaibu Osman, Oluwole Daniel Makinde and David Mwangi Theuri "Mathematical Modelling of Transmission Dynamics of Anthrax in Human and Animal Population",vol.8 no.6,2018

Characteristics and control strategies for Diphtheria-Pertussis co-infection risk in the post COVID-19 era

S.O. Johnson*†, H.O. Edogbanya †‡, J.O. Omolehin§, and O. Johnson¶

Abstract

Currently, the disruptions to routine vaccination programs induced during COVID-19 pandemic have raised worries about possible resurgence of vaccine-preventable diseases like diphtheria and pertussis, particularly in infants and children with zero vaccination. This study aims to assess the risk of diphtheria-pertussis co-dynamics and control strategies in the post-pandemic era using modified SIR-type mathematical model. Our research is hinged on the premise that pathogens can coexist in a host and that diphtheria-pertussis are both preventable by (Diphtheria-Tetanus-Pertussis) DTAP vaccine. Therefore, the presented model captures epidemiological parameters and varying disease control coverage inputs to simulate disease behaviour in a population susceptible to both infections. Key non-optimal control parameters used are vaccination at birth, maternal derived immunity and partial quarantine for diphtheria only. The next generation matrix was used to derive the basic reproduction number R_0 , after which stability analysis was conducted and it was observed that the formulated model exhibits four equilibrium points. The disease-free equilibrium and endemic equilibrium are shown to be locally and globally asymptotically stable. The forward sensitivity index was employed to pinpoint the effects of the hierarchy of parameters within R_0. Furthermore, it was observed that the model would undergo backward bifurcation under certain conditions, Consequently, optimal control inputs should be considered for future research. Finally, theoretical accuracy of the diseases co-existence is validated via Numerical simulations and relevant graphical illustrations are displayed using MATLAB 2021a.

Keywords and phrases: co-dynamics; effective reproduction number; sensitivity analysis; backward bifurcation; gaussian elimination

1 Introduction

The current trend in re-emergence of vaccine-preventable respiratory infectious diseases persist to be a global health concern with the increasing disruption on routine immunization by recent COVID-19 Pandemic [1, 2]. WHO and UNICEF Report available up to 2021 [3] estimated that about 25 million children missed out on DTP (Diphtheria-Tetanus-Pertussis) routine vaccines. According to [4], respiratory system disease affecting the lungs and other organs have long been a concern in children, pathogenic bacteria and virus that infect a human being can also be nested inside individual (host) itself. Hence, great importance is attributed to the characterization of co-infection by understanding how such pathogens intera t directly or indirectly through a carrier or its immigratory system [5, 6, 7, 8]. Diphtheria and pertussis are bacterial respiratory diseases with varying degrees of infection risk, both of which can be prevented by the DTaP (Diphtheria-Tetanus-Pertussis) vaccine [9, 10, 11]. Diphtheria, caused by the *Corynebacterium* species as noted by [12], can result in serious complications such

*Corresponding Author; E-mail: oladipuposamueljohnson@gmail.com
†Department of Mathematics, Federal University Lokoja, Kogi, Nigeria
‡E-mail: helen.edogbanya@fulokoja.edu.ng
§Department of Mathematics, Federal University Lokoja, Kogi, Nigeria; E-mail: joseph.omolehin@fulokoja.edu.ng
¶Department of Public Health, Ladoke Akintola University of Technology, Ogbomosho, Oyo, Nigeria; E-mail: olukunlelaiwola@gmail.com

as paralysis or death if the infection becomes chronic. The disease spreads through droplets or close contact with an infected individual, as the *bacterium Corynebacterium diphtheriae* releases a toxin that causes the illness. Pertussis, commonly known as whooping cough, is a highly contagious respiratory infection caused by the *bacterium Bordetella pertussis*. It spreads through droplets from an infected individual [13]. While severe pertussis can result in serious illness and even death, particularly in newborns and infants, the disease often goes undetected [14]. Research indicates that adolescents and adults, who may be asymptomatic carriers, are the primary source of infection for vulnerable infants. Recently, the co-interaction of pathogens has garnered significant attention from mathematicians worldwide. For example, [15] analyzed a co-dynamic model of pertussis-pneumonia, which includes a compartment for MDI (maternal-derived immunity) and temporary immunity among infected infants. Additionally, various studies have investigated the co-dynamic effects of pneumonia with other diseases, such as the HIV/AIDS-pneumonia co-infection dynamics studied by [16], and [17] examination of COVID-19 and bacterial pneumonia co-infection dynamics. In [18], a model was proposed for pneumonia-meningitis co-infection, while [19] studied influenza-meningitis co-infection, with a focus on quarantine and recovery rates. Additionally, [20] examined optimal control strategies for co-infections between chronic hepatitis B virus (HBV) and SARS-CoV-2, presenting a dynamic model that explores various equilibria and highlights the occurrence of backward bifurcation triggered by co-infection. The authors of [21, 22] utilized the Normalized Forward Sensitivity Index to assess the hierarchical influence of parameters on the reproduction number within the model. Furthermore, [22] investigated the potential coexistence of diphtheria and pertussis through mathematical modeling.

2 Model formulation

The diphtheria-pertussis co-infection model presented, comprises of eight different compartments, where, the total population at time (t) denoted as $N(t)$ is given by

$$N(t) = S(t) + I_{AD}(t) + I_{SD}(t) + I_{AP}(t) + I_{SP}(t) + I_{SDP}(t) + Q_{SD}(t) + R(t) \tag{1}$$

the compartments are Susceptible individuals $S(t)$, the infected individuals with diphtheria in asymptomatic stage $I_{AD}(t)$, the infected individuals with diphtheria in symptomatic stage $I_{SD}(t)$, the infected individuals with pertussis in asymptomatic stage $I_{AP}(t)$, the infected individuals with pertussis in symptomatic stage $I_{SP}(t)$, the infected individuals with both diphtheria and pertussis in there symptomatic stage $I_{SDP}(t)$, individuals who has recovered from diphtheria, pertussis or dual infection. $R(t)$, Quarantine of individuals showing clinical symptoms of diphtheria $Q_{SD}(t)$. In the model formulation, we assumed that $\kappa = bN(1-V)$ is the total proportion of zero vaccinated individuals where b is the birth rate and V is the vaccinated at birth. we also assume that due to vaccination during pregnancy, the mother would have passed on strong immunity to the infant via placenta at fetus stage. Therefore, the Susceptible or Vulnerable compartment S increases by the influx of non-vaccinated individuals and individuals who recovers from asymptomatic stage due to Maternal Derived Immunity (MDI) represented by $\xi_D I_{AD}$ and $\xi_P I_{AP}$ respectively.

Furthermore, The Susceptible compartment could get infected with diphtheria only at the rate $\Phi_D = \frac{\beta_D(\alpha_D I_{AD} + I_{SD})}{N}$, Pertussis only at rate $\Phi_P = \frac{\beta_P(\alpha_P I_{AP} + I_{SP})}{N}$, and dual infection at rate $\Phi_{DP} = \frac{\beta_{DP} I_{SDP}}{N}$ respectively. Individuals at the symptomatic stage of diphtheria and pertussis could get infected with a second infection at rates $\gamma_1 \frac{\beta_P(\alpha_P I_{AP} + I_{SP})}{N} I_{SD}$ and $\gamma_2 \frac{\beta_D(\alpha_D I_{AD} + I_{SD})}{N} I_{SP}$ respectively, where γ_1 and γ_2 denotes vulnerability to a second infection. We also assume that vaccinated individuals at birth are immune against disease and flows directly into the recovered compartment R at rate VbN. Other parameter used are described in Table 1

Based on the model description and assumptions above, we formulated the model governing equation (2).

Table 1: Values of parameters used in simulation.

Parameter	Symbol	Value	Cite
β_D	Effective contact rate for Diphtheria	0.57/day	[23]
β_P	Effective contact rate for Pertussis	0.5-1/day	[15]
β_{DP}	Diphtheria-Pertussis contact rate	0.2/day	fitted
ξ_D	MDI against Diphtheria infection	0.35	[15],
ξ_P	MDI against Pertussis	0.35	[15, 30]
ξ_{DP}	MDI Dual infection	0.35	[15]
Ω	Recovery rate of Quarantine	0.1-0.9	Assumed
η_D	Diphtheria Recovery rate.	0.5	[15]
η_P	Pertussis Recovery rate	$[\frac{1}{14}, 0.0206$	[15]
η_{DP}	Diphtheria-Pertussis Recovery rate	0.15/day	[19]
ϖ_D	Diphtheria induced death rate	0.05	[23]
ϖ_P	Pertussis induced death rate	0.0309	[15]
ϖ_{DP}	Disease induced death rate of Dual infection	0.005/day	[23]
μ	Natural death rate	0.006	[23]
θ	Diphtheria infected Quarantined	0.1/day	Assumed
V	Vaccination	0.1-1.2	Assumed
α_D, α_P	Modification parameter	0.5	[15]
γ_1, γ_2	Modification parameter	1	[19]
b	Birth rate	0.019	[23]
ϕ_D, ϕ_P	Progression to symptomatic infected stage	$[\frac{3}{7}]$/day , $[\frac{7}{7}]$/day	Fitted

$$
\begin{aligned}
\frac{dS}{dt}(t) &= bN(1-V) + \xi_D I_{AD} + \xi_P I_{AP} \\
&\quad - \left(\frac{\beta_D(\alpha_D I_{AD} + I_{SD})}{N} + \frac{\beta_P(\alpha_P I_{AP} + I_{SP})}{N} + \frac{\beta_{DP} I_{SDP}}{N} \right) S - \mu S \\
\frac{dI_{AD}}{dt}(t) &= \frac{\beta_D(\alpha_D I_{AD} + I_{SD})}{N} S - (\phi_D + \xi_D + \mu) I_{AD} \\
\frac{dI_{SD}}{dt}(t) &= \phi_D I_{AD} - (\theta + \eta_D + \varpi_D + \mu) I_{SD} - \gamma_1 \frac{\beta_P(\alpha_P I_{AP} + I_{SP})}{N} I_{SD} \\
\frac{dI_{AP}}{dt}(t) &= \frac{\beta_P(\alpha_P I_{AP} + I_{SP})}{N} S - (\phi_P + \xi_P + \mu) I_{AP} \\
\frac{dI_{SP}}{dt}(t) &= \phi_P I_{AP} - (\eta_P + \varpi_P + \mu) I_{SP} - \gamma_2 \frac{\beta_D(\alpha_D I_{AD} + I_{SD})}{N} I_{SP} \\
\frac{dI_{SDP}}{dt}(t) &= \frac{\beta_{DP} I_{SDP}}{N} S + \gamma_1 \frac{\beta_P(\alpha_P I_{AP} + I_{SP})}{N} I_{SD} + \gamma_2 \frac{\beta_D(\alpha_D I_{AD} + I_{SD})}{N} I_{SP} \\
&\quad - (\eta_{DP} + \varpi_{DP} + \mu) I_{SDP} \\
\frac{dQ_{SD}}{dt}(t) &= \theta I_{SD} - (\Omega + \mu) Q_{SD} \\
\frac{dR}{dt}(t) &= VbN + \eta_P I_{SP} + \eta_D I_{SD} + \eta_{DP} I_{SDP} + \Omega Q_{SD} - \mu R
\end{aligned}
\tag{2}
$$

$S(0) > 0, I_{AD}(0) > 0, I_{SD}(0) > 0, I_{AP}(0) > 0, I_{SP}(0) > 0, I_{SDP}(0) > 0, Q_{SD}(0) > 0$

Model Schematic Diagram is seen in Figure 1:

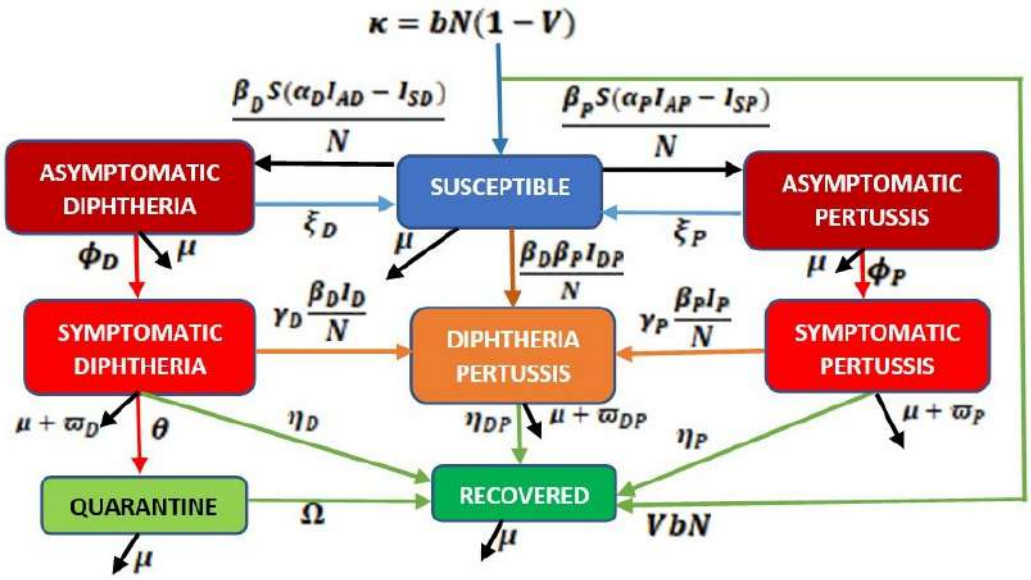


Figure 1: Schematic Diagram of Diphtheria-Pertussis transmission dynamics.

3 Analysis of the model

3.1 Model existence and uniqueness

To ensure that this diphtheria-pertussis transmission model is both mathematically and epidemiological sound, the dynamic system outlined in equation (2) must satisfy the subsequent theorems. We recall that the infection forces is $\Phi_D = \frac{\beta_D(\alpha_D I_{AD} + I_{SD})}{N}$, $\Phi_P = \frac{\beta_P(\alpha_P I_{AP} + I_{SP})}{N}$, and $\Phi_{DP} = \frac{\beta_{DP} I_{SDP}}{N}$ respectively which will subsequently be used interchangeably.

Theorem 1 (non-negativity or positively of model). If the initial value conditions for $S(0) > 0, I_{AD}(0) > 0, I_{SD}(0) > 0, I_{AP}(0) > 0, I_{SP}(0) > 0, I_{SDP}(0) > 0, R(0) > 0, Q_{SP}(0) > 0$ and $t(0) > 0 \ \forall \ t\epsilon[0, t_0]$ then, $S(t), I_{AD}(t), I_{SD}(t), I_{AP}(t), I_{SP}(t), I_{SDP}(t), R(t)$ and $Q_{SD}(t)$ Maintains positivity throughout in $\mathbb{R}^8_+$.

Proof. Giving that we are dealing with human populations, it is presupposed that all the employed parameter are non-negative. From equation (2), we assume that the Susceptible compartment is,

$$\frac{dS}{dt} = \kappa + \xi_D I_{AD} + \xi_P I_{AP} - (\Phi_D + \Phi_P + \Phi_{DP} + \mu)S \geq -(\Phi_D + \Phi_P + \Phi_{DP} + \mu)S \tag{3}$$

By separating variables in equation (3) and applying the integrating factor method, we derive

$$\frac{dS}{dt} \geq -(\Phi_D + \Phi_P + \Phi_{DP} + \mu)S \equiv \frac{dS}{S} \geq -(\Phi_D + \Phi_P + \Phi_{DP} + \mu)dt$$

$$\begin{aligned} \int_0^S \frac{dS}{S} &\geq -\int_0^t (\Phi_D + \Phi_P + \Phi_{DP} + \mu)dt \\ \ln|S(t)| &\geq -(\Phi_D + \Phi_P + \Phi_{DP} + \mu)t + C \\ S(t) &\geq Ce^{-(\Phi_D + \Phi_P + \Phi_{DP} + \mu)t} \end{aligned}$$

Hence, if $(t = 0)$ we have $(S(t) \geq S(0)e^{-(\Phi_D + \Phi_P + \Phi_{DP} + \mu)t} \geq 0)(\forall t > 0)$ since $(\Phi_D + \Phi_P + \Phi_{DP} + \mu) > 0$. Similarly, we can show that $(I_{AD}(t), I_{SD}(t), I_{AP}(t), I_{SP}(t), I_{SDP}(t), R(t))$ and $Q_{SD}(t)$ are non-negative.

Theorem 2 (Boundedness). The closed set given by $B^* = (S, I_{AD}, I_{SD}, I_{AP}, I_{SP}, I_{SDP}, R, Q_{SD}) \in \mathbb{R}^8_+ : S + I_{AD} + I_{SD} + I_{AP} + I_{SP} + I_{SDP} + R + Q_{SD} \leq \frac{\kappa}{\mu}\}$ is positively invariant with respect to the dynamic system equation (2).

Proof. Adding equation (2) and equating it to zero at initial time ($t = \varpi_D = \varpi_P = \varpi_{DP} = 0$) gives:

$$\frac{dN}{dt} + \mu N(t) \leq \kappa \tag{4}$$

Again, applying the integrating factor method to equation (4) and employing Gronwall's-Bellman inequality [21], followed by simplification, results in:

$$N(t) \leq \frac{\kappa}{\mu} + (N(0) - \frac{\kappa}{\mu})e^{-\mu t}, \Rightarrow N(t) \leq \frac{\kappa}{\mu}$$

As $t \to \infty$, the equation (2) has the solution in B^* and thus positively invariant.

Theorem 3 (Existence and uniqueness). Starting from the Initial values of the equation (2) , which are $S(0) > 0, I_{AD}(0) > 0, I_{SD}(0) > 0, I_{AP}(0) > 0, I_{SP}(0) > 0, I_{SDP}(0) > 0, R(0) > 0, Q_{SD}(0) > 0$, then $t \in \mathbb{R}$, the solutions $S(t)$, $I_{AD}(t)$, $I_{SD}(t)$, $I_{AP}(t)$, $I_{SP}(t)$, $I_{SDP}(t)$, $Q_{SD}(t)$, $R(t)$ exist in $\mathbb{R}^8_+$.

Proof. If the model equation (2) can be expressed in the form $\dot{x} = f(x)$ where,

$$\dot{x} = \begin{pmatrix} S \\ I_{AD} \\ I_{SD} \\ I_{AP} \\ I_{SP} \\ I_{SDP} \\ Q_{SD} \\ R \end{pmatrix}$$

$$f(x) = \begin{bmatrix} \kappa + \xi_D I_{AD} + \xi_P I_{AP} - (\Phi_D + \Phi_P + \Phi_{DP})\, S - \mu S \\ \Phi_D S - (\phi_D + \xi_D + \mu) I_{AD} \\ \phi_D I_{AD} - (\theta + \eta_D + \varpi_D + \mu) I_{SD} - \gamma_1 \Phi_P I_{SD} \\ \Phi_P S - (\phi_P + \xi_P + \mu) I_{AP} \\ \phi_P I_{AP} - (\eta_P + \varpi_P + \mu) I_{SP} - \gamma_2 \Phi_D I_{SP} \\ \Phi_{DP} S + \gamma_1 \Phi_P I_{SD} + \gamma_2 \Phi_D I_{SP} - (\eta_{DP} + \varpi_{DP} + \mu) I_{SDP} \\ \theta Q_{SD} - (\Omega + \mu) Q_{SD} \\ \eta_P I_{SD} + \eta_D I_{SP} + \eta_{SDP} I_{SDP} + \Omega Q_{SD} - \mu R \end{bmatrix} \tag{5}$$

Then equation (5) is proved by the existence and uniqueness theorem, since f has a continuous first derivative in $\mathbb{R}^8_+$ and is locally Lipschitz, therefore, there exists a unique, positive, and bounded solution for the governing equation (2) in $\mathbb{R}^8_+$.

3.1.1 Equilibrium solutions

Here, The equilibrium points is derived by equating all compartments in equation (2) to zero, i.e.,

$$\frac{dN}{dt} = \frac{dS}{dt} + \frac{dI_{AD}}{dt} + \frac{dI_{SD}}{dt} + \frac{dI_{AP}}{dt} + \frac{dI_{SP}}{dt} + \frac{dI_{SDP}}{dt} + \frac{dQ_{SD}}{dt} + \frac{dR}{dt} = 0$$

Upon diphtheria-pertussis initial outbreak which is the Disease Free Equilibrium we obtain:

$$\begin{aligned} N_0 &= (S_0 + I_{AD0} + I_{SD0} + I_{AP0} + I_{SP0} + I_{SDP0} + Q_{SD0} + R_0) \\ &= (\frac{\kappa}{\mu}, 0, 0, 0, 0, 0, 0, 0) \end{aligned}$$

Solving for the endemic Equilibria

In the absence of pertussis disease: $E_D^* = (S^*, I_{AD}^*, I_{SD}^*, 0, 0, 0, R^*)$ This account for the endemic equilibrium point of Diphtheria disease denoted as,

$$S^* = \frac{bN(1-V) + \xi_D I_{AD}^*}{\Phi_D^* + \mu}, I_{AD}^* = \frac{\beta_D I_{SD}^* S^*}{(\phi_D + \xi_D + \mu) - \beta_D \alpha_D},$$
$$I_{SD}^* = \frac{\phi_D I_{AD}^*}{(\theta + \eta_D + \varpi_D + \mu)}, R^* = \frac{VbN + \eta_D I_{SD}^*}{\mu}.$$

In the absence of Diphtheria disease: $E_P^* = (S^*, 0, 0, I_{AP}^*, I_{SP}^*, 0, R^*)$ This account for the endemic equilibrium point of pertussis disease, denoted as,

$$S^* = \frac{bN(1-V) + \xi_P I_{AP}^*}{\Phi_P^* + \mu}, I_{AP}^* = \frac{\beta_P I_{SP}^* S^*}{(\phi_P + \xi_P + \mu) - \beta_P \alpha_P},$$
$$I_{SP}^* = \frac{\phi_P I_{AP}^*}{(\theta + \eta_P + \varpi_P + \mu)}, R^* = \frac{VbN + \eta_P I_{AP}^*}{\mu}$$

In the presence of both diphtheria and pertussis co-infection state, $E_D^* = (S^*, I_{AD}^*, I_{SD}^*, I_{AP}^*, I_{SP}^*, I_{SDP}^*, R^*)$ This gives rise to the diphtheria-pertussis endemic equilibrium state given by.

$$S^* = \frac{bN(1-V) + \xi_D I_{AD}^* + \xi_P I_{AP}^*}{\Phi_D^* + \Phi_P^* + \Phi_{DP}^* + \mu}, I_{AD}^* = \frac{\beta_D I_{SD}^* S^*}{(\phi_D + \xi_D + \mu) - \beta_D \alpha_D},$$
$$I_{SD}^* = \frac{\phi_D I_{AD}^*}{(\theta + \eta_D + \varpi_D + \mu) + \gamma_1 \beta_P (\alpha_P I_{AP}^* + I_{SP}^*)},$$
$$I_{AP}^* = \frac{\beta_P I_{SP}^* S^*}{(\phi_P + \xi_P + \mu) - \beta_P \alpha_P}, I_{SP}^* = \frac{\phi_P I_{AP}^*}{(\eta_P + \varpi_P + \mu) + \gamma_1 \beta_D (\alpha_D I_{AD}^* + I_{SD}^*)},$$
$$I_{SDP}^* = \frac{\gamma_1 \beta_P (\alpha_P I_{AP}^* + I_{SP}^*) + \gamma_2 \beta_D (\alpha_D I_{AD}^* + I_{SD}^*)}{(\eta_{DP} + \xi_{DP} + \varpi_{DP} + \mu) - \beta_{DP}},$$
$$R^* = \frac{VbN + \eta_D I_{AD}^* + \eta_P I_{AP}^* + \eta_{DP} I_{SDP}^*}{\mu}$$

In a special case where the three infection forces are at steady state $\Phi_D^* = \frac{\beta_D I_{SD}^*}{N^*}$, $\Phi_P^* = \frac{\beta_P I_{SP}^*}{N^*}$, and $\Phi_{DP}^* = \frac{\beta_{DP} I_{SDP}^*}{N^*}$. The equation (2) possess co-existence endemic equilibria.

$$S^* = \frac{\kappa + \xi_D I_{AD}^* + \xi_P I_{AP}^*}{\Phi_D^* + \Phi_P^* + \Phi_{DP}^* + \mu}, I_{AD}^* = \frac{\Phi_D^* (\kappa + \xi_D I_{AD}^* + \xi_P I_{AP}^*)}{k_1 (\Phi_D^* + \Phi_P^* + \Phi_{DP}^* + \mu)},$$
$$I_{SD}^* = \frac{\alpha_D \Phi_D^* (\kappa + \xi_D I_{AD}^* + \xi_P I_{AP}^*)}{k_1 k_2 (\Phi_D^* + \Phi_P^* + \Phi_{DP}^* + \mu)}, I_{AP}^* = \frac{\Phi_P^* (\kappa + \xi_D I_{AD}^* + \xi_P I_{AP}^*)}{k_3 (\Phi_D^* + \Phi_P^* + \Phi_{DP}^* + \mu)},$$
$$I_{SP}^* = \frac{\alpha_P \Phi_P^* (\kappa + \xi_D I_{AD}^* + \xi_P I_{AP}^*)}{k_3 k_4 (\Phi_D^* + \Phi_P^* + \Phi_{DP}^* + \mu)}, I_{SDP}^* = \frac{\Phi_{DP}^* (\kappa + \xi_D I_{AD}^* + \xi_P I_{AP}^*)}{k_5 (\Phi_D^* + \Phi_P^* + \Phi_{DP}^* + \mu)},$$
$$R^* = \frac{(\kappa + \xi_D I_{AD}^* + \xi_P I_{AP}^*) (\Phi_D^* \eta_D \alpha_D k_3 k_4 k_5 + \Phi_P^* \eta_P \alpha_P k_1 k_2 k_5 + \Phi_{DP}^* \eta_{DP} k_1 k_2 k_3 k_4)}{\mu k_1 k_2 k_3 k_4 k_5 (\Phi_D^* + \Phi_P^* + \Phi_{DP}^* + \mu)}$$

3.2 Basic reproduction number

The Basic reproduction number R_0 which represents average number of secondary infections produced by an infected and infectious individual. Which implies that When $R_0 > 1$, the disease will persist within the population, particularly infants [24]. The next generation matrix is used to derive the basic reproduction number[24, 25] $R_0 = \rho F V^{-1}$, where ρ is the spectral radius and transition and transmission matrix are denoted by $F_i(a)$ and $V_i(a)$ at N_0 Respectively. Now let

$$k_1 = (\phi_D + \xi_D + \mu) I_{AD}, k_2 = (\theta + \eta_D + \varpi_D + \mu) I_{SD}, k_3 = (\phi_P + \xi_P + \mu) I_{AP},$$
$$k_4 = (\eta_P + \varpi_P + \mu) I_{SP}, k_5 = (\eta_{PD} + \varpi_{PD} + \mu) I_{SPD}.$$

$$FV^{-1} = \begin{bmatrix} \beta_D\alpha_D S & \beta_D S & 0 & 0 & 0 \\ 0 & 0 & 0 & 0 & 0 \\ 0 & 0 & \beta_P\alpha_P S & \beta_P S & 0 \\ 0 & 0 & 0 & 0 & 0 \\ 0 & 0 & 0 & 0 & \beta_{DP} S \end{bmatrix} \times \begin{bmatrix} \frac{1}{k_1} & 0 & 0 & 0 & 0 \\ \frac{\phi_D}{k_1 k_2} & \frac{1}{k_2} & 0 & 0 & 0 \\ 0 & 0 & \frac{1}{k_3} & 0 & 0 \\ 0 & 0 & \frac{\phi_P}{k_3 k_4} & \frac{1}{k_4} & 0 \\ 0 & 0 & 0 & 0 & \frac{1}{k_5} \end{bmatrix}$$

The Gaussian Elimination method was used to determine V^{-1} and dominant eigenvalue of FV^{-1} is given by

$$R_0 = \rho FV^{-1} = \max\{R_{0D}, R_{0P}, R_{0DP}\}$$

$$R_0 = \max\left\{\frac{b(1-v)}{\mu}\left(\frac{\beta_D(\alpha_D k_2 + \phi_D)}{k_1 k_2}, \frac{\beta_P(\alpha_P k_4 + \phi_P)}{k_3 k_4}, \frac{\beta_{DP}}{k_5}\right)\right\}$$

where, $S = \frac{\kappa}{\mu} = \frac{b(1-v)}{\mu}$

3.3 Stability analysis

The stability analysis of the disease free equilibrium point is carried out.

3.3.1 Local stability analysis of DFEP

Theorem 4 The diseases free equilibrium point is locally asymptomatic stable if $R_0 < 1$ and unstable if $R_0 > 1$, *Proof.* Jacobian matrix of the model equation (2) estimated at the disease-free equilibrium which yields

$$J_{dfe} = \begin{bmatrix} -\mu & -\beta_D\alpha_D & -\beta_D & \beta_P\alpha_P & -\beta_P & -\beta_{DP} & 0 \\ 0 & \beta_D\alpha_D - k_1 & \beta_D & 0 & 0 & 0 & 0 \\ 0 & \phi_D & -k_2 & 0 & 0 & 0 & 0 \\ 0 & 0 & 0 & \beta_P\alpha_P - k_3 & \beta_P & 0 & 0 \\ 0 & 0 & 0 & \phi_D & -k_4 & 0 & 0 \\ 0 & 0 & 0 & 0 & 0 & \beta_{DP} - k_5 & 0 \\ 0 & 0 & \eta_D & 0 & \eta_P & \eta_{SDP} & -\mu \end{bmatrix} \quad (6)$$

Then characteristic equation is expanded and determined using $|J_{dfe} - \lambda I| = 0$, where $\lambda_1 = 0$ twice and solutions of the equations is given by the remaining 2×2 , 1×1 sub-matrices below $R_{0D} k_1 k_2 = \beta_D(\alpha_D k_2 + \phi_D)$,

$$J_{dfe} = \begin{bmatrix} (\beta_D\alpha_D - k_1) - \lambda & \beta_D \\ \phi_D & -k_2 - \lambda \end{bmatrix} = \lambda^2 + (k_1 + k_2 - \beta_D\alpha_D)\lambda + k_1 k_2(1 - R_{0D}) = 0$$

$R_{0P} k_3 k_4 = \beta_P(\alpha_P k_4 + \phi_P)$,

$$J_{dfe} = \begin{bmatrix} (\beta_P\alpha_P - k_3) - \lambda & \beta_P \\ \phi_D & -k_4 - \lambda \end{bmatrix} = \lambda^2 + (k_3 + k_4 - \beta_P\alpha_P)\lambda + k_3 k_4(1 - R_{0P}) = 0$$

$(\beta_{DP} - k_5) - \lambda = \lambda + k_5(1 - R_{0DP})$

Thus, by Routh-hurwitz Stability criteria, all the roots of equation (6) have negative real parts $\Leftrightarrow$ $R_{0D} < 1$, $R_{0P} < 1$ and $R_{0DP} < 1$ Respectively. Therefore the disease free equilibrium is Asymptotic stable if $R_0 = \max\{R_{0D}, R_{0P}, R_{0DP}\} < 0$.

3.3.2 Global stability analyses of DFEP and EEP

In this section, we will use Lyapunov function method to show the global asymptotic stability of DFE and EEP by the following theorems

Theorem 5 The pertussis-free equilibrium is globally asymptotically stable $\Leftrightarrow R_0 \leq 1$.

Proof. to prove that the pertussis-free equilibrium is globally asymptotically stable, we will employ the Lyapunov function method by [27] . Now we will Consider a Lyapunov function candidate,

$$V_{AD} = \frac{I_{AD}}{\phi_D + \xi_D + \mu}$$

Taking the time derivative of V_{AD}:

$$\frac{dV_{AD}}{dt} = \frac{1}{\phi_D + \xi_D + \mu}\frac{dI_{AD}}{dt}$$

Substituting the value of $\frac{dI_{AD}}{dt}$:

$$\frac{dV_{AD}}{dt} = \frac{(\beta_D\alpha_D S - (\phi_D + \xi_D + \mu))I_{AD}}{\phi_D + \xi_D + \mu}$$

$$\Rightarrow \frac{dV_{AD}}{dt} = \frac{\beta_D\alpha_D S}{\phi_D + \xi_D + \mu}I_{AD} - I_{AD}$$

$$\Rightarrow \frac{dV_{AD}}{dt} \leq \left(\frac{\beta_D\alpha_D S}{\phi_D + \xi_D + \mu} - 1\right) I_{AD}$$

$$\Rightarrow \frac{dV_{AD}}{dt} \leq \left(\frac{b(1-V)\beta_D\alpha_D}{\mu(\phi_D + \xi_D + \mu)} - 1\right) I_{AD}$$

$$\frac{dV_{AD}}{dt} \leq (R_{0AD} - 1)I_{AD}$$

The above analysis shows that $\frac{dV_{AD}}{dt} \leq 0 \Leftrightarrow R_{0AD} \leq 1$ and also, $\frac{dV_{AD}}{dt} = 0 \Leftrightarrow I_{AD} = 0$ or R_{0AD} Thus, the pertussis-free equilibrium is globally asymptotically stable if $R_{0AD} \leq 1$.

Theorem 6 The diphtheria-free equilibrium is globally asymptotically stable $\Leftrightarrow R_{0AP} \leq 1$.

Proof. to prove that the diphtheria-free equilibrium is globally asymptotically stable, we will employ the Lyapunov function method by [27]. Now we will Consider a Lyapunov function candidate,

$$V_{AP} = \frac{I_{AP}}{\phi_P + \xi_P + \mu}$$

Taking the time derivative of V_{AP}:

$$\frac{dV_{AP}}{dt} = \frac{1}{\phi_P + \xi_P + \mu}\frac{dI_{AP}}{dt}$$

Substituting the value of $\frac{dI_{AP}}{dt}$:

$$\frac{dV_{AP}}{dt} = \frac{(\beta_P\alpha_P S - (\phi_P + \xi_P + \mu))I_{AP}}{\phi_P + \xi_P + \mu}$$

$$\Rightarrow \frac{dV_{AP}}{dt} = \frac{\beta_P\alpha_P S}{\phi_P + \xi_P + \mu}I_{AP} - I_{AP}$$

$$\Rightarrow \frac{dV_{AP}}{dt} \leq \left(\frac{\beta_P\alpha_P S}{\phi_P + \xi_P + \mu} - 1\right) I_{AP}$$

$$\Rightarrow \frac{dV_{AP}}{dt} \leq \left(\frac{b(1-V)\beta_P\alpha_P}{\mu(\phi_P+\xi_P+\mu)} - 1\right) I_{AP}$$

$$\frac{dV_{AP}}{dt} \leq (R_{0AP} - 1)I_{AP}$$

The above analysis shows that $\frac{dV_{AP}}{dt} \leq 0 \Leftrightarrow R_{0AP} \leq 1$ and also, $\frac{dV_{AP}}{dt} = 0 \Leftrightarrow I_{AP} = 0$ or R_{0AP} Thus, the pertussis-free equilibrium is globally asymptotically stable if $R_{0AP} \leq 1$.

Theorem 7 The co-infection endemic equilibrium of the basic model equation (2) is globally asymptotically stable.$\Leftrightarrow R_{0AP} \leq 1$

Proof. Using the common quadratic Lyapunov function method as in [27] and Considering a Lyapunov function candidate,

$$G(S, I_{AD}, I_{SD}, I_{AP}, I_{SP}, I_{SDP}, Q, R) =$$
$$\tfrac{1}{2}[(S - S^*) + (I_{AD} - I^*_{AD}) + (I_{SD} - I^*_{SD}) + (I_{AP} - I^*_{AP})$$
$$+(I_{SP} - I^*_{SP}) + (I_{SDP} - I^*_{SDP}) + (Q_{SD} - Q^*_{SD}) + (R - R^*)]^2$$

The time derivative of the Lyapunov function (G) is given by

$$\frac{dG}{dt} = [(S - S^*) + (I_{AD} - I^*_{AD}) + (I_{SD} - I^*_{SD}) + (I_{AP} - I^*_{AP})$$
$$+(I_{SP} - I^*_{SP}) + (I_{SDP} - I^*_{SDP}) + (Q_{SD} - Q^*_{SD}) + (R - R^*)][\tfrac{dS}{dt} + \tfrac{dI_{AD}}{dt}$$
$$+\tfrac{dI_{SD}}{dt} + \tfrac{dI_{AP}}{dt} + \tfrac{dI_{SP}}{dt} + \tfrac{dI_{SDP}}{dt} + \tfrac{dQ_{SD}}{dt} + \tfrac{dR}{dt}]$$

$$\frac{dG}{dt} = [(S - S^*) + (I_{AD} - I^*_{AD}) + (I_{SD} - I^*_{SD}) + (I_{AP} - I^*_{AP})$$
$$+(I_{SP} - I^*_{SP}) + (I_{SDP} - I^*_{SDP}) + (Q_{SD} - Q^*_{SD})$$
$$+(R - R^*)][\kappa - \mu(S + I_{AD} + I_{SD} + I_{AP} + I_{SP} + I_{SDP} + R + Q_{SD})]$$

given that

$$\kappa = \mu(S + I_{AD} + I_{SD} + I_{AP} + I_{SP} + I_{SDP} + R + Q_{SD})$$

$$\frac{dG}{dt} = [(S - S^*) + (I_{AD} - I^*_{AD}) + (I_{SD} - I^*_{SD}) + (I_{AP} - I^*_{AP})$$
$$+(I_{SP} - I^*_{SP}) + (I_{SDP} - I^*_{SDP}) + (Q - Q)^*)$$
$$+(R - R)^*][\kappa - \mu(S - S^*) + (I_{AD} - I^*_{AD}) + (I_{SD} - I^*_{SD}) + (I_{AP} - I^*_{AP})$$
$$+(I_{SP} - I^*_{SP}) + (I_{SDP} - I^*_{SDP}) + (Q - Q^*) + (R - R^*))]$$
$$= -\mu[(S - S^*) + (I_{AD} - I^*_{AD}) + (I_{SD} - I^*_{SD}) + (I_{AP} - I^*_{AP})$$
$$+(I_{SP} - I^*_{SP}) + (I_{SDP} - I^*_{SDP}) + (Q_{SD} - Q^*_{SD}) + (R - R^*))]^2 \leq 0$$

Here, $\frac{dG}{dt} \leq 0$ Note also that $\frac{dG}{dt} = 0 \Leftrightarrow S = S^*, I_{AD} = I^*_{AD}, I_{SD} = I^*_{SD}, I_{AP} = I^*_{AP}, I_{SP} = I^*_{SP}, I_{SDP} = I^*_{SDP}, Q_{SD} - Q^*_{SD}, R - R^*$. It is seen that by the common quadratic Lyapunov method, the co-infection endemic equilibrium is globally asymptotically stable.

3.3.3 Backward bifurcation analysis

ver time, several researchers globally has accepted that reducing the reproduction number to less than one infectious person $R_0 < 1$ is necessary and sufficient to eradicate a disease. However, in recent times this perspective has been challenged by several mathematicians globally and to this effect, numerous theoretical studies has been done to show that this criterion might not always be enough or adequate. The backward bifurcation phenomenon provides an alternative explanation, since it demonstrates that under certain conditions, even when the Disease-Free Equilibrium is stable and the reproduction number is less than unity $R_0 < 1$, At that point, there might exist a stable endemic equilibrium coexisting simultaneously.

Our aim in this section is to adopt the Castillo Chavez and Song approach [28] to show the existence of backward bifurcation at $R = 1$. Now, replacing the state variables as shown bellow;

$$S = x_1, I_{AD} = x_2, I_{SD} = x_3, I_{AP} = x_4, I_{SP} = x_5, I_{SDP} = x_6, Q_{SD} = x_7, R = x_8$$

so that the total population becomes

$$N = x_1 + x_2 + x_3 + x_4 + x_5 + x_6 + x_7 + x_8$$

Then, equation (2) takes on the new form

$$\begin{aligned}
\frac{dx_1}{dt}(t) &\equiv f_1 = bN(1-V) + \xi_D x_2 + \xi_P x_4 \\
&\quad - \left(\frac{\beta_D(\alpha_D x_2 + x_3)}{N} + \frac{\beta_P(\alpha_P x_4 + x_5)}{N} + \frac{\beta_{DP} x_6}{N} \right) x_1 - \mu x_1 \\
\frac{dx_2}{dt}(t) &\equiv f_2 = \frac{\beta_D(\alpha_D x_2 + x_3)}{N} x_1 - (\phi_D + \xi_D + \mu) x_2 \\
\frac{dx_3}{dt}(t) &\equiv f_3 = \phi_D x_2 - (\theta + \eta_D + \varpi_D + \mu) x_3 - \gamma_1 \frac{\beta_P(\alpha_P x_4 + x_5)}{N} x_3 \\
\frac{dx_4}{dt}(t) &\equiv f_4 = \frac{\beta_P(\alpha_P x_4 + x_5)}{N} x_1 - (\phi_P + \xi_P + \mu) x_4 \\
\frac{dx_5}{dt}(t) &\equiv f_5 = \phi_P x_4 - (\eta_P + \varpi_P + \mu) x_5 - \gamma_2 \frac{\beta_D(\alpha_D x_2 + x_3)}{N} x_5 \\
\frac{dx_6}{dt}(t) &\equiv f_6 = \frac{\beta_{DP} x_6}{N} x_1 + \gamma_1 \frac{\beta_P(\alpha_P x_4 + x_5)}{N} x_3 \\
&\quad + \gamma_2 \frac{\beta_D(\alpha_D x_2 + x_3)}{N} x_5 - (\eta_{DP} + \xi_{DP} + \varpi_{DP} + \mu) x_6 \\
\frac{dx_7}{dt}(t) &\equiv f_7 = VbN + \eta_P I_{SP} + \eta_D x_3 + \eta_{DP} x_6 - \mu x_7
\end{aligned} \tag{7}$$

where,

$$N = \sum_{i=1}^{7} x_i$$

now lets consider a special case when the reproduction number $R_0 = max\{R_{0D}, R_{0P}, R_{0DP}\} = 1$ Also, we suppose that $\beta_D = \beta_D^*$ be chosen as a bifurcation coefficient. from $R_{0D} = 1$, then equation becomes

$$\Rightarrow \quad 1 = \frac{\beta_D(\alpha_D k_2 + \phi_D)}{k_1 k_2} \Rightarrow \quad \beta_D = \beta_D^* = \frac{k_1 k_2}{\alpha_D k_2 + \phi_D}$$

Now, taking the Jacobian matrix of the system of equations at the disease free equilibrium point E_{0D}, denoted by $J(E_{0D})$, which yields

$$J(E_{0D}) = \begin{bmatrix}
-\mu & -\beta_D\alpha_D & -\beta_D & -\beta_P\alpha_P & -\beta_P & 0 & 0 \\
0 & \beta_D\alpha_D - k_1 & \beta_D & 0 & 0 & 0 & 0 \\
0 & \phi_D & -k_2 & 0 & 0 & 0 & 0 \\
0 & 0 & 0 & \beta_P\alpha_P - k_3 & \beta_P & 0 & 0 \\
0 & 0 & 0 & \phi_D & -k_4 & 0 & 0 \\
0 & 0 & 0 & 0 & 0 & -k_5 & 0 \\
0 & 0 & \eta_D & 0 & \eta_P & \eta_{DP} & -\mu
\end{bmatrix}$$

before employing the assumptions in theorem 4.1 of [28], it is vital to note the two types of eigenvectors of the matrix $J(E_{0D})$ for the case $R_{0D} = 1$ of the system equation (7) at the selected $\beta_D = \beta_D^*$ which are the right and left eigenvectors linked with the zero eigenvalues of $J(E_{0D})$. given by $\psi = (\psi_1, \psi_2, \psi_3, \psi_4, \psi_5, \psi_6, \psi_7)^T$ are determined as

$$J(E_{0D}) \cdot \psi = 0$$

implies

$$\begin{bmatrix} -\mu & -\beta_D\alpha_D & -\beta_D & -\beta_P\alpha_P & -\beta_P & 0 & 0 \\ 0 & \beta_D\alpha_D - k_1 & \beta_D & 0 & 0 & 0 & 0 \\ 0 & \phi_D & -k_2 & 0 & 0 & 0 & 0 \\ 0 & 0 & 0 & \beta_P\alpha_P - k_3 & \beta_P & 0 & 0 \\ 0 & 0 & 0 & \phi_P & -k_4 & 0 & 0 \\ 0 & 0 & 0 & 0 & 0 & -k_5 & 0 \\ 0 & 0 & \eta_D & 0 & \eta_P & \eta_{DP} & -\mu \end{bmatrix} \times \begin{bmatrix} \psi_1 \\ \psi_2 \\ \psi_3 \\ \psi_4 \\ \psi_5 \\ \psi_6 \\ \psi_7 \end{bmatrix} = \begin{bmatrix} 0 \\ 0 \\ 0 \\ 0 \\ 0 \\ 0 \\ 0 \end{bmatrix}$$

$\Rightarrow$

In order to observe assumptions 2 in theorem 4.1 of [28], that is making the right eigenvector non-negative from the third equation, solving ψ_3 in terms of ψ_2 gives

$$\psi_3 = \frac{\phi_D\psi_2}{k_2}$$

Substituting ψ_3 above into the second equation $(\beta_D\alpha_D - k_1)\psi_2 + \beta_D\psi_3 = 0 \Rightarrow$

$$\psi_2 = (\beta_D\alpha_D - k_1)\psi_2 + \frac{\beta_D\phi_D\psi_2}{k_2} = (\beta_D\alpha_D - k_1 + \frac{\beta_D\phi_D}{k_2})\psi_2 = 0$$

for $\psi_2 \neq 0$, means that ψ_2 coefficient $(\beta_D\alpha_D - k_1 + \frac{\beta_D\phi_D}{k_2}) = 0$, so that $k_1 = (\beta_D\alpha_D + \frac{\beta_D\phi_D}{k_2})$. Now, in a non-trivial sense, we can say $\psi_2 = \psi_2 > 0$ since it does not necessarily make ψ_2 tend to zero. Therefore, in same vein, $\psi_3 = \frac{\phi_D\psi_2}{k_2} > 0$, $\psi_4 = \psi_4 > 0$, $\psi_5 = \frac{\phi_D\psi_4}{k_4} > 0, \psi_6 = 0$,

$$\nu \cdot J(E_{0D}) = 0$$

implies

$$\begin{bmatrix} \nu_1 \\ \nu_2 \\ \nu_3 \\ \nu_4 \\ \nu_5 \\ \nu_6 \\ \nu_7 \end{bmatrix}^T \times \begin{bmatrix} -\mu & -\beta_D\alpha_D & -\beta_D & -\beta_P\alpha_P & -\beta_P & 0 & 0 \\ 0 & \beta_D\alpha_D - k_1 & \beta_D & 0 & 0 & 0 & 0 \\ 0 & \phi_D & -k_2 & 0 & 0 & 0 & 0 \\ 0 & 0 & 0 & \beta_P\alpha_P - k_3 & \beta_P & 0 & 0 \\ 0 & 0 & 0 & \phi_P & -k_4 & 0 & 0 \\ 0 & 0 & 0 & 0 & 0 & -k_5 & 0 \\ 0 & 0 & \eta_D & 0 & \eta_P & \eta_{DP} & -\mu \end{bmatrix} = \begin{bmatrix} 0 \\ 0 \\ 0 \\ 0 \\ 0 \\ 0 \\ 0 \end{bmatrix}$$

Similarly, the left eigenvectors components of $J(E_{0D})|_{\beta=\beta^*}$, $\nu = (\nu_1, \nu_2, \nu_3, \nu_4, \nu_5, \nu_6, \nu_7)$ satisfying $\psi \cdot \nu = 1$ are: $\nu_2 = \nu_2 > 0$, $\nu_3 = \frac{\beta_D\nu_2}{k_2} > 0$, $\nu_4 = \nu_4 > 0$, $\nu_5 = \frac{\beta_P\nu_4}{k_4} > 0$, $\nu_6 = 0$,
Considering assumption 1 and 2 earlier cited in theorem 4.1 of [28], the sign of a and b in the equations below ensures whether the model undergoes forward or backward bifurcation.

$$a = \sum_{i,j,k=1}^{7} \nu_i\psi_j\psi_k \frac{\partial^2 f_i}{\partial x_j \partial x_k}(0,0) \quad \text{and} \quad b = \sum_{i,j,k=1}^{7} \nu_i\psi_j \frac{\partial^2 f_i}{\partial x_j \partial \beta_D^*}(0,0)$$

$$a = \nu_2 \sum_{i,j,k=1}^{7} \psi_j\psi_k \frac{\partial^2 f_1}{\partial x_j \partial x_k} + \nu_4 \sum_{i,j,k=1}^{7} \psi_j\psi_k \frac{\partial^2 f_1}{\partial x_j \partial x_k}$$

$$\frac{\partial^2 f_2}{\partial x_1 \partial x_2} = \frac{\partial^2 f_2}{\partial x_2 \partial x_1} = -\frac{\beta_D \alpha_D}{N}, \quad \frac{\partial^2 f_2}{\partial x_1 \partial x_3} = \frac{\partial^2 f_2}{\partial x_3 \partial x_1} = -\frac{\beta_D}{N},$$
$$\frac{\partial^2 f_4}{\partial x_1 \partial x_4} = \frac{\partial^2 f_4}{\partial x_4 \partial x_1} = -\frac{\beta_P \alpha_P}{N}, \quad \frac{\partial^2 f_4}{\partial x_1 \partial x_5} = \frac{\partial^2 f_4}{\partial x_5 \partial x_1} = -\frac{\beta_P}{N},$$
$$\frac{\partial^2 f_6}{\partial x_1 \partial x_6} = \frac{\partial^2 f_6}{\partial x_6 \partial x_1} = -\frac{\beta_{DP}}{N}, \quad \frac{\partial^2 f_3}{\partial x_3 \partial x_4} = \frac{\partial^2 f_3}{\partial x_4 \partial x_3} = -\gamma_1 \frac{\beta_P \alpha_P}{N},$$
$$\frac{\partial^2 f_3}{\partial x_3 \partial x_5} = \frac{\partial^2 f_3}{\partial x_5 \partial x_3} = -\gamma_1 \frac{\beta_P}{N}, \quad \frac{\partial^2 f_5}{\partial x_2 \partial x_5} = \frac{\partial^2 f_5}{\partial x_5 \partial x_2} = -\gamma_2 \frac{\beta_D \alpha_D}{N},$$
$$\frac{\partial^2 f_5}{\partial x_3 \partial x_5} = \frac{\partial^2 f_5}{\partial x_5 \partial x_3} = -\gamma_2 \frac{\beta_D}{N}.$$

$$= \nu_2\Big(\frac{\partial^2 f_2}{\partial x_1 \partial x_3} + \frac{\partial^2 f_2}{\partial x_3 \partial x_1}\Big) + \nu_4\Big(\frac{\partial^2 f_4}{\partial x_1 \partial x_5} + \frac{\partial^2 f_4}{\partial x_5 \partial x_1}\Big) + \nu_3\Big(\frac{\partial^2 f_3}{\partial x_3 \partial x_5} + \frac{\partial^2 f_3}{\partial x_5 \partial x_3}\Big) +$$
$$\nu_5\Big(\frac{\partial^2 f_5}{\partial x_3 \partial x_5} + \frac{\partial^2 f_5}{\partial x_5 \partial x_3}\Big) + \nu_6\Big(\frac{\partial^2 f_6}{\partial x_1 \partial x_6} + \frac{\partial^2 f_6}{\partial x_6 \partial x_1}\Big)$$
$$= -\nu_2\Big(\psi_1\psi_2\frac{\beta_D}{N} + \psi_2\psi_1\frac{\beta_D}{N}\Big) - \nu_4\Big(\psi_1\psi_5\frac{\beta_P}{N} + \psi_5\psi_1\frac{\beta_P}{N}\Big) - \nu_3\gamma_1\Big(\psi_3\psi_5\frac{\beta_P}{N} + \psi_5\psi_3\frac{\beta_P}{N}\Big) -$$
$$\nu_5\gamma_2\Big(\psi_3\psi_5\frac{\beta_D}{N} + \psi_5\psi_3\frac{\beta_D}{N}\Big) - \nu_6\Big(\psi_1\psi_6\frac{\beta_{DP}}{N} + \psi_6\psi_1\frac{\beta_{DP}}{N}\Big)$$

Substituting ψ yields

$$= -2\frac{\beta_D}{N}\nu_2\psi_1\psi_2 - 2\frac{\beta_P}{N}\nu_4\psi_5\psi_1 - 2\frac{\beta_P}{N}\nu_3\gamma_1\psi_3\psi_5 - 2\frac{\beta_D}{N}\nu_5\gamma_2\psi_3\psi_5 - 2\frac{\beta_{DP}}{N}\nu_6\psi_1\psi_6$$
$$a = 2\frac{\beta_D}{\mu N}\psi_2\psi_3\nu_2\Big(\beta_D(\alpha_D\psi_2 + \psi_3) + \beta_P(\alpha_P\psi_4 + \psi_5)\Big) - 2\frac{\phi_D\beta_P}{k_4\mu N}\nu_4\psi_4\Big(\beta_D(\alpha_D\psi_2 + \psi_3) + \beta_P(\alpha_P\psi_4 + \psi_5)\Big) \tag{8}$$

$$b = \sum_{i,j,k=1}^{n} \nu_i\psi_j\frac{\partial^2 f_i}{\partial x_j \partial \beta_D^*}(x_0, \beta_D^*) \quad = \nu_2\frac{\partial^2 f_2}{\partial x_1 \partial \beta_D^*} \quad = \nu_2(\alpha_D\psi_2 + \psi_3) > 0 \tag{9}$$

In accordance with theorem 4.1 of [28], based on the coefficients of a and b, the systems of equation (7) will undergo backward bifurcation.

3.3.4 Sensitivity analysis of the reproductive number

In this subsection, the normalized forward sensitivity index of R_0 will be used to pinpoint the strength and weakness of each parameter in the models prediction. Therefore, The Normalized forward sensitivity index of R_0 differentiable with respect to a given parameter β defined as [29]

$$\Upsilon_{\beta_D}^{R_0} = \frac{\beta}{R_0}\frac{\partial R_0}{\partial \beta_D}$$

where

$$R_0 = \frac{b(1-V)(\beta_D(\alpha_D(\theta + \eta_D + \varpi_D + \mu) + \phi_D))}{\mu(\phi_D + \xi_D + \mu)(\theta + \eta_D + \varpi_D + \mu)}$$

Manual calculation of the sensitivity to parameter β_D

$$\frac{\beta_D}{R_0} = \beta_D\frac{\mu(\phi_D + \xi_D + \mu)(\theta + \eta_D + \varpi_D + \mu)}{b(1-V)(\beta_D(\alpha_D(\theta + \eta_D + \varpi_D + \mu) + \phi_D))}$$

$$\frac{\partial R_0}{\partial \beta_D} = \frac{b(1-V)(\alpha_D(\theta + \eta_D + \varpi_D + \mu) + \phi_D)}{\mu(\phi_D + \xi_D + \mu)(\theta + \eta_D + \varpi_D + \mu)}$$

By substituting the values of the epidemiological parameters to the above equations will manually compute the sensitivity of β_D, other parameters can be calculated.

4 Numerical Simulations

In this section, Numerical simulation for diphtheria and pertussis co-infection model is performed, The dynamics of the various compartments in the population was observed. Firstly, The epidemiology parameters in Table 1 was substituted into the three terms of reproduction number derived. The Figure 2, Figure 3 and Figure 4 shows the effect of vaccination V and corresponding contact rates of Diphtheria β_D, Pertussis β_P and diphtheria-pertussis β_{DP} with contour plots respectively.

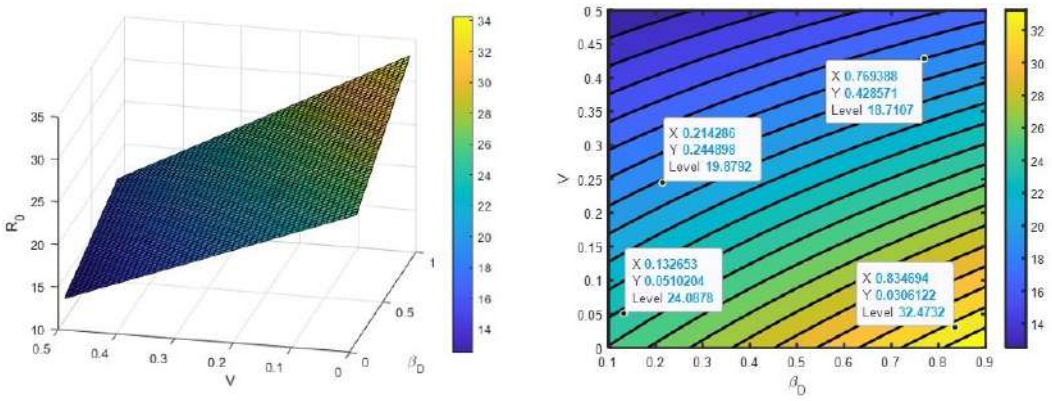


Figure 2: Effect of vaccination V and contact rate of diphtheria β_D on R_0 with contour plot.

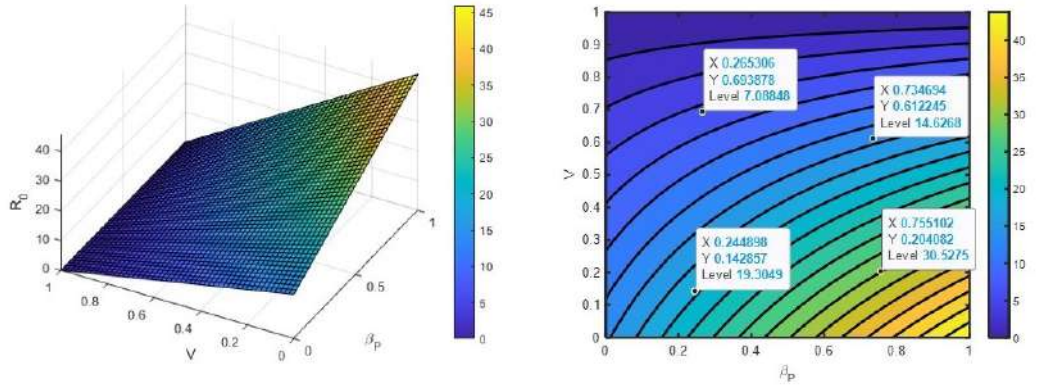


Figure 3: Effect of vaccination V and contact rate of pertussis β_P on R_0 with contour plot.

Furthermore, each parameter sensitivity in reproduction number was examined by varying the vaccination at birth V and quarantine of diphtheria θ as illustrated in the sensitivity bar chart Figure 6, Figure 7, Figure 8 and Figure 9. In Figure 8 We observed that When $V = 0.01$, and quarantine of individuals infected with diphtheria $\theta = 0$ arranging the parameter as regards its magnitude in descending order is $b = 1.0$, $\varpi_D = 0.59155$, $V = 0.5263$, $\beta_P = 0.414355$, $\beta_D = 0.363102$, $\beta_{DP} = 0.3150$, $\phi_P = 0.2524$, $\varpi_P = -0.206208$, $\xi_P = 0.191831$, $\xi_D = 0.168103$, $\eta_P = 0.167155$, $\phi_D = 0.139104$, $\eta_D = -0.0903332$, $\alpha_D = 0.0318801$, $\alpha_P = 0.027965$, $\varpi_D = -0.0215079$

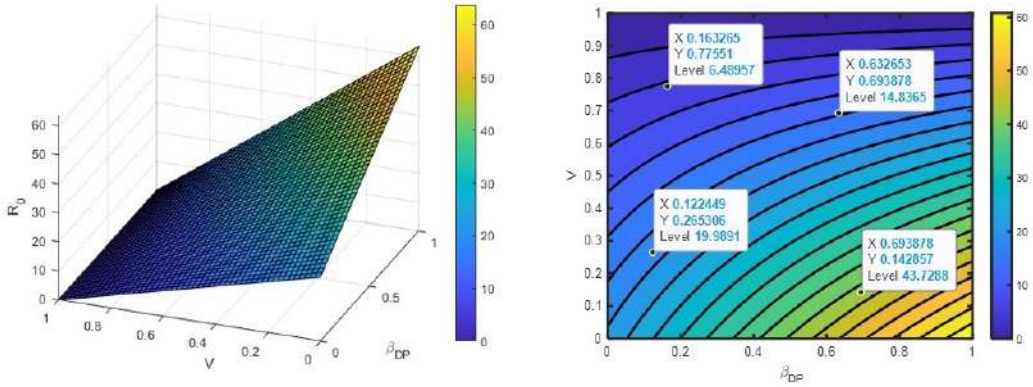
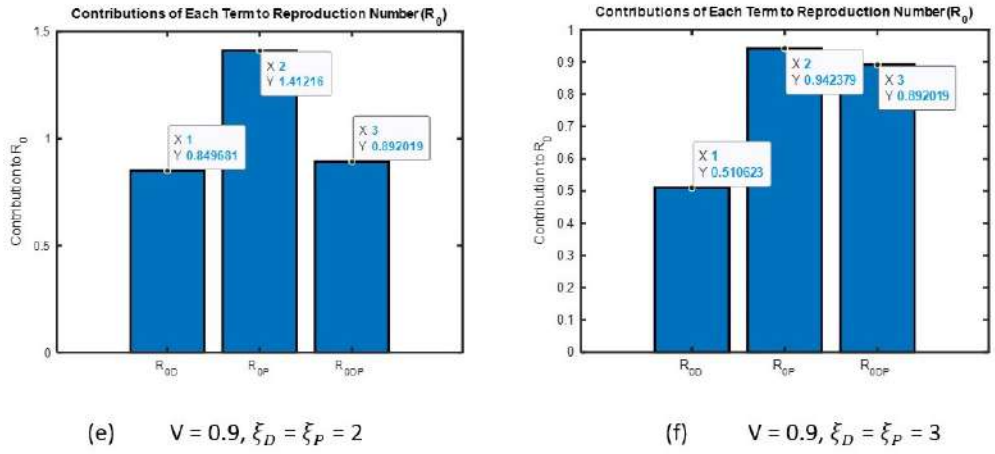
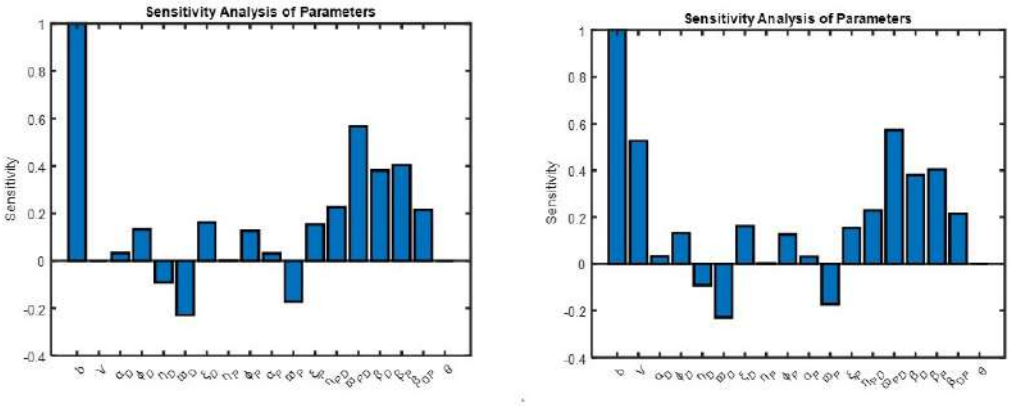


Figure 4: Effect of vaccination V and contact rate of pertussis β_{DP} on R_0 with contour plot.



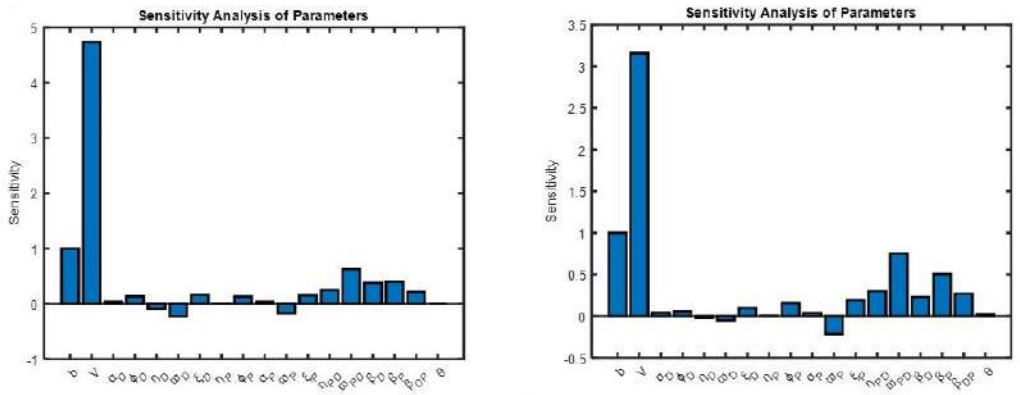
(e) V = 0.9, $\xi_D = \xi_P = 2$ (f) V = 0.9, $\xi_D = \xi_P = 3$

Figure 5: Bar chart showing Effect of Vaccination at Birth V with improved Maternally derived immunity on the three terms of R_0.



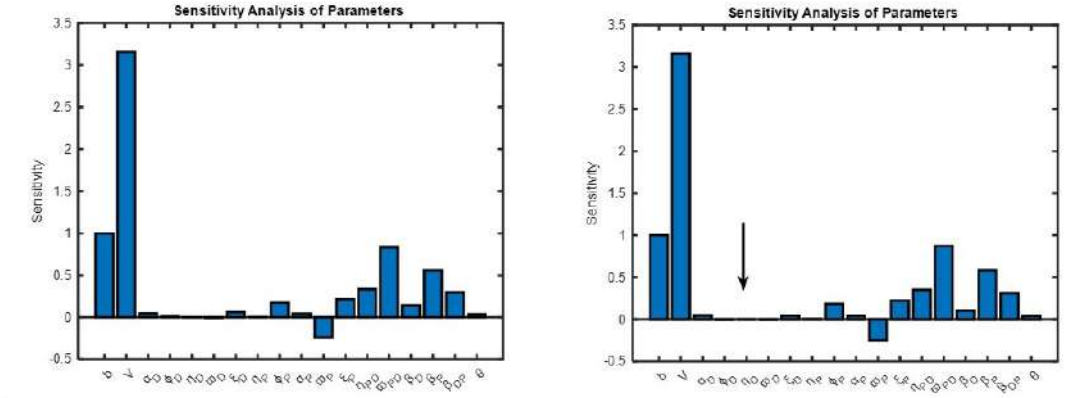
(a) V = θ = 0 (b) V = 0.01, θ = 0

Figure 6: Bar chart showing Effect of Vaccination at Birth V with improved Maternally derived immunity on the three terms of R_0.



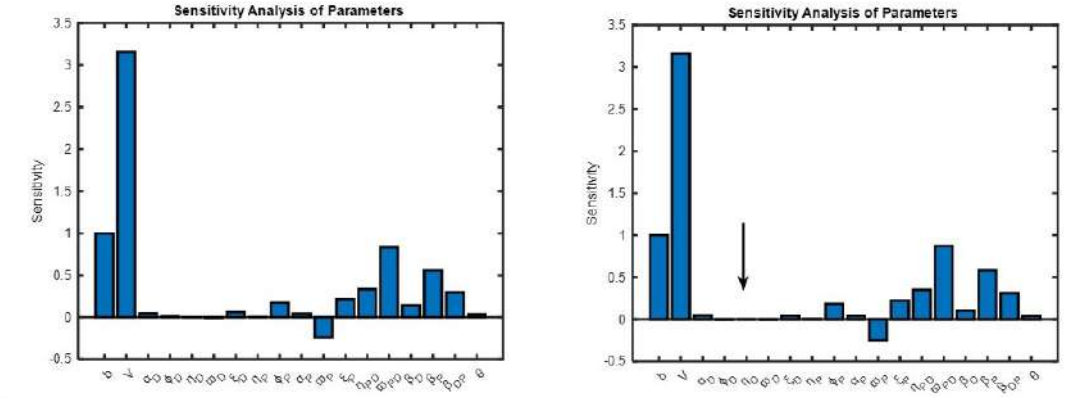
(c) V = 0.09, θ = 0 (d) V = 0.06, θ = 0.1

Figure 7: Impact of parameters on R_0 with vaccination and zero partial quarantine of diphtheria-pertussis model.



(e) V = 0.06, θ =0.3 (f) V = 0.06, θ = 0.6

Figure 8: Impact of parameters on R_0 with vaccination and partial quarantine of diphtheria.



(e) V = 0.06, θ =0.3 (f) V = 0.06, θ = 0.6

Figure 9: Impact of improved vaccination, partial quarantine and maternal derived immunity parameters on R_0.

In the quest to obtain the best disease mitigating parameter for the non-optimal control strategy, a combination of disease controller was explored by varying there values in $(S, I_{AD}, I_{SD}, I_{AP}, I_{SP}, I_{SDP}, Q_{SD}, R)$

model. The initial size of the total population at time $t = 0$ day was $N(0) = 1000$, $S(0) = 900$, $I_{AD0} = 10$, $I_{SD0} = 5$, $I_{AP0} = 15$, $I_{SP0} = 20$, $I_{SDP0} = 25$, $Q = 0$, and $R = 20$ that is $(900, 10, 5, 15, 20, 25, 0, 20)$. The graphical experiment performed on the model dynamics at the initial instance of outbreak using table parameter without disease controller in Figure 10 shows that after $t = 100$ days the model reads $(176, 29, 103, 10, 44, 19, 0, 211)$. The model was also examined by increasing vaccination at birth, Figure 10 and Figure 11 indicates that when $V = 0.6$ and $\xi_D = \xi_P = \theta = 0$ the model compartments is approximately $(120, 12, 52, 0, 18, 4, 0, 992)$ after 100 days, . At a high vaccination administration $V = 0.9$, the model compartments approximately reads $(63, 0, 14, 0, 3, 0, 0, 1374)$.

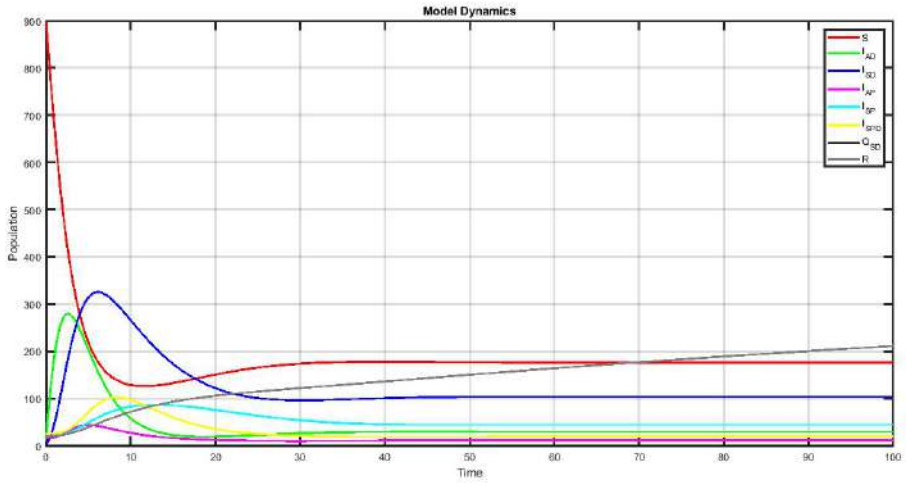


Figure 10: Zero Vaccination on $(S, I_{AD}, I_{SD}, I_{AP}, I_{SP}, I_{SDP}, Q_{SD}, R)$ Model.

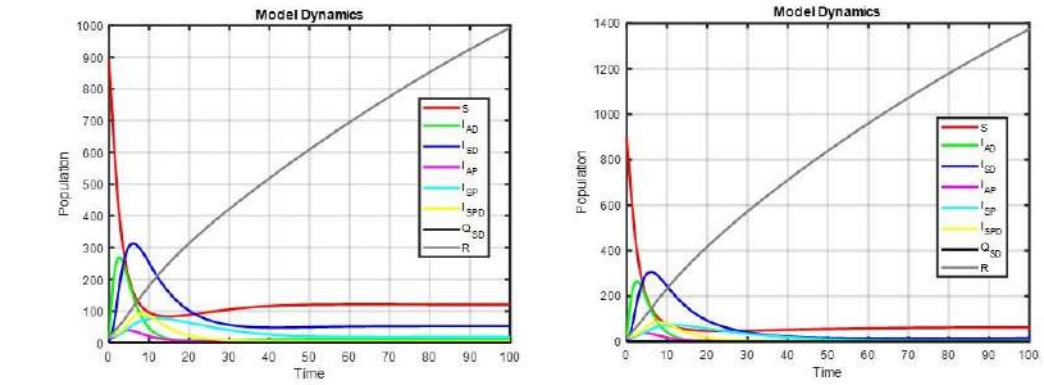
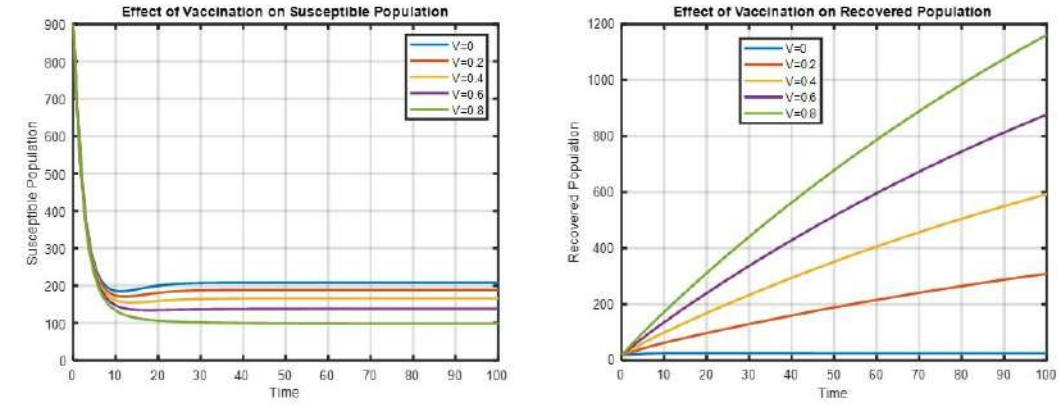
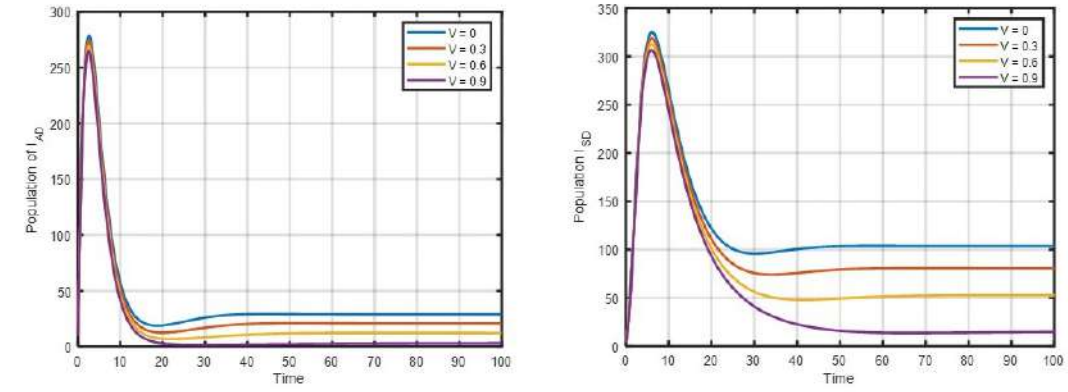


Figure 11: Varying Vaccination impact on $(S, I_{AD}, I_{SD}, I_{AP}, I_{SP}, I_{SDP}, Q_{SD}, R)$ Model.



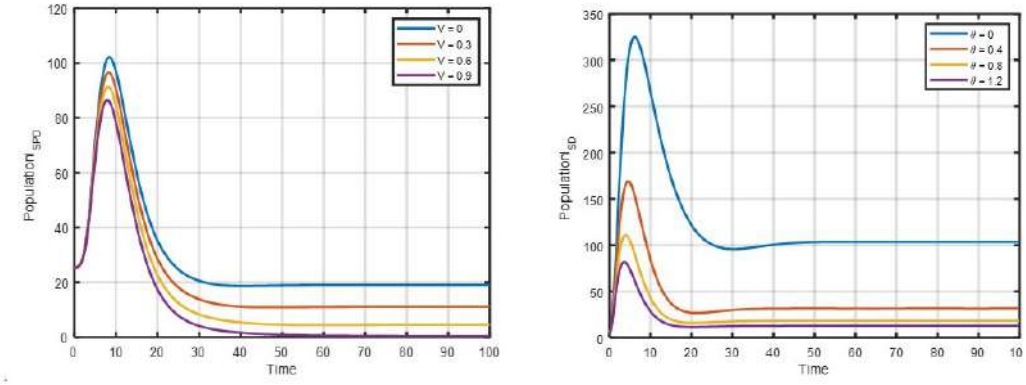
(a) varying vaccine effectiveness on S (b) varying vaccine effectiveness on R

Figure 12: Varying Vaccination effect on Susceptible and Recovered compartment.



(c) varying vaccine effectiveness on I_{AD} (d) varying vaccine effectiveness on I_{SD}

Figure 13: Varying Vaccination effect on Symptomatic and Asymptomatic infectious individuals with Diphtheria.



(e) Partial varying vaccine effectiveness on I_{SDP} (f) varying quarantine effectiveness on I_{SD}

Figure 14: Varying Vaccination on symptomatically infected with diphtheria-pertussis and varying quarantine effect on Symptomatic infectious individuals with Diphtheria.

5 Discussion of results and conclusion

The theoretical results suggest that the $(S, I_{AD}, I_{SD}, I_{AP}, I_{SP}, I_{SDP}, Q_{SD}, R)$ model is both epidemiological and mathematically well-posed. The 3D graphical and contour plots show that increasing vaccination reduces the value of R_0. Furthermore, to emphasize the effectiveness of disease control measures, a bar chart was used to assess the impact of control reinforcement strategies. The findings indicate that combining control measures significantly reduces R_0.

A sensitivity analysis was conducted to identify the most influential parameter in R_0. When $V = 0.06$ and $\theta = 0.6$, the parameters arranged in descending order of influence are: V, ϖ_D, b, θ, β_P, ξ_P, ϕ_P, η_{DP}, β_{DP}, β_D, ξ_D, α_D, θ, α_P, η_P, ϕ_D, η_D, ϖ_D, ϖ_P. Additionally, the impact of disease control measures on each compartment in the model demonstrates that increasing vaccination rates significantly mitigates disease spread.

The model also shows backward bifurcation under certain conditions, Therefore, optimal control strategies should be explored in future research to effectively reduce multiple stable equilibria and control the disease dynamics.

References

[1] Khatiwada, A. P., Shrestha, N., and Shrestha, S. (2021). Will COVID-19 lead to a resurgence of vaccine-preventable diseases?.Infection and Drug Resistance, 119-124.

[2] Agüero, M. L., Castillo, J. B. D., Falleiros-Arlant, L. H., Berezín, E., de Moraes, J. C., Torres-Martínez, C., ... and López-Medina, E. (2023). Risks of low vaccination coverage and strategies to prevent the resurgence of vaccine-preventable diseases in infants in the COVID-19 pandemic scenario: recommendations for Latin America and the Caribbean by the group of experts on infant immunization for Latin America. Expert Review of Vaccines, 22(1), 1091-1101.

[3] Organization, W.H.: COVID-19 Pandemic Fuels Largest Continued Backslide in Vaccinations in Three Decades, https://www.who.int/news/item/15-07-2022- covid-19-pandemic-fuels-largest-continued-backslide-in-vaccinations-in-three decades. Accessed: 2024-05-26 (2022).

[4] Gouveia, N., and Fletcher, T. (2000). Respiratory diseases in children and outdoor air pollution in Sao Paulo, Brazil: a time series analysis. Occupational and environmental medicine, 57(7), 477-483.

[5] Clay, P. A., Duffy, M. A., and Rudolf, V. H. (2020). Within-host priority effects and epidemic timing determine outbreak severity in co-infected populations. Proceedings of the Royal Society B, 287(1922), 20200046.

[6] Cox, F. E. G. (2001). Concomitant infections, parasites and immune responses. Parasitology, 122(S1), S23-S38.

[7] Glidden, Caroline K., Courtney AC Coon, Brianna R. Beechler, Chase McNulty, Vanessa O. Ezenwa, and Anna E. Jolles. "Co-infection best predicts respiratory viral infection in a wild host." Journal of Animal Ecology 90, no. 3 (2021): 602-614.

[8] Griffiths, E. C., Pedersen, A. B., Fenton, A., and Petchey, O. L. (2011). The nature and consequences of coinfection in humans. Journal of Infection, 63(3), 200-206.

[9] Liang, J. L. (2018). Prevention of pertussis, tetanus, and diphtheria with vaccines in the United States: recommendations of the Advisory Committee on Immunization Practices (ACIP). Recommendations and reports, 67.

[10] Murphy, T. V., Slade, B. A., Broder, K. R., Kretsinger, K., Tiwari, T., Joyce, M. P., ... and Moran, J. S. (2008). Prevention of pertussis, tetanus, and diphtheria among pregnant and postpartum women and their infants. Recomm Rep, 57,1-51.

[11] Kuchar, E., Karlikowska-Skwarnik, M., Han, S., and Nitsch-Osuch, A. (2016). Pertussis: history of the disease and current prevention failure. Pulmonary dysfunction and disease, 77-82.

[12] Sadoh, A. E., and Oladokun, R. E. (2012). Re-emergence of diphtheria and pertussis: implications for Nigeria.Vaccine, 30(50), 7221-7228.

[13] Calderón, T. A., Coffin, S. E., and Sammons, J. S. (2015). Preventing the spread of pertussis in pediatric healthcare settings. Journal of the Pediatric Infectious Diseases Society, 4(3), 252-259.

[14] Brooks, D. A., and Clover, R. (2006). Pertussis infection in the United States: role for vaccination of adolescents and adults. The Journal of the American Board of Family Medicine, 19(6), 603-611.

[15] Yakubu, A. A., Abdullah, F. A., and Yatim, Y. M. (2022). Mathematical Model of Pertussis and Pneumonia Co-Infection in Infants with Maternally Derived Immunity. Sains Malaysiana, 51(7), 2197-2209.

[16] Teklu, S. W., and Mekonnen, T. T. (2021). HIV/AIDS-Pneumonia Coinfection Model with Treatment at Each Infection Stage: Mathematical Analysis and Numerical Simulation. Journal of Applied Mathematics, 2021(1), 5444605.

[17] Pérez, A. G. C., and Oluyori, D. A. (2022). A model for COVID-19 and bacterial pneumonia coinfection with community-and hospital-acquired infections. Mathematical Modelling and Numerical Simulation with Applications, 2(4), 197-210.

[18] Tilahun, G. T. (2019). Optimal control analysis of pneumonia and meningitis coinfection. Computational and Mathematical Methods in Medicine, 2019(1), 2658971.

[19] Omame, A., and Abbas, M. (2023). Modeling SARS-CoV-2 and HBV co-dynamics with optimal control. Physica A: Statistical Mechanics and its Applications, 615, 128607.

[20] Johnson, O. S., Edogbanya, H. O., Emmanuel, J., and Olukanni, S. E. (2023). Stability Analysis of COVID-19 Model with Quarantine. International Journal of Mathematical Sciences and Computing, 9(3), 26-45.

[21] Deressa, C.T., Mussa, Y. O., and Duressa, G. F. (2020). Optimal control and sensitivity analysis for transmission dynamics of Coronavirus. Results in Physics, 19, 103642.

[22] Kanchanarat, S., Chinviriyasit, S., and Chinviriyasit, W. (2022). Mathematical assessment of the impact of the imperfect vaccination on diphtheria transmission dynamics. Symmetry, 14(10), 2000.

[23] Izzati, N., and Andriani, A. (2021, April). Dynamical analysis of diphtheria epidemic model with natural immunity rate on exposed individuals. In Journal of Physics: Conference Series (Vol. 1869, No. 1, p. 012117). IOP Publishing.

[24] Burrell, C. J., Howard, C. R., and Murphy, F. A. (2016). Fenner and White's medical virology. Academic Press.

[25] Diekmann, O., Heesterbeek, J. A. P., and Metz, J. A. J. (1990). On the definition and the computation of the basic reproduction ratio R 0 in models for infectious diseases in heterogeneous populations. Journal of mathematical biology, 28, 365-382.

[26] Siddik, S. B. M., Abdullah, F. A., and Ismail, A. I. M. (2020). Mathematical Model of Dengue Virus with Predator-Prey Interactions. Malaysiana, 49(5), 1191-1200.

[27] Vargas-De-León, C. (2009). Constructions of Lyapunov functions for classic SIS, SIR and SIRS epidemic models with variable population size. Foro-Red-Mat: Revista electrónica de contenido matemático, 26(5), 1-12.

[28] Castillo-Chavez, C., and Song, B. (2004). Dynamical models of tuberculosis and their applications. Mathematical Biosciences amd Engineering, 1(2), 361-404.

[29] Johnson, O. S., Edogbanya, H. O., Wakili, A., and John, A. T. (2024). Diphtheria Disease Transmission Dynamics In Low Vaccine Coverage Setting. International Journal of Mathematical Sciences and Optimization: Theory and Applications, 10(2), 79-106.

[30] Edogbanya, H. O., Oladipupo, J. (2024). Mathematical Modeling for Mitigating Pertussis Resurgence in the Post-COVID-19 Era: A Sensitivity Analysis and Intervention Strategies.Federal University Lokoja. DOI: 10.5281/zenodo.10721146

On Lojid Algebras

E. Ilojide*

Abstract

In this paper, lojid algebras are introduced. Properties of classes of lojid algebras are investigated. Associates, commutants and regular maps are introduced and studied. Furthermore, congruences are introduced as a build up to the establishment of quotient lojid algebras.

Keywords and phrases: Lojid algebras, commutants, congruences, translations.

1 Introduction

An algebra of type (2, 0) is a non-empty set, having a constant element, on which is defined a binary operation such that certain axioms are satisfied. BCI algebras and BCK algebras, introduced in [1] and [2], are common varieties of such algebras. There are several other varieties of algebras of type (2, 0). There are also several generalizations of BCI algebras. In [3], BCH algebras were studied. In [4], d algebras were studied. In [5], the notion of BE algebras was introduced. Ideals and upper sets in BE algebras were investigated in [6] and [7]. Pre- commutative algebras were studied in [8]. Fenyves algebras were studied in [9], [10] and [11]. In [12], Q algebras were introduced. Homomorphisms of Q algebras were studied in [13].
Recently, it has been shown in [14], that algebras of type (2,0) have diverse applications in coding theory. Motivated by this, more research interest has been given to the study of algebras of type (2,0). Obic algebras were introduced in [15]. In [16], torian algebras were studied. It was shown that the class of torian algebras is a wider class than the class of obic algebras. Ideals of torian algebras were investigated in [17]. The dual and nuclei of ideals as well as congruences developed on ideals of torian algebras were studied. In [18], right distributive torian algebras were studied. Isomorphism Theorems of torian algebras were studied in [19].
In this paper, lojid algebras are introduced. Properties of classes of lojid algebras are investigated. Associates, commutants and regular maps are introduced and studied. Furthermore, congruences are introduced as a build up to the establishment of quotient lojid algebras.

2 Lojid algebras

In this section, we introduce semi-lojid algebras as a prelude to the introduction of lojid algebras. Thereafter, lojid algebras are introduced. We also establish some properties of lojid algebras. Furthermore, we show that given a lojid algebra, there exist two other lojid algebras which are derived from it by obtaining two binary operations which are induced by the binary operation of the classical lojid algebra.

Definition 2.1. *An algebra* $(X; *, 0)$ *of type (2, 0) is called a semi-lojid algebra if* $x * 0 = x$ *for all* $x \in X$.

*E-mail: ilojidee@funaab.edu.ng; Department of Mathematics, Federal University of Agriculture, Abeokuta, Nigeria

Example 2.2. Let $X = \{0, 1, 2, 3\}$. Define a binary operation $*$ on X by the following table:

$*$	0	1	2	3
0	0	2	3	1
1	1	0	2	2
2	2	3	0	3
3	3	1	1	0

Then $(X; *, 0)$ is a semi-lojid algebra.

Definition 2.3. *Let a be an element of a semi-lojid algebra $(X; *, 0)$. The mapping $L_a : X \to X$ given by $L_a(x) = a * x$ for all $x \in X$, is called a left translation on $(X; *, 0)$.*
Similarly, the mapping $R_a : X \to X$ given by $R_a(x) = x * a$ for all $x \in X$, is called a right translation on $(X; *, 0)$.

We shall write xL_a instead of $L_a(x)$ and xR_a instead of $R_a(x)$.

Remark 2.4. We are interested in semi-lojid algebras in which all the left and right translations are bijections.

Notice that not all the left and right translations in the semi-lojid algebra in Example 2.1. are bijections. We therefore have the following definition:

Definition 2.5. *A semi-lojid algebra $(X; *, 0)$ is called a lojid algebra if all its left and right translations are bijections.*

Example 2.6. Let $X = \{0, 1, 2, 3, 4\}$. Define a binary operation $*$ on X by the following table:

$*$	0	1	2	3	4
0	0	1	3	4	2
1	1	0	4	2	3
2	2	4	1	3	0
3	3	2	0	1	4
4	4	3	2	0	1

Then $(X; *, 0)$ is a lojid algebra.

Example 2.7. Let $X = \{0, 1, 2, 3\}$. Define a binary operation $*$ on X by the following table:

$*$	0	1	2	3
0	0	1	2	3
1	1	0	3	2
2	2	3	0	1
3	3	2	1	0

Then $(X; *, 0)$ is a lojid algebra.

We shall write X for a lojid algebra $(X; *, 0)$ unless there is the need to emphasize the binary operation and the constant element of $(X; *, 0)$.

Definition 2.8. *A lojid algebra X is said to be completely lojid if $xR_x = 0$ for all $x \in X$.*

Example 2.9. The algebra in Example 2.3. is a completely lojid algebra.

Definition 2.10. *Let $(X; *, 0)$ be a lojid algebra. A non-empty subset S of X is called a sub-lojid algebra (or simply a sub-algebra) of $(X; *, 0)$ if $(S; *, 0)$ is a lojid algebra.*

Proposition 2.11. *Let X be a lojid algebra. A subset S (with $0 \in S$) of X is a sub algebra of X if and only if the following hold:*

1. *for any $a, b \in S$, there exists a unique $c \in S$ such that $a * c = b$.*
2. *for any $a, b \in S$, there exists a unique $d \in S$ such that $d * a = b$.*

Proof. Suppose S is a sub-algebra of X. Then S is a lojid algebra, and clearly, items (1) and (2) of the proposition hold.
Conversely, suppose items (1) and (2) hold in S. This implies that the left and right translations for each $a \in S$ are bijections. Hence, S is a lojid algebra.

Corollary 2.12. *A non-empty subset S of a completely lojid algebra X is a sub-algebra of X if and only if the following hold:*

1. *for any $a, b \in S$, there exists a unique $c \in S$ such that $a * c = b$.*
2. *for any $a, b \in S$, there exists a unique $d \in S$ such that $d * a = b$.*

Proof. The proof follows from Proposition 2.1 since if $x \in S$, then $x * x = 0 \in S$.

Definition 2.13. *Let $(X;*,0)$ be a lojid algebra. Define two new binary operations $\vee$ and $\wedge$ on X as follows:*
$x \vee y = yL_x^{-1}$ *and* $x \wedge y = xR_y^{-1}$ *for all* $x, y \in X$.

Notice that $x \vee y = z \Leftrightarrow x * z = y$ and $x \wedge y = z \Leftrightarrow z * y = x$ for all $x, y, z \in X$.
Hence, we have the following Lemma:

Lemma 2.14. *Let $(X;*,0)$ be a lojid algebra. Then $(X;\vee,0)$ and $(X;\wedge,0)$ are lojid algebras.*

Proposition 2.15. *Let $(X;*,0)$ be a lojid algebra. Then the following hold for all $x, y \in X$:*

1. $x * (x \vee y) = y$
2. $(y \wedge x) * x = y$
3. $x \vee (x * y) = y$
4. $(y * x) \wedge x = y$
5. $x * (x \vee y) = (y \wedge x) * x$
6. $x * (x \vee y) = x \vee (x * y)$
7. $x * (x \vee y) = (y * x) \wedge x$
8. $(y \wedge x) * x = x \vee (x * y)$
9. $(y \wedge x) * x = (y * x) \wedge x$
10. $x \vee (x * y) = (y * x) \wedge x$

Proof.

1. Notice that $x * (x \vee y) = x(yL_x^{-1}) = y$
2. Notice that $(y \wedge x) * x = (yR_x^{-1})x = y$
3. notice that $x \vee (x * y) = (x * y)L_x^{-1} = y$
4. Notice that $(y * x) \wedge x = (y * x)R_x^{-1} = y$
5. Follows from (1) and (2)
6. Follows from (1) and (3)
7. Follows from (1) and (4)
8. Follows from (2) and (3)
9. Follows from (2) and (4)
10. Follows from (3) and (4)

Theorem 2.16. *A subset S (with $0 \in S$) of a lojid algebra X is a sub-algebra of X if and only if $x * y,\ x \vee y,\ x \wedge S$ for all $x, y \in S$.*

Proof. Suppose $x * y,\ x \vee y,\ x \wedge S$ for all $x, y \in S$. Let $x, y \in S$. Then there exists a unique $z \in X$ such that $x * z = y$. This implies that $z = x \vee y$. So, $z \in S$. Since X is a lojid algebra, it follows that z is unique in S. Similar argument shows that there exists a unique $p \in S$ such that $p * x = y$. Hence, S is a lojid algebra.
The converse follows from Lemma 2.1. and Proposition 2.2.

Corollary 2.17. *A non-empty subset S of a completely lojid algebra X is a sub-algebra of X if and only if $x * y,\ x \vee y,\ x \wedge S$ for all $x, y \in S$.*

Proof. Clearly, $0 \in S$ since if $x \in X$, then $x * x = 0 \in S$. The result follows therefore from Proposition 2.2. and Theorem 2.1.

3 Associates and Commutants

Definition 3.1. *Let X be a lojid algebra. An element $a \in X$ is said to be left-associative (respectively right-associative, centre-associative) if $xL_aR_y = xR_yL_a$ (respectively $xR_aL_y = xL_yR_a$, $aL_xR_y = aR_yL_x$) for all $x, y \in X$.*

Let X be a lojid algebra. The collection of all left-associative (respectively right-associative, centre-associative) elements of X is denoted by $Ass_L(X)$ (respectively $Ass_R(X), Ass_C(X)$).
Notice that $0 \in Ass_R(X)$ for every lojid algebra X.

Definition 3.2. *A lojid algebra X is said to be bounded if $xL_0 = x$ for all $x \in X$.*

The following Lemma is straightforward from definition.

Lemma 3.3. *Let X be a bounded lojid algebra. Then $0 \in Ass_L(X) \bigcap Ass_C(X)$.*

Theorem 3.4. *Let $(X; *, 0)$ be a lojid algebra. Then $(Ass_R(X), *)$ is a groupoid.*

Proof. Clearly, $0 \in Ass_R(X)$. We show that $Ass_R(X)$ is closed with respect to $*$. Now, let $a, b \in Ass_R(X)$ and let $x, y \in X$. Then $xR_{(a*b)}L_y = y * (x * (a * b)) = y * ((x * a) * b) = (y * (x * a)) * b = ((y * x) * a) * b = (y * x) * (a * b) = xL_yR_{(a*b)}$. So, $Ass_R(X)$ is closed with respect to $*$ as required.

Theorem 3.5. *Let $(X; *, 0)$ be a bounded lojid algebra. Then $(Ass_L(X), *)$ and $(Ass_C(X), *)$ are groupoids.*

Proof. By Lemma 3.1, $0 \in Ass_L(X)$. Now, let $a, b \in Ass_L(X)$ and let $x, y \in X$. Then $xL_{(a*b)}R_y = ((a*b)*x)*y = (a*(b*x))*y = a*((b*x)*y) = a*(b*(x*y)) = (a*b)*(x*y) = xR_yL_{(a*b)}$ as required.
Similar argument shows that $(Ass_C(X), *)$ is a groupoid.

Definition 3.6. *Let X be a lojid algebra. An element $a \in X$ is called an associative element if $a \in Ass_R(X) \bigcap Ass_L(X) \bigcap (Ass_C(X)$.*

The collection of all associative elements of X is called the associate of X. It is denoted by $Ass(X)$. Combining Theorem 3.1. and Theorem 3.2., we have the following Theorem:

Theorem 3.7. *Let X be a bounded lojid algebra. Then $Ass(X)$ is a groupoid.*

Definition 3.8. *Let X be a lojid algebra. An element $a \in Ass(X)$ is called a commutative element if $aR_x = aL_x$ for all $x \in X$.*

The collection of all commutative elements of X is called the commutant of X. It is denoted by $Cmm(X)$.

Let a be an element of a lojid algebra X. Since L_a and R_a are bijections, they belong to the symmetric group $S(X)$ of all permutations of the set X. Now, consider the following sets:
$L(X) = \{L_a, L_a^{-1} : a \in X\}$,
$R(X) = \{R_a, R_a^{-1} : a \in X\}$ and
$T(X) = \{L_a, R_a, L_a^{-1}, R_a^{-1} : a \in X\}$.
The collection of permutations of X which are members of $L(X)$ (respectively $R(X), T(X)$) forms a subgroup of $S(X)$ called the left (respectively right, centre) group of $S(X)$. They are denoted by $L_S(X), R_S(X)$ and $T_S(X)$ respectively.

Theorem 3.9. *Let X be a bounded lojid algebra. Then $Cmm(X)$ is isomorphic to $C(T_S(X))$; where $C(T_S(X))$ is the centre of $T_S(X)$*

Proof. Let $z \in Cmm(X)$. Then we have $L_z R_y = R_y L_z,\ R_z L_y = L_y R_z$ and $L_z = R_z$ for all $y, z \in X$. So, $R_z \in C(T_S(X))$. We show that the mapping $\phi : Cmm(X) \to C(T_S(X))$ defined by $\phi(z) = R_z$ for all $z \in Cmm(X)$, is a homomorphism. Let $z_1, z_2 \in Cmm(X)$. Then $\phi(z_1 * z_2) = R_{(z_1 * z_z)}$ since $xR_{z_1}R_{z_2} = (x * z_1) * z_2 = x * (z_1 * z_2) = xR_{(z_1 * z_2)}$ for all $x \in X$. Clearly, ϕ is bijective and hence an isomorphism.
Similar argument shows that the mapping $\eta : Cmm(X) \to C(T_S(X))$ defined by $\eta(z) = L_z$ for all $z \in Cmm(X)$, is an isomorphism.

Definition 3.10. *Let X be a lojid algebra. A mapping $\alpha \in T_S(X)$ is said to be regular if $\alpha(0) = 0$.*

The collection of all regular mappings on a lojid algebra X is denoted by $D(X)$.

Proposition 3.11. *Let X be bounded lojid algebra. Then the set $P = \{R_{(x,y)}, L_{(x,y)}, T_{(x)}\}$ is contained in $D(X)$; where $R_{(x,y)} = R_x R_y R^{-1}_{(x*y)},\ L_{(x,y)} = L_x L_y L^{-1}_{(y*x)}$ and $T_{(x)} = R_x L_x^{-1}$ for all $x, y \in X$.*

Proof. Notice that $0R_{(x,y)} = 0R_{(x*y)}R^{-1}_{(x*y)} = 0$.
Similar argument shows that $L_{(x*y)}$ and $T_{(x)}$ are regular.
We now pose an Open Problem:
Does the set P in Proposition 3.1 account for all the regular mappings on a bounded lojid algebra?

4 Variants of Invertibility

It is known that the notion of invertibility of elements in an algebraic structure is only meaningful if the structure has an identity element. Although lojid algebras do not have identity elements, in this section, we discuss some variants of invertibility of elements in lojid algebras.
Henceforth, we shall write xy for $x * y$ whenever x, y are elements of a lojid algebra $(X; *, 0)$.

Definition 4.1. *Let X be a lojid algebra. An element $x \in X$ is said to be $\lambda-$ invertible if there exists a bijection λ on X defined by $\lambda(a) = a^\lambda$, $(a \in X)$, such that $a^\lambda(ax) = x$*

If every element of a lojid algebra X is $\lambda-$ invertible, then X is said to be $\lambda-$ invertible.

Definition 4.2. *Let X be a lojid algebra. An element $x \in X$ is said to be $\rho-$ invertible if there exists a bijection ρ on X defined by $\rho(a) = a^\rho$, $(a \in X)$ such that $(xa)a^\rho = x$.*

If every element of a lojid algebra is $\rho-$ invertible, then X is said to be $\rho-$ invertible.

Definition 4.3. *A lojid algebra X which is both $\lambda-$ invertible and $\rho-$ invertible is called an invertible lojid algebra.*

Proposition 4.4. *Let X be an invertible lojid algebra. Then the following hold for all $a, b, x, y \in X$:*

1. *The expression $x = a^\lambda b$ is the solution of $ax = b$*
2. *The expression $y = ba^\rho$ is the solution of $ya = b$*
3. $(ab)^\lambda = b^\rho a^\rho$
4. $(ab)^\rho = b^\lambda a^\lambda$

Proof.

1. Consider the expression $ax = b$. "Multiplying" both sides on the left by a^λ and simplifying gives $x = a^\lambda b$ as required.
2. Consider the expression $ya = b$. "Multiplying" both sides on the right by a^ρ and simplifying gives $y = ba^\rho$ as required.

3. Let $ab = c$. Then $a = cb^{\rho},\ b^{\rho} = c^{\lambda},\ c^{\lambda} = b^{\rho}a^{\rho}$. Thus the conclusion follows.

4. Let $ab = c$. Then $b = a^{\lambda}c,\ a^{\lambda} = bc^{\rho},\ c^{\rho} = b^{\lambda}a^{\lambda}$. Thus the conclusion follows.

Definition 4.5. *A lojid algebra X is said to be partially absorbing if any two elements $x, y \in X$ satisfy $(xy)x^{\rho} = y$.*

Example 4.6. Let $X = \{0, 1, 2, 3, 4\}$. Define a binary operation $*$ on X by the following table:

$*$	0	1	2	3	4
0	0	1	2	3	4
1	1	0	3	4	2
2	2	4	0	1	3
3	3	2	4	0	1
4	4	3	1	2	0

Then $(X; *, 0)$ is a partially absorbing lojid algebra.

The following Lemma follows from definition.

Lemma 4.7. *Let X be a partially absorbing lojid algebra. Then $x(yx^{\rho}) = y$ and $(xy)^{\rho} = x^{\rho}y^{\rho}$ for all $x, y \in X$.*

Definition 4.8. *A lojid algebra X is said to be absorbing if any two elements $x, y \in X$ satisfy $y(xy)^{\rho} = x^{\rho}$.*

Example 4.9. Let $X = \{0, 1, 2, 3, 4, 5\}$. Define a binary operation $*$ on X by the following table:

$*$	0	1	2	3	4	5
0	0	1	2	3	4	5
1	1	2	0	4	5	3
2	2	0	1	5	3	4
3	3	5	4	0	2	1
4	4	3	5	1	0	2
5	5	4	3	2	1	0

Then $(X; *, 0)$ is an absorbing lojid algebra.

Proposition 4.10. *Every partially absorbing lojid algebra is an absorbing lojid algebra.*

Proof. Let X be a partially absorbing lojid algebra. By Lemma 4.1., we have $y(xy)^\rho = y(x^\rho y^\rho) = x^\rho$ as required.

Remark 4.11. The converse of Proposition 4.2 does not hold. Notice that the absorbing lojid algebra in Example 4.2 is not partially absorbing.

5 Congruences and Quotient Algebras

In this section, we discuss the notion of congruences in lojid algebras and use in the establishment of quotient lojid algebras.

Definition 5.1. *Let X be a lojid algebra. A relation $\sim$ on X is called a congruence if the following hold for all $a, b, c, d \in X$:*

1. $ca \sim cb \Rightarrow a \sim b$.
2. $ac \sim bc \Rightarrow a \sim b$.
3. $a \sim b$ *and* $c \sim d \Rightarrow ac \sim bd$.

Example 5.2. Let $X = \{0, 1, 2, 3, 4\}$. Define a binary operation $*$ on X by the following table:

$*$	0	1	2	3	4
0	0	1	3	4	2
1	1	0	4	2	3
2	2	4	1	3	0
3	3	2	0	1	4
4	4	3	2	0	1

Then $(X; *, 0)$ is a lojid algebra. Now, define a relation $\sim$ on X by $x \sim y \Rightarrow x^2 = y^2$. Then $\sim$ is a congruence on X.

Definition 5.3. *Let $(X; *, 0)$ and $(Y; *', 0')$ be lojid algebras. A function $f : X \to Y$ is called a homomorphism if $f(x * y) = f(x) *' f(y)$ for all $x, y \in X$.*

Let X and Y be lojid algebras and let $f : X \to Y$ be a homomorphism. Then f induces a relation $\sim$ on X defined by $a \sim b \Leftrightarrow f(a) = f(b)$. Clearly, $\sim$ is a congruence on X.
Conversely, if $\sim$ is a congruence on a lojid X, then $\sim$ determines a homomorphism $f : X \to Y$. To show this, let $K_a, K_b, ...$ be the congruence classes with respect to $\sim$. Then $bK_a = \{ba_i : a_i \in K_a\} = K_{ba}$. So, we can define $K_a *' K_b = K_{ab}$. Let Y be the collection $\{K_a, K_b, ...\}$ of all congruence classes. Then $(Y; *', K_0)$ is a lojid algebra. The equations $K_x *' K_a = K_b$ and $K_a *' K_y = K_b$ have unique solutions determined by the unique solutions of $x * a = b$ and $a * y = b$ in the lojid algebra $(X; *, 0)$. Let $f : X \to Y$ be such that $f(a) = K_a$ for all $a \in X$. Then $f(a * b) = f(a) *' f(b)$. Hence f is a homomorphism.

We therefore have the following Theorems:

Theorem 5.4. *Let X and Y be lojid algebras. If $f : X \to Y$ is a homomorphism, then f induces a congruence on X.*

Theorem 5.5. *Let X and Y be lojid algebras. If $\sim$ is a congruence on X, then $\sim$ induces a homomorphism $f : X \to Y$.*

Let $(X; *, 0)$ be a lojid algebra, and let $\sim$ be a congruence on X. Let $[x]$ denote the class of $x \in X$. That is, $[x] = \{y \in X : x \sim y\}$. Let $X(\sim)$ be the collection of all congruence classes in X. Define a binary operation $\circ$ on $X(\sim)$ by $[x] \circ [y] = [x * y]$ for all $[x], [y] \in X(\sim)$.

Theorem 5.6. *Let $\sim$ be a congruence on a lojid algebra $(X; *, 0)$. Then $(X(\sim); \circ, [0])$ is a lojid algebra.*

Proof. Clearly $(X(\sim); \circ, [0])$ is a semi-lojid algebra. Also, the maps $L_{[a]} : X(\sim) \to X(\sim)$ and $R_{[a]}$ defined by $L_{[a]}([x]) = [a] \circ [x]$ and $R_{[a]}([x]) = [x] \circ [a]$ respectively for all $[a] \in X(\sim)$ are bijections.

Definition 5.7. *Let $\sim$ be a congruence on a lojid algebra $(X; *, 0)$. The lojid algebra $(X(\sim); \circ, [0])$ is called the quotient lojid algebra induced by $\sim$.*

Theorem 5.8. *Let $\sim$ be a congruence on a lojid algebra X. Then a congruence class K_h has unique solvability property if and only if $h \sim h^2$.*

Proof. Let $K_h = H$. Suppose H has the unique solvability property. Let $a, b \in H$. Then we have $ab \sim h^2$. So, $ab \in H$ or $ab \sim h$, and we have $h \sim h^2$ as required.
Conversely, let H be such that $h \sim h^2$. Let $a, b \in H$. Then $a \sim h,\ b \sim h \Rightarrow ab \sim h^2$ and $ab \sim h \Rightarrow ab \in H$. So, H is closed. We show the existence of solutions of the equation $ax = b$ in H. Let $a, b \in H$. Then $b = ax \sim hx \Rightarrow b \sim h \sim h^2 \Rightarrow hx \sim h^2 \Rightarrow x \sim h \Rightarrow x \in H$. Similar argument shows that for the equation $ya = b$, we have $y \in H$. The uniqueness of the solutions is obvious.

6 Conclusion

In this paper, we have initiated the study of lojid algebras. We hope that this paper would activate further research on the theory of lojid algebras. In particular, we hope that the open problem posed in this paper would be solved in the nearest future. Several notions and concepts which we have studied in lojid algebras could also be extended to other algebras of type (2, 0).

References

[1] K. Iseki, *An Algebra Related with Propositional calculus*, Proc. Japan Acad., 42(1996), 26–29.

[2] Y. Imai and K. Iseki, *On Axiom System of Propositional Calculi*, Proc. Japan Acad., 42(1996), 19–22.

[3] Q. P. Hu and X. Li, *On BCH algebras*, Math. Seminar Notes II, (1983), 313–320.

[4] J. Neggers and H. S. Kim, *On d-algebras*, Mathematica Slovaca, 49(1999), 19–26.

[5] H. S. Kim and Y. H. Kim, *On BE-algebras*, Sci. Math. Jpn. 66(2007),113–116.

[6] S.S. Ahn and K. S. So, *On ideals and upper sets in BE-algebras*, Sci. Math. Jpn. 68(2008), 351–357.

[7] S.S. Ahn and K. S. So, *On Generalized upper sets in BE-algebras*, Bull. Korean Math. Soc. 46(2009), 281–287.

[8] H. S. Kim, J. Neggers and S. S. Ahn, *On Pre-Commutative Algebras*, Mathematics, 7(2019), 336. doi:10.33390/math7040336.

[9] T. G. Jaiyeola, E. Ilojide, M. O. Olatinwo and F. S. Smarandache, *On the Classification of Bol-Moufang Type of Some Varieties of Quasi Neutrosophic Triplet Loops (Fenyves BCI-algebras)*, Symmetry 10(2018),
427. https://doi.org/10.3390/sym10100427.

[10] E. Ilojide, T. G. Jaiyeola and M. O. Olatinwo, *On Holomorphy of Fenyves BCI-algebras*, Journal of the Nigerian Mathematical Society, 38(2),(2019), 139–155.

[11] T. G. Jaiyeola, E. Ilojide, A. J. Saka and K. G. Ilori, *On the Isotopy of Some Varieties of Fenyves Quasi Neutrosophic Triplet Loops(Fenyves BCI-algebras)*, Neutrosophic Sets and Systems, 31(2020), 200–223. DOI: 105281/zenodo.3640219.

[12] J. Neggers, S. A. Sun and S. K. Hee, *On Q-algebras*, International J. of Math. and Math. Sci. 27(2001), 749–757.

[13] E. Ilojide, *Homomorphisms of Q algebras*, Analele Universitatii din Oradea Fascicola Matematica, 28,(2),(2021), 5–13.

[14] M. Ebrahimi and A. Izadara, *The Ideal Entropy of BCI- algebras and its Application in Binary Linear Codes*, Soft Computing, 2019, 23:39–57.

[15] E. Ilojide, *On Obic Algebras*, International Journal of Mathematical Combinatorics, 4(2019), 80–88.

[16] E. Ilojide, *A Note on Torian Algebras*, International Journal of Mathematical Combinatorics, 2(2020), 80–87.

[17] E. Ilojide, On Ideals of Torian Algebras, International Journal of Mathematical Combinatorics, 2(2020), 101–108.

[18] E. Ilojide, *On Right Distributive Torian Algebras*, International Journal of Mathematical Combinatorics ,4(2020), 100–107.

[19] E. Ilojide, *On Isomorphism Theorems of Torian Algebras*, International Journal of Mathematical Combinatorics, 1(2021), 56–61.

[20] J. Neggers, S. A. Sun and S. K. Hee *On Q-algebras*, International Journal of Mathematics and Mathematical Sciences, 27(2001), 749–757.

Eight-order second derivative block linear multistep method for chaotic initial value problems

E. J. Onoja*†, U.W. Sirisena‡, and G.M. Kumleng†§

Abstract

This paper aims to enhance the accuracy and stability of eight-order second derivative linear multistep methods (LMMs) for solving chaotic initial value problems (IVPs). The method is developed using a multistep collocation approach. The newly derived method is applied to plot solution curves, solid lines, and phase portraits, which are compared with those obtained from well-established ordinary differential equations (ODEs) solvers. The results show excellent agreement between the proposed method and the established solvers. The proposed block method demonstrates efficiency and accuracy, making it a suitable choice for solving chaotic and nonlinear ordinary differential equations.

Keywords and phrases: multistep; chaotic; numerical; derivative

1 Introduction

Chaos theory was first reported in the work of Lorenz [1], who discovered it when studying the earth's atmosphere and weather conditions. Since then, chaos theory has attracted the attention of many researchers because of its applicability in numerous everyday activities. The initial value problem is given by

$$y'(x) = f(y(x), y(x)), y(x_0) = y_0 \tag{1}$$

on the interval $I = [x_0, x_N]$ where $y : [x_0, x_N] \to \Re^m$ and $f : [x_0, x_N] \times \Re^m \to \Re^m$ is continuous and differentiable.

Solving chaotic systems (1) has long been a challenge to researchers and remains so due to their complex and dynamic nature. These systems are highly sensitive to tiny changes in the initial conditions, and their solutions can rapidly transition from being stable to instability. This sensitivity

*Corresponding Author; E-mail: janet4chrisrt35@gmail.com, janaet4maths@yahoo.com
†Royal Crown Academy, Rayfield Jos, Nigeria.
‡Department of Mathematics, University of Jos, Plateau State, Nigeria.

and unpredictability make chaotic systems difficult to model and analyze, posing a persistent challenge to researchers.

Chaotic systems exhibit distinct characteristics, including the butterfly effect, non-periodic order, strange attractors, bifurcation, and fractals.

However, chaotic ODEs often deferred analytical solutions, necessitating the use of numerical methods. While, analytical and semi- iterative methods are commonly employed to solve chaotic ODEs, offering advantages over linear multistep methods [2-3], we aim to demonstrate that linear multistep methods can also be successfully utilized to solve chaotic ODEs.

Accordingly, this study focuses on the derivation of an eight-order second derivative linear multistep method and its implementation as a block integrator for solving renowned chaotic initial value problems. By deriving and applying this method, we aim to demonstrate its effectiveness in tackling chaotic systems, which are notoriously challenging to solve numerically.

Theorem 1.1 (Existence and Uniqueness of the solution): Let f(x, y) be defined and continuous for all points (x, y) in region D defined by $a \le x \le b, -\infty < y < \infty$, a and b finite, and let there exist a constant L such that, for every x, y such that (x, y) and (x, y^*) are both in D, $|f(x, y) - f(x, y^*)| \le L|y - y^*|$. Then, if y^* is any given number, there exist a unique solution y(x) of the IVP (1), where y(x) is continuous and differentiable for all (x, y) in D [4].

This work is organized as follows: Section 2 presents the derivation of the eight-order second derivative linear multistep method. Section 3 provides the convergence analysis and plots the regions of absolute stability of the newly derived block integrators. Section 4 offers numerical simulations/sensitivity analysis in graphical form, accompanied by a discussion Finally, Section 5 concludes the work with a summary of the key findings.

2 Derivation of the method

Building on the approach and definition presented in [5-6] for the continuous formulation of the order k-step second derivative linear multistep methods, we have derived the continuous form of the eight-order second derivative linear multistep method, which is presented below and with $\eta = (x - x_n)$.

$$y(x)=\frac{1}{34560h_n^9}[-\eta^9+32h_n\eta^8-446h_n^2\eta^7+3548h_n^3\eta^6-17717h_n^4\eta^5+57438h_n^5\eta^4-12036432h_n^6\eta^3+$$

$$156432h_n^7\eta^2-113472h_n^4\eta+34560h_n^9]y_n-\frac{1}{2160h_n^9}[\eta^9-31h_n\eta^8+415h_n^2\eta^7-3133h_n^3\eta^6+14584h_n^4\eta^5-42844h_n^5\eta^4+77520h_n^6\eta^3$$

$$-78912h_n^7\eta^2+34560h_n^4\eta]y_{n+1}+\frac{1}{192h_n^9}[-\eta^9+30h_n\eta^8-386h_n^2\eta^7+2776h_n^3\eta^6-12165h_n^4\eta^5+33098h_n^5\eta^4-54168h_n^6\eta^3$$

$$+48096h_n^7\eta^2-117280h_n^4\eta]y_{n+2}-\frac{1}{36h_n^9}[2\eta^9-57h_n\eta^8+692h_n^2\eta^7-4661h_n^3\eta^6+18980h_n^4\eta^5-47612h_n^5\eta^4+71376h_n^6\eta^3$$

$$-57920h_n^7\eta^2+19200h_n^4\eta]y_{n+3}-\frac{1}{69h_n^9}[-445\eta^9+12688h_n\eta^8-154246h_n^2\eta^7+1041484h_n^3\eta^6-4256737h_n^4\eta^5+10732084h_n^5\eta^4-16190076h_n^6\eta^3$$

$$+13230288h_n^7\eta^2-44150h_n^4\eta]y_{n+4}+\frac{1}{240h_n^9}[\eta^9-27h_n\eta^8+311h_n^2\eta^7-1993h_n^3\eta^6+7752h_n^4\eta^5-18668h_n^5\eta^4+27024h_n^6\eta^3$$

$$-21312h_n^7\eta^2+6912h_n^4\eta]y_{n+5}-\frac{1}{8640h_n^9}[\eta^9-26h_n\eta^8+290h_n^2\eta^7-1808h_n^3\eta^6+6869h_n^4\eta^5-16214h_n^5\eta^4+23080h_n^6\eta^3$$

$$-17952h_n^7\eta^2+5760h_n^4\eta]y_{n+6}-\frac{1}{576h_n^8}[-19\eta^9+544h_n\eta^8-6634h_n^2\eta^7+44884h_n^3\eta^6-183631h_n^4\eta^5+463036h_n^5\eta^4-698196h_n^6\eta^3$$

$$+570096h_n^7\eta^2-190080h_n^8\eta]f_{n+4}+\frac{1}{96h_n^7}[-\eta^9+28h_n\eta^8-334h_n^2\eta^7+2212h_n^3\eta^6-8869h_n^4\eta^5+21952h_n^5\eta^4-32556h_n^6\eta^3+26208h_n^7\eta^2$$

$$-8640h_n^4\eta]g_{n+4} \qquad (2)$$

Evaluating (2) at $\eta=7h_n$ and its first derivative at $\eta=\{0,h_n,7h_n,4h_n,5h_n,6h_n\}$ yield the block integrators represented in block matrix using finite difference form as:

$$AY_m=BY_{m-1}+CF_m+DF_{m-1}+WG_m+UG_{m-1} \qquad (3)$$

where,

$$A = \begin{vmatrix} 1 & \frac{225}{49} & \frac{900}{49} & \frac{4475}{196} & \frac{45}{49} & \frac{-1}{49} & 0 \\ \frac{-16}{465} & 1 & \frac{64}{31} & \frac{595}{186} & \frac{-16}{155} & \frac{1}{465} & 0 \\ \frac{-13}{2545} & \frac{-139}{2036} & 1 & \frac{9625}{8144} & \frac{-316}{2545} & \frac{527}{91620} & 0 \\ \frac{-64}{2555} & \frac{72}{511} & \frac{1200}{1533} & 1 & \frac{576}{12775} & \frac{-8}{7665} & 0 \\ \frac{5}{681} & \frac{-25}{227} & \frac{500}{227} & \frac{9025}{2724} & 1 & \frac{-5}{681} & 0 \\ \frac{-48}{227} & \frac{675}{227} & \frac{11200}{227} & \frac{-27525}{454} & \frac{2160}{227} & 1 & 0 \\ 14 & -189 & 2835 & \frac{13475}{4} & -378 & 21 & 1 \end{vmatrix}, B = \begin{vmatrix} 0 & 0 & 0 & 0 & 0 & 0 & \frac{-5}{196} \\ 0 & 0 & 0 & 0 & 0 & 0 & \frac{1}{930} \\ 0 & 0 & 0 & 0 & 0 & 0 & \frac{-101}{366480} \\ 0 & 0 & 0 & 0 & 0 & 0 & \frac{197}{38325} \\ 0 & 0 & 0 & 0 & 0 & 0 & \frac{-1}{2724} \\ 0 & 0 & 0 & 0 & 0 & 0 & \frac{5}{454} \\ 0 & 0 & 0 & 0 & 0 & 0 & \frac{-3}{3} \end{vmatrix},$$

$$C = \begin{vmatrix} \frac{-20}{49} & \frac{600}{49} & \frac{575}{49} & 0 & 0 & 0 & 0 \\ 0 & \frac{-12}{31} & \frac{-64}{31} & -\frac{50}{31} & 0 & 0 & 0 \\ 0 & 0 & -\frac{1369}{3054} & \frac{-10205}{18324} & 0 & 0 & -\frac{1}{9162} \\ 0 & 0 & \frac{256}{511} & \frac{264}{511} & 0 & 0 & 0 \\ 0 & 0 & \frac{-200}{227} & \frac{-175}{227} & \frac{60}{227} & 0 & 0 \\ 0 & 0 & \frac{4800}{227} & \frac{5850}{227} & \frac{60}{227} & 0 & 0 \\ 0 & 0 & -1260 & -1565 & 0 & 0 & 0 \end{vmatrix}, D = \begin{vmatrix} 0 & 0 & 0 & 0 & 0 & 0 & 0 \\ 0 & 0 & 0 & 0 & 0 & 0 & 0 \\ 0 & 0 & 0 & 0 & 0 & 0 & 0 \\ 0 & 0 & 0 & 0 & 0 & 0 & \frac{4}{2555} \\ 0 & 0 & 0 & 0 & 0 & 0 & 0 \\ 0 & 0 & 0 & 0 & 0 & 0 & 0 \\ 0 & 0 & 0 & 0 & 0 & 0 & 0 \end{vmatrix}$$

$$W = \begin{vmatrix} 0 & 0 & 0 & \frac{-150}{49} & 0 & 0 & 0 \\ 0 & 0 & 0 & \frac{12}{31} & 0 & 0 & 0 \\ 0 & 0 & 0 & \frac{667}{3054} & 0 & 0 & 0 \\ 0 & 0 & 0 & -\frac{72}{511} & 0 & 0 & 0 \\ 0 & 0 & 0 & \frac{150}{227} & 0 & 0 & 0 \\ 0 & 0 & 0 & \frac{-2700}{227} & 0 & 0 & 0 \\ 0 & 0 & 0 & -630 & 0 & 0 & 0 \end{vmatrix}, U = \begin{vmatrix} 0 & 0 & 0 & 0 & 0 & 0 & 0 \\ 0 & 0 & 0 & 0 & 0 & 0 & 0 \\ 0 & 0 & 0 & 0 & 0 & 0 & 0 \\ 0 & 0 & 0 & 0 & 0 & 0 & 0 \\ 0 & 0 & 0 & 0 & 0 & 0 & 0 \\ 0 & 0 & 0 & 0 & 0 & 0 & 0 \\ 0 & 0 & 0 & 0 & 0 & 0 & 0 \end{vmatrix},$$

is a 7-dimentional vector Y_m, Y_{m-1}, F_m, F_{m-1}, G_m, *and* G_{m-1}having interpolation and collocation points as:

$$Y_m = [y_{n+1}, y_{n+2}, y_{n+3}, y_{n+4}, y_{n+5}, y_{n+6}, y_{n+7}]$$
$$Y_{m-1} = [y_{n-6}, y_{n-5}, y_{n-4}, y_{n-3}, y_{n-2}, y_{n-1}, y_n]$$
$$F_m = [f_{n+1}, f_{n+2}, f_{n+3}, f_{n+4}, f_{n+5}, f_{n+6}, f_{n+7}]$$
$$F_{m-1} = [f_{n-6}, f_{n-5}, f_{n-4}, f_{n-3}, f_{n-2}, f_{n-1}, f_n]$$
$$G_m = [g_{n+1}, g_{n+2}, g_{n+3}, g_{n+4}, g_{n+5}, g_{n+6}, g_{n+7}]$$
$$G_{m-1} = [g_{n-6}, g_{n-5}, g_{n-4}, g_{n-3}, g_{n-2}, g_{n-1}, g_n]$$

3 Stability analysis of the method

The newly derived block integrators are thoroughly examined, with a focus on their local truncations error, order, consistency and zero stability. Additionally, the regions of absolute stability for these bloc integrators will be potted, providing a comprehensive understanding of their numerical properties and performance.

3.1 Convergence analysis

The convergence of the method derived block integrators, presented in Section 2, is conducted as shown in [1, 4] the method (3) is of order greater than one. Furthermore, in [7], it is zero-stable, in [8], is consistent. Therefore, according [11], the method is convergent. A summary of the finding is provided in Table 1. The convergence analysis was performed to determine whether the newly derived block integrators are suitable for solving the chaotic ODEs.

Table 1. Convergence analysis of the new method in block form

Step No.	Evaluation points	Order	Error Constant
Case k=7	$y'(x_n), y'(x_{n+1}),$ $y'(x_{n+3}), y'(x_{n+4}),$ $y'(x_{n+5}), y'(x_{n+6}),$ x_{n+7}	8, 8, 8, 8, 8, 8, 8	$\frac{1}{4116}, -\frac{1}{48825}, \frac{737}{38480400}, \frac{4}{268275}, \frac{1}{57204}, \frac{1}{1589}, \frac{1}{20}$

3.1 Region of absolute stability of the new method

Following the approach outlined in [9], the newly derived bock integrators presented in Section 2 are transformed into general linear methods. The elements of matrices A, B, C, D, W, and U are obtained from equation (2) and substituted into the characteristic equation:

$$del(r(A-Cz-Wz^2)-B-Dz-Uz^2)=0 \tag{11}$$

By solving the characteristic equation, we obtain the stability polynomial and its derivative. These will be substituted into MATLAB code to plot the region of absolute stability. According to [10], the method is A(α)-stable, and this is illustrated in Fig. 1, which shows the region of absolute stability.

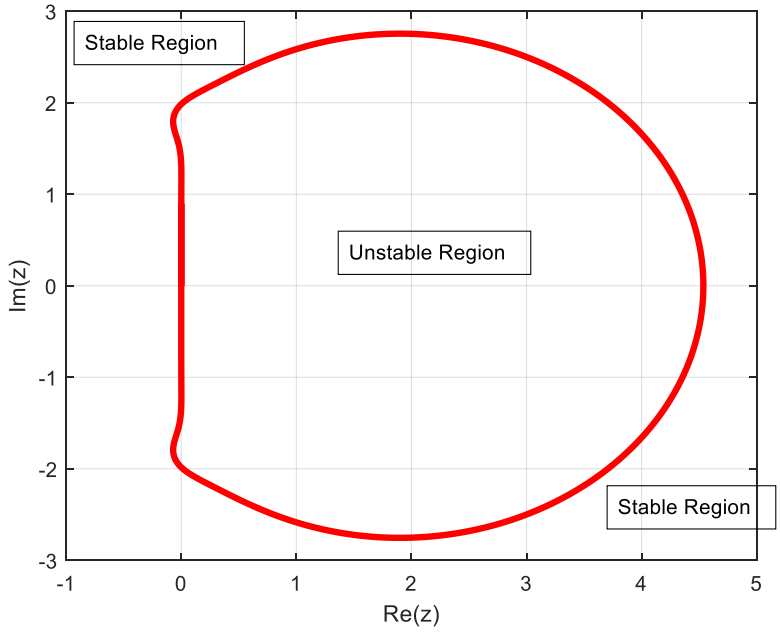


Fig. 1. Region of absolute stability for eight-order second derivative blocks linear multistep method.

4 Numerical simulations/sensitivity analysis

In this section, we apply our newly derived block integrators to solve three real-life problems exhibiting chaotic behaviour, as reported in the literature. Specially, we consider the Lorenz system, Genesio-Tesi and the Rössler system. We then compare the results obtained using our block integrators with those achieved by traditional ODE solvers, demonstrating the effectiveness of our approach in capturing the complex dynamics of these chaotic systems.

The step size, h, was varied across different systems: between 0.1 and 0.0001 for the Lorenz system, 0.1 and 0.001 for the Genesio-Tesi system, and 0.1 and 0.00001 for the Rössler system. The accuracy level set to six decimal places. The results were compared with MATLAB in-built solvers for IVPs of ODEs, specifically: ode45, ode113, ode23s and ode15s. Each of these solvers has its advantages depending on the type of problem type and required order of accuracy.

Model 1: Lorenz system

The Lorenz system [1] was derived from modeling a two-dimensional fluid cell confined between two parallel plates at different temperatures. The variables y_1, y_2, and y_3 represent the rate of convergence of overturning the horizontal temperature difference, and the departure gradient, respectively. The bounded regions of the trajectories converge to an attractor, which is a fractal with a dimension approximately 2.06.

$$
\begin{aligned}
y_1' &= a(y_2 - y_1) \\
y_2' &= -y_1 y_3 + b y_1 - y_2 \\
y_3' &= y_1 y_2 - c y_3
\end{aligned}
$$

where $a = 10, b = 28, c = \frac{8}{3}$ $y_1(0) = 1, y_2(0) = 5, y_3(0) = 10,$ for $x \in [0,10]$ and $h = 10^{-1}$ to 10^{-3}.

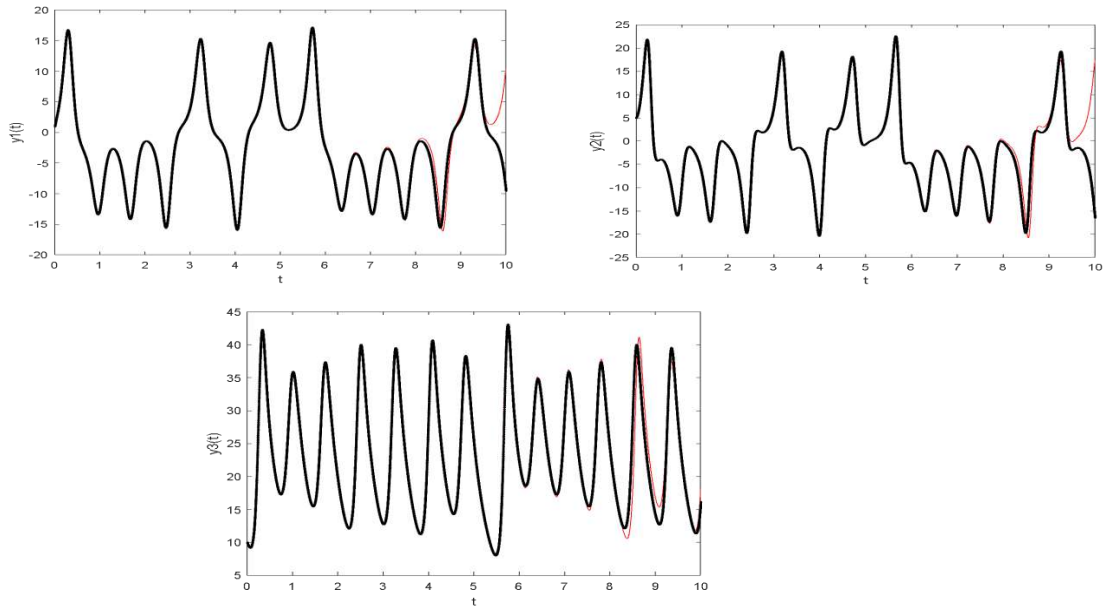


Fig. 2. Comparison of each component of the solutions as a function of time t, showing the plot of the coordinates of the Lorenz system using eight-order second derivative block linear multistep method (red solid lines) and ode45(black dots).

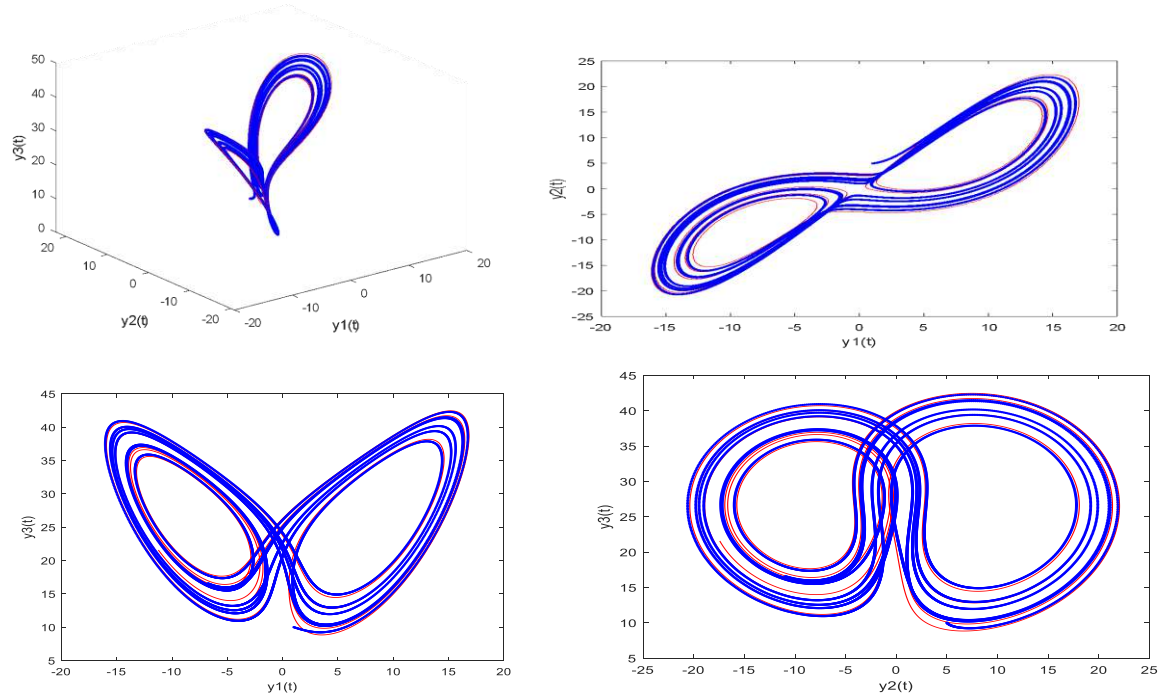


Fig. 3. Comparison of the phase portrait of Lorenz system using the eight-order second derivative block linear multistep method (red solid lines) and ode23s (blue dots).

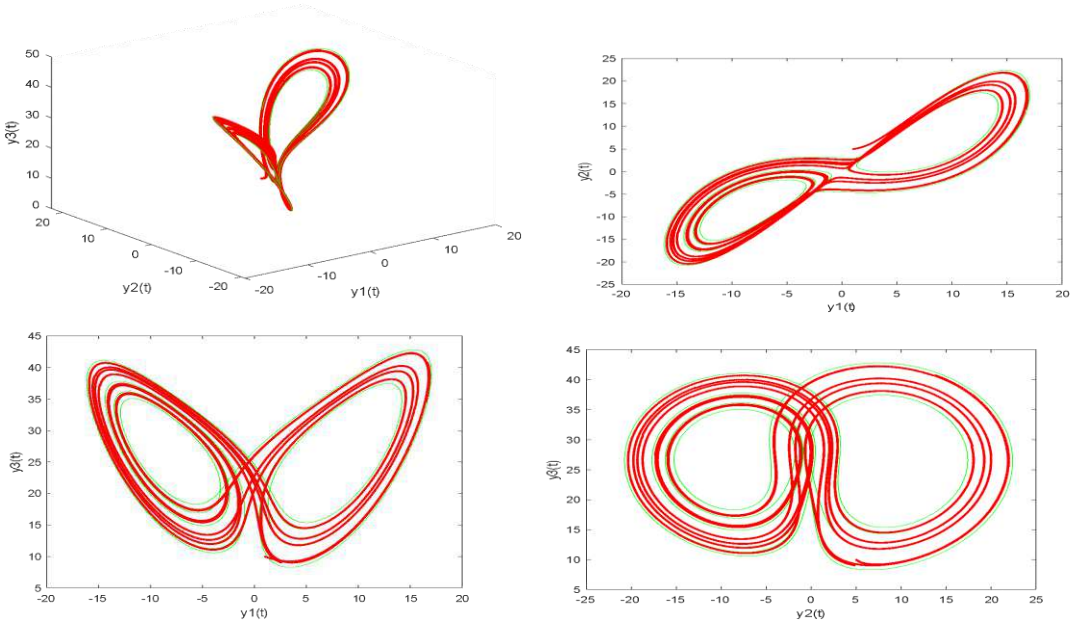


Fig. 4. Comparison of the phase portrait of the Lorenz system using the order eight-order second derivative block linear multistep method(red solid lines) and ode113(green dots).

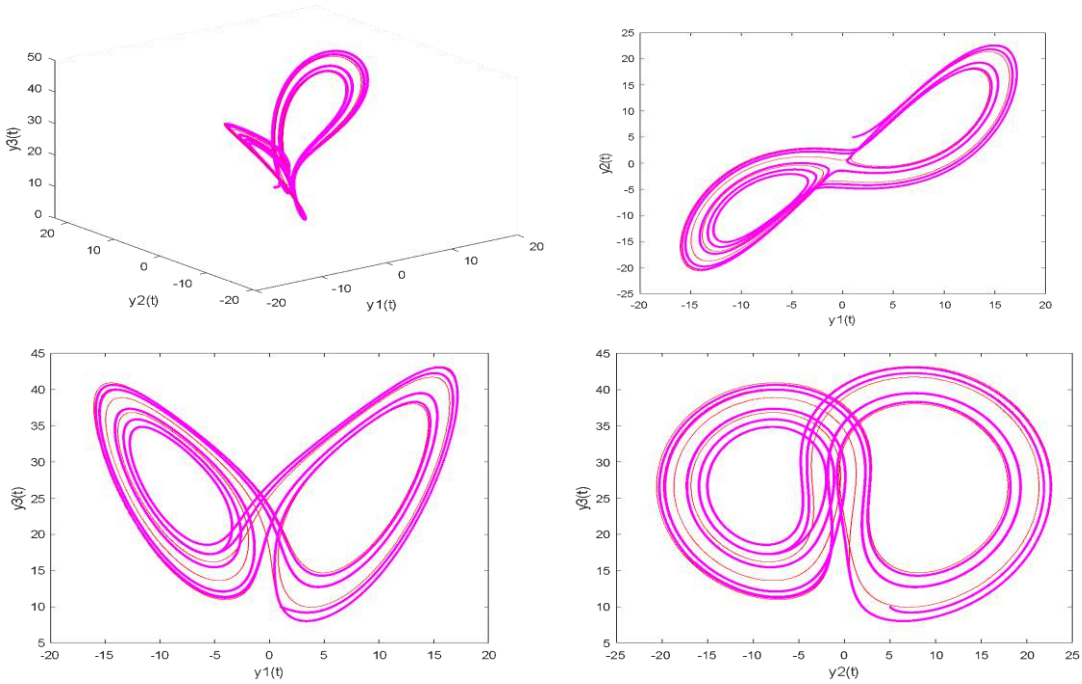


Fig. 5. Comparison of the phase portrait of the Lorenz system using the eight-order second derivative block linear multistep method (red solid lines) and ode45(marble dots).

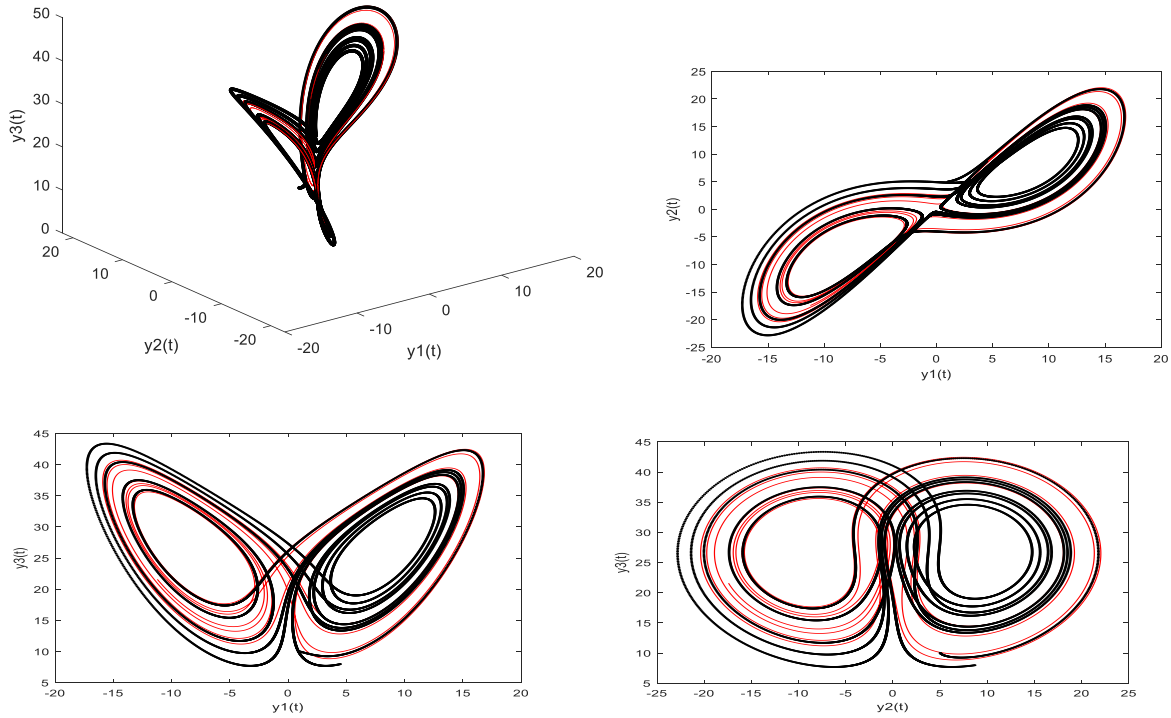


Fig. 6. Comparison of the phase portrait of the Lorenz system using eight-order second derivative block linear multistep method (red solid lines) and ode15s (black dots).

The time series and phase portraits of the approximate solutions obtained from order eight second derivative block linear multistep method for [1] are plotted in 3D and 2D in Figs. 2-6 respectively. The solid lines and the phase portraits compared with results from ODEs solvers(ode15s, ode23s, ode45 and ode113).The excellent agreement between these plots demonstrates the accuracy of our newly derived block integrator with each other. Hence, these show the accuracy of our newly derived integrators. According to the existence and uniqueness theorem (Theorem 1), trajectories cannot merge or cross, ensuring that the strange attractors are unique. In all cases, the solid lines and phase portraits show good agreement with the ODE solvers, further validating our approach.

Model 2: Genesio-Tesi system[12] is another exemplary model that embodies the paradigm chaotic systems. The system is modeled by the following set of IVPs:

$$y_1' = y_2$$
$$y_2' = y_3$$
$$y_3' = cy_1 + by_2 + ay_3 + y_1^2$$

This system was solved for the parameters $a = -1.2, b = -2.92, c = -6$, $y_1(0) = 0.2, y_2(0) = -0.3, y_3(0) = 0.1$ for $x \in [0, 70]$, and $h = 10^{-1}$ to 10^{-3}.

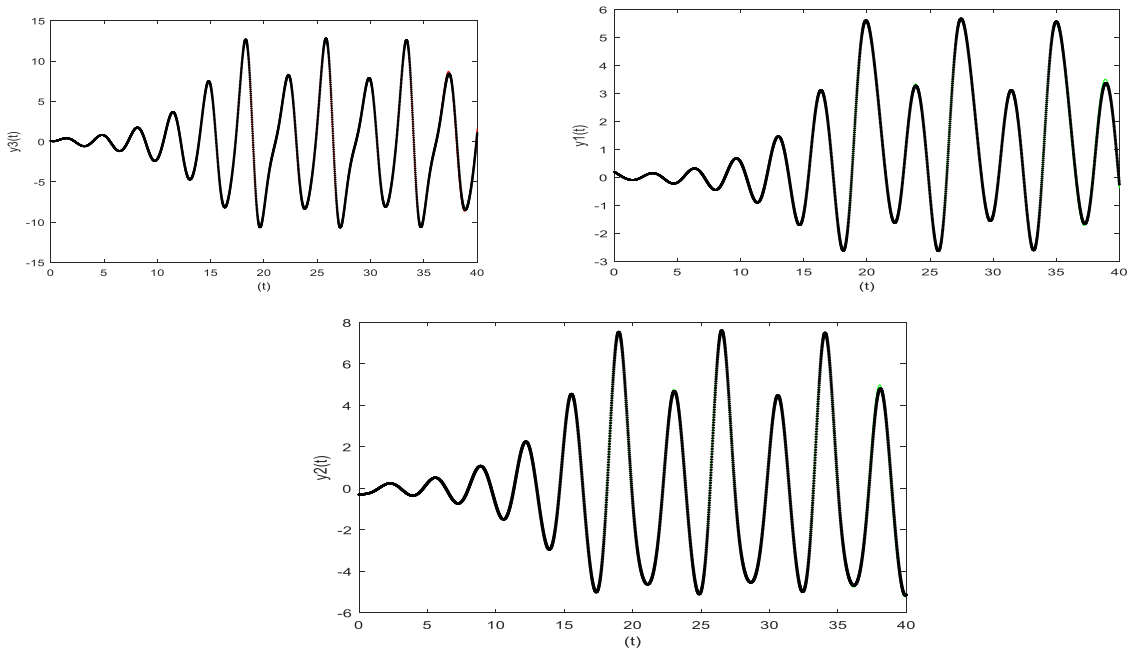


Fig. 7. Comparison of each component of the solutions as a function of time t, showing the plot of the coordinates of the Genesio-Tesi system using the eight-order second derivative block linear multistep method (green solid lines) and ode45(black dots).

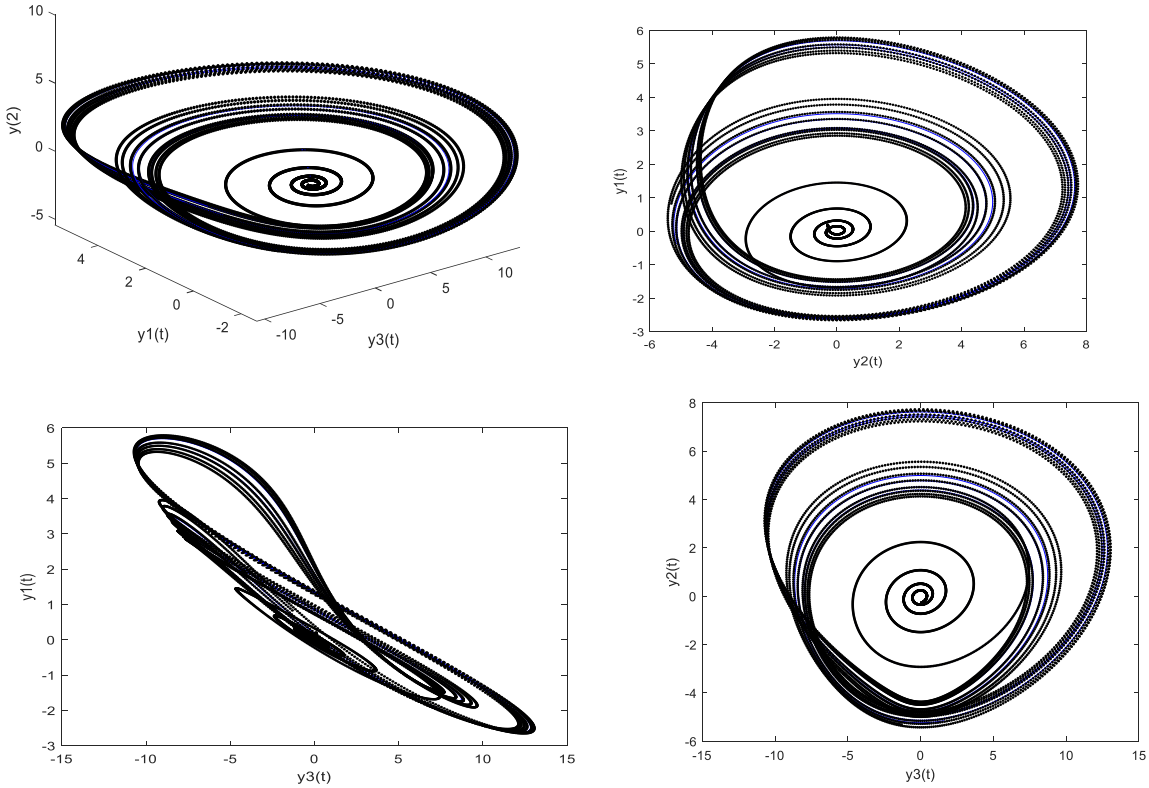


Fig. 8. Comparison of the phase portrait of the Genesio -Tesi system using the order eight second derivative block linear multistep method (blue solid lines) and ode23s (black dots).

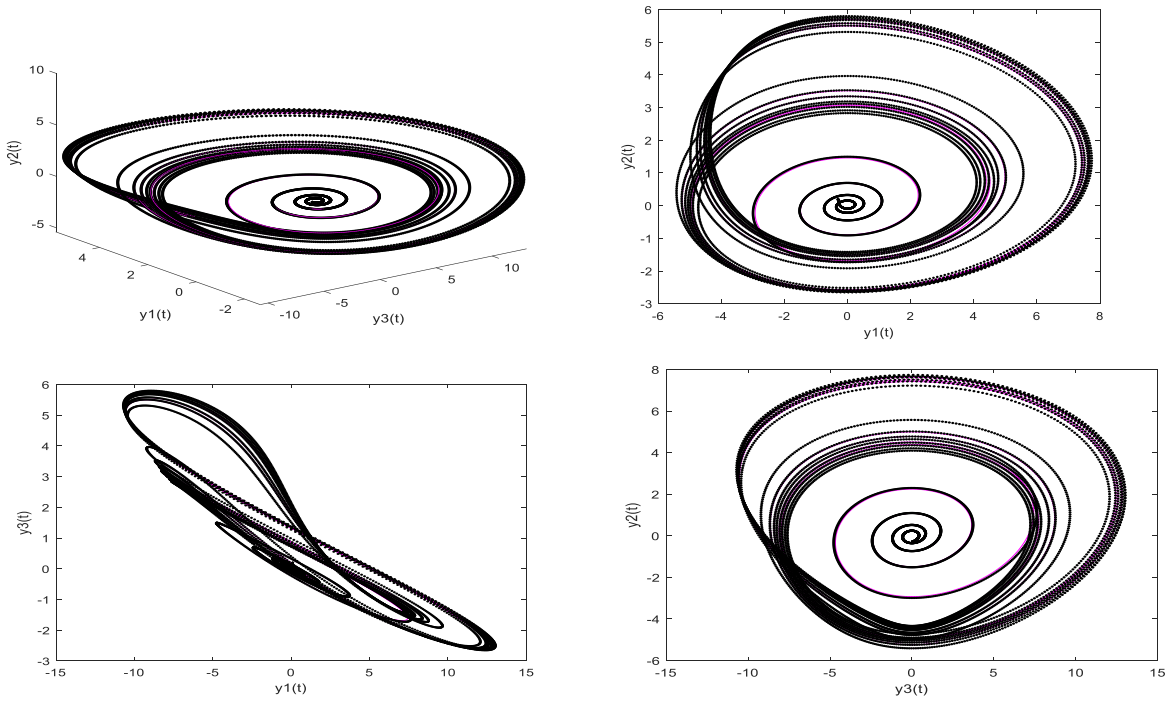


Fig. 9. Comparison of the phase portrait of the Genesio -Tesi system using the eight-order second derivative block linear multistep method (marble solid lines) and ode15s (black dots).

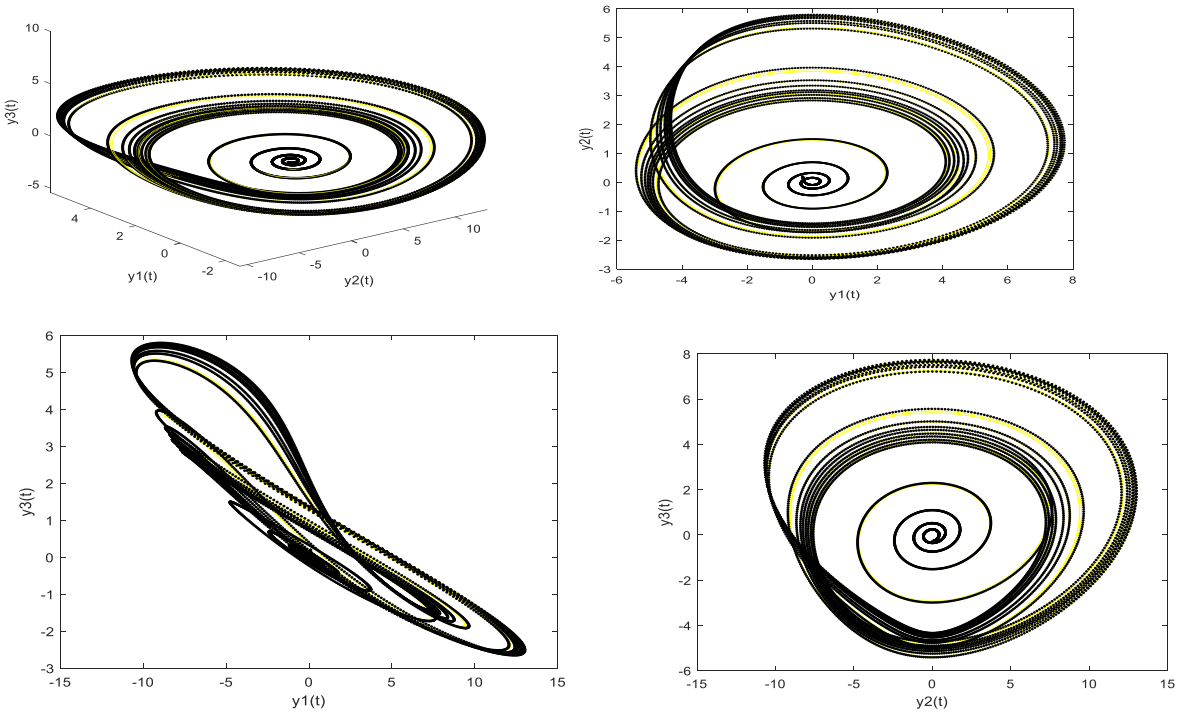


Fig. 10. of the phase portrait of the Genesio -Tesi system using the eight-order second derivative block linear multistep method (yellow solid lines) and ode113(black dots).

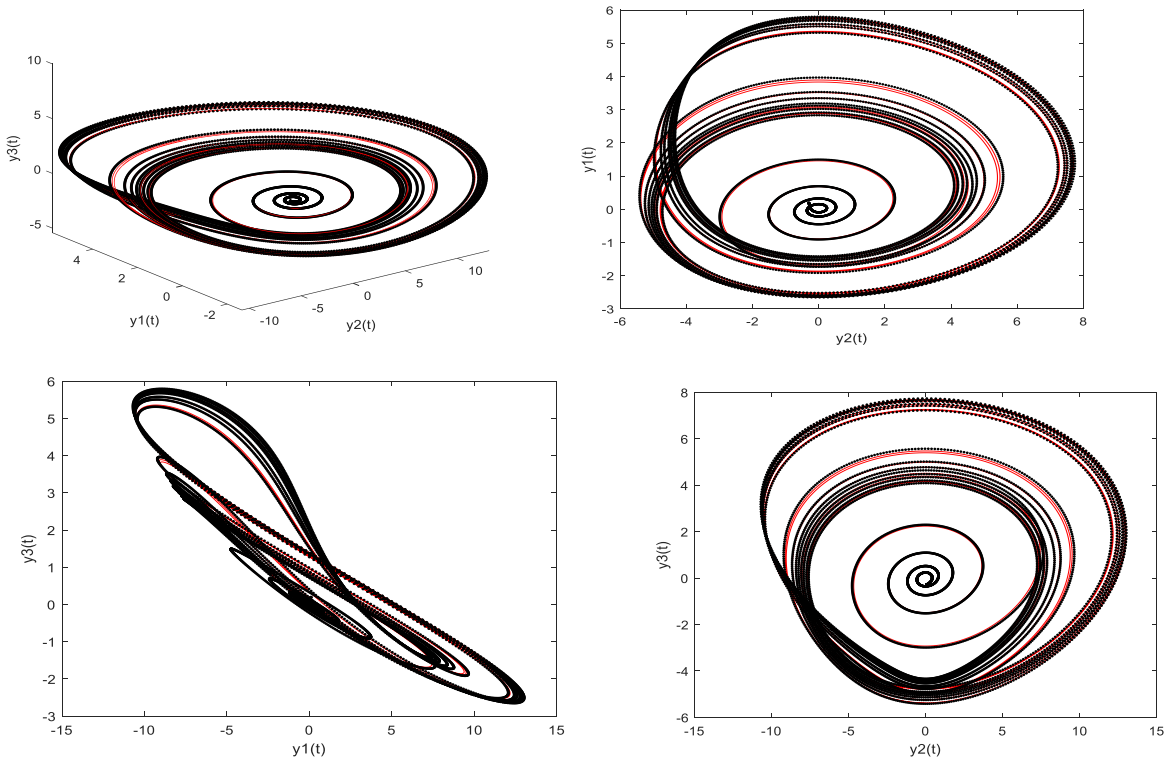


Fig. 11. Comparison of the phase portrait of the Genesio -Tesi system using the eight-order second derivative block linear multistep method(red solid lines) and ode15s(black dots).

The time series and phase portraits of the approximate solutions obtained from order eight second derivative block linear multistep method for[12] are plotted in 3D and 2D in Figs. 7-11 respectively. Similarly, the time series and the phase portraits of the approximate solutions for the [12] are compared with results from ODEs solvers(ode15s, ode23s, ode45 and ode113) in Figs 7-11. The solid lines and phase portraits show excellent agreement between our newly derived block integrator and the ODE solvers, demonstrating their accuracy. According to the existence and uniqueness theorem (Theorem 1), trajectories cannot merge or cross, ensuring that the strange attractors are unique. In all cases, the solid lines and phase portraits show good agreement with the ODE solvers, further validating our approach.

Model 3: Rössler system [13]

$$y_1' = -(y_2 - y_1)$$
$$y_2' = y_1 + ay_2$$
$$y_3' = b + y_1 y_3 - cy_3$$

where, $a = 0.2, b = 0.2, c = 5.7$, $y_1(0) = 0, y_2(0) = 0, y_3(0) = 0$ for $x \in [0,80]$, and $h = 10^{-1}$ to 10^{-3}.

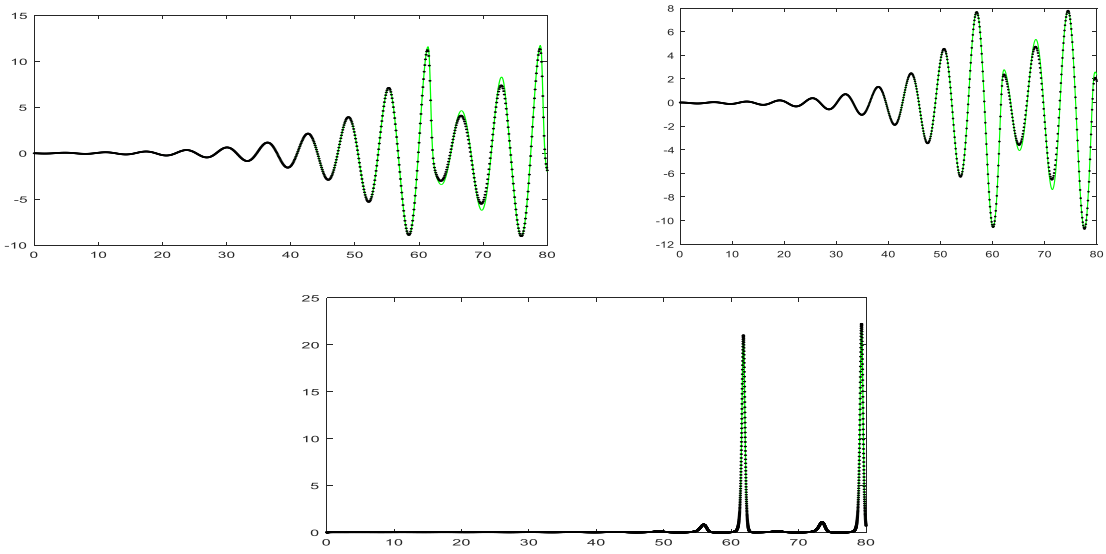


Fig. 12. Comparison of the phase portrait of Rössler system using eight-order second derivative block linear multistep method (green solid lines) and ode23s (black dots).

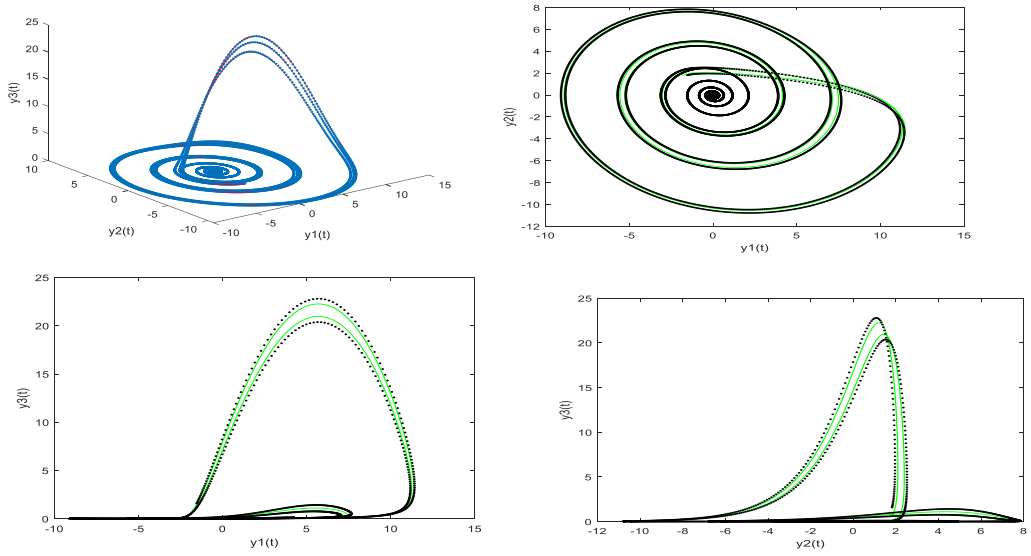


Fig. 13. Comparison of the phase portrait of Rössler system using eight-order second derivative block linear multistep method (solid lines) and ode23s (black dots).

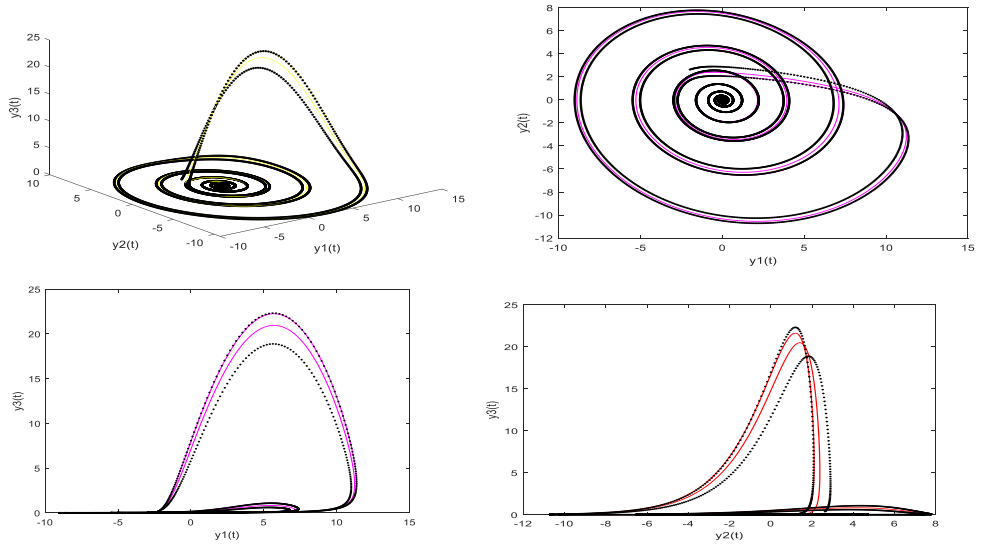


Fig. 14. Comparison of the phase portrait of Rössler system using the eight-order second derivative block linear multistep method (solid lines) and ode15s (dots).

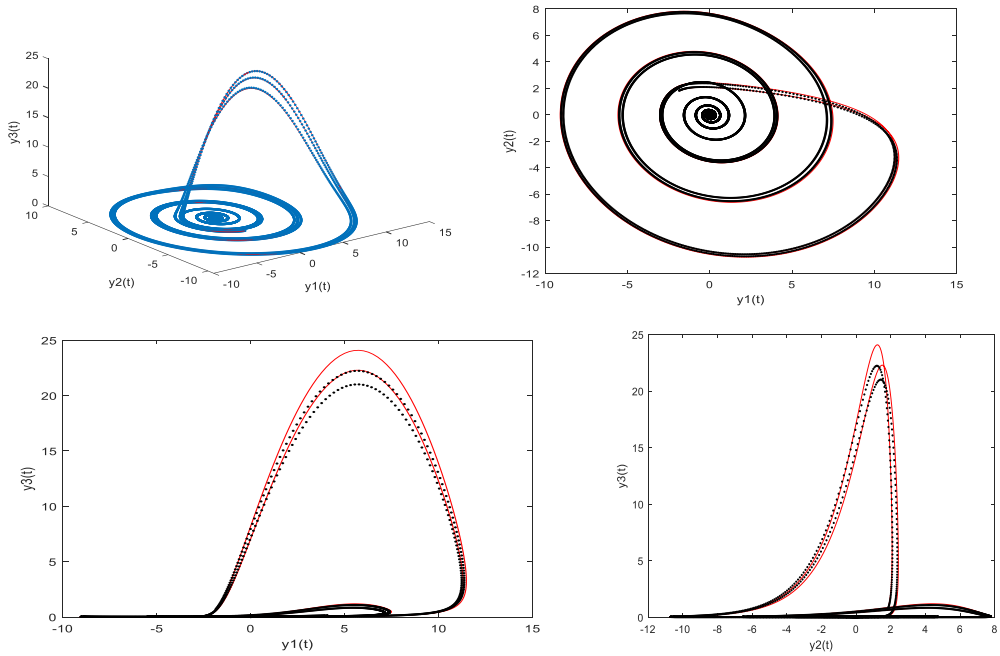


Fig. 15. Comparison of the phase portrait of Rössler system using the order eight second derivative block linear multistep method (solid lines) and ode45 (dots).

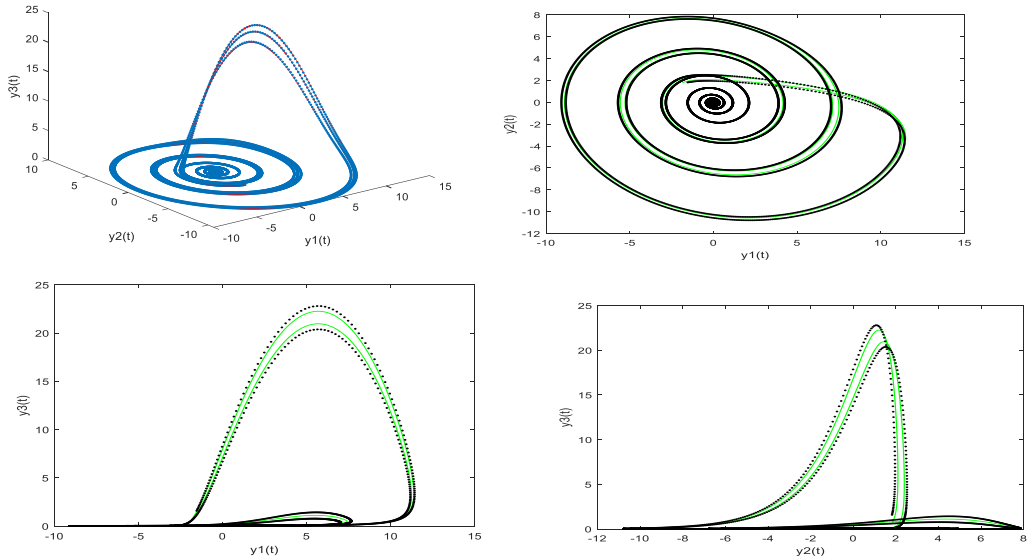


Fig. 16. Comparison of the phase portrait of Rössler system using the order eight second derivative block linear multistep method (solid lines) and ode113 (dots).

The solution curves obtained from the numerical simulations using eight-order second derivative block linear multistep method for[13] are plotted in 3D and 2D in Figs 12-16, respectively. Similarly, the time series and phase portraits of the approximate solutions for[13] are compared with the results from ODEs solvers(ode15s, ode23s, ode45 and ode113) in Figs 12-16. The solid lines and phase portraits show excellent agreement between our newly derived block integrators and the ODE solvers, demonstrating their accuracy. According to the existence and uniqueness theorem (Theorem 1), trajectories cannot merge or cross, ensuring that the strange attractors are unique. In all cases, the solid lines and phase portraits show good agreement with the ODE solvers, further validating our approach.

5 Conclusion

In this study, we have developed an eight-order second derivative block linear multistep method with variable step size for solving nonlinear IVPs of ODEs with chaotic properties. The derived method is convergent and A(α)-stable, is self-starting nature eliminates the use of starting values. Numerical simulations conducted in [12-13] demonstrate the method's efficiency and attractiveness in solving various chaotic, nonlinear, and linear ODEs, as evident from the time series and phase portraits compared with MATLAB ODEs solvers (ode45, ode113, ode23s, and ode15s) notably, our method successfully overcomes the limitations mentioned in [14].

References

[1] Lorenz, E. N. (1963). Deterministic non-periodic flow. Journal of the atmospheric sciences. 20 (2), 130-141.
[2] Alomari, A. K., Noorani, M. S. M., and Nazar, R. (2009). Adaptation of homotopy analysis method for the numeric analytic solution of Chen system. Commun. nonlinear sci. Numer. Simul., 14(5), 23362346. doi:1016/j.cnsns.2008.06.011.
[3] Bonyah, E., Kolebaje, O. T. and Kwasi Awuah-Wereko. (2016). Using multistage Laplace Adomia decomposition method to solve chaotic financial system. British journal of Mathematics and Computer Science, 13(4),1-14.https://doi/10.9734/SBJMCS/2016/22102.
[4] Ricardo, H. J. (2021). A modern introduction to differential equations (Third Ed.). Science direct
[5] Butcher, J. C. (1966). On the convergence of numerical solutions to ordinary differential equations. Math. Comp. 20, 1-10.
[6] Onumanyi, P., Awoyemi, D. O., Jator, S. N., and Sirisena, U.W. (1994). New linear multistep methods with continuous coefficients for first order IVPs. Journal of NMS. 31(1), 37–51.
[7] Onumanyi, P., Sirisena, U. W., and Jator, S. N. (1999). Continuous finite difference approximations for solving differential equations, International Journal of Computer Mathematics **72** (1999) 15. https://dx.doi.org/10.1260/1748-3018.6.1.79.
[8] Lambert, J. D. (1973). Computational methods in ordinary differential equations. New York, John Willey and Sons.
[9] Fatunla, S. O. (1980). Numerical integrators for stiff and highly oscillatory differential equations. Journal of Mathematical Computation. 373. https://doi/10.1090/S0025-5718-1980-0559191-X
[10] Henrici, P. (1962). Discrete variable methods in ordinary differential equations. New York: John Willey, pp 407.
[11] Okuonghae, R. I., and Ikhile, M. N. O. (2011). Continuous Formulation of A(α)-Stable Second Derivative Linear Multistep Methods for Stiff initial values problems in ordinary differential equations. Journal of Algorithms & Computational Technology, vol. 6, 175-190.
https://dx.doi.org/10.1080/00207169908804831.
[12] Dahlquist, G. (1963). A special stability problem for linear multistep methods. Bit.27-43.
[13] Genesio, R., Tesi, A. (1992): A harmonic balance methods for the analysis of chaotic dynamics in nonlinear systems. Automatica, 28, 531-548
https://doi.org/10.1016/0005-1098(92)90177-H.
[14] Rössler, O. E. (1976). An equation for continuous chaos. Phys. Lett. A 57(5), 397–398.
[15] Yao, L. S. (2010). Computed chaos or numerical errors, Nonlinear Analysis Modelling and Control **15**, 109. https://doi.10.15388/NA.2010.15.1.14368.

Mathematical fractional model for the dynamics and control of Diphtheria transmission

E. Abah[*], B. Bolaji[†], W. Atokolo[‡§], G.O. Acheneje[¶], B.I. Omede[‖], J. Amos[*,**] and D. Omeje[††]

Abstract

Diphtheria is an acute bacterial infection primarily affecting the upper respiratory tract, caused by Corynebacterium diphtheriae. This study uses a fractional-order mathematical model to assess the effects of therapy and vaccination on diphtheria transmission dynamics. Initially, the model employs integer-order nonlinear differential equations with minimal vaccination and treatment. To better understand disease dynamics, it is then adapted with fractional-order derivatives and power laws. The research includes a stability analysis of the endemic equilibrium using the Lyapunov function approach and establishes conditions for the existence and uniqueness of solutions in the fractional-order model. To explore factors influencing disease spread, a sensitivity analysis of the basic reproduction number was conducted. Numerical simulations using the fractional Adams–Bashforth–Moulton method offer insights into how model parameters and fractional-order values impact diphtheria dynamics and control. Additional simulations with surface and contour plots revealed that higher contact rates and lower vaccine efficiency would increase diphtheria prevalence. Conversely, improving treatment and immunization programs is expected to reduce the incidence of diphtheria in the general population.

Keywords and phrases: Diphtheria; fractional; Adam-Bashforth-Moulton; transmission

1 Introduction

Exotoxins produced by Corynebacterium bacteria, which cause diphtheria, are known to cause damage to human tissue [1]. Hippocrates, in the fifth century BC, is the first recorded mention of this illness, which has afflicted humans for ages. For a long time, diphtheria has been a leading cause of infant mortality and a devastating menace in both industrialized and developing countries [2]. Many individuals in contemporary and emerging nations are still susceptible to diphtheria despite extensive immunization [3]. The disease is endemic in a number of places, including Brazil, the tropics, South America, Africa, and India, even in locations with high exposure over a period of five to ten years, as recorded cases continue to occur[4],[5],[6]. In the Russian Federation, diphtheria has been on the rise since the early 1990s and has spread to all of the Newly Independent States (NIS). Between 64 Percent

[*]E-mail: abahemmanuel1995@gmail.com; Department of Mathematics Sciences, Prince Abubakar Audu University, Anyiba, Nigeria

[†]Department of Mathematics Sciences, Prince Abubakar Audu University, Anyigba, Nigeria; E-mail: bolarinwa.s.bolaji@gmail.com

[‡]Corresponding Author; E-mail: williamsatokolo@gmail.com

[§]Department of Mathematics Sciences, Prince Abubakar Audu University, Anyigba, Nigeria

[¶]Department of Mathematics Sciences, Prince Abubakar Audu University, Anyigba, Nigeria; E-mail: achenejegodwin@gmail.com

[‖]Department of Mathematics Sciences, Prince Abubakar Audu University, Anyigba, Nigeria; E-mail: benjaminomede197@gmail.com

[**]Department of Mathematics Sciences, Prince Abubakar Audu University, Anyigba, Nigeria; E-mail: amosjeremiah1997@gmail.com

[††]Department of Mathematics Sciences, Prince Abubakar Audu University, Anyigba, Nigeria; E-mail: omejedaniel3269@gmail.com

and 82 percent of people over the age of 15 contract diphtheria each year; by 1999, this had resulted in a considerable number of cases and fatalities. Nearly half of all deaths in several nations occur in individuals between the ages of 40 and 49, who are disproportionately impacted; cases in adults over 50 are less common [3]. The bacteria readily attach themselves to the tissue in the throat, releasing exotoxins that eventually cause a pseudo membrane to form [7],[8]. The initial set of symptoms resembles those of the flu, but they also include fever, swollen lymph nodes, coughing, hoarseness, and shortness of breath. Additionally, some patients may have skin involvement that leads to skin ulcers. Ill health and compromised respiratory defenses increase the severity of diphtheria [9]. The study of mathematical epidemiology has made significant contributions to our understanding of the dynamics of infectious illnesses, their effects, and potential future spread forecasts. Different prevention, detection, control, and rehabilitation programs are compared, evaluated, planned, implemented, and optimized using mathematical models.

To help medical professionals reduce the disease loads of infectious diseases within any community, a variety of mathematical models have been developed by various authors. When studying and examining the dynamics of infectious disease transmission within a population, these models are a priceless resource. For example, Atokolo et al [10] formulated strategies for limiting the Zikavirus's propagation and investigated the fractional order sterile insect technology (SIT) paradigm. The model's analytical solution was created using the Laplace–Adomian decomposition method (LADM), and it perfectly converges to the right value. The response behaviors of the model are more flexible due to its fractional order structure. The report notes that, to the best of current knowledge, this is the first instance of using LADM to solve a SIT model. In order to investigate the epidemiology of Lassa fever, Atokolo et al. [11] combined integer-order nonlinear differential equations with fractional-order derivatives to create a fractional-order mathematical model that allowed them to analyze the dynamics of the illness. Numerical simulations indicate that lower vaccine effectiveness and greater contact rates are positively correlated with the prevalence of Lassa disease. Improving vaccination and treatment plans may help lower this incidence, the report suggests. A stability analysis of the endemic equilibrium is also included in the work. Agahiu et al. [12] offered a mathematical model designed to comprehend the dynamics of the co-infections of the Zika and Chikungunya viruses. The model uses the Laplace Adomians Decomposition Method (LADM) to account for the intricate interactions that take place between human populations and sick insects. Numerical models demonstrate that increasing bed net usage and decreasing mosquito biting rates might significantly control the dynamics of Zika-Chikungunya co-infections in Espirito Santo State, Brazil. Odionyenma et al. [13] provided a fractional derivative model that analyzes the dynamics of the co-infection between Chlamydia and Gonorrhea while ensuring positivity boundedness and uniqueness using the Laplace transform and fixed point theorems. It demonstrates Ulam-Hyers-Rassias stability in comparison to conventional integer-order models, indicating its robustness in accurately and realistically describing the dynamics of Chlamydia-Gonorrhea co-infection. Zhang et al. [14] offered a novel mathematical model for analyzing the COVID-19 pandemic that takes into account five distinct categories: susceptible, exposed, infected, isolated, and recovered people. Using the adaptive predictor-corrector algorithm and the fourth-order Runge-Kutta method, the paper investigates the numerical approximations and dynamics of the model, addressing themes such as positivity, boundedness, basic reproduction number calculation, asymptotic stability, and simulation methodologies. The theoretical conclusions are corroborated by the study's numerical simulations. Ghani et al. [15] offered a fractional mathematical model with variables for innate immunity, treatment, and vaccination for studying diphtheria. The model consists of five compartments: exposed, infected, isolated, recovered, and vulnerable individuals. Analytical proofs are provided for the model's well-posedness, stability characteristics, and predictor-corrector scheme. Numerical simulations are validated using the least squares method, and results are reported that are comparable across different fractional orders. Mangal et al. [16] studied how vaccination campaigns and booster doses affect highly contagious diseases using a fractional-order epidemic model. It looks into stability analysis, Hopf bifurcation occurrences, and the dynamics of disease transmission. The research concludes that awareness programs are a more effective strategy to reduce outbreaks than booster immunizations,

after validating the model with real COVID-19 patient data from Canada and Norway. Rajan et al. [17] used a fractional modeling method to investigate the dynamics of HPV transmission and the connection between HPV and cervical cancer. Compartmental modeling is utilized to identify vulnerable, infected, and recovered populations. The model incorporates a Caputo fractional derivative to account for the development of non-local illnesses and long-term memory effects. The Banach fixed point theorem, Lyapunov functions, and numerical simulations are used in the study to validate its theoretical findings. According to the research, vaccination campaigns can help prevent HPV infection and reduce the risk of cervical cancer. Yunus and Olayiwola [18] highlighted the significance of COVID-19 vaccinations for Nigeria's pandemic control plan. It uses mathematical modeling at the fractional order to evaluate the duration, effectiveness, and impact of immunization campaigns. The findings indicate that immunization strategies with integer ordering are particularly effective in stopping the COVID-19 virus from spreading. As a critical public health measure, the study emphasizes the need for coordinated international efforts to increase vaccination uptake. According to Akogwu [19], the Differential Transform Method (DTM) was employed to obtain the series solution of the SIRV COVID-19 model in Nigeria. The validity of the DTM in solving the model was confirmed through comparison with Maple 21's Classical fourth-order Runge-Kutta method (RK4). The comparison between DTM and RK4 solutions showed a good correlation, validating the accuracy and efficiency of the DTM in solving the model.

The following are the goals of this paper:

- In the fractional instance, establish conditions that guarantee the existence and uniqueness of the model's solution.
- Describe the Lyapunov function approach's stability study of the endemic equilibrium point.
- perform the sensitivity analysis of the model
- Utilizing the fractional Adams–Bashforth–Moulton approach, ascertain numerical solutions.

We found that no research has evaluated the transmission dynamics and control of Diphtheria using a fractional calculus approach combined with the Adams–Bashforth–Moulton method to obtain numerical simulations of the model, despite reviewing several studies on mathematical models and transmission dynamics.

The rest of this essay is structured as follows: The model's formulation is covered in Section 2, its analysis is presented in Section 3, the fractional-order model's numerical findings are presented in Section 4, and concluding thoughts are provided in Section 5.

1.1 Preliminary

In this section, we cover several fundamental concepts and findings from fractional calculus. In this investigation, the fractional Caputo derivatives on the right and left will be utilized [20],[21] . The use of fractional calculus to simulate real-world issues in physics, engineering, biomathematics, and other scientific domains is also highlighted in this work.

Definition 1: let $f \in \Lambda^{\infty}(R)$, then the right and left Function's Caputo fractional derivative f is given by:

$$ {}^{b}D_{t}^{\alpha} f(t) = \left(t^{0}D_{t}^{-(p-\alpha)} \left(\frac{d}{dt} \right)^{p} f(t) \right) $$

$$ {}^{b}D_{t}^{\alpha} f(t) = \frac{1}{\Gamma(p-\alpha)} \int_{0}^{t} \left((t-\lambda)^{p-\alpha-1} f^{p}(\lambda) \right) d\lambda \tag{1} $$

similarly

$$ {}_{T}^{b}D_{t}^{\alpha}f(t)=\left({}_{t}D_{T}^{-(p-\alpha)}\left(\frac{-d}{dt}\right)^{p}f(t)\right) $$

$$ {}_{T}^{b}D_{T}^{\alpha}f(t)=\frac{(-1)^{p}}{\Gamma\left(p-\alpha\right)}\int_{t}^{T}\left((\lambda-t)^{p-\alpha-1}f^{p}\left(\lambda\right)\right)d\lambda $$

Definition 2: The Mittag-Leffler function in generalized form $E_{\phi,\beta}\left(x\right)$ for $x\in R$ is given by:

$$ E_{\phi,\beta}\left(x\right)=\sum_{p=0}^{\infty}\frac{x^{p}}{\Gamma\left(\phi p+\beta\right)},\ \alpha,\beta>0 \tag{2} $$

This alternatively can be shown as

$$ E_{\phi,\beta}\left(x\right)=xE_{\phi,\phi+\beta(x)}+\frac{1}{\Gamma\left(\beta\right)} \tag{3} $$

The function $t^{\beta-1}E_{\phi,\beta}\left(\pm\psi t^{\phi}\right)$is Laplace transformed as

$$ L\left[t^{\beta-1}E_{\phi,\beta(\pm\psi t^{\phi})}\right]\ =\frac{S^{\phi-\beta}}{S^{\phi}\pm\psi} \tag{4} $$

1.2 Proposition

Let $f\in\Lambda^{\infty}(R)\cap b\left(R\right)$ and $\phi\in R,\ p-1<\phi<p$, Consequently, the following requirements are met:

- $$ {}_{t_0}^{b}D_{t}^{\alpha}I^{\alpha}f\left(t\right)=f\left(t\right) $$
- $$ I_{t_0}^{\alpha}D_{t}^{\alpha}f\left(t\right)=f\left(t\right)-\sum\nolimits_{k=0}^{p-k}\frac{t^{k}}{k!}f^{k}\left(t_{o}\right). $$

2 Methodology/Model formulation

The total number of individuals at time t, indicated $N(t)$, is divided into (7) mutually exclusive compartments of susceptible individual $S_d(t)$, Exposed individuals to diphtheria$E_d\left(t\right)$, Vaccinated individual with diphtheria $V_d\left(t\right)$, infected individual with diphtheria $I_d\left(t\right)$, treatment class for individuals with diphtheria$T_d\left(t\right)$, Bacteria Class $B(t)$, and Set of individual that recovered from the disease $R_d\left(t\right)$. Humans' population is represented as;

$$ N\left(t\right)=S_d\left(t\right)+E_d\left(t\right)+I_d\left(t\right)+T_d\left(t\right)+V_d\left(t\right)+R_d\left(t\right) $$

The bacteria class is denoted $B(t)$

Diphtheria Susceptible Individuals S_d is recruited at the rate of Λ, the class reduces by natural death rate μ as well as by the percentage of those that contract the disease after coming into touch with a human who has diphtheria I_d at rates of β and β_1. This class also reduces by the rate α, These susceptible individuals grow by the rate ψ at which the vaccination wanes so that the vaccinated become susceptible again at the rate ω. the dynamics of this class is formulated as;

$$ \frac{dS_d}{dt}=\Lambda-\left(\frac{\beta IS}{N}+\frac{\beta_1 B}{K+B}\right)S_d+\omega R_d+\psi V_d-\alpha S_d-\mu S_d $$

Diphtheria Exposed Individuals E_d rises due to the percentage of people who contract new infections at a rate of β and β_1 respectively. This class reduces by the rate at which the exposed becomes fully infected at rate θ and by natural death rate μ. This population is formulated as follows;

$$\frac{dE_d}{dt} = \left(\frac{\beta I_d S_d}{N} + \frac{\beta_1 B}{K+B}\right) S_d - (\theta + \mu) E_d$$

Diphtheria infected Individuals I_d grows as a result of the exposed class's advancement to the infected class at rate θ. this class reduces by natural mortality rate μ , death due to disease at rate $\delta$and the rate at which the infected are taken for treatment σ, The dynamics of this class is formulated as;

$$\frac{dI_d}{dt} = \theta E_d - (\sigma + \delta + \mu) I_d$$

Diphtheria infected Individuals T_d increases in proportion to the rate at which the afflicted are treated σ, due to both disease induced and natural death at rate δ and μ respectively. Finally, the class reduces as a result of recovery at the rate ε of the treated individuals. The following is a presentation of this population's dynamics;

$$\frac{dT_d}{dt} = \sigma I_d - (\varepsilon + \phi\delta + \mu) T_d$$

Vaccinated individuals against diphtheria V_d population grows due to vaccination rate α and eventually diminishes as a result of the declining vaccination rate and natural death at rate ψ and μ respectively. The dynamics of people who have received a diphtheria vaccination are modeled as follows;

$$\frac{dV_d}{dt} = \alpha S_d - (\psi + \mu) V_d$$

Bacteria class B population grows due to the shedding rate of the bacteria into the infected and treatment classes at the rate P_1 and P_2 respectively. The population reduces by natural death rate μ_B. The following is a presentation of this population's dynamics;

$$\frac{dB}{dt} = P_1 I_d + P_2 T_d - \mu_B B$$

Diphtheria recovered individuals R_d grows due to treatment recovery rate ε. The class eventually decreases because of how quickly the recovered individuals become vulnerable at the rate ω and natural death rate μ.

$$\frac{dR_d}{dt} = \varepsilon T_d - (\omega + \mu) R_d$$

The population-related force of infection is $\lambda = \frac{\beta I_d S_d}{N} + \frac{\beta_1 B}{K+B}$

The model flow diagram that aligns with our hypothesis is displayed in Fig. 1; Similarly, the following describes the mathematical model that matches our presumptions and the above description:

$$\left.\begin{array}{l} \frac{dS_d}{dt} = \Lambda - \lambda S_d + \omega R_d + \psi V_d - \alpha S_d - \mu S_d, \\ \frac{dE_d}{dt} = \lambda S_d - (\theta + \mu) E_d, \\ \frac{dI_d}{dt} = \theta E_d - (\sigma + \delta + \mu) I_d, \\ \frac{dT_d}{dt} = \sigma I_d - (\varepsilon + \phi\delta + \mu) T_d, \\ \frac{dV_d}{dt} = \alpha S_d - (\psi + \mu) V_d, \\ \frac{dB}{dt} = P_1 I_d + P_2 T_d - \mu_B B, \\ \frac{dR_d}{dt} = \varepsilon T_d - (\omega + \mu) R_d. \end{array}\right\} \quad (5)$$

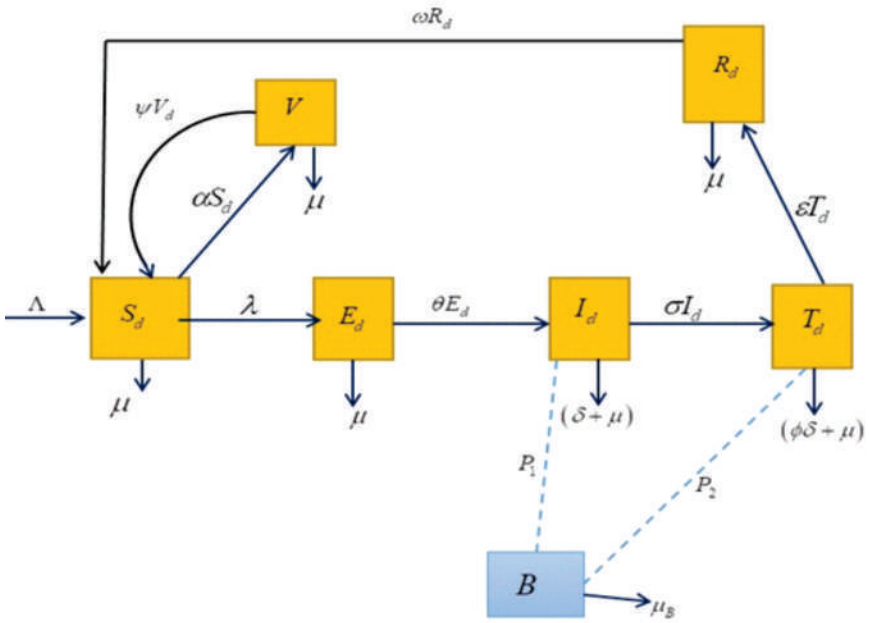


Figure 1: model schematic flow diagram.

2.1 Fractional Diphtheria mathematical model

Using the Caputo fractional derivative operator, we expand the integer model of Diphtheria given in Eq. (5) in this section. Compared to the classical model given in Eq. (5), the new model presented using the Caputo fractional derivative operator has a higher degree of freedom because the output of the fractional order model can be modified to have different responses. Thus, the fractional Diphtheria technique is explained as follows:

$$\left.\begin{aligned} {}^{b}D_t^{\alpha}S_d &= \Lambda - \lambda S_d + \omega R_d + \psi V_d - \alpha S_d - \mu S_d,\\ {}^{b}D_t^{\alpha}E_d &= \lambda S_d - M_1 E_d,\\ {}^{b}D_t^{\alpha}I_d &= \theta E_d - M_2 I_d,\\ {}^{b}D_t^{\alpha}T_d &= \sigma I_d - M_3 T_d,\\ {}^{b}D_t^{\alpha}V_d &= \alpha S_d - M_4 V_d,\\ {}^{b}D_t^{\alpha}B &= P_1 I_d + P_2 T_d - \mu_B,\\ {}^{b}D_t^{\alpha}R_d &= \varepsilon T_d - M_5 R_d. \end{aligned}\right\} \tag{6}$$

Where $M_1 = (\theta + \mu)$, $M_2 = (\sigma + \delta + \mu)$, $M_3 = (\varepsilon + \phi\delta + \mu)$, $M_4 = (\psi + \mu)$, and $M_5 = (\omega + \mu)$. Assuming favorable initial conditions

$$S_d(0) = S_{d0}, E_d(0) = E_{d0}, I_d(0) = I_{d0}, T_d(0) = T_{d0}, V_d(0) = V_{d0}, B(0) = B_0, R_d(0) = R_{d0}. \tag{7}$$

3 Analysis of the model

3.1 Positivity of model solution

We took the initial values' non-negativity into account.

$$\lim Sup.N(t) \leq \frac{\lambda}{\mu},$$

Secondly, If $\lim Sup.N_0(t) \leq \frac{\lambda}{\mu}$, then the feasible domain of our model is provided by;

$$\Omega = \left\{ (S_d, E_d, I_d, T_d, V_d, B, R_d) \subset R_+^7 : S_d + E_d + I_d + T_d + V_d + B + R_d \leq \frac{\lambda}{\mu}, \right\}$$

so that

$$\Omega \subset R_+^7,$$

Hence $\Omega$is positively invariant.

if $S_{d0}, E_{d0}, I_{d0}, T_{d0}, V_{d0}, B_0, R_{d0}$ are non-negative, therefore model (6)'s solution will also be non-negative for $t > 0$ Selecting the first equation from Eq. (6), we have that

$${}^bD_t^\alpha S_d = \Lambda - (\lambda + \alpha + \mu) S_d + \omega R_d + \psi V_d,$$

$${}^bD_t^\alpha S_d + (\lambda + \alpha + \mu) S_d = \Lambda + \omega R_d + \psi V_d,$$

But

$$\Lambda + \omega R_d + \psi V_d \geq 0,$$

then

$${}^bD_t^\alpha S_d + (\lambda + \alpha + \mu) S_d \geq 0$$

Using the acquired Laplace transform;

$$L\left[{}^bD_t^\alpha S_d\right] + L\left[(\lambda + \alpha + \mu) S_d\right] \geq 0$$

$$S^\alpha S_d(s) - S^{\alpha-1} S_d(0) + (\lambda + \alpha + \mu) S_d(s) \geq 0,$$

$$S_d(t) \geq \frac{S^{\alpha-1}}{(S^\alpha + (\lambda + \alpha + \mu))} S_{d0}.$$

Using the inverse Laplace transform, we were able to obtain;

$$S_d(t) \geq E_{\alpha,1}\left(-(\lambda + \alpha + \mu)\right) S_{d0} \tag{8}$$

Given that the term in Eq. (8) on the right is positive, we can now deduce that $S_d \geq 0$ for $t \geq 0$ In the same way, we also have that $E_d \geq 0\,, I_d \geq 0\,, T_d \geq 0\,, V_d \geq 0\,, B \geq 0\,, R_d \geq 0$, since they are positive aspects, the solution will continue to be in for all with positive initial conditions.

3.2 Boundedness of fractional model solution

The total number of people in our model is provided by;

$$N(t) = S_d(t) + E_d(t) + I_d(t) + T_d(t) + V_d(t) + R_d(t).$$

Thus, using our fractional model (6), we can now

$${}^bD_t^\alpha N(t) = {}^bD_t^\alpha S_d(t) + {}^bD_t^\alpha E_d(t) + {}^bD_t^\alpha I_d(t) + {}^bD_t^\alpha T_d(t) + {}^bD_t^\alpha V_d(t) + {}^bD_t^\alpha R_d(t).$$

$${}^bD_t^\alpha N(t) = \Lambda - \mu N(t) \tag{9}$$

Using (9)'s Laplace transformation, we arrived at;

$$L\left[{}^{b}D_{t}^{\alpha}N(t)\right] \leq L\left[\Lambda - \mu N\left(t\right)\right],$$

$$S^{\alpha}N(S) - S^{\alpha-1}N(0) + \mu N(S) \leq \frac{\lambda}{S},$$

$$N(s) \leq \frac{S^{\alpha-1}}{(S^{\alpha}+\mu)}N(0) + \frac{\Lambda}{S\left(S^{\alpha}+\mu\right)} \tag{10}$$

Taking Eq. (10)'s inverse Laplace transform gave us;

$$N(t) \leq E_{\alpha,1}\left(-\mu t^{\alpha}\right)N(0) + \Lambda E_{\alpha,\alpha+1}\left(-\mu t^{\alpha}\right) \tag{11}$$

At $t \to \infty$, the limit of Eq. (11) becomes

$$\lim_{t\to\infty} SupN\left(t\right) = \frac{\Lambda}{\mu}.$$

This means that, if $N \leq \frac{\Lambda}{\mu}$ which implies that, $N(t)$is bounded. We therefore draw the conclusion that epidemiologically, this region Ω is similarly plausible and well posed.

3.3 Existence and uniqueness of our model solution

Let T be a real nonnegative number, given that $Z = [0, T]$. The collection of every continuous function defined on$Z$ is denoted by $N_e^0 Z$ with norm as

$$\|G\| = \sup\left\{\left|G\left(t\right)\right| t, \in Z\right\}.$$

Taking into account model (6) with the starting conditions given in (7), which is modeled as an initial value problem (IVP) in (12)

$$D_t^{\alpha}G\left(t\right) = Q\left(t, G\left(x\right)\right), 0 < t < T < \infty,$$

$$G\left(0\right) = G_0. \tag{12}$$

where $G\left(t\right) = \left(S_d\left(t\right), E_d\left(t\right), I_d\left(t\right), T_d\left(t\right), V_d\left(t\right), B\left(t\right), R_d\left(t\right)\right)$ symbolizes the classes, and Q is a continuous function with the following definition;

$$Q_1\left(t, G\left(t\right)\right) = \begin{pmatrix} Q_1\left(t, S_d\left(t\right)\right) \\ Q_2\left(t, E_d\left(t\right)\right) \\ Q_3\left(t, I_d\left(t\right)\right) \\ Q_4\left(t, T_d\left(t\right)\right) \\ Q_5\left(t, V_d\left(t\right)\right) \\ Q_6\left(t, B\left(t\right)\right) \\ Q_7\left(t, R_d\left(t\right)\right) \end{pmatrix} = \begin{pmatrix} \Lambda - \left(\frac{\beta IS}{N} + \frac{\beta_1 B}{K+B}\right)S_d + \omega R_d + \psi V_d - \alpha S_d - \mu S_d \\ \left(\frac{\beta I_d S_d}{N} + \frac{\beta_1 B}{K+B}\right)S_d - \left(\theta + \mu\right)E_d \\ \theta E_d - \left(\sigma + \delta + \mu\right)I_d \\ \sigma I_d - \left(\varepsilon + \phi\delta + \mu\right)T_d \\ \alpha S_d - \left(\psi + \mu\right)V_d \\ P_1 I_d + P_2 T_d - \mu_B \\ \varepsilon T_d - \left(\omega + \mu\right)R_d \end{pmatrix} \tag{13}$$

Using proposition (2.1), we have that,

$$\begin{gathered}
S_d(t) = S_{d0} + I_t^{\alpha}\left[\Lambda - \left(\frac{\beta IS}{N} + \frac{\beta_1 B}{K+B}\right) S_d + \omega R_d + \psi V_d - \alpha S_d - \mu S_d\right], \\
E_d(t) = E_{d0} + I_t^{\alpha}\left[\left(\frac{\beta I_d S_d}{N} + \frac{\beta_1 B}{K+B}\right) S_d - (\theta+\mu) E_d\right] \\
I_d(t) = I_{d0} + I_t^{\alpha}\left[\theta E_d - (\sigma+\delta+\mu) I_d\right], \\
T_d(t) = T_{d0} + I_t^{\alpha}\left[\sigma I_d - (\varepsilon+\phi\delta+\mu) T_d\right], \\
V_d(t) = V_{d0} + I_t^{\alpha}\left[\alpha S_d - (\psi+\mu) V_d\right], \\
B(t) = B_0 + I_t^{\alpha}\left[P_1 I_d + P_2 T_d - \mu_B\right], \\
R_d(t) = R_d + I_t^{\alpha}\left[\varepsilon T_d - (\omega+\mu) R_d\right].
\end{gathered} \tag{14}$$

Here is how we get the Picard iteration of (14):

$$\begin{gathered}
S_d(t) = S_{d0} + \frac{1}{\Gamma(\alpha)}\int_0^t (t-\lambda)^{\alpha-1} Q_1\left(\lambda, S_{d(n-1)}(\lambda)\right) d\lambda, \\
E_d(t) = E_{d0} + \frac{1}{\Gamma(\alpha)}\int_0^t (t-\lambda)^{\alpha-1} Q_2\left(\lambda, E_{d(n-1)}(\lambda)\right) d\lambda, \\
I_d(t) = I_{d0} + \frac{1}{\Gamma(\alpha)}\int_0^t (t-\lambda)^{\alpha-1} Q_3\left(\lambda, I_{d(n-1)}(\lambda)\right) d\lambda, \\
T_d(t) = T_{d0} + \frac{1}{\Gamma(\alpha)}\int_0^t (t-\lambda)^{\alpha-1} Q_4\left(\lambda, T_{d(n-1)}(\lambda)\right) d\lambda, \\
V_d(t) = V_{d0} + \frac{1}{\Gamma(\alpha)}\int_0^t (t-\lambda)^{\alpha-1} Q_5\left(\lambda, V_{d(n-1)}(\lambda)\right) d\lambda, \\
B(t) = B_0 + \frac{1}{\Gamma(\alpha)}\int_0^t (t-\lambda)^{\alpha-1} Q_6\left(\lambda, B_{(n-1)}(\lambda)\right) d\lambda, \\
R_d = R_{d0} + \frac{1}{\Gamma(\alpha)}\int_0^t (t-\lambda)^{\alpha-1} Q_7\left(\lambda, R_{d(n-1)}(\lambda)\right) d\lambda.
\end{gathered} \tag{15}$$

Now, we changed the initial value problem in Eq. (12) to get ;

$$G(t) = G(0) + \frac{1}{\Gamma(\alpha)}\int_0^t (t-\lambda)^{\alpha-1} Q(\lambda, G(\lambda))\, d\lambda. \tag{16}$$

Lemma 1, Vector satisfies the Lipchitz requirement as stated in Eq. (13) $Q(t, G(t))$ on a set $[0,T]\times R_+^7$ with the Lipchitz constant given as;

$$\zeta = \max\left(\begin{array}{l}(\beta^* + \beta_1^* + \mu), (\theta+\mu), (\sigma+\delta+\mu), (\varepsilon+\phi\delta+\mu), \\ \mu_B, (\psi+\mu), (\omega+\mu).\end{array}\right)$$

Proof

$$\begin{gathered}
\|Q_1(t,S) - Q_1(t,S)\| \\
\left\| \begin{array}{l} \Lambda - \left(\left(\frac{\beta IS}{N} + \frac{\beta_1 B}{K+B}\right) + \mu\right) S_d - \alpha S_d + \omega R_d + \psi V_d \\ - \left(\Lambda - \left(\left(\frac{\beta IS}{N} + \frac{\beta_1 B}{K+B}\right) + \mu\right)\right) S_{d1} - (\alpha S_d + \omega R_d + \psi V_d) \end{array} \right\| \\
\left\| - \left(\frac{\beta IS}{N} + \frac{\beta_1 B}{K+B}\right)(S_d - S_{d1}) + \mu(S_d - S_{d1}) \right\|
\end{gathered}$$

$$\leq \left(\beta_1^* + \beta_{1,2}^*\right) \|(S_d - S_{d1})\| + \|\mu\,(S_d - S_{d1})\|$$

$$\|Q_1\,(t, S_d) - Q_1\,(t, S_{d1})\| \leq \left(\beta_1^* + \beta_{1,2}^* + \mu\right) \|S_d - S_{d1}\|\,.$$

Likewise, we discovered the following:

$$\begin{aligned}
\|Q_2\,(t, E_d) - Q_2\,(t, E_{d1})\| &\leq (\theta + \mu)\,\|E_d - E_{d1}\|\,, \\
\|Q_3\,(t, I_d) - Q_3\,(t, I_{d1})\| &\leq (\sigma + \delta + \mu)\,\|I_d - I_{d1}\|\,, \\
\|Q_4\,(t, T_d) - Q_4\,(t, T_{d1})\| &\leq (\varepsilon + \phi\delta + \mu)\,\|T_d - T_{d1}\|\,, \\
\|Q_5\,(t, V_d) - Q_5\,(t, V_{d1})\| &\leq (\psi + \mu)\,\|V_d - V_{d1}\|\,, \\
\|Q_6\,(t, B) - Q_6\,(t, B_1)\| &\leq \mu_B\,\|B - B_1\|\,, \\
\|Q_7\,(t, R_d) - Q_7\,(t, R_{d1})\| &\leq (\omega + \mu)\,\|R_d - R_{d1}\|\,,
\end{aligned} \tag{17}$$

Where we obtained

$$\|Q\,(t, G\,(t)) - Q\,(t, G_2\,(t))\| \leq \zeta\,\|G_1 - G_2\|\,.$$

$$\zeta = \max\left(\begin{array}{l} (\beta^* + \beta_1^* + \mu)\,, (\theta + \mu)\,, (\sigma + \delta + \mu)\,, (\varepsilon + \phi\delta + \mu)\,, \\ \mu_B, (\psi + \mu)\,, (\omega + \mu)\,. \end{array}\right) \tag{18}$$

Lemma 2. There is a solution to the initially value problems (6), (7) in Eq. (18).

$$G\,(t) \in L_c^0\,(F)\,.$$

We examine the solution of using fixed point theory and Picard-Lindel of $G\,(t) = S\,(G\,(t))$, When the Picard operator, represented as S, is defined as;

$$S : L_C^0\left(F, R_+^*\right) \to L_C^0\left(F, R_+^7\right).$$

$$S\,(G\,(t)) = G\,(0) + \frac{1}{\Gamma\,(\alpha)} \int_0^t (t - \lambda)^{\alpha - 1} G\,(\lambda, G\,(\lambda))\,d\lambda$$

$$\|S\,(G_1\,(t)) - S\,(G_2\,(t))\|$$

$$\left\| \frac{1}{\Gamma\,(\alpha)} \int_0^t (t - \lambda)^{\alpha - 1}\,[Q\,(\lambda, G_1\,(\lambda)) - Q\,(\lambda, G_2\,(\lambda))\,d\lambda] \right\|$$

$$\leq \frac{1}{\Gamma\,(\alpha)} \int_0^t (t - \lambda)^{\alpha - 1}\,\|Q\,(\lambda, G_1\,(\lambda)) - Q\,(\lambda, G_2\,(\lambda))\,d\lambda\|$$

$$\leq \frac{\zeta}{\Gamma\,(\alpha)} \int_0^t (t - \lambda)^{\alpha - 1}\,\|G_1 - G_2\|\,d\lambda$$

$$\|S\,(G_1\,(t)) - S\,(G_2\,(t))\| \leq \frac{\zeta}{\Gamma\,(\alpha + 1)\,S}$$

$\frac{\zeta}{\Gamma(\alpha+1)} S \leq 1$ the answer to Eqs. (6) and (7) is unique since the Picard operator produces a contradiction.

3.4 The basic reproduction number R_0 and model equilibrium points

The model (5)'s disease-free equilibrium point can be written as follows:

$$DDFEP = \left\{S_d^*, E_d^*, I_d^*, T_d^*, B^*, R_d^*\right\} = \left\{\frac{\Lambda\left(\alpha+\mu\right)}{\alpha\mu+\psi\mu+\mu^2}0,0,0,0,\frac{\Lambda\alpha}{\alpha\mu+\psi\mu+\mu^2},0\right\} \tag{19}$$

We utilize the procedure described by [22] to calculate the fundamental reproduction number.

Let $u = (E_d, I_d, T_d, B)$

So, that $\frac{du}{dt} = F - V$

Where; $F = \begin{bmatrix} 0 & \frac{\beta(\psi+\mu)}{\alpha+\psi+\mu} & 0 & \frac{\Lambda\beta_1}{\mu K} \\ 0 & 0 & 0 & 0 \\ 0 & 0 & 0 & 0 \\ 0 & 0 & 0 & 0 \end{bmatrix}$, $V = \begin{bmatrix} M_1 & 0 & 0 & 0 \\ -\theta & M_2 & 0 & 0 \\ 0 & -\sigma & M_3 & 0 \\ 0 & -P_1 & -P_2 & \mu_B \end{bmatrix}$ Mathematically, the basic reproduction number is computed as $R_0 = \rho\left(FV^{-1}\right)$ where ρ is the dominant Eigen value of the system is the dominant Eigen value of the system $\left(FV^{-1}\right)$. Where R_0^d is the basic reproduction number associated with the individuals in the population.

$$R_0 = \frac{\theta\left(\mu K M_3\mu_B\beta\left(\psi+\mu\right)+\left(\alpha+\psi+\mu\right)M_3P_1\Lambda\beta_1+\left(\alpha+\psi+\mu\right)P_2\sigma\Lambda\beta_1\right)}{\left(\alpha+\psi+\mu\right)M_1M_2\mu K M_3\mu_B} \tag{20}$$

Where $M_1 = (\theta+\mu)$, $M_2 = (\sigma+\delta+\mu)$, $M_3 = (\varepsilon+\phi\delta+\mu)$, $M_4 = (\psi+\mu)$, and $M_5 = (\omega+\mu)$.

3.5 Endemic equilibrium point

We looked into the potential for an endemic equilibrium point. Where the disease persists in the population, there is a positive stable state known as the endemic equilibrium point. The variables in the model are not zero at this equilibrium point.

$$(S_d^* \neq 0, E_d^* \neq 0,\ I_d^* \neq 0, T_d^* \neq 0, V_d^* \neq 0, B_d^* \neq 0 \; and \; R_H^* \neq 0)$$

The model equations are solved in terms of the force of infection linked with human populations in order to examine the endemic equilibrium point. Based on the fractional Diphtheria model (6), the endemic equilibrium state is symbolised as follows:

$$\eta^{**} = (S_d^{**}, E_d^{**},\ I_d^{**},\ T_d^{**}, V_d^{**}, B^{**},\ R_H^{**}),$$

Defined as;

$$S_d = \frac{\Lambda M_1M_2M_3M_4M_5}{M_2M_3M_5\left(\left(\alpha+\lambda+\mu\right)M_4-\alpha\psi\right)M_1-\lambda\omega\sigma\theta M_4}$$

$$E_d^{**} = \frac{\lambda\Lambda M_2M_3M_4M_5}{M_2M_3M_5\left(\left(\alpha+\lambda+\mu\right)M_4-\alpha\psi\right)M_1-\lambda\omega\sigma\theta M_4}$$

$$I_d^{**} = \frac{\theta\lambda\Lambda M_3M_4M_5}{M_2M_3M_5\left(\left(\alpha+\lambda+\mu\right)M_4-\alpha\psi\right)M_1-\lambda\omega\sigma\theta M_4}$$

$$T_d^{**} = \frac{\theta\lambda\Lambda M_4M_5\sigma}{M_2M_3M_5\left(\left(\alpha+\lambda+\mu\right)M_4-\alpha\psi\right)M_1-\lambda\omega\sigma\theta M_4}$$

$$V_d^{**} = \frac{\alpha\Lambda M_1M_2M_3M_5}{M_2M_3M_5\left(\left(\alpha+\lambda+\mu\right)M_4-\alpha\psi\right)M_1-\lambda\omega\sigma\theta M_4}$$

$$B^{**} = \frac{\left(\sigma P_2+M_3P_1\right)\Lambda M_5M_4\theta\lambda}{\mu_b\left(M_2M_3M_5\left(\left(\alpha+\lambda+\mu\right)M_4-\alpha\psi\right)M_1-\lambda\omega\sigma\theta M_4\right)}$$

$$R_d^{**} = \frac{\sigma M_4 \Lambda \theta \lambda}{M_2 M_3 M_5 \left(\left(\alpha + \lambda + \mu\right) M_4 - \alpha\psi\right) M_1 - \lambda\omega\sigma\theta M_4}$$

Where $M_1 = (\theta + \mu)$, $M_2 = (\sigma + \delta + \mu)$, $M_3 = (\varepsilon + \phi\delta + \mu)$, $M_4 = (\psi + \mu)$, and $M_5 = (\omega + \mu)$. Substituting the equations above into the force of infection $\lambda^{**} = \frac{\beta I}{N} + \frac{\beta_t B}{K+B}$ we obtained;

$$f(\lambda^{**}) = \lambda^{**} B_1 + B_2 = 0$$

$$B_1 = \left(\left(M_1 M_2 M_3 + \sigma\theta + M_2 M_3\right) M_5 + \sigma\theta\right) M_4 + \begin{pmatrix} -\sigma\theta P_2 - \theta M_3 P_1 + P_1\theta\left(\beta_1 + \beta\right) M_3 \\ +\sigma\theta P_2\left(\beta_1 + \beta\right) \end{pmatrix} M_5 {M_4}^2 \theta\omega\sigma$$
$$- \left(\left(M_1 M_2 M_3 + \sigma\theta + M_2 M_3\right) M_5 + \lambda\sigma\theta\right) M_4 - K M_1 M_2 M_3 \mu_b$$

$$B_2 = M_1 M_2 M_3 \left(\alpha + \lambda + \mu\right) M_5 \left(1 - \frac{\theta\left(\mu K M_3 \mu_B \beta\left(\psi + \mu\right) + \left(\alpha + \psi + \mu\right) M_3 P_1 \Lambda\beta_1 + \left(\alpha + \psi + \mu\right) P_2 \sigma\Lambda\beta_1\right)}{\left(\alpha + \psi + \mu\right) M_1 M_2 \mu K M_3 \mu_B}\right)$$

$$B_2 = M_1 M_2 M_3 \left(\alpha + \lambda + \mu\right) M_5 \left(1 - R_0\right)$$

From above we observed that for $\lambda^{**} > 1$ then $R_0 > 1$ Which implies that, the endemic equilibrium point of model (6) is stable.

3.6 Sensitivity Analysis of the Diphtheria Model

Sensitivity analysis is used to identify the factors that improve an infection's ability to spread and be controlled within a population. With regard to any parameter, let's say p, the sensitivity index of the reproduction number of the Diphtheria model is as follows:

$$\Im_p^{R_0} = \frac{\partial R_0}{\partial p} \times \frac{p}{R_0}$$

$$R_0 = \frac{\theta\left(\mu K M_3 \mu_B \beta\left(\psi + \mu\right) + \left(\alpha + \psi + \mu\right) M_3 P_1 \Lambda\beta_1 + \left(\alpha + \psi + \mu\right) P_2 \sigma\Lambda\beta_1\right)}{\left(\alpha + \psi + \mu\right) M_1 M_2 \mu K M_3 \mu_B}$$

$$\Im_\beta^{R_0} = \frac{\mu K \mu_B \left(\psi + \mu\right)\left(\delta\phi + +\mu\right)\beta}{\left(\alpha + \psi + \mu\right)\left(P_1\mu + \left(\delta\phi +\right) P_1 + \sigma P_2\right)\Lambda\beta_1 + \mu K \mu_B \left(\psi + \mu\right)\left(\delta\phi + +\mu\right)\beta} = 0.1003$$

$$\Im_\theta^{R_0} = \frac{\mu}{\theta + \mu} = 0.0763$$

$$\Im_\phi^{R_0} = -\frac{\delta\left(\alpha + \psi + \mu\right) P_2 \sigma\Lambda\beta_1\phi}{\left(\delta\phi + +\mu\right)\left(\left(\alpha + \psi + \mu\right)\left(P_1\mu + \left(\delta\phi +\right) P_1 + \sigma P_2\right)\Lambda\beta_1 + \mu K \mu_B \left(\psi + \mu\right)\left(\delta\phi + +\mu\right)\beta\right)} = -0.0008$$

$$\Im_\psi^{R_0} = \frac{\mu K \mu_B \alpha\beta\left(\delta\phi + +\mu\right)\psi}{\left(\alpha + \psi + \mu\right)\left(\left(\alpha + \psi + \mu\right)\left(P_1\mu + \left(\delta\phi +\right) P_1 + \sigma P_2\right)\Lambda\beta_1 + \mu K \mu_B \left(\psi + \mu\right)\left(\delta\phi + +\mu\right)\beta\right)} = 0.0516$$

$$\Im_\alpha^{R_0} = -\frac{\mu K \mu_B \left(\psi + \mu\right)\left(\delta\phi + +\mu\right)\beta\alpha}{\left(\alpha + \psi + \mu\right)\left(\left(\alpha + \psi + \mu\right)\left(P_1\mu + \left(\delta\phi +\right) P_1 + \sigma P_2\right)\Lambda\beta_1 + \mu K \mu_B \left(\psi + \mu\right)\left(\delta\phi + +\mu\right)\beta\right)} = -0.0532$$

$$\Im_\delta^{R_0} = -0.0159$$

$$\Im_\varepsilon^{R_0} = -\frac{\left(\alpha + \psi + \mu\right) P_2 \sigma\Lambda\beta_1}{\left(\delta\phi + +\mu\right)\left(\left(\alpha + \psi + \mu\right)\left(P_1\mu + \left(\delta\phi +\right) P_1 + \sigma P_2\right)\Lambda\beta_1 + \mu K \mu_B \left(\psi + \mu\right)\left(\delta\phi + +\mu\right)\beta\right)} = -0.4162$$

$$\Im_{P_1}^{R_0} = \frac{\left(\delta\phi + +\mu\right)\left(\alpha + \psi + \mu\right) P_1 \Lambda\beta_1}{\left(\alpha + \psi + \mu\right)\left(P_1\mu + \left(\delta\phi +\right) P_1 + \sigma P_2\right)\Lambda\beta_1 + \mu K \mu_B \left(\psi + \mu\right)\left(\delta\phi + +\mu\right)\beta} = 0.4615$$

$$\Im_\mu^{R_0} = -0.1441$$

$$\Im_{P_2}^{R_0} = \frac{\sigma\Lambda\beta_1 P_2\left(\alpha + \psi + \mu\right)}{\mu K \mu_B \left(\psi + \mu\right)\left(\delta\phi + +\mu\right)\beta + \left(\delta\phi + +\mu\right)\left(\alpha + \psi + \mu\right) P_1 \Lambda\beta_1 + \sigma\Lambda\beta_1 P_2\left(\alpha + \psi + \mu\right)} = 0.4383$$

$$\Im_{\mu_B}^{R_0} = -\frac{(\alpha+\psi+\mu)\,\Lambda\beta_1\,((\delta\phi++\mu)\,P_1+\sigma P_2)}{(\alpha+\psi+\mu)\,\Lambda\beta_1\,((\delta\phi++\mu)\,P_1+\sigma P_2)+\mu K\mu_B\,(\psi+\mu)\,(\delta\phi++\mu)\,\beta} = -0.8997$$

$$\Im_{\sigma}^{R_0} = -\frac{(\alpha+\psi+\mu)\,\Lambda\beta_1\,((\delta\phi++\mu)\,P_1+\sigma P_2)}{(\alpha+\psi+\mu)\,\Lambda\beta_1\,((\delta\phi++\mu)\,P_1+\sigma P_2)+\mu K\mu_B\,(\psi+\mu)\,(\delta\phi++\mu)\,\beta} = -0.4984$$

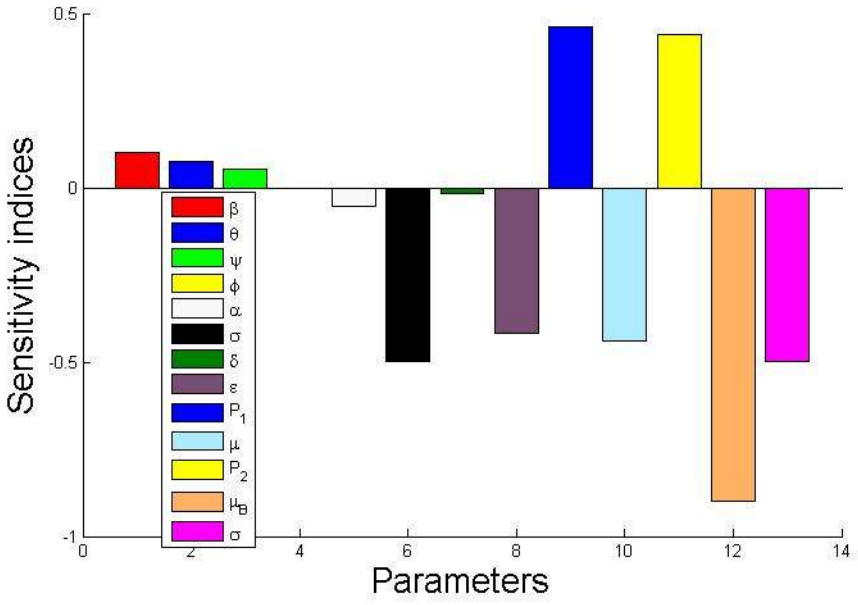


Figure 2: Bar chat of Diphtheria sensitivity Indices

3.7 Interpretation of the diphtheria Sensitivity Analysis

From the sensitivity analysis above, it is observed that the parameters like β, which is the contact rate of susceptible and infected humans, progression rate from exposed class to infected class θ, waning rate of vaccine ψ, shedding rate of bacteria P_1 and P_2 are all with positive sensitivity indices which enhances the spread of Diphtheria within the human population. Also the parameters like ϕ modification parameter that accounts for diphtheria induced death, rate at which susceptible individuals are vaccinated α, rate of treatment σ, the rate at which individuals under treatment recovered ε, disease induced death rate δ, Natural death rate μ and bacteria Natural death rate μ_B are with negative sensitivity indices and will reduces the prevalence of diphtheria within the humans population.

3.8 Global stability analysis at endemic equilibrium state

Using the direct Lyapunov approach for equilibrium point, the global stability is examined. When $R_0 > 1$, the endemic equilibrium point is globally stable, According to epidemiology, this implies that the disease will spread throughout the population regardless of the original population under consideration According to the fractional model (6).

$$\lambda = \frac{\beta I_d S_d}{N} + \frac{\beta_1 B}{K+B}$$

where

$$N \leq \frac{\lambda}{\mu}\ as\ t \to \infty$$

$$\lambda = \beta I_d S_d\,(K+B) + \mu(\beta_1 B)$$

Then, Our fractional model now becomes:

$$\left.\begin{array}{c} {}^{b}D_t^{\alpha}S_d = \Lambda - \lambda_1 S_d + \omega R_d + \psi V_d - \alpha S_d - \mu S_d \\ {}^{b}D_t^{\alpha}E_d = \lambda_1 S_d - M_1 E_d \\ {}^{b}D_t^{\alpha}I_d = \theta E_d - M_2 I_d \\ {}^{b}D_t^{\alpha}T_d = \sigma I_d - M_3 T_d \\ {}^{b}D_t^{\alpha}V_d = \alpha S_d - M_4 V_d \\ {}^{b}D_t^{\alpha}B = P_1 I_d + P_2 T_d - \mu_B \\ {}^{b}D_t^{\alpha}R_d = \varepsilon T_d - M_5 R_d \end{array}\right\} \tag{21}$$

The following outcomes of Equation (21) at equilibrium point
$\lambda = \Lambda - \lambda_1^{**} S_d^{**} + \omega R_d^{**} + \psi V_d^{**} - \alpha S_d^{**} - \mu S_d^{**} = \lambda_1^{**} S_d^{**} - M_1 E_d^{**} = \theta E_d^{**} - M_2 I_d^{**} = \sigma I_d^{**} - M_3 T_d^{**}$
$= \alpha S_d^{**} - M_4 V_d^{*8} = P_1 I_d^{**} + P_2 T_d^{**} - \mu_B B^{**} = \varepsilon T_d^{**} - M_5 R_d^{**}$

Theorem 1.
Model (21) is globally asymptotically stable if $R_0 > 1$
Whenever

$$\left(7 - \frac{S_d^*}{S} + \frac{\lambda_1}{\lambda_1^*}\left(1 - \frac{S_d E_d^*}{S_d^* E_d}\right) - \frac{I_d^* E_d}{I_d E_d^*} - \frac{T_d}{T_d^*} - \frac{T_d^* I_d}{T_d I_d^*}\right) \leq 0$$

Let

$$L(t) = L_H(t)$$

be the non-linear Lyaponov function shown in the following equation (22):

$$\begin{array}{l} L(t) = L_1\left(S_d - S_d^* - S_d^* In\frac{S_d}{S_d^*}\right) + L_2\left(E_d - E_d^* - E_d^* In\frac{E_d}{E_d^*}\right) + L_3\left(I_d - I_d^* - I_d^* In\frac{I_d}{I_d^*}\right) + \\ L_4\left(T_d - T_d^* - T_d^* In\frac{T_d}{T_d^*}\right) + L_5\left(V_d - V_d^* - V_d^* In\frac{V_d}{V_d^*}\right) + L_6\left(B_d - B_d^* - B_d^* In\frac{B_d}{B_d^*}\right) + \\ L_7\left(R_d - R_d^* - R_d^* In\frac{R_d}{R_d^*}\right) \end{array} \tag{22}$$

Using Eq. (22), we obtain the Caputo Fractional order derivative.

$$\begin{array}{l} {}^{b}D_t^{\alpha}L(t) = {}^{b}D_t^{\alpha}L_d(t) \leq L_1\left(1 - \frac{S_d^{**}}{S_d}\right){}^{b}D_t^{\alpha}S_d(t) + L_2\left(1 - \frac{E_d^{**}}{E_d}\right){}^{b}D_t^{\alpha}E_d(t) + L_3\left(1 - \frac{I_d^{**}}{I_d}\right)D_t^{\alpha}I_d(t) \\ +L_4\left(1 - \frac{T_d^{**}}{T_d}\right)D_t^{\alpha}T_d(t) + L_5\left(1 - \frac{V_d^{**}}{V_d}\right)D_t^{\alpha}V_d(t) + L_6\left(1 - \frac{B^{**}}{B}\right)D_t^{\alpha}B(t) \\ +L_7\left(1 - \frac{R_d^{**}}{R_d}\right)D_t^{\alpha}R_d(t) \end{array}$$

$$\begin{array}{l} = \lambda_d S_d^*\left(\left(1 - \frac{S_d^{**}}{S_d}\right){}^{b}D_t^{\alpha}S_d(t) + \left(1 - \frac{E_d^{**}}{E_d}\right){}^{b}D_t^{\alpha}E_d(t)\right) + L_3\left(1 - \frac{I_d^{**}}{I_d}\right){}^{b}D_t^{\alpha}I_d(t) + \left(1 - \frac{T_d^{**}}{T_d}\right){}^{b}D_t^{\alpha}T_d(t) \\ + \left(1 - \frac{V_d^{**}}{V_d}\right){}^{b}D_t^{\alpha}V_d(t) + \left(1 - \frac{B^{**}}{B}\right){}^{b}D_t^{\alpha}B_d(t) + \left(1 - \frac{R_d^{**}}{R_d}\right){}^{b}D_t^{\alpha}R_d(t) \end{array}$$

$$\left(1 - \frac{S_d^*}{S_d}\right){}^{b}D_t^{\alpha} = \left(1 - \frac{S_d^*}{S_d}\right)(\lambda_d^* S_d + \mu S_d^* + \omega R_d^* + \psi V_d^* + \alpha S_d^* - \lambda^* S_d - \omega R_d - \psi V_d + \alpha S_d - \mu S_d)$$

$$
\begin{aligned}
&= \lambda_d^* S_d^* \left(1 - \frac{S_d \lambda_{d1}}{S^{**}\lambda_{d1}^{**}} - \frac{S_d^*}{S_d} + \frac{\lambda_{d1}}{\lambda_{d1}^{**}}\right) + \mu S_d^* \left(2 - \frac{S_d}{S_d^*} - \frac{S_d^*}{S_d}\right) - \omega\left(1 - \frac{R_d}{R_d^*}\right) - \psi\left(1 - \frac{V_d}{V_d^*}\right)\left(1 - \frac{S_d^*}{S_d}\right), \\
\left(1 - \frac{E_d^{**}}{E_d}\right) {}^{b}D_t^{\alpha} E_d &= \left(1 - \frac{E_d^{**}}{E_d}\right)\left(\lambda_{d1}^{**} S_d - \lambda_{d1}^{**} S_d^{**} \frac{E_d}{E_d^{**}}\right), \\
&= \lambda_{d1}^{**} S^{**}\left(1 - \frac{S_d \lambda_{d1}}{S^{**}\lambda_{d1}^{**}} \frac{E_d^{**}}{E_d} - \frac{E_d^{**}}{E_d} + \frac{S_d \lambda_{d1}^{**}}{S^{**}\lambda_{d1}^{**}}\right), \\
\frac{M_1}{\theta}\left(1 - \frac{I_d^*}{I_d}\right) {}^{d}D_t^{\alpha} I_d &= \frac{M_2}{\theta}\left(1 - \frac{I_d^*}{I_d}\right)\left(\theta E_d - M_2 \frac{I_d}{I_d^{**}} I_d^*\right), \\
&= \lambda_{d1}^* S_d^*\left(1 + \frac{E_d}{E_d^*} - \frac{I_d}{I_d^*} - \frac{E_d I_d}{E_d^* I_d^*}\right), \\
\frac{M_1 M_2}{\sigma\theta}\left(1 - \frac{T_d^*}{T_a}\right) {}^{b}D_t^{\alpha} T_d &= \frac{M_1 M_2}{\sigma\theta}\left(1 - \frac{T_d^*}{T_a}\right)\left(\frac{I_d}{I_d^*} - \frac{T_d^*}{T_a}\right), \\
&= \lambda_{d1}^*\left(1 - \frac{T_a}{T_d^*} - \frac{I_d T_d^*}{I_d^* T_a} + \frac{I_d}{I_d^*}\right), \\
\frac{\alpha+\mu}{\alpha}\left(1 - \frac{V_d^*}{V_a}\right) {}^{b}D_t^{\alpha} V_d &= \frac{\alpha+\mu}{\alpha}\left(1 - \frac{V_d^*}{V_a}\right)\left(\alpha S_d - M_4 V_d^* \frac{V_d^*}{V_a}\right), \\
&= \lambda_{d1}^*\left(1 - \frac{S_a}{S_d^*} - \frac{V_d}{V_d^*} - \frac{V_d S_d^*}{V_d^* S_a}\right),
\end{aligned}
\tag{23}
$$

Hence, Eq. (23) now becomes;

$$
\begin{aligned}
&{}^{b}D_t^{\alpha} L(t) \leq \lambda_{d1}^{**} S_d^{**} \\
&\left(7 - \tfrac{S_d}{S_d^*} + \tfrac{\lambda_d}{\lambda_{d1}^*}\left(1 - \tfrac{S_d E_d^*}{S_d^* E_a}\right) - \tfrac{I_d E_d}{I_d^* E_d^*} - \tfrac{T_a}{T_d^*} - \tfrac{T_d I_d}{T_d^* I_d^*}\right) \\
&- (\alpha+\mu) S_d^* \lambda_{d1}^* \left(\left(\tfrac{S_d^*}{S_d} - 1 - In\tfrac{S_d^*}{S_d}\right) + \left(\tfrac{V_d^*}{V_d} - 1 - In\tfrac{V_d^*}{V_d}\right) + \left(\tfrac{R_d^*}{R_d} - 1 - In\tfrac{R_d^*}{R_d}\right)\right) \\
&- \psi V_d^* \lambda_{d1}^* S_d^* \left(1 - \tfrac{V_d}{V_d^*}\right)\left(1 - \tfrac{R_d}{R_d^*}\right)\left(1 - \tfrac{S_d}{S_d^*}\right)
\end{aligned}
$$

Which implies that, ${}^{b}D_t^{\alpha} L(t) \leq \lambda_{d1}^{**} S_d^{**} \beta \frac{(R_0 - 1)}{\mu} \Lambda S^{**}$

$$
\frac{-\beta(R_0-1)}{\mu}\Lambda S^{**}\left[\begin{array}{l}(\alpha+\mu) S_d^*\left(\left(\frac{S_d^*}{S_d} - 1 - In\frac{S_d^*}{S_d}\right) + \left(\frac{V_d^*}{V_d} - 1 - In\frac{V_d^*}{V_d}\right) + \left(\frac{R_d^*}{R_d} - 1 - In\frac{R_d^*}{R_d}\right)\right) \\ +\psi V_d^*\left(1 - \frac{V_d}{V_d^*}\right)\left(1 - \frac{R_d}{R_d^*}\right)\left(1 - \frac{S_d^*}{S_d}\right)\end{array}\right]
$$

Therefore, ${}^{b}D_t^{\alpha} L(t) \leq 0 \ for \ R_0 > 1$. This implies that $\eta^{**} = (S_d^{**}, E_d^{**}, I_d^{**}, I_d^{**}, T_d^{**}, R_d^{**})$, is the endemic equilibrium point, then it is globally asymptotically stable in Ω whenever $R_0 > 1$. according to LaSalle's invariance principle.

4 Fractional order model numerical results

We employed a numerical approach to solve the fractional order Diphtheria model, utilizing the generalized fractional Adams Bashforth–Moulton method described by [23] . Table 1 displays the values of the model parameters that were utilized, and also considers and simulates several values of the fractional order α.

4.1 Implementation of fractional Adams-Bashforth-Moulton method

In this work, the approach outlined by Baskonus and Bulut; Diethelm, is utilized [24],[25]. Using the fractional Adam–Bashforth–Moulton approach, we were able to derive an approximate solution of the

fractional Diphtheria model given in (6). The representation of the fractional model (6) in (23) is as follows:

$$ {}^{b}D_{t}^{\alpha}Y\left(t\right)=Z\left(t,Y\left(t\right)\right),\ 0<t<\varsigma, $$

$$ Y^{(n)}\left(0\right)=Y_{0}^{(n)},\ \ n=1,0,\ ...,Y,Y=[\alpha] \tag{24} $$

where $Y=\left(S_{d}^{*},E_{d}^{*},I_{d}^{*},T_{H}^{*},V_{d}^{*},B_{d}^{*},R_{H}^{*}\right)\in R_{+}^{7}$ and $P\left(t,Y\left(t\right)\right)$ is a real valued function that is continous.
Therefore, the following representation of Eq. (24) can be made using the idea of a fractional integral:

$$ Y\left(t\right)=\sum_{n=0}^{Y-1}Y_{0}^{(n)}\frac{t^{n}}{n!}+\frac{1}{\Gamma\left(\alpha\right)}\int_{0}^{t}\left(t-x\right)^{\alpha-1}P\left(x,Y\left(x\right)\right)dx \tag{25} $$

Using the method described by [24], we let the step size $h=\frac{\varsigma}{N},\ N\in\mathrm{N}$ with a grid that is uniform on $[0,\varsigma]$. Where $t_{c}=cr,\ c=0,1,1,\ ...N$ Therefore, the fractional order model of Diphtheria model presented in (6) can be approximated as:

$$ \begin{aligned}
S_{dk+1}\left(t\right)&=S_{d0}+\tfrac{h^{\gamma}}{\Gamma(\alpha+2)}\left\{\Lambda-\left(\beta I_{d}^{n}+\beta_{1}B^{n}\right)\tfrac{1}{N^{n}(K+B^{n})}+\omega R_{d}^{n}+\psi V_{d}^{n}-\alpha S_{d}^{n}-\mu S_{d}^{n}\right\}+\\
&\tfrac{h^{\alpha}}{\Gamma(\alpha+2)}\sum_{x=0}^{k}dx,k+1\left\{\lambda-\left(\beta I_{dx}+\beta_{1}B_{x}\right)\tfrac{1}{N_{x}}+\omega R_{dx}+\psi V_{dx}-\alpha S_{dx}-\mu S_{dx}\right\},\\
E_{dk+1}\left(t\right)&=E_{d0}+\tfrac{h^{\gamma}}{\Gamma(\alpha+2)}\left\{\left(\beta I_{d}^{n}+\beta_{1}B^{n}\right)\tfrac{S_{d}^{n}}{N^{n}(K+B)}-M_{1}E_{d}^{n}\right\}+\\
&\tfrac{h^{\alpha}}{\Gamma(\alpha+2)}\sum_{x=0}^{k}dx,k+1\left\{\left(\beta I_{dx}+\beta_{1}B_{x}\right)\tfrac{S_{dx}}{N_{x}(K+B_{x})}-M_{1}E_{dx}\right\},\\
I_{dk+1}\left(t\right)&=I_{d0}+\tfrac{h^{\gamma}}{\Gamma(\alpha+2)}\left\{\theta E_{d}^{n}-M_{2}I_{d}^{n}\right\}+\\
&\tfrac{h^{\alpha}}{\Gamma(\alpha+2)}\sum_{x=0}^{k}dx,k+1\left\{\theta E_{dx}-M_{2}I_{dx}\right\},\\
T_{dk+1}\left(t\right)&=T_{d0}+\tfrac{h^{\gamma}}{\Gamma(\alpha+2)}\left\{\sigma I_{d}^{n}-M_{3}T_{d}^{n}\right\}+\\
&\tfrac{h^{\alpha}}{\Gamma(\alpha+2)}\sum_{x=0}^{k}dx,k+1\left\{\sigma I_{dx}-M_{3}T_{dx}\right\},\\
T_{dk+1}\left(t\right)&=T_{d0}+\tfrac{h^{\gamma}}{\Gamma(\alpha+2)}\left\{\alpha S_{d}^{n}-M_{4}V_{d}^{n}\right\}+\\
&\tfrac{h^{\alpha}}{\Gamma(\alpha+2)}\sum_{x=0}^{k}dx,k+1\left\{\alpha S_{dx}-M_{4}V_{dx}\right\},\\
V_{dk+1}\left(t\right)&=V_{d0}+\tfrac{h^{\gamma}}{\Gamma(\alpha+2)}\left\{P_{1}I_{d}^{n}+P_{2}T_{d}^{n}-\mu_{B}B^{n}\right\}+\\
&\tfrac{h^{\alpha}}{\Gamma(\alpha+2)}\sum_{x=0}^{k}dx,k+1\left\{P_{1}I_{dx}+P_{2}T_{dx}-\mu_{B}B_{x}\right\},\\
R_{dk+1}\left(t\right)&=R_{d0}+\tfrac{h^{\gamma}}{\Gamma(\alpha+2)}\left\{\varepsilon T_{d}^{n}-M_{5}R_{d}^{n}\right\}+\\
&\tfrac{h^{\alpha}}{\Gamma(\alpha+2)}\sum_{x=0}^{k}dx,k+1\left\{\varepsilon T_{dx}-M_{5}R_{dx}\right\}.
\end{aligned} \tag{26} $$

Where

$$
\begin{aligned}
S_{dk+1}(t) &= \frac{1}{\Gamma(\alpha)}\sum_{x=0}^{k} e_x k+1\left\{\Lambda-(\beta I_{dx}+\beta_1 B_x)\frac{1}{N_x(K+B_x)}+\omega R_{dx}+\psi V_{dx}-\alpha S_{dx}-\mu S_{dx}\right\},\\
E_{dk+1}(t) &= \frac{1}{\Gamma(\alpha)}\sum_{x=0}^{k} e_x, k+1\left\{(\beta I_{dx}+\beta_1 B_x)\frac{S_{dx}}{N_x(K+B_x)}-M_1 E_{dx}\right\},\\
I_{dk+1}(t) &= \frac{1}{\Gamma(\alpha)}\sum_{x=0}^{k} e_x, k+1\{\theta E_{dx}-M_2 I_{dx}\},\\
T_{dk+1}(t) &= \frac{1}{\Gamma(\alpha)}\sum_{x=0}^{k} e_1, k+1\{\sigma I_{dx}-M_3 T_{dx}\},\\
T_{dk+1}(t) &= \frac{1}{\Gamma(\alpha)}\sum_{x=0}^{k} e_x, k+1\{\alpha S_{dx}-M_4 V_{dx}\},\\
V_{dk+1}(t) &= \frac{1}{\Gamma(\alpha)}\sum_{x=0}^{k} e_x, k+1\{P_1 I_{dx}+P_2 T_{dx}-\mu_B B_x\},\\
R_{dk+1}(t) &= \frac{1}{\Gamma(\alpha)}\sum_{x=0}^{k} e_1, k+1\{\varepsilon T_{dx}-M_5 R_{dx}\}.
\end{aligned}
\tag{27}
$$

Equations (25) and (26) provided us with;

$$dx,_{K+1} = K^{\alpha+1}-(k-\alpha)(k+\alpha)^{\alpha},\ x=0$$

$$(k-x+2)^{\alpha+1}+(k-\alpha)^{\alpha+1}-2(k-x+1)^{\alpha+1},\ 1\le x\le k$$

$$1, x=k+14$$

And

$$e_{x,k+1} = \frac{h^{\alpha}}{\alpha}\left[(k-x+1)^{\alpha}(k-x)^{\alpha}\right],\ 0\le x\le k$$

4.2 parameters descriptions

Table 1: Values of parameters used in the simulation.

Parameters	Symbol	Value (per day)	Source
Recruitment rate of individuals into the susceptible class	Λ	0.29	Assumed
Rate at which susceptible individuals come into contact with diphtheria	β	0.570	[26]
Rate at which exposed individuals progress to infection	θ	0.230	[27]
Rate at which individuals contact bacteria	β_1	0.341	Assumed
Rate at which infected individuals receive treatment	σ	0.36	Assumed
Recovery rate of treated individuals	ε	0.8	Assumed
Vaccination rate for susceptible individuals	α	0.500	[26]
Rate at which vaccine-induced immunity wanes	ψ	0.43	Assumed
Rate at which bacteria are shed into the environment	P_1, P_2	0.007	Assumed
Natural death rate of the bacteria	μ_B	0.047	Assumed
Natural death rate of humans	μ	0.019	[28]
Rate at which recovered individuals become susceptible again	ω	0.7	Assumed
Density of bacteria in the environment	K	0.005	Assumed
Death rate due to diphtheria	δ	0.006	[28]
Modification parameter for death in treated individuals	ϕ	0.1	Assumed

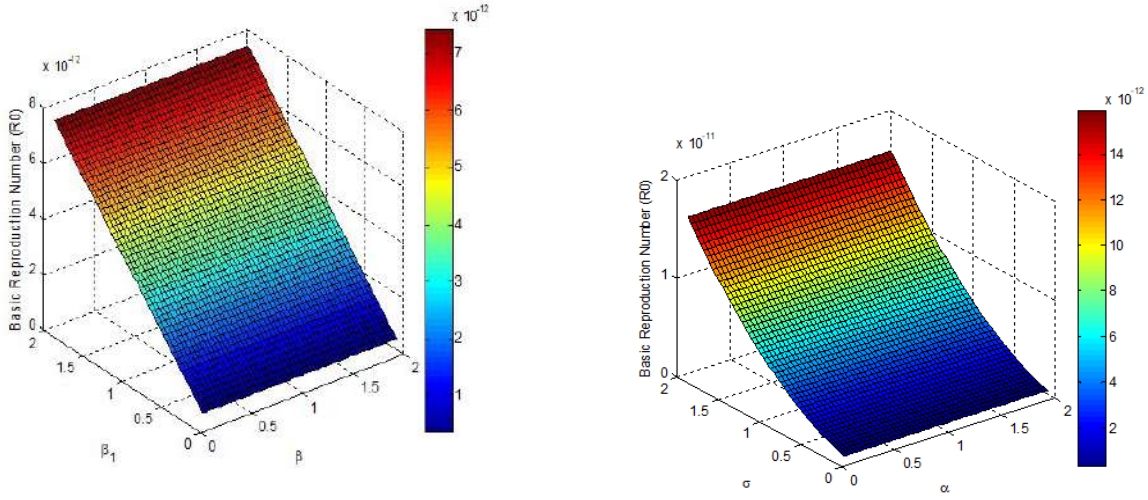
4.3 The fractional Adam-Bashforth Moulton approach is crucial for obtaining the model's numerical solutions

- The fractional Adam–Bashforth Moulton method attains high-order accuracy with just one extra function evaluation every step.
- This method is a helpful tool for numerical solutions of partial and fractional order differential equations and has potential applications in many fields, including engineering, chemistry, and medicine.
- The Adam–Bashforth Moulton method, which is frequently included in packaged ODE solvers, provides automatic error management.

4.4 Fractional order Diphtheria model simulation

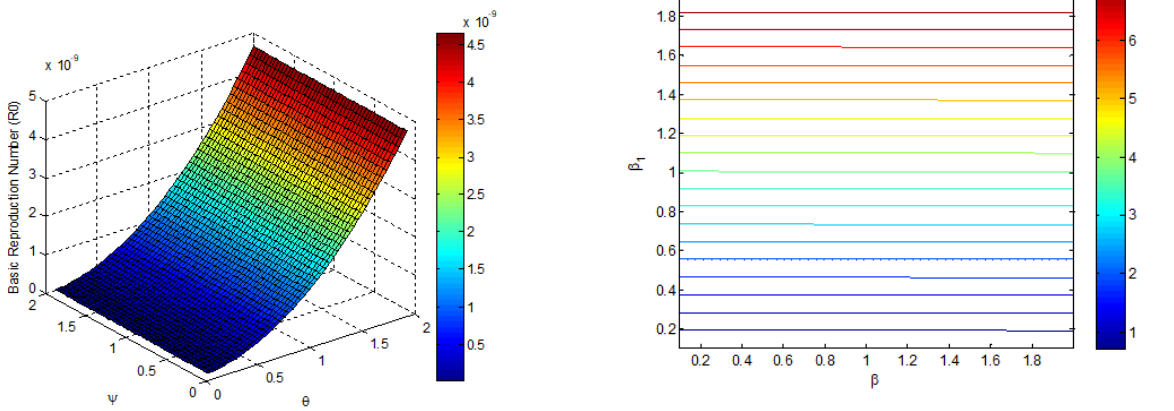
In this section, we present the graphs obtained from numerical simulation of the fractional order Diphtheria.

A closer look at the surface plot in Fig. 3(a) indicates that a rise in the parameters and representing the contact rate between bacteria and susceptible humans, respectively, which increases the incidence of diphtheria in human populations, as demonstrated by the basic reproduction number surpassing one (1). The surface plot in Fig. 3(b) shows the effects of different between and , indicating the percentage of affected people receiving therapy and rate of vaccination in relation to the population's basic reproduction number . It was observed that an increase in these parameters leads to a peak in the value of to a numerical value below one. This implies that the burden of diphtheria among humans will eventually be reduced by improving the treatment rate of affected persons and putting policies in place to encourage vaccination rates. Figure 4(a) shows the impact of varying (the waning rate of the vaccine) and (the progression rate from exposed to infected) on the basic reproduction number . If appropriate measures are not implemented, these factors and can worsen the prevalence of diphtheria, as evidenced by their effect on the basic reproduction number, causing it to rise above one (1). The graph in Figure 4(b) presents a contour plot of in relation to . Analyzing



(a) **Impact of β and β_1 on R_0^d** (b) **Impact of σ and $alpha$ on R_0^d**

Figure 3: **surface plot of the basic reproduction number**

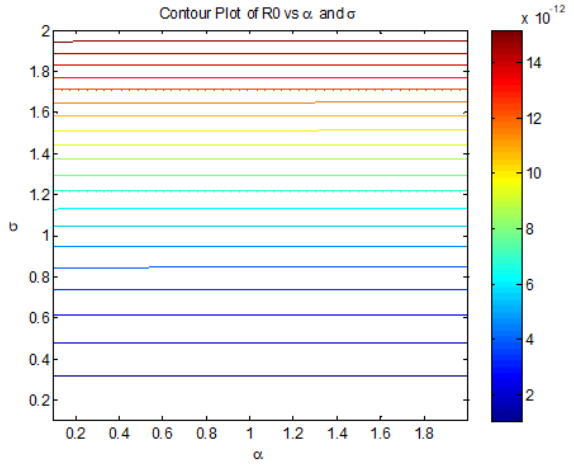


(a) **Impact of ψ and θ on R_0^d**

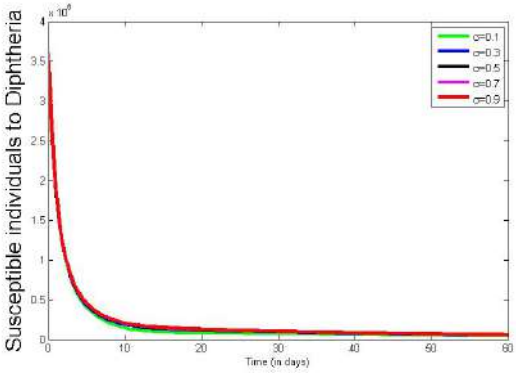
(b) **contour plot showing the Impact of β_1 and β on R_0^d**

Figure 4: **surface plot and contour plot of the basic reproduction number**

the numerical trends in the graph reveals that the maximum value reached by adjusting these parameters is 0.6, which is below unity (1). This observation indicates that increasing these parameters would not lead to a significant diphtheria outbreak in the population. Additionally, raising the values of (the treatment rate of infected individuals) and (the vaccination rate of susceptible individuals) would help reduce the burden of diphtheria among the population. This conclusion is supported by Figure 5(a), where stays below unity (1). The plot in Figure 5(b) shows the effect of varying the fractional order derivative on the susceptible human population over time. The plot clearly indicates that an increase in leads to a decline in the susceptible population. This reduction is due to the implementation of treatment and vaccination strategies, which lowers the number of individuals vulnerable to the disease. Figure 6(a) shows that the exposed population initially rises and then quickly declines as infection rates increase. This indicates that despite the overall population decreasing due to higher infectiousness, there is still a flow of individuals from the susceptible class into the exposed class.

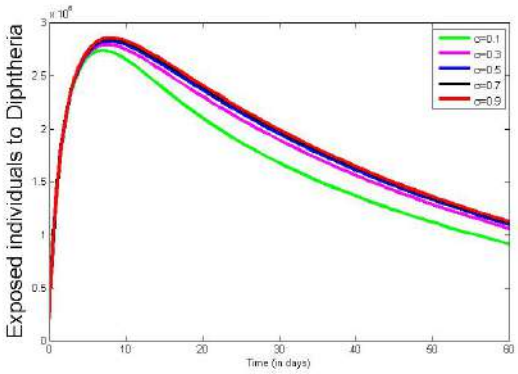


(a) contour plot showing the Impact of α and σ on R_0^d

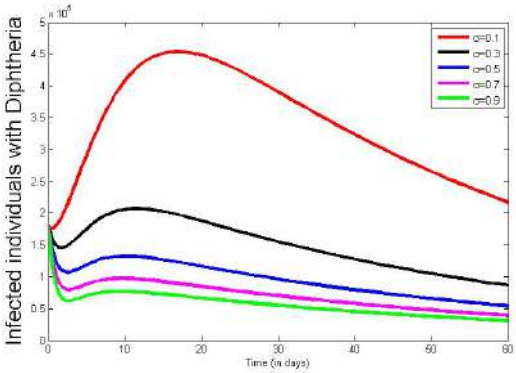


(b) Simulation of Susceptible individuals to Diphtheria

Figure 5: Contour plot on Impact of α and σ on R_0^d and Effect of σ on $S_d(t)$



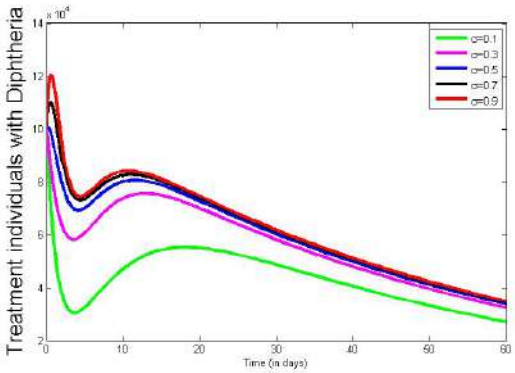
(a) Simulation of Exposed individuals to Diphtheria



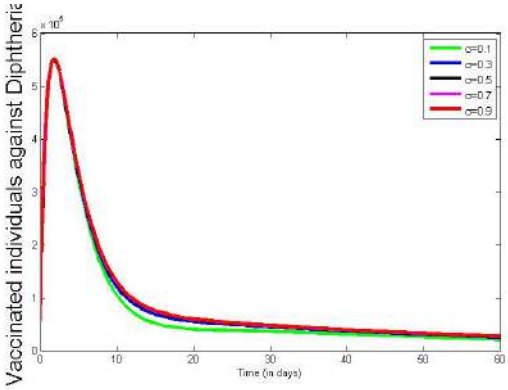
(b) Simulation of Infected individuals with Diphtheria

Figure 6: Effect of σ on $E_d(t)$ and $I_d(t)$

Figure 6(b) illustrates the dynamics of the infected human population over time. Initially, the number of infected individuals increases due to the influx from the exposed class. However, at a certain point, the number of infected individuals begins to decrease due to treatment interventions. This suggests that utilizing treatment and vaccination strategies will ultimately reduce the burden of diphtheria within the population. Figure 7(a) shows how the number of individuals receiving treatment changes over time. Initially, there is an increase in the treated population due to transfers from the infected group. Later, the number of individuals undergoing treatment gradually declines as successful medical interventions lead to recovery from diphtheria. Figure 7(b) shows that the vaccinated segment of the population initially increases as people follow vaccination protocols to prevent diphtheria. However, this population later decreases due to the declining effectiveness of the diphtheria vaccine over time, due to its inherent imperfections. Figure 8(a) shows an increase in the infected human population due to the presence of bacteria in the environment. Additionally, Figure 8(b) shows an increase in the recovered human population as the treatment rate rises. This is due to the effectiveness of the treatment strategies implemented by healthcare providers. This highlights the importance

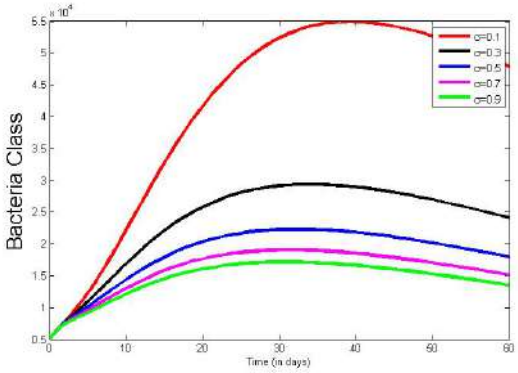


(a) **Simulation of Treatment individuals with Diphtheria**

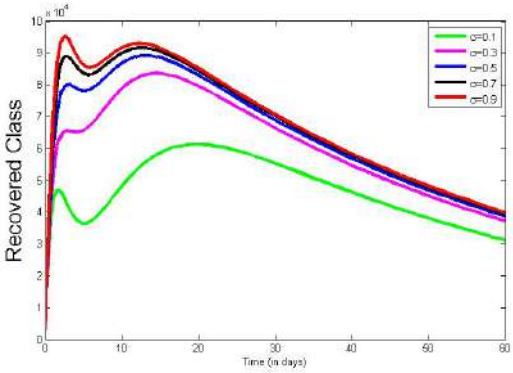


(b) **(b) Simulation of Vaccination individuals against Diphtheria**

Figure 7: **Effect of σ on $T_d(t)$ and $V_d(t)$**

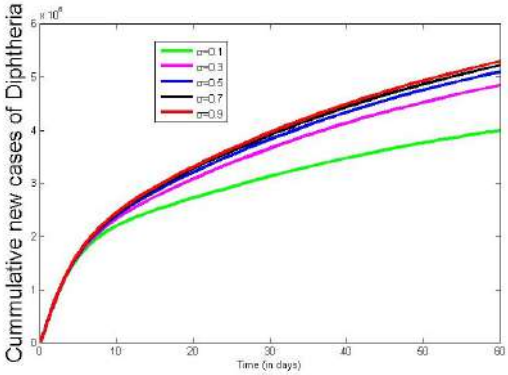


(a) **Simulation of the Bacteria class**



(b) **(b) Simulation of Recovered individuals from Diphtheria**

Figure 8: **Effect of σ on $B(t)$ and $R_d(t)$**



(a) **Cumulative new cases of Diphtheria**

Figure 9: **Effect of σ on the Cumulative new cases of Diphtheria**

of establishing diphtheria treatment facilities by government authorities to help reduce the prevalence of the disease in the population. Figure (9) shows an increase in the cumulative number of new diphtheria cases as the treatment rate between susceptible and infected individuals increases. The graph indicates that increasing the treatment rate leads to a reduction in the cumulative new cases of diphtheria, ultimately reducing the burden and prevalence of

the disease within the population.

5 Conclusion

This manuscript presents a mathematical model for the transmission dynamics and control of diphtheria using the Caputo fractional derivative. Initially, we developed an integer-order nonlinear system with seven differential equations, dividing the human population into six subgroups and including a separate bacteria class, resulting in a total of seven compartments. Acknowledging the importance of fractional modeling, we extended the integer-order model to fractional order using the Caputo operator. We began with a comprehensive theoretical analysis of the fractional diphtheria model, covering aspects such as solution existence, uniqueness, and equilibrium stability. We carried out the sensitivity analysis of the basic reproduction and is observed that the parameters like ϕ modification parameter that accounts for diphtheria induced death, rate at which susceptible individuals are vaccinated α, rate of treatment σ, the rate at which individuals under treatment recovered ε, disease induced death rate δ , natural death rate μ and bacteria natural death rate μ_B are with negative sensitivity indices and will reduces the prevalence of diphtheria within the humans population. Using the fractional Adams–Bashforth–Moulton method, we numerically solved the fractional model. The simulations visually demonstrated the impact of the disease incidence based on different model parameter values and fractional orders of the Caputo operator. Additionally, we conducted simulations by adjusting parameters such as the treatment rate for infected individuals, the vaccination rate for susceptible individuals, the contact rate between susceptible and infected individuals, the progression rate from exposed to infected, and the waning rate of the vaccine. The results indicated that enhancing treatment and vaccination strategies will effectively reduce the prevalence of diphtheria among the population. The study of novel trial functions and rogue waves in generalized breaking soliton equations using the bilinear neural network method, as presented by [29], suggests that this method could also be applied to solve nonlinear partial differential equations in future work.

Funding
There is no financing available.

Conflict of interest
The authors declare that they have no known competing interests.

Author's contribution
Emmanuel Abah: Formulating the model, concept, devising methodology.
Bolarinwa Bolaji: Authoring the final draft of the manuscript, creating visualization and providing supervision.
Godwin Onuche Acheneje: Authoring the initial draft of the manuscript, partaking in reviewing and editing process for the draft manuscript.
William Atokolo: partaking in reviewing and editing process for the draft manuscript.
Benjamin Idoko Omede: Partook in authoring the initial draft of the manuscript, reviewing and editing process for the draft manuscript.
Jeremiah Amos: partaking in reviewing and editing process for the draft manuscript.
Daniel Omeje: partaking in editing process for the draft manuscript.

All authors read through the manuscript and approved submission for publication.

Availability of data

The sources of all the data used in this work are variously cited in the literature.

References

[1] Todar, K. (2008). Diphtheria. University of Wisconsin-Madison Department of Bacteriology, 1-8.

[2] Singh, J., Harit, A. K., Jain, D. C., Panda, R. C., Tewari, K. N., and Bhatia, R. (1999). Diphtheria is declining but continues to kill many children: Analysis of data from a sentinel center in Delhi. Epidemiology and Infection, 123, 209-215.

[3] Galazka, A. M., and Robertson, S. E. (1995). Diphtheria: Changing patterns in the developing world and the industrialized world. European Journal of Epidemiology, 11, 107-117.

[4] Cárdenas, R., Prieto, G., Vargas, J., and Martinez, A. (1972). Corynebacterium diphtheriae. Características de cepas aisladas recientemente en Maracaibo - Venezuela. Kasmera, 4, 185-198.

[5] Formiga, L. C. D. (1985). New possibilities for the laboratory diagnosis of diphtheria. Brazilian Journal of Medical and Biological Research, 18, 401-402.

[6] Kneen, R., Phan, N. G., Solomon, T., Tran, T. M., Nguyen, T. T., Tran, B. L., Wain, J., Day, N. P., Tran, T. H., Parry, C. M., and White, N. J. (1998). Penicillin vs erythromycin in the treatment of diphtheria. Clinical Infectious Diseases, 27, 845-850.

[7] Bachran, C., Sutherland, M., Bachran, D., and Fuchs, H. (2007). Quantification of diphtheria toxin-mediated ADP-ribosylation in a solid-phase assay. Clinical Chemistry, 53(9), 1676-1683.

[8] Brooks, G. F., Carroll, C. K., Butel, J. S., and Morse, A. S. (2007). Jawetz, Melnick and Adelberg's Medical Microbiology (24th ed., pp. 154-217).

[9] Formiga, L. C. D., and Mattos-Guaraldi, A. L. (1993). Diphtheria: Current status and laboratory procedures for diagnosis. Revista Brasileira de Patologia Clínica, 29, 93-96.

[10] Atokolo, W., Aja, R. O., Aniaku, S. E., Onah, I. S., and Mbah, G. C. E. (2022). Approximate solution of the fractional order sterile insect technology model via the Laplace–Adomian decomposition method for the spread of Zika virus disease. International Journal of Mathematics and Mathematical Sciences, 2022, 1–24. https://doi.org/10.1155/2022/2297630

[11] Atokolo, W., Aja, R. O., Omale, D., Ahman, Q. O., Acheneje, G. O., and Amos, J. (2024). Fractional mathematical model for the transmission dynamics and control of Lassa fever. Franklin Open, 100110. https://doi.org/10.1016/j.fraope.2024.100110

[12] Agahiu, N., Bolaji, B., and Atokolo, W. (2024). Approximate solution of fractional order mathematical model on the co-transmission of zika and chikungunya virus using laplace adomian decomposition method. GPH-International Journal of Mathematics, 7(03), 47-81.

[13] Odionyenma, U. B., Ikenna, N., and Bolaji, B. (2023). Analysis of a model to control the co-dynamics of Chlamydia and Gonorrhea using Caputo fractional derivative.

Mathematical Modelling and Numerical Simulation With Applications, 3(2), 111–140. https://doi.org/10.53391/mmnsa.1320175

[14] Zhang, Z., Zeb, A., Egbelowo, O. F., and Erturk, V. S. (2020). Dynamics of a fractional order mathematical model for COVID-19 epidemic. Advances in Difference Equations, 2020(1).https://doi.org/10.1186/s13662-020-02873-w

[15] Ghani, M., Utami, I. Q., Triyayuda, F. W., and Afifah, M. (2022). A fractional SEIQR model on diphtheria disease. Modeling Earth Systems and Environment, 9(2), 2199–2219. https://doi.org/10.1007/s40808-022-01615-z

[16] Mangal, S., Misra, O. P., and Dhar, J. (2023). Modeling the effect of vaccination in fractional-order epidemic model for infectious disease. International Journal of Dynamics and Control, 12(1), 303–317. https://doi.org/10.1007/s40435-023-01331-1

[17] Rajan, P. K., Kuppusamy, M., and Yusuf, A. (2023). A fractional-order modeling of human papillomavirus transmission and cervical cancer. Modeling Earth Systems and Environment, 10(1), 1337–1357. https://doi.org/10.1007/s40808-023-01843-x

[18] Yunus, A. O. and Olayiwola, M. O. (2024). The analysis of a novel covid-19 model with the fractional-order incorporating the impact of the vaccination campaign in nigeria via the laplace-adomian decomposition method. Journal of the Nigerian Society of Physical Sciences, 1830. https://doi.org/10.46481/jnsps.2024.1830

[19] Akogwu, B. (2022). The solution of a mathematical model for COVID-19 transmission and vaccination in Nigeria by using a differential transformation method. FUDMA Journal of Sciences, 6(5), 50-56. https://doi.org/10.33003/fjs-2022-0605-1089

[20] Milici, C., Draganescu, G., and Machado, J. T. (2018). Introduction to fractional differential equations. Springer.

[21] Podlubny, I. (1998). Fractional differential equations: An introduction to fractional derivatives, to methods of their solution and some of their applications. Elsevier.

[22] VandenDriessche, P. and Watmough, J. (2002). Reproduction numbers and subthreshold endemic equilibria for compartmental models of disease transmission. Mathematical Biosciences, 180(1-2), 29-48.

[23] Zhang, R. and Li, M. (2022). Bilinear residual network method for solving the exactly explicit solutions of nonlinear evolution equations. Nonlinear Dynamics, 108. http://dx.doi.org/10.1007/s11071-022-07207-x

[24] Baskonus, H. M. and Bulut, H. (2015). On the numerical solutions of some fractional ordinary differential equations by fractional adams bashforth-moulton method. Open Mathematics, 13, 1.

[25] Diethelm, K. (1999). The FracPECE subroutine for the numerical solution of differential equations of fractional order. Open Mathematics, 13, 1.

[26] Puspita, G., Kharis, M., and Supriyono. (2017). UNNES Journal of Mathematics, 6, 25-3.

[27] Fathoni, M. I., Mardlijah, and Hariyanto. (2015). Proceedings of the national seminar on mathematics and mathematics education. Proceedings of the National Seminar on Mathematics and Mathematics Education, 229–238.

[28] Ministry of National Development Planning (MNDP), Central Bureau of Statistics Indonesia, and United Nations Population Fund (UNFPA) Indonesia. (2013). Indonesia population projection 2010-2035 (pp. 34, 84-468). BPS-Statistic Indonesia.

[29] Zhang, R. F., Li, M.-C., Gan, J. Y., Li, Q., and Lan, Z.-Z. (2022). Novel trial functions and rogue waves of generalized breaking soliton equation via bilinear neural network method. Chaos, Solitons & Fractals, 154. https://doi.org/10.1016/j.chaos.2021.111579

On a class of piecewise continuous Lyapunov functions and eventual stability for nonlinear impulsive Caputo fractional differential equations via new generalized Dini derivative

J.E. Ante*†, S.O. Essang† ‡, J.U. Atsu§, E.O. Ekpenyong¶, and R.D. Effiong‖

Abstract

In this paper, the eventual stability for nonlinear impulsive Caputo fractional differential equations with fixed moments of impulse is examined using the vector Lyapunov functions which is generalized by a class of piecewise continuous Lyapunov functions. Together with the comparison results, sufficient conditions for the eventual stability of impulsive Caputo fractional differential equations are presented. Results obtained are extension and improvements on the existing results.

Keywords and phrases: eventual stability; Caputo derivative; impulsive fractional differential equations; vector Lyapunov functions.

1 Introduction

In the qualitative theory of differential equations, one of the main properties of interest is the stability of solutions since it enables us to compare the behaviour of solutions starting at different points [20]. The theory of impulsive differential equation is richer than the corresponding theory of differential equations [26, 19], as they constitutes very important models in the description of the true state of several real life processes and phenomena.

Many evolution processes are characterized by the fact that at certain moments of time they experience a change of state abruptly. These processes are subject to short term perturbations whose duration is negligible in comparison with the duration of the process. Consequently, it is natural to assume that these perturbations acts instantaneously, that is, in the form of impulses. It is known for example, that many biological phenomena involving thresholds, bursting rhythm models in medicine and biology, optimal control models in economics, pharmacokinetics and frequency modulated systems, do exhibit impulsive effects [26, 18].

Now, the efficient applications of impulsive differential system require the finding of criteria for stability of their solutions [31], and one of the most versatile methods in the study of the stability properties of impulsive systems is the method of Lyapunov function (Lyapunov's second method). The method was originally developed for studying the stability of a fixed point of an autonomous or nonautonomous differential equations. However, as was argued in [5], the method was then extended from fixed points to sets, from differential equation to dynamical systems and to stochastic equations.

There are several approaches in the literature in the study of the stability of solutions, one of which is the Lyapunov's second method. However, the novelty of the Lyapunov's second method over other methods of examining stability properties like the Razumikhin technique, the use of matrix inequality,

*Corresponding Author; E-mail: jackson.ante@topfaith.edu.ng
†Department of Mathematics, Topfaith University, Mkpatak
‡Department of Mathematics, Arthur Jarvis University, Akpabuyo, Nigeria; E-mail: sammykmf@gmail.com
§Department of Mathematics, University of Cross River State, Calabar, Nigeria; E-mail: atsujeremiah@gmail.com
¶Department of Mathematics, University of Calabar, Calabar, Nigeria; E-mail: : ememekpenyong@unical.edu.ng
‖University of Calabar, Calabar, Nigeria. E-mail: raphaeleffiong@gmail.com

etc. stems from the fact that the method allows us to examine the stability of solutions without first solving the given differential equation. Again, the method involves seeking an appropriate continuously differentiable function that is positive definite and whose time derivative along the trajectory curve or solution path is negative semidefinite. This function is called the Lyapunov function. The stability of the zero solution of impulsive differential equations have been extensively studied in [2, 3], [14], [29].

Again, the stability of solutions of differential equations via Lyapunov method has been intensively investigated in the past, and in many real cases, it is obligatory to study the stability of such sets, which are invariant with respect to a given system of differential equation which immediately excludes the stability in the sense of Lyapunov [35]. To allay the problem that will arise subsequently, [26] introduced a new concept called eventual stability, maintaining that, the set under consideration, despite not being invariant in the usual sense, is invariant in the asymptotic sense (see also [39]). Accordingly, the eventual stability of solutions of impulsive differential systems have been extensively studied (see [26], [32], [35] and the references therein).

Furthermore, the study of stability for fractional order systems is quite recent and one of the main difficulties in the application of a Lyapunov function to fractional order differential equations is the appropriate definition of its derivative among the fractional differential equations (see [20]). The stability of fractional order systems is examined in [4, 5, 6, 7, 8, 9, 11, 21, 22, 38]. Using the generalized Caputo fractional Dini derivative and scalar impulsive fractional differential equations, [1] established the comparison results together with sufficient conditions for the stability properties of impulsive fractional differential equations using the scalar Lyapunov function.

In this paper, we extend the study on the stability properties of impulsive Caputo fractional differential equations using scalar Lyapunov function in [1], and the corresponding study on the eventual stability for impulsive differential equations using the scalar Lyapunov function in [35] to the eventual stability of impulsive Caputo fractional differential equations using the vector Lyapunov functions. By adopting the new definition of the Caputo fractional Dini derivative as proposed in [20], and employing the vector Lyapunov functions which is generalized by a class of piecewise continuous functions, together with the comparison results, sufficient conditions for the eventual stability of the set $x(t) = 0$ is established with illustrative example.

2 Preliminaries, notations and definitions

Let $\mathbb{R}^n$ be the n-dimensional Euclidean space with norm $\|.\|$, let Ω be a domain in $\mathbb{R}^n$ containing the origin; $\mathbb{R}_+ = [0, \infty)$, $\mathbb{R} = (-\infty, \infty)$, $t_0 \in \mathbb{R}_+, t > 0$.
Let $J \subset \mathbb{R}_+$ Define the following class of functions $PC^q[J, \Omega] = \alpha : J \to \Omega, \alpha(t)$ is a piecewise continuous function with points of discontinuity $t_k \in J$ at which $\alpha(t)$ exists.
Fractional calculus being the generalization of the classical calculus to non integer order allows for the extension of the classical concepts of derivative and integral to functions with fractional orders. It allows for functions with non integer orders which makes it much more flexible in describing real world systems (see [23], [27] and [30]). There are several definitions of fractional derivatives and fractional integrals

General case

Let the number $n - 1 < q < n, q > 0$ be given, where n is a natural number and $\Gamma(.)$ denotes the gamma function.

Definition 2.1. *The Riemann-Liouville fractional derivative of order q of $x(t)$ is given by (see [30])*

$$ {}^{RL}_{t_0}D^q_t x(t) = \frac{1}{\Gamma(n-q)} \frac{d^n}{dt^n} \int_{t_0}^{t} (t-s)^{n-q-1} x(s) ds, t \geq t_0 $$

Definition 2.2. *The Caputo fractional derivative of order q of $x(t)$ is defined by (see [30])*

$$ {}_{t_0}^{C}D^q x(t) = \frac{1}{\Gamma(n-q)} \int_{t_0}^{t} (t-s)^{n-q-1} x^{(n)}(s) ds, t \geq t_0 $$

The Caputo derivatives has many properties that are similar to those of the standard derivatives, which makes them easier to understand and apply. The initial conditions of fractional differential equations using the Caputo derivative are also easier to interpret in physical context, which is another reason why it is often used in applications of fractional calculus.

Definition 2.3. *The Grunwald-Letnikov fractional derivative of order q of $x(t)$ is given by (see [20])*

$$ D_0^q x(t) = \lim_{h \to 0^+} \frac{1}{h^q} \sum_{r=0}^{[\frac{(t-t_0)}{h}]} (-1)^r ({}^qC_r) x(t-rh), t \geq t_0 $$

and the Grunwald-Letnikov fractional Dini derivative of order q of $x(t)$ is given by (see [20])

$$ D_0^q x(t) = \limsup_{h \to 0^+} \frac{1}{h^q} \sum_{r=0}^{[\frac{(t-t_0)}{h}]} (-1)^r ({}^qC_r) x(t-rh), t \geq t_0 $$

where ${}^qC_r$ are the binomial coefficients and $[\frac{(t-t_0)}{h}]$ denotes the integer part of $\frac{(t-t_0)}{h}$.

Particular case

(when n=1). In most applications, the order of q is often less than 1, so that $q \in (0,1)$. For simplicity of notation, we will use ${}^C D^q$ instead of ${}_{t_0}^{C}D^q$ and the Caputo fractional derivative of order q of the function $x(t)$ is

$$ {}^C D^q x = \frac{1}{\Gamma(1-q)} \int_{t_0}^{t} (t-s)^{-q} x' ds, t \geq t_0 \tag{1} $$

3 Impulses in fractional differential equations

Consider the initial value problem (IVP) for the system of fractional differential equations (FrDE) with a Caputo derivative for $0 < q < 1$,

$$ {}^C D^q x = f(t,x), t \geq t_0, x(t_0) = x_0, \tag{2} $$

where $x \in \mathbb{R}^N, f \in C[\mathbb{R}_+ \times \mathbb{R}^N, \mathbb{R}^N]$, $f(t,0) \equiv 0$ and $(t_0, x_0) \in \mathbb{R}_+ \times \mathbb{R}^N$.
Some sufficient conditions for the existence of the global solutions to (2) are considered in [12], [15], [28], [30], [38]. The IVP for FrDE (2) is equivalent to the following Volterra integral equation (See [1, 16, 37]),

$$ x(t) = x_0 + \frac{1}{\Gamma(q)} \int_{t_0}^{t} (t-s)^{q-1} f(s, x(s)) ds, t \geq t_0 \tag{3} $$

Consider the initial value problem for the system of impulsive fractional differential equations (IFrDE) with a Caputo derivative for $0 < q < 1$,

$$ \begin{aligned} {}^C D^q x = f(t,x), t \geq t_0, t \neq t_k, k = 1, 2, ... \\ \Delta x = I_k(x(t_k)), k \in N, t = t_k \\ x(t_0) = x_0, \end{aligned} \tag{4} $$

where $x, x_0 \in \mathbb{R}^N$, $f : \mathbb{R}_+ \times \mathbb{R}^N \to \mathbb{R}^N$, and $t_0 \in \mathbb{R}_+$, $I_k : \mathbb{R}^N \to \mathbb{R}^N$, $k = 1, 2, ...$
under the following assumptions:

(i) $0 < t_1 < t_2 < ... < t_k < ...$, and $t_k \to \infty$ as $k \to \infty$;

(ii) $f : \mathbb{R}_+ \times \mathbb{R}^N \to \mathbb{R}^N$, is continuous in $(t_{k-1}, t_k]$ and for each $x \in \mathbb{R}^N$, $k = 1, 2, ...$, $\lim_{(t,y)\to(t_k^+,x)} f(t, y) = f(t_k^+, x)$ exists;

(iii) $I_k : \mathbb{R}^N \to \mathbb{R}^N$

In this paper, we assume that $f(t, 0) \equiv 0$, $I_k(0) = 0$ for all k, so that we have the trivial solution for (4), and the points $t_k, k = 1, 2, ...$ are fixed such that $t_1 < t_2 < ...$ and $\lim_{k\to\infty} t_k = \infty$. The system (4) with initial condition $x(t_0) = x_0$ is assumed to have a solution $x(t) = x(t; t_0, x_0) \in PC^q([t_0, \infty), \mathbb{R}^N)$.

Remark 3.1. The second equation in (4) is called the impulsive condition, and the function $I_k(x(t_k))$ gives the amount of jump of the solution at the point t_k.

Definition 3.2. *Let $V : \mathbb{R}_+ \times \mathbb{R}^N \to \mathbb{R}_+^N$. Then V is said to belong to class $\mathcal{L}$ if,*

1. *(i) V is continuous in $(t_{k-1}, t_k] \times \mathbb{R}^{\mathbb{N}}$ and for each $x \in \mathbb{R}^N$, $k = 1, 2, ...$ $\lim_{(t,y)\to(t_k^+,x)} V(t, y) = V(t_k^+, x)$ exists;*

2. *(ii) V is locally Lipschitz with respect to its second argument x and $V(t, 0) \equiv 0$.*

Now, for any function $V(t, x) \in C([t_0, \infty) \times \xi, \mathbb{R}_+^{\mathbb{N}})$ we define the Caputo fractional Dini derivative as:

$$ {}^cD_+^q V(t,x) = \limsup_{h\to 0^+} \frac{1}{h^q}\{V(t,x) - V(t_0,x_0) - \sum_{r=1}^{[\frac{t-t_0}{h}]} (-1)^{r+1} ({}^qC_r)[V(t-rh, x-h^q f(t,x)) - V(t_0,x_0)]\} \tag{5} $$

$t \geq t_0$ where $t \in [t_0, \infty), x, x_0 \in \xi$, and there exists $h > 0$ such that $t - rh \in [t_0, T]$

Definition 3.3. *A function $g \in C[\mathbb{R}^n, \mathbb{R}^n]$ is said to be quasimonotone nondecreasing in x, if $x \leq y$ and $x_i = y_i$ for $1 \leq i \leq n$ implies $g_i(x) \leq g_i(y), \forall i$.*

Definition 3.4. *The set $x(t) \equiv 0$ of (4) is said to be:*
$(S1)$ eventually stable if for every $\epsilon > 0$ there exists a number $T = T(\epsilon) > 0$ for all $t_0 \in \mathbb{R}_+$ and $\delta = \delta(t_0, \epsilon)$ for all $x_0 \in \mathbb{R}^N$ such that $|x_0| < \delta$ implies $|x(t; t_0, x_0)| < \epsilon$ for $t \geq t_0$.

$(S2)$ eventually uniformly stable if the δ in $S1$ is independent of t.

Definition 3.5. *A function $a(r)$ is said to belong to the class $\mathcal{K}$ if $a \in C([0, \psi), \mathbb{R}_+], a(0) = 0$, and $a(r)$ is strictly monotone increasing in r.*

In this paper, we define the following sets:

$$\begin{aligned} \bar{S}_\psi &= \{x \in \mathbb{R}^N : \|x\| \leq \psi\} \\ S_\psi &= \{x \in \mathbb{R}^N : \|x\| < \psi\} \end{aligned}$$

It suffices to say that the inequalities between vectors are understood to be component-wise inequalities.

We will use the comparison results for the impulsive Caputo fractional differential equation of the type

$$\begin{aligned} {}_{t_0}^c D^q u = g(t,u), t \geq t_0, t \neq t_k, k = 1, 2, ... \\ \Delta u = \psi_k(u(t_k)), k \in N, t = t_k \\ u(t_0^+) = u_0, \end{aligned} \tag{6}$$

existing for $t \geq t_0$, where $u \in \mathbb{R}^n, \mathbb{R}_+ = [t_0, \infty), g : \mathbb{R}_+ \times \mathbb{R}^n \to \mathbb{R}^n, g(t, 0) \equiv 0$,
where g is the continuous mapping of $\mathbb{R}_+ \times \mathbb{R}^n$ into $\mathbb{R}^n$. The function $g \in PC[\mathbb{R}_+ \times \mathbb{R}^n_+, \mathbb{R}^n]$ is such that for any initial data $(t_0, u_0) \in \mathbb{R}_+ \times \mathbb{R}^n$, the system (6) with initial condition $u(t_0) = u_0$ is assumed to have a solution $u(t; t_0, u_0) \in PC^q([t_0, \infty), \mathbb{R}^n)$.

Lemma 3.6. *Assume $m \in PC([t_0, T] \times \bar{S}_\psi, \mathbb{R}^N)$ and suppose there exists $t^* \in [t_0, T]$ such that for $\alpha_1 < \alpha_2$, $m(t^*, \alpha_1) = m(t^*, \alpha_2)$ and $m(t, \alpha_1) < m(t, \alpha_2)$ for $t_0 \leq t < t^*$. Then if the Caputo fractional Dini derivative of m exists at t^*, then the inequality ${}^C D^q_+ m(t^*, \alpha_1) - {}^C D^q_+ m(t^*, \alpha_2) > 0$ holds.*

Proof. Let $V(t, x) = m(t, \alpha_1) - m(t, \alpha_2)$.
Applying (5), we have

$$\begin{aligned} {}^C D^q_+(m(t^*, \alpha_1) - m(t^*, \alpha_2)) &= \limsup_{h \to 0^+} \frac{1}{h^q}\{[m(t^*, \alpha_1) - m(t^*, \alpha_2)] - [m(t_0, \alpha_1) - m(t_0, \alpha_2)] \\ &\quad - \sum_{r=1}^{[\frac{t-t_0}{h}]} (-1)^{r+1} qC_r [m(t^* - rh, \alpha_1) - m(t^* - rh, \alpha_2)] \\ &\quad - [m(t_0, \alpha_1) - m(t_0, \alpha_2)]\} \end{aligned}$$

When $m(t^*, \alpha_1) = m(t^*, \alpha_2)$, we have

$$\begin{aligned} {}^C D^q_+(m(t^*, \alpha_1) - m(t^*, \alpha_2)) &= \limsup_{h \to 0^+} \frac{1}{h^q}\{-[m(t_0, \alpha_1) - m(t_0, \alpha_2)] - \sum_{r=1}^{[\frac{t-t_0}{h}]} (-1)^{r+1} qC_r \\ &\quad [m(t^* - rh, \alpha_1) - m(t^* - rh, \alpha_2)] - [m(t_0, \alpha_1) - m(t_0, \alpha_2)]\} \\ &= - \limsup_{h \to 0^+} \frac{1}{h^q}\{[m(t_0, \alpha_1) - m(t_0, \alpha_2)] \\ &\quad + \limsup_{h \to 0^+} \frac{1}{h^q} \sum_{r=1}^{[\frac{t-t_0}{h}]} (-1)^r qC_r [m(t^* - rh, \alpha_1) - m(t^* - rh, \alpha_2)] \\ &\quad - \limsup_{h \to 0^+} \frac{1}{h^q} \sum_{r=1}^{[\frac{t-t_0}{h}]} (-1)^r qC_r [m(t_0, \alpha_1) - m(t_0, \alpha_2)] \\ &= - \limsup_{h \to 0^+} \frac{1}{h^q}\{[m(t_0, \alpha_1) - m(t_0, \alpha_2)] \\ &\quad - \limsup_{h \to 0^+} \frac{1}{h^q} \sum_{r=1}^{[\frac{t-t_0}{h}]} (-1)^r qC_r [m(t_0, \alpha_1) - m(t_0, \alpha_2)] \\ &= - \limsup_{h \to 0^+} \frac{1}{h^q} \sum_{r=0}^{[\frac{t-t_0}{h}]} (-1)^r qC_r [m(t_0, \alpha_1) - m(t_0, \alpha_2)] \end{aligned}$$

Applying equation (3.8) in [1], we have

$${}^c D^q_+(m(t^*, \alpha_1) - m(t^*, \alpha_2)) = -\frac{(t - t_0)^{-q}}{\Gamma(1 - q)}[m(t_0, \alpha_1) - m(t_0, \alpha_2)]$$

By the lemma, we have that

$$m(t, \alpha_1) - m(t, \alpha_2) < 0, \text{for } t_0 \leq t < t^*$$

And so it follows that

$${}^c D^q_+(m(t^*, \alpha_1) - m(t^*, \alpha_2)) > 0$$

4 Fractional differential inequalities and comparison results for impulsive vector fractional differential equations

In this section, we assume that $0 < q < 1$.

Theorem 4.1. *Assume that*

(i) $g \in PC[\mathbb{R}_+ \times \mathbb{R}^n_+, \mathbb{R}^n]$ *and is continuous in* $(t_{k-1}, t_k]$, $k = 1, 2, ...$ *and* $g(t, u)$ *is quasimonotone nondecreasing in* u *for each* $u \in \mathbb{R}^n$ *and* $\lim\limits_{(t,y)\to(t_k^+,u)} g(t, u) = g(t_k^+, u)$ *exists;*

(ii) $V \in PC[\mathbb{R}_+ \times \mathbb{R}^N, \mathbb{R}^N_+]$ *and* $V \in \mathcal{L}$ *such that*
${}^C D^q_+ V(t, x) \leq g(t, V(t, x))$, $t \neq t_k$, $(t, x) \in \mathbb{R}_+ \times \mathbb{R}^N$ *and*
$V(t_k, x + I_k(x(t_k))) \leq \rho_k(V(t, x))$, $t = t_k$, $x \in S_\psi$ *and the function* $\rho_k : \mathbb{R}^N_+ \to \mathbb{R}^N_+$ *is nondecreasing for* $k = 1, 2, ...$

(iii) $r(t) = r(t; t_0, u_0) \in PC^q([t_0, T], \mathbb{R}^n)$ *is the maximal solution of the the IVP for the IFrDE* (6).

Then,

$$V(t, x(t)) \leq r(t), t \geq t_0 \tag{7}$$

where $x(t) = x(t; t_0, x_0) \in PC^q([t_0, T], \mathbb{R}^N)$ *is any solution of* (4) *existing on* $[t_0, \infty)$, *provided that*

$$V(t_0^+, x_0) \leq u_0. \tag{8}$$

Proof. Let $\eta \in \bar{S}_\psi =: \{\eta \in \mathbb{R}^n : \|\eta\| \leq \psi\}$ be a small enough arbitrary vector and consider the initial value problem for the following system of fractional differential equations.

$$\begin{aligned} {}^c D^q u = g(t, u) + \eta, \Delta u = \psi_k(u(t_k)), t = t_k, k = 1, 2, ... \\ u(t_0^+) = u_0 + \eta \end{aligned} \tag{9}$$

for $t \in [t_0, \infty)$.
The function $u_\eta(t, \alpha)$ is a solution of (9), where $\alpha > 0$, if and only if it satisfies the Volterra Integral equation

$$u_\eta(t, \alpha) = u_0 + \eta + \frac{1}{\Gamma(q)} \int_{t_0}^t (t - s)^{q-1} (g(s, u_\eta(s, \alpha)) + \eta) ds, \; t \in [t_0, \infty) \tag{10}$$

Let the function $m(t, \alpha) \in PC([t_0, T] \times \bar{S}_\psi, \mathbb{R}^N)$ be defined as $m(t, \alpha) = V(t, x^*(t))$.
We now prove that

$$m(t, \alpha) < u_\eta(t, \alpha), \quad \text{for} \quad t \in [t_0, \infty) \tag{11}$$

Observe that the inequality (11) holds for $t = t_0$ i.e

$$m(t_0, \alpha) = V(t_0, x_0) \leq u_0 < u_\eta(t_0, \alpha)$$

Assume that the inequality (11) is not true, then there exist a point $t_1 > t_0$ such that

$$m(t_1, \alpha) = u_\eta(t_1, \alpha) \quad \text{and} \quad m(t, \alpha) < u_\eta(t, \alpha) \quad \text{for} \quad t \in [t_0, t_1)$$

It follows from lemma (3.6) that

$${}^C D^q_+ m(t_1, \alpha) - {}^C D^q_+ u_\eta(t_1, \alpha) > 0$$

So that

$${}^C D^q_+ (V(t_1, x(t_1))) > {}^C D^q_+ (u_\eta(t_1, \alpha))$$

and using (9) we arrive at

$$^{C}D_{+}^{q}(V(t_1, x(t_1))) > g(t_1, u_\eta(t_1, \alpha) + \eta) > g(t_1, u(t_1, \alpha))$$

Therefore,

$$^{C}D_{+}^{q}(m(t_1, \alpha)) > g(t_1, u(t_1, \alpha)) \tag{12}$$

For $t \in [t_0, T]$, we maintain that $x^*(t)$ satisfies (4) and the equality,

$$\limsup_{h \to 0^+} \frac{1}{h^q}[x^*(t) - x_0 - S(x^*(t), h)] = f(t, x^*(t)) \tag{13}$$

holds, where $x^*(t)$ is any other solution of (4).

$$S(x^*(t), h) = \sum_{r=1}^{[\frac{t-t_0}{h}]} (-1)^{r+1}({}^{q}C_r)[x^*(t - rh) - x_0)] \tag{14}$$

is the Grunwald Letnikov fractional derivative and $[\frac{t-t_0}{h}]$ is the integer part of $\frac{t-t_0}{h}$.

Multiply equation (13) althrough by h^q we have,

$$\limsup_{h \to 0^+}[x^*(t) - x_0 - S(x^*(t), h)] = h^q f(t, x^*(t))$$

$$x^*(t) - x_0 - \limsup_{h \to 0^+}[S(x^*(t), h)] = h^q f(t, x^*(t))$$

$$x^*(t) - x_0 - [S(x^*(t), h) + \rho(h^q)] = h^q f(t, x^*(t))$$

$$x^*(t) - h^q f(t, x^*(t)) = [S(x^*(t), h) + x_0 + \rho(h^q)] \tag{15}$$

For $t \in [t_0, T]$, we have

$$\begin{aligned}
& m(t, \alpha) - m(t_0, \alpha) - \sum_{r=1}^{[\frac{t-t_0}{h}]} (-1)^{r+1}({}^{q}C_r)[m(t - rh, \alpha) - m(t_0, \alpha)] \\
= \; & V(t, x^*(t)) - V(t_0, x_0) - \sum_{r=1}^{[\frac{t-t_0}{h}]} (-1)^{r+1 q}C_r[V(t - rh, x^*(t) - h^q f(t, x^*(t)) - V(t_0, x_0)] \\
= \; & V(t, x^*(t)) - V(t_0, x_0) - \sum_{r=1}^{[\frac{t-t_0}{h}]} (-1)^{r+1 q}C_r[V(t - rh, x^*(t) - h^q f(t, x^*(t)) - V(t_0, x_0)] \\
& + \sum_{r=1}^{[\frac{t-t_0}{h}]} (-1)^{r+1}({}^{q}C_r)[V(t - rh, S(x^*(t), h) + x_0 + \rho(h^q) - V(t_0, x_0)] \\
& - [V(t - rh, x^*(t - rh) - V(t_0), x_0)]
\end{aligned}$$

Since $V(t, x)$ is locally Lipschtzian in the second variable, we have

$$\leq L|(-1)^{r+1}|| \sum_{r=1}^{[\frac{t-t_0}{h}]} ({}^{q}C_r)[S(x^*(t), h) + x_0 + \rho(h^q) - x^*(t - rh)]||$$

where $L > 0$ is the Lipschitz constant.

$$\leq L\| \sum_{r=1}^{[\frac{t-t_0}{h}]} {}^qC_r[S(x^*(t),h) + \rho(h^q) - (x^*(t-rh) - x_0)]\| \tag{16}$$

Using equations (14), equation (16) becomes,

$$\leq L\| \sum_{r=1}^{[\frac{t-t_0}{h}]} {}^qC_r(\sum_{r=1}^{[\frac{t-t_0}{h}]} (-1)^{r+1q}C_r[x^*(t-rh) - x_0)] + \rho(h^q) - (x^*(t-rh) - x_0)]\|$$

$$\begin{aligned} \leq \quad & L\| \sum_{r=1}^{[\frac{t-t_0}{h}]} {}^qC_r(-1)^{r+1}(\sum_{r=1}^{[\frac{t-t_0}{h}]} {}^qC_r[x^*(t-rh) - x_0)] + \sum_{r=1}^{[\frac{t-t_0}{h}]} {}^qC_r\rho(h^q) \\ & - \sum_{r=1}^{[\frac{t-t_0}{h}]} {}^qC_r(x^*(t-rh) - x_0)]\| \end{aligned}$$

$$\leq L(-1)^{r+1}\| \sum_{r=1}^{[\frac{t-t_0}{h}]} {}^qC_r(x^*(t-rh) - x_0)[\sum_{r=1}^{[\frac{t-t_0}{h}]} {}^qC_r - 1] + \sum_{r=1}^{[\frac{t-t_0}{h}]} {}^qC_r\rho(h^q)\| \tag{17}$$

Substituting equation (17) we obtain

$$\begin{aligned} & = V(t,x^*(t)) - V(t_0,x_0) - \sum_{r=1}^{[\frac{t-t_0}{h}]} (-1)^{r+1q}C_r[V(t-rh, x^*(t) - h^q f(t,x^*(t)) - V(t_0,x_0)] \\ & + L\| \sum_{r=1}^{[\frac{t-t_0}{h}]} (-1)^{r+1q}C_r(x^*(t-rh) - x_0)[\sum_{r=1}^{[\frac{t-t_0}{h}]} (-1)^{r+1q}C_r - 1] + \sum_{r=1}^{[\frac{t-t_0}{h}]} (-1)^{r+1q}C_r\rho(h^q)\| \\ & = V(t,x^*(t)) - V(t_0,x_0) - \sum_{r=1}^{[\frac{t-t_0}{h}]} (-1)^{r+1q}C_r[V(t-rh, x^*(t) - h^q f(t,x^*(t)) - V(t_0,x_0)] \\ & + L\| \sum_{r=1}^{[\frac{t-t_0}{h}]} (-1)^{r+1q}C_r(x^*(t-rh) - x_0)[- \sum_{r=1}^{[\frac{t-t_0}{h}]} (-1)^{rq}C_r - 1] + \sum_{r=1}^{[\frac{t-t_0}{h}]} (-1)^{r+1q}C_r\rho(h^q)\| \end{aligned}$$

Dividing althrough by $h^q > 0$ and taking the *limsup* as $h \to 0^+$ we have,

$$\begin{aligned} {}^CD_+^q m(t,\alpha) = & \limsup_{h\to 0^+} \frac{1}{h^q}[V(t,x^*(t)) - V(t_0,x_0) \\ & - \sum_{r=1}^{[\frac{t-t_0}{h}]} (-1)^{r+1q}C_r[V(t-rh, x^*(t) - h^q f(t,x^*(t)) - V(t_0,x_0)]] \\ & + \limsup_{h\to 0^+} \frac{1}{h^q} L\| \sum_{r=1}^{[\frac{t-t_0}{h}]} (-1)^{r+1q}C_r(x^*(t-rh) - x_0)[- \sum_{r=1}^{[\frac{t-t_0}{h}]} (-1)^{rq}C_r - 1] \\ & + \sum_{r=1}^{[\frac{t-t_0}{h}]} (-1)^{r+1q}C_r\rho(h^q)\| \end{aligned}$$

Recall $\lim_{h\to 0^+}\sum_{r=1}^{[\frac{t-t_0}{h}]}(-1)^{rq}C_r = -1$ *and* $\limsup_{h\to 0^+}\frac{1}{h^q}\rho(h^q) = 0$ so that we obtain,

$$^{C}D_{+}^{q}m(t,\alpha) = ^{C}D_{+}^{q}V(t,x^*(t)) + L\|\sum_{r=1}^{[\frac{t-t_0}{h}]} {}^{q}C_r(x^*(t-rh)-x_0)[-(-1)-1]+0\|$$

$$^{C}D_{+}^{q}m(t,\alpha) = ^{C}D_{+}^{q}V(t,x^*(t)) + 0$$

Using condition (ii) of Theorem 4.1 we have

$$^{C}D_{+}^{q}m(t,\alpha) \le g(t,V(t,x^*(t))) = g(t,m(t,\alpha)) \tag{18}$$

Also,

$$m(t_0^+,\alpha) \le u_0 \; and \; m(t_k^+,\alpha) = V(t_k^+,x(t_k)+I_k(x(t_k)) \le \rho_k(m(t_k)) \tag{19}$$

Now, equation (18) with $t = t_1$ contradicts (12), hence (11) holds.
For $t \in [t_0,T]$, we now show that whenever $\eta_1 < \eta_2$, then

$$u_{\eta_1}(t,\alpha) < u_{\eta_2}(t,\alpha) \tag{20}$$

It is obvious that (20) holds for $t = t_0$. Assume the inequality (20) is not true. Then there exist a point $t_1 > t_0$ such that $u_{\eta_1}(t_1,\alpha) = u_{\eta_2}(t_1,\alpha)$ and $u_{\eta_1}(t,\alpha) < u_{\eta_2}(t,\alpha)$ for $t \in [t_0,t_1)$.
By lemma (3.6), we have that

$$^{C}D_{+}^{q}(u_{\eta_1}(t_1,\alpha) - u_{\eta_2}(t_1,\alpha)) > 0$$

However,

$$\begin{aligned} ^{C}D_{+}^{q}(u_{\eta_1}(t_1,\alpha) - u_{\eta_2}(t_1,\alpha_)) &= {}^{C}D_{+}^{q}u_{\eta_1}(t_1,\alpha) - {}^{C}D_{+}^{q}u_{\eta_2}(t_1,\alpha) \\ &= g(t_1,u(t_1,\alpha)+\eta_1)) - [g(t_1,u(t_1,\alpha)+\eta_2))] \\ &= \eta_1 - \eta_2 < 0 \end{aligned}$$

which is a contradiction and so (20) is true. Thus, equations (11) and (20) guarantee that the family of solutions $\{u_\eta(t,\alpha)\}$, $t \in [t_0,T]$ of (9) is uniformly bounded, i.e. there exists $P > 0$ with $|u_\eta(t,\alpha)| \le P$, with bound P on $[t_0,T]$.
We now show that the family $\{u_\eta(t,\alpha)\}$ is equicontinuous on $[t_0,T]$. Assume $K = sup\{g(t,x) : (t,x) \in [t_0,T]\times[-P,P]\}$. Also, fix a decreasing sequence $\{\eta_i\}_{i=1}^{\infty}(t)$, such that $\lim_{i\to\infty}\eta_i = 0$ and consider a sequence of functions $u_{\eta_i}(t,\alpha)$. Again let $t_1,t_2 \in [t_0,T]$ with $t_1 < t_2$, then we have the following estimate

$$\begin{aligned} \|u_{\eta_i}(t_2,\alpha) - u_{\eta_i}(t_1,\alpha)\| &= \|u_0+\eta_i+\frac{1}{\Gamma(q)}\int_{t_0}^{t_2}(t_2-s)^{q-1}(g(s,u_{\eta_i}(s,\alpha))+\eta_i) \\ &- (u_0+\eta_i+\frac{1}{\Gamma(q)}\int_{t_0}^{t_1}(t_1-s)^{q-1}(g(s,u_{\eta_i}(s,\alpha))+\eta_i))\| \\ &= \frac{1}{\Gamma(q)}\|\int_{t_0}^{t_2}(t_2-s)^{q-1}(g(s,u_{\eta_i}(s,\alpha)))ds \\ &- \int_{t_0}^{t_1}(t_1-s)^{q-1}(g(s,u_{\eta_i}(s,\alpha)))ds\| \\ &\le \frac{k}{\Gamma(q)}\left|\int_{t_0}^{t_2}(t_2-s)^{q-1} - \int_{t_0}^{t_1}(t_1-s)^{q-1}\right|ds \\ &= \frac{k}{\Gamma(q)}\left|-(\int_{t_0}^{t_1}(t_1-s)^{q-1} - \int_{t_0}^{t_2}(t_2-s)^{q-1})\right|ds \\ &= \frac{k}{\Gamma(q)}\left|\int_{t_0}^{t_1}(t_1-s)^{q-1} - (\int_{t_0}^{t_1}(t_2-s)^{q-1} + \int_{t_1}^{t_2}(t_2-s)^{q-1})\right|ds \end{aligned}$$

$$
\begin{aligned}
&= \frac{k}{\Gamma(q)}\left|\int_{t_0}^{t_1}(t_1-s)^{q-1}-\int_{t_0}^{t_1}(t_2-s)^{q-1}-\int_{t_1}^{t_2}(t_2-s)^{q-1}\right|ds\\
&\leq \frac{k}{\Gamma(q)}\left|\int_{t_0}^{t_1}(t_1-s)^{q-1}-\int_{t_0}^{t_1}(t_2-s)^{q-1}\right|ds+\left|\int_{t_1}^{t_2}(t_2-s)^{q-1}\right|ds\\
&= \frac{k}{\Gamma(q)}\left|\frac{(t_1-t_0)^q}{q}+\frac{(t_2-t_1)^q}{q}-\frac{(t_2-t_0)^q}{q}\right|+\frac{(t_2-t_1)^q}{q}\\
&\leq \frac{k}{\Gamma(q+1)}(t_1-t_0)^q+(t_2-t_1)^q-(t_2-t_0)^q+(t_2-t_1)^q\\
&= \frac{k}{\Gamma(q+1)}(t_1-t_0)^q-(t_2-t_0)^q+2(t_2-t_1)^q\\
&\leq \frac{2k}{\Gamma(q+1)}(t_2-t_1)^q<\epsilon
\end{aligned}
$$

provided $\|t_2-t_1\|<\delta=(\frac{\epsilon\Gamma(q+1)}{2k})^{\frac{1}{q}}$, proving that the family of solutions $\{u_{\eta_i}(t;\alpha)\}$ is equi-continuous. By the Arzela-Ascoli theorem, $\{u_{\eta_i}(t;\alpha)\}$ has a subsequence $\{u_{\eta_{i_j}}(t;\alpha)\}$ which converges uniformly to a function $r(t)$ on $[t_0,T]$. We then show that $r(t)$ is a solution of (10). Equation (10) becomes

$$u_{\eta_{i_j}}(t,\alpha)\ =u_{0_{i_j}}+\eta_{i_j}+\frac{1}{\Gamma(q)}\int_{t_0}^{t}(t-s)^{q-1}(g_{i_j}(s,u_{i_j}(s,\eta_{i_j}))+\eta_{i_j})ds \tag{21}$$

Taking the limit as $i_j\to\infty$ in (21), yields

$$r(t)=u_0+\frac{1}{\Gamma(q)}\int_{t_0}^{t}(t-s)^{q-1}(g(s,r(t)))ds \tag{22}$$

Thus, $r(t)$ is a solution of (6) on $[t_0,T]$. We claim that $r(t)$ is the maximal solution of (6). Then from (11), we have that $m(t,\alpha)<u_\eta(t,\alpha)\leq r(t)$ on $[t_0,T]$.

5 Main results

In this section, we will obtain sufficient conditions for the eventual stability of the system (3.3).

Theorem 5.1. *Assume the following*

(i) $g\in PC[\mathbb{R}_+\times\mathbb{R}_+^n,\mathbb{R}^n]$ *satisfies* (A_0) *(ii) and* $g(t,u)$ *is quasi-monotone nondecreasing in* u *with* $g(t,0)\equiv 0$.

(ii) $V\in PC[\mathbb{R}_+\times\mathbb{R}^N,\mathbb{R}_+^N]$ *and* $V\in\mathcal{L}$ *such that*

$$^{C}D_+^qV(t,x)\leq g(t,V(t,x)),t\neq t_k,(t,x)\in\mathbb{R}_+\times\mathbb{R}^N \tag{23}$$

holds for all $(t,x)\in\mathbb{R}_+\times S_\psi$.

(iii) there exists a $\psi_0>0$ *such that* $x_0\in S_\psi$ *implies that* $x+I_k(x)\in S_\psi$ *and* $V(t_k,x+I_k(x))\leq\psi_k(V(t,x))$, $t=t_k,x\in S_\psi$ *and the function* $\psi_k:\mathbb{R}_+^N\to\mathbb{R}_+^N$ *is nondecreasing for* $k=1,2,...$

(iv) $a(\|x\|)\leq V_0(t,x)$, *where* $a\in\mathcal{K}$ *and* $V_0(t,x)=\sum_{i=1}^N V_i(t,x)$
Then the eventual stability of the set of trivial solution $u=0$ *of the IFrDE* (6) *implies the eventual stability of the set of trivial solution* $x=0$ *of* (4).

Proof. Since $V(t,x)$ is positive definite, then

$$a(\|x\|)\leq V_0(t,x),(t,x)\in J\times S_\psi,\ where\ J\subset\mathbb{R}_+ \tag{24}$$

and $a(r)$ is in the k-class. Let $0 < \epsilon < \psi$ and $t_0 \in \mathbb{R}_+$ be given.
Assume that the solution $u = 0$ of (6) is stable. Then given each $a(\epsilon) > 0$, and $t_0 \in \mathbb{R}_+$, there exist a positive function $\delta = \delta(t_0, \epsilon) > 0$ continuous in t_0 such that whenever

$$u_0 = \sum_{i=1}^{n} u_{i0} < \delta, \ we \ \ have \ \sum_{i=1}^{n} u_i(t; t_0, u_0) < a(\epsilon), t \geq t_0 \tag{25}$$

where $u(t; t_0, u_0)$ is any solution of (6).
Choose $u_0 = V(t_0^+, x_0)$
Since $V(t, x)$ is continuous, then by the property of continuity, given $\delta > 0$ there exists a positive function $\delta_1 = \delta_1(t_0, \delta) > 0$ that is continuous in t_0 for each δ, such that

$$\|V(t, x) - V(t_0, x_0)\| < \delta \ implies \ \|x - x_0\| < \delta_1$$

and as $\|V(t, x)\| \to 0$ as $\|x\| \to 0$, then the inequalities,

$$\|x_0\| < \delta_1 \ and \ V(t_0, x_0) < \delta \tag{26}$$

hold simultaneously.
We claim that if

$$\|x_0\| < \delta_0, \ then \ \|x(t, t_0, x_0)\| < \delta.$$

Suppose that this claim is false, then there would exists a point $t_1 > t_0$ and a solution $x(t)$ with $\|x_0\| < \delta$ such that

$$\|x(t_1)\| = \epsilon \ and \ \|x(t)\| \leq \epsilon, t \in [t_0, t_1) \tag{27}$$

so that (24) becomes

$$a(\|x(t_1)\|) \leq V_0(t_1, x(t_1)). \tag{28}$$

This means that $\|x(t)\| < \psi$ for $t \in [t_0, t_1)$
Combining equations (7), (25) and (28) we obtain the estimate

$$a(\|x(t_1)\|) \leq V_0(t_1, x(t_1)) \leq \sum_{i=0}^{n} r_i(t; t_0, u_0)$$

where $r(t) = \sum_{i=0}^{n} r_i(t; t_0, u_0)$ is the maximal solution of (6).

$$a(\epsilon) \leq V_0(t_1, x(t_1)) \leq \sum_{i=1}^{n} r_i(t; t_0, u_0) < a(\epsilon)$$

which leads to a contradiction. Hence, the eventual stability of the trivial solution $u = 0$ of (6) implies the eventual stability of the set of trivial solution $x = 0$ of (4).

6 Application

Let the points $t_k, t_k < t_{k+1}, lim_{k\to\infty} t_k \to \infty$ be fixed. Consider the vector impulsive Caputo fractional differential equations

$$\begin{aligned} {}^{C}D^{q}x_1(t) &= -10x_1 - \frac{x_2^2 cosx_1}{2x_1} + x_1 sinx_2 + \frac{x_2^2 tanx_1}{x_1} \\ {}^{C}D^{q}x_2(t) &= \frac{3x_1^2}{x_2} - x_2 sinx_1 - 5x_2 cosecx_1 - x_1^2 cosx_2 \\ \Delta x_1 &= s_k(x(t_k)), \Delta x_2 = n_k(x(t_k)), k = 1, 2, .. \end{aligned} \tag{29}$$

for $t \geq t_0$, with initial conditions

$$x_1(t_0^+) = x_{10} \quad \text{and} \quad x_2(t_0^+) = x_{20}$$

Consider a vector $V = (V_1, V_2)^T$, where
$V_1(t, x_1, x_2) = x_1^2$ and $V_2(t, x_1, x_2) = x_2^2$, with $x = (x_1, x_2) \in \mathbb{R}^2$, and its associated norm defined by $\|x\| = \sqrt{x_1^2 + x_2^2}$.
Now

$$V_0(t, x) = \sum_{i=1}^{2} V_i(t, x_1, x_2) = x_1^2 + x_2^2$$

and so $b(\|x\|) \leq V_0(t, x) \leq a(\|x\|)$ with $b(r) = r$ and $a(r) = r^2$, implying that $a, b \in \mathcal{K}$. From (5), we compute the Caputo fractional Dini derivative for $V_1(t, x_1, x_2) = x_1^2$ for $t > 0, t \neq t_k$ as follows:

$$\begin{aligned}
{}^{C}D_{+}^{q} V_1(t; x_1, x_2) &= \limsup_{h \to 0^+} \frac{1}{h^q} \big\{ V(t, x) - V(t_0, x_0) \\
&\quad + \sum_{r=1}^{[\frac{t-t_0}{h}]} (-1)^r ({}^{q}C_r)[V(t - rh, x - h^q f(t, x)) - V(t_0, x_0)] \big\} \\
&= \limsup_{h \to 0^+} \frac{1}{h^q} \big\{ x_1^2 - x_{10}^2 + \sum_{r=1}^{[\frac{t-t_0}{h}]} (-1)^r ({}^{q}C_r)[(x_1 - h^q f_1(t; x_1, x_2)^2 - x_{10}^2] \big\} \\
&\leq \limsup_{h \to 0^+} \frac{1}{h^q} \big\{ x_1^2 - x_{10}^2| + \sum_{r=1}^{[\frac{t-t_0}{h}]} (-1)^r ({}^{q}C_r)[x_1^2 - 2x_1 h^q f_1(t; x_1, x_2) \\
&\quad + h^{2q} f_1(t, x_1) - x_{10}^2] \big\} \\
&= \limsup_{h \to 0^+} \frac{1}{h^q} \big\{ x_1^2 - x_{10}^2 + \sum_{r=1}^{[\frac{t-t_0}{h}]} (-1)^r ({}^{q}C_r) x_1^2 \\
&\quad - \sum_{r=1}^{[\frac{t-t_0}{h}]} (-1)^r ({}^{q}C_r) 2x_1 h^q f_1(t; x_1, x_2) - \sum_{r=1}^{[\frac{t-t_0}{h}]} (-1)^r ({}^{q}C_r) h^{2q} f_1(t; x_1, x_2) \big\} \\
&= \limsup_{h \to 0^+} \frac{1}{h^q} \big\{ x_1^2 + \sum_{r=1}^{[\frac{t-t_0}{h}]} (-1)^r ({}^{q}C_r) x_1^2 - x_{10}^2 - \sum_{r=1}^{[\frac{t-t_0}{h}]} (-1)^r ({}^{q}C_r) x_{10}^2 \\
&\quad - 2x_1 \sum_{r=1}^{[\frac{t-t_0}{h}]} (-1)^r ({}^{q}C_r) h^q f_1(t; x_1, x_2)| \big\} \\
&= \limsup_{h \to 0^+} \frac{1}{h^q} \big\{ \sum_{r=0}^{[\frac{t-t_0}{h}]} (-1)^r ({}^{q}C_r) x_1^2 - \sum_{r=0}^{[\frac{t-t_0}{h}]} (-1)^r ({}^{q}C_r) x_{10}^2 \\
&\quad - 2x_1 \sum_{r=1}^{[\frac{t-t_0}{h}]} (-1)^r ({}^{q}C_r) h^q f_1(t; x_1, x_2) \big\}
\end{aligned}$$

Recall that,

$$\limsup_{h \to 0^+} \frac{1}{h^q} \big\{ \sum_{r=0}^{[\frac{t-t_0}{h}]} (-1)^r ({}^{q}C_r) = \frac{x_1^2}{t^q \Gamma(1-q)}, \tag{30}$$

and

$$\lim_{h\to 0^+}\sum_{r=0}^{[\frac{t-t_0}{h}]}(-1)^r{}^qC_r=-1 \tag{31}$$

Substituting (30) and (31), we obtain

$$\begin{aligned}{}^CD_+^qV_1(t;x_1,x_2) &\leq \frac{x_1^2}{t^q\Gamma(1-q)}-\frac{x_{10}^2}{t^q\Gamma(1-q)}+2x_1f_1(t;x_1,x_2)\\ {}^CD_+^qV_1(t;x_1,x_2) &\leq \frac{x_1^2}{t^q\Gamma(1-q)}+2x_1f_1(t;x_1,x_2)\end{aligned}$$

$$\begin{aligned}{}^CD_+^qV_1(t;x_1,x_2) &\leq \frac{x_1^2}{t^q\Gamma(1-q)}+2x_1(-10x_1-\frac{x_2^2cosx_1}{2x_1}+x_1sinx_2+\frac{x_2^2tanx_1}{x_1})\\ &= \frac{x_1^2}{t^q\Gamma(1-q)}-20x_1^2-x_2^2cosx_1+2x_1^2sinx_2+x_2^2tanx_1\end{aligned}$$

As $t\to\infty$, $\frac{x_1^2}{t^q\Gamma(1-q)}\to 0$, so that we have

$$\begin{aligned}&\leq -20x_1^2-x_2^2cosx_1+2x_1^2sinx_2+x_2^2tanx_1\\ &= 2x_1^2(-10+sinx_2)+x_2^2(2tanx_1-cosx_1)\\ &\leq 2x_1^2(-10+|sinx_2|)+x_2^2(2\frac{|sinx_1|}{|cosx_1|}-|cosx_1|)\\ &\leq 2x_1^2(-10+1)+x_2^2(2-1)\\ &= 2x_1^2(-9)+x_2^2(1)\\ &= x_1^2(-18)+x_2^2(1)\end{aligned}$$

Therefore,

$${}^CD_+^qV_1(t;x_1,x_2)\leq -18V_1+V_2 \tag{32}$$

Also, for $x_0\in S_\psi$, for $t=t_k, k=1,2,..$, we have

$$V(t,x(t)+c_k)=|c_k+x(t)|\leq V(t,x(t))$$

Similarly, using (5), we compute the Caputo fractional Dini derivative for $V_2(t,x_1,x_2)=x_2^2$ as follows:

$$\begin{aligned}{}^CD_+^qV_2(t;x_1,x_2) &= \limsup_{h\to 0^+}\frac{1}{h^q}\{V(t,x)-V(t_0,x_0)\\ &\quad+\sum_{r=1}^{[\frac{t-t_0}{h}]}(-1)^r({}^qC_r)[V(t-rh,x-h^qf(t,x))-V(t_0,x_0)]\}\\ &= \limsup_{h\to 0^+}\frac{1}{h^q}\{x_2^2-x_{20}^2+\sum_{r=1}^{[\frac{t-t_0}{h}]}(-1)^r({}^qC_r)[(x_2-h^qf_2(t;x_1,x_2)^2-x_{20}^2]\}\end{aligned}$$

$$
\begin{aligned}
&\leq \limsup_{h\to 0^+}\frac{1}{h^q}\{x_2^2-x_{20}^2|+\sum_{r=1}^{[\frac{t-t_0}{h}]}(-1)^r({}^qC_r)[x_2^2-2x_2h^qf_2(t;x_1,x_2)\\
&\quad +h^{2q}f_2(t,x_2)-x_{20}^2]\}\\
&= \limsup_{h\to 0^+}\frac{1}{h^q}\{x_2^2-x_{20}^2+\sum_{r=1}^{[\frac{t-t_0}{h}]}(-1)^r({}^qC_r)x_2^2\\
&\quad -\sum_{r=1}^{[\frac{t-t_0}{h}]}(-1)^r({}^qC_r)2x_2h^qf_2(t;x_1,x_2)-\sum_{r=1}^{[\frac{t-t_0}{h}]}(-1)^r({}^qC_r)h^{2q}f_2(t;x_1,x_2)\}\\
&= \limsup_{h\to 0^+}\frac{1}{h^q}\{x_2^2+\sum_{r=1}^{[\frac{t-t_0}{h}]}(-1)^r({}^qC_r)x_2^2-x_{20}^2-\sum_{r=1}^{[\frac{t-t_0}{h}]}(-1)^r({}^qC_r)x_{20}^2\\
&\quad -2x_2\sum_{r=1}^{[\frac{t-t_0}{h}]}(-1)^r({}^qC_r)h^qf_2(t;x_1,x_2)|\}\\
&= \limsup_{h\to 0^+}\frac{1}{h^q}\{\sum_{r=0}^{[\frac{t-t_0}{h}]}(-1)^r({}^qC_r)x_2^2-\sum_{r=0}^{[\frac{t-t_0}{h}]}(-1)^r({}^qC_r)x_{20}^2\\
&\quad -2x_2\sum_{r=1}^{[\frac{t-t_0}{h}]}(-1)^r({}^qC_r)h^qf_2(t;x_1,x_2)\}\\
{}^CD_+^qV_2(t;x_1,x_2) &\leq \frac{x_2^2}{t^q\Gamma(1-q)}-\frac{x_{20}^2}{t^q\Gamma(1-q)}+2x_2f_2(t;x_1,x_2)\\
{}^CD_+^qV_2(t;x_1,x_2) &\leq \frac{x_2^2}{t^q\Gamma(1-q)}+2x_2f_2(t;x_1,x_2)\\
{}^CD_+^qV_2(t;x_1,x_2) &\leq \frac{x_2^2}{t^q\Gamma(1-q)}+2x_2(\frac{3x_1^2}{x_2}-x_2sinx_1-5x_2cosecx_1-\frac{x_1^2cosx_2}{x_2})\\
&= \frac{x_1^2}{t^q\Gamma(1-q)}-2x_2^2sinx_1+6x_1^2-10x_2^2cosecx_1-2x_1^2cosx_2\\
&\leq -2x_2^2sinx_1-10x_2^2cosecx_1+6x_1^2-2x_1^2cosx_2\\
&= -2x_2^2(sinx_1+5cosecx_1)+2x_1^2(3-cosx_2)\\
&\leq -2x_2^2(|sinx_1|+\frac{10}{|sinx_1|})+2x_1^2(3-|cosx_2|)\\
&\leq -2x_2^2(1+5)+2x_1^2(3-1)\\
&= -2x_2^2(6)+2x_1^2(2)\\
&= -12V_2+4V_1
\end{aligned}
$$

Therefore,

$$
{}^CD_+^qV_1(t;x_1,x_2)\leq 4V_1-12V_2 \tag{33}
$$

Also, for $x_0\in S_\psi$, for $t=t_k, k=1,2,..$, we have

$$
V(t,x(t)+d_k)=|d_k+x(t)|\leq V(t,x(t))
$$

Combining (33) and (32), we have

$$
{}^CD_+V\leq\begin{pmatrix}-18 & 1\\ 4 & -12\end{pmatrix}\begin{pmatrix}V_1\\ V_2\end{pmatrix}=g(t,V) \tag{34}
$$

Now consider the comparison system

$$^{C}D^{q}u = g(t,u) = Au \tag{35}$$

where $A = \begin{pmatrix} -18 & 1 \\ 4 & -12 \end{pmatrix}$.
The vectorial inequality (34) and all other conditions of Theorem (5.1) are satisfied since the eigenvalues of A are all negative real parts. Hence, the system (35) is eventually stable. Therefore, the set $x(t) = 0$ for the system of IFrDE (29) is eventually stable.

7 Discussions and conclusion

This study provides a significant extension to the theory of nonlinear impulsive Caputo fractional differential equations, particularly in the context of eventual stability with fixed moments of impulse. By employing vector Lyapunov functions generalized through piecewise continuous functions, a broader and more flexible framework for analyzing the stability of such systems was established. The incorporation of comparison results further enriched the analytical approach, facilitating the derivation of sufficient conditions for eventual stability. Compared to existing methods, our approach offers notable improvements by generalizing stability conditions and extending their applicability to a wider class of impulsive fractional systems. The results bridge the gap between classical stability analysis and the unique challenges posed by fractional impulsive systems. This is particularly important for real-world systems where impulsive effects and fractional-order dynamics coexist, such as in biological systems, control engineering, and economic models.

References

[1] Agarwal, R., Hristova, S., and O'regan, D. (2016). Stability of Solutions of Impulsive Caputo Fractional Differential Equations. Electronic Journal of Differential Equations 58, 1-22.

[2] Akpan, E. P., and Akinyele, O. (1992). On the ϕ_0-stability of comparison differential systems. Journal of mathematical analysis and applications 164(2), 307-324.

[3] Ante J.E., Ineh M.P., Achuobi J.O., Akai U.P., Atsu J.U., Offiong N-A.O. (2024). A Novel Lyapunov Asymptotic Eventual Stability Approach for Nonlinear Impulsive Caputo Fractional Differential Equations. AppliedMath 4(4), 1600-1617. https://doi.org/10.3390/appliedmath4040085

[4] Ante, J.E., Itam, O.O., Atsu, J.U., Essang, S.O., Abraham, E.E. & Ineh, M. P. (2024). On the novel auxiliary Lyapunov function and uniform asymptotic practical stability of nonlinear impulsive Caputo fractional differential equations via new modelled generalized Dini derivative. African Journal of Mathematics and Statistics Studies 7, 11-33.

[5] Ante, J.E., Atsu, J.U., Abraham, E.E., Itam, O.O., Oduobuk, E.J. & Inyang, A. B. (2024). On a class of piecewise continuous Lyapunov functions and asymptotic practical stability of nonlinear impulsive Caputo fractional differential equations via new modelled generalized Dini derivative, IEEE-SEM Journal Publication 12, 2320-9151.

[6] Ante, J. E., Atsu, J. U., Maharaj, A., Abraham, E. E., and Narain, O. K. (2024). On a class of piecewise continuous Lyapunov functions and uniform eventual stability of nonlinear impulsive Caputo fractional differential equations via new modelled generalized Dini derivative, Asia Pac. J. Math 11(99), 1-20. https://apjm.apacific.org/PDFs/11-99.pdf.

[7] Ante, J.E., Inyang, A.B., Oduobuk, E.J., and Akai, U.P. (2024). On the vector Lyapunov functions and eventual stability of nonlinear impulsive differential equations, International Journal of Mathematical Analysis and Modelling 7(2), 185–199.

[8] Ante, J.E., Abraham, E. E., Ebere, U.E., Udogworen, W.K., and Akpan, C.S. (2024). On the Global Existence of Solution and Lyapunov Asymptotic Practical stability for Nonlinear Impulsive Caputo Fractional Derivative via Comparison Principle, Sch J Phys Math Stat 11, 160–172.

[9] Atsu, J. U., Ante, J. E., Inyang, A . B., & Akpan, U. D. (2024). A survey on the vector Lyapunov functions and practical stability of nonlinear impulsive Caputo fractional differential equations via new modelled generalized Dini derivative. IOSR Journal of Mathematics 20, 28-42.

[10] Ante, J. E., Essang, S. O., Itam, O. O. & John, E. I. (2024). On the Existence of Maximal Solution and Lyapunov Practical Stability of Nonlinear Impulsive Caputo Fractional Derivative via Comparison Principle. Advanced Journal of Science. Technology and Engineering 4(4), 92-110.

[11] Arnold, L., and Schmalfuss, B., (2001). Lyapunov's Second Method for Random Dynamical systems. Journal of differential equations 177(1), 235-265.

[12] Băleanu, D., and Mustafa, O. G. (2010). On the global existence of solutions to a class of fractional differential equations. Computers and Mathematics with Applications 59(5), 1835-1841.

[13] Burton, T. A. (2011). Fractional Differential Equations and Lyapunov Functionals. Nonlinear Analysis: Theory, Methods and Applications 74(16), 5648-5662.

[14] Devi, J. V., Mc Rae, F. A., and Drici, Z. (2012). Variational Lyapunov method for fractional differential equations. Computers & Mathematics with Applications 64(10), 2982-2989.

[15] Diethelm, K., & Ford, N. J. (2010). The Analysis of Fractional Differential Equations. Lect. Notes Math 2004, 3-12.

[16] Ekoro, S.E., Ofem, A.E., Adie, F.A., Oboyi, J. Ogban, G.I., & Ineh, M.P. (2023). On a faster iterative method for solving nonlinear fractional integro-differential equations with impulsive and integral conditions. Palestine Journal of Mathematics. 12(4), 477–484.

[17] Hale, J. (1977). Theory of Functional Differential Equations. Springer-Verlag, New York, Heidelberg, Berlin.

[18] Igobi, D. K. and Ineh, M. P. (2024). Results on Existence and Uniqueness of Solutions of Dynamic Equation on Time Scale via Generalized Ordinary Differential Equations. International Journal of Applied Mathematics 37(1), 1-20.

[19] Igobi, D. K., Ante, J. E. (2018). Results on Existence and Uniqueness of Solution of Impulsive Neutral Integro-Differential System. Journal of Mathematics Research 10(4). Doi: 10.5539/jmr.v10n4p165

[20] Ineh, M.P., Achuobi, J.O., Akpan, E.P., and Ante, J.E. (2024). CDq On the uniform stability of Caputo fractional differential equations using vector Lyapunov functions. The Journals of the Nigerian Association of Mathematical Physics 68, 51-64.

[21] Ineh, M.P., and Akpan, E.P. (2024). Lyapunov uniform asymptotic stability of Caputo fractional dynamic equations on time scale using a generalized derivative. The Transactions of the Nigerian Association of Mathematical Physics 20, 117-132.

[22] Ineh, M.P., Akpan, E.P. and Nabwey, H.A. (2024). A novel approach to Lyapunov stability of Caputo fractional dynamic equations on time scale using a new generalized derivative. AIMS Mathematics, 9(12), 34406-34434. Doi: 10.3934/math.20241639

[23] Kilbas, A. A., Marichev, O. I., and Samko, S. G. (1993). Fractional integrals and derivatives (theory and applications).

[24] Kulev, G. K. (1992). Uniform asymptotic Stability in Impulsive Perturbed Systems of Differential Equations, Journal of Computational and Applied Mathematics 41, 49-55.

[25] Lakshmikantham, V. (1974). On the Method of Lyapunov Functions. Technical report 16

[26] Lakshmikantham, V., Bainov, D. D., Simeono, P. S. (1989). The Theory of Impulsive Differential Equations. Series in Modern Applied Mathematics No. 6. World Scientific Publishing C. Pte, Ltd.

[27] Li, Y., Chen, Y., and Podlubny, I. (2010). Stability of Fractional-order Nonlinear Dynamic Systems: Lyapunov Direct Method and Generalized Mittag–Leffler Stability. Computers and Mathematics with Applications 59(5), 1810-1821.

[28] Lipcsey, Z., Ugboh, J. A., Esuabana, I. M. and Isaac, I. O. (2020). Existence Theorem for Impulsive Differential Equations with Measurable Right Side for Handling Delay Problems. Hindawi Journal of Mathematics, Vol 2020, Article ID 7089313.

[29] Milman, V. D., Myshkis, A. D. (1960). On Motion Stability with Shocks, Sibirsk. Mat Zh. 1 233-237 (in Russian).

[30] Podlubny, I. (1998). Fractional Differential Equations: An Introduction to Fractional Derivatives, Fractional Differential Equations, to Methods of Their Solution and Some of Their Applications. Elsevier.

[31] Qunli, Z. (2014). A Class of Vector Lyapunov Functions for Stability Analysis of Nonlinear Impulsive Differential Systems. Hindawi Publishing Corporation. Mathematical Problems in Engineering, Article ID 649012.

[32] Sood, A. & Srivastava, S. K. (2016). On Retention of Eventual Stability of Perturbed Impulsive Differential Systems. *J. Math. fund. Sci,* Vol. 48(1), 1-11.

[33] Soliman, A. A. (2003). Stability Criteria of Impulsive Differential Systems. Applied Mathematics and Computation, **134**,, 445-457.

[34] Srivastava, S. K. and Amanpreet, K. (2009). A New Approach to Stability of Impulsive Differential Equations. Int. Journal of Math. Analysis 3(4), 179 - 185.

[35] Stamova, I. (2011). Eventual Stability and Eventual Boundedness for Impulsive Differential Equations with "Supremum". Mathematical Modelling and Analysis 16(2), 304-314.

[36] Ugboh, J. A. and Esuabana, I. M. (2018). Existence and Uniqueness Result for a Class of Impulsive Delay Differential Equations. International Journal of Chemistry, Mathematics and Physics 2(4).

[37] Udo, M. O., Ineh, M. P., Inyang, E. J. & Benneth, P. (2022). Solving nonlinear Volterra integral equations by an efficient method. International Journal of Statistics and Applied Mathematics 7(4), 136-141. https://www.mathsjournal.com/pdf/2022/vol7issue4/PartB/7-4-17-836.pdf

[38] Wu, C. (2020). A General Comparison Principle for Caputo Fractional-order Ordinary Differential Equations. Fractals 28(4), 2050070.

[39] Yoshizawa, T. (1966). Stability Theory by Lyapunov's Second Method. The Mathematical Society of Japan.

Picard-Mann hybrid iteration process for approximating fixed points of contraction mappings

E. Ekuma-Okereke*†, O.D. Koko†‡, C.V. Okpako§, and J.O.Ogbodu¶

Abstract

Fixed point theory has been very remarkable since its introduction and it has evolved greatly by hosting a great number of researches of many sort. Several mathematical problems have been solved by the fixed point method by transforming any of such problem into an operation of the fixed point equation. Fixed point theory is primarily concerned with finding conditions on the ambient space and also on the properties of the mapping so as to find results on the existence and uniqueness of fixed points. In this paper, we construct and introduce a new four-step iteration process called the Picard-Mann hybrid iteration process. We prove that this new iteration process converges to the unique fixed point of contraction mappings. We then show that it converges faster than several other iteration processes mentioned in the body of literature with numerical examples visualized in graphs and tables to substantiate our theoretical assertions. Data dependence and numerical stability is further established. Our results obtained in uniformly convex Banach space generalizes and extend other results cited in the literature.

Keywords and phrases: Fixed points theory; contraction mappings; Picard-Mann hybrid process; uniformly convex Banach space; convergence result.

1 Introduction

Fixed point theory has been very remarkable since its introduction and it has evolved greatly by hosting a great number of researches of many sort. Several mathematical problems have been solved by the fixed point method by transforming any of such problem into an operation of the fixed point equation. Fixed point theory is primarily concerned with finding conditions on the ambient space and also on the properties of the mapping so as to find results on the existence and uniqueness of fixed points.

Historically, Poincare (see [1]) was the first to research on fixed point theory, and was followed by Brouwer. In 1922, Banach established a principle called Banach contraction principle (BCP) in metric spaces (see, [2]). So many authors after Banach have studied fixed point theory away from metric space to Hilbert and general Banach spaces (see [3]-[5]). Notably it has become a flourishing and interesting research area for many researchers seeking approximation of fixed points of different mappings. The theory of fixed point have been applied in many fields like numerical mathematics, differential equations (see [6]).

A plethora of metrical fixed point theorems have been obtained, more or less important from a theoretical point of view, which establish usually the existence, or the existence and uniqueness of fixed points for a certain contractive mapping. Among these fixed point theorems, only a small number are important from a practical point of view, that is, they offer a constructive method for finding the fixed points. Among the last ones only a few give information on the rate of convergence of the method [7].

*Corresponding Author; E-mail: ekuma.okereke@fupre.edu.ng, enyiekumaokereke@gmail.com
†Department of Mathematics, Federal University of Petroleum Resources, Effurun, Nigeria
‡E-mail: kokodogheneovo@gmail.com
§Department of Mathematics, Federal University of Petroleum Resources, Effurun, Nigeria; E-mail: mcvotu@gmail.com
¶Department of Mathematics, Federal University of Petroleum Resources, Effurun, Nigeria; E-mail:ogbodujoseph1987@gmail.com

However, from a practical point of view it is important not only to know the fixed point exists (and, possibly, is unique), but also to be able to construct that fixed point(s). As the constructive methods used in metrical fixed point theory are prevailingly iterative procedures, that is, approximate methods, it is also of crucial importance to have a priori or / and a posteriori error estimates (or, alternatively, rate of convergence) for such a method, [8]. A vast literature is available on iterative methods for studying fixed point problems (FPP), variational inequality problems (VIP), monotone variational inclusion problems (MVIP), equilibrium problems (EP), etc for nonlinear mappings, separately, and on iterative methods to approximate common solutions of these problems. But to construct and study the more general iterative methods for approximating solutions (common solutions) of new generalizations of these problems in the settings of Hilbert spaces and Banach spaces, is still an unexplored field. There are substantial number of iterative methods for studying separately, the fixed point problems for nonlinear mappings, variational inequalities, and equilibrium problems; and for approximating the common solutions of these problems.

Picard, Krasnoselkii and Mann iteration processes (see [9]-[11]) were among the first processes to be introduced in this direction for the approximation of fixed points of contraction mappings in metric spaces and closed convex subset of Banach spaces respectively. Others after followed from these processes.

Ishikawa [12] introduced the Ishikawa iterative technique which is recursively defined as follows:

$$\begin{cases} \omega_1 = \omega \in K, \\ \omega_{n+1} = (1-\alpha_n)\omega_n + \alpha_n \Omega, \\ \theta_n = (1-\beta_n)\omega_n + \beta_n \Omega \omega_n, n \geq 1, \end{cases} \tag{1}$$

where $\{\alpha_n\}$ and $\{\alpha_n\} \in (0,1)$.

Noor [13] introduced a three-step approximation processes for general variational inequalities. The iteration process is defined by the sequence $\{t_n\}$:

$$\begin{cases} t_1 = t \in C \\ t_{n+1} = (1-\alpha_n)t_n + \alpha_n \Omega y_n, \\ y_n = (1-\beta_n t_n + \beta_n \Omega z_n, \\ Z_n = (1-\gamma_n)t_n + \gamma_n \Omega t_n, n \in N, \end{cases} \tag{2}$$

where $\{\alpha_n\}$, $\{\beta_n\}$ and $\{\gamma_n\} \in (0,1)$. This process is also called a three-step approximation process for solving variational inequality problems.

Khan [14] introduced an iterative process called Picard-Mann hybrid iterative process, which is a hybrid of Picard and Mann iterative processes and defined thus:

$$\begin{cases} m_1 = m \in K \\ m_{n+1} = \Omega z_n, \\ z_n = (1-\alpha_n)m_n + \alpha_n \Omega m_n, n \in N, \end{cases} \tag{3}$$

where $\{\alpha_n\} \in (0,1)$. They showed that the process converges faster than all of [9], [10], [11] and [12] iterative processes in the sense of [15].

Thakur [16] introduced a new iterative process defined thus:

$$\begin{cases} x_{n+1} = (1-\alpha_n)\Omega x_n + \alpha_n \Omega y_n, \\ y_n = (1-\beta_n)z_n + \beta_n \Omega z_n, \\ z_n = (1-\gamma_n)x_n + \gamma_n \Omega x_n, \end{cases} \tag{4}$$

where $x_1 \in K$, and $\{\alpha_n\}, \{\beta_n\}, \{\gamma_n\} \in (0,1)$. They showed that the process converges faster than all of iteration processes for contractions in the sense of [15]

Abbas [17], introduced a new iterative process defined thus:

$$\begin{cases} y_1 = y \in K, \\ y_{n+1} = (1-\alpha_n)\Omega w_n + \gamma_n \Omega z_n, \\ w_n = (1-\beta_n)\Omega y_n + \alpha_n \Omega z_n, \\ z_n = (1-\gamma_n) y_n + \beta_n \Omega y_n, \end{cases} \tag{5}$$

where $\{\alpha_n\}, \{\beta_n\}, \{\gamma_n\} \in (0,1)$. They showed that the process developed has rate of convergence that is even faster than that of [18].

[19] introduced the Picard-Krasnoselskii hybrid iterative process which is a hybrid of Picard and Krasnoselskii iteration processes and showed that for nonlinear contractive operators, the iteration process converges faster than all of Picard, Mann, Ishikawa and Krasnoselskii iteration processes for contractions in the sense of [15]. The scheme is defined thus:

$$\begin{cases} y_1 = y \in K, \\ y_{n+1} = \Omega w_n, \\ w_n = (1-\lambda) y_n + \lambda \Omega y_n, \end{cases} \tag{6}$$

where $\lambda \in (0,1)$.

[20] intrdoced a hybrid of Picard and Ishikawa iteration processes called the Picard-Ishikawa hybrid iterative process and showed that it converges faster than all of Picard, Krsanoselskii, Mann, Ishikawa, Noor, Picard-Mann and Picard-Krasnoselskii iteration processes in the sense of [15]. The iterative process is defined thus:

$$\begin{cases} g_1 = g \in K, \\ g_{n+1} = \Omega w_n, \\ w_n = (1-\alpha_n) g_n + \alpha_n \Omega z_n, \\ z_n = (1-\beta_n) g_n + \beta_n \Omega g_n, \end{cases} \tag{7}$$

where $\{\alpha_n\}, \{\beta_n\} \in (0,1)$.

[21], intrdoced a hybrid of Picard (see [9]) and Thakur (see [16]) iteration processes called the Picard-Thakur hybrid iterative process. The iterative process is defined thus:

$$\begin{cases} j_1 = j \in K, \\ j_{n+1} = \Omega k_n, \\ k_n = (1-\alpha_n)\Omega m_n + \alpha_n \Omega l_n, \\ l_n = (1-\beta_n) m_n + \beta_n \Omega m_n, m_n = (1-\gamma_n) j_n + \gamma_n \Omega j_n, n \in N \end{cases} \tag{8}$$

where $\{\alpha_n\}, \{\beta_n\}, \{\gamma_n\} \in (0,1)$.

[22] (cf [23]) introduced a new four-step iteration process, called the Picard-Noor hybrid iterative processis defined thus:

$$\begin{cases} j_1 = j \in K, \\ j_{n+1} = \Omega k_n, \\ k_n = (1-\alpha_n) j_n + \alpha_n \Omega l_n, \\ l_n = (1-\beta_n) j_n + \beta_n \Omega m_n, m_n = (1-\gamma_n) j_n + \gamma_n \Omega j_n, n \in N. \end{cases} \tag{9}$$

They applied their results in solving delay differential equations.

[24] introduced three step iteration process, the SP iteration process, which generates the sequence ω_n defined by:

$$\begin{cases} \omega_1 = \omega, \\ \omega_{n+1} = (1-\alpha_n) w_n + \alpha_n \Omega w_n, \\ w_n = (1-\beta_n) u_n + \beta_n \Omega u_n, \\ u_n = (1-\gamma_n)\omega_n + \gamma_n \Omega \omega_n, n \in \mathbf{N}, \end{cases} \tag{10}$$

There is no iteration process that generalizes and extends other existing processes for a contraction mapping in a uniformly convex Banach space, hence this paper constructs a new hybrid fixed point iteration of Picard and Mann methods to approximate the fixed point of any contraction mapping.

2 Methodology/Model formulation

Let Ω represent an operator (mapping) defined on ambient space. Let ω_1=ω represent an arbitrary initial value from the ambient space. Picard iteration process is defined by the sequence $\{\omega_n\}_{n=0}^{\infty}$ as follows:

$$\begin{cases} \omega_1 = \omega \in K, \\ \omega_{n+1} = \Omega\omega_n, n \geq 1, \end{cases} \tag{11}$$

Independently, Mann iterative process is defined as:

$$\begin{cases} \omega_1 = \omega \in K, \\ \omega_{n+1} = (1-\alpha_n)\omega_n + \alpha_n\Omega\omega_n, n \geq 1, \end{cases} \tag{12}$$

where $\{\alpha_n\} \in [0,1]$.

Since we are interested in having only one recursive process written with respect to ω_{n+1} and generated by an initial value $\omega_1 = \omega$, we observe that both Picard and Mann iterative processes have the recursive sequence ω_{n+1}, we therefore proceed by setting the recursive process in Mann as follows:

Step1:

$$u_n = (1-\alpha_n)\omega_n + \alpha_n\Omega\omega_n, \tag{13}$$

Step 2:

$$w_n = (1-\beta_n)u_n + \beta_n\Omega u_n \tag{14}$$

Step 3:

$$x_n = (1-\gamma_n)w_n + \gamma_n\Omega w_n \tag{15}$$

Finally, we construct a recursive process following Picard iteration process with respect to the three steps of Mann iteration process as follows:

Step 4:

$$\omega_{n+1} = \Omega x_n. \tag{16}$$

Observations

i. The three steps of Mann iteration process has three different control sequences α_n, β_n and γ_n which are elements in the given interval $[0,1]$,

ii. If $\alpha_n = \beta_n = \gamma_n = 0$, then the three steps reduces to one step Picard iteration process,

iii. If If $\alpha_n = \beta_n = \gamma_n = 1$, then the three steps reduces to sequence of composed operators of Picard iteration process form.

Now, the coupled and compact form of these processes is defined below:

$$\begin{cases} \omega_1 = \omega, \\ \omega_{n+1} = \Omega x_n, \\ x_n = (1-\alpha_n)w_n + \alpha_n\Omega w_n, \\ w_n = (1-\beta_n)u_n + \beta_n\Omega u_n, \\ u_n = (1-\gamma_n)\omega_n + \gamma_n\Omega\omega_n, n \in \mathbf{N}, \end{cases} \tag{17}$$

where $\{\alpha_n\}$, $\{\beta_n\}$, and $\{\gamma_n\}$, are real sequences in $[0,1]$.

The following definitions will be used in the sequel.

Definition 2.1. *(Uniformly convex Banach spaces)[22]*
A normed space X is called uniformly convex if for any $\epsilon \in (0,2]$ there exists a $\delta = \delta(\epsilon) > 0$ such that for any $x, y \in X$ with $\|x\| = 1 = \|y\|$ and $\|x - y\| \geq \epsilon$, then $\|\frac{1}{2}(x+y)\| \leq 1 - \delta$.

Definition 2.2. *(Mappings in Normed Vector Space)[1]*
Let $(X, \|.\|)$ be a normed vector space. A mapping $\Omega : X \to X$ is called

(i) Lipschitzian, if $\exists\ L > 0$ satisfying $\|\Omega x - \Omega y\| \leq L.\|x - y\|, \forall x, y \in X$,

(ii) Contraction, when $0 \leq L < 1$ (see [7]),

(iii) Nonexpansive, when $L = 1$, (see [25]).

Definition 2.3. *(Fixed Point Set)[1]*
Let Ω be any mapping defined on $X \neq \emptyset$. Let the fixed point of Ω be denoted by $Fix(\Omega)$. The set of fixed point of Ω is denoted by $Fix(\Omega) = \{x \in X : \Omega(\omega) = \omega\}$. So ω is a point invariant under the transformation Ω.

Definition 2.4. *Approximate operator[1]*
Let $\Omega, \hat{\Omega} : D \to D$ be two operators. We say that $\hat{\Omega}$ is an approximate operator of Ω if for all $\omega \in D$ and for a fixed $\epsilon > 0$ we have

$$\|\Omega - \hat{\Omega}\| \leq \epsilon \tag{18}$$

Definition 2.5. *Stability[26]*
Intuitively, a fixed point iteration procedure is numerically stable if, "small" modifications in the initial data or in the data that are involved in the computation process, will produce a "small" influence on the computed value of the fixed point.

Definition 2.6. *Faster Convergence[15] Let ${a_n}_{n=0}^{\infty}$ and ${b_n}_{n=0}^{\infty}$ be two sequences of real numbers converging to a and b respectively. If*

$$\lim_{n\to\infty} \frac{\|a_n - a\|}{\|b_n - b\|} = 0$$

then ${a_n}_{n=0}^{\infty}$ is said to converge to a faster than ${b_n}_{n=0}^{\infty}$ to b.

3 Analysis of the model

Overtime, we observe that improvements of some iterations can be based on better and convergence results. We have also observed that hybrid models of any iteration process significantly generate improved convergent result as compared to the normal or classical iteration process. The flexibility of fixed point theory and its application has influenced new hybrid iteration process. We have proposed a new iteration process called Picard–Mann Hybrid (HybridPicMan) iteration process in the following theorem.

Theorem 3.1. *Let K be a nonempty closed convex subset of a Banach space $\mathbb{B}$ and let $\Omega : K \to K$ be a contraction map satisfying the contractive condition and such that $Fix(\Omega) \neq \emptyset$. Let ${\omega_n}_{n=1}^{\infty}$ be a sequence generated by the hybrid iterative process defined as follows:*

$$\begin{cases} \omega_1 = \omega, \\ \omega_{n+1} = \Omega x_n, \\ x_n = (1-\alpha_n)w_n + \alpha_n \Omega w_n, \\ w_n = (1-\beta_n)u_n + \beta_n \Omega u_n, \\ u_n = (1-\gamma_n)\omega_n + \gamma_n \Omega \omega_n, n \in \mathbf{N}, \end{cases} \tag{19}$$

where $\{\alpha_n\}$, $\{\beta_n\}$ and $\{\gamma_n\}$, are real sequences in (0,1) satisfying $\sum_{n=0}^{\infty} \alpha_n = 0$. Then $\{\omega_n\}$ converges to a fixed point of Ω.

Proof. Banach's fixed point theorem guarantees the existence and the uniqueness of fixed point say ω^*. All we need do here is to show that the sequence $\{\omega_n\}_{n=1}^{\infty}$ generated by the hybrid iterative process converges to this point ω^* as $n \to \infty$. So let $\omega^* \in Fix(\Omega)$, then using equations (triangle inequality).....we obtain the following conditions (estimates):

$$\begin{aligned}\|u_n - \omega^*\| &= \|(1-\gamma_n)\omega_n + \gamma_n\Omega\omega_n - \omega^*\| \\ &= \|(1-\gamma_n)(\omega_n - \omega^*) + \gamma_n(\Omega\omega_n - \omega^*)\| \\ &\leq (1-\gamma_n)\|\omega_n - \omega^*\| + \gamma_n\|\Omega\omega_n - \omega^*\| \\ &\leq (1-\gamma_n)\|\omega_n - \omega^*\| + L.\gamma_n\|\omega_n - \omega^*\| \\ &= [1-\gamma_n(1-L)]\,\|\omega_n - \omega^*\|. \end{aligned} \tag{20}$$

In addition,

$$\begin{aligned}\|w_n - \omega^*\| &= \|(1-\beta_n)u_n + \beta_n\Omega u_n - \omega^*\| \\ &= \|(1-\beta_n)(u_n - \omega^*) + \beta_n(\Omega u_n - \omega^*)\| \\ &\leq (1-\beta_n)\|u_n - \omega^*\| + \beta_n\|\Omega u_n - \omega^*\| \\ &\leq (1-\beta_n)\|u_n - \omega^*\| + L.\beta_n\|u_n - \omega^*\| \\ &= [1-\beta_n(1-L\,[1-\gamma_n(1-L)])]\,\|\omega_n - \omega^*\| \\ &\leq [1-\beta_n(1-L)]\,\|\omega_n - \omega^*\|. \end{aligned} \tag{21}$$

Also,

$$\begin{aligned}\|x_n - \omega^*\| &= \|(1-\alpha_n)w_n + \alpha_n\Omega w_n - \omega^*\| \\ &= \|(1-\alpha_n)(w_n - \omega^*) + \alpha_n(\Omega w_n - \omega^*)\| \\ &\leq (1-\alpha_n)\|w_n - \omega^*\| + \alpha_n\|\Omega w_n - \omega^*\| \\ &\leq (1-\alpha_n)\|w_n - \omega^*\| + L.\alpha_n\|w_n - \omega^*\| \\ &= [1-\alpha_n(1-L\,[1-\beta_n(1-L)])]\,\|\omega_n - \omega^*\|. \end{aligned} \tag{22}$$

Furthermore,

$$\begin{aligned}\|\omega_{n+1} - \omega^*\| &= \|\Omega x_n - \omega^*\| \\ &= \|\Omega x_n - \Omega\omega^*\| \\ &\leq L\|x_n - \omega^*\| \\ &\leq L \times [1-\alpha_n(1-L\,[1-\beta_n(1-L)])]\,\|\omega_n - \omega^*\|. \end{aligned} \tag{23}$$

Since from our hypothesis, $\beta_n \in (0,1)$ and $0 \leq L < 1$, we then obtain from condition (23) that

$$\begin{aligned}\|\omega_{n+1} - \omega^*\| &= \|\Omega x_n - \omega^*\| \\ &= \|\Omega x_n - \Omega\omega^*\| \\ &\leq L\|x_n - \omega^*\| \\ &\leq L\,[1-\alpha_n(1-L)]\,\|\omega_n - \omega^*\|. \end{aligned} \tag{24}$$

If $n = 0$, we obtain by induction that

$$\|\omega_1 - \omega^*\| \leq L\,[1-\alpha_0(1-L)]\,\|\omega_0 - \omega^*\|. \tag{25}$$

If $n = 1$, we obtain by induction that

$$\begin{aligned}\|\omega_2 - \omega^*\| &\leq L\,[1-\alpha_1(1-L)]\,\|\omega_1 - \omega^*\| \\ &\leq L\,[1-\alpha_1(1-L)]\,.L\,[1-\alpha_0(1-L)]\,\|\omega_0 - \omega^*\| \\ &= L^2\prod_{k=0}^{1}[1-\alpha_k(1-L)]\,\|\omega_0 - \omega^*\|. \end{aligned} \tag{26}$$

If $n = k + 1$, we obtain by induction that

$$\begin{aligned}\|\omega_{k+1} - \omega^*\| &\leq L\left[1 - \alpha_k(1-L)\right]\|\omega_k - \omega^*\| \\ &\leq L^k\left[1 - \alpha_1(1-L)\right].L\left[1 - \alpha_0(1-L)\right]\|\omega_0 - \omega^*\| \\ &= L^{k+1}\prod_{n=0}^{k}\left[1 - \alpha_n(1-L)\right]\|\omega_0 - \omega^*\|. \end{aligned} \tag{27}$$

So that

$$\|\omega_{n+1} - \omega^*\| \leq L^{n+1}\prod_{k=0}^{n}\left[1 - \alpha_k(1-L)\right]\|\omega_0 - \omega^*\|. \tag{28}$$

Therefore,

$$\|\omega_{n+1} - \omega^*\| \leq \mathbb{L}\|\omega_0 - \omega^*\|. \tag{29}$$

where $0 \leq \mathbb{L} = L^{k+1}\prod_{n=0}^{k}\left[1 - \alpha_n(1-L)\right]\| < 1$. Thus $\{\omega_n\}_{n=0}^{\infty}$ is bounded and consequently $\lim_{n\to\infty}\|\omega_n - \omega^*\| = 0$. Hence $\omega_n \to \omega^*$ as $n \to \infty$. This completes the proof of the Theorem.

In this subsection, data dependence and stability results of the Picard-Noor iterative process will be established.

Theorem 3.2. *Let Θ be an approximate mapping of Ω which satisfies the contraction mapping condition given by inequality (18). Given the iterative process of our iterative process of equation (19) whose sequences converges to some fixed point $\omega^* \in Fix(\Omega))$ and we define an iterative sequence θ_n for the mapping Θ with some fixed point $\theta^* \in Fix(\Theta)$ as follows:*

$$\begin{cases} \theta_1 = \theta, \\ \theta_{n+1} = \Theta\hat{x_n}, \\ \hat{x_n} = (1-\alpha_n)\hat{w_n} + \alpha_n\Theta\hat{w_n}, \\ \hat{w_n} = (1-\beta_n)\hat{u_n} + \beta_n\Theta\hat{u_n}, \\ \hat{u_n} = (1-\gamma_n)\theta_n + \gamma_n\Theta\theta_n, n \in \mathbf{N}, \end{cases} \tag{30}$$

where $\{\alpha_n\}$, $\{\beta_n\}$, and $\{\gamma_n\}$, are real sequences in (0,1) satisfying $\sum_{n=0}^{\infty}\alpha_n = 0$ and there exists $\mu > 0$ such that $\|\Omega\omega^* - \Theta\theta^*\| \leq \mu$. Then $\|\omega^* - \theta^*\| \leq \dfrac{5\mu}{1-L}$, where $0 \leq L < 1$.

Proof.

$$\begin{aligned}\|u_n - \hat{u_n}\| &= \|(1-\gamma_n)\omega_n + \gamma_n\Omega\omega_n - (1-\gamma_n)\theta_n - \gamma_n\Theta\theta_n\| \\ &= \|(1-\gamma_n)(\omega_n - \theta_n) + \gamma_n(\Omega\omega_n - \Theta\theta_n\| \\ &\leq (1-\gamma_n)\|\omega_n - \theta_n\| + \gamma_n\|\Omega\omega_n - \Theta\theta_n\| \\ &= (1-\gamma_n)\|\omega_n - \theta_n\| + \gamma_n\|\Omega\omega_n - \Theta\theta_n + \Theta\theta_n - \Theta\theta_n\| \\ &\leq (1-\gamma_n)\|\omega_n - \theta_n\| + \gamma_n\left[\|\Omega\omega_n - \Theta\theta_n\| + \|\Theta\theta_n - \Theta\theta_n\|\right] \\ &\leq (1-\gamma_n)\|\omega_n - \theta_n\| + \gamma_n L\|\omega_n - \theta_n\| + \gamma_n\mu \\ &= (1-\gamma_n(1-L))\|\omega_n - \theta_n\| + \gamma_n\mu. \end{aligned} \tag{31}$$

In addition,

$$\begin{aligned}\|w_n - \hat{w_n}\| &= \|(1-\beta_n)u_n + \beta_n\Omega u_n - (1-\beta_n)u_n - \beta_n\Theta\hat{u_n}\| \\ &= \|(1-\beta_n)(u_n - \hat{u_n}) + \beta_n(\Omega u_n - \Theta\hat{u_n})\| \\ &\leq (1-\beta_n)\|u_n - \hat{u_n}\| + \beta_n\|\Omega u_n - \Theta\hat{u_n}\| \\ &= (1-\beta_n)\|u_n - \hat{u_n}\| + \beta_n\|\Omega u_n - \Theta\hat{u_n} + \Theta\hat{u_n} - \Theta\hat{u_n}\| \\ &\leq (1-\beta_n)\|u_n - \hat{u_n}\| + \beta_n\left[\|\Omega u_n - \Theta\hat{u_n}\| + \|\Theta\hat{u_n} - \Theta\hat{u_n}\|\right] \\ &\leq [(1-\beta_n) + \beta_n L]\|u_n - \hat{u_n}\| + \beta_n\mu. \end{aligned} \tag{32}$$

Also,

$$\begin{aligned}\|x_n - \hat{x_n}\| &= \|(1-\alpha_n)w_n + \alpha_n\Omega w_n - (1-\alpha_n)\hat{w_n} - \alpha_n\Theta\hat{w_n}\| \\ &= \|(1-\alpha_n)(w_n - \hat{w_n} + \alpha_n(\Omega w_n - \Theta\hat{w_n})\| \\ &\leq (1-\alpha_n)\|w_n - \hat{w_n}\| + \alpha_n\|\Omega w_n - \Theta\hat{w_n}\| \\ &= (1-\alpha_n)\|w_n - \hat{w_n}\| + \alpha_n\|\Omega w_n - \Omega\hat{w_n} + \Omega\hat{w_n} - \Theta\hat{w_n}\| \\ &\leq (1-\alpha_n)\|w_n - \hat{w_n}\| + \alpha_n\left[\|\Omega w_n - \Omega\hat{w_n}\| + \|\Omega\hat{w_n} - \Theta\hat{w_n}\|\right] \\ &\leq (1-\alpha_n)\|w_n - \hat{w_n}\| + \alpha_n L\|w_n - \hat{w_n}\| + \alpha_n\mu. \end{aligned} \tag{33}$$

Continuing we have

$$\|x_n - \hat{x_n}\| \leq (1-\alpha_n(1-L[1-\beta_n[1-L[1-\gamma_n(1-L)]]]))\|\omega_n - \theta_n\| + \alpha_n L\beta_n L\gamma_n\mu + \alpha_n L\beta_n\mu + \alpha_n\mu. \tag{34}$$

Furthermore,

$$\begin{aligned}\|\omega_{n+1} - \theta_{n+1}\| &= \|\Omega x_n - \Theta\hat{x_n}\| \\ &= \|\Omega x_n - \Omega\hat{x_n} + \Omega\hat{x_n} - \Theta\hat{x_n}\| \\ &\leq \|\Omega x_n - \Omega\hat{x_n}\| + \|\Omega\hat{x_n} - \Theta\hat{x_n}\| \\ &\leq L\|x_n - \hat{x_n}\| + \mu. \end{aligned} \tag{35}$$

Continuing we have

$$\begin{aligned}\|\omega_{n+1} - \theta_{n+1}\| \leq L(1-\alpha_n(1-L[1-\beta_n[1-L[1-\gamma_n(1-L)]]]))\|\omega_n - \theta_n\| + \alpha_n L\beta_n L\gamma_n\mu + \alpha_n L\beta_n\mu \\ + \alpha_n\mu + \mu. \end{aligned} \tag{36}$$

From our hypothesis, observe that

$$L < 1 \tag{37}$$

$$\beta_n\gamma_n L^2 < 1 \tag{38}$$

$$\beta_n L^2 < 1 \tag{39}$$

$$(1-\beta_n[1-L[1-\gamma_n(1-L)]]) < 1 \tag{40}$$

$$1-\alpha_n \leq \alpha_n \implies 1 = 1-\alpha_n+\alpha_n \leq \alpha_n+\alpha_n = 2\alpha_n. \tag{41}$$

So from (36) we have that

$$\begin{aligned}\|\omega_{n+1} - \theta_{n+1}\| &\leq (1-\alpha_n(1-L))\|\omega_n - \theta_n\| + \alpha_n 3\mu + \mu \\ &\leq (1-\alpha_n(1-L))\|\omega_n - \theta_n\| + \alpha_n 3\mu + (1-\alpha_n+\alpha_n)\mu \\ &\leq (1-\alpha_n(1-L))\|\omega_n - \theta_n\| + \alpha_n 3\mu + 2\alpha_n\mu \\ &\leq (1-\alpha_n(1-L))\|\omega_n - \theta_n\| + \alpha_n(1-L)\frac{5\mu}{(1-L)}. \end{aligned} \tag{42}$$

From (42), let $a_n := \|\omega_n - \theta_n\|$ so that $a_{n+1} := \|\omega_{n+1} - \theta_{n+1}\|$ be a sequence of non-negative real numbers. Let $\hat{\alpha_n} := \alpha_n(1-L) \in (0,1)$ such that $\lim_{n\to\infty}\hat{\alpha_n} = 0, \sum_{n=1}^{\infty}\hat{\alpha_n} = \infty$. Let $\mu_n = \dfrac{5\mu}{(1-L)}$ such that it is non-negative real constants. Now since limit is unique, we have that $\lim_{n\to\infty}\omega_n = \omega^* = \lim_{n\to\infty}\omega_{n+1}$. Since $\lim_{n\to\infty}\theta_n = \theta^* = \lim_{n\to\infty}\theta_{n+1}$, we then have

$$\begin{aligned}\|\omega^* - \theta^*\| &\leq (1-\hat{\alpha_n})\|\omega^* - \theta^*\| + \hat{\alpha_n}\frac{5\mu}{1-L} \\ \hat{\alpha_n}\|\omega^* - \theta^*\| &\leq \hat{\alpha_n}\frac{5\mu}{1-L} \\ \|\omega^* - \theta^*\| &\leq \frac{5\mu}{1-L}. \end{aligned} \tag{43}$$

This completes the proof of data dependence of the iterative process.

4 Numerical simulations/sensitivity analysis

4.1 Stability and Convergence of our Scheme

Firstly, in this section we would numerically show the stability and convergence of our iterative process (19) of Theorem 3.1 using the following examples. Intuitively, a fixed point iteration procedure is numerically stable if, "small" modifications in the initial data or in the data that are involved in the computation process (see [26]), will produce a "small" influence on the computed value of the fixed point.

Example 4.1. Let $K = [1, 6] \subset \mathbb{B} = R$ denote the reals with the usual norm $|.|$ and define the map $\Omega : K \to K$ by

$$\Omega(\omega) := \frac{1}{2}\omega + 1, \forall \omega \in [1, 6]. \tag{44}$$

Then Ω is a contraction map with a constant $L = \frac{1}{2}$ and $Fix(\Omega) = \{2\}$.

Using this example, we perform the following iterations such that the tables and graphs below are generated with Python software, run on HP PC with Intel(R)Core(TM)i7-3520M CPU @ 2.90GHz.

Table 4.1: Numerical values of the sequences $\{u_n\}$, $\{w_n\}$, $\{x_n\}$ and $\{\omega_n\}$ with $\alpha_n = \frac{1}{n+3}, \beta_n = \frac{1}{n+1}, \gamma_n = \frac{1}{n+2} \in (0, 1)$, initial value $x = 6 \in [1, 6]$ and a "good" stopping criteria $\|\omega_n - \omega_{n+1}\| \leq 10^{-7}$.

n	u[n]	w[n]	x[n]	omega[n]	err[n]
0	5.3333333	3.6666667	3.2500000	6.0000000	3.3750000
1	2.5468750	2.4101562	2.3417969	2.6250000	0.4541016
2	2.1538086	2.1281738	2.1121521	2.1708984	0.1148224
3	2.0514030	2.0449777	2.0404799	2.0560760	0.0358361
4	2.0187942	2.0169148	2.0155052	2.0202399	0.0124873
5	2.0072681	2.0066624	2.0061865	2.0077526	0.0046594
6	2.0029214	2.0027127	2.0025432	2.0030933	0.0018217
7	2.0012080	2.0011325	2.0010696	2.0012716	0.0007368
8	2.0005105	2.0004821	2.0004580	2.0005348	0.0003058
9	2.0002195	2.0002085	2.0001990	2.0002290	0.0001295
10	2.0000957	2.0000913	2.0000875	2.0000995	0.0000557
11	2.0000422	2.0000404	2.0000389	2.0000438	0.0000243
12	2.0000188	2.0000181	2.0000174	2.0000194	0.0000107
13	2.0000084	2.0000081	2.0000079	2.0000087	0.0000048
14	2.0000038	2.0000037	2.0000036	2.0000039	0.0000021
15	2.0000017	2.0000017	2.0000016	2.0000018	0.0000010
16	2.0000008	2.0000008	2.0000008	2.0000008	0.0000004
17	2.0000004	2.0000004	2.0000003	2.0000004	0.0000002
18	2.0000002	2.0000002	2.0000002	2.0000002	0.0000001
19	2.0000001	2.0000001	2.0000001	2.0000001	0.0000000
20	2.0000000	2.0000000	2.0000000	2.0000000	0.0000000
21	2.0000000	2.0000000	2.0000000	2.0000000	0.0000000
22	2.0000000	2.0000000	2.0000000	2.0000000	0.0000000
23	2.0000000	2.0000000	2.0000000	2.0000000	0.0000000
24	2.0000000	2.0000000	2.0000000	2.0000000	0.0000000

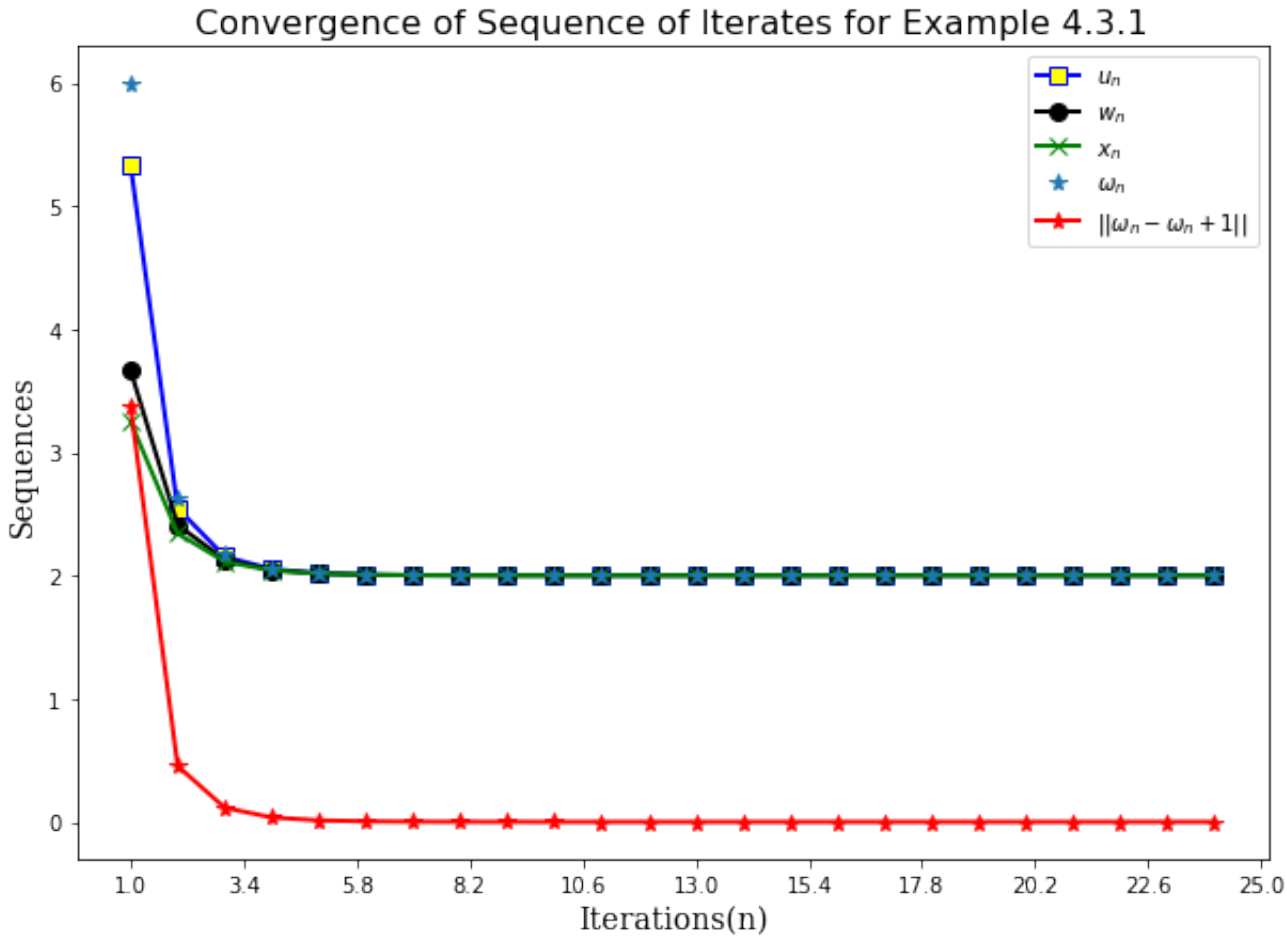


FIGURE 4.1. Graph corresponding to Table 4.1

Table 4.2: Numerical values of the sequences $\{u_n\}$, $\{w_n\}$, $\{x_n\}$ and $\{\omega_n\}$ with $\alpha_n = 0.5, \beta_n = 0.33, \gamma_n = 0.25 \in (0,1)$, initial value $x = 6 \in [1,6]$ and a "good" stopping criteria $\|\omega_n - \omega_{n+1}\| \leq 10^{-7}$.

n	u[n]	w[n]	x[n]	omega[n]	err[n]
0	5.0000000	4.5050000	4.1918750	6.0000000	2.9040625
1	2.8219531	2.6863309	2.6005395	3.0959375	0.7956677
2	2.2252023	2.1880439	2.1645384	2.3002698	0.2180005
3	2.0617019	2.0515211	2.0450810	2.0822692	0.0597287
4	2.0169054	2.0141160	2.0123515	2.0225405	0.0163647
5	2.0046318	2.0038676	2.0033841	2.0061757	0.0044837
6	2.0012690	2.0010597	2.0009272	2.0016921	0.0012285
7	2.0003477	2.0002903	2.0002540	2.0004636	0.0003366
8	2.0000953	2.0000795	2.0000696	2.0001270	0.0000922
9	2.0000261	2.0000218	2.0000191	2.0000348	0.0000253
10	2.0000072	2.0000060	2.0000052	2.0000095	0.0000069
11	2.0000020	2.0000016	2.0000014	2.0000026	0.0000019
12	2.0000005	2.0000004	2.0000004	2.0000007	0.0000005
13	2.0000001	2.0000001	2.0000001	2.0000002	0.0000001
14	2.0000000	2.0000000	2.0000000	2.0000001	0.0000000
15	2.0000000	2.0000000	2.0000000	2.0000000	0.0000000
16	2.0000000	2.0000000	2.0000000	2.0000000	0.0000000
17	2.0000000	2.0000000	2.0000000	2.0000000	0.0000000
18	2.0000000	2.0000000	2.0000000	2.0000000	0.0000000
19	2.0000000	2.0000000	2.0000000	2.0000000	0.0000000
20	2.0000000	2.0000000	2.0000000	2.0000000	0.0000000
21	2.0000000	2.0000000	2.0000000	2.0000000	0.0000000

22	2.0000000	2.0000000	2.0000000	2.0000000	0.0000000
23	2.0000000	2.0000000	2.0000000	2.0000000	0.0000000
24	2.0000000	2.0000000	2.0000000	2.0000000	0.0000000

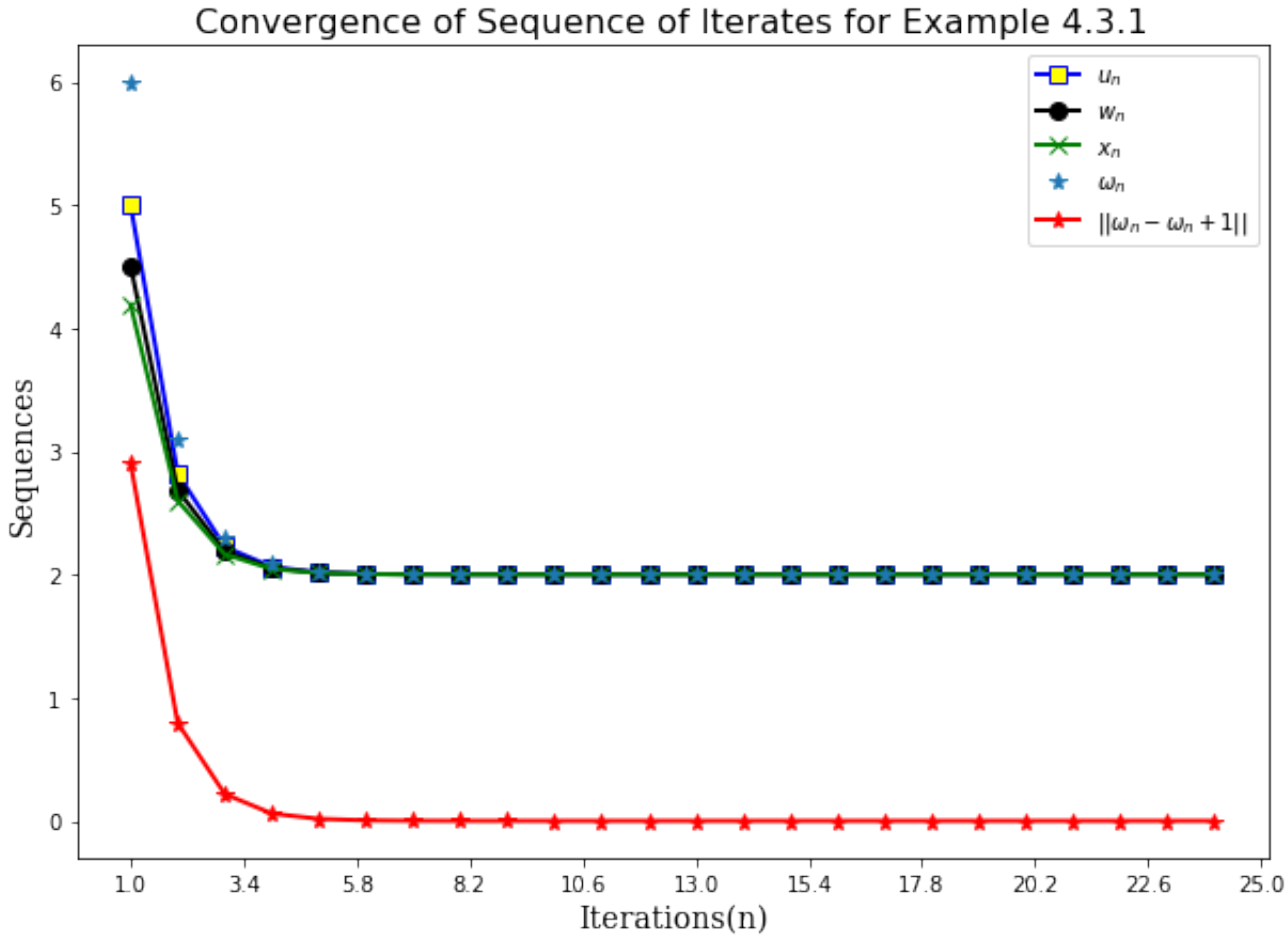


FIGURE 4.2. Graph corresponding to Table 4.2

Table 4.3: Numerical values of the sequences $\{u_n\}$, $\{w_n\}$, $\{x_n\}$ and $\{\omega_n\}$ with $\alpha_n = 0.5, \beta_n = 0.33, \gamma_n = 0.25 \in (0,1)$, initial value $x = 2.5 \in [1,6]$ and a "good" stopping criteria $\|\omega_n - \omega_{n+1}\| \leq 10^{-7}$.

n	u[n]	w[n]	x[n]	omega[n]	err[n]
0	2.3750000	2.3131250	2.2739844	2.5000000	0.3630078
1	2.1027441	2.0857914	2.0750674	2.1369922	0.0994585
2	2.0281503	2.0235055	2.0205673	2.0375337	0.0272501
3	2.0077127	2.0064401	2.0056351	2.0102837	0.0074661
4	2.0021132	2.0017645	2.0015439	2.0028176	0.0020456
5	2.0005790	2.0004834	2.0004230	2.0007720	0.0005605
6	2.0001586	2.0001325	2.0001159	2.0002115	0.0001536
7	2.0000435	2.0000363	2.0000318	2.0000579	0.0000421
8	2.0000119	2.0000099	2.0000087	2.0000159	0.0000115
9	2.0000033	2.0000027	2.0000024	2.0000044	0.0000032
10	2.0000009	2.0000007	2.0000007	2.0000012	0.0000009
11	2.0000002	2.0000002	2.0000002	2.0000003	0.0000002
12	2.0000001	2.0000001	2.0000000	2.0000001	0.0000001
13	2.0000000	2.0000000	2.0000000	2.0000000	0.0000000
14	2.0000000	2.0000000	2.0000000	2.0000000	0.0000000
15	2.0000000	2.0000000	2.0000000	2.0000000	0.0000000

16	2.0000000	2.0000000	2.0000000	2.0000000	0.0000000
17	2.0000000	2.0000000	2.0000000	2.0000000	0.0000000
18	2.0000000	2.0000000	2.0000000	2.0000000	0.0000000
19	2.0000000	2.0000000	2.0000000	2.0000000	0.0000000
20	2.0000000	2.0000000	2.0000000	2.0000000	0.0000000
21	2.0000000	2.0000000	2.0000000	2.0000000	0.0000000
22	2.0000000	2.0000000	2.0000000	2.0000000	0.0000000
23	2.0000000	2.0000000	2.0000000	2.0000000	0.0000000
24	2.0000000	2.0000000	2.0000000	2.0000000	0.0000000

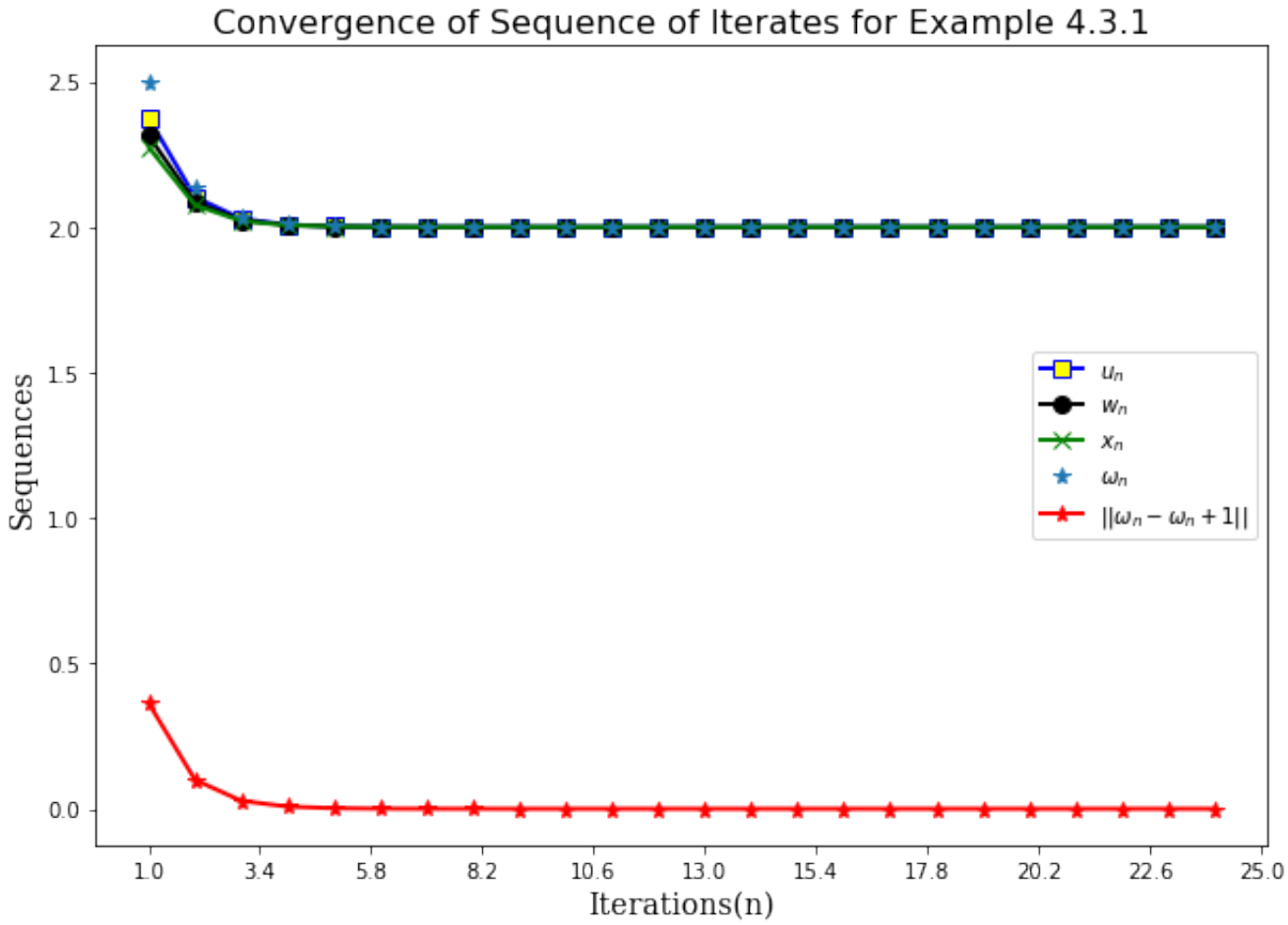


FIGURE 4.3. Graph corresponding to Table 4.3

Table 4.4: Numerical values of the sequences $\{u_n\}$, $\{w_n\}$, $\{x_n\}$ and $\{\omega_n\}$ with $\alpha_n = \frac{1}{n+3}, \beta_n = \frac{1}{n+1}, \gamma_n = \frac{1}{n+2} \in (0,1)$, initial value $x = 2.5 \in [1,6]$ and a "good" stopping criteria $\|\omega_n - \omega_{n+1}\| \leq 10^{-7}$.

n	u[n]	w[n]	x[n]	omega[n]	err[n]
0	2.4166667	2.2083333	2.1562500	2.5000000	0.4218750
1	2.0683594	2.0512695	2.0427246	2.0781250	0.0567627
2	2.0192261	2.0160217	2.0140190	2.0213623	0.0143528
3	2.0064254	2.0056222	2.0050600	2.0070095	0.0044795
4	2.0023493	2.0021144	2.0019382	2.0025300	0.0015609
5	2.0009085	2.0008328	2.0007733	2.0009691	0.0005824
6	2.0003652	2.0003391	2.0003179	2.0003867	0.0002277
7	2.0001510	2.0001416	2.0001337	2.0001589	0.0000921
8	2.0000638	2.0000603	2.0000573	2.0000668	0.0000382
9	2.0000274	2.0000261	2.0000249	2.0000286	0.0000162

10	2.0000120	2.0000114	2.0000109	2.0000124	0.0000070
11	2.0000053	2.0000051	2.0000049	2.0000055	0.0000030
12	2.0000023	2.0000023	2.0000022	2.0000024	0.0000013
13	2.0000011	2.0000010	2.0000010	2.0000011	0.0000006
14	2.0000005	2.0000005	2.0000004	2.0000005	0.0000003
15	2.0000002	2.0000002	2.0000002	2.0000002	0.0000001
16	2.0000001	2.0000001	2.0000001	2.0000001	0.0000001
17	2.0000000	2.0000000	2.0000000	2.0000000	0.0000000
18	2.0000000	2.0000000	2.0000000	2.0000000	0.0000000
19	2.0000000	2.0000000	2.0000000	2.0000000	0.0000000
20	2.0000000	2.0000000	2.0000000	2.0000000	0.0000000
21	2.0000000	2.0000000	2.0000000	2.0000000	0.0000000
22	2.0000000	2.0000000	2.0000000	2.0000000	0.0000000
23	2.0000000	2.0000000	2.0000000	2.0000000	0.0000000
24	2.0000000	2.0000000	2.0000000	2.0000000	0.0000000

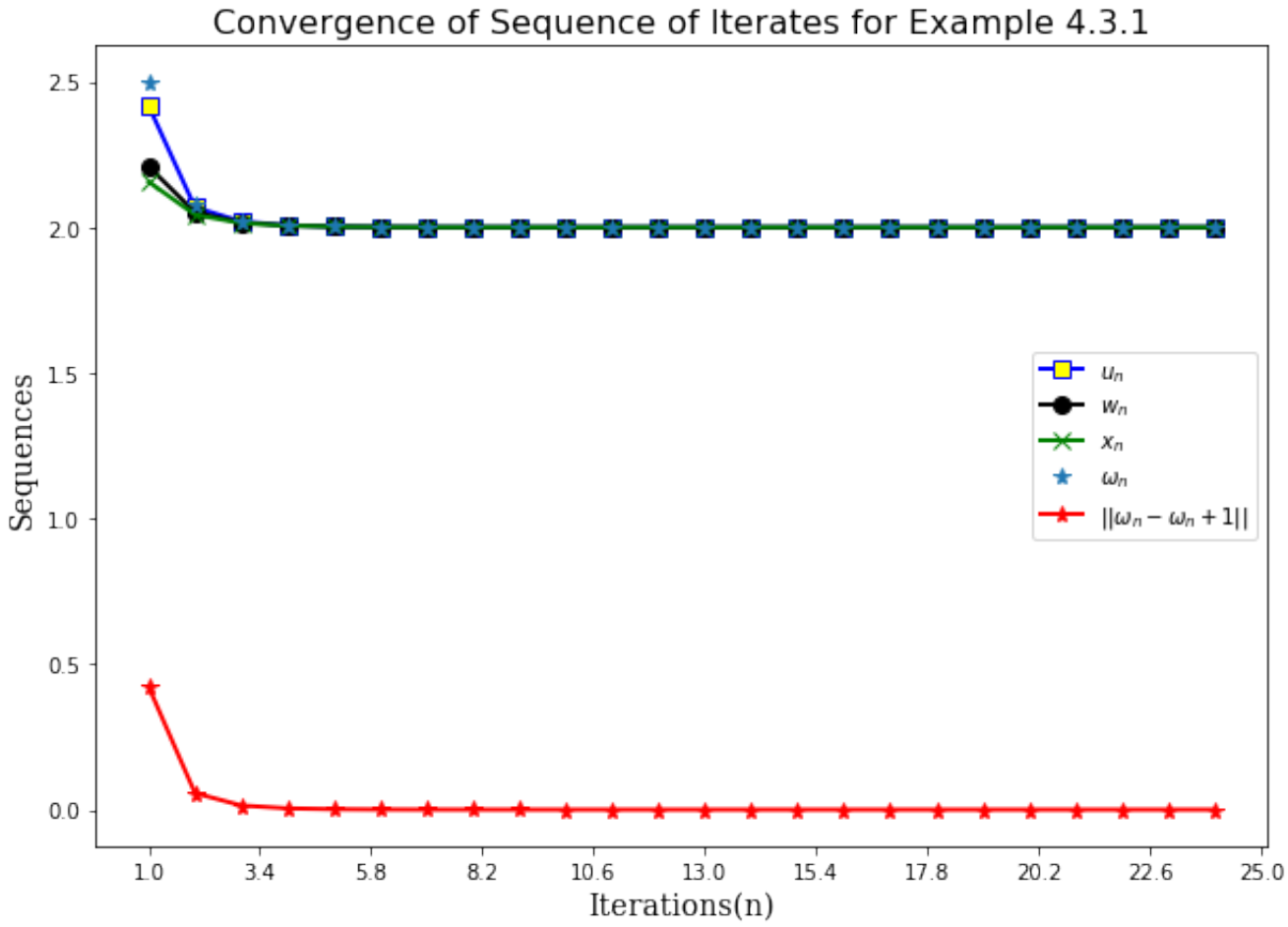


FIGURE 4.4. Graph corresponding to Table 4.4

Example 4.2. Let $K = [1, 10] \subset \mathbb{B} = R$ denote the reals with the usual norm $|.|$ and define the map $\Omega : K \to K$ by

$$\Omega(\omega) := (4\omega + 15)^{\frac{1}{3}}, \forall \omega \in [1, 10]. \tag{45}$$

Then Ω is a contraction map with a constant $L = \frac{1}{(15)^{\frac{1}{3}}}$ and $Fix(\Omega) = \{3\}$.

Proof. We first prove that the fixed point is actually the 3. To see this, we make use of the definition of fixed

point as follows:

$$\begin{aligned} Fix(\Omega) &= \{\omega \in R : \Omega\omega = \omega\} \\ &= \{\omega \in R : (4\omega + 15)^{\frac{1}{3}} = \omega\} \\ &= \{\omega \in R : 4\omega + 15 = \omega^3\} \\ &= \{\omega \in R : \omega^3 - 4\omega - 15 = 0\} \\ &= \{\omega \in R : \omega = 3 \in [1, 10]\}. \end{aligned}$$

Thus $Fix(\Omega) = \{3\}$.

Next, we prove that Ω is $L = \frac{1}{(15)^{\frac{1}{3}}}$ contractive map. Now since $\mathbb{B} = R$, is the reals with the usual norm, we have that the norm becomes absolute norm. That is

$$\|\Omega\omega - \Omega\hat{\omega}\| \leq L\|\omega - \hat{\omega}\|, \forall\omega, \hat{\omega} \in R \tag{46}$$

becomes

$$|\Omega\omega - \Omega\hat{\omega}| \leq L|\omega - \hat{\omega}|, \forall\omega, \hat{\omega} \in R \tag{47}$$

where $\Omega\omega = (4\omega + 15)^{\frac{1}{3}}$ and $\Omega\hat{\omega} = (4\hat{\omega} + 15)^{\frac{1}{3}}$, $\forall\forall\omega, \hat{\omega} \in [1, 10] \subset R$. So using (47), we have

$$|\,(4\omega + 15)^{\frac{1}{3}} - (4\hat{\omega} + 15)^{\frac{1}{3}}\,| \leq \frac{1}{(15)^{\frac{1}{3}}}|\omega - \hat{\omega}|.$$

Thus $L = \frac{1}{(15)^{\frac{1}{3}}} \in [1, 10]$ as expected and that completes the proof of Example 4.2.

Using this example, we perform the following iterations such that the tables and graphs below are generated with Python software, run on HP PC with Intel(R)Core(TM)i7-3520M CPU @ 2.90GHz.

Table 4.5: Numerical values of the sequences $\{u_n\}$, $\{w_n\}$, $\{x_n\}$ and $\{\omega_n\}$ with $\alpha_n = 0.5, \beta_n = 0.33, \gamma_n = 0.25 \in (0, 1)$, initial value $x = 3.5 \in [1, 10]$ and a "good" stopping criteria $\|\omega_n - \omega_{n+1}\| \leq 10^{-7}$.

n	u[n]	w[n]	x[n]	omega[n]	err[n]
0	3.2861584	3.3487968	3.3877021	3.5000000	0.4436285
1	3.0323498	3.0393479	3.0437331	3.0563715	0.0499064
2	3.0037113	3.0045130	3.0050159	3.0064650	0.0057221
3	3.0004265	3.0005186	3.0005764	3.0007429	0.0006575
4	3.0000490	3.0000596	3.0000662	3.0000854	0.0000756
5	3.0000056	3.0000069	3.0000076	3.0000098	0.0000087
6	3.0000006	3.0000008	3.0000009	3.0000011	0.0000010
7	3.0000001	3.0000001	3.0000001	3.0000001	0.0000001
8	3.0000000	3.0000000	3.0000000	3.0000000	0.0000000
9	3.0000000	3.0000000	3.0000000	3.0000000	0.0000000
10	3.0000000	3.0000000	3.0000000	3.0000000	0.0000000
11	3.0000000	3.0000000	3.0000000	3.0000000	0.0000000
12	3.0000000	3.0000000	3.0000000	3.0000000	0.0000000
13	3.0000000	3.0000000	3.0000000	3.0000000	0.0000000
14	3.0000000	3.0000000	3.0000000	3.0000000	0.0000000

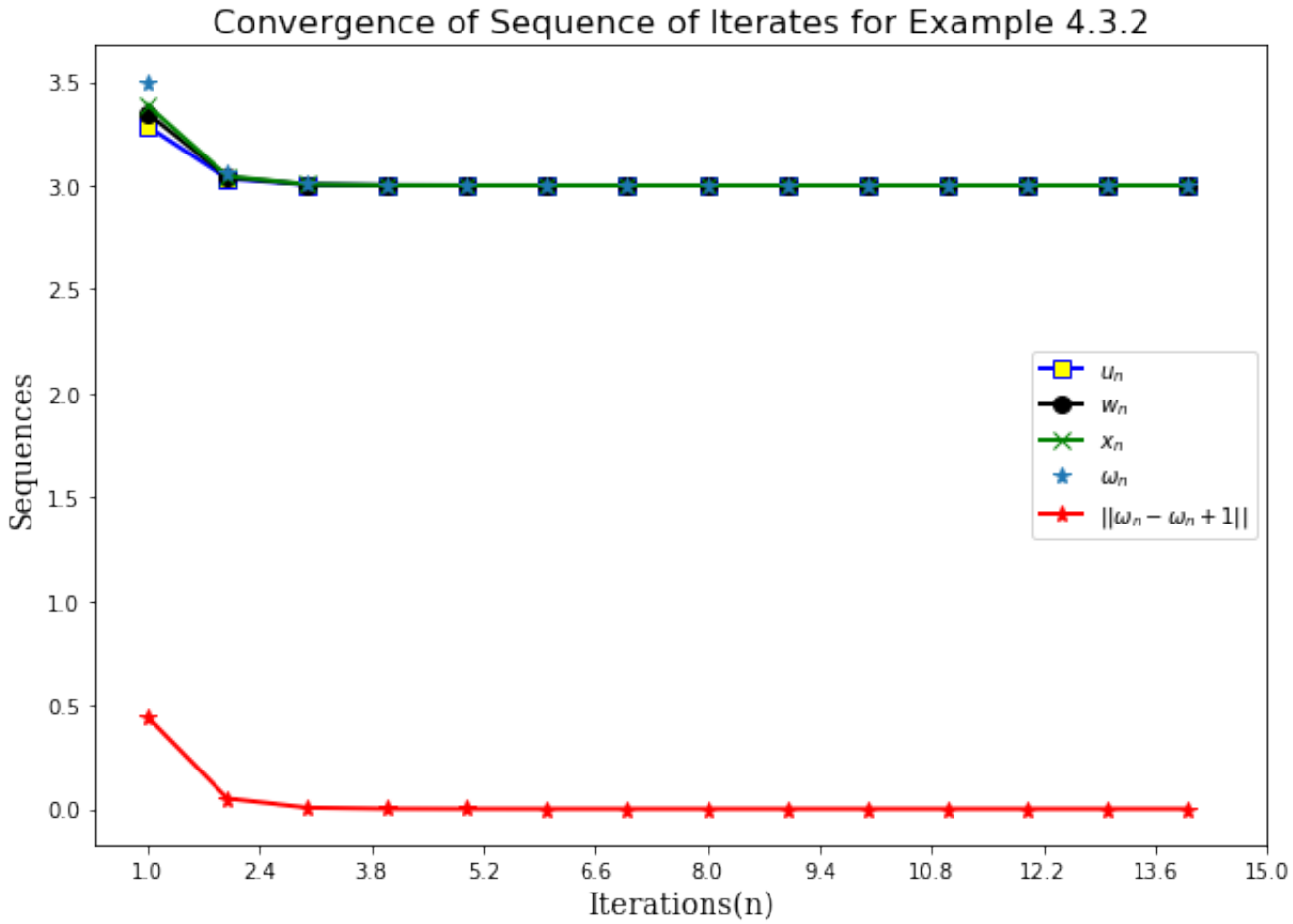


FIGURE 4.5. Graph corresponding to Table 4.5

Table 4.6: The numerical values of the sequences $\{u_n\}$, $\{w_n\}$, $\{x_n\}$ and $\{\omega_n\}$ with $\alpha_n = \frac{1}{n+3}, \beta_n = \frac{1}{n+1}, \gamma_n = \frac{1}{n+2} \in (0,1)$, initial value $\omega_1 = 3.5 \in [1,10]$ "good" stopping criteria $\|\omega_n - \omega_{n+1}\| \leq 10^{-7}$.

n	u[n]	w[n]	x[n]	omega[n]	err[n]
0	3.3574389	3.0520458	3.2538454	3.5000000	0.4628551
1	3.0292319	3.0207347	3.0257862	3.0371449	0.0333296
2	3.0031653	3.0026998	3.0029615	3.0038153	0.0033766
3	3.0003764	3.0003429	3.0003611	3.0004387	0.0003852
4	3.0000470	3.0000442	3.0000457	3.0000535	0.0000467
5	3.0000060	3.0000058	3.0000059	3.0000068	0.0000059
6	3.0000008	3.0000008	3.0000008	3.0000009	0.0000008
7	3.0000001	3.0000001	3.0000001	3.0000001	0.0000001
8	3.0000000	3.0000000	3.0000000	3.0000000	0.0000000
9	3.0000000	3.0000000	3.0000000	3.0000000	0.0000000
10	3.0000000	3.0000000	3.0000000	3.0000000	0.0000000
11	3.0000000	3.0000000	3.0000000	3.0000000	0.0000000
12	3.0000000	3.0000000	3.0000000	3.0000000	0.0000000
13	3.0000000	3.0000000	3.0000000	3.0000000	0.0000000
14	3.0000000	3.0000000	3.0000000	3.0000000	0.0000000

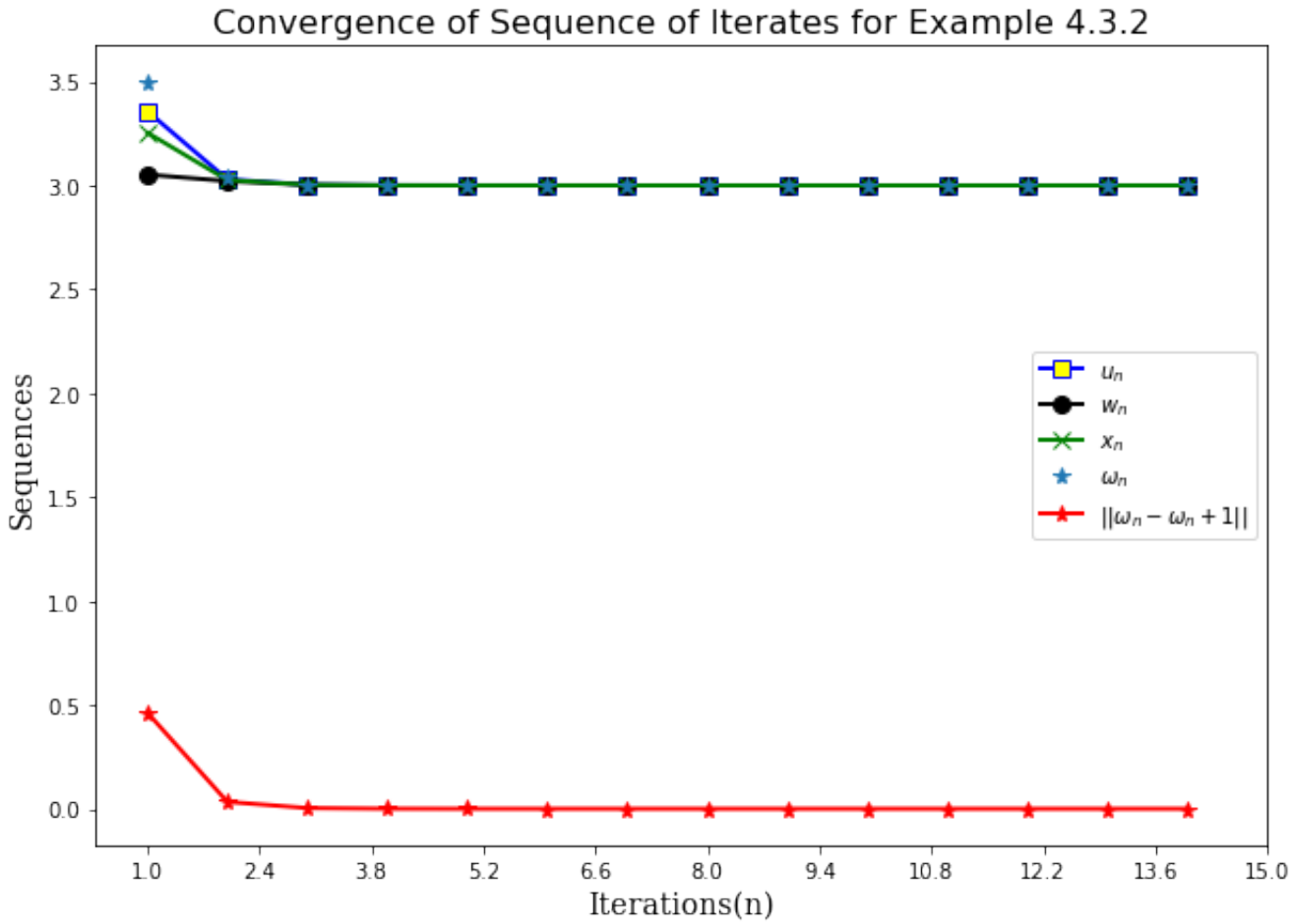


FIGURE 4.6. Graph corresponding to Table 4.6

Table 4.7: The numerical values of the sequences $\{u_n\}$, $\{w_n\}$, $\{x_n\}$ and $\{\omega_n\}$ with $\alpha_n = 0.5, \beta_n = 0.33, \gamma_n = 0.25 \in (0,1)$, initial value $\omega = 10 \in [1,10]$ and a "good" stopping criteria $\|\omega_n - \omega_{n+1}\| \leq 10^{-7}$.

n	u[n]	w[n]	x[n]	omega[n]	err[n]
0	6.9014762	7.8525786	8.3984174	10.0000000	6.3508373
1	3.3712034	3.4527639	3.5032795	3.6491627	0.5763827
2	3.0417619	3.0508001	3.0564618	3.0727800	0.0644385
3	3.0047884	3.0058228	3.0064717	3.0083415	0.0073830
4	3.0005502	3.0006691	3.0007436	3.0009585	0.0008483
5	3.0000632	3.0000769	3.0000855	3.0001102	0.0000975
6	3.0000073	3.0000088	3.0000098	3.0000127	0.0000112
7	3.0000008	3.0000010	3.0000011	3.0000015	0.0000013
8	3.0000001	3.0000001	3.0000001	3.0000002	0.0000001
9	3.0000000	3.0000000	3.0000000	3.0000000	0.0000000
10	3.0000000	3.0000000	3.0000000	3.0000000	0.0000000
11	3.0000000	3.0000000	3.0000000	3.0000000	0.0000000
12	3.0000000	3.0000000	3.0000000	3.0000000	0.0000000
13	3.0000000	3.0000000	3.0000000	3.0000000	0.0000000
14	3.0000000	3.0000000	3.0000000	3.0000000	0.0000000

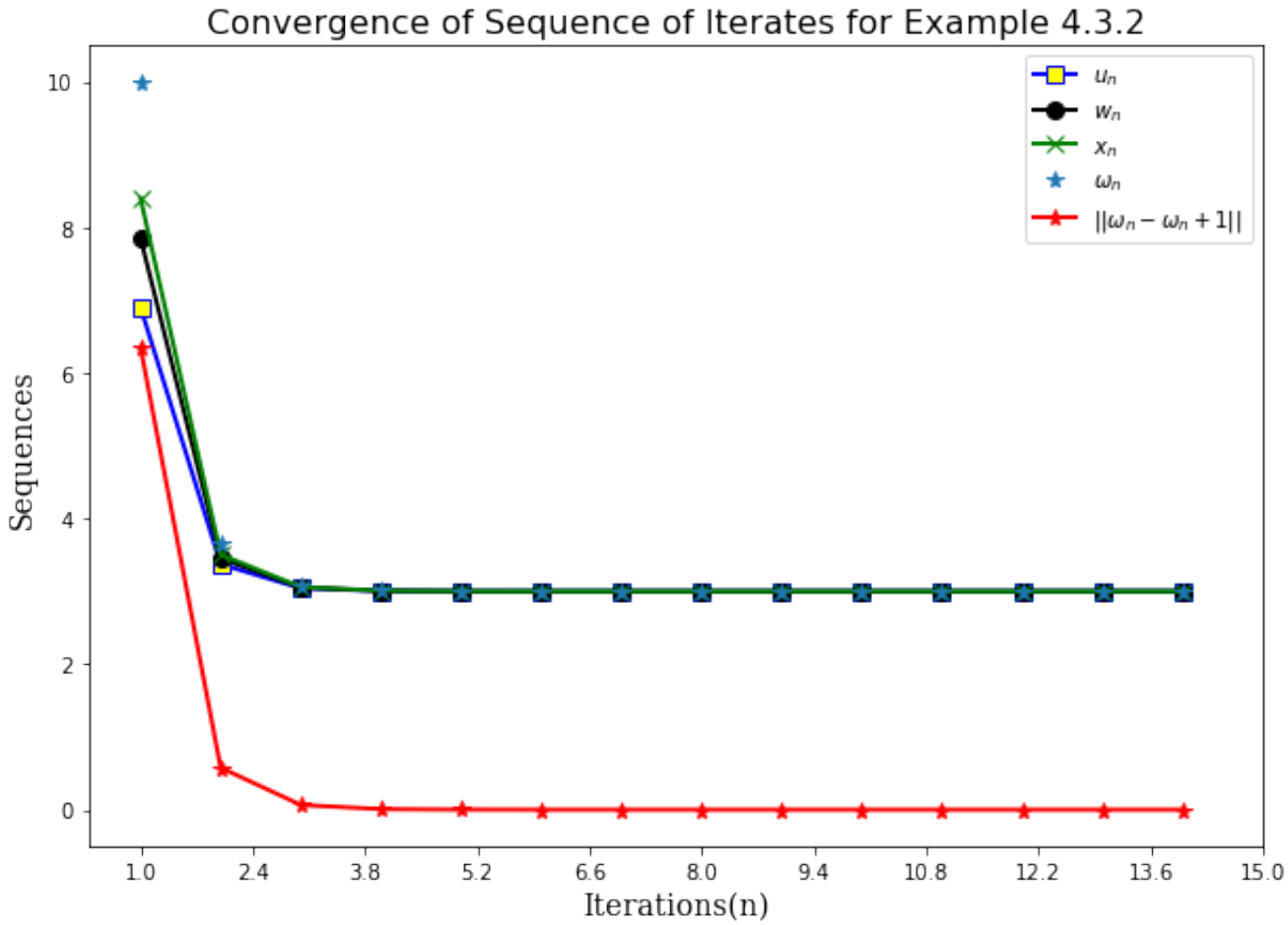


FIGURE 4.7. Graph corresponding to Table 4.7

Table 4.8: The numerical values of the sequences $\{u_n\}$, $\{w_n\}$, $\{x_n\}$ and $\{\omega_n\}$ with $\alpha_n = \frac{1}{n+3}, \beta_n = \frac{1}{n+1}, \gamma_n = \frac{1}{n+2} \in (0,1)$, initial value $\omega = 10 \in [1,10]$ and a "good" stopping criteria $\|\omega_n - \omega_{n+1}\| \leq 10^{-7}$.

n	u[n]	w[n]	x[n]	omega[n]	err[n]
0	7.9343175	3.6020891	6.5433352	10.0000000	6.5469301
1	3.3562207	3.2524706	3.3143620	3.4530699	0.4072026
2	3.0380498	3.0324537	3.0356005	3.0458673	0.0406024
3	3.0045174	3.0041160	3.0043339	3.0052649	0.0046230
4	3.0005638	3.0005302	3.0005480	3.0006419	0.0005607
5	3.0000725	3.0000694	3.0000711	3.0000812	0.0000707
6	3.0000095	3.0000092	3.0000094	3.0000105	0.0000091
7	3.0000013	3.0000012	3.0000013	3.0000014	0.0000012
8	3.0000002	3.0000002	3.0000002	3.0000002	0.0000002
9	3.0000000	3.0000000	3.0000000	3.0000000	0.0000000
10	3.0000000	3.0000000	3.0000000	3.0000000	0.0000000
11	3.0000000	3.0000000	3.0000000	3.0000000	0.0000000
12	3.0000000	3.0000000	3.0000000	3.0000000	0.0000000
13	3.0000000	3.0000000	3.0000000	3.0000000	0.0000000
14	3.0000000	3.0000000	3.0000000	3.0000000	0.0000000

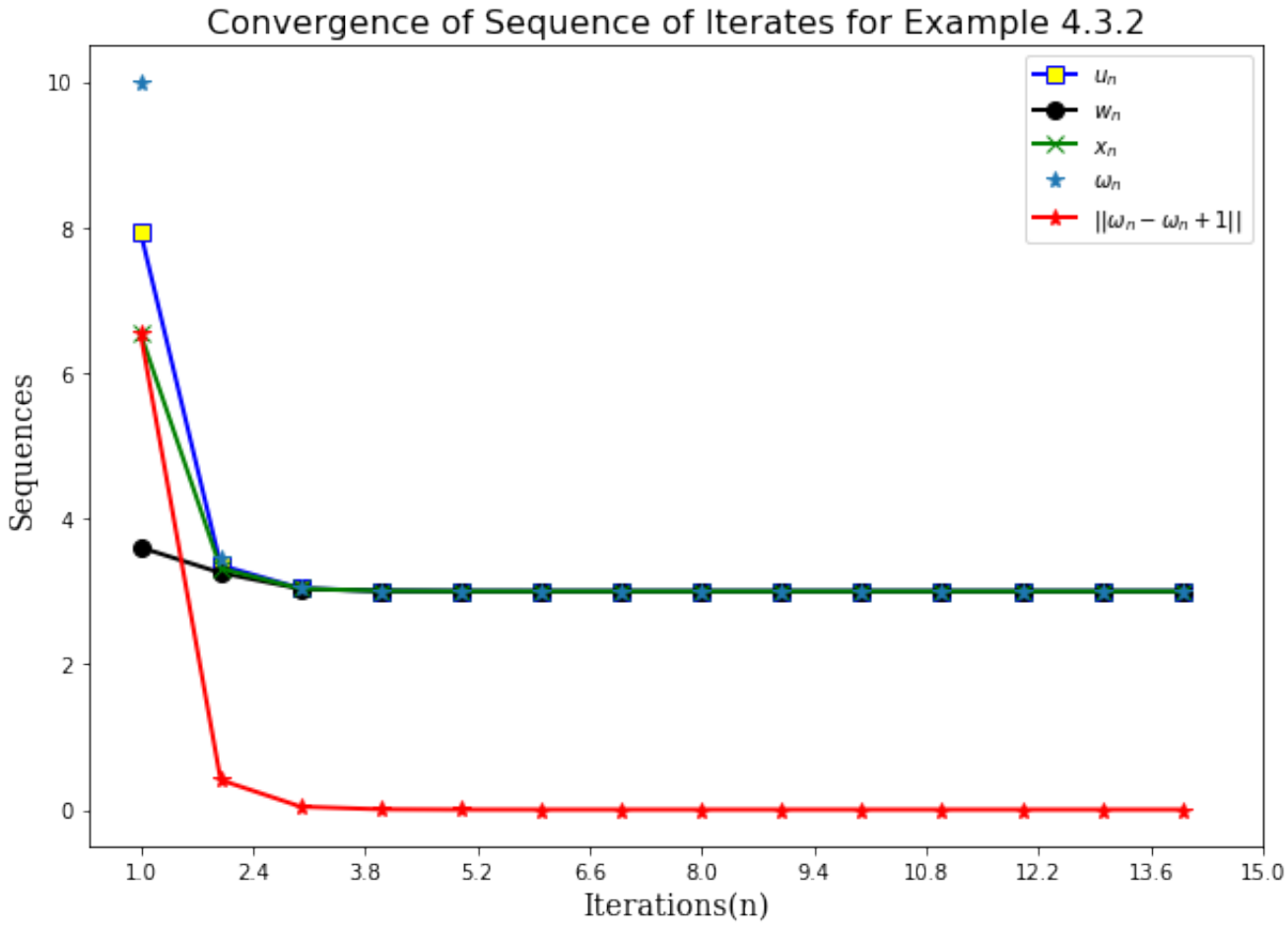


FIGURE 4.8. Graph corresponding to Table 4.8

Table 4.9: The numerical values of the sequences $\{u_n\}$, $\{w_n\}$, $\{x_n\}$ and $\{\omega_n\}$ with $\alpha_n = 0.5, \beta_n = 0.33, \gamma_n = 0.25 \in (0,1)$, initial value $\omega = 3 \in [1,10]$ and a "good" stopping criteria $\|\omega_n - \omega_{n+1}\| \leq 10^{-7}$.

n	u[n]	w[n]	x[n]	omega[n]
0	3.0000000	3.0000000	3.0000000	3.0000000
1	3.0000000	3.0000000	3.0000000	3.0000000
2	3.0000000	3.0000000	3.0000000	3.0000000
3	3.0000000	3.0000000	3.0000000	3.0000000
4	3.0000000	3.0000000	3.0000000	3.0000000
5	3.0000000	3.0000000	3.0000000	3.0000000
6	3.0000000	3.0000000	3.0000000	3.0000000
7	3.0000000	3.0000000	3.0000000	3.0000000
8	3.0000000	3.0000000	3.0000000	3.0000000
9	3.0000000	3.0000000	3.0000000	3.0000000
10	3.0000000	3.0000000	3.0000000	3.0000000
11	3.0000000	3.0000000	3.0000000	3.0000000
12	3.0000000	3.0000000	3.0000000	3.0000000
13	3.0000000	3.0000000	3.0000000	3.0000000
14	3.0000000	3.0000000	3.0000000	3.0000000

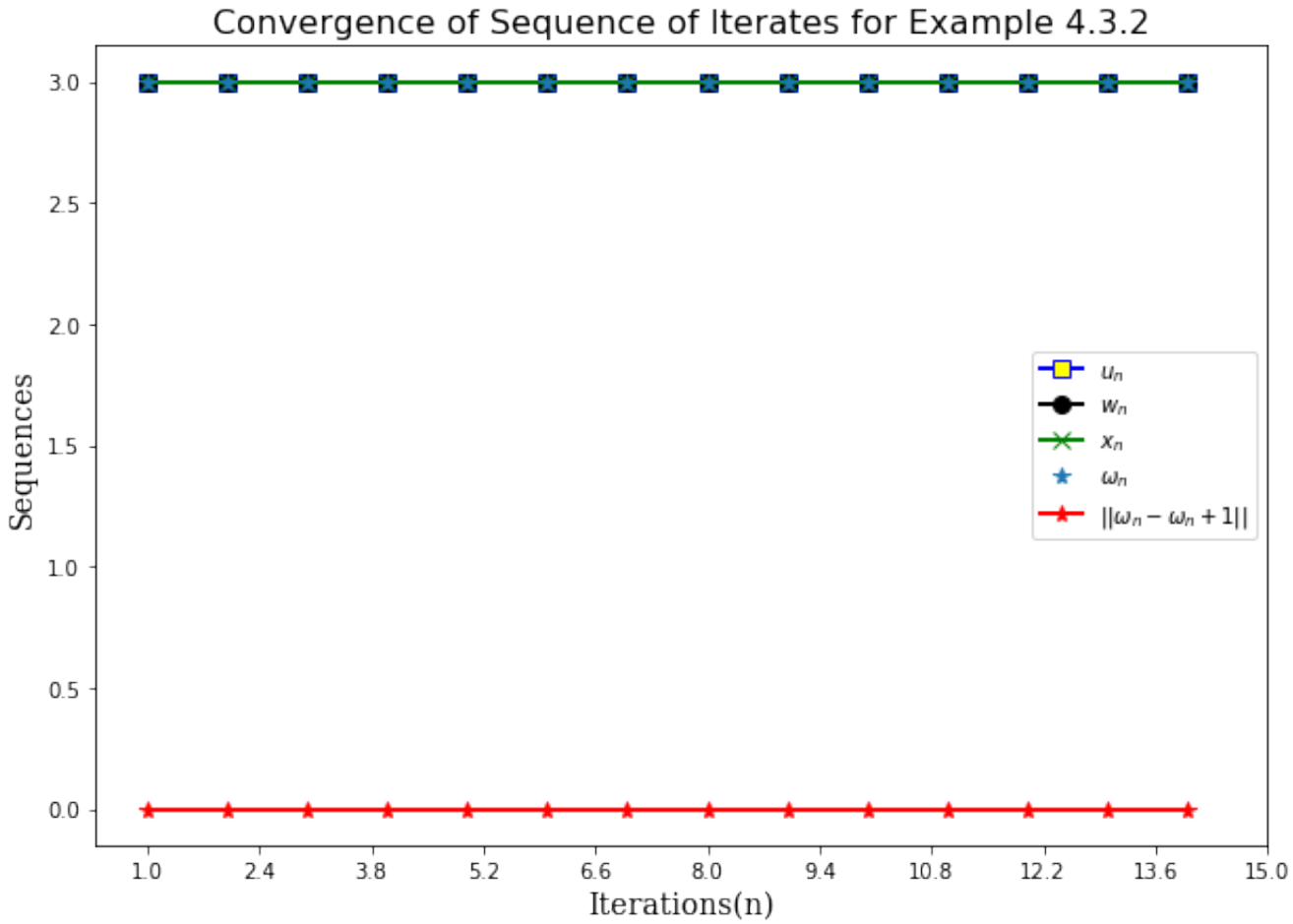


FIGURE 4.9. Graph corresponding to Table 4.9

4.2 Comparison of the rate of convergence of several iteration processes

Table 4.10: The numerical values of the sequences $\{u_n\}$, $\{w_n\}$, $\{x_n\}$ and $\{\omega_n\}$ with $\alpha_n = 0.5, \beta_n = 0.33, \gamma_n = 0.25, \lambda = 0.5 \in (0,1)$, initial value $\omega = 3.5 \in [1,6]$ and a "good" stopping criteria $\|\omega_n - \omega_{n+1}\| \leq 10^{-7}$.

n	HybridPicMann[n]	PicNoor[n]	Picard[n]	Mann[n]	Krasnoselskii[n]
0	3.5000000	3.5000000	3.5000000	3.5000000	3.5000000
1	2.4101562	2.6367188	2.7500000	3.1250000	3.1250000
2	2.1121521	2.2702738	2.3750000	2.8437500	2.8437500
3	2.0306666	2.1147256	2.1875000	2.6328125	2.6328125
4	2.0083854	2.0486986	2.0937500	2.4746094	2.4746094
5	2.0022929	2.0206716	2.0468750	2.3559570	2.3559570
6	2.0006270	2.0087746	2.0234375	2.2669678	2.2669678
7	2.0001714	2.0037247	2.0117188	2.2002258	2.2002258
8	2.0000469	2.0015810	2.0058594	2.1501694	2.1501694
9	2.0000128	2.0006711	2.0029297	2.1126270	2.1126270
10	2.0000035	2.0002849	2.0014648	2.0844703	2.0844703
11	2.0000010	2.0001209	2.0007324	2.0633527	2.0633527
12	2.0000003	2.0000513	2.0003662	2.0475145	2.0475145
13	2.0000001	2.0000218	2.0001831	2.0356359	2.0356359
14	2.0000000	2.0000092	2.0000916	2.0267269	2.0267269
15	2.0000000	2.0000039	2.0000458	2.0200452	2.0200452
16	2.0000000	2.0000017	2.0000229	2.0150339	2.0150339
17	2.0000000	2.0000007	2.0000114	2.0112754	2.0112754
18	2.0000000	2.0000003	2.0000057	2.0084566	2.0084566
19	2.0000000	2.0000001	2.0000029	2.0063424	2.0063424

20	2.0000000	2.0000001	2.0000014	2.0047568	2.0047568
21	2.0000000	2.0000000	2.0000007	2.0035676	2.0035676
22	2.0000000	2.0000000	2.0000004	2.0026757	2.0026757
23	2.0000000	2.0000000	2.0000002	2.0020068	2.0020068
24	2.0000000	2.0000000	2.0000001	2.0015051	2.0015051

Table 4.11: The numerical values of the sequences $\{u_n\}$, $\{w_n\}$, $\{x_n\}$ and $\{\omega_n\}$ with $\alpha_n = 0.5, \beta_n = 0.33, \gamma_n = 0.25, \lambda = 0.5 \in (0,1)$, initial value $\omega = 3.5 \in [1,6]$ and a "good" stopping criteria $\|\omega_n - \omega_{n+1}\| \leq 10^{-7}$.

n	Ishikawa[n]	Noor[n]	PicMann[n]
0	3.5000000	3.5000000	3.5000000
1	3.0631250	3.0553906	2.5625000
2	2.7534898	2.7425662	2.2109375
3	2.5340359	2.5224650	2.0791016
4	2.3784980	2.3676031	2.0296631
5	2.2682604	2.2586432	2.0111237
6	2.1901296	2.1819798	2.0041714
7	2.1347543	2.1280398	2.0015643
8	2.0955071	2.0900880	2.0005866
9	2.0676907	2.0633854	2.0002200
10	2.0479758	2.0445975	2.0000825
11	2.0340028	2.0313786	2.0000309
12	2.0240995	2.0220778	2.0000116
13	2.0170805	2.0155338	2.0000044
14	2.0121058	2.0109295	2.0000016
15	2.0085800	2.0076899	2.0000006
16	2.0060811	2.0054106	2.0000002
17	2.0043100	2.0038068	2.0000001
18	2.0030547	2.0026785	2.0000000
19	2.0021650	2.0018846	2.0000000
20	2.0015344	2.0013260	2.0000000
21	2.0010875	2.0009329	2.0000000
22	2.0007708	2.0006564	2.0000000
23	2.0005463	2.0004618	2.0000000
24	2.0003872	2.0003250	2.0000000

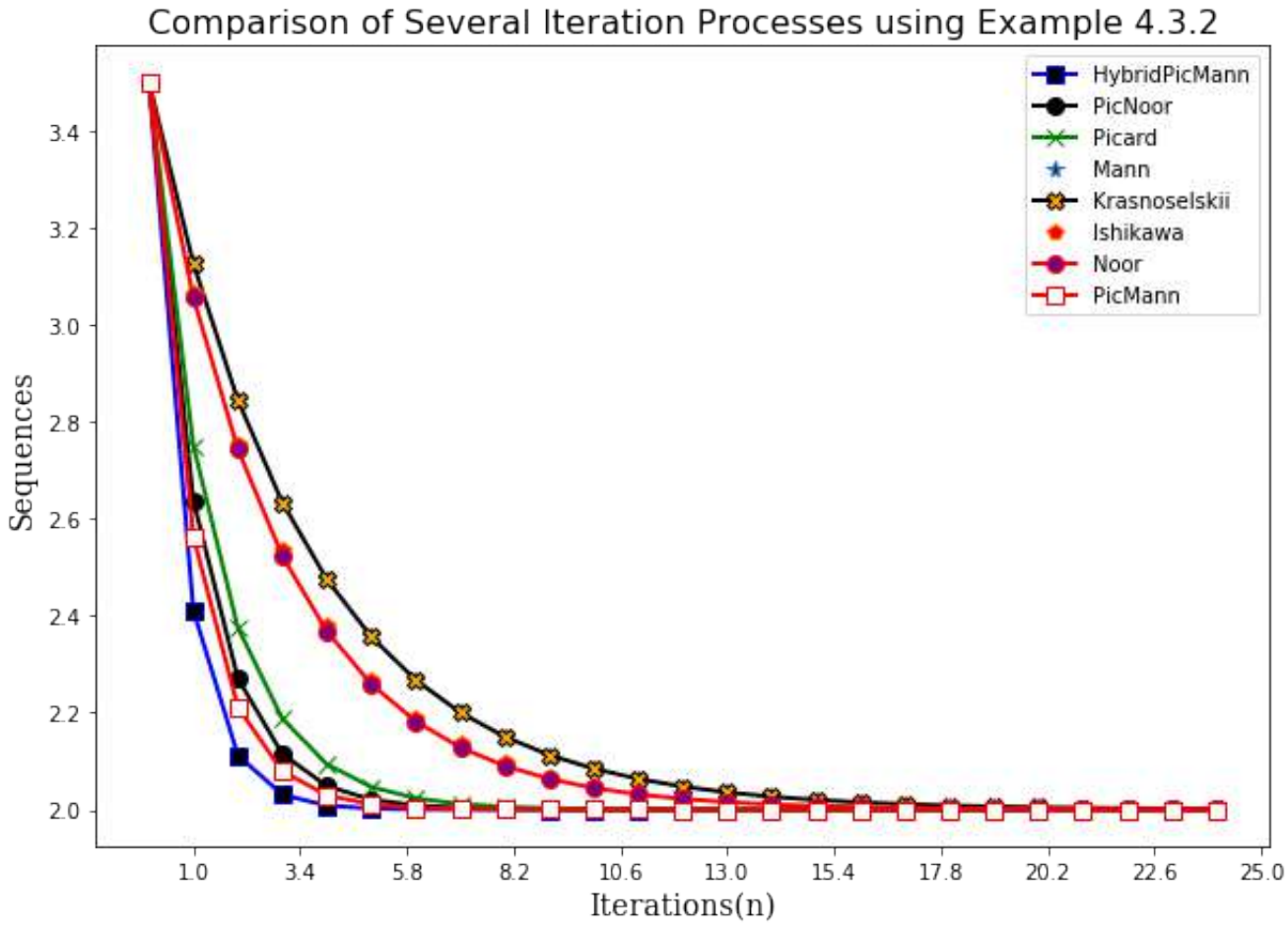


FIGURE 4.10. Graph corresponding to Table 4.10 and Table 4.11

Table 4.12: The numerical values of the sequences $\{u_n\}$, $\{w_n\}$, $\{x_n\}$ and $\{\omega_n\}$ with $\alpha_n = 0.5, \beta_n = 0.33, \gamma_n = 0.25, \lambda = 0.5 \in (0,1)$, initial value $\omega = 3.5 \in [1,10]$ and a "good" stopping criteria $\|\omega_n - \omega_{n+1}\| \leq 10^{-7}$.

n	HybridPicMann[n]	PicNoor[n]	Picard[n]	Mann[n]	Krasnoselskii[n]
0	3.5000000	3.5000000	3.5000000	3.5000000	3.5000000
1	3.0236702	3.0563637	3.0723168	3.2861584	3.2861584
2	3.0011338	3.0064632	3.0106756	3.1639834	3.1639834
3	3.0000543	3.0007426	3.0015807	3.0940416	3.0940416
4	3.0000026	3.0000853	3.0002342	3.0539547	3.0539547
5	3.0000001	3.0000098	3.0000347	3.0309634	3.0309634
6	3.0000000	3.0000011	3.0000051	3.0177718	3.0177718
7	3.0000000	3.0000001	3.0000008	3.0102012	3.0102012
8	3.0000000	3.0000000	3.0000001	3.0058558	3.0058558
9	3.0000000	3.0000000	3.0000000	3.0033616	3.0033616
10	3.0000000	3.0000000	3.0000000	3.0019297	3.0019297
11	3.0000000	3.0000000	3.0000000	3.0011078	3.0011078
12	3.0000000	3.0000000	3.0000000	3.0006360	3.0006360
13	3.0000000	3.0000000	3.0000000	3.0003651	3.0003651
14	3.0000000	3.0000000	3.0000000	3.0002096	3.0002096
15	3.0000000	3.0000000	3.0000000	3.0001203	3.0001203
16	3.0000000	3.0000000	3.0000000	3.0000691	3.0000691
17	3.0000000	3.0000000	3.0000000	3.0000397	3.0000397
18	3.0000000	3.0000000	3.0000000	3.0000228	3.0000228
19	3.0000000	3.0000000	3.0000000	3.0000131	3.0000131
20	3.0000000	3.0000000	3.0000000	3.0000075	3.0000075

21	3.0000000	3.0000000	3.0000000	3.0000043	3.0000043
22	3.0000000	3.0000000	3.0000000	3.0000025	3.0000025
23	3.0000000	3.0000000	3.0000000	3.0000014	3.0000014
24	3.0000000	3.0000000	3.0000000	3.0000008	3.0000008

Table 4.13: The numerical values of the sequences $\{u_n\}$, $\{w_n\}$, $\{x_n\}$ and $\{\omega_n\}$ with $\alpha_n = 0.5, \beta_n = 0.33, \gamma_n = 0.25, \lambda = 0.5 \in (0,1)$, initial value $\omega = 3.5 \in [1,10]$ and a "good" stopping criteria $\|\omega_n - \omega_{n+1}\| \leq 10^{-7}$.

n	Ishikawa[n]	Noor[n]	PicMann[n]
0	3.5000000	3.5000000	3.5000000
1	3.2761249	3.2757664	3.0418085
2	3.1526115	3.1522093	3.0035506
3	3.0843848	3.0840478	3.0003019
4	3.0466713	3.0464210	3.0000257
5	3.0258165	3.0256424	3.0000022
6	3.0142816	3.0141657	3.0000002
7	3.0079009	3.0078258	3.0000000
8	3.0043710	3.0043235	3.0000000
9	3.0024182	3.0023886	3.0000000
10	3.0013379	3.0013196	3.0000000
11	3.0007402	3.0007291	3.0000000
12	3.0004095	3.0004028	3.0000000
13	3.0002266	3.0002225	3.0000000
14	3.0001253	3.0001229	3.0000000
15	3.0000693	3.0000679	3.0000000
16	3.0000384	3.0000375	3.0000000
17	3.0000212	3.0000207	3.0000000
18	3.0000117	3.0000115	3.0000000
19	3.0000065	3.0000063	3.0000000
20	3.0000036	3.0000035	3.0000000
21	3.0000020	3.0000019	3.0000000
22	3.0000011	3.0000011	3.0000000
23	3.0000006	3.0000006	3.0000000
24	3.0000003	3.0000003	3.0000000

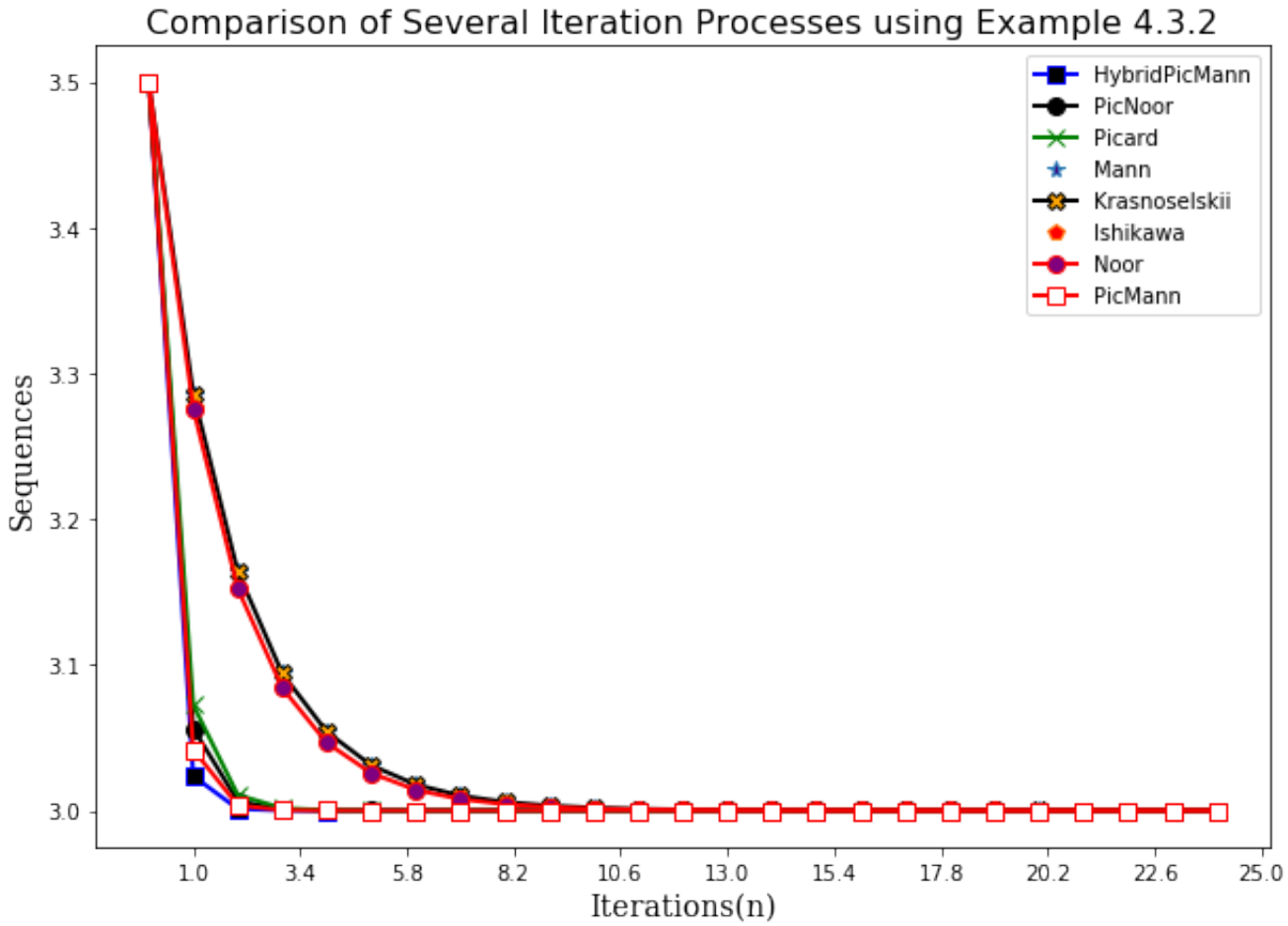


FIGURE 4.5. Graph corresponding to Table 4.12 and Table 4.13

5 Discussions and Conclusion

We introduced a new four-step iteration process called Picard-Mann hybrid iterative process. We proved that it converges to the unique fixed points of contractive mappings. We further showed with a good stopping criteria that the new scheme converges faster than several other listed and cited iteration processes with numerically performed examples using Python program. Our results showed numerical stability and data dependence. In view of the results proved in this work, it is evident that the Picard-Manns' hybrid iteration process is a generalization of the results of [9], [10], [11]-[22].

References

[1] Berinde, V. (2007). Iterative approximation of fixed points. Springer 1912.

[2] Zamfirescu, T.(1972). Fixed point theorems in metric spaces. Arch. Math. 23(1), 292–298.

[3] Browder, F.(1965). Nonexpansive nonlinear operators in a Banach space. Proc. Natl. Acad. Sci. U.S.A. 54(4), 1041–1044.

[4] Göhde, D.(1965). Zum Prinzip der kontraktiven Abbildung. Math. Nachr. 30(3–4), 251–258.

[5] Kirk, W. (1965). A fixed point theorem for mappings which do not increase distances. Am. Math. Mon. 72(9), 1004–1006.

[6] Okeke, G. A., Ofem, A. E. (2022). A novel iterative scheme for solving delay differential equations and nonlinear integral equations in Banach spaces. Math. Meth. Appl. Sci., 1–24.

[7] Berinde, V. (2004). On the convergence of the Ishikawa iteration in the class of quasi contractive operators. Acta Mathematica Universitatis Comenianae, 73(1), 119–126.

[8] Rhoades, B.,and Xue, Z. (2010). Comparison of the rate of convergence among Picard, Mann, Ishikawa, and Noor iterations applied to quasicontractive maps. Fixed Point Theory and Applications, 2010, 1–12.

[9] Picard, È. (1890). Memoire sur la theorie des equations aux derivees partielles et la methode des approximations successives. Journal de Mathématiques Pures et Appliquées, 6, 145–210.

[10] Krasnosel'skii, M. A. (1955). Two remarks on the method of successive approximations. Uspekhi matematicheskikh nauk, 10:1, 123–127.

[11] Mann, W. R. (1953). Mean value method in iteration. Proc. Amer. Math.Soc., 4, 506-510.

[12] Ishikawa, S. (1974). Fixed points by a new iteration method. Proceeding of the American Mathematical Society, 44:1, 147–150.

[13] Noor, M. A. (2000). New approximation scheme for general variational inequalities. Journal of Mathematical Analysis and Application, 251, 217–229.

[14] Khan, S. H. (2013). A Picard-Mann hybrid iterative process. Fixed Point Theory and Application, 2013, 69, doi:10.1186/1687-1812-2013-69.

[15] Berinde, V. (2002). Iterative Approximation of Fixed Points. Efemeride, Baia Mare.

[16] Thakur, B. S., Thakur, D., and Postolache, M. (2016). A new iterative scheme for numerical reckoning fixed points of Suzuki's generalized nonexpansive mappings. Applied Mathematics and Computation, 275, 147–155.

[17] Abbas, M., and Nazir, T. (2014). Some new faster iteration process applied to constrained minimization and feasibility problems. Matematicki Vesnik, 66:2, 223–234.

[18] Agarwal, R. P., O'Regan, D., and Sahu, D. R. (2007). Iterative construction of fixed points of nearly asymptotically nonexpansive mappings. J. Nonlinear Convex Anal., 8:1, 61–79.

[19] Okeke, G. A., & Abbas, M. (2017). A solution of delay differential equations via Picard–Krasnoselskii hybrid iterative process. Arabian Journal of Mathematics,6, 21–29.

[20] Okeke, G. A. (2019). Convergence analysis of the Picard–Ishikawa hybrid iterative process with applications. Afrika Matematika, 30, 817–835.

[21] Jia, J., Shabbir, K., Ahmad, K., Shah, N.A., and Botmart, T. (2022). Strong convergence of a new hybrid iterative scheme for nonexpansive mappings and application. Journal of Function Spaces, https://doi.org/10.1155/2022/4855173.

[22] Okeke, G. A., Anozie, E. H., Udo, A. V., and Olaoluwa, H. (2024). A novel fixed point iteration process applied in solving delay differential equations. Journal of the Nigerian Mathematical Society. 43(2), 115-143.

[23] Eke, K. and Akewe, H.(2019). Equivalence of Picard-type hybrid iterative algorithms for contractive mappings. Asian J. Sci. Res. 12(3), https://doi.org/10.3923/ajsr.2019.298.307.

[24] Phuengrattana, W., and Suantai, S.(2010). On the rate of convergence of Mann, Ishikawa, Noor and SP iterations for countinuous functions on an arbitrary interval. J. Comput. Appl. Math. 235(9), 3006–3014.

[25] Takahashi, W.(2000). Nonlinear Functional Analysis. Yokohama Publishers, Yokohama.

[26] Yu, T.M., Shahid, A., Shabbir, K., Shah, N., and Li, Y.M.(2021). An iteration process for a general class of contractive-like operators: convergence, stability and polynomiography. AIMS Mathematics 6(7), 6699–6714.

Stabilizers of Lojid algebras

E. Ilojide*

Abstract

In this paper, the notion of stabilizers are introduced and studied in lojid algebras. It is shown that to every lojid stabilizer, there is a corresponding lojid adjoint. The properties of stabilizers and their corresponding adjoints are investigated in some classes of lojid algebras.

Keywords and phrases: Lojid algebras; congruences; translations; stabilizers; adjoints

1 Introduction

An algebra of type (2, 0) is a non-empty set, having a constant element, on which is defined a binary operation such that certain axioms are satisfied. BCI algebras and BCK algebras, introduced in [1] and [2], are common varieties of such algebras. There are several other varieties of algebras of type (2, 0). There are also several generalizations of BCI algebras. In [3], BCH algebras were studied. In [4], d algebras were studied. In [5], the notion of BE algebras was introduced. Ideals and upper sets in BE algebras were investigated in [6] and [7]. Pre- commutative algebras were studied in [8]. Fenyves algebras were studied in [9], [10] and [11]. In [12], Q algebras were introduced. Homomorphisms of Q algebras were studied in [13].

Recently, it has been shown in [14] that algebras of type (2,0) have diverse applications in coding theory. Motivated by this, more research interest has been given to the study of algebras of type (2,0). Obic algebras were introduced in [15]. In [16], torian algebras were studied. It was shown that the class of torian algebras is a wider class than the class of obic algebras. Ideals of torian algebras were investigated in [17]. The dual and nuclei of ideals as well as congruences developed on ideals of torian algebras were studied. In [18], right distributive torian algebras were studied. Isomorphism Theorems of torian algebras were studied in [19]. In [20], lojid algebras were introduced. Properties of classes of lojid algebras were investigated Associates, commutants and regular maps were introduced and studied. Furthermore, congruences were introduced as a build up to the establishment of quotient lojid algebras.

In this paper, the notion of stabilizers are introduced and studied in lojid algebras. It is shown that to every lojid stabilizer, there is a corresponding lojid adjoint. The properties of stabilizers and their corresponding adjoints are investigated in some classes of lojid algebras.

2 Preliminaries

In this section, some basic concepts necessary for a proper understanding of this paper are discussed.

Definition 2.1. [20] An algebra $(X; *, 0)$ of type (2, 0) is called a semi-lojid algebra if $x * 0 = x$ for all $x \in X$.

Example 2.2. [20]. Let $X = \{0, 1, 2, 3\}$. Define a binary operation $*$ on X by the following table:

Then $(X; *, 0)$ is a semi-lojid algebra.

*Department of Mathematics, Federal University of Agriculture, Abeokuta, Nigeria; E-mail: ilojidee@funaab.edu.ng

$*$	0	1	2	3
0	0	2	3	1
1	1	0	2	2
2	2	3	0	3
3	3	1	1	0

Definition 2.3. [20]. Let a be an element of a semi-lojid algebra $(X; *, 0)$. The mapping $L_a : X \to X$ given by $L_a(x) = a * x$ for all $x \in X$, is called a left translation on $(X; *, 0)$.
Similarly, the mapping $R_a : X \to X$ given by $R_a(x) = x * a$ for all $x \in X$, is called a right translation on $(X; *, 0)$.

We shall write xL_a instead of $L_a(x)$ and xR_a instead of $R_a(x)$.

Definition 2.4. [20]. A semi-lojid algebra $(X; *, 0)$ is called a lojid algebra if all its left and right translations are bijections.

Example 2.5. [20]. Let $X = \{0, 1, 2, 3, 4\}$. Define a binary operation $*$ on X by the following table:

$*$	0	1	2	3	4
0	0	1	3	4	2
1	1	0	4	2	3
2	2	4	1	3	0
3	3	2	0	1	4
4	4	3	2	0	1

Then $(X; *, 0)$ is a lojid algebra.

Example 2.6. [20]. Let $X = \{0, 1, 2, 3\}$. Define a binary operation $*$ on X by the following table:

$*$	0	1	2	3
0	0	1	2	3
1	1	0	3	2
2	2	3	0	1
3	3	2	1	0

Then $(X; *, 0)$ is a lojid algebra.

We shall write X for a lojid algebra $(X; *, 0)$ unless there is the need to emphasize the binary operation and the constant element of $(X; *, 0)$.

Definition 2.7. [20]. A lojid algebra X is said to be completely lojid if $xR_x = 0$ for all $x \in X$.

Example 2.8. [20]. The algebra in Example 2.3. is a completely lojid algebra.

Definition 2.9. [20]. Let $(X; *, 0)$ be a lojid algebra. A non-empty subset S of X is called a sub-lojid algebra (or simply a sub-algebra) of $(X; *, 0)$ if $(S; *, 0)$ is a lojid algebra.

3 Stabilizers and Adjoints

In this section, we present the notions of stabilizers in lojid algebras. By introducing a new binary operation in lojid algebras, we study adjoints of stabilizers.

Definition 3.1. A self map f on a lojid algebra is said to be regular if $f(0) = 0$.

Definition 3.2. A self map f on a lojid algebra $(X; *, 0)$ is called a stabilizer if $f(x * y) = f(x) * f(y)$ for all $x, y \in X$.

Proposition 3.3. *Every stabilizer on a completely lojid algebra is regular.*

Proof. The proof is straightforward.

Definition 3.4. Let $(X; *, 0)$ be a lojid algebra. Define a binary operation $\odot$ on X by $x \odot y = y*(y*x)$ for all $x, y \in X$.

Definition 3.5. Let f be a stabilizer on a lojid algebra $(X; *, 0)$. A map $g : X \to X$ is called a right adjoint of f if $g(x * y) = (g(x) * f(y)) \odot (f(x) * g(y))$ for all $x, y \in X$.
If $g(x * y) = (f(x) * g(y)) \odot (g(x) * f(y))$ for all $x, y \in X$, then g is called a left adjoint of f
If g is both a right adjoint and a left adjoint of f, then g is called an adjoint of f.

Example 3.6. Let N^* be the set of non-negative integers. Define a binary operation $*$ on N^* by

$$x * y = \begin{cases} 0, & x \leq y \\ x - y, & x > y \end{cases}$$

Then $(N^*; *, 0)$ is a lojid algebra. Define the self map f on N^* by $f(x) = 7x$ for all $x \in N^*$. Then f is a stabilizer on N^*. The self map g on N^* defined by $g(x) = 0$ for all $x \in N^*$ is an adjoint of f.

Definition 3.7. A lojid algebra X is said to be prime if $0R_x = 0$ for all $x \in X$.

Definition 3.8. A lojid algebra X is said to be composite if $0R_x = x$ for all $x \in X$.

Definition 3.9. A self map f on a lojid algebra X is called a module if $f(x) = 0$ for all $x \in X$.

Proposition 3.10. *Let f be a stabilizer on a completely lojid algebra $(X; *, 0)$, and let g be a regular right adjoint of f. Then $(f(x) * g(x)) * ((f(x) * g(x)) * (g(x) * f(x))) = (f(y) * g(y)) * ((f(y) * g(y)) * (g(y) * f(y)))$ for all $x, y \in X$.*

Proof. Notice that $0 = g(0) = g(x * x) = (g(x) * f(x)) \odot (f(x) * g(x)) = (f(x) * g(x)) * ((f(x) * g(x)) * (g(x) * f(x)))$. So, $(f(x) * g(x)) * ((f(x) * g(x)) * (g(x) * f(x))) = 0$
Now, replacing x with y in the last expression, we have $(f(y)*g(y))*((f(y)*g(y))*(g(y)*f(y))) = 0$.
Hence, the conclusion follows.

Corollary 3.11. *Let f be a stabilizer on a completely lojid algebra $(X; *, 0)$, and let g be a regular right adjoint of f.*

1. *If f is a module, then $(0 * g(x)) * ((0 * g(x)) * g(x)) = (0 * g(y)) * ((0 * g(y)) * g(y))$ for all $x, y \in X$.*
2. *If g is a module, then $f(x) * (f(x) * (0 * f(x) = f(y) * (f(y) * (0 * f(y)$ for all $x, y \in X$.*

Proof.

1. Since f is a module, then expression $(f(x) * g(x)) * ((f(x) * g(x)) * (g(x) * f(x))) = (f(y) * g(y)) * ((f(y) * g(y)) * (g(y) * f(y)))$ in Proposition 3.10 becomes $(0*g(x))*((0*g(x))*g(x)) = (0 * g(y)) * ((0 * g(y)) * g(y))$ for all $x, y \in X$ as required.

2. Since g is a module, then expression $(f(x) * g(x)) * ((f(x) * g(x)) * (g(x) * f(x))) = (f(y) * g(y)) * ((f(y) * g(y)) * (g(y) * f(y)))$ in Proposition 3.10 becomes $f(x) * (f(x) * (0 * f(x) = f(y) * (f(y) * (0 * f(y)$ for all $x, y \in X$ as required.

Proposition 3.12. *Let f be a stabilizer on a lojid algebra X, and let g be a right adjoint of f. Then the following hold for all $x, y \in X$:*

1. $(f(0) * g(x)) * ((f(0) * g(x)) * (g(0) * f(x))) = g(0 * x)$
2. *If X is prime, then* $(f(0) * g(x)) * ((f(0) * g(x)) * (g(0) * f(x))) = g(0)$
3. *If f is regular, then* $(0 * g(x)) * ((0 * g(x)) * g(0) * f(x))) = g(0 * x)$
4. *If X is prime and f is regular, then g is regular*
5. *If g is regular, then* $((f(0) * g(x)) * ((f(0) * g(x)) * (0 * f(x))) = g(0 * x)$
6. *If X is composite, then* $((f(0) * g(x)) * ((f(0) * g(x)) * (g(0) * f(x))) = g(x)$
7. *If X is composite and f is regular, then* $g(x) * (g(x) * (g(0) * f(x))) = g(x)$
8. *If f is composite and g is regular, then* $((f(0) * g(x)) * ((f(0) * g(x)) * f(x)) = g(x)$
9. *If f is a module, then* $(0 * g(x)) * ((0 * g(x)) * g(0) = g(0 * x)$
10. *If g is a module, then* $f(0) * (f(0) * (0 * f(x))) = 0$
11. *If g is a module, then* $f(0) * (f(0) * (0 * f(x))) = f(0) * (f(0) * (0 * f(y)))$

Proof.

1. Notice that $g(0*x) = (g(0)*f(x)) \odot (f(0)*g(x)) = (f(0)*g(x))*((f(0)*g(x))*(g(0)*f(x)))$ as required.
2. Apply 'primeness' to (1)
3. Apply regularity of f in (2)
4. Combine (2) and (3)
5. Apply regularity of g to (1)
6. Apply 'compositeness' of X to (1)
7. Apply regularity of f to (6)
8. Apply regularity of g to (6)
9. Apply 'moduleness' to f in (1)
10. Apply 'moduleness' to g in (1)
11. Follows from (10) after replacing x with y

Corollary 3.13. *Let f be a stabilizer on a completely lojid algebra X, and let g be a right adjoint of f. Then the following hold for all $x, y \in X$:*

1. $(0 * g(x)) * ((0 * g(x)) * (g(0) * f(x))) = g(0 * x)$
2. *If X is prime, then g is regular*
3. *If X is composite, then* $g(x) * (g(x) * (g(0) * f(x))) = g(x)$

4. *If g is a module, then* $0 * (0 * (0 * f(x))) = 0$
5. *if g is a module, then* $0 * (0 * (0 * f(x))) = 0 * (0 * (0 * f(y)))$

Proof.

1. Follows from Proposition 3.3 and Proposition 3.12(1).
2. Follows from Proposition 3.3 and Proposition 3.12(4).
3. Follows from Proposition 3.3 and Proposition 3.12(7).
4. Follows from Proposition 3.3 and Proposition 3.12(10).
5. Follows from (4) after replacing x with y.

Proposition 3.14. *Let f be a stabilizer on a completely lojid algebra $(X; *, 0)$, and let g be a regular right adjoint on f. If f is a module, then the following hold for all $x, y \in X$:*

1. $((0 * g(x)) * ((0 * g(x)) * g(x)) = 0$
2. $((0 * g(x)) * ((0 * g(x)) * g(x)) = ((0 * g(y)) * ((0 * g(y)) * g(y))$
3. $g(0 * x) = 0$
4. $g(0 * x) = g(0 * y)$
5. $((0 * g(x)) * ((0 * g(x)) * g(x)) = g(0 * x)$

Proof.

1. Notice that $0 = g(0) = g(x * x) = (g(x) * f(x)) \odot (f(x) * g(x)) = ((0 * g(x)) * ((0 * g(x)) * g(x))$ as required.
2. This follows from (1) after replacing x with y
3. Notice that $g(0 * x) = (g(0) * f(x)) \odot (f(0) * g(x)) = 0$
4. This follows from (3) after replacing x with y
5. This follows from (1) and (3)

Proposition 3.15. *Let f be a stabilizer on a completely lojid algebra X, and let g be a regular left adjoint of f. Then $(g(x) * f(x)) * ((g(x) * f(x)) * (f(x) * g(x))) = (g(y) * f(y)) * ((g(y) * f(y)) * (f(y) * g(y)))$ for all $x, y \in X$.*

Proof. Notice that $0 = g(0) = g(x * x) = (f(x) * g(x)) \odot (g(x) * f(x)) = (g(x) * f(x)) * ((g(x) * f(x)) * (f(x) * g(x)))$. By replacing x with y, the conclusion follows.

Corollary 3.16. *Let f be a stabilizer on a completely lojid algebra X, and let g be a regular left adjoint of f. Then the following hold for all $x, y \in X$:*

1. *If f is a module, then* $g(x) * (g(x) * (0 * g(x))) = g(y) * (g(y) * (0 * g(y)))$
2. *If g is a module, then* $(0 * f(x)) * ((0 * f(x)) * f(x)) = (0 * f(y)) * ((0 * f(y)) * f(y))$

Proposition 3.17. *Let f be a stabilizer on a completely lojid algebra X, and let g be a left adjoint of f. Then the following hold for all $x, y \in X$:*

1. $(g(0) * f(x)) * ((g(0) * f(x)) * (f(0) * g(x))) = g(0 * x)$
2. *If X is prime, then* $(g(0) * f(x)) * ((g(0) * f(x)) * (f(0) * g(x))) = g(0)$

3. *If f is regular, then* $(g(0) * f(x)) * ((g(0) * f(x)) * (0 * g(x))) = g(0 * x)$
4. *If X is prime and f is regular, then g is regular*
5. *If g is regular, then* $(0 * f(x)) * ((0 * f(x)) * (f(0) * g(x))) = g(0 * x)$
6. *If X is composite, then* $(g(0) * f(x)) * ((g(0) * f(x)) * (f(0) * g(x))) = g(x)$
7. *If X is composite and f is regular, then* $(g(0) * f(x)) * ((g(0) * f(x)) * g(x)) = g(x)$
8. *If X is composite and g is regular, then* $f(x) * (f(x) * (f(0) * g(x))) = g(x)$
9. *If f is a module, then* $g(0) * (g(0) * (0 * g(x))) = g(0 * x)$
10. *if g is a module, then* $(0 * f(x)) * ((0 * f(x)) * f(0)) = 0$
11. *If g is a module, then* $(0 * f(y)) * ((0 * f(y)) * f(0))$

Proof.

1. Notice that $g(0*x) = (f(0)*g(x)) \odot (g(0)*f(x)) = (g(0)*f(x))*((g(0)*f(x))*(f(0)*g(x)))$ as required.
2. Apply 'primeness' of X to (1)
3. Apply regularity to f in (1)
4. Follows from (ii) and (3)
5. Apply regularity of g to (1)
6. Apply 'compositeness' of X to (1)
7. Apply regularity of f to (6)
8. Apply regularity of g to (6)
9. Apply 'moduleness' of f to (1)
10. Apply 'moduleness' of g to (1)
11. Follows from (10) after replacing x with y

Corollary 3.18. *Let f be a stabilizer on a completely lojid algebra X, and let g be a left adjoint of f. Then the following hold for all $x, y \in X$:*

1. $(g(0) * f(x)) * ((g(0) * f(x)) * (0 * g(x))) = g(0 * x)$
2. *If X is prime, then g is regular*
3. *If X is composite, then* $(g(0) * f(x)) * ((g(0) * f(x)) * g(x)) = g(x)$

Proof.

1. Follows from Proposition 3.3 and Proposition 3.17(1).
2. Follows from Proposition 3.3 and Proposition 3.17(4).
3. Follows from Proposition 3.3 and Proposition 3.17(6).

Proposition 3.19. *Let f be a stabilizer on a completely lojid algebra X, and let g be a regular left adjoint of f. If f is a module, then the following hold for all $x, y \in X$:*

1. $g(x) * (g(x) * (0 * g(x))) = 0$
2. $g(x) * (g(x) * (0 * g(x))) = g(y) * (g(y) * (0 * g(y)))$
3. $g(0 * x) = 0 * (0 * (0 * g(x)))$

Proof.

1. Notice that $0 = g(0) = g(x * x) = g(x) * (g(x) * (0 * g(x)))$ as required.
2. Follows from (1) after replacing x with y
3. Notice that $g(0 * x) = (f(0) * g(x)) \odot (g(0) * f(x)) = 0 * (0 * (0 * g(x)))$ as required.

By Proposition 3.10 and Proposition 3.15, we have have the following Theorem:

Theorem 3.20. *Let f be a stabilizer on a completely lojid algebra $(X; *, 0)$, and let g be a regular adjoint of f. Then the following hold for all $x, y \in X$:*

1. $(f(x) * g(x)) * ((f(x) * g(x)) * (g(x) * f(x))) = (f(y) * g(y)) * ((f(y) * g(y)) * (g(y) * f(y)))$
2. $(g(x) * f(x)) * ((g(x) * f(x)) * (f(x) * g(x))) = (g(y) * f(y)) * ((g(y) * f(y)) * (f(y) * g(y)))$

Proof.

1. Notice that $0 = g(0) = g(x * x) = (g(x) * f(x)) \odot (f(x) * g(x)) = (f(x) * g(x)) * ((f(x) * g(x)) * (g(x) * f(x)))$. So, $(f(x) * g(x)) * ((f(x) * g(x)) * (g(x) * f(x))) = 0$
   Now, replacing x with y in the last expression, we have $(f(y) * g(y)) * ((f(y) * g(y)) * (g(y) * f(y))) = 0$. Hence, the conclusion follows.
2. Notice that $0 = g(0) = g(x * x) = (f(x) * g(x)) \odot (g(x) * f(x)) = (g(x) * f(x)) * ((g(x) * f(x)) * (f(x) * g(x)))$. By replacing x with y, the conclusion follows.

By Corollary 3.11 and Corollary 3.16, we have the following Corollary:

Corollary 3.21. *Let f be a stabilizer on a completely lojid algebra $(X; *, 0)$, and let g be a regular adjoint of f. Then the following hold for all $x; y \in X$:*

1. *If f is a module, then* $(0 * g(x)) * ((0 * g(x) * g(x)) = (0 * g(y)) * ((0 * g(y)) * g(y)))$ *and* $g(x) * (g(x) * (0 * g(x))) = g(y) * (g(y) * (0 * g(y)))$
2. *If g is a module, then* $f(x) * (f(x) * (0 * f(x))) = f(y) * (f(y) * (0 * f(y)))$ *and* $(0 * f(x)) * ((0 * f(x)) * f(x)) = (0 * f(y)) * ((0 * f(y)) * f(y))$

By Proposition 3.12 and Proposition 3.17, we have the following Theorem:

Theorem 3.22. *Let f be a stabilizer on a lojid algebra $(X; *, 0)$, and let g be an adjoint of f. Then the following hold for all $x, y \in X$:*

1. $(f(0) * g(x)) * ((f(0) * g(x)) * (g(0) * f(x))) = (g(0) * f(x)) * ((g(0) * f(x)) * (f(0) * g(x)))$
2. *If X is prime, then* $(f(0) * g(x)) * ((f(0) * g(x)) * (g(0) * f(x))) = (g(0) * f(x)) * ((g(0) * f(x)) * (f(0) * g(x)))$
3. *If f is regular, then* $(0 * g(x)) * ((0 * g(x)) * (g(0) * f(x))) = (g(0) * f(x)) * ((g(0) * f(x)) * (0 * g(x)))$
4. *If X is prime and f is regular, then g is regular.*
5. *If g is regular, then* $((f(0) * g(x)) * ((f(0) * g(x)) * (0 * f(x))) = (0 * f(x)) * ((0 * f(x)) * (f(0) * g(x)))$

6. *If X is composite, then* $((f(0)*g(x))*((f(0)*g(x))*(g(0)*f(x)))=(g(0)*f(x))*((g(0)*f(x))*((f(0)*g(x))))$
7. *If X is composite and f is regular, then* $g(x)*(g(x)*(g(0)*f(x)))=(g(0)*f(x))*((g(0)*f(x))*g(x))$
8. *If X is composite and g is regular, then* $((f(0)*g(x))*((f(0)*g(x))*f(x))=f(x)*(f(x)*(f(0)*g(x)))$
9. *If f is a module, then* $(0*g(x))*((0*g(x))*g(0))=g(0)*(g(0)*(0*g(x)))$
10. *If g is a module, then* $f(0)*(f(0)*(0*f(x)))=(0*f(x))*((0*f(x))*f(0))$
11. *If g is a module, then* $f(0)*(f(0)*(0*f(x)))=f(0)*(f(0)*(0*f(y)))$ *and* $(0*f(x))*((0*f(x))*f(0)=(0*f(y))*((0*f(y))*f(0))$

Proof.

1. Since g is an adjoint of f, then by Proposition 3.12 and Proposition 3.17, we have $(f(0)*g(x))*((f(0)*g(x))*(g(0)*f(x)))=(g(0)*f(x))*((g(0)*f(x))*(f(0)*g(x)))$ as required.
2. Since X is prime, then by Proposition 3.12 and Proposition 3.17, we have $(f(0)*g(x))*((f(0)*g(x))*(g(0)*f(x)))=(g(0)*f(x))*((g(0)*f(x))*(f(0)*g(x)))$ as required.
3. Since f is regular, then by Proposition 3.12 and Proposition 3.17, we have $(0*g(x))*((0*g(x))*(g(0)*f(x)))=(g(0)*f(x))*((g(0)*f(x))*(0*g(x)))$ as required.
4. Since X is prime and f is regular, then by Proposition 3.12 and Proposition 3.17, g is regular as required.
5. Since g is regular, then by Proposition 3.12 and Proposition 3.17, we have $((f(0)*g(x))*((f(0)*g(x))*(0*f(x)))=(0*f(x))*((0*f(x))*(f(0)*g(x)))$ as required.
6. Since X is composite, then by Proposition 3.12 and Proposition 3.17, we have $((f(0)*g(x))*((f(0)*g(x))*(g(0)*f(x)))=(g(0)*f(x))*((g(0)*f(x))*((f(0)*g(x))))$ as required.
7. Since X is composite and f is regular, then by Proposition 3.12 and Proposition 3.17, we have $g(x)*(g(x)*(g(0)*f(x)))=(g(0)*f(x))*((g(0)*f(x))*g(x))$ as required.
8. Since X is composite and g is regular, then by Proposition 3.12 and Proposition 3.17, we have $((f(0)*g(x))*((f(0)*g(x))*f(x))=f(x)*(f(x)*(f(0)*g(x)))$ as required.
9. Since f is a module, then by Proposition 3.12 and Proposition 3.17, we have $(0*g(x))*((0*g(x))*g(0))=g(0)*(g(0)*(0*g(x)))$ as required.
10. Since g is a module, then by Proposition 3.12 and Proposition 3.17, we have $f(0)*(f(0)*(0*f(x)))=(0*f(x))*((0*f(x))*f(0))$ as required.
11. Since g is a module, then by Proposition 3.12 and Proposition 3.17, we have $f(0)*(f(0)*(0*f(x)))=f(0)*(f(0)*(0*f(y)))$ and $(0*f(x))*((0*f(x))*f(0)=(0*f(y))*((0*f(y))*f(0))$ as required.

By Corollary 3.13 and Corollary 3.18, we have the following Corollary:

Corollary 3.23. *Let f be a stabilizer on a completely lojid algebra $(X;*,0)$, and let g be an adjoint of f. Then the following hold for all $x,y\in X$:*

1. $(0*g(x))*((0*g(x))*(g(0)*f(x)))=(g(0)*f(x))*((g(0)*f(x))*(0*g(x)))$
2. *If X is prime, then g is regular.*
3. *If X is composite, then* $g(x)*(g(x)*(g(0)*f(x)))=(g(0)*f(x))*((g(0)*f(x))*g(x))$

By Proposition 3.14 and Proposition 3.19, we have the following Theorem:

Theorem 3.24. *Let f be a stabilizer on a completely lojid algebra $(X; *, 0)$, and let g be an adjoint of f. Then the following hold for all $x, y \in X$:*

1. $((0 * g(x)) * ((0 * g(x)) * g(x)) = g(x) * (g(x) * (0 * g(x)))$
2. $(0 * g(x)) * ((0 * g(x)) * g(x)) = (0 * g(y)) * ((0 * g(y)) * g(y))$ *and* $g(x) * (g(x) * (0 * g(x))) = g(y) * (g(y) * (0 * g(y)))$
3. $0 * (0 * (0 * g(x))) = 0$

References

[1] K. Iseki (1996). An Algebra Related with Propositional calculus, Proc. Japan Acad., 42, 26–29.

[2] Y. Imai and K. Iseki (1996). On Axiom System of Propositional Calculi, Proc. Japan Acad., 42, 19–22.

[3] Q. P. Hu and X. Li (1983). On BCH algebras, Math. Seminar Notes II, 313–320.

[4] J. Neggers and H. S. Kim (1999). On d-algebras, Mathematica Slovaca, 49, 19–26.

[5] H. S. Kim and Y. H. Kim (2007). On BE-algebras, Sci. Math. Jpn. 66,113–116.

[6] S.S. Ahn and K. S. So (2008). On ideals and upper sets in BE-algebras, Sci. Math. Jpn. 68, 351–357.

[7] S.S. Ahn and K.S. So (2009). On Generalized upper sets in BE-algebras, Bull. Korean Math. Soc. 46, 281–287.

[8] H.S. Kim, J. Neggers and S.S. Ahn (2019). On Pre-Commutative Algebras, Mathematics, 7(2019), 336. doi:10.33390/math7040336.

[9] T.G. Jaiyeola, E. Ilojide, M.O. Olatinwo and F.S. Smarandache (2018). On the Classification of Bol- Moufang Type of Some Varieties of Quasi Neutrosophic Triplet Loops (Fenyves BCI-algebras), Symmetry 10, 427. https://doi.org/10.3390/sym10100427.

[10] E. Ilojide, T.G. Jaiyeola and M.O. Olatinwo (2019). On Holomorphy of Fenyves BCI-algebras, Journal of the Nigerian Mathematical Society, 38(2), 139–155.

[11] T.G. Jaiyeola, E. Ilojide, A.J. Saka and K.G. Ilori (2020). On the isotopy of some varieties of Fenyves Quasi Neutrosophic triplet loops(Fenyves BCI-algebras), Neutrosophic Sets and Systems, 31, 200–223. DOI: 105281/zenodo.3640219.

[12] J. Neggers, S.A. Sun and S.K. Hee (2001). On Q-algebras, International J. of Math. and Math. Sci. 27, 749–757.

[13] E. Ilojide (2021). Homomorphisms of Q algebras, Analele Universitatii din Oradea Fascicola Matematica, 28(2), 5–13.

[14] M. Ebrahimi and A. Izadara (2019). The ideal entropy of BCI- algebras and its application in binary linear codes, Soft Computing,23, 39–57.

[15] E. Ilojide (2019). On Obic Algebras, International Journal of Mathematical Combinatorics, 4, 80–88.

[16] E. Ilojide (2020). A note on Torian Algebras, International Journal of Mathematical Combinatorics, 2, 80–87.

[17] E. Ilojide (2020). On ideals of Torian Algebras, International Journal of Mathematical Combinatorics, 2, 101–108.

[18] E. Ilojide (2020). On right distributive Torian Algebras, International Journal of Mathematical Combinatorics ,4, 100–107.

[19] E. Ilojide (2021). On Isomorphism Theorems of Torian Algebras, International Journal of Mathematical Combinatorics, 1, 56–61.

[20] E. Ilojide (2024). On Lojid Algebras, International Journal of Mathematical Analysis and Modelling, 7(2), 369–379.

[21] J. Neggers, S.A. Sun and S.K. Hee (2001). On Q-algebras, International Journal of Mathematics and Mathematical Sciences, 27, 749–757.

Algorithm for approximating common fixed points of family of strictly pseudo-contractive mappings in Hilbert spaces

E. Ekuma-Okereke*†, J.O. Ogbodu†‡, C.V. Okpako§, and O.D. Koko¶

Abstract

It is our purpose in this paper to construct and study a Halpern-type algorithm with inertial and error terms for approximating common fixed points of strictly pseudo-contractive mappings in the framework of real Hilbert spaces. We prove strong convergence theorem for the sequence generated by the algorithm under certain mild conditions on the control sequences. Numerical examples are given to illustrate the effectiveness of this algorithm. Our result is intended to complement and extend some well known results in the literature.

Keywords and phrases: Common fixed points; strictly pseudo-contractive mappings; Halpern-type algorithm; inertial and error terms; strong convergence theorem

1 Introduction

Let H be a real Hilbert space. Let $T_i : H \to H, i = 1, 2, ..., \mathbb{N}$ be any mapping for each i defined on H. Let $\cap_{i=1}^{N} Fix(T_i)$ represent finite intersection of a non-empty, closed and convex family of mappings which is a subset of H, where

$$Fix(T_i) := \{x \in H : x = T_i(x), \text{ for each } i \geq 1\}, \tag{1}$$

is the fixed point set of a family of mappings and $\mathbb{N}$ is the set of all natural numbers. Let $P_{\cap_{i=1}^{N} Fix(T_i)}(x)$ denote a metric projection of H onto $\cap_{i=1}^{N} Fix(T_i)$ defined by

$$\|x - P_{\cap_{i=1}^{N} Fix(T_i)}(x)\| = \inf\{\|x - z\| : z \in \cap_{i=1}^{N} Fix(T_i)\}, \forall \tag{2}$$

and the metric projection holds true if and only if it satisfies the variational inequality

$$\langle x - P_{\cap_{i=1}^{N} Fix(T_i)}(x), z - P_{\cap_{i=1}^{N} Fix(T_i)}(x)\rangle \leq 0. \tag{3}$$

Using this characterization, we get that a metric projection $P_{\cap_{i=1}^{N} Fix(T_i)}(x)$ is nonexpansive, that is $\|P_{\cap_{i=1}^{N} Fix(T_i)}(x) - P_{\cap_{i=1}^{N} Fix(T_i)}(y)\|^2 \leq \|x - y\|^2, \forall x, y \in H$.

A mapping $T : H \to H$ is called

(a) Lipschitzian if there exists $L \geq 0$ such that

$$\|Tx - Ty\|^2 \leq L\|x - y\|^2, \forall x, y \in H, \tag{4}$$

*Corresponding Author; E-mail: ekuma.okereke@fupre.edu.ng, enyiekumaokereke@gmail.com

†Department of Mathematics, Federal University of Petroleum Resources, Effurun, Nigeria

‡E-mail: ogbodujoseph1987@gmail.com

§Department of Mathematics, Federal University of Petroleum Resources, Effurun, Nigeria; E-mail: mcvotu@gmail.com

¶Department of Mathematics, Federal University of Petroleum Resources, Effurun, Nigeria; E-mail:kokodogheneovo@gmail.com

(b) quasi nonexpansive if

$$\|Tx - p\|^2 \leq \|x - p\|^2, \forall x \in H, p \in Fix(T). \tag{5}$$

(c) strictly pseudocontractive [1] if there exists a constant $k \in [0, 1)$ such that

$$\|Tx - Ty\|^2 \leq \|x - y\|^2 + k\|(x - y) - (Tx - Ty)\|^2, \forall x, y \in H. \tag{6}$$

or equivalently, if there exists a constant $\lambda > 0$ such that

$$\langle x - y, Tx - Ty\rangle \leq \|x - y\|^2 - \lambda\|(x - y) - (Tx - Ty)\|^2, \forall x, y \in H. \tag{7}$$

(d) demicontraction (or k-demicontractive) (see [2]) if there exists a constant $k \in [0, 1)$ and $Fix(T) \neq \emptyset$ such that

$$\|Tx - Tp\|^2 \leq \|x - p\|^2 + k\|x - Tx\|^2, \forall x \in H, p \in Fix(T). \tag{8}$$

The mapping T is called a contraction if $0 \leq L < 1$. It is called nonexpansive if $L = 1$. It is demiclosed at a point $p \in Fix(T)$ if $Fix(T)$ contains a sequence $\{x_n\}_{n=1}^{\infty}$ which converges weakly to $\bar{x} \in Fix(T)(x_n \rightharpoonup \bar{x})$ and Tx_n converges strongly to p $(Tx_n \to p)$ and $T\bar{x} = p$.

Many authors have proposed and studied different iterative schemes for the approximation of fixed points of contractive, nonexpansive and pseudo-contractive mappings in Hilbert space, (see for example, [2], [3], [4]).

If given contraction mapping (i.e) $T : H \to H$, and if there exists a constant $L \in [0, 1)$ such that

$$d(Tx, Ty) \leq L.d(x, y), \text{ for all } x, y \in H, \tag{9}$$

then T has a unique fixed point $p \in H$ and the n^{th} iterate of x under T, (i.e) the Picard iteration (see [5])for some $x_0 \in H$, the sequence $\{x_n\}$ given by

$$x_n = T^n(x_0), n \geq 1, \tag{10}$$

converges to the fixed point p as $n \to \infty$ and for each $x \in H$. However, we observed that if the mapping T is not a (strict) contraction, that is, if there is no $L \in [0, 1)$, then the Picard's iterative technique fails to converge to its fixed point. Hence the need for more consideration of some other iterative techniques. In the literature, some authors have considered mappings with compactness conditions to guarantee strong convergence since strong convergence has advantage over weak convergence.

In the iterative approximation of fixed points of nonexpansive maps and strictly pseudocontractive mappings, the iterative schemes of Mann [6]:

$$x_{n+1} = (1 - \alpha_n)x_n + \alpha_n Tx_n, n \geq 0, \tag{11}$$

where $\{\alpha_n\} \subset [0, 1]$. and Ishikawa [7]:

$$x_{n+1} = (1 - \alpha_n)x_n + \alpha_n Tx_n \left[(1 - \beta_n)x_n + \beta_n Tx_n\right], n \geq 0, \tag{12}$$

where $\{\alpha_n\}, \{\beta_n\} \subset$ are suitable control sequences in $[0, 1]$, play an important role. However, the two iteration schemes yield weak convergence only, and require the "compactness" assumption either on the mappings or the domain of the mappings or even both to yield the desired strong convergence. Often strong conditions are needed to impose on the fixed point point set, $Fix(T)$, to obtain the strong convergence by using Mann or the Ishikawa iteration process. For example, Qilhou in [8] required that $Fix(T)$ is finite where T is a continuous pseudocontractive-type self-mapping of a nonempty convex compact of a Hilbert space and in [9] required that the interior of $Fix(T)$ is nonempty. Recently many new algorithms have been constructed and studied to achieve strong convergence with mild assumptions on the mappings, their ambient domain, their fixed point sets and other necessary components, see ([2],

[10]). Meanwhile, the Halpern ([11]), iterative method generated by $\{x_n\}$ and for $x_0 \in H$ is defined recursively by

$$x_{n+1} = \alpha_n x_0 + (1-\alpha_n)Tx_n, n \geq 0. \tag{13}$$

where $\alpha_n = 0$ satisfies certain necessary conditions to guarantee strong convergence of the sequence generated by (13).

Several authors have studied nonexpansive mapping and pseudocontractive mappings and proposed different iterative methods to approximate the fixed points of their mappings in Hilbert spaces but without the inertial and error terms (see for example [12], [13], [21], [15], [16], [17]). To be sure, the study of fixed point of nonexpansive mappings and its generalization is important in many areas of Mathematical applications (see for example [4]). Besides, there have been a growing interest among authors to speed up the rate of convergence of algorithms. The inertial method introduced by Polyak (see [10], [18], [19]) is one of the methods for speeding up the convergence rates. This method was firstly introduced by Polyak in 1964 as acceleration process which solves a smooth convex minimization problem (see [?]). It is a two-step iterative technique in which the next iterate is defined recursively with the use of the previous two iterates as follows: initialize $x_{-1}, x_0 \in X$ and let $\{x_n\}$ be generated by

$$x_{n+1} = x_n - \alpha P(x_n) + \beta(x_n - x_{n-1}), n \geq 0, \tag{14}$$

where P is an operator usually linear defined on a Banach space X, and $\alpha, \beta \in (0,1)$. It is easy to observe that when $P \equiv 0$, then (14) reduces to

$$x_{n+1} = x_n + \beta(x_n - x_{n-1}), n \geq 0, \tag{15}$$

Recently, [4], studied fixed point of nonexpansive mappings using the following algorithm:

$$\begin{cases} z_n = x_n + \tau_n(x_n - x_{n-1}), \\ x_{n+1} = \alpha_n x_0 + \beta_n y_n + \eta_n T y_n + e_n, n \geq 1, \end{cases} \tag{16}$$

where $\{\alpha_n\}_{n=1}^{\infty}, \{\beta_n\}_{n=1}^{\infty}, \{\eta_n\}_{n=1}^{\infty}$ are sequences in $(0,1)$, $\{\theta_n\}_{n=1}^{\infty}$ is a positive sequences and e_n is an error sequence satisfying some convergence conditions. The sequence $\{x_n\}$ generated by the algorithm (16) converges strongly to metric projection of H onto $Fix(T)$, which is the fixed point of nonexpansive mapping. They applied it to solve compressed sensing problem.

Similarly, the authors in citeagb, studied fixed point of strictly pseudo-contractive mapping and zeros of inverse strongly monotone operators using the same algorithm as (16) and the sequences satisfying suitable convergence conditions. The sequence $\{x_n\}$ converges strongly to metric projection of H onto $Fix(T)$, which is the fixed point of strictly pseudo-contractive mapping.

Consequently, Ekuma-Okereke, et.al [20] proposed and studied a modified Mann-type iterative procedure with inertial term for the approximation of fixed point of strictly pseudo-contractive mappings defined on a closed and convex subset of real Hilbert spaces. below is their algorithm: Let the sequence $\{x_n\} \in C$ be generated by choosing $x_1 < x_0 \in C$ and using the procedure

$$\begin{cases} z_n = x_n + \tau_n(x_n - x_{n-1}), \\ y_n = \alpha_n x_0 + (1-\alpha_n)z_n, \\ x_{n+1} = P_C(\beta_n y_n + (1-\beta_n)Ty_n), n \geq 1, \end{cases} \tag{17}$$

where $\{\beta_n\}_{n=1}^{\infty} \in (k,1)$ for any $k \in [0,1)$, $\{\alpha_n\}_{n=1}^{\infty} \in (0,1)$, $\{\theta_n\}_{n=1}^{\infty}$ is a positive sequence satisfying required convergence conditions and P_C is the metric projection onto a nonempty, closed and convex subset subset C of H. Then $\{x_n\}$ generated by (17)converges strongly to metric projection of C onto $Fix(T)$.

Question 1. Is it possible to construct an algorithm with inertial and error terms that converges strongly to a common fixed point of a family of strictly pseudocontractive mappings more general than nonexpansive mappings?

Thus, we are inspired by the above results to construct a Halpern-type iterative with inertial and error terms algorithm for approximating a common fixed point of a family of strictly pseudocontractive mappings in a real Hilbert space. It is intended that our method complement and extend some results cited here.

2 Methodology/Model formulation

This section formulate a Halpern algorithm with inertial-like and error terms for approximating a common fixed point of a finite family of strictly pseudo-contractive mappings and then discuss its convergence analysis in the next section.

Model/Algorithm Hypotheses

(C_1) Let H be a real Hilbert Space.

(C_2) Let $T_i : H \to H, i = 1, 2, ..., N$, represent a strictly pseudo-contractive mappings.

(C_3) Let $F = \cap_{i=1}^{N} F(T_i) \neq \emptyset$.

(C_4) Let $\{\beta_n^0\}_{n=1}^{\infty}, \{\beta_n^i\}_{n=1}^{\infty} \in (0,1)$ for each i, $\{\alpha_n\}_{n=1}^{\infty} \in (0,1)$ be positive sequences and $\{\zeta_n\}_{n=1}^{\infty}$ be an error sequence which positive.

Let the sequences satisfy the following conditions:

(i) $\lim_{n\to\infty} \alpha_n = 0, \sum_{n=1}^{\infty} \alpha_n = \infty, \sum_{n=1}^{\infty} \zeta_n < \infty, \lim_{n\to\infty}, \dfrac{\zeta_n}{\alpha_n} = 0,$

(ii) $\liminf_{n\to\infty} \gamma_n^i[\beta_n - (1-\alpha_n)k] > 0$, where $\beta_n = (1-\alpha_n)\beta_n^0, \gamma_n^i = (1-\alpha_n)\sum_{i=1}^{N} \beta_n^i$

(iii) $\alpha_n + \beta_n + \gamma_n^i = 1, \sum_{i=0}^{N} \beta_n^i = 1$

(iv) $\tau \in [0,1)$ such that $0 \leq \tau_n \leq 1$ with

$$\tau_n := \begin{cases} \min\{\frac{\zeta_n}{\|x_n - x_{n-1}\|}, \tau\}, \text{ whenever } x_n \neq x_{n-1} \\ \tau, \text{ otherwise .} \end{cases}$$

Algorithm 2.1

==========

Initialization: Let $x_1, x_0 \in H$. Given x_{n-1}, x_n, then calculate x_{n+1} as follows:

Step 1: Compute

$$z_n = x_n + \zeta_n(x_n - x_{n-1}) \tag{18}$$

where

$$\tau_n := \begin{cases} \min\{\frac{\theta_n}{\|x_n - x_{n-1}\|}, \tau\}, \text{ whenever } x_n \neq x_{n-1} \\ \tau, \text{ otherwise .} \end{cases}$$

Step 2: Compute

$$x_{n+1} = \alpha_n x_0 + (1-\alpha_n)\left(\beta_n^0 z_n + \sum_{i=1}^{N} \beta_n^i T_i z_n + \frac{\zeta_n}{1-\alpha_n}\right), n \geq 1. \tag{19}$$

Set $n := n+1$ and go to **Step 1.** Stop if $x_{n+1} = x_n = x_{n-1} = z_n$.

==========

The following Lemmas are needed in the sequel.

Lemma 2.1. *cf.([21]) Let H be a real Hilbert space. Given $x, y \in H$, then the inequality holds:*

$$\|x+y\|^2 \leq \|x\|^2 + 2\langle y, x+y\rangle. \tag{20}$$

Lemma 2.2. *cf.([21]) Let H be a real Hilbert space. Given $x, y \in H$, then the equality hold:*

$$\|\alpha x + \beta y\|^2 = \alpha(\alpha+\beta)\|x\|^2 + \beta(\alpha+\beta)\|y\|^2 - \alpha\beta\|x-y\|^2, \forall x, y \in H, \alpha, \beta \in \mathbb{R} \tag{21}$$

Lemma 2.3. *cf.([22]) Let H be a real Hilbert space. For all $x_i \in H, \alpha_i \in [0,1], i = 0, 1, 2, ..., n$ satisfying $\alpha_0 + \alpha_1 + \alpha_2 + ... + \alpha_n = 1$, then we have the equality condition as follows:*

$$\|\alpha_0 x_0 + \alpha_1 x_1 + \alpha_2 x_2 + ... + \alpha_n x_n\|^2 = \sum_{i=0}^{n} \alpha_i \|x_i\|^2 - \sum_{0 \le i,j \le n} \alpha_{i,j}\|x_i - x_j\|^2. \tag{22}$$

Lemma 2.4. *([2]) Let C represent a non-empty, closed and convex subset of a real Hilbert space H. Let $T : C \to C$, represent a strictly pseudo-contractive mapping. Then*

(i) $(1-T)$ is demiclosed at 0 and $x_n - Tx_n \to 0$, then $x = Tx$,

(ii) $Fix(T)$ is closed and convex subset of C.

Lemma 2.5. *([23]) Let $\{a_n\}_{n=1}^{\infty}, \{c_n\}_{n=1}^{\infty}, \{e_n\}_{n=1}^{\infty}$ be sequences contain in $[0, \infty)$, $\{b_n\}_{n=1}^{\infty} \subset (0,1)$ and $\{d_n\}_{n=1}^{\infty}$ be a sequence contain in $(-\infty, +\infty)$ such that*

$$a_{n+1} \le [1 - b_n + c_n]a_n + d_n + e_n, n \ge 1. \tag{23}$$

If $\sum_{n=1}^{\infty} c_n < \infty, \sum_{n=1}^{\infty} e_n \infty$, then

(i) if $d_n \le M b_n$ for some $M \ge 0$, then $\{a_n\}_{n=1}^{\infty}$ is bounded.

(ii) if $\lim_{n\to\infty} b_n = 0, \sum_{n=1}^{\infty} c_n = \infty$ and $\limsup_{n\to\infty} \frac{d_n}{b_n} \le 0$, then $\lim_{n\to\infty} a_n = 0$.

Lemma 2.6. *([24]) Let $\{\alpha_n\}_{n=1}^{\infty}$ be a sequence of non-negative real numbers satisfying the following relation:*

$$a_{n+1} \le (1-\alpha_n)a_n + \alpha_n \delta_n, n \ge n_0 \tag{24}$$

where $\{\alpha_n\}_{n=1}^{\infty}$ is a sequence in $(0,1)$, $\{\delta_n\}$ is a sequence in $(-\infty, +\infty)$ satisfying the following conditions:

(i) $\lim_{n\to\infty} \alpha_n = 0, \sum_{n=1}^{\infty} \alpha_n = \infty$,

(ii) $\lim_{n\to\infty} sup \delta_n \le 0$. Then $\lim_{n\to\infty} a_n = 0$.

Lemma 2.7. *([25]) Let $\{\alpha_n\}_{n=1}^{\infty}$ be a sequence of real numbers such that there exists a nondecreasing subsequence $\{n_i\}$ of $\{n\}$ that is $a_{n_i} < a_{n_{i+1}}$ $\forall i \in N$. Then there exists a nondecreasing subsequence $\{m_k\} \subset N$ such that $m_k \to \infty$ and the following properties are satisfied for all (sufficiently large number) $k \in N$: $a_{m_k} \le a_{m_{k+1}}$ and $a_k \le a_{m_{k+1}}$. In fact, $m_k = max\{j \le k : a_j \le a_{j+1}\}$.*

3 Analysis of the model

Theorem 3.1. *Suppose that conditions $C_1 - C_4$ are satisfied. Then the sequence $\{x_n\}$ generated by **Algorithm 2.1** converges strongly to a point $x^* \in F$.*

Proof. We first show that the sequence $\{x_n\}$ generated by **Algorithm 2.1** is bounded. To do this, we set $\beta_n = (1-\alpha_n)\beta_n^0, \gamma_n^i = (1-\alpha_n)\sum_{i=1}^{N} \beta_n^i$ with $\alpha_n + \beta_n + \gamma_n^i = 1$. Also, we let $p \in F$. In view

of Lemma 2.3 and the property of T_i for each i, we get

$$\begin{aligned}
\|x_{n+1}-p\|^2 &= \|\alpha_n x_0 + (1-\alpha_n)\left(\beta_n^0 z_n + \sum_{i=1}^{N}\beta_n^i T_i z_n + \frac{\zeta_n}{1-\alpha_n}\right) - p\|^2 \\
&= \|\alpha_n x_0 + (1-\alpha_n)\beta_n^0 z_n + (1-\alpha_n)\sum_{i=1}^{N}\beta_n^i T_i z_n + \zeta_n - p\|^2 \\
&= \|\alpha_n(x_0-p) + (1-\alpha_n)\beta_n^0(z_n-p) + (1-\alpha_n)\sum_{i=1}^{N}\beta_n^i(T_i z_n - p)\|^2 + \|\zeta_n\|^2 \\
&+ 2\langle \zeta_n, \alpha_n(x_0-p) + (1-\alpha_n)\beta_n^0(z_n-p) + (1-\alpha_n)\sum_{i=1}^{N}\beta_n^i(T_i z_n - p)\rangle \\
&\leq \alpha_n\|x_0-p\|^2 + \beta_n\|z_n-p\|^2 + \gamma_n^i\|T_i z_n - p\|^2 + \|\zeta_n\|^2 \\
&- \alpha_n\beta_n\|x_0-z_n\|^2 - \alpha_n\gamma_n^i\|x_0 - T_i z_n\|^2 - \beta_n\gamma_n^i\|z_n - T_i z_n\|^2 \\
&+ 2\|\zeta_n\|\left[\alpha_n\|x_0-p\| + \beta_n\|z_n-p\| + \gamma_n^i\|T_i z_n - p\|\right] \\
&\leq \alpha_n\|x_0-p\|^2 + \beta_n\|z_n-p\|^2 + \gamma_n^i\left(\|z_n-p\|^2 + k\|z_n - T_i z_n\|^2\right) + \|\zeta_n\|^2 \\
&- \alpha_n\beta_n\|x_0-z_n\|^2 - \alpha_n\gamma_n^i\|x_0 - T_i z_n\|^2 - \beta_n\gamma_n^i\|z_n - T_i z_n\|^2 \\
&+ 2\|\zeta_n\|\left[\alpha_n\|x_0-p\| + \beta_n\|z_n-p\| + \gamma_n^i L\|z_n - p\|\right]. \\
&\leq \alpha_n\|x_0-p\|^2 + \left[\beta_n + \gamma_n^i\right]\|z_n-p\|^2 - \gamma_n^i(\beta_n - k)\|z_n - T_i z_n\|^2 + \|\zeta_n\|^2 \\
&- \alpha_n\beta_n\|x_0-z_n\|^2 - \alpha_n\gamma_n^i\|x_0 - T_i z_n\|^2 - \beta_n\gamma_n^i\|z_n - T_i z_n\|^2 \\
&+ 2\|\zeta_n\|\left[\alpha_n\|x_0-p\| + \beta_n\|z_n-p\| + \gamma_n^i L\|z_n - p\|\right]. \qquad (25)
\end{aligned}$$

Furthermore,

$$\begin{aligned}
\|z_n-p\|^2 &= \|x_n + \tau_n(x_n - x_{n-1}) - p\|^2 \\
&= \|(x_n-p) + \tau_n(x_n - x_{n-1})\|^2 \\
&= \|x_n-p\|^2 + \tau_n^2\|x_n - x_{n-1}\|^2 + 2\langle \tau_n(x_n - x_{n-1}, x_n - p)\rangle \\
&\leq \|x_n-p\|^2 + \tau_n^2\|x_n - x_{n-1}\|^2 + 2\tau_n\|x_n - x_{n-1}\|.\|x_n-p\|^2 + 2\tau_n\|x_n - x_{n-1}\| \\
&= [1 + 2\tau_n\|x_n - x_{n-1}\|].\|x_n-p\|^2 + \tau_n^2\|x_n - x_{n-1}\|^2 + 2\tau_n\|x_n - x_{n-1}\|. \qquad (26)
\end{aligned}$$

Substituting (26) into (25), we get

$$\begin{aligned}
\|x_{n+1}-p\|^2 &\leq \alpha_n\|x_0-p\|^2 + \left[\beta_n + \gamma_n^i\right] \\
&\times [1 + 2\tau_n\|x_n - x_{n-1}\|].\|x_n-p\|^2 + \tau_n^2\|x_n - x_{n-1}\|^2 + 2\tau_n\|x_n - x_{n-1}\| \\
&- \gamma_n^i(\beta_n - k)\|z_n - T_i z_n\|^2 + \|\zeta_n\|^2 \\
&- \alpha_n\beta_n\|x_0-z_n\|^2 - \alpha_n\gamma_n^i\|x_0 - T_i z_n\|^2 - \beta_n\gamma_n^i\|z_n - T_i z_n\|^2 \\
&+ 2\|\zeta_n\|\left[\alpha_n\|x_0-p\| + [\beta_n + \gamma_n^i L] \times [1 + 2\tau_n\|x_n - x_{n-1}\|].\|x_n-p\|^2 + \tau_n^2\|x_n - x_{n-1}\|^2 + 2\tau_n\|x_n - \right. \\
&\leq [1 - \alpha_n + 2(\beta_n + \gamma_n^i\tau_n)\|x_n - x_{n-1}\| \\
&+ 2(\beta_n + \gamma_n^i L)\|\zeta_n\|(1 + 2\tau_n\|x_n - x_{n-1})\|x_n - p\|^2 \\
&+ [(\beta_n + \gamma_n^i) + 2(\beta_n + \gamma_n^i L)\|\zeta_n\|] \times [\tau_n^2\|x_n - x_{n-1}\|^2 + 2\tau_n\|x_n - x_{n-1}\|] \\
&+ \alpha_n\|x_n-p\|^2 + 2\alpha_n\|\zeta_n\|\|x_0-p\| + \|\zeta_n\|^2 + 2(\beta_n + \gamma_n^i L)\|\zeta_n\|. \qquad (27)
\end{aligned}$$

If $\lim_{n\to\infty}\frac{\|\zeta_n\|}{\alpha_n}=0$, the above inequality (27) can be expressed thus

$$\begin{aligned}\|x_{n+1}-p\|^2 \leq [1-\alpha_n+2\alpha_n(\beta_n+\gamma_n^i)\frac{\tau_n}{\alpha_n}\|x_n-x_{n-1}\| \\ +2(\beta_n+\gamma_n^iL)\alpha_n\times\frac{\|\zeta_n\|}{\alpha_n}(1+2\tau_n\|x_n-x_{n-1}\|)]\|x_n-p\|^2 \\ +[\alpha_n(\beta_n+\gamma_n^i)+2(\beta_n+\gamma_n^iL)\alpha_n\times\frac{\|\zeta_n\|}{\alpha_n}]\times[\alpha_n^2\times\frac{\tau_n^2}{\alpha_n^2}\|x_n-x_{n-1}\|^2+2\alpha_n\frac{\tau_n}{\alpha_n}\|x_n-x_{n-1}\|] \\ +\alpha_n\|x_n-p\|^2+2\alpha_n^2\frac{\|\zeta_n\|}{\alpha_n}\|x_0-p\|+\alpha_n^2\frac{\|\zeta_n\|^2}{\alpha_n^2}+2(\beta_n+\gamma_n^iL)\alpha_n\frac{\|\zeta_n\|}{\alpha_n}. \qquad (28)\end{aligned}$$

By our hypothesis,there exists a positive integer N such that

$$\{2(\beta_n+\gamma_n^i)\frac{\tau_n}{\alpha_n}\|x_n-x_{n-1}\|+2(\beta_n+\gamma_n^iL)\times\frac{\|\zeta_n\|}{\alpha_n}(1+2\tau_n\|x_n-x_{n-1}\|)\}\leq\frac{1}{2},\forall n\geq N. \qquad (29)$$

In addition, we can find a positive constant M such that

$$\begin{aligned}2\{(\beta_n+\gamma_n^i)+2(\beta_n+\gamma_n^iL)\frac{\|\zeta_n\|}{\alpha_n}[\frac{\tau_n^2}{\alpha_n^2}\|x_n-x_{n-1}\|^2+2\frac{\tau_n}{\alpha_n}\|x_n-x_{n-1}\|] \\ +\|x_n-p\|^2+2\alpha_n\frac{\|\zeta_n\|}{\alpha_n}\|x_0-p\|+\alpha_n\frac{\|\zeta_n\|^2}{\alpha_n^2}+2(\beta_n+\gamma_n^iL)\frac{\|\zeta_n\|}{\alpha_n}\}\leq M \qquad (30)\end{aligned}$$

Substituting (29) and (30) into (28), we get

$$\|x_{n+1}-p\|^2\leq[1-\frac{\alpha_n}{2}]\|x_n-p\|^2+\frac{\alpha_n}{2}M,\forall n\geq N. \qquad (31)$$

Following from Lemma (2.5), the sequence $\{x_n\}$ is bounded. On the other hand, if $\sum_{n=1}^{\infty}\|\zeta_n\|<\infty$, let N be a positive integer such that

$$2(\beta_n+\gamma_n^i)\frac{\tau_n}{\alpha_n}\|x_n-x_{n-1}\|\leq\frac{1}{2},\forall n\geq N.$$

In addition, let M_1, M_2 and M_3 be positive integers such that

$$+2(\beta_n+\gamma_n^i)(1+2\tau_n\|x_n-x_{n-1}\|)\}\leq M_1,$$

$$2(\beta_n+\gamma_n^i)[\frac{\tau_n^2}{\alpha_n^2}\|x_n-x_{n-1}\|^2+2\frac{\tau_n}{\alpha_n}\|x_n-x_{n-1}\|]+\|x_n-p\|^2+2\|\zeta_n\|\|x_0-p\|\leq M_2,$$

and

$$[2(\beta_n+\gamma_n^iL)\left(\tau_n^2\|x_n-x_{n-1}\|^2+2\tau_n\|x_n-x_{n-1}+1\right)+\|\zeta_n\|]\|\zeta_n\|\leq M_3.$$

From (27), we get

$$\|x_{n+1}-p\|^2\leq[1-\frac{\alpha_n}{2}+M_1\|\zeta_n\|]\|x_n-p\|^2+\frac{\alpha_n}{2}M_2+\|\zeta_n\|M_3,\forall n\geq N. \qquad (32)$$

Following from Lemma 2.5 the sequence $\{x_n\}$ is bounded. Now, from Lemma 2.1

$$\begin{aligned}\|z_n-p\|^2&=\|x_n+\tau_n(x_n-x_{n-1})-p\|^2 \\ &=\|x_n-p\|^2+\tau_n^2\|x_n-x_{n-1}\|^2+2\langle\tau_n(x_n-x_{n-1},x_n-p)\rangle \\ &\leq\|x_n-p\|^2+\tau_n\|x_n-x_{n-1}\|^2+2\tau_n\langle x_n-x_{n-1},x_n-p\rangle. \qquad (33)\end{aligned}$$

Note that,

$$\begin{aligned}\|x_{n-1}-p\|^2 &= \|x_{n-1}-x_n+x_n-p\|^2\\ &= \|x_n-p\|^2-2\langle x_n-x_{n-1},x_n-p\rangle+\|x_n-x_{n-1}\|,\end{aligned} \tag{34}$$

(34) implies that

$$2\langle x_n-x_{n-1},x_n-p\rangle = -\|x_{n-1}-p\|^2+\|x_n-p\|^2+\|x_n-x_{n-1}\|. \tag{35}$$

Plugging (35) into (33) gives

$$\begin{aligned}\|z_n-p\|^2 &\le \|x_n-p\|^2+\tau_n\|x_n-x_{n-1}\|^2+\tau_n[-\|x_{n-1}-p\|^2+\|x_n-p\|^2+\|x_n-x_{n-1}\|]\\ &= \|x_n-p\|^2+2\tau_n\|x_n-x_{n-1}\|^2+\tau_n[\|x_n-p\|^2-\tau_n\|x_{n-1}-p\|^2].\end{aligned} \tag{36}$$

On the other hand, we show that the sequence $\{x_n\}$ generated by **Algorithm 2.1** converges to the metric projection mapping of H onto $\cap_{i=1}^{N}Fix(T_i)$. To do this, we let $p=P_{\cap_{i=1}^{N}Fix(T_i)}x_0$. In view of the construction of algorithm (18)-(19), Lemmas 2.1, 2.2 and the approach used to get inequality (27), we get

$$\begin{aligned}\|x_{n+1}-p\|^2 &= \|\alpha_n x_0+\beta_n z_n+\gamma_n^i T_i z_n+\zeta_n-p\|^2\\ &= \|\alpha_n(x_0-p+\frac{\zeta_n}{\alpha_n})+\beta_n(z_n-p)+\gamma_n^i(T_iz_n-p)\|^2\\ &\le \|\beta_n(z_n-p)+\gamma_n^i(T_iz_n-p)\|^2+2\langle\alpha_n(x_0-p+\frac{\zeta_n}{\alpha_n},x_{n+1}-p)\rangle\\ &= \beta_n(\beta_n+\gamma_n^i)\|(z_n-p)\|^2+\gamma_n^i(\beta_n+\gamma_n^i)\|T_iz_n-p\|^2-\beta_n\gamma_n^i\|T_iz_n-z_n\|^2\\ &+2\langle\alpha_n(x_0-p+\frac{\zeta_n}{\alpha_n},x_{n+1}-p)\rangle\\ &\le \beta_n(\beta_n+\gamma_n^i)\|(z_n-p)\|^2+\gamma_n^i(\beta_n+\gamma_n^i)[\|z_n-p\|^2+k\|z_n-T_iz_n\|^2]-\beta_n\gamma_n^i\|T_iz_n-z_n\|^2\\ &+2\langle\alpha_n(x_0-p+\frac{\zeta_n}{\alpha_n},x_{n+1}-p)\rangle\\ &= (\beta_n+\gamma_n^i)^2\|(z_n-p)\|^2-\gamma_n^i[\beta_n-(\beta_n+\gamma_n^i)k]\|z_n-T_iz_n\|^2+2\langle\alpha_n(x_0-p+\frac{\zeta_n}{\alpha_n},x_{n+1}-p)\rangle\\ &\le (1-\alpha_n)\|z_n-p\|^2-\gamma_n^i[\beta_n-(\beta_n+\gamma_n^i)k]\|z_n-T_iz_n\|^2\\ &+2\langle\alpha_n(x_0-p+\frac{\zeta_n}{\alpha_n},x_{n+1}-p)\rangle.\end{aligned} \tag{37}$$

Plugging (36) into (37), we get

$$\begin{aligned}\|x_{n+1}-p\|^2 &\le (1-\alpha_n)[\|x_n-p\|^2+2\tau_n\|x_n-x_{n-1}\|^2+\tau_n[\|x_n-p\|^2-\tau_n\|x_{n-1}-p\|^2]\\ &-\gamma_n^i[\beta_n-(\beta_n+\gamma_n^i)k]\|z_n-T_iz_n\|^2\\ &+2\langle\alpha_n(x_0-p+\frac{\zeta_n}{\alpha_n},x_{n+1}-p)\rangle\\ &= (1-\alpha_n)\|x_n-p\|^2-\gamma_n^i[\beta_n-(\beta_n+\gamma_n^i)k]\|z_n-T_iz_n\|^2\\ &+2\tau_n(1-\alpha_n)\|x_n-x_{n-1}\|^2+\tau_n[\|x_n-p\|^2-\|x_{n-1}-p\|^2]\\ &+2\langle\alpha_n(x_0-p+\frac{\zeta_n}{\alpha_n},x_{n+1}-p)\rangle\end{aligned} \tag{38}$$

Next, we consider two cases to complete the proof of our Theorem.

Case 1. If we suppose to find $n_0\in N$ such that $\{\|x_n-p\|\}_{n=n_0}^{\infty}$ is decreasing, then we can get $\{\|x_n-p\|\}_{n=n_0}^{\infty}$ is convergent and hence

$$\|x_n-p\|-\|x_{n+1}-p\|\to 0, n\to\infty. \tag{39}$$

Consequently,

$$\|x_{n-1} - p\| - \|x_n - p\| \to 0, n \to \infty \tag{40}$$

and

$$\begin{aligned} \|x_n - x_{n-1}\| &= \|x_n - p + p - x_{n-1}\| \\ &\leq \|x_n - p\| + \|x_{n-1} - p\| \to 0, n \to \infty \end{aligned} \tag{41}$$

In view of (38) we get

$$\begin{aligned} \gamma_n^i[\beta_n - (\beta_n + \gamma_n^i)k]\|z_n - T_i z_n\|^2 &\leq \|x_n - p\|^2 - \|x_{n+1} - p\|^2 - \alpha_n\|x_n - p\|^2 \\ &+ 2\tau_n(1 - \alpha_n)\|x_n - x_{n-1}\|^2 + \tau_n[\|x_n - p\|^2 - \|x_{n-1} - p\|^2] \\ &+ 2\langle \alpha_n(x_0 - p + \frac{\zeta_n}{\alpha_n}, x_{n+1} - p)\rangle. \end{aligned} \tag{42}$$

Invoking (39), (40), (41) and conditions (i) and (ii) of our hypothesis, we get

$$\|z_n - T_i z_n\| \to 0, \text{ for each i=1,2,3,...,N}, n \to \infty. \tag{43}$$

Now from the definition of z_n and conditions (i) and (v), we get

$$\begin{aligned} \|z_n - x_n\|^2 &= \|x_n + \tau_n(x_n - x_{n-1}) - x_n\|^2 \\ &= \|\tau_n(x_n - x_{n-1})\|^2 \\ &\leq \tau_n\|x_n - x_{n-1}\|^2 \\ &\leq \alpha_n \frac{\theta_n}{\alpha_n} \to 0, n \to \infty. \end{aligned}$$

Thus,

$$\|z_n - x_n\| \to 0, n \to \infty. \tag{44}$$

Since $\{z_n\}$ is bounded, we choose a subsequence $\{z_{n_i}\}$ of $\{z_n\}$ such that $z_{n_i} \rightharpoonup z \in H$ and

$$\begin{aligned} \limsup_{n\to\infty}\langle x_0 - p, z_n - p\rangle &= \limsup_{i\to\infty}\langle x_0 - p, z_{n_i} - p\rangle \\ &= \langle x_0 - p, z - p\rangle. \end{aligned} \tag{45}$$

Now, in view of (44), it follows that $x_{n_i} \rightharpoonup z \in H$. From (43) and Lemma 2.4, we get $z \in \cap_{i=1}^N F(T_i)$. By invoking (38) and Lemma 2.6 we find that $\lim_{n\to\infty}\|x_n - p\| = 0$. Consequently, $x_n \to p = P_{\cap_{i=1}^N F(T_i)}x_0$.

Case 2. Suppose we find a subsequence n_i of $n \neq n_0$ such that $\{\|x_n - p\|\}_{n=n_i}^{\infty}$ is decreasing, that is

$$\|x_{n_i} - p\| \leq \|x_{n_i+1} - p\|, \forall i \in N.$$

Now invoking Lemma 2.7, and following the same line of argument as in Case 1, we find that $x_n \to p = p = P_{\cap_{i=1}^N F(T_i)}x_0$.

Corollary 3.2. *Suppose that $T_i : H \to H$, $i = 1$ represent strictly pseudo-contractive self mapping and if conditions C_1, C_3, C_4 are satisfied. Then the sequence $\{x_n\}$ generated by iterative algorithm 2.1 converges strongly to an element of the set of fixed point of a single strictly pseudo-contractive mapping.*

Proof. Set $i = 1$, then the result holds for a single pseudo-contractive mapping and this reduces to the results of [2] and [19] respectively.

Corollary 3.3. *Suppose that $T_i : H \to H$, $i = 1, 2, ..., N$ represent nonexpansive self mappings and if conditions C_1, C_3, C_4 are satisfied with $k = 0$. Then the sequence $\{x_n\}$ generated by iterative algorithm 2.1 converges strongly to a common element of the set of fixed points of a family of nonexpansive mappings.*

Proof. If we set $k = 0$ and $T_i : H \to H, i = 1, 2, ..., N$ such that T_i represent nonexpansive self mappings in the proof of Theorem 3.1, then we get the conclusion of Corollary 3.3.

Corollary 3.4. *Suppose that $T_i : H \to H$, $i = 1$ represent a single nonexpansive self mapping and conditions C_1, C_3, C_4 are satisfied. Then the sequence $\{x_n\}$ generated by iterative algorithm 2.1 converges strongly to an element of the set of fixed point of a single nonexpansive mapping.*

Proof. If we set $k = 0$ and $T : H \to H$ such that T represent a single nonexpansive self mapping in the proof of Theorem 3.1, then we get the conclusion of Corollary 3.4 and our result reduces to that of [4].

4 Numerical simulations/sensitivity analysis

In this section we would demonstrate the effectiveness, implementation and strong convergence results of our algorithm (18)-(19) of Theorem 3.1 as discussed. All codes are written in Python software, run on HP PC with Intel(R)Core(TM)i7-3520M CPU @ 2.90GHz.

Example 4.1. (See [2])
Let $H = R$ denote the reals with the usual norm $|.|$ and the inner product $\langle x, y\rangle = xy$, let R denote the reals and define $T : R \to R$ by

$$T(x) := \begin{cases} -3x + 1 & \text{if } x \in (-\infty, 0] \\ \frac{1}{2}(x + 2) & \text{if } x \in (0, \infty). \end{cases} \tag{46}$$

Then T is $\frac{1}{2}$ strictly pseudo-contractive mapping with $Fix(T) = \{2\}$.

Proof. We first prove that the fixed point is actually the 2. To see this, we make use of the definition of fixed point as follows:

$$\begin{aligned} Fix(T) &= \{x \in R : Tx = x\} \\ &= \{x \in R : \frac{1}{2}(x + 2) = x\} \\ &= \{x \in R : \frac{1}{2}x + 1 = x\} \\ &= \{x \in R : x + 2 = 2x\} \\ &= \{x \in R : x = 2 \in (0, \infty)\}. \end{aligned}$$

Thus $Fix(T) = \{2\}$.

Next, we prove that T is $\frac{1}{2}$-strictly pseudo-contractive mapping. Now since $H = R$, is the reals with the usual norm, we have that the norm becomes absolute norm. That is

$$\|Tx - Ty\|^2 \leq \|x - y\|^2 + k\|(x - y) - (Tx - Ty)\|^2, \forall x, y \in R \tag{47}$$

becomes

$$|Tx - Ty|^2 \leq |x - y|^2 + k|(x - y) - (Tx - Ty)|^2, \forall x, y \in R \tag{48}$$

where $Tx = -3x + 1$ and $Ty = -3y + 1, \forall x, y \in (-\infty, 0]$. So using (48), we have

$$\begin{aligned}
|-3x+1-(-3y+1)|^2 &\leq |x-y|^2 + k|(x-y)-(-3x+1-(-3y+1))|^2, \forall x, y \in R \\
|-3x+3y|^2 &\leq |x-y|^2 + k|(x-y)+3x-3y|^2, \forall x, y \in R \\
|-3(x-y)|^2 &\leq |x-y|^2 + k|(x-y)+3(x-y)|^2, \forall x, y \in R \\
9|x-y|^2 &\leq |x-y|^2 + k|(x-y)(1+3)|^2, \forall x, y \in R \\
9|x-y|^2 &\leq |x-y|^2 + 16k|x-y|^2, \forall x, y \in R \\
9|x-y|^2 &\leq (1+16k)|x-y|^2, \forall x, y \in R \\
9 &\leq (1+16k) \\
8 &\leq 16k \\
1 &\leq 2k \\
k &= \frac{1}{2}.
\end{aligned}$$

Thus $k = \frac{1}{2} \in [0, 1)$ as expected and that completes the proof of the example.

Example 4.2. Two Strictly Pseudo-contrative mappings with a common fixed points
Let $H = R$ denote the reals with the usual norm $|.|$ and the inner product $\langle x, y\rangle = xy$, let R denote the reals and define $T_i : R \to R$ for each $i = 1, 2$ by

$$T_1(x) := \begin{cases} -3x + 1 & \text{if } x \in (-\infty, 0] \\ \frac{1}{2}(x+2) & \text{if } x \in (0, \infty). \end{cases} \tag{49}$$

and

$$T_2(x) := \begin{cases} 2 & \text{if } x \in [0, \infty) \\ -3x & \text{if } x \in (-\infty, 0). \end{cases} \tag{50}$$

Then T_1 and T_2 are strictly pseudo-contractive mappings with constant $k = \frac{1}{2}$ and $\cap_{i=1}^{2} Fix(T_i) = \{2\}$, for each $i = 1, 2$.

Next, we implement our method in Python Program using this example to show the convergence of the method to the common fixed point of these mappings. Now we construct the following initialization. Let $\alpha_n = \frac{1}{n+1}$ so that $\lim_{n\to\infty} \alpha_n = 0, \sum_{n=1}^{\infty} \alpha_n = \infty$. Let $\zeta_n = \frac{1}{1+n^2}$ such that $\lim_{n\to\infty} \zeta_n = 0, \lim_{n\to\infty}, \frac{\zeta_n}{\alpha_n} = 0$.Let $\tau_n = \min\{\frac{1}{3}, 1\} = \frac{1}{3}$. Let $\beta_n^i = \frac{2^{i-1}}{3^i}, \forall i = 1, 2, ..., N$ which implies that $\sum_{i=1}^{N} \beta_n^i = \sum_{i=1}^{N} \frac{2^{i-1}}{3^i} < 1$. This implies that $\beta_n^0 = 1 - \sum_{i=1}^{N} \frac{2^{i-1}}{3^i}$, such that our hypothesis are satisfied. With a stopping criterion of $\|x_n - x_{n+1}\| \leq 10^{-7}$, the results of Algorithm 2.1 are displayed:

n	z[n]	x[n]	err[n]
1	1.3300000	1.0000000	0.2208333
2	1.2937083	1.2208333	0.0798843
3	1.1145873	1.1409491	0.0943320
4	1.0154875	1.0466170	0.0441352
5	0.9879172	1.0024818	0.0001889
6	1.0022306	1.0022929	0.0263274
7	1.0373084	1.0286203	0.0394170
8	1.0810450	1.0680373	0.0444176
9	1.1271128	1.1124550	0.0450747

10	1.1724044	1.1575297	0.0435867
100	1.8830614	1.8826797	0.0011343
500	1.9761197	1.9761040	0.0000475
1000	1.9880298	1.9880259	0.0000119
10000	1.9988005	1.9988005	0.0000001
10003	1.9988007	1.9988006	0.0000001
10004	1.9988008	1.9988007	0.0000001
10005	1.9988009	1.9988009	0.0000001
10006	1.9988010	1.9988010	0.0000001
10007	1.9988011	1.9988011	0.0000001
10008	1.9988013	1.9988012	0.0000001
10009	1.9988014	1.9988013	0.0000001
10010	1.9988015	1.9988015	0.0000001
10011	1.9988016	1.9988016	0.0000001
13392	1.9991041	1.9991041	0.0000001
15487	1.9992253	1.9992253	0.0000001
15488	1.9992253	1.9992253	0.0000001
15489	1.9992254	1.9992254	0.0000000

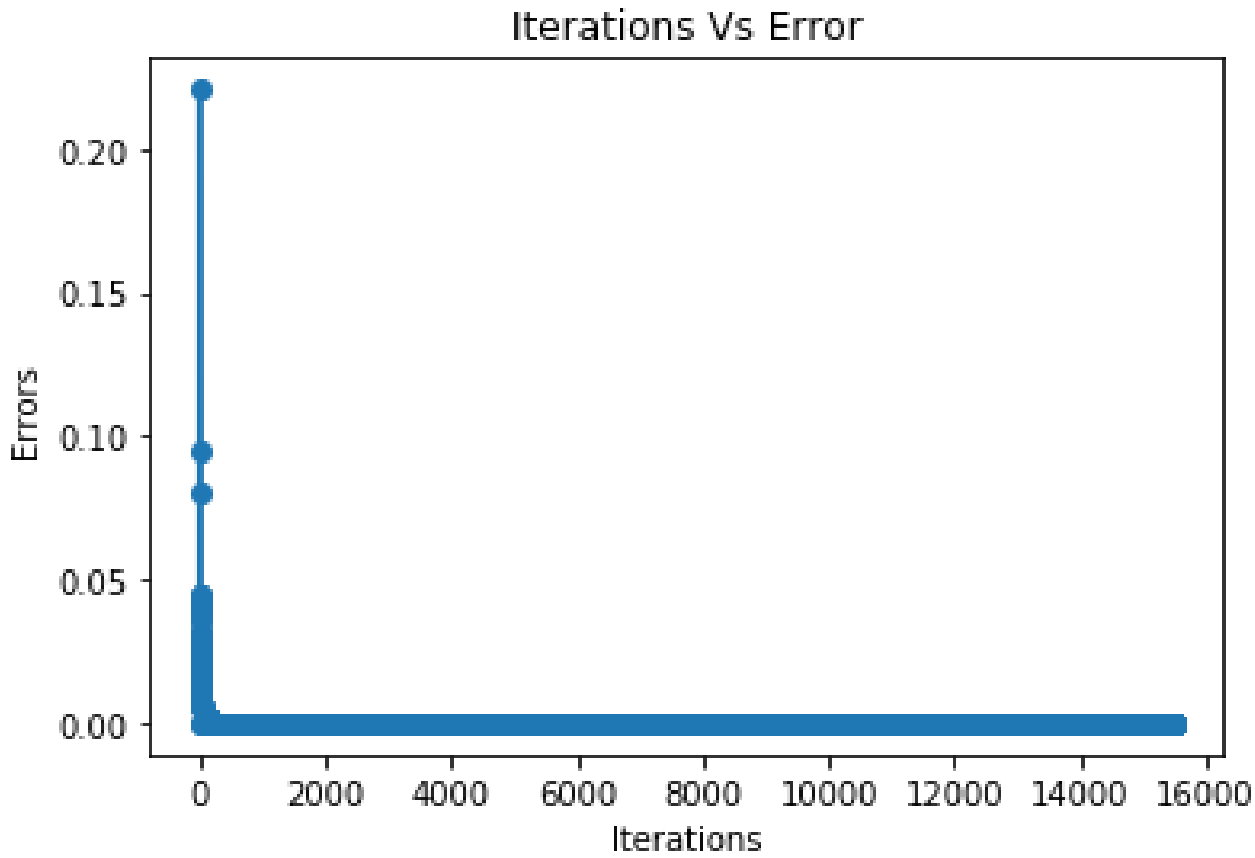


Fig. 1

n	z[n]	x[n]	err[n]
1	1.3300000	1.0000000	0.2766667
2	1.3679667	1.2766667	0.0242370

3	1.2444314	1.2524296	0.0302139
4	1.2122451	1.2222157	0.0164719
5	1.2441233	1.2386876	0.0465091
6	1.3005447	1.2851967	0.0564273
7	1.3602450	1.3416240	0.0551856
8	1.4150208	1.3968096	0.0496985
9	1.4629086	1.4465081	0.0434322
10	1.5042729	1.4899403	0.0377019
50	1.8837069	1.8829398	0.0022357
51	1.8859134	1.8851756	0.0021521
52	1.8880379	1.8873277	0.0020731
53	1.8900849	1.8894007	0.0019983
54	1.8920585	1.8913990	0.0019275
55	1.8939626	1.8933266	0.0018604
56	1.8958009	1.8951870	0.0017967
57	1.8975766	1.8969837	0.0017363
58	1.8992929	1.8987200	0.0016788
59	1.9009528	1.9003988	0.0016241
60	1.9025589	1.9020229	0.0015721
61	1.9041138	1.9035950	0.0015225
62	1.9056199	1.9051175	0.0014752
63	1.9070795	1.9065927	0.0014301
64	1.9084948	1.9080228	0.0013870
65	1.9098676	1.9094099	0.0013459
66	1.9111999	1.9107558	0.0013065
67	1.9124934	1.9120623	0.0012689
68	1.9137499	1.9133312	0.0012328
69	1.9149708	1.9145640	0.0011983
70	1.9161577	1.9157622	0.0011652
71	1.9173119	1.9169274	0.0011334
72	1.9184348	1.9180608	0.0011029
73	1.9195276	1.9191637	0.0010736
74	1.9205916	1.9202373	0.0010455
75	1.9216279	1.9212829	0.0010185
76	1.9226375	1.9223014	0.0009925
77	1.9236214	1.9232938	0.0009675
78	1.9245806	1.9242613	0.0009434
79	1.9255161	1.9252047	0.0009202
80	1.9264286	1.9261249	0.0008979
81	1.9273191	1.9270228	0.0008763
82	1.9281883	1.9278991	0.0008555
83	1.9290370	1.9287546	0.0008355
84	1.9298658	1.9295901	0.0008161
85	1.9306756	1.9304063	0.0007974
86	1.9314668	1.9312037	0.0007794
87	1.9322403	1.9319831	0.0007619
88	1.9329964	1.9327450	0.0007451
89	1.9337359	1.9334901	0.0007287
90	1.9344593	1.9342188	0.0007130
91	1.9351670	1.9349318	0.0006977
92	1.9358597	1.9356294	0.0006829

93	1.9365377	1.9363123	0.0006686
94	1.9372015	1.9369809	0.0006547
95	1.9378516	1.9376356	0.0006412
96	1.9384884	1.9382768	0.0006282
97	1.9391123	1.9389050	0.0006155
98	1.9397236	1.9395205	0.0006033
99	1.9403228	1.9401237	0.0005913
100	1.9409102	1.9407151	0.0005798
10950	1.9994521	1.9994521	0.0000001
10951	1.9994522	1.9994522	0.0000001
10952	1.9994522	1.9994522	0.0000001

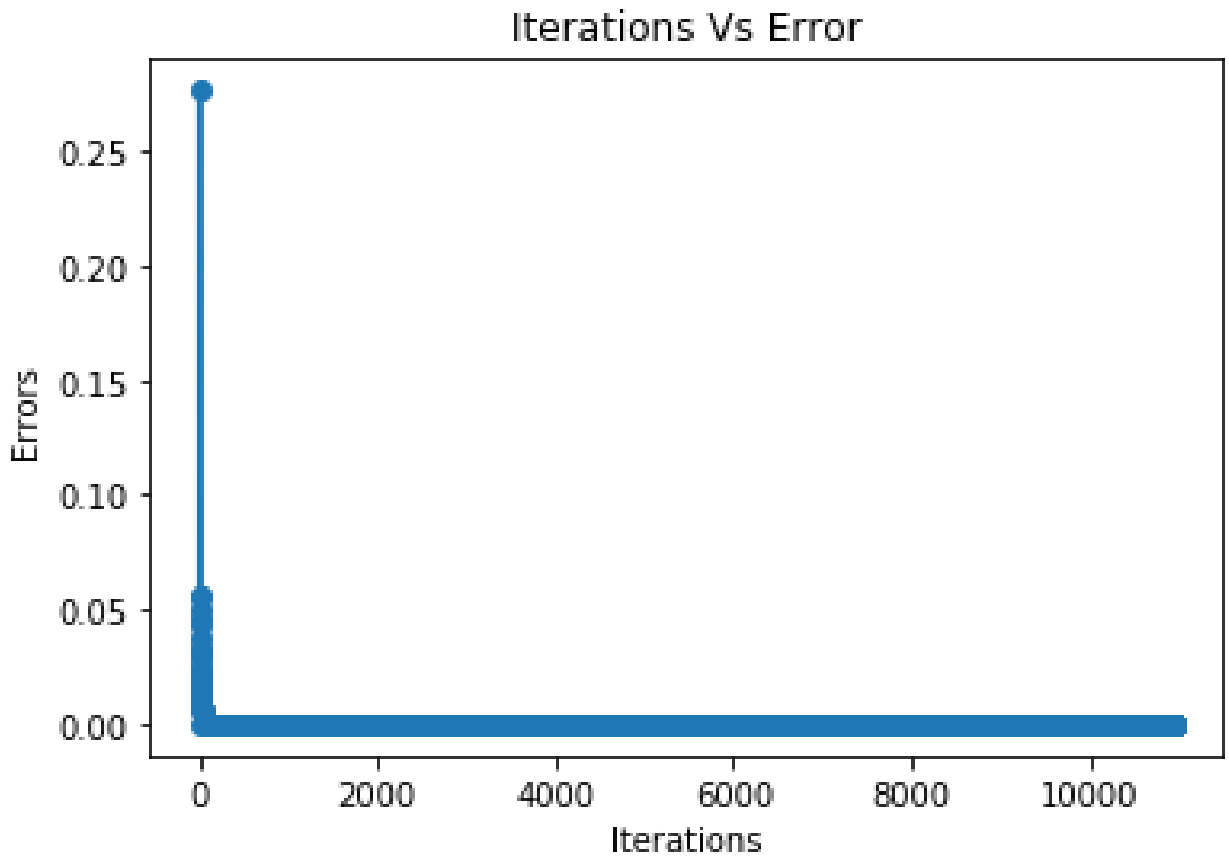


Fig. 2

5 Discussions and Conclusion

We observed that the choice of the control sequences of $\{\alpha_n\}, \{\beta_n^i\}$, $\{\zeta_n\}$ and $\{\tau_n\}$ satisfying the convergence hypothesis, influenced to a great deal, the strong convergence of the Algorithm 2.1 to the common fixed point of the family of mappings. With a stopping criteria of $\|x_{n+1} - x_n\| \leq 10^{-7}$, the computation can be truncated after many iterations. If the stooping criteria is higher at $\|x_{n+1} - x_n\| \leq 10^{-5}$, then truncating the computation early may have a negligible computational error. Consequently, $\|x_n - p\| = \|x_n - 1\| \to F = \cap_{i=1}^{N} F(T_i)$ as $n \to \infty$. Thus, we introduced the Halpern type algorithm with inertial and error terms for approximating the common fixed point of a family of strictly pseudo-contractive mappings defined on a real Hilbert spaces. We proved strong convergence theorem for it. We supported our paper with a some examples to illustrate the effectiveness of our algorithm. We

observed that our algorithm performed favourably with a "good" stopping criteria $\|x_n - x_{n+1}\| \leq 10^{-7}$. Therefore, our algorithm is a good fit for approximating fixed points of strictly pseudo-contractive mappings in Hilbert spaces.

References

[1] Browder, F.E.and Petryshyn, W.V.(1967). Construction of fixed points of nonlinear mappings in Hilbert spaces, J. Math. Anal. Appl. 20, 197-228.

[2] Agbebaku, D.F., Nwokoro, P.U., Osilike, M.O., Chima, E.E. and Onah, A.C.(2021). The Iterative Algorithm with Inertial and Error Terms for Fixed Points of Strictly Pseudo-contractive Mappings and Zeros of Inverse Strongly Monotone Operators. Appl. Set-Valued Anal. Optim. 3(1), 95-107.

[3] Chidume, C.E. and Shahzad, N. (2010). Weak convergence theorems for a finite family of strict pseudocontractions. Nonlinear Anal. 72, 1257-1265.

[4] Shehu, Y., Iyiola, O.S. and Ogbuisi, F.U. (2020). Iterative method with inertial terms for nonexpansive mappings: applications to compressed sensing. Numer. Algor. 83, 1321-1347.

[5] Berinde, V., and Berinde, M. (2005). The fastest Krasnoselskij iteration for approximating fixed points of strictly pseudo-contractive mappings. Carpathian J. Math. 21(1-2), 13-20.

[6] Mann, W.R. (1953). Mean value methods in iteration. Proc. Amer. Math. Soc. 4, 506-510.

[7] Ishikawa, S. (1974). Fixed point by a new iteration method. Proc. Amer. Math. Soc. 44, 147-150.

[8] Qihou, L. (1990). The convergence theorems of the sequence of Ishikawa iterates for hemicontractive mappings. J. Math. Anal. Appl. 148, 55-62.

[9] Zegeye, H., Shahzad, N. and Alghamdi, M. A. (2011). Convergence of Ishikawa's iteration method for pseudocontractive mappings. Nonlinear Analysis 74, 7304-7311.

[10] Gidey, H. H., Zegeye, O. A., Boikanyo, D. K., and Belay, Y. A. (2023). An inertial-like algorithm for solving common fixed point problems of a family of continuous Pseudocontractive mappings. Numerical Functional Analysis and Optimization, Taylor and Francis, pp. 1-24.

[11] Halpern, B.(1968). Fixed points of non-expanding maps. Bull. Amer. Math. Soc., 73, 957-961.

[12] Zegeye, H.,and Shazad, N. (2013). An algorithm for a common fixed point of a family of pseudocontractive mappings. Fixed Point Theory Appl. 2013(1),1–14.

[13] Daman, O. A., and Zegeye, H. (2012). Strong convergence theorems for a common fixed point of a finite family of pseudocontractive mappings. Int. J. Math. Math. Sci., DOI: 10.1155/2012/405315

[14] Chidume, C. E. (1981). On the approximation of fixed points of nonexpansive mapping. Houston J. Math. 7, 345–554.

[15] Jung, J. S. (2011). Some results on a general iterative method for k-strictly pseudocontractive mappings. Fixed Point Theory Appl. 2011(1),1–11.

[16] Berinde, V. (2007). Iterative approximation of fixed points lecture notes in Mathematics. Springer, Berlin.

[17] Nakajo, K., and Takahashi, W. (2003). Strong convergence theorems for nonexpansive mappings and nonexpansive semigroups. J. Math. Anal. Appl., 279(2003), 372–379.

[18] Ekuma-Okereke, E., and Okoro, F. M. (2020). Common Solution for Nonlinear Operators in Banach Spaces, GU J Sci., 33(3), 737-749.

[19] Ekuma-Okereke, E., Okoro, F., and Abhulimen, C. E. (2021). Two modified hybrid inertial algorithms for Bregman weak relatively nonexpansive mapping in Banach spaces. Nigerian Journal of Mathematics and Applications, 31(2021), 149-174.

[20] Ekuma-Okereke, E., Okoro, F., and Abhulimen, C. E. (2022) Iterative Procedure with inertial term for the approximation of fixed point of strictly pseudo-contractive mapping with application to monotone variational inclusion problem in Hilbert spaces. International Journal of Mathematical Analysis and Modelling, 5(3).

[21] Chidume, C. E. (2009). Geometric Properties of Banach Spaces and Nonlinear Iterations. Springer 1965.

[22] Jeong, J. U. (2015). Convergence Theorems of Common Elements for Pseudo-contractive Mappings and Monotone Mappings. Hindawi Publishing Corporation Abstract and Applied Analysis, 2015(2015), 9 pages. http://dx.doi.org/10.1155/2015/383579.

[23] Nwokoro, P.U., Osilike, M.O., Agbebaku, D.F., Chima, E.E., and Onah, A.C. (2020). A new Halpern-type averaging algorithm with inertial and error terms for fixed points of asymptotically nonexpansive maps. J. Math. Comput. Sci., 10(2020), 1538-1558.

[24] Xu, H.-K. (2002). Another control condition in an iterative method for nonexpansive mappings. Bulletin of the Australian Mathematical Society, 65(1), 109–113.

[25] Mainge, P.E. (2008). Strong convergence of projected subgradient methods for nonsmooth and nonstrictly convex minimization. Set-Valued Anal. 16(2008), 899-912.

On the monoid of partial isometries with fixed set

M.M. Zubairu [*†] and **Z.D. Lawan** [†‡§]

Abstract

Denote $[n]$ to be a finite n-chain $\{1, 2, \ldots, n\}$, and let $\mathcal{DP}_n$ denote the semigroup of all partial isometries on $[n]$. For a nonempty subset D of $[n]$, let $\mathrm{Fix}([n], D)$ be the set of all maps in $\mathcal{DP}_n$ which fix all elements of D. Then $\mathrm{Fix}([n], D)$ is a subsemigroup of $\mathcal{DP}_n$. In this paper, we show that the semigroup $\mathrm{Fix}([n], D)$ is a semilattice of idempotents, and further, we obtain the cardinality and the rank of the semigroup.

Keywords and phrases: partial isometries; fixed sets; semilattice; rank.

1 Introduction and Preliminaries

In the study of transformation semigroups, many authors have investigated the algebraic, combinatorial, and rank properties of the semigroup of full transformations with fixed subsets of a chain. In many instances, the subsemigroup of a transformation semigroup, when considering fixed subsets of a chain, exhibits different algebraic, combinatorial, and rank properties. This fact has led many authors to study various subsemigroups with fixed subsets within different transformation semigroups; for examples, see [6, 13, 14, 15, 18]. It has now become customary that, upon encountering any class of transformation semigroup, one of the questions usually raised is the structural properties of its subsemigroup with fixed sets.

Denote $[n]$ to be a finite n chain $\{1, 2, \ldots, n\}$, $\mathcal{P}_n$ to be the semigroup of partial transformations and $\mathcal{I}_n$ to be an inverse subsemigroup of $\mathcal{P}_n$ (consisting of all partial injective maps in $\mathcal{P}_n$). For any transformation α, we shall denote the domain of α, image set of α and $|\mathrm{Im}\ \alpha|$ by $\mathrm{Dom}\ \alpha$, $\mathrm{Im}\ \alpha$, $h(\alpha)$, respectively. Let

$$\mathcal{DP}_n = \{\alpha \in \mathcal{I}_n : (\text{for all } x, y \in \mathrm{Dom}\ \alpha)\ |x\alpha - y\alpha| = |x - y|\} \tag{1}$$

be the semigroup of partial isometries on $[n]$ and

$$\mathcal{ODP}_n = \{\alpha \in \mathcal{DP}_n : (\text{for all } x, y \in \mathrm{Dom}\ \alpha)\ x \leq y \Rightarrow x\alpha \leq y\alpha\} \tag{2}$$

be the semigroup of order-preserving partial isometries of $[n]$. Clearly $\mathcal{ODP}_n$ is a subsemigroup of $\mathcal{DP}_n$.

Among the algebraic and combinatorial properties of the semigroups $\mathcal{DP}_n$ and $\mathcal{ODP}_n$ obtained include the number of their maximal subsemigroups [12], the combinatorial properties [2], the rank properties [1], the presentation [16], and the natural partial orders [11], among other results. Moreover, [5] obtained the rank of the two-sided ideals $\mathcal{DP}_{n,r} = \{\alpha \in \mathcal{DP}_n : |\mathrm{Im}\ \alpha| \leq r\}$ and $\mathcal{ODP}_{n,r} = \{\alpha \in \mathcal{ODP}_n : |\mathrm{Im}\ \alpha| \leq r\}$ $(2 \leq r \leq n-1)$ to be $\mathrm{rank}(\mathcal{DP}_{n,r}) = \mathrm{rank}(\mathcal{ODP}_{n,r}) = \binom{n}{r}$.

The authors of [2] obtained $F(n; p)$ to be $\frac{2(2n-p+1)}{p+1}\binom{n}{p}$ (where $F(n, p) = \{\alpha \in \mathcal{DP}_n : |\mathrm{Im}\ \alpha| = p\}$). In particular, they obtained the order of the semigroup to be $|\mathcal{DP}_n| = 3 \cdot 2^{n+1} - (n+2)^2 - 1$.

[*]Corresponding Author; E-mail: mmzubairu.mth@buk.edu.ng
[†]Department of Mathematical Sciences, Bayero University, Kano, Nigeria
[‡]E-mail: zdlawan.sce@buk.edu.ng
[§]Department of Science, School of Continuing Education, Bayero University, Kano, P.M.B 3011, Nigeria

Now let D be a non empty subset of $[n]$ and $\mathcal{DP}_n$ be as defined in equation (1), and let

$$\text{Fix}([n], D) = \{\alpha \in \mathcal{DP}_n : d\alpha = d, \text{for all } d \in D\}. \tag{3}$$

Notice that for all $\alpha, \beta \in \text{Fix}([n], D)$ and $d \in D$, $d(\alpha\beta) = (d\alpha)\beta = d\beta = d$. Thus, $\text{Fix}([n], D)$ is a subsemigroup of $\mathcal{DP}_n$. Moreover, it is clear that $Id_{[n]} \in \text{Fix}([n], D)$ (where $Id_{[n]}$ denote the identity map on $[n]$) for every nonempty subset $D \subseteq [n]$. Thus, $\text{Fix}([n], D)$ is a monoid. Notice also that if $D = [n]$ then $\text{Fix}([n], D) = \{Id_{[n]}\} \cong \mathbb{Z}_1$. So, for the remaining content of the paper, we shall assume $\emptyset \neq D \subsetneq [n]$.

On this note, we investigate the algebraic, combinatorial, and rank properties of $\text{Fix}([n], D)$. Section 1 of this paper contains the definitions of basic terms so as to give the reader a proper understanding. In Section 2, we show that the semigroup $\text{Fix}([n], D)$ is a semilattice of idempotents, and in Section 3, we obtain the cardinality and the rank of the semigroup. For $\alpha, \beta \in \text{Fix}([n], D)$, we shall write the composition of α and β as $x(\alpha \circ \beta) = ((x)\alpha)\beta$ for all $x \in \text{Dom } \alpha$.

Let S be a semigroup, for a subset A of S, A is said to be a *generating set of* S if every element of S can be written as a product of elements of A. If A generates S we simply write $\langle A \rangle = S$. The rank of a finite semigroup S is defined and denoted by

$$\text{rank}(S) = \min\{|A| : A \subset S, \langle A \rangle = S\}.$$

An element $a \in S$ is an idempotent if $a^2 = a$. The collection of all idempotent of S is usually denoted by $E(S)$. A map $\alpha \in \text{Fix}([n], D)$ is an idempotent if and only if $\text{Im } \alpha = F(\alpha) = \{x \in \text{Dom } \alpha : x\alpha = x\}$. We shall denote $f(\alpha)$ to be $|F(\alpha)|$. A semigroup S is said to be a *semilattice* if for all $a, b \in S$: $a^2 = a$ and $ab = ba$. For basic concept in semigroup theory, we refer the reader to [4, 7, 10].

To begin our investigation, we record the following results from [1].

Lemma 1 ([1], Lemma 1.2). *Let $\alpha \in \mathcal{DP}_n$. Then we have the following conditions:*

(a) The map α is either order-preserving or order-reversing. Equivalently, α is either a translation or a reflection.

(b) If $h(\alpha) = p$, then $f(\alpha) = 0$ or 1 or p.

(c) If α is order-preserving and $f(\alpha) \geq 1$, then α is a partial identity.

Throughout this paper, unless otherwise specified, we shall consider $D = \{d_1, d_2, \ldots, d_r\} \subseteq [n]$ with $0 < r < n$, and $d_i < d_j$ if and only if $i < j$. Obviously, since $D \neq \emptyset$, then by our assumption, we shall have $1 \leq r < n$. Moreover, as a consequence of Lemma 1, we have the following lemma.

Lemma 2. *Every $\alpha \in \text{Fix}([n], D)$ can be expressed as*

$$\alpha = \begin{pmatrix} d_1 & \cdots & d_r & b_1 & \cdots & b_p \\ d_1 & \cdots & d_r & b_1 & \cdots & b_p \end{pmatrix},$$

where $r + p < n$ and $\{b_j : 1 \leq j < r + p\} \subseteq [n] \setminus D$.

Notice that $\{b_j : 1 \leq j < r + p\}$ may not necessarily be part of $\text{Dom } \alpha$ and also if $r + p = n$, then $\alpha = Id_{[n]}$. Consequently by Lemma 1, we readily have the following remark.

Remark 1.1. Let $\alpha \in \text{Fix}([n], D)$. Then α is a partial identity and hence every element of $\text{Fix}([n], D)$ is an idempotent.

Now for the remaining content of the paper, unless or otherwise specified we shall refer to $\alpha, \beta \in \text{Fix}([n], D)$ to be expressed as

$$\alpha = \begin{pmatrix} d_1 & \cdots & d_r & b_1 & \cdots & b_p \\ d_1 & \cdots & d_r & b_1 & \cdots & b_p \end{pmatrix} \text{and } \beta = \begin{pmatrix} d_1 & \cdots & d_r & c_1 & \cdots & c_m \\ d_1 & \cdots & d_r & c_1 & \cdots & c_m \end{pmatrix}, \tag{4}$$

where $r + p < n$, $r + m < n$.

The following result shows that the monoid $\text{Fix}([n], D)$ is commutative.

Lemma 3. *The monoid* $\text{Fix}([n], D)$ *is commutative.*

Proof. Let $\alpha, \beta \in \text{Fix}([n], D)$ be as expressed in equation (4). Then we may assume without loss of generality that $m \leq p$. Thus, there are two cases to consider.

Case 1: If $\{b_i : 1 \leq i \leq p\} \cap \{c_i : 1 \leq i \leq m\} = \emptyset$. Then,

$$\alpha\beta = \begin{pmatrix} d_1 & \cdots & d_r \\ d_1 & \cdots & d_r \end{pmatrix} = \beta\alpha.$$

Case 2: If $\{b_i : 1 \leq i \leq p\} \cap \{c_i : 1 \leq i \leq m\} \neq \emptyset$. Then $\{b_i : 1 \leq i \leq p\} \cap \{c_i : 1 \leq i \leq m\} = \{a_i : 1 \leq i \leq t \text{ for some } t \leq m\}$. Thus,

$$\alpha\beta = \begin{pmatrix} d_1 & \cdots & d_r & a_1 & \cdots & a_t \\ d_1 & \cdots & d_r & a_1 & \cdots & a_t \end{pmatrix} = \beta\alpha.$$

The result now follows.

Hence, we have actually proved the following result.

Theorem 1. *Let* $\text{Fix}([n], D)$ *be as defined in equation* (3)*, then* $\text{Fix}([n], D)$ *is a semilattice of idempotents.*

2 Green's relations on the monoid $\text{Fix}([n], D)$

The main aim of this section is to describe Green's relations on the monoids $\text{Fix}([n], D)$. For the definitions of Green's relations, we refer the reader to [7, 10].

Theorem 2. *Let* $\alpha, \beta \in \text{Fix}([n], D)$ *be as expressed in equation* (4) *with* $m = p$*. Then*

(i) $(\alpha, \beta) \in \mathcal{L}$ *if and only* $\alpha = \beta$*;*

(ii) $(\alpha, \beta) \in \mathcal{R}$ *if and only* $\alpha = \beta$*.*

Proof. (i) Let $\alpha, \beta \in \text{Fix}([n], D)$ be as expressed in equation (4) such that $(\alpha, \beta) \in \mathcal{L}$. This means that there exist $\gamma_1, \gamma_2 \in \text{Fix}([n], D)$ such that

$$\alpha = \gamma_1\beta \text{ and } \beta = \gamma_2\alpha.$$

Notice that $\text{Dom}\ \alpha = \{d_1, \ldots, d_r, b_1, \ldots, b_p\}$ and $\text{Dom}\ \beta = \{d_1, \ldots, d_r, c_1, \ldots, c_p\}$. Now for $d_i \in \text{Dom}\ \alpha$ $(1 \leq i \leq r)$ (which is also in $\text{Dom}\ \beta$)

$$d_i\alpha = d_i\gamma_1\beta = (d_i\gamma_1)\beta = d_i\beta.$$

Also, for $b_i \in \text{Dom}\ \alpha$ and $c_i \in \text{Dom}\ \beta$ $(1 \leq i \leq p)$,

$$b_i\alpha = (b_i\gamma_1)\beta = b_i\beta \text{ and}$$

$$c_i\beta = (c_i\gamma_2)\alpha = c_i\alpha.$$

Thus $\alpha = \beta$. The converse follows easily.

(ii) Let $\alpha, \beta \in \text{Fix}([n], D)$ be as expressed in equation (4) such that $(\alpha, \beta) \in \mathcal{R}$. This means that there exists $\gamma_1, \gamma_2 \in \text{Fix}([n], D)$ such that

$$\alpha = \beta\gamma_1 \text{ and } \beta = \alpha\gamma_2.$$

Notice that $\text{Dom}\ \alpha = \{d_1, \ldots, d_r, b_1, \ldots, b_p\}$ and $\text{Dom}\ \beta = \{d_1, \ldots, d_r, c_1, \ldots, c_p\}$. Now for $d_i \in \text{Dom}\ \alpha$ $(1 \leq i \leq r)$

$$d_i\alpha = d_i\beta\gamma_1 = (d_i\beta)\gamma_1 = d_i\gamma_1 = d_i,$$

$$d_i\beta = d_i\alpha\gamma_2 = (d_i\alpha)\gamma_2 = d_i\gamma_2 = d_i.$$

Thus, we have $d_i\alpha = d_i\beta$. Moreover, for $b_i \in \text{Dom}\ \alpha$ and $c_i \in \text{Dom}\ \beta$ $(1 \leq i \leq p)$,

$$b_i\alpha = b_i\beta\gamma_1 = (b_i\beta)\gamma_1 = b_i\gamma_1 = b_i. \tag{5}$$

Notice that β is defined on b_i, i.e., $b_i \in \text{Dom}\ \beta$. Hence,

$$b_i\beta = (b_i\alpha)\gamma_2 = b_i\gamma_2 = b_i. \tag{6}$$

From equation (5) and (6) we have $b_i\alpha = b_i\beta$.

In a similar way, one can show that $c_i\beta = c_i\alpha$. Thus $\alpha = \beta$.

Consequently we have the following corollary.

Corollary 1. *On the semigroup* $\text{Fix}([n], D)$, $\mathcal{L} = \mathcal{R} = \mathcal{J} = \mathcal{D} = \mathcal{H}$.

Now as a consequence of corollary 1, we readily have the following result.

Theorem 3. *Every* H_α $(\alpha \in \text{Fix}([n], D))$ *is a maximal subgroup of* $\text{Fix}([n], D)$ *isomorphic to the trivial group* $\mathbb{Z}_1$.

3 The combinatorial and rank properties of $\text{Fix}([n], D)$

In this section, we determine the cardinality and the rank of the monoid $\text{Fix}([n], D)$. These properties heavily depend on the size of the subset D, as we shall see below.

Now for $0 \leq k \leq n - r$, let $F(n;\ k) = |J_k|$ where $J_k = \{\alpha \in \text{Fix}([n], D) : |\text{Im}\ \alpha \setminus D| = k\}$. We now record the following results.

Proposition 1. *For* $0 \leq k \leq n - r$,

$$F(n, k) = \binom{n-r}{k}.$$

Proof. Let $D \subsetneq [n]$ such that $|D| = r$, i.e., we fixed r elements from the chain $[n]$. Out of the remaining $n-r$ elements we can select k $(0 \leq k \leq n-r)$ elements to formulate a partial identity from the $n - r$ elements. This can be done in $\binom{n-r}{k}$ ways, as required.

Theorem 4. *Let* $\text{Fix}([n], D)$ *be as defined in equation* (3). *Then* $|\text{Fix}([n], D)| = 2^{n-r}$.

Proof. Using Proposition 1, we see that

$$|\text{Fix}([n], D)| = \sum_{k=0}^{n-r} F(n,\ k) = \sum_{k=0}^{n-r} \binom{n-r}{k} = 2^{n-r},$$

as required.

Now for $0 \leq p \leq n - r - 1$, let

$$L(n - r,\ p) = \{\alpha \in \text{Fix}([n], D) : |\text{Im}\ \alpha \setminus D| \leq p\} \tag{7}$$

and recall that

$$J_k = \{\alpha \in \text{Fix}([n], D) : |\text{Im}\ \alpha \setminus D| = k\}.$$

Obviously, $J_0 \cup J_1 \cup \ldots \cup J_p = L(n - r,\ p)$, which is a two sided ideal of $\text{Fix}([n], D)$ for all p.

We now state the following lemma.

Lemma 4. *Every element in* J_k $(0 \leq k \leq p \leq n - r - 2)$ *can be express as a product of elements in* J_{k+1}.

Proof. Let $\alpha \in J_k$. Then α can be expressed as

$$\alpha = \begin{pmatrix} d_1 & \cdots & d_r & b_1 & \cdots & b_k \\ d_1 & \cdots & d_r & b_1 & \cdots & b_k \end{pmatrix}.$$

Now, since $p \leq n - r - 2$, we can choose two elements say $x, y \in [n] \setminus \text{Dom}\ \alpha$ such that $x \neq y$ and let

$$\beta = \begin{pmatrix} d_1 & \cdots & d_r & b_1 & \cdots & b_k & x \\ d_1 & \cdots & d_r & b_1 & \cdots & b_k & x \end{pmatrix}$$

and

$$\gamma = \begin{pmatrix} d_1 & \cdots & d_r & b_1 & \cdots & b_k & y \\ d_1 & \cdots & d_r & b_1 & \cdots & b_k & y \end{pmatrix}.$$

Then clearly $\beta, \gamma \in J_{k+1}$ and obviously $\alpha = \beta\gamma$.

Consequently, we have the following corollary.

Corollary 2. $J_k \subseteq \langle J_{k+1} \rangle$ $(0 \leq k \leq p \leq n-r-2)$.

We now use the following Lemmas to deduce the rank of the two sided ideal $L(n-r, p)$.

Lemma 5. *For* $0 \leq p \leq n-r-1$, *the ideal* $L(n-r, p)$ *has* $\binom{n-r}{p}$ $\mathcal{D}-$*classes of height* p.

Proof. The result follows from Proposition 1.

Lemma 6. *Let* $0 \leq p \leq n-r-1$ *and* $G = \{\alpha \in L(n-r, p) : |\text{Im } \alpha \setminus D| = p\}$. *Then* G *is the minimum generating set of* $L(n-r, p)$.

Proof. Notice that $J_p = G$. Now by Corollary 2, we see that $J_{p-1} \subseteq \langle J_p \rangle$. Similarly, $J_{p-2} \subseteq \langle J_{p-1} \rangle, \ldots, J_0 \subseteq \langle J_1 \rangle$. Consequently, $J_0 \cup J_1 \cup J_2 \cup \ldots \cup J_p \subseteq \langle J_p \rangle$, i.e., $L(n-r, p) \subseteq \langle J_p \rangle$. Thus G is a generating set of $L(n-r, p)$. Notice that $L(n-r, p)$ is $\mathcal{D}$ trivial as such every $\mathcal{D}-$class in J_p contains one and only one element since $\mathcal{D} = \mathcal{J}$. This element is maximal and hence J_p is the unique minimum generating set.

Proposition 2. *For* $0 \leq p \leq n-r-1$, *rank* $(L(n-r, p)) = \binom{n-r}{p}$.

Proof. The proof follows directly from Lemma 5 and 6.

Consequently, we deduce the following results.

Lemma 7. *rank* $(\text{Fix}([n], D) \setminus \{id_{\{n\}}\}) = n-r$.

Proof. Notice that if $p = n-r-1$ then $\text{Fix}([n], D) \setminus \{id_{[n]}\} = L(n-r, n-r-1)$. Thus the results now follows easily from Proposition 2.

We now have the following result.

Theorem 5. *Let* $\text{Fix}([n], D)$ *be as expressed in equation* (3). *Then rank* $(\text{Fix}([n], D)) = n-r+1$.

Proof. Notice that $\text{Fix}([n], D) = \text{Fix}([n], D) \setminus \{id_{[n]}\} \cup \{id_{[n]}\}$. Thus rank $(\text{Fix}([n], D))$ = rank $(\text{Fix}([n], D) \setminus \{id_{[n]}\})$+ rank $(\{id_{[n]}\})$. Now the result follows using Lemma 7.

3.1 Isomorphism property in $\text{Fix}([n], D)$

In this subsection, we give a necessary and sufficient conditions for the monoids $\text{Fix}([n], D_1)$ and $\text{Fix}([n], D_2)$ to be isomorphic, where $D_1, D_2 \subseteq [n]$.

Lemma 8. *Let* D_1 *and* D_2 *be nonempty subsets of* $[n]$. *Then* $\text{Fix}([n], D_1) \cong \text{Fix}([n], D_2)$ *if and only if* $|D_1| = |D_2|$.

Proof. Let $|D_1| = r$, $|D_2| = k$ and suppose that there exists an isomorphism $\varphi : \text{Fix}([n], D_1) \to \text{Fix}([n], D_2)$. This means that $|\text{Fix}([n], D_1)| = |\text{Fix}([n], D_2)|$. This implies

$$2^{n-r} = 2^{n-k}, \text{ and as such } r = k.$$

Thus $|D_1| = |D_2|$, as required.

Conversely, suppose $|D_1| = |D_2|$. Then $|[n] \setminus D_1| = |[n] \setminus D_2|$. Now let $D_1 = \{d_1 < \ldots < d_r\}, D_2 = \{d'_1 < \ldots < d'_r\}, [n] \setminus D_1 = \{a_1 < \ldots < a_r\}$ and $[n] \setminus D_2 = \{a'_1 < \ldots < a'_r\}$. Define θ as

$$\theta = \begin{pmatrix} d_1 & \cdots & d_r & a_1 & \cdots & a_k \\ d'_1 & \cdots & d'_r & a'_1 & \cdots & a'_k \end{pmatrix}.$$

Clearly θ is a bijection and hence

$$\theta^{-1} = \begin{pmatrix} d'_1 & \cdots & d'_r & a'_1 & \cdots & a'_k \\ d_1 & \cdots & d_r & a_1 & \cdots & a_k \end{pmatrix}.$$

Now, define $\phi : \text{Fix}([n], D_1) \to \text{Fix}([n], D_2)$ by $\alpha\phi = \theta^{-1}\alpha\theta$ for all $\alpha \in \text{Fix}([n], D_1)$. Clearly, ϕ is an isomorphism.

4 Conclusion

In this paper, we successfully studied the subsemigroup $\text{Fix}([n], D)$ of the semigroup $\mathcal{DP}_n$, consisting of all partial isometries of a finite chain $[n]$. We established that the subsemigroup is a monoid and forms a semilattice of idempotents. Furthermore, we determined its cardinality and rank. These results provide a deeper understanding of the algebraic structure of the monoid $\text{Fix}([n], D)$.

References

[1] Alkharousi, F., Kehinde, R. and Umar, A. (2016). On the semigroup of partial isometries of a finite chain, Comm. Algebra, 44(2), 639–647.

[2] Alkharousi, F., Kehinde, R. and Umar, A. (2014). Combinatorial results for certain semigroups of partial isometries of a finite chain, Australas . J. Combin., 58(3), 365–375.

[3] Garba, G. U. (1994). On the idempotents ranks of certain semigroups of order-preserving transformation, Port. Math., 51(2).

[4] Ganyushkin, O. and Mazorchuk, V. (2009). Classical Finite Transformation Semigroups. Springer−Verlag, London.

[5] Bugay, L., Yagci, M. and Ayik, H. (2018). The ranks of certain semigroups of partial isometries, Semigroup Forum, 97(2), 214-222.

[6] Honyam, P., Sanwong, J. (2013). Semigroups of transformations with fixed sets, Questiones Mathematicae, 36(1), 79–92.

[7] Higgins, P. M. (1992). Techniques of semigroup theory. Oxford university Press.

[8] Howie, J.M., Robertson, E.F. and Schein, B. M. (1988). A combinatorial property of finite full transformation semigroups, Proc. R. Soc. Edinb., 109A, 319–328.

[9] Howie, J. M. (1966). The Subsemigroup generated by the idempotents of a full transformation semigroup, J. Lond. Math. Soc., 41, 707–716.

[10] Howie, J. M. (1995). Foundamentals of Semigroup Theory. Oxford University Press.

[11] Namnak, C., Laysirikul, E. and Sawatraksa, N. (2018). Natural patial order on the semigroups of partial isometries of a finite chain, Thai. J. Math., 97–108.

[12] Demitrova, I. (2013). The maximal subsemigroups of the semigroups of all partial order preserving isometries. Proceeding of the 5th International Scientific CONFERENCE-FMNS. Vol. 1. Mathematics and Informatics, 95–101.

[13] Nuttawoot, N., Chollawat, P. (2021). Domination parameters on Cayley digraphs of transformation semigroups with fixed sets, Turk. J. Math., 45(4), 1775-1788.

[14] Nuttawoot, N., Chollawat, P. (2020) On connectedness and completeness of Cayley digraphs of transformation semigroups with fixed sets,Int. Elect. J. Algebra, 28(28), 110-126.

[15] Chaiya, Y., Honyam, P. and Sanwong, J. (2016). Natural partial orders on the semigroups of full transformation with fixed sets, Int. J. Math. Math. Sci., 2759090.

[16] Fernandes, V.H., Quinteiro, T.M. (2016). Presentations for monoids of finite partial isometries, Semigroup Forum, 93(1), 97–110.

[17] Umar, A. and Al-Kharousi, F. (2012). Studies in semigroup of contraction mappings of a finite chain. The Research council of Oman Research grant proposal No. ORG/CBS/12/007.

[18] Chaiya, y., Honyam, p. and Sanwong, J. (2017). Maximal subsemigroups and finiteness conditions on transformation semigroups with fixed sets, Turk. J. Math., **41**(1).

A hybrid method of block pulse with Bernstein polynomial for numerical solution of linear ill-posed first kind Fredholm Integal equation

H.S. Musa[*†] and **S.L. Bichi**[†‡]

Abstract

This study presents an effective method for approximating solutions to first-kind Fredholm integral equations using a hybrid approach combining Block-Pulse and Bernstein polynomials. The method transforms the integral equation into a system of linear algebraic equations by exploiting the properties of the hybrid functions. Additionally, we estimate the error bound under the L_2 norm to assess the accuracy of the approach. To validate the method's effectiveness, we apply it to some test problems with known exact solutions, demonstrating its reliability and efficiency.

Keywords and phrases: First kind Fredholm integral equation; Hybrid functions; Convergence analysis;

1 Introduction

Integral equations are vital mathematical tools extensively used in applied sciences, including mathematics, physics, and engineering, often serving as alternative formulations for differential equations. Among these, Fredholm integral equations are particularly significant due to their applications in various scientific fields. First-kind Fredholm integral equations arise in radiography, spectroscopy, cosmic radiation studies, image processing, and signal processing. In physics, they are instrumental in plasma diagnostics, physical electronics, nuclear physics, and optical imaging. Furthermore, several mathematical problems, such as harmonic continuation, the backward heat equation, numerical inversion of the Laplace transform, and numerical differentiation, can be reformulated as first-kind Fredholm integral equations [1, 2, 3]. These equations are characterised by the presence of the unknown function $f(t)$ solely within the integral sign. Furthermore, first-kind Fredholm integral equations typically exhibit the following form:

$$\int_a^b k(t,s)f(s)ds = g(s) \qquad s \in D, \tag{1}$$

The presence of $f(t)$ within the integral sign introduces specific challenges. First-kind Fredholm integral equations often manifest as ill-posed problems, which can either lack a solution entirely or, if a solution exists, it may not be unique and may not exhibit continuous dependence on the data $g(s)$ [4]. It is widely recognized that analytically solving first-kind Fredholm integral equations is typically difficult, and exact solutions are rare. Consequently, a computational approach to solving these equations becomes crucial in scientific investigation.

Tikhonov introduced various regularisation methods to address first-kind integral equations [5, 6] with Rajan [7] analyzing its convergence under the supremum norm. Wazwaz [4] utilised a regularisation method in conjunction with existing techniques to manage ill-posed first-kind Fredholm integral

[*]Corresponding Author; E-mail: shajara292@gmail.com
[†]Department of Mathematical Sciences, Bayero University, Kano, Nigeria
[‡]slawanbh@gmail.com

equations. Molabahrami [8] combined regularisation and integral mean value theorem methods to address ill-posedness in both linear and nonlinear first-kind Fredholm integral equations. Suliman *et.al* [9] introduced a constrained perturbation regularization for linear least-squares problems termed constrained perturbation regularisation. Additionally,[10] proposed the homotopy regularization method for solving both linear and nonlinear first-kind Fredholm integral equations, demonstrating its effectiveness in overcoming ill-posedness. Despite these advancements, there remains a need for methods that combine the computational efficiency of basis functions with the robustness of regularization techniques. Block-Pulse functions were originally introduced in electrical engineering by Harmuth, after which numerous researchers explored their applications [11, 12]. Bernstein polynomials have found applications across various fields of mathematics [13, 14].

Recently, hybrid functions have seen extensive use in addressing diverse types of integral equations [15, 16], integro-differential equations [17, 18], and control problems [19, 20]. One of the key attributes of these hybrid functions is their efficiency and broad applicability. Examples include hybrid Chebyshev and block-pulse functions [21, 22], hybrid Legendre and block-pulse functions [23, 24, 25], hybrid Taylor and block-pulse functions [26], hybrid Fourier and block-pulse functions [27], hybrid Bernstein polynomials and block-Pulse functions [28, 29], hybrid improved block pulse and Bernstein polynomials [30].

However,the hybridization of block-pulse and Bernstein polynomial have been successful in other contexts but remains underexplored, particularly in the context of ill-posed first-kind Fredholm integral equations. Hybrid block pulse and Bernstein polynomial have independently demonstrated strengths in numerical computations. Their combination could provide a synergistic effect, enhancing both accuracy and computational efficiency.

1.1 Preliminaries

In this section, we revisit certain definitions and characteristics of Bernstein polynomials and Block-Pulse functions.

Definition 1.1. ***Definition 1.1*** *(Bernstein polynomials) The Bernstein polynomials of* m^{th} *degree are defined on the interval* $[a, b]$ *as:*

$$B_{i,m}(t) = \binom{m}{i} \frac{(t-a)^i (b-t)^{m-i}}{(b-a)^m} \quad a \le t \le b, \;\; i = 0, 1, 2, \cdots m, \tag{2}$$

where;

$$\binom{m}{i} = \frac{m!}{i!(m-i)!}.$$

The Bernstein polynomials constitute a basis on $L^2[a, b]$ comprisig of $m+1$ polynomials of degree m. Consequently any polynomial of $m - th$ degree can be expressed as linear combination of $B_{i,m}(t)$ for $i = 0, 1, \cdots m$ [31].

Lemma 1

Consider the N-set of block-pulse function $\{b_n(t) n = 1, 2, \cdots N\}$ be defined over the interval $[0, 1)$ as:

$$b_n(t) = \begin{cases} 1 & \frac{n-1}{N} \le t < \frac{n}{N} \\ \\ 0 & otherwise \end{cases}, \tag{3}$$

where N is a positive integer and $b_n(t)$ is the n^{th} block-pulse function. The fundamental characteristics include disjointness, orthogonality, and completeness [32].

Proof.

The property of disjointness can be readily derived from the definition of block-pulse functions, as outlined below:

$$b_n(t)b_m(t) = \begin{cases} b_n(t) & n = m \\ \\ 0 & n \neq m \end{cases}, \tag{4}$$

where $n, m = 1, 2, \cdots, N$.

The block pulse functions also exhibit orthogonality within the interval $t \in [0, T)$:

$$\int_0^T b_n(t)b_m(t)dt = \begin{cases} h & n = m \\ \\ 0 & n \neq m \end{cases}, \tag{5}$$

where $n, m = 1, 2, \cdots, N$.

This characteristic is directly inferred from the disjointness of block pulse functions. The orthogonality property of block pulse functions serves as the foundation for expanding functions into their block pulse series.

For the completeness property, as the number of block pulse functions N approaches infinity, the set of block pulse functions becomes complete. For any function f belonging to $L^2([0, 1))$Parseval's identity holds:

$$\int_0^1 f(t)dt = \sum_{n=0}^{\infty} f_n^2 ||b_n(t)||_2,$$

where;

$$f_n = \frac{1}{h}\int_0^1 f(t)b_n(t)dt. \tag{6}$$

Definition 1.2. *Definition 1.2 (Hybrid block pulse and Bernstein polynomial HBB [33]). The combination of block-pulse and Bernstein polynomial functions are defined over the interval* $[0, 1)$ *for* $i = 0, 1, 2 \cdots m$ *and* $n = 1, 2 \cdots N$ *as:*

$$h_{n,i} = \begin{cases} B_{i,m}(Nt - n + 1) & \frac{n-1}{N} \leq t < \frac{n}{N} \\ \\ 0 \quad otherwise \end{cases}. \tag{7}$$

2 Methodology

2.1 Function approximation

A function $f(t) \in L^2[0, 1)$ can be expanded in terms of hybrid functions as follows:

$$f(t) \approx \sum_{n=1}^{N}\sum_{i=0}^{m} c_{n,i}h_{n,i} = C^T\Omega(t), \tag{8}$$

where;

$\Omega^T(t) = [h_{1,0}(t), h_{1,1}(t) \cdots h_{1,m}(t) \quad \cdots \quad h_{N,0}(t), h_{N,1}(t) \ \cdots \ h_{N,m-1}(t), h_{N,m}(t)]$ and

$$C^T = [c_{1,0}, c_{1,1} \cdots c_{1,m} \quad \cdots \quad c_{N,0}, c_{N,1} \ \cdots \ c_{N,m-1}, c_{N,m}],$$

and we have

$$C^T = \frac{\langle f, \Omega(t)\rangle}{\langle \Omega(t), \Omega(t)\rangle},$$

then

$$C = J^{-1}\left(\int_0^1 f(t)\Omega(t)^T dt\right).$$

Similarly, the function $k\,(t,s) \in L^2([0,1)\times[0,1)$ can be estimated as:

$$k\,(t,s) \approx \Omega^T(t)K\Omega(s), \tag{9}$$

where K is an $N(m+1)\times N(m+1)$ matrix called the kernel matrix and enteries of the matrix is given by:

$$k_{i,j} = \frac{\langle h_i(t),(k(t,s)h_j(s))\rangle}{\langle h_i(t),h_i(t)\rangle\langle h_j(s)h_j(s)\rangle} \quad i,j = 1,2\cdots N(m+1), \tag{10}$$

$$K = J^{-1}\langle\Omega(t),k(t,s),\Omega(s)\rangle J^{-1}. \tag{11}$$

2.2 Integration of cross product

The integration of the cross product of two hybrid function vectors $\Omega(t)$ is defined by:

$$J = \int_0^1 \Omega(t)\Omega(t)^T dt, \tag{12}$$

where;

$$J = \frac{1}{N}\begin{bmatrix} Q_1 & \vec{0} & ... & \vec{0} \\ \vec{0} & Q_2 & ... & \vec{0} \\ \vdots & & & \\ \vec{0} & \vec{0} & ... & Q_N \end{bmatrix}. \tag{13}$$

and $\vec{0}$ is an $(m+1)\times(m+1)$ matrix, also $Q_n(n=1,2,\cdots N)$ is an $(m+1)\times(m+1)$ defined by;

$$\begin{aligned}(Q_n) &= \begin{bmatrix} \frac{\binom{m}{i}\binom{m}{j}}{(2m+1)\binom{2m}{i+j}} & \frac{\binom{m}{i}\binom{m}{j}}{(2m+1)\binom{2m}{i+j}} & \cdots & \frac{\binom{m}{i}\binom{m}{j}}{(2m+1)\binom{2m}{i+j}} \\ \frac{\binom{m}{i}\binom{m}{j}}{(2m+1)\binom{2m}{i+j}} & \frac{\binom{m}{i}\binom{m}{j}}{(2m+1)\binom{2m}{i+j}} & \cdots & \frac{\binom{m}{i}\binom{m}{j}}{(2m+1)\binom{2m}{i+j}} \\ \vdots & & & \\ \frac{\binom{m}{i}\binom{m}{j}}{(2m+1)\binom{2m}{i+j}} & \frac{\binom{m}{i}\binom{m}{j}}{(2m+1)\binom{2m}{i+j}} & \cdots & \frac{\binom{m}{i}\binom{m}{j}}{(2m+1)\binom{2m}{i+j}} \end{bmatrix} n = 1,2,\cdots N, \\ i,j &= 0,1,2\cdots m.\end{aligned} \tag{14}$$

We now present a numerical direct approach for solving equation (1) using a hybrid function comprised of block pulse and Bernstein polynomial. For this purpose, we approximate the functions in equation(1) , as mentioned earlier, in the form;

$$f(t) \approx F^T\Omega(t), \tag{15}$$

$$k(t,s) \approx \Omega^T(t)K\Omega(s), \tag{16}$$

and

$$g\,(t) \approx G^T\Omega(t), \tag{17}$$

where K is an $N(m+1)\times N(m+1)$ dimensional matrix and G is a known $N(m+1)\times 1$ vector. In equation (15), F is an unknown $N(m+1)\times 1$ vector. By substituting equation(15)-(17) in to equation (1), we have;

$$\int_0^1 \Omega^T(t)K\Omega(s)\Omega^T(s)Fds = \Omega^T(t)G, \tag{18}$$

or

$$\Omega^T(t)K\int_0^1 \Omega(s)\Omega^T(s)Fds = \Omega^T(t)G. \tag{19}$$

using equation (12), equation (19) can be replaced by

$$\Omega^T(t)KJF = \Omega^T(t)G \tag{20}$$

Therefore, we have the following linear system of equations:

$$(KJ)F = G \tag{21}$$

by solving the linear system (21) we find the unknown vector F,where K is an $N(m+1)\times N(m+1)$ matrix and J is the dual operational matrix of $\Omega(t)$ which is an $N(m+1)\times N(m+1)$ matrix derived from the previous section, F is an unknown $N(m+1)\times 1$ vector and G is an known $N(m+1)\times 1$ vector.

3 Error analysis

The objective of this section is to outline the convergence characteristics of the proposed numerical method. We aim to demonstrate that, under suitable conditions, the approximate solution derived from our approach converges to the exact solution of Equation (1). To achieve this, we provide the following theorem and lemma for convergence analysis.

Lemma 2. Let $f\in C^{m+1}[0,1)$ is an $m+1$ times continuously differentiable function such that $f\approx \sum_{n=1}^{N} f_n$ and let $Y_n = span\left\{h_{n0}(t), h_{n1}(t)\cdots h_{nm}(t)\right\}\ n=1,2,\cdots N$. If $C_n^T\Omega_n(t)$ is the best approximation to f_n from Y_n , where $C_n=[c_{n0},c_{n1}...c_{nm}]^T$
and $\Omega_n(t)=[h_{n0}(t), h_{n1}(t)\cdots h_{nm}(t)]^T$ then $p_{N(m+1)}(f)(t)=C^T\Omega(t)$ approximates $f(t)$ with the following error bound:

$$\begin{aligned} \left\|f(t)-p_{N(m+1)}(f)(t)\right\|_2 &\leq \frac{\mu}{(m+1)!N^{m+1}\sqrt{(2m+3)}}. \\ where\ \mu &= \max_{t\in[0,1)}\left|f^{m+1}(t)\right| \end{aligned} \tag{22}$$

Proof. The Taylor expansion for the function $f_n(t)$ is given as:

$$\begin{aligned} f_n(t) &= f_n\left(\frac{n-1}{N}\right)+f_n'\left(\frac{n-1}{N}\right)\left(t-\frac{(n-1)}{N}\right)+...+\frac{f_n^m}{m!}\left(\frac{n-1}{N}\right)\left(t-\frac{(n-1)}{N}\right)^m \\ &\quad +\frac{f_n^{m+1}}{m+1!}\left(\frac{n-1}{N}\right)\left(t-\frac{(n-1)}{N}\right)^{m+1}+... \\ t &\in \left[\frac{n-1}{N},\frac{n}{N}\right), \end{aligned} \tag{23}$$

for which it is known that:

$$\left|f_n(t)-\tilde{f}_n(t)\right| \leq \left|f^{m+1}(\theta)\right|\frac{\left(t-\frac{n-1}{N}\right)^{m+1}}{(m+1)!},\quad \theta\in\left[\frac{n-1}{N},\frac{n}{N}\right),\quad n=1,2,\cdots N.$$

Since $C_n^T\,\Omega_n(t)$ is the best approximation to $\tilde{f}_n$ from Y_n we have;

$$\left\|f_n(t)-C_n^T\Omega_n(t)\right\|_2^2=\left\|f_n(t)-\tilde{f}_n(t)\right\|_2^2=\int_{\frac{n-1}{N}}^{\frac{n}{N}}\left|f_n(t)-\tilde{f}_n(t)\right|^2dt.$$

Now;

$$\begin{aligned}\left\|f_n(t)-C_n^T\Omega_n(t)\right\|_2^2 &\leq \left(\frac{\mu}{(m+1)!}\right)^2\int_{\frac{n-1}{N}}^{\frac{n}{N}}\left(t-\frac{n-1}{N}\right)^{2m+2}dt,\\ &= \left(\frac{\mu}{(m+1)!}\right)^2\frac{1}{(2m+3)\,N^{2m+3}},\end{aligned}\tag{24}$$

where $\mu=\max\left|f^{m+1}(\theta)\right|\quad\theta\in[0,1)$.
Now,

$$\begin{aligned}\left\|f-C^T\Omega(t)\right\|_2^2 &\leq \sum_{n=1}^{N}\left\|\left(f_n(t)-C_n^T\Omega_n(t)\right)\right\|_2^2\\ &\leq \frac{\mu^2}{((m+1)!)^2\,N^{2m+2}(2m+3)}.\end{aligned}\tag{25}$$

By taking the square root of equation (25) we have the bound;

$$\left\|f-C^T\Omega(t)\right\|_2\leq\frac{\mu}{(m+1)!N^{m+1}\sqrt{(2m+3)}}.$$

Theorem 3.1. Theorem 3.1 *In equation (1) suppose that $k(t,s)$ is continuous on the square $[0,1)^2$ and f belong to $C^{m+1}[0,1)$ with $m\geq 1$. Furthermore assume the approximate solution*

$$f(t)\simeq\sum_{n=1}^{N}\sum_{i=0}^{m}f_{ni}h_{ni}(t)=F^T\Omega(t)$$

is given by the hybrid block pulse and Bernstein polynomial method, Now if A is non-singular then

$$\left\|f(t)-\sum_{n=1}^{N}\sum_{i=0}^{m}f_{ni}h_{ni}(t)\right\|_2\leq\left\|A^{-1}\right\|_2\frac{N(m+1)\,c_2}{(m+1)!N^{m+1}}\frac{\sqrt{\frac{4m^3-m}{N(m+1)}}}{m\sqrt{(2m+3)}}.\tag{26}$$

Proof. The estimation provided in (26) is derived as follows:
Let

$$f(t)\simeq f_{N(m+1)}(t)=\sum_{n=1}^{N}\sum_{i=0}^{m}f_{ni}h_{ni}(t),\tag{27}$$

where f_{ni} are unknown coefficients determined by solving the linear system in equation (21). Also suppose;

$$p_{N(m+1)}(f)(t)=\sum_{n=1}^{N}\sum_{i=0}^{m}c_{ni}h_{ni}(t),\tag{28}$$

our goal is to find a bound for $\left\|f(t)-f_{N(m+1)}(t)\right\|_2$, so

$$\left\|f(t)-f_{N(m+1)}(t)\right\|_2\leq\left\|f(t)-p_{N(m+1)}(f)(t)\right\|_2+\left\|p_{N(m+1)}(f)(t)-f_{N(m+1)}(t)\right\|_2,\tag{29}$$

from lemma 2 we have

$$\begin{aligned} \left\| f(t) - p_{N(m+1)}(f)(t) \right\|_2 &\leq \frac{\mu}{(m+1)!N^{m+1}\sqrt{(2m+3)}}, \\ where\ \mu &= \max \left| f^{m+1}(t) \right| \quad t \in [0,1). \end{aligned} \tag{30}$$

We now find a bound for $\left\| p_{N(m+1)}(f)(t) - f_{N(m+1)}(t) \right\|_2$,

$$\begin{aligned} \left\| p_{N(m+1)}(f)(t) - f_{N(m+1)}(t) \right\|_2^2 &= \int_0^1 \left| p_{N(m+1)}(f)(t) - f_{N(m+1)}(t) \right|^2 dt \\ &= \int_0^1 \left| \sum_{n=1}^{N} \sum_{i=0}^{m} (c_{ni} - f_{ni}) h_{ni}(t) \right|^2 dt \\ &\leq \int_0^1 \left(\sum_{n=1}^{N} \sum_{i=0}^{M} |(c_{ni} - f_{ni})| \, |h_\gamma(t)| \right)^2 dt, \end{aligned} \tag{31}$$

where $|h_\gamma(t)| = \sup |h_{ni}(t)| \quad n = 1, 2, \cdots N \quad i, j = 0, 1, \cdots m$ then;

$$\begin{aligned} \left\| p_{N(m+1)}(f)(t) - f_{N(m+1)}(t) \right\|_2^2 &\leq \int_0^1 \sum_{n=1}^{N} \sum_{i=0}^{M} |(c_{ni} - f_{ni})|^2 |h_\gamma(t)|^2 dt \\ &= \sum_{n=1}^{N} \sum_{i=0}^{M} |(c_{ni} - f_{ni})|^2 \alpha \\ &= \|C - F\|_2^2 \alpha, \end{aligned} \tag{32}$$

where $\alpha = \int_0^1 |h_\gamma(t)|^2 dt$.
This implies,

$$\left\| p_{N(m+1)}(f)(t) - f_{N(m+1)}(t) \right\|_2 \leq \|C - F\|_2 \sqrt{\alpha}, \tag{33}$$

if we substitute $f_{N(m+1)}$ as an approximate solution in equation (1) then;

$$\int_0^1 k(t,s) f_{N(m+1)}(s) ds = g(t),$$

but if we use $p_{N(m+1)}(f)(t)$ as an approximate solution in equation (1) we have:

$$\int_0^1 k(t,s) p_{N(m+1)}(f)(s) ds = \tilde{g}(t),$$

by using the numerical method of hybrid block and Bernstein polynomial in equation (21) we have;

$$F = (KJ)^{-1} G = A^{-1} G, \tag{34}$$

$$C = (KJ)^{-1} \tilde{G} = A^{-1} \tilde{G}, \tag{35}$$

where

$$F = [f_{10} \ldots f_{1m} \quad f_{20} \ldots f_{2m} \quad \ldots \quad f_{N0} \ldots f_{Nm}]^T,$$

$$C = [c_{10}...c_{1m} \quad c_{20}...c_{2m} \quad ... \quad c_{N0}...c_{Nm}],$$
$$G = [g_{10}...g_{1m} \quad g_{20}...g_{2m} \quad ... \quad g_{N0}...g_{Nm}]^T,$$
$$\tilde{G} = [\tilde{g}_{10}...\tilde{g}_{1m} \quad \tilde{g}_{20}...\tilde{g}_{2m} \quad ... \quad \tilde{g}_{N0}...\tilde{g}_{Nm}]^T,$$

Also, we observe $C - F = A^{-1}\left(\tilde{G} - G\right)$,
We have the following bound of $\|C - F\|_2$ as

$$\|C - F\|_2 \leq \left\|A^{-1}\right\|_2 \left\|\left(\tilde{G} - G\right)\right\|_2 \tag{36}$$

then it is enough to find a bound for $\left\|\left(\tilde{G} - G\right)\right\|_2$ but before then we need a bound for $\|(\tilde{g}(t) - g(t))\|_2$, Now from equation 1;

$$\begin{aligned} g(t) &= \int_0^1 k(t,s) f(s)\, ds - \int_0^1 k(t,s) p_{N(m+1)}(f)(s)\, ds + \int_0^1 k(t,s) p_{N(m+1)}(f)(s)\, ds, \\ \tilde{g}(t) &= g(t) - \int_0^1 k(t,s)\left(f(s) - p_{N(m+1)}(f)(s)\right) ds, \end{aligned}$$

therefore;

$$\begin{aligned} \|(\tilde{g}(t) - g(t))\|_2^2 &= \int_0^1 \left| \int_0^1 k(t,s)\left(f(s) - p_{N(m+1)}(f)(s)\right) ds \right|^2 dt, \\ &\leq \int_0^1 \left(\int_0^1 \left| k(t,s)\left(f(s) - p_{N(m+1)}(f)(s)\right) ds \right| \right)^2 dt \\ &= \int_0^1 \left(\int_0^1 |k(t,s)| \left| \left(f(s) - p_{N(m+1)}(f)(s)\right) \right| ds \right)^2 dt, \end{aligned}$$

If we assume $c_0 = \sup |k(t,s)| \quad t, s \in [0,1)$ we have;

$$\begin{aligned} \|(\tilde{g}(t) - g(t))\|_2^2 &\leq c_0^2 \left(\int_0^1 \left| \left(f(s) - p_{N(m+1)}(f)(s)\right) \right| ds \right)^2 \\ &\leq c_0^2 \left(\left\| \left(f(s) - p_{N(m+1)}(f)(s)\right) \right\|_2 \right)^2 \\ &\leq c_0^2 \left(\frac{\mu}{(m+1)! N^{m+1} \sqrt{(2m+3)}} \right)^2, \end{aligned} \tag{37}$$

taking square roots of both sides of equation (37) we have;

$$\|(\tilde{g}(t) - g(t))\|_2 \leq \frac{\mu c_0}{(m+1)! N^{m+1} \sqrt{(2m+3)}}. \tag{38}$$

Now we find a bound for $\left\|\tilde{G} - G\right\|_2$ since;

$$g_{ni} = \frac{(2m+1)\binom{2m}{i+j}}{\binom{m}{i}\binom{m}{j}} \int_0^1 g(t) h_{ni}(t)\, dt \quad n = 1, 2, \cdots N \quad i, j = 0, 1, \cdots m, \tag{39}$$

and

$$\tilde{g}_{ni} = \frac{(2m+1)\binom{2m}{i+j}}{\binom{m}{i}\binom{m}{j}} \int_0^1 \tilde{g}(t)\, h_{ni}(t)\, dt \quad n = 1, 2, \cdots N \quad i, j = 0, 1, \cdots m. \tag{40}$$

Then we have;

$$\begin{aligned}
\left\|\tilde{G} - G\right\|_2^2 &= \sum_{n=1}^{N}\sum_{i=0}^{m} |(\tilde{g}_{ni} - g_{ni})|^2 \\
&\leq N(m+1) \sup_{1\leq n\leq .N; 0\leq i,j\leq m} \left(\left| \frac{(2m+1)\binom{2m}{i+j}}{\binom{m}{i}\binom{m}{j}} \int_0^1 h_{ni}(t)\,(\tilde{g}(t) - g(t))\, dt \right|^2 \right) \\
&\leq N(m+1) \sup_{1\leq n\leq .N; 0\leq i,j\leq m} \left(\frac{(2m+1)\binom{2m}{i+j}}{\binom{m}{i}\binom{m}{j}} \int_0^1 |h_{ni}(t)\,(\tilde{g}(t) - g(t))|\, dt \right)^2 \\
&= N(m+1) \sup_{1\leq n\leq .N; 0\leq i,j\leq m} \left(\frac{(2m+1)\binom{2m}{i+j}}{\binom{m}{i}\binom{m}{j}} \int_0^1 |h_{ni}(t)|\, |(\tilde{g}(t) - g(t))|\, dt \right)^2 \\
&\leq N(m+1) \sup_{1\leq n\leq .N; 0\leq i,j\leq m} \left(\frac{(2m+1)\binom{2m}{i+j}}{\binom{m}{i}\binom{m}{j}} \|h_{ni}(t)\|_2 \|(\tilde{g}(t) - g(t))\|_2 \right)^2 \\
&= N(m+1) \sup_{1\leq n\leq .N; 0\leq i,j\leq m} \left(\frac{1}{\sqrt{\left(\frac{\binom{m}{i}\binom{m}{j}}{(2m+1)\binom{2m}{i+j}}\right)}} \|(g(t) - \tilde{g}(t))\|_2 \right)^2 .
\end{aligned} \tag{41}$$

Substitute equation (38) in equation (41) we have;

$$\left\|\tilde{G} - G\right\|_2^2 \leq \frac{c_1 N(m+1)}{(m+1)!N^{m+1}} \frac{\sqrt{\frac{4m^3-m}{N(m+1)}}}{m\sqrt{(2m+3)}}. \tag{42}$$

Consequently, by substituting equation (42) in the inequality (36) we can conclude:

$$\|C - F\|_2 \leq \left\|A^{-1}\right\|_2 \frac{N(m+1)\, c_1}{(m+1)!N^{m+1}} \frac{\sqrt{\frac{4m^3-m}{N(m+1)}}}{m\sqrt{(2m+3)}} \quad where\ c_1 = \mu c_0, \tag{43}$$

so by substituting equation (43) in equation (33) we have;

$$\left\|P_{N(m+1)}(f)(t) - f_{N(m+1)}(t)\right\|_2 \leq \left\|A^{-1}\right\|_2 \frac{N(m+1)\, c_2}{(m+1)!N^{m+1}} \frac{\sqrt{\frac{4m^3-m}{N(m+1)}}}{m\sqrt{(2m+3)}}. \tag{44}$$

Finally substitute equation (30)and equation (44) in equation (29) we have;

$$\begin{aligned}
\left\|f(t) - f_{N(m+1)}(t)\right\|_2 &= \left\|f(t) - p_{N(m+1)}(f)(t)\right\|_2 + \left\|p_{N(m+1)}(f)(t) - f_{N(m+1)}(t)\right\|_2 \\
&\leq \frac{\mu}{(m+1)!N^{m+1}\sqrt{(2m+3)}} + \left\|A^{-1}\right\|_2 \frac{N(m+1)\, c_2}{(m+1)!N^{m+1}} \frac{\sqrt{\frac{4m^3-m}{N(m+1)}}}{m\sqrt{(2m+3)}} \\
&\leq \frac{1}{(m+1)!N^{m+1}\sqrt{(2m+3)}} \left(\mu + \left\|A^{-1}\right\|_2 N(m+1)\, c_2 \sqrt{\frac{4m^3-m}{N(m+1)}} \right).
\end{aligned}$$

4 Numerical examples

In this section, we provide some examples demonstrating the approximation of solutions for first-kind Fredholm integral equations using the numerical method detailed in the preceding section. We conduct these numerical experiments using Maple 18 software.

Example 1. Consider the first kind Fredholm integral equation

$$\int_0^1 \sin(ts) f(s)\, ds = \frac{\sin(t) - t\cos(t)}{t^2}$$

with exact solution $f(t) = t$. The absolute errors of improved block pulse method for $t \in [0, 1]$ is shown in Table (1).

Table 1. Numerical results yeilded by the proposed method for Example 1.

t_i	$exact$	$HBBM\ N = 3,\ M = 3$
0	0	
0.1	0.1	0.6674604728
0.2	0.2	0.5592445614
0.3	0.3	0.3329531755
0.4	0.4	0.1257379315
0.5	0.5	0.1700910529
0.6	0.6	0.2859762479
0.7	0.7	0.0824780603
0.8	0.8	0.2093223047
0.9	0.9	0.0010252419

Example 2 Consider the first kind Fredholm integral equation

$$\int_0^1 \sin(t+s) f(s)\, ds = \frac{1}{4}\left(1 - \cos(2)\cos(t) + (2 + \sin(t)\sin(t))\right)$$

with exact solution $f(t) = \cos(t)$. The absolute errors of improved block pulse method for $t \in [0, 1]$ is shown in Table (2).

Table 2. Numerical results yeilded by the proposed method for Example 2.

t_i	$exact$	$HBBM\ N = 2,\ M = 2$
0.1	0.9950041653	0.9290675127
0.2	0.9800665778	0.3244888834
0.3	0.9553364891	1.567859402
0.4	0.9210609940	0.5496316061
0.5	0.8775825619	0.3792593930
0.6	0.8253356149	0.3395967964
0.7	0.7648421873	0.6352944497
0.8	0.6967067093	0.2229385196
0.9	0.6216099683	0.2822716825

5 Discussions and conclusion

In this research work, we introduced the hybrid block-pulse Bernstein method to solve linear ill-posed first-kind Fredholm integral equations. By leveraging the properties of hybrid functions, we transformed the problem into a solvable linear system of algebraic equations, which were effectively solved using Maple 18 software. Our error bound estimation and convergence analysis demonstrated the robustness of the method. The numerical examples further confirmed the effectiveness of this approach, and the proposed method offers a promising tool for solving complex Fredholm integral equations in applied sciences. Future work could explore incorporating regularization techniques with the hybrid functions to further enhance solution stability. Additionally, the use of preconditioning methods or multigrid techniques may improve computational efficiency. Extending the hybrid approach to nonlinear illposed first kind Fredholm integral equation could also open new avenues for solving complex real-world problems more efficiently.

References

[1] te Riele, H. J. (1985). A program for solving first kind Fredholm integral equations by means of regularization. Computer physics communications, 36(4), 423-432.

[2] Kosarev, E. L. (1980). Applications of integral equations of the first kind in experiment physics. Computer Physics Communications, 20(1), 69-75.

[3] Weese, J. (1992). A reliable and fast method for the solution of Fredhol integral equations of the first kind based on Tikhonov regularization. Computer physics communications, 69(1), 99-111.

[4] Wazwaz, A. M. (2011). The regularization method for Fredholm integral equations of the first kind. Computers and Mathematics with Applications, 61(10), 2981-2986.

[5] Tikhonov, A. N., Goncharsky, A. V., Stepanov, V. V. E., Yagola, A. G. E., Tikhonov, A. N., Goncharsky, A. V., ... and Yagola, A. G. (1995). Numerical methods for the approximate solution of ill-posed problems on compact sets (pp. 65-79). Springer Netherlands.

[6] Tikhonov, A. N., and Arsenin, V. I. A. K. (1977). Solutions of ill-posed problems. (No Title).

[7] Rajan, M. P. (2003). Convergence analysis of a regularized approximation for solving Fredholm integral equations of the first kind. Journal of mathematical analysis and applications, 279(2), 522-530.

[8] Molabahrami, A. (2013). An algorithm based on the regularization and integral mean value methods for the Fredholm integral equations of the first kind. Applied Mathematical Modelling, 37(23), 9634-9642.

[9] Suliman, M. A., Ballal, T., and Al-Naffouri, T. Y. (2018). Perturbation-based regularization for signal estimation in linear discrete ill-posed problems. Signal Processing, 152, 35-46.

[10] Rasekh, M., and Fakhri, N. (2023). The Use of Homotopy Regularization Method for Linere and Nonlinner Fredholm Integral Equations of the First Kind. Journal of Mathematics and Statistics Studies, 4(1), 19-25.

[11] Rao, G. P. (Ed.). (1983). Piecewise constant orthogonal functions and their application to systems and control. Berlin, Heidelberg: Springer Berlin Heidelberg.

[12] Datta, K. B., and Mohan, B. M. (1995). Orthogonal functions in systems and control (Vol. 9). World Scientific.

[13] Mandal, B. N., and Bhattacharya, S. (2007). Numerical solution of some classes of integral equations using Bernstein polynomials. Applied Mathematics and computation, 190(2), 1707-1716.

[14] Yousefi, S. A., and Behroozifar, M. (2010). Operational matrices of Bernstein polynomials and their applications. International Journal of Systems Science, 41(6), 709-716.

[15] Hsiao,C. H. (2009). Hybrid function method for solving Fredholm and Volterra integral equations of the second kind. Journal of Computational and Applied Mathematics, 230(1), 59-68.

[16] Sohrabi, S. (2013). Study on convergence of hybrid functions method for solution of nonlinear integral equations. Applicable Analysis, 92(4), 690-702.

[17] Maleknejad, K., and Kajani, M. T. (2004). Solving linear integro-differential equation system by Galerkin methods with hybrid functions. Applied Mathematics and Computation, 159(3), 603-612.

[18] Maleknejad, K., Basirat, B., and Hashemizadeh, E. (2011). Hybrid Legendre polynomials and Block-Pulse functions approach for nonlinear Volterra–Fredholm integro-differential equations. Computers and Mathematics with applications, 61(9), 2821-2828.

[19] Marzban, H. R., and Razzaghi, M. (2003). Hybrid functions approach for linearly constrained quadratic optimal control problems. Applied Mathematical Modelling, 27(6), 471-485.

[20] Maleknejad, K., and Ebrahimzadeh, A. (2014). An efficient hybrid pseudo-spectral method for solving optimal control of Volterra integral systems. Mathematical Communications, 19(2), 417-435.

[21] Kajani, M. T., and Vencheh, A. H. (2005). Solving second kind integral equations with hybrid Chebyshev and block-pulse functions. Applied Mathematics and Computation, 163(1), 71-77.

[22] Wang, X. T., and Li, Y. M. (2009). Numerical solutions of integrodifferential systems by hybrid of general block-pulse functions and the second Chebyshev polynomials. Applied mathematics and Computation, 209(2), 266-272.

[23] Hashemizadeh, E., Maleknejad, K., and Basirat, B. (2011). Hybrid functions approach for the nonlinear Volterra–Fredholm integral equations. Procedia Computer Science, 3, 1189-1194.

[24] Marzban, H. R., Tabrizidooz, H. R., and Razzaghi, M. (2011). A composite collocation method for the nonlinear mixed Volterra–Fredholm–Hammerstein integral equations. Communications in Nonlinear Science and Numerical Simulation, 16(3), 1186-1194.

[25] Maleknejad, K., and Saeedipoor, E. (2017). An efficient method based on hybrid functions for Fredholm integral equation of the first kind with convergence analysis. Applied Mathematics and Computation, 304, 93-102.

[26] Maleknejad, K., and Mahmoudi, Y. (2004). Numerical solution of linear Fredholm integral equation by using hybrid Taylor and block-pulse functions. Applied Mathematics and Computation, 149(3), 799-806.

[27] Asady, B., Kajani, M. T., Vencheh, A. H., and Heydari, A. (2005). Solving second kind integral equations with hybrid Fourier and block–pulse functions. Applied Mathematics and Computation, 160(2), 517-522.

[28] Alipour, M., Baleanu, D., and Babaei, F. (2014, January). Hybrid Bernstein block-pulse functions method for second kind integral equations with convergence analysis. In Abstract and Applied Analysis (Vol. 2014). Hindawi.

[29] Masouri, Z. (2012). Numerical expansion-iterative method for solving second kind Volterra and Fredholm integral equations using block-pulse functions. Advanced Computational Techniques in Electromagnetics, 20, 7-17.

[30] Musa, H. S. A., and Bichi, S. L. (2024). A Hybrid Method of Improved Block Pulse with Bernstein Polynomials for Numerical Solution of Linear Ill-Posed First Kind Fredholm Integral Equation. Dutse Journal of Pure and Applied Sciences, 10(4b), 20-34.

[31] Maleknejad, K., Basirat, B., and Hashemizadeh, E. (2012). A Bernstein operational matrix approach for solving a system of high order linear Volterra–Fredholm integro-differential equations. Mathematical and Computer Modelling, 55(3-4), 1363-1372.

[32] Jiang, Z., and Schaufelberger, W. (1992). Block pulse functions and their applications in control systems (Vol. 179). Berlin: Springer-Verlag.

[33] Kilbas, A. A., Srivastava, H. M., and Trujillo, J. J. (2006). Theory and applications of fractional differential equations (Vol. 204). elsevier.

A fractional-order transmission dynamics for Diphtheria and Pertussis co-infection

J.O. Omolehin*†, O.S. Johnson†‡, and I.O. Babarinsa†§

Abstract

Resurgence of vaccine preventable infectious illnesses like diphtheria and pertussis place a heavy burden on global health especially in developing countries. In this article, a modified SIR-type fractional-order compartmental model was used to study the transmission dynamics of pertussis and diphtheria co-infection. Fractional-order models through fractional calculus provides heuristic approach to improving flexibility, convergence, and accuracy in long-term disease predictions. In Particular, the Laplace-Adomian decomposition method (LADM) is applied to solve the complexity of diphtheria-pertussis co-dynamics model by adding fractional derivatives to account for non-integer order dynamics. The approximate solutions of the model is obtained in the form of an infinite series which shows convergence to equilibrium point. The efficiency and reliability of (LADM) is demonstrated in different time intervals by the numerical simulations.

Keywords and phrases: Co-infection; fractional-order; Laplace-Adomian decomposition method; Caputo fractional derivative.

1 Introduction

The rise in vaccine-preventable respiratory infections is a global health concern, worsened by disruptions to routine immunization during the COVID-19 pandemic [1–4]. In 2021, the WHO and UNICEF report [5] found that about 25 million children missed their DTP vaccines. Respiratory diseases remain a significant threat to children's health. It is crucial to understand how different pathogens interact within a host, as co-infections are common and can influence disease severity and outcomes. [7–10].

Diphtheria and pertussis are bacterial respiratory diseases that can be prevented with the DTaP vaccine [11–14]. Diphtheria, caused by Corynebacterium species, can cause serious complications such as paralysis or death and spreads through droplets or close contact with an infected person [15]. In addition, Whooping cough (pertussis) is extremely contagious and spreads easily through the air. It poses a serious health risk, particularly in infants, and can be difficult to diagnose [17–19]. Studies show that asymptomatic adolescents and adults are the main carriers, spreading the disease to infants.

Recently, mathematicians have focused on studying the interaction between these pathogens using a fractional-order compartmental approach to account for non-integer dynamics, convergence, and long-term prediction accuracy [20, 21]. For example, [20] applied Laplace Adomian Decomposition Method (LADM) to study COVID-19 and Influenza dynamics, while [21] used it for COVID-19 and Monkeypox. [22] used fractional calculus in an SEIR model without vaccination, showing the importance of timely vaccination. [23] developed a fractional order model for malaria and COVID-19 co-infection, suggesting that preventive measures could reduce the risk of co-infection and potentially eliminate both diseases.

*Corresponding Author; E-mail: oladipuposamueljohnson@gmail.com
†Department of Mathematics, Federal University Lokoja, Kogi, Nigeria
‡E-mail: oladipuposamueljohnson@gmail.com
§E-mail: olayiwola.babarinsa@fulokoja.edu.ng

2 Model formulation

In this article, the Caputo derivative is used as a differential operator. This section outlines the key terms and concepts used in this study.

2.1 Preliminary Definitions

Definition [24] Let $f(t)$ be a function defined on the interval $0 < t < \infty$, the following integral converges in a certain region of s, where $F(s)$ is the Laplace transform of $f(t)$, $\mathscr{L}$ is Laplace operator and s is a complex parameter.

$$F(s) = \mathscr{L}[f(t)] = \int_0^\infty f(t)e^{-st}dt \tag{1}$$

Proposition [25,26]. Let $0 < q < 1$, then the Laplace transformation of the Caputo derivative is given by

$$\mathscr{L}\{{}^C\mathcal{D}^q f(t)\} = \mathscr{L}[f(t)] - s^{q-1}f(0), \tag{2}$$

Definition [27] Let $q \in [0, 1]$ The Caputo fractional time derivative of a function f of order q is defined by:

$$\mathscr{L}\{{}^C\mathcal{D}_0^q f(t)\} = \frac{1}{\Gamma(n-q)}\int_0^t (t-s)^{n-q-1}f^{(n)}(s)ds \tag{3}$$

Where q represents the integer part of q. Therefore, when $n = 1$ the Caputo derivative becomes:

$$\mathscr{L}\{{}^C\mathcal{D}_0^q f(t)\} = \frac{1}{\Gamma(1-q)}\int_0^t \frac{f(s)}{(t-s)^q}ds \tag{4}$$

The diphtheria-pertussis dual infection model with total population $N(t)$ consist of eight sub-population given by

$$N(t) = S(t) + I_{AD}(t) + I_{SD}(t) + I_{AP}(t) + I_{SP}(t) + I_{SDP}(t) + Q_{SD}(t) + R(t) \tag{5}$$

The following Table 1 gives a summary Definition of model parameters and variables:

Table 1: Values of parameters used in simulation.

Variables	Description	Unit
$S(t)$	susceptible	People
$I_{AD}(t)$	asymptomatic diphtheria infected	People
$I_{SD}(t)$	symptomatic diphtheria infected	People
$I_{AP}(t)$	asymptomatic pertussis infected	People
$I_{SP}(t)$	symptomatic pertussis infected	People
$I_{SDP}(t)$	diphtheria-pertussis co-infected	People
$Q_{SD}(t)$	quarantined diphtheria infected	People
$R(t)$	Recovered	People

This article models a population where the susceptible group (S) grows due to two factors: the addition of unvaccinated individuals $bN(1-V)$ and the movement of vaccinated newborns directly into the recovered group VbN.

Furthermore, S get infected with diphtheria only with infection force $\Phi_D = \frac{\beta_D(\alpha_D I_{AD}+I_{SD})}{N}$, Pertussis only with infection force $\Phi_P = \frac{\beta_P(\alpha_P I_{AP}+I_{SP})}{N}$, and diphtheria- Pertussis dual infection force $\Phi_{DP} = \frac{\beta_{DP} I_{SDP}}{N}$ respectively. Individuals exhibiting symptoms of diphtheria or pertussis are

Table 2: Values of parameters used in simulation.

Parameters	Description	Values	Cite
β_D	Contact rate for Diphtheria	0.57/day	[30]
β_P	Contact rate for Pertussis	0.5-1/day	[28]
β_{DP}	Diphtheria and Pertussis dual transmission	0.2/day	fitted
Ω	Recovery rate of Quarantine	0.1-0.9	Assumed
η_D	Diphtheria Recovery rate.	0.5	[28]
η_P	Pertussis Recovery rate	$[\frac{1}{14}, 0.0206$	[28]
η_{DP}	Dual infection Recovery rate	0.15/day	[29]
ϖ_D	Disease induced death rate of Diphtheria	0.05	[30]
ϖ_P	Disease induced death rate of Pertussis	0.0309	[28]
ϖ_{DP}	Disease induced death rate of Dual infection	0.005/day	[30]
μ	Natural death rate	0.006	[30]
θ	Diphtheria Quarantined rate	0.1/day	Assumed
V	Vaccination	0.1-1.2	Assumed
α_D, α_P	Modification parameter	0.5	[28]
γ_1, γ_2	Modification parameter	1	[29]
b	Birth rate	0.019	[30]
ϕ_D, ϕ_P	Progression to symptomatic infected stage	$[\frac{3}{7}]$/day , $[\frac{7}{7}]$/day	Fitted

susceptible to secondary infections at rates $\gamma_1 \frac{\beta_P(\alpha_P I_{AP}+I_{SP})}{N} I_{SD}$ and $\gamma_2 \frac{\beta_D(\alpha_D I_{AD}+I_{SD})}{N} I_{SP}$.The model parameters are listed in Table 2, with the governing equations in equation (6).

$$\begin{aligned}
\frac{dS}{dt}(t) &= bN(1-V) - (\Phi_D + \Phi_P + \Phi_{DP})\, S - \mu S,\\
\frac{dI_{AD}}{dt}(t) &= \Phi_D S - (\phi_D + \mu) I_{AD},\\
\frac{dI_{SD}}{dt}(t) &= \phi_D I_{AD} - (\theta + \eta_D + \varpi_D + \mu) I_{SD} - \gamma_1 \Phi_P I_{SD},\\
\frac{dI_{AP}}{dt}(t) &= \Phi_P S - (\phi_P + \mu) I_{AP},\\
\frac{dI_{SP}}{dt}(t) &= \phi_P I_{AP} - (\eta_P + \varpi_P + \mu) I_{SP} - \gamma_2 \Phi_D I_{SP},\\
\frac{dI_{SDP}}{dt}(t) &= \phi_{DP} S + \gamma_1 \Phi_P I_{SD} + \gamma_2 \Phi_D I_{SP} - (\eta_{DP} + \varpi_{DP} + \mu) I_{SDP},\\
\frac{dQ_{SD}}{dt}(t) &= \theta I_{SD} - (\Omega + \mu) Q_{SD},\\
\frac{dR}{dt}(t) &= VbN + \eta_P I_{AP} + \eta_D I_{AD} + \eta_{SDP} I_{SDP} - \mu R.
\end{aligned} \tag{6}$$

$$S(0) > 0,\ I_{AD}(0) > 0,\ I_{SD}(0) > 0,\ I_{AP}(0) > 0,\ I_{SP}(0) > 0,\ I_{SDP}(0) > 0,\ Q_{SD}(0) > 0$$

3 Fractional-order of Diphtheria-Pertussis co-infection model

This section incorporates the Caputo fractional derivative into our diphtheria-pertussis co-infection model. Fractional calculus is applied because it effectively models systems and processes exhibiting memory and hereditary characteristics [22]. Therefore, the fractional-order model is constructed as follows:

$$
\begin{aligned}
{}^{C}\mathcal{D}^{q}S(t) &= bN(1-V) - (\Phi_D + \Phi_P + \Phi_{DP})\,S - \mu S,\\
{}^{C}\mathcal{D}^{q}I_{AD}(t) &= \Phi_D S - (\phi_D + \mu)I_{AD},\\
{}^{C}\mathcal{D}^{q}I_{SD}(t) &= \phi_D I_{AD} - (\theta + \eta_D + \varpi_D + \mu)I_{SD} - \gamma_1\Phi_P I_{SD},\\
{}^{C}\mathcal{D}^{q}I_{AP}(t) &= \Phi_P S - (\phi_P + \mu)I_{AP},\\
{}^{C}\mathcal{D}^{q}I_{SP}(t) &= \phi_P I_{AP} - (\eta_P + \varpi_P + \mu)I_{SP} - \gamma_2\Phi_D I_{SP},\\
{}^{C}\mathcal{D}^{q}I_{SDP}(t) &= \Phi_{DP} S + \gamma_1\Phi_P I_{SD} + \gamma_2\Phi_D I_{SP} - (\eta_{DP} + \varpi_{DP} + \mu)I_{SDP},\\
{}^{C}\mathcal{D}^{q}Q_{SD}(t) &= \theta I_{SD} - (\Omega + \mu)Q_{SD},\\
{}^{C}\mathcal{D}^{q}R(t) &= VbN + \eta_P I_{SP} + \eta_D I_{SD} + \eta_{SDP} I_{SDP} + \Omega Q_{SD} - \mu R.
\end{aligned}
\tag{7}
$$

With the following initial conditions;

$$S(0) > 0,\ I_{AD}(0) > 0,\ I_{SD}(0) > 0,\ I_{AP}(0) > 0,\ I_{SP}(0) > 0,\ I_{SDP}(0) > 0,\ Q_{SD}(0) > 0,\ R_(0) = 0.$$

3.1 Applying Laplace-Adomian Decomposition method solution

Here, we will apply Laplace transformation to convert the governing system of differential equations (6) into a system of algebraic equations. Furthermore, apply the Laplace Adomian Decomposition Method (LADM) to solve equation (7), and obtain the solution in terms of series;

$$
\begin{aligned}
\mathscr{L}\{{}^{C}\mathcal{D}^{q}S(t)\} &= \mathscr{L}\{bN(1-V) - (\Phi_D + \Phi_P + \Phi_{DP})\,S - \mu S\},\\
\mathscr{L}\{{}^{C}\mathcal{D}^{q}I_{AD}(t)\} &= \mathscr{L}\{\Phi_D S - (\phi_D + \mu)I_{AD}\},\\
\mathscr{L}\{{}^{C}\mathcal{D}^{q}I_{SD}(t)\} &= \mathscr{L}\{\phi_D I_{AD} - (\theta + \eta_D + \varpi_D + \mu)I_{SD} - \gamma_1\Phi_P I_{SD}\},\\
\mathscr{L}\{{}^{C}\mathcal{D}^{q}I_{AP}(t)\} &= \mathscr{L}\{\Phi_P S - (\phi_P + \mu)I_{AP}\},\\
\mathscr{L}\{{}^{C}\mathcal{D}^{q}I_{SP}(t)\} &= \mathscr{L}\{\phi_P I_{AP} - (\eta_P + \varpi_P + \mu)I_{SP} - \gamma_2\Phi_D I_{SP}\},\\
\mathscr{L}\{{}^{C}\mathcal{D}^{q}I_{SDP}(t)\} &= \mathscr{L}\{\Phi_{DP} S + \gamma_1\Phi_P I_{SD} + \gamma_2\Phi_D I_{SP} - (\eta_{DP} + \varpi_{DP} + \mu)I_{SDP}\},\\
\mathscr{L}\{{}^{C}\mathcal{D}^{q}Q_{SD}(t)\} &= \mathscr{L}\{\theta I_{SD} - (\Omega + \mu)Q_{SD}\},\\
\mathscr{L}\{{}^{C}\mathcal{D}^{q}R(t)\} &= \mathscr{L}\{VbN + \eta_P I_{SP} + \eta_D I_{SD} + \eta_{SDP} I_{SDP} + \Omega Q_{SD} - \mu R\}.
\end{aligned}
\tag{8}
$$

which is equivalent to;

$$
\begin{aligned}
s^{q}\mathscr{L}\{S(t)\} - s^{q-1}S(0) &= \mathscr{L}\{bN(1-V) - (\Phi_D + \Phi_P + \Phi_{DP})\,S - \mu S\},\\
s^{q}\mathscr{L}\{I_{AD}(t)\} - s^{q-1}I_{AD}(0) &= \mathscr{L}\{\Phi_D S - (\phi_D + \mu)I_{AD}\},\\
s^{q}\mathscr{L}\{I_{SD}(t)\} - s^{q-1}I_{SD}(0) &= \mathscr{L}\{\phi_D I_{AD} - (\theta + \eta_D + \varpi_D + \mu)I_{SD} - \gamma_1\Phi_P I_{SD}\},\\
\mathscr{L}\{I_{AP}(t)\} - s^{q-1}I_{AP}(0) &= \mathscr{L}\{\Phi_P S - (\phi_P + \mu)I_{AP}\},\\
s^{q}\mathscr{L}\{I_{SP}(t)\} - s^{q-1}I_{SP}(0) &= \mathscr{L}\{\phi_P I_{AP} - (\eta_P + \varpi_P + \mu)I_{SP} - \gamma_2\Phi_D I_{SP}\},\\
s^{q}\mathscr{L}\{I_{SDP}(t)\} - s^{q-1}I_{SDP}(0) &= \mathscr{L}\{\Phi_{DP} S + \gamma_1\Phi_P I_{SD} + \gamma_2\Phi_D I_{SP} - (\eta_{DP} + \varpi_{DP} + \mu)I_{SDP}\},\\
s^{q}\mathscr{L}\{Q_{SD}(t)\} - s^{q-1}Q_{SD}(0) &= \mathscr{L}\{\theta I_{SD} - (\Omega + \mu)Q_{SD}\},\\
s^{q}\mathscr{L}\{R(t)\} - s^{q-1}R(0) &= \mathscr{L}\{VbN + \eta_P I_{SP} + \eta_D I_{SD} + \eta_{SDP} I_{SDP} + \Omega Q_{SD} - \mu R\}.
\end{aligned}
\tag{9}
$$

Substituting the initial conditions and Dividing equation (9) by (s^q) we have

$$
\begin{aligned}
\mathscr{L}\{S(t)\} &= \frac{S_0}{s} + \frac{\kappa}{s^{q+1}} - [\frac{1}{s^q}\mathscr{L}\{(\Phi_D + \Phi_P + \Phi_{DP})\, S - \mu S\}],\\
\mathscr{L}\{I_{AD}(t)\} &= \frac{I_{AD_0}}{s} + [\frac{1}{s^q}\mathscr{L}\{\Phi_D S - (\phi_D + \mu) I_{AD}\}],\\
\mathscr{L}\{I_{SD}(t)\} &= \frac{I_{SD_0}}{s} + [\frac{1}{s^q}\mathscr{L}\{\phi_D I_{AD} - (\theta + \eta_D + \varpi_D + \mu) I_{SD} - \gamma_1 \Phi_P I_{SD}\}],\\
\mathscr{L}\{I_{AP}(t)\} &= \frac{I_{AP_0}}{s} + [\frac{1}{s^q}\mathscr{L}\{\Phi_P S - (\phi_P + \mu) I_{AP}\}],\\
\mathscr{L}\{I_{SP}(t)\} &= \frac{I_{SP_0}}{s} + [\frac{1}{s^q}\mathscr{L}\{\phi_P I_{AP} - (\eta_P + \varpi_P + \mu) I_{SP} - \gamma_2 \Phi_D I_{SP}\}],\\
\mathscr{L}\{I_{SDP}(t)\} &= \frac{I_{SDP_0}}{s} + [\frac{1}{s^q}\mathscr{L}\{\Phi_{DP} S + \gamma_1 \Phi_P I_{SD} + \gamma_2 \Phi_D I_{SP} - (\eta_{DP} + \varpi_{DP} + \mu) I_{SDP}\}],\\
\mathscr{L}\{Q_{SD}(t)\} &= \frac{Q_{SD_0}}{s} + [\frac{1}{s^q}\mathscr{L}\{\theta I_{SD} - (\Omega + \mu) Q_{SD}\}],\\
\mathscr{L}\{R(t)\} &= \frac{R_0}{s} + [\frac{1}{s^q}\mathscr{L}\{VbN + \eta_P I_{SP} + \eta_D I_{SD} + \eta_{SDP} I_{SDP} + \Omega Q_{SD} - \mu R\}].
\end{aligned}
\tag{10}
$$

Expressing the obtained solutions as an infinite series,

$S(t) = \sum_{n=0}^{\infty} S_n(t)$, $I_{AD}(t) = \sum_{n=0}^{\infty} I_{AD_n}(t)$, $I_{SD}(t) = \sum_{n=0}^{\infty} I_{SD_n}(t)$ $I_{AP}(t) = \sum_{n=0}^{\infty} I_{AP_n}(t)$, $I_{SP}(t) = \sum_{n=0}^{\infty} I_{SP_n}(t)$, $I_{SDP}(t) = \sum_{n=0}^{\infty} I_{SDP_n}(t)$, $Q_{SD}(t) = \sum_{n=0}^{\infty} Q_{SD_n}(t))$, $R(t) = \sum_{n=0}^{\infty} I_{R_n}(t)$.

$S(t)I_{AD}(t)$, $S(t)I_{DP}(t)$, $S(t)I_{AP}(t)$, $S(t)I_{SD}(t)$, and $S(t)I_{SDP}(t)$, are the non-linear term in the model and it can be decomposed by Adomian polynomial.

$I_{AD}(t)S(t) = \sum_{n=0}^{\infty} A_n$, $I_{SD}(t)S(t) = \sum_{n=0}^{\infty} B_n$, $I_{AP}(t)S(t) = \sum_{n=0}^{\infty} C_n$, $I_{SP}(t)S(t) = \sum_{n=0}^{\infty} D_n$, $I_{SDP}(t)S(t) = \sum_{n=0}^{\infty} E_n$.

where A_n, B_n, C_n, D_n and E_n are Adomian polynomials [21].

$$
\begin{aligned}
A_n &= \frac{1}{\Gamma(n+1)}\frac{d^n}{d\lambda^n}\Big[\sum_{k=0}^{\infty}\lambda^k I_{AD}(k)\sum_{k=0}^{\infty}\lambda^k S(k)\Big]_{\lambda=0}\\
B_n &= \frac{1}{\Gamma(n+1)}\frac{d^n}{d\lambda^n}\Big[\sum_{k=0}^{\infty}\lambda^k I_{SD}(k)\sum_{k=0}^{\infty}\lambda^k S(k)\Big]_{\lambda=0}\\
C_n &= \frac{1}{\Gamma(n+1)}\frac{d^n}{d\lambda^n}\Big[\sum_{k=0}^{\infty}\lambda^k I_{AP}(k)\sum_{k=0}^{\infty}\lambda^k S(k)\Big]_{\lambda=0}\\
D_n &= \frac{1}{\Gamma(n+1)}\frac{d^n}{d\lambda^n}\Big[\sum_{k=0}^{\infty}\lambda^k I_{SP}(k)\sum_{k=0}^{\infty}\lambda^k S(k)\Big]_{\lambda=0}\\
E_n &= \frac{1}{\Gamma(n+1)}\frac{d^n}{d\lambda^n}\Big[\sum_{k=0}^{\infty}\lambda^k I_{SDP}(k)\sum_{k=0}^{\infty}\lambda^k S(k)\Big]_{\lambda=0}.
\end{aligned}
\tag{11}
$$

The first three terms of polynomials $A(n), B(n), C(n), D(n)$ and $E(n)$ calculated as

$$
A(n) = \begin{cases} A_0 = S_0 I_{AD_0},\\ A_1 = S_1 I_{AD_0} + S_0 I_{AD_1},\\ A_2 = S_2 I_{AD_0} + S_1 I_{AD_1} + S_0 I_{AD_2}\\ \vdots \end{cases}
\qquad
B(n) = \begin{cases} B_0 = S_0 I_{SD_0},\\ B_1 = S_1 I_{SD_0} + S_0 I_{SD_1},\\ B_2 = S_2 I_{SD_0} + S_1 I_{SD_1} + S_0 I_{SD_2}\\ \vdots \end{cases}
$$

$$C(n) = \begin{cases} C_0 = S_0 I_{AP_0}, \\ C_1 = S_1 I_{AP_0} + S_0 I_{AP_1}, \\ C_2 = S_2 I_{AP_0} + S_1 I_{AP_1} + S_0 I_{AP_2} \\ \vdots \end{cases} \quad D(n) = \begin{cases} D_0 = S_0 I_{SP_0}, \\ D_1 = S_1 I_{SP_0} + S_0 I_{SP_1}, \\ D_2 = S_2 I_{SP_0} + S_1 I_{SP_1} + S_0 I_{SP_2} \\ \vdots \end{cases}$$

$$E(n) = \begin{cases} E_0 = S_0 I_{SDP_0}, \\ E_1 = S_1 I_{SDP_0} + S_0 I_{SDP_1}, \\ E_2 = S_2 I_{SDP_0} + S_1 I_{SDP_1} + S_0 I_{SDP_2} \\ \vdots \end{cases}$$

Substituting the infinite series into equation (9), by matching the terms on both sides we obtain the following iterative algorithm

$$\mathscr{L}\{\sum_{n=0}^{\infty} S_{n+1}\} = \frac{S_n}{s} + \frac{1}{s^q}\mathscr{L}\Big[bN(1-V) - \Big(\frac{\beta_D(\alpha_D \sum_{n=0}^{\infty} A(n) + \sum_{n=0}^{\infty} B(n))}{N} + \frac{\beta_P(\alpha_P \sum_{n=0}^{\infty} C(n) + \sum_{n=0}^{\infty} D(n))}{N} + \frac{\beta_{DP} \sum_{n=0}^{\infty} E(n)}{N}\Big) - \mu \sum_{n=0}^{\infty} S_n\Big],$$

$$\mathscr{L}\{\sum_{n=0}^{\infty} I_{AD_{n+1}}\} = \frac{I_{AD_n}}{s} + \frac{1}{s^q}\mathscr{L}\Big[\frac{\beta_D(\alpha_D \sum_{n=0}^{\infty} A(n) + \sum_{n=0}^{\infty} B(n))}{N} - (\phi_D + \mu)\sum_{n=0}^{\infty} I_{AD_n}\Big],$$

$$\mathscr{L}\{\sum_{n=0}^{\infty} I_{SD_{n+1}}\} = \frac{I_{SD_n}}{s} + \frac{1}{s^q}\mathscr{L}\Big[\phi_D \sum_{n=0}^{\infty} I_{AD_n} - (\theta + \eta_D + \varpi_D + \mu)\sum_{n=0}^{\infty} I_{SD_n} - \gamma_1 \frac{\beta_P(\alpha_P \sum_{n=0}^{\infty} C(n) + \sum_{n=0}^{\infty} D(n))}{N} \sum_{n=0}^{\infty} I_{SD_n}\Big],$$

$$\mathscr{L}\{\sum_{n=0}^{\infty} I_{AP_{n+1}}\} = \frac{I_{AP_n}}{s} + \frac{1}{s^q}\mathscr{L}\Big[\frac{\beta_P(\alpha_P \sum_{n=0}^{\infty} C(n) + \sum_{n=0}^{\infty} D(n))}{N} - (\phi_P + \mu)\sum_{n=0}^{\infty} I_{AP_n}\Big],$$

$$\mathscr{L}\{\sum_{n=0}^{\infty} I_{SP_{n+1}}\} = \frac{I_{SP_n}}{s} + \frac{1}{s^q}\mathscr{L}\Big[\phi_P \sum_{n=0}^{\infty} I_{AP_n} - (\eta_P + \varpi_P + \mu)\sum_{n=0}^{\infty} I_{SD_n} - \gamma_2 \frac{\beta_D(\alpha_D \sum_{n=0}^{\infty} A(n) + \sum_{n=0}^{\infty} B(n))}{N} \sum_{n=0}^{\infty} I_{SP_n}\Big],$$

$$\mathscr{L}\{\sum_{n=0}^{\infty} I_{SDP_{n+1}}\} = \frac{I_{SDP_n}}{s} + \frac{1}{s^q}\mathscr{L}\Big[\frac{\beta_{DP} \sum_{n=0}^{\infty} E(n)}{N} + \gamma_1 \frac{\beta_P(\alpha_P \sum_{n=0}^{\infty} C(n) + \sum_{n=0}^{\infty} D(n))}{N} \sum_{n=0}^{\infty} I_{SD_n} + \gamma_2 \frac{\beta_D(\alpha_D \sum_{n=0}^{\infty} A(n) + \sum_{n=0}^{\infty} B(n))}{N} \sum_{n=0}^{\infty} I_{SP_n} - (\eta_{DP} + \varpi_{DP} + \mu)\sum_{n=0}^{\infty} I_{SDP_n}\Big],$$

$$\mathscr{L}\{\sum_{n=0}^{\infty} Q_{SD_{n+1}}(t)\} = \frac{Q_{SD_n}}{s} + \frac{1}{s^q}\mathscr{L}\Big[\theta \sum_{n=0}^{\infty} I_{SD_n} - (\Omega + \mu)\sum_{n=0}^{\infty} Q_{SD_n}\Big],$$

$$\mathscr{L}\{\sum_{n=0}^{\infty} R_{n+1}\} = \frac{R_0}{s} + \frac{1}{s^q}\mathscr{L}\Big[VbN + \eta_P \sum_{n=0}^{\infty} I_{AP_n} + \eta_D \sum_{n=0}^{\infty} I_{AD_n} + \eta_{SDP} \sum_{n=0}^{\infty} I_{SP_n} - \mu \sum_{n=0}^{\infty} R_n\Big]. \tag{12}$$

Evaluating the Laplace transform of the second equation at the RHS of equation (12), [21] we get

$$\mathscr{L}\{\sum_{n=0}^{\infty} S_{n+1}\} = \frac{S_n}{s} + \Big[bN(1-V) - \Big(\frac{\beta_D(\alpha_D \sum_{n=0}^{\infty} A(n) + \sum_{n=0}^{\infty} B(n))}{N} + \frac{\beta_P(\alpha_P \sum_{n=0}^{\infty} C(n) + \sum_{n=0}^{\infty} D(n))}{N} + \frac{\beta_{DP} \sum_{n=0}^{\infty} E(n)}{N}\Big) - \mu \sum_{n=0}^{\infty} S_n\Big] \frac{1}{s^{q+1}},$$

$$\mathscr{L}\{\sum_{n=0}^{\infty} I_{AD_{n+1}}\} = \frac{I_{AD_n}}{s} + \Big[\frac{\beta_D(\alpha_D \sum_{n=0}^{\infty} A(n) + \sum_{n=0}^{\infty} B(n))}{N} - (\phi_D + \mu) \sum_{n=0}^{\infty} I_{AD_n}\Big] \frac{1}{s^{q+1}},$$

$$\mathscr{L}\{\sum_{n=0}^{\infty} I_{SD_{n+1}}\} = \frac{I_{SD_n}}{s} + \Big[\phi_D \sum_{n=0}^{\infty} I_{AD_n} - (\theta + \eta_D + \varpi_D + \mu) \sum_{n=0}^{\infty} I_{SD_n} - \gamma_1 \frac{\beta_P(\alpha_P \sum_{n=0}^{\infty} C(n) + \sum_{n=0}^{\infty} D(n))}{N} \sum_{n=0}^{\infty} I_{SD_{n+1}}\Big] \frac{1}{s^{q+1}},$$

$$\mathscr{L}\{\sum_{n=0}^{\infty} I_{AP_{n+1}}\} = \frac{I_{AP_n}}{s} + \Big[\frac{\beta_P(\alpha_P \sum_{n=0}^{\infty} C(n) + \sum_{n=0}^{\infty} D(n))}{N} - (\phi_P + \mu) \sum_{n=0}^{\infty} I_{AP_n}(t)\Big] \frac{1}{s^{q+1}},$$

$$\mathscr{L}\{\sum_{n=0}^{\infty} I_{SP_{n+1}}\} = \frac{I_{SP_n}}{s} + \Big[\phi_P \sum_{n=0}^{\infty} I_{AP_n} - (\eta_P + \varpi_P + \mu) \sum_{n=0}^{\infty} I_{SD_n} - \gamma_2 \frac{\beta_D(\alpha_D \sum_{n=0}^{\infty} A(n) + \sum_{n=0}^{\infty} B(n))}{N} \sum_{n=0}^{\infty} I_{SP_{n+1}}\Big] \frac{1}{s^{q+1}},$$

$$\mathscr{L}\{\sum_{n=0}^{\infty} I_{SDP_{n+1}}\} = \frac{I_{SDP_n}}{s} + \Big[\frac{\beta_{DP} \sum_{n=0}^{\infty} E(n)}{N} + \gamma_1 \frac{\beta_P(\alpha_P \sum_{n=0}^{\infty} C(n) + \sum_{n=0}^{\infty} D(n))}{N} \sum_{n=0}^{\infty} I_{SD_n} + \gamma_2 \frac{\beta_D(\alpha_D \sum_{n=0}^{\infty} A(n) + \sum_{n=0}^{\infty} B(n))}{N} \sum_{n=0}^{\infty} I_{SP_n} - (\eta_{DP} + \varpi_{DP} + \mu) \sum_{n=0}^{\infty} I_{SDP_n}\Big] \frac{1}{s^{q+1}},$$

$$\mathscr{L}\{\sum_{n=0}^{\infty} Q_{SD_{n+1}}\} = \frac{Q_{SD_n}}{s} + \Big[\theta \sum_{n=0}^{\infty} I_{SD_n} - (\Omega + \mu) \sum_{n=0}^{\infty} Q_{SD_n}\Big] \frac{1}{s^{q+1}},$$

$$\mathscr{L}\{\sum_{n=0}^{\infty} R_{n+1}\} = \frac{R_n}{s} + \Big[VbN + \eta_P \sum_{n=0}^{\infty} I_{SP_n} + \eta_D \sum_{n=0}^{\infty} I_{SD_n} + \eta_{SDP} \sum_{n=0}^{\infty} I_{SP_n} - \mu \sum_{n=0}^{\infty} R_n\Big] \frac{1}{s^{q+1}}. \tag{13}$$

Taking the inverse Laplace transform of equation (13)

$$
\begin{aligned}
\sum_{n=0}^{\infty} S_{n+1} &= S_n + \Big[bN(1-V) - \Big(\frac{\beta_D(\alpha_D \sum\limits_{n=0}^{\infty} A(n) + \sum\limits_{n=0}^{\infty} B(n))}{N} \\
&\quad + \frac{\beta_P(\alpha_P \sum\limits_{n=0}^{\infty} C(n) + \sum\limits_{n=0}^{\infty} D(n))}{N} + \frac{\beta_{DP} \sum\limits_{n=0}^{\infty} E(n)}{N}\Big) - \mu \sum_{n=0}^{\infty} S_n\Big]\frac{t^q}{\Gamma(q+1)}, \\
\sum_{n=0}^{\infty} I_{AD_{n+1}} &= I_{AD_n} + \Big[\frac{\beta_D(\alpha_D \sum\limits_{n=0}^{\infty} A(n) + \sum\limits_{n=0}^{\infty} B(n))}{N} - (\phi_D + \mu)\sum_{n=0}^{\infty} I_{AD_n}\Big]\frac{t^q}{\Gamma(q+1)}, \\
\sum_{n=0}^{\infty} I_{SD_{n+1}} &= I_{SD_n} + \Big[\phi_D \sum_{n=0}^{\infty} I_{AD_n} - (\theta + \eta_D + \varpi_D + \mu)\sum_{n=0}^{\infty} I_{SD_n} \\
&\quad - \gamma_1 \frac{\beta_P(\alpha_P \sum\limits_{n=0}^{\infty} C(n) + \sum\limits_{n=0}^{\infty} D(n))}{N} \sum_{n=0}^{\infty} I_{SD_1}\Big]\frac{t^q}{\Gamma(q+1)}, \\
\sum_{n=0}^{\infty} I_{AP_{n+1}} &= I_{AP_n} + \Big[\frac{\beta_P(\alpha_P \sum\limits_{n=0}^{\infty} C(n) + \sum\limits_{n=0}^{\infty} D(n))}{N} - (\phi_P + \mu)\sum_{n=0}^{\infty} I_{AP_n}\Big]\frac{t^q}{\Gamma(q+1)}, \\
\sum_{n=0}^{\infty} I_{SP_{n+1}} &= I_{SP_n} + \Big[\phi_P \sum_{n=0}^{\infty} I_{AP_n} - (\eta_P + \varpi_P + \mu)\sum_{n=0}^{\infty} I_{SD_n} \\
&\quad - \gamma_2 \frac{\beta_D(\alpha_D \sum\limits_{n=0}^{\infty} A(n) + \sum\limits_{n=0}^{\infty} B(n))}{N} \sum_{n=0}^{\infty} I_{SP_1}\Big]\frac{t^q}{\Gamma(q+1)}, \\
\sum_{n=0}^{\infty} I_{SDP_{n+1}} &= I_{SDP_n} + \Big[\frac{\beta_{DP} \sum\limits_{n=0}^{\infty} E(n)}{N} + \gamma_1 \frac{\beta_P(\alpha_P \sum\limits_{n=0}^{\infty} C(n) + \sum\limits_{n=0}^{\infty} D(n))}{N} \sum_{n=0}^{\infty} I_{SD_n} \\
&\quad + \gamma_2 \frac{\beta_D(\alpha_D \sum\limits_{n=0}^{\infty} A(n) + \sum\limits_{n=0}^{\infty} B(n))}{N} \sum_{n=0}^{\infty} I_{SP_n} - (\eta_{DP} + \varpi_{DP} + \mu)\sum_{n=0}^{\infty} I_{SDP_n}\Big]\frac{t^q}{\Gamma(q+1)}, \\
\sum_{n=0}^{\infty} Q_{SD_{n+1}} &= Q_{SD_n} + \Big[\theta \sum_{n=0}^{\infty} I_{SD_n} - (\Omega + \mu)\sum_{n=0}^{\infty} Q_{SD_n}\Big]\frac{t^q}{\Gamma(q+1)}, \\
\sum_{n=0}^{\infty} R_{n+1} &= R_n + \Big[VbN + \eta_P \sum_{n=0}^{\infty} I_{AP_n} + \eta_D \sum_{n=0}^{\infty} I_{AD_n} + \eta_{SDP} \sum_{n=0}^{\infty} I_{SP_n} - \mu \sum_{n=0}^{\infty} R_n\Big]\frac{t^q}{\Gamma(q+1)}.
\end{aligned}
\tag{14}
$$

for $n = 0$

$$
\begin{aligned}
S_1 &= S_0 + \Big[bN(1-V) - \Big(\frac{\beta_D(\alpha_D A_0 + B_0)}{N} + \frac{\beta_P(\alpha_P C_0 + D_0)}{N} + \frac{\beta_{DP} E_0}{N}\Big) \\
&\quad - \mu S_0\Big]\frac{t^q}{\Gamma(q+1)}, \\
I_{AD_1} &= I_{AD_0} + \Big[\frac{\beta_D(\alpha_D A_0 + B_0)}{N} - (\phi_D + \mu) I_{AD_0}\Big]\frac{t^q}{\Gamma(q+1)}, \\
I_{SD_1} &= I_{SD_0} + \Big[\phi_D I_{AD_0} - (\theta + \eta_D + \varpi_D + \mu) I_{SD_0} - \gamma_1 \frac{\beta_P(\alpha_P C_0 + D_0)}{N} I_{SD_0}\Big]\frac{t^q}{\Gamma(q+1)}, \\
I_{AP_1} &= I_{AP_0} + \Big[\frac{\beta_P(\alpha_P C_0 + D_0)}{N} - (\phi_P + \mu) I_{AP_0}\Big]\frac{t^q}{\Gamma(q+1)}, \\
I_{SP_1} &= I_{SP_0} + \Big[\phi_P I_{AP_0} - (\eta_P + \varpi_P + \mu) I_{SD_0} - \gamma_2 \frac{\beta_D(\alpha_D A_0 + B_0)}{N} I_{SP_0}\Big]\frac{t^q}{\Gamma(q+1)}, \\
I_{SDP_1} &= I_{SDP_0} + \Big[\frac{\beta_{DP} E_0}{N} + \gamma_1 \frac{\beta_P(\alpha_P C_0 + D_0)}{N} I_{SD_0} \\
&\quad + \gamma_2 \frac{\beta_D(\alpha_D A_0 + B_0)}{N} I_{SP_0} - (\eta_{DP} + \varpi_{DP} + \mu) I_{SDP_0}\Big]\frac{t^q}{\Gamma(q+1)}, \\
Q_{SD_1} &= Q_{SD_0} + \Big[\theta I_{SD_0} - (\Omega + \mu) Q_{SD_0}\Big]\frac{t^q}{\Gamma(q+1)}, \\
R_1 &= R_0 + \Big[VbN + \eta_P I_{AP_0} + \eta_D I_{AD_0} + \eta_{SDP} I_{SP_0} - \mu R_0\Big]\frac{t^q}{\Gamma(q+1)}.
\end{aligned}
\tag{15}
$$

4 Numerical Simulations

In this section, we will use the parameters in Table 2 and assign initial values to the compartments. The Figure 1 illustrates Effect of Varying q on the System Variables at $n = 0$ using equation (15) with $S(0) = 990,\ I_{AD}(0) = 10,\ I_{SD}(0) = 5,\ I_{AP}(0) = 7,\ I_{SP}(0) = 4,\ I_{SDP}(0) > 3,\ Q_{SD}(0) = 2$ respectively.

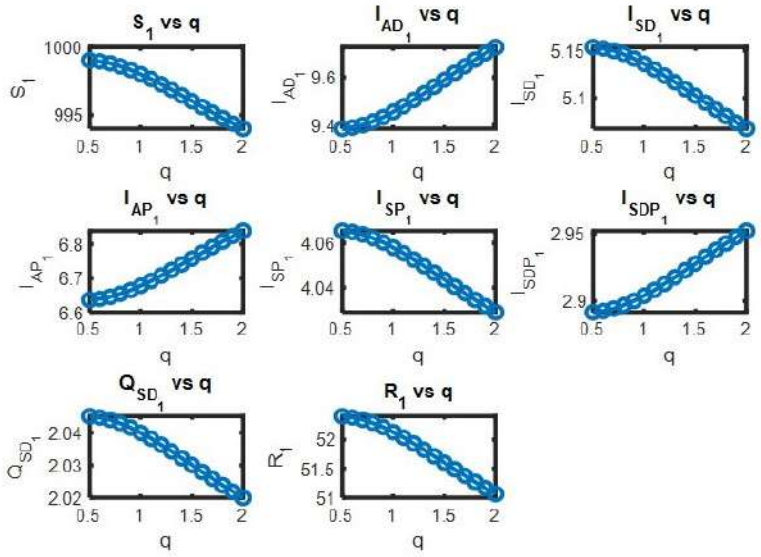


Figure 1: Effect of Varying q on the System Variables at $n = 0$.

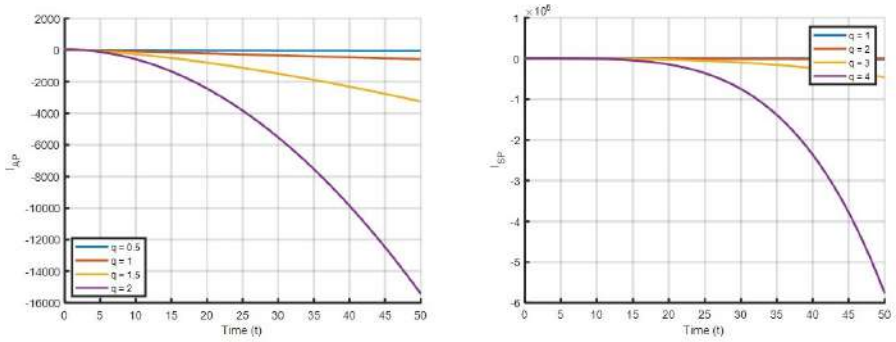


Figure 2: Plots on the effect of varying q on I_{AP} and I_{SP} compartments over time.

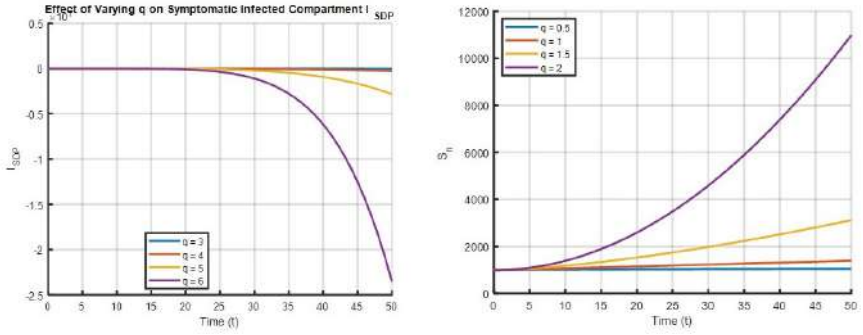


Figure 3: Plots on the effect of varying q on I_{SDP} and S compartments over time.

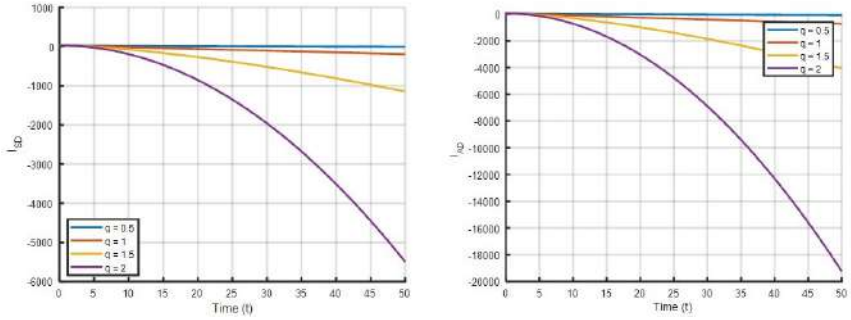


Figure 4: Plots on the effect of varying q on I_{SD} and I_{AD} compartments over time.

5 Conclusion

In this article, we developed a fractional-order compartmental model to investigate the transmission dynamics of Diphtheria and Pertussis co-infections within the human population. To analyze and solve the model, we applied the Laplace-Adomian Decomposition Method, yielding a series of solutions that demonstrably converge to exact values. Our findings highlight the critical role of fractional-order models in understanding and controlling disease outbreaks.

References

[1] Khatiwada, A. P., Shrestha, N., and Shrestha, S. (2021). Will COVID-19 lead to a resurgence of vaccine-preventable diseases?. Infection and Drug Resistance, 119-124.

[2] Agüero, M. L., Castillo, J. B. D., Falleiros-Arlant, L. H., Berezín, E., de Moraes, J. C., Torres-Martínez, C., ... and López-Medina, E. (2023). Risks of low vaccination coverage and strategies

to prevent the resurgence of vaccine-preventable diseases in infants in the COVID-19 pandemic scenario: recommendations for Latin America and the Caribbean by the group of experts on infant immunization for Latin America. Expert Review of Vaccines, 22(1), 1091-1101.

[3] Johnson, O. S., Edogbanya, H. O., Wakili, A., and John, A. T. (2024). Diphtheria Disease Transmission Dynamics In Low Vaccine Coverage Setting. International Journal of Mathematical Sciences and Optimization: Theory and Applications, 10(2), 79-106.

[4] Johnson, O. S., Edogbanya, H. O., Emmanuel, J., and Olukanni, S. E. (2023). Stability Analysis of COVID-19 Model with Quarantine. International Journal of Mathematical Sciences and Computing, 9(3), 26-45.

[5] Organization, W.H.: COVID-19 Pandemic Fuels Largest Continued Backslide in Vaccinations in Three Decades, https://www.who.int/news/item/15-07-2022- covid-19-pandemic-fuels-largest-continued-backslide-in-vaccinations-in-three decades. Accessed: 2024-05-26 (2022).

[6] Gouveia, N., and Fletcher, T. (2000). Respiratory diseases in children and outdoor air pollution in Sao Paulo, Brazil: a time series analysis. Occupational and environmental medicine, 57(7), 477-483.

[7] Clay, P. A., Duffy, M. A., and Rudolf, V. H. (2020). Within-host priority effects and epidemic timing determine outbreak severity in co-infected populations. Proceedings of the Royal Society B, 287 (1922), 20200046.

[8] Cox, F. E. G. (2001). Concomitant infections, parasites and immune responses. Parasitology, 122 (S1), S23-S38.

[9] Glidden, Caroline K., Courtney AC Coon, Brianna R. Beechler, Chase McNulty, Vanessa O. Ezenwa, and Anna E. Jolles. "Co-infection best predicts respiratory viral infection in a wild host." Journal of Animal Ecology 90, no. 3 (2021): 602-614.

[10] Griffiths, E. C., Pedersen, A. B., Fenton, A., and Petchey, O. L. (2011). The nature and consequences of coinfection in humans. Journal of Infection, 63(3), 200-206.

[11] Liang, J. L. (2018). Prevention of pertussis, tetanus, and diphtheria with vaccines in the United States: recommendations of the Advisory Committee on Immunization Practices (ACIP). Recommendations and reports, 67.

[12] Johnson, S. O., Edogbanya, H. O., Omolehin, J. O., and Johnson, O. (2024). Characteristics and control strategies for Diphtheria-Pertussis co-infection risk in the post COVID-19 era. International Journal of Mathematical Analysis and Modelling, 7(2).

[13] Murphy, T. V., Slade, B. A., Broder, K. R., Kretsinger, K., Tiwari, T., Joyce, M. P., ... and Moran, J. S. (2008). Prevention of pertussis, tetanus, and diphtheria among pregnant and postpartum women and their infants. Recomm Rep, 57, 1-51.

[14] Kuchar, E., Karlikowska-Skwarnik, M., Han, S., and Nitsch-Osuch, A. (2016). Pertussis: history of the disease and current prevention failure. Pulmonary dysfunction and disease, 77-82.

[15] Sadoh, A. E., and Oladokun, R. E. (2012). Re-emergence of diphtheria and pertussis: implications for Nigeria. Vaccine, 30 (50), 7221-7228.

[16] Calderón, T. A., Coffin, S. E., and Sammons, J. S. (2015). Preventing the spread of pertussis in pediatric healthcare settings. Journal of the Pediatric Infectious Diseases Society, 4(3), 252-259.

[17] Brooks, D. A., and Clover, R. (2006). Pertussis infection in the United States: role for vaccination of adolescents and adults. The Journal of the American Board of Family Medicine, 19 (6), 603-611.

[18] Edogbanya, H. O., and Johnson, O. S. 1.20 Sensitivity Analysis of Pertussis Transmission Dynamics. DEPARTMENT OF MATHEMATICS FACULTY OF SCIENCE, 27.

[19] Helen O. E., and O. S. Johnson. (2024). Mathematical Modeling for Mitigating Pertussis Resurgence in the Post-COVID-19 Era: A Sensitivity Analysis and Intervention Strategies. International Journal of Novel Research in Physics Chemistry and Mathematics, 11(1), 12–28. https://doi.org/10.5281/zenodo.10721146

[20] Meenakshi, A., Renuga, E., Čep, R., and Karthik, K. (2024). Analysis of Caputo Fractional-Order Co-Infection COVID-19 and Influenza SEIR Epidemiology by Laplace Adomian Decomposition Method. Mathematics, 12(12), 1876.

[21] Acheneje, G. O., Omale, D., Agbata, B. C., Atokolo, W., Shior, M. M., and Bolarinwa, B. (2024). Approximate Solution of the Fractional Order Mathematical Model on the Transmission Dynamics on The Co-Infection of COVID-19 and Monkeypox Using the Laplace-Adomian Decomposition Method. International Journal of Mathematics and Statistics Studies, 12(3), 17-51.

[22] Zeng, Y. (2022). A Laplace Adomian Decomposition Method for Fractional Order Infection Model. J. Appl. Math. Comput, 6, 529-534.

[23] Abioye, A. I., Peter, O. J., Ogunseye, H. A., Oguntolu, F. A., Ayoola, T. A., and Oladapo, A. O. (2023). A fractional-order mathematical model for malaria and COVID-19 co-infection dynamics. Healthcare Analytics, 4, 100210.

[24] Schiff, J. L. (2013). The Laplace transform: theory and applications. Springer Science and Business Media.

[25] Caputo, M. (1969). Elasticita e dissipazione. Zanichelli.

[26] Caputo, M., and Fabrizio, M. (2015). A new definition of fractional derivative without singular kernel. Progress in Fractional Differentiation and Applications, 1(2), 73-85

[27] Meenakshi, A., Renuga, E., Čep, R., and Karthik, K. (2024). Analysis of Caputo Fractional-Order Co-Infection COVID-19 and Influenza SEIR Epidemiology by Laplace Adomian Decomposition Method. Mathematics, 12(12), 1876.

[28] Yakubu, A. A., Abdullah, F. A., and Yatim, Y. M. (2022). Mathematical Model of Pertussis and Pneumonia Co-Infection in Infants with Maternally Derived Immunity. Sains Malaysiana, 51(7), 2197-2209.

[29] Omame, A., and Abbas, M. (2023). Modeling SARS-CoV-2 and HBV co-dynamics with optimal control. Physica A: Statistical Mechanics and its Applications, 615, 128607.

[30] Izzati, N., and Andriani, A. (2021, April). Dynamical analysis of diphtheria epidemic model with natural immunity rate on exposed individuals. In Journal of Physics: Conference Series (Vol. 1869, No. 1, p. 012117). IOP Publishing.

A mathematical model for transmission dynamics of COVID-19 in Nigeria and its post effects

B.C. Agbata[*], D.F. Agbebaku[†‡], C.E. Odo[§], J.T. Ojih[**], M.M. Shior[††], and I.G. Ezugorie[‡‡]

Abstract

This study presents a mathematical model formulated through a system of differential equations to analyze the dynamics of COVID-19 in Nigeria and its post effects. The total population (N), is divided into six compartments: susceptible (S), vaccinated (V), exposed (E), infected (I), deceased (D), and recovered (R). Our primary objective is to conduct a comprehensive mathematical analysis of the disease and elucidate its post-effects. Qualitative analyses such as identification of invariant regions, positivity of solutions, and stability analyses are performed. The basic reproduction number is obtained using the next-generation matrix, and its epidemiological significance such as threshold for epidemic spread, intervention decision and estimation of herd immunity are discussed. Sensitivity analysis is conducted to determine the most influential parameters and numerical simulation is carryout using MATLAB which revealed the model behavior in real-life. Post-effects of COVID-19 in Nigeria which include increased in poverty levels, reduced income, job losses, strain in healthcare system, educational disruption are identified. Our findings underscore the importance of implementing targeted public health interventions to mitigate the socio-economic impact of the pandemic, strengthen the healthcare system's resilience, and address the educational disruptions. Recommendations include prioritizing vaccination efforts to achieve herd immunity, enhancing healthcare infrastructure and capacity, implementing social protection measures to support vulnerable populations, and adopting innovative approaches to facilitate remote learning and educational recovery.

Keywords and phrases: COVID-19, Post effects of COVID-19, Epidemiology, Basic reproduction number, Sensitivity analysis.

[*]Department of Mathematics and Statistics, Faculty of Science, Confluence University of Science and Technology, Osara, Nigeria
[†] Corresponding author E-mail: dennis.agbebaku@unn.edu.ng
[‡] Department of Mathematics, University of Nigeria, Nsukka, Nigeria
[§] Department of Mathematics, Federal Polytechnic, Bida, Niger State, Nigeria
[**] Department of Primary Education Studies, Kogi State College of Education, Ankpa, Nigeria
[††] Department of Mathematics/ Computer Science, Benue State University, Makurdi, Nigeria
[‡‡] Department of Industrial Mathematics/ Applied Statistics, Enugu State University of Science and Technology, Enugu, Nigeria

1 Introduction

The COVID-19 pandemic, caused by the novel Coronavirus SARS-CoV-2, has emerged as one of the most significant global health crises in recent history. The virus belongs to the family Coronaviridae and is characterized by its high transmissibility and ability to cause severe respiratory illness, ranging from mild symptoms to acute respiratory distress syndrome and death[1, 2] primary mode of transmission is through respiratory droplets produced when an infected individual coughs, sneezes, or talks, although airborne and surface transmission also contribute to its spread [1].

In Nigeria, COVID-19 was first reported on February 27, 2020, when an Italian citizen tested positive for the virus in Lagos, the country's largest city [1, 3]. Since then, the virus has spread to various states within the country, prompting significant public health interventions and mitigation measures by the Nigerian government and health authorities [3]. The transmission dynamics of COVID-19 in Nigeria are influenced by factors such as population density, mobility patterns, healthcare infrastructure, and socio-economic disparities. Preventing the spread of COVID-19 relies on a combination of public health measures, including hand hygiene, respiratory etiquette, physical distancing, wearing face masks, and vaccination [2]. These interventions aim to reduce the likelihood of viral transmission and mitigate the burden on healthcare systems. Vaccination campaigns have been initiated globally and in Nigeria to immunize populations against COVID-19 and achieve herd immunity [1, 2, 4].While several treatments and vaccines have been developed to combat COVID-19, management primarily focuses on supportive care to alleviate symptoms and prevent complications [2, 4]. Severe cases may require hospitalization, oxygen therapy, and in some instances, mechanical ventilation in intensive care units. Additionally, antiviral medications, corticosteroids, and monoclonal antibodies have been used to treat hospitalized patients with COVID-19 [1, 2]. Diagnosing COVID-19 involves various methods, including molecular tests (such as reverse transcription-polymerase chain reaction or RT-PCR) to detect viral RNA, antigen tests to identify viral proteins, and serological tests to detect antibodies produced in response to infection [1, 2]. Prompt and accurate diagnosis is crucial for initiating appropriate management and implementing public health measures to prevent further transmission.

Adekunle *et al* [5], developed a compartmental mathematical model to simulate the dynamics of COVID-19 transmission in Nigeria. Their model incorporated parameters such as population size, contact rates, and intervention measures. The main findings revealed that early implementation of non-pharmaceutical interventions (NPIs) significantly reduced the spread of the virus and mitigated the burden on the healthcare system. The study concluded that a combination of NPIs, including social distancing and mask-wearing, was essential for controlling the pandemic in Nigeria. Ogunnaike *et al*l [6], developed a susceptible-exposed-infectious-recovered (SEIR) compartmental model to assess the impact of intervention strategies on COVID-19 transmission dynamics in Nigeria. The model considered factors such as population density, mobility, and healthcare capacity. Their findings suggested that early implementation of stringent control measures, coupled with widespread testing

and contact tracing, could effectively suppress the spread of the virus and reduce the number of cases and deaths. Adekunle *et all* [7], developed a dynamic compartmental model to predict the spread of COVID-19 in Nigeria under different scenarios. Their model incorporated parameters such as transmission rates, contact patterns, and the effectiveness of control measures. The study found that without intervention, the virus would overwhelm the healthcare system. However, early implementation of interventions such as lockdowns and mass testing could mitigate the impact of the pandemic and reduce the number of cases and deaths. Teslya *et al* [8], developed a mathematical model to investigate COVID-19 transmission dynamics in various population density settings globally. Their model considered factors such as population density, mobility, and the effectiveness of intervention measures. The study found that population density significantly influenced the transmission rate of COVID-19, with higher-density areas experiencing faster spread. The findings underscored the importance of tailored intervention strategies based on population density to control the pandemic. Flaxman *et al* [9], employed a Bayesian approach to model COVID-19 transmission dynamics in different regions of the United States. Their model incorporated data on reported cases, testing rates, and intervention measures. The study identified regional variations in transmission rates and the effectiveness of control measures. The findings highlighted the importance of targeted interventions and surveillance strategies tailored to regional dynamics to effectively control the spread of the virus. This study aims to contribute to the understanding of COVID-19 transmission dynamics in Nigeria through mathematical modeling, with the goal of informing evidence-based policy decisions and interventions to control the spread of the virus and minimize its socio-economic consequences.

The novelty of this study lies in its comprehensive integration of mathematical modeling, epidemiological analysis, and socio-economic impact assessment to provide a holistic understanding of COVID-19 dynamics in Nigeria. Unlike previous studies that focus solely on disease transmission or economic consequences, this research uniquely formulates a system of differential equations incorporating vaccination as a distinct compartment, allowing for a nuanced exploration of its role in controlling the epidemic. The study not only derives the basic reproduction number and conducts stability and sensitivity analyses but also bridges the gap between mathematical epidemiology and real-world policy implications by linking the model outcomes to critical socio-economic effects such as poverty, healthcare strain, job losses, and educational disruptions. The use of MATLAB for numerical simulations enhances the study's practical relevance by demonstrating real-life disease progression and intervention impacts. Furthermore, its emphasis on post-pandemic recovery strategies, including healthcare resilience, targeted social protections, and innovative educational solutions, underscores its originality in addressing both immediate and long-term consequences of the pandemic. This multi-faceted approach provides a novel framework that can guide policymakers in developing data-driven interventions tailored to Nigeria's unique demographic and economic landscape.

2 Post effects of COVID-19 in Nigeria

The COVID-19 pandemic has left a lasting impact on Nigeria, extending beyond its initial health crisis to profoundly affect various facets of society, economy, and governance. One significant post-effect is the strain on the country's healthcare system, which has been overwhelmed by the surge in cases and strained resources. This strain has exposed underlying weaknesses in Nigeria's healthcare infrastructure, including shortages of medical supplies, inadequate facilities, and challenges in healthcare workforce management [10]. Moreover, the diversion of attention and resources towards managing the pandemic has disrupted routine healthcare services, leading to delays in accessing essential medical care for non-COVID-19 conditions. These disruptions have the potential to exacerbate existing health disparities and contribute to worsened health outcomes in the long term, particularly among vulnerable populations.

The economic repercussions of COVID-19 in Nigeria have been profound, with widespread disruptions to livelihoods, businesses, and economic activities. The implementation of lockdowns and containment measures to curb the spread of the virus resulted in mass unemployment, income losses, and economic instability [11]. Small and medium-sized enterprises (SMEs), which are the backbone of Nigeria's economy, were particularly hard-hit, facing challenges such as reduced demand, supply chain disruptions, and financial constraints. The socio-economic fallout from the pandemic has exacerbated poverty, inequality, and social tensions, posing significant challenges to Nigeria's development aspirations and efforts to achieve sustainable growth and prosperity [12].

3 Model formulation

The total population $N(t)$ is divided into six epidemiological compartments. The susceptible humans $S(t)$ exposed humans $E(t)$, the infected humans $I(t)$, the deceased $D(t)$, treatment class $T(t)$, recovered humans $R(t)$. Individuals are recruited into the susceptible population at rate Λ, the susceptible population reduces at the rate α_1, that is, the rate at which a susceptible individuals became exposed to the disease. ω_1 is the vaccination rate of susceptible individual and ω_2, ω_3 are the rates at which vaccinated individuals became exposed and infected respectively due to vaccine failure. The exposed population is further reduced by α_2 which is the rate at which exposed human interacted with COVID-19 infected individuals, γ represents disease induced death rate whereas ρ is the burial rate of deceased population and α_3 denotes recovery rate of infected individuals. Population of every compartment is reduced at the rate μ which represents natural death rate.

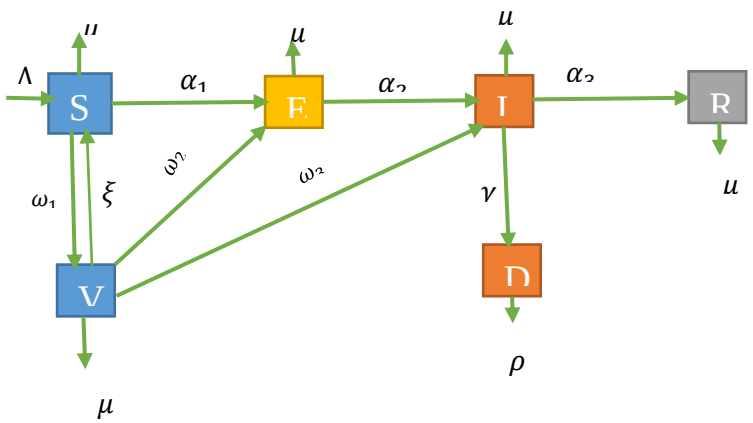


Fig. 1. Schematic Diagram for the model.

Figure 1, gives the schematic diagram for the model, Schematic diagram is essential tools in modeling as it visually illustrates the structure, relationships, and interactions within a mathematical or conceptual framework [2, 13]. This diagram provides a clear representation of system components and their connections, making complex models more accessible to modelers and stakeholders alike [14]. In mathematical modeling, they typically depict how variables, parameters, and equations interact, showing causal relationships and dependencies that govern system behavior [13]. Schematic diagrams aid in conceptualizing model architecture, defining initial conditions and constraints, and outlining system dynamics under different scenarios.

The model Equations

$$\left.\begin{aligned}
\frac{dS}{dt} &= \Lambda + \xi V - (\alpha_1 + \omega_1 + \mu)S \\
\frac{dV}{dt} &= \omega_1 S - (\xi + \omega_2 + \omega_3 + \mu)V \\
\frac{dE}{dt} &= \alpha_1 S + \omega_2 V - (\alpha_2 + \mu)E \\
\frac{dI}{dt} &= \alpha_2 E + (\alpha_3 + \gamma + \mu)I \\
\frac{dD}{dt} &= \gamma I - \rho D \\
\frac{dR}{dt} &= \alpha_3 I - \mu R
\end{aligned}\right\} \quad (1)$$

$$\alpha_1 = \frac{\beta(I + D)}{N}$$

3.1 Model Variables and Descriptions

Table 1. Description of parameters and variables

Variable	Description
S	Susceptible humans
V	Vaccinated individuals
E	Exposed individuals
I	Infected individuals
D	Diseased compartment
R	Recovered individuals
Parameter	**Description**
Λ	Constant recruitment level
ω_1	Vaccination rate

β	Contact rate of susceptible individuals with infected individuals
α_2	Infectious rate of exposed individuals
γ	Disease induced rate
ω_2	Rate at which the vaccinated individuals becomes exposed due to vaccine failure
ω_3	Rate at which the vaccinated individuals became infected due to vaccine failure
μ	Natural death rate
ρ	Burial rate of diseased humans
α_3	Recovering rate
ξ	Rate at which vaccinated individuals become Susceptible

Table 1, gives the parameters and variables used for the study, Parameters and variables are essential elements in mathematical modeling, each playing distinct yet complementary roles in defining and simulating complex systems [13]. Parameters are constants that characterize the system's properties and initial conditions, setting the framework within which the model operates. They control the model's behavior and are crucial for sensitivity analysis, identifying which parameters significantly impact model outcomes. Variables, on the other hand, represent the changing quantities within the system, such as outputs of interest or dynamic states over time [14, 15]. They depend on parameters and other variables, providing insights into system behavior and enabling predictions and scenario analyses. Together, parameters and variables form the foundation of mathematical models, translating real-world complexities into structured frameworks for analysis, prediction, and understanding of diverse phenomena across scientific and engineering disciplines [13].

3.2 Invariant Region of the Model

The model solutions are feasible for all $t > 0$, if they enter the invariant region D, which is given by:

$$D=\left\{\left(S,V,E,I,D,R\right):S>0,\mathrm{V}>0,,E>0,I>0,\mathrm{D}>0,R>0,N<\frac{\Lambda}{\mu}\right\}$$

Proof

The total population of the model is given as

$$N\left(t\right)=S+V+E+I+D+R$$

Adding the differential equations is

$$N^{'}\left(t\right)=S^{'}+V^{'}+E^{'}+I^{'}+D^{'}+R^{'}$$

On evaluating the algebraic terms, we obtain

$$N^{'}(t)=\Lambda-\left(S+V+E+I+D+R\right)\mu-\rho D$$

$$N^{'}(t)=\Lambda-\mu N-\rho D$$

$$\frac{dN}{dt}\leq\Lambda-\mu N$$

$$\frac{dN}{dt}+\mu N=\Lambda$$

Multiplying through by the integrating factor e^{ut}, gives

$$d\left(Ne^{ut}\right)\leq\Lambda e^{ut}dt$$

Integrating both sides

$$\int d\left(Ne^{ut}\right)\leq\int\Lambda e^{ut}dt$$

$$N(\mathrm{t})\leq\frac{\Lambda}{\mu}+K_{0}e^{-ut}$$

Therefore, D remains a positively invariant set within the trajectory outlined by model (1), ensuring that no solution trajectory exits through the boundary of region D. Consequently, within this domain, the model can be deemed both epidemiologically and mathematically well-defined [16].

3.3 Epidemiological meaning of the fraction $\frac{\Lambda}{\mu}$

In the model, the ratio $\frac{\Lambda}{\mu}$ holds significance in understanding the demographic dynamics of the population concerning the spread of COVID-19. The constant recruitment rate (Λ) signifies the pace at which new individuals join the population, either through birth or migration. In the case of COVID-19, this influx of susceptible individuals into the population could contribute to the pool of

people at risk of contracting the disease. Conversely, the natural death rate (μ) represents the rate at which individuals in the population perish due to causes unrelated to COVID-19 infection. This encompasses deaths from old age, diseases other than COVID-19, accidents, and other non-COVID-19-related factors [16, 17].

Thus, the ratio $\frac{\Lambda}{\mu}$ indicates the equilibrium between the addition of new susceptible individuals to the population and the removal of individuals through natural mortality. Concerning COVID-19, a higher ratio $\frac{\Lambda}{\mu}$ implies a population with a greater influx of susceptible individuals, potentially heightening the likelihood of COVID-19 transmission and outbreaks. Conversely, a lower ratio indicates a population where natural deaths are more prevalent, possibly diminishing the pool of susceptible individuals and thus the potential for COVID-19 transmission [18, 19].

Comprehending the $\frac{\Lambda}{\mu}$ ratio within the COVID-19 disease model aids in assessing the population's vulnerability to COVID-19 outbreaks and assists in devising effective vaccination strategies and public health interventions.

3.4 Positivity of solution of the model

It is necessary to show that all state variable of the model in are non-negative for all time (t), for the model to be epidemiologically and mathematically feasible in the region D given by [16, 20]:

$$D = \left\{ (S, V, E, I, D, R) \in R_+^6 : (S + V + E + I + D + R) \leq N \right\}$$

This can be done by considering,

$$\left\{ (S, V, E, I, D, R) \geq 0 \in R_+^6 \right\}$$

Lemma 1:

Supposed the initial data for the given model (1) be $(S,V,E,I,D,R)>0$. Then the solutions (S,V,E,I,D,R) of the model (1) are positive for all time $t>0$

Proof

Let $t_1=\sup\{t>0: S>0, V>0, E>0, I>0, D>0, R>0\in[0,t]\}$. Thus $t>0.$

We have from the first equation that

$$\frac{dS}{dt}=\Lambda+\xi V-\alpha_1 S-(\omega_1+\mu)\mathrm{S}$$

$$\frac{dS}{dt}\geq-(\omega_1+\mu)$$

$$\int\frac{dS}{dt}\geq-\int(\omega_1+\mu)\,\mathrm{dt}$$

$$\ln S\geq-(\omega_1+\mu)\,\mathrm{t}+\mathrm{c}$$

$$\mathrm{S(t)}\geq Ce^{-(\omega_1+\mu)t}$$

Applying the given initial, t = 0, S(0) = C

Therefore, $\mathrm{S(t)}\geq S(0)e^{-(\omega_1+\mu)t}$ and $(\omega_1+\mu)>0$

Similarly, it can be demonstrated that $V,E,I,D,R>0$

4 Asymptotic stability of the disease-free equilibrium of the model

The equilibrium state where there is no infection (or absence of the disease), a point where $E=I=D=R=0$ is called the disease-free equilibrium point (DFE) which is given

$$\eta_0=\{S^*,\mathrm{V}^*,E^*,I^*,D^*,R^*>0\}=\left\{\frac{\Lambda(\xi+\mu)}{\xi\omega_1-(\omega_1+\mu)(\xi+\mu)},\frac{\omega_1\Lambda}{\mu^2+\xi\alpha_1+\omega_1+(\xi+\omega_1)\mu},0,0,0,0\right\}$$

4.1 Basic reproduction number (R_0) of the model

The basic reproduction number R_0 is a fundamental concept in epidemiology that measures the average number of secondary infections generated by a single infected individual in a population where everyone is susceptible to the disease. In simpler terms, it represents the potential for a disease to spread within a population [18]. R_0 is defined as the expected number of secondary cases produced by a single infected individual in a population where everyone is susceptible to the disease and no control measures are in place [16]. It serves as a crucial epidemiological parameter for understanding the transmission dynamics of infectious disease. An R_0 greater than 1 indicates that, on average, each infected individual is spreading the disease to more than one other person, leading to sustained transmission and potential outbreaks. Conversely, an R_0 less than 1 suggests that the disease is unlikely to cause an epidemic as each infected individual infects fewer than one other person, leading to the disease eventually dying out. [18, 21]. Hence, it follows that

$R_0 = \rho\left(FV^{-1}\right)$ ρ is given by dominant eigenvalue of FV^{-1}

$$F = \begin{bmatrix} 0 & \frac{\beta(\xi+\mu)}{\mu+\xi+\omega_1} & \frac{\beta(\xi+\mu)}{\mu+\xi+\omega_1} \\ 0 & 0 & 0 \\ 0 & 0 & 0 \end{bmatrix} \quad V = \begin{bmatrix} K_2 & 0 & 0 \\ -\alpha_2 & K_3 & 0 \\ 0 & -\gamma & \rho \end{bmatrix}$$

$$F.V^{-1} = \begin{bmatrix} \frac{\beta(\xi+\mu)\alpha_2}{(\mu+\xi+\omega_1)\mathrm{K}_2 K_3} + \frac{\beta(\xi+\mu)\alpha_2\gamma}{(\mu+\xi+\omega_1)\mathrm{K}_2 K_3\rho} & \frac{\beta(\xi+\mu)}{(\mu+\xi+\omega_1)K_3} + \frac{\beta(\xi+\mu)\gamma}{(\mu+\xi+\omega_1)K_3\rho} & \frac{\beta(\xi+\mu)}{(\mu+\xi+\omega_1)\rho} \\ 0 & 0 & 0 \\ 0 & 0 & 0 \end{bmatrix}$$

Therefore, the basic reproduction number of the model is

$$R_0 = \frac{\beta\alpha_2(\beta+\gamma)(\xi+\mu)}{(\mu+\xi+\omega_1)\mathrm{K}_2 K_3\rho}$$

$$R_0 = \frac{\beta\alpha_2(\gamma\mu+\gamma\xi+\mu\rho+\rho\xi)}{(\mu+\xi+\omega_1)\mathrm{K}_2 K_3\rho}$$

4.2 Local asymptotic stability of the DFE of the model

Theorem 1

The disease-free equilibrium points of the is locally asymptotically stable (LAS) if $R_0 < 1$*, and unstable if* $R_0 > 1$.

Proof

Using Jacobian matrix to prove the local stability of the disease-free equilibrium point

$$J(\varepsilon_0) = \begin{bmatrix} -(\omega_1+\mu) & \xi & 0 & \frac{-\beta(\xi+\mu)}{\mu+\xi+\omega_1} & \frac{-\beta(\xi+\mu)}{\mu+\xi+\omega_1} & 0 \\ \omega_1 & -K_1 & 0 & 0 & 0 & 0 \\ 0 & \omega_2 & -K_2 & \frac{\beta(\xi+\mu)}{\mu+\xi+\omega_1} & \frac{\beta(\xi+\mu)}{\mu+\xi+\omega_1} & 0 \\ 0 & 0 & \alpha_2 & -K_3 & 0 & 0 \\ 0 & 0 & 0 & \gamma & -\rho & 0 \\ 0 & 0 & 0 & \alpha_3 & 0 & -\mu \end{bmatrix}$$

Since the diagonal of the first and last column consist of only the diagonal element, we can reduce $J(\varepsilon_0)$ to

$$J_1(\varepsilon_0) = \begin{bmatrix} \xi & 0 & -\frac{-B(\xi+\mu)}{\mu+\xi+\omega_1} & \frac{-\beta(\xi+\mu)}{\mu+\xi+\omega_1} \\ -K_1 & 0 & 0 & 0 \\ \omega_2 & -K_2 & \frac{\beta(\xi+\mu)}{\mu+\xi+\omega_1} & \frac{\beta(\xi+\mu)}{\mu+\xi+\omega_1} \\ 0 & \alpha_2 & -K_3 & 0 \end{bmatrix}$$

The characteristics polynomial of $J_1(\varepsilon_0)$ is

$$\lambda^5-\left(-\rho-K_3-K_2-K_1-\omega_1-\mu\right)\lambda^4+$$
$$\frac{\left(\begin{array}{l}\left(-\xi+\rho+K_1+K_2+K_3\right)\omega_1{}^2\\+\left(\begin{array}{l}\left(-\xi+2\rho+2K_1+2K_2+2K_3\right)\mu-\xi^2\\+\left(\rho+K_1+K_2+K_3\right)\xi+\left(\rho+K_2+K_3\right)K_1\\+\left(\rho+K_3\right)K_2+K_3\rho\end{array}\right)\omega_1\\+\left(\begin{array}{l}\left(\rho+K_1+K_2+K_3\right)\mu+\left(\rho+K_2+K_3\right)K_1\\+\left(\rho+K_3\right)K_2+K_3\rho-\beta\alpha_2\end{array}\right)(\mu+\xi)\end{array}\right)}{\mu+\xi+\omega_1}\lambda^3+$$
$$\frac{\left(\begin{array}{l}\left(\left(\rho+K_2+K_3\right)\xi+\left(-K_1-K_2-K_3\right)\rho+\left(-K_1-K_3\right)K_2-K_1K_3\right)\omega_1{}^2\\+\left(\begin{array}{l}\left(\left(\rho+K_2+K_3\right)\xi+\left(-2K_1-2K_2-2K_3\right)\rho+\left(-2K_1-2K_3\right)K_2+\beta\alpha_2-2K_1K_3\right)\mu+\left(\rho+K_2+K_3\right)\xi^2\\+\left(\left(-K_1-K_2-K_3\right)\rho+\left(-K_1-K_3\right)K_2+\beta\alpha_2-K_1K_3\right)\xi+\left(\left(-K_1-K_3\right)K_2-K_1K_3\right)\rho-K_1K_2K_3\end{array}\right)\omega_1\\+(\mu+\xi)\left(\begin{array}{l}\left(\left(-K_1-K_2-K_3\right)\rho+\left(-K_1-K_3\right)K_2+\beta\alpha_2-K_1K_3\right)\mu\\+\left(\left(-K_1-K_3\right)K_2+\beta\alpha_2-K_1K_3\right)\rho-K_1K_2K_3+\alpha_2\beta\left(K_1+\gamma\right)\end{array}\right)\end{array}\right)}{\mu+\xi+\omega_1}\lambda^2+$$
$$\frac{\left(\begin{array}{l}\left(\left(\left(K_2+K_3\right)\xi+\left(-K_2-K_3\right)K_1-K_2K_3\right)\rho+K_2K_3\left(\xi-K_1\right)\right)\omega_1{}^2\\+\left(\begin{array}{l}\left(\left(K_2+K_3\right)\xi+\left(-2K_2-2K_3\right)K_1+\beta\alpha_2-2K_2K_3\right)\mu+\left(K_2+K_3\right)\xi^2\\+\left(\left(-K_2-K_3\right)K_1+\beta\alpha_2-K_2K_3\right)\xi-K_1K_2K_3\\+\left(\left(K_2K_3-\beta\alpha_2\right)\xi+\left(-2K_2K_3+\beta\alpha_2\right)K_1-\alpha_2\beta\left(\omega_2-\gamma\right)\right)\mu-\xi\left(\left(-K_2K_3+\beta\alpha_2\right)\xi+\left(K_2K_3-\beta\alpha_2\right)K_1+\alpha_2\beta\left(\omega_2-\gamma\right)\right)\end{array}\right)\rho\right)\omega_1\\+(\mu+\xi)\left(\left(\left(\left(-K_2-K_3\right)K_1+\beta\alpha_2-K_2K_3\right)\mu+K_1\left(-K_2K_3+\beta\alpha_2\right)\right)\rho+\left(K_1\left(-K_2K_3+\beta\alpha_2\right)+\alpha_2\beta\gamma\right)\mu+\alpha_2K_1\beta\gamma\right)\end{array}\right)}{\mu+\xi+\omega_1}\lambda+$$
$$-\rho K_2K_3\left(\xi-K_1\right)\omega_1{}^2+\left(\begin{array}{l}\left(\left(-K_2K_3+\beta\alpha_2\right)\rho+\alpha_2\beta\gamma\right)\xi^2\\+\left(\begin{array}{l}\left(\left(-K_2K_3+\beta\alpha_2\right)\mu+\beta\left(\omega_2-K_1\right)\alpha_2+K_1K_2K_3\right)\rho\\+\alpha_2\beta\gamma\left(\mu+\omega_2-K_1\right)\end{array}\right)\xi\\+\mu\left(\left(\beta\left(\omega_2-K_1\right)\alpha_2+2K_1K_2K_3\right)\rho+\alpha_2\beta\gamma\left(\omega_2-K_1\right)\right)\end{array}\right)\omega_1$$
$$\frac{+\mu\rho K_1K_2K_3(\mu+\xi)\mu^2K_1K_2K_3\left(\mu+\xi+\omega_1\right)\rho\left(1-R_0\right)}{\mu+\xi+\omega_1}$$

Applying Routh-Hurwitz criterion to the Characteristics polynomial, we have that

$$\left(1-R_0\right)>0$$
$$\Rightarrow R_0<1$$

Thus, the DFE point of the model is locally asymptotically stable.

Where $K_1=(\xi+\omega_2+\omega_3+\mu), \mathrm{K}_2=(\alpha_2+\mu), \mathrm{K}_3=(\alpha_3+\gamma+\mu),$

4.3 Epidemiological implication of basic reproduction less than 1 ($R_0<1$)

When the basic reproduction number (R_0) is less than 1, it indicates that, on average, each infected individual will transmit the COVID-19 virus to fewer than one other individual during their infectious period. This finding holds significant epidemiological implications for the dynamics of COVID-19

transmission and control efforts. A basic reproduction number below 1 suggests that the disease is not self-sustaining within the population. In other words, the chain of transmission is not perpetuated, and the number of new infections generated by each existing case is insufficient to maintain the disease at endemic levels. Instead, the infection tends to die out over time as the number of susceptible individuals decreases due to immunity acquired through vaccination or recovery from previous infection [16–18]. From an epidemiological perspective, a basic reproduction number below 1 is a promising sign for disease control and elimination efforts. It signifies that the spread of COVID-19 is inherently limited within the population, making it more feasible to implement interventions aimed at reducing transmission and preventing outbreaks. With an R_0 less than 1, there's a reduced risk of widespread COVID-19 transmission within the community. Control measures such as vaccination campaigns, contact tracing, isolation of cases, and public health education can be more effective in containing the disease and preventing its resurgence. Vaccination strategies, in particular, play a crucial role in boosting population immunity and reducing the pool of susceptible individuals, further lowering the likelihood of COVID-19 transmission [19, 22].

Furthermore, a basic reproduction number below 1 indicates the potential for achieving COVID-19 elimination in a given population. Elimination occurs when the disease is no longer continuously transmitted within a defined geographic area or population group. By maintaining high vaccination coverage and implementing robust surveillance systems to detect and respond to sporadic cases, it becomes possible to interrupt the chain of transmission and achieve sustained COVID-19 control [17].

A basic reproduction number less than 1 provides valuable information to epidemiologists, health workers, and policymakers, assisting them in several key ways:

1. Guiding Control Strategies: Epidemiologists rely on the R_0 value to assess disease transmission potential and devise appropriate control measures. An R_0 below 1 indicates that the disease is not self-sustaining, guiding decisions on the intensity and duration of interventions such as vaccination campaigns and case isolation [23].
2. Optimizing Resource Allocation: Health workers and policymakers can allocate resources more effectively based on the R_0 value. With R_0 below 1, resources can be prioritized for interventions in areas with the highest risk of transmission, ensuring maximum impact [22].
3. Informing Vaccination Strategies: For vaccine-preventable diseases like COVID-19, knowledge of R_0 below 1 underscores the importance of achieving high vaccination coverage. This information guides vaccination strategies and coverage targets to interrupt transmission [19].
4. Supporting Policy Decisions: Policymakers use epidemiological data, including R_0, to make informed decisions about public health policies. An R_0 below 1 provides evidence of effective control measures, supporting continued investment in disease prevention programs [17].

5. Monitoring Progress towards Goals: Epidemiologists monitor progress towards disease control and elimination goals using R_0 as a metric. Regular surveillance of disease dynamics helps detect changes in R_0 and ensures ongoing progress towards elimination targets [24] .

4.4 Global asymptotic stability of the disease-free equilibrium point

To investigate the global stability of the disease-free equilibrium, we apply the method implemented by Castillo-Chavez and Song.

We write the equation in the uninfected class as

$$\frac{dX}{dt} = F\left(X, Z\right)$$

And we re-write the equation in the infected class as

$$\frac{dz}{dt} = G(X, Z)$$

where $X = S \in R^1_+$ represents the uninfected compartment and

$Z = \left(E, I, D, R\right) \in R^4_+$ represents the infected compartment

$\varepsilon_0 = (X^*, 0)$ denotes the disease-free equilibrium of the system, and it globally asymptotically stable if it satisfies the following conditions:

$H_1 : \frac{dX}{dt} = F\left(X^*, 0\right), X^*$ is globally asymptotically stable

$H_2 : \frac{dZ}{dt} = D_Z G\left(X^*, 0\right) Z - \hat{G}\left(X, Z\right)$

$\hat{G}\left(X, Z\right) \geq 0$ for all $\left(X, Z\right) \in D$ and where $D_Z G\left(X^*, 0\right)$ is an M- matrix (i.e the diagonal elements are no-negative and it is also the Jacobian of $\hat{G}\left(X, Z\right) \geq 0$ evaluated at $(X^*, 0)$.

If the system satisfies the above condition, then the theorem below holds [18, 21].

Theorem 2

The equilibrium point $\varepsilon_0 = (X^*, 0)$. *is globally asymptotically stable if* $R_0 \leq 1$ *and* H_1, H_2 are satisfied.

$$F(X, Z) = \begin{bmatrix} \Lambda + \xi \mathrm{V} - (\alpha_1 + \omega_1 + \mu)\mathrm{S} \\ \omega_1 S - (\xi + \omega_2 + \omega_2 + \mu)\mathrm{V} \\ \alpha_3 I - \mu R \end{bmatrix}$$

$$G(X, Z) = \begin{bmatrix} \alpha_1 S + \omega_2 \mathrm{V} - (\alpha_2 + \mu)\mathrm{E} \\ \alpha_2 E - (\alpha_3 + \gamma + \mu)\mathrm{I} \\ \gamma \mathrm{I} - \rho \mathrm{D} \end{bmatrix}$$

At disease free equilibrium,

H_1:

$$\frac{dS}{dt} = \Lambda + \xi V - (\omega_1 + \mu)S$$

$$\frac{dR}{dt} = 0$$

H_2:

$$D_Z G\left(X^*, 0\right) Z = \begin{bmatrix} \alpha_1 S + \omega_2 \mathrm{V} - (\alpha_2 + \mu)\mathrm{E} \\ \alpha_2 E - (\alpha_3 + \gamma + \mu)\mathrm{I} \\ \gamma \mathrm{I} - \rho \mathrm{D} \end{bmatrix}$$

$$\hat{G}\left(X, Z\right) = D_Z G\left(X^*, 0\right) Z - G\left(X, Z\right)$$

$$\hat{G}\left(X, Z\right) = \begin{pmatrix} \beta\left(I + D\right)\left(1 - \frac{S}{N}\right) \\ 0 \\ 0 \end{pmatrix}$$

Clearly, $1 \geq \frac{S}{N}$ this implies that $\hat{G}\left(X, Z\right) \geq 0$

Clearly, $1 \geq S$ this means that $\hat{G}\left(X, Z\right) \geq 0$.

Hence, the disease free equilibrium of the given model is globally asymptotically stable [16].

5 Endemic equilibrium point of the model

The endemic equilibrium point is the steady state where there is persistence or prevalence of a disease in the population.

To obtain the endemic equilibrium we set the RHS of the differential equations in (1) to zero and solve for the state variables.

Thus, at the endemic equilibrium point,

$$\frac{dS}{dt} = \frac{dV}{dt} = \frac{dE}{dt} = \frac{dI}{dt} = \frac{dD}{dt} = \frac{dR}{dt} = 0.$$

Let $\varepsilon^{**} = \left(S^{**}, V^{**}, E^{**}, I, ^{**} D^{**}, R^{**}\right)$ be the endemic equilibrium point.

We have that,

$$S^{**} = \frac{\Lambda(\xi + \omega_2 + \omega_3 + \mu)}{\xi\omega_1 - (\alpha_1 + \omega_1 + \mu)(\xi + \omega_2 + \omega_3 + \mu)}$$

$$V^{**} = \frac{\omega_1 \Lambda}{\mu^2 + \left(\xi + \alpha_1 + \omega_1 + \omega_3 + \omega_2\right)\mu + \left(\xi + \omega_3 + \omega_2\right)\alpha_1 + \omega_1\left(\omega_3 + \omega_2\right)}$$

$$E^{**} = \frac{\Lambda\alpha_1}{\left(\alpha_1 + \omega_1 + \mu\right)\left(\alpha_2 + \mu\right)}$$

$$I^{**} = \frac{\Lambda\alpha_1\alpha_{2_}}{\left(\alpha_1 + \omega_1 + \mu\right)\left(\alpha_2 + \mu\right)\left(\alpha_3 + \gamma + \mu\right)}$$

$$D^{**} = \frac{\Lambda\gamma\alpha_1\alpha_{2_}}{\rho\left(\alpha_1 + \omega_1 + \mu\right)\left(\alpha_2 + \mu\right)\left(\alpha_3 + \gamma + \mu\right)}$$

$$R^{**} = \frac{\Lambda\alpha_1\alpha_2\alpha_3}{\mu\left(\alpha_1 + \omega_1 + \mu\right)\left(\alpha_2 + \mu\right)\left(\alpha_3 + \gamma + \mu\right)}$$

5.1 Sensitivity analysis of the model

Sensitivity analysis is a crucial tool in assessing the robustness and reliability of models, especially complex ones like those used to simulate the spread of diseases such as COVID-19. In the context of COVID-19 modeling, sensitivity analysis involves examining how changes in model parameters impact the model outputs, such as infection rates, mortality rates, and other epidemiological indicators. Sensitivity analysis helps researchers understand which parameters have the most significant influence on model outcomes and how uncertainties in those parameters might affect model predictions bata[15, 25]. Regarding the effects of R_0 with negative and positive values, it's essential to note that R_0 represents the average number of secondary infections in a completely susceptible population. Therefore, in realistic scenarios, R_0 is typically a positive value greater than zero. However, in theoretical contexts or models, negative values of R_0 might be used to represent scenarios where the disease is dying out or when interventions are so effective that transmission rates become negative

(i.e., cases decrease over time). In practice, negative values of R_0 are not observed because they imply disease extinction [14, 26].

The sensitivity index of the reproduction number of the model with respect to any parameter say x is given by:

$$\Im_x^{R_0} = \frac{\partial R_0}{\partial x} \times \frac{x}{R_0}$$

Given that

$$\Im_\beta^{R_0} = 1$$

$$\Im_{\alpha_2}^{R_0} = \frac{\mu}{\alpha_2 + \mu} = 0.2307$$

$$\Im_\rho^{R_0} = -\frac{\gamma}{\rho + \gamma} = -0.1071$$

$$\Im_\gamma^{R_0} = \frac{\left(\alpha_3 + \mu - \rho\right)\gamma}{\left(\alpha_3 + \gamma + \mu\right)\left(\rho + \gamma\right)} = -0.1431$$

$$\Im_\xi^{R_0} = \frac{\omega_1 \xi}{\left(\mu + \xi + \omega_1\right)\left(\xi + \mu\right)} = 0.1531$$

$$\Im_\mu^{R_0} = -2\frac{\mu\begin{pmatrix}\mu^3 + \left(2\xi + \alpha_2/2 + \alpha_3/2 + \gamma_c/2 + \omega_1/2\right)\mu^2 \\ +\xi\left(\xi + \alpha_2 + \alpha_3 + \gamma_c + \omega_1\right)\mu + \left(\alpha_2/2 + \alpha_3/2 + \gamma/2\right)\xi^2 \\ +1/2\omega_1\left(\alpha_2 + \alpha_3 + \gamma\right)\xi - 1/2\alpha_2\omega_1\left(\alpha_3 + \gamma\right)\end{pmatrix}}{\left(\mu + \xi + \omega_1\right)\left(\alpha_2 + \mu\right)\left(\alpha_3 + \gamma_c + \mu\right)\left(\xi + \mu\right)} = -0.2334$$

$$\Im_{\alpha_3}^{R_0} = -\frac{\alpha_3}{\alpha_3 + \gamma_c + \mu} = -0.7467$$

$$\Im_{\omega_1}^{R_0} = -\frac{\omega_1}{\mu + \xi + \omega_1} = -0.1534$$

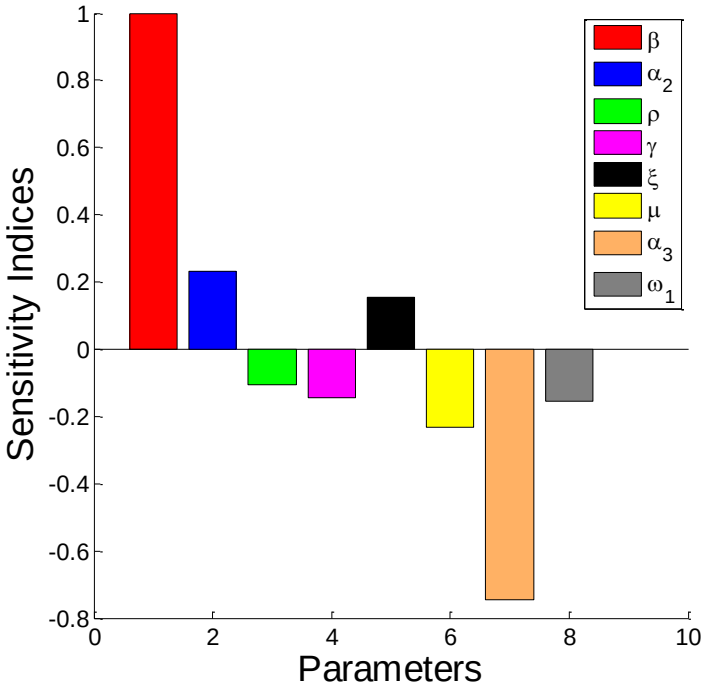


Fig. 2. Sensitivity bar chat

Figure 2, gives a sensitivity bar chart, the Sensitivity bar chart is a crucial visual tool in modeling that illustrates how alterations in input parameters impact model outputs [13]. They pinpoint pivotal parameters by emphasizing those that significantly influence predictions, directing efforts toward refining parameter estimation and management to improve model precision [15].

6 Numerical simulations of the model

Numerical simulation is a critical tool in mathematical modeling of infectious diseases like COVID-19, enabling researchers to understand the dynamics of disease transmission, evaluate intervention strategies, and forecast the course of epidemics. It offers a powerful tool for understanding disease

dynamics, assessing intervention strategies, and guiding public health decision-making. By combining mathematical models with computational techniques, researchers can generate valuable insights into the spread of infectious diseases and inform effective responses to epidemics.

Table 2. Parameter values and their source

Parameter	Value	Source
Λ_{SS}	0.02755	[2]
μ	2.500	[4]
ω_1	0.020	[4]
β	0.1000	[27]
α_1	0.40	Assumed
α_2	0.7	[28]
γ	0.167	Assumed
ω_2	0.002	Assumed
ω_3	0.09091	Assumed

Table 2, gives parameter values used for numerical simulation, Parameter values in numerical simulation are fundamental to modeling, serving multiple critical roles to ensure model accuracy and applicability. They define essential system characteristics such as physical constants, material properties, initial conditions, and boundary constraints [13, 15]. These parameters are calibrated against empirical data to align model predictions with observed behavior, thereby enhancing the model's reliability and predictive power . Sensitivity analysis systematically evaluates the impact of parameter variations on model outputs, identifying influential parameters that significantly affect outcomes and guiding model refinement efforts [13].

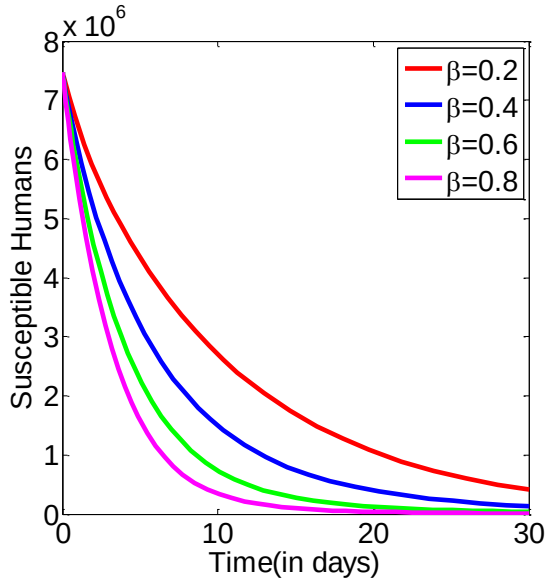


Fig. 3a. Graph of susceptible human against time.

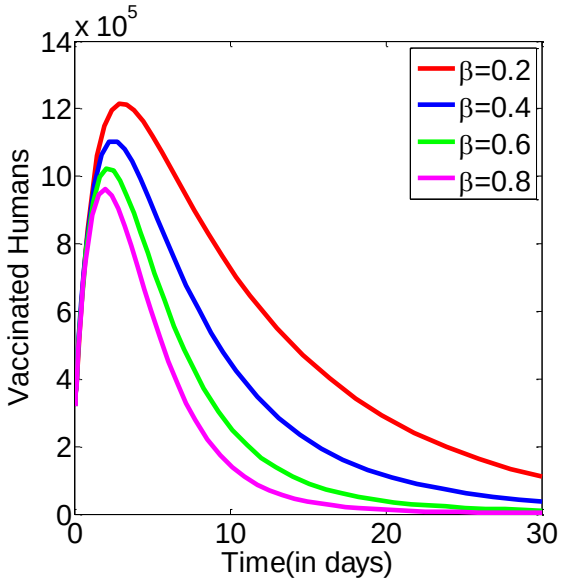


Fig. 3b..Graph of vaccinated humans against time

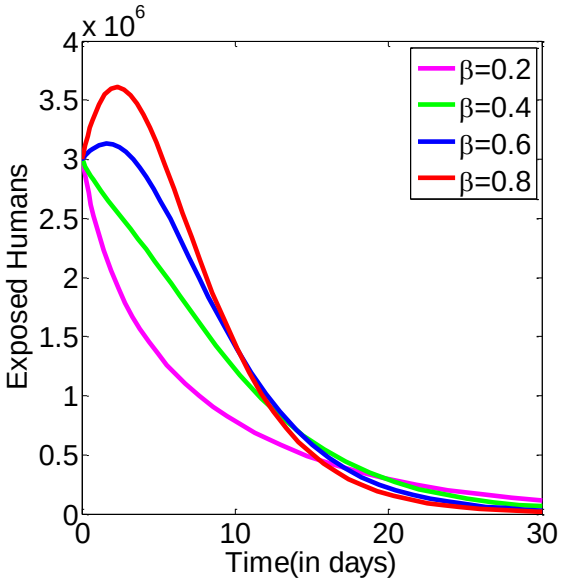


Fig. 3c. Graph of exposed humans against time.

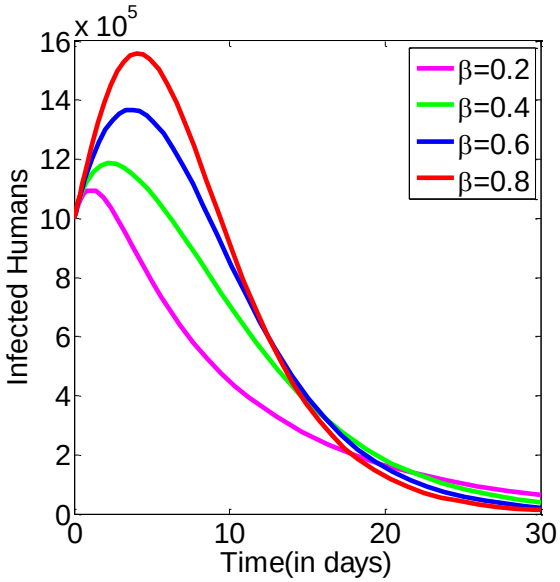


Fig. 3d. Graph of infected humans against time

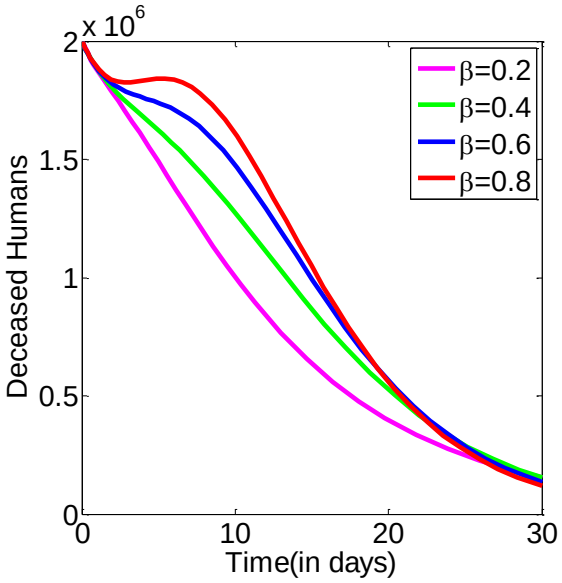


Fig. 3e. Graph of deceased humans against time.

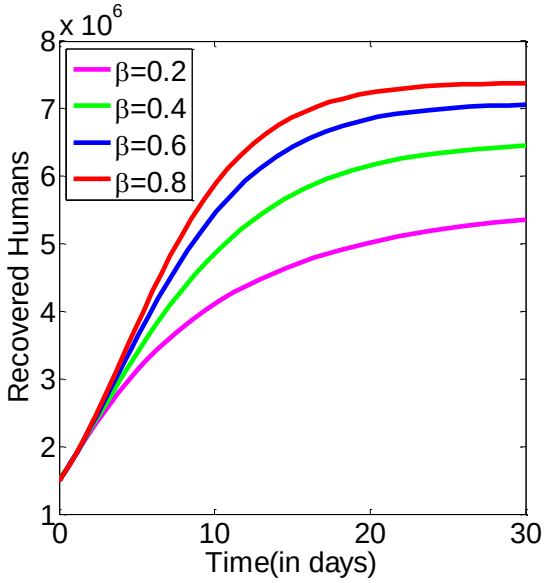


Fig. 3f. Graph of recovered humans against time

7 Conclusion

From the sensitivity analysis and the resulting bar chart in Figure 2, it is evident that parameters with positive sensitivity indices contribute to the transmission of COVID-19 within the human population. For instance, the contact rate β exhibits a positive sensitivity index, indicating that reducing the contact rate between uninfected and infected individuals could effectively halt the spread of COVID-19. Conversely, parameters such as the vaccination rate ω_1, which has a negative sensitivity index, are crucial in mitigating the prevalence of COVID-19. This highlights the importance of increasing vaccination rates to control the disease effectively.

In Figure 3a, the number of susceptible individuals decreases to zero over time, while Figure 3b illustrates a rapid increase in vaccinated individuals followed by a decline due to increased contact rates between susceptible and infected humans. Figure 3c shows an initial increase and subsequent rapid decrease in the number of exposed individuals, indicating effective disease control. In Figure 3d, the number of infected individuals decreases markedly over time, leading to fewer deaths in Figure 3e and a high recovery rate as depicted in Figure 3f. These simulations emphasized that high vaccination rates and reduced contact rates are crucial factors in achieving control over COVID-19.

In conclusion, even though the spread of COVID-19 in Nigeria has declined, our study remains significant in its potential for future preparedness and response efforts. Despite the absence of active transmission, understanding the dynamics of COVID-19 transmission and its post-effects remains

crucial for preemptive measures and contingency planning. By developing a mathematical model and conducting qualitative analysis including sensitivity analysis, and numerical simulations, our study provides a framework for evaluating the potential impact of COVID-19 reintroduction or future outbreaks in Nigeria. The significance of this study lies in its capacity to inform proactive strategies for maintaining public health vigilance, optimizing healthcare resources, and mitigating the socio-economic consequences of any future resurgence of COVID-19. Through evidence-based insights into transmission dynamics and post-effects, policymakers, public health authorities, and stakeholders can develop targeted response plans, refine surveillance systems, and strengthen healthcare infrastructure to ensure swift and effective responses to emerging threats.

Furthermore, the results from this study can be extrapolated to other infectious disease outbreaks and public health emergencies, enhancing Nigeria's overall preparedness and resilience. By leveraging mathematical modeling and data-driven analysis, we can foster a culture of proactive risk management and evidence-based decision-making, ultimately safeguarding the health and well-being of the Nigerian population in the face of future health challenges.

Funding

Not Applicable

Declaration of competing interests

The authors declare that they have no competing interests

Ethics Approval

Not Applicable

Availability of data.

The data used in this study are referenced and presented in Table 2 above.

Consent for Publication

The Authors hereby declare that the manuscript has neither been published previously nor is under consideration for publication elsewhere; that is publication is approved by all authors.

Acknowledgement:

Not Applicable

References

[1] Agbata BC, Emmanuel O, Bashir Tenuche., William Obeng-Denteh (2020) Mathematical model and Analysis of COVID-19 transmission dynamics with a cases study of Nigeria and its computer simulation. Continental journal of Biological Sciences, 13:1–16
[2] World Health Organization (2020) Coronavirus disease (COVID-19) pandemic. In: https://www.who.int/emergencies/diseases/novel-coronavirus-2019.
[3] Nigeria Centre for Disease Control (NCDC). (2020) Covid-19 Nigeria. In: https://covid19.ncdc.gov.ng/.
[4] World Health Organization (2023) Trends in COVID-19 cases, World. In: https://covid19.who.int/region/afro/country/ng.
[5] Adekunle AI, Olaniyan AB, Emebo ON,, Suleiman IM (2021) Mathematical modeling of the COVID-19 outbreak in Nigeria., e07374 ed. Heliyon
[6] Samui P, Mondal J, Khajanchi S (2020) A mathematical model for COVID-19 transmission dynamics with a case study of India. Chaos Solitons Fractals 140:110173
[7] Adekunle AI, Akanbi MO, Adeniyi O V., Suleiman IM (2021) Dynamic modeling of COVID-19 in Nigeria. Results Phys 28:104251
[8] Teslya A, Pham TM, Godijk NG, Kretzschmar ME, Bootsma MC (2020) Mathematical modeling of COVID-19 transmission dynamics in different population density settings. . BMC Public Health 20:1856
[9] Flaxman S, Mishra S, Gandy A, Unwin HJT, Mellan TA, Coupland H, Ghani AC (2020) Modelling COVID-19 transmission in the United States: A Bayesian approach identifying regional differences. :2004.14101 . arXiv preprint arXiv2002 14101
[10] Otu A, Ebenso B, Labonte R, Yaya S (2020) Tackling COVID-19: can the African continent play the long game? J Glob Health 10:
[11] Adepoju P, Pitan OS, Ogundipe AA, Sonola AD (2021) Evaluating the Effects of COVID-19 Pandemic on Nigeria's Economy: Way Forward. Journal of Public Affairs e2763
[12] Adedoyin F, Osabohien R, Adewuyi A, Bekun F (2021) Impact of COVID-19 on Economic Policy Uncertainty and Socio-Economic Well-Being in Nigeria. Journal of Public Affairs, e2665 e2665
[13] Odeh JO, Agbata BC, Ezeafulukwe AU, Madubueze CE, Acheneje GO, Topman NN (2024) A mathematical model for the control of chlamydia disease with treatment strategy. JMAR 7:1–20
[14] Agbata BC, Omale D, Ojih PB, Omatola IU (2019) Mathematical analysis of Chickenpox transmission dynamics with control measures. Dio 10:6–23
[15] Agbata B.C, Ode O.J, Ani B.N, Odo C.E, Olorunnishola O.A. (2019) Mathematical assessment of the transmission dynamics of HIV/AIDS with treatment effects. IJMSS 7:40–52
[16] van den Driessche P, Watmough J. (2002) Reproduction number and sub-threshold endemic equilibria for computational models of disease transmission. J Math Biosci 180:29–48
[17] Gao S, Yang S, Ma W, Chen J., Wang L. (2016) Mathematical Models for Communicable Diseases. 10:276–289

[18] Diekmann O, Heesterbeek JAP (2000) Mathematical epidemiology of infectious diseases: model building, analysis and interpretation. John Wiley & Sons
[19] Fine P. (2019) Herd Immunity: History, Theory, Practice. p. . Academic Press;
[20] Hethcote HW (2000) The mathematics of infectious diseases. SIAM review 42:599–653
[21] Okon I M, Acheneje G O, Agbata B C, Onalo P O, Odeh OJ, Shior MM. (2023) A mathematical model for computation of alcoholism epidemics in Nigeria: A case of Lokoja metropolis. ICIET
[22] Brauer F, Castillo-Chavez C, Feng Z, others (2019) Mathematical models in epidemiology. Springer
[23] Britton NF, Britton NF (2003) Essential mathematical biology. Springer
[24] Diekmann O, Heesterbeek JAP, Roberts MG (2010) The construction of next-generation matrices for compartmental epidemic models. J R Soc Interface 7:873–885
[25] Keeling MJ, Rohani P (2008) Modeling Infectious Diseases in Humans and Animals. . Princeton University Press.
[26] Chowell G, Viboud C, Simonsen L, Miller MA, Acuna-Soto R (2010) Mortality patterns associated with the 1918 influenza pandemic in Mexico: evidence for a spring herald wave and lack of preexisting immunity in older populations. J Infect Dis 202:567–575
[27] Ojih PB, Agbata B.C., Omatola IU, Olorunnishola OA (2019) Mathematical model for the control of cholera disease with vaccination and treatment strategies. A direct mode of transmission approach. . Continental journal of Biological Sciences 12:1–16
[28] Peter OJ, Ibrahim MO, Akinduko OB, Rabiu M (2017) Mathematical model for the control of typhoid fever. IOSR Journal of Mathematics 13:60–66

Estimation of different types of entropies for the Gumbel Type-2 distribution

D.O. Omosigho[*†], A.D. Adefolarin[*], and N.A. Adeleye[‡]

Abstract

The estimation of the entropy of a random system is relevant in many scientific applications. This article is aimed at the analysis of the entropy of the Gumbel type-2 distribution, an aspect of the statistical analysis which has not been employed. On this basis, six different entropy measures are considered and expressed analytically. A numerical study is performed to discuss the behavior of these measures. In addition, we considered the method of maximum likelihood estimation approach to obtain the parameter estimates of the Gumbel type-2 distribution. Maximum likelihood estimates for the considered entropy measures are thus derived. The convergence properties of these estimates are proved through a simulated data, showing their numerical efficiency. Concrete applications to two real data sets are provided.

Keywords and phrases: entropy; maximum likelihood estimation; gumbel type-2 distribution; random system.

1 Introduction

Entropy, which is one of the important terms in statistical mechanics, was originally defined in physics especially in the second law of thermodynamics. In statistical theory, Entropy is defined as a measure of uncertainty associated with a distribution. In every probability distribution there is some element of uncertainty associated with it and Entropy is used to provide a reasonable explanation for the level of uncertainty present. Entropy can also be considered as a measure of randomness of a probabilistic system. The concept of Entropy was redefined by [12] as a measure of information, which provides a quantitative measure for the level of uncertainty of a random system. It is a measure of average uncertainty in a random variable. When a system is in a number of states randomly with equal probability of occurrences entropy attains its maximum value and reach minimum value i.e., 0 when the system is in one particular state, which indicates that there is no uncertainty in its description.

[*]Department of Mathematics and Statistics, Federal Polytechnic Ado-Ekiti, Nigeria
[†]Corresponding author
[‡]Department of Statistics, Ogun State Institute of Technology, Igbesa, Ogun State, Nigeria

Let X be a random variable with a continuous distribution function (CDF) $F(x)$ and probability density function (PDF) $f(x)$. The differential entropy $J(X)$ of the random variable is defined by [7] as:

$$J((X) = J(f) = -\int_{-\infty}^{\infty} f(x)F(x)dx$$

It could be observed that a very sharply peaked distribution has very low entropy, whereas if the probability is spread out, the entropy is higher. In this sense, $J(X)$ is a measure of uncertainty associated with f. Furthermore, as $J(f)$ increases, $f(x)$ approaches uniformity. Thus, entropy can be taking as a tool for measuring the uniformity of a distribution,[8]. Thus, entropy can be viewed as measuring the uniformity of a distribution, [8] Many authors have studied different techniques for estimating entropy for different life distributions. [4] developed and studied the entropy of upper record values and provided several upper and lower bounds for this entropy by using the hazard rate function. [5] examined the entropy in the Weibull distribution for progressive censoring. [6] developed and studied the estimators for the entropy function of a Rayleigh distribution based on doubly-generalized Type II hybrid censored samples by making use of maximum likelihood estimator (MLE), approximate MLEs and Bayes estimators.

The units of entropy majorly depend on the base of logarithm. If the base of the logarithm is e, then entropy is measured in nats and if the base of the logarithm is 2, then the entropy is measured in bits. Entropy is used to study a wide range of physical, biological and chemical phenomenon. We observe that the movement of molecule in biological sciences is random so, to study the different properties of the molecules we have to find the entropy of probability distribution of the molecule. In the present study, we have derived the expressions for seven different types of entropy for Gumbel type-2 distribution and also carried out a numerical study on this entropy formation.

2 Methodology/Model formulation

In probability theory, the Gumbel type-2 probability density function is given as

$$f(x;\alpha,\varphi) = \alpha\varphi x^{-\varphi-1}e^{-\alpha x^{-\varphi}}, \qquad x > 0; \alpha, \varphi > 0. \tag{1}$$

The graph of probability density function of Gumbel type-2 distribution for various values of the parameters is given below in figure 1

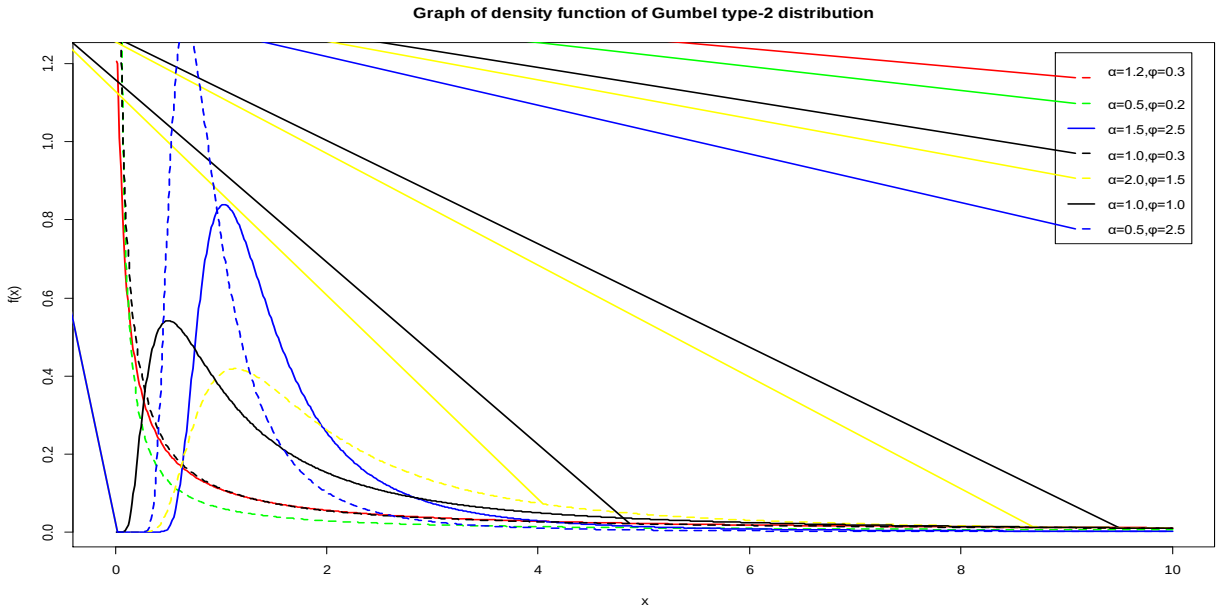


Figure 1. The graph of probability density function of Gumbel type-2 distribution.

2.1 An integral result

The following result given in Lemma 1 shows that a certain integral involving the PDF of the Gumbel type-2 distribution is pertinent in obtaining some properties of different measures of entropy that will be considered in this work.

Lemma 1: Let $\lambda > 0$, $f(x;\alpha,\varphi)$ be specified by equation (1) and

$$I_\lambda(\alpha,\varphi) = \int_{-\infty}^{+\infty} f(x;\alpha,\varphi)^\lambda dx, \tag{2}$$

Then, $I_\lambda(\alpha,\varphi)$ exist if and only if $\min(\alpha,\varphi) > \max\left(1 - {}^1/_\lambda, 0\right)$, and is given as

$$I_\lambda(\alpha,\varphi) = \alpha^\lambda \varphi^{\lambda-1}[\alpha\varphi]^{{}^{1-\lambda(\varphi+1)}/_\lambda}\Gamma[(\lambda-1)(\varphi+1)+1] \tag{3}$$

Equation (3) is a very important concept that is used in deriving different measures of entropy of Gumbel type-2 considered in this work.

2.2 Various entropy measures

Various approaches can be used to estimate the entropy of Gumbel type-2. The important entropy measures which is mostly applicable in literature is presented in Table 1 for a general distribution with pdf denoted by $f(x;\alpha,\varphi)$. Also, we adhere to basic assumptions that allow for the use of different entropy measures which is $\lambda > 0$ and $\lambda \neq 1$.

From Table 1, which summarizes different type of entropy considered, we can emphatically say that the integral $\int_{-\infty}^{+\infty} f(x;\alpha,\varphi)^{\lambda}dx$ is very important in determining the considered entropy measures. Now, we consider different entropy measures of Gumbel type-2 distribution. Based on Lemma 1, it is pertinent that α, φ and λ satisfy $min\ (\alpha,\varphi) > max\left(1-{}^{1}/_{\lambda}, 0\right)$.

Table 1. Important entropy measures of a distribution with pdf $\boldsymbol{f(x;\alpha,\varphi)}$ at $\boldsymbol{\lambda}$

Name of entropy	***Notation***	Reference	***Expression***
Renyi	$R_{\lambda}(\alpha,\varphi)$	[10]	$\frac{1}{1-\lambda} log\left[\int_{-\infty}^{+\infty} f(x;\rho)^{\lambda}dx\right]$
Tsallis	$T_{\lambda}(\alpha,\varphi)$	[13]	$\frac{1}{\lambda-1}\left[1-\int_{-\infty}^{+\infty} f(x;\rho)^{\lambda}dx\right]$
Arimoto	$A_{\lambda}(\alpha,\varphi)$	[2]	$\frac{\lambda}{1-\lambda}\left(\left[\int_{-\infty}^{+\infty} f(x;\rho)^{\lambda}dx\right]^{\frac{1}{\lambda}}-1\right)$
Havrda and Charvat	$HC_{\lambda}(\alpha,\varphi)$	[9]	$\frac{1}{2^{1-\lambda}-1}\left[\int_{-\infty}^{+\infty} f(x;\rho)^{\lambda}dx-1\right]$
Award and Alawneh 1	$AA1_{\lambda}(\alpha,\eta)$	Awad and Alawneh (1987)	$\frac{1}{1-\lambda} log\left[\left(\underset{x\in R}{\mathrm{Sup}} f(x,\rho)\right)^{1-\lambda}\int_{-\infty}^{+\infty} f(x;\rho)^{\lambda}dx\right]$
Award and Alawneh 2	$AA2_{\lambda}(\alpha,\eta)$	Awad and Alawneh (1987)	$\frac{1}{2^{1-\lambda}-1}\left[\left(\underset{x\in R}{\mathrm{Sup}} f(x,\rho)\right)^{1-\lambda}\int_{-\infty}^{+\infty} f(x;\rho)^{\lambda}dx-1\right]$

2.2.1 Renyi entropy: Based on Table 1, equation (1) and Lemma 1, the Renyi entropy of the Gumbel type-2 distribution can be expressed as

$$R_{\lambda}(\alpha,\eta) = \frac{1}{1-\lambda} log[I_{\lambda}(\alpha,\varphi)]$$
$$= \frac{1}{1-\lambda} log\left\{\alpha^{\lambda}\varphi^{\lambda-1}[\alpha\varphi]^{1-{}^{\lambda(\varphi+1)}/_{\lambda}}\Gamma[(\lambda-1)(\varphi+1)+1]\right\} \quad (4)$$

2.2.2 Havrada and Charvat entropy: From Table 1, equation (1) and proposition 1, Havrda and Charvat entropy of the Gumbel type-2 distribution can be expressed as

$$HC_\lambda(\alpha,\eta) = \frac{1}{2^{1-\lambda}-1}\left(I_\lambda(\alpha,\eta)-1\right)$$
$$= \frac{1}{2^{1-\lambda}-1}\left\{\alpha^\lambda \varphi^{\lambda-1}[\alpha\varphi]^{1-{}^{\lambda(\varphi+1)}/_{\lambda}}\Gamma[(\lambda-1)(\varphi+1)+1]-1\right\} \quad (5)$$

2.2.3 Arimoto entropy: from Table 1, equation (1) and proposition 1, Arimoto entropy of the Gumbel type-2 distribution can be obtained as

$$A_\lambda(\alpha,\eta) = \frac{\lambda}{1-\lambda}\left\{[I_\lambda(\alpha,\varphi)]^{\frac{1}{\lambda}}-1\right\}$$
$$A_v(\alpha,\eta) = \frac{\lambda}{1-\lambda}\left(\left[\alpha^\lambda \varphi^{\lambda-1}[\alpha\varphi]^{1-{}^{\lambda(\varphi+1)}/_{\lambda}}\Gamma[(\lambda-1)(\varphi+1)+1]\right]^{\frac{1}{\lambda}}-1\right) \quad (6)$$

2.2.4 Tsallis entropy: From Table 1, equation (1) and proposition 1, Tsallis entropy of the Gumbel type-2 distribution can be represented by

$$T_\lambda(\alpha,\eta) = \frac{1}{\lambda-1}\left\{1-[I_\lambda(\alpha,\varphi)]^{\frac{1}{\lambda}}\right\}$$
$$= \frac{1}{\lambda-1}\left(1-\alpha^\lambda \varphi^{\lambda-1}[\alpha\varphi]^{1-{}^{\lambda(\varphi+1)}/_{\lambda}}\Gamma[(\lambda-1)(\varphi+1)+1]\right) \quad (7)$$

2.2.5 Award and Alawneh 1: From Table 1, equation (1), and proposition 1, Award and Alawneh 1 entropy of Gumbel type-2 distribution can be obtained as

$$AA1_\lambda(\alpha,\eta) = \frac{1}{1-\lambda} log\left[\left(\operatorname*{Sup}_{x\in R} f(x,\rho)\right)^{1-\lambda}\int_{-\infty}^{+\infty} f(x;\rho)^\lambda dx\right] \quad (8)$$

Before going further, there is need to determine $sup_{0<x<\infty} f(x;\alpha,\varphi)$, which is provided ion the following lemma.

Lemma 2. Let $\boldsymbol{f}(x;\alpha,\varphi)$ be given as in (1). Then, $sup_{0<x<\infty} f(x;\alpha,\varphi)$ is finite if and only if $\alpha > 0$ and $\varphi > 0$, based on this we have

$$sup_{0<x<\infty} f(x;\alpha,\varphi) = \alpha\varphi\left(\frac{\alpha\varphi}{\varphi+1}\right)^{-\varphi-1/\varphi} e^{-\alpha\left(\frac{\alpha\varphi}{\varphi+1}\right)^{-1}}$$

Proof. We have

$$f'(x;\alpha,\varphi) = \alpha\varphi\left[(-\varphi-1)x^{-\varphi-2}e^{-\alpha x^{-\varphi}} + x^{-\varphi-1}(\alpha\varphi x^{-\varphi-1})e^{-\alpha x^{-\varphi}}\right]$$

Therefore, taking $f'(x;\alpha,\varphi)=0$ implies that

$$x_* = \left(\frac{\alpha\varphi}{\varphi+1}\right)^{1/\varphi}$$

Since $f'(x;\alpha,\varphi) > 0$ for $x < x_*$ and $f'(x;\alpha,\varphi) < 0$ for $x > x_*$, x_* is considered as a maximum point for $f(x;\alpha,\varphi)$. Hence

$$\lim_{0<x<\infty} f(x;\alpha,\varphi) = f(x_*;\alpha,\varphi) = \alpha\varphi {x_*}^{-\varphi-1} e^{-\alpha {x_*}^{-\varphi}}$$
$$= \alpha\varphi \left(\frac{\alpha\varphi}{\varphi+1}\right)^{-\varphi-1/\varphi} e^{-\alpha\left(\frac{\alpha\varphi}{\varphi+1}\right)^{-1}}$$

It should be noted that, taking $\varphi = 1$, we have $f(x;\alpha,\varphi) = {4e^{-2}}/{\alpha}$ and for $\alpha = 1$, we have $f(x;\alpha,\varphi) = \varphi^{-1/\varphi}(\varphi+1)^{1+1/\varphi} e^{-\left(1+1/\varphi\right)}$.

2.2.6 Award and Alawneh 2: From Table 1, equation (1), and proposition 1, Award and Alawneh 2 entropy of Gumbel type-2 distribution can be obtained as

$$AA2_\lambda(\alpha,\eta) = \frac{1}{2^{1-\lambda}-1}\left[\left(\sup_{x\in R} f(x,\rho)\right)^{1-\lambda} \int_{-\infty}^{+\infty} f(x;\rho)^\lambda dx - 1\right] \quad (9)$$

Theoretically, it is complicated to study the characteristics behaviour of these entropy measures. Based on this reason, a numerical study will be used to obtain the values of the forms of entropy under study in the next section.

3 Estimation of the entropy measures

The estimation of the parameters of the Gumbel type-2 model using the maximum likelihood is well known in statistical literature and details can be found. Suppose $x_1,\ldots,x_n$ is observed from a random variable X having a Gumbel type-2 distribution with parameters α and φ. The maximum likelihood estimation (MLEs) of α and φ, say, $\hat{\alpha}$ and $\hat{\varphi}$, are defined by

$$(\hat{\alpha}\,,\hat{\varphi}) = argmax_{(\alpha,\varphi)\in(0,+\infty)^2} l(\alpha,\varphi),$$

where $l(\alpha,\varphi)$ represent the likelihood function specified by

$$l(\alpha,\varphi) = nlog\alpha + nlog\varphi - (\varphi+1)\sum_{i=1}^{n} log(x_i) - \alpha\sum_{i=1}^{n} {x_i}^{-\varphi}$$

The MLEs are the solutions of the two equations given as follows:

$$\frac{\partial l}{\partial\alpha} = \frac{n}{\alpha} - \sum_{i=1}^{n} {x_i}^{-\varphi} = 0, \quad \frac{\partial l}{\partial\varphi} = \frac{n}{\varphi} - \sum_{i=1}^{n} log(x_i) - \alpha\sum_{i=1}^{n} {x_i}^{-\varphi}\, log(x_i) = 0$$

and this implies that $\hat{\alpha}$ and $\hat{\varphi}$ satisfies the following simple relation

$$\hat{\alpha} = \frac{n}{\sum_{i=1}^{n} {x_i}^{-\varphi}}$$

Then, it follows that the properties of these MLEs follow the usual maximum likelihood theory. Based on this one can easily obtained the MLEs of the entropy measures.

3.1 Numerical values

We now investigate the numerical values for the six entropy measures presented in subsection 2.2 under the following configuration of the parameters: configuration 1, $\alpha = 0.5$ with $\varphi = \{1.5, 2.0, 2.5, 3.0, 3.5, 4.0, 4.5, 5.0, 5.5, 6.0\}$ and $\lambda = 1.5$, configuration 2, $\alpha = 0.5$ with

$\varphi = \{1.5, 2.0, 2.5, 3.0, 3.5, 4.0, 4.5, 5.0, 5.5, 6.0\}$ and $\lambda = 3.5$, configuration 3, $\varphi = 0.5$ with $\alpha = \{1.5, 2.0, 2.5, 3.0, 3.5, 4.0, 4.5, 5.0, 5.5, 6.0\}$ and $\lambda = 1.5$ configuration 4, $\varphi = 0.5$ with $\alpha = \{1.5, 2.0, 2.5, 3.0, 3.5, 4.0, 4.5, 5.0, 5.5, 6.0\}$ and $\lambda = 3.5$. The findings of all the six entropy measures are presented for this configurations in Table $2 - 5$, respectively.

Table 2-5 presents the numerical values for all the entropy measures considered for different values of the parameters of the Gumbel type-2 model.

Table 2. Numerical values of the considered entropy of the Gumbel type-2 distribution at $\boldsymbol{\alpha = 0.5}$ and $\boldsymbol{\lambda = 1.5}$

$\boldsymbol{\varphi}$	$R_\lambda(\alpha, \varphi)$	$T_\lambda(\alpha, \varphi)$	$A_\lambda(\alpha, \varphi)$	$HC_\lambda(\alpha, \varphi)$	$AA1_\lambda(\alpha, \eta)$	$AA2_\lambda(\alpha, \eta)$
1.5	0.9651	0.7656	0.8253	−0.9246	2.6130	2.4898
2.0	0.5256	0.4622	0.4821	−0.1586	2.1902	2.2721
2.5	0.4697	0.3371	0.4094	−0.0957	2.1887	2.0506
3.0	0.1225	0.1188	0.1200	−0.0246	1.8357	1.4889
3.5	−0.2420	−0.2572	−0.2520	0.0533	1.5320	1.8270
4.0	−0.5720	−0.6622	−0.6301	0.1371	1.2664	1.6017
4.5	−0.8720	−1.0930	−1.0194	0.2264	1.0314	1.3756
5.0	−1.1464	−1.5478	−1.3962	0.3206	0.8205	1.1489
5.5	−1.3989	−2.0254	−1.7823	0.4195	0.6292	0.9216
6.0	−1.6327	−2.5244	−2.1698	0.5228	0.4545	0.6939

From Table 2, it can be observed that the values of Renyi, Tsallis, Arimoto, Award and Alawneh 1 and Award and Alawneh 2 entropy increases as the value of $\boldsymbol{\varphi}$ increases and decrease for Havrada and Charvat entropy.

Table 3. Numerical values of the considered entropy of the Gumbel type-2 distribution at $\boldsymbol{\alpha = 0.5}$ and $\boldsymbol{\lambda = 3.5}$

$\boldsymbol{\varphi}$	$R_\lambda(\alpha, \varphi)$	$T_\lambda(\alpha, \varphi)$	$A_\lambda(\alpha, \varphi)$	$HC_\lambda(\alpha, \varphi)$	$AA1_\lambda(\alpha, \eta)$	$AA2_\lambda(\alpha, \eta)$
1.5	0.349	0.233	0.309	−2.709	2.068	1.208
2.0	0.217	0.168	0.201	−1.950	1.865	1.203
2.5	0.080	0.072	0.078	−0.843	1.745	1.199
3.0	−0.169	−0.206	−0.176	2.394	1.665	1.189
3.5	−0.049	−0.052	−0.049	0.600	1.572	1.196
4.0	−0.267	−0.379	−0.294	4.417	1.547	1.191
4.5	−0.371	−0.610	−0.423	7.106	1.533	1.188
5.0	−0.460	−0.864	−0.545	10.064	1.347	1.163
5.5	−0.541	−1.152	−0.645	13.447	1.259	1.151
6.0	−0.620	−1.483	−0.780	17.276	1.147	1.143

From Table 3, it can be observed that the values of Renyi, Tsallis, Arimoto, Award and Alawneh 1 and Award and Alawneh 2 entropy increases as the value of $\boldsymbol{\varphi}$ increases and decrease for Havrada and Charvat entropy.

Table 4. Numerical values of the considered entropy of the Gumbel type-2 distribution at $\boldsymbol{\varphi = 0.5}$ and $\boldsymbol{\lambda = 3.5}$

$\boldsymbol{\alpha}$	$R_\lambda(\alpha,\varphi)$	$T_\lambda(\alpha,\varphi)$	$A_\lambda(\alpha,\varphi)$	$HC_\lambda(\alpha,\varphi)$	$AA1_\lambda(\alpha,\eta)$	$AA2_\lambda(\alpha,\eta)$
1.5	2.962	1.545	1.882	−0.320	4.754	3.097
2.0	3.537	1.659	2.077	−0.344	4.753	3.097
2.5	3.984	1.727	2.205	−0.358	4.755	3.097
3.0	4.348	1.773	2.296	−0.368	4.753	3.097
3.5	4.656	1.805	2.365	−0.394	4.753	3.097
4.0	4.923	1.829	2.419	−0.379	4.754	3.097
4.5	5.159	1.848	2.463	−0.383	4.754	3.097
5.0	5.371	1.863	2.499	−0.386	4.754	3.097
5.5	5.561	1.866	2.530	−0.389	4.754	3.097
6.0	5.733	1.876	2.556	−0.391	4.752	3.097

From Table 4, it can be observed that the values of Renyi, Tsallis, Arimoto entropy decreases Award and Alawneh 1 and Award and Alawneh 2 entropy remain constant while Havrada and Charvat entropy increases as the value of $\boldsymbol{\alpha}$ increases.

Table 5. Numerical values of the considered entropy of the Gumbel type-2 distribution at $\boldsymbol{\varphi = 0.5}$ and $\boldsymbol{\lambda = 3.5}$

$\boldsymbol{\alpha}$	$R_\lambda(\alpha,\varphi)$	$T_\lambda(\alpha,\varphi)$	$A_\lambda(\alpha,\varphi)$	$HC_\lambda(\alpha,\varphi)$	$AA1_\lambda(\alpha,\eta)$	$AA2_\lambda(\alpha,\eta)$
1.5	1.942	0.397	1.050	−4.621	3.733	1.215
2.0	2.528	0.399	1.170	−4.649	3.798	1.215
2.5	2.967	0.400	1.234	−4.654	3.738	1.215
3.0	3.407	0.400	1.277	−4.655	3.812	1.215
3.5	3.684	0.400	1.299	−4.656	3.781	1.215
4.0	3.905	0.400	1.314	−4.657	3.736	1.215
4.5	4.141	0.400	1.327	−4.657	3.736	1.215
5.0	4.352	0.400	1.338	−4.657	3.736	1.215
5.5	4.542	0.400	1.345	−4.657	3.736	1.215
6.0	4.716	0.400	1.352	−4.657	3.736	1.215

From Table 5, it can be observed that the values of Renyi entropy decreases, Tsallis entropy increases and remain constant for $\boldsymbol{\alpha = 2.5 - 6.0}$, Arimoto entropy decreases, Havrada and Charvat, Award and Alawneh 1 and Award and Alawneh 2 entropy remain constant for all values of $\boldsymbol{\alpha}$.

4 Illustrative example

For illustrative purposes, we present here a real data analysis using the proposed methods. . The data set refers to [10] which consists of thirty successive values of March precipitation (in inches) in Minneapolis/St Paul. To evaluate whether the data fit the Gumbel type-2 distribution or not also, to check for the goodness of fit, we compute the Anderson–Darling statistic and Cramer-von Misses statistic which values is respectively given as 0.7723 and 0.1261 with associated p-value of 0.4924. Since the p-value is quite high that is p-value > 0.05, we cannot reject the null hypothesis that the data are coming from the Gumbel type-2 distribution. The ordered data are as follows: 0.32, 0.47, 0.52 , 0.59, 0.77, 0.81, 0.90, 0.96, , 1.18, 1.20 , 1.20, , 1.35, 1.43, 1.74, 1.95, 1.51, 1.62, 1.31, 0.81, 1.87, 1.89, 2.05, 2.10, , 2.20, 2.48, 2.81, 3.00, 3.09, 3.37, 4.75.

5 Conclusion

This article studied the entropy of the Gumbel type-2 distribution which covered both the theoretical and practical aspects. In particular, six different entropy measures were examined. After determining the closed-form expressions of these measures, an estimation strategy was developed to evaluate them in a practical setting. A real-life data set is used to show how the different entropies can be estimated. The finding of this study aims to be applied by the statistician to assess the entropy of diverse data with values on such as modern rate, unit interval, percentage and proportion type data.

References

[1] Abo-Eleneen, Z. A. (2011). The entropy of progressively censored samples. Entropy, 13, 437–449.

[2] Arimoto, S. (1971). Information-theoretical considerations on estimation problems. Information and Control, Vol. 19, 3, pg. 181–194.

[3] Awad, A. M., and Alawneh, A. J. (1987). Application of entropy to a life-time model. IMA Journal of Mathematical Control and Information, 4, 2, 143–148.

[4] Baratpour, S. Ahmadi, J. and Arghami, N.R. (2007). Entropy properties of record statistics. Stat. Pap. 2007, 48, 197–213.

[5] Cramer, E., and Bagh, C. (2011). Minimum and maximum information censoring plans in progressive censoring. Communication in Statistics Theory and Methods, 40, 2511–2527.

[6] Cho, Y., Sun, H. and Lee, K. (2014). An estimation of the entropy for a Rayleigh distribution based on doubly-generalized Type-II hybrid censored samples. Entropy, 16, 3655–3669.

[7] Cover, T. M. and Thomas, J. A. (2005). Elements of Information Theory; Wiley: Hoboken, NJ, USA, 2005.

[8] Jiheel, A. K. and Shanubhoque, A. (2014). Shrinkage estimation of the entropy function for the exponential distribution under different loss functions using progressive Type II censored sample. International Journal of Mathematics and Computer Research 2014, 2, 394–402

[9] Havrda, J., and Charvat, F. (1967). Quantification method of classification processes, concept of structural entropy. Kybernetika, Vol. 3, pg. 30–35.

[10] Hinkley, D. (1977).On Quick Choice of Power Transformations. Journal of the Royal Statistical Society, Series(c), Applied Statistics, 26(1), 67–69.

[11] Renyi A. (1960). "On measures of entropy and information". Proc. 4th Berkeley Symposium on Mathematical Statistics and Probability. Vol. 1, pg. 47-561.
[12] Shannon, C. E. (1948). "A mathematical theory of communication". The Bell System Technical, Vol. 1, pg. 379–423.
[13] Tsallis, C. (1988). "Possible generalization of Boltzmann-Gibbs statistics". Journal of Statistical Physics, Vol., 52, Pg. 479–487.

Laplace-Adomian Decomposition method for solving fractional-order mathematical model of Monkeypox transmission dynamics

B.C. Agbata[*], W. Obeng-Denteh[†], D.F. Agbebaku[‡§], M.M. Shior[**], D.J. Yahaya[††] and A.Y. Danjuma[‡‡]

Abstract

In this study, we developed a model to understand and predict the spread of Monkeypox among humans and rodents, both of which are important in the disease's transmission. Our model categorized the human population into six groups: susceptible individuals who have not been exposed, exposed individuals who have encountered the virus, infected individuals, quarantined individuals, those receiving treatment, and those who have recovered. For rodents, we considered three groups: susceptible, exposed, and infected animals, as they also play a key role in spreading Monkeypox. To explore how different control measures could impact the spread of the disease, we used a mathematical approach known as the Laplace Adomian Decomposition Method (LADM) to get an approximate solution to the model. This allows us to estimate the outcomes of various strategies in managing the disease. Our findings shed light on how actions like quarantining, treating infected individuals, and reducing the number of susceptible rodents can work together to slow or stop the spread of Monkeypox. This model gives public health officials a clearer picture of where to focus efforts to prevent outbreaks and protect communities.

Keywords and phrases: numerical methods; human-rodent interactions; mathematical epidemiology; series solution; numerical simulations

[*] Department of Mathematics and Statistics, Confluence University of Science and Technology, Osara, Nigeria.
[†] Department of Mathematics, Kwame Nkrumah University of Science and Technology, Kumasi, Ghana.
[‡] Corresponding author E-mail: dennis.agbebaku@unn.edu.ng
[§] Department of Mathematics, University of Nigeria, Nsukka
[**] Department of Mathematics/ Computer Science, Benue State University Makurdi, Nigeria
[††] Department of Mathematics and Statistics, Confluence University of Science and Technology, Osara, Nigeria.
[‡‡] Department of Actuarial Science, Confluence University of Science and Technology, Osara, Nigeria.

1 Introduction

Monkeypox has re-emerged as a global public health concern, shifting from sporadic outbreaks in endemic regions of Central and West Africa to a worldwide spread. The recent outbreak was declared a public health emergency of international concern by the World Health Organization (WHO) in July 2022 [1] after cases rapidly spread across North America, Europe, and other regions [3]. This change in monkeypox's epidemiology has underscored the urgent need for enhanced surveillance and understanding of transmission, especially as the virus increasingly affects diverse populations outside historically affected areas [1,2]. Monkeypox is caused by the Monkeypox virus (MPXV), a member of the Orthopoxvirus genus, and it is closely related to the smallpox virus. MPXV can transmit through direct contact with bodily fluids, respiratory droplets, or contaminated objects. Unlike in previous outbreaks, recent studies suggest transmission through close, often sexual contact, especially among men who have sex with men (MSM), though the virus remains capable of infecting anyone [2,3]. This shift in transmission patterns has led public health agencies to prioritize community education and risk reduction strategies, especially for vulnerable groups. The clinical presentation of monkeypox typically includes fever, rash, lymphadenopathy, and muscle aches. The incubation period ranges from 5 to 21 days, with symptoms lasting two to four weeks. Unlike smallpox, monkeypox typically causes a milder disease, but it can still lead to severe complications, particularly in immunocompromised individuals [3]. A recent study highlighted that those with untreated HIV infection or weakened immune systems are at greater risk of severe illness and mortality if infected with monkeypox [1,3]. To control the spread of monkeypox, health authorities have expanded diagnostic and testing capabilities. For instance, the U.S. Centers for Disease Control and Prevention (CDC) increased testing capacities significantly to accommodate the growing number of cases in 2022. Vaccination campaigns using the JYNNEOS vaccine, initially stockpiled for smallpox, have also been implemented as a preventive measure, especially for high-risk groups [2] . Additionally, tecovirimat (Tpoxx) is available under expanded access protocols as a treatment option, particularly for severe cases [2,3]. The resurgence of Monkeypox highlights the interconnectedness of global health and the need for preparedness. This recent outbreak underscores the importance of international collaboration in epidemiological research, timely surveillance, and robust public health response strategies. By improving diagnostic and treatment options, expanding access to vaccines, and implementing targeted interventions, health authorities aim to prevent future outbreaks and manage those at risk effectively [2,3].

The Laplace Adomian Decomposition Method (LADM) is a powerful analytical technique used to solve complex differential equations commonly encountered in mathematical modeling, including epidemiological studies. LADM combines the Laplace transform with Adomian Decomposition to break down differential equations into a series of manageable sub-problems. This hybrid approach leverages the Laplace transform's ability to simplify differential equations and Adomian's method of decomposing nonlinear terms, allowing for effective solutions in systems that are otherwise challenging to solve analytically [7,8]. LADM's adaptability to various boundary conditions and its

ability to handle nonlinear equations without requiring linearization make it a suitable choice for modeling infectious disease dynamics, such as monkeypox.

One of the main advantages of using LADM in monkeypox modeling is its effectiveness in obtaining approximate solutions that converge rapidly, often without the need for iterative approximation, as seen in traditional numerical methods. This characteristic is particularly beneficial in epidemiological modeling, where accurate, timely predictions of disease spread and control measures are crucial. For example, LADM allows researchers to explore various compartments in monkeypox transmission, such as susceptible, exposed, infected, and recovered populations, while efficiently estimating the impact of intervention strategies [5, 6]. By providing explicit, analytical expressions for these population compartments over time, LADM enhances the accuracy of disease models and aids in better understanding and predicting the dynamics of infectious diseases like monkeypox.LADM also supports sensitivity analysis, which assesses how changes in model parameters—such as transmission and recovery rates—impact the overall system dynamics. This feature is essential in infectious disease research, where understanding parameter sensitivity helps identify which factors are most influential in controlling outbreaks [4]. In monkeypox modeling, LADM's capacity for parameter sensitivity analysis aids in evaluating the effectiveness of public health interventions, such as vaccination and quarantine measures. Overall, LADM's combination of flexibility, accuracy, and computational efficiency makes it an invaluable tool in developing reliable epidemiological models that can inform and optimize strategies for disease control.

Mathematical modeling is a fundamental tool in scientific research for understanding and predicting complex systems across disciplines, particularly in epidemiology, where it plays a critical role in studying disease dynamics. Models use mathematical equations to represent real-world processes, allowing researchers to simulate and analyze the behavior of systems under various conditions [9]. In infectious disease modeling, for example, compartmental models like SIR (Susceptible, Infected, Recovered) and SEIR (Susceptible, Exposed, Infected, Recovered) categorize populations into compartments that describe disease progression stages. These models help estimate parameters like transmission and recovery rates, enabling scientists to assess the potential impact of public health interventions [10]. Additionally, mathematical models support decision-making in public health by providing insights into outbreak control, vaccine distribution, and policy effects. Recent advancements in modeling methods, including stochastic and agent-based models, have further enhanced their accuracy and applicability to real-world scenarios, emphasizing their importance in epidemiology and beyond [11].

Recent researchers have focused on a variety of mathematical models to assess monkeypox interventions, estimate transmission dynamics, and predict spread patterns across different conditions. [12] developed a stochastic compartmental model, separating populations into Susceptible, Exposed, Infectious, and Recovered (SEIR) categories, to estimate the reproduction number of monkeypox during the 2022 outbreak in non-endemic countries. Their findings highlighted that regions with dense populations and high mobility had higher reproduction numbers, underlining the impact of early

interventions like quarantine and isolation. [13] applied a compartmental model to evaluate vaccination strategies in the UK's 2022 outbreak, emphasizing that even with limited vaccine supplies, targeting high-risk populations could substantially reduce transmission rates. Their model also pointed to the significance of timely vaccine distribution and rapid case detection.

[14] presented a deterministic model simulating monkeypox transmission in West Africa, incorporating both zoonotic and human-to-human transmission. Their analysis indicated that human transmission plays an increasing role, especially in urban settings, and recommended enhanced public health surveillance. [15] introduced a dynamic model that examined how behavior changes, such as social distancing and improved hygiene, affect monkeypox spread. The study showed that these behavioral shifts reduce the effective reproduction number, highlighting the importance of public health campaigns during outbreaks. Lastly, [16] developed a network-based model to simulate monkeypox spread in social and sexual networks, focusing on the heterogeneity of contact patterns within certain communities. Their research emphasized that interventions like vaccination are particularly effective in high-contact subpopulations, such as MSM (men who have sex with men), which are more vulnerable to outbreaks.

The novelty of this study lies in its dual-host modeling approach, which simultaneously considers both human and rodent populations to capture the complex transmission dynamics of Monkeypox—a factor often overlooked in previous models that focus primarily on human-to-human spread. By incorporating distinct epidemiological compartments for both species, this study provides a more comprehensive framework for understanding the role of zoonotic reservoirs in sustaining outbreaks. Furthermore, the use of the Laplace Adomian Decomposition Method (LADM) to obtain approximate solutions introduces an innovative mathematical approach that enhances the model's analytical tractability, allowing for more efficient evaluation of disease control strategies. Unlike conventional numerical methods, LADM provides a semi-analytical solution that improves accuracy and computational efficiency, making it particularly valuable for real-time policy assessments. Additionally, this study uniquely bridges theoretical epidemiology with practical public health interventions by evaluating the synergistic effects of multiple control measures, such as quarantining, treatment, and rodent population management, offering actionable insights for outbreak prevention. By integrating mathematical modeling with applied disease control strategies, this research presents a novel and impactful contribution to Monkeypox epidemiology, equipping policymakers with targeted recommendations to mitigate future outbreaks.

2 Materials and methods

We develop a deterministic compartmental model on the transmission dynamics of Monkeypox consisting of human and rodent population [22]. The human population comprises of six epidemiological groups, Susceptible humans $S_h(t)$, exposed humans $E_h(t)$, infected humans $I_h(t)$, quarantined humans $Q_h(t),$, treated humans $T_h(t)$ and recovered humans $R_h(t)$. The rodent

population is subdivided into three compartments namely: Susceptible rodents $S_r(t)$, exposed humans $E_r(t)$, infected rodents $I_r(t)$. The recruitment rate of human population is given as Λ_h and β_{rh} is the effective contact rate with the probability of human been infected with Monkeypox virus due to contact with infected rodent. β_{hh} denotes effective contact rate and the probability human been infected with monkeypox virus due to contact with infectious human and ω_h is the progression rate from exposed human to highly infected human whereas the treatment rate of infected humans is ρ_h and the recovery rate of treated humans is τ_h. θ_h is the quarantined rate of exposed humans whereas γ_h is the rate at which quarantined humans become susceptible and the recovery rate of quarantined humans is ψ_h. Natural death occurs in the humans and rodents' population at the rates μ_h and μ_r respectively. The infected humans and rodents' population decrease by the disease induced death rates δ_h and δ_r respectively. Λ_r is rodents' recruitment rate and β_{rr} is the effective contact rate with the probability of rodent been infected per contact rate with already infected rodent. ω_r is the progression rate from exposed rodent population to highly infectious rodent population and is immunity loss rate. The transition from one epidemiological compartment to another is illustrated in figure 1 below.

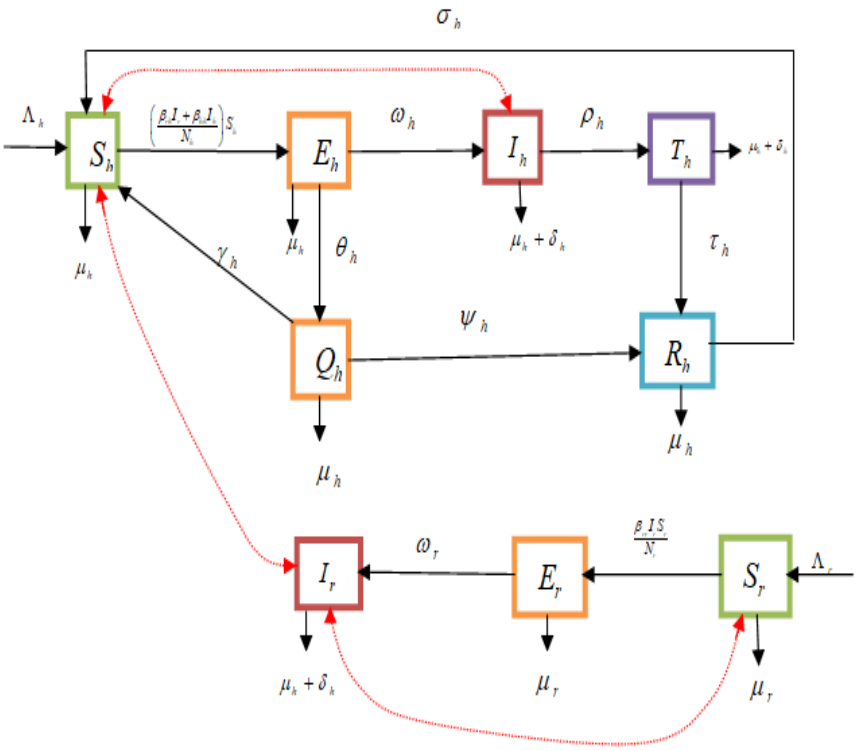


Figure 1. Schematic diagram for the model [22] .

Table 1. Description of variables and parameters

Variables	Description
$S_h(t)$	Susceptible human
$E_h(t)$	Exposed human
$Q_h(t)$	Isolated/quarantined human
$I_h(t)$	Infected human
$T_h(t)$	Treated human
$R_h(t)$	Recovered human
$S_r(t)$	Susceptible rodent
$E_r(t)$	Exposed rodent
$I_r(t)$	Infected rodents
Λ_h	Human recruitment rate
β_{rh}	Rodent contact rate to human
β_{hh}	Human to human contact rate
β_{rr}	Rodent to rodent to contact rate
ω_h	Progression rate from exposed human to infected human
ρ_h	Human treatment rate
θ_h	Quarantined rate of exposed humans
γ_h	Quarantined rate of susceptible humans
ψ_h	Recovery rate of quarantined individual
τ_h	Recovery rate of infected human
γ_h	Rate at which quarantined human become susceptible
σ_h	Immunity loss rate for human population
δ_h	Disease induced death rate for human
δ_r	Disease induce death rate for rodents
μ_h	Natural death rate for human
μ_r	Natural death rate for rodents
ω_r	Progression rate from exposed rodent to infected rodent

2.1 Model equations

The model is governed by the following set of differential equations.

$$\frac{dS_h}{dt} = \Lambda_h + \sigma_h R_h + \alpha_h Q_h - \frac{(\beta_{rh} \mathrm{I}_r + \beta_{hh} \mathrm{I}_h)\mathrm{S}_h}{N_h} - \mu_h S_h$$

$$\frac{dE_h}{dt} = \frac{(\beta_{rh} \mathrm{I}_r + \beta_{hh} \mathrm{I}_h)\mathrm{S}_h}{N_h} - (\omega_h + \theta_h + \mu_h)\mathrm{E}_h$$

$$\frac{dI_h}{dt} = \omega_h E_h - (\rho_h + \delta_h + \mu_h) I_h$$

$$\frac{dQ_h}{dt} = \theta_h E_h - (\alpha_h + \psi_h + \mu_h)\mathrm{Q}_h \qquad (1)$$

$$\frac{dT_h}{dt} = \rho_h I_h - (\tau_h + \delta_h + \mu_h)\mathrm{T}_h$$

$$\frac{dR_h}{dt} = \psi_h Q_h + \tau_h T_h - (\sigma_h + \mu_h)\mathrm{R}_h$$

$$\frac{dS_r}{dt} = \Lambda_r - \frac{\beta_{rr} I_r S_r}{N_r} - \mu_r \mathrm{S}_r$$

$$\frac{dE_r}{dt} = \frac{\beta_{rr} I_r S_r}{N_r} - (\omega_r + \mu_r)\mathrm{E}_r$$

$$\frac{dI_r}{dt} = \omega_r \mathrm{E}_r - (\delta_r + \mu_r)\mathrm{I}_r \quad \text{P7}$$

where $\lambda_h = \frac{(\beta_{rh} I_r + \beta_{hh} I_h)}{N_h}$, $\lambda_r = \frac{\beta_{rr} I_r}{N_r}$

2.1.1 Model Analysis

Total human population,

$N_h = S_h + E_h + I_h + \mathrm{Q}_h + T_h + R_h$

The differential equation yields

$\frac{dN_h}{dt} = \Lambda_h - \delta_h I_h - \mu_h N_h$

Total rodent population,

$N_r = S_r + E_r + I_r$

The differential equation also gives

$\frac{dN_r}{dt} = \Lambda_r - (\mu_r + \Lambda_r) N_r$

Lemma 1

Let $(S_h, E_h, I_h, Q_h, T_h, R_h, S_r, E_r, I_r)$ be the solution of the model (1) with initial conditions in a epidemiological feasible region $D = D_h \times D_r$ with [22]:

$$D_h = S_h, E_h, I_h, Q_h, T_h, R_h \in R_+^6 : N_h \leq \frac{\Lambda_h}{\mu_h}$$

and

$$D_r = S_r, E_r, I_r \in R_+^3 : N_r \leq \frac{\Lambda_r}{\mu_r}$$

Then D is non-negative invariant

From the result of [23], we obtain

$$0 \leq N_h(t) \leq N_h(0) e^{-\mu_h(t)} + \frac{\Lambda_h}{\mu_h}\left(1 - e^{-\mu_h(t)}\right)$$

and

$$0\, N_r(t) \leq N_r(0) e^{-(\mu_r + \Lambda_r)t} + \frac{\Lambda_h}{\mu_h}\left(1 - e^{-(\mu_r + \Lambda_r)t}\right)$$

Therefore, the set D is positively invariant for all t

Asymptotic Stability of the Disease-Free Equilibrium of the Monkeypox Model

The disease-free equilibrium is given below [22]

$$\eta_0 = \left\{S_h^*, E_h^*, I_h^*, Q_h^*, T_h^*, R_h^*, S_r^*, E_r^*, I_r^*\right\} = \left\{\frac{\Lambda_h}{\mu_h}, 0, 0, 0, 0, 0, \frac{\Lambda_r}{\mu_r}, 0, 0\right\}$$

Basic Reproduction Number

In this article, R_0 is obtained using the next generation operator method on the dynamic system (1), as detailed below [22].

Hence, it follows that

$R_0 = \rho\left(FV^{-1}\right)$ where ρ is the dominant eigenvalue of FV^{-1}

$$F=\begin{bmatrix} 0 & \beta_{hh} & 0 & 0 & 0 & \beta_{rh} \\ 0 & 0 & 0 & 0 & 0 & 0 \\ 0 & 0 & 0 & 0 & 0 & 0 \\ 0 & 0 & 0 & 0 & 0 & 0 \\ 0 & 0 & 0 & 0 & 0 & \beta_{rr} \\ 0 & 0 & 0 & 0 & 0 & 0 \end{bmatrix}, V=\begin{bmatrix} P_1 & 0 & 0 & 0 & 0 & 0 \\ -\omega_h & P_2 & 0 & 0 & 0 & 0 \\ \theta_h & 0 & P_3 & 0 & 0 & 0 \\ 0 & -\rho_h & 0 & P_4 & 0 & 0 \\ 0 & 0 & 0 & 0 & P_6 & 0 \\ 0 & 0 & 0 & 0 & -\omega_t & P_7 \end{bmatrix}$$

$$J=\begin{bmatrix} \frac{\beta_{hh}\omega_h}{P_2P_1} & \frac{\beta_{hh}}{P_2} & 0 & 0 & \frac{\beta_{rh}\omega_r}{P_6P_7} & \frac{\beta_{rh}}{P_7} \\ 0 & 0 & 0 & 0 & 0 & 0 \\ 0 & 0 & 0 & 0 & 0 & 0 \\ 0 & 0 & 0 & 0 & 0 & 0 \\ 0 & 0 & 0 & 0 & \frac{\beta_{rr}\omega_r}{P_6P_7} & \frac{\beta_{rr}}{P_7} \\ 0 & 0 & 0 & 0 & 0 & 0 \end{bmatrix}$$

The eigenvalues of FV^{-1} are

$$R_0^r=\frac{\beta_{rr}\omega_r}{P_6P_7}$$

$$R_0^h=\frac{\beta_{hh}\omega_h}{P_2P_1}$$

$$R_0=\left(R_0^h,R_0^r\right)$$

Jacobian Matrix (LAS)

$$J=\begin{bmatrix} \frac{\beta_{hh}\omega_h}{P_2P_1} & \frac{\beta_{hh}}{P_2} & 0 & 0 & \frac{\beta_{rh}\omega_r}{P_6P_7} & \frac{\beta_{rh}}{P_7} \\ 0 & 0 & 0 & 0 & 0 & 0 \\ 0 & 0 & 0 & 0 & 0 & 0 \\ 0 & 0 & 0 & 0 & 0 & 0 \\ 0 & 0 & 0 & 0 & \frac{\beta_{rr}\omega_r}{P_6P_7} & \frac{\beta_{rr}}{P_7} \\ 0 & 0 & 0 & 0 & 0 & 0 \end{bmatrix}$$

The reduced Jacobian matrix becomes

$$J_1=\begin{bmatrix} -P_1 & \beta_{hh} & 0 & \beta_{rh} \\ \omega_h & -P_2 & 0 & 0 \\ 0 & 0 & -P_6 & \beta_{rr} \\ 0 & 0 & \omega_r & -P_7 \end{bmatrix}$$

The characteristic polynomial becomes

$$\lambda^4+\left(P_7+P_6+P_2+P_1\right)\lambda^3+\left(P_2P_1+P_6P_1+P_7P_1+P_6P_2+P_7P_2+P_7P_6-\beta_{hh}\omega_h-\omega_r\beta_{rr}\right)\lambda^2$$
$$+\left(P_1P_2P_6+P_1P_2P_7+P_1P_6P_7-\omega_r\beta_{rr}P_1+P_2P_6P_7-\omega_r\beta_{rr}P_2-P_6\beta_{hh}\omega_h-P_7\beta_{hh}\omega_h\right)\lambda$$
$$+P_1P2\left(1-R_0^r\right)+P_6P_7\left(1-R_0^h\right)$$

Applying the Routh Hurwitz criterion, we observe that the DFE is locally asymptotically stable.

$P_1=(\omega_h+\theta_h+\mu_h)$ $P_2=(\rho_h+\delta_h+\mu_h)$ $P_3=(\alpha_h+\psi_h+\mu_h)$ $P_4=(\tau_h+\delta_h+\mu_h)$ $P_5=(\sigma_h+\mu_h)$

$P_6=(\omega_r+\mu_r)$ $P_7=(\delta_r+\mu_r)$.

Global Asymptotic Stability of the Disease Free Equilibrium Point of the Monkeypox Model.

To investigate the global stability of the disease free equilibrium, we use the technique implemented by Castillo-Chavez and song [22, 24].

To do this, we write the equation in the uninfected class as

$$\frac{dX}{dt}=F\left(X,Z\right)$$

And we re-write the equation in the infected class as

$$\frac{dZ}{dt} = G(X, Z)$$

Where $X = (S_h, R_h, S_r) \in R^3_+$ denotes the uninfected population and

$Z = (E_h, Q_h, I_h, T_h, E_r, I_r) \in R^6_+$ denotes the infected population

$\eta_0 = (X^*, 0)$ represent the disease free equilibrium of the system, and it is globally asymptotically stable if it satisfies the following conditions [22]:

$H_1 : \frac{dX}{dt} = F(X^*, 0), X^*$ is globally asymptotically stable

$H_2 : \frac{dZ}{dt} = D_Z G(X^*, 0) Z - \hat{G}(X, Z)$

$\hat{G}(X, Z) \geq 0$ for all $(X, Z) \in D$ and where $D_Z G(X^*, 0)$ is an M- matrix, the diagonal elements are non-negative and it is also the Jacobian of $\hat{G}(X, Z) \geq 0$ evaluated at $(X^*, 0)$.

If the system satisfies the above condition, then the theorem below holds.

Theorem 2 [22]

The equilibrium point $\eta_0 = (X^*, 0)$. *is globally asymptotically stable if*

$R_0 \leq 1$, *conditions* H_1 *and* H_2 *are satisfied*

$$F(X, Z) = \begin{bmatrix} \Lambda_h + \sigma_h R_h + \alpha_h Q_h - \frac{(\beta_{rh} I_r + \beta_{hh} I_h) S_h}{N_h} - \mu_h S_h, \\ \psi_h Q_h + \tau_h T_h - (\sigma_h + \mu_h) R_h, \\ \Lambda_r - \frac{\beta_{rr} I_r S_r}{N_r} - \mu_r S_r \end{bmatrix},$$

$$G(X, Z) = \begin{bmatrix} \frac{(\beta_{rh} I_r + \beta_{hh} I_h) S_h}{N_h} - (\omega_h + \theta_h + \mu_h) E_h \\ \omega_h E_h - (\rho_h + \delta_h + \mu_h) I_h \\ \theta_h E_h - (\gamma_h + \mu_h + \delta_h) I_h \\ \theta_h E_h - (\alpha_h + \psi_h + \mu_h) Q_h \\ \rho_h I_h - (\tau_h + \delta_h + \mu_h) T_h \\ \frac{\beta_{rr} I_r S_r}{N_r} - (\omega_r + \mu_r) E_r \\ \omega_r E_r - (\delta_r + \mu_r) I_r \end{bmatrix}$$

At disease free equilibrium,

H_1 :

$$\frac{dS_h}{dt} = \Lambda_h - \mu_h S_h$$
$$\frac{dS_r}{dt} = \Lambda_r - \mu_r S_r$$
$$\frac{dR_h}{dt} = 0$$

H_2 :

$$D_z G(X^*,0)Z = \begin{bmatrix} (\beta_{rh} I_r + \beta_{hh} I_h) - (\omega_h + \theta_h + \mu_h)E_h \\ \omega_h E_h - (\rho_h + \delta_h + \mu_h)I_h \\ \theta_h E_h - (\gamma_h + \mu_h + \delta_h) I_h \\ \theta_h E_h - (\alpha_h + \psi_h + \mu_h)Q_h \\ \rho_h I_h - (\tau_h + \delta_h + \mu_h)T_h \\ \beta_{rr} I_r S_r - (\omega_r + \mu_r)E_r \\ \omega_r E_r - (\delta_r + \mu_r)I_r \end{bmatrix}$$

$$\hat{G}(X,Z) = D_Z G(X^*,0)Z - G(X,Z)$$

$$\hat{G}(X,Z) = \begin{bmatrix} (\beta_{rh} I_r + \beta_{hh} I_h)\left(1 - \frac{S_h}{N_h}\right) \\ 0 \\ 0 \\ 0 \\ \beta_{rr} I_r \left(1 - \frac{S_r}{N_r}\right) \\ 0 \end{bmatrix}$$

Clearly, $1 \geq \frac{S_h}{N_h}, 1 \geq \frac{S_h}{N_h}$ this implies that $\hat{G}(X,Z) \geq 0$.

Therefore, the disease-free equilibrium of the Monkeypox only model is globally asymptotically stable.

2.2 Fractional order of the Monkeypox model

The Caputo derivative is measured as a differential operator in our model. We present in this segment some well-known definitions and effects that we shall be using throughout this research.

Definition 1 The Caputo fractional order derivative of a function (f) on the interval $[O,T]$ is defined by:

$$\left[{}^{C}D_{0}^{\beta}f(t)\right]=\frac{1}{\Gamma(n-\beta)}\int_{0}^{t}(t-s)^{n-\beta-1}f^{(n)}(s)ds, \tag{2}$$

Where $n=[\beta]+1$ and $[\beta]$ represents the integer part of β. In particular, for $0<\beta<1,$ the Caputo derivative becomes:

$$\left[{}^{C}D_{0}^{\beta}f(t)\right]=\frac{1}{\Gamma(1-\beta)}\int_{0}^{t}\frac{f(s)}{(t-s)^{\beta}}ds, \tag{3}$$

Definition 2 Laplace transform of Caputo derivatives is defined as

$$\mathcal{L}[{}^{C}D^{\beta}q(t)]=S^{\beta}h(S)-\sum_{K=0}^{n}S^{\beta-i-1}y^{k}(0),\quad n-1<\beta<n,\ n\in N, \tag{4}$$

For arbitrary $c_i\in R, i=0,1,2,...n-1,\ n=[\beta]+1$ and $[\beta]$ represents the non-integer part of β .

Lemma 1. The following results hold for fractional differentiation equations

$$I^{\beta}[{}^{c}D^{\beta}h](t)=h(t)+\sum_{i=0}^{n-1}\frac{h^{(t)}(0)}{i!}t^{i}, \tag{5}$$

For arbitrary $\beta>0, i=0,1,2,...,n-1,$ where $n=[\beta]+1$ and $[\beta]$ represents the integer part of β Introducing fractional-order into the model, we now present a new model described by the following Introducing fractional order derivative into the model we present new mathematical model describe by set of fractional difference of order β for $0<\beta<1$

$$\left.\begin{aligned}
D^{\beta}\left(S_h\right) &= \Lambda_h + \sigma_h R_h + \alpha_h Q_h - (\mu_h + \lambda_h)s_h,\\
D^{\beta}\left(E_h\right) &= \lambda_h S_h - (\omega_h + \theta_h + \mu_h)E_h,\\
D^{\beta}\left(I_h\right) &= \omega_h E_h - (\rho_h + \delta_h + \mu_h)I_h,\\
D^{\beta}\left(Q_h\right) &= \theta_h E_h - (\alpha_h + \psi_h + \mu_h)Q_h,\\
D^{\beta}\left(T_h\right) &= \rho_h I_h - (\tau_h + \delta_h + \mu_h)T_h,\\
D^{\beta}\left(R_h\right) &= \psi_h Q_h + \tau_h T_h - (\sigma_h + \mu_h)R_h,\\
D^{\beta}\left(S_r\right) &= \Lambda_r - (\mu_r + \lambda_r)S_r,\\
D^{\beta}\left(E_r\right) &= \lambda_r S_r - (\omega_r + \mu_r)E_r,\\
D^{\beta}\left(I_r\right) &= \omega_r E_r - (\delta_r + \mu_r)I_r.
\end{aligned}\right\} \qquad (6)$$

2.3 The Laplace-Adomian Decomposition Method (LADM) Implementation

We considered the general procedure of this method with the initial conditions. Applying Laplace transforms to both sides of the equation (1), and then we have:

$$\left.\begin{aligned}
S^{\beta}\mathcal{L}(S_h) - S^{\beta-1}S_h(0) &= \mathcal{L}\left[\Lambda_h + \sigma_h R_h + \alpha_h Q_h - (\mu_h + \lambda_h)S_h\right]\\
S^{\beta}\mathcal{L}(E_h) - S^{\beta-1}E_h(0) &= \mathcal{L}\left[\lambda_h S_h - (\omega_h + \theta_h + \mu_h)E_h\right]\\
S^{\beta}\mathcal{L}(I_h) - S^{\beta-1}I_h(0) &= \mathcal{L}\left[\omega_h E_h - (\rho_h + \delta_h + \mu_h)I_h\right]\\
S^{\beta}\mathcal{L}(Q_h) - S^{\beta-1}Q_h(0) &= \mathcal{L}\left[\theta_h E_h - (\alpha_h + \psi_h + \mu_h)Q_h\right]\\
S^{\beta}\mathcal{L}(T_h) - S^{\beta-1}T_r(0) &= \mathcal{L}\left[\rho_h I_h - (\tau_h + \delta_h + \mu_h)T_h\right]\\
S^{\beta}\mathcal{L}(R_h) - S^{\beta-1}R_h(0) &= \mathcal{L}\left[\psi_h Q_h + \tau_h T_h - (\sigma_h + \mu_h)R_h\right]\\
S^{\beta}\mathcal{L}(S_r) - S^{\beta-1}S_r(0) &= \mathcal{L}\left[\Lambda_r - (\mu_r + \lambda_r)S_r\right]\\
S^{\beta}\mathcal{L}(E_r) - S^{\beta-1}E_r(0) &= \mathcal{L}\left[\lambda_r S_r - (\omega_r + \mu_r)E_r\right]\\
S^{B}L(I_r) - S^{\beta-1}I_r(0) &= \mathcal{L}\left[\omega_r E_r - (\delta_r + \mu_r)I_r\right]
\end{aligned}\right\} \qquad (7)$$

With initial conditions

$$S_h(0) = n_1,\ \ E_h(0) = n_2,\ I_h(0) = n_3,\ Q_h(0) = n_4,\ T_h(0) = n_5,\ R_h(0) = n_6,\ S_r(0) = n_7,$$

$$E_r(0) = n_8,\ I_r(0) = n_9$$

Dividing eqn. (7) by (S^{β}) we have:

$$\left.\begin{aligned}
\mathcal{L}(S_h) &= \frac{n_1}{S} + \frac{1}{S^{\beta}}\mathcal{L}\left[\Lambda_h + \sigma_h R_h + \alpha_h Q_h - (\mu_h + \lambda_h)S_h\right] \\
\mathcal{L}(E_h) &= \frac{n_2}{S} + \frac{1}{S^{\beta}}\mathcal{L}\left[\lambda_h S_h - (\omega_h + \theta_h + \mu_h)E_h\right] \\
\mathcal{L}(I_h) &= \frac{n_3}{S} + \frac{1}{S^{\beta}}\mathcal{L}\left[\omega_h E_h - (\rho_h + \delta_h + \mu_h)I_h\right] \\
\mathcal{L}(Q_h) &= \frac{n_4}{S} + \frac{1}{S^{\beta}}\mathcal{L}\left[\theta_h E_h - (\alpha_h + \psi_h + \mu_h)Q_h\right] \\
\mathcal{L}(T_h) &= \frac{n_5}{S} + \frac{1}{S^{\beta}}\mathcal{L}\left[\rho_h I_h - (\tau_h + \delta_h + \mu_h)T_h\right] \\
\mathcal{L}(R_h) &= \frac{n_6}{S} + \frac{1}{S^{\beta}}\mathcal{L}\left[\psi_h Q_h + \tau_h T_h - (\sigma_h + \mu_h)R_h\right] \\
\mathcal{L}(S_r) &= \frac{n_7}{S} + \frac{1}{S^{\beta}}\mathcal{L}\left[\Lambda_r - (\mu_r + \lambda_r)S_r\right] \\
\mathcal{L}(E_r) &= \frac{n_8}{S} + \frac{1}{S^{\beta}}\mathcal{L}\left[\lambda_r S_r - (\omega_r + \mu_r)E_r\right] \\
\mathcal{L}(I_r) &= \frac{n_9}{S} + \frac{1}{S^{\beta}}\mathcal{L}\left[\omega_r E_r - (\delta_r + \mu_r)I_r\right]
\end{aligned}\right\} \qquad (8)$$

Decomposing the non-linear term of equation (6) whereby we assume the solution of $S_h(t), E_h(t), I_h(t), Q_h(t), T_h(t), R_r(t), S_r(t), E_r(t), I_r(t)$ are in the form of infinite series given by:

$$S_h(t) = \sum_{n=0}^{\infty} S_h(n), \quad E_h(t) = \sum_{n=0}^{\infty} E_h(n), \quad I_h(t) = \sum_{n=0}^{\infty} I_h(n), \quad Q_h(t) = \sum_{n=0}^{\infty} Q_h(n), \quad T_h(t) = \sum_{n=0}^{\infty} T_h(n),$$
$$R_h(t) = \sum_{n=0}^{\infty} R_h(n), \quad S_r(t) = \sum_{n=0}^{\infty} S_r(n), \quad E_r(t) = \sum_{n=0}^{\infty} E_r(n), \quad I_r(t) = \sum_{n=0}^{\infty} I_r(n), \qquad (9)$$

We have three (5) non-linear terms. The non-linear term in equation (6) are decomposed by Adomian polynomial as follows:

$$I_r(t)S_h(t) = \sum_{n=0}^{\infty} A(n), \qquad I_h(t)S_h(t) = \sum_{n=0}^{\infty} B(n), \qquad I_r(t)S_r(t) = \sum_{n=0}^{\infty} C(n), \tag{10}$$

Where $A(n), B(n), C(n),$ are Adomian polynomials given by

$$A(n) = \frac{1}{\Gamma(n+1)} \frac{d^n}{d\lambda^n} \left[\sum_{k=0}^{n} \lambda^k I_r(k) \sum_{k=0}^{n} \lambda^k S_h(k) \right]_{\lambda=0}$$

$$B(n) = \frac{1}{\Gamma(n+1)} \frac{d^n}{d\lambda^n} \left[\sum_{k=0}^{n} \lambda^k I_h(k) \sum_{k=0}^{n} \lambda^k S_h(k) \right]_{\lambda=0} \tag{11}$$

$$C(n) = \frac{1}{\Gamma(n+1)} \frac{d^n}{d\lambda^n} \left[\sum_{k=0}^{n} \lambda^k I_r(k) \sum_{k=0}^{n} \lambda^k S_r(k) \right]_{\lambda=0}$$

The polynomials are given by

$$\begin{aligned} A(0) &= I_r(0)S_h(0), \\ A(1) &= I_r(0)S_h(1) + I_r(1)S_h(0), \\ A(2) &= I_r(0)S_h(2) + I_r(1)S_h(1) + I_r(2)S_h(0). \end{aligned} \tag{12}$$

$$\begin{aligned} B(0) &= I_h(0)S_h(0), \\ B(1) &= I_h(0)S_h(1) + I_h(1)S_h(0), \\ B(2) &= I_h(0)S_h(2) + I_h(1)S_h(1) + I_h(2)S_h(0). \end{aligned}$$

$$\begin{aligned} C(0) &= I_r(0)S_r(0), \\ C(1) &= I_r(0)S_r(1) + I_r(1)S_r(0), \\ C(2) &= I_r(0)S_r(2) + I_r(1)S_r(1) + I_r(2)S_r(0). \end{aligned}$$

Substituting equation (9), (10) into equation (8) we obtained:

$$
\begin{aligned}
\mathcal{L}\left\{\sum_{n=0}^{\infty} S_h(n)\right\} &= \frac{n_1}{S}+\frac{1}{S^{\beta}}\mathcal{L}\left[\Lambda_h+\sigma_h\sum_{n=0}^{\infty}R_h(n)+\alpha_h\sum_{n=0}^{\infty}Q_h(n)-\left(\frac{\beta_{rh}\sum_{n=0}^{\infty}A(n)+\beta_{hh}\sum_{n=0}^{\infty}B(n)}{N_h}\right)-\mu_h\sum_{n=0}^{\infty}S_h(n)\right]\\
\mathcal{L}\left\{\sum_{n=0}^{\infty} E_h(n)\right\} &= \frac{n_2}{S}+\frac{1}{S^{\beta}}\mathcal{L}\left[\left(\frac{\beta_{rh}\sum_{n=0}^{\infty}A(n)+\beta_{hh}\sum_{n=0}^{\infty}B(n)}{N_h}\right)-\left(\omega_h+\theta_h+\mu_h\right)\sum_{n=0}^{\infty}E_h(n)\right]\\
\mathcal{L}\left\{\sum_{n=0}^{\infty} I_h(n)\right\} &= \frac{n_3}{S}+\frac{1}{S^{\beta}}\mathcal{L}\left[\omega_h\sum_{n=0}^{\infty}E_h(n)-\left(\rho_h+\delta_h+\mu_h\right)\sum_{n=0}^{\infty}I_h(n)\right]\\
\mathcal{L}\left\{\sum_{n=0}^{\infty} Q_h(n)\right\} &= \frac{n_4}{S}+\frac{1}{S^{\beta}}\mathcal{L}\left[\theta_h\sum_{n=0}^{\infty}E_h(n)-(\alpha_h+\psi_h+\mu_h)\sum_{n=0}^{\infty}Q_h(n)\right]\\
\mathcal{L}\left\{\sum_{n=0}^{\infty} T_h(n)\right\} &= \frac{n_5}{S}+\frac{1}{S^{\beta}}\mathcal{L}\left[\rho_h\sum_{n=0}^{\infty}Q_h(n)-(\tau_h+\delta_h+\mu_h)\sum_{n=0}^{\infty}T_h(n)\right]\\
\mathcal{L}\left\{\sum_{n=0}^{\infty} R_h(n)\right\} &= \frac{n_6}{S}+\frac{1}{S^{\beta}}\mathcal{L}\left[\psi_h\sum_{n=0}^{\infty}Q_h(n)+\tau_h\sum_{n=0}^{\infty}T_h(n)-(\sigma_h+\mu_h)\sum_{n=0}^{\infty}R_h(n)\right]\\
\mathcal{L}\left\{\sum_{n=0}^{\infty} S_r(n)\right\} &= \frac{n_7}{S}+\frac{1}{S^{\beta}}\mathcal{L}\left[\Lambda_r-\frac{\beta_{rr}\sum_{n=0}^{\infty}C(n)}{N_r}-\mu_r\sum_{n=0}^{\infty}S_r(n)\right]\\
\mathcal{L}\left\{\sum_{n=0}^{\infty} E_r(n)\right\} &= \frac{n_8}{S}+\frac{1}{S^{\beta}}\mathcal{L}\left[\frac{\beta_{rr}\sum_{n=0}^{\infty}C(n)}{N_r}-(\omega_r+\mu_r)\sum_{n=0}^{\infty}E_r(n)\right]\\
\mathcal{L}\left\{\sum_{n=0}^{\infty} I_r(n)\right\} &= \frac{n_9}{S}+\frac{1}{S^{\beta}}\mathcal{L}\left[\omega_r\sum_{n=0}^{\infty}E_r(n)-(\delta_r+\mu_r)\sum_{n=0}^{\infty}I_r(n)\right]
\end{aligned}
\tag{13}
$$

Evaluating the Laplace transform of the 2nd terms in the RHS of (16), we obtain

$$
\begin{aligned}
\mathcal{L}\left\{\sum_{n=0}^{\infty} S_h(n)\right\} &= \frac{n_1}{S} + \left[\Lambda_h + \sigma_h \sum_{n=0}^{\infty} R_h(n) + \alpha_h \sum_{n=0}^{\infty} Q_h(n) - \left(\frac{\beta_{rh} \sum_{n=0}^{\infty} A(n) + \beta_{hh} \sum_{n=0}^{\infty} B(n)}{N_h}\right) - \mu_h \sum_{n=0}^{\infty} S_h(n)\right] \frac{1}{S^{\beta+1}} \\
\mathcal{L}\left\{\sum_{n=0}^{\infty} E_h(n)\right\} &= \frac{n_2}{S} + \left[\left(\frac{\beta_{rh} \sum_{n=0}^{\infty} A(n) + \beta_{hh} \sum_{n=0}^{\infty} B(n)}{N_h}\right) - \left(\omega_h + \theta_h + \mu_h\right) \sum_{n=0}^{\infty} E_h(n)\right] \frac{1}{S^{\beta+1}} \\
\mathcal{L}\left\{\sum_{n=0}^{\infty} I_h(n)\right\} &= \frac{n_3}{S} + \left[\omega_h \sum_{n=0}^{\infty} E_h(n) - \left(\rho_h + \delta_h + \mu_h\right) \sum_{n=0}^{\infty} I_h(n)\right] \frac{1}{S^{\beta+1}} \\
\mathcal{L}\left\{\sum_{n=0}^{\infty} Q_h(n)\right\} &= \frac{n_4}{S} + \left[\theta_h \sum_{n=0}^{\infty} E_h(n) - (\alpha_h + \psi_h + \mu_h) \sum_{n=0}^{\infty} Q_h(n)\right] \frac{1}{S^{\beta+1}} \\
\mathcal{L}\left\{\sum_{n=0}^{\infty} T_h(n)\right\} &= \frac{n_5}{S} + \left[\rho_h \sum_{n=0}^{\infty} Q_h(n) - (\tau_h + \delta_h + \mu_h) \sum_{n=0}^{\infty} T_h(n)\right] \frac{1}{S^{\beta+1}} \\
\mathcal{L}\left\{\sum_{n=0}^{\infty} R_h(n)\right\} &= \frac{n_6}{S} + \left[\psi_h \sum_{n=0}^{\infty} Q_h(n) + \tau_h \sum_{n=0}^{\infty} T_h(n) - (\sigma_h + \mu_h) \sum_{n=0}^{\infty} R_h(n)\right] \frac{1}{S^{\beta+1}} \\
\mathcal{L}\left\{\sum_{n=0}^{\infty} S_r(n)\right\} &= \frac{n_7}{S} + \left[\Lambda_r - \frac{\beta_{rr} \sum_{n=0}^{\infty} C(n)}{N_r} - \mu_r \sum_{n=0}^{\infty} S_r(n)\right] \frac{1}{S^{\beta+1}} \\
\mathcal{L}\left\{\sum_{n=0}^{\infty} E_r(n)\right\} &= \frac{n_8}{S} + \left[\frac{\beta_{rr} \sum_{n=0}^{\infty} C(n)}{N_r} - (\omega_r + \mu_r) \sum_{n=0}^{\infty} E_r(n)\right] \frac{1}{S^{\beta+1}} \\
\mathcal{L}\left\{\sum_{n=0}^{\infty} I_r(n)\right\} &= \frac{n9}{S} + \left[\omega_r \sum_{n=0}^{\infty} E_r(n) - (\delta_r + \mu_r) \sum_{n=0}^{\infty} I_r(n)\right] \frac{1}{S^{\beta+1}}
\end{aligned}
\tag{14}
$$

Taking the inverse Laplace transform of both sides of (14)

$$\left.\begin{aligned}
\sum_{n=0}^{\infty} S_h(n) &= n_1 + \left[\Lambda_h + \sigma_h \sum_{n=0}^{\infty} R_h(n) + \alpha_h \sum_{n=0}^{\infty} Q_h(n) - \left(\frac{\beta_{rh} \sum_{n=0}^{\infty} A(n) + \beta_{hh} \sum_{n=0}^{\infty} B(n)}{N_h}\right) - \mu_h \sum_{n=0}^{\infty} S_h(n)\right] \frac{t^{\beta}}{\Gamma(\beta+1)} \\
\sum_{n=0}^{\infty} E_h(n) &= n_2 + \left[\left(\frac{\beta_{rh} \sum_{n=0}^{\infty} A(n) + \beta_{hh} \sum_{n=0}^{\infty} B(n)}{N_h}\right) - \left(\omega_h + \theta_h + \mu_h\right) \sum_{n=0}^{\infty} E_h(n)\right] \frac{t^{\beta}}{\Gamma(\beta+1)} \\
\sum_{n=0}^{\infty} I_h(n) &= n_3 + \left[\omega_h \sum_{n=0}^{\infty} E_h(n) - \left(\rho_h + \delta_h + \mu_h\right) \sum_{n=0}^{\infty} I_h(n)\right] \frac{t^{\beta}}{\Gamma(\beta+1)} \\
\sum_{n=0}^{\infty} Q_h(n) &= n_4 + \left[\theta_h \sum_{n=0}^{\infty} E_h(n) - (\alpha_h + \psi_h + \mu_h) \sum_{n=0}^{\infty} Q_h(n)\right] \frac{t^{\beta}}{\Gamma(\beta+1)} \\
\sum_{n=0}^{\infty} T_h(n) &= n_5 + \left[\rho_h \sum_{n=0}^{\infty} Q_h(n) - (\tau_h + \delta_h + \mu_h) \sum_{n=0}^{\infty} T_h(n)\right] \frac{t^{\beta}}{\Gamma(\beta+1)} \\
\sum_{n=0}^{\infty} R_h(n) &= n_6 + \left[\psi_h \sum_{n=0}^{\infty} Q_h(n) + \tau_h \sum_{n=0}^{\infty} T_h(n) - (\sigma_h + \mu_h) \sum_{n=0}^{\infty} R_h(n)\right] \frac{t^{\beta}}{\Gamma(\beta+1)} \\
\sum_{n=0}^{\infty} S_r(n) &= n_7 + \left[\Lambda_r - \frac{\beta_{rr} \sum_{n=0}^{\infty} C(n)}{N_r} - \mu_r \sum_{n=0}^{\infty} S_r(n)\right] \frac{t^{\beta}}{\Gamma(\beta+1)} \\
\sum_{n=0}^{\infty} E_r(n) &= n_8 + \left[\frac{\beta_{rr} \sum_{n=0}^{\infty} C(n)}{N_r} - (\omega_r + \mu_r) \sum_{n=0}^{\infty} E_r(n)\right] \frac{t^{\beta}}{\Gamma(\beta+1)} \\
\sum_{n=0}^{\infty} I_r(n) &= n_9 + \left[\omega_r \sum_{n=0}^{\infty} E_r(n) - (\delta_r + \mu_r) \sum_{n=0}^{\infty} I_r(n)\right] \frac{t^{\beta}}{\Gamma(\beta+1)}
\end{aligned}\right\} \quad (15)$$

When $n=0$ we obtain,

$$S_h(0) = n_1,\ \ E_h(0) = n_2,\ I_h(0) = n_3,\ Q_h(0) = n_4,\ T_h(0) = n_5,\ R_h(0) = n_6,\ S_r(0) = n_7,$$

$$E_r(0) = n_8,\ I_r(0) = n_9 \quad (16)$$

When $n=1$, we obtain,

$$
\left.
\begin{aligned}
S_h(1) &= \left[\Lambda_h + \sigma_h R_h(0) + \alpha_h Q_h(0) - \left(\frac{\beta_{rh} A(0) + \beta_{hh} B(0)}{N_h} \right) - \mu_h S_h(0) \right] \frac{t^\beta}{\Gamma(\beta+1)} \\
E_h(1) &= \left[\left(\frac{\beta_{rh} A(0) + \beta_{hh} B(0)}{N_h} \right) - \left(\omega_h + \theta_h + \mu_h \right) E_h(0) \right] \frac{t^\beta}{\Gamma(\beta+1)} \\
I_h(1) &= \left[\omega_h E_h(0) - \left(\rho_h + \delta_h + \mu_h \right) I_h(0) \right] \frac{t^\beta}{\Gamma(\beta+1)} \\
Q_h(1) &= \left[\theta_h E_h(0) - (\alpha_h + \psi_h + \mu_h) Q_h(0) \right] \frac{t^\beta}{\Gamma(\beta+1)} \\
T_h(1) &= \left[\rho_h Q_h(0) - (\tau_h + \delta_h + \mu_h) \mathrm{T}_h(0) \right] \frac{t^\beta}{\Gamma(\beta+1)} \\
R_h(1) &= \left[\psi_h Q_h(0) + \tau_h T_h(1) - (\sigma_h + \mu_h) R_h(0) \right] \frac{t^\beta}{\Gamma(\beta+1)} \\
S_r(1) &= \left[\Lambda_r - \frac{\beta_{rr} C(0)}{N_r} - \mu_r S_r(0) \right] \frac{t^\beta}{\Gamma(\beta+1)} \\
E_r(1) &= \left[\frac{\beta_{rr} C(0)}{N_r} - (\omega_r + \mu_r) E_r(0) \right] \frac{t^\beta}{\Gamma(\beta+1)} \\
I_r(1) &= \left[\omega_r E_r(0) - (\delta_r + \mu_r) I_r(0) \right] \frac{t^\beta}{\Gamma(\beta+1)}
\end{aligned}
\right\} \quad (17)
$$

When $n = 2$, we obtain,

$$
\left.
\begin{aligned}
S_h(2) &= \left[\Lambda_h + \sigma_h R_h(1) + \alpha_h Q_h(1) - \left(\frac{\beta_{rh} A(1) + \beta_{hh} B(1)}{N_h} \right) - \mu_h S_h(1) \right] \frac{t^\beta}{\Gamma(\beta+1)} \\
E_h(2) &= \left[\left(\frac{\beta_{rh} A(1) + \beta_{hh} B(1)}{N_h} \right) - \left(\omega_h + \theta_h + \mu_h \right) E_h(1) \right] \frac{t^\beta}{\Gamma(\beta+1)} \\
I_h(2) &= \left[\omega_h E_h(1) - \left(\rho_h + \delta_h + \mu_h \right) I_h(1) \right] \frac{t^\beta}{\Gamma(\beta+1)} \\
Q_h(2) &= \left[\theta_h E_h(1) - (\alpha_h + \psi_h + \mu_h) Q_h(1) \right] \frac{t^\beta}{\Gamma(\beta+1)} \\
T_h(2) &= \left[\rho_h Q_h(1) - (\tau_h + \delta_h + \mu_h) \mathrm{T}_h(1) \right] \frac{t^\beta}{\Gamma(\beta+1)} \\
R_h(2) &= \left[\psi_h Q_h(1) + \tau_h T_h(1) - (\sigma_h + \mu_h) R_h(1) \right] \frac{t^\beta}{\Gamma(\beta+1)} \\
S_r(2) &= \left[\Lambda_r - \frac{\beta_{rr} C(1)}{N_r} - \mu_r S_r(1) \right] \frac{t^\beta}{\Gamma(\beta+1)} \\
E_r(2) &= \left[\frac{\beta_{rr} C(1)}{N_r} - (\omega_r + \mu_r) E_r(1) \right] \frac{t^\beta}{\Gamma(\beta+1)} \\
I_r(2) &= \left[\omega_r E_r(1) - (\delta_r + \mu_r) I_r(1) \right] \frac{t^\beta}{\Gamma(\beta+1)}
\end{aligned}
\right\} \quad (18)
$$

When $n = n+1$, we obtain,

$$
\left.
\begin{aligned}
S_h(n+1) &= \left[\Lambda_h + \sigma_h R_h(n) + \alpha_h Q_h(n) - \left(\frac{\beta_{rh} A(n) + \beta_{hh} B(n)}{N_h} \right) - \mu_h S_h(n) \right] \frac{t^\beta}{\Gamma(\beta+1)} \\
E_h(n+1) &= \left[\left(\frac{\beta_{rh} A(n) + \beta_{hh} B(n)}{N_h} \right) - \left(\omega_h + \theta_h + \mu_h \right) E_h(n) \right] \frac{t^\beta}{\Gamma(\beta+1)} \\
I_h(n+1) &= \left[\omega_h E_h(n) - \left(\rho_h + \delta_h + \mu_h \right) I_h(n) \right] \frac{t^\beta}{\Gamma(\beta+1)} \\
Q_h(n+1) &= \left[\theta_h E_h(n) - (\alpha_h + \psi_h + \mu_h) Q_h(n) \right] \frac{t^\beta}{\Gamma(\beta+1)} \\
T_h(n+1) &= \left[\rho_h Q_h(n) - (\tau_h + \delta_h + \mu_h) \mathrm{T}_h(n) \right] \frac{t^\beta}{\Gamma(\beta+1)} \\
R_h(n+1) &= \left[\psi_h Q_h(n) + \tau_h T_h(1) - (\sigma_h + \mu_h) R_h(n) \right] \frac{t^\beta}{\Gamma(\beta+1)} \\
S_r(n+1) &= \left[\Lambda_r - \frac{\beta_{rr} C(n)}{N_r} - \mu_r S_r(n) \right] \frac{t^\beta}{\Gamma(\beta+1)} \\
E_r(n+1) &= \left[\frac{\beta_{rr} C(n)}{N_r} - (\omega_r + \mu_r) E_r(n) \right] \frac{t^\beta}{\Gamma(\beta+1)} \\
I_r(n+1) &= \left[\omega_r E_r(n) - (\delta_r + \mu_r) I_r(n) \right] \frac{t^\beta}{\Gamma(\beta+1)}
\end{aligned}
\right\} \quad (19)
$$

The series solution of each compartment can be expressed as:

$$
\begin{aligned}
S_h(t) &= S_h(0) + S_h(1) + S_h(2) + \ldots \\
E_h(t) &= E_h(0) + E_h(1) + E_h(2) + \ldots \\
I_h(t) &= I_h(0) + I_h(1) + I_h(2) + \ldots \\
Q_h(t) &= Q_h(0) + Q_h(1) + Q_h(2) + \ldots \\
T_h(t) &= T_h(0) + T_h(1) + T_h(2) + \ldots \\
R_h(t) &= R_h(0) + R_h(1) + R_h(2) + \ldots \\
S_r(t) &= S_r(0) + S_r(1) + S_r(2) + \ldots
\end{aligned}
\quad (20)
$$

$$E_r(t) = E_r(0) + E_r(1) + E_r(2) + \ldots$$

$$I_r(t) = I_r(0) + I_r(1) + I_r(2) + \ldots$$

2.5 Numerical solution of Laplace Adomian Decomposition Method (LADM)

Numerical simulation plays a key role in mathematical epidemiology, allowing researchers to model and explore how diseases spread within populations. These models are often built on systems of differential equations that represent important factors, such as infection and recovery rates, as well as patterns of movement within the population. By solving these equations over time, simulations can forecast how a disease may progress under different conditions. Additionally, numerical simulations help in estimating parameters and analyzing sensitivity within epidemiological models [20]. Parameter estimation involves matching model outputs with real-world data to determine key values, like transmission rates or initial conditions, while sensitivity analysis examines how changes in these parameters impact the model's predictions. This approach helps ensure that the predictions are reliable and provides insights into which factors most influence disease spread. Simulations also allow researchers to test various scenarios and intervention strategies, such as the effects of vaccination programs, social distancing, or healthcare capacity changes on disease dynamics [22]. This makes simulation a critical tool for guiding public health responses and policies, offering valuable support for planning interventions during outbreaks. Overall, numerical simulations are essential for deepening our understanding of disease dynamics, shaping effective public health strategies, and preparing for future epidemics.

Therefore, we conduct the numerical solution of the model using the initial conditions and parameter values in MATLAB, the Laplace Adomian Decomposition Method (LADM) gives us an approximate solution in in terms of an infinite series presented as:

$$\left.\begin{aligned}
S_h(t) &= 30000 - 350.97\frac{t^{\beta}}{\Gamma(\beta+1)} - 524.37\frac{t^{2\beta}}{\Gamma(2\beta+1)} + \ldots \\
E_h(t) &= 10000 - 208.64\frac{t^{\beta}}{\Gamma(\beta+1)} + 5142.89\frac{t^{2\beta}}{\Gamma(2\beta+1)} + \ldots \\
I_h(t) &= 7000 + 252.41\frac{t^{\beta}}{\Gamma(\beta+1)} - 3656.46\frac{t^{2\beta}}{\Gamma(2\beta+1)} + \ldots \\
Q_h(t) &= 5000 + 164.37\frac{t^{\beta}}{\Gamma(\beta+1)} + 175.37\frac{t^{2\beta}}{\Gamma(2\beta+1)} + \ldots \\
T_h(t) &= 4500 - 309.92\frac{t^{\beta}}{\Gamma(\beta+1)} - 798800\frac{t^{2\beta}}{\Gamma(2\beta+1)} + \ldots \\
R_h(t) &= 4000 - 544.13\frac{t^{\beta}}{\Gamma(\beta+1)} - 798850\frac{t^{2\beta}}{\Gamma(2\beta+1)} + \ldots \\
S_r(t) &= 6000 - 104.53\frac{t^{\beta}}{\Gamma(\beta+1)} - 1.66\frac{t^{2\beta}}{\Gamma(2\beta+1)} + \ldots \\
E_r(t) &= 3000 - 16.09\frac{t^{\beta}}{\Gamma(\beta+1)} - 3.19\frac{t^{2\beta}}{\Gamma(2\beta+1)} + \ldots \\
I_r(t) &= 1500 - 327.38\frac{t^{\beta}}{\Gamma(\beta+1)} + 149.01\frac{t^{2\beta}}{\Gamma(2\beta+1)} + \ldots
\end{aligned}\right\} \quad (21)$$

For $\beta = 1$, the series solution of our model becomes,

$$\left.\begin{aligned}
S_h(t) &= 200000 - 429.97t - 262.185t^2 + \ldots \\
E_h(t) &= 150000 - 25080.46t + 2571.445t^2 + \ldots \\
I_h(t) &= 13000 + 25298.11t - 1828.23t^2 + \ldots \\
Q_h(t) &= 9000 + 168.73t + 87.685t^2 + \ldots \\
T_h(t) &= 10000 - 419.29t - 399400t^2 + \ldots \\
R_h(t) &= 8000 - 466.31t + 3991425t^2 + \ldots \\
S_r(t) &= 9000 - 194.35t - 0.834t^2 + \ldots \\
E_r(t) &= 10000 - 12.49t - 1.595t^2 + \ldots \\
I_r(t) &= 8000 - 1427.93t + 129.51t^2 + \ldots
\end{aligned}\right\} \quad (22)$$

Table 2. **Parameter Values used in the Model**

Parameters	Value	Sources
Λ_h	0.029	Assumed
Λ_r	0.9	Assumed
β_{rh}	0.00025	[19]
β_{hh}	0.00006	[20]
β_{rr}	0.027	[20]
ω_h	0.07	Assumed
ρ_h	0.002	[20]
θ_h	0.2	[20]
μ_r	0.00200	Assumed
τ_h	0.02	[20]
α_h	0.0001	[17]
σ_h	0.00001	Assumed
δ_h	0.02	[20]
δ_r	0.5	[18]
μ_h	0.05	Assumed
ω_r	0.007	Assumed

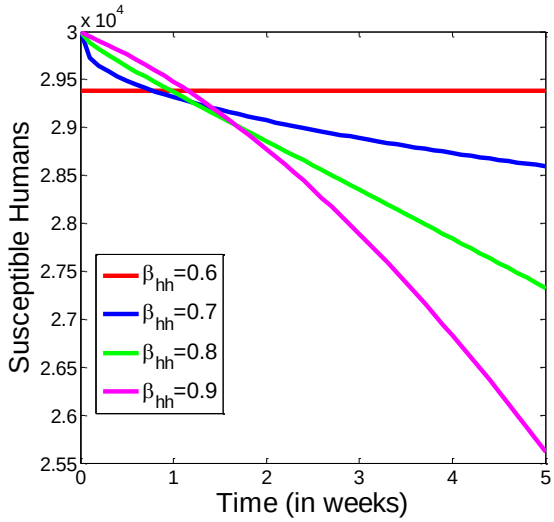


Figure 2a: Graph of susceptible humans

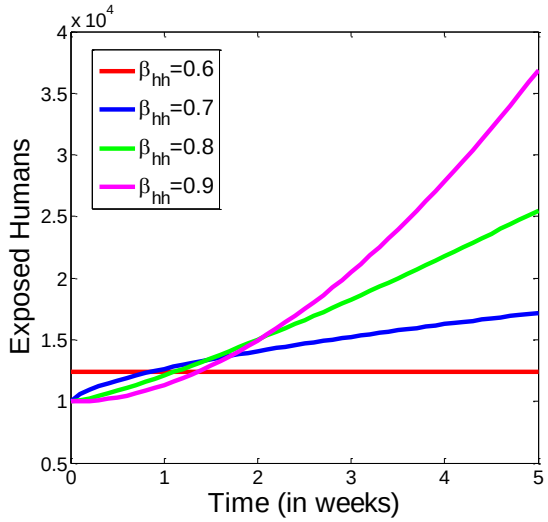


Figure 2b: Graph of Exposed humans

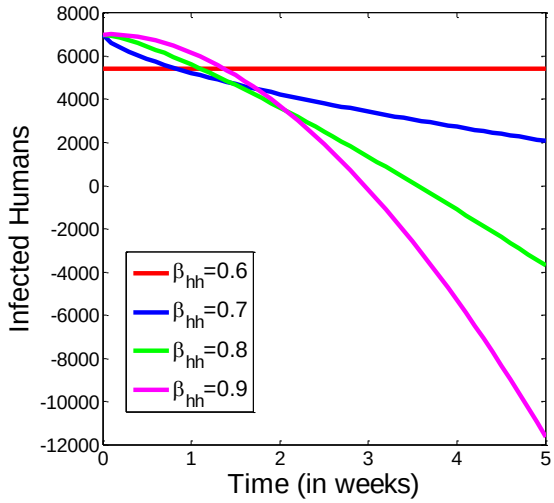


Figure 2c: Graph of infected humans humans

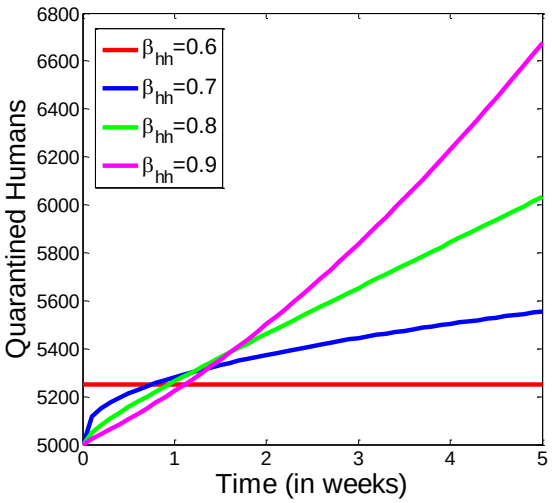
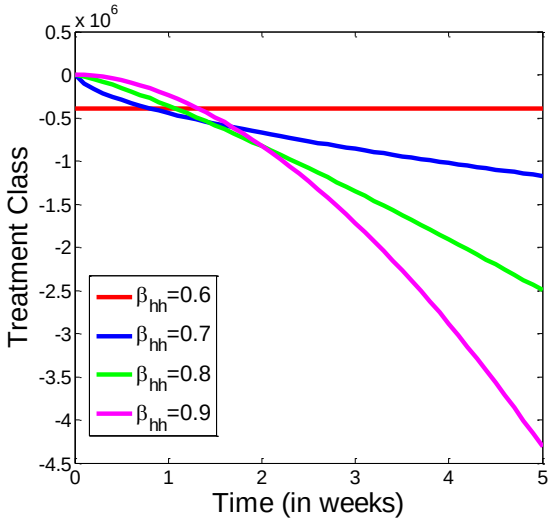


Figure 2d: Graph of quarantined



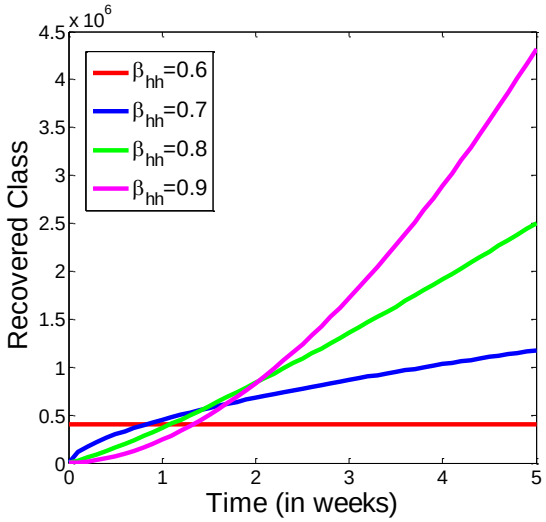
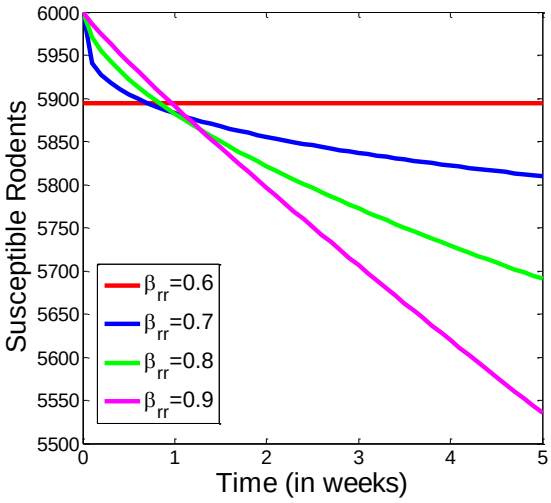


Figure 2e: Graph of treatment classFigure 2f: Graph of recovered humans



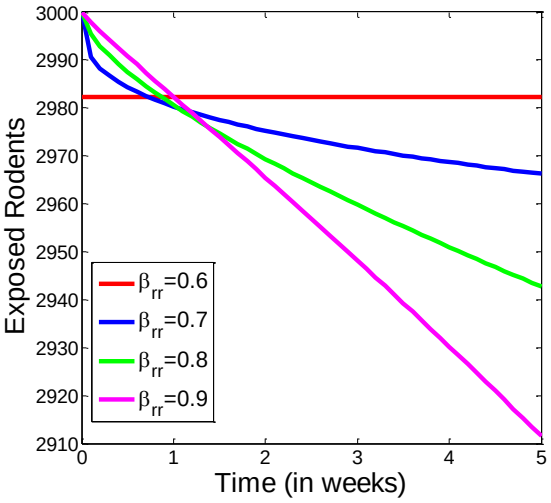


Figure 2g: Graph of susceptible rodents Figure 2h: Graph of Exposed rodents

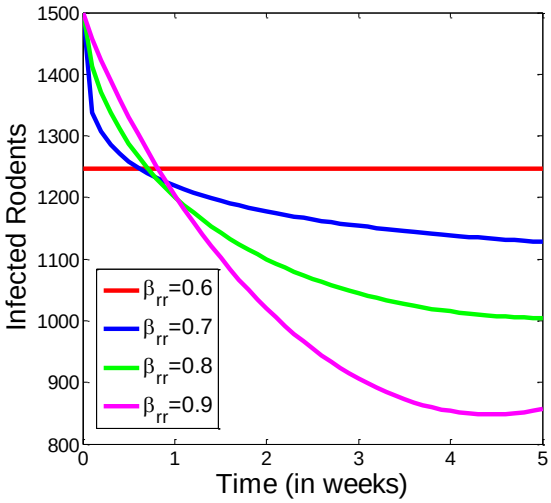


Figure 2i: Graph of infected rodents

In Figure 2a, we observe a steady decline in the graph of susceptible humans over time. This trend suggests effective control of the monkeypox virus, as fewer individuals within the population remain susceptible. This decrease implies that, eventually, almost no new cases are likely to emerge as the susceptible population approaches zero. However, Figure 2b shows an initial increase in the number of exposed humans. This rise occurs as susceptible individuals become exposed to the virus before prevention measures take full effect. After this initial increase, the exposed population also declines, indicating that interventions reduce the risk of exposure over time. In Figure 2c, the number of infected humans decreases steadily. This decline is likely due to effective quarantine measures, as shown in Figure 2d. Quarantine helps prevent the virus from spreading among the population by isolating infected individuals. As a result, the number of humans requiring treatment, illustrated in Figure 2e, also decreases. This decrease in active treatment cases is a promising sign, as it aligns with the observed high recovery rate in Figure 2f. Together, these trends suggest that both treatment and quarantine measures are effectively managing human cases of monkeypox, leading to an increase in recovered individuals. In Figure 2g, the graph of susceptible rodents also shows a significant decline over time. This trend indicates that control measures are not only effective for humans but are also helping reduce the number of susceptible rodents, which play a role in the transmission cycle. Figure 2h mirrors this effect in the exposed rodent population. Initially, there may be an increase in exposed rodents, but over time, the number of exposed rodents decreases as the virus is brought under control in their population as well. Finally, Figure 2i illustrates a complete decline in the number of infected rodents, eventually reaching zero. This result is a clear indicator of successful disease control. By eliminating the rodent population as a reservoir for the virus, the likelihood of further outbreaks decreases significantly, pointing to effective measures in controlling monkeypox transmission within both human and rodent populations.

3. Convergence analysis for the Laplace-Adomian Decomposition Method (LADM).

The solution of (1) is expressed in the forms of infinite series which converged uniformly to its exact solution. To verify the convergence of the series (21), we employ the method used in [18]. For sufficient conditions of convergence of the LADM, we present the following theorem:

Theorem 1

Let X be a Banach space and $T: X \to X$ *be a constructive nonlinear operator such that for* $(x),(x)' \in X,\ \left\|T(x)-T(x')\right\|, 0<k<1.$ *Then, T has a unique point x such that* $Tx = x$ *,where* $x = (S_H, E_H, I_H, R_H, S_M, E_M, I_M, S_W, E_W, I_W)$. *The series given () can be written by applying the Adomian decomposition method as follows:*

$$x_n = Tx_{n-1}, x_{n-1},$$

$$= \sum_{i=1}^{n-1} x_i,\ n = 1,2,3,...$$

And we assume that $x_0 \in B_r(x)$, *where* $B_r(x) = \left\{x \in X : \left\|x' - x\right\| < r\right\}$; *then, we have as follows:*

(i) $x_n \in B_r(x)$

(ii) $\lim_{n\to\infty} x_n = x$

Proof

For condition (i), invoking mathematical induction,

For n=1, we have as follows:

$$\left\|x_0 - x\right\| = \left\|T(x_0) - T(x)\right\| \le \left\|x_0 - x\right\|.$$

If this is true for m-1, then

$$\left\|x_0 - x\right\| \le k^{m-1}\left\|x_0 - x\right\|.$$

This gives the following:

$$\left\|x_m - x\right\| = \left\|T(x_{m-1}) - T(x)\right\| \le k\left\|x_{m-1} - x\right\| \le k^n\left\|x_0 - x\right\|.$$

Therefore,

$$\|x_m - x\| \leq k^n \|x_0 - x\| \leq k^n r < r.$$

This directly implies that $x_n \in B_r(x)$.

Also, for (ii), we have that since $\|x_m - x\| \leq k^n \|x_0 - x\|$ and $\lim_{n\to\infty} k^n = 0$, we can write $\lim_{n\to\infty} x_n = x$.

4 Conclusion

Our research presents a practical model for understanding how monkeypox spreads between humans and rodents, highlighting key strategies to control the disease. The results show that reducing the number of susceptible humans over time, combined with measures like quarantining and treating those infected, is highly effective in limiting the spread of monkeypox among people. In the rodent population, reducing the number of both susceptible and exposed animals plays an essential role in minimizing overall infection risks for humans. By using the Laplace Adomian Decomposition Method, we were able to predict how the disease would likely behave under different public health strategies. Our findings emphasize the importance of quickly isolating infected individuals, providing timely treatment, and managing rodent populations to reduce potential sources of infection. This model offers valuable insights for public health planning, suggesting that a comprehensive approach targeting both human and rodent populations is essential to controlling monkeypox. This framework could be adapted for similar zoonotic diseases, providing a basis for developing proactive strategies to prevent outbreaks and protect public health.

References

[1] World Health Organization (2022) . https://www.who.int/europe/news-room/23-07-2022-who-director-general-declares-the-ongoing-monkeypox-outbreak-a-public-health-event-of-international-concern

[2] CDC. (2023). Epidemiologic and clinical features of mpox-associated deaths in the United States. Retrieved from https://www.cdc.gov.

[3] Frontiers. (2023). Insights into monkeypox pathophysiology, global prevalence, clinical manifestation, and treatments. Retrieved from https://www.frontiersin.org

[4] Abdelrahman, M. M., & El-Sayed, A. M. (2020). Application of Laplace-Adomian Decomposition Method for solving some epidemiological models. Mathematics and Computers in Simulation, 173, 35-43.

[5] Chowdhury, M. S. H., Hamid, M. A., & Rahman, M. M. (2021). Analytical solution of SEIR model of infectious disease by using Laplace Adomian Decomposition Method. Results in Applied Mathematics, 10, 100168.

[6] Kanth, A. R., & Arshad, M. (2018). The use of Laplace Adomian Decomposition Method in solving biological models. Journal of Applied Mathematics and Physics, 6(4), 743-751.

[7] Kaya, D., & Cimen, S. (2015). A comparative analysis of Adomian Decomposition and Laplace-Adomian Decomposition Methods. Computers & Mathematics with Applications, 70(7), 1453-1461.
[8] Singh, J., & Kumar, M. (2019). Laplace-Adomian Decomposition Method for solving nonlinear problems. International Journal of Mathematical Analysis and Applications, 6(4), 15-21.
[9] Brauer, F., Castillo-Chavez, C., & Feng, Z. (2019). Mathematical Models in Epidemiology. New York: Springer.
[10] Kucharski, A. J., Russell, T. W., Diamond, C., Liu, Y., Edmunds, J., Funk, S., & Eggo, R. M. (2020). Early dynamics of transmission and control of COVID-19: A mathematical modelling study. The Lancet Infectious Diseases, 20(5), 553-558.
[11] Vynnycky, E., & White, R. (2018). An Introduction to Infectious Disease Modelling. Oxford University Press.
[12] Endo, A., Murayama, H., Abbott, S., Ratnayake, R., Pearson, C. A. B., Edmunds, W. J., & Funk, S. (2022). Estimating the reproduction number of monkeypox in non-endemic countries. Eurosurveillance, 27(22), 2200486.
[13] Grant, R., Hayes, S., Pybus, O. G., & Frost, S. D. (2023). Evaluating vaccination strategies against monkeypox transmission in the UK. Journal of Infectious Diseases, 227(3), 1024-1033.
[14] Yinka-Ogunleye, A., Aruna, O., Dalhat, M., Ogoina, D., McCollum, A. M., & Nkomo, P. (2022). Modeling zoonotic and human-to-human transmission of monkeypox in West Africa. Tropical Medicine & International Health, 27(4), 451-459.
[15] Al-Najjar, H., Al-Azzam, M., Al-Dabbas, B., & Mansour, A. (2023). Impact of behavior change on monkeypox transmission: A dynamic modeling approach. *Computational and Mathematical Methods in Medicine, 2023, 375162.
[16] Hebert-Dufresne, L., Althouse, B. M., Scarpino, S. V., & Allard, A. (2022). Network-based modeling of monkeypox transmission in social and sexual networks. Epidemics, 38, 100527.
[17] Agbata, B. C., Odeh, O. J., Anni, B. N., Odo, C. E., & Olorunnishola, O. A. (2019). Mathematical assessment of the transmission dynamics of HIV/AIDS with treatment as control effects. International Journal of Mathematics and Statistics Studies, 7(4), 40-52.
[18] Agbata, B. C., Shior, M. M., Obeng-Denteh, W., Omotehinwa, T. O., Paul, R. V., Kwabi, P. A., & Asante-Mensa, F. (2023). A mathematical model of COVID-19 transmission dynamics with effects of awareness and vaccination program. Journal of Global Scientific Academy, 21(2), 59-61.
[19] Odeh, J. O., Agbata, B. C., Ezeafulukwe, A. U., Madubueze, C. E., Acheneje, G. O., & Topman, N. N. (2024). A mathematical model for the control of chlamydia disease with treatment strategy. Journal of Mathematical Analysis and Research, 7(1), 1-20.
[20] Olumuyiwa, J. P., Sumit, K., Nitu, K., Festus, A. O., Kayode, O., & Rabiu, M. (2021). Transmission dynamics of monkeypox virus: A mathematical modeling approach. Modeling Earth System and Environment. https://dio.org/10.1007/s40808-021-013313-2
[21] Agbata, B.C., Obeng-Denteh, W., Amoah-Mensah, J. Kwabi, P.A., Shior, M.M., Asante Mensa, F, Abraham, S (2024). Numerical solution of fractional order model of measles disease with double dose vaccination. DUJOPAS. 10(3b): 202-217
[22] Agbata, B.C, Obeng-Denteh, W, Raimonda Dervish, Kwabi P.A., Habeed A. Aal-Rkhais, Asente-Mensa, F Ezugorie I.G, Arivi S.S. (2024). Mathematical modeling and analysis of Monkeypox transmission dynamics with treatment and quarantine interventions. *DUJOPAS*, 10 (4b): 78-96
[23] Somma, S. A., Akinwande, N. I., & Chado, U. D. (2019). A mathematical model of monkeypox virus transmission dynamics. Ife Journal of Science, 21(1), 195–204.

[24] Castillo-Chavez, C., & Song, B. (2004). Mathematical models of epidemics. *Mathematical Biosciences, 188*(2), 35-58. https://doi.org/10.1016/j.mbs.2004.03.005Malaria is a very deadly disease, which has taken a toll on human activities [1]. As seen in [2,3], evidences abound as to the source of the latest epidemic.

Half Logistic Generalized Inverse Rayleigh distribution for modeling Breast Cancer data

O.I. Oseghale*† and E. S. Micah†

Abstract

This article introduced a three-parameter extension of the Generalized Inverse Rayleigh distribution called half-logistic Generalized Rayleigh distribution, which has sub-models the Generalized Rayleigh and Rayleigh distribution. The proposed model is quite flexible and adaptable to model any kind of life-time data. Its probability density function may sometimes be unimodal and its corresponding hazard rate may be of monotone or non-monotone shape. Standard statistical properties such as it ordinary and incomplete moments, quantile function, moment generating function, reliability function, Lorenz and Bonferroni curves. The maximum likelihood method is used to obtain the estimates of the model parameters. An application of the newly developed model to breast cancer data is presented.

Keywords and phrases: maximum likelihood estimation**;** monotone shape; entropy

1 Introduction

Over the last century, many significant distributions have been introduced to serve as models in applied sciences. Among them, the so-called generalized beta distribution introduced by [18] is at the top of the list in terms of usefulness. The main feature of the generalized beta distribution is to be very rich; It includes a plethora of named distributions (to our knowledge, over thirty). In this paper, we focus our attention on one of the most attractive of these distributions, known as the inverse Lomax (IL) distribution. [22] introduced the inverse Rayleigh (IR) distribution as a model for analyzing reliability and survival data. The model underwent further investigation by [23], he observed that the lifetime distributions of various experimental units could be closely approximated with the inverse

* Corresponding author: innocentoseghale@gmail.com
† Federal University, Otuoke, Bayelsa State, Nigeria

Rayleigh distribution. Additionally, Voda explored its properties and provided a maximum likelihood (ML) estimator for the scale parameter. [12] carried an in-depth analysis of the inverse Rayleigh distribution. [17] developed a percentile estimator for the scale parameter θ of one-parameter inverse Rayleigh distribution and investigated its asymptotic efficiency. [14] established Bayesian prediction bounds for both Rayleigh and inverse Rayleigh lifetime models. [20] addressed both Bayesian and non-Bayesian issues related to parameter estimation in the IR distribution [3] propose a two-parameter extension of the inverse Rayleigh distribution, employing the half-logistic transformation to address limitations in modeling moderately right-skewed or near-symmetrical lifetime data. Their theoretical contributions encompass mathematical properties and empirical evidence, demonstrating the model's effectiveness in handling diverse right-skewed datasets.

The work in [6] present the inverse Rayleigh probability distribution as a robust model for estimating extreme wind speeds, crucial in wind power production and mechanical safety assessment. [7] introduce the compound inverse Rayleigh distribution as a model tailored for extreme wind speeds, essential in wind power generation and turbine safety evaluation. They provide a useful practical framework for real-world data analysis, accompanied by a novel Bayesian estimation approach, supported by extensive numerical simulations and robustness assessments. In a different context, [4] introduce the beta generalized inverse Rayleigh distribution, a four-parameter lifetime model, and conduct a comprehensive investigation into its properties and applications, further expanding the domain of inverse Rayleigh-based distributions.

Several generalizations of the inverse Rayleigh distribution have been recently proposed by numerous authors, with the aim of enhancing its adaptability. For example, [13] introduced an extension of the inverse Rayleigh distribution, termed the Burr XII inverse Rayleigh model, by integrating the Burr XII family framework initially introduced by [10]. [2] explored the use of the inverse Rayleigh distribution in mixture models to analyze the complex nature of engineering systems' lifetimes. [5] introduced the exponential transformed inverse Rayleigh distribution.

The generation of new distributions by adding one or more parameters to standard distributions enhances their applicability to complex data across various fields. Motivated by this approach, several authors have proposed different methods for generating new distributions. These include the Marshall–Olkin-G distribution by [15] the Beta-G distribution introduced by [11], the Kumaraswamy-G distribution by [8] and the McDonald-G distribution by [1]. [19] developed the transmuted-G class of distributions.

2 Methodology/Model formulation

The techniques for modifying the classical distributions are usually referred to as generators in literature and are capable of improving the goodness-of-fit of the modified distributions. These features have been established by the results of many generators ([8];[11]). Recently, [1] proposed an extension of the beta-generated family of distributions developed by [11]) and called it the transformed-transformer (T-X) family of distributions. According to [1] the CDF of the T-X family is defined as

$$G(x) = \int_0^{-log(1-F(t))} r(t)dt = R\{-log[1-F(t)]\} \quad (1)$$

Here, we define $r(t)$ as the probability density function (PDF) of the random variable T, R(t) is the CDF of T and $F(x)$ is the CDF of the random variable X. Although, the $T-X$ method have been embraced by several researchers, [24] proposed an extension of it in order to improve on some of the drawbacks of the $T-X$ method. The new family defined by [24] is called the exponentiated $T-X$ family of distributions.

In this work, our attention is focus on one of the most attractive of these distributions, known as the Generalized Rayleigh (GR) distribution. If the random variable X has a GIR distribution when its cumulative distribution function (CDF) can be represented by

$$F(x;\eta,\varphi) = 1-\left(1-e^{-(\theta x)^{-2}}\right)^{\varphi}; x>0,\varphi,\theta>0 \quad (2)$$

The corresponding probability density function to equation (2) is given as

$$f(x;\eta,\varphi) = \frac{2\varphi}{\theta^2 x^3} e^{-(\theta x)^{-2}}\left(1-e^{-(\theta x)^{-2}}\right)^{\varphi-1}; x>0,\varphi,\theta>0 \quad (3)$$

where φ is a shape parameter and θ is a scale parameter. If $\varphi = 1$, GIR reverses back to the well-known Inverse Rayleigh distribution. The main motivations behind the half logistic generated family are as follows. First, it is proved in [24] that the combined effect of the considered ratio and power transformations can significantly enrich the parental distribution, improving the flexibility of the mode, median, skewness and tail, with a positive impact on the analyses of practical data sets. However, the half logistic generated family remains underexploited and, based on the previous promising studies, needs more thorough attention.

2.1 Half Logistic Generalized Rayleigh distribution

Based on the work of [9], the CDF of half-logistic generalized family is defined by:

$$G(x;\lambda,\varsigma)=\frac{1-[1-F(x;\varsigma)]^{\lambda}}{1+[1-F(x;\varsigma)]^{\lambda}},\quad x\in R \tag{4}$$

where λ is a positive shape parameter and $F(x;\varsigma)$ represents a CDF of a continuous distribution, otherwise known as the baseline distribution. Here, ς represents a vector of parameter(s) related to the corresponding baseline distribution. The chief motivations behind the half-logistic family of distributions are as follows. [9] showed that the effect of the power transformation can enormously enrich the baseline distribution, improving the flexibility of the median, mode, skewness and tail, which provides a positive impact on the analyses of real-life data sets. The normal, Frechet, Weibull, and inverse Lomax distributions have been considered as baseline in the previous work using the half-logistic generated family by [12]. In recent studies, [29] developed and studied the type 1 half logistic Gompertz distribution, the Half-Logistic Generalized Weibull Distribution, type I half-logistic Topp-Leone distribution was proposed and studied by [29]. [30] proposed and studied the half logistic generalized Rayleigh distribution. However, the half logistic-g family has not been completely explored and, based on the studies carried out in the past, more work needs to be done to fully explore the richness of this generated family of distribution. In this paper, we consider the baseline distribution as Inverse Generalised Rayleigh (IGR) distribution.

Thus, we introduce a new flexible lifetime distribution with three parameters called the half-logistic Generalized Rayleigh ($HLGIR$) distribution. The CDF of the $HLGIR$ distribution with parameter vector $\zeta=(\theta,\varphi,\lambda)$ is obtained by inserting (3.1) into (3.3) as

$$G(x;\lambda,\varphi,\theta)=\frac{1-\left[1-\left(1-e^{-(\theta x)^{-2}}\right)^{\varphi}\right]^{\lambda}}{1+\left[\left[1-\left(1-e^{-(\theta x)^{-2}}\right)^{\varphi}\right]\right]^{\lambda}},\quad x\in R \tag{5}$$

The associated PDF to (5) is given by

$$g(x;\lambda,\varphi,\theta)=\frac{2\varphi e^{-(\theta x)^{-2}}\left(1-e^{-(\theta x)^{-2}}\right)^{\varphi-1}\left[1-\left(1-e^{-(\theta x)^{-2}}\right)^{\varphi}\right]^{\lambda-1}}{\theta^{2}x^{3}\left(1+\left[1-\left(1-e^{-(\theta x)^{-2}}\right)^{\varphi}\right]^{\lambda}\right)^{2}},\quad x\in R \tag{6}$$

where φ and λ are positive shape parameters and θ is a positive scale parameter.

The survival $(S(x))$, hazard $(h(x))$,and the cumulative hazard $(H(x))$ are, respectively, given as

$$S(x;\zeta) = 1 - G(x;\zeta) = \frac{2\left[1-\left(1-e^{-(\theta x)^{-2}}\right)^{\varphi}\right]^{\lambda}}{1+\left[1-\left(1-e^{-(\theta x)^{-2}}\right)^{\varphi}\right]^{\lambda}}, \qquad x \in R \qquad (7)$$

and $S(x;\zeta) = 1$ for $x \leq 0$,

$$h(x;\zeta) = \frac{g(x;\zeta)}{S(x;\zeta)} = \frac{2\varphi e^{-(\theta x)^{-2}}\left(1-e^{-(\theta x)^{-2}}\right)^{\varphi-1}}{\theta^2 x^3\left[1-\left(1-e^{-(\theta x)^{-2}}\right)^{\varphi}\right]\left(1+\left[\left[1-\left(1-e^{-(\theta x)^{-2}}\right)^{\varphi}\right]\right]^{\lambda}\right)}, \qquad (8)$$

and $h(x;\zeta) = 0$ for $x \leq 0$, and

$$H(x) = -log[S(x;\zeta)]$$
$$= \log(2) + \lambda log\left[1-\left(1-e^{-(\theta x)^{-2}}\right)^{\varphi}\right] - log\left[1+\left[\left[1-\left(1-e^{-(\theta x)^{-2}}\right)^{\varphi}\right]\right]^{\lambda}\right]. \qquad (8)$$

and $H(x;\zeta) = 0$ for $x \leq 0$. The graph of distribution, density, survival function(sf) and hazard function (hf) are respectively, given in Figures 3.1, 3.2, 3.3 and 3.4 for various hypothetical values of the parameters of the distributions.

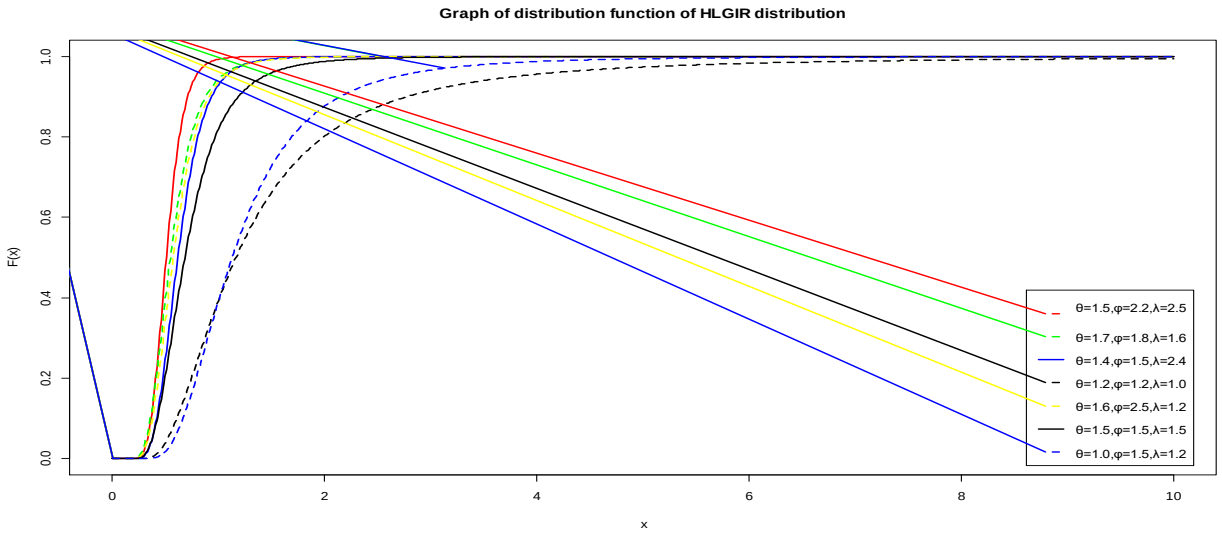


Figure 3.1. Graph of the CDF of *HLGIR* distribution

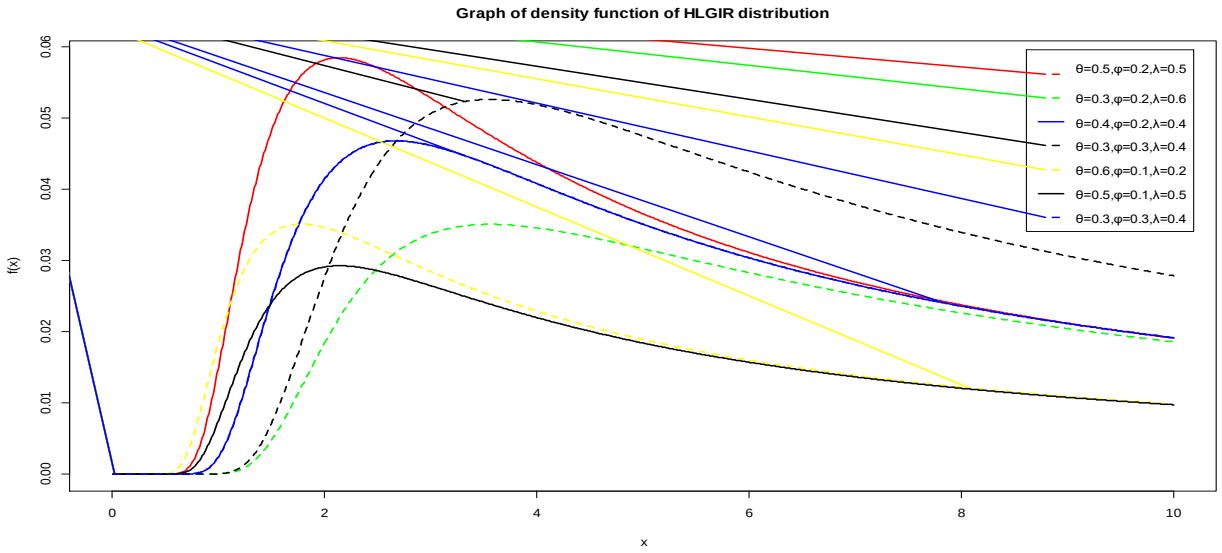


Figure 3.2. Graph of the CDF of *HLGIR* distribution

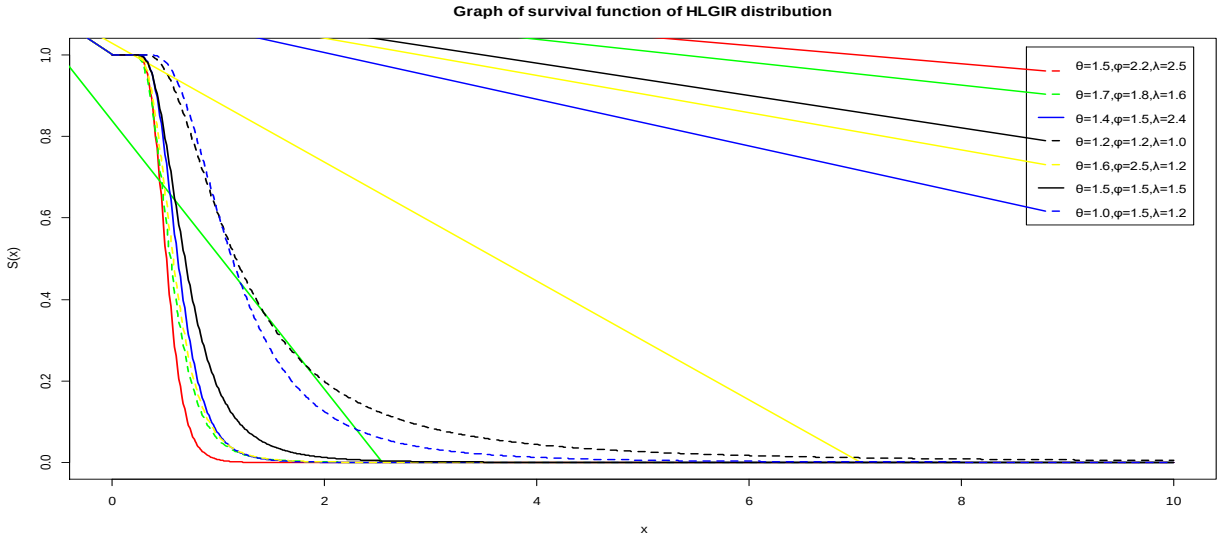
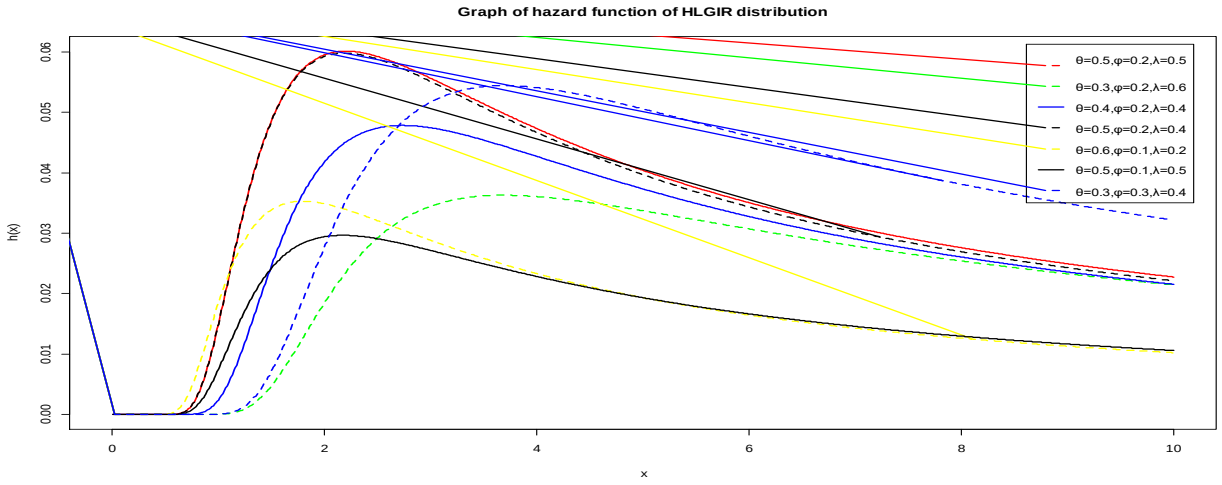


Figure 3.3. Graph of the survival function and the hazard function of *HLGIR* distribution

- From figure 3.3 it can be observed that the failure rate function of the *HLGIR* model exhibits the form of bathtub-shaped.



✓ The graph of the hazard function in figure 3.4 for various parameter values for $HLGIR$ distribution indicates that the new model exhibits various shapes such as monotonically increasing, decreasing, and upside-down bathtub shapes. This property clearly explains the flexibility of $HLGIR$ distribution and its applicability in modeling non-monotonic and monotonic hazard behavior which are often encountered in real-life data.

3.1 Important representation

In this subsection, an important tool for the expansion of the PDF for $HLGIR$ is provided. From the generalized binomial series given by

$$(1+v)^{-b} = \sum_{i=0}^{\infty} (-1)^i \binom{b+i-1}{i} v^i \tag{9}$$

For $|v| < 1$ and b is a positive real non-integer. Then, by applying the binomial theorem (9) in (6), the density function of $HLGIR$ distribution becomes

$$g(x) = \frac{2\varphi}{\theta^2} \sum_{i,j,k=0}^{\infty} (-1)^{i+j+k} \binom{i+1}{i} \binom{\lambda(i+1)-1}{j} \binom{\varphi(j+1)}{k} x^{-3} e^{-(k+1)(\varphi x)^{-2}} \tag{10}$$

3.1 Statistical characteristics of $HLGIR$ distribution

3.1.1 The quantiles, median and the upper quartile

An expression for the quantile and the median of $HLGR$ are obtained in this subsection.

The quantile x_q of the $HLGR$ is represented as follows

$$x_q = \frac{1}{\theta}\left\{-log\left(1-\left[1-\left(\frac{1-q}{1+q}\right)^{1/\lambda}\right]^{1/\varphi}\right)\right\}^{-1/2} \tag{11}$$

The median and the upper quartile of HLGIR are found by putting $q = 0.5$ and 0.75 in (11), respectively, as follows:

$$x_{0.5} = \frac{1}{\theta}\left\{-log\left(1-\left[1-\left(\frac{0.5}{1.5}\right)^{1/\lambda}\right]^{1/\varphi}\right)\right\}^{-1/2} \tag{12}$$

and

$$x_{0.75} = \frac{1}{\theta}\left\{-log\left(1-\left[1-\left(\frac{0.25}{1.25}\right)^{1/\lambda}\right]^{1/\varphi}\right)\right\}^{-1/2} \tag{13}$$

3.2 The ordinary and incomplete moments of $HLGIR$ distribution

Moments are the anticipated outcome of a particular function of a random variable. Due to the mathematical tractability of the various kinds of moments of $HLGIR$ distribution, the moments can be calculated directly. In a similar vein, Bonferroni and Lorenz curves, the mean waiting time, and the mean residual life can be computed using the first incomplete moment. Thus, the r^{th} ordinary moment of a distribution is given by

$$\mu_r' = E(x)^r$$

Thus the r^{th} moment of $HLGIR$ distribution is given by

$$\mu_r' = \int_{-\infty}^{\infty} x^r f(x;,\theta\lambda)dx \tag{14}$$

Putting equation (10) in (14), we have

$$\mu_r' = \frac{2\varphi}{\theta^2}\sum_{i,j,k=0}^{\infty}(-1)^{i+j+k}\binom{i+1}{i}\binom{\lambda(i+1)-1}{j}\binom{\varphi(j+1)}{k}\int_{-\infty}^{\infty}x^{r-3}e^{-(k+1)(\varphi x)^{-2}}dx \tag{15}$$

Letting $m = (k+1)(\varphi x)^{-2}$, $x = \frac{1}{\varphi}(k+1)^{1/2}m^{-1/2}$ $dx = -\frac{1}{2\varphi}(k+1)^{1/2}m^{-3/2}dm$ and substitute it in (15), we have

$$\mu_r' = \frac{1}{\theta^2}\sum_{i,j,k=0}^{\infty}(-1)^{i+j+k}\binom{i+1}{i}\binom{\lambda(i+1)-1}{j}\binom{\varphi(j+1)}{k}\frac{(k+1)^{1-r/2}}{\varphi^{r-3}}\int_{0}^{\infty}m^{\frac{-r}{2}}e^{-m}dx$$

Finally, we have,

$$\mu_r' = \frac{1}{\theta^2}\sum_{i,j,k=0}^{\infty}(-1)^{i+j+k}\binom{i+1}{i}\binom{\lambda(i+1)-1}{j}\binom{\varphi(j+1)}{k}\frac{(k+1)^{1-r/2}}{\varphi^{r-3}}\Gamma\left(1-{}^{r}/_{2}\right) \tag{16}$$

Where $\Gamma(.)$ is a gamma function. It should be noted that the mean (μ_1') and the variance $(\sigma^2 = \mu_2' - \{\mu_1'\}^2)$ of $HLGIL$ can respectively, be obtained by taking $r = 1,2$.

The mean is given by

$$\mu_1' = \frac{1}{\theta^2}\sum_{i,j,k=0}^{\infty}(-1)^{i+j+k}\binom{i+1}{i}\binom{\lambda(i+1)-1}{j}\binom{\varphi(j+1)}{k}\frac{(k+1)}{\varphi^{-2}}\Gamma\left({}^{1}/_{2}\right) \tag{17}$$

The variance is given as

$$\sigma^2 = \frac{1}{\theta^2}\sum_{i,j,k=0}^{\infty}(-1)^{i+j+k}\binom{i+1}{i}\binom{\lambda(i+1)-1}{j}\binom{\varphi(j+1)}{k}\frac{1}{\varphi^{-1}} - \left[\frac{1}{\theta^2}\sum_{i,j,k=0}^{\infty}(-1)^{i+j+k}\binom{i+1}{i}\binom{\lambda(i+1)-1}{j}\binom{\varphi(j+1)}{k}\frac{(k+1)}{\varphi^{-2}}\Gamma\left({}^{1}/_{2}\right)\right]^2 \tag{18}$$

3.3 Incomplete Moments 0f $HLGIL$ distribution

Thus the r^{th} moment of $HLGIR$ distribution is given by

$$v_r' = \int_0^t x^r f(x;\varphi,\theta,\lambda)dx \tag{19}$$

Putting equation (10) in (19), we have

$$v_r' = \frac{2\varphi}{\theta^2}\sum_{i,j,k=0}^{\infty}(-1)^{i+j+k}\binom{i+1}{i}\binom{\lambda(i+1)-1}{j}\binom{\varphi(j+1)}{k}\int_0^t x^{r-3}e^{-(k+1)(\varphi x)^{-2}}dx \tag{20}$$

Letting $m=(k+1)(\varphi x)^{-2}$, $x=\frac{1}{\varphi}(k+1)^{1/2}m^{-1/2}$ $dx=-\frac{1}{2\varphi}(k+1)^{1/2}m^{-3/2}dm$ and substitute it in (20), we have

$$v_r' = \frac{1}{\theta^2}\sum_{i,j,k=0}^{\infty}(-1)^{i+j+k}\binom{i+1}{i}\binom{\lambda(i+1)-1}{j}\binom{\varphi(j+1)}{k}\frac{(k+1)^{1-r/2}}{\varphi^{r-3}}\int_0^t m^{\frac{-r}{2}}e^{-m}dx \tag{21}$$

Finally, we have,

$$v_r' = \frac{1}{\theta^2}\sum_{i,j,k=0}^{\infty}(-1)^{i+j+k}\binom{i+1}{i}\binom{\lambda(i+1)-1}{j}\binom{\varphi(j+1)}{k}\frac{(k+1)^{1-r/2}}{\varphi^{r-3}}$$
$$\times\Gamma\left(1-{}^{r}/_{2},(k+1)(\varphi t)^{-2}\right) \tag{22}$$

The first incomplete moment is obtained by taking $r=1$, and we have

$$v_1' = \frac{1}{\theta^2}\sum_{i,j,k=0}^{\infty}(-1)^{i+j+k}\binom{i+1}{i}\binom{\lambda(i+1)-1}{j}\binom{\varphi(j+1)}{k}\frac{(k+1)}{\varphi^{-2}}\Gamma((k+1)(\varphi t)^{-2}) \tag{23}$$

3.4 Moments generating function

The moment generating function (MGF) of a random variable X provides an alternative method that can be used in describing the characteristics of a distribution. Mathematically, the MGF is defined as

$$\mathcal{M}_X(t) = E(e^{tX}) = \sum_{r=0}^{\infty} \frac{t^r}{r!} E(X^r). \tag{24}$$

Putting (23) in (24) for $E(X^r)$ for $HLGIL$ model, we obtain

$$\mathcal{M}_X(t) = \frac{1}{\theta^2} \sum_{i,j,k,r=0}^{\infty} \frac{t^r}{r!} (-1)^{i+j+k} \binom{i+1}{i} \binom{\lambda(i+1)-1}{j} \binom{\varphi(j+1)}{k} \frac{(k+1)^{1-r/2}}{\varphi^{r-3}} \Gamma\left(1 - r/2\right) \tag{25}$$

By setting $t = it$ in (25), we derived an expression for the characteristics function of the $HLGIL$ model as

$$\zeta_X(t) = \frac{1}{\theta^2} \sum_{i,j,k,r=0}^{\infty} \frac{t^r}{r!} (-1)^{i+j+k} \binom{i+1}{i} \binom{\lambda(i+1)-1}{j} \binom{\varphi(j+1)}{k} \frac{(k+1)^{1-r/2}}{\varphi^{r-3}} \Gamma\left(1 - r/2\right) \tag{26}$$

3.5 Mean deviation about the Mean and the Median

The mean deviation, about the mean and the median, are used to determine the degree of spread (scatter) in a population. Let $\mu = (X)$ and M be the median and the mean of the $HLGIL$ distribution given by (12) and (23) respectively

The mean deviation of $HLGIL$ model about the mean can be calculated as

$$\Gamma_1(X) = E|X - \mu| = \int_0^{\infty} |X - \mu| f(x; \varphi, \theta, \lambda) dx, \tag{27}$$

$$= 2\mu F(\mu; v, w, \lambda) - 2\mu + 2 \int_{\mu}^{\infty} x f(x; \varphi, \theta, \lambda) dx$$

$$= 2\mu \left\{ \frac{1 - \left[1 - \left(1 - e^{-(\theta x)^{-2}}\right)^{\varphi}\right]^{\lambda}}{1 + \left[\left[1 - \left(1 - e^{-(\theta x)^{-2}}\right)^{\varphi}\right]\right]^{\lambda}} \right\} - 2\mu + \frac{2}{\theta^2} \sum_{i,j,k=0}^{\infty} (-1)^{i+j+k} \binom{i+1}{i} \binom{\lambda(i+1)-1}{j}$$

$$\times \binom{\varphi(j+1)}{k} \frac{(k+1)^{1-r/2}}{\varphi^{r-3}} \Gamma\left(1-{}^{r}/_{2}, (k+1)(\varphi\mu)^{-2}\right) \tag{28}$$

The mean deviation about the median can also be calculated as

$$\Gamma_2(X) = E|X-M| = \int_0^{\infty} |X-M| f(x)dx, \tag{29}$$

$$= -\mu + 2\int_m^{\infty} xf(x;\varphi,\theta,\lambda)dx$$

$$= -\boldsymbol{\mu} + \frac{2}{\theta^2} \sum_{i,j,k=0}^{\infty} (-1)^{i+j+k} \binom{i+1}{i} \binom{\lambda(i+1)-1}{j} \binom{\varphi(j+1)}{k} \frac{(k+1)^{1-r/2}}{\varphi^{r-3}}$$

$$\Gamma\left(1-{}^{r}/_{2}, (k+1)(\varphi m)^{-2}\right) \tag{30}$$

3.6 Bonferroni and Lorenz curves

The Bonferroni and Lorenz curves have been found suitable to have applications not only in economics to study income and poverty analysis, but also in other fields like demography, insurance, and reliability. The Bonferroni and Lorenz curves are defined by

$$B(p) = \frac{1}{p\mu} \int_0^q xf(x;\lambda,\varphi,\theta)dx \tag{31}$$

and

$$L(p) = \frac{1}{\mu} \int_0^q xf(x;\lambda,\varphi,\theta)dx \tag{32}$$

Respectively, where $\mu = E(X)$ and $q = F^{-1}(p)$. In the case of $HLGIR$ distribution, we obtain

$$B(p) = \frac{1}{\mu\theta^2 p}\sum_{i,j,k=0}^{\infty}(-1)^{i+j+k}\binom{i+1}{i}\binom{\lambda(i+1)-1}{j}\binom{\varphi(j+1)}{k}\frac{(k+1)}{\varphi^{-2}}\Gamma((k+1)(\varphi t)^{-2}) \tag{33}$$

and

$$L(p) = \frac{1}{\mu\theta^2}\sum_{i,j,k=0}^{\infty}(-1)^{i+j+k}\binom{i+1}{i}\binom{\lambda(i+1)-1}{j}\binom{\varphi(j+1)}{k}\frac{(k+1)}{\varphi^{-2}}\Gamma((k+1)(\varphi t)^{-2}) \tag{34}$$

4.0 Application of $HLGIR$ to Breast cancer data

Here, we demonstrate the flexibility of Half logistic Generalized Inverse Power Lomax distribution using two lifetime data sets. The first data represent 121 breast cancer patients' survival times during a specific period from 1929 to 1938. The data source [26] studied these datasets. The observations are listed as follows: 0.3, 0.3, 4.0, 5.0, 5.6, 6.2, 6.3, 6.6, 6.8, 7.4, 7.5, 8.4, 8.4,10.3, 11.0, 11.8, 12.2, 12.3, 13.5, 14.4, 14.4, 14.8, 15.5, 15.7,16.2, 16.3, 16.5, 16.8, 17.2, 17.3, 17.5, 17.9, 19.8, 20.4, 20.9,21.0, 21.0, 21.1, 23.0, 23.4, 23.6, 24.0, 24.0, 27.9, 28.2, 29.1,30.0, 31.0, 31.0, 32.0, 35.0, 35.0, 37.0, 37.0, 37.0, 38.0, 38.0,38.0, 39.0, 39.0, 40.0, 40.0, 40.0, 41.0, 41.0, 41.0, 42.0, 43.0, 43.0, 43.0, 44.0, 45.0, 45.0, 46.0, 46.0, 47.0, 48.0, 49.0, 51.0, 51.0, 51.0, 52.0, 54.0, 55.0, 56.0, 57.0, 58.0, 59.0, 60.0, 60.0, 60.0, 61.0, 62.0, 65.0, 65.0, 67.0, 67.0, 68.0, 69.0, 78.0, 80.0, 83.0, 88.0, 89.0, 90.0, 93.0, 96.0, 103.0, 105.0, 109.0, 109.0, 111.0, 115.0, 117.0, 125.0, 126.0, 127.0, 129.0, 129.0, 139.0,154.0. Then the fit of the Half logistic Generalized Inverse Rayleigh model is compared with those of some competitive model such as Half logistic Inverse Rayleigh distribution (HLIR) by [27] and the inverse Rayleigh model. The maximum likelihood estimation procedure was used to determine the estimates of the parameters of the models considered. We compute statistical measures which represent the measures of goodness of fits and this includes Akaike Information Criterion (AIC), Bayesian Information Criterion (BIC), Consistent Akaike Information Criterion (CAIC), and Hana Quin Information Criterion (HQIC). The model with the smallest AIC, BIC, CAIC, and HQIC is assumed to be the best fit model in the class of models considered. Table 4.1 shows that the breast cancer data is over-dispersed, positively skewed. Figure 4.1 shows that the Breast cancer data contains no outlier observation and it has a wider spread.

Table 4.1 Exploratory data analysis of Breast cancer data

$Min.$	q_1	$median$	$mean$	q_3	max	$Range$	$Skewness$	$Kurtosis$	$variance$
0.0004	0.0095	0.7405	0.9765	1.4122	3.8474	3.8470	1.0432	3.4021	1244.46

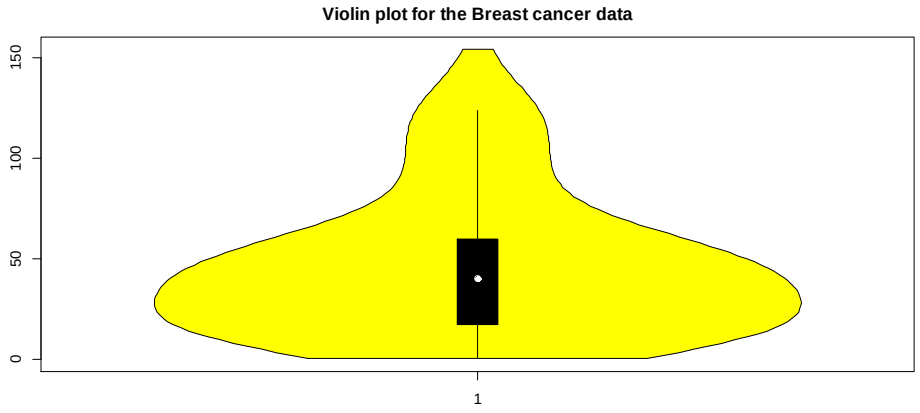


Figure 4.1. Violin plot of Breast cancer data

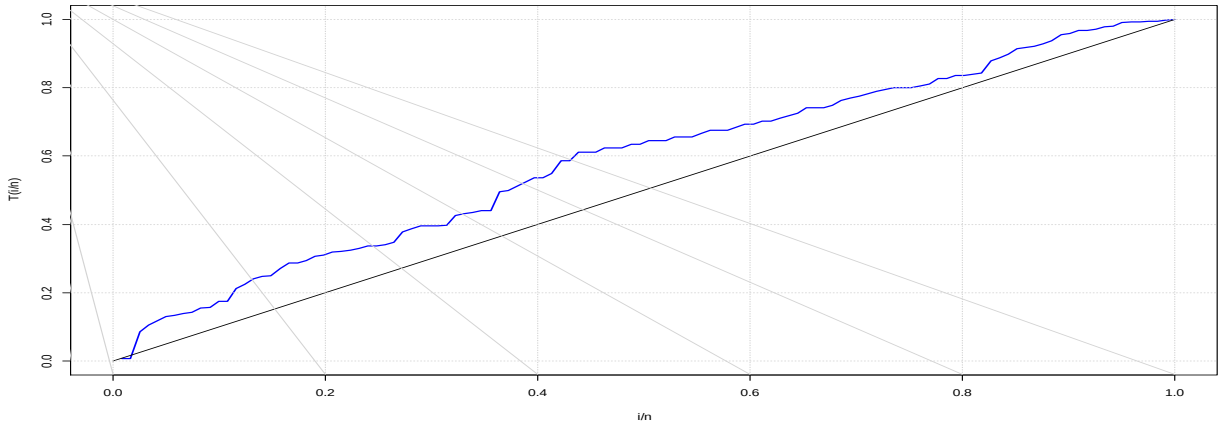


Figure 4.2. Total time on test (TTT) Plot for Breast cancer data.

Table 4.2 Measures of goodness of fit of Breast cancer data

	Parameter estimate			*Measures of goodness of fit*				
Model	θ	φ	λ	$-l$	*AIC*	*CAIC*	*HQIC*	*BIC*
HLGIR	1.213 (0.012)	3.569 (0.012)	0.003 (0.005)	276.76	559.52	559.72	562.92	567.90
HLIR	7.070 (5.897)	– (–)	0.0015 (0.0117)	419.60	843.20	843.29	845.47	848.79
IR	5.338 (0.485)	– (–)	– (–)	1092.55	2187.10	2187.12	2188.23	2189.89

From Table 4.2, we observe that $HLGIR$ model has a better fit than its existing sub-model models which includes $HLIR$, and IR model because it possesses the smallest $AIC, CAIC, HQIC,$ and BIC. This result shows that the $HLGIR$ is more suitable for modeling breast cancer data than other models considered in the study.

5 Discussions and conclusion

It is evident in this study that the new model developed show the potentiality of a process or phenomenon under consideration. In the field of statistics many of these models were developed through generalization, combination, or through modification of existing models to develop new one. In this research, we have presented a new generalized distribution called the Half Logistic Generalized Inverse Rayleigh distribution. The new distribution was developed using the Half logistic generalized family of distributions introduced in the literature. Some mathematical properties of the new developed generalized distribution were studied which includes: Renyi entropy, Bonferroni and Lorenz curve, ordinary moments and incomplete moments, moment generating function, mean deviations, quantile function, and also the parameters of the developed model are estimated using the maximum likelihood estimation procedure. An application of the newly developed model to breast cancer data demonstrates its attractiveness in modeling lifetime data.

References

[1] Alexander, C.; Cordeiro, G.M.; Ortega, E.M.M.; Sarabia, J.M. (2012). Generalized beta-generated distributions. Comput. Stat. Data Anal. 2, 56, 1880–1897.

[2] Ali, S. (2015). Mixture of the inverse Rayleigh distribution: Properties and estimation in a Bayesian framework. Appl. Math. Model., 39, 515–530.

[3] Almarashi, A.M.; Badr, M.M.; Elgarhy, M.; Jamal, F.; Chesneau, C. (2020). Statistical inference of the half-logistic inverse Rayleigh distribution. Entropy, 22, 449.

[4] Bakoban, R.A.; Al-Shehri, A.M. (2021). A new generalization of the generalized inverse Rayleigh distribution with applications. Symmetry, 13, 711.

[5] Banerjee, P.; Bhunia, S. (2022). Exponential transformed inverse Rayleigh distribution: Statistical properties and different methods of estimation. Austrian J. Stat., 51, 60–75.

[6] Chiodo, E.; Noia, L.P.D. (2020). Stochastic extreme wind speed modeling and bayes estimation under the inverse Rayleigh distribution. Appl. Sci., 10, 5643.

[7] Chiodo, E.; Fantauzzi, M.; Mazzanti, G. (2022). The compound inverse Rayleigh as an extreme wind speed distribution and its bayes estimation. Energies, 15, 861.

[8] Cordeiro, G. M. and de Castro, M. (2011). A new family of generalized distributions. Journal of Statistical Computation and Simulation, 81(7):883–898

[9] Cordeiro, G. M., Alizadeh, M. and Marinho, M.R.P.D. (2015). The type I half-logistic family of distributions, Journal of Statistical Computation and Simulation, 86, 707-728.

[10] Cordeiro, G.M.; Yousof, H.M.; Ramires, T.G.; Ortega, E.M. (2018). The Burr XII system of densities: Properties, regression model and applications. J. Stat. Comput. Simul., 88, 432–456.

[11] Eugene, N., Lee, C., and Famoye, F. (2002). The beta-normal distribution and its applications. Communications in Statistics-Theory and Methods, 31(4):497–512.

[12] Gharraph, M. K. (1993). Comparison of estimators of location measures of an inverse Rayleigh distribution. Egypt. Stat. J., 37, 295–309.

[13] Goual, H.; Yousof, H.M. (2020). Validation of Burr XII inverse Rayleigh model via a modified chi-squared goodness-of-fit test. J. Appl. Stat. 2020, 47, 393–423.

[14] Howlader, H.A.; Hossain, A.M.; Makhnin, O. (2009). Bayesian prediction bounds for Rayleigh and inverse Rayleigh lifetime models. J. Appl. Stat. Sci., 17, 131.

[15] Marshall, A.W. and Olkin, I. (1997). A new method for adding a parameter to a family of distributions with application to the exponential and Weibull families. Biometrika, 84, 641–652.

[16] Mudholkar, G. S. and Srivastava, D. K. (1993). Exponentiated Weibull family for analyzing bathtub failure-rate data. IEE Transactions on Reliability, 42:299–302.

[17] Mukherjee, S.P.; Maiti, S.S. (1996). A percentile estimator of the inverse Rayleigh parameter. IAPqR Trans. 1996, 21, 63–66.

[18] McDonald, J.B.; Xu, Y.J. (1995). A generalization of the beta distribution with applications. J. Econom., 66, 133–152.

[19] Shaw, W.T.; Buckley, I.R. (2009). The alchemy of probability distributions: Beyond Gram-Charlier expansions, and a skew-kurtotic-normal distribution from a rank transmutation map. arXiv, arXiv:0901.0434

[20] Soliman, A.; Essam, A.; Amin, A.; Abd-El Aziz, A.A. (2010). Estimation and Prediction from Inverse Rayleigh Distribution Based on Lower Record Values. Appl. Math. Sci., 4, 3057–3066.

[22] Treyer, V.N. (1964). Inverse Rayleigh (IR) model. Proc. USSR Acad. Sci.

[23] Voda, V.G. (972). On the inverse Rayleigh distributed random variable. Rep. Statis. App. Res. JUSE, 19, 13–21.

[24] Alzaatreh, A. Lee, C. and Famoye, F. 2013). A new method for generating families of continuous distributions. Metron, 71, 63-79 (2013).

[25] Fayomi, A. (2019). Type I half logistic power Lomax distribution: Statistical properties and application. Adv. Appl. 54, 85–98.

[26] Tahir, M.H.; Cordeiro, G.M.; Mansoor, M.; Zubair, M. (2013). The Weibull-Lomax distribution: Properties and applications. Hacet. J. Math. Stat., 44, 461–480.

[27] Al-Marzouki, S.A. New Generalization of Power Lomax Distribution. (2018). Int. J. Math. Appl. 7, 59–68.

[28] Anwar,M.; Bibi, A. (2018). The Half-Logistic Generalized Weibull Distribution. J. Probab. Stat.,12, 8767826.

[29] Ogunde, A. A., Oseghale, O. I. and Audu, A. T. (2017). Performance Rating of the Type Half Logistic Gompertz Distribution: An Analytical Approach, American Journal of Mathematics and Statistics, Vol. 7 (3), 93-98.

[30] Ogunde, A. A., Subhankar, D. and Almetawally, E. M. (2024). Half logistic Generalized Distribution for modeling Hydrological Data. Annals of Data Science, Springer-Verlag GmbH Germany.

Controlling the dynamics of Diabetes Mellitus with mathematical model

K.A. Adeyemo[*], T.A. Lawal[†], I.A. Azeez[‡], E. Philemon[§], K.I. Falade[**], F.C. Nwachukwu[††], A. Omame[‡‡], N. O. Lasisi[§§], and P.O. Aye[***]

Abstract

A suitably and mathematically well posed model of the dynamics of diabetes mellitus; incorporating three control parameters, was formulated. The obtained equilibrium point shows that there is no disease free equilibrium (DFE) but endemic equilibrium point (EEP) of the model, The Analysis of the model shows that the endemic equilibrium point of the model is both locally asymptotically stable (LAS) and globally asymptotically stable (GAS). Homotopy perturbation method was used to obtain the model solution. Nigeria diabetes values and parameters are used to obtain the sensitivity analysis of the sensitive parameters, and graphical simulations of the numerical solution of the state variables. The study provides a comprehensive guidance for the prevention and control of Type 1, Type 2 and gestational diabetes.

***Keywords and phrases*:** model; diabetes mellitus; equilibrium point; model solution; graphical simulation.

1 Introduction

Diabetes mellitus is an endocrine-metabolic disorder characterised by persistent hyperglycaemia (high blood sugar) due to insulin shortage, inadequate insulin production or ineffective use of the insulin produced [1]. This condition lowers life expectancy, quality of life and increases the risk of micro

[*]Corresponding Author. Department of Computer and Mathematics, Faculty of Science, Nigeria Police Academy Wudil, Kano, Nigeria; E-mail: k.2a.adeyemo@gmail.com
[†]Department of Biochemistry and Forensic Science, Faculty of Science, Nigeria Police Academy Wudil, Kano, Nigeria; E-mail: lawalat40gmail.com
[‡] Department of Family Medicine, Faculty of Medical Sciences, ABUA, Nigeria
[§] Department of Computer and Mathematics, Faculty of Science, Nigeria Police Academy Wudil, Kano, Nigeria; E-mail: edwardphile@polac.edu.ng
[**] Department of Mathematics, ADUSTECH, Wudil, Kano State, Nigeria; E-mail: faladekazeem2016@kustwudil.edu.ng
[††] Department of Biochemistry and Forensic Science, Faculty of Science, Nigeria Police Academy Wudil, Kano, Nigeria; E-mail: nwachukwuchukwuedozie@gmail.com
[‡‡] Department of Mathematics, School of Physical Sciences, Federal University of Technology, Owerri, Nigeria; E-mail: omame2020@gmail.com
[§§] Department of Mathematics and Statistics, Federal Polytechnic, Kaura Namoda, Zamfara State, Nigeria; E-mail: nurudeenlasisi2009@yahoo.com
[***] Department of Mathematical Sciences, Adekunle Ajasin University, Akingba-Akoko, Ondo State, Nigeria; E-mail; ayepatricko@gmail.com

vascular damage (retinopathy, nephropathy, and neuropathy) as well as macro vascular damage (ischemic heart disease, stroke, and peripheral vascular disease) [2-11].

It results from either ineffectiveness of insulin or a hereditary or acquired deficit non pancreatic insulin production [12]. According to the World Health Organization, the number of persons with diabetes increased from an estimated 30 million in 1985 to over 171 million in 2000. By 2030, it is predicted that there would be over 366 million, with emerging nations experiencing a notable surge in the number, especially among individuals between the ages of 45 and 64 [13-14]. The population of diabetics is currently rising significantly in several countries [15]. Neonatal diabetes mellitus (NDM) is a severe and monogenic form of diabetes mellitus (DM) which is characterized by onset of insulin requiring hyperglycaemia within the first month of life [16]; type 1 diabetes can occur before six months of life [17] or in the first six months [15]. NDM can be either transient or permanent. Nearly half of the individuals with NDM are permanent [15]. Type 1 diabetes, or insulin-dependent diabetes, and type 2 diabetes, or non-insulin-dependent diabetes, are the two major forms of diabetes mellitus. Five to ten percent of cases of diabetes are type 1 diabetes mellitus, generally referred to as insulin-dependent diabetes mellitus (IDDM). IDDM, which is most common in adolescents and young adults due to pancreatic insufficiency, is a condition in which the body fails to manufacture insulin [18]. Type 1 diabetes has an unknown aetiology and, at this point in time, is not preventive [19]. Nonetheless, there have been theories regarding autoimmune cell destruction. Sudden symptoms include excessive excretion of urine (polyuria), thirst (polydipsia), constant hunger, weight loss, vision changes, and fatigue [19,20]. Type 2 diabetes mellitus is also known as non-insulin-dependent diabetes mellitus (NIDDM), in which the body does not produce enough insulin or makes improper use of secreted insulin [21]. It is the most common form of diabetes, accounting for 90–95% of diabetes. Type 2 diabetes is nearing epidemic proportions due to an increased number of elderly people and a greater prevalence of obesity and sedentary lifestyles [21]. Symptoms may be like those of type 1 diabetes but are often less marked. Thus, the disease may be diagnosed several years after onset, once complications have already arisen [19]. Gestational diabetes is a disorder that occurs when a woman without diabetes develops hyperglycaemia during pregnancy [19, 21]. Gestational diabetes can cause health problems for both the mother and the baby. Gestational diabetes increases the risk of pre-eclampsia, depression, and requiring a Caesarean section, and babies born to mothers with poorly treated gestational diabetes are at increased risk of being too large, having low blood sugar after birth, and having jaundice [19]. If untreated, it can result in a stillbirth [13, 16, 19]. In 90% of cases, gestational diabetes will resolve after the baby is born [19]. Women, however, are at an increasing risk of developing type 2 diabetes [16].

This study improved on the existing studies by incorporating all types of diabetes, stages before, when, and after, diabetes is discovered, in determining the compartments and the control parameters in the formulated mathematical model. One of the three control parameters, is assumed to be moderately consumption of medicinal plants (strictly organic plants) in human daily diets. Properties of some of the many medicinal plants were studied in the work of [18]. The formulated mathematically well posed model is qualitatively and quantitatively analysed in order to be suitable for individual, health personnel, government and nongovernmental organisations, whenever solution to problem of diabetes is required.

1.1 Motivational Problem

Awareness to prevent, control and manage the problematic rising trend of diabetes mellitus and its complications on human population, requires mathematical model for both qualitative and quantitative analysis towards an improved quality of human lives on any part of the earth surface.

2 Materials and Methods

2.1 Model formulation

The total population at time t, denoted by N(t), and is sub divided into mutually exclusive compartments of healthy individuals H(t); susceptible individuals to diabetes, S(t); individuals with diabetes, D(t); and individuals with diabetes who are either receiving treatment or managed, using medicine or herbs, disciplined eating habit, exercises and other chiropractic approaches, M(t).

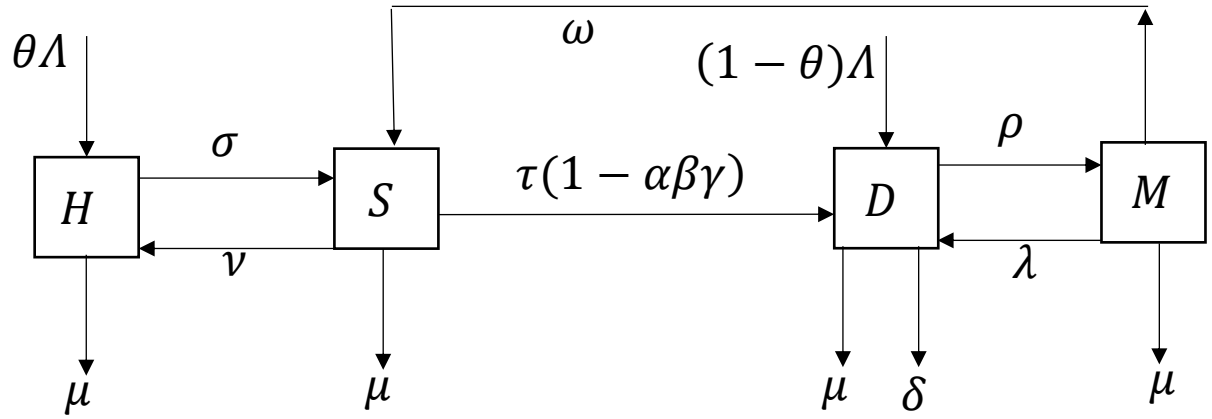


Figure I: Flow Diagram of the Model

2.2 The Mathematical Model

$$\left(\begin{array}{c} \dot{H} = \theta\Lambda - (\mu+\sigma)H + \nu S \\ \dot{S} = \sigma H - [\tau(1-\alpha\beta\gamma) + \nu + \mu)]\mathrm{S} + \omega M \\ \dot{D} = (1-\theta)\Lambda + \tau(1-\alpha\beta\gamma)S - (\lambda+\mu+\delta)D + \rho M \\ \dot{M} = \lambda D - (\omega+\rho+\mu)M \end{array}\right] \quad (1)$$

Table 1: Parameters and their meanings

Parameters	Description
Λ	Birth rate of human being
θ	Proportion of birth into the healthy compartment
$1-\theta$	Proportion of birth into the diabetes compartment
σ	Rate at which healthy individuals become susceptible to diabetes
τ	Rate of incidence of diabetes from susceptible to diabetes compartment
α	Public campaign that enhanced diabetes awareness
β	Control parameter due to regular exercise and other chiropractic activities
γ	Control parameter due to consistent and disciplined eating habit, i.e. herbal medicinal food (Organic)
λ	Rate at which neonatal and gestational diabetes are being moved for treatment
ν	Rate at which susceptible individuals move to the healthy compartment
μ	Natural mortality rate of human beings
δ	Mortality rate due to diabetes
ω	Rate at which transient and gestational diabetes move to susceptible compartment
ρ	Rate at which managed diabetes move back to diabetes compartment

Table 2: State Variables and their meanings

Variables	**Description**
H	Healthy compartment
S	Susceptible compartment
D	Diabetes compartment
M	Treatment/Managed Diabetes compartment
N	Total human population

Theorem1: Consider the feasible region, $\Sigma = \left\{ H, S, D, M \in R_+^4 : 0 \le N \le \frac{\Lambda}{\mu} \right\}$, Σ is a positively invariant set and a global attractor of the model

Let $H_0 \ge 0, S_0 \ge 0, D_0 \ge 0, M_0 \ge 0.$ and $H_0 + S_0 + D_0 + M_0 = N_0,$ then there exist solutions, H(t), S(t), D(t) and M(t) for the dynamical system (1) with the initial data H_0, S_0, D_0 and M_0 at time t = 0, that are defined for all $t \ge 0$. Adding the four equations of the model (1) and applying the standard comparison theorem [22] we have,

$$\frac{dN}{dt} \le \Lambda - \mu N \tag{2}$$

Applying integrating factor to equation (2) gives

$$N(t) \le \frac{\Lambda}{\mu} + [N(0) - \frac{\Lambda}{\mu}]e^{-\mu t} \tag{3}$$

In particular, $N(0) \le \frac{\Lambda}{\mu}$ implies $N(t) \le \frac{\Lambda}{\mu}$. Hence Σ is positively invariant and an attractor, so that no solution path leaves through any boundary of Σ.

Lemma 1: The region Σ is positively invariant for the system (1) and if $D_0 > 0,$ then $H_0 > 0, S > 0, M > 0$ for all time t, greater than zero and M is bounded by $\dot{M} = \max\left\{ M_0, \frac{\lambda}{\omega + \rho + \mu} \right\}$

The feasible region, Σ is positively invariant and the state variables are nonnegative, Solution of the model exists and unique.

Proof:

The right hand side of the system (1) is continuously differentiable and hence it is locally Lipschitz and therefore, there exist a unique solution H(t), S(t), D(t), M(t) to the system (1) with the initial data H_0, S_0, D_0, M_0 that is defined on a maximum forward interval of existence, [23]. Suppose that the initial condition is positive, $H_0 > 0$, $S_0 > 0$, $D_0 > 0$, $M_0 > 0$. We assumed by contradiction as it was in [24], that the state variables of the system (1) are positive if we suppose that there exists first time, t_1: $H(t_1) = 0$ and $H(t) > 0$, $S(t) > 0$, $D(t) > 0$, $M(t) > 0$, $0 < t < t_1$ or there exists t_2: $S(t_2) = 0$ and $H(t) > 0$, $S(t) > 0$, $D(t) > 0$, $M(t) > 0$, $0 < t < t_2$ or t_3: $D(t_3) = 0$ and $H(t) > 0$, $S(t) > 0$, $D(t) > 0$, $M(t) > 0$, $0 < t < t_3$ or t_4 : $M(t) = 0$ and $H(t) > 0$, $S(t) > 0$, $D(t) > 0$, $M(t) > 0$, $0 < t < t_4$. If $H(t_1) = 0$, $\Rightarrow \frac{dH(t_1)}{dt} = \lim_{t \to t_1} \frac{H(t_1) - H(t)}{t_1 - t} < 0$. Similarly $\frac{dS(t_1)}{dt} < 0, \frac{dD(t_1)}{dt} < 0, \frac{dM(t_1)}{dt} < 0$. Putting $H(t_1) = 0$ in the first equation of the system (1) implies $\frac{dH(t_1)}{dt} = \theta\Lambda + \nu S > 0$ which contradict our assumption. This implies that $H(t_1) \neq 0$, and H(t) will remain positive for all t, Similarly, S(t), D(t), M(t) are shown to be positive for all t.

To show that M is bounded by $\dot{M} = \max\{M_0, \frac{\lambda}{\omega + \rho + \mu}\}$ we need to show that $M \leq \xi$ for $t \geq 0$ and that $\xi \geq \frac{\lambda}{k_4}$ if $M_0 \leq \xi$. Suppose that the above inequalities do not hold, then there exist a time t_1 with $M''(t_1) > 0$ and $M'(t) > \xi$. Using the fourth equation for M in the system (1) gives $\frac{dM(t_1)}{dt} = \lambda D(t_1) - k_4 M(t_1) \leq \lambda(D(t_1) - 1) < 0.$ Since $(D(t_1) - 1) < 0$ and $\lambda > 0$ $\Rightarrow$ contradiction, therefore $\Rightarrow M(t) < \xi$ for all $t \geq 0.$ Suppose that $M(0) > \xi \geq \frac{\lambda}{k_4}.$ To show that $M(t) \leq M(0)$ for all $t \geq 0.$ We assume if there exists a time $t_2 > 0$ then $M(t_2) \geq M(0)$ and $M'(t_2) > 0$. However, since $M(t_2) > \frac{\lambda}{k_4}$ $\frac{dM(t_1)}{dt} = \lambda D(t_1) - k_4 M(t_1) \leq \lambda(D(t_1) - 1) \leq 0. \Rightarrow$ contradiction, because $M'(t_2) > 0$.

Therefore, M(t) is bounded from above by $\dot{M}$ that is $\dot{M} = \max\{M_0, \frac{\lambda}{k_4}\}$. Therefore, the model is epidemiologically meaningful and mathematically well posed, that is the model is suitable for analysis [25] ■

2.3 Equilibrium point of the model

Model (1) implies

$$\begin{bmatrix} \dot{H} = \theta\Lambda - k_1 H + \nu S \\ \dot{S} = \sigma H - k_2 \mathrm{S} + \omega M \\ \dot{D} = (1-\theta)\Lambda + k_0 S - k_3 D + \rho M \\ \dot{M} = \lambda D - k_4 M \end{bmatrix} \tag{4}$$

At the equilibrium point,

$$\dot{H} = \dot{S} = \dot{D} = \dot{M} = 0 \tag{5}$$

Equation (5) implies the endemic equilibrium point of the system (4)

$$\varepsilon_E = \begin{bmatrix} H^{\square} = \dfrac{\begin{pmatrix} k_4\theta\Lambda(k_1k_2-\nu\sigma)[(k_1k_2-\nu\sigma)(k_4-\lambda\rho)-k_1\lambda\tau(1-\alpha\beta\gamma)+ \\ \nu\{k_4\theta\sigma\Lambda[(k_1k_2-\nu\sigma)(k_4-\lambda\rho)-k_1\lambda\tau(1-\alpha\beta\gamma)]+ \\ k_1k_4\lambda[\theta\Lambda\sigma\tau(1-\alpha\beta\gamma)+(k_1k_2-\nu\sigma)(1-\theta)\Lambda]\} \end{pmatrix}}{k_1k_4(k_1k_2-\nu\sigma)[(k_1k_2-\nu\sigma)(k_4-\lambda\rho)-k_1\lambda\tau(1-\alpha\beta\gamma)]} \\ S^{\square} = \dfrac{\begin{matrix} k_4\theta\sigma\Lambda[(k_1k_2-\nu\sigma)(k_4-\lambda\rho)-k_1\lambda\tau(1-\alpha\beta\gamma)]+ \\ k_1k_4\lambda[\theta\Lambda\sigma\tau(1-\alpha\beta\gamma)+(k_1k_2-\nu\sigma)(1-\theta)\Lambda] \end{matrix}}{k_4(k_1k_2-\nu\sigma)[(k_1k_2-\nu\sigma)(k_4-\lambda\rho)-k_1\lambda\tau(1-\alpha\beta\gamma)]} \\ D^{\square} = \dfrac{k_4[\theta\sigma\Lambda\tau(1-\alpha\beta\gamma)+(k_1k_2-\nu\sigma)(1-\theta)\Lambda]}{(k_1k_2-\nu\sigma)(k_4-\lambda\rho)-k_1\lambda\tau(1-\alpha\beta\gamma)} \\ M^{\square} = \dfrac{\lambda[\theta\sigma\Lambda\tau(1-\alpha\beta\gamma)+(k_1k_2-\nu\sigma)(1-\theta)\Lambda]}{(k_1k_2-\nu\sigma)(k_4-\lambda\rho)-k_1\lambda\tau(1-\alpha\beta\gamma)} \end{bmatrix} \tag{6}$$

2.4 Model Solution, Using Homotopy Perturbation Method (HPM)

To use HPM, as it was in [26-28] the model (4) implies

$$\begin{pmatrix} \dot{H} + k_1 H - \nu S - \theta\Lambda &= 0 \\ \dot{S} - \sigma H + k_2 S + \omega M &= 0 \\ \dot{D} - \tau(1-\alpha\beta\gamma)S + k_3 D - (1-\theta)\Lambda + \rho M &= 0 \\ \dot{M} - \lambda D + k_4 M &= 0 \end{pmatrix} \tag{7}$$

With the initial conditions: $H(0) = H_0, S(0) = S_0, D(0) = D_0, M(0) = M_0$

Let

$$\begin{pmatrix} H(t) &= n_0 + pn_1 + p^2 n_2 + ... \\ S(t) &= x_0 + px_1 + p^2 x_2 + ... \\ D(t) &= y_0 + py_1 + p^2 y_2 + ... \\ M(t) &= z_0 + pz_1 + p^2 z_2 + ... \end{pmatrix} \quad (8)$$

Applying HPM to the first equation of the system (7) gives $(1-p)\dot{H} + p(\dot{H} + k_1 H - \nu S - \theta\Lambda) = 0$

$$\Rightarrow \dot{H} + pk_1 H - p\nu S - p\theta\Lambda = 0 \quad (9)$$

Substitute the first two equations in the system (8) into the equation (9), simplifying and then collecting the coefficients of power of p, gives

$$\begin{bmatrix} p^0 &\Rightarrow & n_0' &= 0 \\ p^1 &\Rightarrow & n_1' + k_1 n_0 - \nu x_0 - \theta\Lambda &= 0 \\ p^2 &\Rightarrow & n_2' + k_1 n_1 - \nu x_1 &= 0 \end{bmatrix} \quad (10)$$

Similarly applying HPM to second, third and the fourth equations of the system (7), give the system (11), (12) and (13)

$$\begin{bmatrix} p^0 &\Rightarrow & x_0' &= 0 \\ p^1 &\Rightarrow & x_1' - \sigma n_0 + k_2 x_0 + \omega z_0 &= 0 \\ p^2 &\Rightarrow & x_2' - \sigma n_1 + k_2 x_1 + \omega z_1 &= 0 \end{bmatrix} \quad (11)$$

$$\begin{bmatrix} p^0 &\Rightarrow & y_0' &= 0 \\ p^1 &\Rightarrow & y_1' - \tau(1-\alpha\beta\gamma)x_0 + k_3 y_0 + \rho z_0 - (1-\theta)\Lambda &= 0 \\ p^2 &\Rightarrow & y_2' - \tau(1-\alpha\beta\gamma)x_1 + k_3 y_1 + \rho z_1 &= 0 \end{bmatrix} \quad (12)$$

$$\begin{bmatrix} p^0 &\Rightarrow & z_0' &= 0 \\ p^1 &\Rightarrow & z_1' - \lambda y_0 + k_4 z_0 &= 0 \\ p^2 &\Rightarrow & z_2' - \lambda y_1 + k_4 z_1 &= 0 \end{bmatrix} \quad (13)$$

Solving the first equations of the system (11) – (13) $\Rightarrow$

$$n_0 = H_0, \quad x_0 = S_0, \quad y_0 = D_0, \quad z_0 = M_0 \quad (14)$$

Substitute (14) into the second equations of the system (10) – (13) then integrate $\Rightarrow$

$$\begin{pmatrix} n_1 &= & (\nu S_0 + \theta\Lambda - k_1 H_0)t \\ x_1 &= & (\sigma H_0 - k_2 S_2 + \omega M_0)t \\ y_1 &= & (\tau(1-\alpha\beta\gamma)S_0 - k_3 D_0 - \rho M_0 + (1-\theta)\Lambda)t \\ z_1 &= & (\lambda D_0 - k_4 M_0)t \end{pmatrix} \quad (15)$$

Substitute (15) into the third equations of the system (10) – (13) then integrate $\Rightarrow$

$$\left(\begin{array}{rcl} n_2 &=& [\nu(\sigma H_0 - k_2 S_0 + \omega M_0) - k_1(\nu S_0 + \theta\Lambda - k_1 H_0)]\frac{t^2}{2} + \ldots \\ x_2 &=& [\sigma(\nu S_0 + \theta\Lambda - k_1 H_0) - k_2(\sigma H_0 - k_2 S_0 + \omega M_0) - \omega(\lambda D_0 - k_4 M_0)]\frac{t^2}{2} + \ldots \\ y_2 &=& \{\tau(1-\alpha\beta\gamma)(\sigma H_0 - k_2 S_2 + \omega M_0) - k_3[\tau(1-\alpha\beta\gamma)S_0 - k_3 D_0 - \rho M_0 + (1-\theta)\Lambda)] - \rho(\lambda D_0 - k_4 M_0)\}\frac{t^2}{2} + \ldots \\ z_2 &=& \lambda[\tau(1-\alpha\beta\gamma)S_0 - k_3 D_0 - \rho M_0 + (1-\theta)\Lambda] - k_4(\lambda D_0 - k_4 M_0)\}\frac{t^2}{2} + \ldots \end{array}\right) \quad (16)$$

Substitute for $n_0, n_1, n_2, x_0, x_1, x_2, y_0, y_1, y_2, z_0, z_1, z_2$ in the system (8) and the then let $p \to 1$ we therefore obtain the model solution as given in the system (17)

$$\left(\begin{array}{rl} H(t) = & H_0 + (\nu S_0 + \theta\Lambda - k_1 H_0)t + [\nu(\sigma H_0 - k_2 S_0 + \omega M_0) - \\ & k_1(\nu S_0 + \theta\Lambda - k_1 H_0]\frac{t^2}{2} + \ldots \\ S(t) = & S_0 + (\sigma H_0 - k_2 S_0 + \omega M_0)t + [\sigma(\nu S_0 + \theta\Lambda - k_1 H_0) - \\ & k_2(\sigma H_0 - k_2 S_0 + \omega M_0) - \omega(\lambda D_0 - k_1 M_0)]\frac{t^2}{2} + \ldots \\ D(t) = & D_0 + \big(\tau(1-\alpha\beta\gamma)\big)S_0 - k_3 D_0 - \rho M_0 + (1-\theta)\Lambda)t + \\ & \{\big(\tau(1-\alpha\beta\gamma)\big)(\sigma H_0 - k_2 S_0 + \omega M_0 - k_3[\big(\tau(1-\alpha\beta\gamma)\big)S_0 - \\ & k_3 D_0 - \rho M_0 + (1-\theta)\Lambda - \rho(\lambda D_0 - k_4 M_0\}\frac{t^2}{2} + \ldots \\ M(t) = & M_0 + (\lambda D_0 - k_4 M_0)t + \{\lambda[\tau(1-\alpha\beta\gamma)S_0 - k_3 D_0 - \\ & \rho M_0 + (1-\theta)\Lambda] - k_4(\lambda D_0 - k_4 M_0)\}\frac{t^2}{2} + \ldots \end{array}\right) \quad (17)$$

3 Local stability of the endemic equilibrium point

Lemma 2: The model (4) has a unique endemic equilibrium whenever $\tau > 0$

Theorem 2: Consider the model (4). The associated unique endemic equilibrium of the model (4) denoted by ε_E is Locally Asymptotically Stable (LAS) if all the eigenvalues of the characteristic equation associated with the linearized System (4) have negative real parts.

Proof: Model (1) $\Rightarrow \frac{dN}{dt} = \Lambda - (\mu + \delta)N$, so that $N \to \frac{\Lambda}{\mu + \delta} = N^{\square}$ as $t \to \infty$, hence, using substitution

$H = N^{\square} - S - D - M$, model (1) can be re-written as

$$\left(\begin{array}{c} \dot{S} = \sigma\left(N^{\square} - S - D - M\right) - [\tau(1-\alpha\beta\gamma) + \nu + \mu)]\mathrm{S} + \omega M \\ \dot{D} = (1-\theta)\Lambda + \tau(1-\alpha\beta\gamma)S - (\lambda + \mu + \delta)D + \rho M \\ \dot{M} = \lambda D - (\omega + \rho + \mu)M \end{array}\right) \quad (18)$$

Linearizing system (8) gives

$$\left(\begin{array}{c} \dot{S} = \{\sigma x - [\tau(1-\alpha\beta\gamma) + \nu + \mu)]\}\mathrm{S} + xD + (x+\omega)M \\ \dot{D} = (1-\theta)\Lambda + \tau(1-\alpha\beta\gamma)S - (\lambda + \mu + \delta)D + \rho M \\ \dot{M} = \lambda D - (\omega + \rho + \mu)M \end{array}\right) \quad (19)$$

The Jacobian of the system (19) evaluated at ε_E is given as

$$\left(\begin{array}{ccc} \{\sigma x - [\tau(1-\alpha\beta\gamma) + \nu + \mu)]\} & x & (x+\omega) \\ \tau(1-\alpha\beta\gamma) & -(\lambda + \mu + \delta) & \rho \\ 0 & \lambda & -(\omega + \rho + \mu) \end{array}\right) \quad (20)$$

The proof of Theorem 2 is based on using a Krasnoselskii sublinearity trick (see, for instance, [29-31]. It entails showing that the system (19), $z'(t) = Mf(\bar{x})z$ has solution of the form

$$z(t) = z_0 e^{\omega_1 t} \quad (21)$$

with $z_0 \in C \setminus \{0\}, z_0 = (z_1, z_2, z_3), z_i \in C, \omega_1 \in C,$ and $\mathrm{Re}(\omega_1) < 0$ where C denotes complex numbers. Substituting a solution of the form (21) into the system (19) gives

$$\left(\begin{array}{c} \omega_1 z_1 = \{\sigma x - [\tau(1-\alpha\beta\gamma) + \nu + \mu)]\}z_1 + xz_2 + (x+\omega)z_3 \\ \omega_1 z_2 = (1-\theta)\Lambda + \tau(1-\alpha\beta\gamma)z_1 - (\lambda + \mu + \delta)z_2 + \rho z_3 \\ z_3 = \lambda z_2 - (\omega + \rho + \mu)z_3 \end{array}\right) \quad (22)$$

System (22) becomes

$$\left(\begin{array}{c} (1+\frac{\omega_1}{k_2})z_1 = \frac{\sigma H^{\square}}{k_2} z_1 + \frac{H^{\square}}{k_2} z_2 + \frac{(H^{\square} + \omega)}{k_2} z_3 \\ (1+\frac{\omega_1}{k_3})z_2 = \frac{(1-\theta)\Lambda}{k_3} + \frac{k_0}{k_3} z_1 + \frac{\rho}{k_3} z_3 \\ (1+\frac{\omega_1}{k_4})z_3 = \frac{\lambda}{k_4} z_2 \end{array}\right) \quad (23)$$

The simplification of results in

$$\begin{pmatrix} [1+F_1(\omega_1)] & = & (Mz)_1 \\ [1+F_2(\omega_2)] & = & (Mz)_2 \\ [1+F_2(\omega_3)] & = & (Mz)_3 \end{pmatrix} \tag{24}$$

with

$$M = \begin{pmatrix} \frac{\sigma H^{\square}}{k_2} & \frac{k_0 k_3 (k_4+\omega_1)}{k_4(1+\omega_1)(k_4+\omega_1)-\lambda\rho} & \frac{k_0 k_3}{k_4(1+\omega_1)(k_4+\omega_1)-\lambda\rho} \\ \frac{k_0}{k_3} & 0 & 0 \\ 0 & \frac{\lambda}{k_4} & 0 \end{pmatrix} \tag{25}$$

The equilibrium $\varepsilon_E = \{S^{\square}, D^{\square}, M^{\square}\} \Rightarrow \varepsilon_E = M\varepsilon_E$, where the matrix M has non-negative entries. It should be mentioned that, $(Mz)_i$, with i = 1, 2, 3 denotes the i^{th} coordinates of the vector Mz. If z is a solution of (21), such that [29- 31] and which is in the form $[1+F_i(\omega)] = (Mz)_i$ for $i = 1,2,3$ then it is possible to find a minimum positive real number, s, such that

$$\|z\| \le s\varepsilon_E \tag{26}$$

where, $\|z\| = (\|z_1\|, \|z_2\|, \|z_3\|)$ $\|.\|$ is a norm in C. Our mission is to show that $\mathrm{Re}(\omega) < 0$. Suppose by contradiction that, $\mathrm{Re}(\omega) \ge 0$, then there are $\omega = 0$ and $\omega \ne 0$ for consideration.

Case 1, $\omega = 0$ is not applicable to the model (4) because there is no disease free. The determinant of this system is given by

$$\Delta = -K_2 \cdot -K_3 \cdot -K_4 < 0 \tag{27}$$

Since determinant Δ is negative, it implies that the system (4) has a unique solution.

Case 2, $\omega \neq 0$

By assumption if $\mathrm{Re}(\omega) > 0$ then $[1+F_i(\omega)] > 1$ for $i = 1,2,3$ If $F(\omega) = \min_i[1+F_i(\omega)]$ then

$F(\omega) > 1 \Rightarrow \frac{s}{F(\omega)} < s.$ Since, s is the minimum positive real number such that $\|z\| \leq s\varepsilon_E$, then

$$\|z\| > \frac{s}{F(\omega)}\varepsilon_E \qquad (28)$$

Taking the norm of both sides of the second equation in (24) implies

$$F(\omega)\|z_2\| \leq \|1+F_2(\omega)\|\|z_2\| = \|(Mz)_2\| \leq M\|z_2\| \leq sM(\varepsilon_E)_2 = s(\varepsilon_E)_2 = s(D^{\square}) \qquad (29)$$

(29) implies, $\|z_2\| \leq \frac{s}{F(\omega)}(D^{\square})$ which contradicts (28). Hence, $\mathrm{Re}(\omega_1) < 0$ Thus, all eigenvalues of the characteristic equations associated with the linearized system (19) have negative real parts so that the unique endemic equilibrium (ε_E) point is locally asymptomatically stable whenever $\tau > 0$

3.1 Global Stability Analysis (GAS) of the Endemic Equilibrium Point

To determine GAS, as it was in [32] and applied quantitatively in [26] we obtain the Lyapunov Equation (quadratic Lyapunov function) of the system (4) as $A^TP + PA = -Q \Rightarrow A^TP + PA = -I$ if Q = I from the model (7), where

$$P = \begin{pmatrix} P_{11} & P_{12} & P_{13} & P_{14} \\ P_{21} & P_{22} & P_{23} & P_{24} \\ P_{31} & P_{32} & P_{33} & P_{34} \\ P_{41} & P_{42} & P_{43} & P_{44} \end{pmatrix}, \text{ and } Q = \begin{pmatrix} 1 & 0 & 0 & 0 \\ 0 & 1 & 0 & 0 \\ 0 & 0 & 1 & 0 \\ 0 & 0 & 0 & 1 \end{pmatrix}$$

Then the Jacobian matrix of the system (4) is

$$A=\begin{pmatrix} -k_1 & \nu & 0 & 0 \\ \sigma & -k_2 & 0 & \omega \\ 0 & k_0 & -k_3 & \rho \\ 0 & 0 & \lambda & -k_4 \end{pmatrix} \Rightarrow A^T=\begin{pmatrix} -k_1 & \sigma & 0 & 0 \\ \nu & -k_2 & k_0 & 0 \\ 0 & 0 & -k_3 & \lambda \\ 0 & \omega & \rho & -k_4 \end{pmatrix}$$

To determine the variables in the matrix P, we assumed, $\begin{pmatrix} a=k_1+k_2 & b=k_1+k_3 & c=k_1+k_4 \\ d=k_2+k_3 & e=k_2+k_4 & f=k_3+k_4 \end{pmatrix}$.
From the Lyapunov equation we derived the system (30) in order obtain the entries of the matrix P.

$$\begin{pmatrix} 2k_1P_{11}+\sigma P_{12}+\sigma P_{21} &=& -1 \\ \nu P_{11}-aP_{12}-k_0P_{13}+\sigma P_{22} &=& 0 \\ -bP_{13}+\lambda P_{14}+\sigma P_{23} &=& 0 \\ -cP_{14}+\omega P_{12}+\rho P_{13}+\sigma P_{24} &=& 0 \\ \nu P_{11}-aP_{21}+\sigma P_{22}+k_0P_{31} &=& 0 \\ \nu P_{12}-2k_2P_{22}-k_0P_{23}+k_0P_{32}+\nu P_{21} &=& -1 \\ \nu P_{13}-dP_{23}+\lambda P_{24}+k_0P_{33} &=& 0 \\ \nu P_{14}+\omega P_{22}+\rho P_{23}-eP_{24}+k_0P_{34} &=& 0 \\ -bP_{31}+\sigma P_{32}+\lambda P_{41} &=& 0 \\ \nu P_{31}-dP_{32}-k_0P_{33}+\lambda P_{22} &=& 0 \\ 2k_3P_{33}+\lambda P_{34}+\lambda P_{43} &=& -1 \\ \omega P_{32}+\rho P_{33}-fP_{34}+\lambda P_{44} &=& 0 \\ \omega P_{21}+\rho P_{31}-cP_{41}+\sigma P_{42} &=& 0 \\ \omega P_{22}+\rho P_{32}+\nu P_{41}-eP_{42}-k_0P_{43} &=& 0 \\ \omega P_{23}+\rho P_{33}-fP_{43}+\lambda P_{44} &=& 0 \\ \omega P_{24}+\rho P_{34}+\omega P_{42}+\rho P_{43}-2k_4P_{44} &=& -1 \end{pmatrix} \quad (30)$$

Solving the System (30), we obtained a diagonal matrix in which the diagonal entries are positive and all other entries are zeros. $P_{11}=\frac{1}{2k_1}>0, P_{22}=\frac{X}{Y}>0, P_{33}=\frac{1}{2k_3}>0, P_{44}=\frac{q}{(L+M+H)}>0$

$$X=k_1(2ak_1-\sigma\nu)[k_1(\sigma\nu-2ak_1)^2-2(a\nu\sigma)^2][(\sigma\nu-2ak_1)\nu+2ak_0][k_1(\sigma\nu-2ak_1)-a\nu\sigma]$$

$$Y=4a\sigma[k_1(\sigma\nu-2ak_1)-a\nu\sigma][k_2(\sigma\nu-2ak_1)+a\sigma\nu][(\sigma\nu-2ak_1)\nu+2ak_0][k_1(\sigma\nu-2ak_1)-a\nu\sigma]$$

$$\text{Matrix } P=\begin{pmatrix} P_{11} & P_{12} & P_{13} & P_{14} \\ P_{21} & P_{22} & P_{23} & P_{24} \\ P_{31} & P_{32} & P_{33} & P_{34} \\ P_{41} & P_{42} & P_{43} & P_{44} \end{pmatrix} \text{ becomes } P=\begin{pmatrix} P_{11} & 0 & 0 & 0 \\ 0 & P_{22} & 0 & 0 \\ 0 & 0 & P_{33} & 0 \\ 0 & 0 & 0 & P_{44} \end{pmatrix}$$

$$\Delta_1 = P_{11} > 0, \Delta_2 = \begin{vmatrix} P_{11} & 0 \\ 0 & P_{22} \end{vmatrix} > 0, \ \Delta_3 = \begin{vmatrix} P_{11} & 0 & 0 \\ 0 & P_{22} & 0 \\ 0 & 0 & P_{33} \end{vmatrix} > 0 \text{ and } \Delta_4 = \begin{vmatrix} P_{11} & 0 & 0 & 0 \\ 0 & P_{22} & 0 & 0 \\ 0 & 0 & P_{33} & 0 \\ 0 & 0 & 0 & P_{44} \end{vmatrix} > 0$$

P is positive definite matrix which therefore implies that EEP is Globally Asymptotically Stable

3.2 Variables and estimation of parameter values

Variables and Parameters values are obtained based on Nigeria Population, with their respective sources, stated in the Table 3 and 4 respectively.

Table 3: Values of Variables and the Sources

S N	Variables	Value	Source
1	H(0)	41,634,136	Estimated based on number [5, 6, 13]
2	S(0)	31,688,476	Estimated based on [5, 6, 13]
3	D(0)	96,812,400	[5, 6, 13]
4	M(0)	48,406,200	50% of D (0), based on [5, 6, 13]
5	N(0)	218,541,212	[5, 6, 13]

Table 4: Values of Parameters and the Sources

S N	Variables	Value	Source
1	τ	0.043	[6]
2	Λ	0.036	[17]
3	θ	0.999	[14]
4	1-θ	0.001	[14]

5	μ	0.009	[17]
6	ν	0.55	[33]
7	σ	0.101	[34]
8	α	0.95	Suggestion
9	β	0.95	Suggestion
10	γ	0.95	Suggestion
11	ω	0.8	[9]
12	λ	0.338	[35]
13	δ	0.316	Estimated based on type 1, 2 & gest.
14	ρ	0.20	[9]

3.3 Numerical Solution of the Model

Considering the four level of controls in the model solution (17), the numerical solution of the model solution is obtained as shown in (31) – (18)

$$\begin{pmatrix} \alpha=\beta=\gamma=0.00 \Rightarrow & H(t)=41,634,136+12,837,906.9t+2,486,737.6t^2+\ldots \\ \alpha=\beta=\gamma=0.25 \Rightarrow & H(t)=41,634,136+12,848,906.9t+3,952,592.4t^2+\ldots \\ \alpha=\beta=\gamma=0.95 \Rightarrow & H(t)=41,634,136+12,848,906.9t+5,693,301.4t^2+\ldots \\ \alpha=\beta=\gamma=1.00 \Rightarrow & H(t)=41,634,136+12,848,906.9t+6,225,669.6t^2+\ldots \end{pmatrix} \quad (31)$$

$$\begin{pmatrix} \alpha=\beta=\gamma=0.00 \Rightarrow & S(t)=31,688,476+11,609,885.0t-16,390,245.4t^2+\ldots \\ \alpha=\beta=\gamma=0.25 \Rightarrow & S(t)=31,688,476+11,803,051.5t-13,915,475t^2+\ldots \\ \alpha=\beta=\gamma=0.95 \Rightarrow & S(t)=31,688,476+23,272,695.4t-17,527,478.4t^2+\ldots \\ \alpha=\beta=\gamma=1.00 \Rightarrow & S(t)=31,688,476+25,216,1t-15,007,565.2t^2+\ldots \end{pmatrix} \quad (32)$$

$$\begin{pmatrix} \alpha=\beta=\gamma=0.00 \Rightarrow & D=96,812,400-60,241,816.5t+43,610,202.0t^2+\ldots \\ \alpha=\beta=\gamma=0.25 \Rightarrow & D=96,812,400-42,740,905.0t+21,969,634.9t^2+\ldots \\ \alpha=\beta=\gamma=0.95 \Rightarrow & D=96,812,400-71,924,407.0t+26,303,901.6t^2+\ldots \\ \alpha=\beta=\gamma=1.00 \Rightarrow & D=96,812,400-73,867,861.0t+26,099,122.5t^2+\ldots \end{pmatrix} \quad (33)$$

$$\begin{pmatrix} \alpha=\beta=\gamma=0.00 \Rightarrow & M(t)=48,406,200-16,119,264.6t+9,160,893.9t^2+\ldots \\ \alpha=\beta=\gamma=0.25 \Rightarrow & M(t)=48,406,200-16,119,264.6t-2,084,398.1t^2+\ldots \\ \alpha=\beta=\gamma=0.95 \Rightarrow & M(t)=48,406,200-16,119,264.6t-4,022,789.6t^2+\ldots \\ \alpha=\beta=\gamma=1.00 \Rightarrow & M(t)=48,406,200-16,119,264.6t-4,359,446.4t^2+\ldots \end{pmatrix} \quad (34)$$

$$\begin{pmatrix} D(1)=49,043,660.4+33,791,821.1\tau-15,844,238\tau^2 \\ D(2)=49,043,225.7+41,106,829.5\tau-15,353,129.7\tau^2 \\ D(3)=48,455,574.+4,810,325.9\tau-322,271.8\tau^2 \\ D(4)=24,470,108.8 \end{pmatrix} \quad (35)$$

$$\begin{pmatrix} \varsigma=\alpha\beta\gamma \Rightarrow & H(t)=58,630,731.1+3,748,746.7\varsigma \\ \varsigma=\alpha\beta\gamma \Rightarrow & S(t)=61,612,246.7+50,859,283.5\varsigma-8,950,306.4\varsigma^2 \\ \varsigma=\alpha\beta\gamma \Rightarrow & D(t)=63,971,808.9-8,671,610.1\varsigma-2,931,184.0\varsigma^2 \\ \varsigma=\alpha\beta\gamma \Rightarrow & M(t)=32,881,948.7-5,859,199.2\varsigma \end{pmatrix} \quad (36)$$

3.4 Graphical Simulation of the Model Solution with four level of Controls

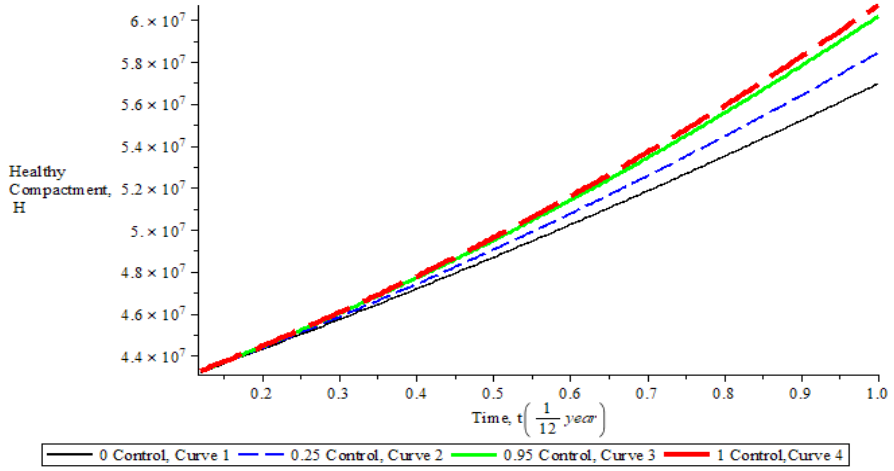


Figure 1: Effects of various controls on the Simulation of healthy Compartment

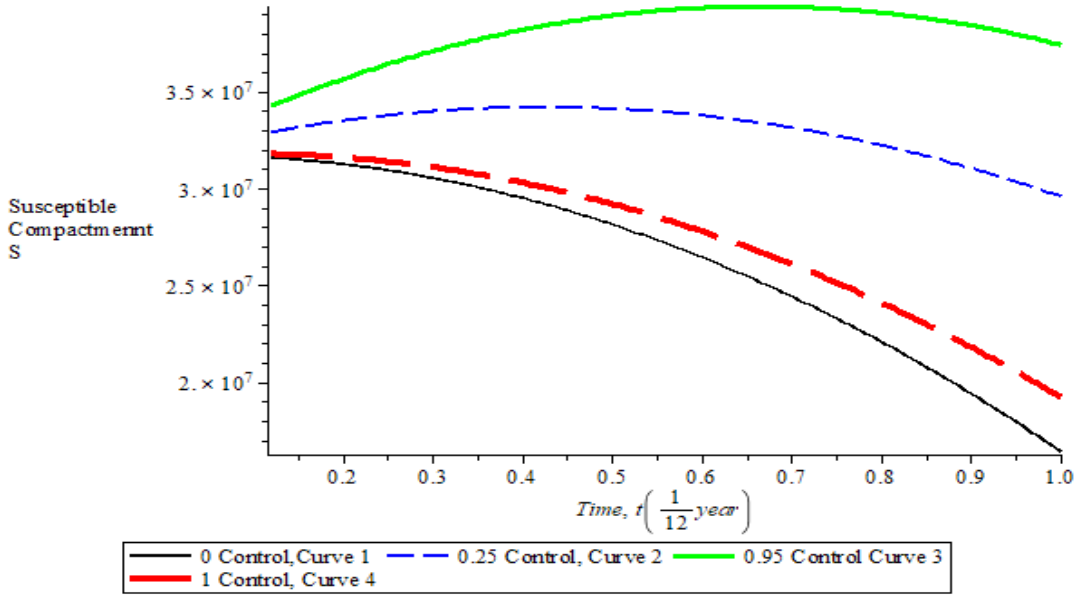


Figure 2: Effects of various controls on the Simulation of Susceptible Compartment

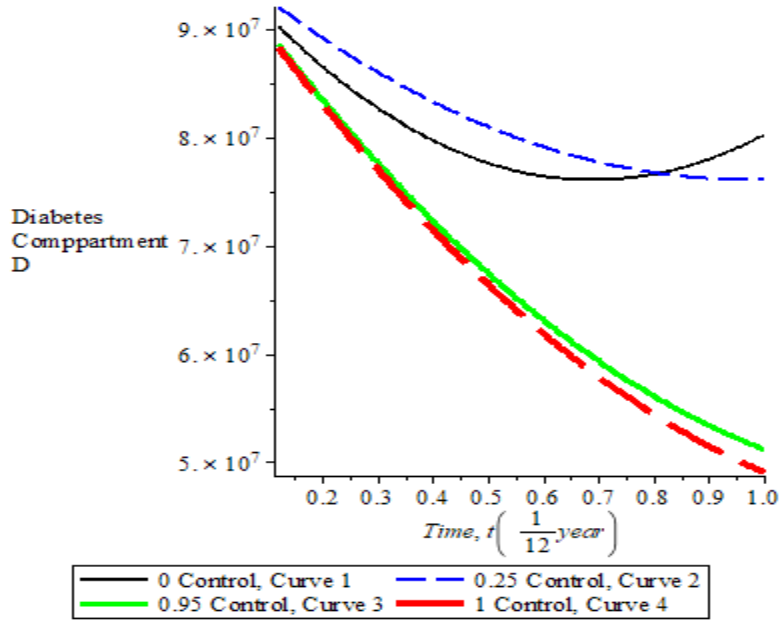


Figure 3: Effects of various controls on the Simulation of Diabetes Compartment

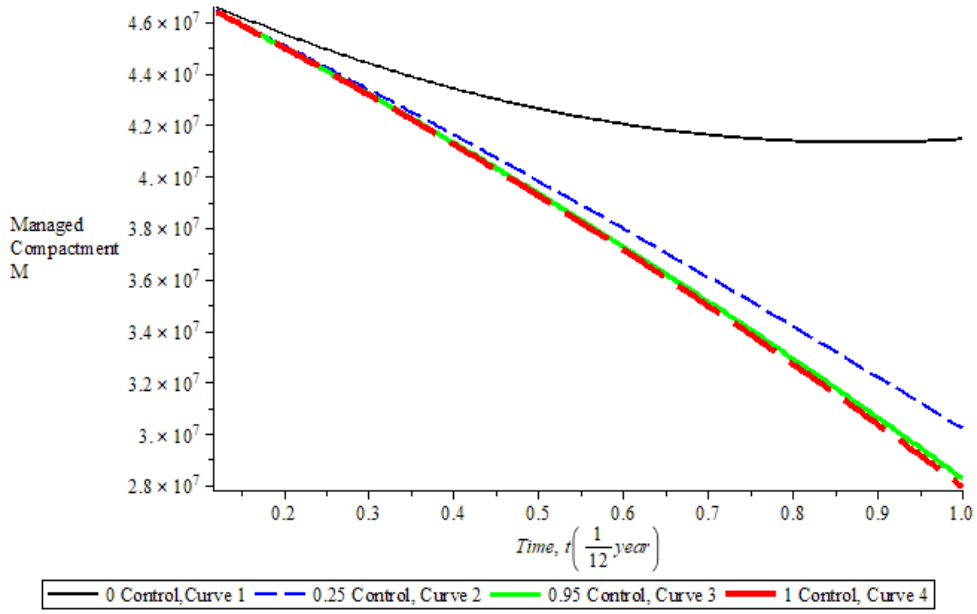


Figure 4: Effects of various controls on the Simulation of Managed Compartment

3.5 Sensitivity Analysis of the sensitive parameters

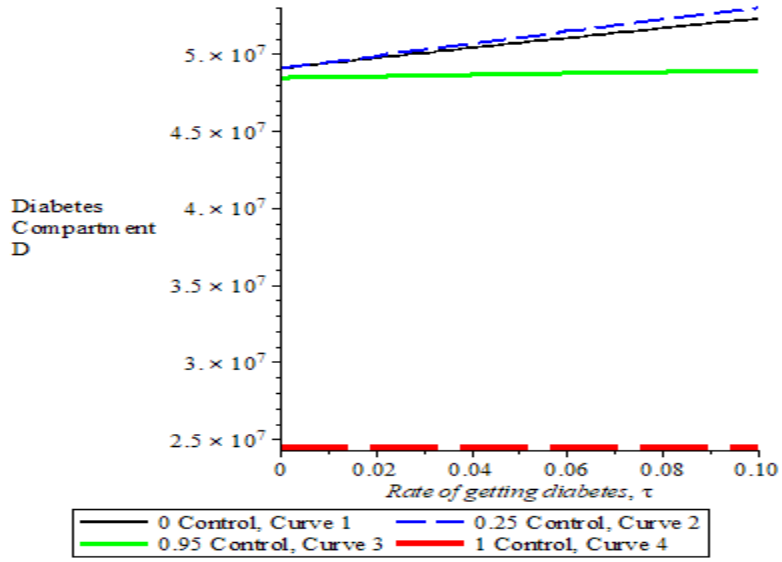


Figure 5: Effect of incidence of diabetes on the Diabetes Compartment

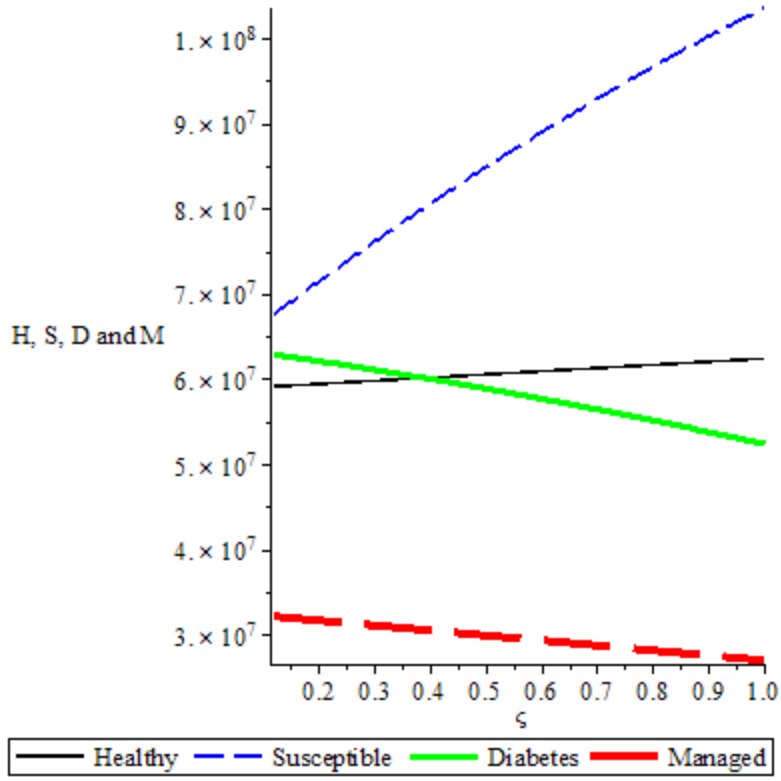


Figure 5: Effect of Control on the State Variables

4 Results and discussion

Equilibrium point of the formulated, mathematically, well posed model, indicates that Diabetes Mellitus has no disease free equilibrium (DFE) point, but endemic equilibrium point (EEP) and it is proved that the EEP is locally and globally asymptotically stable, that is (LAS and GAS). Graphical Simulation of the Numerical Solution of the healthy Compartment of the total population shows that the incorporated control parameters impacted positively on the healthy Compartment. The Numerical Simulation shows is directly impacted based on the sequence of the controls, that is, the positive effects are in accordance with the respective sizes of the controls. Level 0, no measure reflected the least population, while 0.25, 0.95 and 1.00 reflected positive effects proportional to their sizes; Therefore, the higher the control, the higher the size of the healthy compartment.

In the Simulation of the susceptible population, the effect of zero, 0, no measure, rapidly depleted the population, because of unhindered movement of susceptible individuals to the diabetes compartment. Impact of one, 1 control measure is faster than 0.25 and 0.95 control measures because of effect of public enlightenment campaign on the people. The higher the healthy population, the lower the susceptible population, as indicated in the figure 1 and 2. Based on the level of control and the initial value of the curve.

The Diabetes Mellitus population is positively impacted by 0.95 and 1.00 control measures, than 0.25 measure and no measure, by reducing the population of the compartment of diabetes, in proportion to the level of control.

The effects of control of measures on the managed compartment are positively impacted as 0.25, 0.95 and 1.00 reduce the respective population while the effect of no measure is negative, as the population is on the increase.

On the sensitivity analysis of the incidence of diabetes mellitus, no control measure, 0 and 0.25 show increasing trend on the population of the diabetes mellitus compartment.
The population of diabetes is kept constant with the control measure of 0.95 and 1 on the simulation of the diabetes population. The constant value in 0.95 is higher than the constant value in 1.00; this shows a perfect control will keep diabetes mellitus at bay.

5 Conclusion

Prevention, controlling and managing the rising trend of the associated complications of diabetes mellitus on human population; will be effectively checked if either control measure 0.95, $\alpha = \beta = \gamma = 0.95,$ or 1.00, $\alpha = \beta = \gamma = 1.00,$ is, adequately adopted; as incorporated in the Mathematical Model of the study; by Diabetes Patient or Health Personnel or Governmental Agencies or Nongovernmental Agencies; for type 1 diabetes or type 2 diabetes or gestational diabetes, if the advice from the study is strictly adhered.

5.1 Recommendation

Each of the three types of diabetes: type 1, type 2 and gestational diabetes can be uniquely studied mathematically.

6.0 Declarations:

6.1 Authors Contribution Statement

K. A. Adeyemo, T.A. Lawal, E. Philemon, I. A. Azeez, K.I. Falade, F. C Nwachukwu, A. Omame, N.O. Lasisi and P.O. Aye were all involved in the rigorous work of this study from conceiving the idea of the study, writing the abstract; introduction to the study; formulation of the model, solving the model equations, designing the analysis, collection of data, the results and discussion; and drawing the conclusion from the study.

6.2 Funding statement

The Authors, K.A. Adeyemo, T.A. Lawal; E. Philemon and I. A. Azeez were supported by Tertiary Education Trust Fund (TETFUND) for Institution Based Research (I. B.R)

6.3 Data availability statement

Data included in article/supplied materials are referenced in the article.

6.4 Declaration of interest statement

The authors declare no conflict of interest.

Acknowledgements
We sincerely appreciate Nigeria Police Academy and other Institutions involved in providing conducive academic environment for the pursuit of this research. The authors are grateful to the editor and the anonymous reviewers for their invaluable comments and constructive criticisms, which have improved the manuscript

References

[1] W.H.O. (2021) Definition of Diabetes
[2] Nansseru J. R. N., Ngo –Um S. S and Balti E. V. (2016) Incidence, prevalence and genetic determinants of neonatal diabetes mellitus: a systemic review and meta –analysis protocol, Systemic Review: Volume 5(188), 0369-0373, Doi: 10:1186/s13643.0369-3
[3] Shankar PR, Partha P, Shenoy N, Subish P, Vijay B, Dubey AK, Nepal. (2007) Knowledge and perceptions about diabetes in the community: a survey among individuals attending a diabetes-screening programme in pokhara city, western Nepal Pharm cology online, Manipal College of Medical Sciences Pokhara Volume 1: 148-161
[4] W. H. O. (2018) Diabetes, httpps://www.who.int/news-room/fact-sheet/detail/diabetes.
[5] W.H.O. (2014) Global Health Estimates: Death by cause, Age, Sex and Country, Geneva 2002-2012, www.who.org or www.idf.who.org
[6] https://www.wordometers.info>world-population>nigeria population
[7] Neelesh J., Sanjay and Sapna M. (2010) Anti diabetic potential of medicinal plants, Acta poloniae pharmaceutical-Drug Research, Volume 10(1): 113-118.
[8] Patel K. P., Joshi H. M., Majmuar F. D and Patel V. J. (2013) Newer Approaches in the treatment of diabetes mellitus. NHL Journal of medicinal Sciences, Volume 2(1): 6-11
[9] Wellness, Be well Boston, 2024
[10] Kumar V. K., Sharathnath P., Yogeswaran P., Harani A.,Sudhakar K., Sudha P., David B. (2010) Medicinal potency of Mamordica charantia, International of pharmaceutical Sciences, Review and Research. Volume 1(2):95-106
[11] Ekam V. S., Ebong P. E., Johnson J. T and Dasofunjo K. (2013) Effect of activity directed fractions of Vernonia amygdalna on total body weight and blood glucose levels of diabetic wistar albino rats. International Journal of Science and Technology, Volume 2(1): 153 -157
[12] Mahora R., Stoicescu S –M., (2016) Congenital Diabetes Mellitus, Medica –a Journal of Clinical Medicine Volume 11(2): 154 -157
[13] International Diabetes Federation (I.D.F) (2021), Diabetes in Nigeria
[14] Beltran J., Busiah K., Vaivre—Douret L., Fauret., A. L., Berdugo M., Cave H and Polak M. (2020) Neonatal Diabetes Mellitus. Front. Pediatr 8: 540718 doi: 10 3389/fped.540718
[15] Chinenye S. and Young L. (2011) State of Diabetes in Nigeria, The Nigerian Health Journal , Volume 11(4): 101-106
[16] Alhassan A. J., Sule M. S., El-ta'alu A. B., and Lawal A. T. (2017) In vitro Inhibitory Activities of Persea Americana Seed Extracts on α -Amylase and α -Glucosidase. Bayero Journal of Pure and Applied Sciences, Volume 10(1), 546-552
[17] Wikipedia https://en.wikipedia.org>>wiki>Demographics of Nigeria
[18]Nagmoti D. M and Archana R. J. (2013) In vitro inhibitory effects of pithecellobiumdulce(Roxb) Benth seeds on intestinal α -glucosidase and pancreatic α -amylase, J Biochem Tech, Volume 4(3): 616-621.

[19] C.D.C (2024) Prevention of Gestational Diabetes, https://www.cdc.gov
[20] Donovan P. J., Mcintyre. H. D. (2010) Drugs for gestational diabetesAustralian presciber, 10. 18773austprescr.2010.066 33(5) https://www.nih.gov
[21] Implications of gestational diabetes (ADA, 2019).
[22] Lakshmiantham S., Leela S and Martynyuk A. A. (1989) Stability Analysis of nonlinear system Marcel Deker, Inc., New York and Basel
[23]Perko L. (2000) Differential equations and dynamical systems. Springer ; New York
[24] Huo, H. F., Chang, S. J.,&Li, Y. N. (2010).Stability of two strain tuberculosis model with general contact rate.Abstract and Applied Analysis. ID 293747, 31 pages. Doi: 10.1155/2010/293747.
[25] Hethccote H. W. (2000).The mathematics of infectious diseases, SIAM Rev, 42(4):599-653
[26] Aye P. O., Adeyemo K. A., Oke A. S and Omotoye A. E. (2021) Analysis of Mathematical Model for the Dynamics of Diabetes Mellitus and Its Complications. Applied Mathematics and Computational Intelligence, University Malaysia Perlis, U – Map, Volume 10(1), 57-77
[27]He J. H. (2000) A coupling homotopy perturbation technique and perturbation technique for nonlinear problems, International Journal of Non-Linear Mechanics. Volume 35: 37-43
[28]He J. H. (2000). New perturbation technique which is also valid for large parameters, Journal Sound and Vibration. Volume 229: 1257-1263
[29]Dessalegn, Y. M annd Gumel A. B. (2010) Global Asymptotic Properties of an SEIRS Model with Multiple Infectious Stages. J. Math. Anal. Appl.366: 202 -217. www.elsvier.com/locate/jmaa
[30] Adeyemo, K. A., Akinwande N I., and Lasisi N. O. (2020) Local Stability Analysis of the Unique Endemic Equilibrium Point of a Mathematical Model for the Transmission and Control of Zika Virus disease Dynamics. Caliphate journal of science and technology (CaJoST), 2, 175 -181.
[31] Garba, S. M., &Gumel, A. B., (2010).Mathematical recipe for HIV elimination in Nigeria.Journal of the Nigerian Mathematical Society. 29, 51-112
[32]Hedrick J.K and Girard A. (2005) Control of nonlinear dynamical system, theory and application. Class note: 62-83
[33] Estimated based on ADA (2020)
[34] Bashir M.A., Yahaya M.M., Yusuf A.H., Mukhtar. (2021) Prediabetes Burden in Nigeria, A Systemic Review and Meter-Analysis, Front Public Health Sec. Clinical Diabetes, Volume 9, https//doi.org/10.3389/fpbh.2021.762429
[35]Bao S.Y., Han S.Y., Wang H., Bao W., Ao W. (2016b). Improvement Effects of Agiophyllum Oligosaccharides on General Characterization and Glucose and Lipid Metabolism of Diabete GK Rats. J. Jilin Univ. (Medicine Edition) 42, 1059–1065. [Google Scholar]

Mathematical model for controllability of covid-19 investigating the impact of protective measures, for optimal solution to lower the disease burden in Nigeria

S.C. Nwasuka*, U.A. Osisiogu†, and T.E. Efor‡

Abstract

This work presents a non–linear deterministic mathematical model, analyzed to study the controllability of Covid-19 incorporating all-round protection, hospitalization, treatment and early burial of death due to covid-19 measures. We introduce a protection measure(A), that will cooperate with all government guidelines and observe personal hygiene, early burial of covid-19 death to extend B.I. Omede 2022 work. The existence of the disease-free equilibrium (DFE) state was established which shows the state in which there is no covid-19 infection for stability. The effective reproduction number and the local stability of the DFE were computed using the next generation and linearization approach respectively. The sensitivity analysis shows that the parameter with the highest positive sensitivity index is *a* proportion of susceptible ones that are not protecting themselves from covid-19 infection. The value, +1.014, of the sensitivity index of *a* shows that personal protection and other forms of protection, play important role in the control of spread of the disease. From numerical simulations, it was observed that the introduction of protective parameters leads to significant impact on the reduction of the spread of the disease. Moreso, it was discovered that effective implementation of protective measures without relaxing it will help in reducing the spread of the disease.

Keywords and phrases: early burial; Covid 19; reproduction number; model-fitting; protective measures

1 Introduction

The COVID-19 pandemic, first reported in Wuhan, China, in December 2019, rapidly escalated globally, with over 196 million confirmed cases and 4.2 million deaths by July 2021 [1]. Nigeria, among 210 affected countries, recorded its first case on February 27, 2020 a 44-year-old Italian citizen returning from Milan [16]. By May 2020, Nigeria reported 2,558 cases, 87 deaths (3.4% case fatality

*Corresponding author. Department of Mathematics and Computer Science, Clifford University, Owerrinta, Abia State, Nigeria; E-mail: snwasuka@gmail.com
†Department of Industrial Mathematics, Ebonyi State University, Abakaliki, Ebonyi State, Nigeria; E-mail: uosisiogu@gmail.com
‡Department of Industrial Mathematics, Ebonyi State University, Abakaliki, Ebonyi State, Nigeria; E-mail: tesyefor@gmail.com

rate, CFR), and significant demographic trends: 69% male patients, 23% aged 21–30 years, and 15.2% regional CFR variation [3]. As of April 2024, Nigeria's cumulative totals reached 267,188 cases, 3,155 deaths, and 259,953 recoveries, though global tracking ceased due to inconsistent reporting [16]. Common symptoms included fever, dry cough, and breathing difficulties, with less frequent reports of muscle pain, diarrhea, and sore throat [1].

Transmission evolved from travel-related importation to community spread, including asymptomatic carriers [2], complicating containment efforts. Coronaviruses, known for causing illnesses from common colds to severe syndromes like SARS and MERS, were identified as the cause of COVID-19, declared a pandemic by the WHO in March 2020 [1]. Nigeria, flagged as high-risk by the WHO due to travel links with China [1], activated its highest public health emergency (Level 3) following the index case [3].

The Nigeria Centre for Disease Control (NCDC) spearheaded responses, deploying Rapid Response Teams, contact tracing, and designating COVID-19 treatment facilities [3]. Despite these measures, challenges emerged: public skepticism toward government motives, misinformation, and low adherence to protocols like masking and distancing [3]. Weak healthcare infrastructure, urban overcrowding, and poverty further strained responses, prompting calls for context-specific adaptations by global health experts like Dr. Wafaa El-Sadr [4].

Mathematical models played a critical role in predicting outbreak trajectories and evaluating intervention efficacy [4]. While unable to provide precise long-term forecasts, models helped estimate short-term healthcare demands (e.g., ICU beds, ventilators) and informed policy decisions on lockdowns and reopening timelines [4]. Early models in China suggested peak transmission by late January 2020 [5], but Nigeria's heterogeneous data highlighted regional disparities in CFR (0.2%–15%) and resource allocation [3]. Models emphasized prioritizing interventions (e.g., testing, isolation) over speculative death tolls [4], underscoring the importance of adaptive, evidence-based policies. Key challenges included reconciling public compliance with epidemiological guidelines [3], addressing healthcare inequities, and mitigating economic impacts. Nigeria's young population (median age 18) initially suggested lower vulnerability, yet comorbidities and limited healthcare access exacerbated risks [3]. The NCDC's daily updates aimed to enhance transparency, but persistent case growth reflected systemic gaps in enforcement and education [3].

Nigeria's COVID-19 experience underscores the interplay of global health governance [1], localized responses [16], and socioeconomic realities. While mathematical models provided strategic insights [5,4,2], their limitations highlighted the need for flexible, equity-focused policies. Strengthening healthcare systems, combating misinformation [16], and fostering community trust remain critical for future pandemic preparedness, particularly in low-resource settings. The pandemic's legacy emphasizes the value of integrating scientific rigor with contextual adaptability to mitigate health crises effectively [7].

2 Methodology/Model formulation

We present a deterministic compartmental model [7] which describes the transmission dynamics of covid-19 in the presence of some control measures. The model is a system of nine (9) nonlinear ordinary differential equations, which captures the dynamics of the disease in Nigeria. In this model, the human population is divided into nine (9) compartments namely:

Susceptible (S): This is a class of individuals who are prone to contract covid-19 disease. Since covid-19 is an epidemic that has affected every part of Nigeria, we assume that the entire population of Nigeria is susceptible to covid-19 infection.

Protection class (A): This is the class is a fraction of susceptible who employs several available protection measures against covid-19.
Exposed class (E): This is the class of people who have contracted covid-19 but have not shown symptoms of the disease.
Asymptomatically Infectious (I_{as}): This is the fraction of the exposed class who are not showing symptoms even after the incubation period has elapsed.
Symptomatically Infectious (I_s): This is the fraction of the exposed class who are showing symptoms at the expiration of the incubation period of the disease.
Hospitalized (H): The class contains a fraction of asymptomatically and symptomatically infectious classes who are isolated and are receiving treatments in isolation centers.
Quarantine class (Q): This is the class of symptomatically infectious humans who self-isolates themselves.
Dead (D): This comprises the fractions of the infectious classes who die due to the disease and the rate burial of the infected dead are done early to avoid re-infection
Recoveries(R): This contains fractions of the infected classes who have recovered from covid-19 infection naturally or after being treated.

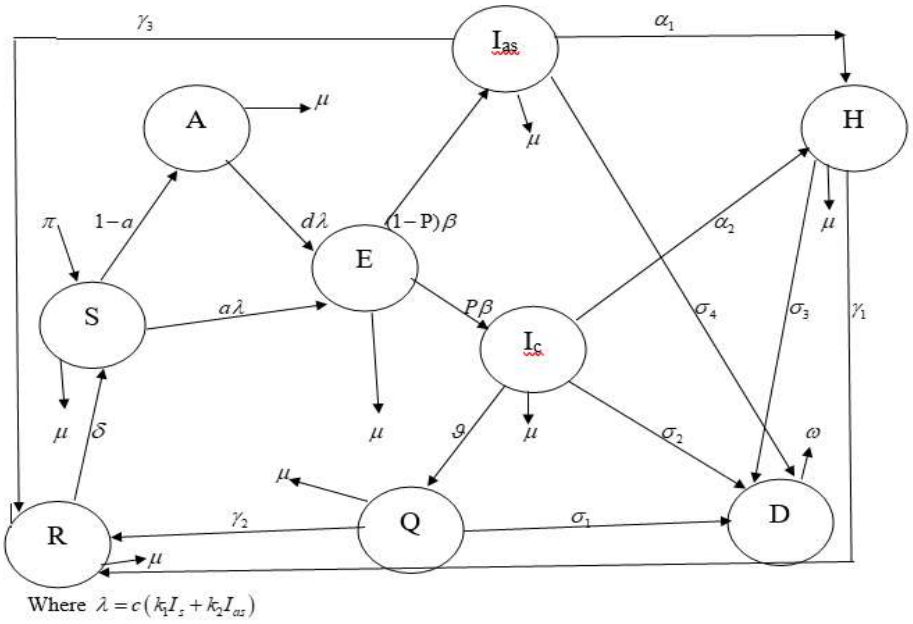
Hence, the total population N is given by $N = S + A + E + I_{as} + I_s + H + Q + D + R$. The recruitment of humans into the susceptible class is through migration into the country from foreign countries, and through birth of young ones. Here, the recruitment is put at the rate π. It is assumed that a fraction a of the susceptible contracts covid-19 through contact with asymptomatically and symptomatically infectious humans at the rate $ac(\varkappa_1 I_s + \varkappa_2 I_{as})$, where c is the rate of contact with the infectious classes, $\varkappa_1$ and $\varkappa_1$ are the probabilities a contact with I_s and I_{as}, respectively will result to infections. The remaining fraction (1-a) of the susceptible are assumed to protect themselves from being infected by the disease. However, the proportion d of this class is assumed to relax their protection and become infected with the disease at the rate $dc^0(\varkappa_1 I_s + \varkappa_2 I_{as})$, where c^0 is the rate at which the proportion d have contacts with the infectious classes. The exposed class becomes either symptomatically infectious or asymptomatically infectious in the proportions p and $(1-p)$, respectively, at the incubation rate β. The asymptomatically infectious and symptomatically classes are assumed to be hospitalized at the rates a_1 and a_2, respectively, whereas the proportion q of the symptomatically infectious class self-isolates themselves. The disease-induced death for the classes $I_{as}, I_s, H,$ and Q are put at σ_4, σ_2, and σ_3, and σ_1 respectively. The hospitalized class, the self-isolation class and the asymptomatically infectious class recover from the the disease at the rates γ_1, γ_2, and γ_3, respectively, while the natural death rate for all the classes is μ and ω is the rate infected dead burial are conducted early to avoid contacts and re-infection. However, since covid-19 is not known to confer life-long immunity after infection, we assume that the proportion δ, of recovery class becomes susceptible to the disease after recovery. Therefore, the rate of change of each class is given by the system of ordinary differential equations.

We present a deterministic compartmental model which describes the transmission dynamics of covid-19 in the presence of protective measures. The model is a system of nine (9) nonlinear ordinary differential equations, which captures the dynamics of the disease in Nigeria. In this model, the human population is divided into nine (9) compartments namely: Susceptible (S), Protection class (A), Exposed class (E), Symptomatically Infectious (I_s), Hospitalized (H), Quarantine class (Q), Dead (D), Recoveries(R) and Asymptomatically Infectious (I_{as})

Table 1: Description of the Parameter used in this model

Parameter	***Description***
π	rate of recruitment into the susceptible class
a	proportion of the susceptible class that are protected
c	rate of contact between infected class and those that are not protected
d	proportion of protected class that lose their protection
c_0	rate of contact between infected class and those that are protected
$\varkappa_1$	probability that a contact with symptomatomatically infectious persons will result to infection
$\varkappa_2$	probability that a contact with asymptomatomatically infectious persons will result to infection
a_1	the rate at which the asymptomatically infectious persons are hospitalized and treated
a_2	the rate at which the symptomatically infectious persons are hospitalized and treated
σ_1	death rate for self-isolated persons
σ_2	death rate for symptomatically infected persons
σ_3	death rate for hospitalized persons
σ_4	death rate for asymptomatically infected persons
ρ	proportion of exposed class that becomes symptomatically infectious
β	incubation rate of corona virus
γ_1	rate of recovery for hospitalized persons
γ_2	rate of recovery for self-isolated persons
γ_3	rate of recovery for asymptomatically infected persons
q	the proportion of symptomatically infectious humans that self-isolate
δ	proportion of recovered class that becomes susceptible
μ	human natural death rate
ω	The rate of early burials of death due to covid-19 to avoid re-infection

Figure 1: A compartmentalized diagram showing the covid-19 model with control measure



The System equation of the model

$$\frac{dS(t)}{dt} = \pi + \delta R - ac(k_1 I_s + k_2 I_{as})S - (1-a)S - \mu S$$

$$\frac{dA(t)}{dt} = (1-a)S(t) - cd(k_1 I_s + k_2 I_{as})A - \mu A$$

$$\frac{dE(t)}{dt} = ac(k_1 I_s + k_2 I_{as})S + cd(k_1 I_s + k_2 I_{as})\,\mathrm{A} - (\beta + \mu)\,\mathrm{E(t)}$$

$$\frac{dI_{as}(t)}{dt} = (1-p)\beta E - (\alpha_1 + \sigma_4 + \gamma_3 + \mu)I_{as}(t)$$

$$\frac{dI_s(t)}{dt} = p\beta E - (\alpha_2 + \sigma_2 + q + \mu)I_s(t) \qquad (1)$$

$$\frac{dH(t)}{dt} = \alpha_1 I_{as} + \alpha_2 I_s - (\sigma_3 + \gamma_1 + \mu)H(t)$$

$$\frac{dQ(t)}{dt} = qI_s - (\sigma_1 + \gamma_2 + \mu)Q(t)$$

$$\frac{dD(t)}{dt} = \sigma_1 Q + \sigma_2 I_s + \sigma_3 H + \sigma_4 I_{as} - \omega D(\mathrm{t})$$

$$\frac{dR_h(t)}{dt} = \gamma_1 H + \gamma_2 Q + \gamma I_{as} - (\delta + \mu)R_h(t)$$

2.1 Disease-free equilibrium

The equilibrium points of the model system are the steady state solutions obtained when the right hand of the system (1) is to zero. That is the solution to the equations
Disease-free equilibrium points of the model are the solutions to (1) when equated to (0) obtained when there is no disease in the population. That is the solution obtained when
$A = E = I_{as} = I_s = H = Q = D = 0$.

With this definition, the components of the disease-free equilibrium point corresponding to the classes where there can be disease infections are zero. Let E_0 denote the disease-free equilibrium of the model, with this definition, the components of the disease-free equilibrium point corresponding to the classes where there can be disease infections are zero. Let E_0 denote the disease-free equilibrium of the model, then we have

$$E_0 = (S^*, \mathrm{A}^*, \mathrm{E}^*, \mathrm{I}^*_{\mathrm{as}}, \mathrm{I}^*_{\mathrm{s}}, H^*, \mathrm{Q}^*, \mathrm{D}^*, \mathrm{R}^*) = \left(\frac{\pi}{1-a+\mu}, \frac{(1-a)\pi}{\mu(1+\mu-a)}, 0,0,0,0,0,0,0 \right). \quad (2)$$

The disease-free equilibrium is necessary in the determination of the basic reproduction number of the disease.

Using the next generation matrix, we got the reproduction number as;

$$\frac{dE(t)}{dt} = ac(k_1 I_s + k_2 I_{as})S + cd(k_1 I_s + k_2 I_{as})A - (\beta+\mu)E(t),$$

$$\frac{dI_{as}(t)}{dt} = (1-p)\beta E - (\alpha_1 + \sigma_4 + \gamma_3 + \mu)I_{as}(t),$$

$$\frac{dI_s(t)}{dt} p\beta E - (\alpha_2 + \sigma_2 + q + \mu)I_s(t), \quad (3)$$

$$\frac{dH(t)}{dt} = \alpha_1 I_{as} + \alpha_2 I_s - (\sigma_3 + \gamma_1 + \mu)H(t),$$

$$\frac{dQ(t)}{dt} = qI_s - (\sigma_1 + \gamma_2 + \mu)Q(t),$$

From the subsystem, we have

$$F = \begin{pmatrix} ac(k_1 I_s + k_2 I_{as})S + cd(k_1 I_s + k_2 I_{as})A \\ 0 \\ 0 \\ 0 \\ 0 \end{pmatrix}, V = \begin{pmatrix} (\beta+\mu)E \\ -(1-p)\beta E + (\alpha_1 + \sigma_4 + \gamma_3 + \mu)I_{as} \\ -p\beta + (\alpha_2 + \sigma_2 + q + \mu)I_s \\ -\alpha_1 I_{as} - \alpha_2 I_s + (\sigma_3 + \gamma_1 + \mu)H \\ -qI_s + (\sigma_1 + \gamma_2 + \mu)Q(t) \end{pmatrix}$$

Then, F is the Jacobian matrix of F evaluated at the disease-free equilibrium and V is the Jacobian matrix of V evaluated at the disease-free equilibrium. Hence, we have

$$F = \begin{pmatrix} 0 & \frac{ac\kappa_2\pi}{(1-a+\mu)} + \frac{dc\kappa_2\pi(1-a)}{\mu(1+\mu-a)} & \frac{ac\kappa_1\pi}{(1-a+\mu)} + \frac{dc\kappa_1\pi(1-a)}{\mu(1+\mu-a)} & 0 & 0 \\ 0 & 0 & 0 & 0 & 0 \\ 0 & 0 & 0 & 0 & 0 \\ 0 & 0 & 0 & 0 & 0 \\ 0 & 0 & 0 & 0 & 0 \end{pmatrix}$$

$$V = \begin{pmatrix} \beta+\mu & 0 & 0 & 0 & 0 \\ -(1-p)\beta & \alpha_1+\sigma_4+\gamma_3+\mu & 0 & 0 & 0 \\ -p\beta & 0 & \alpha_2+\sigma_2+q+\mu & 0 & 0 \\ 0 & -\alpha_1 & -\alpha_2 & \sigma_3+\gamma_1+\mu & 0 \\ 0 & 0 & -q & 0 & \sigma_1+\gamma_2+\mu \end{pmatrix}$$

The inverse of V is non-negative, and is given by

$$V^{-1} = \begin{pmatrix} \frac{1}{\beta+\mu} & 0 & 0 & 0 & 0 \\ \frac{(1-p)\beta}{(\beta+\mu)(\alpha_1+\sigma_4+\gamma_3+\mu)} & \frac{1}{(\alpha_1+\sigma_4+\gamma_3+\mu)} & 0 & 0 & 0 \\ \frac{(\alpha_1(1-p)\beta(\alpha_2+\sigma_2+q+\mu)+p\beta\alpha_2(\alpha_1+\sigma_4+\gamma_3+\mu)}{(\beta+\mu)(\alpha_1+\sigma_4+\gamma_3+\mu)(\alpha_2+\sigma_2+q+\mu)(\sigma_3+\gamma_1+\mu)} & \frac{\alpha_1}{(\alpha_1+\sigma_4+\gamma_3+\mu)(\sigma_3+\gamma_1+\mu)} & \frac{\alpha_2}{(\alpha_2+\sigma_2+q+\mu)(\sigma_3+\gamma_1+\mu)} & \frac{1}{(\sigma_3+\gamma_1+\mu)} & 0 \\ \frac{pq\beta}{(\beta+\mu)(\alpha_2+\sigma_2+q+\mu)(\sigma_1+\gamma_2+\mu)} & 0 & \frac{q}{(\alpha_2+\sigma_2+q+\mu)(\sigma_1+\gamma_2+\mu)} & 0 & \frac{1}{\sigma_1+\gamma_2+\mu} \end{pmatrix}$$

The next generation matrix is therefore given by

$$K = FV^{-1} = \begin{pmatrix} \frac{ack_2\pi(1-p)\beta}{(1-a+\mu)(\beta+\mu)(\alpha_1+\sigma_4+\gamma_3+\mu)} + \frac{ack_1\pi p\beta}{(1-a+\mu)(\beta+\mu)(\alpha_2+\sigma_2+q+\mu)} & \frac{ac\pi}{(1-a+\mu)(\alpha_1+\sigma_4+\gamma_3+\mu)} & \frac{ac\pi}{(1-a+\mu)(\alpha_2+\sigma_2+q+\mu)} & 0 & 0 \\ 0 & 0 & 0 & 0 & 0 \\ 0 & 0 & 0 & 0 & 0 \\ 0 & 0 & 0 & 0 & 0 \\ 0 & 0 & 0 & 0 & 0 \end{pmatrix}$$

The egienvalues of K are 0,0,0,0 and

$\frac{(1-p)\beta acK_2\pi}{(1-a+\mu)(\beta+\mu)(\alpha_1+\sigma_4+\gamma_3+\mu)} + \frac{p\beta acK_1\pi}{(1-a+\mu)(\beta+\mu)(\alpha_2+\sigma_2+q+\mu)}$. Therefore, the basic reproduction number of the disease is

$R_0 = \frac{(1-p)\beta acK_2\pi}{(1-a+\mu)(\beta+d)(\alpha_1+\sigma_4+\gamma_3+\mu)} + \frac{p\beta acK_1\pi}{(1-a+\mu)(\beta+\mu)(\alpha_2+\sigma_2+q+\mu)}$. The basic reproduction number can be written in the form

$R_0 = R_{0a} + R_{0s}$

where $R_{0a} := \frac{(1-p)\beta acK_2\pi}{(1-a+\mu)(\beta+\mu)(\alpha_1+\sigma_4+\gamma_3+\mu)}$ is the average number of people that would be asymptomatically infected by a single infectious individual, where

$R_{0s} := \frac{p\beta acK_1\pi}{(1-a+\mu)(\beta+\mu)(\alpha_2+\sigma_2+q+\mu)}$ is the average number of people that would be asymptomatically infected by single infectious individuals.

3 Analysis of the model

The stability or otherwise of the disease-free equilibrium point, E_0 is determined by the sign of the real part of all the eigenvalues of the Jacobian matrix of $f(X)$ evaluated at E_0. Let $J(E_0)$ be the Jacobian matrix of $f(X(t))$ evaluated at E_0. If all the eigenvalues of $J(E_0)$ have negative real parts, then E_0 is unstable. Therefore, we need to show that all the eigenvalues of $J(E_0)$ have negative real part. First we write $f(X(t))$ in the form

$$f(X(t)) = \begin{pmatrix} f_1 \\ f_2 \\ f_3 \\ f_4 \\ f_5 \\ f_6 \\ f_7 \\ f_8 \\ f_9 \end{pmatrix} = \begin{pmatrix} \pi + \delta R - ac(k_1 I_s + k_2 I_{as})S - (1-a)S - \mu S \\ (1-a)S - cd(k_1 I_s + k_2 I_{as})A - \mu A \\ ac(\mathrm{k}_1 I_s + k_2 I_{as})S + cd(k_1 I_s + k_2 I_{as})A - (\beta + \mu)E \\ (1-p)\beta E - (\alpha_1 + \sigma_4 + \gamma_3 + \mu)I_{as} \\ P\beta - (\alpha_2 + \sigma_2 + q + \mu)I_s \\ \alpha_1 I_{as} + \alpha_2 I_s - (\sigma_3 + \gamma_1 + \mu)H \\ qI_s - (\sigma_1 + \gamma_2 + \mu)Q \\ \sigma_1 Q + \sigma_2 I_s + \sigma_3 H + \sigma_4 I_{as} - \omega D(t) \\ \gamma_1 H + \gamma_2 Q + \gamma_3 I_{as} - (\delta + \mu)R \end{pmatrix}$$

The Jacobian matrix of $f(X)$ valuated at the disease-free equilibrium point E_0 is

$$\mathrm{J}(E_o) = \begin{pmatrix} (-d+1-a) & 0 & 0 & -\mathrm{ack}_2 S^* & -\mathrm{ack}_1 S^* & 0 & 0 & 0 & \delta \\ 1-a & -d & 0 & 0 & 0 & 0 & 0 & 0 & 0 \\ 0 & 0 & -(\beta+d) & ack_2 S^* & ack_1 S^* & 0 & 0 & 0 & 0 \\ 0 & 0 & (1-p)\beta & -G_1 & 0 & 0 & 0 & 0 & 0 \\ 0 & 0 & p\beta & 0 & -G_2 & 0 & 0 & 0 & 0 \\ 0 & 0 & 0 & \alpha_1 & \alpha_2 & -G_3 & 0 & 0 & 0 \\ 0 & 0 & 0 & 0 & q & 0 & -G_4 & 0 & 0 \\ 0 & 0 & 0 & \sigma_4 & \sigma_2 & \sigma_3 & \sigma_1 & 0 & 0 \\ 0 & 0 & 0 & \gamma_3 & 0 & \gamma_1 & \gamma_2 & 0 & -(\delta+\mu) \end{pmatrix}$$

where $G_1 = \alpha_1 + \sigma_4 + \gamma_3 + \mu$, $G_2 = \alpha_2 + \sigma_2 + q + \mu$, $\sigma_3 + \gamma_1 + \mu$, $G_4 = \sigma_1 + \gamma_2 + \mu$. The eigenvalues of $J(E_0)$ are $0, -\mu, -(\mu + 1 - a), -(\delta + \mu)$ and the eigenvalues of the sub-matrix

$$J_s(E_0)=\begin{pmatrix} -(\beta+d) & ack_2S^* & ack_1S^* & 0 & 0 \\ (1-p)\beta & -(\alpha_1+\sigma_4+\gamma_3+\mu) & 0 & 0 & 0 \\ p\beta & 0 & -(\alpha_2+\sigma_2+q+\mu) & 0 & 0 \\ 0 & \alpha_1 & \alpha_2 & -(\sigma_3+\gamma_1+\mu) & 0 \\ 0 & 0 & q & 0 & -(\sigma_1+\gamma_2+\mu) \end{pmatrix}$$

At this stage, notice that the matrices F,V and $J_s(E_0)$ are related by $F-V=J_s(E_0)$. In Driesseche and Watmough (2002). It is shown that all the eigenvalues of eigenvalues of the matrix F-V or equivalently, $J_s(\mathrm{E}_0)$ are all negative or have negative real parts if $p(FV^{-1})<1$. This shows that the disease -free equilibrium E_0 is locally asymptotically stable if $R_0<1,$ and unstable if $R_0>1$. Epidemiologically, this means that the disease can be eradicated in the population when, if the initial sizes of the compartments are in the basin of attraction of the disease –free equilibrium.

3.1 Global stability of the disease-free equilibrium

In the last subsection, we proved that the disease-free equilibrium E_0. Is locally asymptotically stable when the control reproduction number $\mathrm{R_e}<1$. The aim of this subsection is to determine the stability or otherwise of the disease-free equilibrium E_0 in the global sense. That is if the solution to the system of equations tends to the disease-free equilibrium

$$\frac{dX_1(t)}{dt}=F_1(X_1,X_2) \qquad 4$$

$$\frac{dX_2(t)}{dt}=F_2(X_1,X_2),F2(X_1,0)=0 \qquad 5$$

where the first equation represents the system for the uninfected compartments, while the second equation represents the system for the infected compartment in this case, $X_1(t)=(S(t),\mathrm{A(t)}),R(t)$ and $X_2(t)=(E(t),I_{as}(t),I_s(t),H(t),Q(t),D(t)$. Also, the right-hand sides are given by

$$F_1(X_1,X_2)=\begin{pmatrix} \pi+\delta R-ac(K_1I_s+K_2I_{as})\mathrm{S}-(1-\mathrm{a})\mathrm{S}-\mu\mathrm{S} \\ (1-\mathrm{a})\mathrm{S(t)}-\mathrm{cd}(\mathrm{K}_1I_s+K_2I_{as})A-\mu A \\ \gamma_1H+\gamma_2Q+\gamma_3I_{as}-(\delta+\mu)R_h(t) \end{pmatrix}$$

$$F_2(X_1, X_2) = \begin{pmatrix} ac(K_1 I_s + K_2 I_{as})S + cd(K_1 I_s + K_2 I_{as})A - (\beta + \mu)E(t) \\ (1-P)\beta E - (\alpha_1 + \sigma_4 + \gamma_3 + \mu)I_{as}(t) \\ \mathrm{p}\,\beta\,\mathrm{E} - (\alpha_2 + \sigma_2 + q + \mu)I_s(t) \\ \alpha_1 I_{as} + \alpha_2 I_s - (\sigma_3 + \gamma_1 + \mu)H(t) \\ \mathrm{qI_s} - (\sigma_1 + \gamma_2 + \mu)Q(t) \\ \sigma_1 Q + \sigma_2 I_s + \sigma_3 H + \sigma_4 I_{as} - \omega D(t) \end{pmatrix}$$

The two conditions that must be satisfied to guarantee global stability of the disease-free equilibrium are

i. In the system $\frac{dX_1(t)}{dt} = F_1(X_1, 0)$, the disease-free equilibrium $\left(\frac{\pi}{1+\mu-a}, \frac{\pi(1-a)}{\mu(1+\mu-a)}, 0\right)$ must be globally asymptotically stable. That is $\left(S(t), A(t), R(t)\right) \to \left(\frac{\pi}{1+\mu-a}, \frac{\pi(1-a)}{\mu(1+\mu-a)}, 0\right) as\, t \to \infty$.

ii. In the system $\frac{dX_2}{dt} = F_2(X_1, X_2)$, we must have $BX_2 - F_2\left(X_1, X_2\right) \geq 0$, where B is the Jacobian matrix of $F_2(X_1, X_2)$ evaluated at the disease-free equilibrium, E_0. The solution to (9) is

$$S(t) = \frac{\pi}{1+\mu-a} + \frac{\delta R(0)}{1+a-\delta} e^{-(\delta+\mu)t} + K_0 e^{-(1+\mu-a)t}$$

$$A(t) = A(0)e^{-\mu t} + \frac{\pi(1-a)}{\mu(1+\mu-a)}(1-e^{-\mu t}) + \frac{R(0)(1-a)}{1-a-\delta}\left(e^{-\mu t} - e^{-(\delta+\mu)t}\right) + K_0\left(e^{-\mu t} - e^{-(1+\mu-a)t}\right) \quad (6)$$

$$R(t) = R(0)e^{-(\delta+\mu)t},$$

where $K_0 = S(0) - \frac{\pi}{1+\mu-a} - \frac{\delta R(0)}{1-a-\delta}$.

We see that as $t \to \infty, \left(S(t), A(t), R(t)\right) \to \left(\frac{\pi}{1+\mu-a}, \frac{\pi(1-a)}{\mu(1+\mu-a)}, 0\right)$. That is $\left(S(t), A(t), R(t)\right)$ tends to the disease-free equilibrium. Therefore, the equilibrium point $\left(\frac{\pi}{1+\mu-a}, \frac{\pi(1-a)}{\mu(1+\mu-a)}, 0\right)$ is globally asymptotically stable. The matrix B is given by

$$B=\begin{pmatrix} -(\beta+\mu) & \frac{ack_2\pi}{1+\mu-a} & \frac{ack_1\pi}{1+\mu-a} & 0 & 0 & 0 \\ (1-p)\beta & -(\alpha_1+\sigma_4+\gamma_3+\mu) & 0 & 0 & 0 & 0 \\ p\beta & 0 & -(\alpha_2+\sigma_2+q+\mu) & 0 & 0 & 0 \\ 0 & \alpha_1 & \alpha_2 & -(\sigma_3+\gamma_1+\mu) & 0 & 0 \\ 0 & 0 & q & 0 & -(\sigma_1+\gamma_2+\mu) & 0 \\ 0 & \sigma_4 & \sigma_2 & \sigma_3 & \sigma_1 & 0 \end{pmatrix}$$

Therefore,

$$BX_2 - F_2(X_1, X_2) = \begin{pmatrix} ac(k_2I_s + k_1I_{as}) & \left(\frac{\pi}{1+\mu-a} - S(t)\right) - cd(k_2I_s + k_1I_{as}) \\ 0 \\ 0 \\ 0 \\ 0 \\ 0 \end{pmatrix} \quad (7)$$

In (7), the quantity $ac(k_2I_s + K_1I_{as})\left(\frac{\pi}{1+\mu-a} - S(t)\right)$ is positive since from (11), we have that $S(t) \le \frac{\pi}{1+\mu-a} \forall t.$

Furthermore, one sees that if the parameter, d, which represents the fraction of individuals who are not consistent with their protection against Covid-19, is zero, the first element in the matrix becomes positive, which makes the matrix become nonnegative. In this case, the disease-free equilibrium becomes globally asymptotically stable. Let the contact rate, e be the bifurcation parameter such that $R_0 = 1$ implies that

$$\frac{ack_2\pi(1-p)\beta(\mu a + d(1-a))}{\mu(1-a+\mu)(\beta+\mu)(\alpha_1+\sigma_4+\gamma_3+\mu)} + \frac{ack_1\pi p\beta(\mu a + d(1-a))}{\mu(1-a+\mu)(\beta+\mu)(\alpha_2+\sigma_2+q+\mu)} = 1$$

$$\Rightarrow \frac{(1-p)\beta ack_2\pi(\mu a+d(1-a))(\alpha_2+\sigma_2+q+\mu)+p\beta ack_1\pi(\mu a+d(1-a))(\alpha_1+\sigma_4+\gamma_3+\mu)}{\mu(1-a+\mu)(\beta+d)(\alpha_1+\sigma_4+\gamma_3+\mu)(\alpha_2+\sigma_2+q+\mu)}=1$$

Therefore at $R_0=1$, the bifurcation parameter is

$$c^*=\frac{\mu(1-a+\mu)(\beta+d)(\alpha_1+\sigma_4+\gamma_3+\mu)(\alpha_2+\sigma_2+q+\mu)}{\beta a\pi\left[(1-p)k_2(\mu a+d(1-a))(\alpha_2+\sigma_2+q+\mu)\,pk_1(\mu a+d(1-a))(\alpha_1+\sigma_4+\gamma_3+\mu)\right]}$$

We now make change of variables in the model system as follows: $x_1=S(t), \mathrm{x}_2=A(t), \mathrm{x}_3=E(t), \mathrm{x}_4=I_{as}(t), X_5=I_s(t), x_6=H(t), x_7=Q(t), \mathrm{x}_8=D(t), x_9=R(t).$

Then the right –hand side of the model system becomes

$$f\left(X(t),c^*\right)=\begin{pmatrix} f_1\\ f_2\\ f_3\\ f_4\\ f_5\\ f_6\\ f_7\\ f_8\\ f_9 \end{pmatrix}=\mu\begin{pmatrix} \pi+\delta x9-ac^*(k_1x_5+k_2x_4)x_1-(1-a)x_1-\mu x_1\\ (1-a)x_1-c^*d(k_1x_5+k_2x_4)x_2-\mu x_2\\ ac^*(k_1x_5+k_2x_4)x_1+c*d(k_1x_5+k_2x_4)x_2-(\beta+\mu)x_3\\ (1-p)\beta x_3-(\alpha_1+\sigma_4+\gamma_3+\mu)x_4\\ p\beta x_3-(\alpha_2+\sigma_2+q+\mu)x_5\\ \alpha_1x_4+\alpha_2x_5-(\sigma_3+\gamma_1+\mu)x_6\\ qx_5-(\sigma_1+\gamma_2+\mu)\,\mathrm{x}_7\\ \sigma_1x_7+\sigma_2x_5+\sigma_3x_6+\sigma_4x_4\\ \gamma_1x_6+\gamma_2x_7+\gamma_3x_4-(\delta+\mu)x_9 \end{pmatrix}$$

Then the Jacobian matrix of $f(X(t),c^*)$ at the disease-free equilibrium E_0 is given by

$$J(E_0,c^*)=\begin{pmatrix} -a_1 & 0 & 0 & -a_2 & -a_3 & 0 & 0 & 0 & \delta \\ a_4 & -\mu & 0 & -a_5 & -a_6 & 0 & 0 & 0 & 0 \\ 0 & 0 & -a_7 & a_8 & a_9 & 0 & 0 & 0 & 0 \\ 0 & 0 & a_{10} & -a_{11} & 0 & 0 & 0 & 0 & 0 \\ 0 & 0 & a_{12} & 0 & -a_{13} & 0 & 0 & 0 & 0 \\ 0 & 0 & 0 & \alpha_1 & \alpha_2 & -a_{14} & 0 & 0 & 0 \\ 0 & 0 & 0 & 0 & q & 0 & -a_{15} & 0 & 0 \\ 0 & 0 & 0 & \sigma_4 & \sigma_2 & \sigma_3 & \sigma_1 & 0 & 0 \\ 0 & 0 & 0 & \gamma_3 & 0 & \gamma_1 & \gamma_2 & 0 & -a_{16} \end{pmatrix} \quad (8)$$

where

$$a_1=(1+\mu-a),\ a_2=\frac{ac^*k_2\pi}{1+\mu-a},\ a_3=\frac{ac^*k_1\pi}{1+\mu-a},\ a_4=1-a,\ a_5=\frac{c^*d\pi k_2(1-a)}{\mu(1+\mu-a)},\ a_6=\frac{c^*d\pi k_1(1-a)}{\mu(1+\mu-a)},\ a_7=\beta+\mu$$

$$a_8=\frac{ac^*k_2\pi}{1+\mu-a}+\frac{c^*d\pi k_2(1-a)}{\mu(1+\mu-a)},\ a_9=\frac{ac^*k_1\pi}{1+\mu-a}+\frac{c^*d\pi k_1(1-a)}{\mu(1+\mu-a)},\ a_{10}=(1-P)\beta,\ a_{11}=\alpha_1+\sigma_4+\gamma_3+\mu,$$

$$a_{12}=\alpha_2+\sigma_2+q+\mu,\ a_{13}=\sigma_3+\gamma_1+\mu,\ a_{14}=\sigma_1+\gamma_2+\mu,\ a_{15}=\delta+\mu$$

The matrix $J(E_0;c^*)$ possesses one zero eigenvalue, while the remaining eigenvalues have negative real part. Therefore, the disease-free equilibrium E_0 is non-hyperbolic. Hence, we can apply the theorem above to analyze the dynamics of the model around the bifurcation parameter value $c=c^*$ .The right eigenvector $w(w_1\ w_2\ w_3 \ldots w_g)^T$ corresponding to the zero eigenvalue satisfies the following system of equations

$$-a_1w_1 - a_2w_4 - a_3w_6 + \delta w_9 = 0$$

$$a_4w_1 - \mu w_2 - a_5w_4 - a_cw_5 = 0$$

$$-a_7w_3 + a_8w_4 + a_9w_5 = 0$$

$$a_{10}w_3 - a_{11}w_4 = 0$$

$$a_{12}w_3 - a_{13}w_5 = 0$$

$$\alpha_1w_4 + \alpha_2w_5 - a_{14}w_6 = 0$$

$$qw_3 - a_{15}w_7 = 0$$

$$\sigma_4w_4 + \sigma_2w_5 + \sigma_3w_6 + \sigma_1w_7 = 0$$

$$\gamma_3w_4 + \gamma_1w_6 + \gamma_2w_7 - a_{16}w_9 = 0 \qquad (7)$$

On the other hand, the left eigenvector corresponding to the zero eigenvalue $w = (v_1\, v_2\, v_3 ... v_9)^T$ satisfies the system

$$-a_1v_1 + a_4v_2 = 0$$

$$-\mu v_2 = 0$$

$$-a_7v_3 + a_{10}v_4 + a_{12}v_5 = 0$$

$$-a_2v_1 - a_5v_2 + a_8v_3 - a_{11}v_4 + \alpha_1v_6 + \sigma_4v_8 + \gamma_3v_9 = 0$$

$$-a_3v_1 - a_6v_2 + a_9v_3 - a_{13}v_5 + \beta_2v_6 + qv_7 + \sigma_2v_8 = 0$$

$$-a_{14}v_6 + \sigma_3v_8 + \gamma_1v_9 = 0$$

$$-a_{15}v_7 + \sigma_1v_8 + \gamma_2v_9 = 0$$

$$\delta v_1 - a_{16}v_9 = 0 \qquad (9)$$

The solution to (14) is obtained in terms of w_3 as

$$w_1 = \left(-\frac{a_2a_{10}}{a_1a_{11}} - \frac{a_3}{a_1}\left(\frac{\alpha_1a_{10}}{a_{11}a_{14}} + \frac{\alpha_2a_{12}}{a_{13}a_{14}}\right) + \frac{\delta}{a_1}\left(\frac{\gamma_3a_{10}}{a_{16}a_{11}} + \frac{\alpha_1\gamma_1a_{10}}{a_{11}a_{14}a_{16}} + \frac{\alpha_2\gamma_1a_{12}}{a_{13}a_{14}a_{16}} + \frac{q\gamma_2a_{12}}{a_{13}a_{15}a_{16}} \right) w3 \right.$$

$$w_2 = \left(\frac{a_4}{\mu} \left(-\frac{a_2 a_{10}}{a_1 a_{11}} - \frac{a_3}{a_1} \right) \frac{\alpha_1 a_{10}}{a_{11} a_{14}} + \frac{\alpha_2 a_{12}}{a_{13} a_{14}} \right) + \frac{\delta}{a_1} \left(\frac{\gamma_3 a_{10}}{a_{16} a_{11}} + \frac{\alpha_1 \gamma_1 a_{10}}{a_{11} a_{14} a_{16}} + \frac{\alpha_2 \gamma_1 a_{12}}{a_{13} a_{14} a_{16}} + \frac{q \gamma_2 a_{12}}{a_{13} a_{15} a_{16}} \left(-\frac{a_4 a_{10}}{\mu a_{11}} - \frac{a_6 a_{12}}{\mu a_{13}} \right) \right) w3$$

$$w_3 > 0, w_4 = \frac{a_{10}}{a_{11}} w_3, w_5 = \frac{a_{12}}{a_{13}} w_3, w_6 = \left(\frac{\alpha_1 a_{10}}{a_{11} a_{14}} + \frac{\alpha_2 a_{12}}{a_{13} a_{14}} \right) w_3, \quad w_7 = \frac{q a_{12}}{a_{13} a_{15}} w_3$$

$$wg = \left(\frac{\gamma_3 a_{10}}{a_{16} a_{11}} + \frac{\alpha_1 \gamma_1 a_{10}}{a_{11} a_{14} a_{16}} + \frac{\alpha_2 \gamma_1 a_{12}}{a_{13} a_{14} a_{16}} + \frac{q \gamma_2 a_{12}}{a_{13} a_{15} a_{16}} \right) w_3$$

From (9), the compartments v_1, v_2, v_8 and v_9 are all zeros since they correspond to the states that are not infected by the virus disease [8]. Solving for other components in terms of v_3, we obtain $v_3 > 0, v_4 = \frac{a_8}{a_{11}} v_3,\ v_5 = \frac{a_9}{a_{13}} v_3,\ v_6 = 0, v_7 = 0.$ Since v_3, v_4 and v_5 are the only non-zero left eigenvectors, the relevant components of $f\left(X(t), c^*\right)$ are f_3, f_4 and f_5. Futhermore, the second order partial derivatives of f_4 and f_5 are all zeros since these components are linear in each variable, and do not contain the bifurcation parameter, c^*. Therefore, the parameters a and b in the bifurcation theorem become

$$\phi_1 = v_3 \sum_{i,j}^{9} w_i w_j \frac{\partial^2 f_3(0,0)}{\partial x, \partial x_j}, \qquad 9$$

$$\phi_2 = v_3 \sum_{i}^{9} w_i \frac{\partial^2 f_3(0,0)}{\partial x, \partial c^*} \qquad 10$$

The second orders partial derivatives with respect to each relevant variable evaluate at disease-free equilibrium are

$$\frac{\partial^2 f_3(0,0)}{\partial x_1^{\,2}} = 0, \frac{\partial^2 f_3(0,0)}{\partial x_1 \partial x_2} = 0, \frac{\partial^2 f_3(0,0)}{\partial x_1 \partial x_3} = 0, \frac{\partial^2 f_3(0,0)}{\partial x_1 \partial x_4} = ac^* k_2, \frac{\partial^2 f_3(0,0)}{\partial x_1 \partial x_5} = ac^* k_1, \frac{\partial^2 f_3(0,0)}{\partial x^2_{\,2}} = 0$$

$$, \frac{\partial^2 f_3(0,0)}{\partial x_2 \partial x_3} = 0, \frac{\partial^2 f_3(0,0)}{\partial x_2 \partial x_4} = dc^* K_2, \frac{\partial^2 f_3(0,0)}{\partial x_2 \partial x_5} = dc^* K_1, \frac{\partial^2 f_3(0,0)}{\partial x_1 \partial c^*} = 0, \frac{\partial^2 f_3(0,0)}{\partial x_4 \partial c^*} = \frac{aK_2 \pi}{1+\mu-a} + \frac{d\pi(1-a)K_2}{\mu(1+\mu-a)},$$

$\frac{\partial^2 f_3(0,0)}{\partial x_5 \partial c^*} = \frac{aK_1 \pi}{1+\mu-a} + \frac{d\pi(1-a)K_1}{\mu(1+\mu-a)}$. Using these partial derivatives, we have

$$\phi_1 = v_3 c^* (w_1 a + w_2 d)(w_4 K_2 + w_5 K_1), \qquad 12$$

$$\phi_2 = v_3 \left[K_2 w_4 (a x_1^* + d x^*_{\,2}) + K_1 w_5 (a x_1^* + d x^*_{\,2}) \right] \qquad 13$$

where $x_1^* = \frac{\pi}{1+\mu-a}$, $x_2^* = \frac{\pi(1-a)}{\mu(1+\mu-a)}$. We see that $\phi_2 > 0$. Therefore, forward bifurcation occurs in the model if $\phi_1 < 0$, otherwise, backward bifurcation occurs in the model.

The control reproduction number R_0, of the model is a function of parameters. In this section, we investigate how much and how R_0 depends on each of these parameters. That is, we conduct sensitivity analysis on the control.

4 Numerical simulations/sensitivity analysis

Parameter Values used in this model reproduction number. Sensitivity analysis helps to determine how sensitive R_0 is to various key parameters of the model. It also helps to discover parameters of the model that increase or decrease R_0.

Sensitivity analysis identifies parameters influencing COVID-19 spread. Parameters with positive indices (a, c, $\varkappa_1$, $\varkappa_2$, π, β, d) must be reduced; those with negative indices (α_1, α_2, σ_2, σ_4, q, p, γ_3) require increase. The highest positive index is a (+1.014), representing non-protected susceptibles, underscoring personal protection importance. Reducing a lowers exposure, decreasing transmission and the basic reproduction number. This highlights targeted interventions to curb spread by minimizing unprotected populations and enhancing protective measures.

Table 3:

PARAMETER	SENSITIVITY INDEX
c	+0.9992
c_0	+0.0007646
$\varkappa_2$	+0.2082
$\varkappa_1$	+0.0002669
π	+1
β	+0.0272
d	+0.00076469
a	+1.014
α_1	-0.1237
α_2	-0.2224
σ_2	-0.07113
σ_4	-0.0552
q	-0.4719
ρ	-0.447
γ_3	-0.4719

Numerical simulation of the results

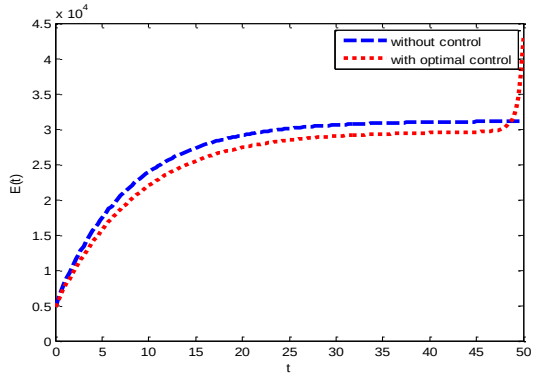


Figure 2: Exposed Humans

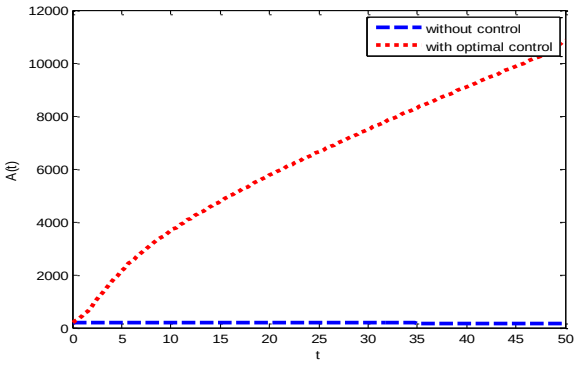


Figure 3: Graph of the protected class

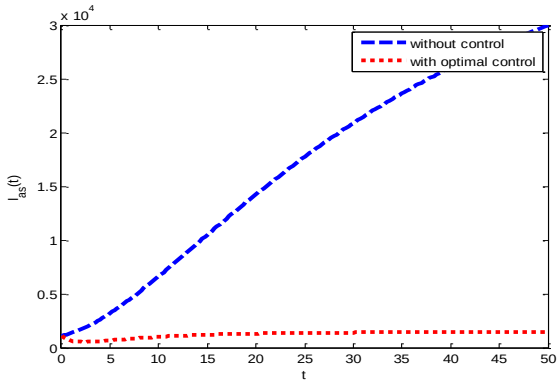


Figure 4: Graph of Asymptomatically infectious Humans

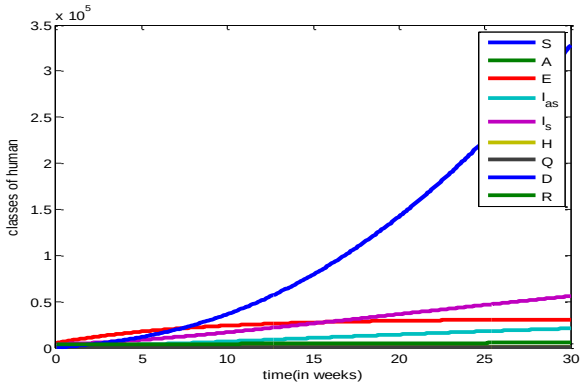


Figure 5: Graph for all the classes of Humans

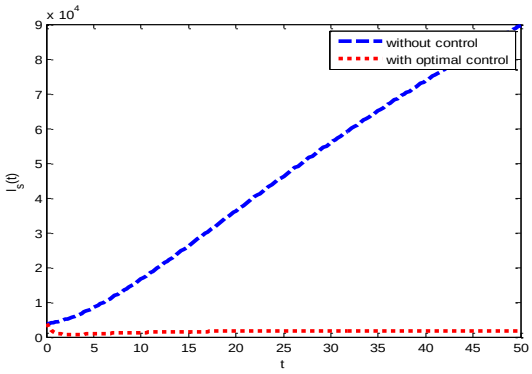


Figure 6: Symptomatically infectious Human

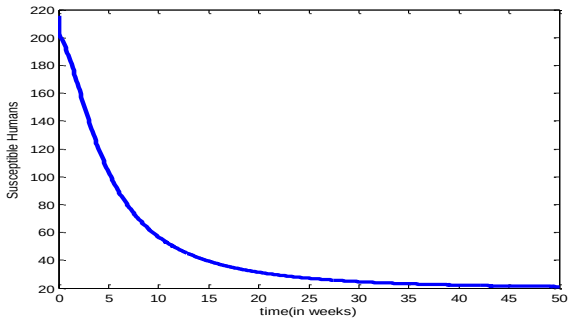


Figure 7: Susceptible humans

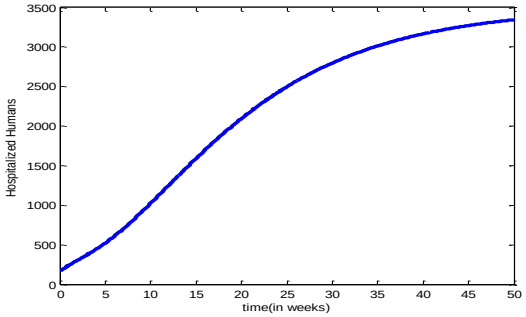


Figure 8: Hospitalized Humans

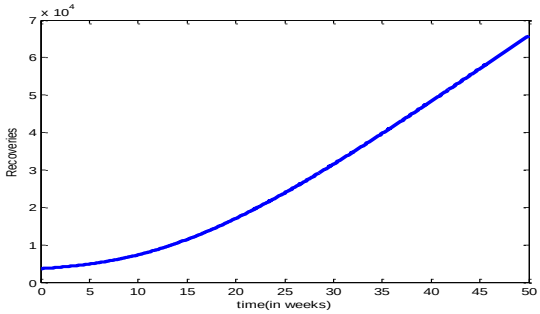


Figure 9: Recovered Humans

5 Discussion and Conclusion

The result of the implementation is presented graphically in figures 2,3,4 and 6. The figures show the effect of optimally applying the stated control measures in controlling the spread of covid-19. Specifically, we show the effect of optimal control on the number of persons that are exposed to covid-19, the number of persons that are symptomatically and asymptomatically infectious, and the number of covid-19 casualties. Each figure shows the number of people in these classes when there is no control and when optimal control is applied. The effect of applying optimal protection measures is shown in figure 2. We observe that when optimal control is applied, more people tend to control themselves as compared to when control is not applied. In figure 1, the effect of optimal control on the number of people exposed to covid-19 is presented. The graph shows that the number of people exposed to covid-19 is reduced when optimal control is applied. However, there is a sharp increase in the number of exposed persons when optimal control is applied. This sharp and sudden increase could be attributed to the inability of some people in the protection class to continue to observe adequate protection measures. In figure 4 and figure 6, we see that the number of people that are symptomatically and asymptomatically infectious are reduced when optimal control is applied. This is

the number of people that are exposed to covid-19 has been reduced. Lastly, the number of casualties can be seen to decrease when optimal control.

It can be concluded that if there are no interventions to control the spread of the disease, the disease will not be wiped out from the population. It was also observed that the best combination is protection, early burial of death due to covid-19, hospitalized and quarantine. We further noted that there is a direct correlation between asymptomatically class and the reproduction numbers, that is, as the rate of secondary infective increase also the rate of symptomatic increases. We finally observed that when protective measures are observed, quarantine, hospitalized and treatment policy is strictly adhered to and no delay in the burial of death due to covid-19, the disease will be completely wiped out of the population and thus reducing the rate of infection which increases the recovery rate in all classes.

References

[1] WHO (2020). Disease (COVID-19) pandemic, Advice for the public. Retrieved October 10, 2020.www.who.ng.org
[2] Wang C, Zhao H (2020) The impact of Covid 19 on Anxiety in Chinese University Students Front. Psychol. 11:1168. Dol: 10.3389/fpsyg.2020. 01168
[3] NCDC (2020) covid-19 fact sheet. www.ncdc.ng.org
[4] Hafeez, A.A., et al., (2020). Mathematical Modeling for infectious viral disease: The COVID-19 Perspective. Journal Public Affairs/Early View.
[5] China-WHO Joint Mission, (2020). Report of the WHO- China Joint Mission on Coronavirus Disease 2019 (COVID-19). World Health Organization. Retrieved form https://www.who.intl.
[6] Center for Disease Control and Prevention (CDC), (2020). How COVID-19 spreads. Retrieved April 3, 2020 from https://web-archive.org/web/20200403001235.
[7] B. I. Omede1,4 · U. B. Odionyenma2 · A. A. Ibrahim3 · Bolarinwa Bolaji,(2020). Third wave of COVID-19: mathematical model with optimal control strategy for reducing the disease burden in Nigeria International Journal of Dynamics and Control,https://doi.org/10.1007/s40435-022-00982-
[8] Cao, W., Ziwei F, Guogiang H, Mei H., Xinrong Xu, Jiaxin D, Jianzhong Z.(2020) . The psychological impact of the Covid-19 Epidemic on College Students in China. Psychiatry Research, 287, Article ID: 112934. Doi.org/10.1016/j.psychres.2020. 112934. Scientific research an academic publisher
[9] David J.C., Scott J.B., Keith, M.O., Mary,L.W. (2020). Coronavirus Disease 2019 (COVID-19). Assistant Professor of medicine and Pediatrics, Adult and Pediatric Infectious Disease, Rutgers New Jersey Medical School.
[10] Daniel, D.O. (2020). Mathematical Model for the transmission of Covid-19 with Nonlinear Forces of Infection and the Need for Prevention Measure in Nigeria, Journal of Infectious Disease and Epidemiology. ISSN: 2474-3658. DOI: 10.23937/2474-3658/1510158.
[11] Donald C.M. (2020). The Virus can be stopped, but only with harsh steps, Experts say. Retrieved September 30, 2020.
[12] Chan, J.F, Yuan,S., (2020): A familiar cluster of pneumonia associated with the 2019 novel coronavirus indicating person-to-person transmission: a study of a family cluster. Lancet 2020; 395;514

[13] Meng L, Hua F and Bian Z. (2020) Coronavirus Disease 2019 (Covid-19): emerging and Future Challenges for Dental and Oral Medicine,Journal of dental Research doi.org/10.1177/002203452091424
[14] Batista, V.C., Helder, S.L.,.Marcos. A.A. Protective behaviors for COVID-19 among Brazillian adults and elderly living with multi-morbidity: the ELSI-COVID-19 initiative. CSP cadernos De Saude Publica
[15] Anwar, Z., Ebraheem A.,Vedat, S., (2020): "Mathematical Model for Coronavirus Disease 2019 (COVID-19) Containing Isolation Class". Biomed Research International, vol 5. 2020, Article ID 3452402, p4.
[16] Abba BG, Enahoro A, Iboi, Calistus N, Ngonghala, Elamin H, Elibasha. Nigeria: a primer on using Mathematics to understand COVID-19 dynamics; modeling, analysis and simulations. Journal of infectious Disease Modeling. 2021;6:148-168.

International Journal of Mathematical Analysis and Modelling

Scope: The International Journal of Mathematical Analysis and Modelling (IJMAM), formerly known as the Journal of the Nigerian Society for Mathematical Biology, is the official journal of the Nigerian Society for Mathematical Biology, designed to disseminates original research findings in all areas of pure and applied mathematics. The aim of the journal is to cause to be published, original research, that shows the connection between pure and applied mathematicians, statisticians, operations researchers, physicists, engineers, computer scientists and specialists in any field of human endeavour such as in agriculture, medicine, pharmacy, life sciences, physical sciences, engineering, social sciences, humanities, arts, etc., at the crossroad of theoretical, experimental and field studies with the mathematical sciences, in order to provide solutions to problems that cut across these fields through exchange of ideas and collaborations.

Submitted papers should provide rigorous mathematical analysis of any real-world problem being discussed; at the same time, the results obtained should be useful and easily understandable by non-mathematicians. The journal will accept different kinds of articles, ranging from review articles to special invitations. All submitted manuscript will be assessed by the Editor-in-Chief before being sent out for peer-review.

Areas covered in the IJMAM include, mathematical modelling, numerical analysis, fluid mechanics, real and complex analysis, functional analysis, operator theory, statistics, algebra, computational mathematics and differential equations. Articles that show the connections between different areas of mathematics when solving real-world problems are especially welcome in the IJMAM.

Manuscript Information and guidelines for Authors

This is to invite you to submit high-quality research articles to the International Journal of Mathematical Analysis and Modelling (IJMAM), formerly known as the Journal of the Nigerian Society for Mathematical Biology.

Manuscripts should be written using LaTeX only. Initial submissions for review can be in MS Word or PDF. However, the accepted manuscript should be in LaTeX; we do not accept manuscripts in any other format including MS Word, for publication. The article should be concise and details of well-established mathematical methods should be omitted. Articles that do not contain significant mathematical content and results will not be accepted for publication.

Citations within the manuscript should be done using the number system i.e., “Following the idea in [7], we have that …”. Theorems, Lemmas, Propositions,

Remarks, e.t.c., should be numbered using the Section number where they appear e.g., Theorem 2.1 will appear in Section 2.

References should follow the format shown below:

[1] Anderson, R. M. and May, M. (1991). Infectious Diseases of Humans: dynamics and Control, Oxford University Press, UK.

[2] Castillo-Chavez C. and Song B. (2004). Dynamical models of tuberculosis and their applications, Math. Biosci. Eng., 1: 361-404.

References should be arranged in the order in which the articles are cited in the work, and not in alphabetical order, which should be the last section in the manuscript.

Manuscripts should be submitted to the Editor-in-Chief, via the journal's website, which can be accessed using www.tnsmb.org, or via the following email address: mcsb@uniben.edu or ijmam.nsmb@gmail.com.

There is a publication charge for each accepted article. Payment details will be corresponded to the author(s) at the time of manuscript acceptance for publication in the IJMAM.

Subscription rates: This is subject to change from time to time. Please, contact the Editor-in-Chief for the current rates, for local and foreign subscriptions.

International Journal of Mathematical Analysis and Modelling

(Formerly Journal of the Nigerian Society for Mathematical Biology)

Volume 7, Issues 1&2, 2024

Contents

Issue 1

Mathematical analysis for the dynamics of Feline immunodeficiency virus in cats population
Salisu Usaini and Musa Usman 1 – 11

Uniqueness of solution of multi-term fractional order Volterra Integro-differential equations with convergence analysis
D. Umar and S.L. Bichi 12 – 22

The application of Least Squares Method and Shifted Chebychev Polynomials for solving fourth order Volterra Integro-Differential Equations
A.K. Bello, A.M. Ayinde, A.S. Daodu and A.A. Ishaq 23 – 38

Type II Half Logistic Inverse Exponential distribution: properties and application to tax data
D.O. Omosigho, K.T. Amzat, and O.E. Adeniji 39 – 50

Transient analysis of short circuit faults in hybrid networks
J.S. Zangina, M.A. Suleiman, and A. Ahmed 51 – 61

An Investment Model for a DC Pension System with Refund Clause under Quadratic Utility
K.N.C. Njoku 62 – 74

Stability analysis of an HIV/AIDS model with saturated incidence
O.A. Odebiyi and J.K. Oladejo 75 – 98

Revealing some of the hidden mathematical models of educational theories
C.V. Obasi, E.N. Didigwu, and I.G. Ezugorie 99 – 121

Optimal control and sensitivity analysis of age-structured mathematical model of Diphtheria infection
E.S. Udofia, J.I. Uwakwe, and H.S. Thomas 122 – 143

Algorithm for semigroup bases I
M.I. Sampson, Z. Lipcsey, E.O. Akak, F.A. Efiong and M.A. Essien 144 – 152

Issue 2

Utility maximization and portfolio management with administrative fee and dividend
E.E. Akpanibah, L.E. Georgey, and W.V. German 1 – 15

The influence of aquatic mosquitoes on Lymphatic Filariasis transmission dynamics: mathematical model approach
A. Abokwara and C.E. Madubueze 16 – 32

Approximate common solution of variational inequality and fixed point problems for family of nonexpansive semigroup
A.H. Ugwu, I.G. Ezugorie, E.C. Agbo, and E.U. Ofoedu 33 – 54

Numerical solution approximation of nonlinear functional integral by Homotopy perturbation method
C.E. Chika 55 – 61

A theoretical investigation of the impact of a 2-dose vaccination strategy on Monkeypox transmission dynamics at population level
I.I. Ako 62 – 77

Complex Ebola Virus Disease fractional order model in the Caputo sense with Laplace Adomian Decomposition Method model solution
Q.O. Ahman, R.O. Aja, W. Atokolo, D. Omale, N.E. Didigwu, C.S. Ugwu, A.L. Ozioko, S.O. Joseph, V.I. Ezaegu, R.V. Paul, and G.C.E. Mbah 78 – 113

Mathematical model for transmission dynamics of Malaria disease: impact of invasive alien plants
C.J. Alhassan, D. Okuonghae, and K.O. Achema 114 – 143

On the nilpotents of the semigroup of partial contractions of a finite chain
M.M. Zubairu and B. Ali 144 – 152

Detection and correction of heteroscedasticity and its effect on modelling of Nigerian economic data
E.O. Idowu, E.M. Ikegwu, A.A. Fadiji and M.U. Evro 153 – 158

Options pricing using combination of Brownian motion with a random time component
C.A. Onyegbuchulem, B.O. Onyegbuchulem, and U. Alwell 159 – 167

An effective new one-step block integrator for the numerical solution of system of first order differential equation arising from epidemiology models
M.I. Modebei, O.O. Olaiyay, O.E. Faniyi, and O.F. Anorue 168 – 177

Mathematical model showing preventive measure as a key to reducing Coronavirus disease (COVID-19) spread
C. Okoye, M.B. Okofu, N.K. Nubila, C.L. Ejikeme, and D.F. Agbebaku 178 – 184

On the vector Lyapunov functions and eventual stability of nonlinear impulsive differential equations
J.E. Ante, A.B. Inyang, E.J. Oduobuk, and U.P. Akai 185 – 199

Effect of thermal radiation and chemical reaction on unsteady MHD plane – Poiseuille flow of fourth-grade fluid in horizontal parallel plates
K.M. Joseph, E.A. Andi, E.J. Adoyi, C.O. Akusu, and C. Onwubuoua 200 – 223

Fractional order model of dynamical behavior and qualitative analysis of Anthrax with infected vector and saturation
A.C. Loyinmi and A.L. Ijaola 224 – 264

An infection-age-structured modelling for Monkey-Pox disease dynamics incorporating control measures
N.O. Lasisi, O.J. Ejiwole, E. Azuaba, and A. A. Ibrahim 265 – 282

An equivalence in a selected family of cyclic subsemigroups and algorithm for generating systems of semigroup
M.I. Sampson, C. F. Igiri, J.O. Achuobi, C.T. Madubuike, and L.E. Effiong 283 – 292

Application of Jensen's integral formulae on polynomials with entire functions of positive real parts and Gauss mean value theorem
G.N. Emenogu, I.C. Yemisi, E.I. Edugbe, C. Chigozie, and B.O. Osu 293 – 323

A generalize Picard's successive iteration method for the nth order initial valued problem
A.K. Bello, A.M. Ayinde, A.A. Ishaq, M.T. Raji and A.E. Adenipekun 324 – 335

Mathematical model of the transmission dynamics of Anthrax disease
C. Omeh, G.C.E. Mbah, D. Nnaji, I.G. Ezema, A.Y. Danjuma., and E.O. Oshilim 336 – 348

Characteristics and control strategies for Diphtheria-Pertussis co-infection risk in the post COVID-19 era
S.O. Johnson, H.O. Edogbanya, J.O. Omolehin, and O. Johnson 349 – 368

On Lojid Algebras
E. Ilojide 369 – 379

Eight-order second derivative block linear multistep method for chaotic initial value problems
E. J. Onoja, U.W. Sirisena, and G.M. Kumleng 380 – 397

Mathematical fractional model for the dynamics and control of Diphtheria transmission
E. Abah, B. Bolaji, W. Atokolo, G.O. Acheneje, B.I. Omede, J. Amos, and D. Omeje 398 – 422

On a class of piecewise continuous Lyapunov functions and eventual stability for nonlinear impulsive Caputo fractional differential equations via new generalized Dini derivative
J.E. Ante, S.O. Essang, J.U. Atsu, E.O. Ekpenyong, and R.D. Effiong 423 – 439

Picard-Mann hybrid iteration process for approximating fixed points of contraction mappings
E. Ekuma-Okereke, O.D. Koko, C.V. Okpako, and J.O. Ogbodu 440 – 463

Stabilizers of Lojid algebras
E. Ilojide 464 – 473

Algorithm for approximating common fixed points of family of strictly pseudo-contractive mappings in Hilbert spaces
E. Ekuma-Okereke, J.O. Ogbodu, C.V. Okpako, and O.D. Koko 474 – 489

On the monoid of partial isometries with fixed set
M.M. Zubairu and Z.D. Lawan 490 – 496

A hybrid method of block pulse with Bernstein polynomial for numerical solution of linear ill-posed first kind Fredholm Integal equation
H.S. Musa and S.L. Bichi 497 – 509

A fractional-order transmission dynamics for Diphtheria and Pertussis co-infection
J.O. Omolehin, O.S. Johnson, and I.O. Babarinsa 510 – 522

A mathematical model for transmission dynamics of COVID-19 in Nigeria and its post effects
B.C. Agbata, D.F. Agbebaku, C.E. Odo, J.T. Ojih, M.M. Shior, and I.G. Ezugorie 523 – 547

Estimation of different types of entropies for the Gumbel Type-2 distribution
D.O. Omosigho, A.D. Adefolarin, and N.A. Adeleye 548 – 557

Laplace-Adomian Decomposition method for solving fractional-order mathematical model of Monkeypox transmission dynamics
B.C. Agbata, W. Obeng-Denteh, D.F. Agbebaku, M.M. Shior, D.J. Yahaya, and A.Y. Danjuma 558 – 588

Half Logistic Generalized Inverse Rayleigh distribution for modeling Breast Cancer data
O.I. Oseghale and E. S. Micah 589 – 606

Controlling the dynamics of Diabetes Mellitus with mathematical model
K.A. Adeyemo, T.A. Lawal, I.A. Azeez, E. Philemon, K.I. Falade, F.C. Nwachukwu, A. Omame, N. O. Lasisi, and P.O. Aye 607 – 628

Mathematical model for controllability of covid-19 investigating the impact of protective measures, for optimal solution to lower the disease burden in Nigeria
S.C. Nwasuka, U.A. Osisiogu, and T.E. Efor 629 – 649